MAGIC-TDAS 07-04
070918/S. Commichau

Geomagnetic Field Effects on the Imaging Technique Part I: Results from dedicated MC Studies

S. Commichau and A. Biland

ETH Zurich

September 2007

Abstract

This note summarizes results from MC studies on Geomagnetic Field (GF) effects on the imaging technique. The studies were performed using dedicated MC data. MC γ-rays were generated for energies between 30 GeV and 1 TeV using the standard MAGIC MC software and MARS.

The results from the MC studies show that the shape and the orientation of γ-ray shower images can be significantly altered due to the influence of the GF. Moreover, the MC studies also show that not only low-energy γ-rays around 30 GeV are affected by the GF but also TeV γ-rays. Depending on the orientation of the γ-rays with respect to the direction of the GF, the pointing of the shower images can be degraded and images get systematically rotated. The pointing information can be irrecoverable for some orientations of the γ-rays. As a result, the γ/hadron separation capability of the analysis will be significantly degraded. The influence of the GF also reduces the γ efficiency and degrades the energy estimation.

Contents

1 Introduction

Among all IACTs being currently in operation, the MAGIC telescope aims at the detection of very low-energy γ-rays in the order of 60 GeV and below [6]. Since γ/hadron separation becomes more and more complicated at γ-ray energies close to the threshold energy of MAGIC, it is crucial to investigate the impact of the Geomagnetic Field (GF) on EAS.
The influence of the GF on EAS was already qualitatively discussed in 1953 [16]. Charged secondary particles in EAS are deflected by the GF which causes a broadening of the EAS. It was pointed out that the east-west separation of electrons and positrons in EAS due to the Lorentz force can be non negligible compared to the displacement due to Coulomb scattering. The effect on γ-ray induced EAS is expected to be bigger than on hadron induced EAS, as their shape is initially more regular and the scattering angles occurring in nuclear interactions are typically much larger than that produced by the deflection of secondary charged particles due to the influence of the GF [16]. The Cherenkov images on ground can be affected in a way that the threshold energy of an IACT increases [10] as well as its γ/hadron separation capability is expected to be deteriorated.
This note summarizes results from dedicated MC simulations. The objectives of the MC studies was to find out about the impact of the GF on the analysis methods that are widely used to extract the γ-ray signal from a VHE γ-ray source. A second note will be dedicated to results from studies on GF effects in real data.
The first part of this note reviews some general information on the origin and the features of the GF. The influence of the GF on the development of EAS as well as on the Cherenkov light distribution on ground is briefly reviewed and discussed. The second part summarizes results from dedicated MC studies on the GF effects and discusses the influence of the GF on the analysis of MAGIC data. The studies are carried out at the level of the Hillas parameters.

1.1 The Geomagnetic Field

In the most simple model, the GF in space can be approximated by the magnetic field that is generated by a dipole magnet located at the center of the Earth. Figure 1 shows a simplified representation of the GF. In reality, the magnetic field lines do not strictly follow those of a dipole magnet. Furthermore, the dipole center does not coincide with the center of the Earth and the dipole axis is not parallel to the spin axis of the Earth, i.e. north and south geographic poles and north and south magnetic poles are not located in the same plane. The geographic north of the Earth is close to the magnetic south, but the dipole axis is tilted from the spin axis by $\sim 11°$ [13].
The solar wind, a stream of charged particles that are ejected from the upper atmosphere of the sun, modifies the GF. Field lines going toward the sun get compressed, while the field lines on the opposite side form the so-called Earth's magnetotail. In this way, the solar wind determines the overall shape of the GF. The solar wind mostly consists of high-energy electrons and protons that are able to overcome the sun's gravitional attraction. To date, the mechanism by which the particles attain the high kinetic energy of $\mathcal{O}(1\,\mathrm{keV})$ is not well understood [7]. Although a fraction of the kinetic energy can be attributed to the high temperature of the corona, there is another process required, being able to provide additional energy. This process may involve strong magnetic fields in the solar atmosphere. The solar wind not only temporarily deforms the GF (on timescales hours and days) due to coronal mass ejections, but also modulates the GF according to the eleven-year cycle of the solar activity of the sun. Coronal mass ejections are believed to be caused by a temporary release of magnetic energy at the sun. The sudden disturbances of the GF induced by the solar wind, also called magnetic storms, can last from hours to several days. These locally occurring disturbances of the GF can reach some

500 nT [13].
The main part of the GF is generated by internal sources. The intensity of the generated field ranges from 20 μT to 70 μT. External sources, related to ionized currents in the upper atmosphere, have a small share on the GF, which is in the order of some 100 nT [13]. Although the magnetic properties of iron and its abundance in the Earth suggest that the Earth represents a big magnet, the high temperature existing in the inner core rebuts this assumption. It is known that all materials lose their magnetism at the so-called Curie temperature, and the Curie temperature of iron is already reached at an average depth of 25 km [13]. The Curie temperature increases with increasing pressure, but the change is small compared to the average increase in temperature towards the Earth's interior.

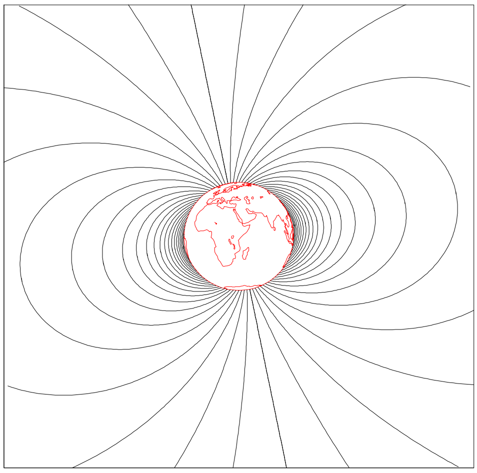

Figure 1: A simplified representation of the GF [5]. In first order, the GF closely resembles a dipole magnet situated at the center of the Earth. On closer inspection, the GF appears to be variable in time and position. The axis of the GF dipole component is not only offset from the center of the Earth, but also tilted with respect to the Earth's spin axis by $\sim 11°$ [13].

The Earth's crust by itself, i.e. the outer layer of some 20 km thickness, cannot account for the GF observed in space. The complete magnetization of the material in the outer layer of the Earth would contribute only marginally to the dipole field [13]. Furthermore, time variations of the dipole location as well as the evidence for an ancient dipole reversal indicate that the GF is probably generated by liquid motion of material in certain layers deep inside the Earth. To date, the liquid outer core at depths between about 2900 km and 5200 km is believed to hold a massive ring of current whose flow may generate the dipole field of the Earth. There is a number of so-called current-source models that explain the occurrence of the GF by means of a "self-excited dynamo" model [13]. These models comprise time constants that are probably much larger than the period of reliable observations of the GF field, which have been carried out to this day. The occurrence of dipole reversals as well as the relation between the change in the Earth's spin and the secular change of the dipole declination is described by these self-excited dynamo models, however. Nowadays, dipole reversals are expected to happen every 200 thousand years.
Given its irregularity and temporal variability, the GF must be measured in many places all around the world to get a satisfactory and comprehensive picture of its orientation and strength. The surveying and mapping of the GF is done by means of satellites as well as by a large number of Earth-based and

satellite-born geomagnetic observatories throughout the world, such as the International Real-time Magnetic Observatory Network (INTERMAGNET) [23], which measures the magnitude of the GF components and their change over time down to time-scales of hours. Because the orientation and strength of the GF continuously changes, it is impossible to make an accurate prediction of the GF components at any point in the very distant future. But, from the information collected on the GF over period of years, it is possible to introduce a mathematical representation of the GF, a so-called main field model. There are two global main field models, the World Magnetic Model (WMM) and the International Geomagnetic Reference Field Model (IGRF), which are constantly updated and distributed by the National Geophysical Data Center (NGDC) [33]. While the WMM is the standard navigation model for the U.S. and U.K. Departments of Defense and National Air Transportation Association (NATA), the IGRF is the international research reference model, providing the most accurate estimate for the GF components all around the world. Based on the measurements of the geomagnetic observatories, the WMM and the IGRF are updated every five years.

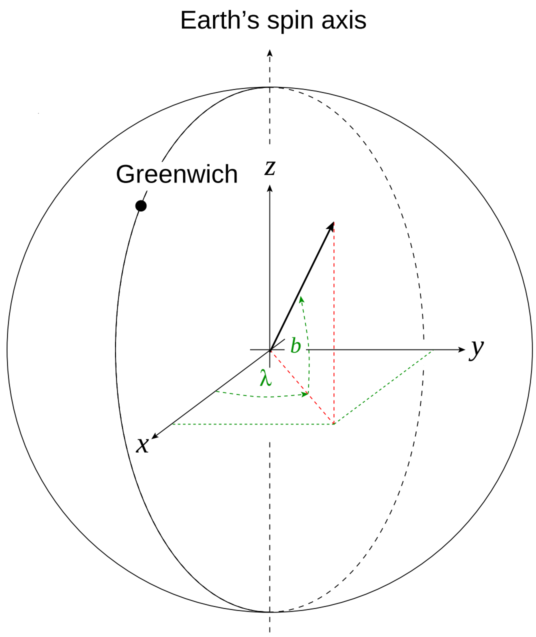

Figure 2: Definition of the geographic coordinate system. The z-axis is aligned with the Earth's spin axis and the x-axis points towards the Greenwich meridian at ($b = 52°$,$\lambda = 0°$).

It is common to express the GF by the gradient of a magnetic scalar potential V. Then, the GF can be obtained from

$$\vec{B} = -\nabla V. \tag{1}$$

The spherical symmetry of the problem allows to perform the harmonic analysis of the scalar potential V of the GF in terms of the following expansion [13]:

$$V(r, \lambda, b) = r_{\mathrm{E}} \sum_{n=1}^{N} \sum_{m=0}^{n} \left(\frac{r_{\mathrm{E}}}{r}\right)^{n+1} \left(g_{n,m} \cos(m\lambda) + h_{n,m} \sin(m\lambda)\right) P_n^m(\sin b). \tag{2}$$

(r, λ, b) is a system of spherical coordinates. The polar axis of the corresponding spherical coordinate system coincides with the z-axis of a Cartesian coordinate system situated at the Earth's center. The z-

axis of the Cartesian coordinate system is aligned with the Earth's spin axis, and the x-axis is oriented towards the Greenwich meridian (figure 2). r_{E} denotes the mean radius of the Earth (6371.2 km), r the radial distance from the center of the Earth, λ the longitude eastwards from Greenwich, b the geographic latitude, and $P_n^m(\sin b)$ the associated Legendre function of degree n and m. The associated Legendre functions are normalized according to the convention of Schmidt [12]. N, the maximum spherical harmonic degree of the expansion, defines the precision of the approximation. The most accurate model for the GF, the IGRF, describes the GF in terms of a series expansion like the one in equation 2. The spherical harmonic coefficients $g_{n,m}$ and $h_{n,m}$ are adjusted to best fit the GF measurements. The maximum degree of the expansion is usually set to $N = 5$. The spherical harmonic coefficients are updated every five years. Coefficients for dates lying between neighboring five-year epochs are interpolated using the coefficients as well as their first time derivations of the corresponding neighboring intervals. So far, coefficients are available back to the year 1900.
The main contribution in the spherical harmonic expansion, defined by equation 2, comes from the terms with $n = 1$. The contributions of higher-order terms of the series expansion are considered as a perturbation of the dipole-like component of the GF. In the so-called centered dipole model, the terms with $n = 1$ can be identified with the magnetic potential produced by a dipole situated in the center of the Earth whose axis is inclined with respect to the Earth's spin axis. For $n = 1$, the magnetic scalar potential of the GF, approximated by the first term of the resulting series expansion, reads

$$V(r, \lambda, b) = r_{\mathrm{E}} \left(\frac{r_{\mathrm{E}}}{r}\right)^2 B_0 \sin b, \quad B_0 = \sqrt{g_{1,0}^2 + g_{1,1}^2 + h_{1,1}^2}. \tag{3}$$

The coordinates b and λ are now measured in a spherical coordinate system with its center situated at the Earth's center and the polar axis coinciding with the direction of the dipole [26]. The coordinate system, whose polar axis is aligned with the dipole, is referred to as the geomagnetic system. The geomagnetic coordinate system is connected to the geomagnetic reference system through a rotation around the y-axis and a rotation around the z-axis. $B_0 \approx 3 \cdot 10^{-5}\,\mathrm{T} = 0.3\,\mathrm{G}$ denotes the mean value of the GF on the geomagnetic equator at the Earth's surface. Thus, in the centered dipole approximation, the main component of the GF is given by

$$\vec{B}(r, \lambda, b) = -\nabla V(r, \lambda, b) = \left(\frac{r_{\mathrm{E}}}{r}\right)^3 B_0 \left(\cos b\, \vec{e}_b + 2 \sin b\, \vec{e}_r\right). \tag{4}$$

Another approach, the so-called eccentered dipole model, is used to approximate the GF with a magnetic dipole that is not necessarily located at the center of the Earth [13]. The eccentric dipole has the same moment as the centered dipole and the same orientation of its axis, but in terms of the geographic Cartesian coordinate system. The dipole is placed in a way that the quadrupole term is made to vanish, maximizing the dipole term. The eccentered dipole model is somewhat more appropriate for studies of magnetospheric particle dynamics, as charged particles, arriving from space, are guided by the eccentered dipole field.
Usually, the GF is described by seven parameters [13]. The total intensity F, the inclination I, the declination D, the horizontal intensity H, the north and the east components, X and Y, respectively, and the vertical component Z. All components are provided by both the IGRF model and the WMM. Nevertheless, at any point of the Earth, the direction and intensity of the GF is completely determined by only three parameters. The values for F, I, X and Y, respectively, can be derived from D, H and Z. Figure 3 shows the decomposition of the total intensity F of the GF in a Cartesian coordinate system whose x-axis is aligned with the spin axis of the Earth. The y-axis points eastwards and the z-axis points inwards into the Earth. The vertical intensity Z is the z-component of the GF, which is considered positive when pointing down. The horizontal intensity H points to the magnetic south,

while its projection on the x-axis, X, points to the geographic north. The declination D, sometimes called magnetic variation, is the difference between the true meridians and the magnetic meridians, i.e. D is determined by the angle between the magnetic and the geographic north pole. D, usually measured in degrees, is considered positive east of the geographic north and negative when being west of the geographic north. The inclination I is the angle under which the magnetic field lines dip into the surface of the Earth. The magnetic inclination varies from $+90°$ (perpendicular to the surface) at the magnetic poles to $0°$ (parallel to the surface) at the magnetic equator. The total GF F intensity can be expressed in terms of the horizontal intensity H and the vertical intensity Z:

$$F = \sqrt{Z^2 + H^2}. \tag{5}$$

The relation between inclination I, horizontal intensity H and vertical intensity Z reads

$$\tan(I) = \frac{Z}{H}. \tag{6}$$

The north and the east components, X and Y respectively, can be calculated from H and D:

$$X = H\cos(D), \quad Y = H\sin(D). \tag{7}$$

Up-to-date values for the components of the GF can be found at the web pages of the NGDC [33]. The NGDC web pages also provide a collection of programs to estimate the components of the GF based on either the WMM or the IGRF model. The errors on the field components are very small. For example, the errors on the components D and I are $\mathcal{O}(500\,\mathrm{nT})$ and $\mathcal{O}(30')$, respectively.
Figure 4 shows the main field isomagnetic contours in geographic coordinates (Mercator projection) at 10 km a.s.l., calculated for November 2006 according to the epoch 2005 WMM. The locations of the new generation IACTs being currently in operation are indicated. Of all the four observatory sites, the one of the CANGAROO experiment [32] exhibits the highest value for the absolute GF strength. Instead, the H.E.S.S. observatory site shows the lowest value, although the global minimum in the total GF, called South Atlantic/South American anomaly, is located at about (30° S, 50° W).
Table 1 lists the values and the annual change of the GF components. The regular changes of the components are also called secular variations. The estimation of the values was done for November 2006 according to the epoch 2005 IGRF model.
The Lorentz force exerted on charged particles in an EAS depends both on ZA and azimuth angle that correspond to the direction of the primary particle. For a particle of charge q, traveling at a velocity $\vec{v}$ trough a magnetic field of strength $\vec{B}$, the Lorentz force $\vec{F}$ reads

$$\vec{F} = \frac{\mathrm{d}\vec{p}}{\mathrm{d}t} = q\left(\vec{v} \times \vec{B}\right) = \frac{q}{m}\left(\vec{p} \times \vec{B}\right) \propto \vec{B}_\perp. \tag{8}$$

Therein $\vec{p}$ denotes the momentum of the particle and $\vec{B}_\perp$ the component of the magnetic field strength perpendicular to the direction of movement of the particle.
For sake of simplification, the reference frame is usually chosen such that the y-component of the magnetic field strength vanishes. In a reference frame rotated clockwise by the angle D around the z-axis, the magnetic field reads $\vec{B} = (B_x, B_y, B_z)^\mathrm{T} = (H, 0, Z)^\mathrm{T}$. In such a reference frame, the magnetic field strength perpendicular to the direction of movement of the particle can be written as

$$\vec{B}_\perp(\theta,\phi) = -\sin\theta\sin\phi B_z\vec{e}_x + (\sin\theta\cos\phi B_z - \cos\theta B_x)\vec{e}_y + \sin^2\theta B_x\vec{e}_z. \tag{9}$$

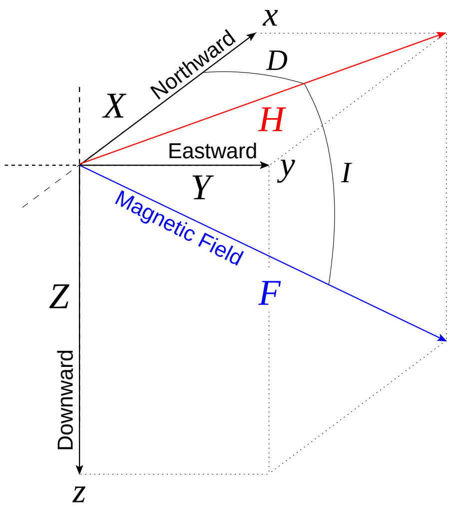

Figure 3: Decomposition of the total intensity F of the GF in a Cartesian coordinate system, whose x-axis is aligned with the spin axis of the Earth. The y-axis points eastwards and the z-axis points inwards to the center of the Earth. H points to the magnetic south, while its x-component, X, points to the geographic north. The declination D is given by the angle between the magnetic south and the geographic north pole. The inclination I is the angle under which the magnetic field lines dip into the surface of the Earth.

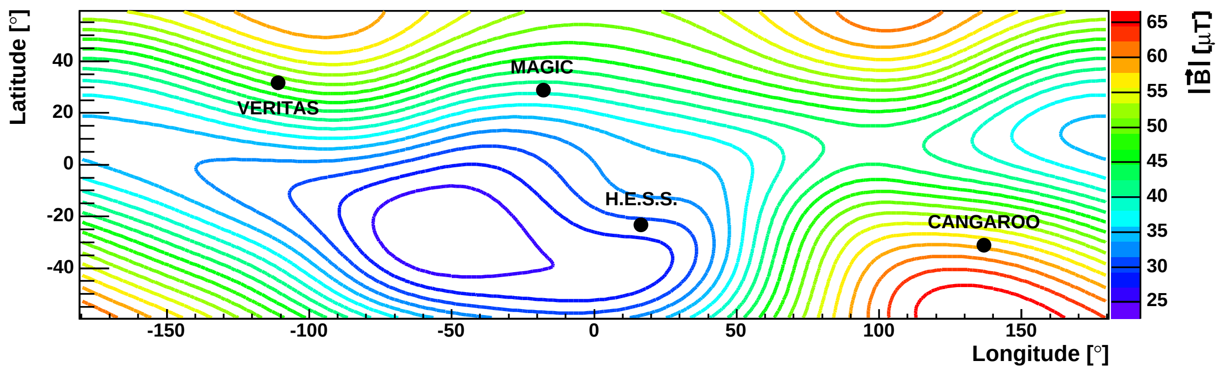

Figure 4: Iso-contours of the absolute value of the GF in geographic coordinates (Mercator projection) for 10 km a.s.l., calculated for November 2006 according to the epoch 2005 WMM [33]. The locations of the new generation IACTs being currently in operation are indicated. Of all four observatory sites, the one of the CANGAROO experiment exhibits the highest value for the absolute GF strength. Instead, the H.E.S.S. observatory site shows the lowest value. The minimum in the total GF at about (30° S, 50° W) is called South Atlantic/South American anomaly.

Therein the $\vec{e}_i$, $i = \{x, y, z\}$ denote the unit vectors of the tilted reference frame, and the angles ϕ and θ correspond to the azimuth angle and the ZA under which the particle is traveling (figure 17).
The angle α between the shower axis and the direction of the GF can be expressed in terms of the azimuth angle and the ZA:

$$\alpha \equiv \sphericalangle(\vec{B}, \vec{p}) = \arcsin\left(\frac{|\vec{B}_\perp(\theta, \phi)|}{|\vec{B}|}\right). \tag{10}$$

Figure 5 shows the angle α between the shower axis and the direction of the GF versus azimuth angle (for La Palma). The ZA was varied between 0° and 60° in steps of 10°. Depending on the ZA, the angle α takes values between $\sim 0°$ and 90°. For each ZA, the maximum Lorentz force coincides with the maximum angle α. For instance, at about 40° ZA the maximum Lorentz force is reached at 180° azimuth angle.

Main Field		**Secular Change**	
D (declination)	−7.021° (west)	ΔD	0.136°/year
I (inclination)	38.631° (down)	ΔI	−0.058°/year
H (horizontal intensity)	30130.57 nT	ΔH	31.04 nT/year
X (north component of the horizontal intensity)	29904.63 nT	ΔX	39.45 nT/year
Y (east component of the horizontal intensity)	−3683.00 nT	ΔY	67.04 nT/year
Z (vertical intensity)	24079.34 nT	ΔZ	−24.82 nT/year
F (total intensity)	38570.27 nT	ΔF	8.78 nT/year

Table 1: Present values (November 2006) and the annual change of the GF components at the Roque de los Muchachos observatory on the Canary Island of La Palma (28.8° N, 17.9° W) at 10 km a.s.l., calculated according to the epoch 2005 IGRF model [33].

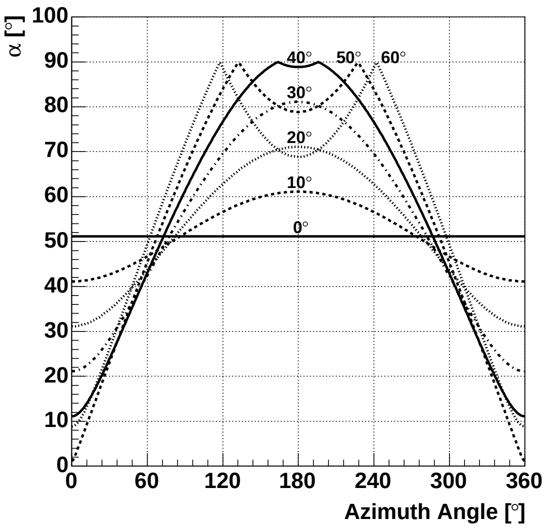

Figure 5: The angle between the shower axis and the direction of the GF versus azimuth angle and different ZAs between 0° and 60° (for La Palma).

Another representation of the relation between maximum Lorentz force, azimuth angle and ZA is shown in figure 6. The vertical component $|\vec{B}_\perp|$ of the GF strength at the Roque de los Muchachos observatory on La Palma (28.8° N, 17.9° W) is shown for 10 km a.s.l., calculated in November 2006 for the epoch 2005 IGRF model [33].

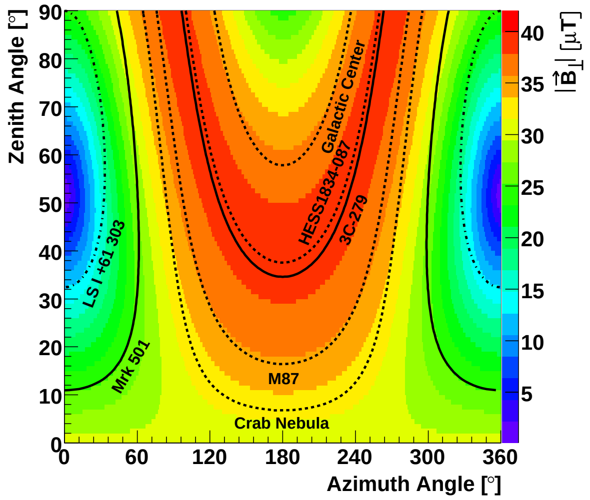

(a) The absolute value of the vertical component of the GF strength for alt-azimuth coordinates.

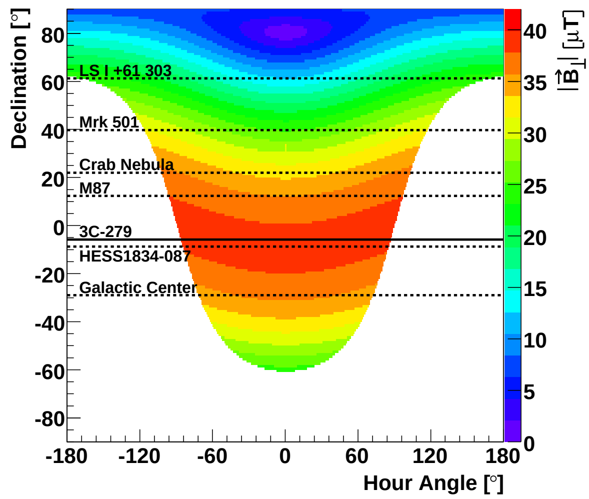

(b) The absolute value of the vertical component of the GF strength for equatorial coordinates and $0° \leq \mathrm{ZA} \leq 90°$.

Figure 6: The absolute value of the vertical component of the GF strength at the Roque de los Muchachos observatory on La Palma (28.8° N, 17.9° W) for 10 km a.s.l., together with the trajectories of some established and potential VHE γ-ray sources. The GF components were calculated for November 2006 according to the epoch 2005 IGRF model [33].

Figure 6 (a) shows the absolute value of the vertical GF component for local, i.e. alt-azimuth coordinates. The trajectories of several selected sources at different declination angles are indicated. It is remarkable that the absolute value of the vertical GF component is symmetric in azimuth. The minimum influence of the GF is expected to occur at the magnetic north at $\mathrm{ZA} = (90° - I) \approx 51°$, where the angle α between the shower axis and the GF lines becomes smallest. I denotes the inclination angle under which the GF lines dip into the surface of the Earth (table 1). The maximum influence of the GF on EAS occurs in direction of the magnetic south at $\mathrm{ZA} = I \approx 39°$.
Figure 6 (b) shows the absolute value of the vertical GF component for equatorial coordinates. The figure was obtained for $0° \leq \mathrm{ZA} \leq 90°$. The trajectories of several selected sources at different declination angles are indicated. For all sources, the field strength changes very little along the source trajectory. That is, if there is a non negligible systematic GF effect on the reconstruction methods, this effect is approximately constant along the trajectory of a certain source. Moreover, large ZA observations are not necessarily more affected by the GF than observations carried out at low ZA.
Except for M87, MAGIC has detected VHE γ-ray emission from all sources whose trajectories are indicated in figures 6 (a) and (b) [1, 2, 3, 4, 38]. Observations of the source HESS 1834-087 or 3C-279 should be most of all affected by the GF. The maximum effect is expected to occur for sources with declinations between $-20°$ and $+10°$.
Figure 7 shows the absolute value of the vertical component of the GF strength at the γ-ray observatories MAGIC, H.E.S.S., VERITAS and CANGAROO. While the GF strength at the H.E.S.S. site exhibits the lowest maximum value among all observatory sites, the one of the CANGAROO experiment exhibits the highest maximum field strength. Furthermore, the GF strength at the CANGAROO

site varies by up to 90 %.

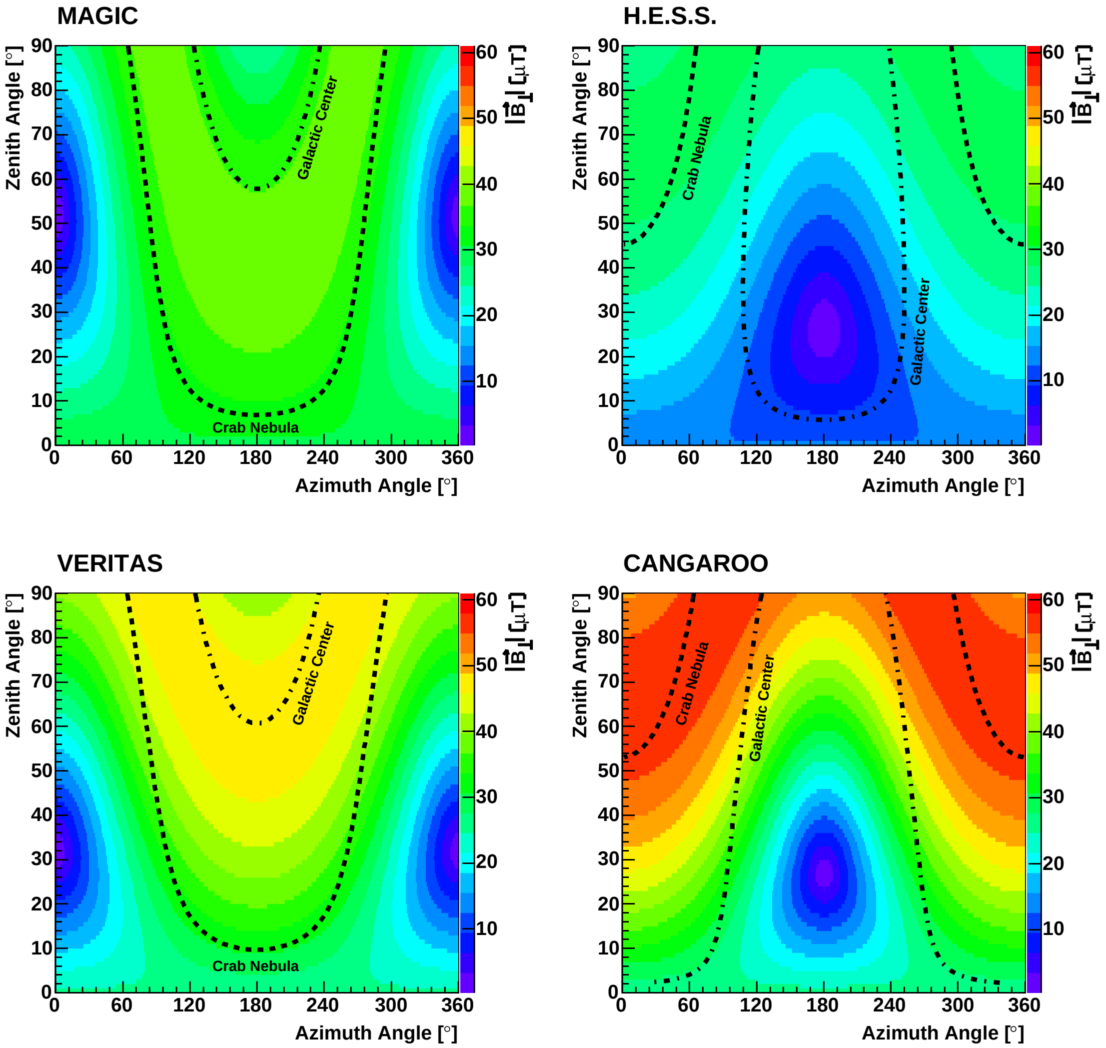

Figure 7: The absolute value of the vertical component of the GF strength at the γ-ray observatories MAGIC, H.E.S.S., VERITAS and CANGAROO, together with the trajectories of the Crab nebula and the Galactic Center. The GF components at 10 km a.s.l. were calculated for November 2006 according to the epoch 2005 IGRF model [33].

For low-ZA observations below $\sim 10°$, the MAGIC and VERITAS sites exhibit about the same GF strength over the entire range of the azimuth angle. In comparison to the other observatory sites, the H.E.S.S. site exhibits the lowest GF strength for observations carried out at ZA $\lesssim 10°$. Thus, with regard to possible GF effects, the H.E.S.S. observatory site exhibits most favorable conditions for observations of the GC, while the VERITAS observatory site, apart from the large ZA under which GC observations have to be carried out, provides rather bad conditions for observations of the GC. For GC observations carried out under $\sim 60°$ ZA at the MAGIC observatory site, the absolute value of the vertical GF component is $\sim 37\,\mu$T, which is comparable to the GF strength for Crab nebula observations carried out under similar ZA. Therefore, if there is a significant GF effect on the image

analysis, the effect should be comparable (see following TDAS note). It was shown elsewhere [28] that IACT measurements of TeV γ-rays from the Crab nebula were not significantly affected when the GF strength was below $35\,\mu$T. However, IACTs currently in operation as well as future instruments will be more sensitive to GF effects. We were able to show that even low-ZA measurements of sub-TeV γ-rays from the Crab nebula are affected for a GF strength of about $33\,\mu$T [18] (see following TDAS note).
The study the influence of the GF on the reconstruction methods using real MAGIC data is complicated for several reasons. First of all, the source needs to be strong and stable, preferably without any time variability. Secondly, the change of the telescope performance must be as small as possible in order to be able to disentangle a possible influence of the GF from all other influences which may mimic a GF effect. As already pointed out, the change of the intensity of the GF along a source trajectory is very little. For example, in case of the MAGIC site, Crab nebula observations restricted to ZA $< 60^\circ$ involve changes of the GF intensity of at most 5 %. In addition, the influence of the GF on the reconstruction methods for the VHE γ-ray signal is expected to be energy dependent. Because the energy threshold of an IACT strongly depends on the ZA under which observations are carried out, it is not trivial to extract a possible GF effect just from the comparison of observations carried out at different ZA intervals. Beside the Crab nebula, all other sources are either faint or variable in time. Therefore, it is much more straightforward to carry out first of all MC simulations to investigate possible GF effects on the reconstruction methods.
The impact of the GF on EAS as well as on the Cherenkov light distribution on ground is briefly discussed in the next two sections. Rather detailed reports on the GF effects on EAS and on the Cherenkov light distribution on ground can be found elsewhere [34, 37, 39].

1.2 The Influence of the Geomagnetic Field on EAS

The Lorentz force acts on the movement of secondary charged particles in EAS. As the Lorentz force exerted on oppositely charged particles in a magnetic field points at diametrically opposed directions, the GF is expected to laterally broaden the EAS. It was discussed firstly in 1953 that the displacement from the rectilinear path due to the Lorentz force on electrons and positrons in EAS can be of the same order as the displacement due to Coulomb scattering [16]. The magnetic deflection modifies the electron and positron distribution around the core of a γ-ray induced EAS rather than that of the low-energy electrons and positrons being more offset from the core. Below the critical energy $E_\mathrm{C} \approx 83\,\mathrm{MeV}$, electrons and positrons lose their energy predominantly by ionization of air molecules as well as Compton scattering, i.e. low-energy electrons and positrons are carried away by single large-angle scatterings.
Figure 8 shows the two-dimensional projection of the trajectories of secondary particles from a MC simulated γ-ray induced EAS, color coded by the particle species [39]. The energy of the primary γ-ray was set to 10 GeV and the GF was disabled. Even though a value of 10 GeV is well below the threshold energy of all IACTs currently in operation, the figure obtained with this somewhat extreme input parameter allows to illustrate the influence of the GF on EAS. The ZA was set to 70° and the azimuth angle was set to 90° to obtain a front view on the shower. Positron trajectories are colored red, while electron trajectories are colored green, and secondary photons (not Cherenkov photons!) are indicated as blue traces. Within statistical fluctuations, the shapes of the electron and positron components are comparable. Apart from differences due to intrinsic fluctuations of the EAS development, there is no systematic difference between both components. Figure 9 was generated under the same conditions but enabled GF. The overall shape of the EAS (upper left figure) is different from the one in figure 8. The influence of the GF becomes more obvious when comparing the electron

and the positron component, which are now clearly separated due to their opposite deflections by the GF. At the beginning, just after the interaction of the primary γ-ray with one of the atmospheric molecules, the deflection of the positive and the negative components is rather small.

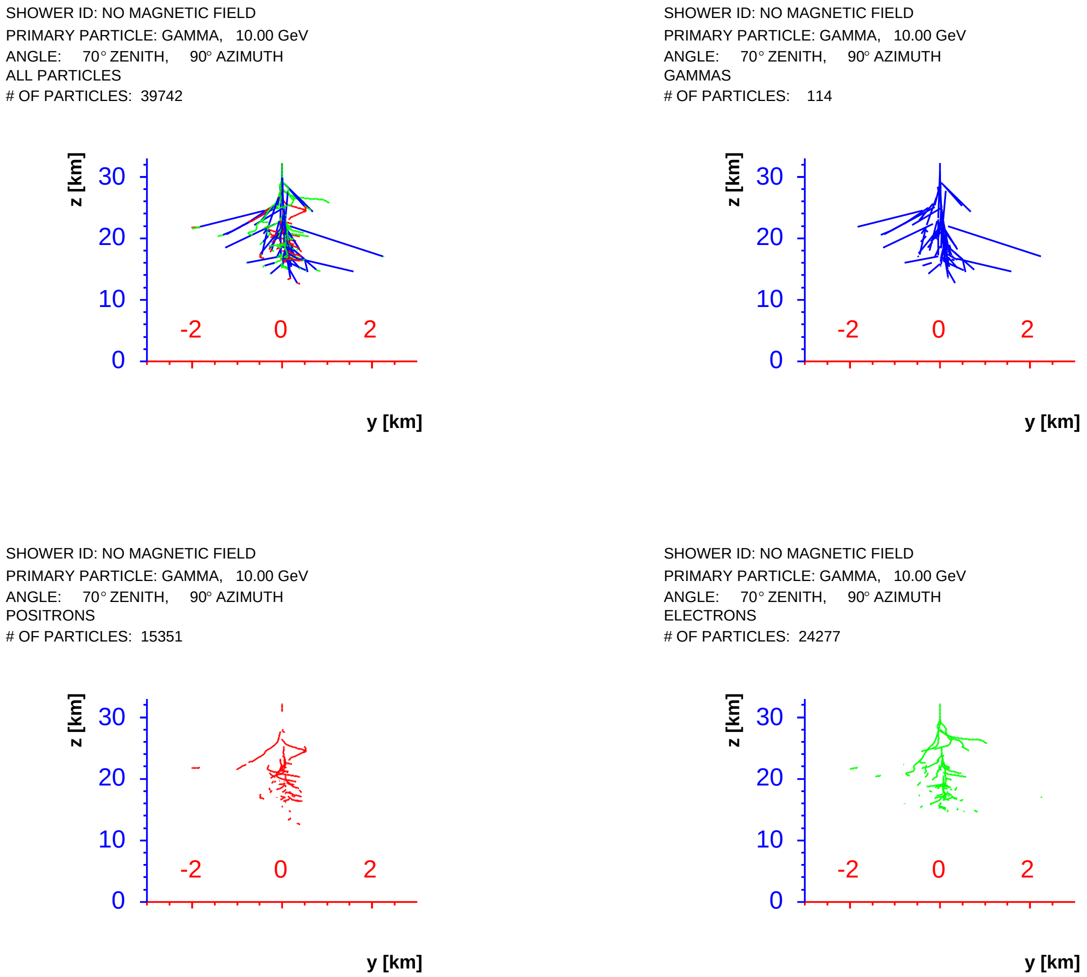

Figure 8: The two-dimensional projection of the trajectories of secondary particles from a MC simulated γ-ray induced EAS. The energy of the primary γ-ray was set to 10 GeV and the GF was disabled. The EAS was simulated for very large ZA of 70°. Electron trajectories are colored green, whereas the ones of positrons are colored red. Apart from differences due to intrinsic fluctuations of the EAS development, there is no systematic difference between the shape of the electron and the positron component in the EAS (adopted from [39]).

At this stage, the primary energy is distributed over a small number of secondary particles. During the development of the EAS downwards, the number of secondary particles increases fast and the primary γ-ray energy is distributed over a large number of secondaries. The charged secondary particles, carrying only a fraction of the energy of the primary γ-ray, are deflected stronger. The influence of the GF on the electron and positron component in γ-ray induced EAS was studied in detail in [39].

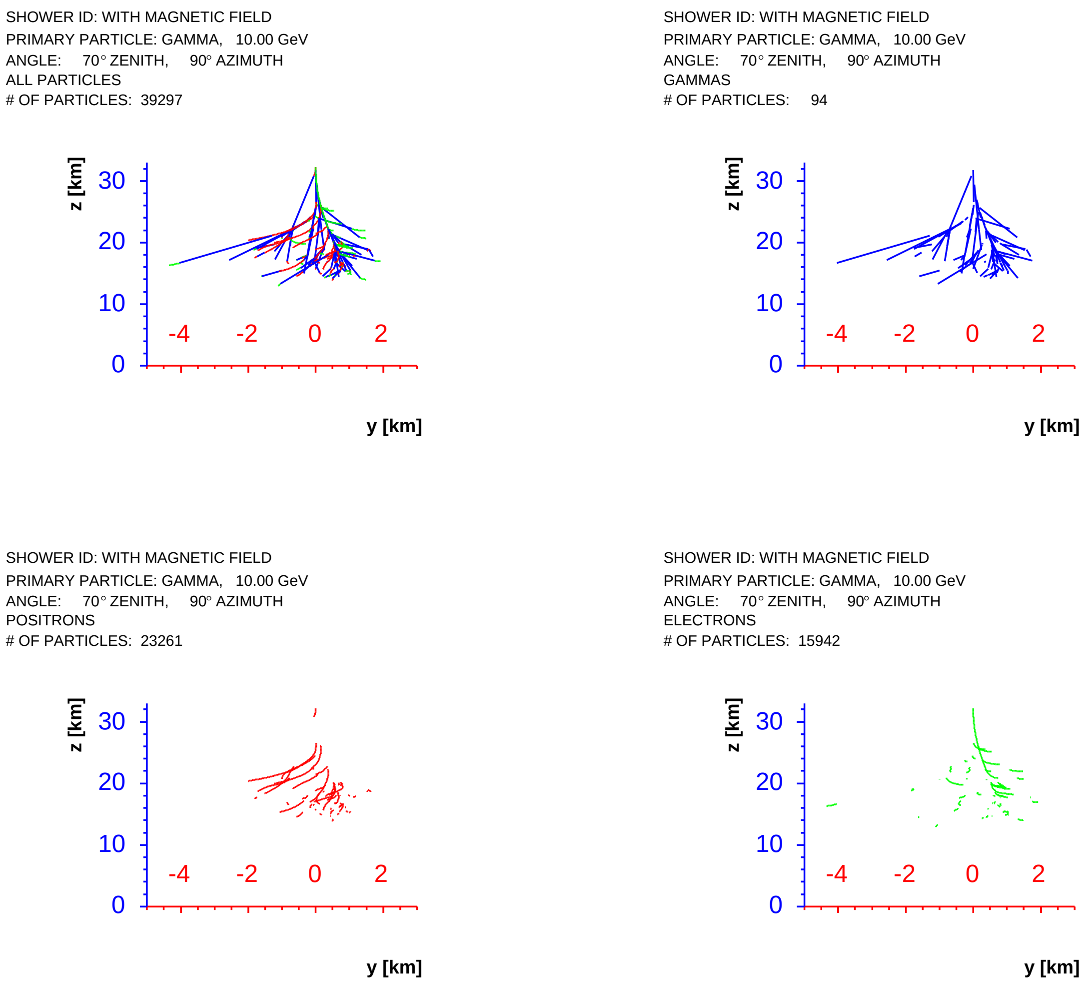

Figure 9: The two-dimensional projection of the trajectories of secondary particles from a MC simulated γ-ray induced EAS. The energy of the primary γ-ray was set to 10 GeV. The EAS was simulated for very large ZA of 70°. Electron trajectories are colored green, whereas the ones of the positrons are colored red. Both the electron and the positron component of the EAS are clearly separated, which is due to their (opposite) deflection by the GF (adopted from [39]).

The photon component (blue) of the EAS in figure 9 appears to be modified too. The modification of the neutral component in γ-ray EAS is indirectly related to the GF, since most of the secondary photons are produced in pair production processes involving secondary electrons and positrons, which are subject to deflection. Provided that most of the positrons and electrons in an EAS have enough energy to emit Cherenkov radiation, the distribution of Cherenkov photons on ground will be significantly modified. The change of the Cherenkov image on ground depends on the angle included by the trajectory of the primary γ-ray and the field lines of the GF. The largest change of the Cherenkov image is expected to occur for telescope orientations for which the vertical component of the GF

strength is maximal (figure 6).
In case of hadron induced EAS, the deflection of secondary charged particles, such as nucleons and mesons, is expected to be smaller. Nuclear interactions involved in the development of hadron induced EAS cause a much larger lateral displacement than that due to the GF.

1.3 The Influence of the GF on the Cherenkov Light Distribution

As all charged particles in EAS are deflected due to the GF, the distribution of Cherenkov photons on ground will also be changed. Figure 10 shows the average distribution of Cherenkov photons on ground as obtained from a MC simulation. For each figure, 15 individual EAS events were averaged. The γ-ray energy was set to 50 GeV and the ZA to 50°. The GF was disabled in both cases.[1] As expected, both images appear to be very similar. Independent of the azimuth angle the shape and the intensity level of the Cherenkov light distribution is very similar for both orientations. Differences between the images can be attributed to intrinsic fluctuations of the EAS development. The elliptical shape of the images is of geometrical origin, i.e. due to the fact that the Cherenkov cones emanating from the EAS are snipped on ground under an angle that corresponds to the ZA. For 0° ZA the Cherenkov images on ground look like a circle.

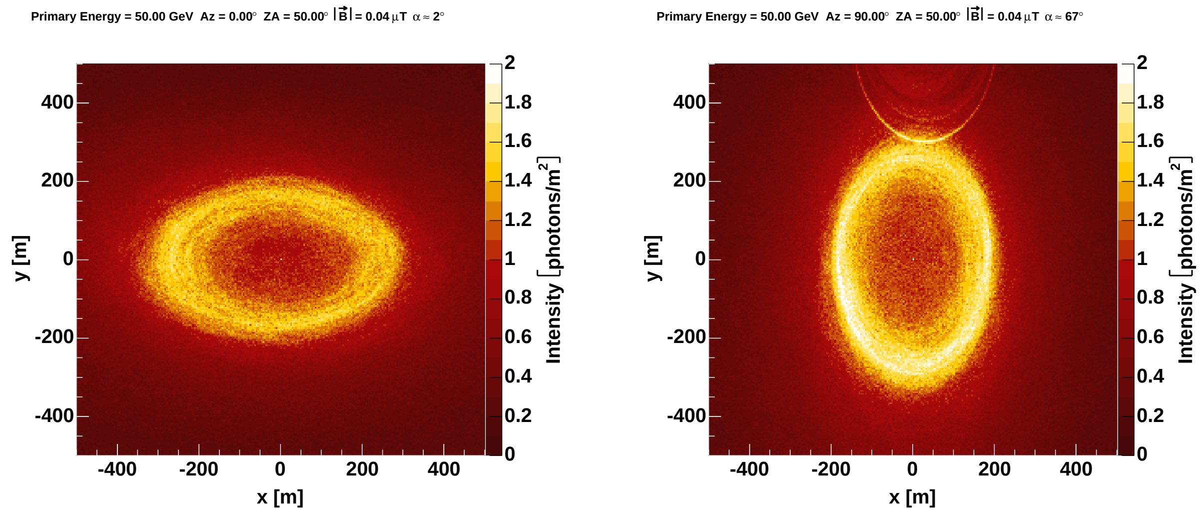

(a) (b)

Figure 10: MC simulated distributions of Cherenkov photons on ground for γ-ray induced EAS. The γ-ray energy was set to 50 GeV, the ZA to 50° and the azimuth angle to 0° (a) and 90° (b), respectively. The GF was disabled in both cases. Both images appear to be very similar. Differences can be attributed to intrinsic fluctuations of the EAS development.

To demonstrate the influence of the GF on the Cherenkov light distribution on ground, the MC simulation was rerun with enabled GF. Figure 11 shows the average distribution of Cherenkov photons on ground for a γ-ray of 50 GeV energy. Again, 15 events were averaged for each figure. The ZA was set to 50° and the azimuth angle was set to 0°, 45°, 90° and 135°. While figure 11 (a) is very similar to figure 10 (a), all other images appear to have significantly altered. As can be seen from figure 6

[1] Because the CORSIKA simulation program requires non-zero input values for the GF components, the field components were set to the thousandth part of their nominal values.

(section 1.1), at $\sim 50^\circ$ ZA, the vertical component of the GF strength is maximal at azimuth angles of $\sim 135^\circ$ and $\sim 225^\circ$, respectively.

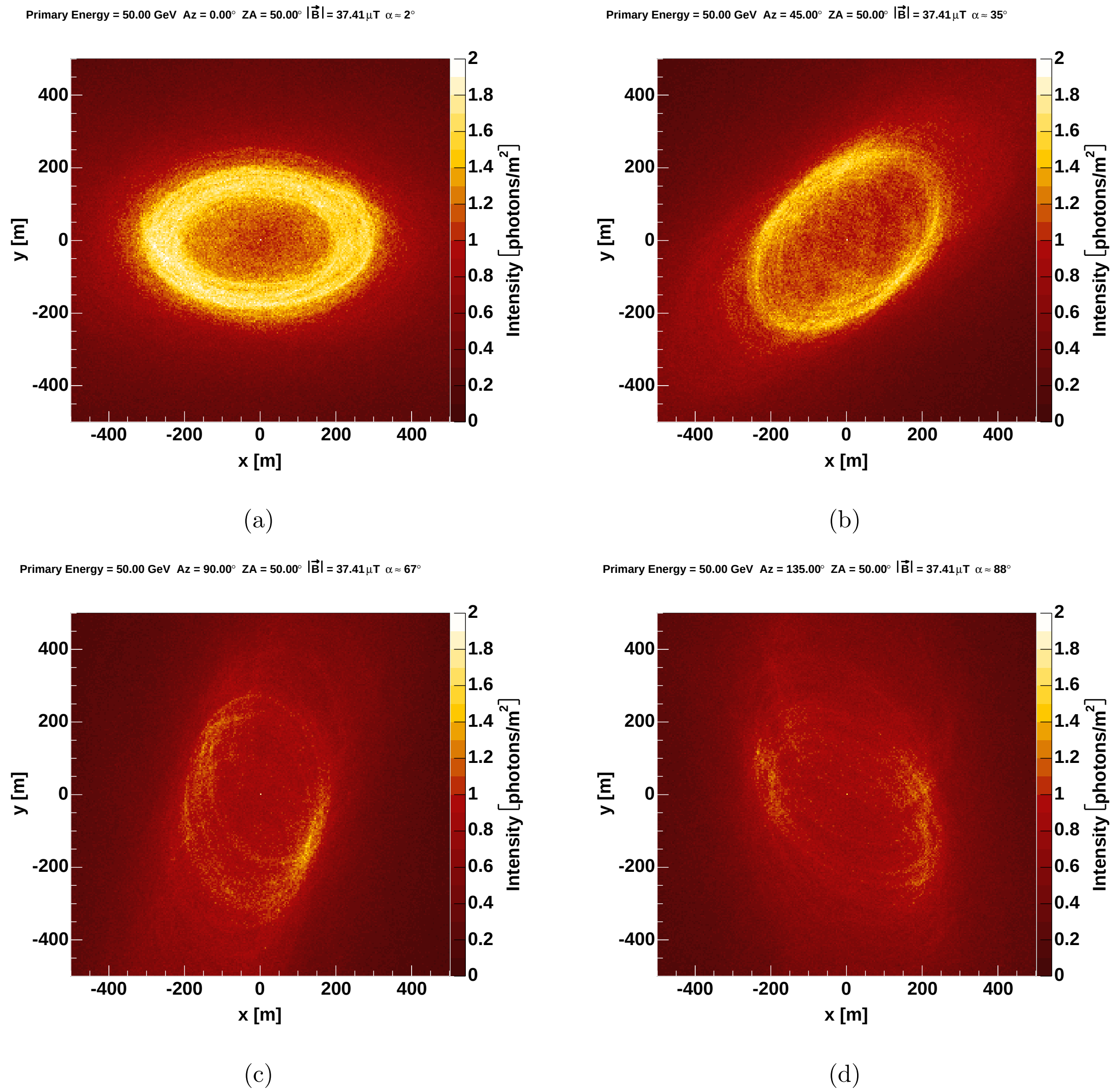

Figure 11: MC simulated distributions of Cherenkov photons on ground for γ-ray induced EAS. The γ-ray energy was set to 50 GeV, the ZA to 50° and the azimuth angle to 0° (a) 45° (b) 90° (c) and 135° (d), respectively. The GF was enabled in all cases. Differences between the Cherenkov images can be attributed to the influence of the GF on the EAS development.

At 45° azimuth angle and 50° ZA, the GF strength has already increased by more than a factor four with respect to 0° azimuth angle, resulting in a significant change of the Cherenkov light distribution (figure 11 (b)). The image appears to be rather faint compared to that obtained for 0° azimuth angle. Furthermore, the Cherenkov photons are widely spread along the secondary diagonal. The attenuation of the intensity of the Cherenkov images becomes even more pronounced for increasing azimuth angle.

For 50° ZA, the maximum field strength is reached at $\sim 135°$ azimuth angle. As can be seen from figure 11 (d), the corresponding intensity distribution of Cherenkov photons appears to be strongly attenuated compared to that obtained for 0° azimuth angle. Moreover, the distribution of Cherenkov photons is widely dispersed along the y-direction. Obviously, there is a strong correlation between the angle α and the Cherenkov density. The Cherenkov density decreases with increasing angle α, which is given in the header of the figures. Therefore, depending on the energy of the primary γ-ray and the orientation of its trajectory, the GF is expected to significantly reduce the performance of an IACT at those low energies. The decrease of the Cherenkov photon density at the telescope level reduces the number of Cherenkov photons that are collected by the mirror. As a result, the threshold energy of the detector will be increased as well as the effective collection area of the IACT will be affected [10, 24, 25, 28, 34, 36]. Furthermore, if the influence of the GF is not properly taken into account, the energy of a γ-ray may be significantly underestimated. The thinned out distribution of Cherenkov photons can make a primary γ-ray of certain energy look like a γ-ray of much lower energy. The angular dispersion of the images will also have an effect on the angular resolution of an IACT. It was shown elsewhere that the distortions of the Cherenkov images on ground not only depend on the orientation of the trajectory of the primary γ-ray with respect to the GF lines, but also strongly depend on its energy [24, 25, 34, 36, 39].

1.3.1 GF Effects on the Lateral Cherenkov Light Distribution

The figures 12 - 15 show the average lateral Cherenkov distribution of MC simulated γ-rays on ground as a function of the impact parameter r for several energies of the primary γ-ray. The energy was set to 50 GeV, 100 GeV, 300 GeV and 1 TeV, respectively. The ZA was varied between 20° and 60° in steps of 20°, and the azimuth angle between 0° and 180° in steps of 90°. Up to 100 events were averaged for each orientation and energy of the primary γ-ray.
As mentioned in the previous section, Cherenkov images on ground have, for a geometrical reason, an elliptical shape for ZA greater than zero. While the left column corresponds always to the semi-major axis of the Cherenkov ellipse on ground, the right one corresponds to the semi-minor axis. The angle between the direction of the momentum of the primary γ-ray and the direction of the GF lines is given in brackets behind the value of the azimuth angle in the legend.
The average lateral Cherenkov density significantly decreases with increasing ZA. For example, the comparison of the intensity of Cherenkov photons at the hump for 20° ZA and 60° ZA (in 12 (a) at about 120 m and in 12 (e) at about 400 m impact parameter) shows that the intensity decreases from $\sim$ 8 photons/m^2 to only $\sim$ 0.7 photons/m^2. The Cherenkov photons originating from a γ-ray impinging at large ZA propagate longer through the atmosphere and therefore suffer from absorption. Furthermore, at large ZA, Cherenkov photons are distributed over a wider area resulting in a lower intensity.
The average lateral Cherenkov distribution shown in figure 12 exhibits some dependence on the azimuth angle. While the change of the intensity between 0° and 180° azimuth angle (solid black line and dash-dotted blue line) is less than 10 %, the change between 0° and 90° azimuth angle (solid black line and dashed red line) is greater, especially for large impact parameters r. For 90° azimuth angle, the lateral distribution of Cherenkov photons is clearly broadened along the semi-major axis, which is aligned in east-west direction, i.e. perpendicular to the GF lines.
Even though the opposite way around, the same effect occurs for the Cherenkov distribution along the semi-minor axis (figures 12 (b), (d) and (f)). For 20° ZA (figure 12 (b)), the Cherenkov distributions described by the solid black line and the dash-dotted blue line, i.e. the ones obtained for 0° and 180° azimuth angle, respectively, appear to be enhanced with respect to the one described by the dashed red line, especially at large impact parameters r. At larger ZA, the solid black curve is of similar shape as the dashed red curve, which can be explained by the decrease of the angle between the GF lines and the direction of the primary γ-ray.
At higher ZA, the influence of the GF becomes more pronounced. For 40° ZA, depending on the azimuth angle, the Cherenkov photon intensity changes by up to 30 % (figure 12 (c) and (d)). For 60° ZA and for the azimuth angles taken into consideration, the change of the Cherenkov photon intensity on ground is of the same order of magnitude as for 40° ZA (figure 12 (e) and (f)).
At higher energies of the primary γ-ray, the influence of the GF on the shape of the lateral distribution of Cherenkov photons becomes smaller. For 100 GeV γ-rays (figure 13) at ZA up to 40°, there is almost no difference between the intensity of Cherenkov photons up to the hump at some 100 m impact parameter. At larger impact parameters beyond the hump of the Cherenkov distribution, the difference of the Cherenkov distributions is more pronounced.
At 300 GeV (figure 14) and 1 TeV energies (figure 15) of the primary γ-ray, respectively, the influence of the GF on the lateral distribution of Cherenkov photons gets smaller and smaller. Because high-energy EAS contain more charged particles with higher momentum, which are deflected less by the Lorentz force, the influence of the GF becomes lower with increasing energy of the primary γ-ray. The influence of the GF on the Cherenkov light distribution originating from low-energy γ-rays of energies between 10 GeV and 100 GeV was studied in [34, 37].

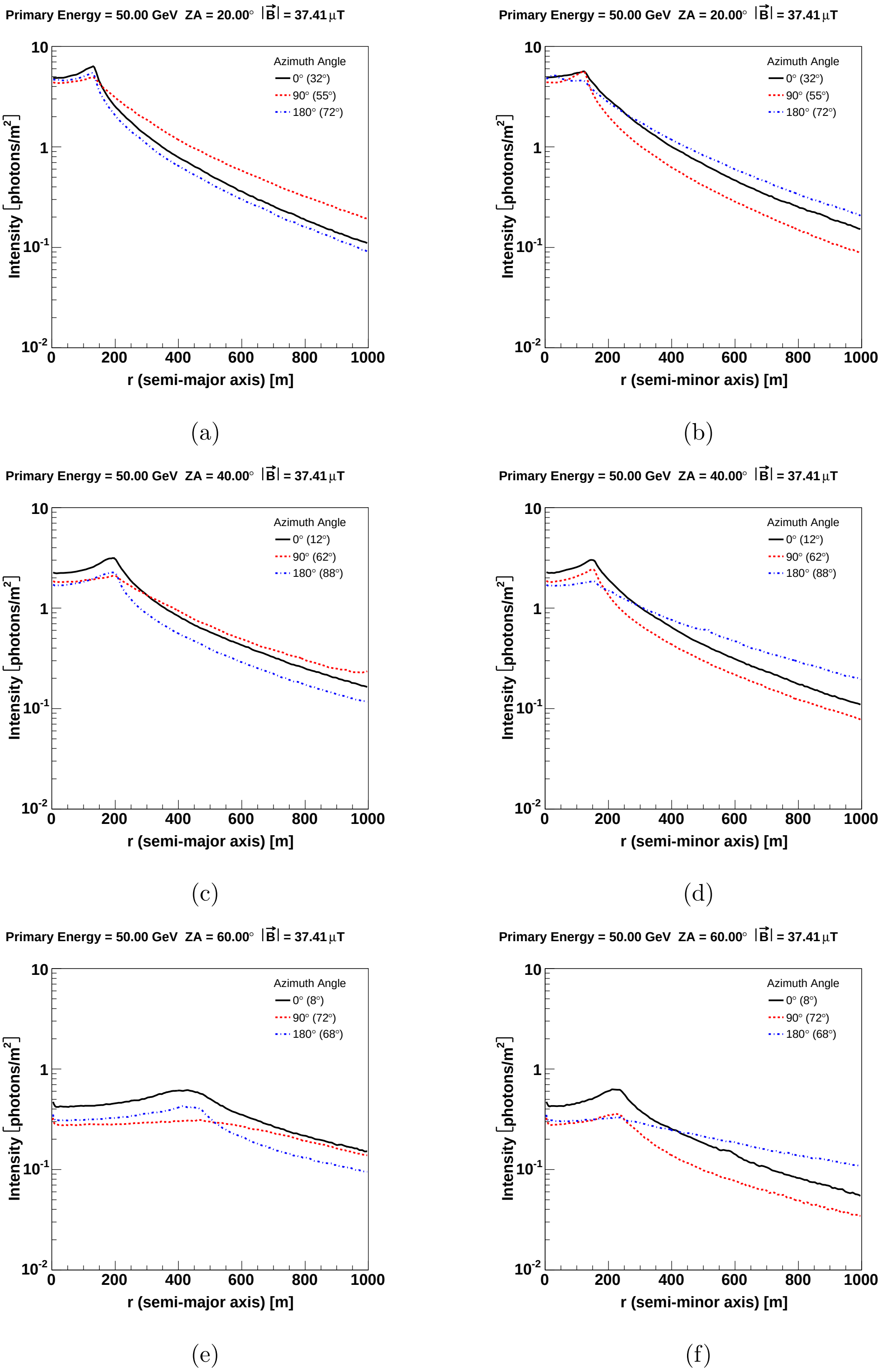

Figure 12: Average lateral distributions of Cherenkov photons on ground for γ-ray induced EAS. The primary γ-ray energy was set to 50 GeV, the ZA was set to 20°, 40° and 60°, and the azimuth angle to 0°, 90° and 180°, respectively. The left column corresponds to the semi-major axis of the Cherenkov ellipse on ground, while the right one to the semi-minor axis.

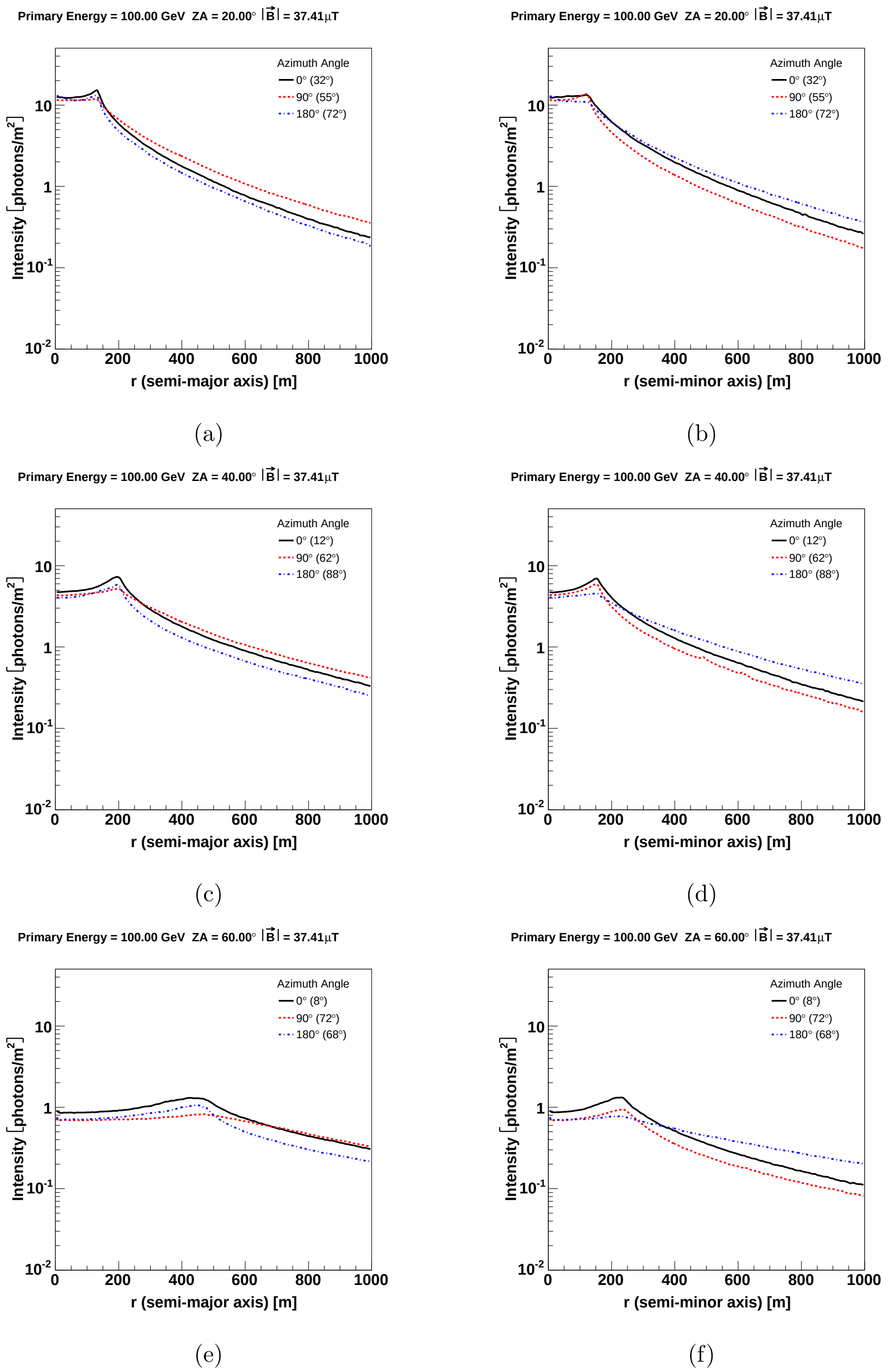

Figure 13: Average lateral distributions of Cherenkov photons on ground for γ-ray induced EAS. The primary γ-ray energy was set to 100 GeV, the ZA was set to 20°, 40° and 60°, and the azimuth angle to 0°, 90° and 180°, respectively. The left column corresponds to the semi-major axis of the Cherenkov ellipse on ground, while the right one to the semi-minor axis.

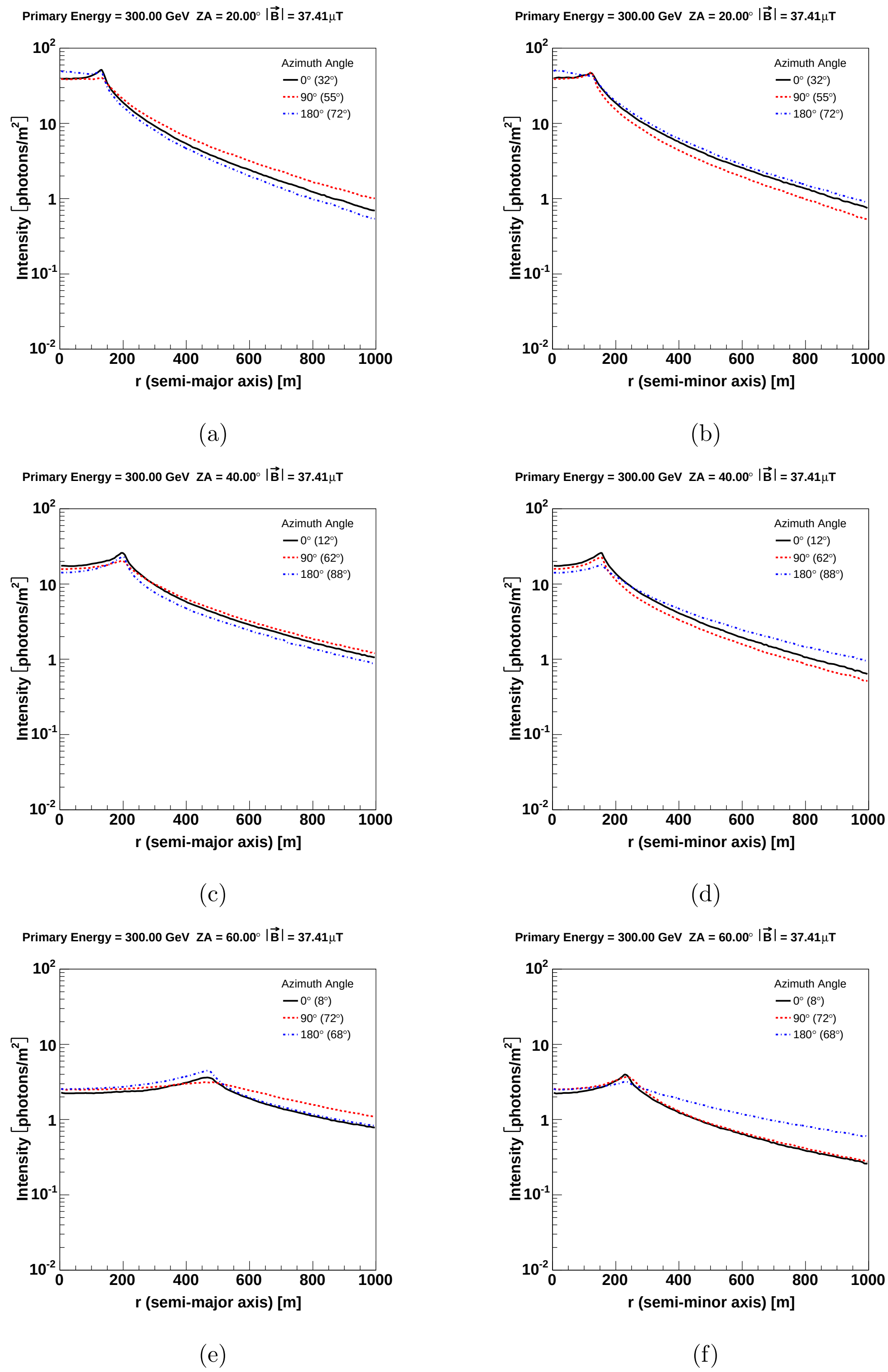

Figure 14: Average lateral distributions of Cherenkov photons on ground for γ-ray induced EAS. The primary γ-ray energy was set to 300 GeV, the ZA was set to 20°, 40° and 60°, and the azimuth angle to 0°, 90° and 180°, respectively. The left column corresponds to the semi-major axis of the Cherenkov ellipse on ground, while the right one to the semi-minor axis.

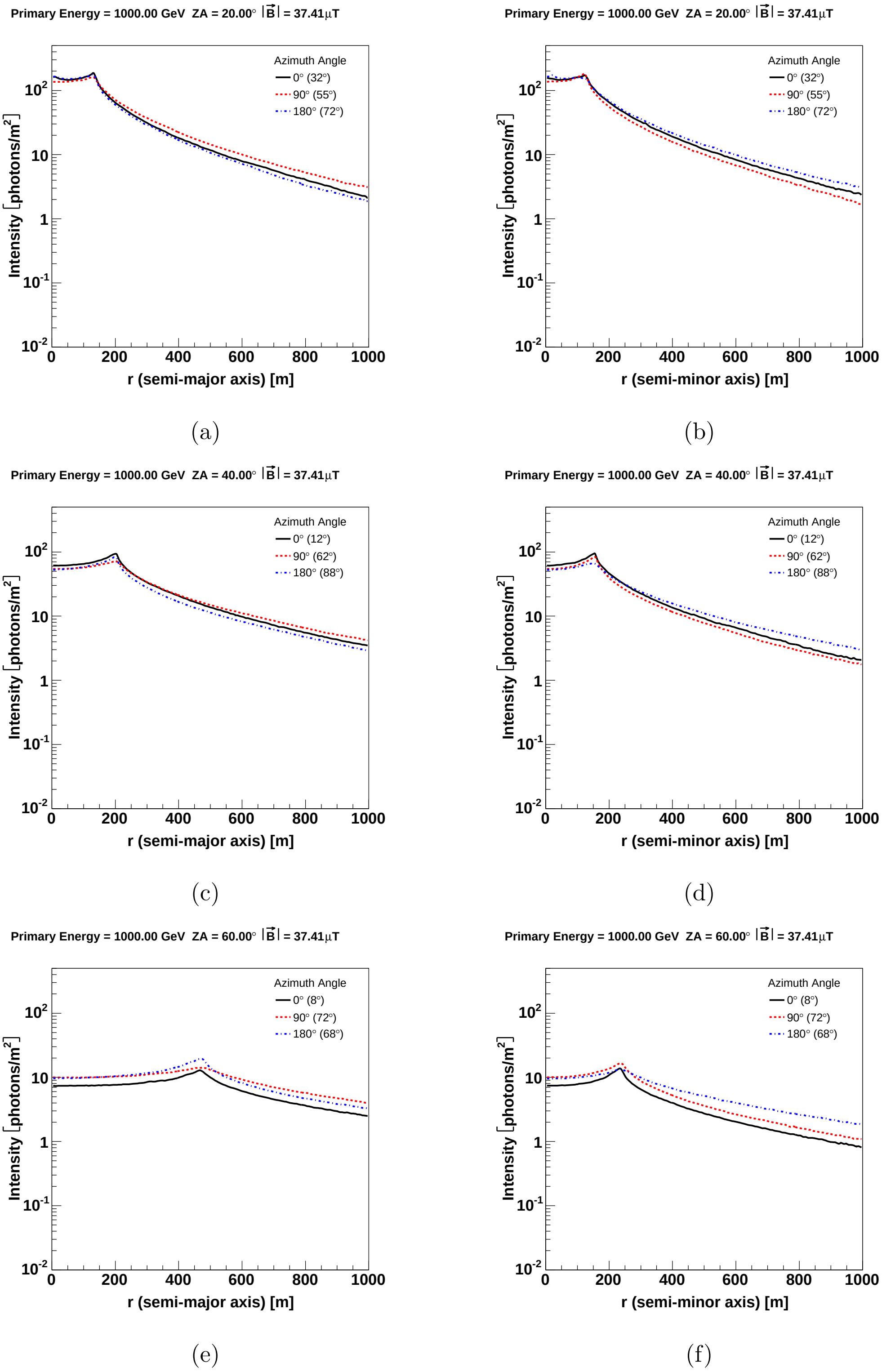

Figure 15: Average lateral distributions of Cherenkov photons on ground for γ-ray induced EAS. The primary γ-ray energy was set to 1000 GeV, the ZA was set to 20°, 40° and 60°, and the azimuth angle to 0°, 90° and 180°, respectively. The left column corresponds to the semi-major axis of the Cherenkov ellipse on ground, while the right one to the semi-minor axis.

2 Dedicated MC Production

The MC data used for the studies of the GF effects were produced following for most instances the standard MAGIC MC production chain. Showers were generated with the CORSIKA MC simulation program (MMCS version 6.19) [21, 36], processed further with the Reflector program (program version 0.6) [31] and the Camera program (program version 0.7) [8].

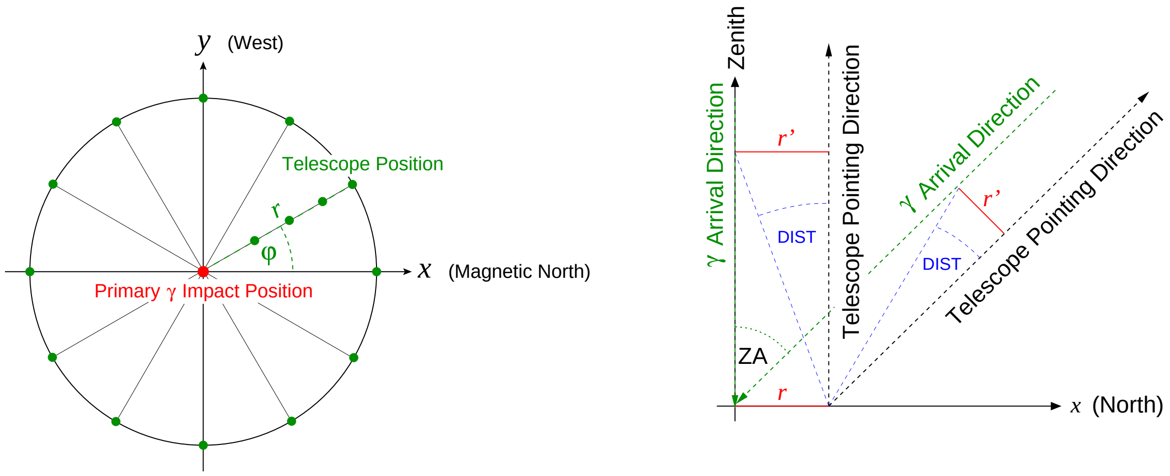

(a) The telescope positions (green) and the primary γ-ray impact point (red) on the ground.

(b) The relation between the true impact parameter r' and the DIST parameter.

Figure 16: (a) The telescope positions (green) and the primary γ-ray impact point (red) on the ground. The simulations were done for fixed impact parameters $r = 20$ m,... 220 m and fixed angles $\varphi = 0°$, $30°$,... $330°$. (b) The relation between the true impact parameter r' and the DIST parameter. In direction of the inclination of the telescope the true impact parameter r' and the DIST parameter scale like cos(ZA).

To investigate the extent of the GF effect on the EAS development in greater detail, the EAS were simulated for fixed impact positions (r, φ), i.e. in the range $r = 20\,\text{m}, \ldots 220\,\text{m}$ and $\varphi = 0°, 30°, \ldots 330°$, as illustrated in figure 16 (a).[1] The telescope position (green) was varied within the limits mentioned before, and the impact point of the primary γ-ray (red) was always fixed at the origin of the coordinate system. In this way, for not too big impact parameters, the telescope is always located somewhere in the Cherenkov pool on ground. The telescope is always oriented in the direction of the primary γ-ray. The impact parameter was varied in steps of 20 m and the angle φ in steps of 30°.
The true impact parameter r' varies like $r\sqrt{\cos^2(\mathrm{Az}-\varphi)(\cos^2(\mathrm{ZA})-1)+1}$ between $r\cos(\mathrm{ZA})$ and r (figure 16 (b)). Thus, in direction of the inclination of the telescope the DIST parameter scales like cos(ZA). For some combinations $(r, \varphi, \mathrm{ZA}, \mathrm{Az})$ of the input parameters the average DIST of the shower images lies below a lower cut usually applied to the data, e.g. DIST $> 0.2°$ - $0.3°$.
About 10^5 events were generated for 30, 50, 70, 120, 170, 300, 450 and 1000 GeV γ-rays.
As the production of MC data is rather time consuming, the generation of γ showers with a continuous energy distribution as well as continuous impact parameter distribution was omitted (except for the studies of the GF effects on the DISP method, which is discussed in section 3.1.3).
The choice of discrete values for the γ-ray energy allows to investigate the energy dispersion of the

[1] For the production of standard MC data the EAS core location is randomly placed somewhere in a circle on the plane perpendicular to the direction of the EAS.

showers due to the GF. Since the energy estimation of showers is based on the image parameter SIZE, it is important to know how its value depends on the GF.
As the absolute value of the vertical component of the GF is symmetric in azimuth (figure 6), the azimuth angle was varied in steps of 30°, from 0° to only 180°. The ZA was changed in steps of 20° in the range between 0° and 60°.
The simulation of the electronic noise as well as NSB was done as in the standard MC production. The diffuse NSB level for the inner pixels was set to 0.183 Phe/ns.
The optical PSF of the telescope was set to 1.4 cm (each axis) and the reflectivity of the mirrors was set to 73 %, which is a rather conservative value, as the mirror reflectivity was lastly measured to be about 77 % [19]. The MC simulations for this work were performed before that date.
The trigger condition simulated in the MC is the one that is commonly used for data acquisition as well as for the standard MC production (4 next-neighbor coincidence).

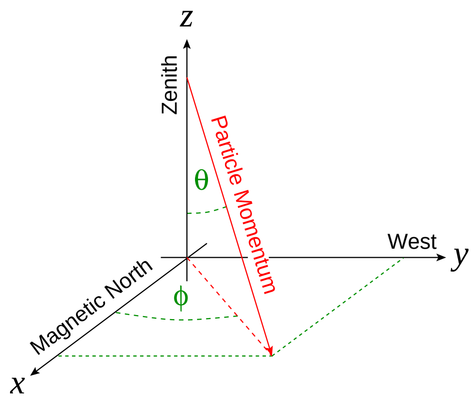

Figure 17: The coordinate system of the CORSIKA MC simulation program [21]. The coordinate system is in line with the geomagnetic system such that the GF has only two components. The angle θ corresponds to the ZA and the angle $\phi \neq \varphi$ to the azimuth angle.

Figure 17 shows the coordinate system of the CORSIKA simulation program. The coordinate system is in line with the geomagnetic system such that the GF can be locally described by only two components, i.e. $\vec{B} = (B_x, 0, B_z)^{\mathrm{T}}$ (section 1.1). The values used for the MC simulation are $B_x = 29.5\,\mu\mathrm{T}$ and $B_z = 23.0\,\mu\mathrm{T}$, respectively.
As a reference, MC data were produced with disabled GF. This was done only for 0° azimuth angle, but in the same ZA range as the MC dataset produced with enabled GF. In case of disabled GF, the MC generated γ showers should not exhibit a dependency on the azimuth angle.
In addition to the MC datasets mentioned beforehand, smaller MC training samples with continuous impact parameter distribution were produced. For these datasets the EAS core location is randomly placed somewhere in a circle on the plane perpendicular to the direction of the EAS, as it is the case in the standard MC data. These additional data, later on used for the optimization of the DISP parameters (section 3.1.3), were produced with disabled GF but for the same set of input parameters (Energy, ZA, Az) as the datasets mentioned above.

3 Analysis & Results

The MC generated γ showers were calibrated using MARS (version 0.11.2) [11, 30, 29]. To find out about the influence of the image cleaning, the calculation of the image parameters was done for three different absolute image cleaning levels. The cleaning levels were set to 4.0 Phe (core pixels) and

2.0 Phe (boundary pixels), to 7.0 Phe (core pixels) and 4.0 Phe (boundary pixels) as well as to 10.0 Phe (core pixels) and 5.0 Phe (boundary pixels), respectively. The first set of image cleaning levels (in the following referred to as *soft image cleaning*) are rather low compared to the others (in the following referred to as *intermediate image cleaning* and *hard image cleaning*). The *hard image cleaning* is used in the standard analysis for γ-ray energies above 100 GeV.

3.1 GF Effects on the Image Parameters

For this work, all image parameters that are commonly used for the extraction of the γ-ray signal were calculated. As demonstrated in section 1.3, the GF affects the shape, the orientation as well as the intensity of the Cherenkov light distribution on ground. Therefore, the GF is expected to affect the reconstructed shower images in the camera plane of the telescope, which was already shown elsewhere [10, 14, 24, 25, 28, 34, 36, 39].

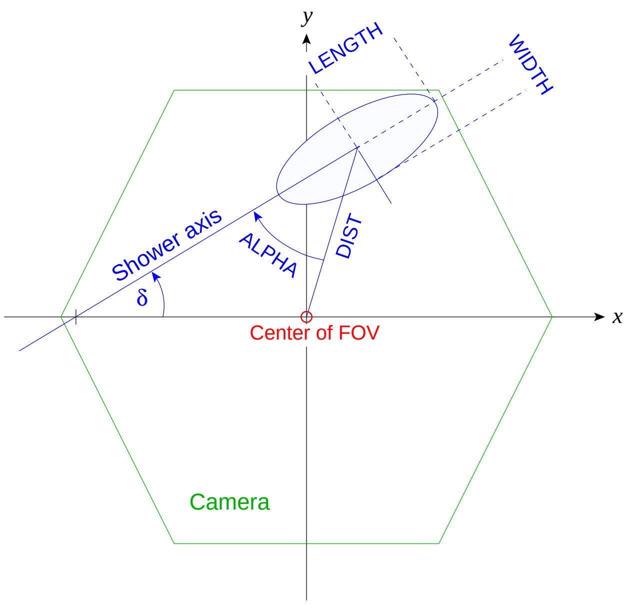

Figure 18: Shower images in the camera are parameterized by the Hillas parameters [22]. The definition of the basic image parameters is illustrated. Light distributions are approximated by an ellipse. Major and minor axis of the ellipse represent the shape of the shower image. Both parameters ALPHA and δ are related to the orientation of the image. The parameter DIST describes the distance between camera center and centroid of the light distribution.

Figure 19 qualitatively demonstrates the influence of the GF on some of the image parameters that describe shape and orientation of the images. On each camera display, ten Hillas ellipses are superimposed. The primary γ-ray energy was set to 450 GeV and the ZA to 40°. While figure (a) contains Hillas ellipses for showers generated at 0° azimuth angle where the GF strength is minimal (figure 6), figure (b) is obtained for showers generated at 180° azimuth angle where the GF strength is maximal, i.e. the angle between the GF lines and the direction of the primary γ-ray is about 90° (figure 5). In the latter case, the shape and orientation of the Hillas ellipses has clearly changed with respect to the ones plotted in figure 19 (a). The Hillas ellipses appear to be more roundish, and the angle of the major image axis enclosed with the y-axis has a much larger spread. As the telescope axis is parallel to the shower axis, the major image axis should enclose small angles with the y-axis, which is the case for 0° azimuth angle (figure 19 (a)). The dispersion of the alignment with respect to the y-axis will cause the distribution of the image parameter ALPHA to appear broadened. The broadening of the ALPHA distribution affects the reconstruction of the γ signal, which, in the ideal case, shows up at small values of the image parameter ALPHA. Therefore, the influence of the GF can cause a loss of signal events, i.e. the number of excess events from the ALPHA distribution is lower than the one which could be expected in the absence of the GF.

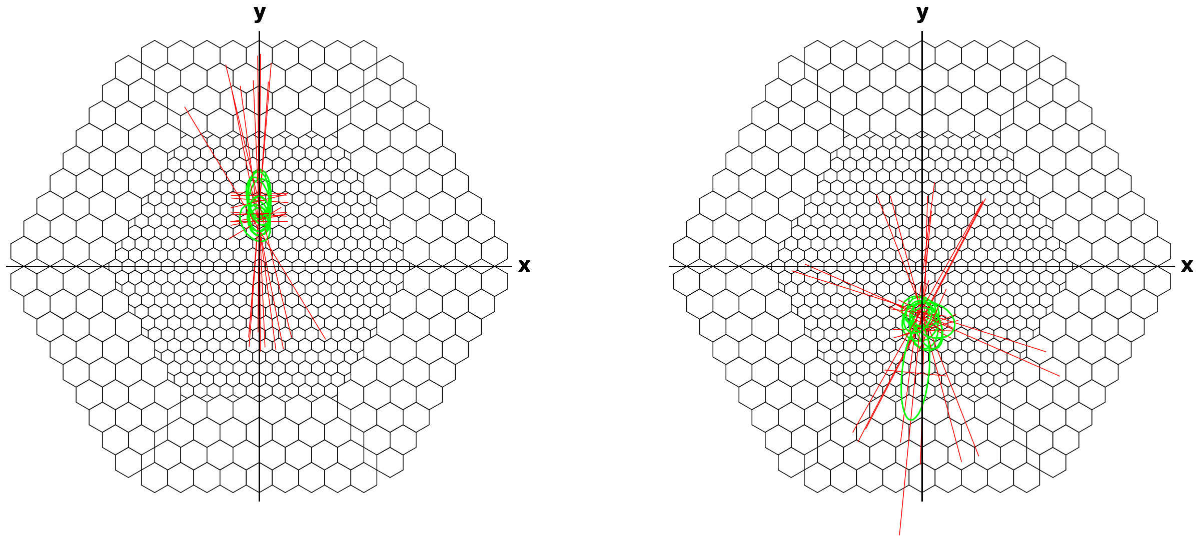

(a) Hillas ellipses superimposed on the MAGIC camera display for MC generated γ-rays of 450 GeV energy at 40° ZA and 0° azimuth angle.

(b) Hillas ellipses superimposed on the MAGIC camera display for MC generated γ-rays of 450 GeV energy at 40° ZA and 180° azimuth angle.

Figure 19: The influence of the GF is qualitatively demonstrated in terms of Hillas ellipses obtained from MC generated γ showers. On each camera display, ten Hillas ellipses are superimposed. The primary γ-ray energy was set to 450 GeV and the ZA to 40°. The GF was enabled. While figure (a) contains Hillas ellipses for showers generated at 0° azimuth angle, figure (b) is obtained for showers generated at 180° azimuth angle, where the influence of the GF is maximal.

Apart from that, the influence of the GF on the other image parameters that describe the shape of shower images, like the WIDTH and LENGTH parameters, may affect the γ/hadron separation capability of the analysis. It was already shown that the image parameters WIDTH and LENGTH, also very important for the background suppression, are subject to changes due to the influence of the GF [15, 24, 25, 34, 36, 39].

In the preceding section it was shown that the GF can thin out the distribution of Cherenkov light on ground. The reduction of the number density of Cherenkov photons will affect the γ efficiency. In other words, the detection probability for the primary γ-ray depends on its arrival direction with respect to the GF lines. Both the number of γ-ray candidates derived from the ALPHA distribution as well as the γ efficiency derived from MC simulations are used to estimate the differential flux of a VHE γ-ray source. Provided that the influence of the GF on the image parameters depends on the energy of the γ shower [24, 25, 34, 36, 39], the GF can affect not only the level of the observed γ-ray flux, but also the shape of the reconstructed differential energy spectrum. The shape of the differential energy spectrum derived for a certain source as well as the absolute flux level is generally used to probe assumptions on the physical processes taking place at the source. It is therefore very important to investigate the effect of the GF on the image parameters in great detail, and to possibly correct the differential energy spectrum for effects of the GF.

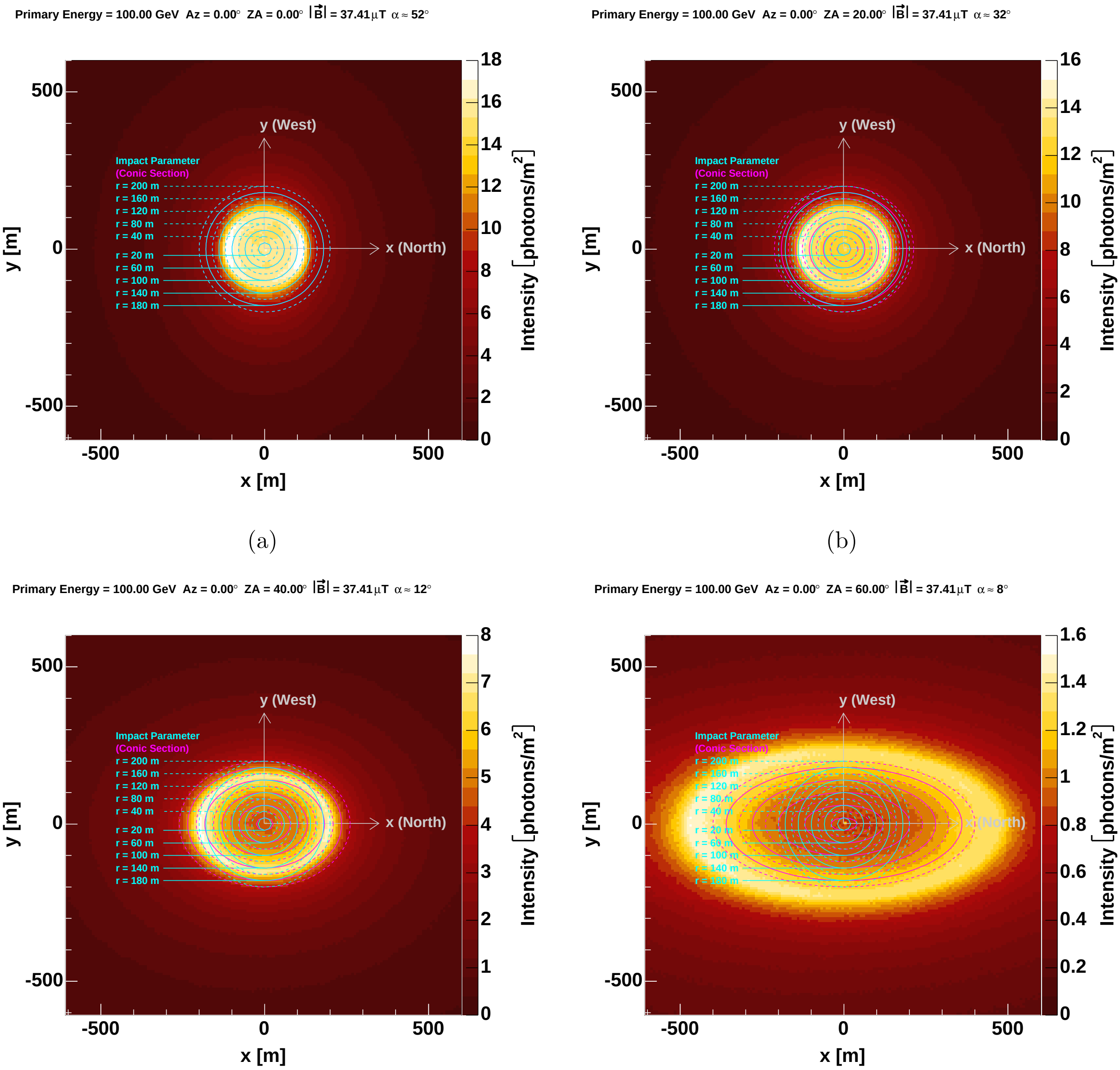

(a) (b) (c) (d)

Figure 20: MC simulated distributions of Cherenkov photons on ground for γ-ray induced EAS. The primary γ-ray energy was set to 100 GeV. The azimuth angle was set to 0° and the ZA was set to 0° (a) 20° (b) 40° (c) and 60° (d), respectively. The GF was enabled in all cases. The origin of the coordinate system is placed at the point of intersection of the primary γ-ray's trajectory with the ground. The Telescope is placed at fixed positions on the light blue circles.

To clean the MC dataset, weak pre-selection cuts have been applied: for all data, the parameter

NUMCOREPIXELS was required to be greater than four, i.e. only showers having a minimum of four core pixels were kept, and the DIST parameter was required to be greater than 0.1°. A lower cut on the number of core pixels ensures that the moments used for the image parameter calculation are well defined. The lower cut on the image parameter DIST is motivated by the fact that the image parameter ALPHA is not defined for too small DIST values, since shower images located in the camera center appear to be roundish without any preferential direction.

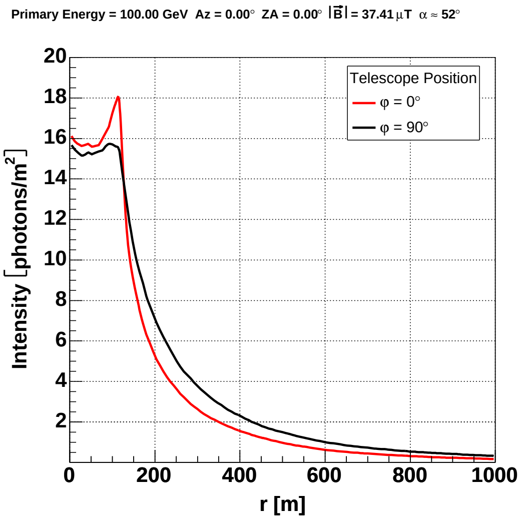

Figure 21: Average lateral distribution of MC simulated Cherenkov photons on ground for γ-ray induced EAS. The γ-ray energy was set to 100 GeV. Both the azimuth angle as well as the ZA were set to 0°. The red line would be measured by a telescope situated on the x-axis of the CORSIKA coordinate system, while the black corresponds to a telescope situated on the y-axis.

Because of the strategy which was selected for the MC production (section 2), the interpretation of the reconstructed data has to be done carefully. For instance, the positioning of the telescope at fixed radii around the primary γ-ray impact point on ground (figure 16) causes the GF effects and geometrical effects on the image parameters to be entangled. For ZA greater than 0°, the maximum intensity of Cherenkov photons, the so-called hump, is not any more located on a circle centered at the intersection point of the primary γ-ray's trajectory with the ground. Instead, the maximum intensity is located on an ellipse whose semi-minor axis corresponds to the impact parameter r, while its semi-major axis scales like $r\cos^{-1}(\mathrm{ZA})$.
Figure 20 shows the MC simulated distributions of Cherenkov photons on ground for γ-ray induced EAS of 100 GeV energy. The azimuth angle was set to 0° and the ZA was varied between 0° and 60° in steps of 20°. The GF was enabled in all cases. About 150 events were averaged.
In absence of the GF, figure 20 (a) would be symmetric with respect to the origin of the gray coordinate system superimposed to the distribution of Cherenkov photons. That is, along the light blue circles that are superimposed to the distribution and centered at the origin of the coordinate system, the average intensity would remain constant. Instead, the distribution of Cherenkov photons appears to be asymmetric which is due to the fact that positrons and electrons in EAS are deflected to opposite directions. The intensity of Cherenkov photons along the y-axis is smaller than the one on the x-axis. As a result, the estimated energy of the primary γ-ray will be underestimated if this effect is not

properly taken into account. Thus, by using inappropriate MC produced at wrong azimuth angles, the energy may be systematically under- or overestimated. Another representation of this effect is given in figure 21 where the average lateral distribution of Cherenkov photons along the x-axis and y-axis, respectively, is shown. While the red curve corresponds to the intensity measured by a telescope situated at the x-axis ($\varphi = 0°$), the black curve would be measured along the y-axis ($\varphi = 90°$).

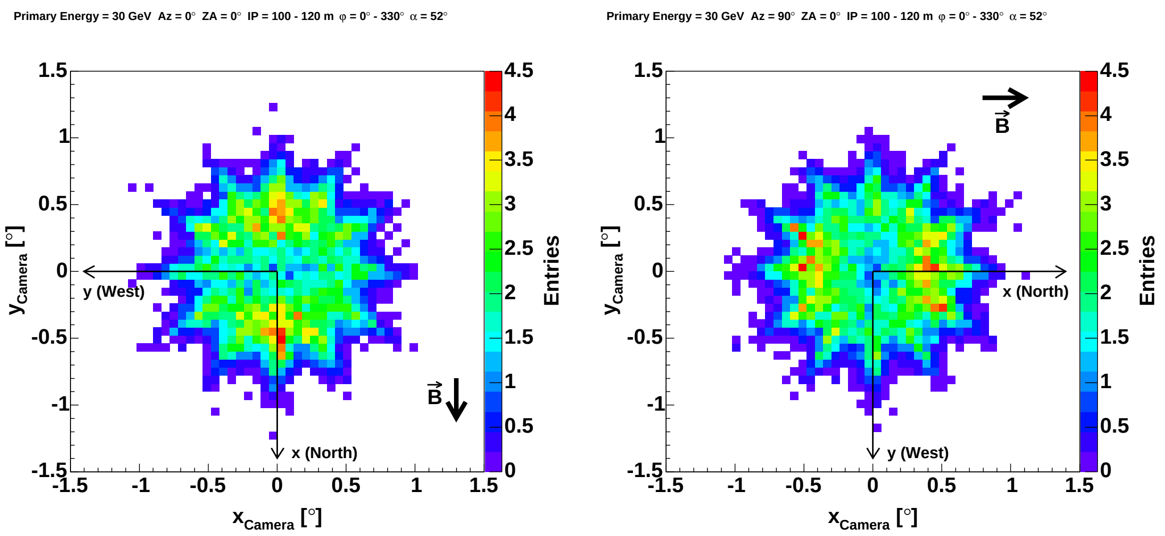

(a) (b)

Figure 22: Frequency distributions of reconstructed image centroids for MC generated γ-ray showers. The energy was set to 30 GeV. The ZA was set to 0°, while the azimuth angle was set to 0° (a) and 90° (b), respectively. The soft image cleaning was applied.

At 0° ZA, the asymmetry of the distribution of Cherenkov photons due to the GF is independent of the azimuth angle, as the angle α stays constant with increasing azimuth angle (figure 5). For ZA greater than 0°, the influence of the GF depends on the azimuth angle. The distribution of Cherenkov photons shown in figure 20 (b), obtained for 20° ZA, is not only asymmetric in the same way as the one shown in figure 20, but in addition, it appears to be elongated along the x-axis. In absence of the GF, the average intensity of Cherenkov photons measured along the pink circles would be constant. In the MC data produced for these studies, the telescope is always placed on the light blue circles. Therefore, the GF effects as well as geometrical effects are entangled.

The reconstructed intensity not only changes because of the GF, but also because the telescope is not always located at the hump of the distribution of Cherenkov photons. At 20° ZA, the deviation from a circle is at most 6 m which roughly corresponds to the width of the hump (figures 12 (a) - 15 (a)). At larger ZA, the deviation of the Cherenkov distribution from a circle becomes greater, i.e. for 40° ZA it extends up to 30 m and for 60° ZA it extends up to 100 m.

Figure 20 (d) exhibits an additional south-north asymmetry of geometrical origin. Because of the inclination of the EAS with respect to the x-axis, half of all Cherenkov photons cover a greater distance through the atmosphere, which results in a certain attenuation. The path difference Δs depends on the impact parameter r and the ZA. For instance, at 40° ZA and $r = 120$ m it amounts to $\Delta s = 2\,r\,\tan(\mathrm{ZA}) \approx 200$ m, and for 60° ZA it is $\Delta s \approx 420$ m.

Figure 22 shows the frequency distributions of the reconstructed image centroids of MC generated γ-ray showers of 30 GeV energy for two different azimuth angles. The ZA was set to 0° ZA and the azimuth set to 0° and 90°, respectively. For 0° azimuth angle (figure 22 (a)), the x-axis of the camera reference system is aligned with the y-axis of the CORSIKA reference system (figure 17). Due to the influence of the GF, the number of showers above the analysis threshold reconstructed along the x-axis of the camera reference system is lower than the one reconstructed along the y-axis.

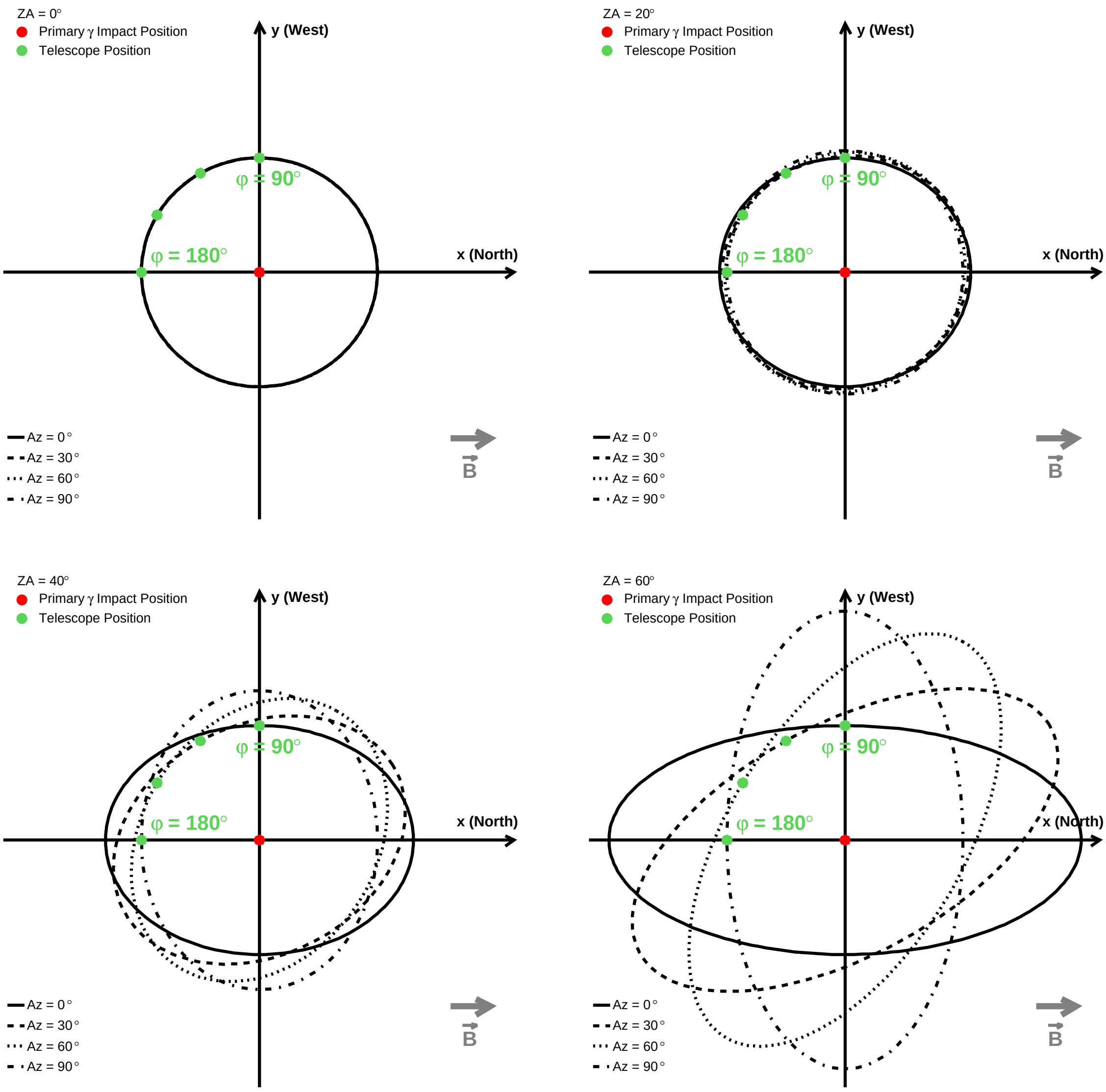

Figure 23: Possible telescope positions on the ground and the orientation of the hump in the lateral Cherenkov light distribution. Depending on the orientation of the telescope, one is confronted with a different situation. The ellipses correspond to the position of the maximum intensity of Cherenkov photons (the hump in the lateral distribution is located at $r \approx 120\,\mathrm{m}$ for 0° ZA). The telescope positions are indicated as green spots and the primary γ-ray impact point is indicated as a red spot. The projection of the GF on ground is indicated in the lower right part of the figure.

A comparable distribution of centroids, even though rotated anti-clockwise, is obtained for 90° azimuth

angle (figure 22 (b)). The latter is expected, because for 0° ZA the lateral component of the GF stays constant with increasing azimuth angle.
According to the relation between the coordinate system of the CORSIKA MC program and the one of the Reflector program [31], the image parameter δ, the azimuth angle and the angle φ are related through

$$\delta = 90^\circ + \text{azimuth angle} - \varphi. \tag{11}$$

Therein δ is defined as the angle between the major axis of the shower image in the camera and the x-axis of the camera coordinate system (figure 18).

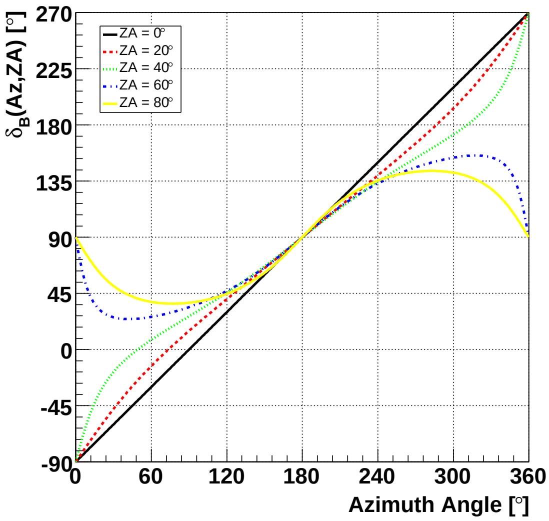

Figure 24: The angle between the projection of the GF in the camera and the x-axis of the camera coordinate system versus azimuth angle and different ZAs between 0° and 80°.

As already pointed out, for fixed impact parameters r as well as fixed angles φ and ZA $> 0^\circ$ the telescope is not always located on the hump of the Cherenkov distribution on ground. Therefore, to disentangle both the geometrical effect and the influence of the GF, it is appropriate to place the telescope always on the hump, i.e. on the semi-minor axis of the ellipses of maximum intensity. To achieve this, the angle φ must be set to $\varphi = \text{azimuth angle} + 90^\circ$, while the impact parameter r is kept constant. Figure 23 illustrates the situation. The circles and ellipses, respectively, correspond to the position of the maximum intensity (the hump in the lateral distribution at an impact parameter of $r \approx 120\,\text{m}$) of the Cherenkov photon distribution. For ZA $> 0^\circ$, each circle changes to an ellipse whose orientation is defined by the azimuth angle. The telescope positions are indicated as green spots and the primary γ-ray impact point is indicated as a red spot. The projection of the GF on ground (not in the telescope camera!) is indicated in the lower right part of the figure.
The projection of the GF in the camera coordinate system is obtained from the transformation of coordinates between the CORSIKA and the MAGIC coordinate system, which is described in [31]. According to this transformation the GF vector $\vec{B} = (B_x, 0, B_z)^{\mathrm{T}}$ is rotated by the azimuth angle around the z-axis of the CORSIKA coordinate system and by the ZA around the new y'-axis, i.e.

$$\vec{B}'' = R_{y'}(\text{ZA})\, R_z(\text{Az})\, \vec{B}. \tag{12}$$

The projection of the GF in the camera coordinate system is then given by

$$\vec{B}_{\text{Camera}}(\text{Az},\text{ZA}) = (-B_{y''}, -B_{x''})^{\text{T}} = (\sin(\text{Az})B_x, \sin(\text{ZA})B_z - \cos(\text{ZA})\sin(\text{Az})B_x)^{\text{T}}. \tag{13}$$

The angle $\delta_B(\text{Az},\text{ZA}) = \sphericalangle(\vec{B}_{\text{Camera}}(\text{Az},\text{ZA}), \vec{e}_{x,\text{Camera}})$ between the projection of the GF in the camera and the x-axis of the camera coordinate system versus azimuth angle for different inclinations of the telescope is shown in figure 24. From the figure it can be seen that only for ZA $= 0°$ the angle $\delta_B(\text{Az},\text{ZA})$ and the azimuth angle are linearly related.

3.1.1 The Influence of the GF on Shape and Orientation of the Shower Images

As the γ/hadron separation is based on the shape and orientation of the shower images, it is important to investigate the influence of the GF on the image parameters that are commonly used for the background discrimination.

The Influence of the GF on the Image Parameters WIDTH and LENGTH

To investigate the influence of the GF on the image parameters WIDTH and LENGTH, it is helpful to depict the reconstructed γ-ray images in the camera. Furthermore, to disentangle the influence of the GF on the shape of the images and the one on the orientation of the images, it is, for the first instance, suggestive to ignore the information on the distortion of the image parameter DIST and the parameter δ.

Figure 25 shows the Hillas ellipses for primary γ-rays of 30 GeV energy, two different image cleaning levels and two ranges of the impact parameter, i.e. 40 - 60 m as well as 100 - 120 m. The ZA was set to 0°. In this case, as the absolute value of the GF strength is symmetric in the azimuth angle (figure 6), it is sufficient to consider only one azimuth angle. The minor and major axes of the Hillas ellipses are obtained from the mean values of the distributions of the image parameters WIDTH and LENGTH. For each telescope position (r, φ), the ellipses are placed at the average DIST value that was obtained for disabled GF. The nominal orientation δ of the ellipses is given by equation 11. Compared to the images which have survived the soft image cleaning (figures 25 (a) and (c)), the images obtained after application of the hard image cleaning levels appear to be significantly smaller. The latter is expected, as the application of the hard image cleaning levels result in a removal of more boundary pixels which do not contribute any more to the size of the images. Undistorted shower images, which were obtained for disabled GF, are displayed as blue ellipses (dotted lines), whereas distorted shower images, which were obtained for enabled GF, are displayed as red ellipses (solid lines). As indicated by the black curve in the upper right part of the figures 25 (a) - (d), for 0° ZA, the Cherenkov light distributions on ground are circularly shaped. The coordinate system of the MC program CORSIKA (figure 17) is centered on the camera display, and the coordinate system of the telescope camera is indicated in the lower left part of the figures 25 (a) - (d). The projection of the GF is indicated in the lower right part of the figures. Only for 0° ZA the projection of the GF is parallel to the x-axis of the CORSIKA coordinate system.

As can be seen from figure 25 (a) (soft image cleaning), on average, the distortion of the image parameters WIDTH and LENGTH is rather small. In case of larger image cleaning levels (figure 25 (b)), the Hillas ellipses obtained for enabled GF appear to be slightly different from the ones obtained for disabled GF. Images lying on the x-axis of the camera coordinate system ($\varphi = 90°, 270°$) are slightly stretched horizontally with respect to the direction of the GF. Instead, images lying on the y-axis of the camera coordinate system appear to be more roundish than the one obtained for disabled GF. This effect was already shown qualitatively in [15]. In both cases, i.e. for $\delta = 0°, 180°$

as well as $\delta = 90°, 270°$, the average pointing of the shower images is expected to be maintained and the parameter ALPHA should remain mostly unaffected. The angle δ is counted anti-clockwise from the positive x-axis of the camera coordinate system (figure 18 for the definition of the angle δ). At intermediate angles $\delta \neq 0°, 90°, 180°, 270°$ the shower images are expected to be affected too, although the figures do not allow to draw a conclusion (at least at the γ-ray energies considered for this plot). At larger impact parameters (figures 25 (c) - (d)) the situation is similar, although the average WIDTH and LENGTH of the shower images appear to be slightly less affected than in case of smaller impact parameters.

At ZA $> 0°$, the situation is somewhat different, as the angle α between the shower axis and the direction of the GF is a function of the azimuth angle, i.e. the absolute value of the GF strength changes with increasing azimuth angle (figure 6). Figure 26 shows the Hillas ellipses for primary γ-rays of 30 GeV energy, two different image cleaning levels and impact parameters between 100 m and 120 m. The ZA was set to 20°. The Hillas ellipses depicted in figure 26 (a) are similar to the ones in figure 25 (a), although the influence of the GF is expected to be smaller, as the angle between the direction of the shower axis and the GF lines is smaller ($\alpha = 32°$). The shapes of the Hillas ellipses obtained for 180° azimuth angle are comparable to the ones obtained for 0° azimuth angle. The shape of the distorted γ-ray images does not systematically change as a function of the angle δ. Instead, the variation of the shape of the images is rather due to limited statistics and a significant difference between the images obtained for disabled GF and the ones obtained for enabled GF is hardly visible. At 30 GeV and 20° ZA the trigger efficiency is in the order of 10 % (section 3.1.4). Therefore, at higher energies where much more events survive the image cleaning, the influence of the GF on the image parameters WIDTH and LENGTH is expected to appear more articulated.

Figures 27 - 34 show the Hillas ellipses for primary γ-rays between 50 GeV and 170 GeV energy, different image cleaning levels and telescope orientations. The figures indicate that the shape of the γ-ray images for enabled GF does not significantly change as a function of the angle δ. However, for 170 GeV, 20° ZA and 180° there is a slight dependency on the angle δ. Images lying on the x-axis of the camera coordinate system ($\varphi = 90°, 270°$) are slightly stretched horizontally with respect to the direction of the GF. Instead, images lying on the y-axis of the camera coordinate system appear to be more roundish than the one obtained for disabled GF.

The influence of the GF on the shape of the shower images becomes more pronounced at higher energies. Figure 35 shows the Hillas ellipses for primary γ-rays of 300 GeV energy, two different image cleaning levels and two ranges of the impact parameter, i.e. 40 - 60 m as well as 100 - 120 m. The ZA was set to 0°. As can be seen from the figures, the Hillas ellipses obtained for enabled GF appear to be different from the ones obtained for disabled GF. The distortion of the images occurs at impact parameters 40 - 60 m as well as between 100 m and 120 m, independently of the image cleaning level. Again, images lying on the x-axis of the camera coordinate system ($\varphi = 90°, 270°$) are slightly stretched horizontally with respect to the direction of the GF. Instead, images lying on the y-axis of the camera coordinate system appear to be more roundish than the one obtained for disabled GF. In both cases, i.e. for $\delta = 0°, 180°$ as well as $\delta = 90°, 270°$, the average pointing of the shower images is expected to be maintained, and the parameter ALPHA should remain unaffected. Shower images pointing at intermediate angles $\delta \neq 0°, 90°, 180°, 270°$ are altered compared to the ones obtained for disabled GF. Because these images are neither oriented horizontally nor vertically with respect to the direction of the GF, the sideways extension of these showers images is expected to result in a systematic rotation away from the source position (camera center) [15]. Therefore, at least at intermediate angles δ, the distribution of the parameter ALPHA is expected to be broadened.

Figure 37 shows the Hillas ellipses for primary γ-rays of 300 GeV energy, two different image cleaning levels and impact parameter between 100 m and 120 m. The ZA was set to 40°, and the azimuth angle was set to 0° and 180°, respectively. The Hillas ellipses depicted in figure 37 (a) and (b) that were obtained for enabled GF are altered slightly less than the corresponding ellipses in figure 37 (c) and (d), which is due to the fact that the influence of the GF is weaker. In the latter case, the angle between the direction of the shower axis and the GF lines is $\alpha = 87°$.

Figures 38 (a) - (d) show the images obtained for 300 GeV, 40° ZA and increasing azimuth angle. As expected, images perpendicular to the projected direction of the GF in the camera are slightly stretched and the ones lying parallel to the projected direction of the GF are more roundish.

The effects mentioned beforehand appear to be more pronounced for γ-ray of 450 GeV energy (figures 35 - 42). Even at 1 TeV the images are subject to GF effects (figures 43 - 46).

From the figures presented beforehand it can be concluded that, for very low energies, the influence of the GF on the WIDTH and LENGTH of the shower images is, within statistics, in the order of the one presumably resulting from intrinsic fluctuations in the shower development. For higher energies, the influence of the GF on the shape of the Hillas ellipses is clearly visible.

As yet it was not investigated to what extent the alternation of the shape of the shower images degrades the γ/hadron separation. But, even for very unfavorable orientations of the shower axis with respect to the GF lines (large angle α) the standard γ/hadron separation should be feasible, even though it might be degraded. Apart from the influence of the GF on the shape of the shower images, its influence on the orientation of the images is of major importance, as it directly affects the distribution of the parameter ALPHA commonly used to extract the γ signal.

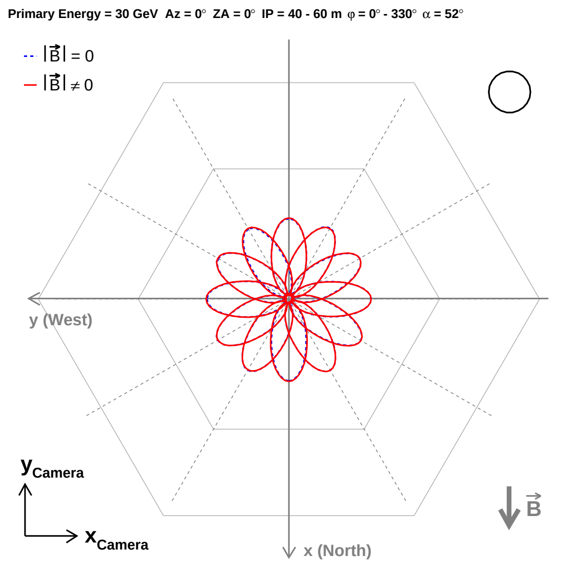

(a) Soft image cleaning, impact parameter 40 - 60 m.

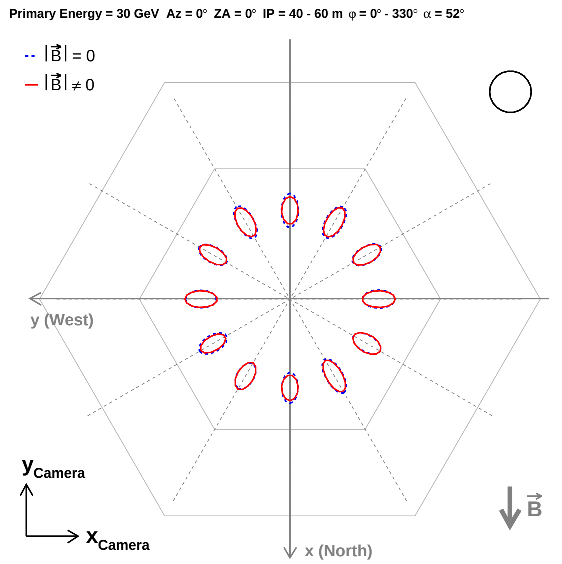

(b) Hard image cleaning, impact parameter 40 - 60 m.

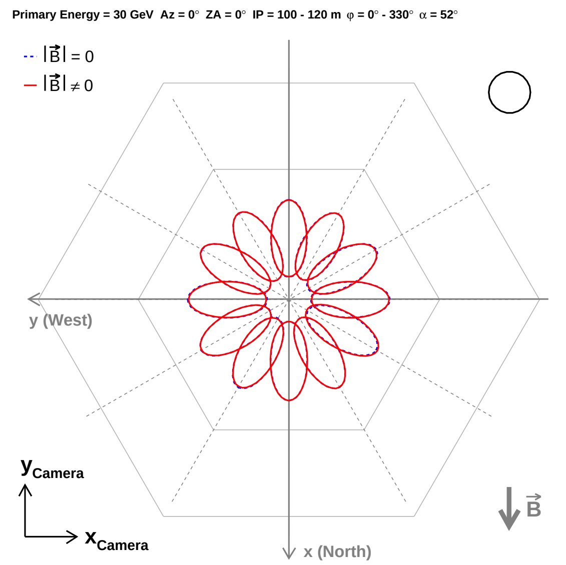

(c) Soft image cleaning, impact parameter 100 - 120 m.

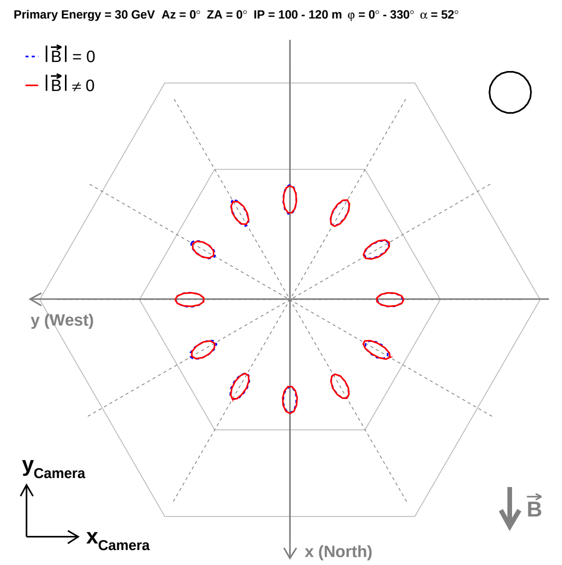

(d) Hard image cleaning, impact parameter 100 - 120 m.

Figure 25: Hillas ellipses for MC γ-rays of 30 GeV energy, two different image cleaning levels and two impact parameter windows. The ZA was set to 0° and the azimuth angle to 0°. The angle φ was varied over the full range between 0° and 330°. To demonstrate the influence of the GF on the image parameters WIDTH and LENGTH, the distortion of the orientation (δ) and the parameter DIST was ignored. While the red ellipses (solid lines) were obtained for enabled GF, the blue ones (dashed lines) were obtained for disabled GF. The black curve in the upper right part of the figure indicates the ellipticity (zero for 0° ZA) of the Cherenkov light distribution on ground.

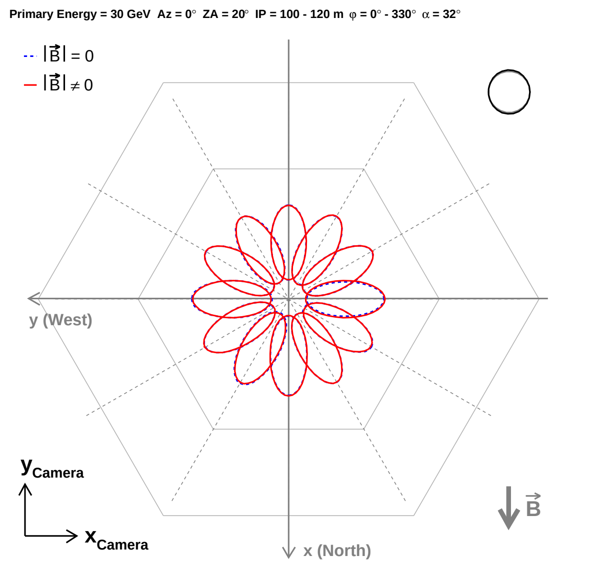

(a) Soft image cleaning, ZA 20°, azimuth angle 0°, impact parameter 100 - 120 m.

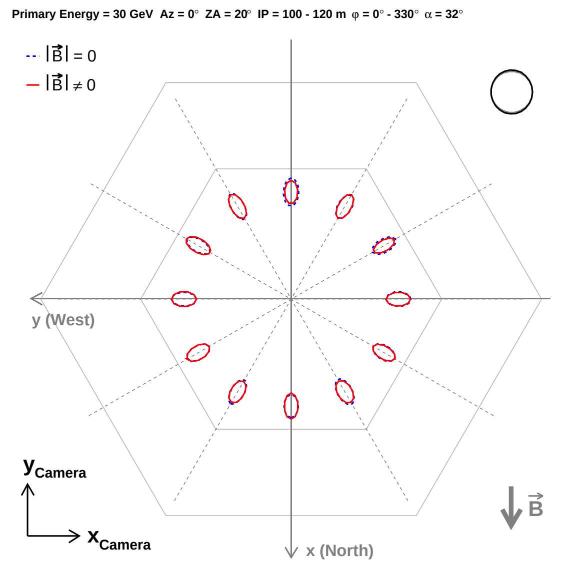

(b) Hard image cleaning, ZA 20°, azimuth angle 0°, impact parameter 100 - 120 m.

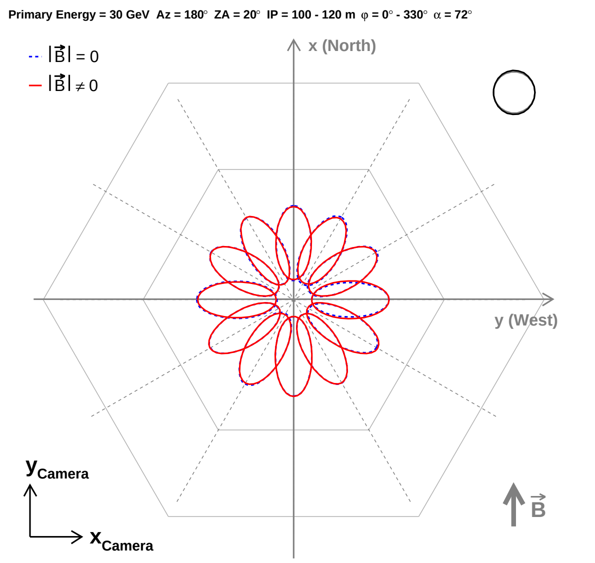

(c) Soft image cleaning, ZA 20°, azimuth angle 180°, impact parameter 100 - 120 m.

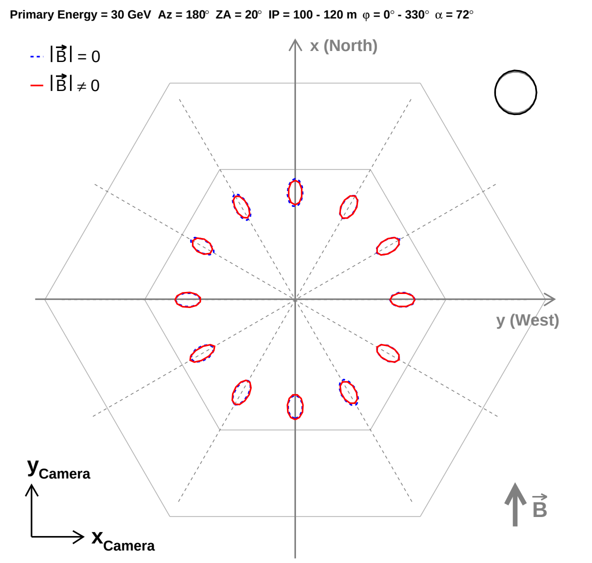

(d) Hard image cleaning, ZA 20°, azimuth angle 180°, impact parameter 100 - 120 m.

Figure 26: Hillas ellipses for MC γ-rays of 30 GeV energy, two different image cleaning levels and impact parameters between 100 m and 120 m. The ZA was set to 20° and the azimuth angle to 0° and 180°, respectively. The angle φ was varied over the full range between 0° and 330°. To demonstrate the influence of the GF on the image parameters WIDTH and LENGTH, the distortion of the orientation (δ) and the parameter DIST was ignored. While the red ellipses (solid lines) were obtained for enabled GF, the blue ones (dashed lines) were obtained for disabled GF. The black curve in the upper right part of the figure indicates the ellipticity of the Cherenkov light distribution on ground.

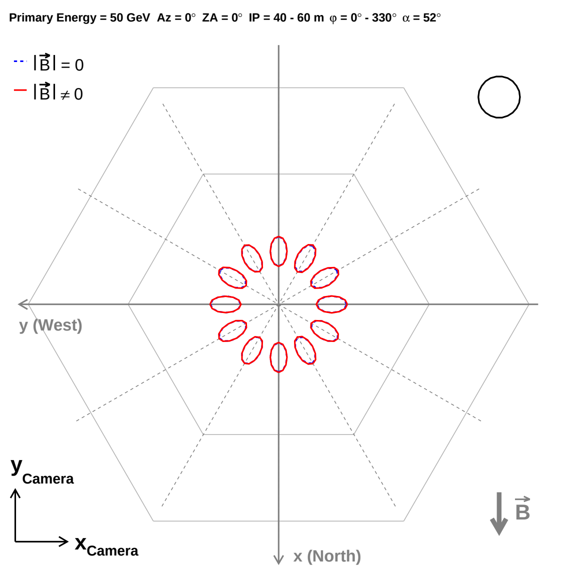

(a) Intermediate image cleaning, impact parameter 40 - 60 m.

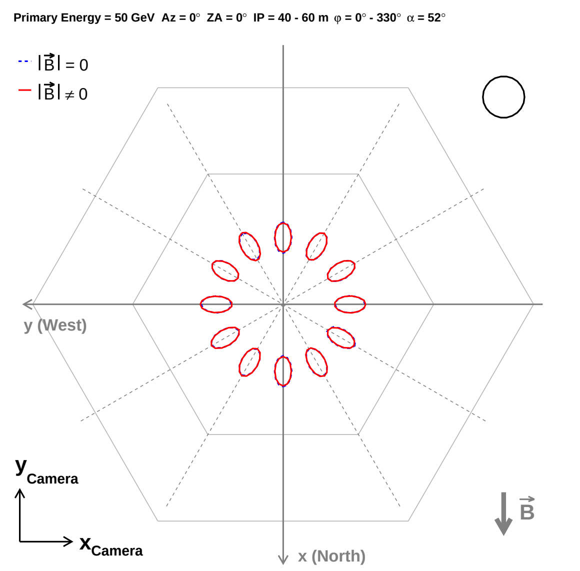

(b) Hard image cleaning, impact parameter 40 - 60 m.

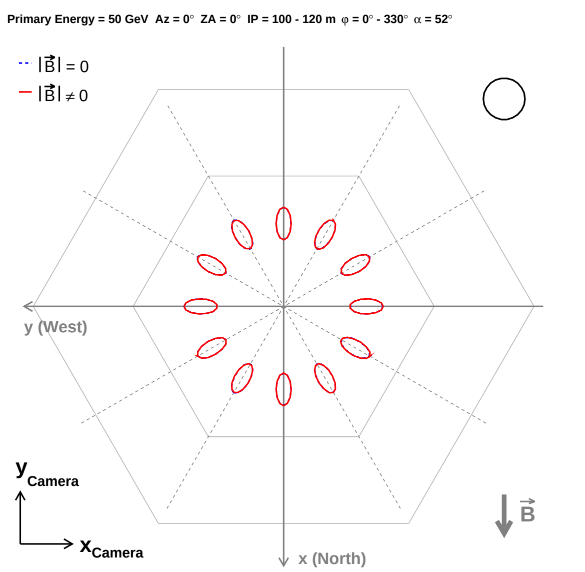

(c) Intermediate image cleaning, impact parameter 100 - 120 m.

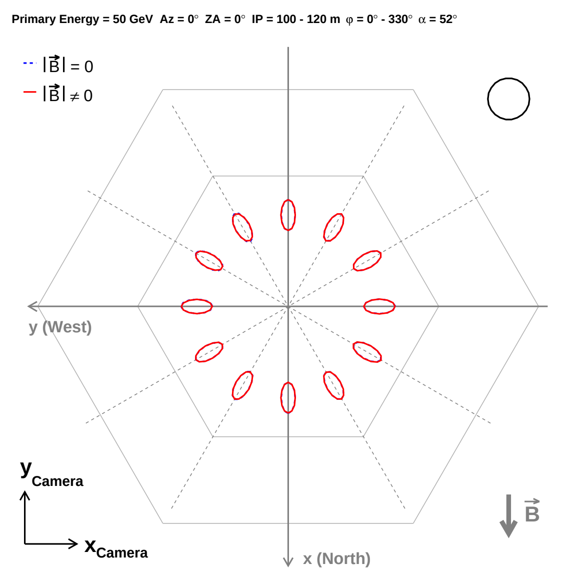

(d) Hard image cleaning, impact parameter 100 - 120 m.

Figure 27: Hillas ellipses for MC γ-rays of 50 GeV energy, two different image cleaning levels and two impact parameter windows. The ZA was set to 0° and the azimuth angle to 0°. The angle φ was varied over the full range between 0° and 330°. To demonstrate the influence of the GF on the image parameters WIDTH and LENGTH, the distortion of the orientation (δ) and the parameter DIST was ignored. While the red ellipses (solid lines) were obtained for enabled GF, the blue ones (dashed lines) were obtained for disabled GF. The black curve in the upper right part of the figure indicates the ellipticity (zero for 0° ZA) of the Cherenkov light distribution on ground.

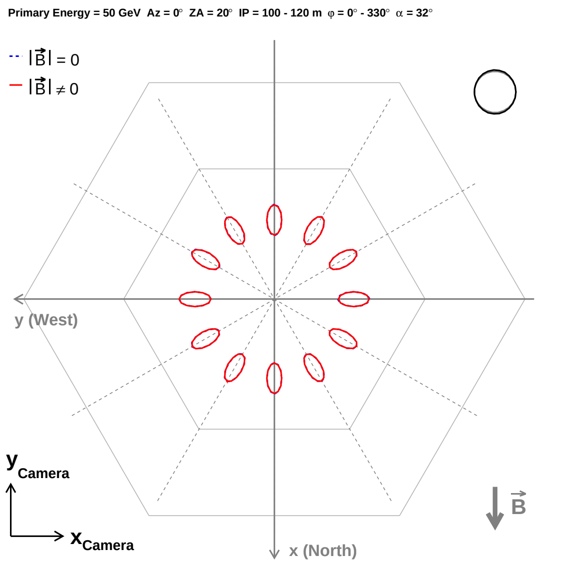

(a) Intermediate image cleaning, ZA 20°, azimuth angle 0°, impact parameter 100 - 120 m.

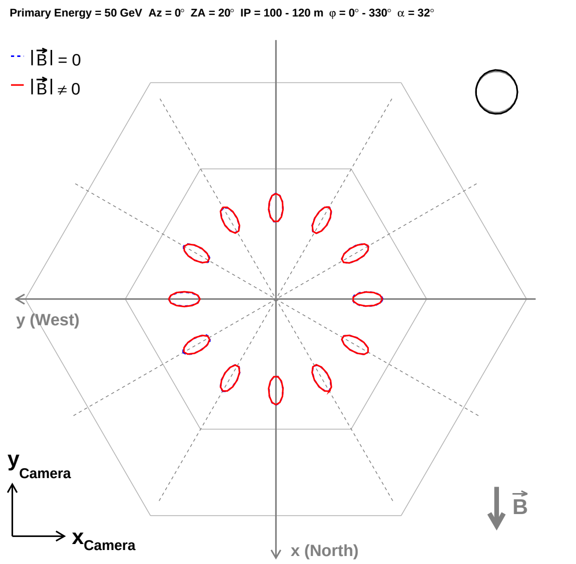

(b) Hard image cleaning, ZA 20°, azimuth angle 0°, impact parameter 100 - 120 m.

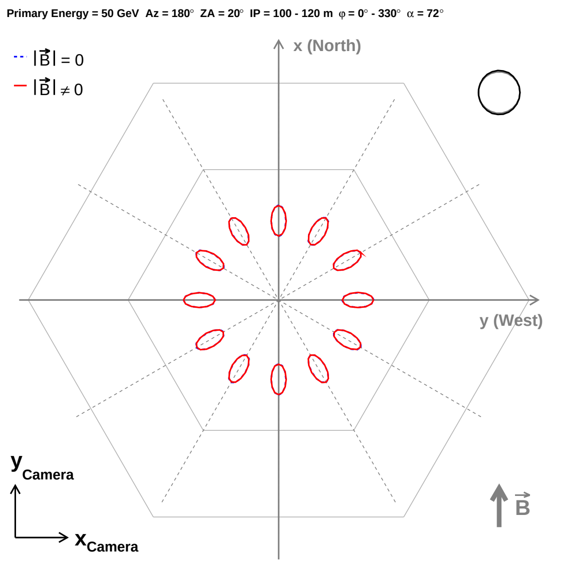

(c) Intermediate image cleaning, ZA 20°, azimuth angle 180°, impact parameter 100 - 120 m.

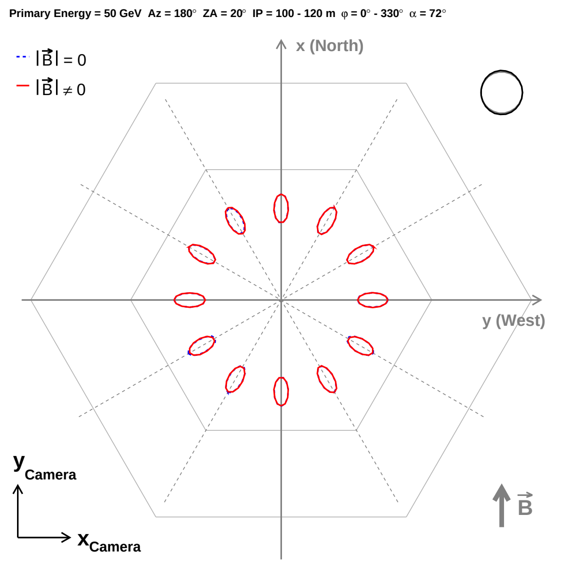

(d) Hard image cleaning, ZA 20°, azimuth angle 180°, impact parameter 100 - 120 m.

Figure 28: Hillas ellipses for MC γ-rays of 50 GeV energy, two different image cleaning levels and impact parameters between 100 m and 120 m. The ZA was set to 20° and the azimuth angle to 0° and 180°, respectively. The angle φ was varied over the full range between 0° and 330°. To demonstrate the influence of the GF on the image parameters WIDTH and LENGTH, the distortion of the orientation (δ) and the parameter DIST was ignored. While the red ellipses (solid lines) were obtained for enabled GF, the blue ones (dashed lines) were obtained for disabled GF. The black curve in the upper right part of the figure indicates the ellipticity of the Cherenkov light distribution on ground.

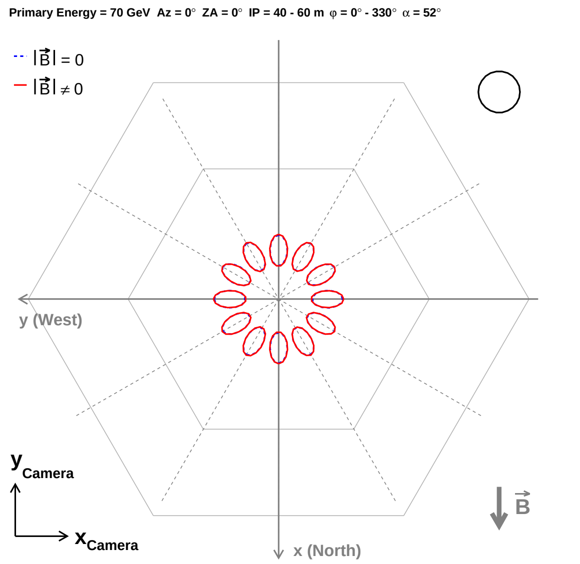

(a) Intermediate image cleaning, impact parameter 40 - 60 m.

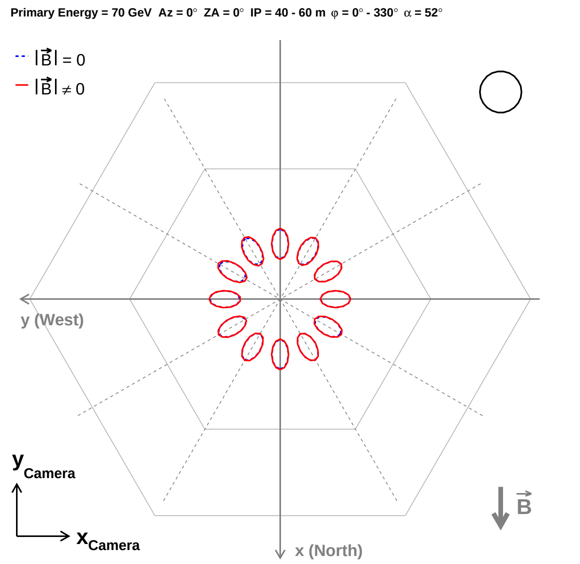

(b) Hard image cleaning, impact parameter 40 - 60 m.

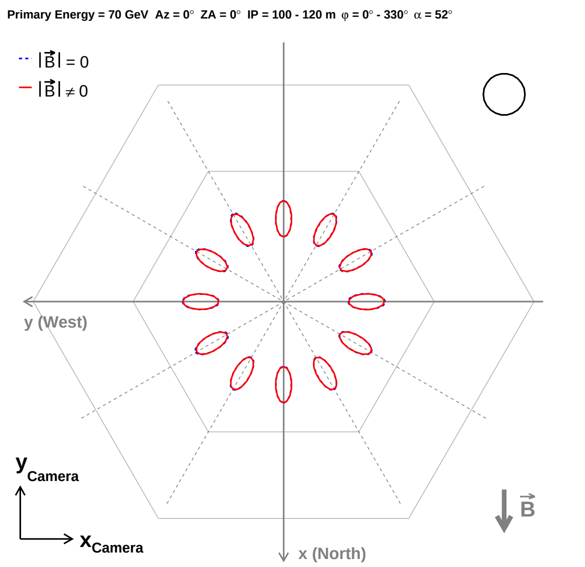

(c) Intermediate image cleaning, impact parameter 100 - 120 m.

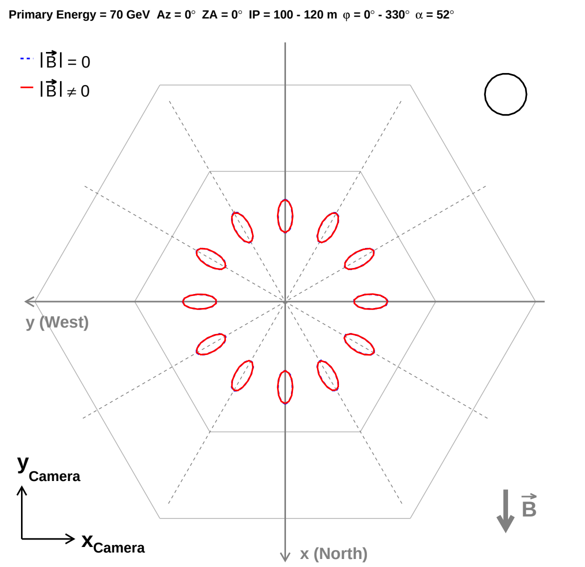

(d) Hard image cleaning, impact parameter 100 - 120 m.

Figure 29: Hillas ellipses for MC γ-rays of 70 GeV energy, two different image cleaning levels and two impact parameter windows. The ZA was set to 0° and the azimuth angle to 0°. The angle φ was varied over the full range between 0° and 330°. To demonstrate the influence of the GF on the image parameters WIDTH and LENGTH, the distortion of the orientation (δ) and the parameter DIST was ignored. While the red ellipses (solid lines) were obtained for enabled GF, the blue ones (dashed lines) were obtained for disabled GF. The black curve in the upper right part of the figure indicates the ellipticity (zero for 0° ZA) of the Cherenkov light distribution on ground.

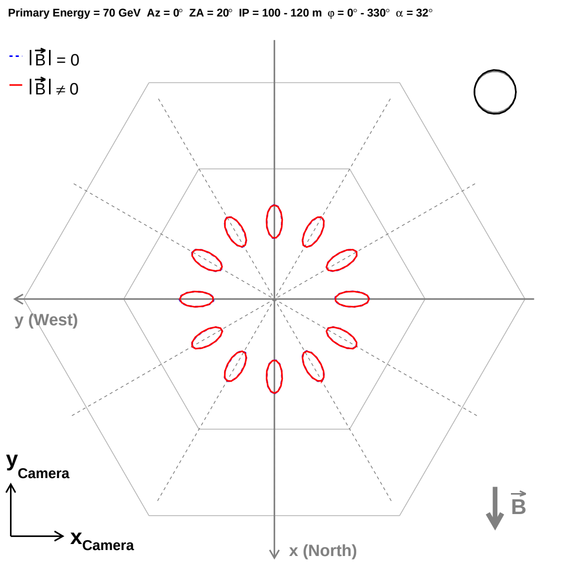

(a) Intermediate image cleaning, ZA 20°, azimuth angle 0°, impact parameter 100 - 120 m.

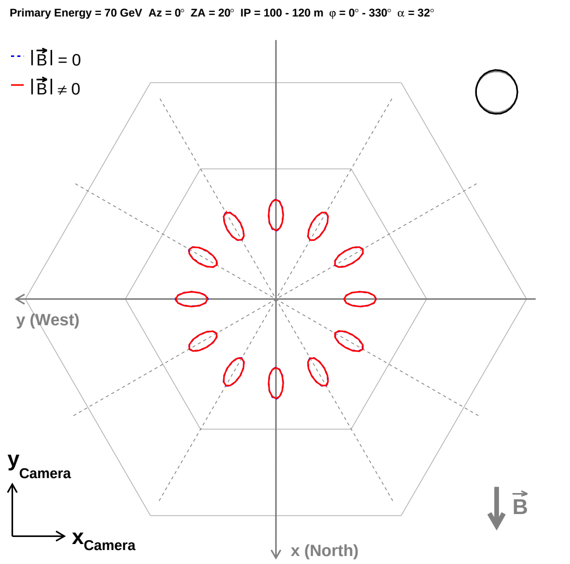

(b) Hard image cleaning, ZA 20°, azimuth angle 0°, impact parameter 100 - 120 m.

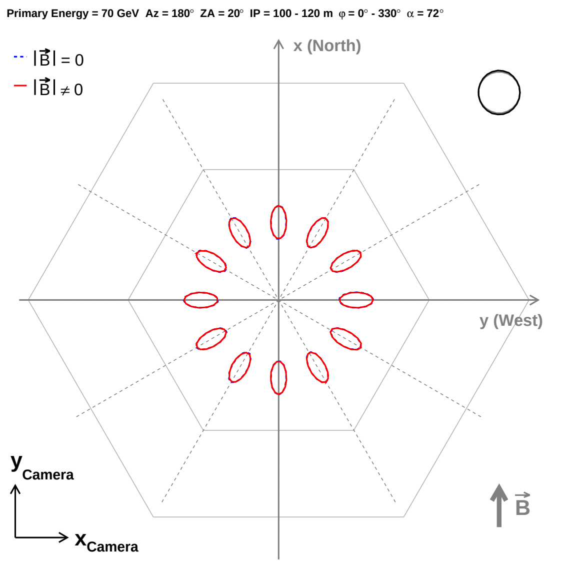

(c) Intermediate image cleaning, ZA 20°, azimuth angle 180°, impact parameter 100 - 120 m.

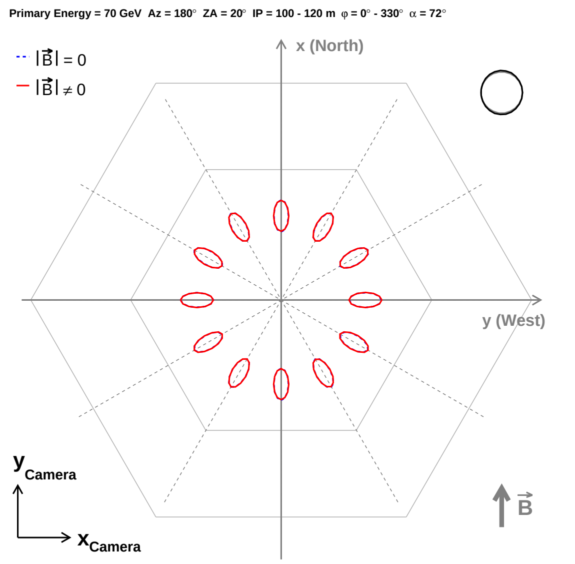

(d) Hard image cleaning, ZA 20°, azimuth angle 180°, impact parameter 100 - 120 m.

Figure 30: Hillas ellipses for MC γ-rays of 70 GeV energy, two different image cleaning levels and impact parameters between 100 m and 120 m. The ZA was set to 20° and the azimuth angle to 0° and 180°, respectively. The angle φ was varied over the full range between 0° and 330°. To demonstrate the influence of the GF on the image parameters WIDTH and LENGTH, the distortion of the orientation (δ) and the parameter DIST was ignored. While the red ellipses (solid lines) were obtained for enabled GF, the blue ones (dashed lines) were obtained for disabled GF. The black curve in the upper right part of the figure indicates the ellipticity of the Cherenkov light distribution on ground.

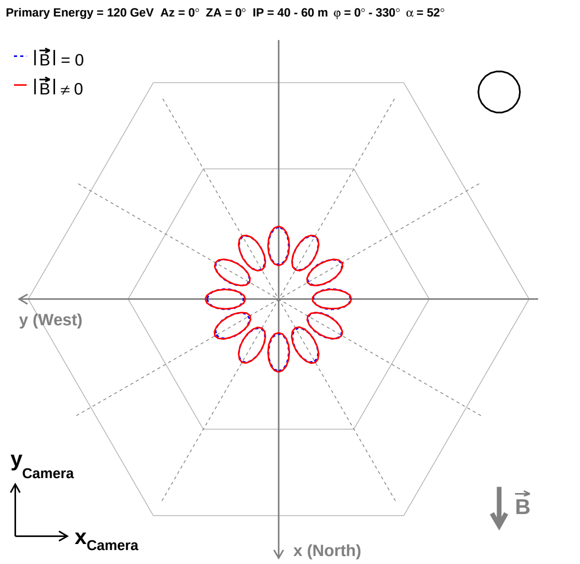

(a) Intermediate image cleaning, impact parameter 40 - 60 m.

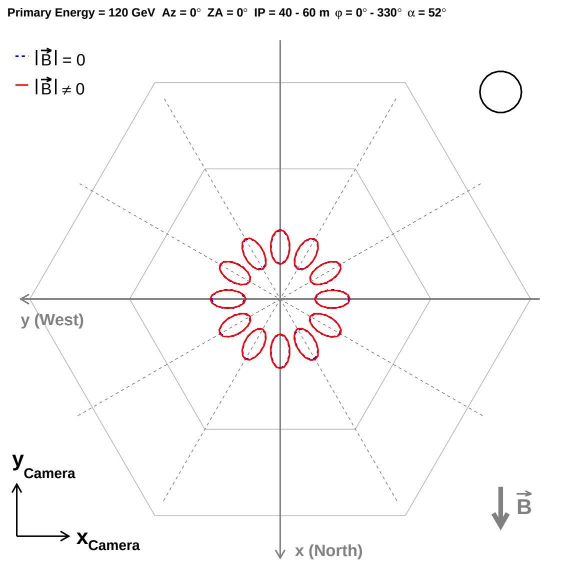

(b) Hard image cleaning, impact parameter 40 - 60 m.

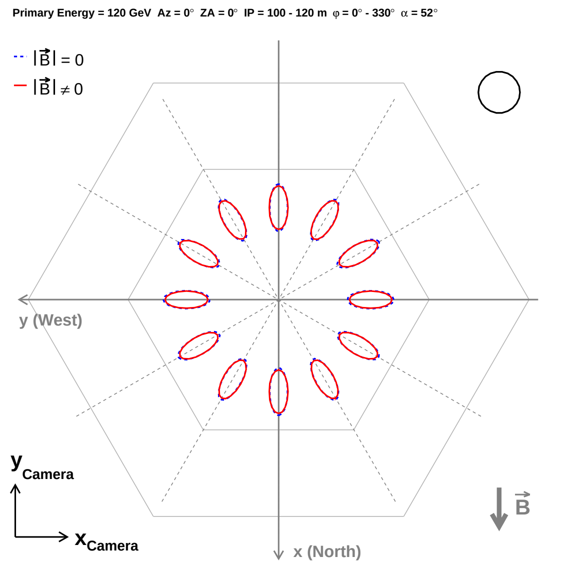

(c) Intermediate image cleaning, impact parameter 100 - 120 m.

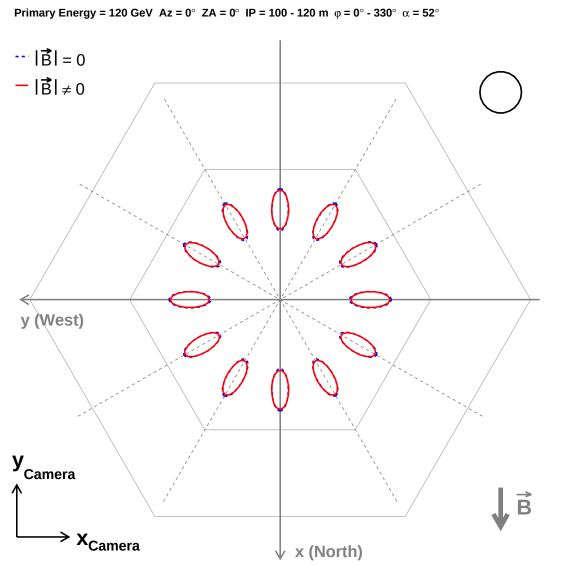

(d) Hard image cleaning, impact parameter 100 - 120 m.

Figure 31: Hillas ellipses for MC γ-rays of 120 GeV energy, two different image cleaning levels and two impact parameter windows. The ZA was set to 0° and the azimuth angle to 0°. The angle φ was varied over the full range between 0° and 330°. To demonstrate the influence of the GF on the image parameters WIDTH and LENGTH, the distortion of the orientation (δ) and the parameter DIST was ignored. While the red ellipses (solid lines) were obtained for enabled GF, the blue ones (dashed lines) were obtained for disabled GF. The black curve in the upper right part of the figure indicates the ellipticity (zero for 0° ZA) of the Cherenkov light distribution on ground.

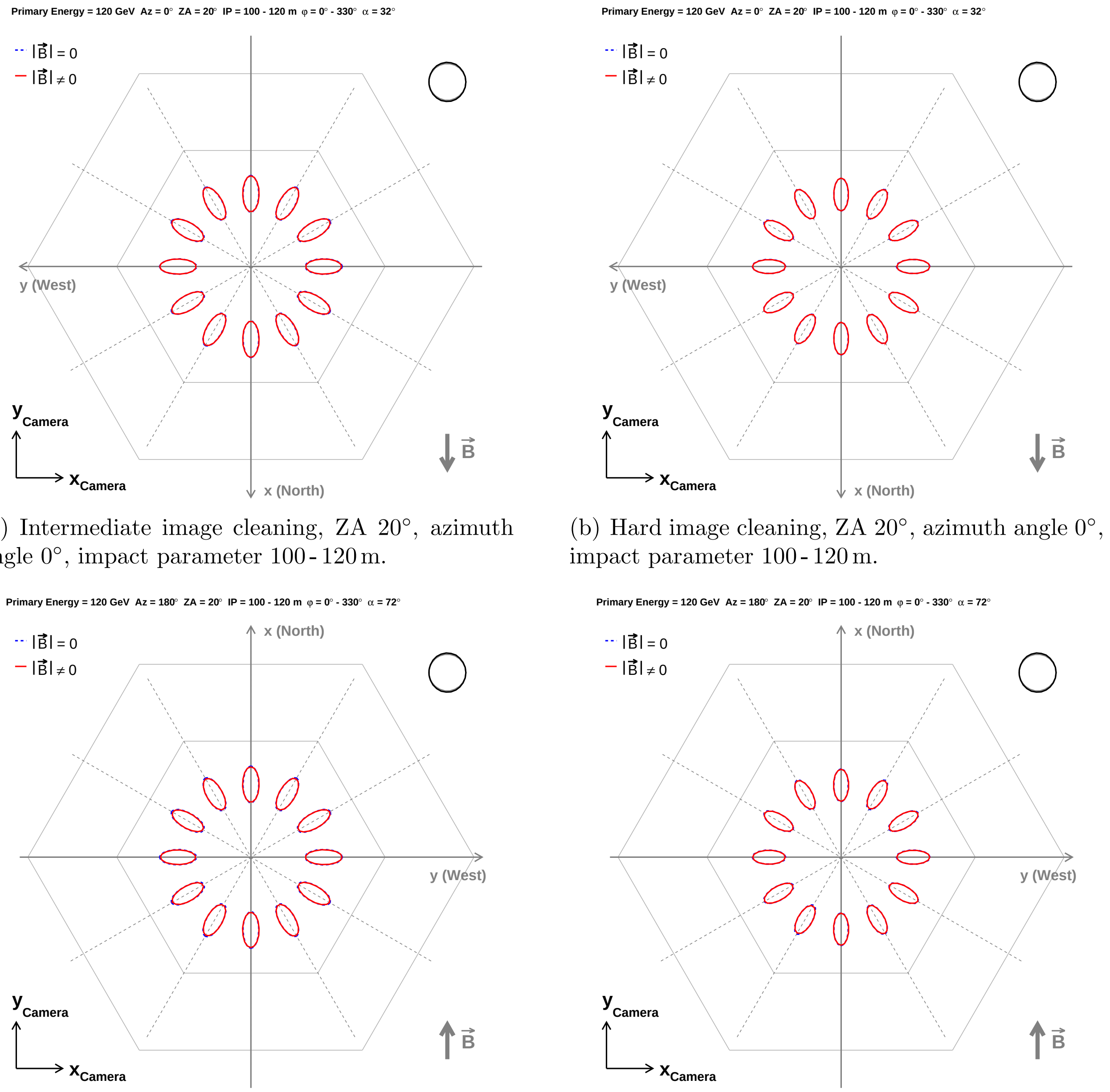

(a) Intermediate image cleaning, ZA 20°, azimuth angle 0°, impact parameter 100 - 120 m.

(b) Hard image cleaning, ZA 20°, azimuth angle 0°, impact parameter 100 - 120 m.

(c) Intermediate image cleaning, ZA 20°, azimuth angle 180°, impact parameter 100 - 120 m.

(d) Hard image cleaning, ZA 20°, azimuth angle 180°, impact parameter 100 - 120 m.

Figure 32: Hillas ellipses for MC γ-rays of 120 GeV energy, two different image cleaning levels and impact parameters between 100 m and 120 m. The ZA was set to 20° and the azimuth angle to 0° and 180°, respectively. The angle φ was varied over the full range between 0° and 330°. To demonstrate the influence of the GF on the image parameters WIDTH and LENGTH, the distortion of the orientation (δ) and the parameter DIST was ignored. While the red ellipses (solid lines) were obtained for enabled GF, the blue ones (dashed lines) were obtained for disabled GF. The black curve in the upper right part of the figure indicates the ellipticity of the Cherenkov light distribution on ground.

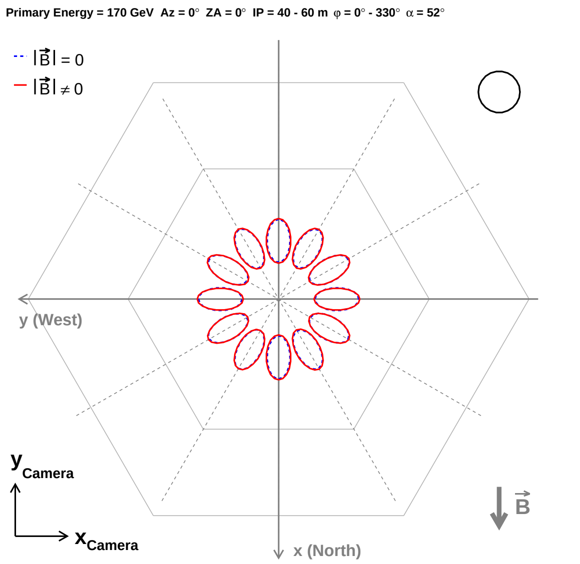

(a) Intermediate image cleaning, impact parameter 40 - 60 m.

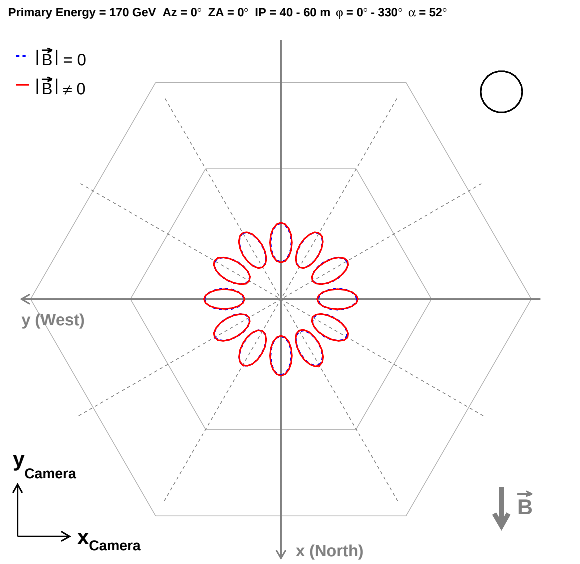

(b) Hard image cleaning, impact parameter 40 - 60 m.

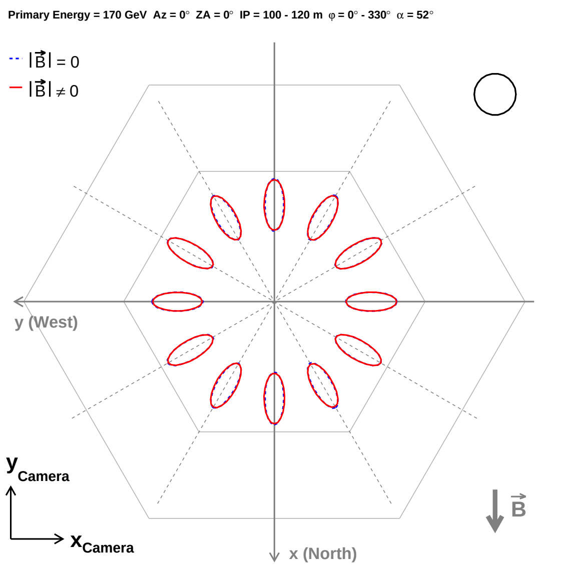

(c) Intermediate image cleaning, impact parameter 100 - 170 m.

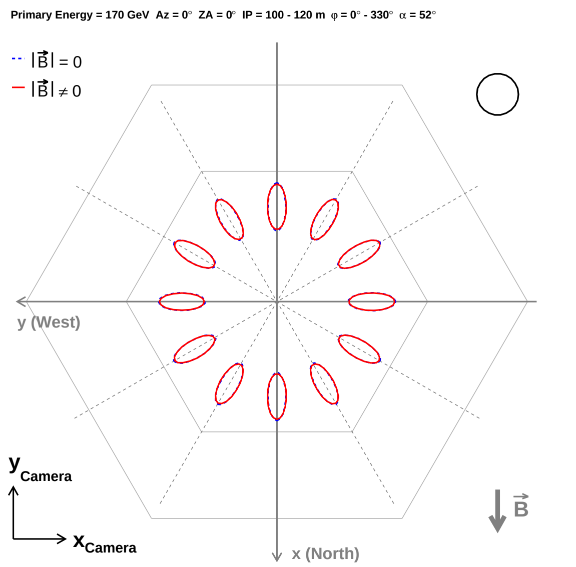

(d) Hard image cleaning, impact parameter 100 - 120 m.

Figure 33: Hillas ellipses for MC γ-rays of 170 GeV energy, two different image cleaning levels and two impact parameter windows. The ZA was set to 0° and the azimuth angle to 0°. The angle φ was varied over the full range between 0° and 330°. To demonstrate the influence of the GF on the image parameters WIDTH and LENGTH, the distortion of the orientation (δ) and the parameter DIST was ignored. While the red ellipses (solid lines) were obtained for enabled GF, the blue ones (dashed lines) were obtained for disabled GF. The black curve in the upper right part of the figure indicates the ellipticity (zero for 0° ZA) of the Cherenkov light distribution on ground.

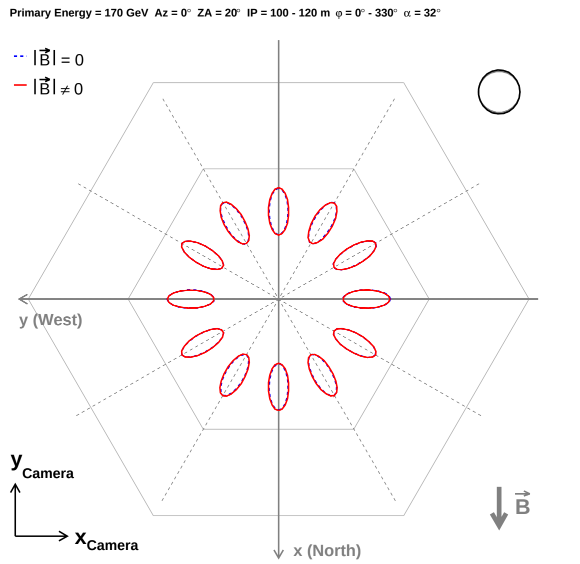

(a) Intermediate image cleaning, ZA 20°, azimuth angle 0°, impact parameter 100 - 120 m.

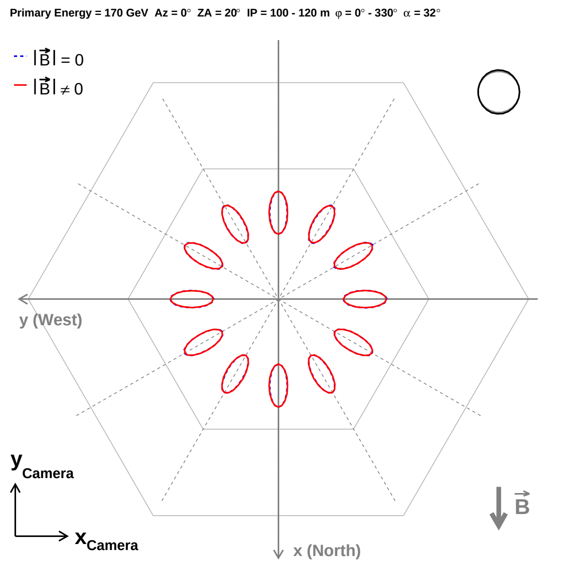

(b) Hard image cleaning, ZA 20°, azimuth angle 0°, impact parameter 100 - 120 m.

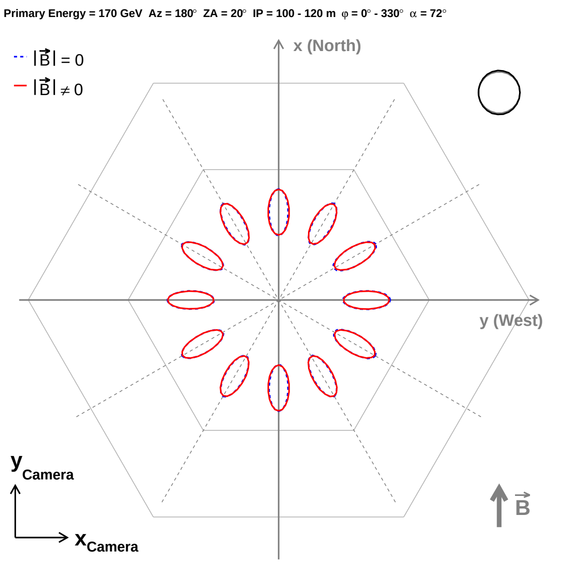

(c) Intermediate image cleaning, ZA 20°, azimuth angle 180°, impact parameter 100 - 120 m.

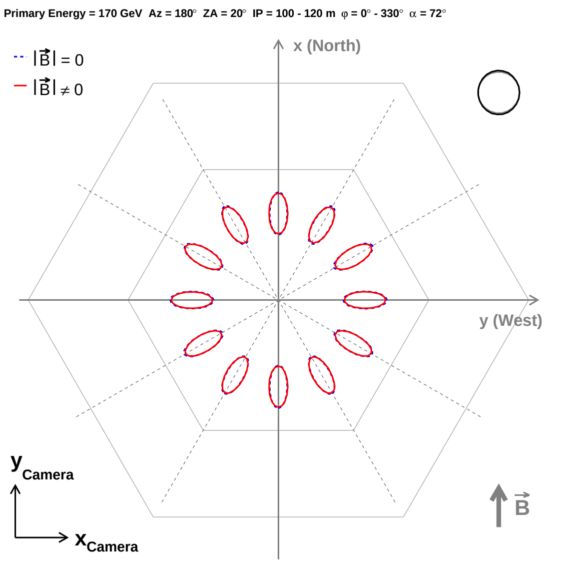

(d) Hard image cleaning, ZA 20°, azimuth angle 180°, impact parameter 100 - 120 m.

Figure 34: Hillas ellipses for MC γ-rays of 170 GeV energy, two different image cleaning levels and impact parameters between 100 m and 120 m. The ZA was set to 20° and the azimuth angle to 0° and 180°, respectively. The angle φ was varied over the full range between 0° and 330°. To demonstrate the influence of the GF on the image parameters WIDTH and LENGTH, the distortion of the orientation (δ) and the parameter DIST was ignored. While the red ellipses (solid lines) were obtained for enabled GF, the blue ones (dashed lines) were obtained for disabled GF. The black curve in the upper right part of the figure indicates the ellipticity of the Cherenkov light distribution on ground.

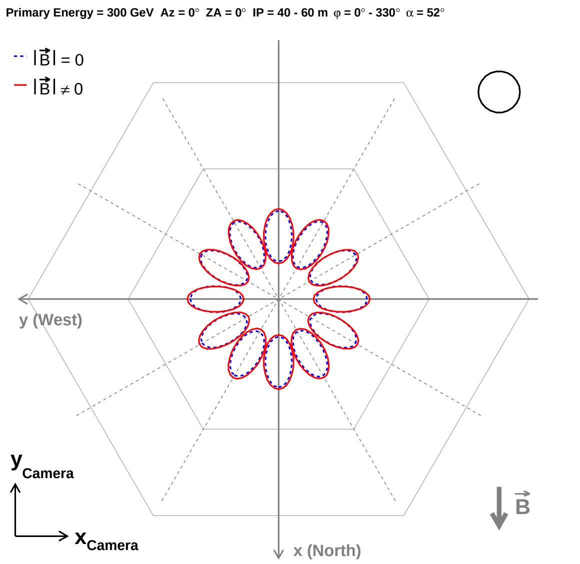

(a) Intermediate image cleaning, impact parameter 40 - 60 m.

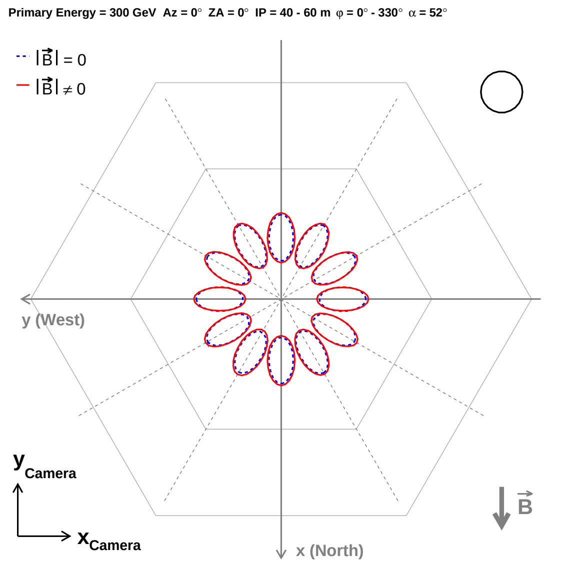

(b) Hard image cleaning, impact parameter 40 - 60 m.

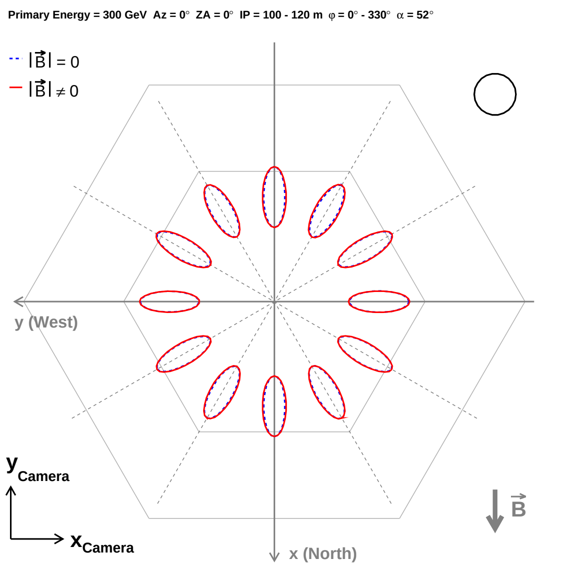

(c) Intermediate image cleaning, impact parameter 100 - 120 m.

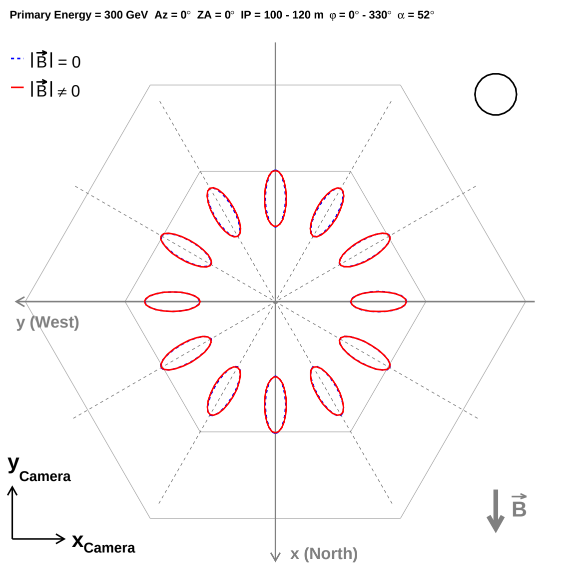

(d) Hard image cleaning, impact parameter 100 - 120 m.

Figure 35: Hillas ellipses for MC γ-rays of 300 GeV energy, two different image cleaning levels and two impact parameter windows. The ZA was set to 0° and the azimuth angle to 0°. The angle φ was varied over the full range between 0° and 330°. To demonstrate the influence of the GF on the image parameters WIDTH and LENGTH, the distortion of the orientation (δ) and the parameter DIST was ignored. While the red ellipses (solid lines) were obtained for enabled GF, the blue ones (dashed lines) were obtained for disabled GF. The black curve in the upper right part of the figure indicates the ellipticity (zero for 0° ZA) of the Cherenkov light distribution on ground.

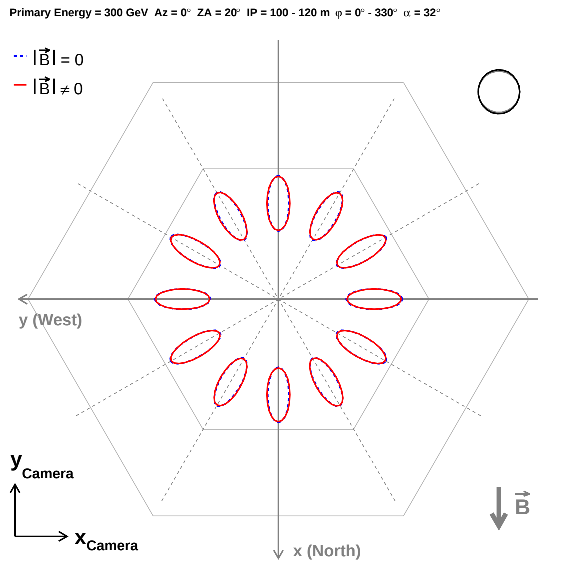

(a) Intermediate image cleaning, ZA 20°, azimuth angle 0°, impact parameter 100 - 120 m.

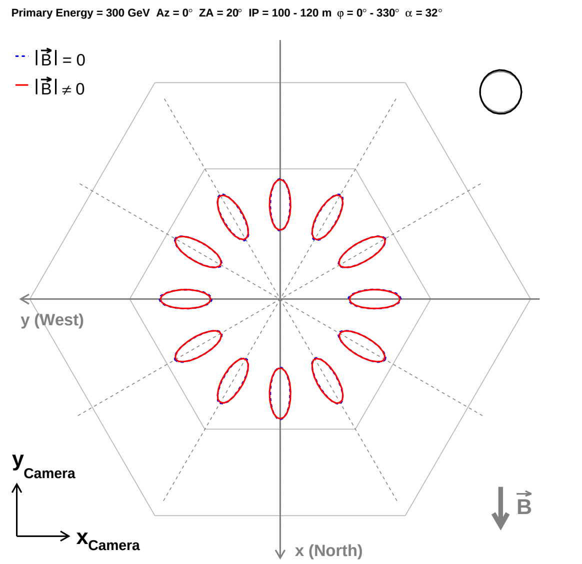

(b) Hard image cleaning, ZA 20°, azimuth angle 0°, impact parameter 100 - 120 m.

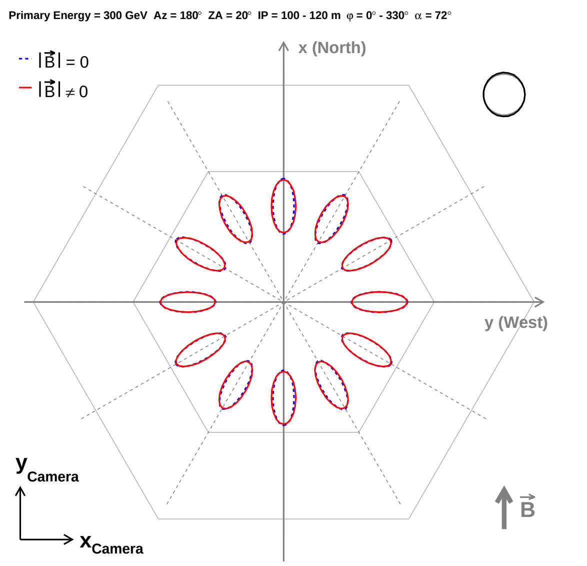

(c) Intermediate image cleaning, ZA 20°, azimuth angle 180°, impact parameter 100 - 120 m.

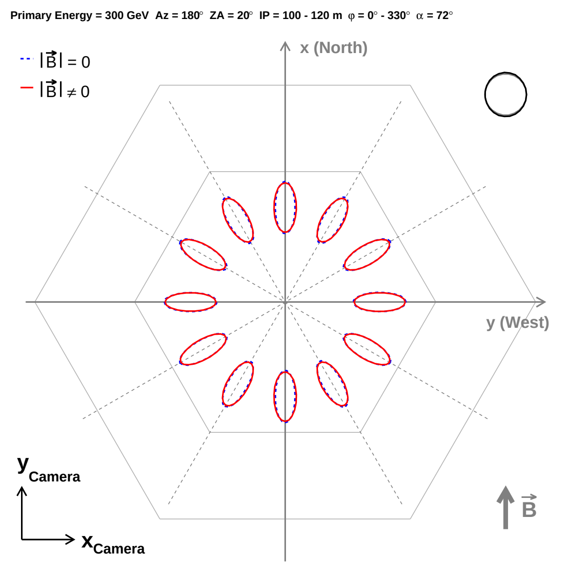

(d) Hard image cleaning, ZA 20°, azimuth angle 180°, impact parameter 100 - 120 m.

Figure 36: Hillas ellipses for MC γ-rays of 300 GeV energy, two different image cleaning levels and impact parameters between 100 m and 120 m. The ZA was set to 20° and the azimuth angle to 0° and 180°, respectively. The angle φ was varied over the full range between 0° and 330°. To demonstrate the influence of the GF on the image parameters WIDTH and LENGTH, the distortion of the orientation (δ) and the parameter DIST was ignored. While the red ellipses (solid lines) were obtained for enabled GF, the blue ones (dashed lines) were obtained for disabled GF. The black curve in the upper right part of the figure indicates the ellipticity of the Cherenkov light distribution on ground.

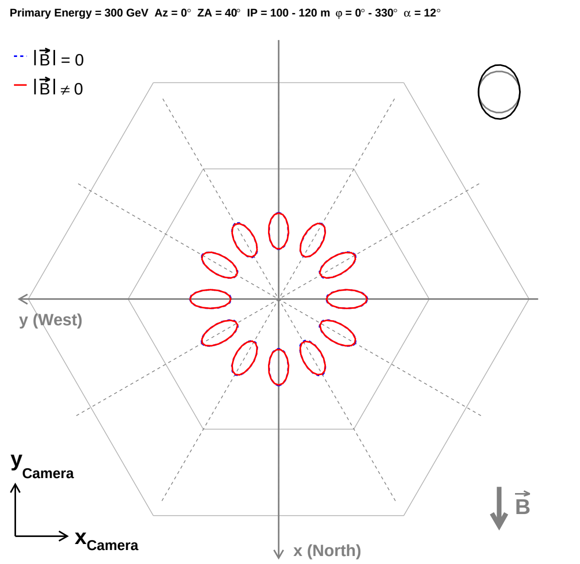

(a) Intermediate image cleaning, ZA 40°, azimuth angle 0°, impact parameter 100 - 120 m.

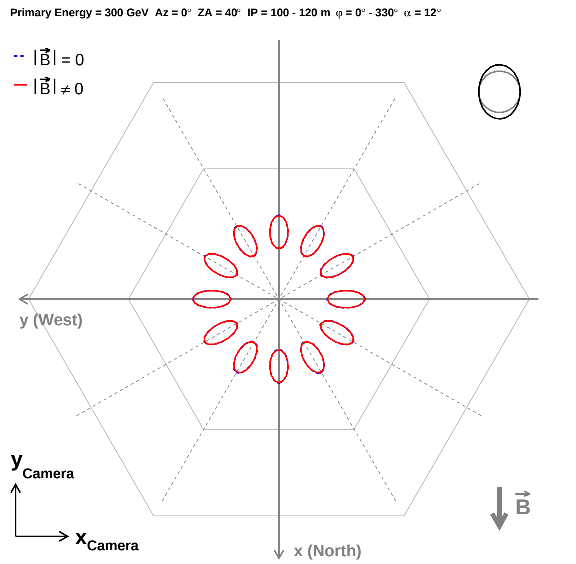

(b) Hard image cleaning, ZA 40°, azimuth angle 0°, impact parameter 100 - 120 m.

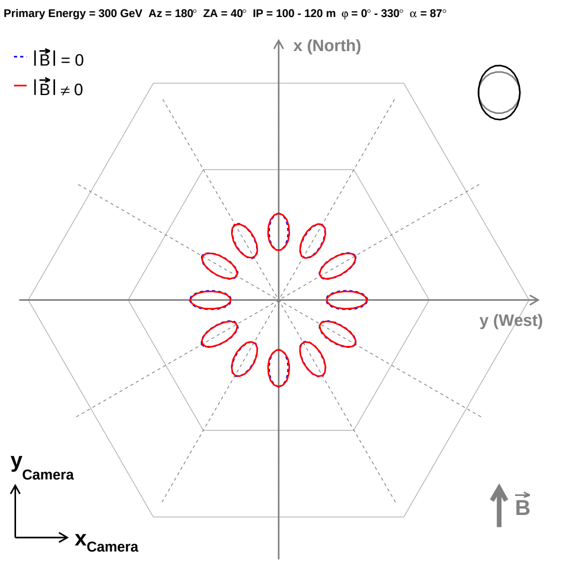

(c) Intermediate image cleaning, ZA 40°, azimuth angle 180°, impact parameter 100 - 120 m.

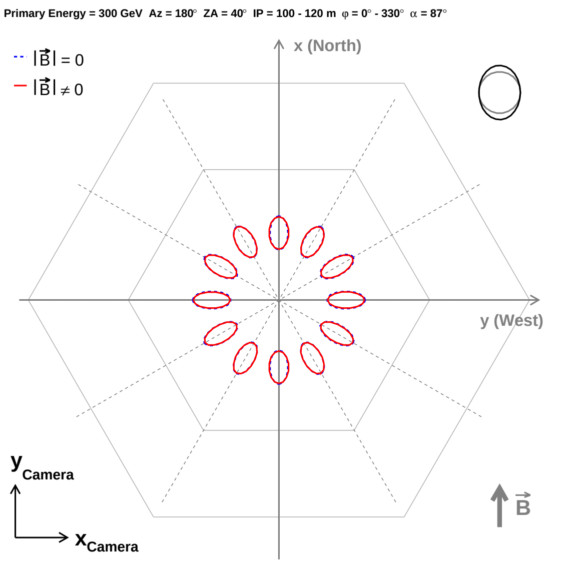

(d) Hard image cleaning, ZA 40°, azimuth angle 180°, impact parameter 100 - 120 m.

Figure 37: Hillas ellipses for MC γ-rays of 300 GeV energy, two different image cleaning levels and impact parameters between 100 m and 120 m. The ZA was set to 40° and the azimuth angle to 0° and 180°, respectively. The angle φ was varied over the full range between 0° and 330°. To demonstrate the influence of the GF on the image parameters WIDTH and LENGTH, the distortion of the orientation (δ) and the parameter DIST was ignored. While the red ellipses (solid lines) were obtained for enabled GF, the blue ones (dashed lines) were obtained for disabled GF. The black curve in the upper right part of the figure indicates the ellipticity of the Cherenkov light distribution on ground.

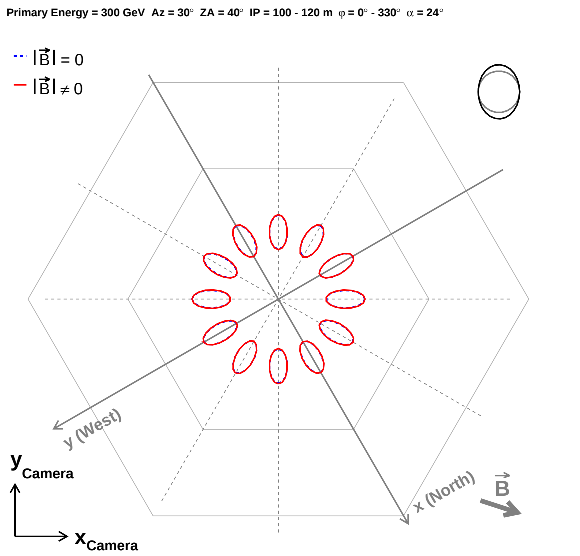

(a) Hard image cleaning, ZA 40°, azimuth angle 30°, impact parameter 100 - 120 m.

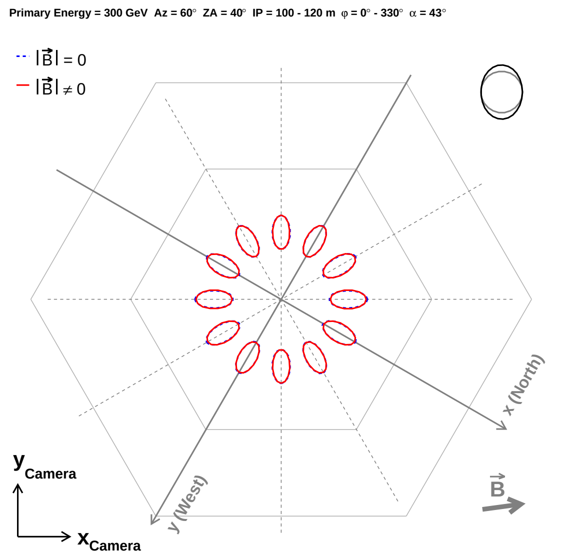

(b) Hard image cleaning, ZA 40°, azimuth angle 60°, impact parameter 100 - 120 m.

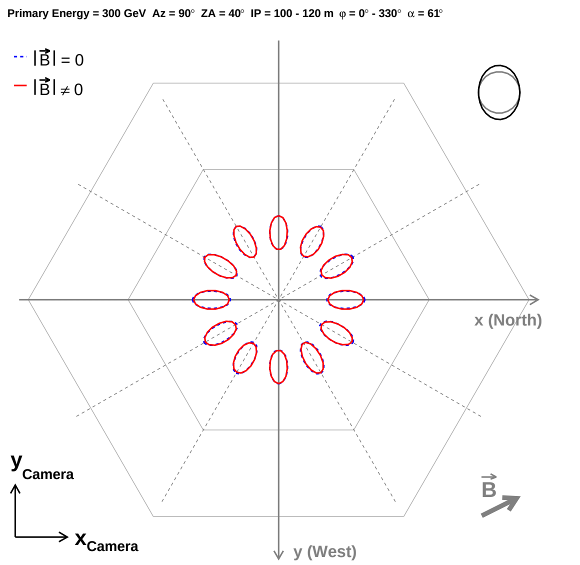

(c) Hard image cleaning, ZA 40°, azimuth angle 90°, impact parameter 100 - 120 m.

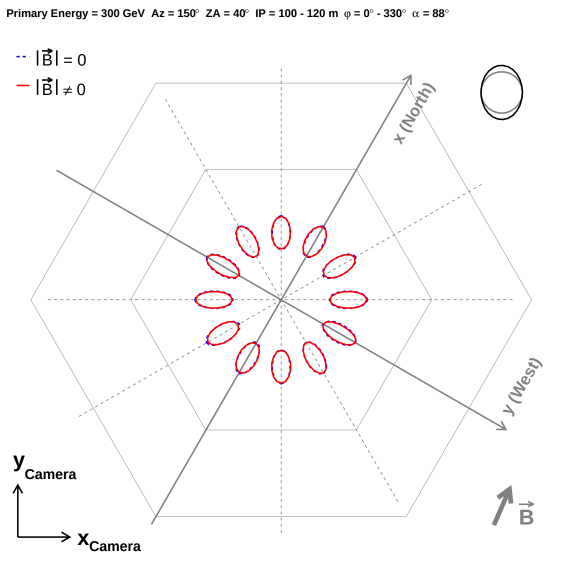

(d) Hard image cleaning, ZA 40°, azimuth angle 150°, impact parameter 100 - 120 m.

Figure 38: Hillas ellipses for MC γ-rays of 300 GeV energy and impact parameters between 100 m and 120 m. The hard image cleaning level was applied. The ZA was set to 40°, respectively, and the azimuth angle to 30°, 60°, 90° and 150°, respectively. The angle φ was varied over the full range between 0° and 330°. To demonstrate the influence of the GF on the image parameters WIDTH and LENGTH, the distortion of the orientation (δ) and the parameter DIST was ignored. While the red ellipses (solid lines) were obtained for enabled GF, the blue ones (dashed lines) were obtained for disabled GF. The black curve in the upper right part of the figure indicates the ellipticity of the Cherenkov light distribution on ground.

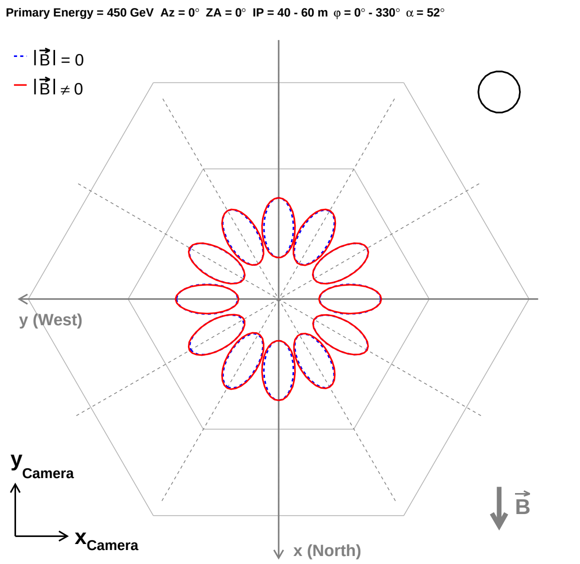

(a) Intermediate image cleaning, impact parameter 40 - 60 m.

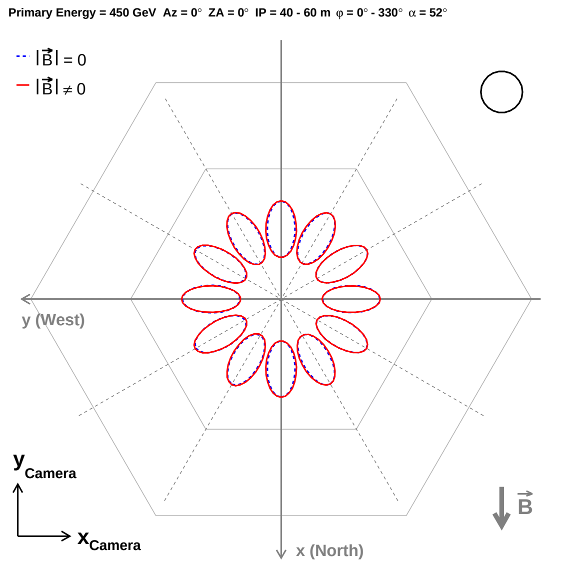

(b) Hard image cleaning, impact parameter 40 - 60 m.

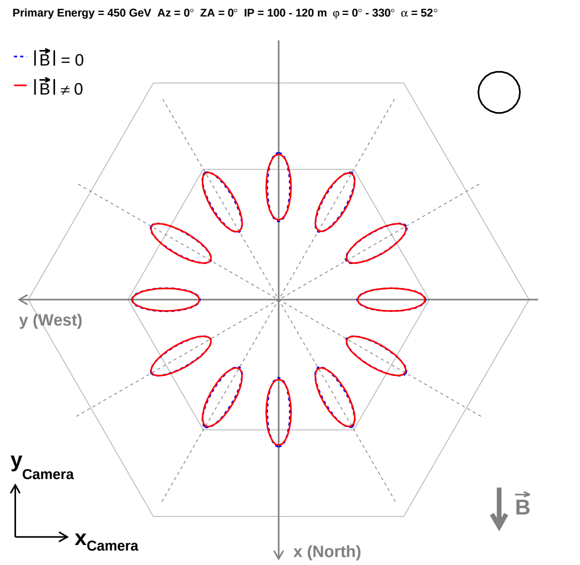

(c) Intermediate image cleaning, impact parameter 100 - 120 m.

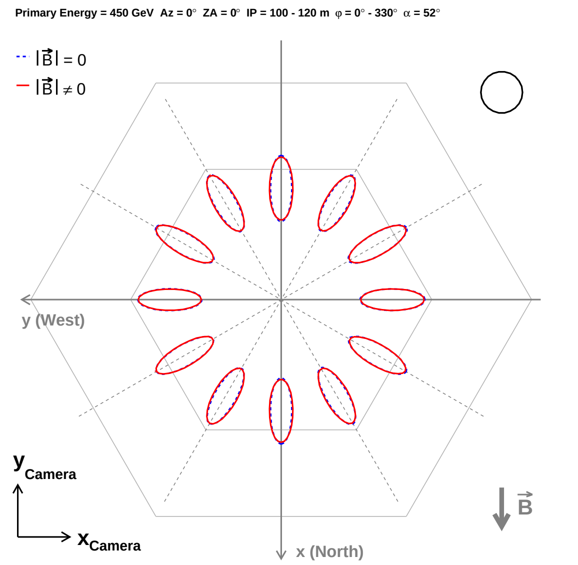

(d) Hard image cleaning, impact parameter 100 - 120 m.

Figure 39: Hillas ellipses for MC γ-rays of 450 GeV energy, two different image cleaning levels and two impact parameter windows. The ZA was set to 0° and the azimuth angle to 0°. The angle φ was varied over the full range between 0° and 330°. To demonstrate the influence of the GF on the image parameters WIDTH and LENGTH, the distortion of the orientation (δ) and the parameter DIST was ignored. While the red ellipses (solid lines) were obtained for enabled GF, the blue ones (dashed lines) were obtained for disabled GF. The black curve in the upper right part of the figure indicates the ellipticity (zero for 0° ZA) of the Cherenkov light distribution on ground.

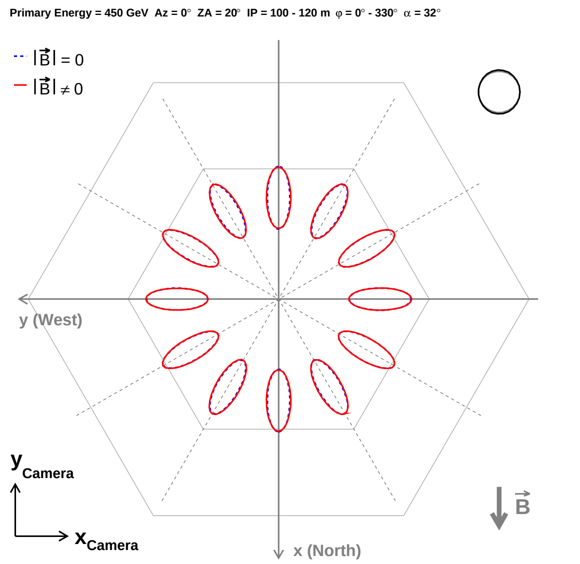

(a) Intermediate image cleaning, ZA 20°, azimuth angle 0°, impact parameter 100 - 120 m.

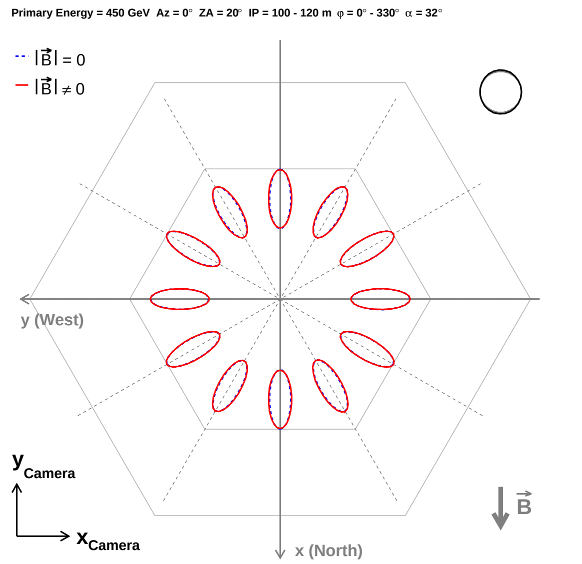

(b) Hard image cleaning, ZA 20°, azimuth angle 0°, impact parameter 100 - 120 m.

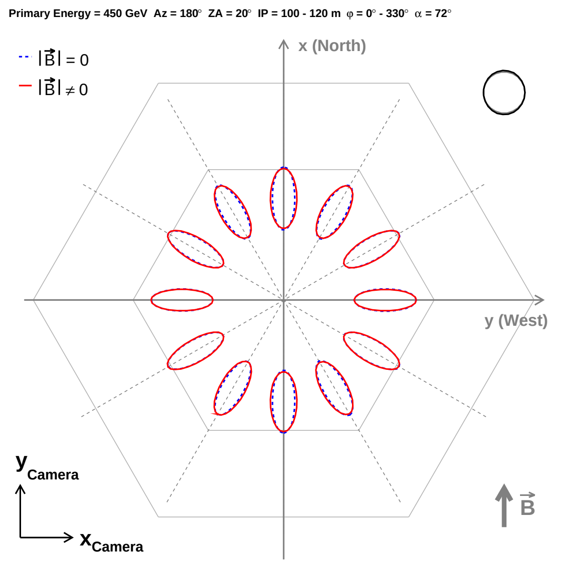

(c) Intermediate image cleaning, ZA 20°, azimuth angle 180°, impact parameter 100 - 120 m.

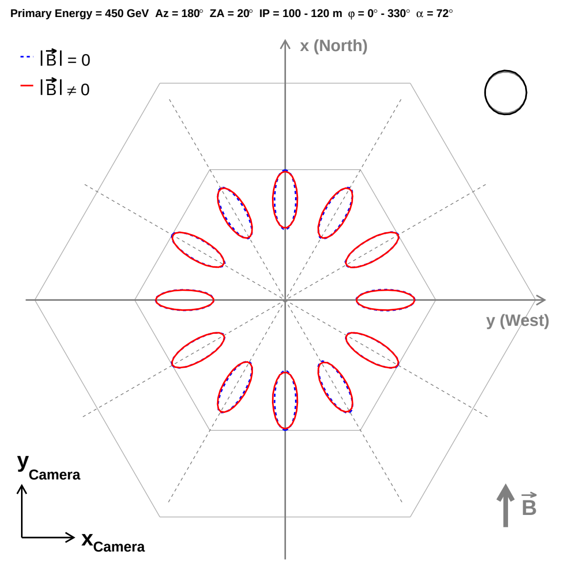

(d) Hard image cleaning, ZA 20°, azimuth angle 180°, impact parameter 100 - 120 m.

Figure 40: Hillas ellipses for MC γ-rays of 450 GeV energy, two different image cleaning levels and impact parameters between 100 m and 120 m. The ZA was set to 20° and the azimuth angle to 0° and 180°, respectively. The angle φ was varied over the full range between 0° and 330°. To demonstrate the influence of the GF on the image parameters WIDTH and LENGTH, the distortion of the orientation (δ) and the parameter DIST was ignored. While the red ellipses (solid lines) were obtained for enabled GF, the blue ones (dashed lines) were obtained for disabled GF. The black curve in the upper right part of the figure indicates the ellipticity of the Cherenkov light distribution on ground.

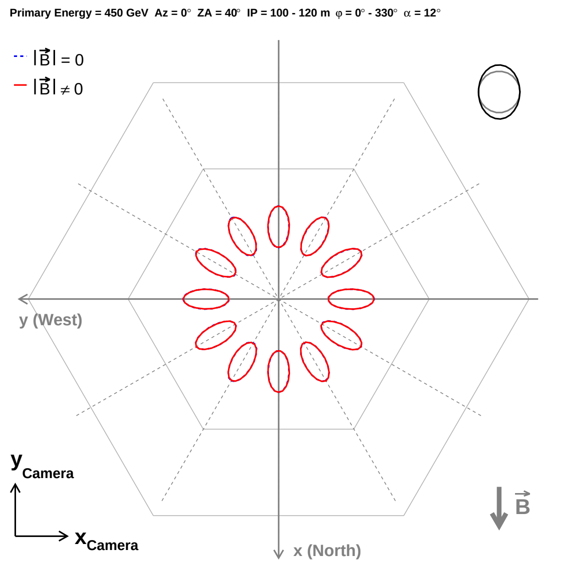

(a) Intermediate image cleaning, ZA 40°, azimuth angle 0°, impact parameter 100 - 120 m.

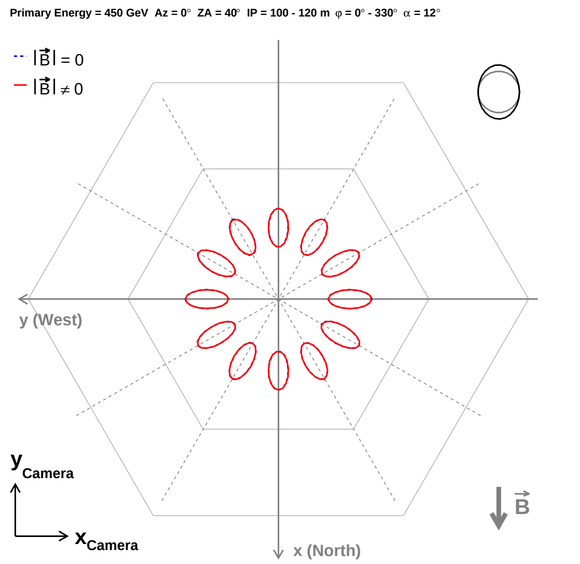

(b) Hard image cleaning, ZA 40°, azimuth angle 0°, impact parameter 100 - 120 m.

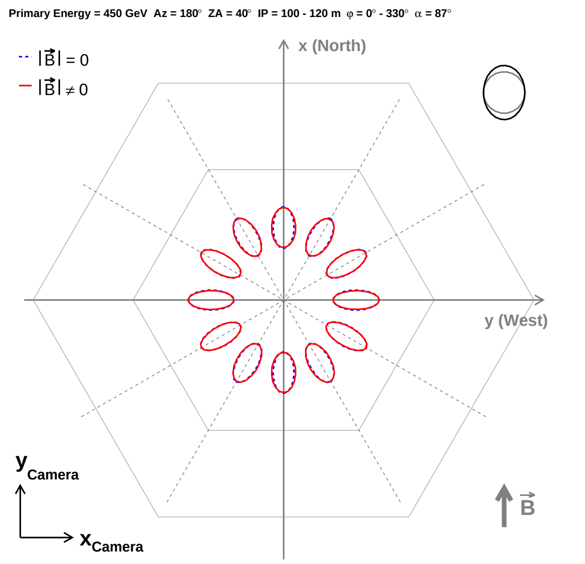

(c) Intermediate image cleaning, ZA 40°, azimuth angle 180°, impact parameter 100 - 120 m.

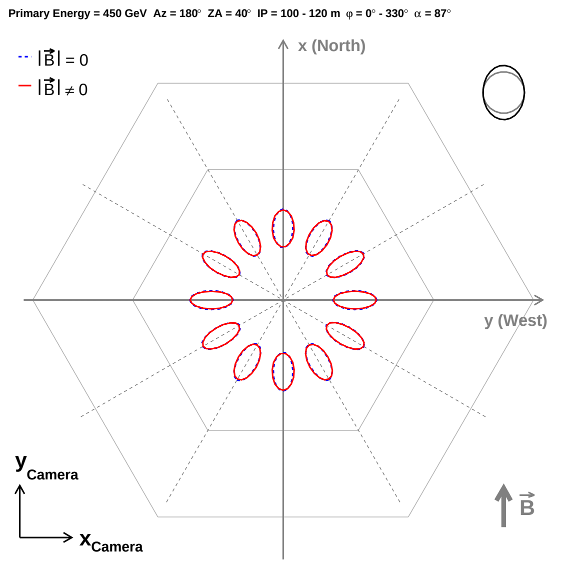

(d) Hard image cleaning, ZA 40°, azimuth angle 180°, impact parameter 100 - 120 m.

Figure 41: Hillas ellipses for MC γ-rays of 450 GeV energy, two different image cleaning levels and impact parameters between 100 m and 120 m. The ZA was set to 40° and the azimuth angle to 0° and 180°, respectively. The angle φ was varied over the full range between 0° and 330°. To demonstrate the influence of the GF on the image parameters WIDTH and LENGTH, the distortion of the orientation (δ) and the parameter DIST was ignored. While the red ellipses (solid lines) were obtained for enabled GF, the blue ones (dashed lines) were obtained for disabled GF. The black curve in the upper right part of the figure indicates the ellipticity of the Cherenkov light distribution on ground.

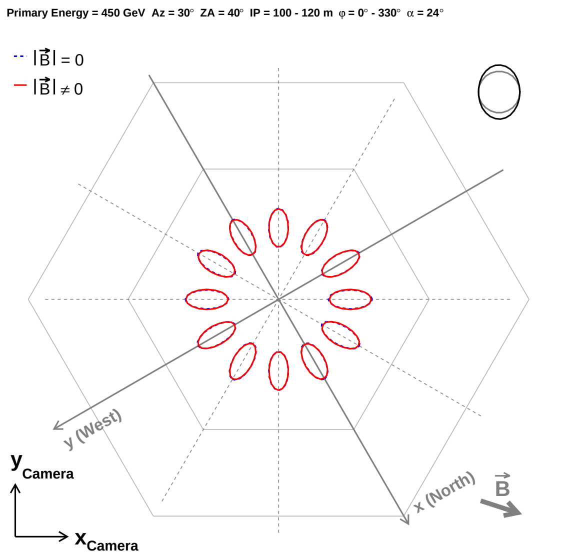

(a) Hard image cleaning, ZA 40°, azimuth angle 30°, impact parameter 100 - 120 m.

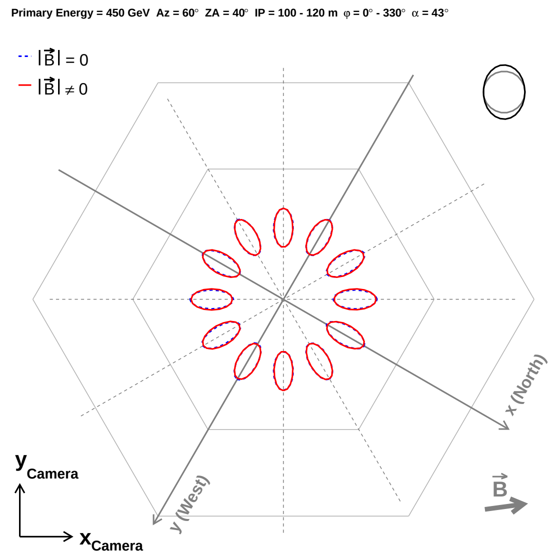

(b) Hard image cleaning, ZA 40°, azimuth angle 60°, impact parameter 100 - 120 m.

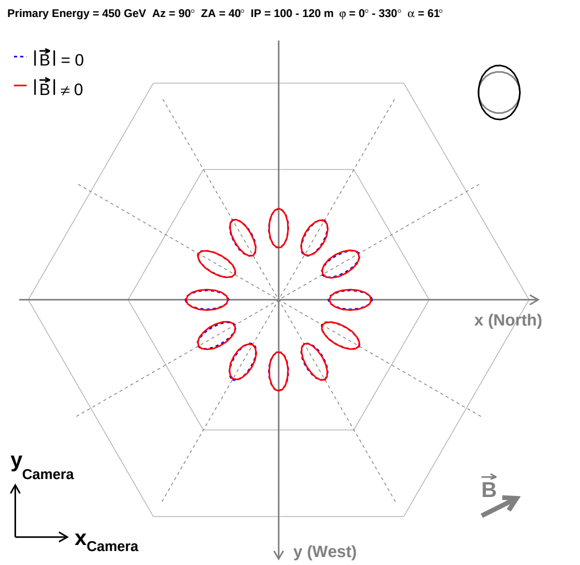

(c) Hard image cleaning, ZA 40°, azimuth angle 90°, impact parameter 100 - 120 m.

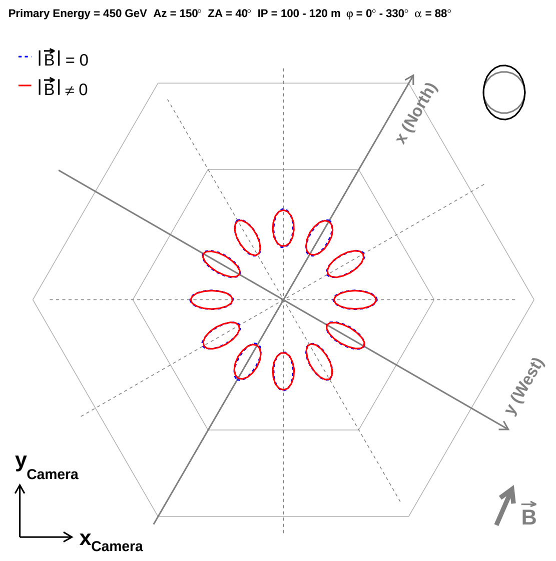

(d) Hard image cleaning, ZA 40°, azimuth angle 150°, impact parameter 100 - 120 m.

Figure 42: Hillas ellipses for MC γ-rays of 450 GeV energy and impact parameters between 100 m and 120 m. The hard image cleaning level was applied. The ZA was set to 40°, respectively, and the azimuth angle to 30°, 60°, 90° and 150°, respectively. The angle φ was varied over the full range between 0° and 330°. To demonstrate the influence of the GF on the image parameters WIDTH and LENGTH, the distortion of the orientation (δ) and the parameter DIST was ignored. While the red ellipses (solid lines) were obtained for enabled GF, the blue ones (dashed lines) were obtained for disabled GF. The black curve in the upper right part of the figure indicates the ellipticity of the Cherenkov light distribution on ground.

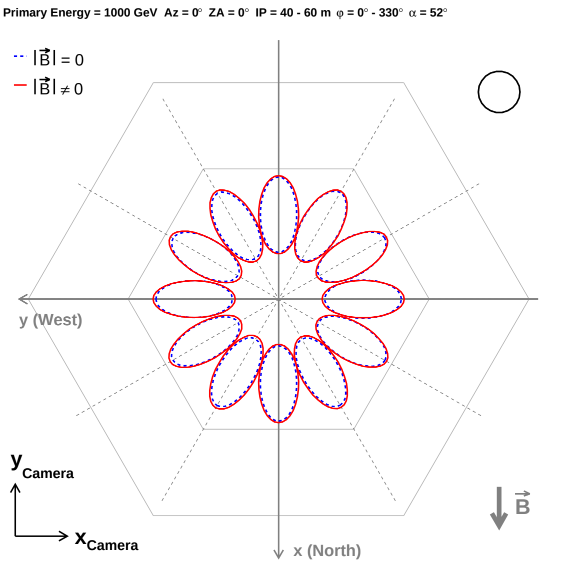

(a) Intermediate image cleaning, impact parameter 40 - 60 m.

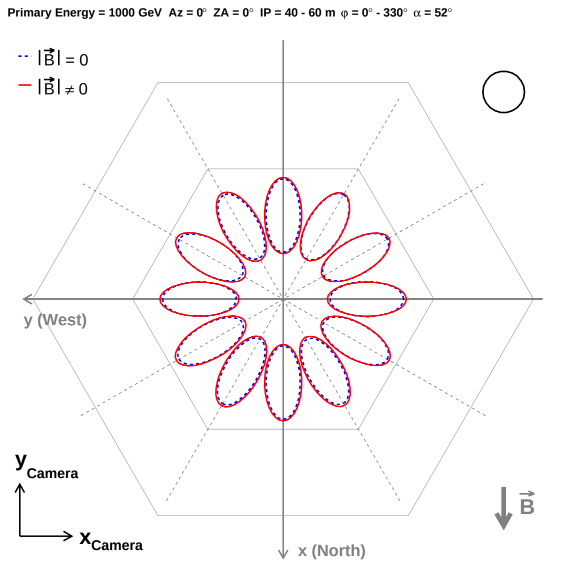

(b) Hard image cleaning, impact parameter 40 - 60 m.

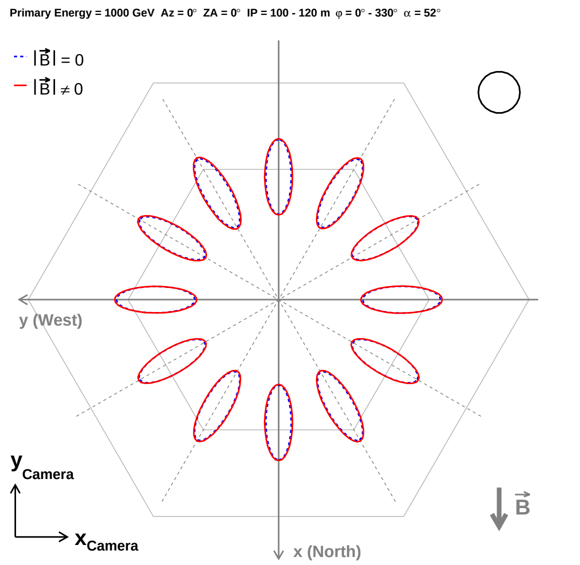

(c) Intermediate image cleaning, impact parameter 100 - 120 m.

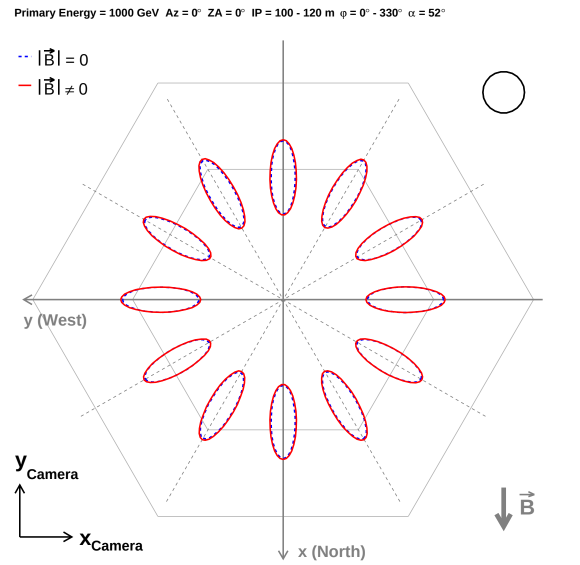

(d) Hard image cleaning, impact parameter 100 - 120 m.

Figure 43: Hillas ellipses for MC γ-rays of 1 TeV energy, two different image cleaning levels and two impact parameter windows. The ZA was set to 0° and the azimuth angle to 0°. The angle φ was varied over the full range between 0° and 330°. To demonstrate the influence of the GF on the image parameters WIDTH and LENGTH, the distortion of the orientation (δ) and the parameter DIST was ignored. While the red ellipses (solid lines) were obtained for enabled GF, the blue ones (dashed lines) were obtained for disabled GF. The black curve in the upper right part of the figure indicates the ellipticity (zero for 0° ZA) of the Cherenkov light distribution on ground.

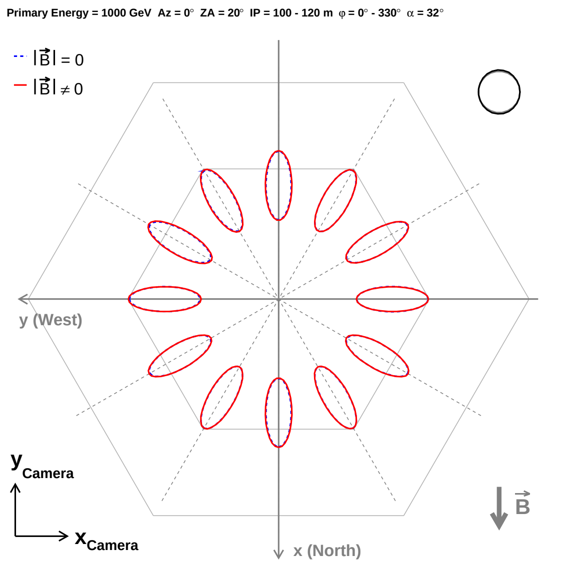

(a) Intermediate image cleaning, ZA 20°, azimuth angle 0°, impact parameter 100 - 120 m.

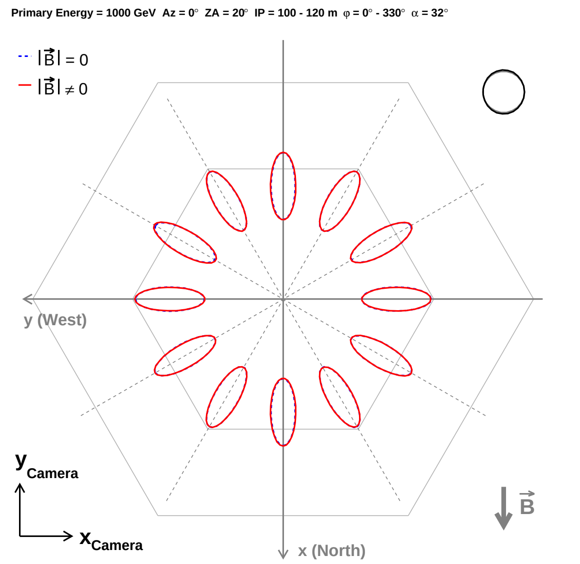

(b) Hard image cleaning, ZA 20°, azimuth angle 0°, impact parameter 100 - 120 m.

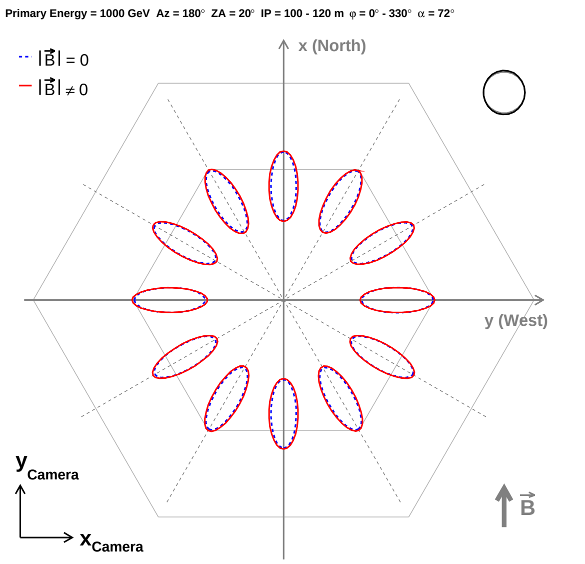

(c) Intermediate image cleaning, ZA 20°, azimuth angle 180°, impact parameter 100 - 120 m.

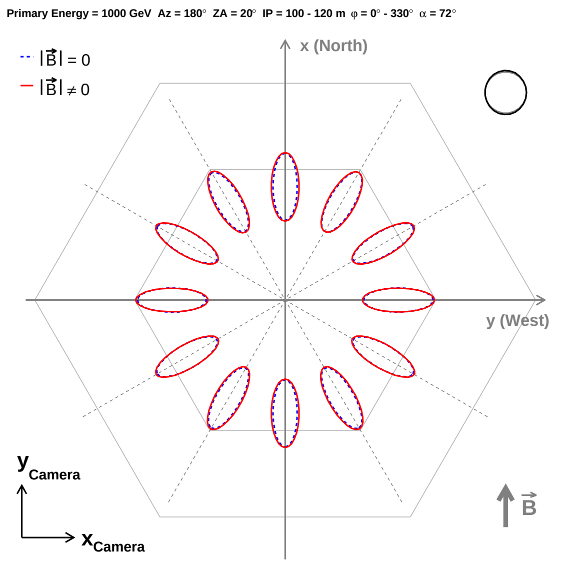

(d) Hard image cleaning, ZA 20°, azimuth angle 180°, impact parameter 100 - 120 m.

Figure 44: Hillas ellipses for MC γ-rays of 1 TeV energy, two different image cleaning levels and impact parameters between 100 m and 120 m. The ZA was set to 20° and the azimuth angle to 0° and 180°, respectively. The angle φ was varied over the full range between 0° and 330°. To demonstrate the influence of the GF on the image parameters WIDTH and LENGTH, the distortion of the orientation (δ) and the parameter DIST was ignored. While the red ellipses (solid lines) were obtained for enabled GF, the blue ones (dashed lines) were obtained for disabled GF. The black curve in the upper right part of the figure indicates the ellipticity of the Cherenkov light distribution on ground.

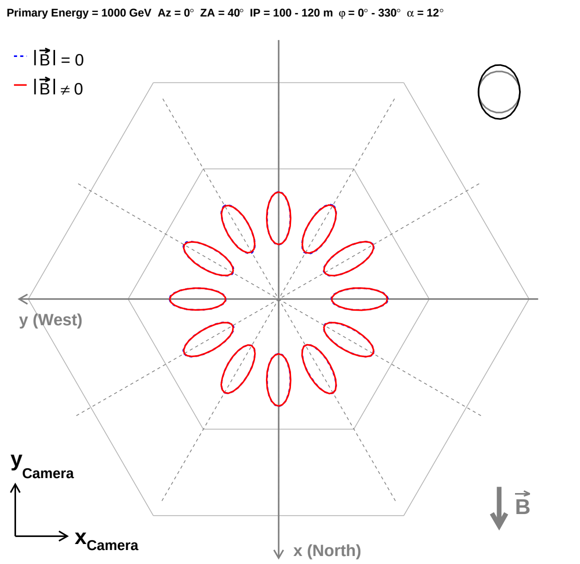

(a) Intermediate image cleaning, ZA 40°, azimuth angle 0°, impact parameter 100 - 120 m.

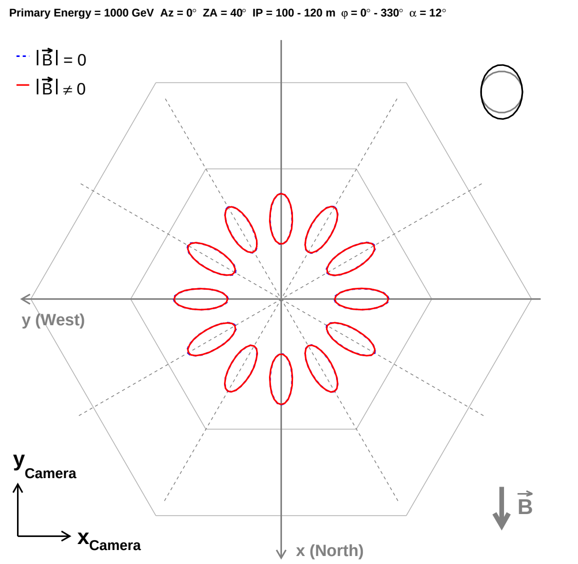

(b) Hard image cleaning, ZA 40°, azimuth angle 0°, impact parameter 100 - 120 m.

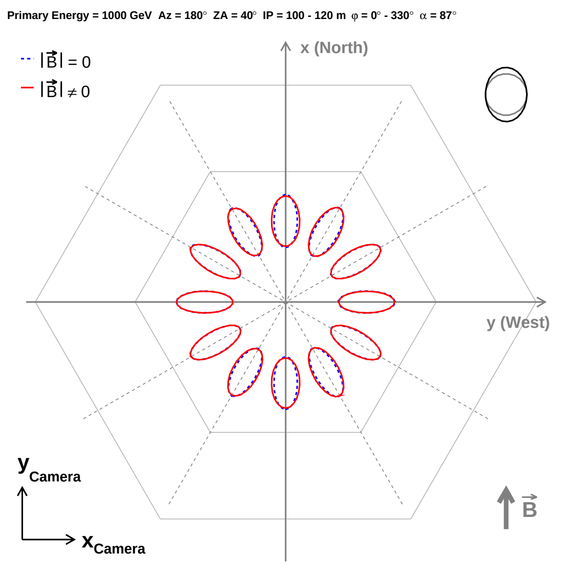

(c) Intermediate image cleaning, ZA 40°, azimuth angle 180°, impact parameter 100 - 120 m.

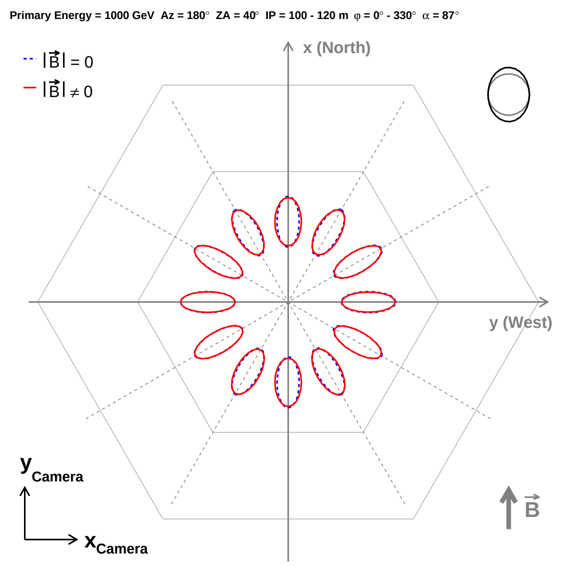

(d) Hard image cleaning, ZA 40°, azimuth angle 180°, impact parameter 100 - 120 m.

Figure 45: Hillas ellipses for MC γ-rays of 1 TeV energy, two different image cleaning levels and impact parameters between 100 m and 120 m. The ZA was set to 40° and the azimuth angle to 0° and 180°, respectively. The angle φ was varied over the full range between 0° and 330°. To demonstrate the influence of the GF on the image parameters WIDTH and LENGTH, the distortion of the orientation (δ) and the parameter DIST was ignored. While the red ellipses (solid lines) were obtained for enabled GF, the blue ones (dashed lines) were obtained for disabled GF. The black curve in the upper right part of the figure indicates the ellipticity of the Cherenkov light distribution on ground.

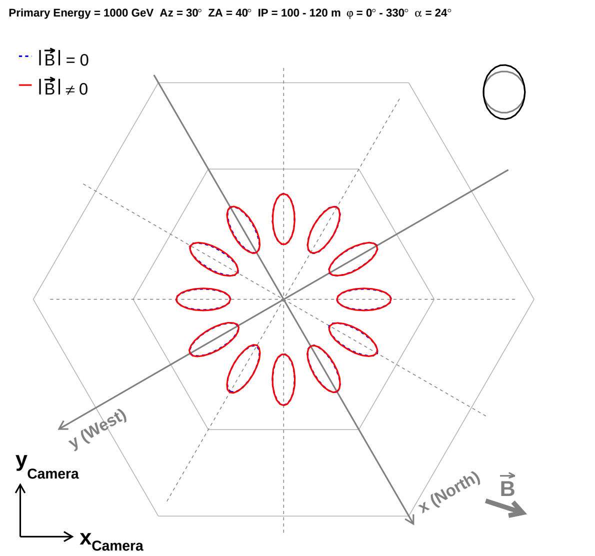

(a) Hard image cleaning, ZA 40°, azimuth angle 30°, impact parameter 100 - 120 m.

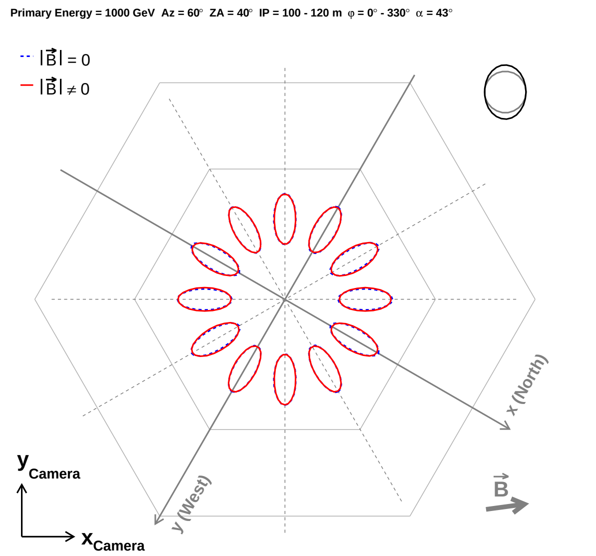

(b) Hard image cleaning, ZA 40°, azimuth angle 60°, impact parameter 100 - 120 m.

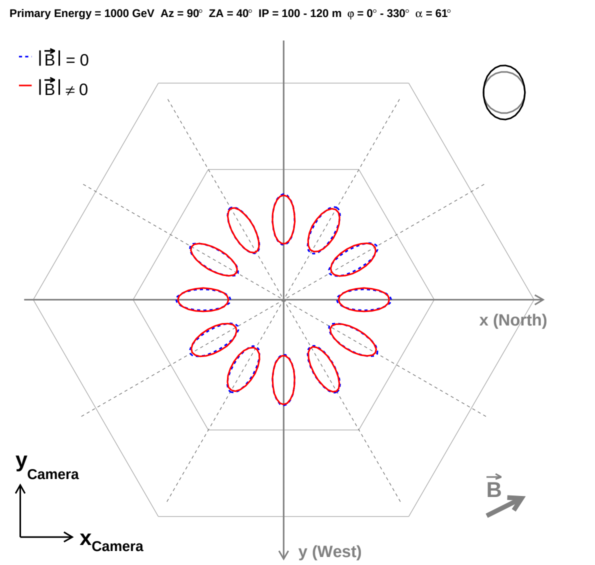

(c) Hard image cleaning, ZA 40°, azimuth angle 90°, impact parameter 100 - 120 m.

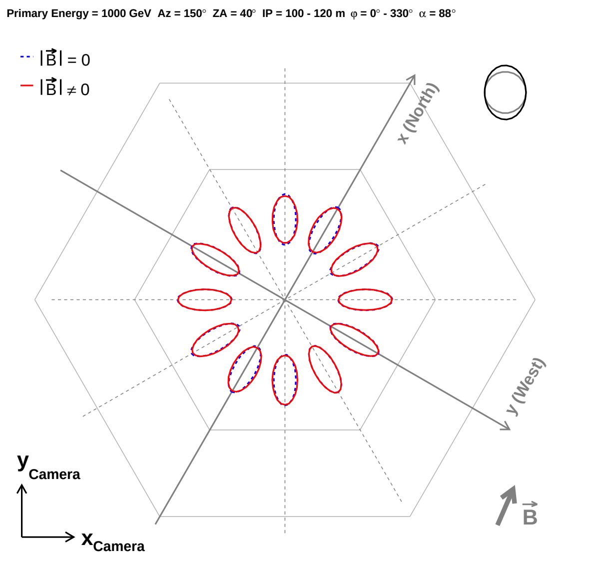

(d) Hard image cleaning, ZA 40°, azimuth angle 150°, impact parameter 100 - 120 m.

Figure 46: Hillas ellipses for MC γ-rays of 1 TeV energy and impact parameters between 100 m and 120 m. The hard image cleaning level was applied. The ZA was set to 40°, respectively, and the azimuth angle to 30°, 60°, 90° and 150°, respectively. The angle φ was varied over the full range between 0° and 330°. To demonstrate the influence of the GF on the image parameters WIDTH and LENGTH, the distortion of the orientation (δ) and the parameter DIST was ignored. While the red ellipses (solid lines) were obtained for enabled GF, the blue ones (dashed lines) were obtained for disabled GF. The black curve in the upper right part of the figure indicates the ellipticity of the Cherenkov light distribution on ground.

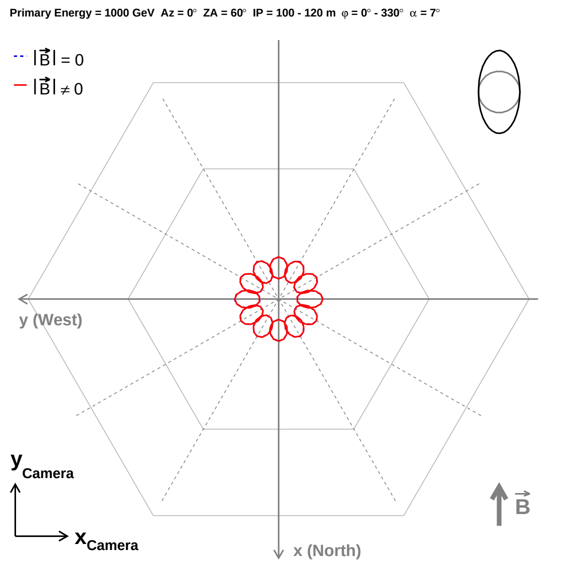

(a) Intermediate image cleaning, ZA 60°, azimuth angle 0°, impact parameter 100 - 120 m.

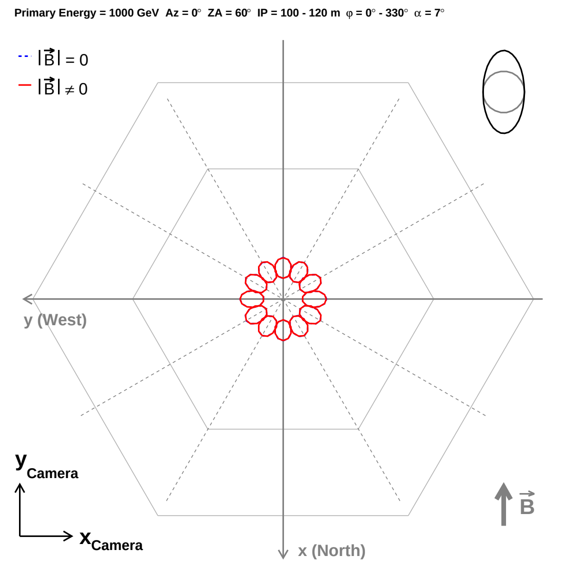

(b) Hard image cleaning, ZA 60°, azimuth angle 0°, impact parameter 100 - 120 m.

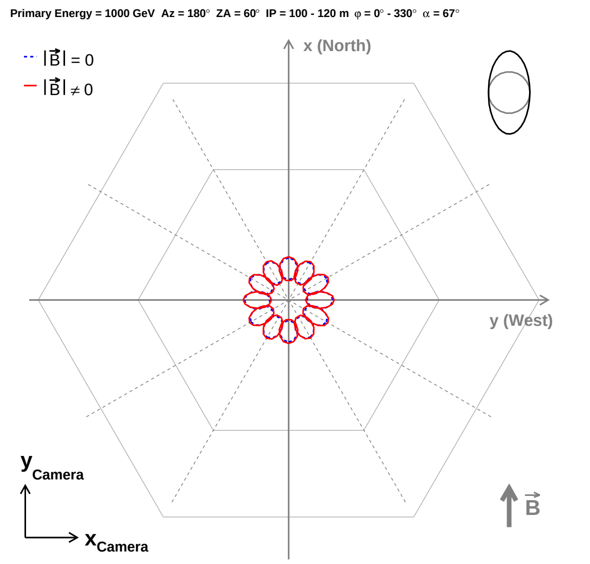

(c) Intermediate image cleaning, ZA 60°, azimuth angle 180°, impact parameter 100 - 120 m.

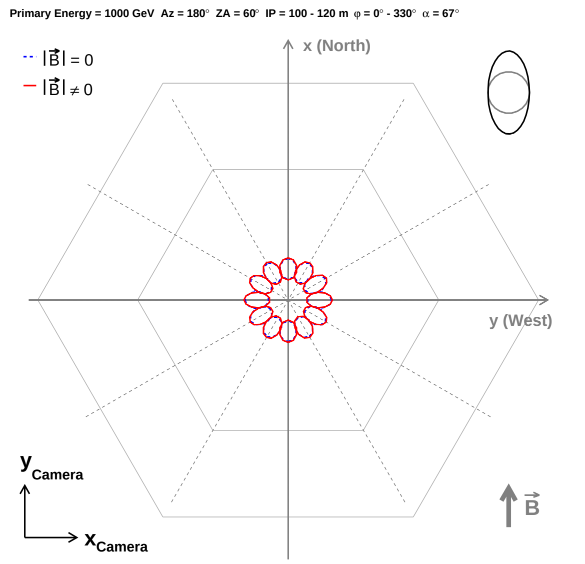

(d) Hard image cleaning, ZA 60°, azimuth angle 180°, impact parameter 100 - 120 m.

Figure 47: Hillas ellipses for MC γ-rays of 1 TeV energy, two different image cleaning levels and impact parameters between 100 m and 120 m. The ZA was set to 60° and the azimuth angle to 0° and 180°, respectively. The angle φ was varied over the full range between 0° and 330°. To demonstrate the influence of the GF on the image parameters WIDTH and LENGTH, the distortion of the orientation (δ) and the parameter DIST was ignored. While the red ellipses (solid lines) were obtained for enabled GF, the blue ones (dashed lines) were obtained for disabled GF. The black curve in the upper right part of the figure indicates the ellipticity of the Cherenkov light distribution on ground.

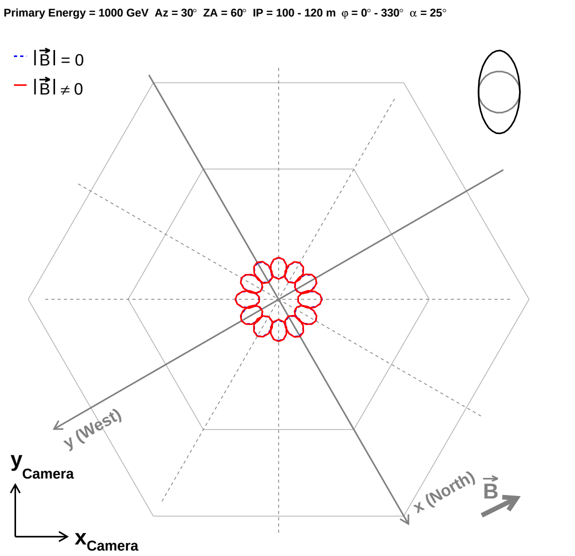

(a) Hard image cleaning, ZA 60°, azimuth angle 30°, impact parameter 100 - 120 m.

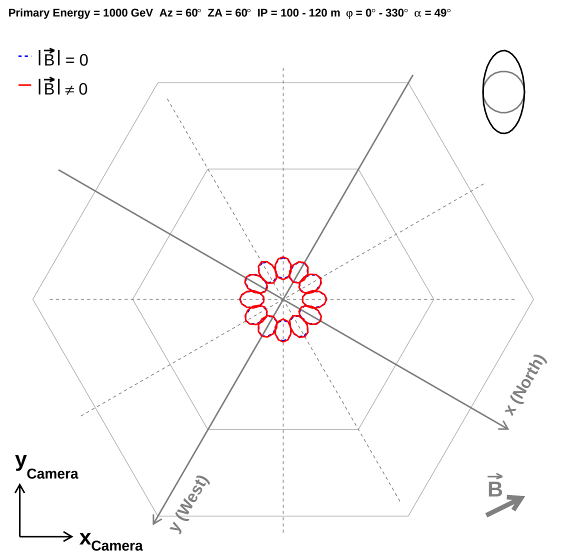

(b) Hard image cleaning, ZA 60°, azimuth angle 60°, impact parameter 100 - 120 m.

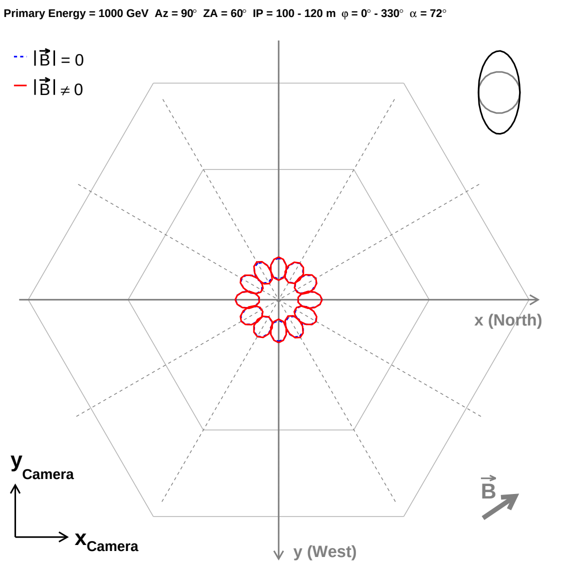

(c) Hard image cleaning, ZA 60°, azimuth angle 90°, impact parameter 100 - 120 m.

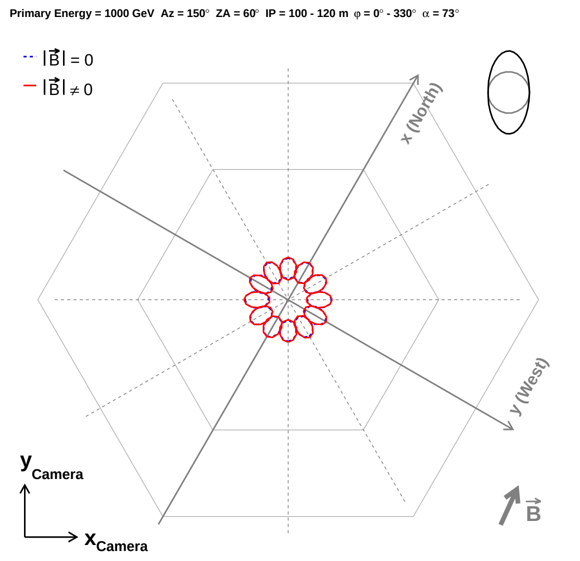

(d) Hard image cleaning, ZA 60°, azimuth angle 150°, impact parameter 100 - 120 m.

Figure 48: Hillas ellipses for MC γ-rays of 1 TeV energy and impact parameters between 100 m and 120 m. The hard image cleaning level was applied. The ZA was set to 60°, respectively, and the azimuth angle to 30°, 60°, 90° and 150°, respectively. The angle φ was varied over the full range between 0° and 330°. To demonstrate the influence of the GF on the image parameters WIDTH and LENGTH, the distortion of the orientation (δ) and the parameter DIST was ignored. While the red ellipses (solid lines) were obtained for enabled GF, the blue ones (dashed lines) were obtained for disabled GF. The black curve in the upper right part of the figure indicates the ellipticity of the Cherenkov light distribution on ground.

The Influence of the GF on the Orientation of γ-Ray Shower Images

The investigation of the influence of the GF on the orientation of shower images is important because it allows to draw a conclusion to what extent the GF affects the analysis of Cherenkov images. This is particularly important for the γ/hadron separation, which is partially based on the image orientation. Figures 49 - 80 show the Hillas ellipses for MC generated γ-rays with energies between 30 GeV and 1 TeV and different MC input parameters. All angles φ between $0°$ and $330°$ were considered. For each position (r, φ) of the telescope, the corresponding ellipse is positioned according to the average value of the DIST parameter and the average angle δ. The angle δ is counted anti-clockwise from the positive x-axis of the camera coordinate system indicated in the lower left part of the figures (see figure 18 for the definition of the angle δ). The coordinate system of the MC program CORSIKA, (figure 17) is always centered on the camera displays. The projection of the GF is indicated in the lower right part of the figures. As pointed out in the preceding section only for $0°$ ZA the projection of the GF is parallel to the x-axis of the CORSIKA coordinate system. The black curve in the upper right part of the figure indicates the ellipticity of the Cherenkov light distribution on ground. The red ellipses (solid lines) were obtained for enabled GF and the blue ones (dashed lines) were obtained for disabled GF.
For some combinations of the MC input parameters the shower images shown in the figures 49 - 80 appear to be systematically rotated. The magnitude of the rotation is clearly correlated with the size of the angle α, which is measured between the direction of the primary γ-ray and the direction of the GF. The images in figures 72 show that the shower images are rotated away from the direction of the GF and the degree of the rotation increases with increasing azimuth angle, i.e. increasing angle α. However, the average orientation of the images is preserved for configurations where the connecting line between the shower axis and the telescope optical axis is parallel or perpendicular to the projection of the GF in camera, i.e. the corresponding shower images are not rotated. For $0°$ or $180°$ azimuth angle shower images are not rotated if they are situated at $\delta = 0°$, $90°$, $180°$ and $270°$. Instead, images lying at intermediate angles are systematically rotated towards or away from the projection of the GF. The degree of the rotation and the size of the rotation angle depend on various parameters like the γ-ray energy, the ZA, the azimuth angle, the impact parameter and the orientation of the shower with respect to the telescope. Figures 49 - 80 show that the rotation angle can be very large even for high γ-ray energies of around 450 GeV. The dependency of the rotation angle on the γ-ray energy and the impact parameter will be discussed in greater detail in the next section.
Due to the rotation of the shower images the major image axes do not point any more towards the camera center and the γ/hadron separation is expected to be significantly degraded. Rotated shower images will result in a broadened ALPHA distribution.
It is worth mentioning that for ZA $> 0°$ the major image axes obtained for disabled GF are not any more parallel to the gray dotted lines crossing the camera center. The gray dotted lines correspond to the nominal orientations of the shower images according to the telescope positions (r, φ). The rotation results from the impact parameter definition in the production of the MC data (section 2) but it does not affect the pointing of the images. As already mentioned, for ZA $> 0°$, the true impact parameter r' as well as the DIST parameter scale like cos(ZA) in direction of the telescopes' inclination, resulting in an elliptical arrangement of the images in the camera display (e.g. figure 65).

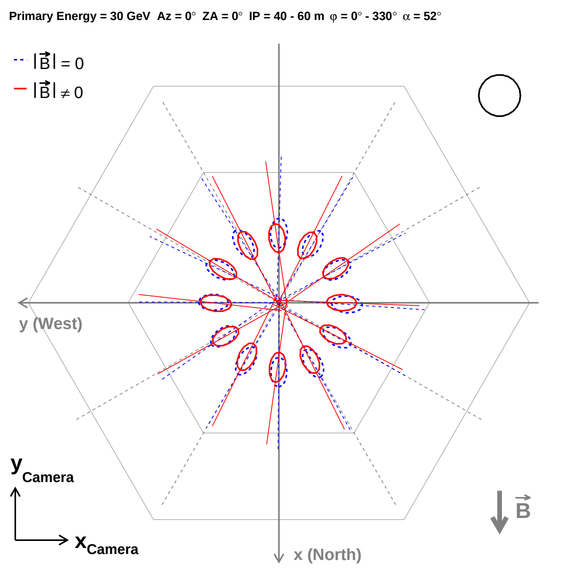

(a) Intermediate image cleaning, ZA 0°, azimuth angle 0°, impact parameter 40 - 60 m.

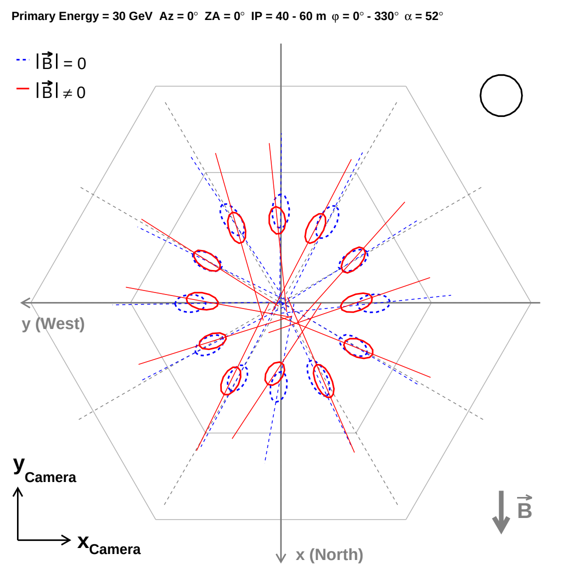

(b) Hard image cleaning, ZA 0°, azimuth angle 0°, impact parameter 40 - 60 m.

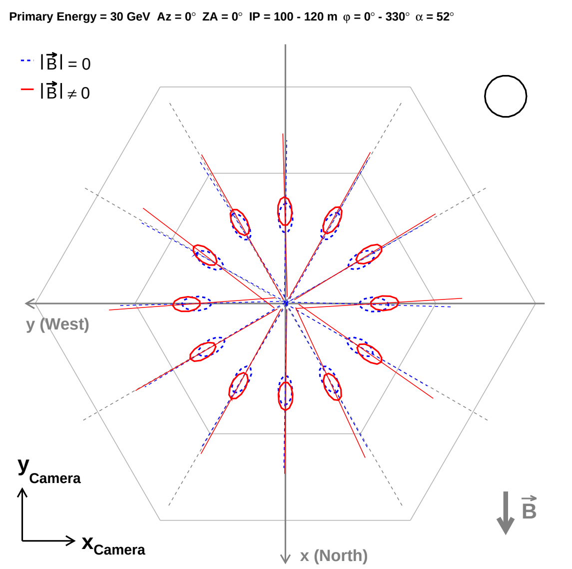

(c) Intermediate image cleaning, ZA 0°, azimuth angle 0°, impact parameter 100 - 120 m.

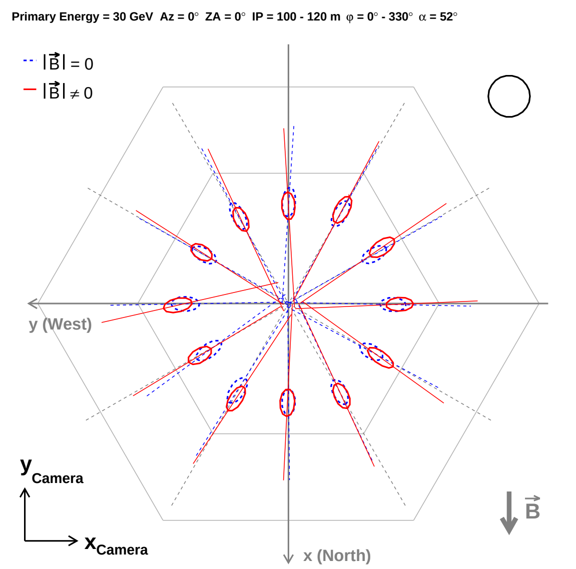

(d) Hard image cleaning, ZA 0°, azimuth angle 0°, impact parameter 100 - 120 m.

Figure 49: Hillas ellipses for MC γ-rays of 30 GeV energy, two different image cleaning levels and two impact parameter windows. The ZA was set to 0° and the azimuth angle to 0°. The angle φ was varied over the full range between 0° and 330°. While the red ellipses (solid lines) were obtained for enabled GF, the blue ones (dashed lines) were obtained for disabled GF. The black curve in the upper right part of the figure indicates the ellipticity of the Cherenkov light distribution on ground.

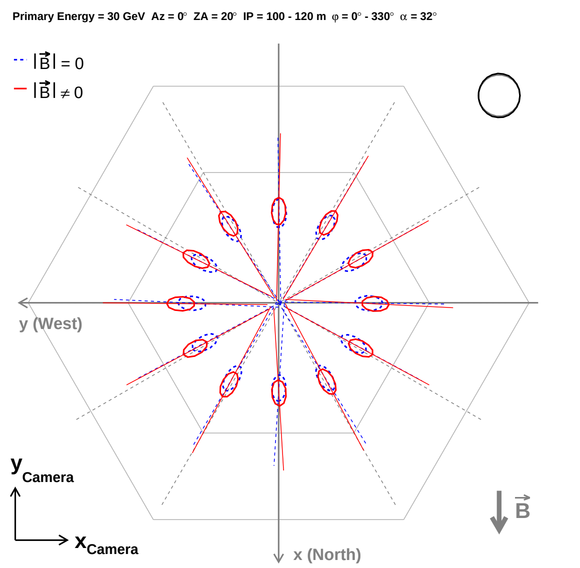

(a) Intermediate image cleaning, ZA 20°, azimuth angle 0°, impact parameter 100 - 120 m.

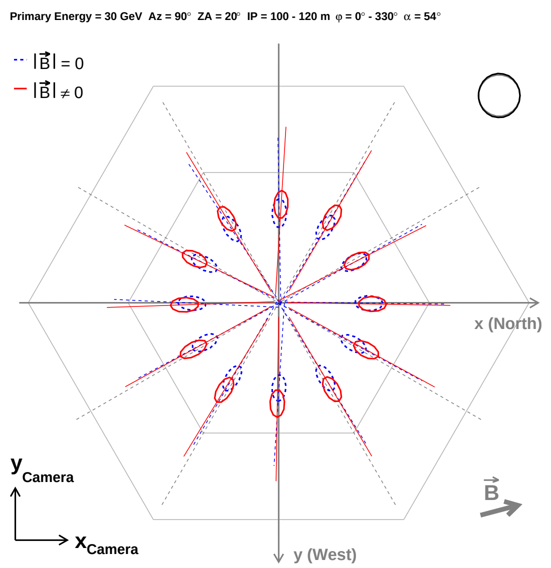

(b) Intermediate image cleaning, ZA 20°, azimuth angle 90°, impact parameter 100 - 120 m.

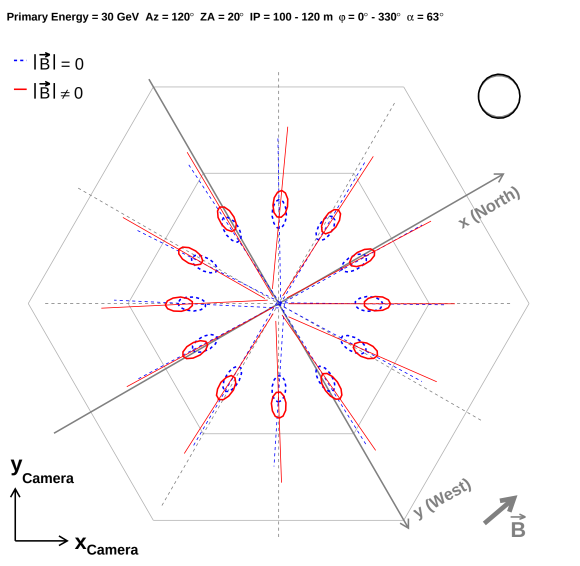

(c) Intermediate image cleaning, ZA 20°, azimuth angle 120°, impact parameter 100 - 120 m.

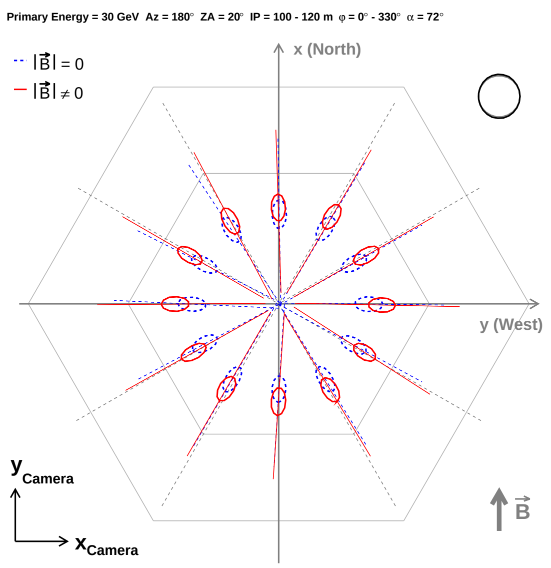

(d) Intermediate image cleaning, ZA 20°, azimuth angle 180°, impact parameter 100 - 120 m.

Figure 50: Hillas ellipses for MC γ-rays of 30 GeV energy and impact parameters between 100 m and 120 m. The ZA was set to 20° and the azimuth angle to 0° , 90°, 120° and 180°, respectively. The angle φ was varied over the full range between 0° and 330°. While the red ellipses (solid lines) were obtained for enabled GF, the blue ones (dashed lines) were obtained for disabled GF. The black curve in the upper right part of the figure indicates the ellipticity of the Cherenkov light distribution on ground.

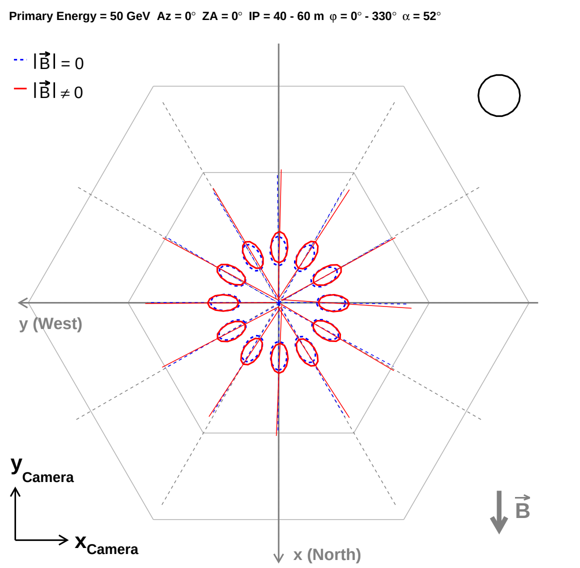

(a) Intermediate image cleaning, ZA 0°, azimuth angle 0°, impact parameter 40 - 60 m.

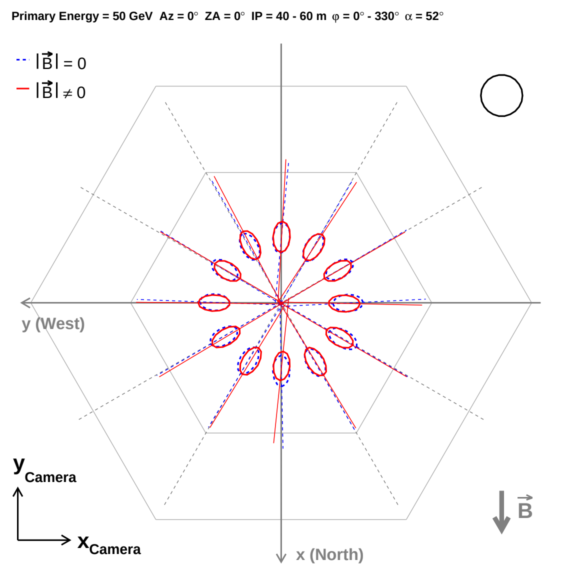

(b) Hard image cleaning, ZA 0°, azimuth angle 0°, impact parameter 40 - 60 m.

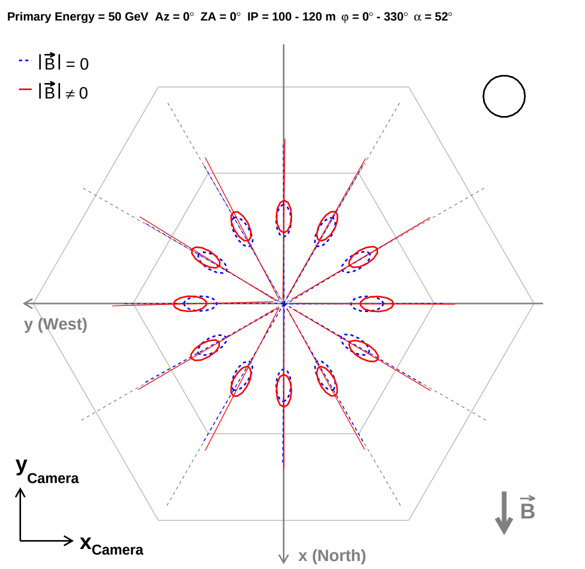

(c) Intermediate image cleaning, ZA 0°, azimuth angle 0°, impact parameter 100 - 120 m.

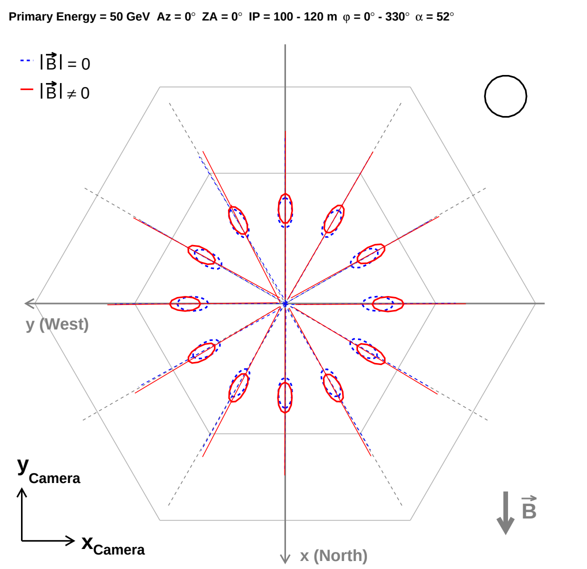

(d) Hard image cleaning, ZA 0°, azimuth angle 0°, impact parameter 100 - 120 m.

Figure 51: Hillas ellipses for MC γ-rays of 50 GeV energy, two different image cleaning levels and two impact parameter windows. The ZA was set to 0° and the azimuth angle to 0°. The angle φ was varied over the full range between 0° and 330°. While the red ellipses (solid lines) were obtained for enabled GF, the blue ones (dashed lines) were obtained for disabled GF. The black curve in the upper right part of the figure indicates the ellipticity of the Cherenkov light distribution on ground.

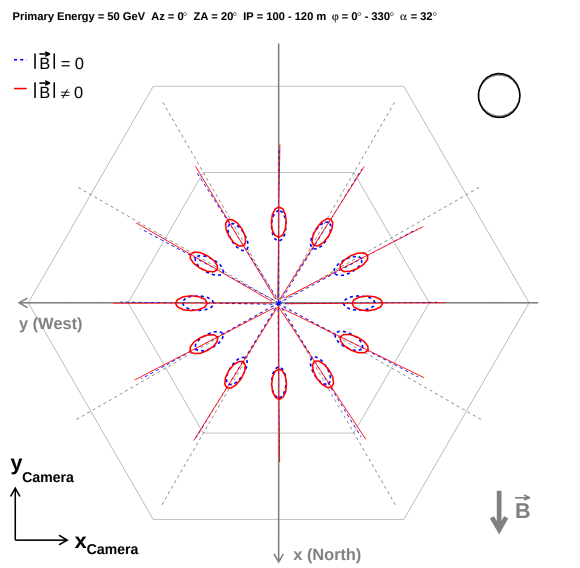

(a) Intermediate image cleaning, ZA 20°, azimuth angle 0°, impact parameter 100 - 120 m.

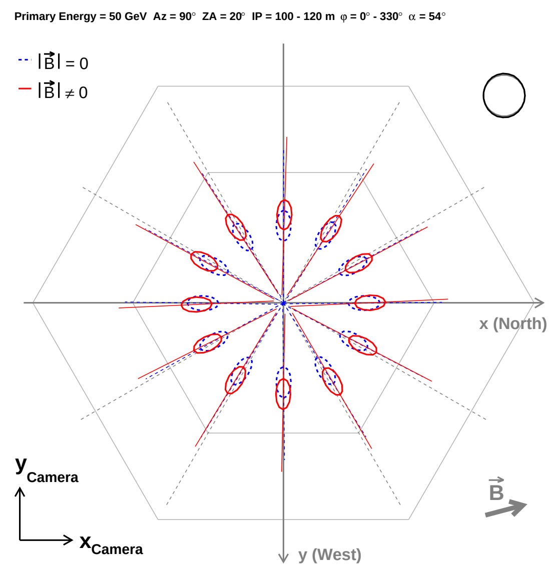

(b) Intermediate image cleaning, ZA 20°, azimuth angle 90°, impact parameter 100 - 120 m.

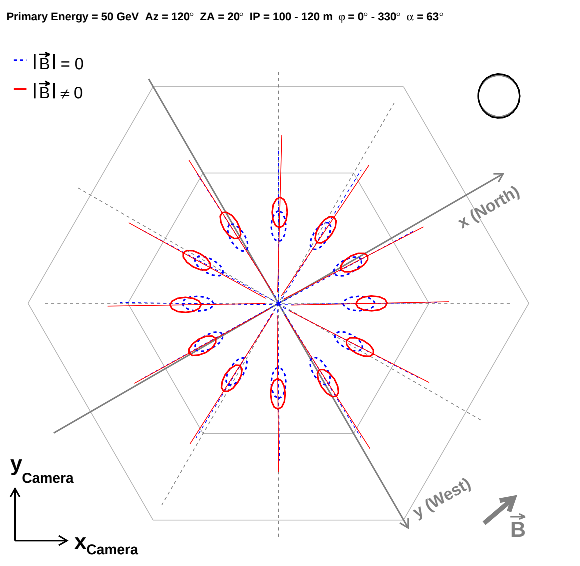

(c) Intermediate image cleaning, ZA 20°, azimuth angle 120°, impact parameter 100 - 120 m.

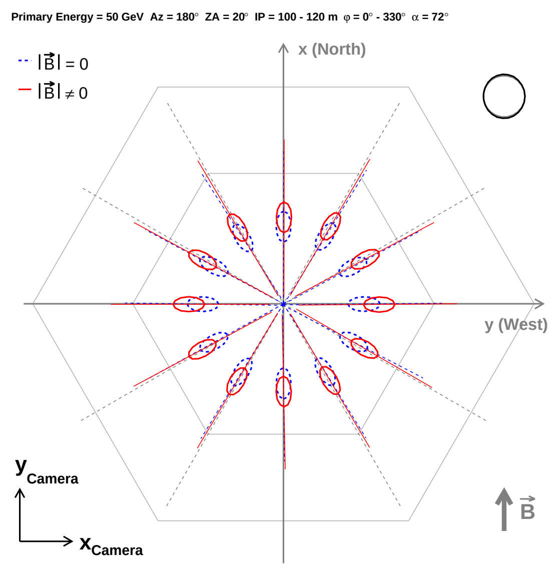

(d) Intermediate image cleaning, ZA 20°, azimuth angle 180°, impact parameter 100 - 120 m.

Figure 52: Hillas ellipses for MC γ-rays of 50 GeV energy and impact parameters between 100 m and 120 m. The ZA was set to 20° and the azimuth angle to 0° , 90°, 120° and 180°, respectively. The angle φ was varied over the full range between 0° and 330°. While the red ellipses (solid lines) were obtained for enabled GF, the blue ones (dashed lines) were obtained for disabled GF. The black curve in the upper right part of the figure indicates the ellipticity of the Cherenkov light distribution on ground.

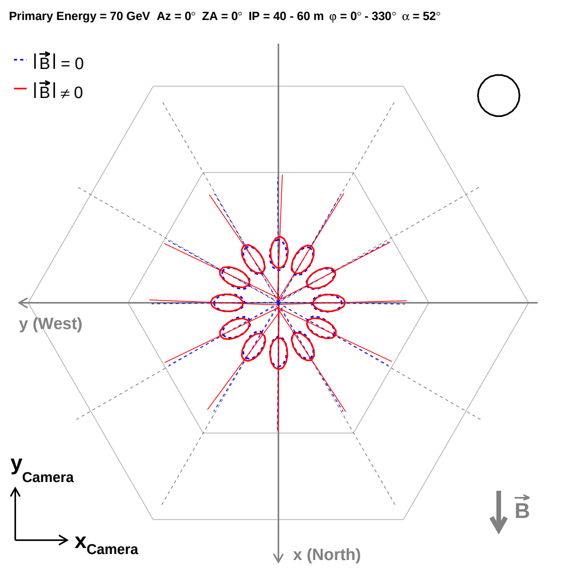

(a) Intermediate image cleaning, ZA 0°, azimuth angle 0°, impact parameter 40 - 60 m.

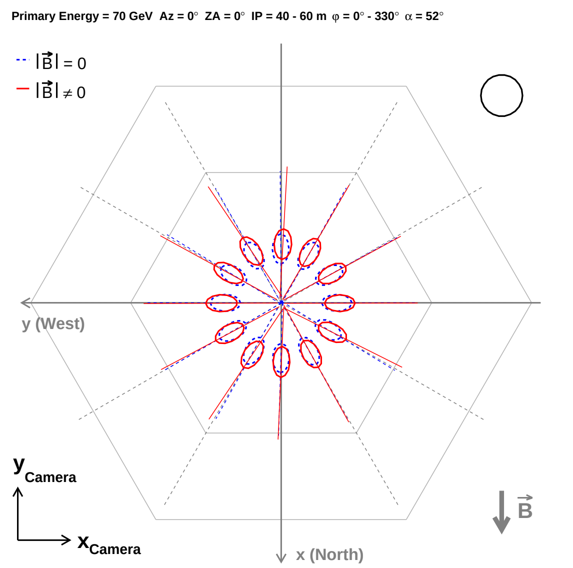

(b) Hard image cleaning, ZA 0°, azimuth angle 0°, impact parameter 40 - 60 m.

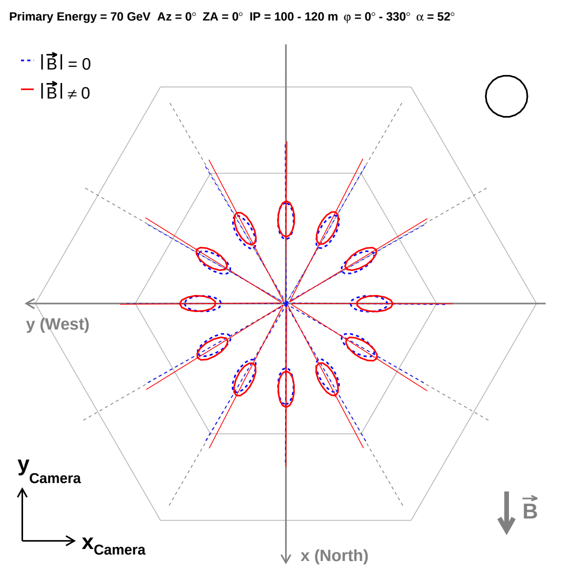

(c) Intermediate image cleaning, ZA 0°, azimuth angle 0°, impact parameter 100 - 120 m.

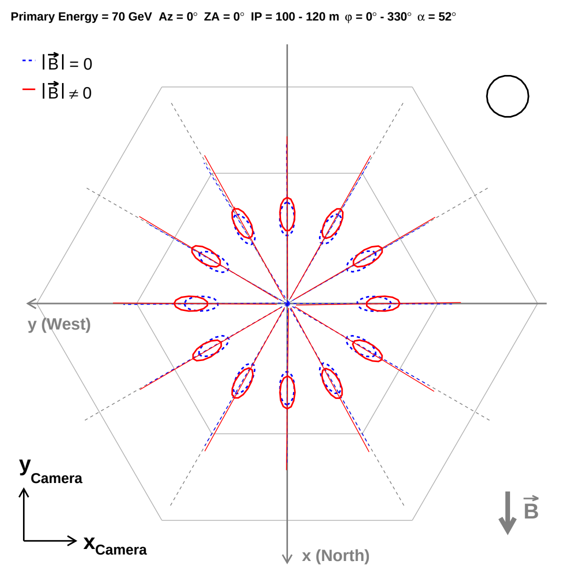

(d) Hard image cleaning, ZA 0°, azimuth angle 0°, impact parameter 100 - 120 m.

Figure 53: Hillas ellipses for MC γ-rays of 70 GeV energy, two different image cleaning levels and two impact parameter windows. The ZA was set to 0° and the azimuth angle to 0°. The angle φ was varied over the full range between 0° and 330°. While the red ellipses (solid lines) were obtained for enabled GF, the blue ones (dashed lines) were obtained for disabled GF. The black curve in the upper right part of the figure indicates the ellipticity of the Cherenkov light distribution on ground.

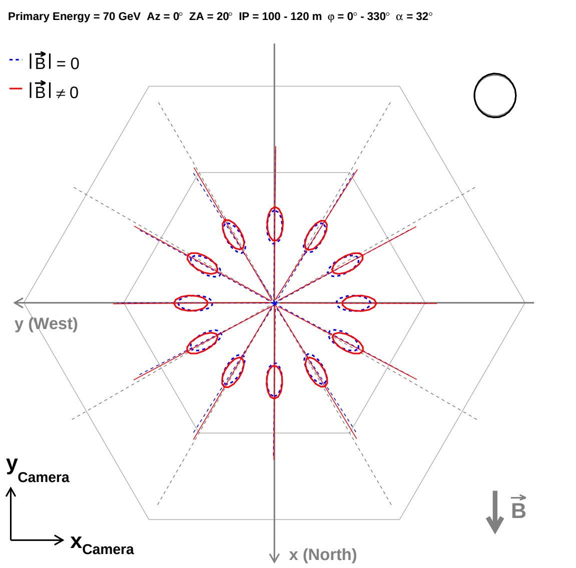

(a) Intermediate image cleaning, ZA 20°, azimuth angle 0°, impact parameter 100 - 120 m.

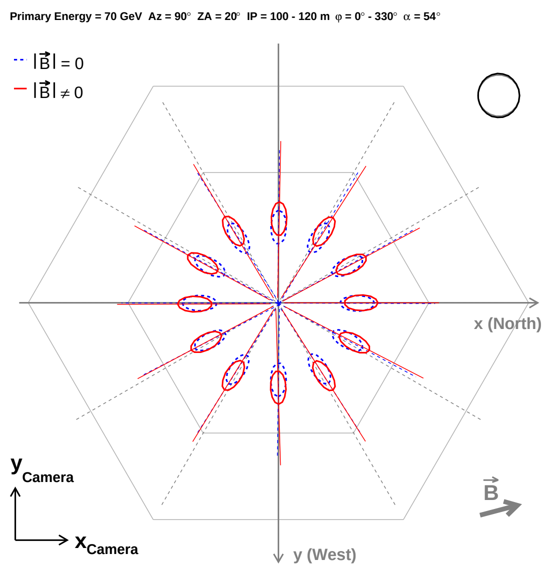

(b) Intermediate image cleaning, ZA 20°, azimuth angle 90°, impact parameter 100 - 120 m.

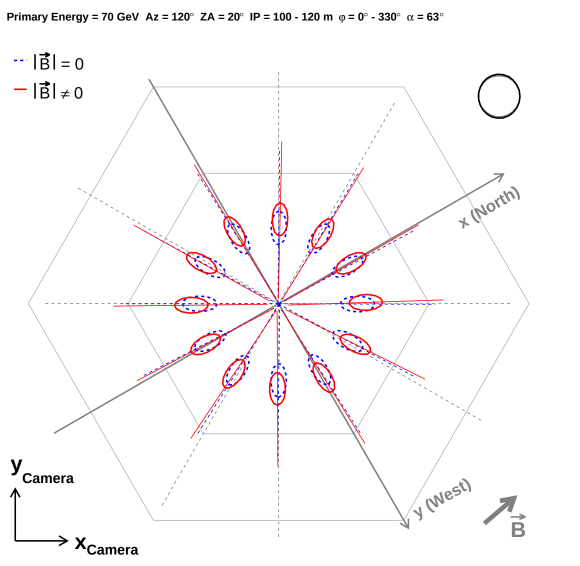

(c) Intermediate image cleaning, ZA 20°, azimuth angle 120°, impact parameter 100 - 120 m.

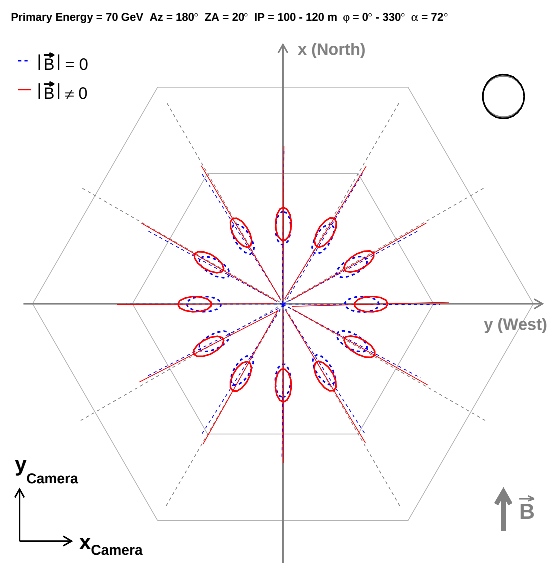

(d) Intermediate image cleaning, ZA 20°, azimuth angle 180°, impact parameter 100 - 120 m.

Figure 54: Hillas ellipses for MC γ-rays of 70 GeV energy and impact parameters between 100 m and 120 m. The ZA was set to 20° and the azimuth angle to 0° , 90°, 120° and 180°, respectively. The angle φ was varied over the full range between 0° and 330°. While the red ellipses (solid lines) were obtained for enabled GF, the blue ones (dashed lines) were obtained for disabled GF. The black curve in the upper right part of the figure indicates the ellipticity of the Cherenkov light distribution on ground.

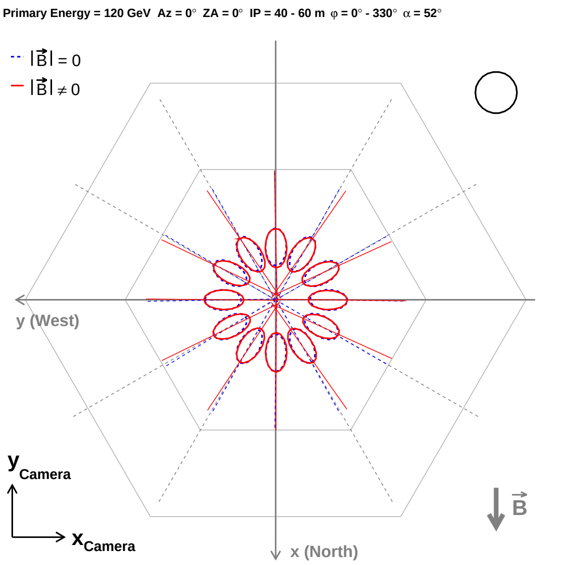

(a) Intermediate image cleaning, ZA 0°, azimuth angle 0°, impact parameter 40 - 60 m.

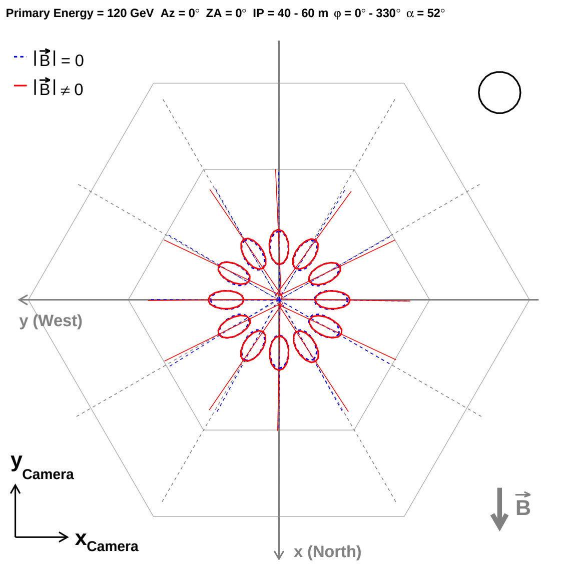

(b) Hard image cleaning, ZA 0°, azimuth angle 0°, impact parameter 40 - 60 m.

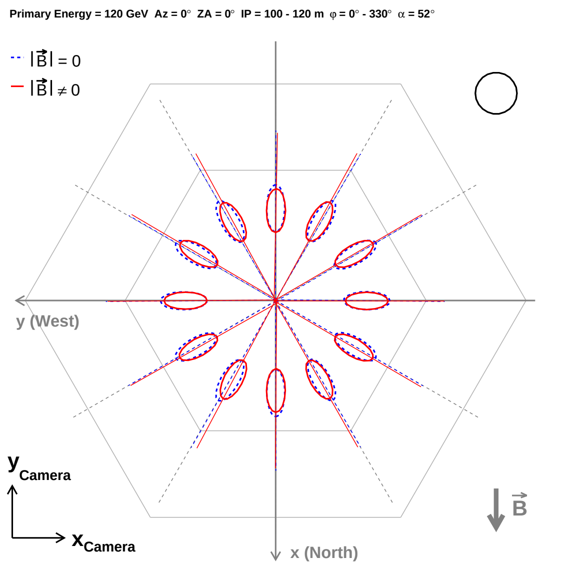

(c) Intermediate image cleaning, ZA 0°, azimuth angle 0°, impact parameter 100 - 120 m.

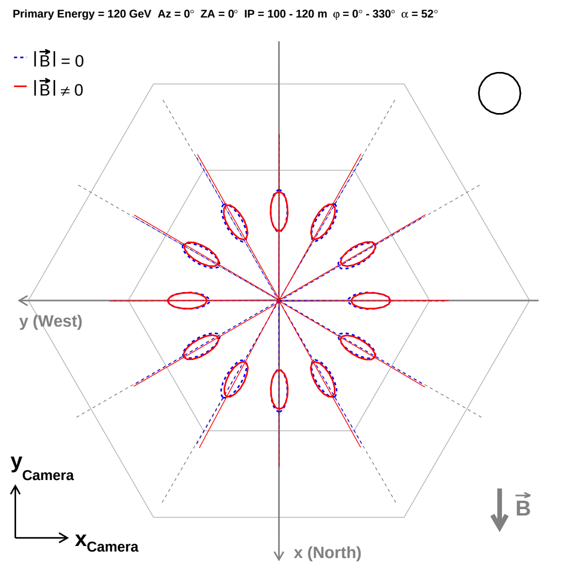

(d) Hard image cleaning, ZA 0°, azimuth angle 0°, impact parameter 100 - 120 m.

Figure 55: Hillas ellipses for MC γ-rays of 120 GeV energy, two different image cleaning levels and two impact parameter windows. The ZA was set to 0° and the azimuth angle to 0°. The angle φ was varied over the full range between 0° and 330°. While the red ellipses (solid lines) were obtained for enabled GF, the blue ones (dashed lines) were obtained for disabled GF. The black curve in the upper right part of the figure indicates the ellipticity of the Cherenkov light distribution on ground.

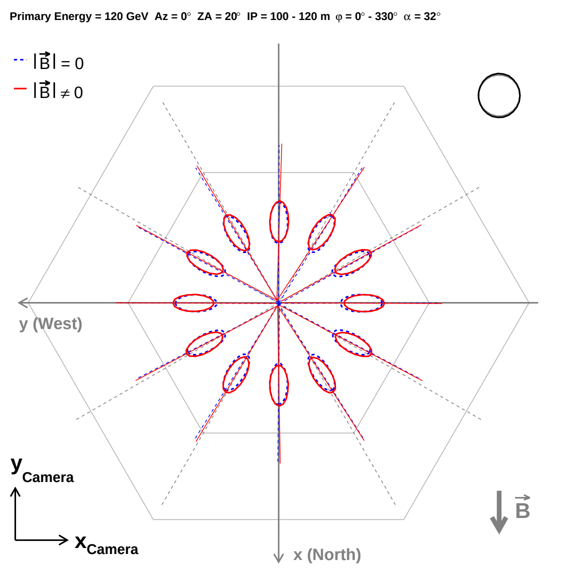

(a) Intermediate image cleaning, ZA 20°, azimuth angle 0°, impact parameter 100 - 120 m.

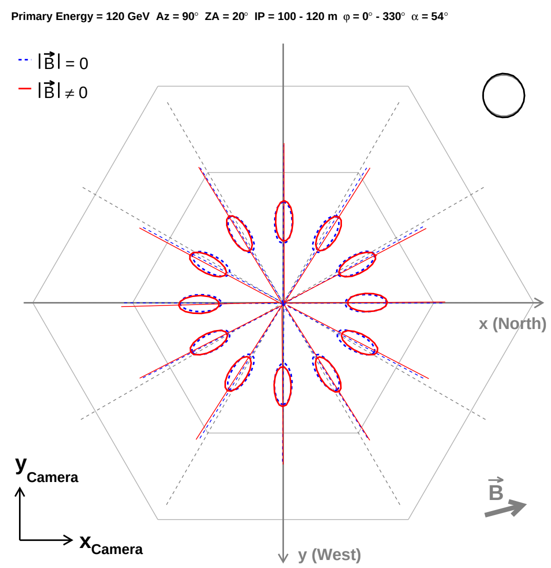

(b) Intermediate image cleaning, ZA 20°, azimuth angle 90°, impact parameter 100 - 120 m.

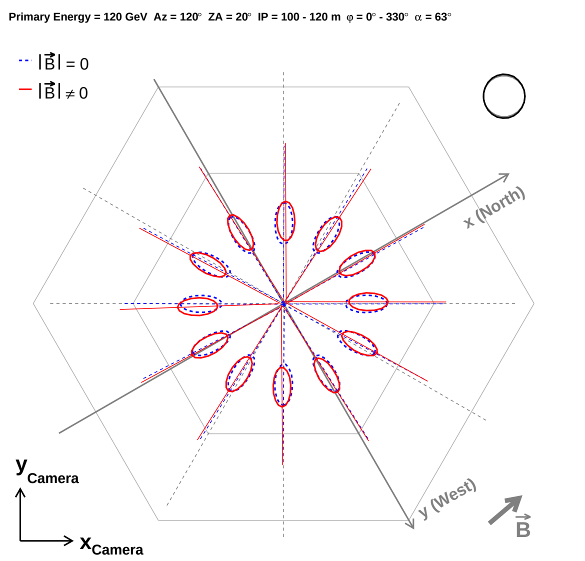

(c) Intermediate image cleaning, ZA 20°, azimuth angle 120°, impact parameter 100 - 120 m.

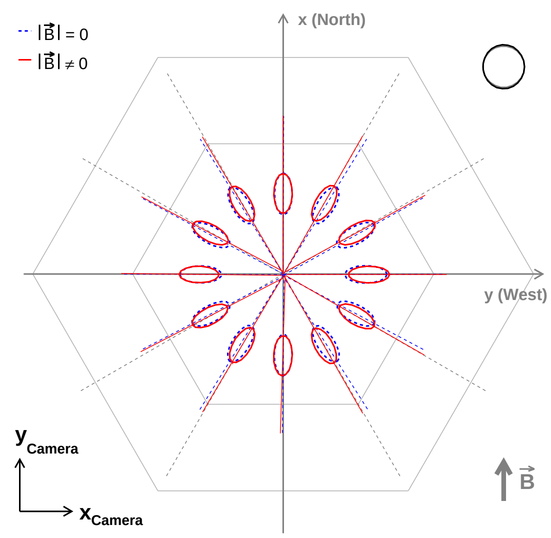

(d) Intermediate image cleaning, ZA 20°, azimuth angle 180°, impact parameter 100 - 120 m.

Figure 56: Hillas ellipses for MC γ-rays of 120 GeV energy and impact parameters between 100 m and 120 m. The ZA was set to 20° and the azimuth angle to 0° , 90°, 120° and 180°, respectively. The angle φ was varied over the full range between 0° and 330°. While the red ellipses (solid lines) were obtained for enabled GF, the blue ones (dashed lines) were obtained for disabled GF. The black curve in the upper right part of the figure indicates the ellipticity of the Cherenkov light distribution on ground.

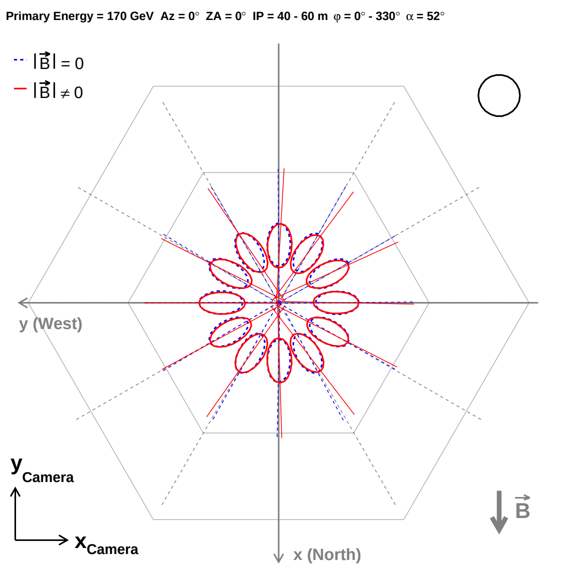

(a) Intermediate image cleaning, ZA 0°, azimuth angle 0°, impact parameter 40 - 60 m.

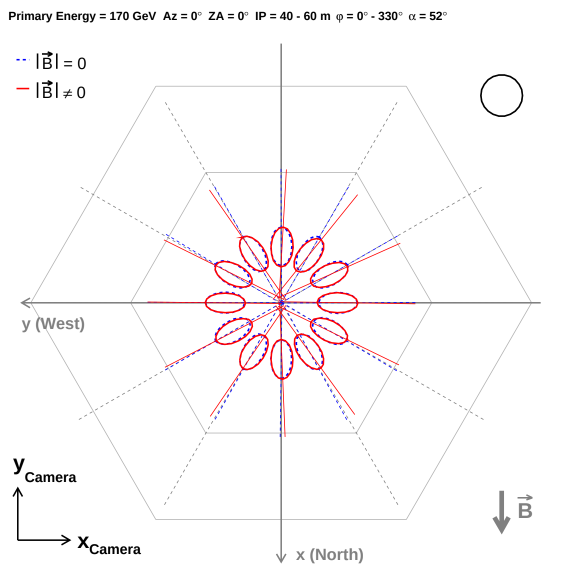

(b) Hard image cleaning, ZA 0°, azimuth angle 0°, impact parameter 40 - 60 m.

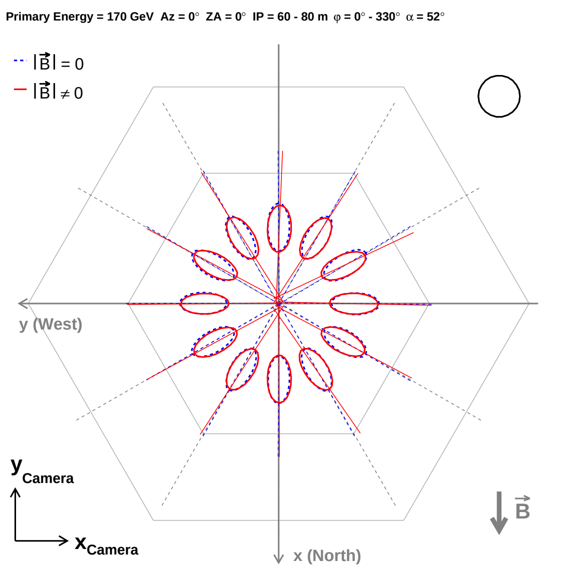

(c) Intermediate image cleaning, ZA 0°, azimuth angle 0°, impact parameter 60 - 80 m.

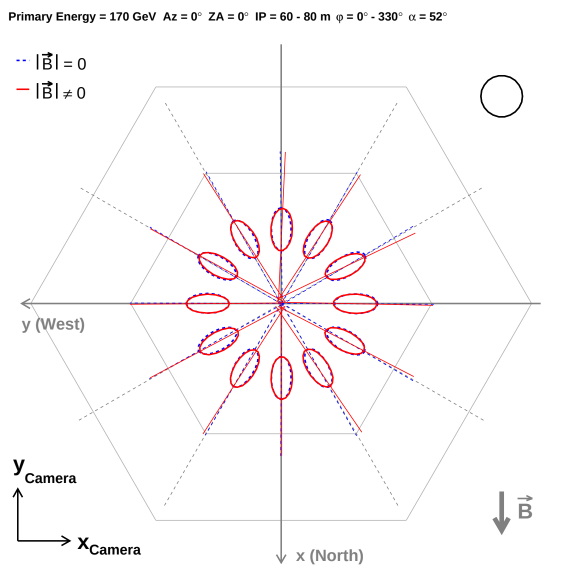

(d) Hard image cleaning, ZA 0°, azimuth angle 0°, impact parameter 60 - 80 m.

Figure 57: Hillas ellipses for MC γ-rays of 170 GeV energy, two different image cleaning levels and two impact parameter windows. The ZA was set to 0° and the azimuth angle to 0°. The angle φ was varied over the full range between 0° and 330°. While the red ellipses (solid lines) were obtained for enabled GF, the blue ones (dashed lines) were obtained for disabled GF. The black curve in the upper right part of the figure indicates the ellipticity of the Cherenkov light distribution on ground.

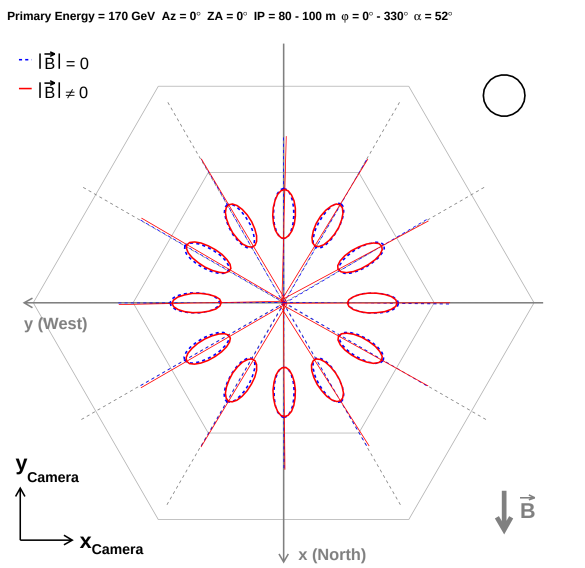

(a) Intermediate image cleaning, ZA 0°, azimuth angle 0°, impact parameter 80 - 100 m.

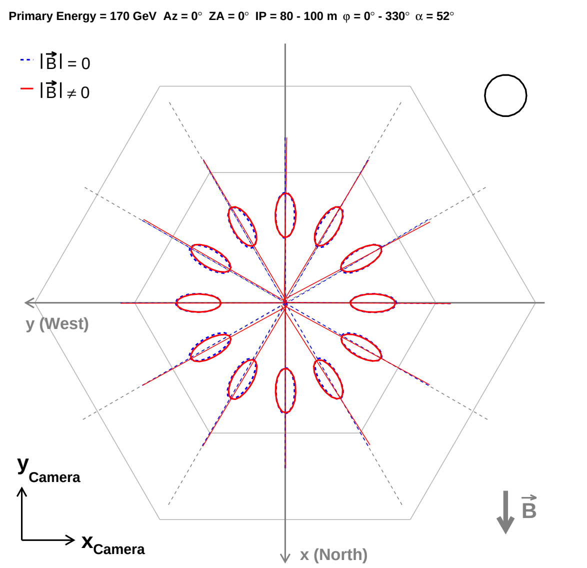

(b) Hard image cleaning, ZA 0°, azimuth angle 0°, impact parameter 80 - 100 m.

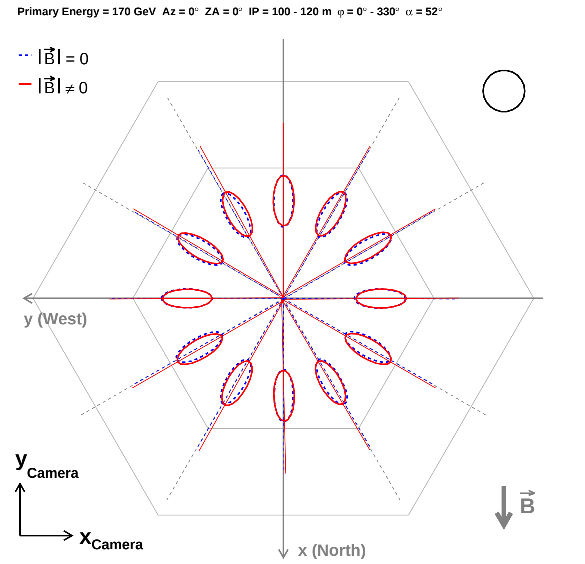

(c) Intermediate image cleaning, ZA 0°, azimuth angle 0°, impact parameter 100 - 120 m.

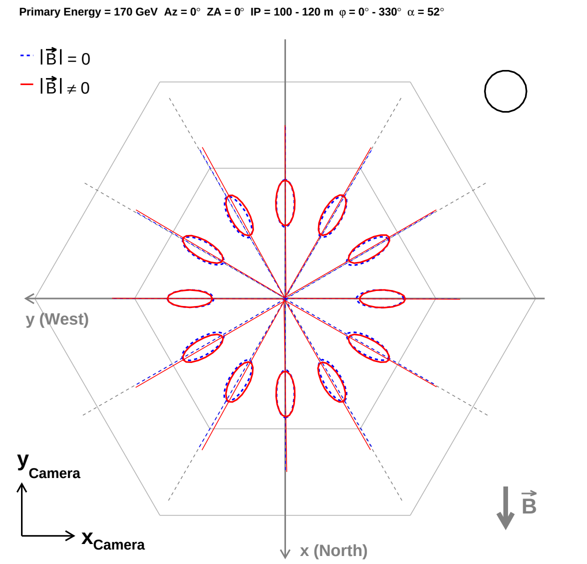

(d) Hard image cleaning, ZA 0°, azimuth angle 0°, impact parameter 100 - 120 m.

Figure 58: Hillas ellipses for MC γ-rays of 170 GeV energy, two different image cleaning levels and two impact parameter windows. The ZA was set to 0° and the azimuth angle to 0°. The angle φ was varied over the full range between 0° and 330°. While the red ellipses (solid lines) were obtained for enabled GF, the blue ones (dashed lines) were obtained for disabled GF. The black curve in the upper right part of the figure indicates the ellipticity of the Cherenkov light distribution on ground.

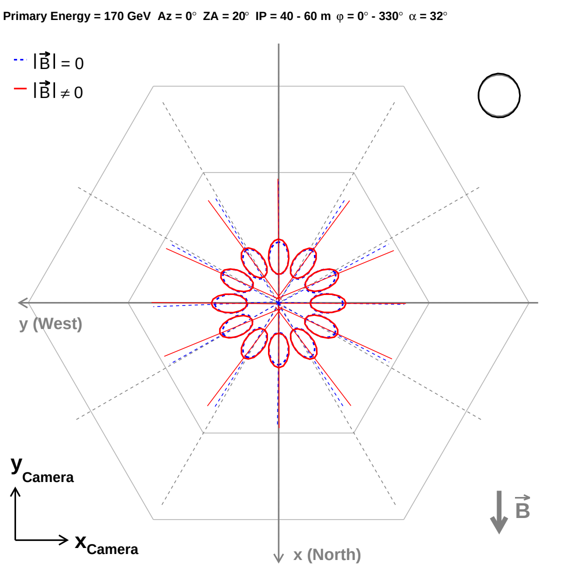

(a) Hard image cleaning, ZA 20°, azimuth angle 0°, impact parameter 40 - 60 m.

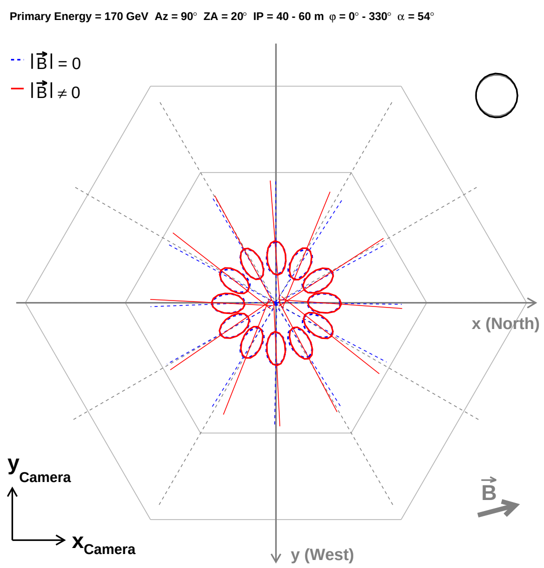

(b) Hard image cleaning, ZA 20°, azimuth angle 90°, impact parameter 40 - 60 m.

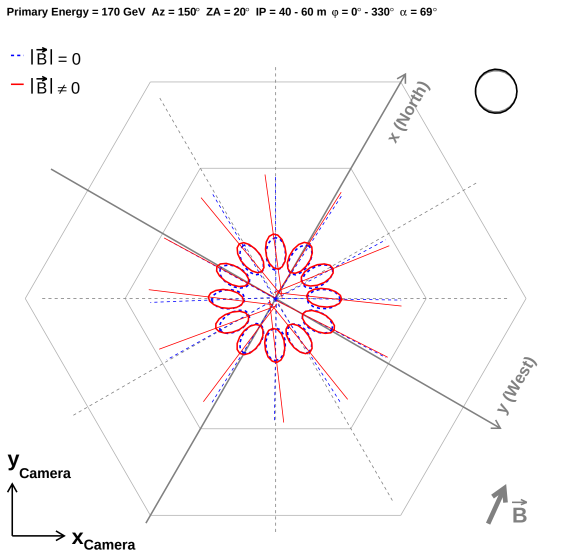

(c) Hard image cleaning, ZA 20°, azimuth angle 150°, impact parameter 40 - 60 m.

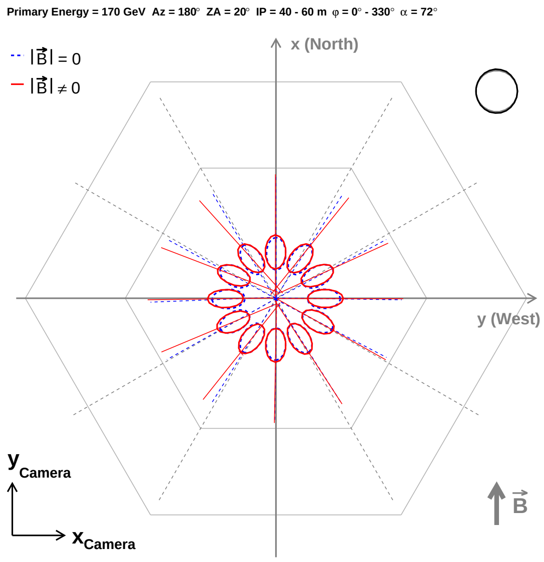

(d) Hard image cleaning, ZA 20°, azimuth angle 180°, impact parameter 40 - 60 m.

Figure 59: Hillas ellipses for MC γ-rays of 170 GeV energy and impact parameters between 40 m and 60 m. The ZA was set to 20° and the azimuth angle to 0° , 90°, 120° and 180°, respectively. The angle φ was varied over the full range between 0° and 330°. While the red ellipses (solid lines) were obtained for enabled GF, the blue ones (dashed lines) were obtained for disabled GF. The black curve in the upper right part of the figure indicates the ellipticity of the Cherenkov light distribution on ground.

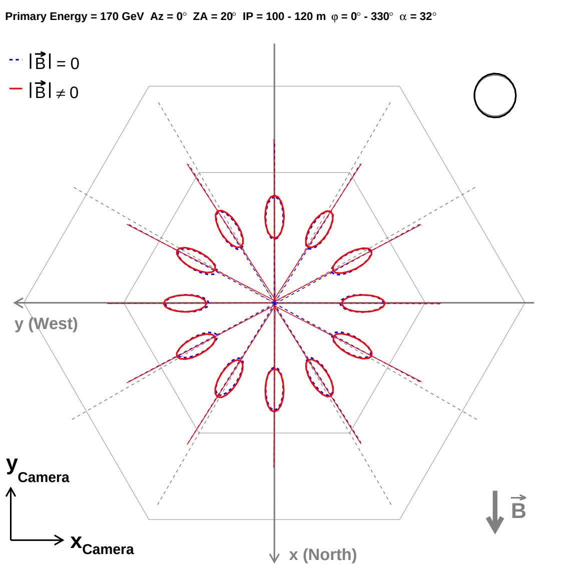

(a) Hard image cleaning, ZA 20°, azimuth angle 0°, impact parameter 100 - 120 m.

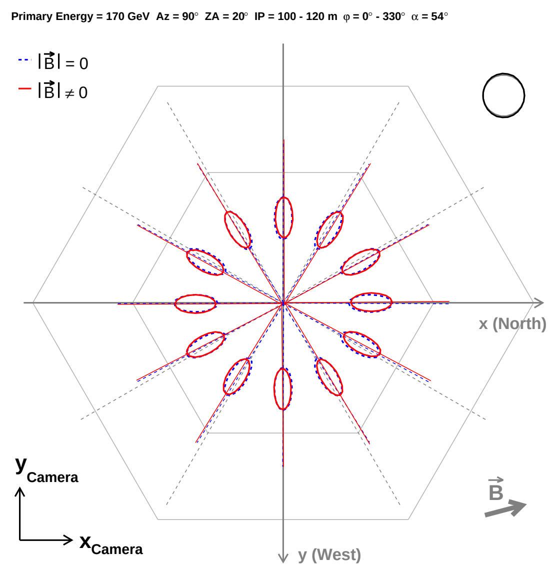

(b) Hard image cleaning, ZA 20°, azimuth angle 90°, impact parameter 100 - 120 m.

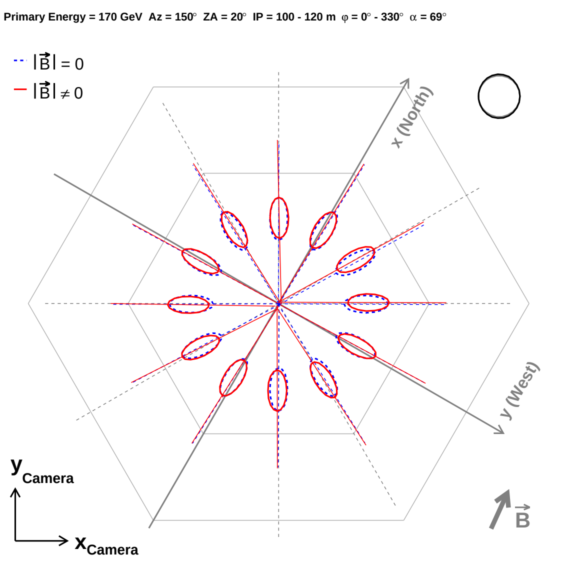

(c) Hard image cleaning, ZA 20°, azimuth angle 150°, impact parameter 100 - 120 m.

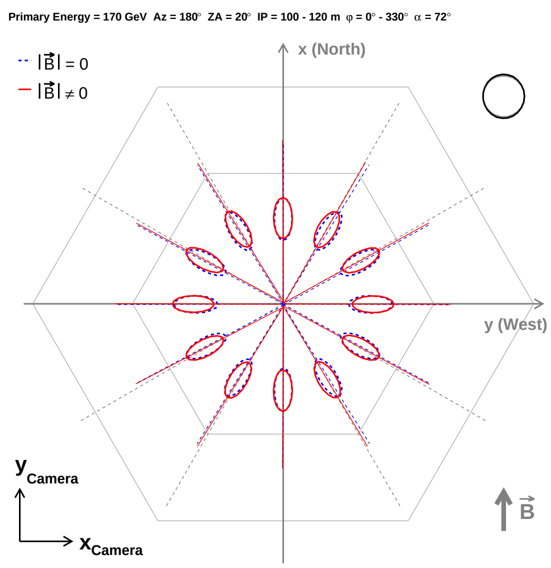

(d) Hard image cleaning, ZA 20°, azimuth angle 180°, impact parameter 100 - 120 m.

Figure 60: Hillas ellipses for MC γ-rays of 170 GeV energy and impact parameters between 60 m and 100 m. The ZA was set to 20° and the azimuth angle to 0° , 90°, 150° and 180°, respectively. The angle φ was varied over the full range between 0° and 330°. While the red ellipses (solid lines) were obtained for enabled GF, the blue ones (dashed lines) were obtained for disabled GF. The black curve in the upper right part of the figure indicates the ellipticity of the Cherenkov light distribution on ground.

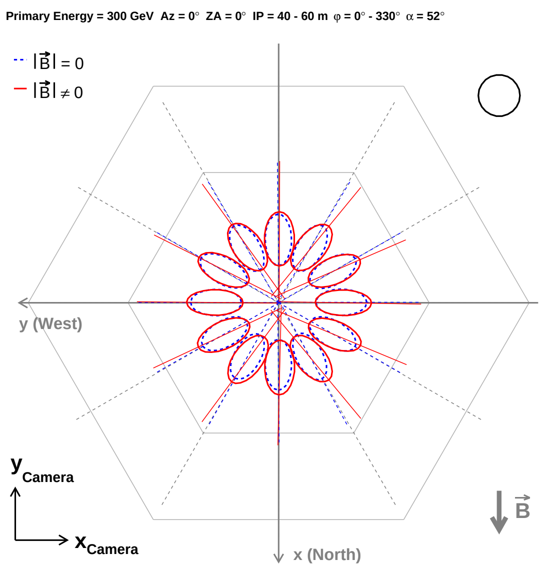

(a) Intermediate image cleaning, ZA 0°, azimuth angle 0°, impact parameter 40 - 60 m.

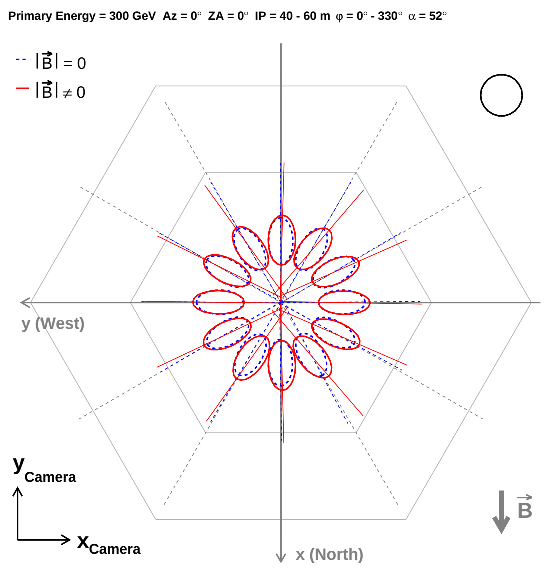

(b) Hard image cleaning, ZA 0°, azimuth angle 0°, impact parameter 40 - 60 m.

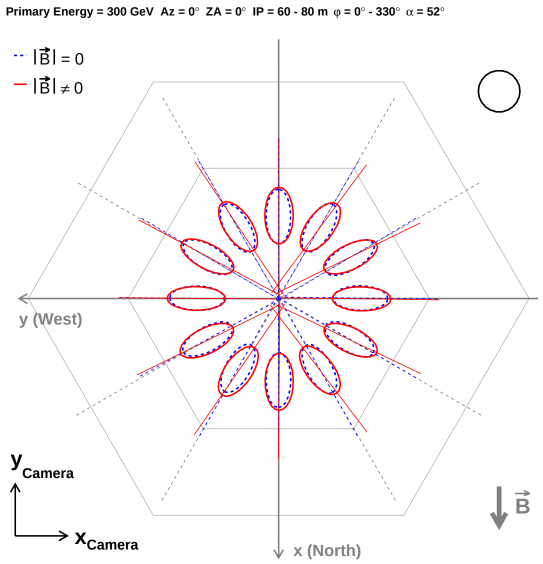

(c) Intermediate image cleaning, ZA 0°, azimuth angle 0°, impact parameter 60 - 80 m.

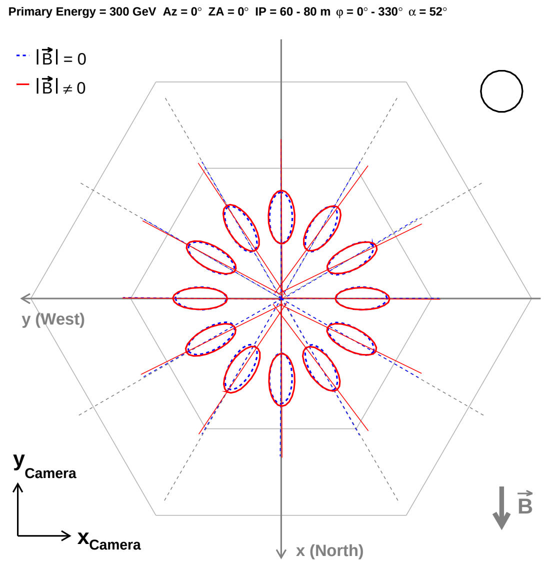

(d) Hard image cleaning, ZA 0°, azimuth angle 0°, impact parameter 60 - 80 m.

Figure 61: Hillas ellipses for MC γ-rays of 300 GeV energy, two different image cleaning levels and two impact parameter windows. The ZA was set to 0° and the azimuth angle to 0°. The angle φ was varied over the full range between 0° and 330°. While the red ellipses (solid lines) were obtained for enabled GF, the blue ones (dashed lines) were obtained for disabled GF. The black curve in the upper right part of the figure indicates the ellipticity of the Cherenkov light distribution on ground.

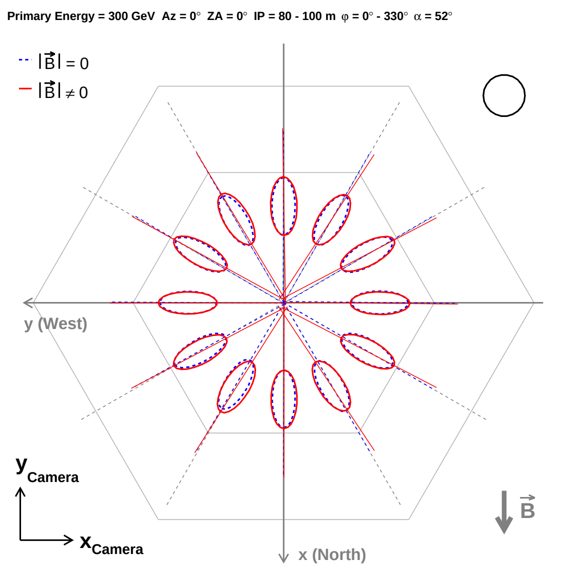

(a) Intermediate image cleaning, ZA 0°, azimuth angle 0°, impact parameter 80 - 100 m.

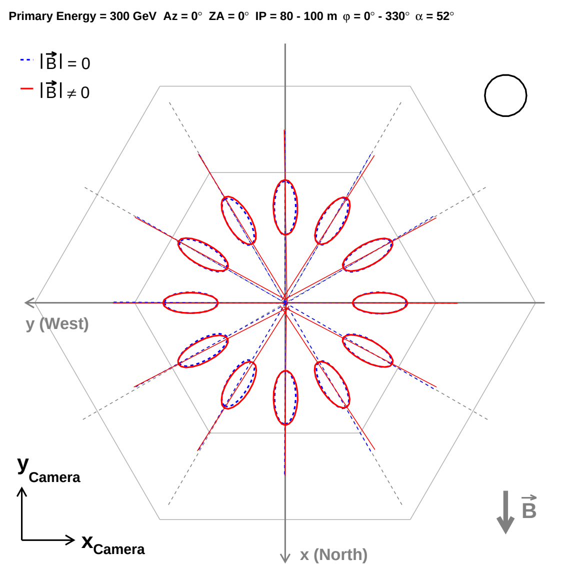

(b) Hard image cleaning, ZA 0°, azimuth angle 0°, impact parameter 80 - 100 m.

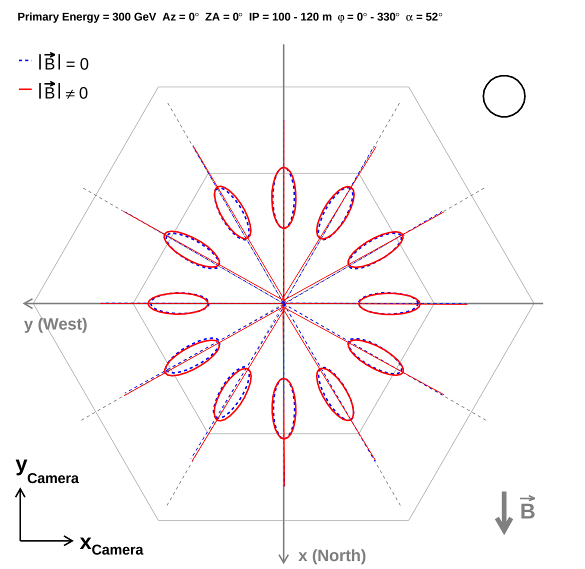

(c) Intermediate image cleaning, ZA 0°, azimuth angle 0°, impact parameter 100 - 120 m.

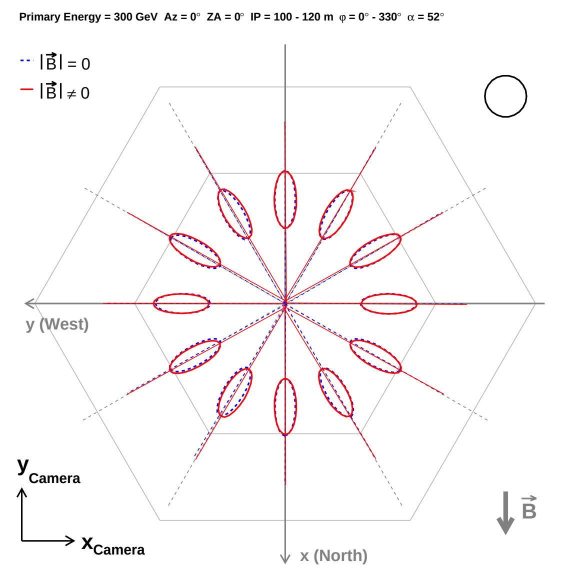

(d) Hard image cleaning, ZA 0°, azimuth angle 0°, impact parameter 100 - 120 m.

Figure 62: Hillas ellipses for MC γ-rays of 300 GeV energy, two different image cleaning levels and two impact parameter windows. The ZA was set to 0° and the azimuth angle to 0°. The angle φ was varied over the full range between 0° and 330°. While the red ellipses (solid lines) were obtained for enabled GF, the blue ones (dashed lines) were obtained for disabled GF. The black curve in the upper right part of the figure indicates the ellipticity of the Cherenkov light distribution on ground.

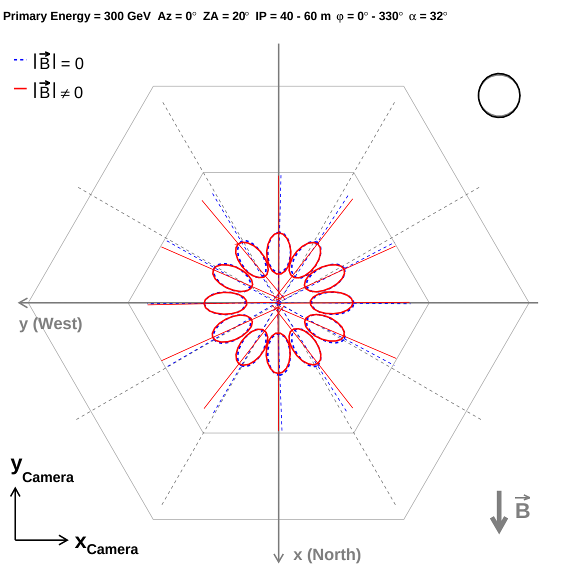

(a) Hard image cleaning, ZA 20°, azimuth angle 0°, impact parameter 40 - 60 m.

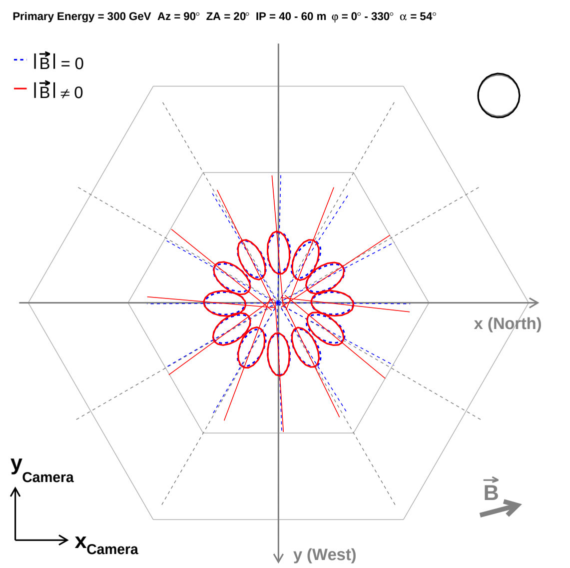

(b) Hard image cleaning, ZA 20°, azimuth angle 90°, impact parameter 40 - 60 m.

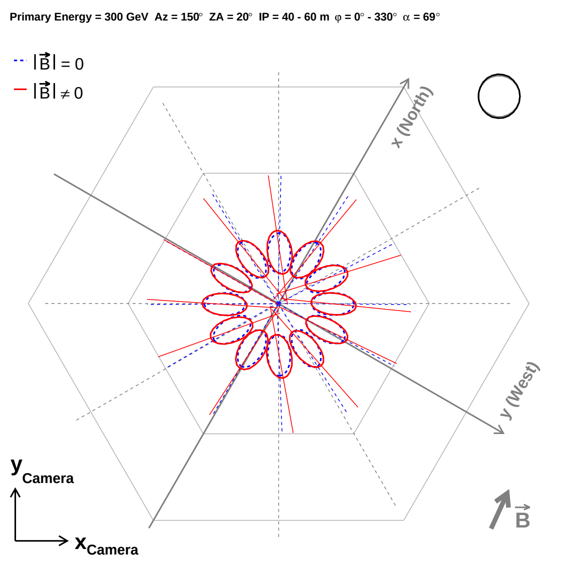

(c) Hard image cleaning, ZA 20°, azimuth angle 150°, impact parameter 40 - 60 m.

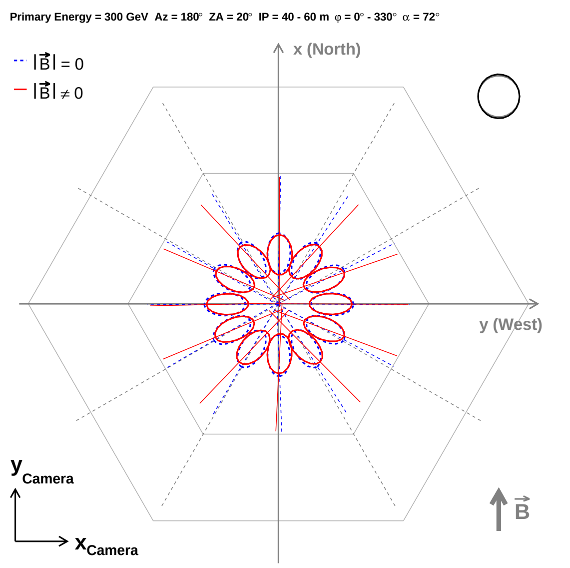

(d) Hard image cleaning, ZA 20°, azimuth angle 180°, impact parameter 40 - 60 m.

Figure 63: Hillas ellipses for MC γ-rays of 300 GeV energy and impact parameters between 40 m and 60 m. The ZA was set to 20° and the azimuth angle to 0° , 90°, 120° and 180°, respectively. The angle φ was varied over the full range between 0° and 330°. While the red ellipses (solid lines) were obtained for enabled GF, the blue ones (dashed lines) were obtained for disabled GF. The black curve in the upper right part of the figure indicates the ellipticity of the Cherenkov light distribution on ground.

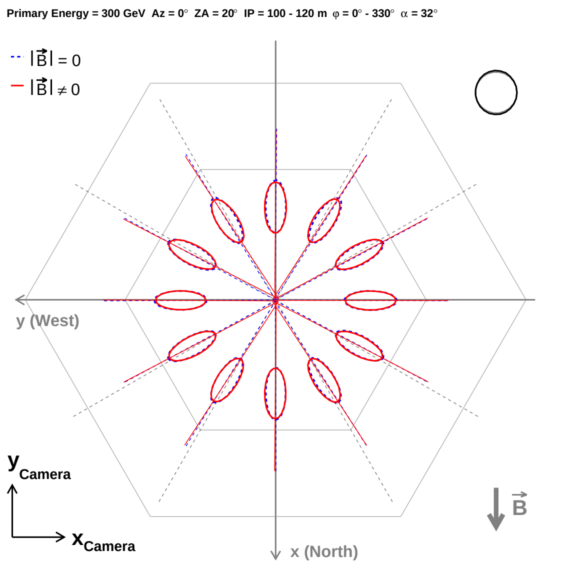

(a) Hard image cleaning, ZA 20°, azimuth angle 0°, impact parameter 100 - 120 m.

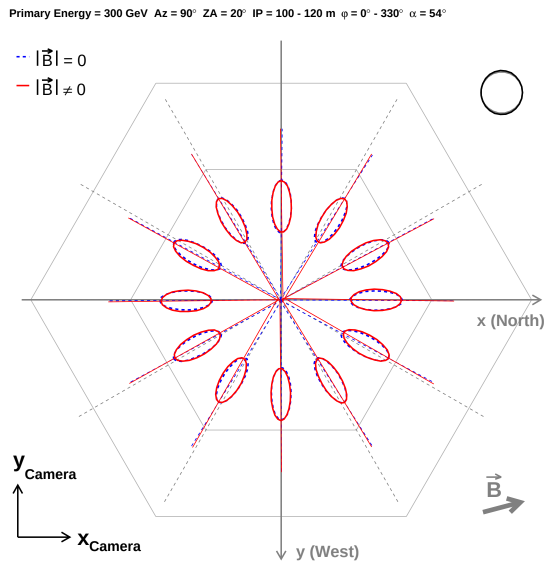

(b) Hard image cleaning, ZA 20°, azimuth angle 90°, impact parameter 100 - 120 m.

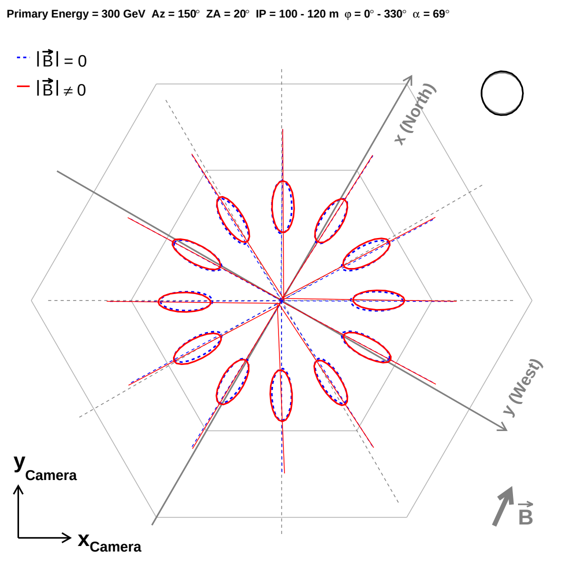

(c) Hard image cleaning, ZA 20°, azimuth angle 150°, impact parameter 100 - 120 m.

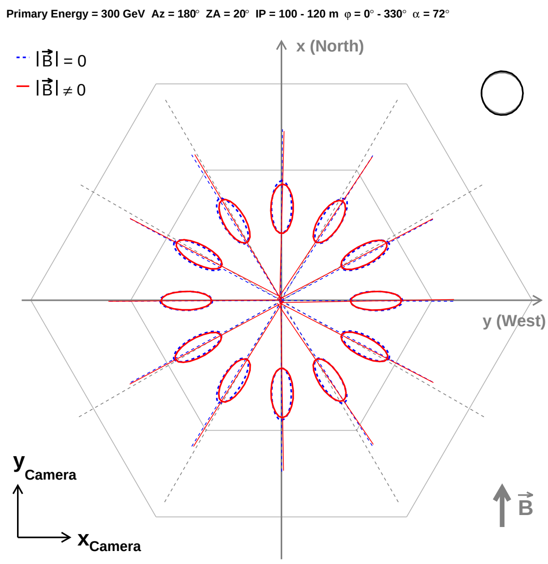

(d) Hard image cleaning, ZA 20°, azimuth angle 180°, impact parameter 100 - 120 m.

Figure 64: Hillas ellipses for MC γ-rays of 300 GeV energy and impact parameters between 60 m and 100 m. The ZA was set to 20° and the azimuth angle to 0° , 90°, 150° and 180°, respectively. The angle φ was varied over the full range between 0° and 330°. While the red ellipses (solid lines) were obtained for enabled GF, the blue ones (dashed lines) were obtained for disabled GF. The black curve in the upper right part of the figure indicates the ellipticity of the Cherenkov light distribution on ground.

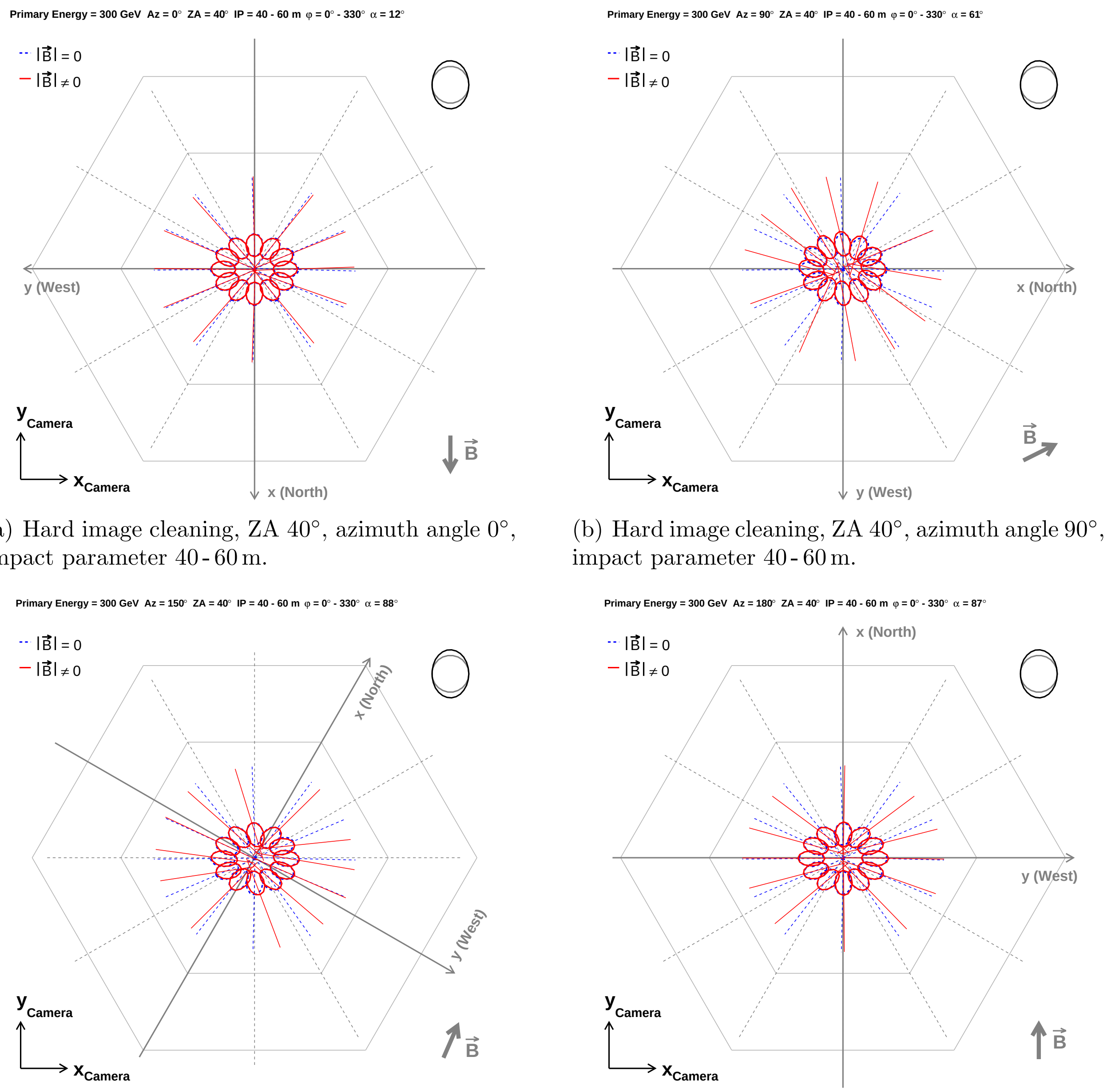

(a) Hard image cleaning, ZA 40°, azimuth angle 0°, impact parameter 40 - 60 m.

(b) Hard image cleaning, ZA 40°, azimuth angle 90°, impact parameter 40 - 60 m.

(c) Hard image cleaning, ZA 40°, azimuth angle 150°, impact parameter 40 - 60 m.

(d) Hard image cleaning, ZA 40°, azimuth angle 180°, impact parameter 40 - 60 m.

Figure 65: Hillas ellipses for MC γ-rays of 300 GeV energy and impact parameters between 40 m and 60 m. The ZA was set to 40° and the azimuth angle to 0° , 90°, 120° and 180°, respectively. The angle φ was varied over the full range between 0° and 330°. While the red ellipses (solid lines) were obtained for enabled GF, the blue ones (dashed lines) were obtained for disabled GF. The black curve in the upper right part of the figure indicates the ellipticity of the Cherenkov light distribution on ground.

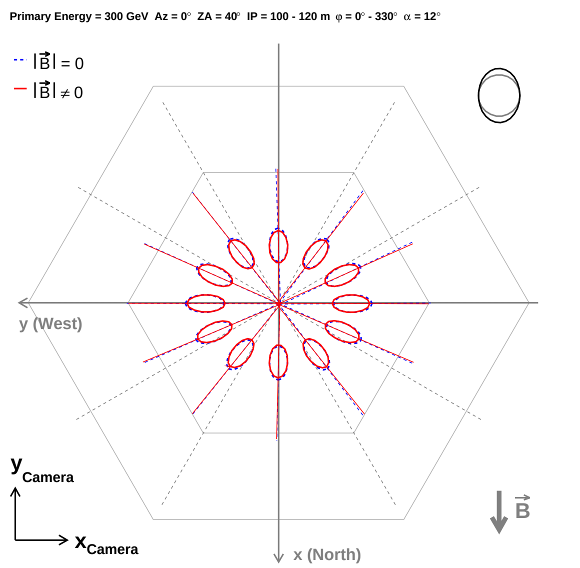

(a) Hard image cleaning, ZA 40°, azimuth angle 0°, impact parameter 100 - 120 m.

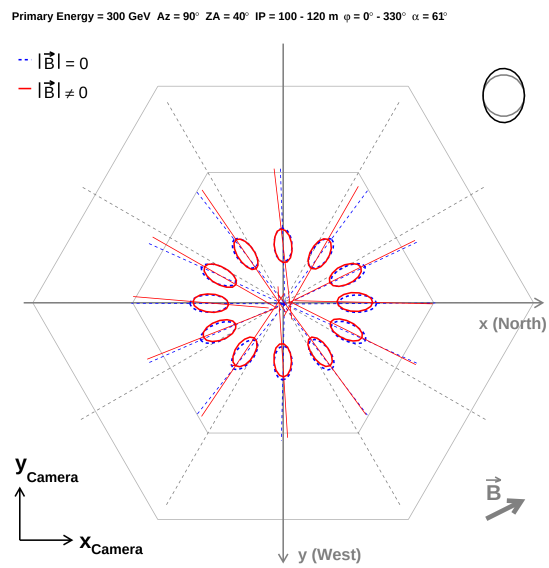

(b) Hard image cleaning, ZA 40°, azimuth angle 90°, impact parameter 100 - 120 m.

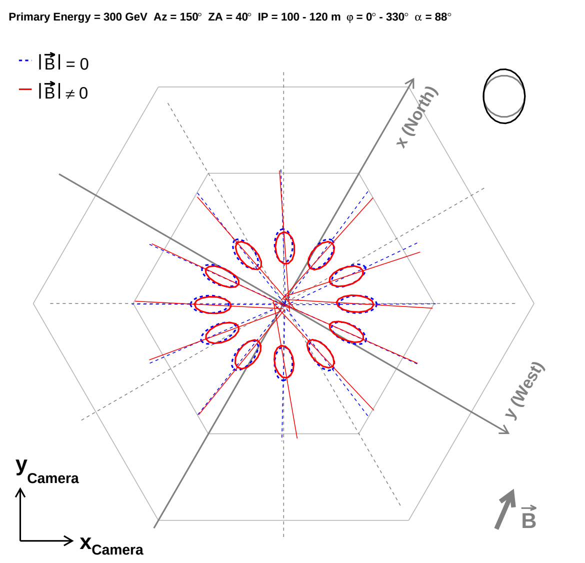

(c) Hard image cleaning, ZA 40°, azimuth angle 150°, impact parameter 100 - 120 m.

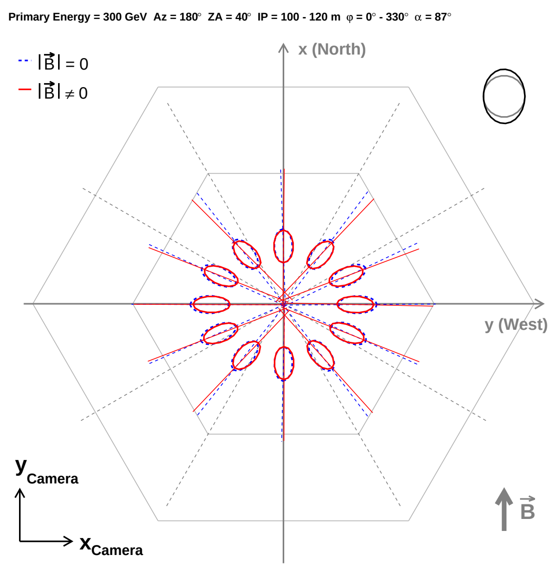

(d) Hard image cleaning, ZA 40°, azimuth angle 180°, impact parameter 100 - 120 m.

Figure 66: Hillas ellipses for MC γ-rays of 300 GeV energy and impact parameters between 60 m and 100 m. The ZA was set to 40° and the azimuth angle to 0° , 90°, 150° and 180°, respectively. The angle φ was varied over the full range between 0° and 330°. While the red ellipses (solid lines) were obtained for enabled GF, the blue ones (dashed lines) were obtained for disabled GF. The black curve in the upper right part of the figure indicates the ellipticity of the Cherenkov light distribution on ground.

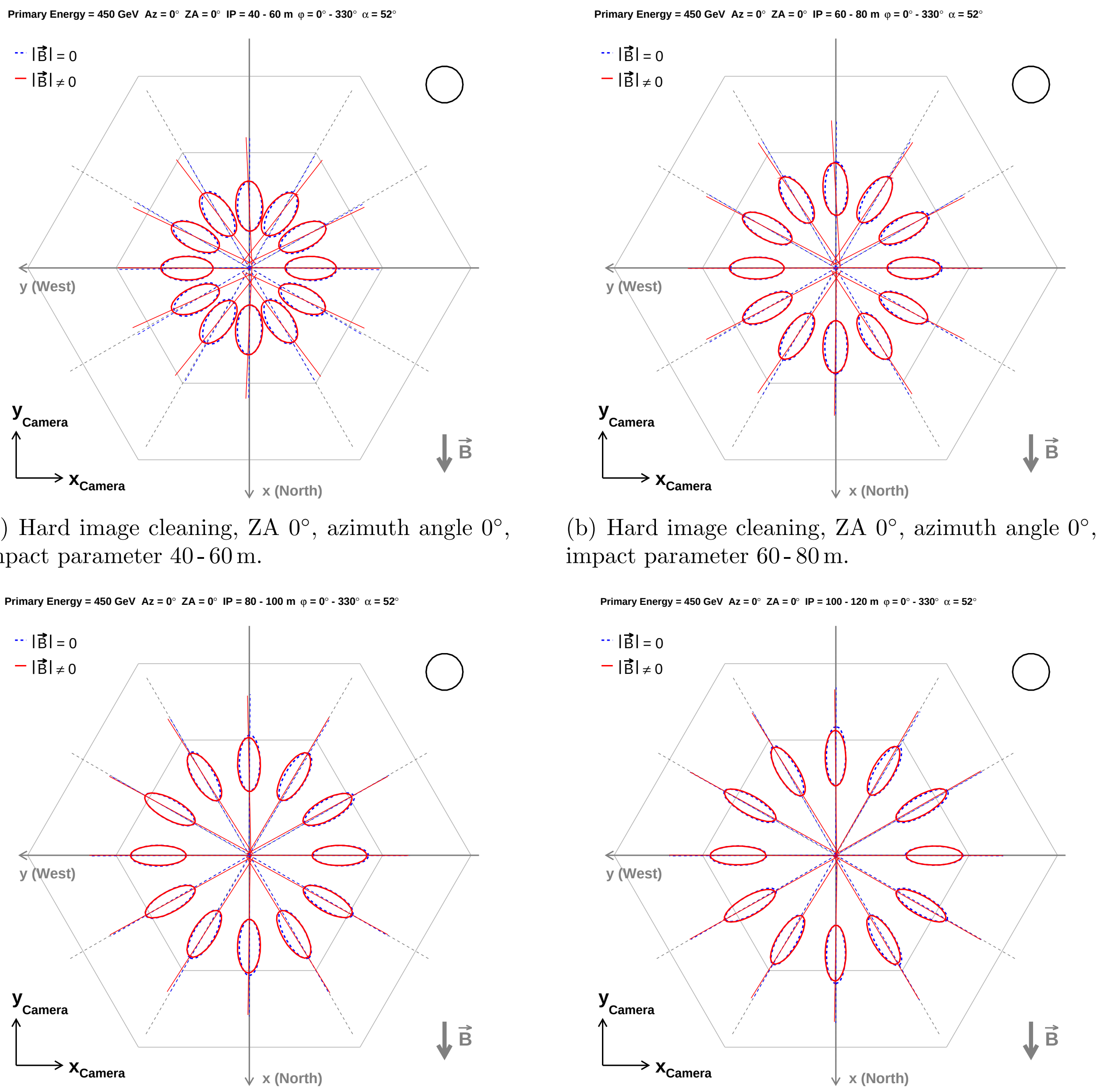

(a) Hard image cleaning, ZA 0°, azimuth angle 0°, impact parameter 40 - 60 m.

(b) Hard image cleaning, ZA 0°, azimuth angle 0°, impact parameter 60 - 80 m.

(c) Hard image cleaning, ZA 0°, azimuth angle 0°, impact parameter 80 - 100 m.

(d) Hard image cleaning, ZA 0°, azimuth angle 0°, impact parameter 100 - 120 m.

Figure 67: Hillas ellipses for MC γ-rays of 450 GeV energy and four impact parameter windows. The ZA was set to 0° and the azimuth angle to 0°. The angle φ was varied over the full range between 0° and 330°. While the red ellipses (solid lines) were obtained for enabled GF, the blue ones (dashed lines) were obtained for disabled GF. The black curve in the upper right part of the figure indicates the ellipticity of the Cherenkov light distribution on ground.

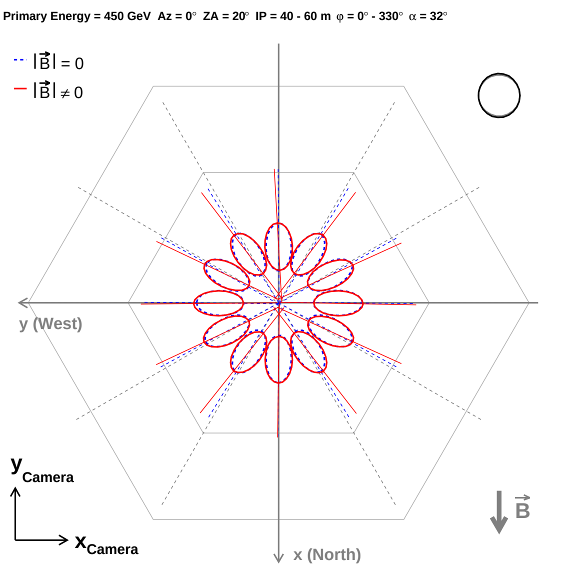

(a) Hard image cleaning, ZA 20°, azimuth angle 0°, impact parameter 40 - 60 m.

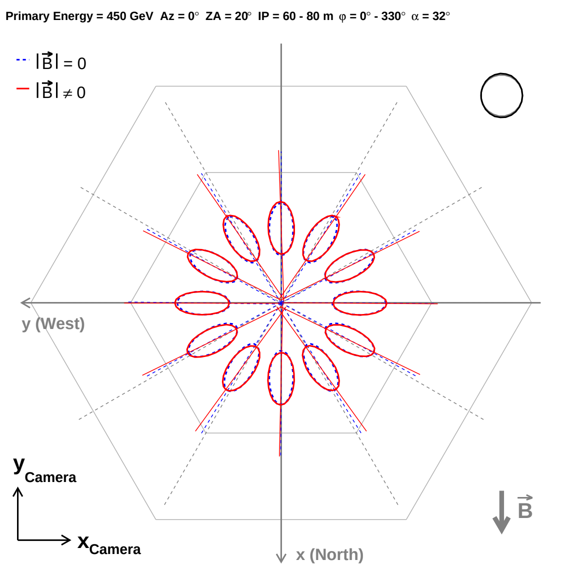

(b) Hard image cleaning, ZA 20°, azimuth angle 0°, impact parameter 60 - 80 m.

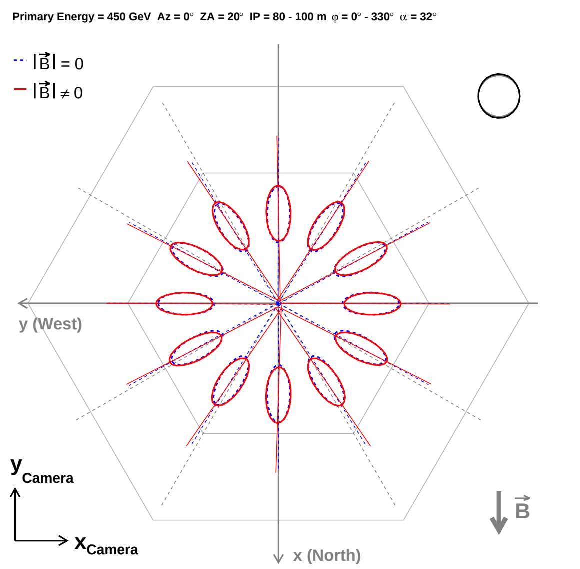

(c) Hard image cleaning, ZA 20°, azimuth angle 0°, impact parameter 80 - 100 m.

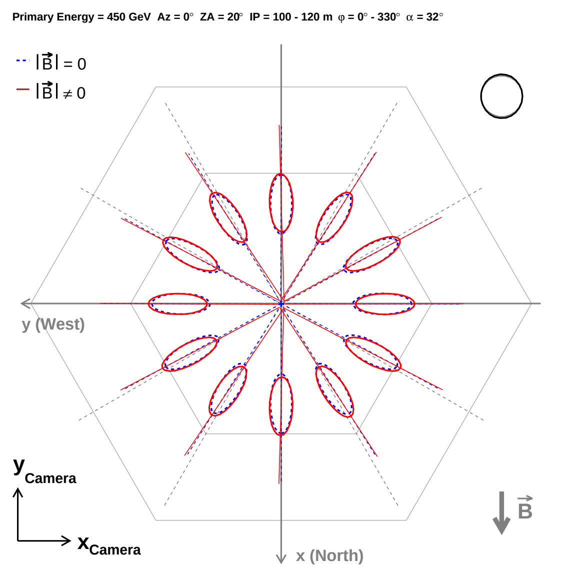

(d) Hard image cleaning, ZA 20°, azimuth angle 0°, impact parameter 100 - 120 m.

Figure 68: Hillas ellipses for MC γ-rays of 450 GeV energy and four impact parameter windows. The ZA was set to 20° and the azimuth angle to 0°. The angle φ was varied over the full range between 0° and 330°. While the red ellipses (solid lines) were obtained for enabled GF, the blue ones (dashed lines) were obtained for disabled GF. The black curve in the upper right part of the figure indicates the ellipticity of the Cherenkov light distribution on ground.

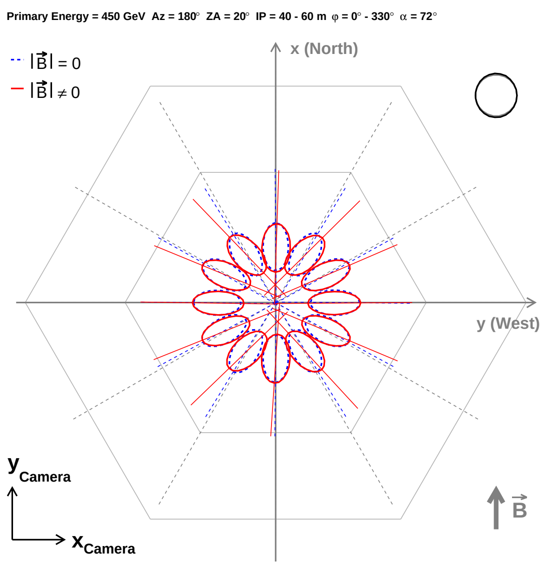

(a) Hard image cleaning, ZA 20°, azimuth angle 180°, impact parameter 40 - 60 m.

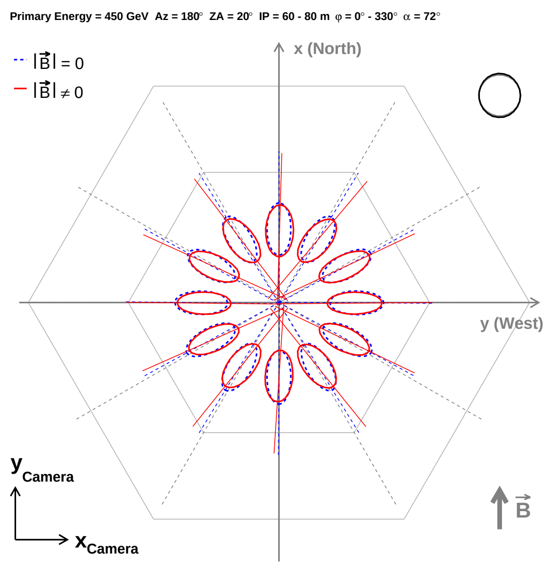

(b) Hard image cleaning, ZA 20°, azimuth angle 180°, impact parameter 60 - 80 m.

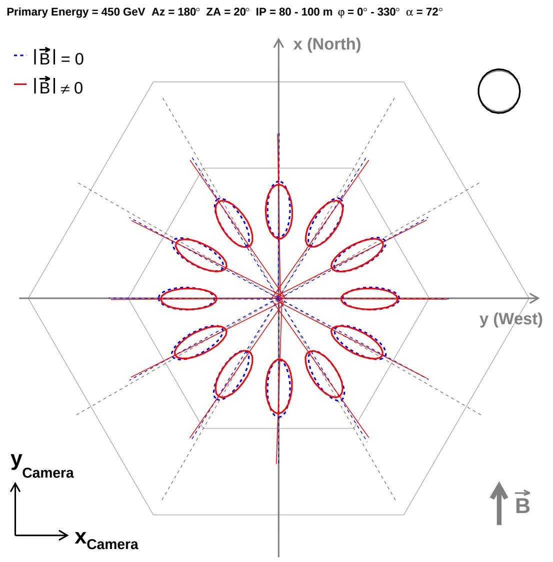

(c) Hard image cleaning, ZA 20°, azimuth angle 180°, impact parameter 80 - 100 m.

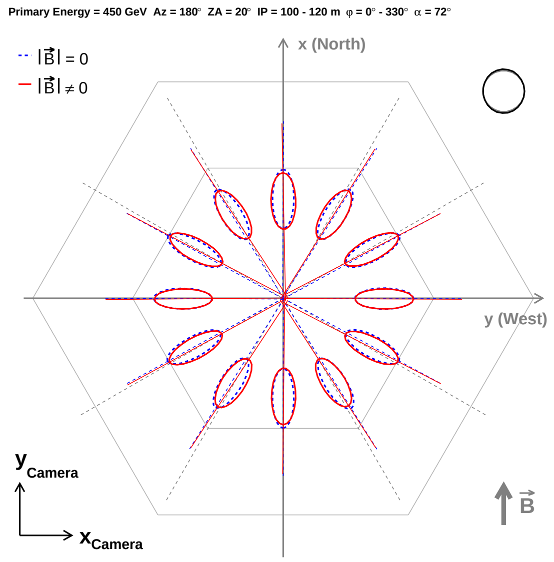

(d) Hard image cleaning, ZA 20°, azimuth angle 180°, impact parameter 100 - 120 m.

Figure 69: Hillas ellipses for MC γ-rays of 450 GeV energy and four impact parameter windows. The ZA was set to 20° and the azimuth angle to 180°. The angle φ was varied over the full range between 0° and 330°. While the red ellipses (solid lines) were obtained for enabled GF, the blue ones (dashed lines) were obtained for disabled GF. The black curve in the upper right part of the figure indicates the ellipticity of the Cherenkov light distribution on ground.

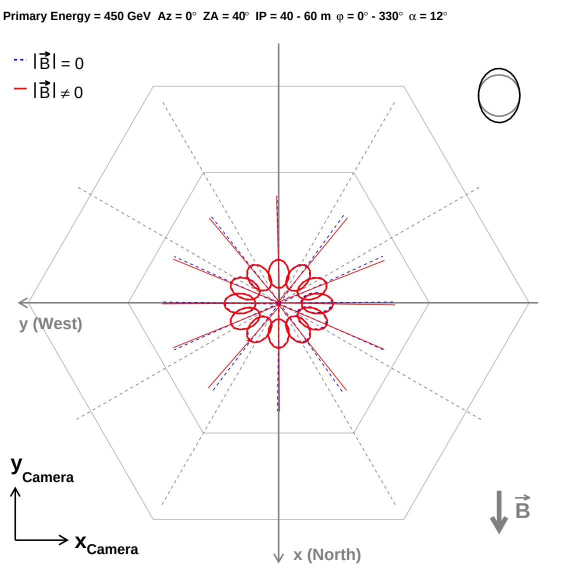

(a) Hard image cleaning, ZA 40°, azimuth angle 0°, impact parameter 40 - 60 m.

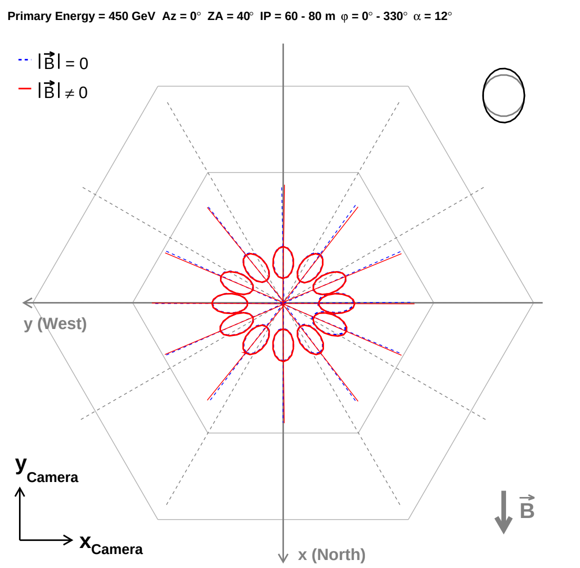

(b) Hard image cleaning, ZA 40°, azimuth angle 0°, impact parameter 60 - 80 m.

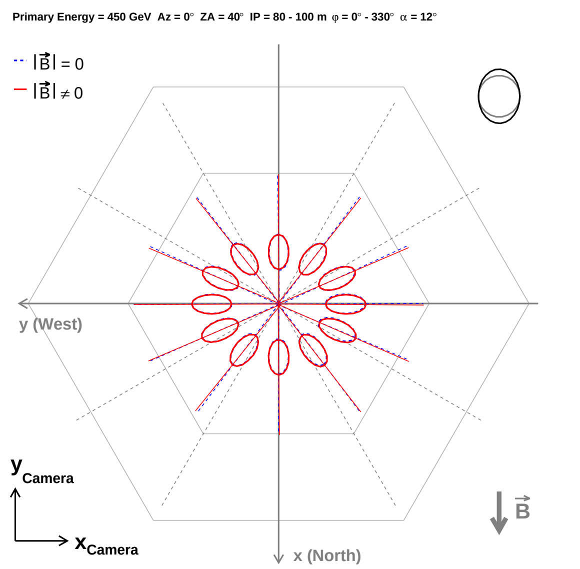

(c) Hard image cleaning, ZA 40°, azimuth angle 0°, impact parameter 80 - 100 m.

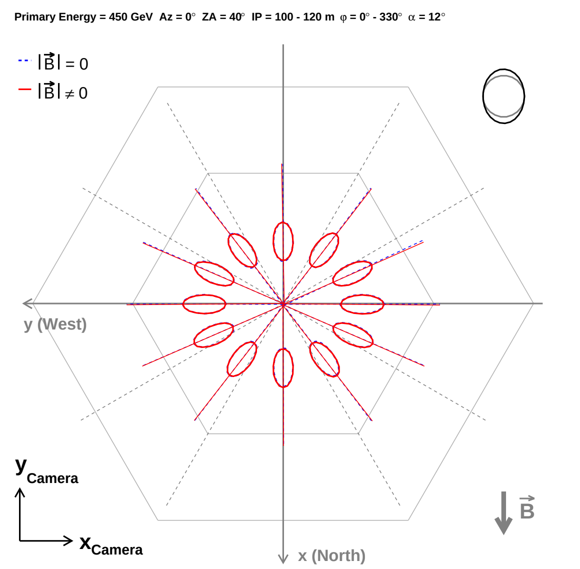

(d) Hard image cleaning, ZA 40°, azimuth angle 0°, impact parameter 100 - 120 m.

Figure 70: Hillas ellipses for MC γ-rays of 450 GeV energy and four impact parameter windows. The ZA was set to 40° and the azimuth angle to 0°. The angle φ was varied over the full range between 0° and 330°. While the red ellipses (solid lines) were obtained for enabled GF, the blue ones (dashed lines) were obtained for disabled GF. The black curve in the upper right part of the figure indicates the ellipticity of the Cherenkov light distribution on ground.

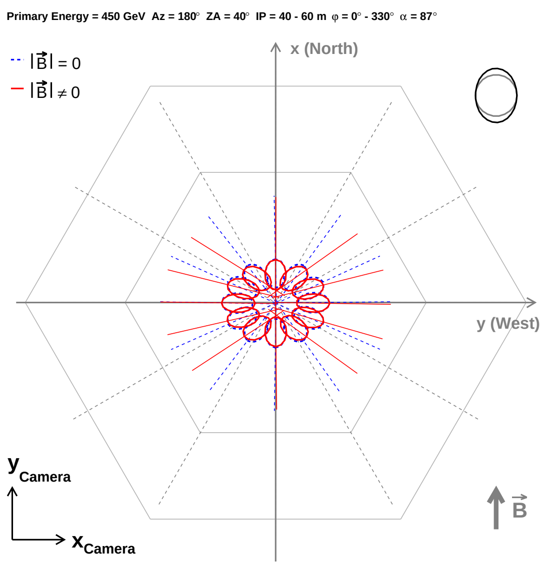

(a) Hard image cleaning, ZA 40°, azimuth angle 180°, impact parameter 20 - 60 m.

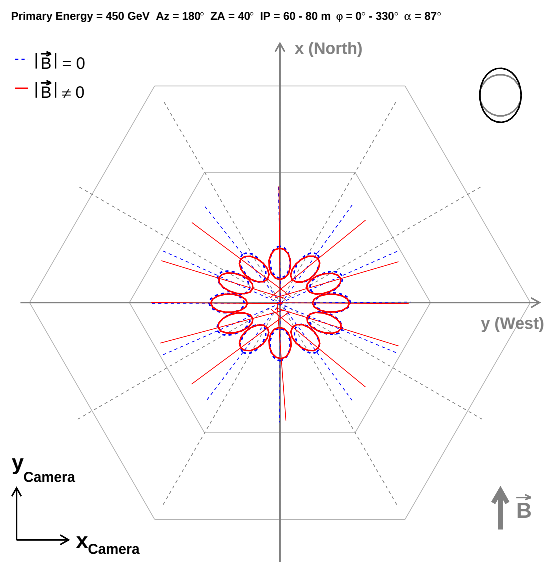

(b) Hard image cleaning, ZA 40°, azimuth angle 180°, impact parameter 60 - 80 m.

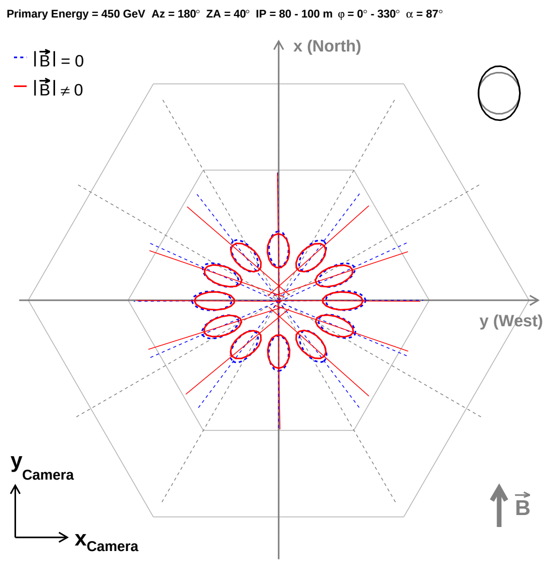

(c) Hard image cleaning, ZA 40°, azimuth angle 180°, impact parameter 80 - 100 m.

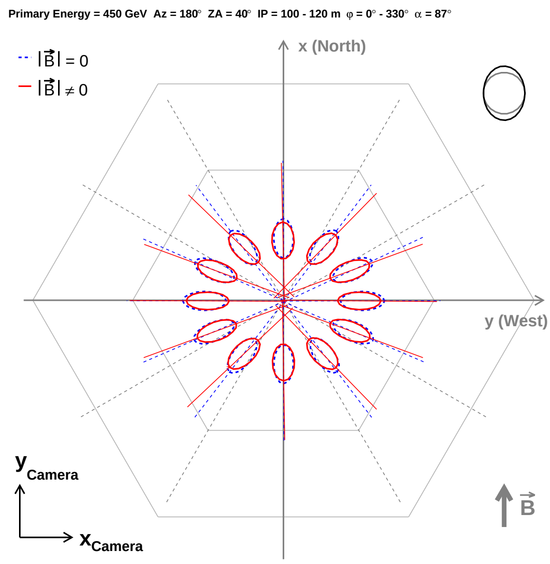

(d) Hard image cleaning, ZA 40°, azimuth angle 180°, impact parameter 100 - 120 m.

Figure 71: Hillas ellipses for MC γ-rays of 450 GeV energy and four impact parameter windows. The ZA was set to 40° and the azimuth angle to 180°. The angle φ was varied over the full range between 0° and 330°. While the red ellipses (solid lines) were obtained for enabled GF, the blue ones (dashed lines) were obtained for disabled GF. The black curve in the upper right part of the figure indicates the ellipticity of the Cherenkov light distribution on ground.

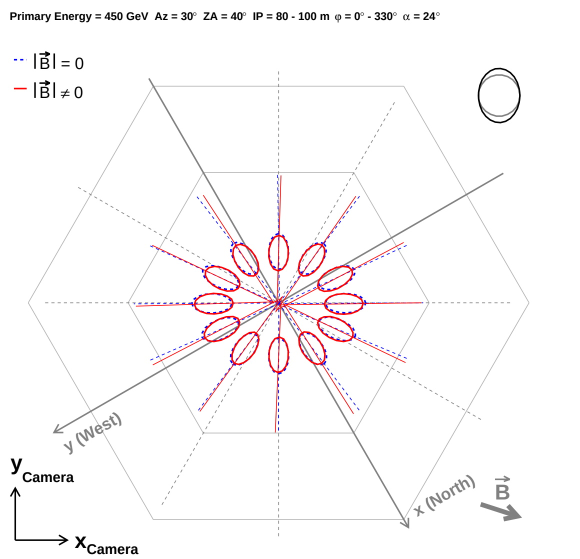

(a) Hard image cleaning, ZA 40°, azimuth angle 30°.

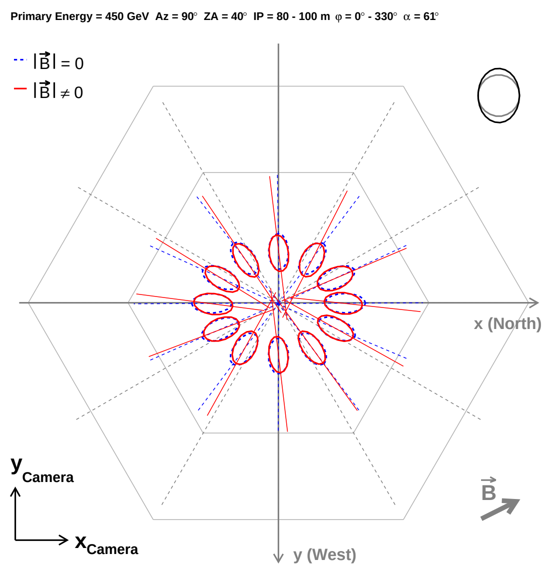

(b) Hard image cleaning, ZA 40°, azimuth angle 90°.

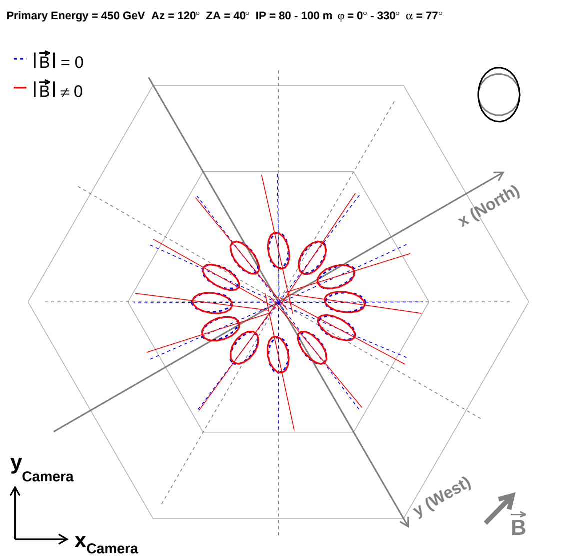

(c) Hard image cleaning, ZA 40°, azimuth angle 120°.

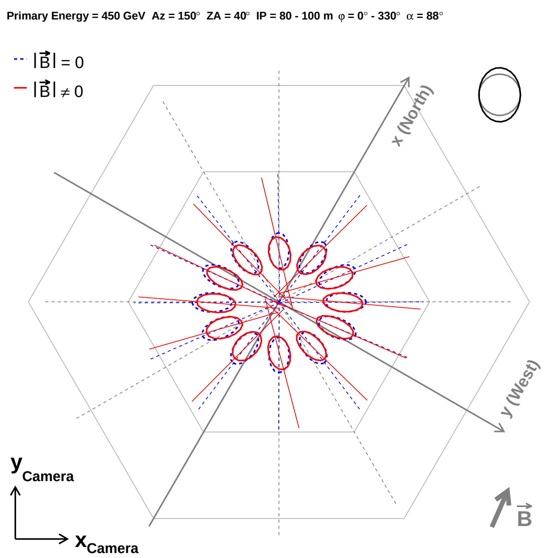

(d) Hard image cleaning, ZA 40°, azimuth angle 150°.

Figure 72: Hillas ellipses for MC γ-rays of 450 GeV energy and impact parameters between 80 m and 100 m. The ZA was set to 40° and the azimuth angle to 30°, 90°, 120° and 150°. The angle φ was varied over the full range between 0° and 330°. While the red ellipses (solid lines) were obtained for enabled GF, the blue ones (dashed lines) were obtained for disabled GF. The black curve in the upper right part of the figure indicates the ellipticity of the Cherenkov light distribution on ground.

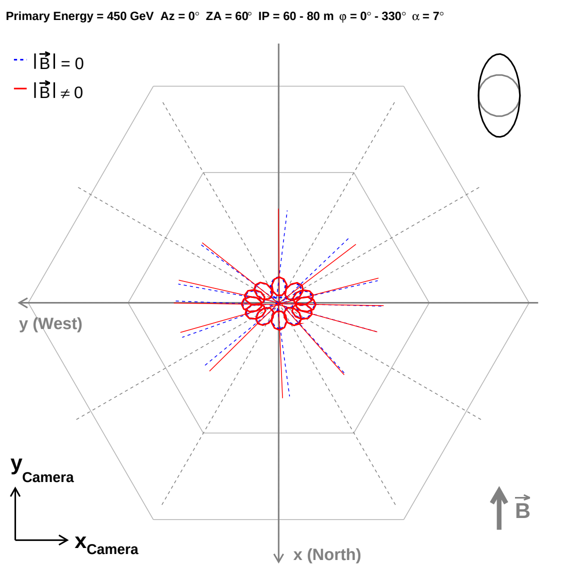

(a) Hard image cleaning, ZA 60°, azimuth angle 0°, impact parameter 60 - 80 m.

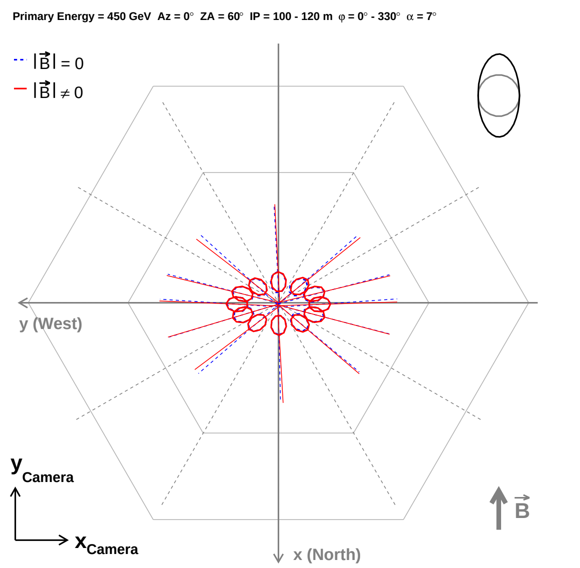

(b) Hard image cleaning, ZA 60°, azimuth angle 0°, impact parameter 100 - 120 m.

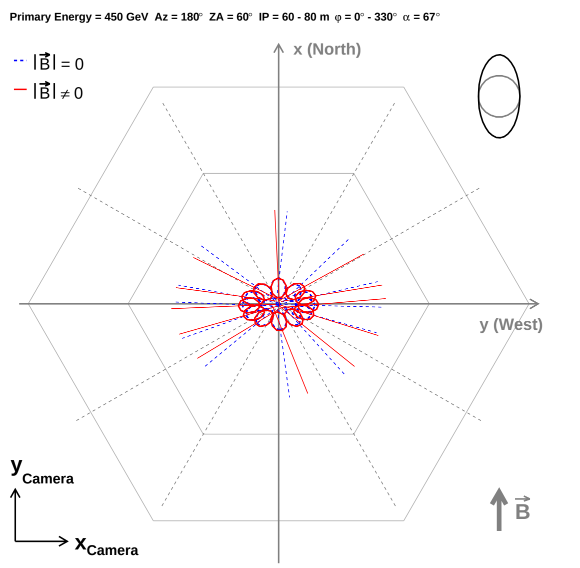

(c) Hard image cleaning, ZA 60°, azimuth angle 180°, impact parameter 60 - 80 m.

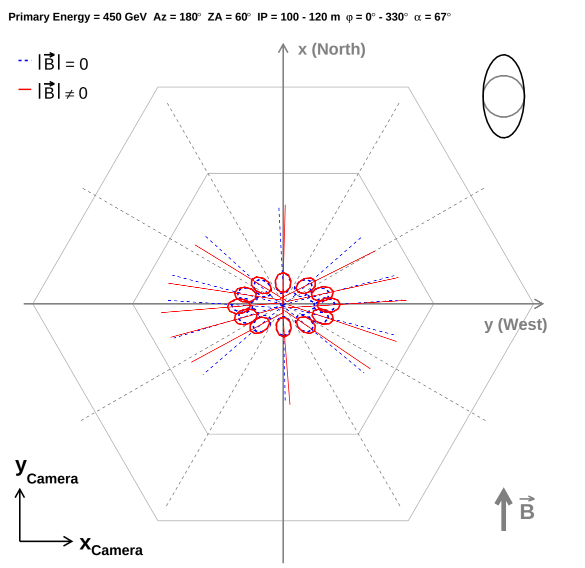

(d) Hard image cleaning, ZA 60°, azimuth angle 180°, impact parameter 100 - 120 m.

Figure 73: Hillas ellipses for MC γ-rays of 450 GeV energy and two impact parameter windows. The ZA was set to 60° and the azimuth angle to 0° and 180°. The angle φ was varied over the full range between 0° and 330°. While the red ellipses (solid lines) were obtained for enabled GF, the blue ones (dashed lines) were obtained for disabled GF. The black curve in the upper right part of the figure indicates the ellipticity of the Cherenkov light distribution on ground.

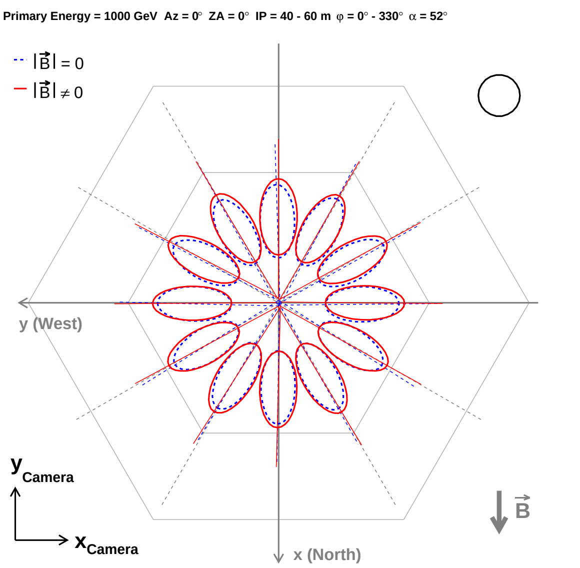

(a) Hard image cleaning, ZA 0°, azimuth angle 0°, impact parameter 40 - 60 m.

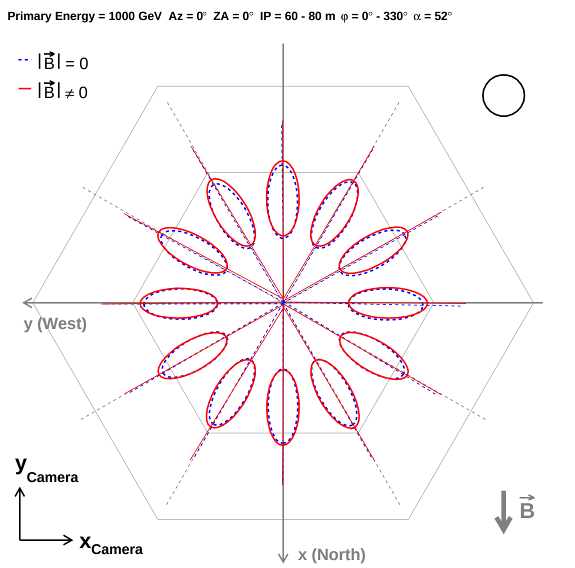

(b) Hard image cleaning, ZA 0°, azimuth angle 0°, impact parameter 60 - 80 m.

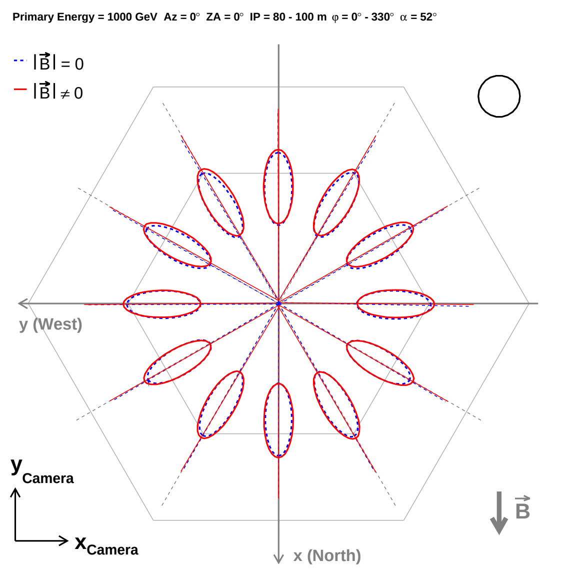

(c) Hard image cleaning, ZA 0°, azimuth angle 0°, impact parameter 80 - 100 m.

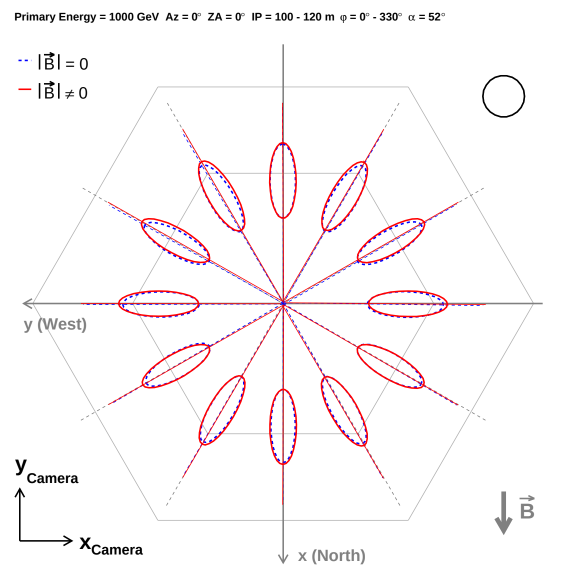

(d) Hard image cleaning, ZA 0°, azimuth angle 0°, impact parameter 100 - 120 m.

Figure 74: Hillas ellipses for MC γ-rays of 1 TeV energy and four impact parameter windows. The ZA was set to 0° and the azimuth angle to 0°. The angle φ was varied over the full range between 0° and 330°. While the red ellipses (solid lines) were obtained for enabled GF, the blue ones (dashed lines) were obtained for disabled GF. The black curve in the upper right part of the figure indicates the ellipticity of the Cherenkov light distribution on ground.

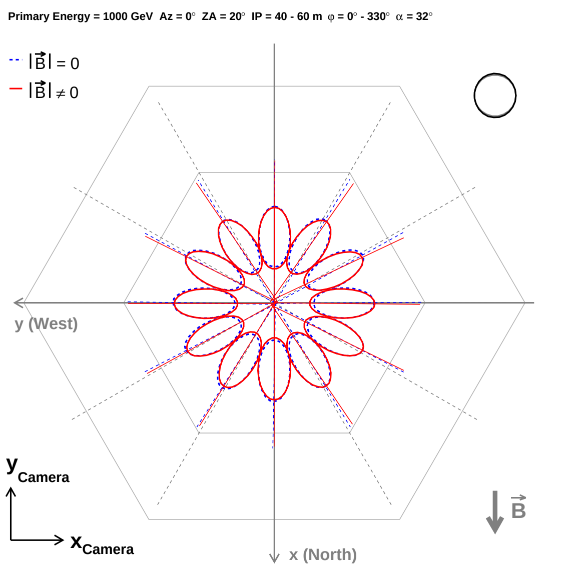

(a) Hard image cleaning, ZA 20°, azimuth angle 0°, impact parameter 40 - 60 m.

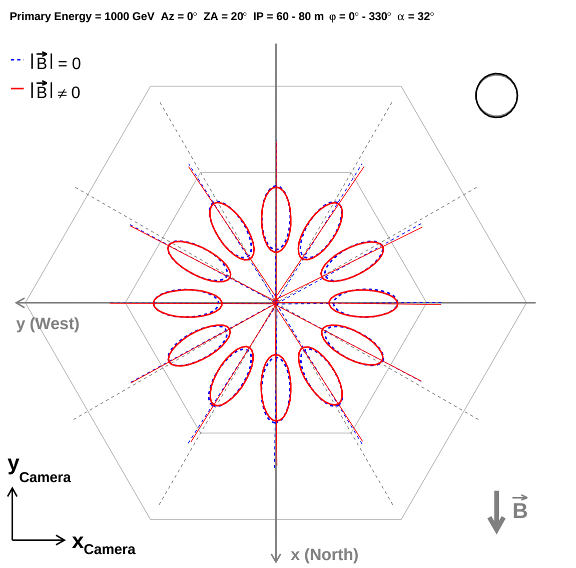

(b) Hard image cleaning, ZA 20°, azimuth angle 0°, impact parameter 60 - 80 m.

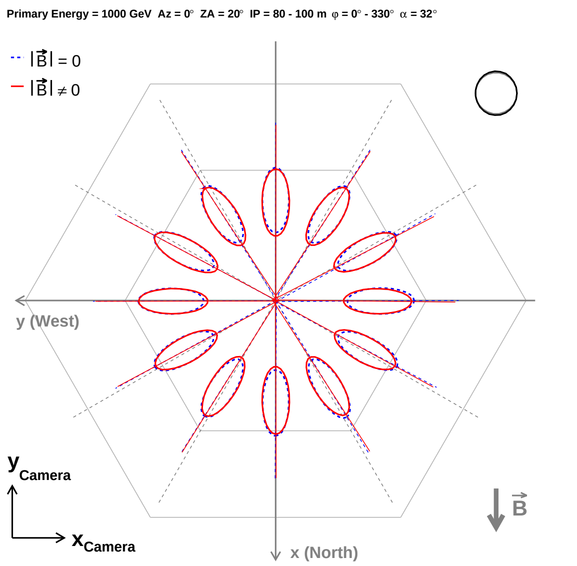

(c) Hard image cleaning, ZA 20°, azimuth angle 0°, impact parameter 80 - 100 m.

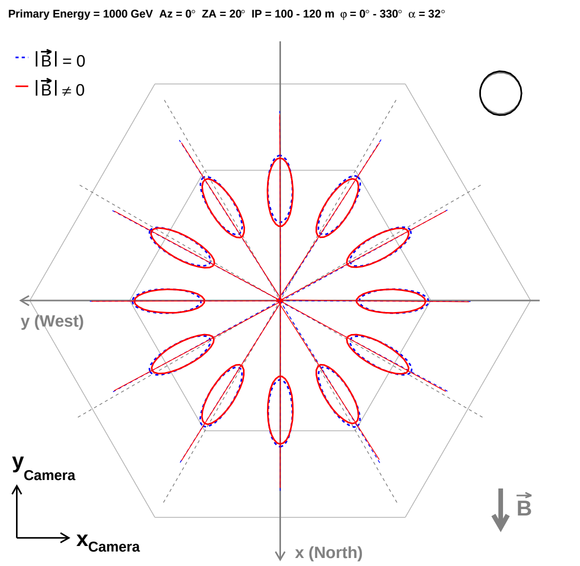

(d) Hard image cleaning, ZA 20°, azimuth angle 0°, impact parameter 100 - 120 m.

Figure 75: Hillas ellipses for MC γ-rays of 1 TeV energy and four impact parameter windows. The ZA was set to 20° and the azimuth angle to 0°. The angle φ was varied over the full range between 0° and 330°. While the red ellipses (solid lines) were obtained for enabled GF, the blue ones (dashed lines) were obtained for disabled GF. The black curve in the upper right part of the figure indicates the ellipticity of the Cherenkov light distribution on ground.

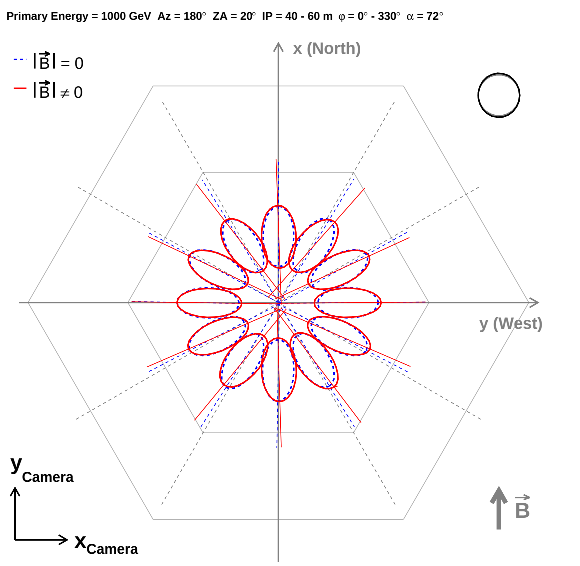

(a) Hard image cleaning, ZA 20°, azimuth angle 180°, impact parameter 40 - 60 m.

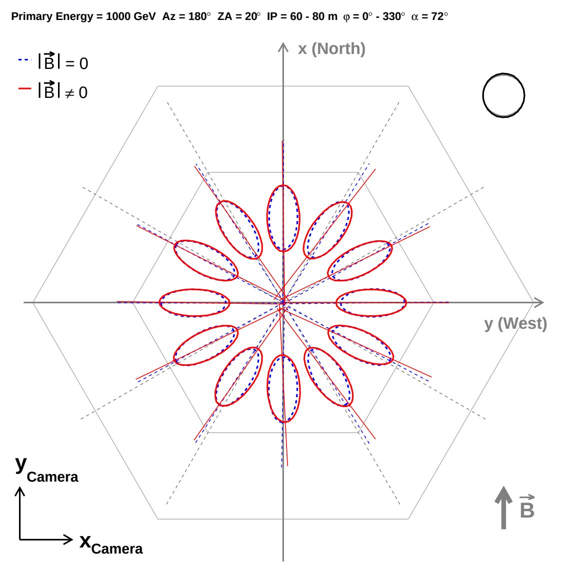

(b) Hard image cleaning, ZA 20°, azimuth angle 180°, impact parameter 60 - 80 m.

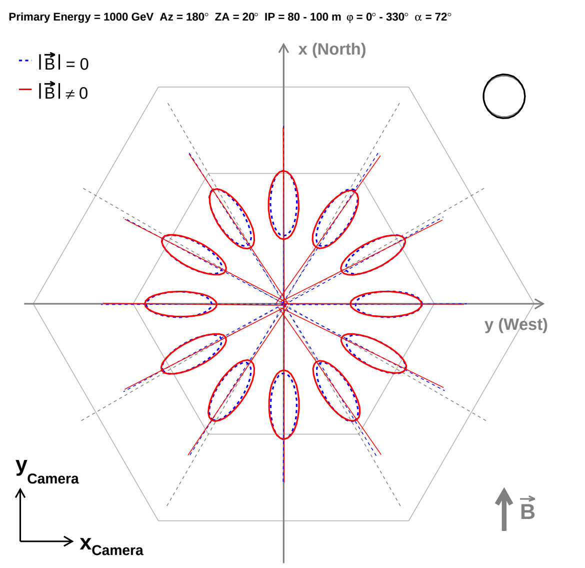

(c) Hard image cleaning, ZA 20°, azimuth angle 180°, impact parameter 80 - 100 m.

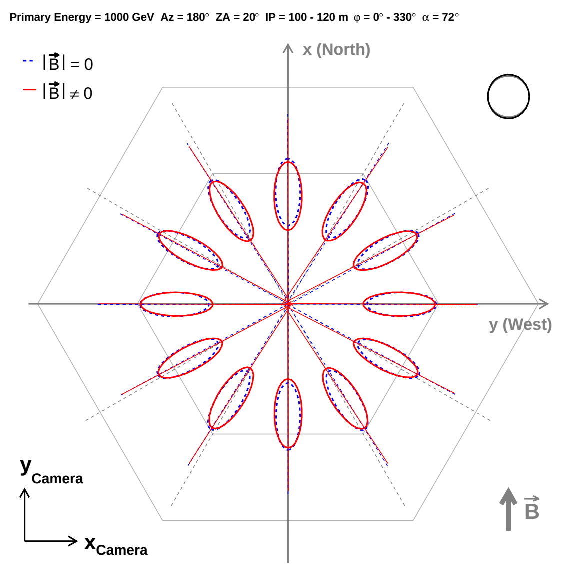

(d) Hard image cleaning, ZA 20°, azimuth angle 180°, impact parameter 100 - 120 m.

Figure 76: Hillas ellipses for MC γ-rays of 1 TeV energy and four impact parameter windows. The ZA was set to 20° and the azimuth angle to 180°. The angle φ was varied over the full range between 0° and 330°. While the red ellipses (solid lines) were obtained for enabled GF, the blue ones (dashed lines) were obtained for disabled GF. The black curve in the upper right part of the figure indicates the ellipticity of the Cherenkov light distribution on ground.

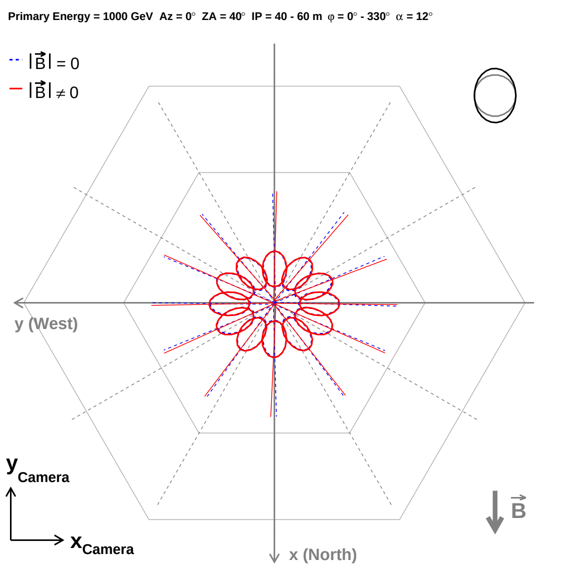

(a) Hard image cleaning, ZA 40°, azimuth angle 0°, impact parameter 40 - 60 m.

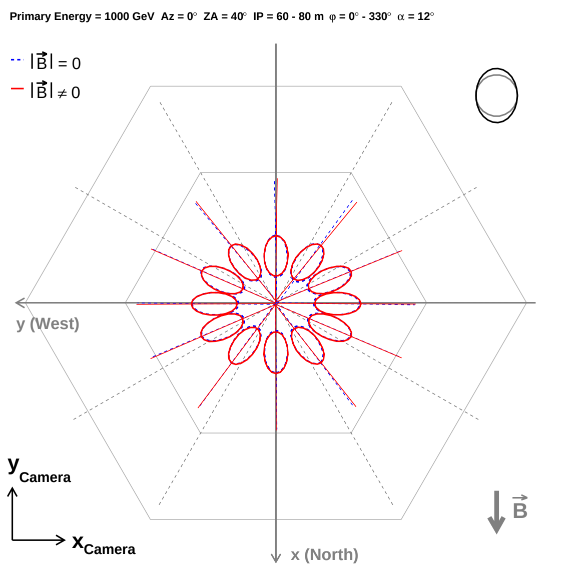

(b) Hard image cleaning, ZA 40°, azimuth angle 0°, impact parameter 60 - 80 m.

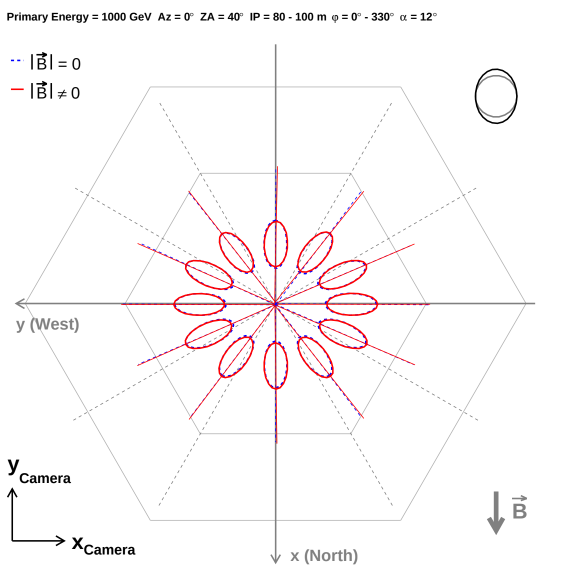

(c) Hard image cleaning, ZA 40°, azimuth angle 0°, impact parameter 80 - 100 m.

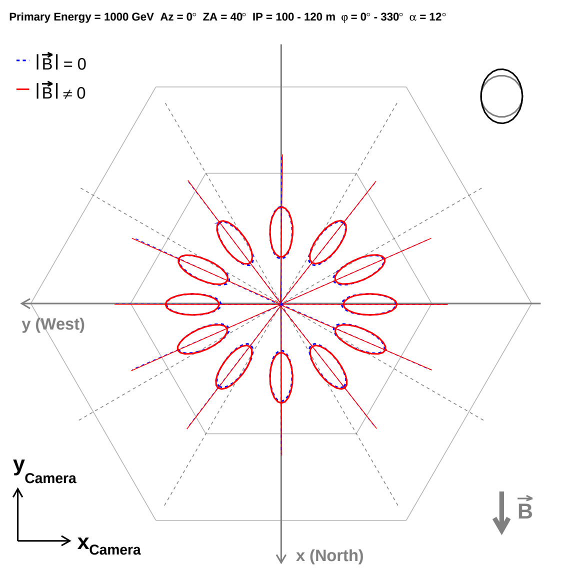

(d) Hard image cleaning, ZA 40°, azimuth angle 0°, impact parameter 100 - 120 m.

Figure 77: Hillas ellipses for MC γ-rays of 1 TeV energy and four impact parameter windows. The ZA was set to 40° and the azimuth angle to 0°. The angle φ was varied over the full range between 0° and 330°. While the red ellipses (solid lines) were obtained for enabled GF, the blue ones (dashed lines) were obtained for disabled GF. The black curve in the upper right part of the figure indicates the ellipticity of the Cherenkov light distribution on ground.

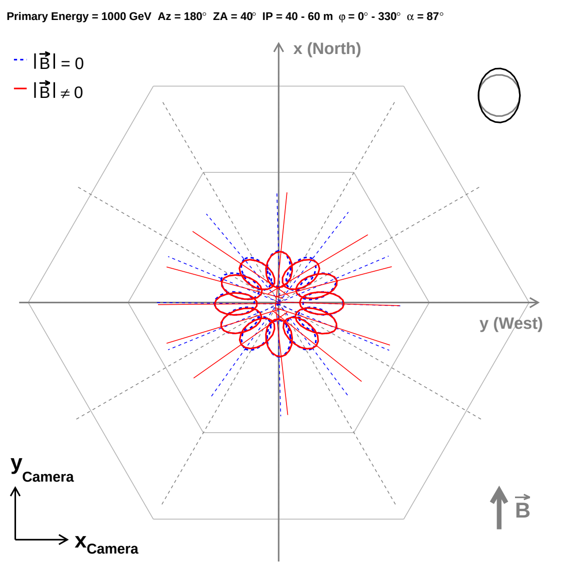

(a) Hard image cleaning, ZA 40°, azimuth angle 180°, impact parameter 20 - 60 m.

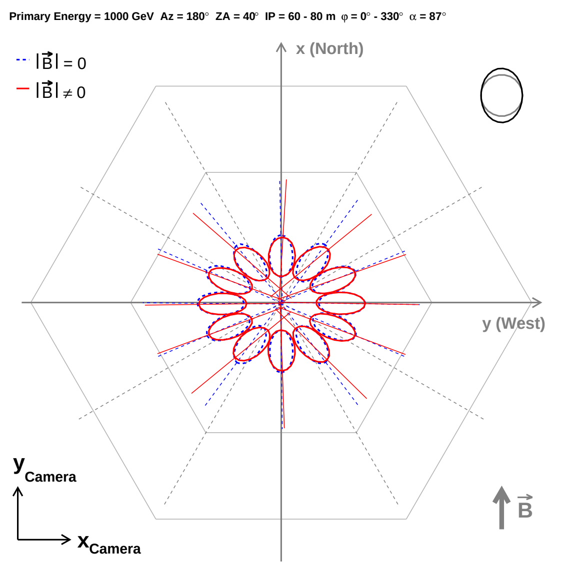

(b) Hard image cleaning, ZA 40°, azimuth angle 180°, impact parameter 60 - 80 m.

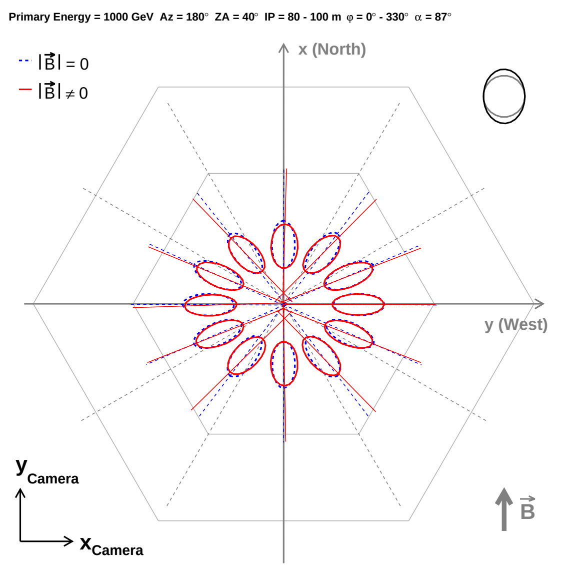

(c) Hard image cleaning, ZA 40°, azimuth angle 180°, impact parameter 80 - 100 m.

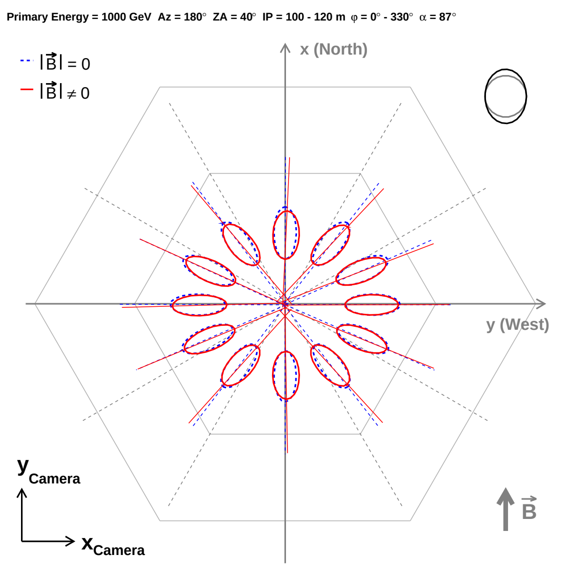

(d) Hard image cleaning, ZA 40°, azimuth angle 180°, impact parameter 100 - 120 m.

Figure 78: Hillas ellipses for MC γ-rays of 1 TeV energy and four impact parameter windows. The ZA was set to 40° and the azimuth angle to 180°. The angle φ was varied over the full range between 0° and 330°. While the red ellipses (solid lines) were obtained for enabled GF, the blue ones (dashed lines) were obtained for disabled GF. The black curve in the upper right part of the figure indicates the ellipticity of the Cherenkov light distribution on ground.

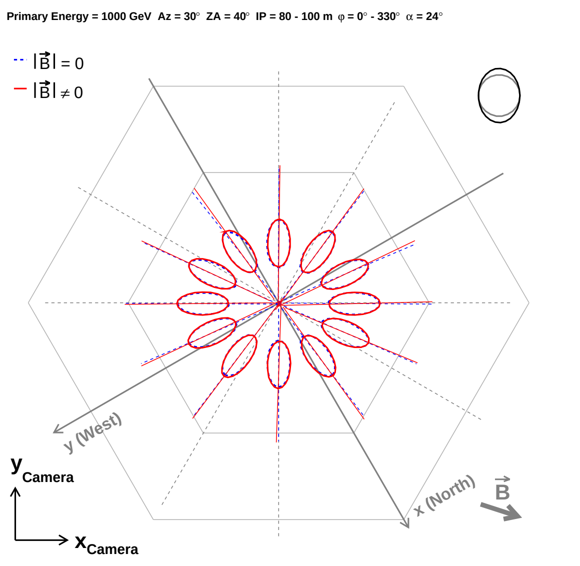

(a) Hard image cleaning, ZA 40°, azimuth angle 30°.

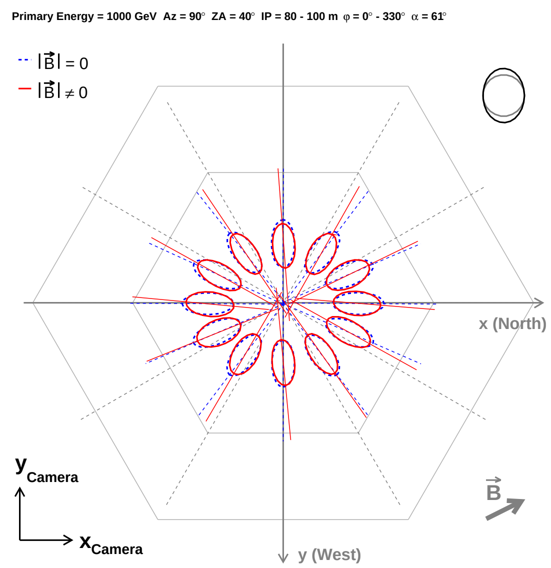

(b) Hard image cleaning, ZA 40°, azimuth angle 90°.

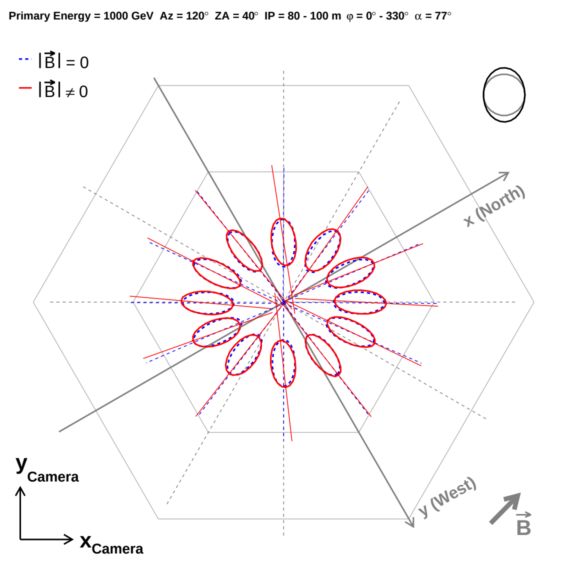

(c) Hard image cleaning, ZA 40°, azimuth angle 120°.

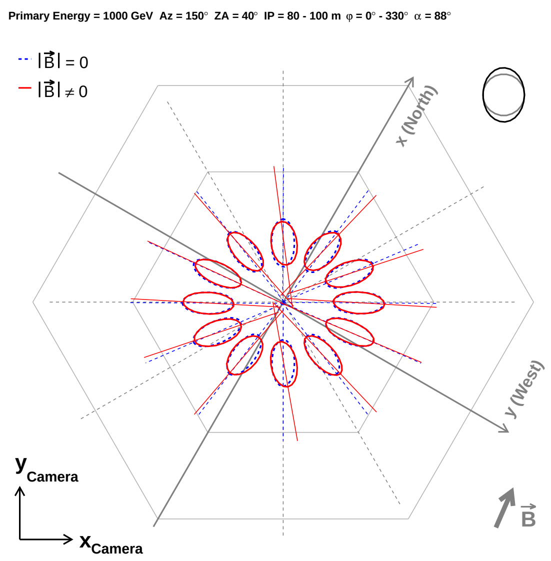

(d) Hard image cleaning, ZA 40°, azimuth angle 150°.

Figure 79: Hillas ellipses for MC γ-rays of 1 TeV energy and impact parameters between 80 m and 100 m. The ZA was set to 40° and the azimuth angle to 30°, 90°, 120° and 150°. The angle φ was varied over the full range between 0° and 330°. While the red ellipses (solid lines) were obtained for enabled GF, the blue ones (dashed lines) were obtained for disabled GF. The black curve in the upper right part of the figure indicates the ellipticity of the Cherenkov light distribution on ground.

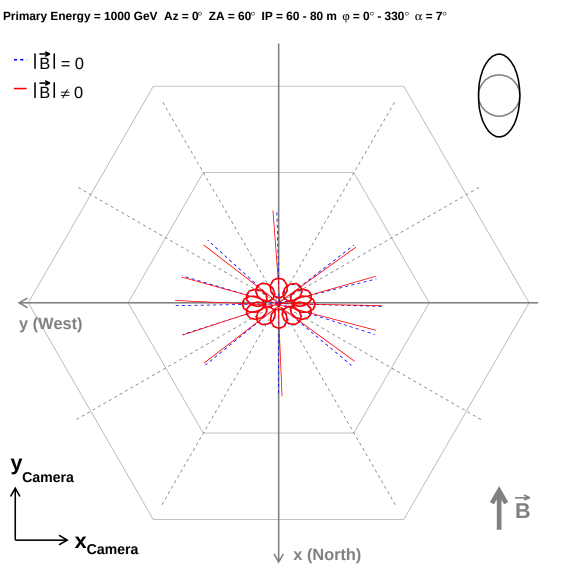

(a) Hard image cleaning, ZA 60°, azimuth angle 0°, impact parameter 60 - 80 m.

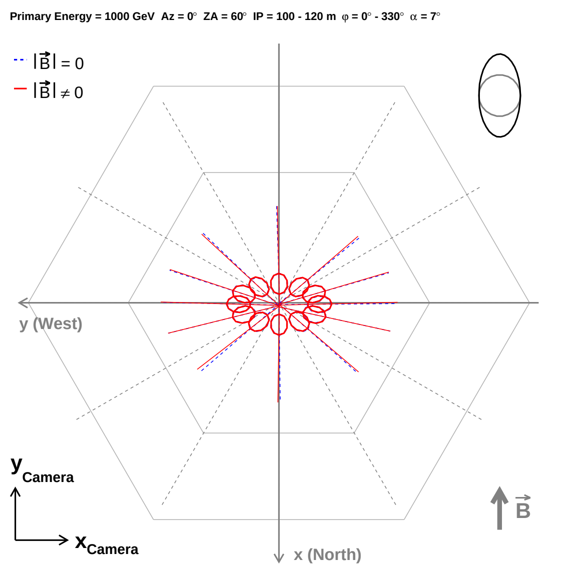

(b) Hard image cleaning, ZA 60°, azimuth angle 0°, impact parameter 100 - 120 m.

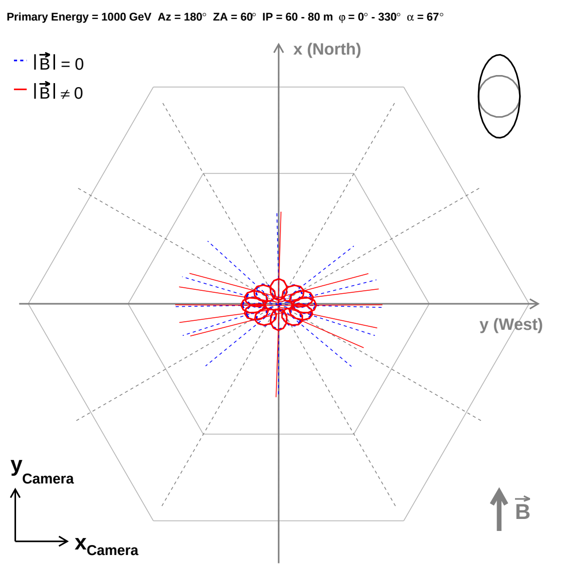

(c) Hard image cleaning, ZA 60°, azimuth angle 180°, impact parameter 60 - 80 m.

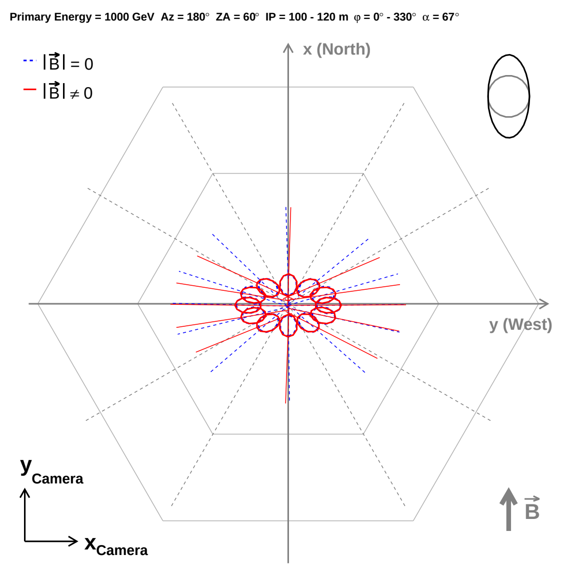

(d) Hard image cleaning, ZA 60°, azimuth angle 180°, impact parameter 100 - 120 m.

Figure 80: Hillas ellipses for MC γ-rays of 1 TeV energy and two impact parameter windows. The ZA was set to 60° and the azimuth angle to 0° and 180°. The angle φ was varied over the full range between 0° and 330°. While the red ellipses (solid lines) were obtained for enabled GF, the blue ones (dashed lines) were obtained for disabled GF. The black curve in the upper right part of the figure indicates the ellipticity of the Cherenkov light distribution on ground.

The Rotation Angle of MC γ-Ray Shower Images on closer Inspection

It was shown in the preceding section that γ-ray shower images can be significantly rotated away from their nominal orientation. Furthermore, is was demonstrated that the rotation angle of shower images depends on various parameters like the γ-ray energy, the ZA, the azimuth angle, the impact parameter and the orientation of the shower with respect to the telescope. This paragraph focuses on the dependency of the rotation angle on the γ-ray energy, the impact parameter and the orientation of the primary γ-rays.

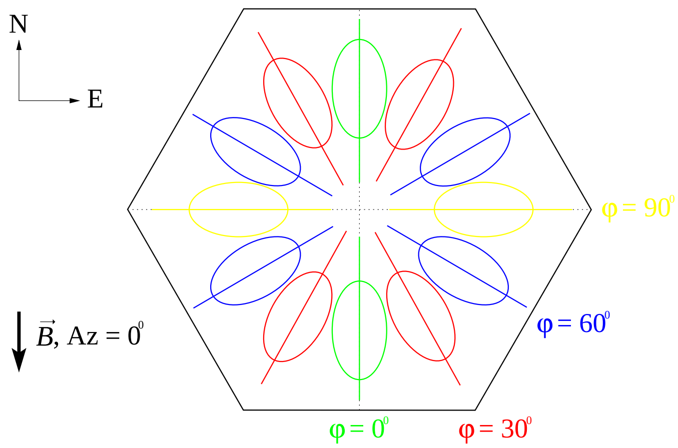

Figure 81: The relation between the telescope positions and image orientation in the camera. The green images correspond to the case where the connecting line between shower axis and telescope optical axis is parallel to the north-south direction, i.e. the telescope is situated on the x-axis of the CORSIKA coordinate system ($\varphi = 0°$). The yellow images are obtained when the telescope is situated on the y-axis of the CORSIKA coordinate system ($\varphi = 90°$).

To compare equivalent arrangements we considered only two azimuth angles, i.e. 0° and 180°. For all other arrangements, i.e. for azimuth angles $\neq 0°$, 180° and ZA $> 0°$ the shower images in the camera are not situated at equivalent positions with respect to the projection of the GF in the camera (see e.g. figures 59, 65 and 72).
Figure 81 shows the relation between the telescope positions and image orientation in the camera. From the preceeding section we know that the green and the yellow images are not rotated whereas the blue and the red images can be rotated due to the influence of the GF. The color code used for the following figures corresponds to the one in figure 81.
Figures 82 - 85 show the rotation angle versus γ-ray energy for two impact parameter windows (40 m - 60 m and 100 m - 120 m), different orientations of the telescope and the intermediate image cleaning. The figures show that the rotation of the images becomes largest for small impact parameters. Furthermore, for all telescope orientations which are unfavorable with regard to the influence of the GF (large vertical transversal GF component) the rotation angle increases between $\sim$ 100 GeV and $\sim$ 400 GeV (e.g. figure 83). The (red) images obtained for $\varphi = 30°$, 150°, 210° and 330° are rotated most of all. It is remarkable that the rotation angle is largest for energies well above 100 GeV. There are indications that the direction of rotation reverses for energies around 100 - 150 GeV (figure 82 (b)). However, due to the limited statistics at those energies the error on the rotation angle is comparatively large.
Figures 86 - 93 show the rotation angle versus true impact parameter (see section 2) for different energies and telescope orientations. The intermediate image cleaning was applied. At low energies

(∼ 50 GeV) the rotation angle is comparatively small. Nevertheless, at higher energies the rotation angle clearly depends on the true impact parameter. The figures also show that the rotation of the images becomes largest for small impact parameters. At energies below ∼ 170 GeV the rotation angle changes its sign depending on the impact parameter (e.g. figure 86 (d)) whereas at higher energies (∼ 300 GeV) the rotation angle stays predominantly positive and approaches zero for large impact parameters (≲ 100 m, e.g. figure 89 (c)).

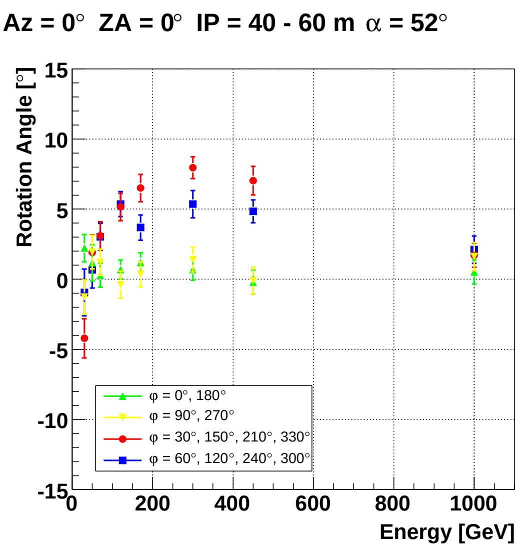

(a) 0° azimuth angle, 0° ZA, impact parameter 40 m - 60 m.

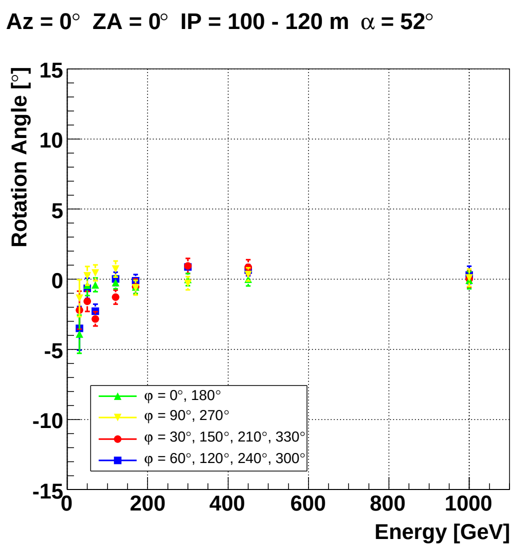

(b) 0° azimuth angle, 0° ZA, impact parameter 100 m - 120 m.

Figure 82: Rotation angle versus energy for MC γ-rays, impact parameters between 40 m and 120 m, 0° ZA and 0° azimuth angle. The intermediate image cleaning was applied.

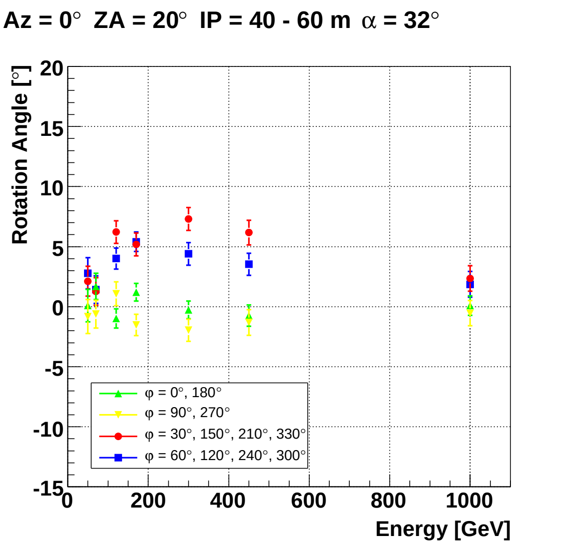

(a) 0° azimuth angle, 20° ZA, impact parameter 40 m - 60 m.

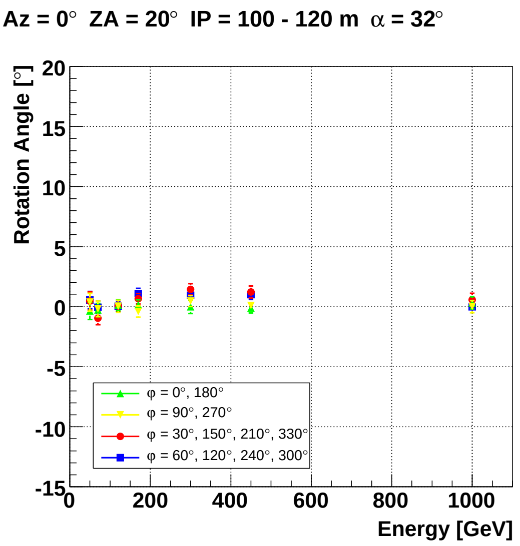

(b) 0° azimuth angle, 20° ZA, impact parameter 100 m - 120 m.

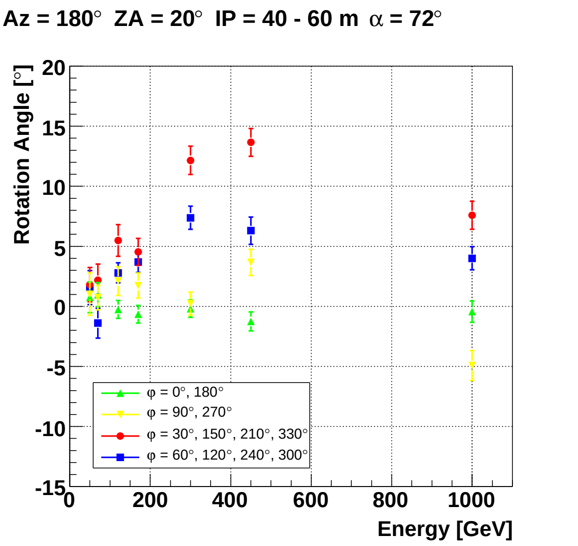

(c) 180° azimuth angle, 20° ZA, impact parameter 40 m - 60 m.

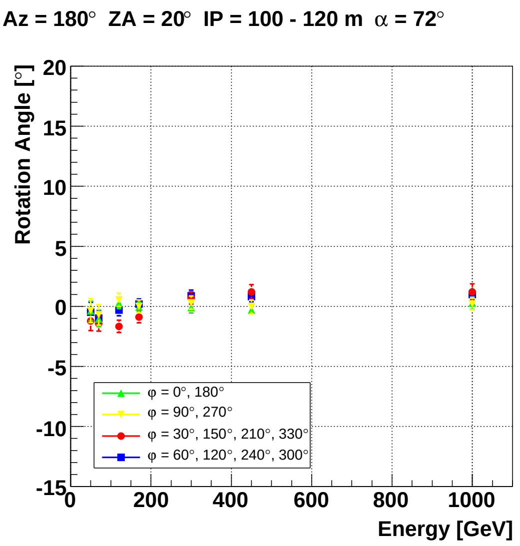

(d) 180° azimuth angle, 20° ZA, impact parameter 100 m - 120 m.

Figure 83: Rotation angle versus energy for MC γ-rays, impact parameters between 40 m and 120 m, 20° ZA, 0° and 180° azimuth angle. The intermediate image cleaning was applied.

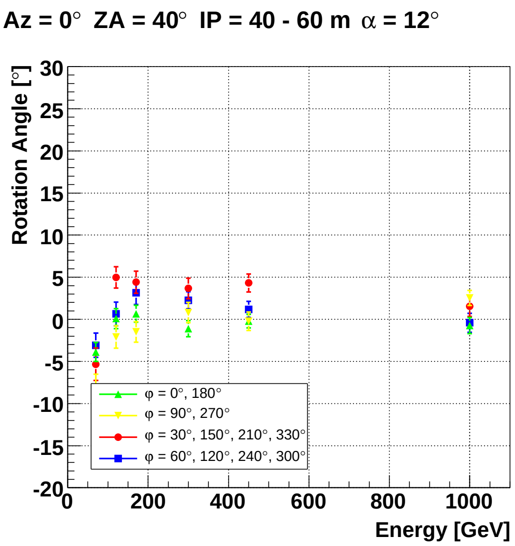

(a) 0° azimuth angle, 40° ZA, impact parameter 40 m - 60 m.

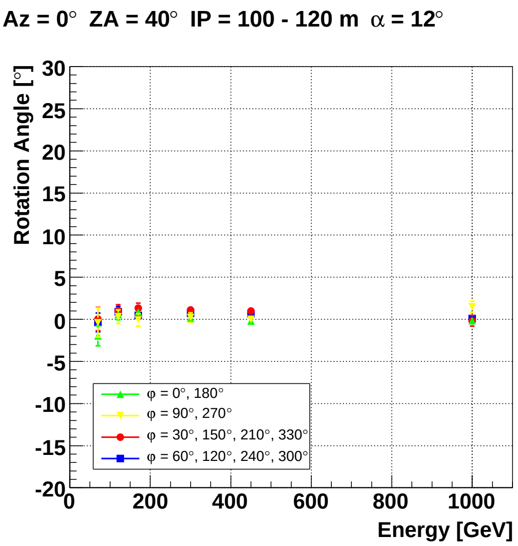

(b) 0° azimuth angle, 40° ZA, impact parameter 100 m - 120 m.

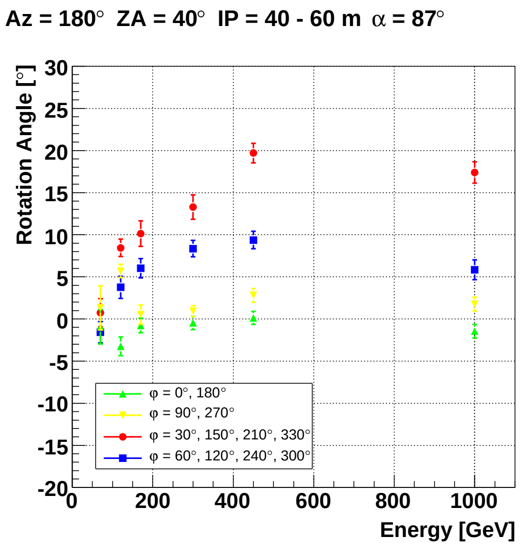

(c) 180° azimuth angle, 40° ZA, impact parameter 40 m - 60 m.

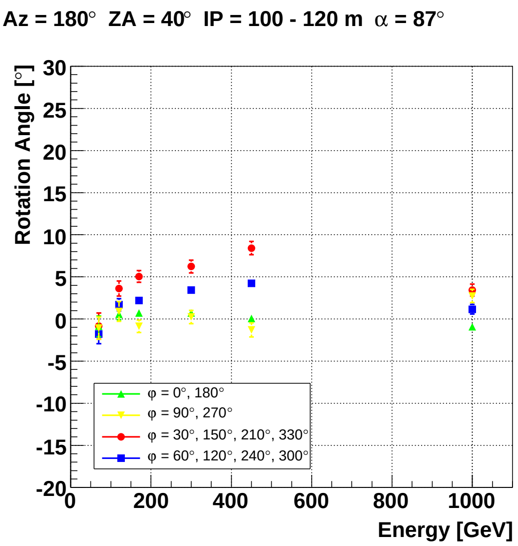

(d) 180° azimuth angle, 40° ZA, impact parameter 100 m - 120 m.

Figure 84: Rotation angle versus energy for MC γ-rays, impact parameters between 40 m and 120 m, 40° ZA, 0° and 180° azimuth angle. The intermediate image cleaning was applied.

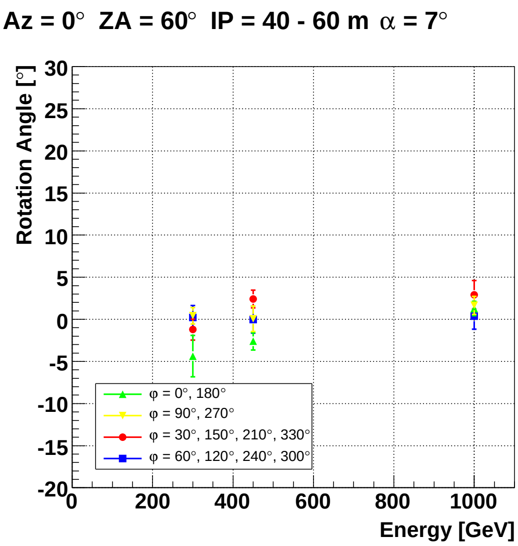

(a) 0° azimuth angle, 60° ZA, impact parameter 40 m - 60 m.

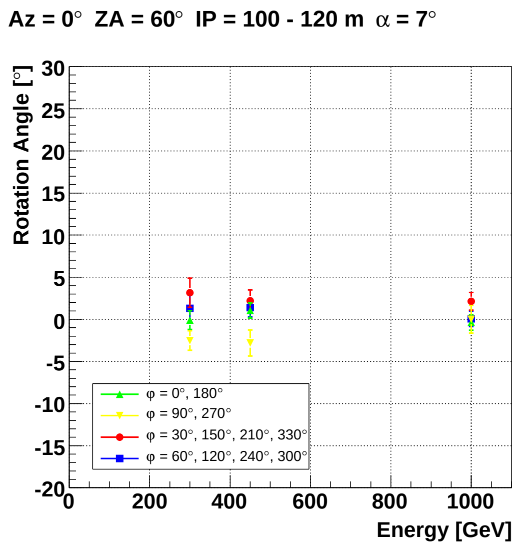

(b) 0° azimuth angle, 60° ZA, impact parameter 100 m - 120 m.

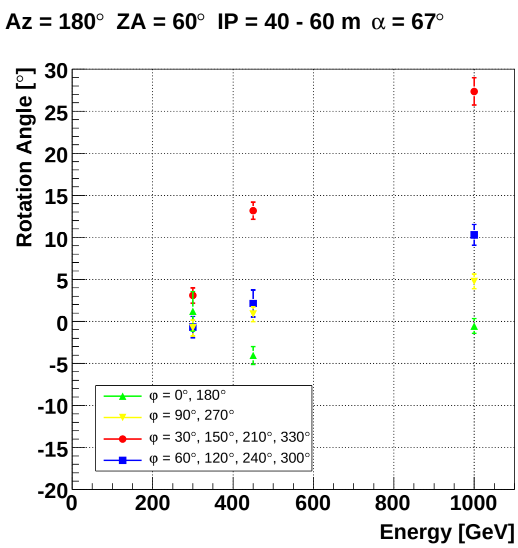

(c) 180° azimuth angle, 60° ZA, impact parameter 40 m - 60 m.

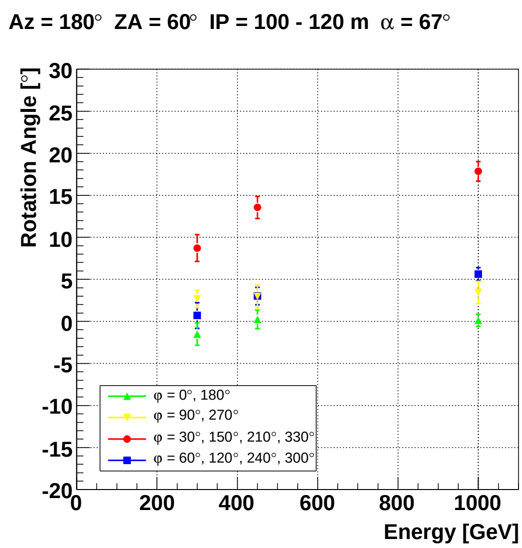

(d) 180° azimuth angle, 60° ZA, impact parameter 100 m - 120 m.

Figure 85: Rotation angle versus energy for MC γ-rays, impact parameters between 40 m and 120 m, 60° ZA, 0° and 180° azimuth angle. The intermediate image cleaning was applied.

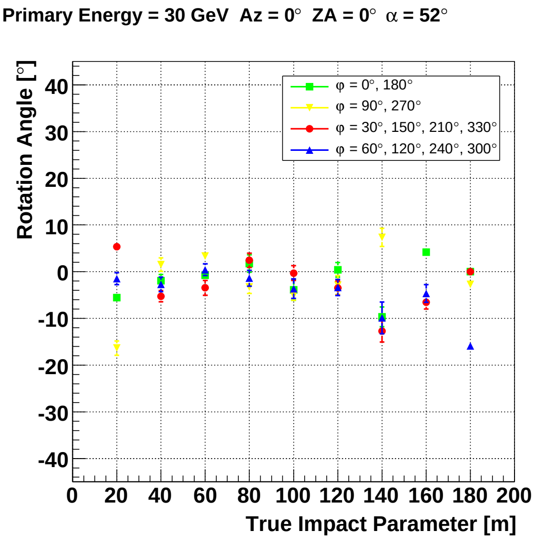

(a) 0° azimuth angle, 0° ZA, 30 GeV energy.

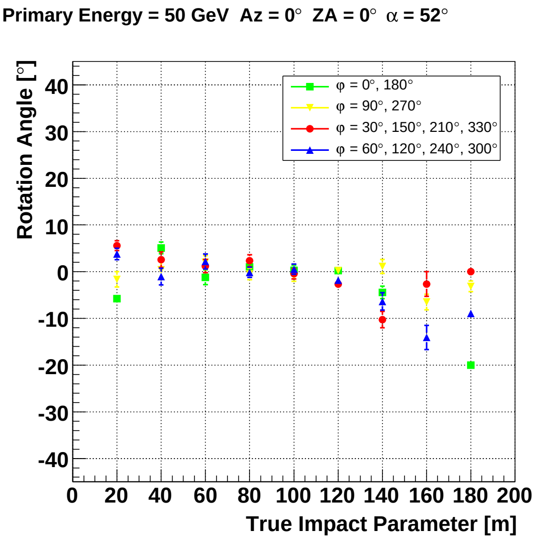

(b) 0° azimuth angle, 0° ZA, 50 GeV energy.

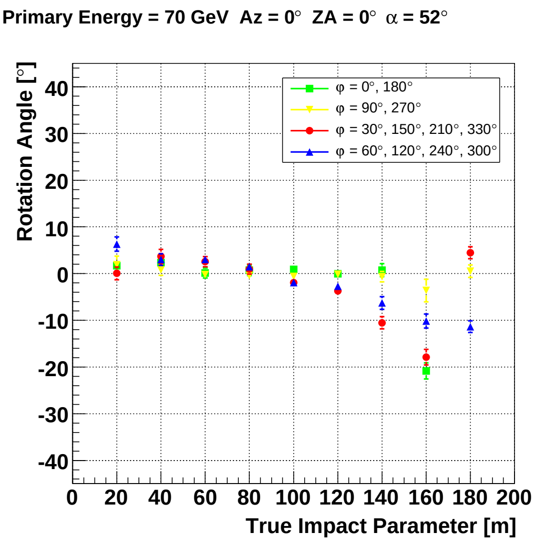

(c) 0° azimuth angle, 0° ZA, 70 GeV energy.

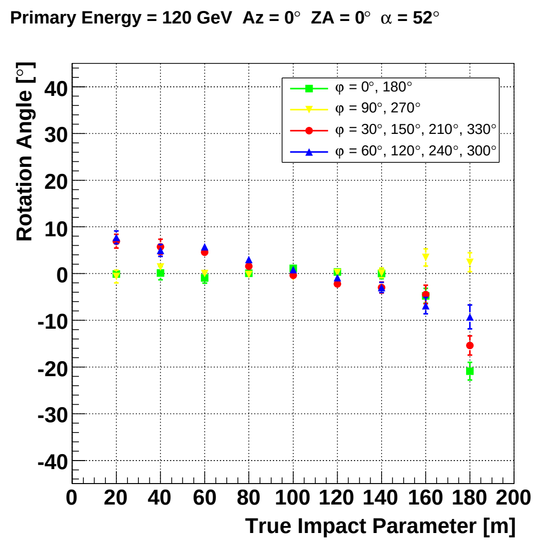

(d) 0° azimuth angle, 0° ZA, 120 GeV energy.

Figure 86: Rotation angle versus true impact parameter for 0° ZA, 0° azimuth angle, 30 GeV, 50 GeV, 70 GeV and 120 GeV MC γ-rays. The intermediate image cleaning was applied.

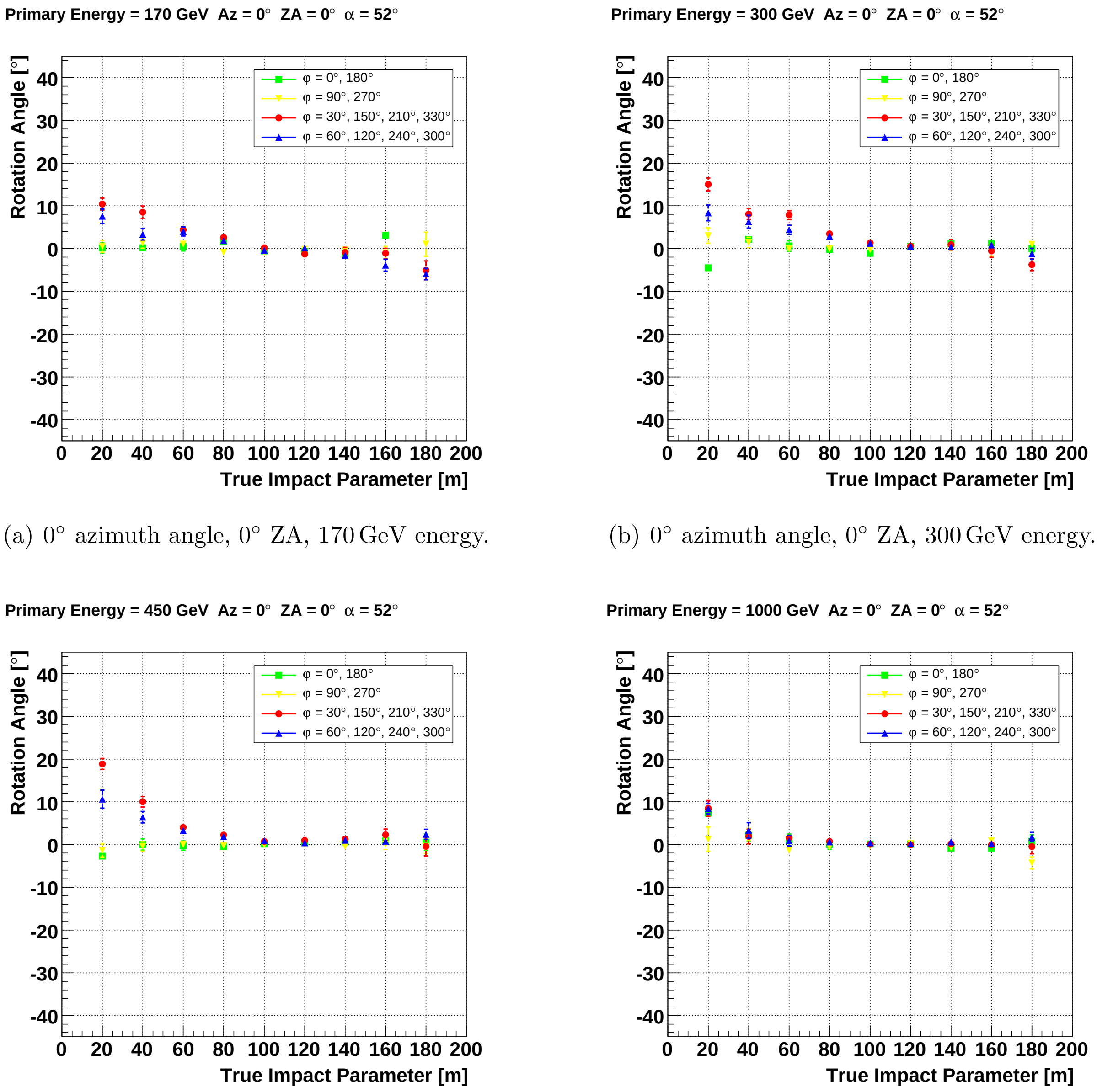

(a) 0° azimuth angle, 0° ZA, 170 GeV energy.

(b) 0° azimuth angle, 0° ZA, 300 GeV energy.

(c) 0° azimuth angle, 0° ZA, 450 GeV energy.

(d) 0° azimuth angle, 0° ZA, 1000 GeV energy.

Figure 87: Rotation angle versus true impact parameter for 0° ZA, 0° azimuth angle, 170 GeV, 300 GeV, 450 GeV and 1000 GeV MC γ-rays. The intermediate image cleaning was applied.

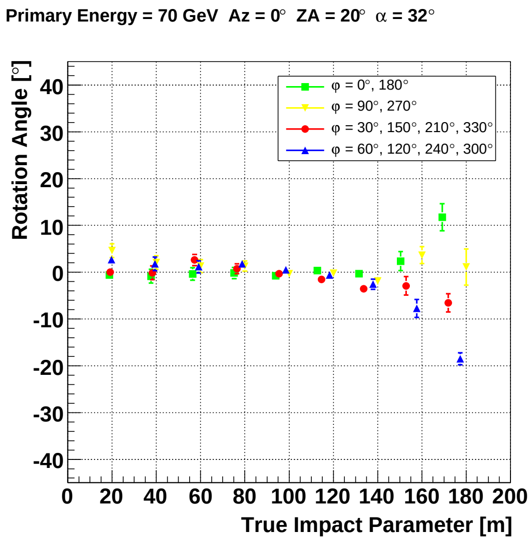

(a) 0° azimuth angle, 20° ZA, 70 GeV energy.

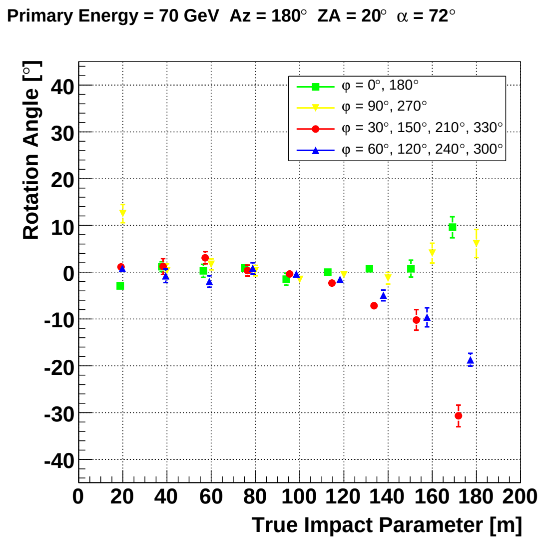

(b) 180° azimuth angle, 20° ZA, 70 GeV energy.

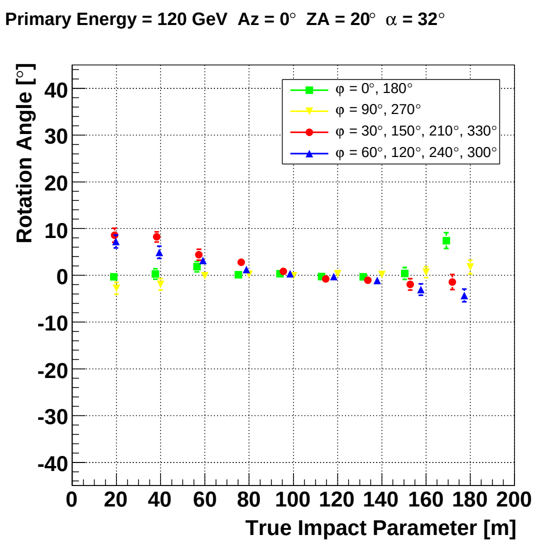

(c) 0° azimuth angle, 20° ZA, 120 GeV energy.

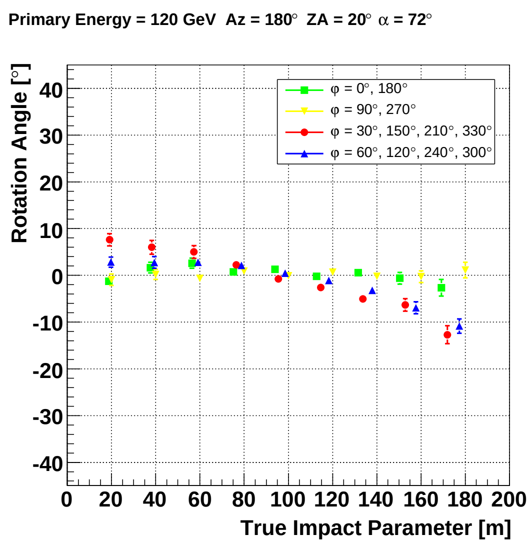

(d) 180° azimuth angle, 20° ZA, 120 GeV energy.

Figure 88: Rotation angle versus true impact parameter for 20° ZA, 0° and 180° azimuth angle, 70 GeV and 120 GeV MC γ-rays. The intermediate image cleaning was applied.

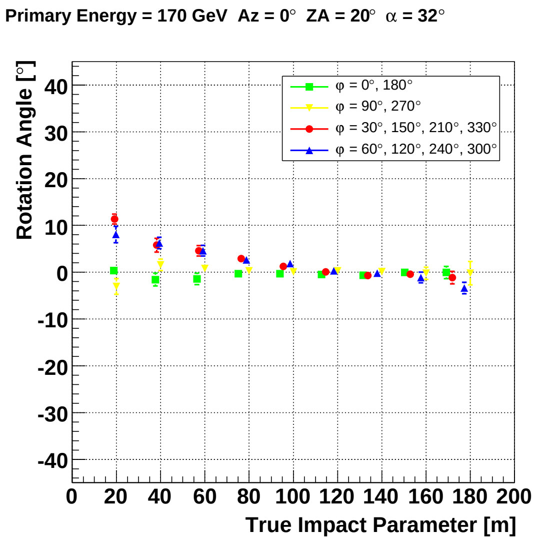

(a) 0° azimuth angle, 20° ZA, 170 GeV energy.

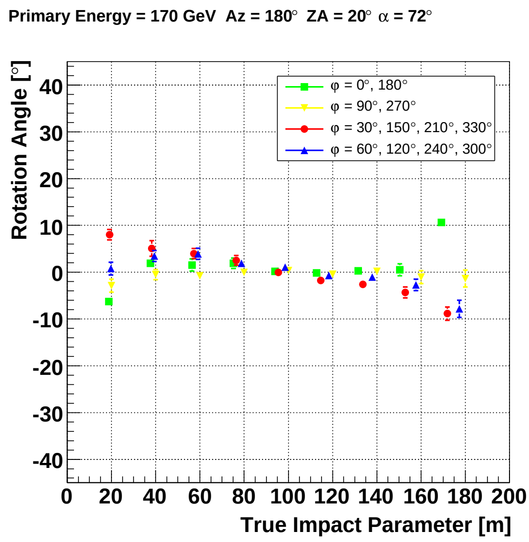

(b) 180° azimuth angle, 20° ZA, 170 GeV energy.

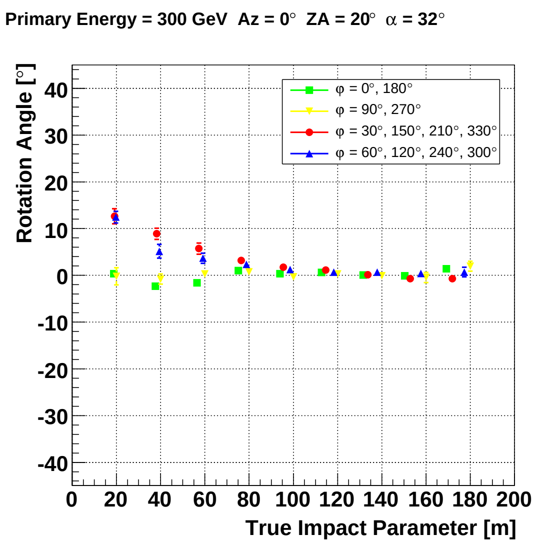

(c) 0° azimuth angle, 20° ZA, 300 GeV energy.

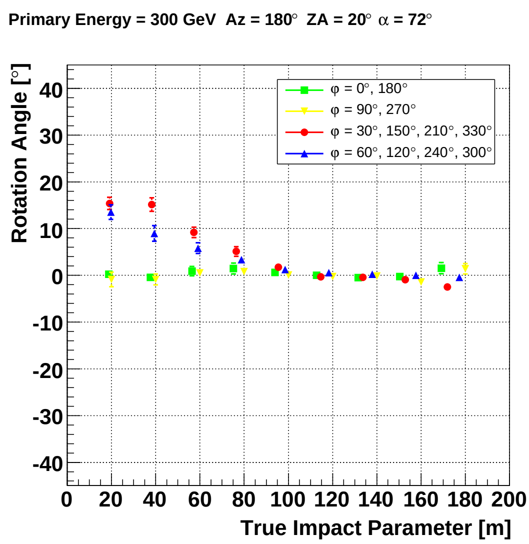

(d) 180° azimuth angle, 20° ZA, 300 GeV energy.

Figure 89: Rotation angle versus true impact parameter for 20° ZA, 0° and 180° azimuth angle, 170 GeV and 300 GeV MC γ-rays. The intermediate image cleaning was applied.

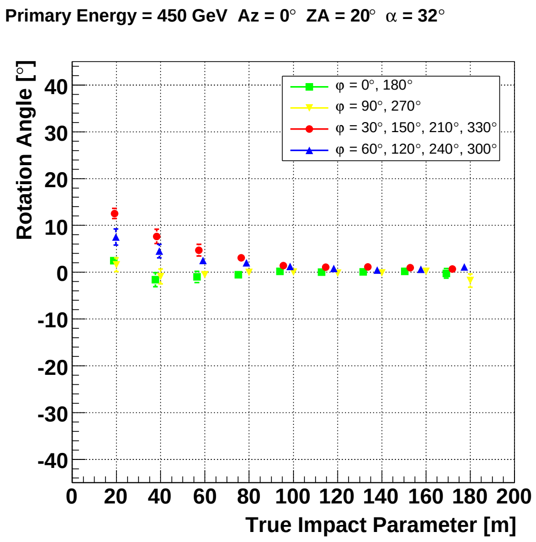

(a) 0° azimuth angle, 20° ZA, 450 GeV energy.

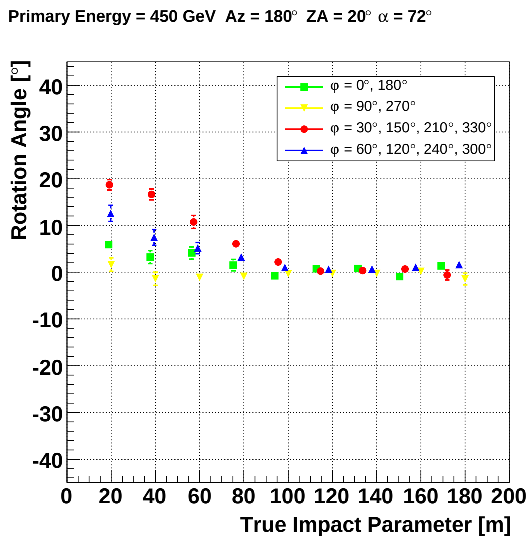

(b) 180° azimuth angle, 20° ZA, 450 GeV energy.

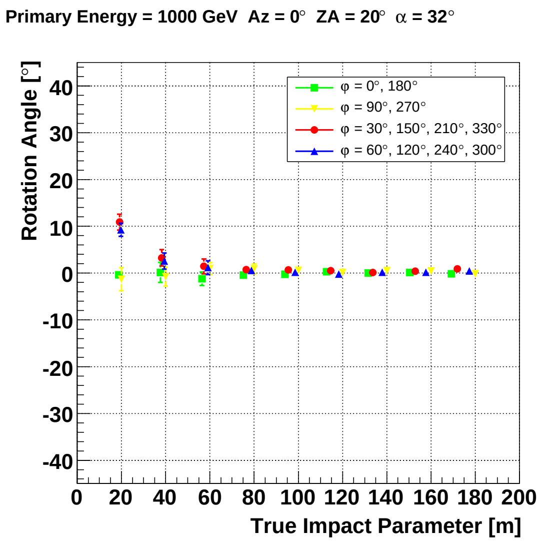

(c) 0° azimuth angle, 20° ZA, 1000 GeV energy.

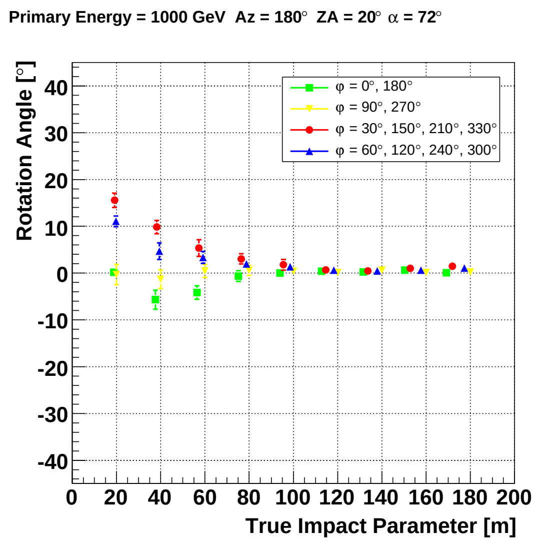

(d) 180° azimuth angle, 20° ZA, 1000 GeV energy.

Figure 90: Rotation angle versus true impact parameter for 20° ZA, 0° and 180° azimuth angle, 450 GeV and 1000 GeV MC γ-rays. The intermediate image cleaning was applied.

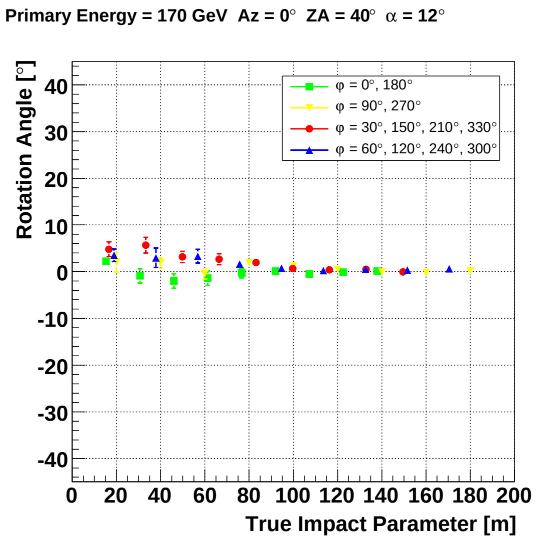

(a) 0° azimuth angle, 40° ZA, 170 GeV energy.

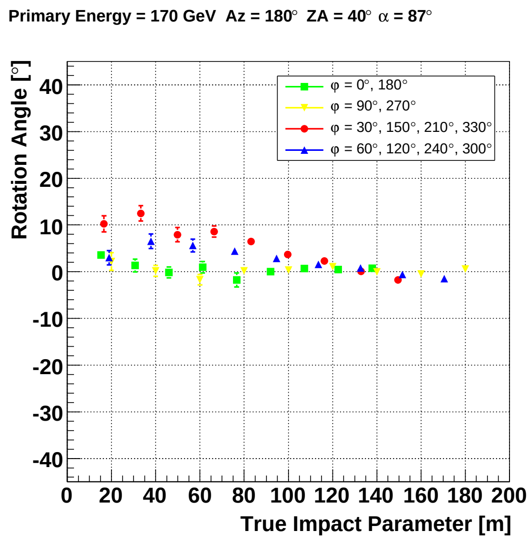

(b) 180° azimuth angle, 40° ZA, 170 GeV energy.

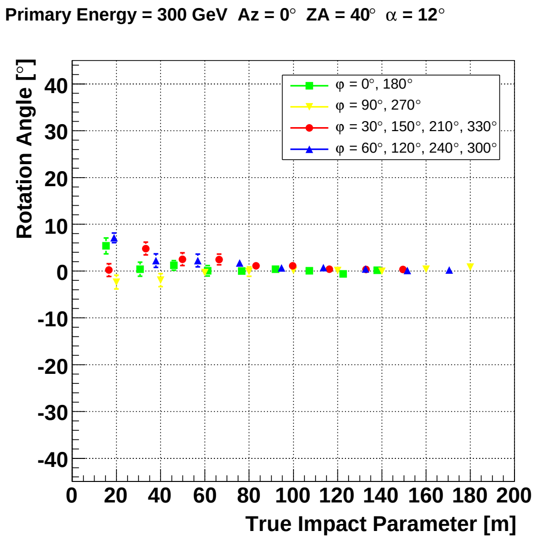

(c) 0° azimuth angle, 40° ZA, 300 GeV energy.

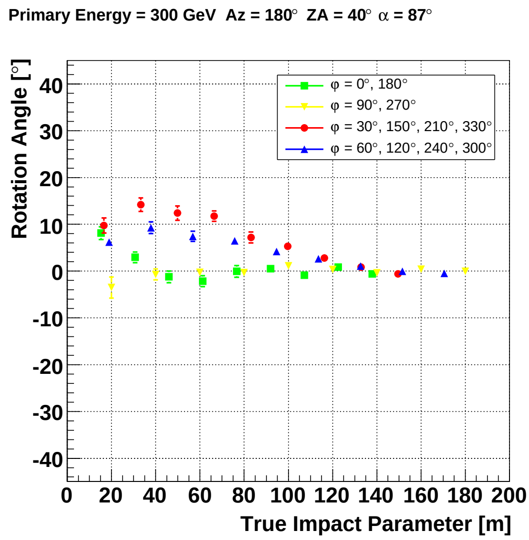

(d) 180° azimuth angle, 40° ZA, 300 GeV energy.

Figure 91: Rotation angle versus true impact parameter for 20° ZA, 0° and 180° azimuth angle, 170 GeV and 300 GeV MC γ-rays. The intermediate image cleaning was applied.

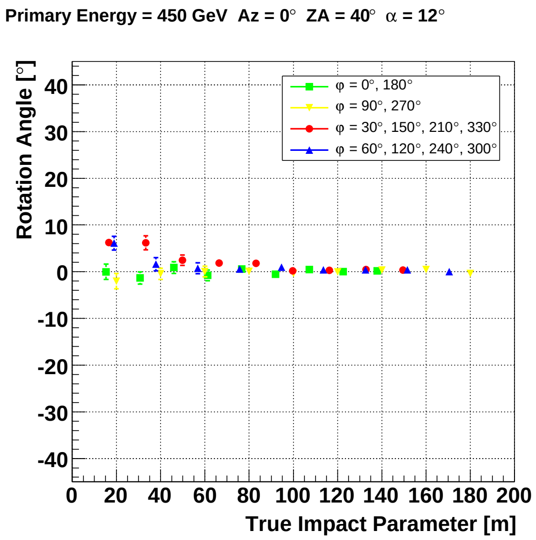

(a) 0° azimuth angle, 40° ZA, 450 GeV energy.

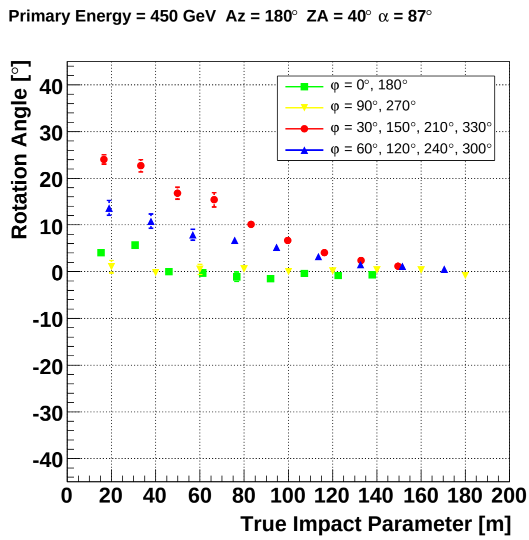

(b) 180° azimuth angle, 40° ZA, 450 GeV energy.

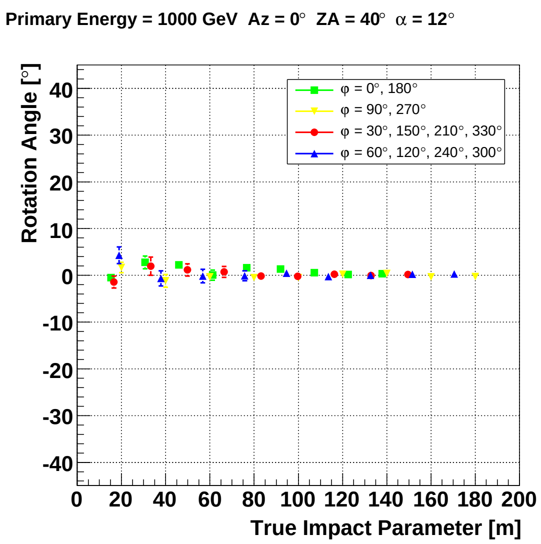

(c) 0° azimuth angle, 40° ZA, 1000 GeV energy.

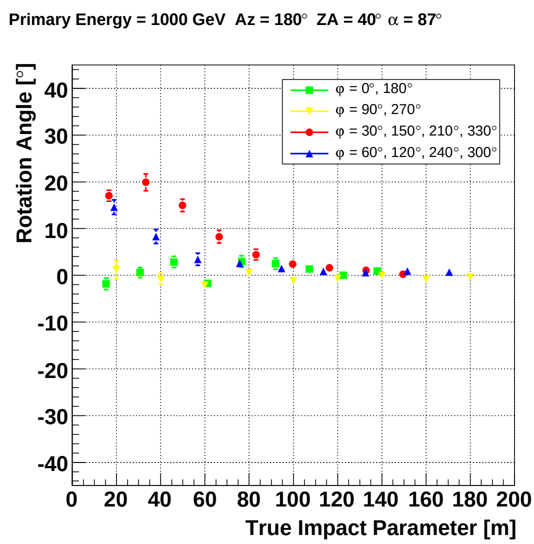

(d) 180° azimuth angle, 40° ZA, 1000 GeV energy.

Figure 92: Rotation angle versus true impact parameter for 40° ZA, 0° and 180° azimuth angle, 450 GeV and 1000 GeV MC γ-rays. The intermediate image cleaning was applied.

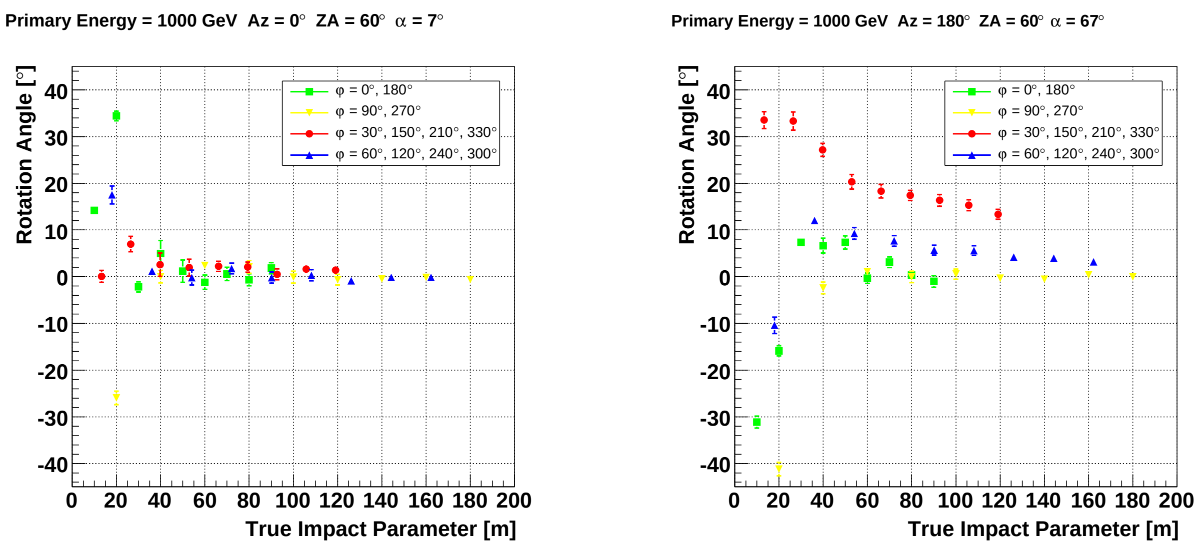

(a) 0° azimuth angle, 60° ZA.

(b) 180° azimuth angle, 60° ZA.

Figure 93: Rotation angle versus true impact parameter for 60° ZA, 0° and 180° azimuth angle and 1000 GeV MC γ-rays. The intermediate image cleaning was applied.

3.1.2 The Influence of the GF on the Image Parameter ALPHA

Although it was shown in the preceding paragraph that the GF can strongly alter the average orientation of shower images and therefore the pointing of γ-rays originating from a VHE γ-ray source under study, it remains important to investigate the influence of the GF on the image parameter ALPHA. The study of the average rotation of γ-ray induced shower images is not sufficient to conclude on the influence of the GF on the parameter ALPHA. In the preceding section it was demonstrated that shower images which are not oriented parallel or perpendicular to the projection of the GF in the camera can be significantly rotated away from the camera center. Although images oriented either parallel or perpendicular to the projection of the GF are not rotated the corresponding ALPHA distributions may be significantly broadened. It was shown elsewhere that the ALPHA distribution can be strongly affected by the influence of the GF [10, 14, 15, 24, 25, 28, 34, 36, 39]. However, it has not been investigated so far how the shape of the ALPHA distribution depends on the telescope position in the Cherenkov light pool on ground.

Figure 94 (a) (left panel) shows the normalized distributions of the image parameter ALPHA for MC γ-rays of 30 GeV, various telescope orientations and impact parameters between 20 m and 200 m. The soft image cleaning was applied. To get an impression of the average degradation of the ALPHA distribution with increasing GF strength, all telescope positions between $\varphi = 0° \ldots 330°$ were considered. The angle α (in parentheses) between the direction of the GF and the direction of the EAS, the azimuth angle as well as the percentage of γ showers lying within $|\text{ALPHA}| \leq 9°$ are given in the legend. As can be seen from the figures, the ALPHA distributions are rather flat, independent of the azimuth angle. The influence of the GF is hardly visible, even for 20° ZA, where the angle α increases with increasing azimuth angle (figure 94 (a), right panel).

Figure 94 (b) (left panel) shows the normalized ALPHA distributions obtained for a similar configuration of MC input parameters as before, but for the hard image cleaning. The application of the higher image cleaning levels results in a stronger peaked ALPHA distribution at around zero, but the influence of the GF is again hardly visible. At 20°, the situation is similar (figure 94 (b), right panel). The ALPHA distributions are rather dominated by fluctuations due to limited statistics of the dataset than by the influence of the GF, as the width of the ALPHA distributions does not exhibit a clear dependency on the strength of the GF.

Figure 95 shows the normalized ALPHA distributions for MC γ-rays of 450 GeV and similar MC simulation input parameters as before. At 0° ZA (upper left panel of the figure), the ALPHA distribution obtained for disabled GF is narrower than the ones obtained for enabled GF. The percentage of γ showers lying within $|\text{ALPHA}| \leq 9°$ is reduced by $\sim 10\,\%$ compared to the case of disabled GF. The ALPHA distributions obtained for enabled GF and different azimuth angles are compatible to each other, which is expected, as the angle α does not depend on the azimuth angle.

For ZA $> 0°$, the shape of the ALPHA distribution also depends on the azimuth angle, i.e. on the strength of the GF. Depending on the direction of the MC γ-ray, the influence of the GF on the shower development can result in a significant broadening of the ALPHA distribution. The percentage of γ showers lying within $|\text{ALPHA}| \leq 9°$ decreases with increasing azimuth angle. For 20° ZA (upper right panel in the figure) and enabled GF it decreases by $\sim 10\,\%$ and for 40° ZA (lower left panel in the figure) it decreases by up to $\sim 15\,\%$. Furthermore, the width of the ALPHA distributions increases with increasing ZA. At 60° ZA, the ALPHA distribution happens to be significantly broadened due to the decrease of the intensity of Cherenkov photons on ground, but also because the angular distance between telescope pointing direction and direction of the the shower (DIST) gets smaller for some positions of the telescope. The ALPHA distributions are rather dominated by fluctuations due to limited statistics of the dataset than by the influence of the GF. Normally, in case of ON-source observations,

the γ signal is expected to show up in an excess at small absolute values of the image parameter ALPHA, typically at $|\mathrm{ALPHA}| \lesssim 5° - 10°$. Therefore, in case of unfavorable pointing directions with regard to the influence of the GF, a certain fraction of the signal will be lost.
Figure 96 shows the normalized distribution of the image parameter ALPHA for MC γ-rays of 1 TeV and similar MC simulation input parameters as before. As can be seen from the ALPHA distributions the GF effects occur also at TeV energies. This was already noticed in the previous sections where the results from studies of GF effects on the shape and orientation of shower images were presented.

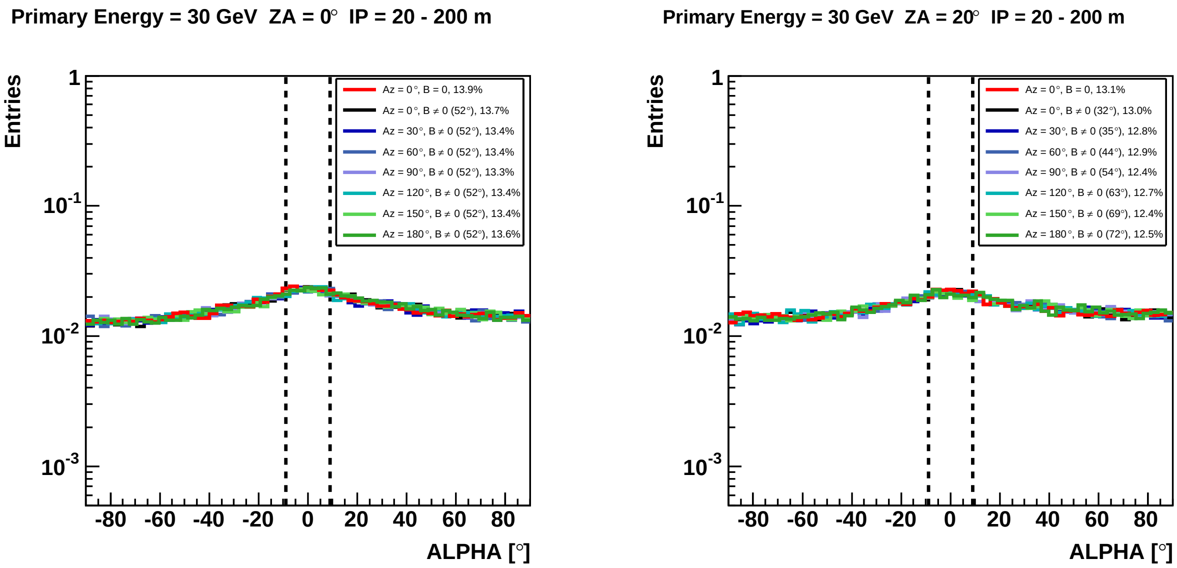

(a) Soft image cleaning.

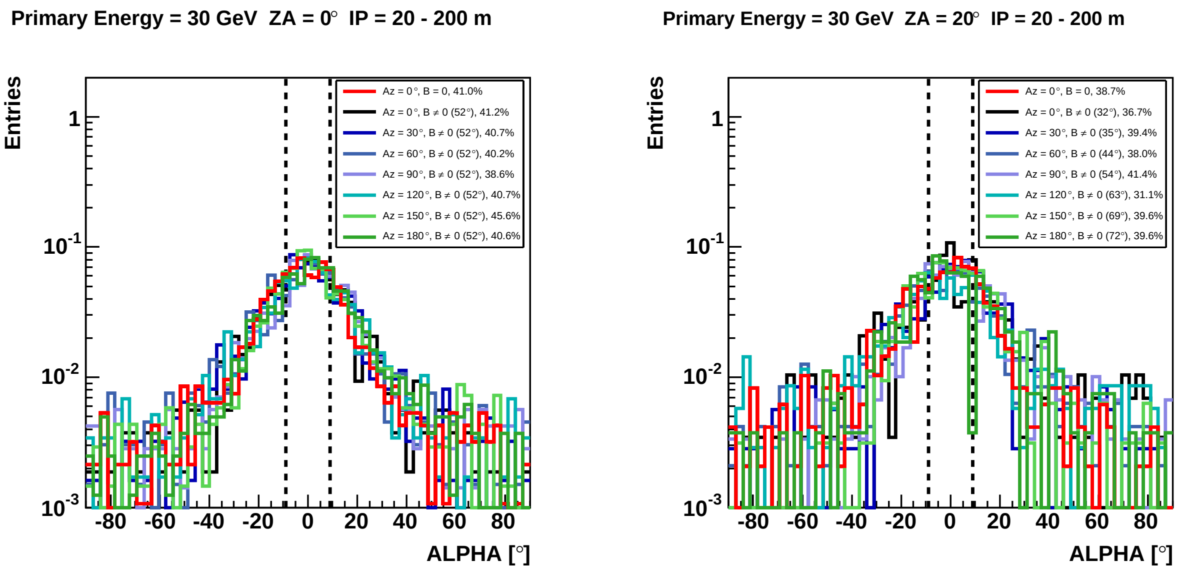

(b) Hard image cleaning.

Figure 94: Normalized distributions of the image parameter ALPHA for MC γ-rays of 30 GeV energy, impact parameters between 20 m and 200 m and various orientations of the telescope. The the entire range of the angle φ between 0° and 330° was considered and two image cleaning levels were considered.

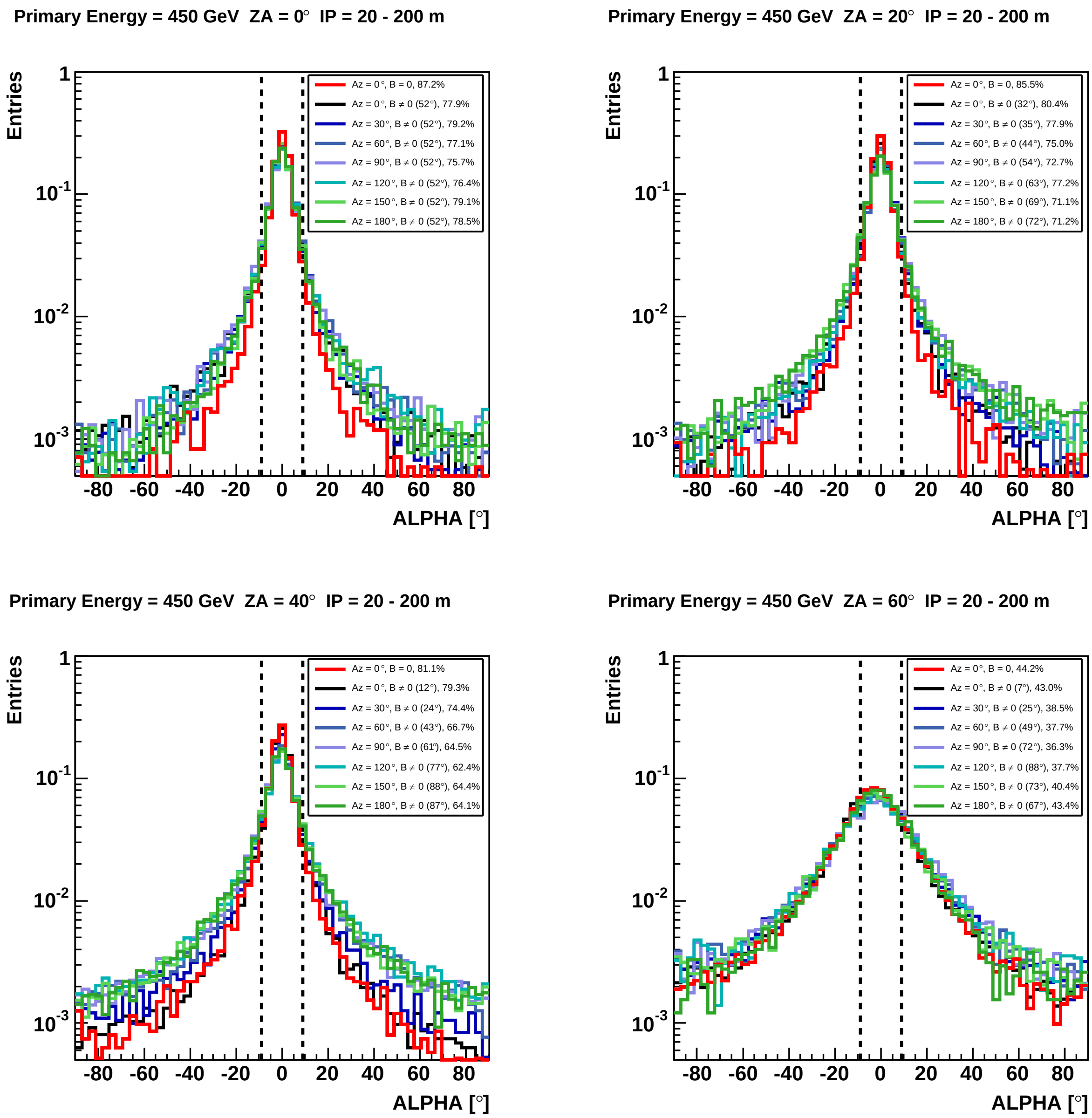

Figure 95: Normalized distributions of the image parameter ALPHA for MC γ-rays of 450 GeV energy, impact parameters between 20 m and 200 m and various orientations of the telescope. The hard image cleaning was applied, and the entire range of the angle φ between 0° and 330° was considered.

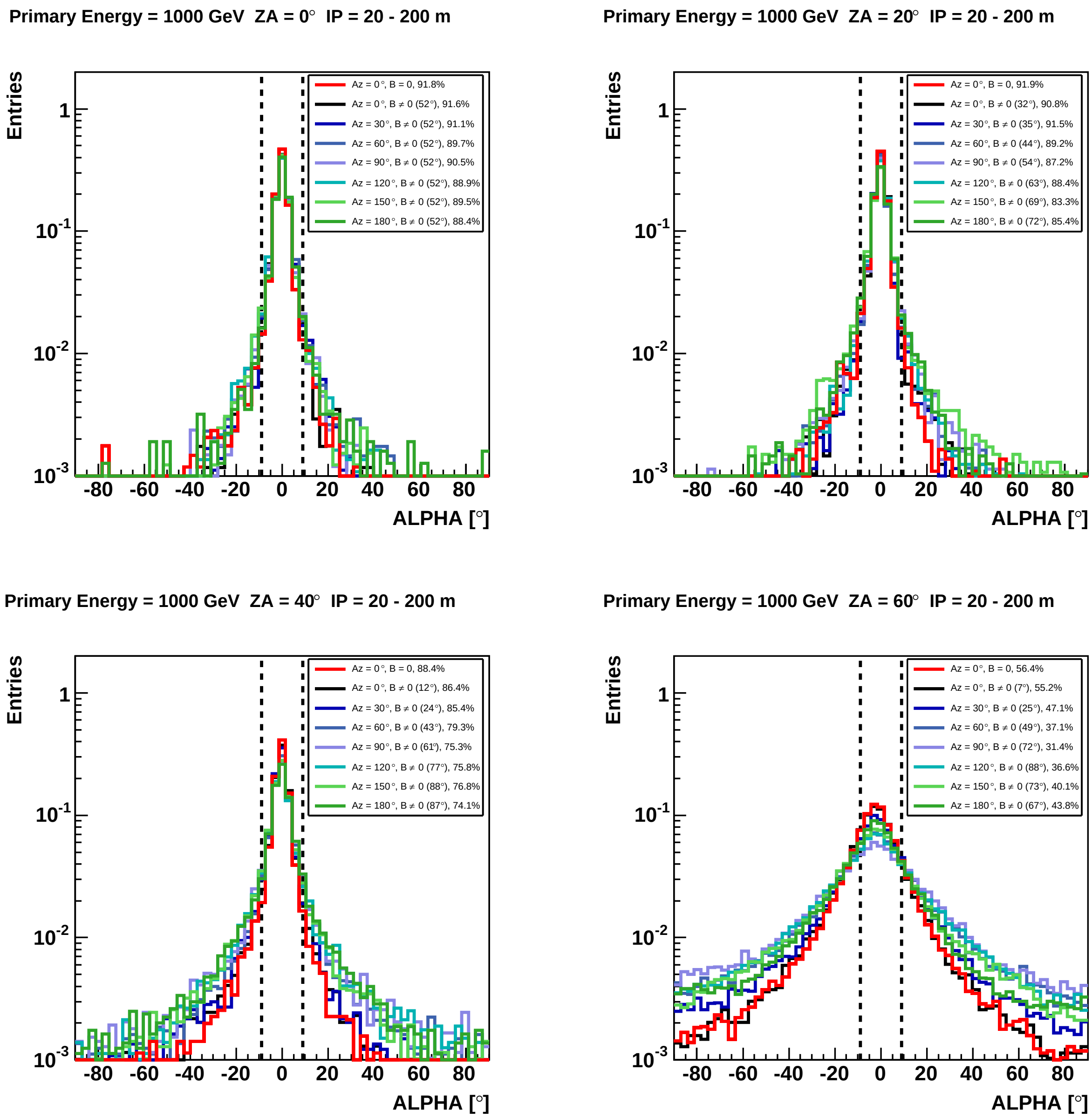

Figure 96: Normalized distributions of the image parameter ALPHA for MC γ-rays of 1 TeV energy, impact parameters between 20 m and 200 m and various orientations of the telescope. The hard image cleaning was applied, and the entire range of the angle φ between 0° and 330° was considered.

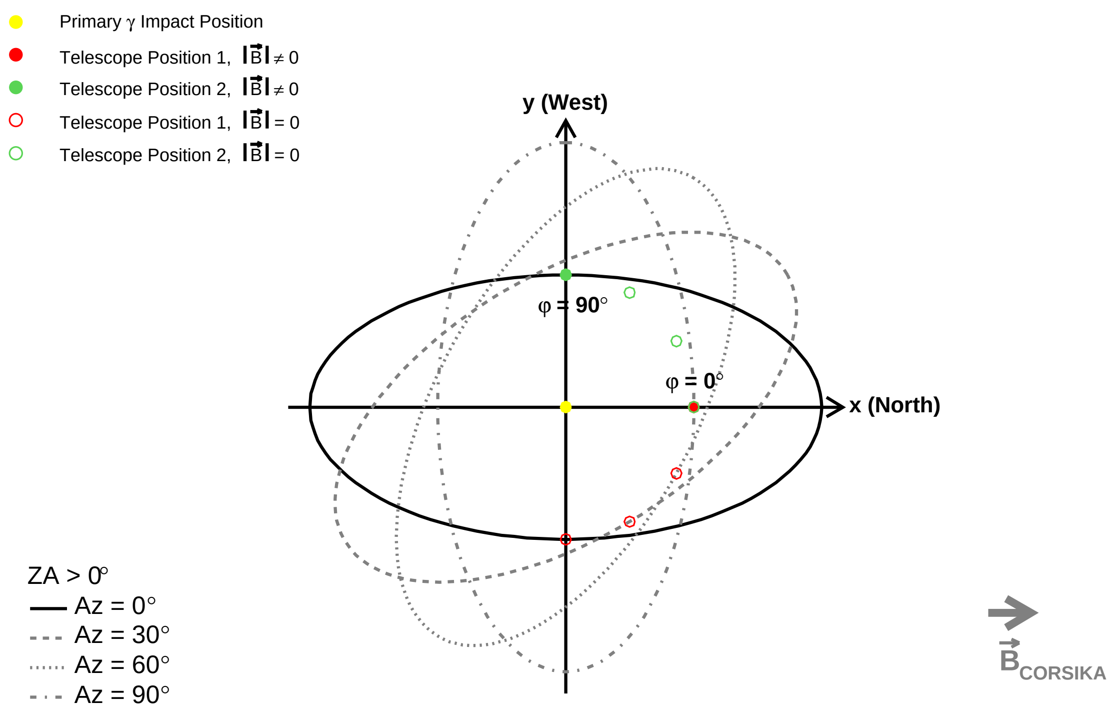

Figure 97: To investigate the GF effects on the ALPHA distribution two telescope positions were considered: for enabled GF in the MC simulation the telescope was situated at $\varphi = 90°$ (telescope position 2, filled green circle) as well as $\varphi = 0°$ (telescope position 1, filled red circle), while for disabled GF the telescope was placed at equivalent positions $\varphi = 90° -$ azimuth angle (telescope position 2, open green circles) as well as $\varphi = 360° -$ azimuth angle (telescope position 1, open red circles). By the choice of this arrangement, the telescope is not always situated on the hump of the Cherenkov light distribution on ground. However, the connecting line between the impact point of the primary γ-ray (filled yellow circle) and the telescope position is either parallel (telescope position 1) or vertical (telescope position 2) to the north-south direction. Note: for ZA $> 0°$ the corresponding shower images are not always parallel or vertical to the projection of the GF in the camera.

In section 3.1.1 it was shown that the influence of the GF can severely affect the average pointing of γ-rays. The extent of the disturbance depends on the position (r, φ) of the telescope with respect to the direction of the EAS and the energy of the primary γ-ray. The rotation of the shower images will of course affect the ALPHA distribution, but it is unclear if a de-rotation of the images will help to recover events which are otherwise lost due to their large value for ALPHA. As mentioned beforehand, the average pointing (δ) is maintained for shower images which are oriented either parallel or perpendicular to the projection of the GF in the camera, i.e. the pointing corresponds to the one of images obtained for disabled GF. However, the corresponding ALPHA distribution could be significantly broadened. Therefore, to find out how the shape of the ALPHA distribution depends on the position of the telescope with respect to the direction of the EAS, it is suggestive to investigate the dependency of the shape of the ALPHA distribution on the angle φ.
As mentioned in section 3.1, for ZA $> 0°$, GF effects as well as geometrical effects on the image

parameters are entangled. To disentangle both effects, it is helpful to chose a certain arrangement for the telescope position with respect to the direction of the MC γ-ray. Figure 97 shows an arrangement where the telescope is not always situated on the hump of the Cherenkov light distribution on ground. As can be seen from the figure, the distance between the telescope position 2 (filled green circle) and the maximum of the Cherenkov light distribution on ground (indicated by the dashed, dotted and dash-dotted gray ellipse) increases with increasing azimuth angle. For ZA $= 0°$ the connecting line between the impact point of the MC γ-ray (filled yellow circle) and the telescope position is either parallel (telescope position 1, located on the x-axis of the CORSIKA coordinate system, filled red circle) or vertical (telescope position 2, located on the y-axis of the CORSIKA coordinate system, filled green circle) to the direction of the GF. Therefore the corresponding shower images are oriented parallel or vertical to the projection of the GF in the camera. For ZA $> 0°$ this is not always the case (see section 3.1).

For enabled GF in the MC simulation the telescope was situated at $\varphi = 90°$ (telescope position 2) as well as $\varphi = 0°$ (telescope position 1). Since for disabled GF MC data were produced only for 0° azimuth angle, the telescope had to be placed at equivalent positions $\varphi = 90° -$ azimuth angle (telescope position 2, open green circles) as well as $\varphi = 360° -$ azimuth angle (telescope position 1, open red circles). Otherwise the ALPHA distributions for enabled and disabled GF would not have been comparable.

Figure 98 shows the normalized distributions of the image parameter ALPHA for MC γ-rays of 30 GeV energy, impact parameters between 20 m and 180 m and various orientations of the telescope as well as different image cleaning levels. The angle φ was set to 0° (x-axis of the CORSIKA coordinate system, pointing to the north, figure 17) and 90° (y-axis of the CORSIKA coordinate system, pointing to the west), corresponding to $\delta = 90°$ and $\delta = 0°$. The angle α between the direction of the GF and the one of the primary γ-ray is given in the figure caption. The ALPHA distributions obtained for enabled GF and $\varphi = 0°$ (telescope position 1) is drawn as a red solid line, while the one obtained for enabled GF but $\varphi = 90°$ (telescope position 2) is drawn as a green solid line. The ALPHA distributions obtained for disabled GF are drawn as red and green dotted lines. The black dotted line indicates the region considered being the signal region. To get an impression of the extent of the disturbance due to the influence of the GF, the percentage of γ showers lying within $|\text{ALPHA}| \leq 9°$ was calculated. The corresponding values, calculated for both telescope positions and for enabled as well as disabled GF, are given in the legend.

The normalized ALPHA distributions in figure 98 (a), obtained after application of the soft image cleaning, appear to be rather flat and do not show a strong dependence on the strength of the GF. The percentage of events contained within $|\text{ALPHA}| \leq 9°$ is all about the same.

A similar situation is shown in figure 98 (b). The ALPHA distributions were obtained for the same MC input parameters, but after application of the intermediate image cleaning. In case of enabled GF, the percentage of events contained within $|\text{ALPHA}| \leq 9°$ is slightly lower than for disabled GF.

The ALPHA distributions for 20° ZA (figures 98 (c) - (d)) look similar to the ones obtained for 0° ZA. In figure 98 (d) for enabled GF and telescope position 2 (green solid line), the percentage of events contained within $|\text{ALPHA}| \leq 9°$ is slightly greater than in case of disabled GF (green dotted line). But, as mentioned beforehand, the ALPHA distributions at 30 GeV are rather dominated by fluctuations due to limited statistics of the dataset than by the influence of the GF.

Figures 99 - 101 show the ALPHA distributions for γ-rays of 50 GeV energy and four impact parameter windows. The intermediate image cleaning was applied. As can be seen from the figures, at 50 GeV energy the ALPHA distributions can be altered depending on the position (r, φ) of the telescope. The ALPHA distributions obtained for enabled GF and $\varphi = 0°$ (telescope position 1, red solid lines) are degraded compared to the ones obtained for disabled GF (red dotted line). At higher energies (figures

102 - 107) the dependency of the shape of the ALPHA distribution on the telescope position is more pronounced, i.e. the ALPHA distributions obtained for enabled GF and $\varphi = 0°$ (telescope position 1, red solid lines) are significantly degraded compared to the ones obtained for disabled GF (red dotted line).
Figure 108 shows the normalized distributions of the image parameter ALPHA for MC γ-rays of 170 GeV energy and four impact parameter windows. The hard image cleaning was applied. As can be seen from the figures, the ALPHA distributions can be significantly altered depending on the position (r, φ) of the telescope. The ALPHA distributions obtained for enabled GF and $\varphi = 0°$ (telescope position 1, red solid lines) are significantly degraded compared to the ones obtained for disabled GF (red dotted line). The percentage of events contained within $|\text{ALPHA}| \leq 9°$ can be reduced by more than 20 % (figure 108 (b)). However, for impact parameters between 20 m and 60 m, the ALPHA distributions obtained for enabled GF and $\varphi = 90°$ (telescope position 2, green solid line) appear to be enhanced with respect to the case of disabled GF, where somewhat less shower images are contained within $|\text{ALPHA}| \leq 9°$ (figure 108 (a)). Thus, if the telescope is situated on the y-axis of the CORSIKA coordinate system, perpendicular to the direction of the GF, the pointing of γ-ray showers can be enhanced. The latter configuration corresponds to images elongated in direction of the major image axis (figure 39, section 3.1.1).
At 0° ZA, the result is independent of the azimuth angle (figure 109), since the distribution of Cherenkov light on ground is, on average, circular. The ALPHA distributions obtained for different azimuth angles are compatible with each other, irrespective of the orientation of the telescope. Furthermore, the ALPHA distributions for telescope position 2 appear to be always enhanced compared to the ones obtained at position 1.
The normalized ALPHA distributions shown in figure 110 were obtained for similar MC input parameters, but 20° ZA and two different azimuth angles, i.e. 0° and 180°, respectively. The ALPHA distributions obtained for enabled GF and telescope position 2 are always in excess of the ones obtained for disabled GF. The ALPHA distributions obtained for enabled GF and telescope position 1 appear to be significantly disturbed. In case of telescope position 1, the percentage of γ-ray showers contained within $|\text{ALPHA}| \leq 9°$ can differ by up to ~ 30 % (figure 110 (d)). For 180°, the influence of the GF on the image parameter ALPHA is apparently more pronounced than for 0° azimuth angle, as the angle α between the shower axis and the direction of the GF is greater. It should be kept in mind that for ZA $> 0°$ and azimuth angle 0° and 180°, the γ-ray showers collected by the telescope located at position 1 have a smaller angular distance (DIST) than the ones collected at position 2 (figure 16). For greater impact parameters between 100 m and 200 m (figures 111 (a) - (d)) the situation is similar, but for impact parameters beyond 140 m, the difference between the ALPHA distributions obtained for enabled GF at the telescope positions 1 and 2 becomes smaller.
Figure 112 shows the normalized ALPHA distributions for MC γ-rays of 170 GeV energy and impact parameters between 60 m and 100 m. The ZA was set to 20° and the azimuth angle to 30°, 60°, 90° and 150°. For these azimuth angles, the telescope position 2 is not always located on or close to the maximum intensity of the Cherenkov distribution on ground. The degradation of the ALPHA distribution for telescope position 2 is rather low, while the one for the γ-ray showers collected at telescope position 1 can be greater than 20 %. It is noteworthy that for ZA $> 0°$ and intermediate azimuth angles $\neq 0°$, 180° the shower images are not oriented perpendicular or vertical to the direction of the GF in the camera (see section 3.1 or figures 59 - 60), i.e. the ALPHA distributions correspond to rotated images.
At 40° ZA the influence of the GF is more pronounced (figures 113 - 114), and the GF strength strongly increases with increasing azimuth angle. At 180° azimuth angle, the GF strength is almost maximal ($\alpha = 87°$), while at 0° azimuth angle it is very low ($\alpha = 12°$). It is noteworthy that the ALPHA

distributions obtained for large α at telescope position 2 (figures 113 (b) and (d), 180° azimuth angle, strong GF) are significantly enhanced compared to the ones obtained for telescope position 1 and small α (figures 113 (a) and (c), 0° azimuth angle, weak GF). Thus, for some orientations of the EAS with respect to the telescope pointing direction, the pointing of γ-ray showers can be significantly enhanced.

Figure 115 shows the normalized ALPHA distributions for MC γ-rays of 170 GeV energy and impact parameters between 60 m and 100 m. The ZA was set to 40° and the azimuth angle to 30°, 60°, 90° and 150°. Except for 150° azimuth angle (figure 115 (b)) where the telescope position 2 is close to the maximum of the Cherenkov light distribution on ground, the influence of the GF is rather small. For these configurations the corresponding shower images are not oriented perpendicular or vertical to the direction of the GF in the camera.

Figure 123 shows the normalized distributions of the image parameter ALPHA for MC γ-rays of 450 GeV energy, four impact parameter windows, 0° ZA and 0° azimuth angle. As for lower energies, the ALPHA distributions obtained for telescope position 2 and enabled GF appear to be enhanced compared to the corresponding distributions obtained for disabled GF. The distributions obtained for telescope position 1 and enabled GF appear to be degraded compared to the corresponding distributions obtained for disabled GF. Except for impact parameters beyond 100 m where the ALPHA distributions are narrower, the degradation is in the order of 20 %.

The normalized ALPHA distributions shown in figures 126 - 129 were obtained for 20° as well as 40° ZA but intermediate azimuth angles between 30° and 150°. Except for 150° azimuth angle, the ALPHA distributions obtained for enabled GF appear to be significantly degraded compared to the ones obtained for disabled GF. It is noteworthy that the pointing of γ-rays collected at telescope position 1 (close to the maximum of the Cherenkov light distribution on ground) is severely degraded for 90° azimuth angle. The degradation is in the order of 40 % (figure 129 (d)). The pointing of those events cannot be entirely recovered using the information on the average rotation of the images, as the parameter ALPHA is distributed over a wide range and does not exhibit a piling up at a certain value, i.e. there is no systematic rotation away from the camera center (section 3.1.1).

At larger ZA (figures 124 - 125 and 127 - 128), the influence of the GF becomes more pronounced. For some combinations of MC input parameters, the ALPHA distribution obtained for telescope position 1 and enabled GF is severely degraded. At 40°, ZA 180° azimuth angle (strong GF) and impact parameters between 20 m and 60 m (figure 127 (b)), the ALPHA distribution obtained for telescope position 1 and enabled GF is completely disturbed, looking background-like. In contrast to this, the pointing of γ-ray showers collected at telescope position 2 can be significantly enhanced. As mentioned beforehand, the latter configuration corresponds to images elongated in direction of the major image axis (figure 41, section 3.1.1). For greater impact parameters, the pointing of the γ-rays is less affected by the GF.

Figure 130 shows the normalized ALPHA distributions for MC γ-rays of 1 TeV energy and impact parameters between 100 m and 140 m. The ZA was set to 40° and 60° and the azimuth angle to 0° and 180°. As can be seen from the figure, even at 1 TeV the pointing of γ-rays can be severely affected by the influence of the GF. In case of enabled GF, the ALPHA distribution obtained for 60° ZA and 180° azimuth angle at the telescope position 1 is completely disturbed. Apart from the arrangement discussed beforehand (figure 97), there exist more possible configurations all of which result in degraded ALPHA distributions.

In conclusion it can be stated that, for selected arrangements where shower images are oriented vertical to the projection of the GF in the telescope camera, the pointing of the γ-ray showers is not necessarily degraded but can be enhanced instead. Arrangements where shower images are oriented parallel to the projection of the GF in the telescope camera result in degraded ALPHA distributions even though the corresponding images are not rotated. The pointing of these shower images cannot be recovered by de-rotation. For pointing directions where the shower images are oriented neither parallel nor vertical to the projection of the GF in the telescope camera the influence of the GF on the development of EAS will, on average, degrade the pointing of γ showers. The angular distribution of the γ-ray images will be blurred and in addition the images will be rotated away from their nominal orientation.

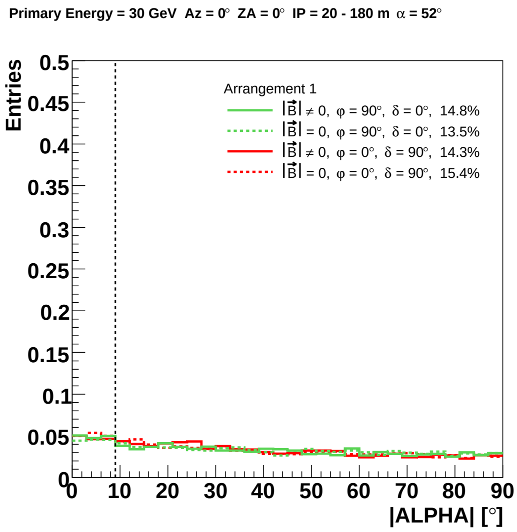

(a) Soft image cleaning, ZA 0°, azimuth angle 0°, impact parameter 20 - 180 m.

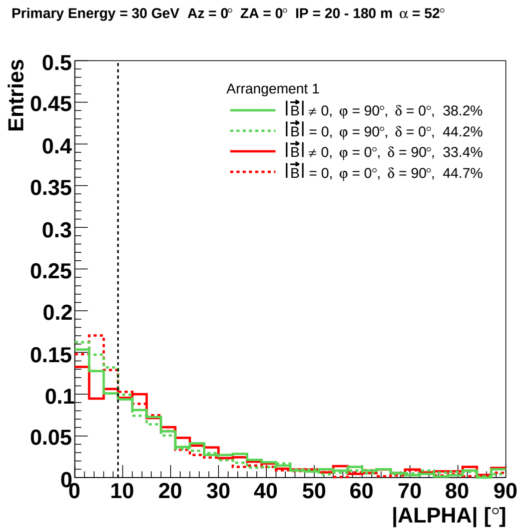

(b) Intermediate image cleaning, ZA 0°, azimuth angle 0°, impact parameter 20 - 180 m.

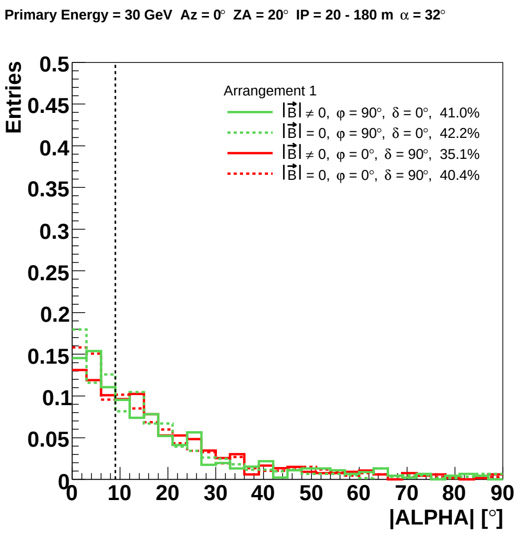

(c) Intermediate image cleaning, ZA 20°, azimuth angle 0°, impact parameter 20 - 180 m.

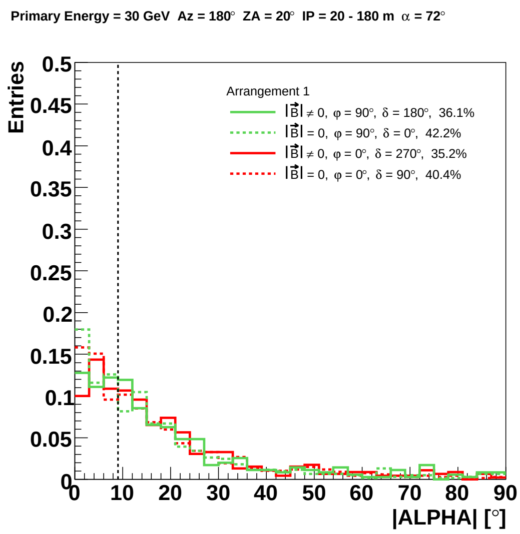

(d) Intermediate image cleaning, ZA 20°, azimuth angle 180°, impact parameter 20 - 180 m.

Figure 98: Normalized distributions of the image parameter ALPHA for MC γ-rays of 30 GeV energy, impact parameters between 20 m and 180 m and various orientations of the telescope. The angle φ was set to 0° and 90°, respectively.

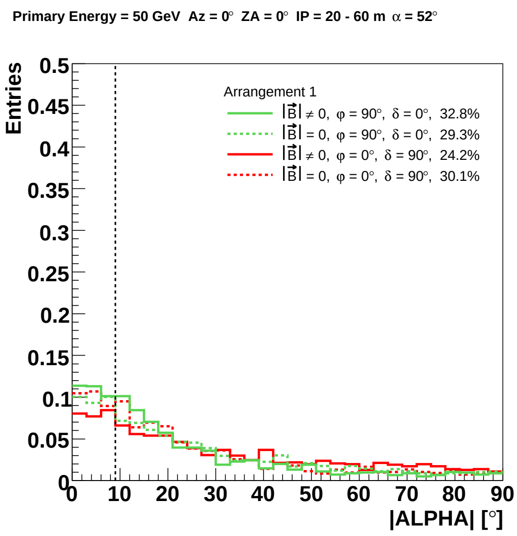

(a) Intermediate image cleaning, ZA 0°, azimuth angle 0°, impact parameter 20 - 60 m.

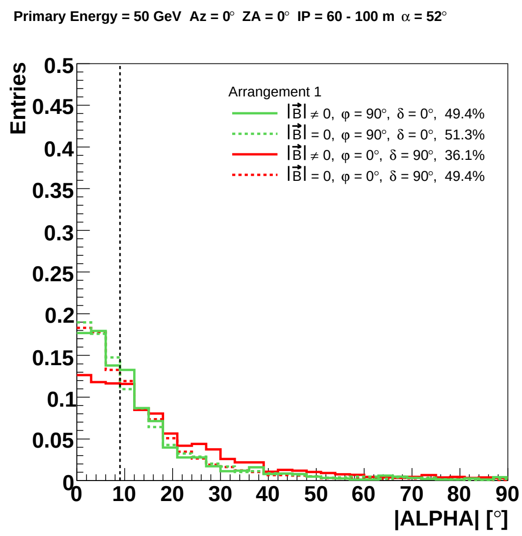

(b) Intermediate image cleaning, ZA 0°, azimuth angle 0°, impact parameter 20 - 100 m.

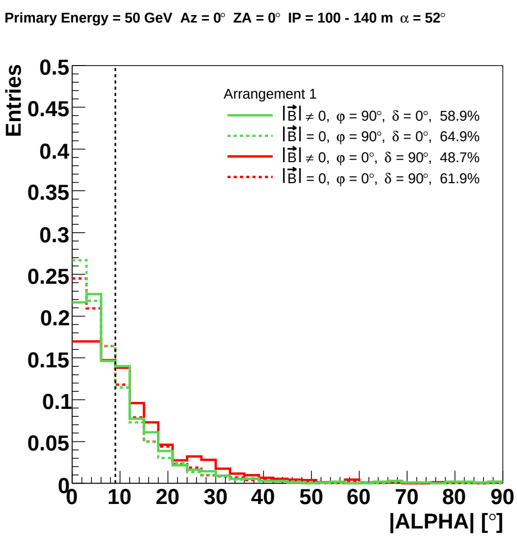

(c) Intermediate image cleaning, ZA 0°, azimuth angle 0°, impact parameter 100 - 140 m.

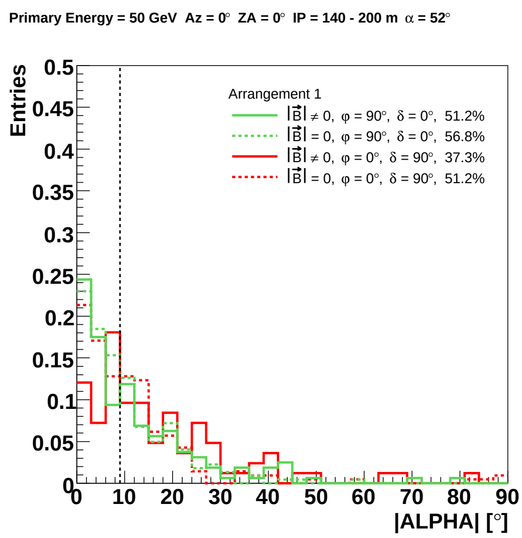

(d) Intermediate image cleaning, ZA 0°, azimuth angle 0°, impact parameter 140 - 200 m.

Figure 99: Normalized distributions of the image parameter ALPHA for MC γ-rays of 50 GeV energy, four impact parameter windows, 0° ZA and 0° azimuth angle. The angle φ was set to 0° and 90°, respectively.

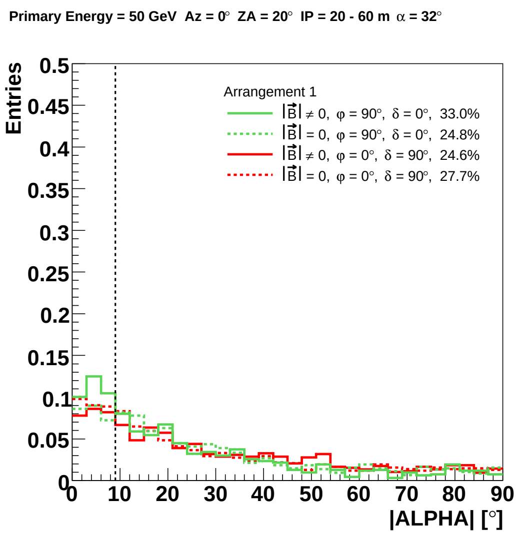

(a) Intermediate image cleaning, ZA 20°, azimuth angle 0°, impact parameter 20 - 60 m.

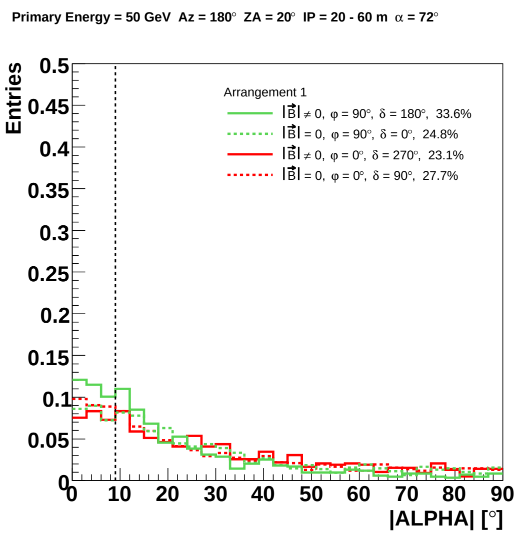

(b) Intermediate image cleaning, ZA 20°, azimuth angle 180°, impact parameter 20 - 60 m.

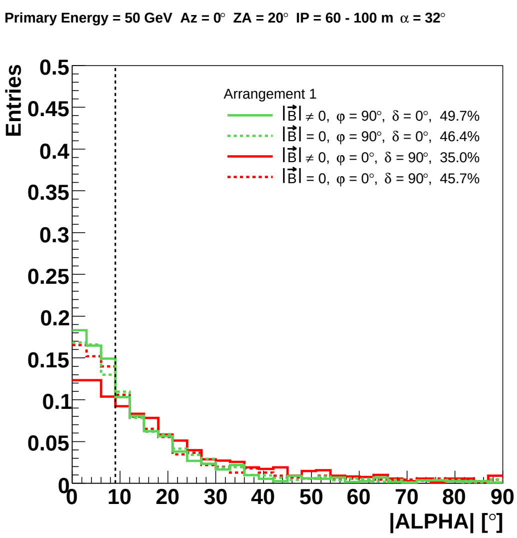

(c) Intermediate image cleaning, ZA 20°, azimuth angle 0°, impact parameter 60 - 100 m.

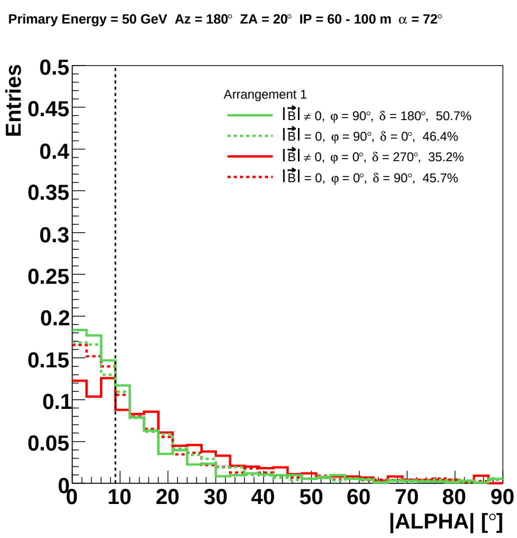

(d) Intermediate image cleaning, ZA 20°, azimuth angle 180°, impact parameter 60 - 100 m.

Figure 100: Normalized distributions of the image parameter ALPHA for MC γ-rays of 50 GeV energy, two impact parameter windows, 20° ZA, 0° and 180° azimuth angle. The angle φ was set to 0° and 90°, respectively.

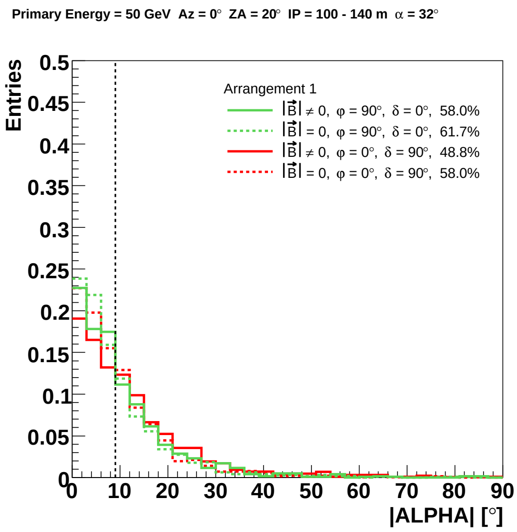

(a) Intermediate image cleaning, ZA 20°, azimuth angle 0°, impact parameter 100 - 140 m.

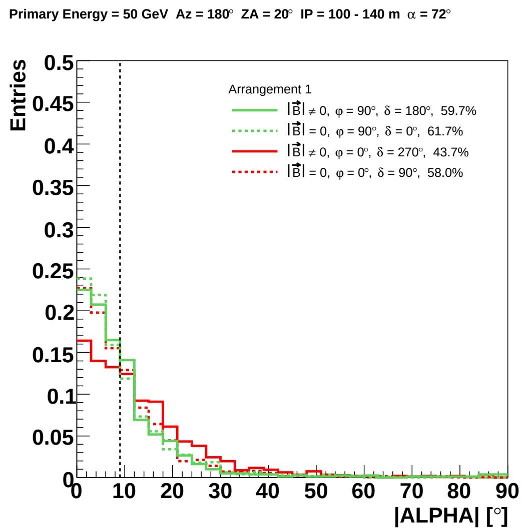

(b) Intermediate image cleaning, ZA 20°, azimuth angle 180°, impact parameter 100 - 140 m.

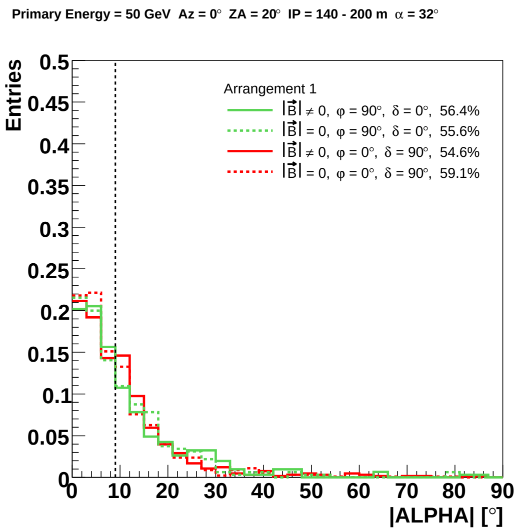

(c) Intermediate image cleaning, ZA 20°, azimuth angle 0°, impact parameter 140 - 200 m.

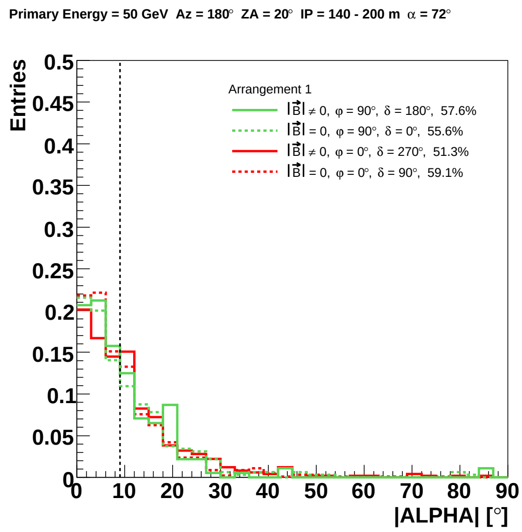

(d) Intermediate image cleaning, ZA 20°, azimuth angle 180°, impact parameter 140 - 200 m.

Figure 101: Normalized distributions of the image parameter ALPHA for MC γ-rays of 50 GeV energy, two impact parameter windows, 20° ZA, 0° and 180° azimuth angle. The angle φ was set to 0° and 90°, respectively.

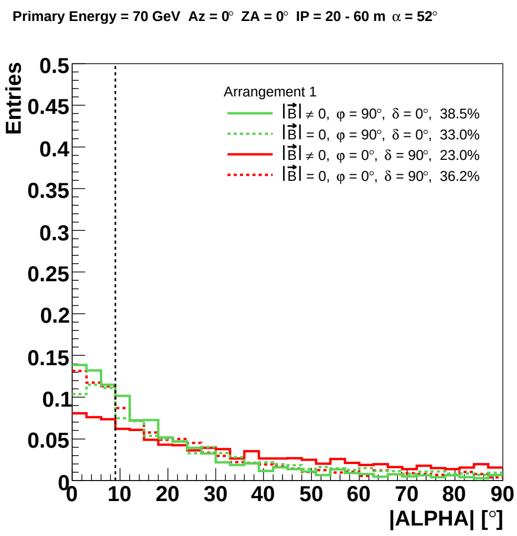

(a) Intermediate image cleaning, ZA 0°, azimuth angle 0°, impact parameter 20 - 60 m.

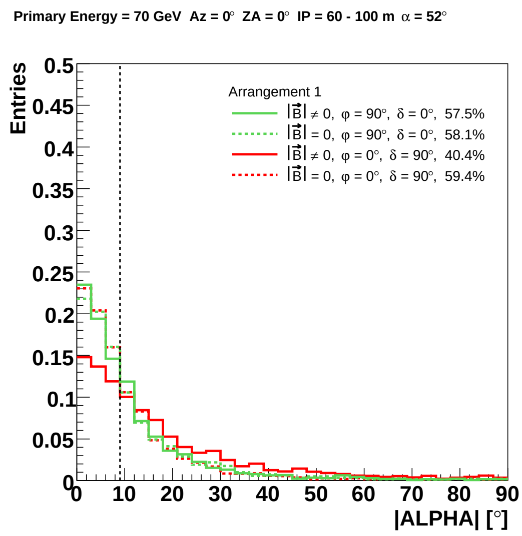

(b) Intermediate image cleaning, ZA 0°, azimuth angle 0°, impact parameter 60 - 100 m.

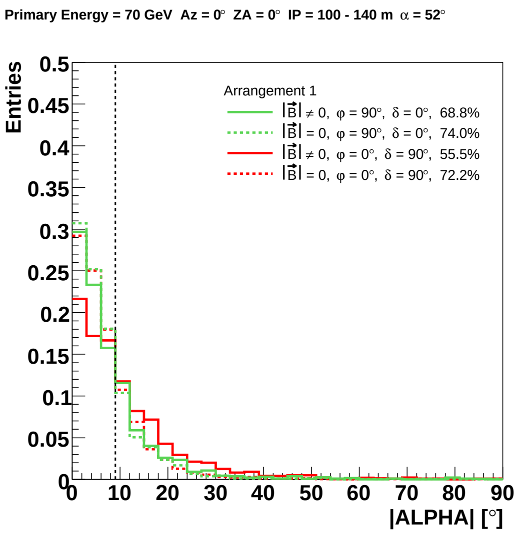

(c) Intermediate image cleaning, ZA 0°, azimuth angle 0°, impact parameter 100 - 140 m.

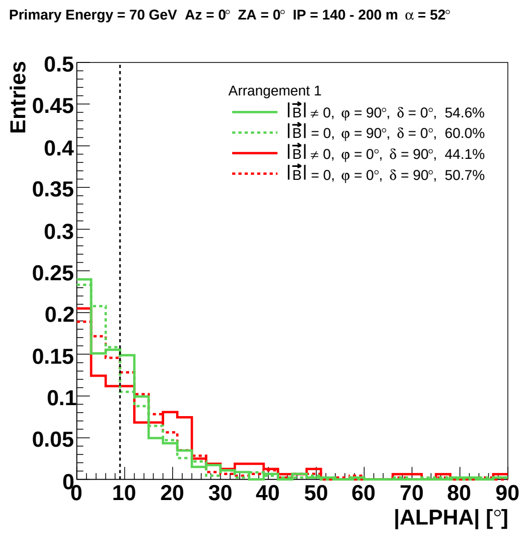

(d) Intermediate image cleaning, ZA 0°, azimuth angle 0°, impact parameter 140 - 200 m.

Figure 102: Normalized distributions of the image parameter ALPHA for MC γ-rays of 70 GeV energy, four impact parameter windows, 0° ZA and 0° azimuth angle. The angle φ was set to 0° and 90°, respectively.

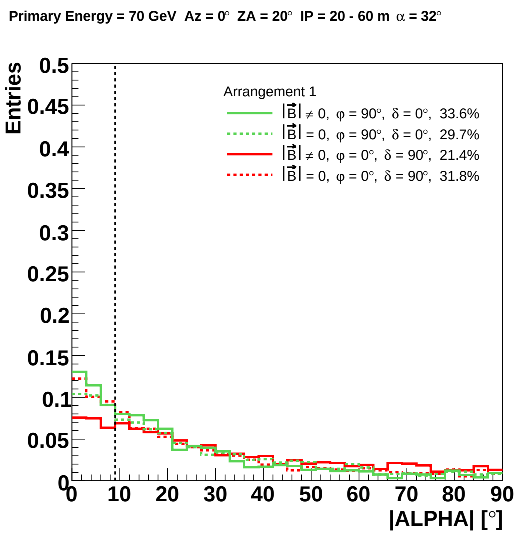

(a) Intermediate image cleaning, ZA 20°, azimuth angle 0°, impact parameter 20 - 60 m.

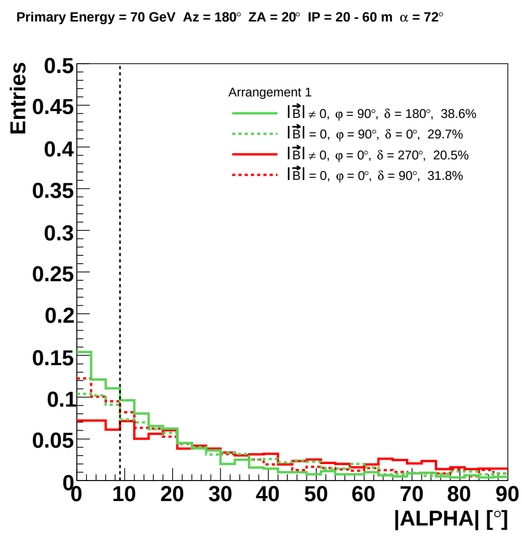

(b) Intermediate image cleaning, ZA 20°, azimuth angle 180°, impact parameter 20 - 60 m.

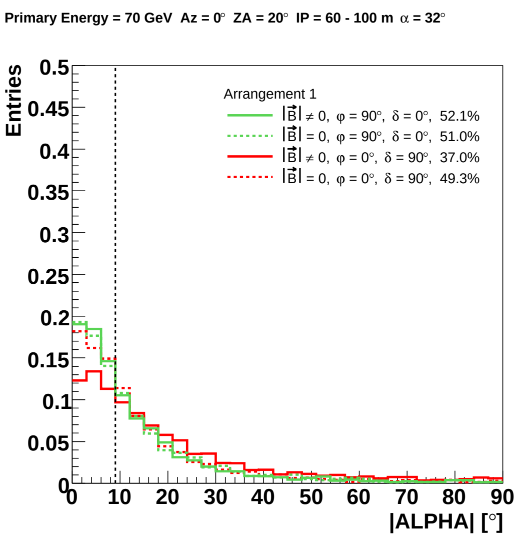

(c) Intermediate image cleaning, ZA 20°, azimuth angle 0°, impact parameter 60 - 100 m.

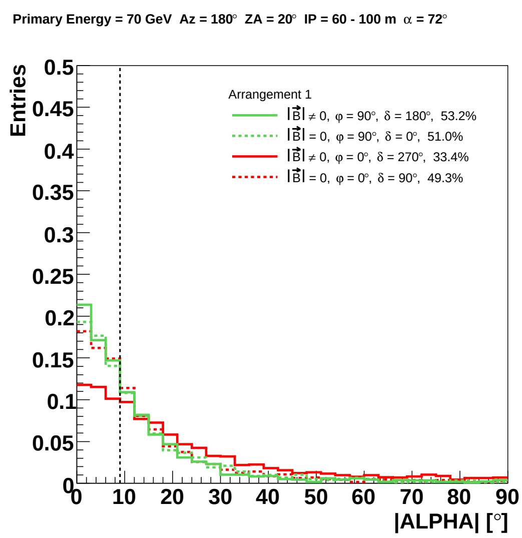

(d) Intermediate image cleaning, ZA 20°, azimuth angle 180°, impact parameter 60 - 100 m.

Figure 103: Normalized distributions of the image parameter ALPHA for MC γ-rays of 70 GeV energy, two impact parameter windows, 20° ZA, 0° and 180° azimuth angle. The angle φ was set to 0° and 90°, respectively.

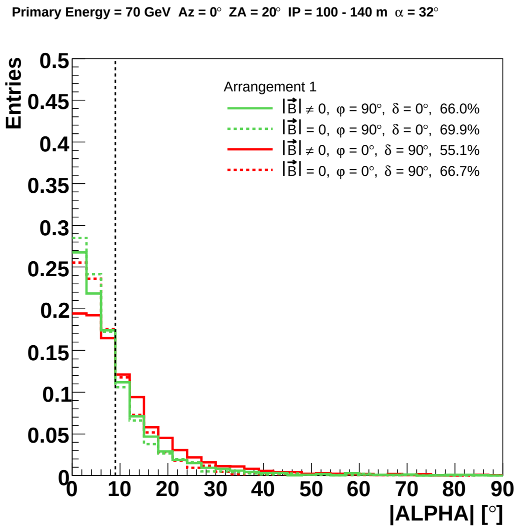

(a) Intermediate image cleaning, ZA 20°, azimuth angle 0°, impact parameter 100 - 140 m.

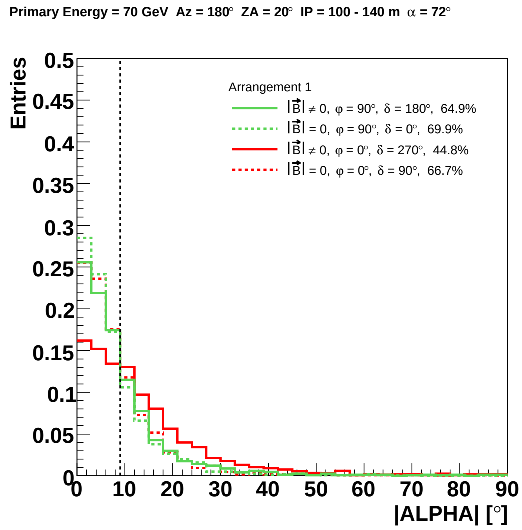

(b) Intermediate image cleaning, ZA 20°, azimuth angle 180°, impact parameter 100 - 140 m.

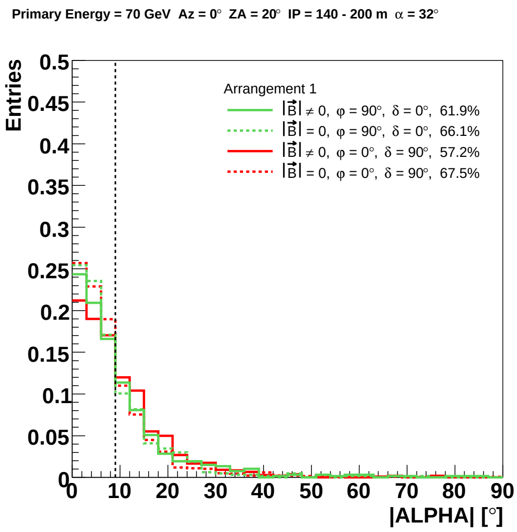

(c) Intermediate image cleaning, ZA 20°, azimuth angle 0°, impact parameter 140 - 200 m.

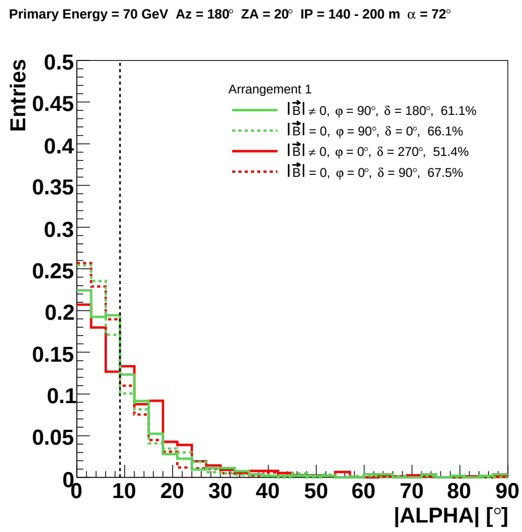

(d) Intermediate image cleaning, ZA 20°, azimuth angle 180°, impact parameter 140 - 200 m.

Figure 104: Normalized distributions of the image parameter ALPHA for MC γ-rays of 70 GeV energy, two impact parameter windows, 20° ZA, 0° and 180° azimuth angle. The angle φ was set to 0° and 90°, respectively.

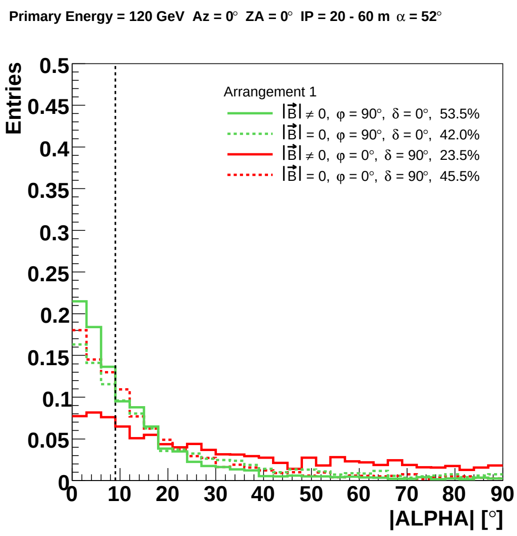

(a) Intermediate image cleaning, ZA 0°, azimuth angle 0°, impact parameter 20 - 60 m.

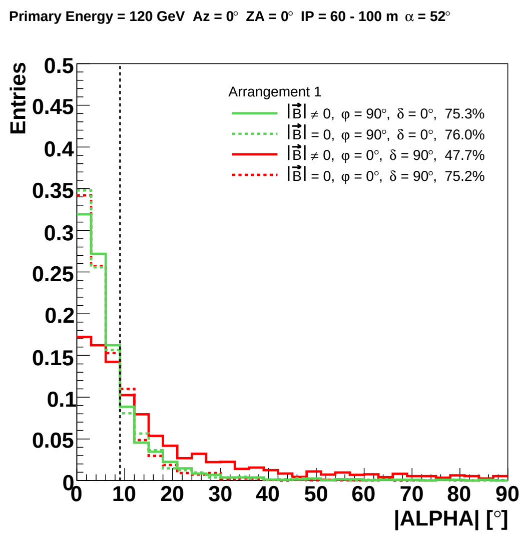

(b) Intermediate image cleaning, ZA 0°, azimuth angle 0°, impact parameter 60 - 100 m.

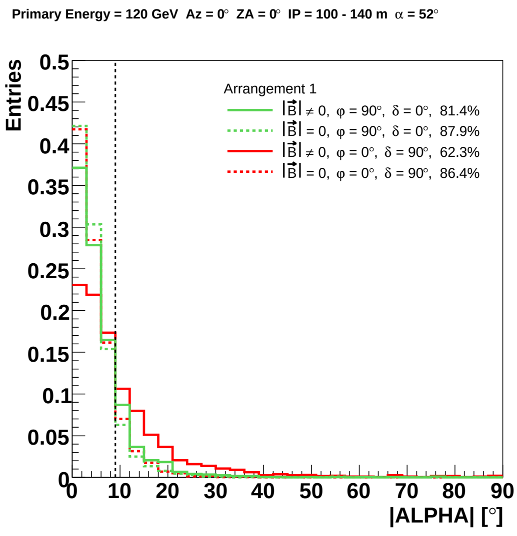

(c) Intermediate image cleaning, ZA 0°, azimuth angle 0°, impact parameter 100 - 140 m.

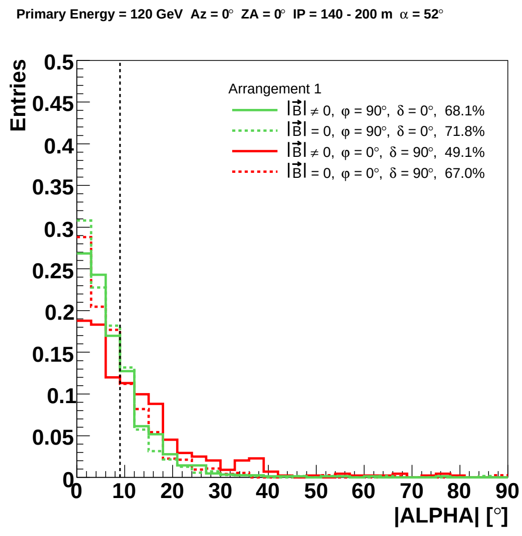

(d) Intermediate image cleaning, ZA 0°, azimuth angle 0°, impact parameter 140 - 200 m.

Figure 105: Normalized distributions of the image parameter ALPHA for MC γ-rays of 120 GeV energy, four impact parameter windows, 0° ZA and 0° azimuth angle. The angle φ was set to 0° and 90°, respectively.

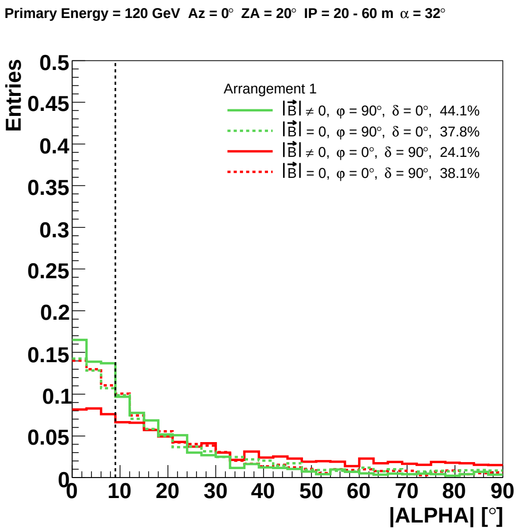

(a) Intermediate image cleaning, ZA 20°, azimuth angle 0°, impact parameter 20 - 60 m.

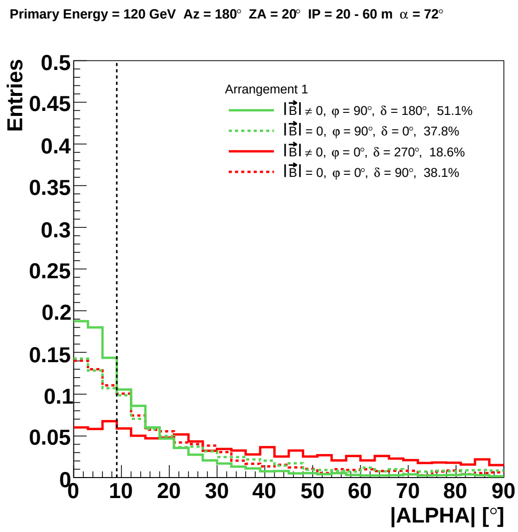

(b) Intermediate image cleaning, ZA 20°, azimuth angle 180°, impact parameter 20 - 60 m.

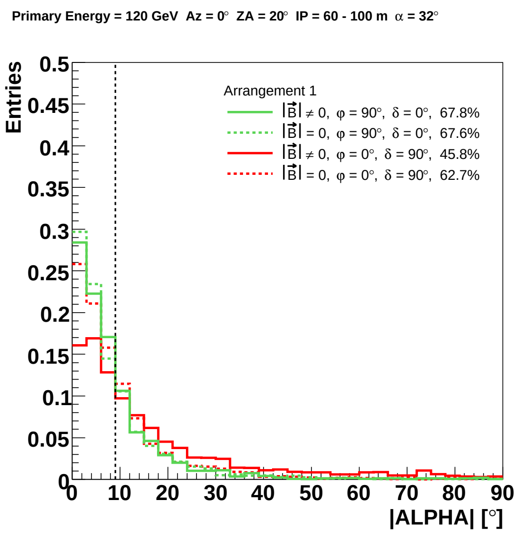

(c) Intermediate image cleaning, ZA 20°, azimuth angle 0°, impact parameter 60 - 100 m.

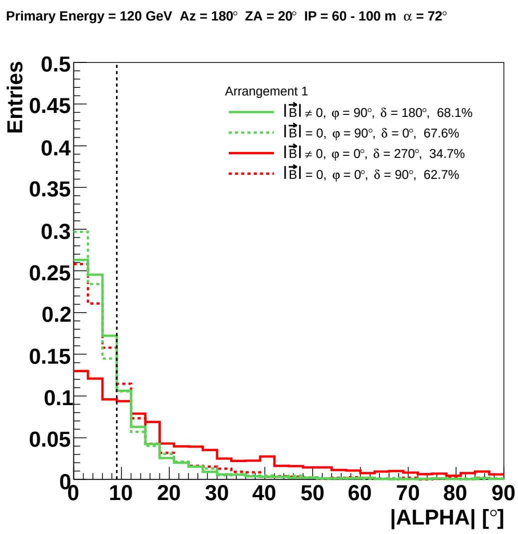

(d) Intermediate image cleaning, ZA 20°, azimuth angle 180°, impact parameter 60 - 100 m.

Figure 106: Normalized distributions of the image parameter ALPHA for MC γ-rays of 120 GeV energy, two impact parameter windows, 20° ZA, 0° and 180° azimuth angle. The angle φ was set to 0° and 90°, respectively.

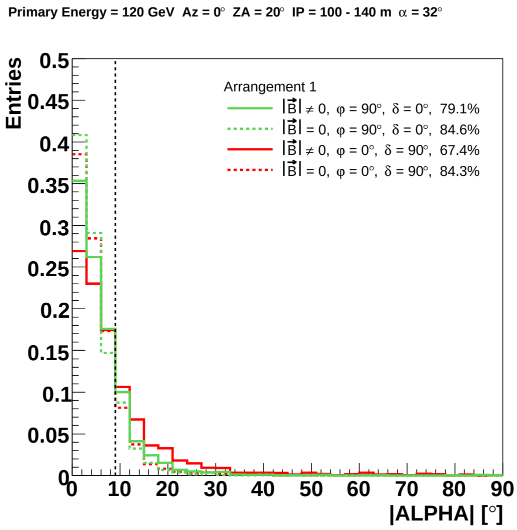

(a) Intermediate image cleaning, ZA 20°, azimuth angle 0°, impact parameter 100 - 140 m.

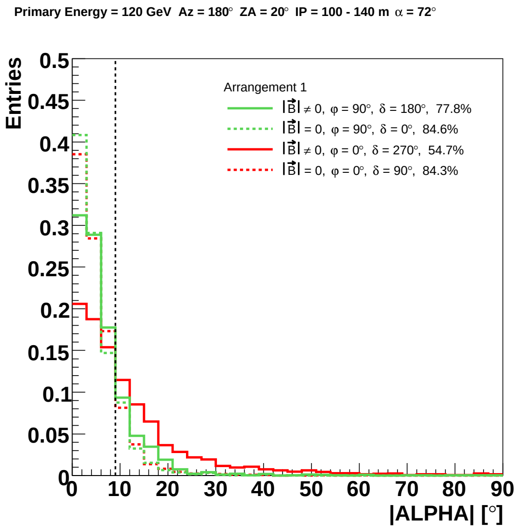

(b) Intermediate image cleaning, ZA 20°, azimuth angle 180°, impact parameter 100 - 140 m.

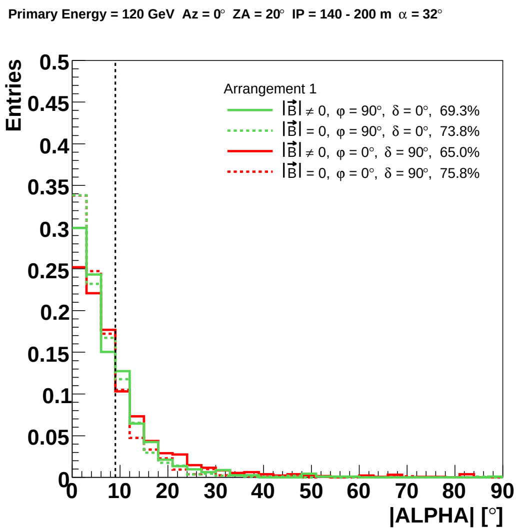

(c) Intermediate image cleaning, ZA 20°, azimuth angle 0°, impact parameter 140 - 200 m.

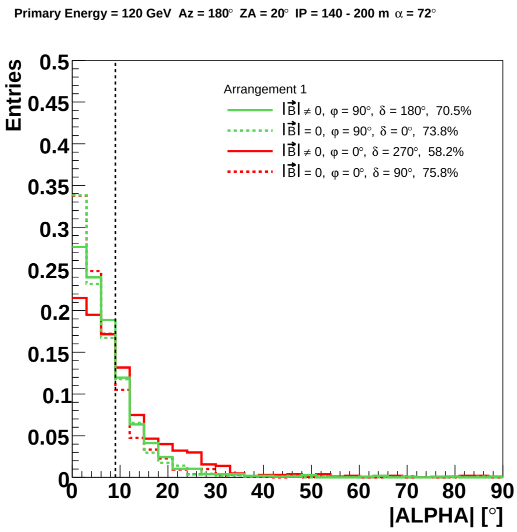

(d) Intermediate image cleaning, ZA 20°, azimuth angle 180°, impact parameter 140 - 200 m.

Figure 107: Normalized distributions of the image parameter ALPHA for MC γ-rays of 120 GeV energy, two impact parameter windows, 20° ZA, 0° and 180° azimuth angle. The angle φ was set to 0° and 90°, respectively.

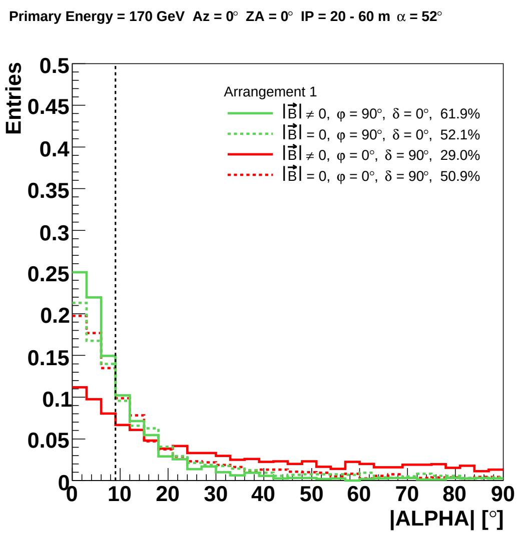

(a) Hard image cleaning, ZA 0°, azimuth angle 0°, impact parameter 20 - 60 m.

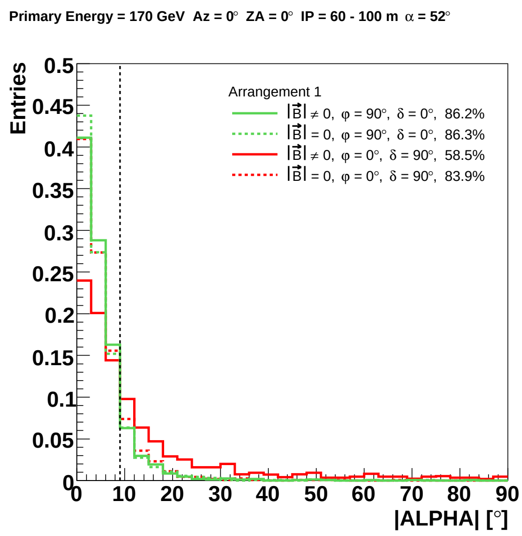

(b) Hard image cleaning, ZA 0°, azimuth angle 0°, impact parameter 60 - 100 m.

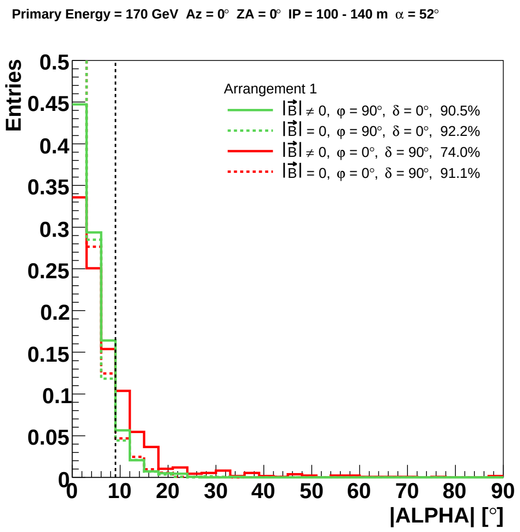

(c) Hard image cleaning, ZA 0°, azimuth angle 0°, impact parameter 100 - 140 m.

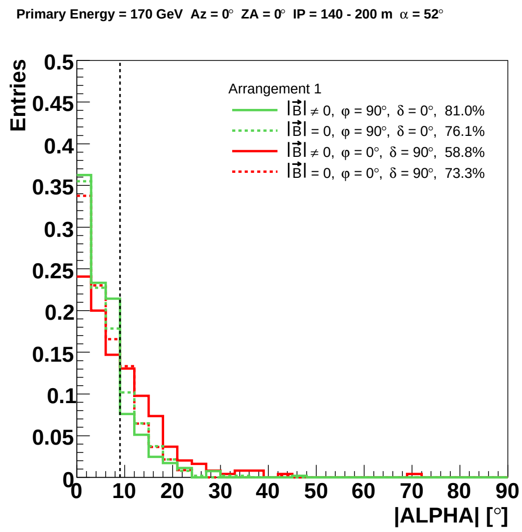

(d) Hard image cleaning, ZA 0°, azimuth angle 0°, impact parameter 140 - 200 m.

Figure 108: Normalized distributions of the image parameter ALPHA for MC γ-rays of 170 GeV energy, four impact parameter windows, 0° ZA and 0° azimuth angle. The angle φ was set to 0° and 90°, respectively.

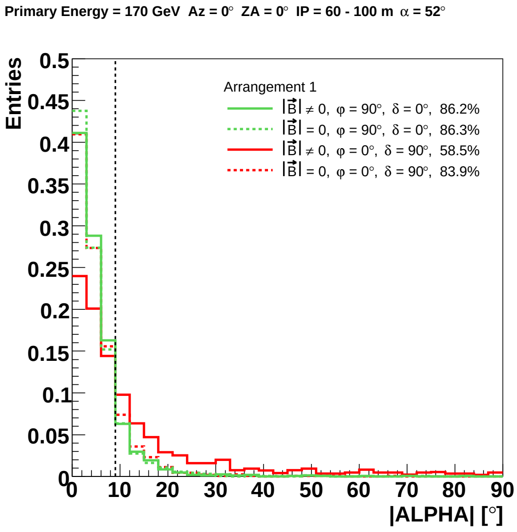

(a) Hard image cleaning, ZA 0°, azimuth angle 0°, impact parameter 60 - 100 m.

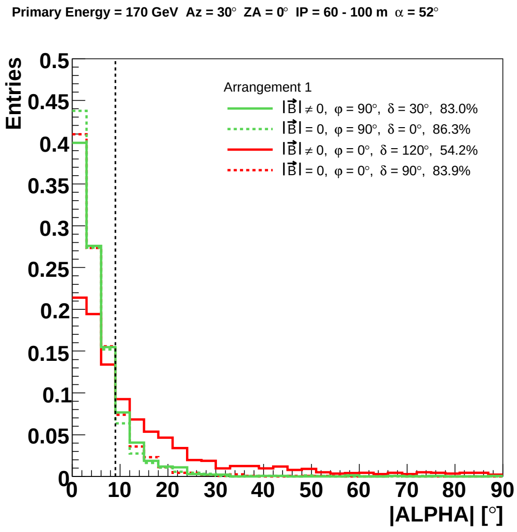

(b) Hard image cleaning, ZA 0°, azimuth angle 30°, impact parameter 60 - 100 m.

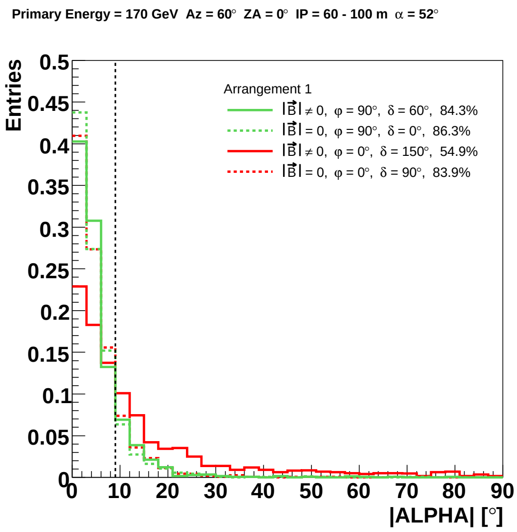

(c) Hard image cleaning, ZA 0°, azimuth angle 60°, impact parameter 60 - 100 m.

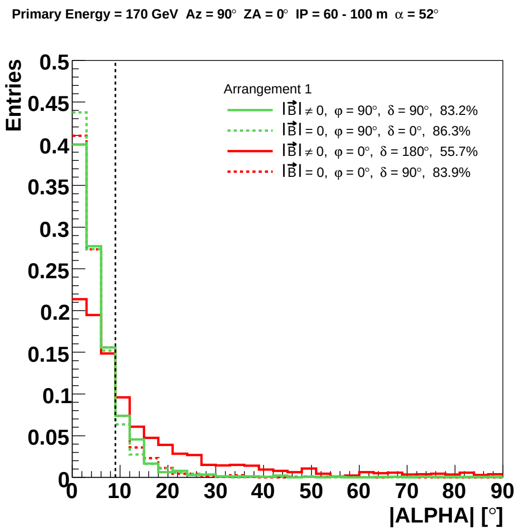

(d) Hard image cleaning, ZA 0°, azimuth angle 90°, impact parameter 60 - 100 m.

Figure 109: Normalized distributions of the image parameter ALPHA for MC γ-rays of 170 GeV energy, impact parameters between 60 m and 100 m, 0° ZA and azimuth angles between 0° and 90°. The angle φ was set to 0° and 90°, respectively.

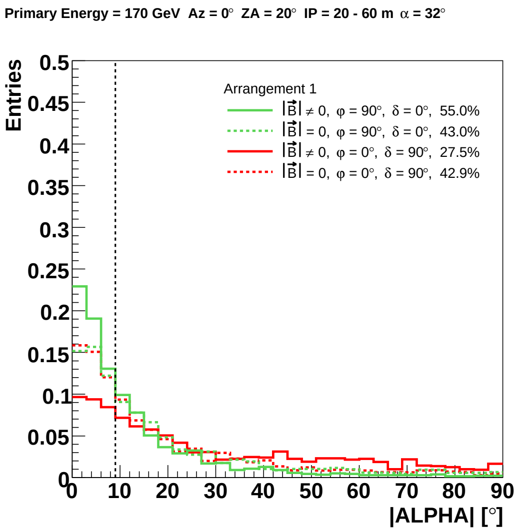

(a) Hard image cleaning, ZA 20°, azimuth angle 0°, impact parameter 20 - 60 m.

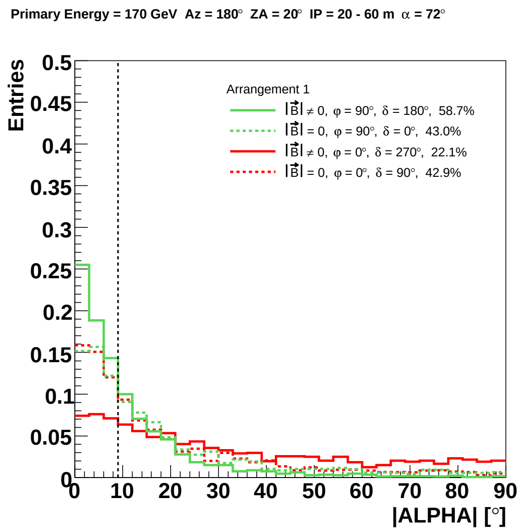

(b) Hard image cleaning, ZA 20°, azimuth angle 180°, impact parameter 20 - 60 m.

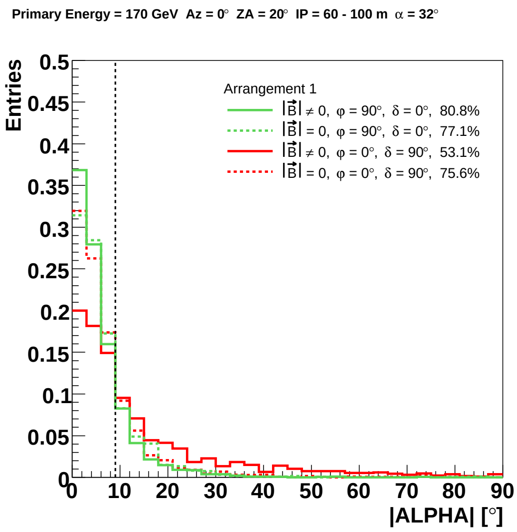

(c) Hard image cleaning, ZA 20°, azimuth angle 0°, impact parameter 60 - 100 m.

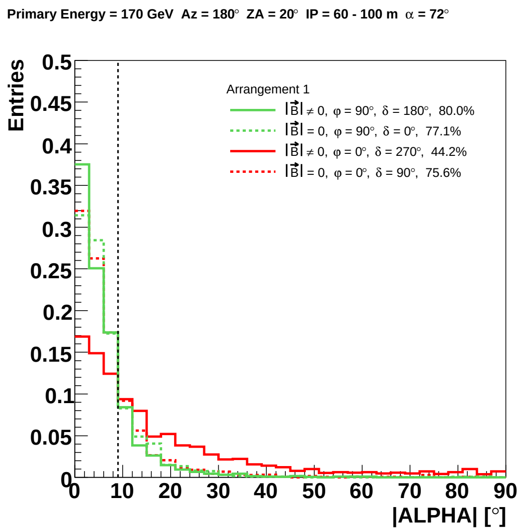

(d) Hard image cleaning, ZA 20°, azimuth angle 180°, impact parameter 60 - 100 m.

Figure 110: Normalized distributions of the image parameter ALPHA for MC γ-rays of 170 GeV energy, two impact parameter windows, 20° ZA, 0° and 180° azimuth angle. The angle φ was set to 0° and 90°, respectively.

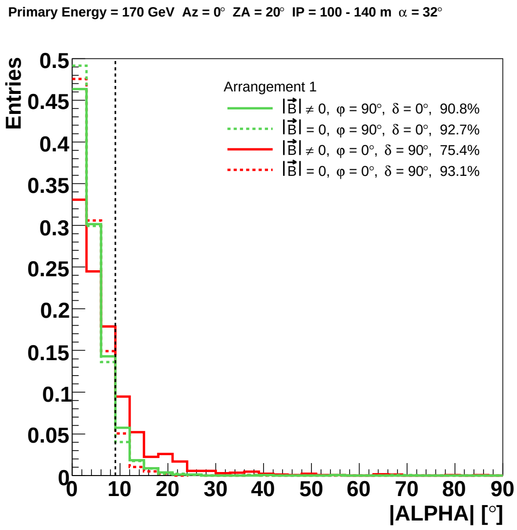

(a) Hard image cleaning, ZA 20°, azimuth angle 0°, impact parameter 100 - 140 m.

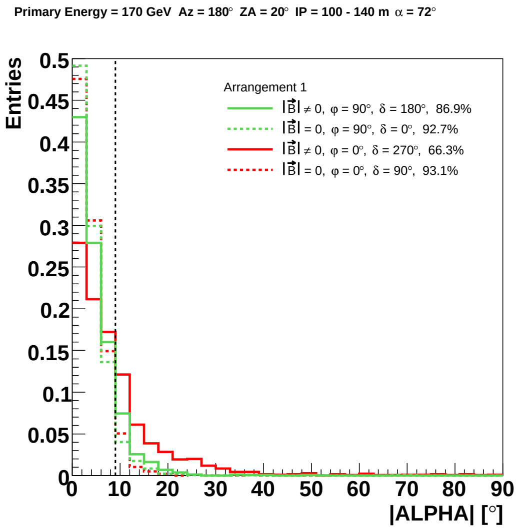

(b) Hard image cleaning, ZA 20°, azimuth angle 180°, impact parameter 100 - 140 m.

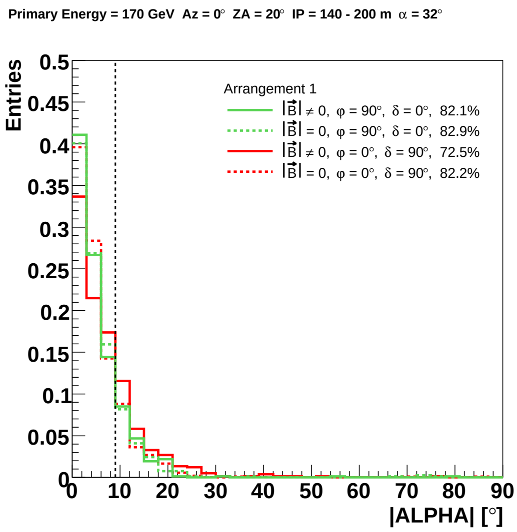

(c) Hard image cleaning, ZA 20°, azimuth angle 0°, impact parameter 140 - 200 m.

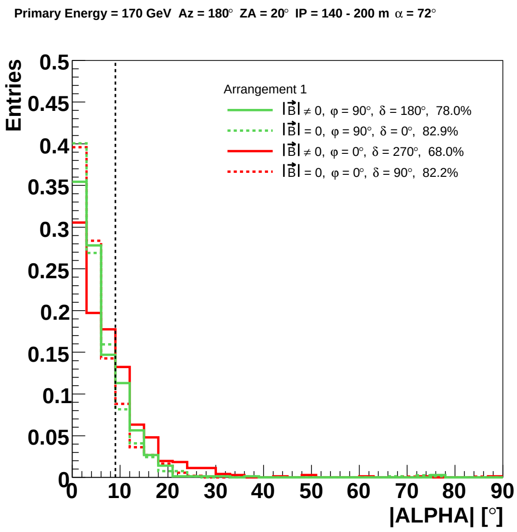

(d) Hard image cleaning, ZA 20°, azimuth angle 180°, impact parameter 140 - 200 m.

Figure 111: Normalized distributions of the image parameter ALPHA for MC γ-rays of 170 GeV energy, two impact parameter windows, 20° ZA, 0° and 180° azimuth angle. The angle φ was set to 0° and 90°, respectively.

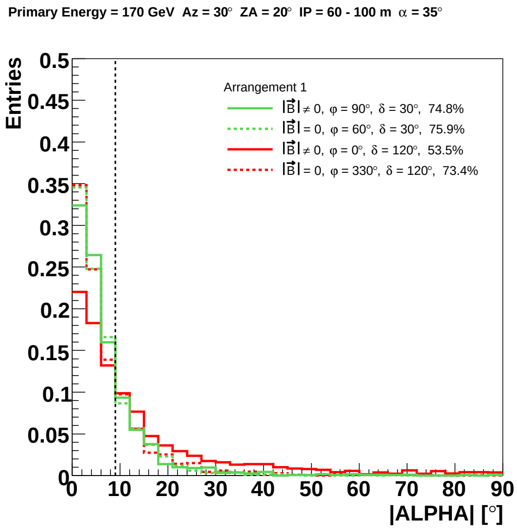

(a) Hard image cleaning, ZA 20°, azimuth angle 30°, impact parameter 60 - 100 m.

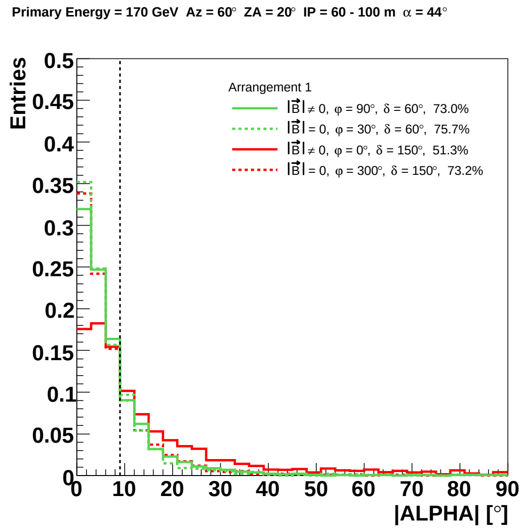

(b) Hard image cleaning, ZA 20°, azimuth angle 60°, impact parameter 60 - 100 m.

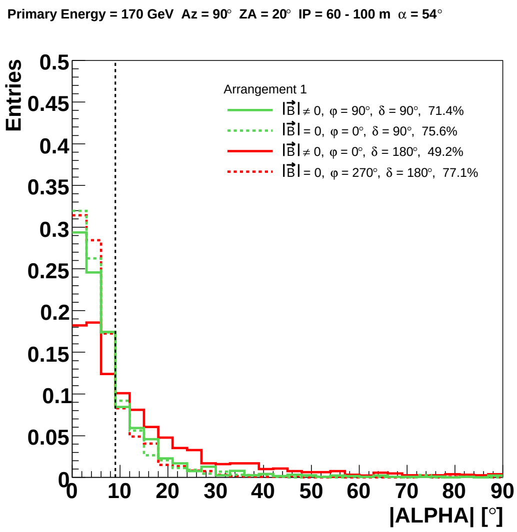

(c) Hard image cleaning, ZA 20°, azimuth angle 90°, impact parameter 60 - 100 m.

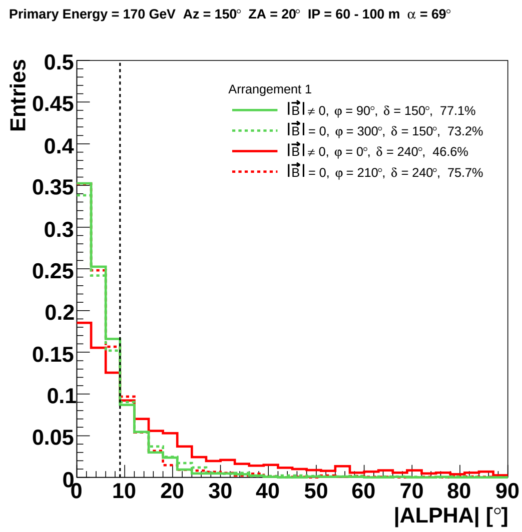

(d) Hard image cleaning, ZA 20°, azimuth angle 150°, impact parameter 60 - 100 m.

Figure 112: Normalized distributions of the image parameter ALPHA for MC γ-rays of 170 GeV energy, impact parameters between 60 m and 100 m, 20° ZA, 30°, 60°, 90° and 150° azimuth angle. The angle φ was set to 0° and 90°, respectively.

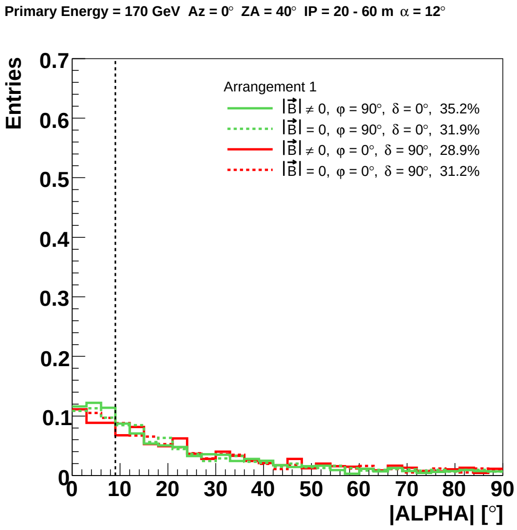

(a) Hard image cleaning, ZA 40°, azimuth angle 0°, impact parameter 20 - 60 m.

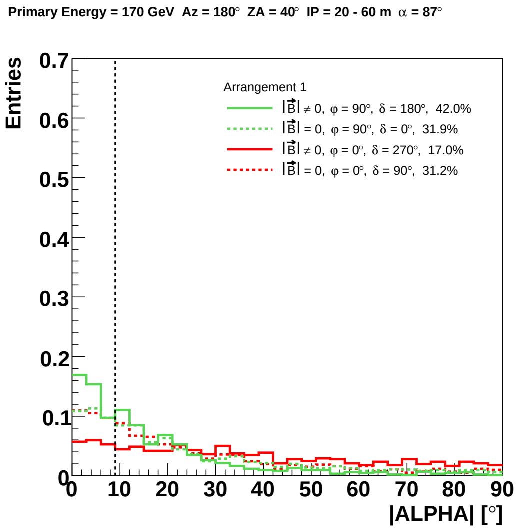

(b) Hard image cleaning, ZA 40°, azimuth angle 180°, impact parameter 20 - 60 m.

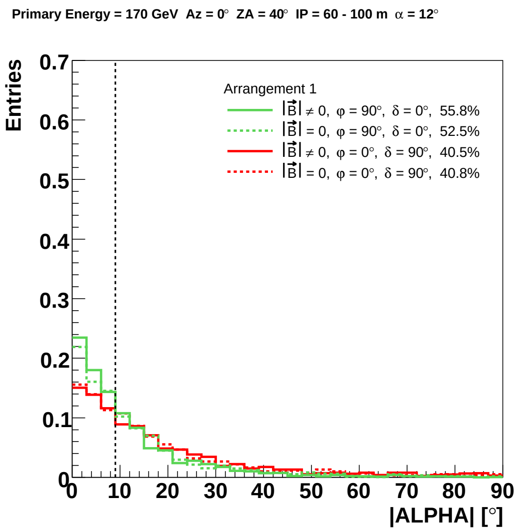

(c) Hard image cleaning, ZA 40°, azimuth angle 0°, impact parameter 60 - 100 m.

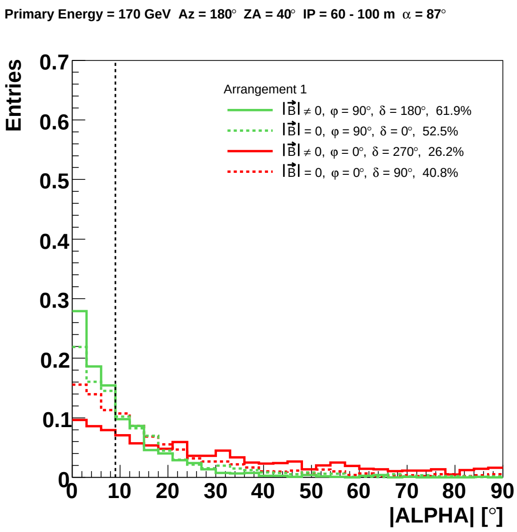

(d) Hard image cleaning, ZA 40°, azimuth angle 180°, impact parameter 60 - 100 m.

Figure 113: Normalized distributions of the image parameter ALPHA for MC γ-rays of 170 GeV energy, two impact parameter windows, 40° ZA, 0° and 180° azimuth angle. The angle φ was set to 0° and 90°, respectively.

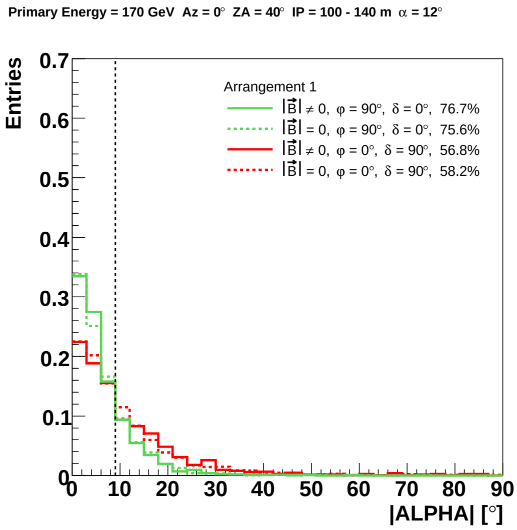

(a) Hard image cleaning, ZA 40°, azimuth angle 0°, impact parameter 100 - 140 m.

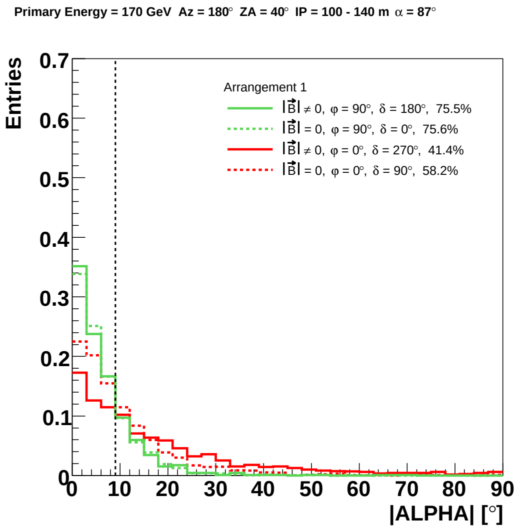

(b) Hard image cleaning, ZA 40°, azimuth angle 180°, impact parameter 100 - 140 m.

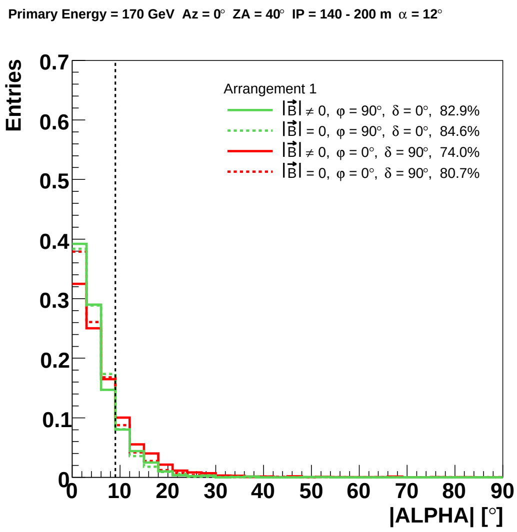

(c) Hard image cleaning, ZA 40°, azimuth angle 0°, impact parameter 140 - 200 m.

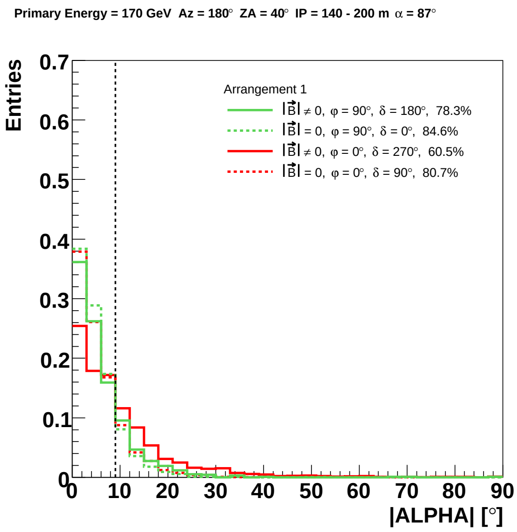

(d) Hard image cleaning, ZA 40°, azimuth angle 180°, impact parameter 140 - 200 m.

Figure 114: Normalized distributions of the image parameter ALPHA for MC γ-rays of 170 GeV energy, two impact parameter windows, 40° ZA, 0° and 180° azimuth angle. The angle φ was set to 0° and 90°, respectively.

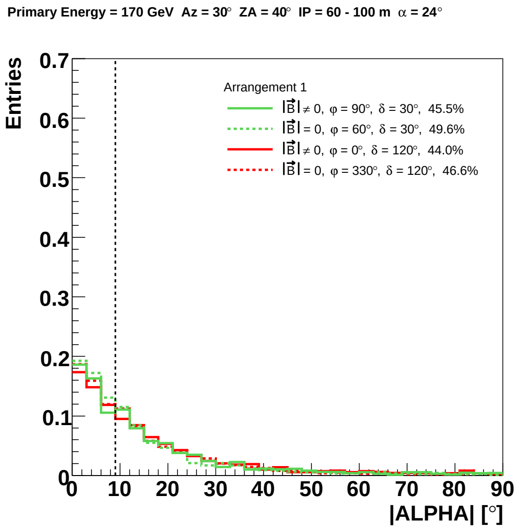

(a) Hard image cleaning, ZA 40°, azimuth angle 30°, impact parameter 60 - 100 m.

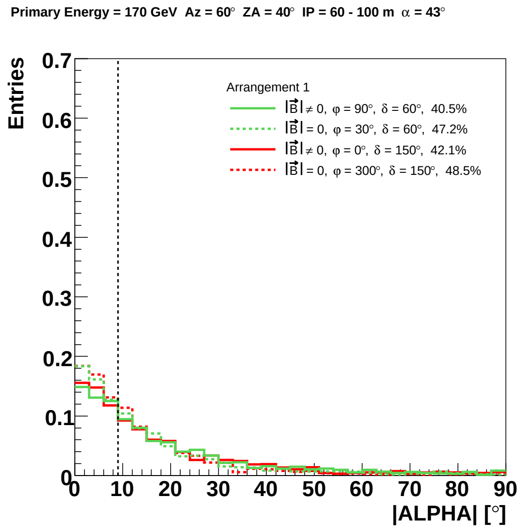

(b) Hard image cleaning, ZA 40°, azimuth angle 60°, impact parameter 60 - 100 m.

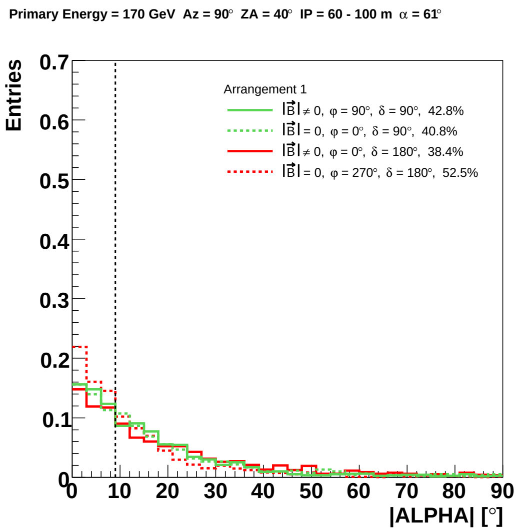

(c) Hard image cleaning, ZA 40°, azimuth angle 90°, impact parameter 60 - 100 m.

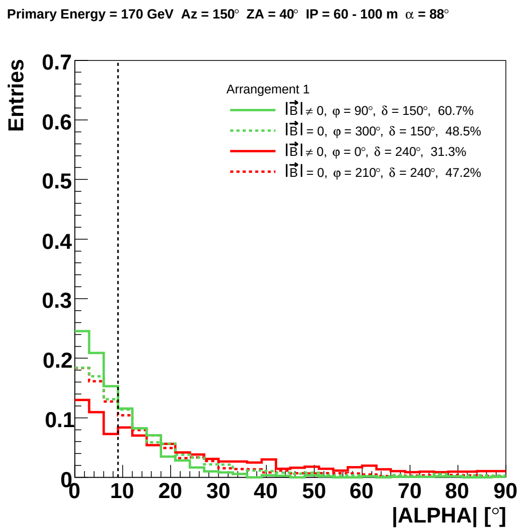

(d) Hard image cleaning, ZA 40°, azimuth angle 150°, impact parameter 60 - 100 m.

Figure 115: Normalized distributions of the image parameter ALPHA for MC γ-rays of 170 GeV energy, two impact parameter windows, 40° ZA, 30°, 60°, 90° and 150° azimuth angle. The angle φ was set to 0° and 90°, respectively.

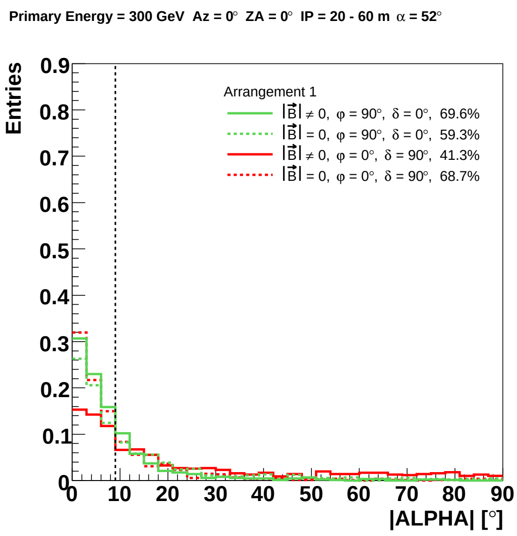

(a) Hard image cleaning, ZA 0°, azimuth angle 0°, impact parameter 20 - 60 m.

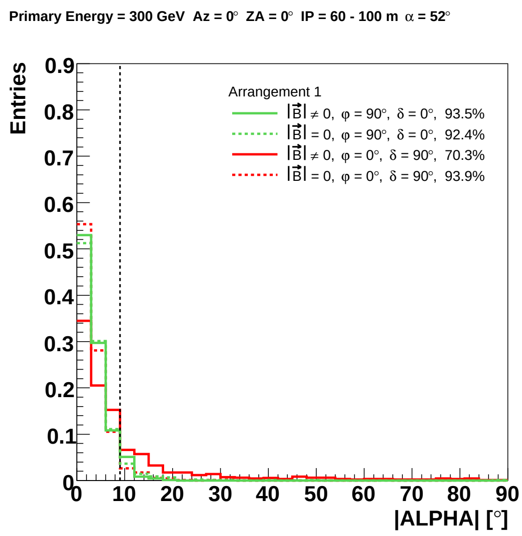

(b) Hard image cleaning, ZA 0°, azimuth angle 0°, impact parameter 60 - 100 m.

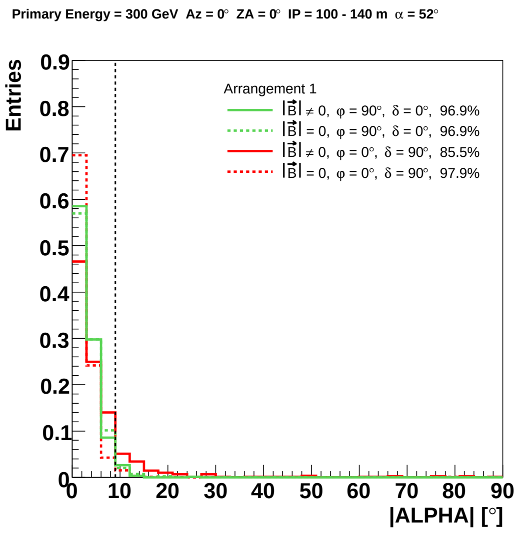

(c) Hard image cleaning, ZA 0°, azimuth angle 0°, impact parameter 100 - 140 m.

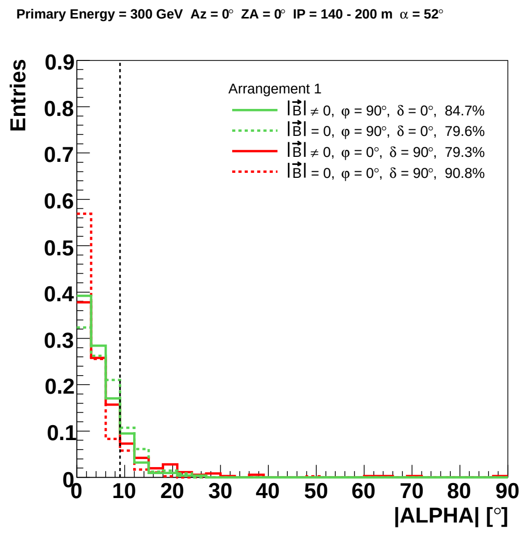

(d) Hard image cleaning, ZA 0°, azimuth angle 0°, impact parameter 140 - 200 m.

Figure 116: Normalized distributions of the image parameter ALPHA for MC γ-rays of 300 GeV energy, four impact parameter windows, 0° ZA and 0° azimuth angle. The angle φ was set to 0° and 90°, respectively.

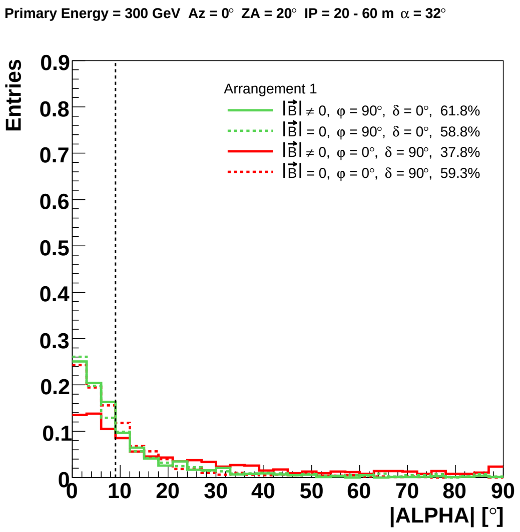

(a) Hard image cleaning, ZA 20°, azimuth angle 0°, impact parameter 20 - 60 m.

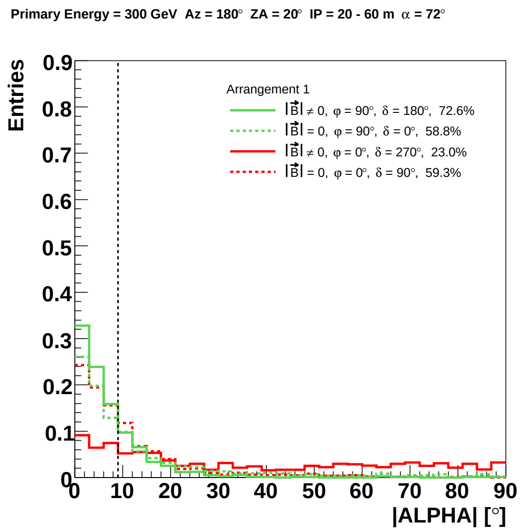

(b) Hard image cleaning, ZA 20°, azimuth angle 180°, impact parameter 20 - 60 m.

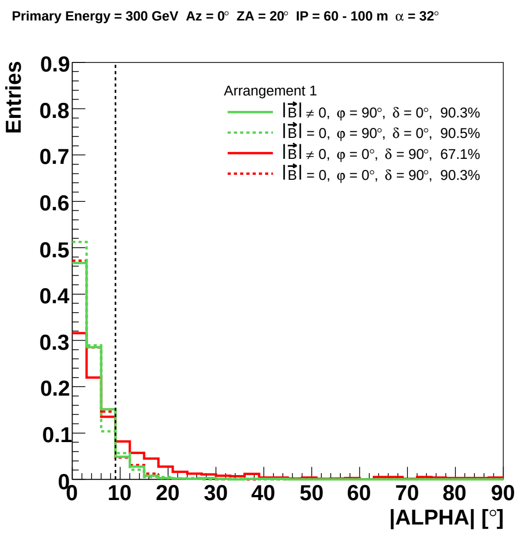

(c) Hard image cleaning, ZA 20°, azimuth angle 0°, impact parameter 60 - 100 m.

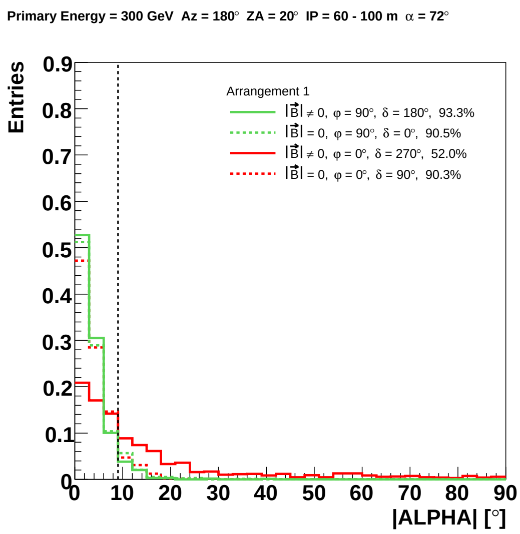

(d) Hard image cleaning, ZA 20°, azimuth angle 180°, impact parameter 60 - 100 m.

Figure 117: Normalized distributions of the image parameter ALPHA for MC γ-rays of 300 GeV energy, two impact parameter windows, 20° ZA, 0° and 180° azimuth angle. The angle φ was set to 0° and 90°, respectively.

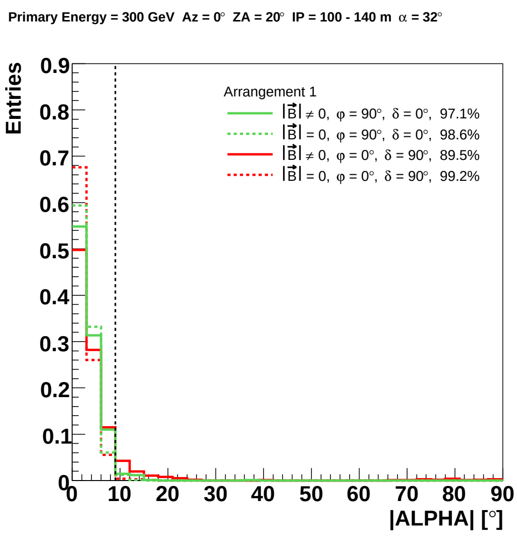

(a) Hard image cleaning, ZA 20°, azimuth angle 0°, impact parameter 100 - 140 m.

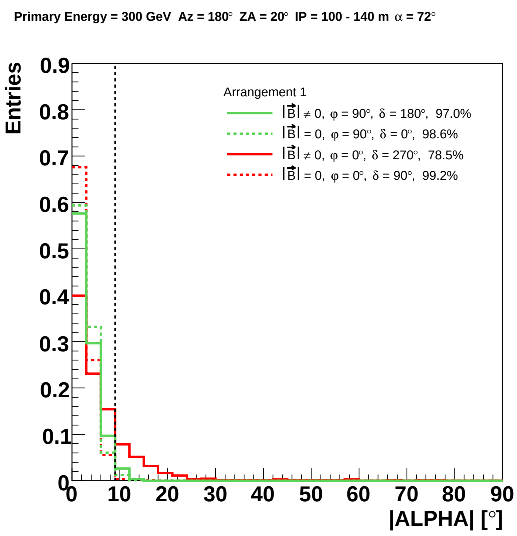

(b) Hard image cleaning, ZA 20°, azimuth angle 180°, impact parameter 100 - 140 m.

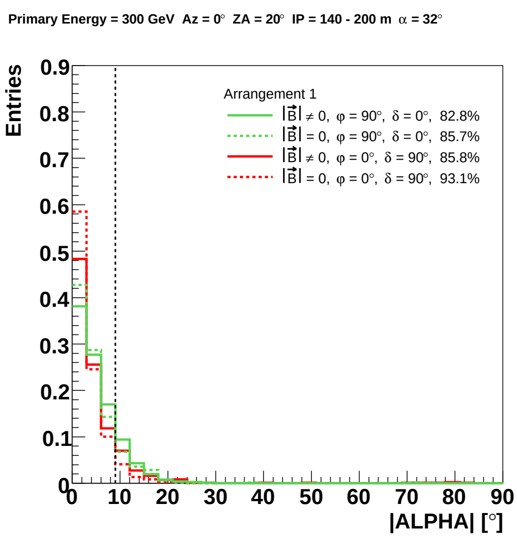

(c) Hard image cleaning, ZA 20°, azimuth angle 0°, impact parameter 140 - 200 m.

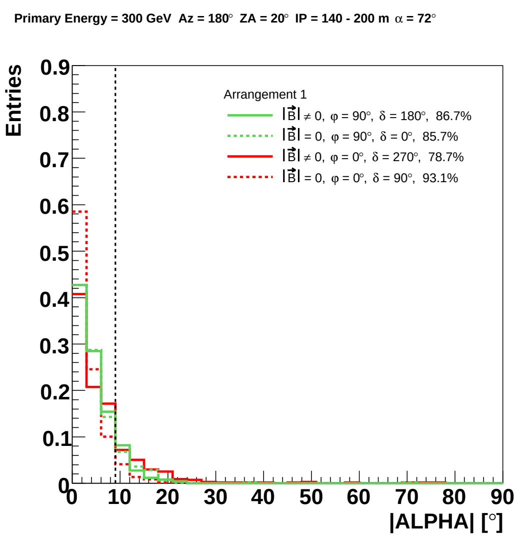

(d) Hard image cleaning, ZA 20°, azimuth angle 180°, impact parameter 140 - 200 m.

Figure 118: Normalized distributions of the image parameter ALPHA for MC γ-rays of 300 GeV energy, two impact parameter windows, 20° ZA, 0° and 180° azimuth angle. The angle φ was set to 0° and 90°, respectively.

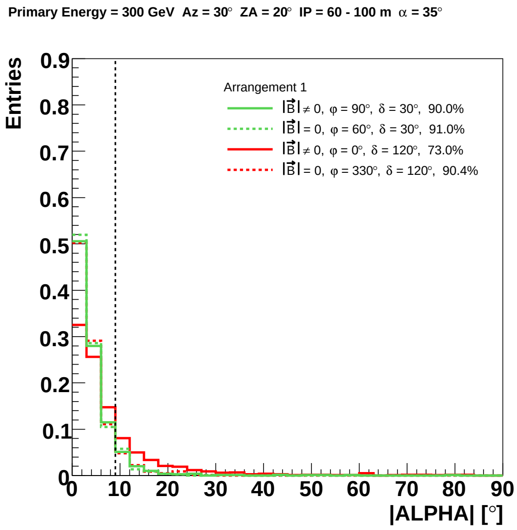

(a) Hard image cleaning, ZA 20°, azimuth angle 30°, impact parameter 60 - 100 m.

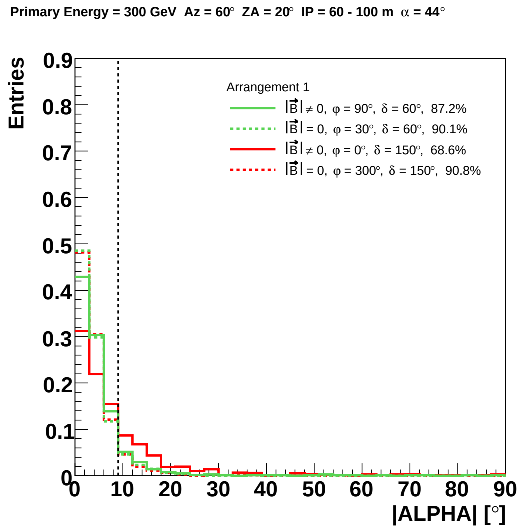

(b) Hard image cleaning, ZA 20°, azimuth angle 60°, impact parameter 60 - 100 m.

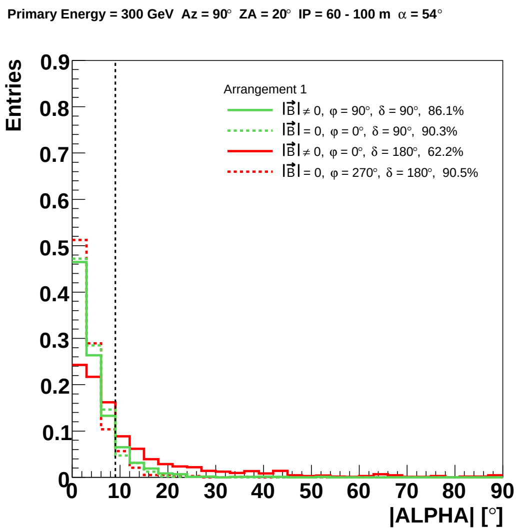

(c) Hard image cleaning, ZA 20°, azimuth angle 90°, impact parameter 60 - 100 m.

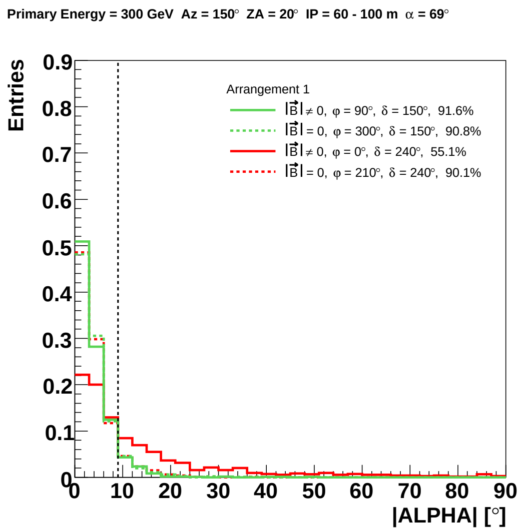

(d) Hard image cleaning, ZA 20°, azimuth angle 150°, impact parameter 60 - 100 m.

Figure 119: Normalized distributions of the image parameter ALPHA for MC γ-rays of 300 GeV energy, impact parameters between 60 m and 100 m, 20° ZA, 30°, 60°, 90° and 150° azimuth angle. The angle φ was set to 0° and 90°, respectively.

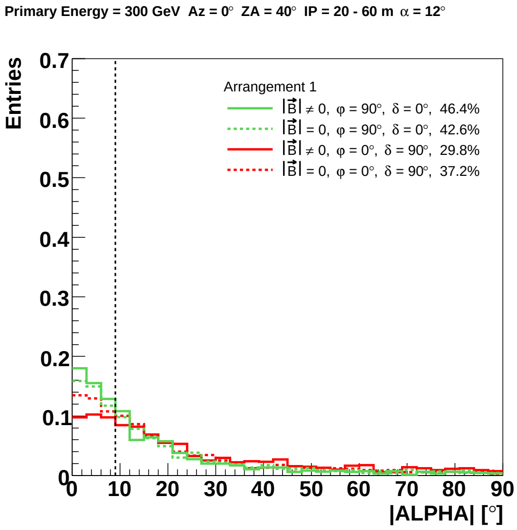

(a) Hard image cleaning, ZA 40°, azimuth angle 0°, impact parameter 20 - 60 m.

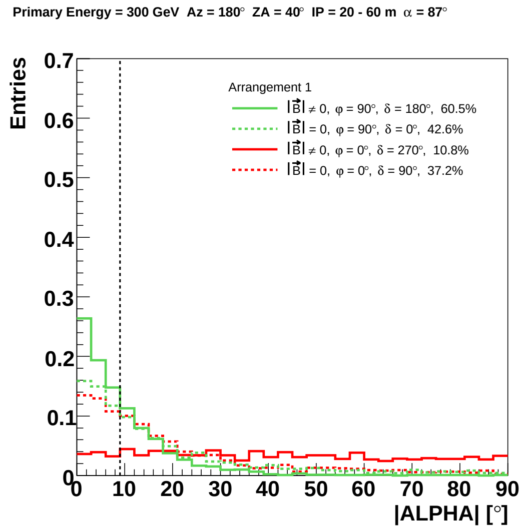

(b) Hard image cleaning, ZA 40°, azimuth angle 180°, impact parameter 20 - 60 m.

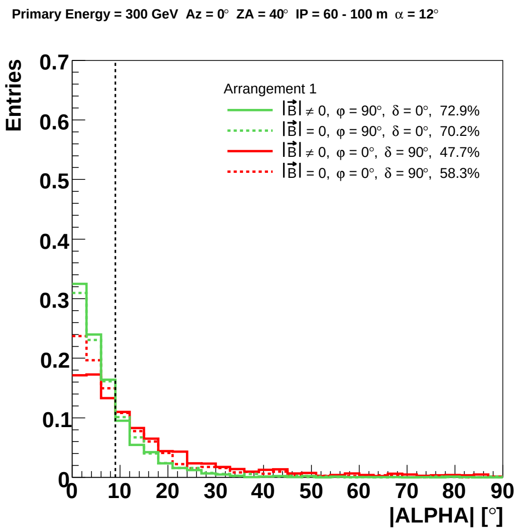

(c) Hard image cleaning, ZA 40°, azimuth angle 0°, impact parameter 60 - 100 m.

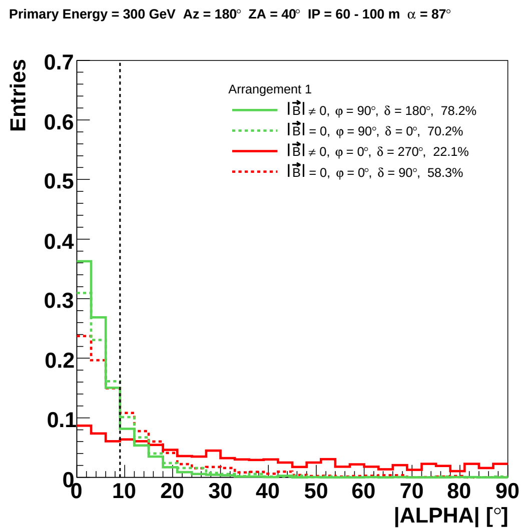

(d) Hard image cleaning, ZA 40°, azimuth angle 180°, impact parameter 60 - 100 m.

Figure 120: Normalized distributions of the image parameter ALPHA for MC γ-rays of 300 GeV energy, impact parameters between 60 m and 100 m, 40° ZA, 0° and 180° azimuth angle. The angle φ was set to 0° and 90°, respectively.

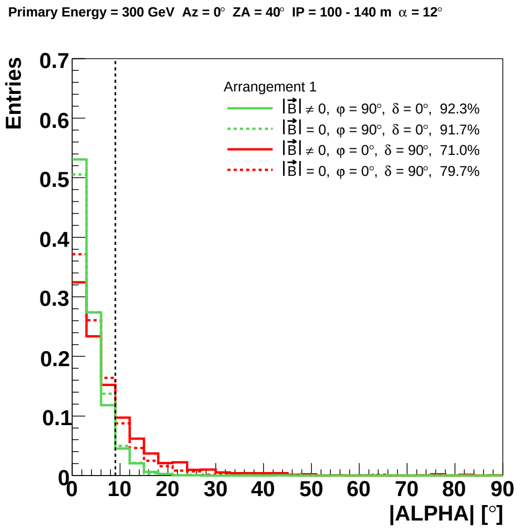

(a) Hard image cleaning, ZA 40°, azimuth angle 0°, impact parameter 100 - 140 m.

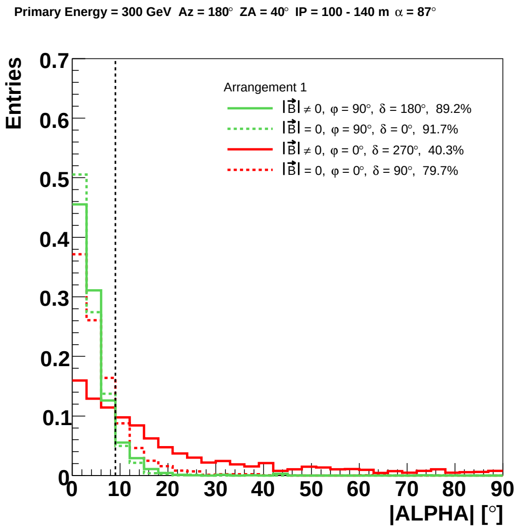

(b) Hard image cleaning, ZA 40°, azimuth angle 180°, impact parameter 100 - 140 m.

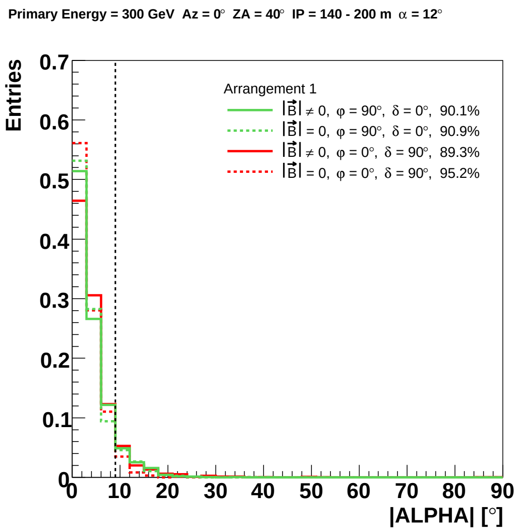

(c) Hard image cleaning, ZA 40°, azimuth angle 0°, impact parameter 140 - 200 m.

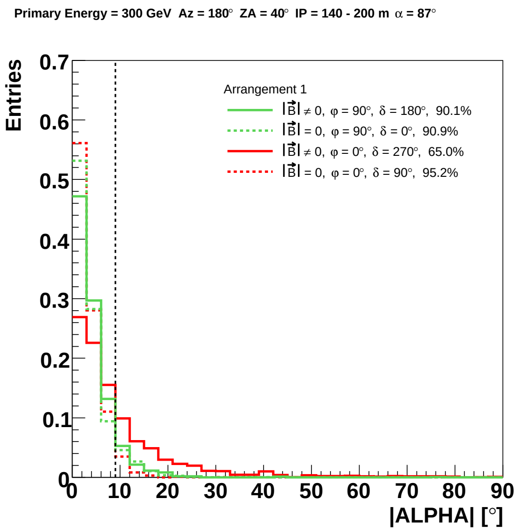

(d) Hard image cleaning, ZA 40°, azimuth angle 180°, impact parameter 140 - 200 m.

Figure 121: Normalized distributions of the image parameter ALPHA for MC γ-rays of 300 GeV energy, two impact parameter windows, 40° ZA, 0° and 180° azimuth angle. The angle φ was set to 0° and 90°, respectively.

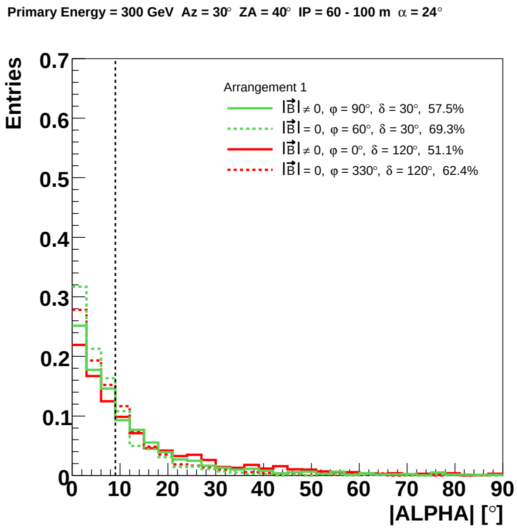

(a) Hard image cleaning, ZA 40°, azimuth angle 30°, impact parameter 60 - 100 m.

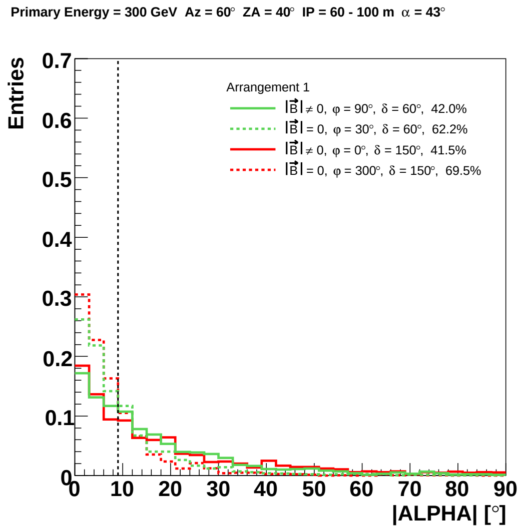

(b) Hard image cleaning, ZA 40°, azimuth angle 60°, impact parameter 60 - 100 m.

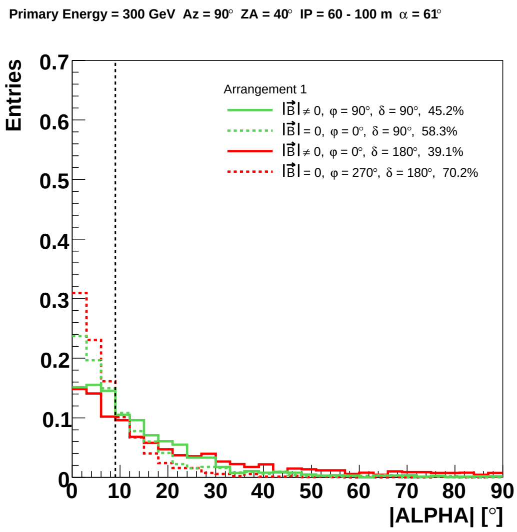

(c) Hard image cleaning, ZA 40°, azimuth angle 90°, impact parameter 60 - 100 m.

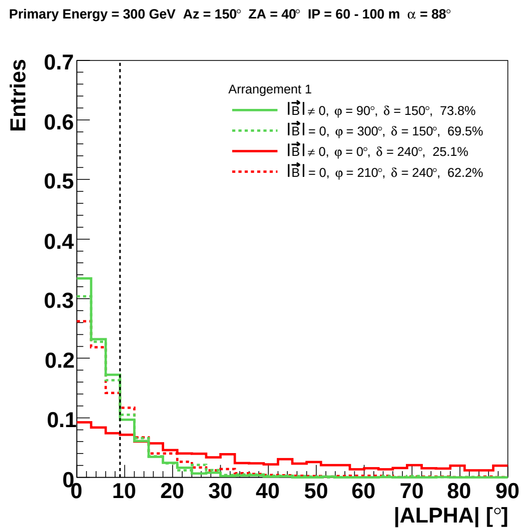

(d) Hard image cleaning, ZA 40°, azimuth angle 150°, impact parameter 60 - 100 m.

Figure 122: Normalized distributions of the image parameter ALPHA for MC γ-rays of 300 GeV energy, impact parameters between 60 m and 100 m, 40° ZA, 30°, 60°, 90° and 150° azimuth angle. The angle φ was set to 0° and 90°, respectively.

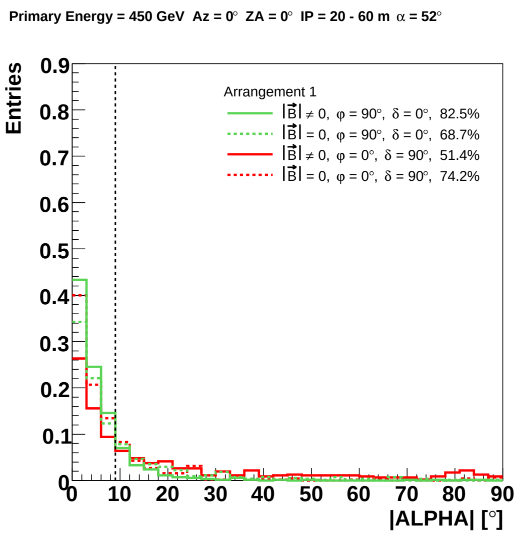

(a) Hard image cleaning, ZA 0°, azimuth angle 0°, impact parameter 20 - 60 m.

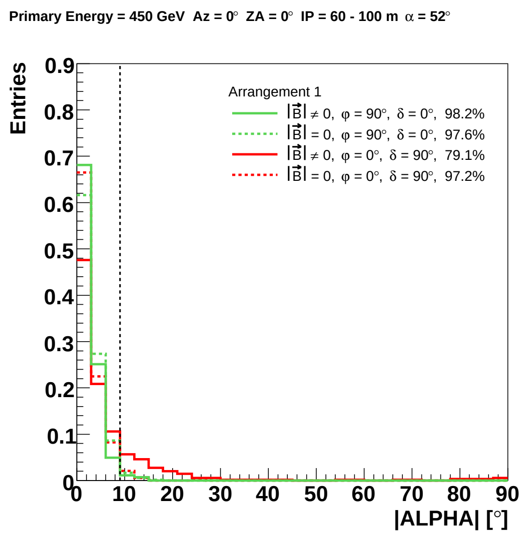

(b) Hard image cleaning, ZA 0°, azimuth angle 0°, impact parameter 60 - 100 m.

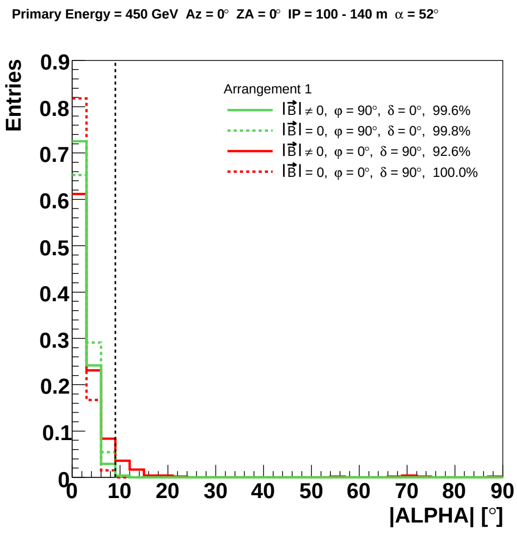

(c) Hard image cleaning, ZA 0°, azimuth angle 0°, impact parameter 100 - 140 m.

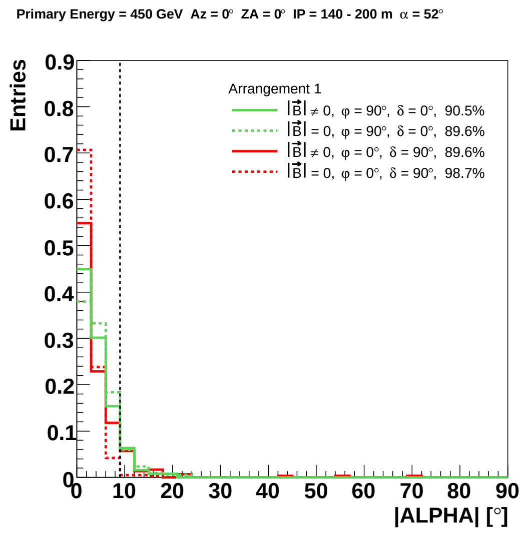

(d) Hard image cleaning, ZA 0°, azimuth angle 0°, impact parameter 140 - 200 m.

Figure 123: Normalized distributions of the image parameter ALPHA for MC γ-rays of 450 GeV energy, four impact parameter windows, 0° ZA and 0° azimuth angle. The angle φ was set to 0° and 90°, respectively.

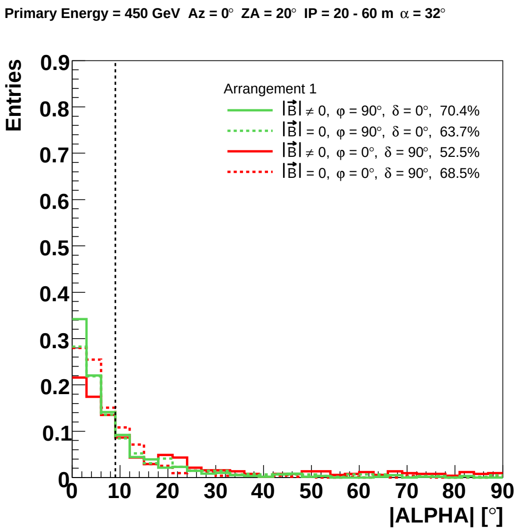

(a) Hard image cleaning, ZA 20°, azimuth angle 0°, impact parameter 20 - 60 m.

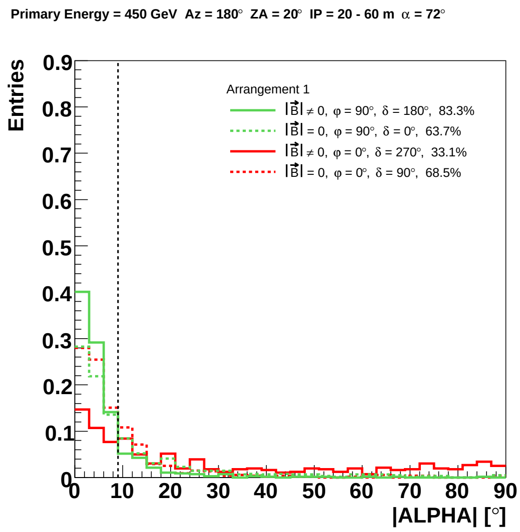

(b) Hard image cleaning, ZA 20°, azimuth angle 180°, impact parameter 20 - 60 m.

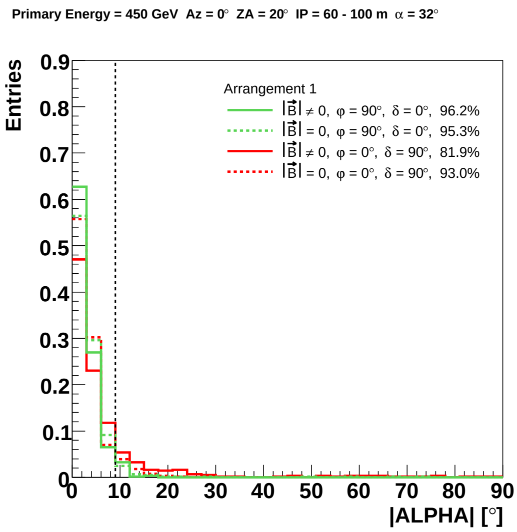

(c) Hard image cleaning, ZA 20°, azimuth angle 0°, impact parameter 60 - 100 m.

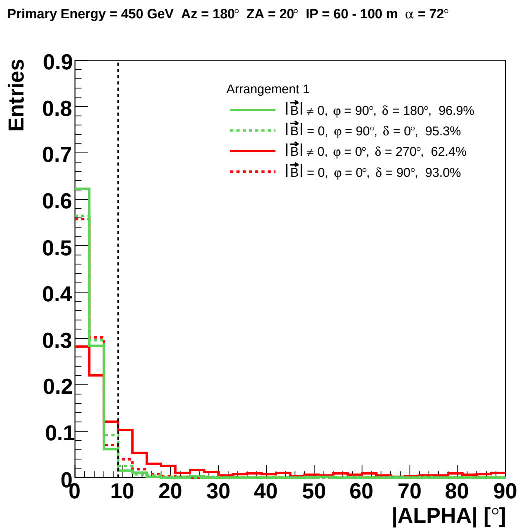

(d) Hard image cleaning, ZA 20°, azimuth angle 180°, impact parameter 60 - 100 m.

Figure 124: Normalized distributions of the image parameter ALPHA for MC γ-rays of 450 GeV energy, two impact parameter windows, 20° ZA, 0° and 180° azimuth angle. The angle φ was set to 0° and 90°, respectively.

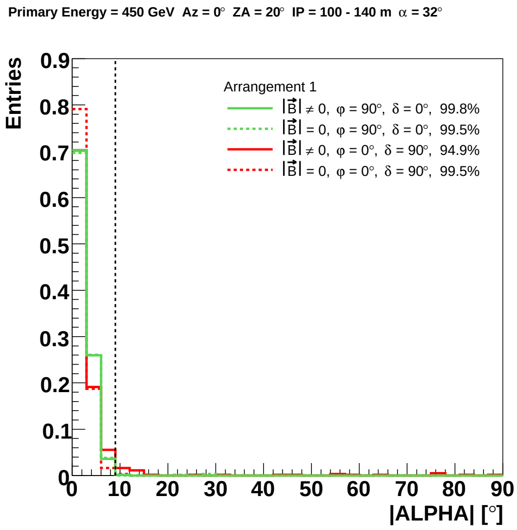

(a) Hard image cleaning, ZA 20°, azimuth angle 0°, impact parameter 100 - 140 m.

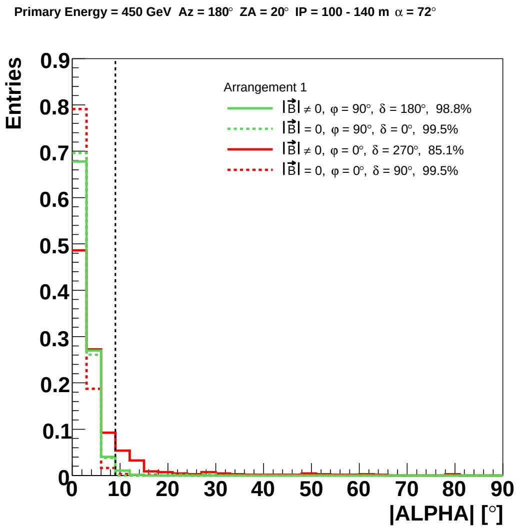

(b) Hard image cleaning, ZA 20°, azimuth angle 180°, impact parameter 100 - 140 m.

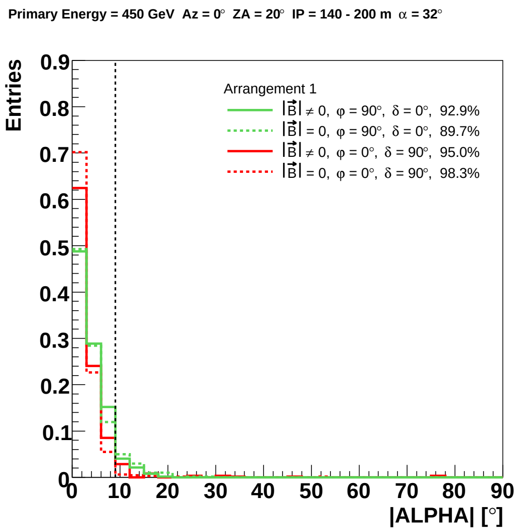

(c) Hard image cleaning, ZA 20°, azimuth angle 0°, impact parameter 140 - 200 m.

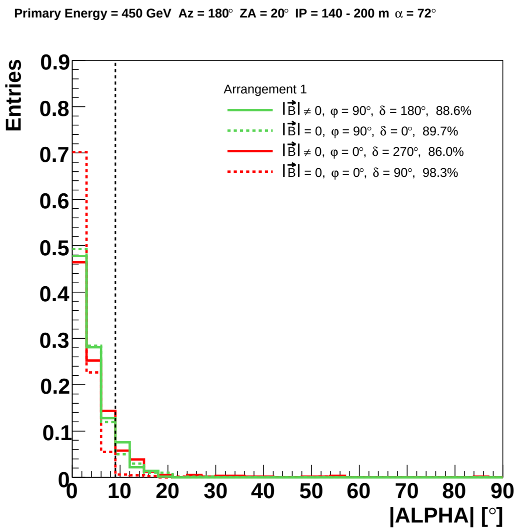

(d) Hard image cleaning, ZA 20°, azimuth angle 180°, impact parameter 140 - 200 m.

Figure 125: Normalized distributions of the image parameter ALPHA for MC γ-rays of 450 GeV energy, two impact parameter windows, 20° ZA, 0° and 180° azimuth angle. The angle φ was set to 0° and 90°, respectively.

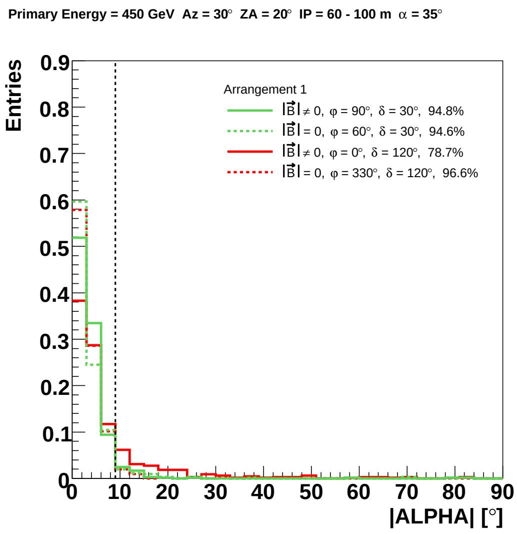

(a) Hard image cleaning, ZA 20°, azimuth angle 30°, impact parameter 60 - 100 m.

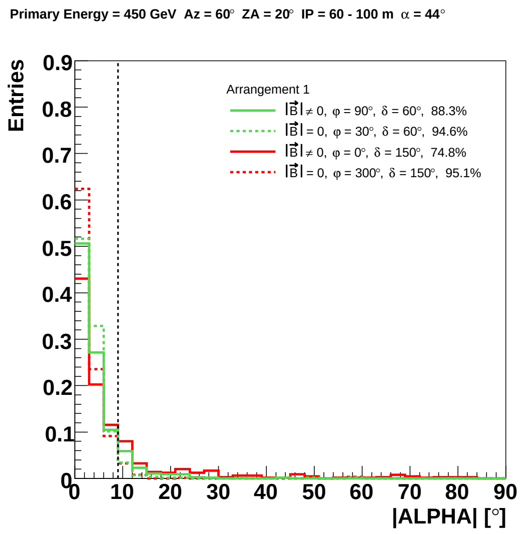

(b) Hard image cleaning, ZA 20°, azimuth angle 60°, impact parameter 60 - 100 m.

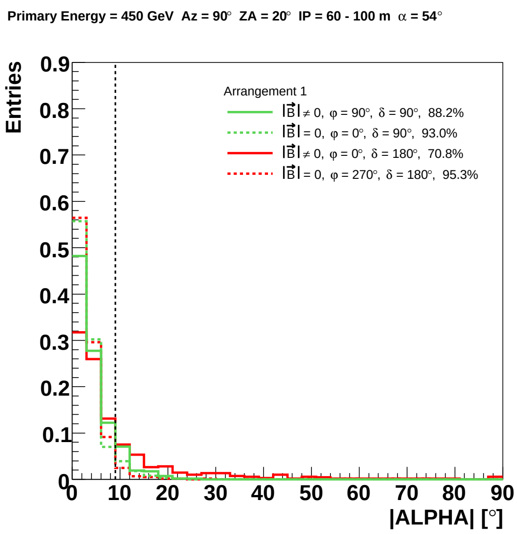

(c) Hard image cleaning, ZA 20°, azimuth angle 90°, impact parameter 60 - 100 m.

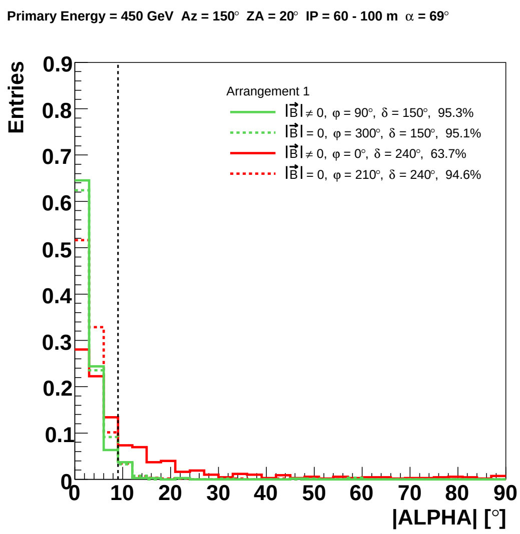

(d) Hard image cleaning, ZA 20°, azimuth angle 150°, impact parameter 60 - 100 m.

Figure 126: Normalized distributions of the image parameter ALPHA for MC γ-rays of 450 GeV energy, impact parameters between 60 m and 100 m, 20° ZA, 30°, 60°, 90° and 150° azimuth angle. The angle φ was set to 0° and 90°, respectively.

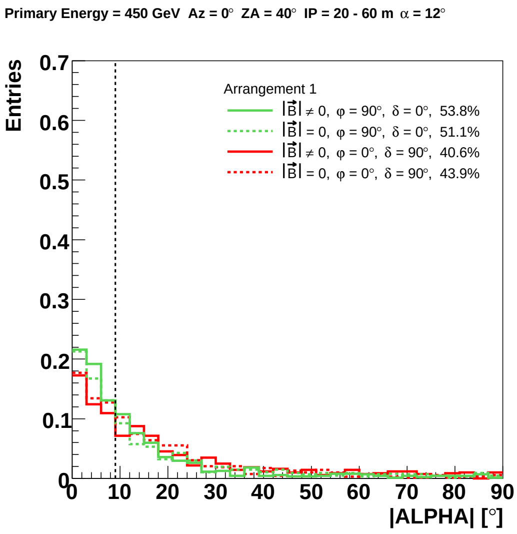

(a) Hard image cleaning, ZA 40°, azimuth angle 0°, impact parameter 20 - 60 m.

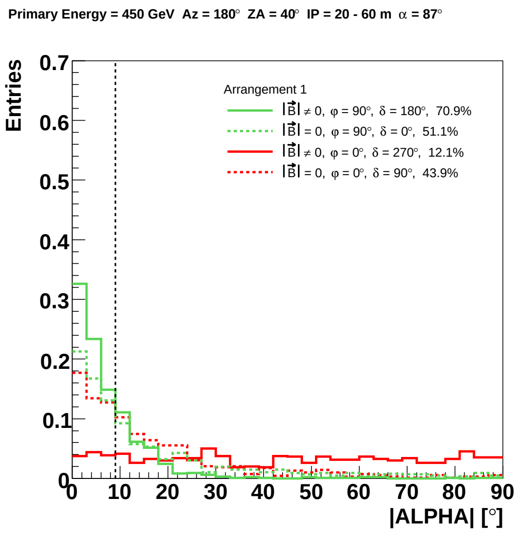

(b) Hard image cleaning, ZA 40°, azimuth angle 180°, impact parameter 20 - 60 m.

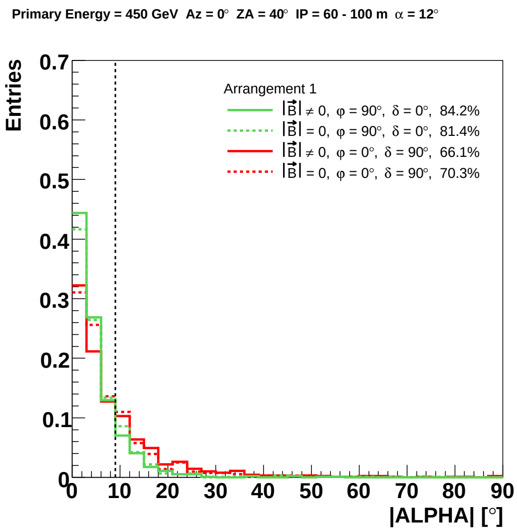

(c) Hard image cleaning, ZA 40°, azimuth angle 0°, impact parameter 60 - 100 m.

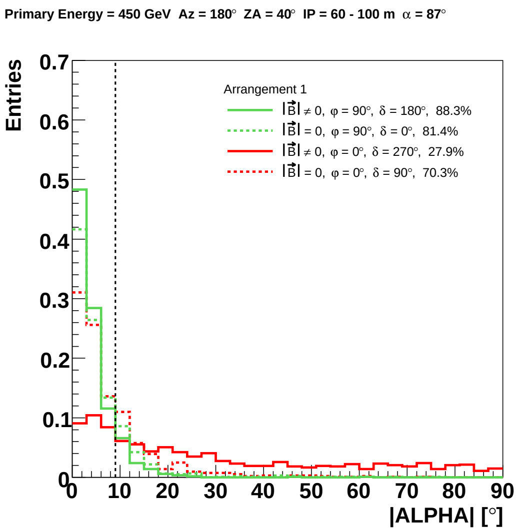

(d) Hard image cleaning, ZA 40°, azimuth angle 180°, impact parameter 60 - 100 m.

Figure 127: Normalized distributions of the image parameter ALPHA for MC γ-rays of 450 GeV energy, impact parameters between 60 m and 100 m, 40° ZA, 0° and 180° azimuth angle. The angle φ was set to 0° and 90°, respectively.

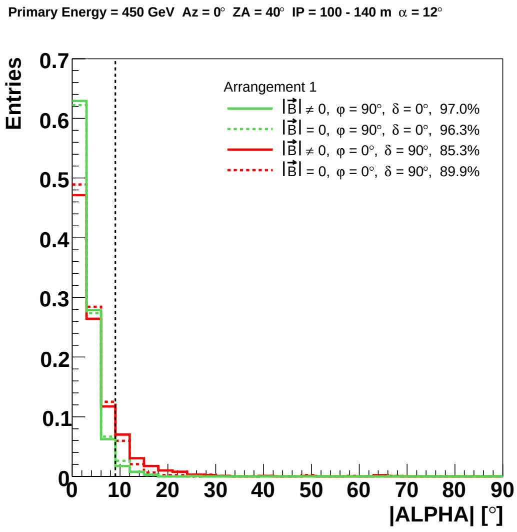

(a) Hard image cleaning, ZA 40°, azimuth angle 0°, impact parameter 100 - 140 m.

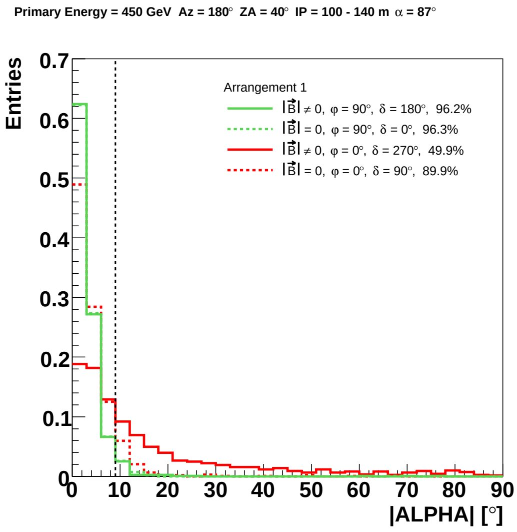

(b) Hard image cleaning, ZA 40°, azimuth angle 180°, impact parameter 100 - 140 m.

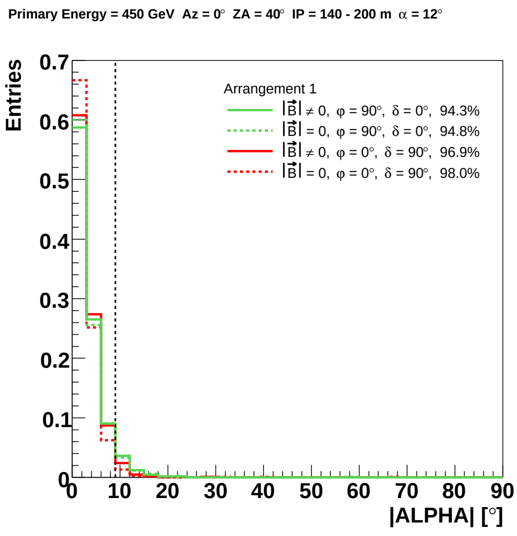

(c) Hard image cleaning, ZA 40°, azimuth angle 0°, impact parameter 140 - 200 m.

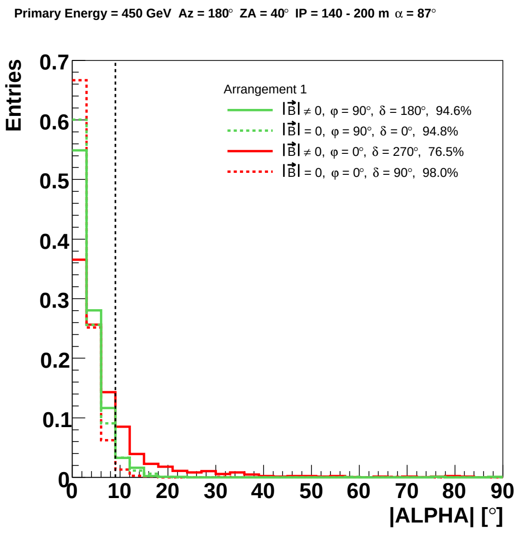

(d) Hard image cleaning, ZA 40°, azimuth angle 180°, impact parameter 140 - 200 m.

Figure 128: Normalized distributions of the image parameter ALPHA for MC γ-rays of 450 GeV energy, two impact parameter windows, 40° ZA, 0° and 180° azimuth angle. The angle φ was set to 0° and 90°, respectively.

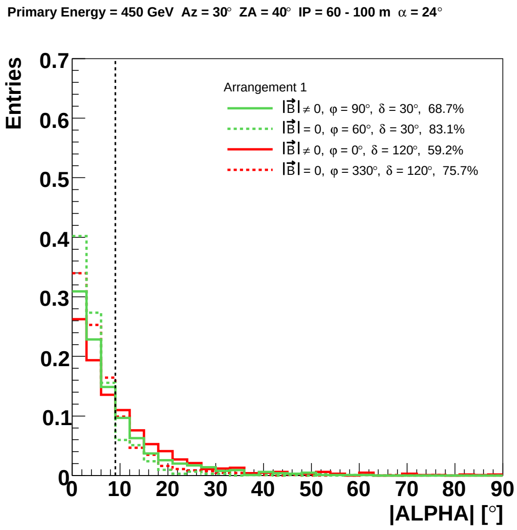

(a) Hard image cleaning, ZA 40°, azimuth angle 30°, impact parameter 60 - 100 m.

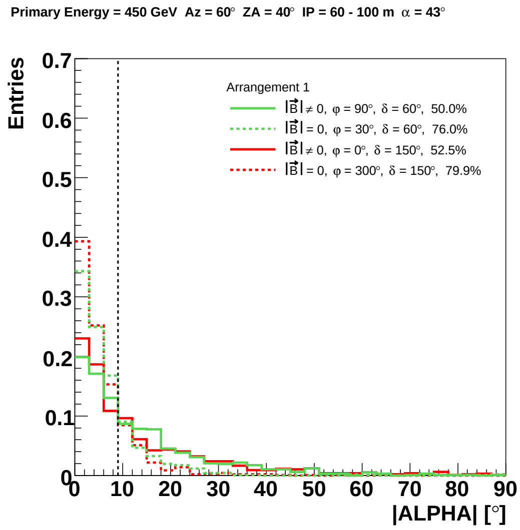

(b) Hard image cleaning, ZA 40°, azimuth angle 60°, impact parameter 60 - 100 m.

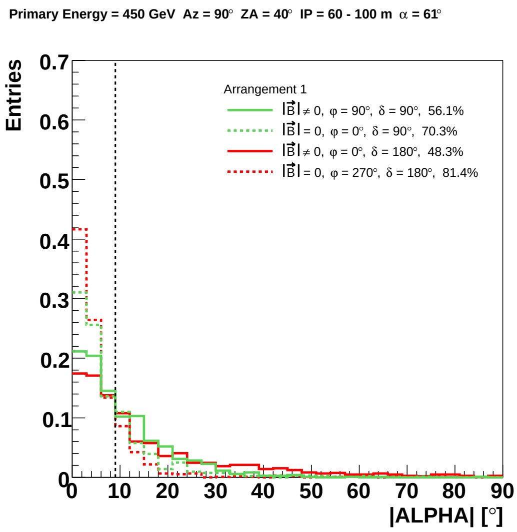

(c) Hard image cleaning, ZA 40°, azimuth angle 90°, impact parameter 60 - 100 m.

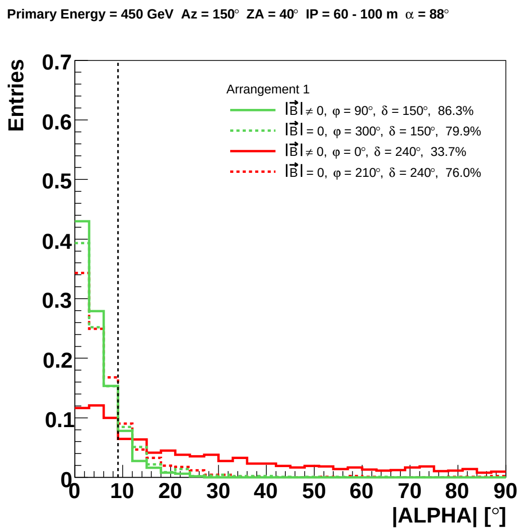

(d) Hard image cleaning, ZA 40°, azimuth angle 150°, impact parameter 60 - 100 m.

Figure 129: Normalized distributions of the image parameter ALPHA for MC γ-rays of 450 GeV energy, impact parameters between 60 m and 100 m, 40° ZA, 30°, 60°, 90° and 150° azimuth angle. The angle φ was set to 0° and 90°, respectively.

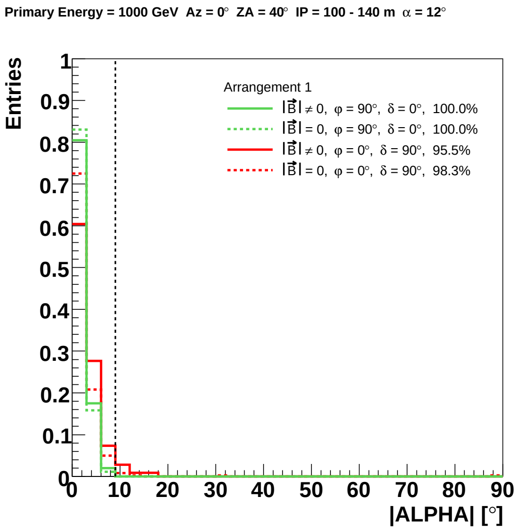

(a) Hard image cleaning, ZA 40°, azimuth angle 0°, impact parameter 100 - 140 m.

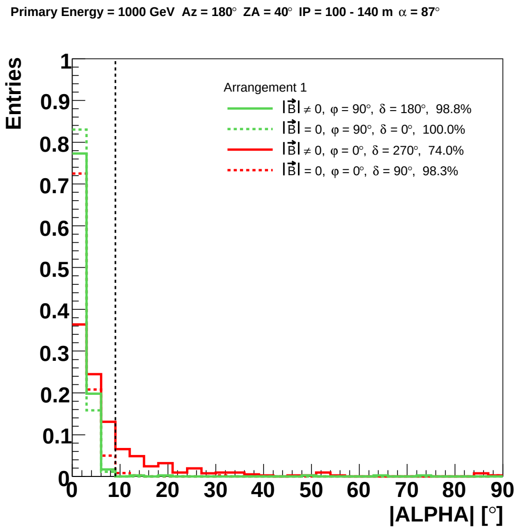

(b) Hard image cleaning, ZA 40°, azimuth angle 180°, impact parameter 100 - 140 m.

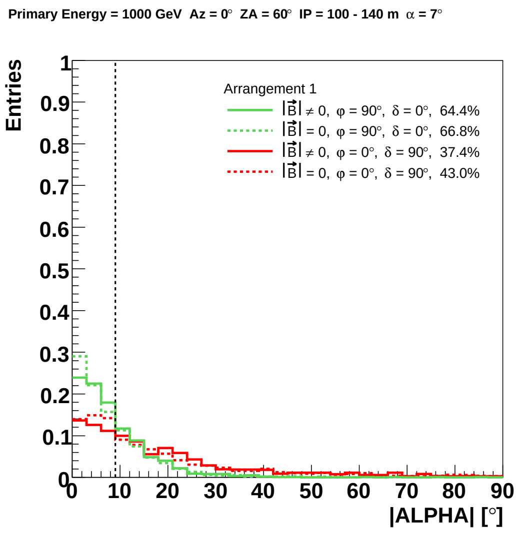

(c) Hard image cleaning, ZA 60°, azimuth angle 0°, impact parameter 100 - 140 m.

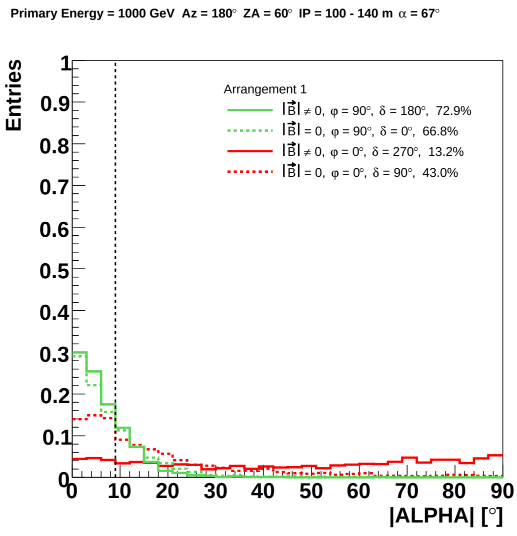

(d) Hard image cleaning, ZA 60°, azimuth angle 180°, impact parameter 100 - 140 m.

Figure 130: Normalized distributions of the image parameter ALPHA for MC γ-rays of 450 GeV energy, two impact parameter windows, 40° and 60° ZA, 0° and 180° azimuth angle. The angle φ was set to 0° and 90°, respectively.

The Recovery of the γ-Ray Signal by De-Rotation of Shower Images

E_γ = 170 GeV, Az = 0°, ZA = 40°, Hard Image Cleaning

δ_n[°]	$\Delta\delta$[°]	DIST[°]	RMS$_{\|ALPHA\|}$[°]	δ_n[°]	$\Delta\delta$[°]	DIST[°]	RMS$_{\|ALPHA\|}$[°]
IP = 60 m				IP = 80 m			
1.73 ± 0.76	+1.02 ± 1.53	0.329 ± 0.002	16.4 (17.9)	0.92 ± 0.61	+1.89 ± 1.14	0.425 ± 0.004	13.4 (14.1)
22.43 ± 0.70	−0.38 ± 0.93	0.305 ± 0.002	15.8 (19.2)	23.43 ± 0.61	+1.50 ± 1.00	0.396 ± 0.004	13.1 (13.5)
54.48 ± 0.85	+2.87 ± 1.70	0.268 ± 0.003	19.5 (20.3)	53.20 ± 0.55	+2.52 ± 1.16	0.347 ± 0.003	17.7 (16.7)
88.81 ± 0.71	−4.13 ± 1.59	0.247 ± 0.003	20.1 (21.1)	92.10 ± 0.77	−1.76 ± 1.68	0.321 ± 0.003	18.8 (16.0)
127.37 ± 0.15	+0.36 ± 0.62	0.267 ± 0.003	20.3 (17.3)	125.58 ± 0.62	−1.57 ± 1.42	0.357 ± 0.003	16.2 (13.7)
151.50 ± 0.24	−6.55 ± 0.98	0.310 ± 0.003	18.2 (19.8)	157.83 ± 0.69	−0.05 ± 1.31	0.397 ± 0.004	10.6 (12.5)
179.60 ± 0.76	+3.29 ± 1.53	0.325 ± 0.003	17.3 (17.5)	179.08 ± 0.69	+0.09 ± 1.15	0.426 ± 0.004	11.1 (14.1)
207.69 ± 0.62	+2.46 ± 1.75	0.312 ± 0.003	17.3 (19.8)	204.98 ± 0.37	+1.38 ± 0.75	0.403 ± 0.004	11.9 (14.8)
235.25 ± 0.47	+1.89 ± 1.34	0.278 ± 0.003	22.3 (19.7)	233.34 ± 0.68	+3.64 ± 1.44	0.362 ± 0.003	15.9 (16.5)
269.83 ± 0.60	−0.98 ± 1.69	0.258 ± 0.003	20.3 (19.5)	271.67 ± 0.54	+1.72 ± 1.29	0.341 ± 0.002	18.0 (17.2)
308.62 ± 0.62	+0.39 ± 1.39	0.277 ± 0.003	19.9 (20.4)	307.97 ± 0.59	+1.01 ± 0.90	0.364 ± 0.003	16.3 (15.0)
337.80 ± 0.85	+1.38 ± 1.33	0.315 ± 0.003	18.0 (20.2)	336.93 ± 0.84	−0.03 ± 1.38	0.408 ± 0.004	13.5 (11.5)
IP = 100 m				IP = 120 m			
0.50 ± 0.29	+1.44 ± 0.72	0.506 ± 0.004	8.8 (9.8)	360.00 ± 0.33	+0.36 ± 0.67	0.579 ± 0.005	5.7 (5.9)
24.78 ± 0.35	+1.11 ± 0.78	0.479 ± 0.004	9.7 (11.9)	23.48 ± 0.26	+0.21 ± 0.53	0.549 ± 0.004	6.4 (6.6)
52.87 ± 0.74	+0.75 ± 1.26	0.425 ± 0.003	13.0 (13.4)	51.52 ± 0.50	−0.33 ± 1.00	0.498 ± 0.004	10.5 (7.7)
90.32 ± 0.30	+2.02 ± 0.91	0.391 ± 0.003	19.9 (14.3)	89.77 ± 0.51	−0.10 ± 1.31	0.469 ± 0.005	10.7 (12.4)
125.81 ± 0.51	−4.13 ± 1.03	0.426 ± 0.003	13.6 (11.6)	128.65 ± 0.35	+1.51 ± 0.93	0.500 ± 0.004	12.7 (7.3)
157.01 ± 0.51	−0.93 ± 0.95	0.477 ± 0.004	9.4 (9.8)	156.02 ± 0.40	+0.69 ± 0.68	0.550 ± 0.005	8.0 (7.5)
180.55 ± 0.57	+0.93 ± 0.86	0.501 ± 0.004	9.2 (8.4)	180.20 ± 0.27	+0.04 ± 0.54	0.576 ± 0.004	5.2 (5.2)
203.79 ± 0.57	+1.31 ± 1.00	0.483 ± 0.004	10.9 (9.2)	203.03 ± 0.33	+0.64 ± 0.62	0.557 ± 0.005	7.4 (7.6)
233.09 ± 0.50	+2.08 ± 1.16	0.439 ± 0.003	12.2 (10.3)	234.04 ± 0.48	+2.04 ± 0.83	0.508 ± 0.004	10.6 (6.8)
271.84 ± 0.80	+3.60 ± 1.32	0.407 ± 0.004	16.3 (13.3)	271.55 ± 0.56	+0.42 ± 0.99	0.473 ± 0.004	8.7 (8.2)
307.25 ± 0.52	−1.50 ± 1.11	0.440 ± 0.002	8.7 (8.8)	306.83 ± 0.42	−1.97 ± 0.91	0.506 ± 0.005	9.9 (7.1)
337.14 ± 0.35	−0.99 ± 1.00	0.484 ± 0.004	9.9 (9.9)	336.99 ± 0.34	+1.05 ± 0.61	0.563 ± 0.005	8.7 (6.0)

Table 2: The nominal angle δ_n, average displacement $\Delta\delta$, average value of the parameter DIST, RMS of the ALPHA distribution for enabled GF and impact parameters between 60 m and 120 m. The RMS of the ALPHA distribution for disabled GF is given parentheses. The primary γ-ray energy was set to 170 GeV, the ZA to 40° and the azimuth angle to 0°.

E_γ = 170 GeV, Az = 180°, ZA = 40°, Hard Image Cleaning

δ_n[°]	$\Delta\delta$[°]	DIST[°]	RMS$_{\|ALPHA\|}$[°]	δ_n[°]	$\Delta\delta$[°]	DIST[°]	RMS$_{\|ALPHA\|}$[°]
IP = 60 m				IP = 80 m			
1.73 ± 0.76	−1.29 ± 1.25	0.350 ± 0.003	11.5 (17.9)	0.92 ± 0.61	+1.25 ± 1.21	0.441 ± 0.004	8.7 (14.1)
22.43 ± 0.70	+3.72 ± 1.67	0.324 ± 0.003	16.8 (19.2)	23.43 ± 0.61	+3.82 ± 1.45	0.426 ± 0.005	14.6 (13.5)
54.48 ± 0.85	+12.57 ± 1.95	0.292 ± 0.003	27.4 (20.3)	53.20 ± 0.50	+7.20 ± 0.84	0.381 ± 0.004	22.3 (16.7)
88.81 ± 0.71	−3.61 ± 1.21	0.280 ± 0.003	21.7 (21.1)	92.10 ± 0.77	−1.30 ± 0.87	0.355 ± 0.005	21.8 (16.0)
127.37 ± 0.15	−6.58 ± 0.56	0.296 ± 0.003	20.9 (17.3)	125.58 ± 0.62	−9.71 ± 1.74	0.383 ± 0.004	17.7 (13.7)
151.50 ± 0.24	−6.94 ± 1.70	0.324 ± 0.004	14.4 (19.8)	157.83 ± 0.69	−3.32 ± 1.16	0.425 ± 0.005	11.7 (12.5)
179.60 ± 0.76	−0.71 ± 1.06	0.343 ± 0.004	13.3 (17.5)	179.08 ± 0.69	−0.25 ± 1.26	0.448 ± 0.005	10.9 (14.1)
207.69 ± 0.62	+9.99 ± 1.30	0.321 ± 0.003	13.6 (19.8)	204.98 ± 0.37	+3.76 ± 1.12	0.419 ± 0.005	13.7 (14.8)
235.25 ± 0.47	+10.78 ± 0.98	0.286 ± 0.003	25.1 (19.7)	233.34 ± 0.68	+11.72 ± 1.63	0.369 ± 0.003	23.6 (16.5)
269.83 ± 0.60	+1.69 ± 0.99	0.262 ± 0.003	23.9 (19.5)	271.67 ± 0.54	+1.41 ± 1.22	0.338 ± 0.003	25.3 (17.2)
308.62 ± 0.62	−5.01 ± 1.43	0.287 ± 0.003	20.9 (20.4)	307.97 ± 0.59	−9.17 ± 1.18	0.366 ± 0.003	19.3 (15.0)
337.80 ± 0.85	+0.27 ± 1.24	0.333 ± 0.005	12.7 (20.2)	336.93 ± 0.84	−1.74 ± 1.52	0.424 ± 0.003	10.7 (11.5)
IP = 100 m				IP = 120 m			
0.50 ± 0.29	+1.56 ± 0.58	0.537 ± 0.006	5.7 (9.8)	360.00 ± 0.33	+0.60 ± 0.78	0.615 ± 0.002	5.2 (5.9)
24.78 ± 0.35	+1.80 ± 0.72	0.515 ± 0.004	8.1 (11.9)	23.48 ± 0.26	+0.06 ± 0.79	0.582 ± 0.007	5.5 (6.6)
52.87 ± 0.74	+4.77 ± 1.43	0.471 ± 0.003	15.0 (13.4)	51.52 ± 0.50	+3.90 ± 1.05	0.543 ± 0.006	18.1 (7.7)
90.32 ± 0.30	−0.58 ± 1.36	0.434 ± 0.004	22.0 (14.3)	89.77 ± 0.51	+1.38 ± 1.84	0.510 ± 0.005	21.2 (12.4)
125.81 ± 0.51	−2.37 ± 1.19	0.469 ± 0.004	15.5 (11.6)	128.65 ± 0.35	−3.08 ± 0.87	0.540 ± 0.005	13.3 (7.3)
157.01 ± 0.51	−2.77 ± 1.15	0.523 ± 0.005	8.7 (9.8)	156.02 ± 0.40	−0.94 ± 1.18	0.599 ± 0.006	9.4 (7.5)
180.55 ± 0.57	+3.18 ± 1.02	0.539 ± 0.006	6.4 (8.4)	180.20 ± 0.27	+1.59 ± 0.62	0.616 ± 0.006	4.7 (5.2)
203.79 ± 0.57	+3.68 ± 1.19	0.508 ± 0.005	11.4 (9.2)	203.03 ± 0.33	+2.00 ± 0.66	0.590 ± 0.006	7.5 (7.6)
233.09 ± 0.50	+7.48 ± 1.69	0.462 ± 0.004	14.0 (10.3)	234.04 ± 0.48	+1.82 ± 1.01	0.533 ± 0.005	12.6 (6.8)
271.84 ± 0.80	+3.82 ± 1.18	0.427 ± 0.003	20.3 (13.3)	271.55 ± 0.56	+2.22 ± 0.84	0.496 ± 0.005	16.3 (8.2)
307.25 ± 0.52	−4.88 ± 1.19	0.457 ± 0.005	12.7 (8.8)	306.83 ± 0.42	−3.25 ± 0.96	0.529 ± 0.006	14.6 (7.1)
337.14 ± 0.35	+0.41 ± 0.92	0.514 ± 0.005	8.5 (9.9)	336.99 ± 0.34	−0.24 ± 0.96	0.590 ± 0.007	7.9 (6.0)

Table 3: The nominal angle δ_n, average displacement $\Delta\delta$, average value of the parameter DIST, RMS of the ALPHA distribution for enabled GF and impact parameters between 60 m and 120 m. The RMS of the ALPHA distribution for disabled GF is given parentheses. The primary γ-ray energy was set to 170 GeV, the ZA to 40° and the azimuth angle to 180°.

$E_\gamma = 450\,\mathrm{GeV}$, Az = 0°, ZA = 40°, Hard Image Cleaning

δ_n[°]	$\Delta\delta$[°]	DIST[°]	$\mathrm{RMS}_{\lvert\mathrm{ALPHA}\rvert}$[°]	δ_n[°]	$\Delta\delta$[°]	DIST[°]	$\mathrm{RMS}_{\lvert\mathrm{ALPHA}\rvert}$[°]
IP = 60 m				**IP = 80 m**			
0.10 ± 0.31	$+0.13 \pm 0.93$	0.358 ± 0.004	7.6 (12.1)	0.74 ± 0.51	$+0.91 \pm 0.93$	0.468 ± 0.003	6.2 (10.6)
23.41 ± 0.62	$+1.50 \pm 1.14$	0.335 ± 0.003	8.4 (9.1)	24.35 ± 0.52	$+1.49 \pm 0.93$	0.441 ± 0.006	9.1 (3.9)
54.65 ± 0.93	$+2.49 \pm 1.24$	0.292 ± 0.003	12.5 (7.8)	53.60 ± 0.52	$+1.64 \pm 0.93$	0.387 ± 0.003	13.0 (4.7)
91.52 ± 0.83	$+2.71 \pm 1.24$	0.267 ± 0.003	16.3 (11.6)	90.85 ± 0.62	$+1.42 \pm 1.14$	0.357 ± 0.004	16.4 (5.9)
128.06 ± 0.52	-1.00 ± 1.03	0.293 ± 0.003	11.2 (6.2)	128.44 ± 0.52	-0.51 ± 0.93	0.388 ± 0.004	6.4 (5.0)
156.64 ± 0.62	-1.00 ± 1.24	0.337 ± 0.003	5.7 (6.8)	154.96 ± 0.52	-1.69 ± 1.03	0.440 ± 0.004	3.9 (6.7)
179.48 ± 0.41	$+0.09 \pm 1.34$	0.356 ± 0.003	7.1 (8.2)	180.59 ± 0.41	$+0.65 \pm 0.83$	0.466 ± 0.004	3.7 (3.9)
203.50 ± 0.41	$+0.66 \pm 0.83$	0.342 ± 0.003	8.3 (9.0)	203.95 ± 0.52	$+0.88 \pm 0.83$	0.448 ± 0.004	5.4 (6.6)
232.64 ± 0.62	$+1.64 \pm 1.55$	0.305 ± 0.002	12.0 (11.2)	233.32 ± 0.52	$+2.20 \pm 0.93$	0.404 ± 0.003	8.5 (6.3)
270.28 ± 0.62	$+0.17 \pm 0.93$	0.283 ± 0.003	12.2 (11.9)	269.27 ± 0.52	-2.12 ± 1.24	0.372 ± 0.004	7.9 (9.3)
305.49 ± 0.62	-3.15 ± 1.34	0.303 ± 0.003	9.4 (10.1)	306.92 ± 0.52	$+0.12 \pm 1.03$	0.405 ± 0.003	10.0 (11.2)
337.26 ± 0.62	$+0.63 \pm 1.24$	0.345 ± 0.003	5.4 (7.7)	337.30 ± 0.41	$+0.96 \pm 0.83$	0.451 ± 0.004	5.0 (7.5)
IP = 100 m				**IP = 120 m**			
359.99 ± 0.31	$+0.67 \pm 0.72$	0.570 ± 0.007	4.5 (8.7)	0.29 ± 0.21	$+0.55 \pm 0.62$	0.650 ± 0.008	2.7 (2.7)
25.23 ± 0.41	$+1.40 \pm 0.72$	0.541 ± 0.005	3.7 (3.6)	24.97 ± 0.31	$+0.94 \pm 0.52$	0.623 ± 0.006	2.4 (1.9)
52.56 ± 0.41	$+0.67 \pm 0.72$	0.477 ± 0.003	6.2 (4.2)	53.42 ± 0.31	$+0.55 \pm 0.62$	0.560 ± 0.005	4.1 (3.2)
90.71 ± 0.52	-0.38 ± 0.93	0.441 ± 0.005	9.1 (3.9)	90.27 ± 0.21	-0.67 ± 0.72	0.519 ± 0.005	3.8 (3.7)
126.90 ± 0.31	-1.15 ± 0.72	0.476 ± 0.006	3.5 (5.1)	126.89 ± 0.41	-0.29 ± 0.62	0.556 ± 0.005	2.6 (5.3)
156.29 ± 0.31	-0.97 ± 0.72	0.537 ± 0.005	2.3 (3.7)	156.23 ± 0.31	-0.02 ± 0.52	0.622 ± 0.007	2.3 (2.4)
179.92 ± 0.41	-0.74 ± 0.83	0.567 ± 0.004	2.5 (2.9)	179.95 ± 0.21	-0.29 ± 0.41	0.648 ± 0.004	2.2 (2.6)
203.57 ± 0.41	$+0.27 \pm 0.83$	0.546 ± 0.006	5.0 (2.7)	203.14 ± 0.21	-0.55 ± 0.41	0.632 ± 0.007	2.8 (2.6)
232.85 ± 0.52	$+1.40 \pm 0.83$	0.491 ± 0.004	6.6 (9.5)	232.26 ± 0.41	-0.60 ± 0.83	0.577 ± 0.005	5.0 (10.2)
270.28 ± 0.31	$+0.59 \pm 0.72$	0.458 ± 0.003	6.4 (6.5)	270.20 ± 0.21	-0.46 ± 0.62	0.539 ± 0.006	4.0 (3.5)
307.19 ± 0.41	-1.51 ± 0.83	0.495 ± 0.003	5.0 (5.7)	307.18 ± 0.31	$+0.37 \pm 0.62$	0.579 ± 0.005	4.0 (4.1)
336.92 ± 0.41	$+0.26 \pm 0.72$	0.549 ± 0.007	3.1 (4.8)	336.47 ± 0.21	$+0.24 \pm 0.41$	0.633 ± 0.005	2.3 (2.4)

Table 4: The nominal angle δ_n, average displacement $\Delta\delta$, average value of the parameter DIST, RMS of the ALPHA distribution for enabled GF and impact parameters between 60 m and 120 m. The RMS of the ALPHA distribution for disabled GF is given parentheses. The MC γ-ray energy was set to 450 GeV, the ZA to 40° and the azimuth angle to 0°.

$E_\gamma = 450\,\mathrm{GeV}$, Az = 180°, ZA = 40°, Hard Image Cleaning

δ_n[°]	$\Delta\delta$[°]	DIST[°]	$\mathrm{RMS}_{\lvert\mathrm{ALPHA}\rvert}$[°]	δ_n[°]	$\Delta\delta$[°]	DIST[°]	$\mathrm{RMS}_{\lvert\mathrm{ALPHA}\rvert}$[°]
IP = 60 m				**IP = 80 m**			
0.10 ± 0.31	$+0.50 \pm 0.59$	0.340 ± 0.005	5.3 (12.1)	0.74 ± 0.51	$+1.17 \pm 0.80$	0.444 ± 0.005	3.3 (10.6)
23.41 ± 0.62	$+8.06 \pm 0.81$	0.328 ± 0.004	18.6 (9.1)	24.35 ± 0.52	$+6.86 \pm 0.90$	0.428 ± 0.002	3.7 (3.9)
54.65 ± 0.93	$+16.67 \pm 1.88$	0.294 ± 0.002	25.7 (7.8)	53.60 ± 0.52	$+13.23 \pm 1.18$	0.386 ± 0.005	26.1 (4.7)
91.52 ± 0.83	$+0.07 \pm 1.21$	0.275 ± 0.003	25.3 (11.6)	90.85 ± 0.62	$+0.88 \pm 1.76$	0.359 ± 0.004	26.7 (5.9)
128.06 ± 0.52	-17.44 ± 1.18	0.293 ± 0.004	17.7 (6.2)	128.44 ± 0.52	-12.50 ± 1.94	0.382 ± 0.004	17.2 (5.0)
156.64 ± 0.62	-7.71 ± 1.38	0.325 ± 0.005	10.6 (6.8)	154.96 ± 0.52	-6.79 ± 1.09	0.428 ± 0.005	7.7 (6.7)
179.48 ± 0.41	$+0.06 \pm 0.70$	0.342 ± 0.005	4.6 (8.2)	180.59 ± 0.41	$+0.78 \pm 0.79$	0.445 ± 0.005	3.2 (3.9)
203.50 ± 0.41	$+9.53 \pm 0.98$	0.322 ± 0.004	15.0 (9.0)	203.95 ± 0.52	$+8.06 \pm 0.99$	0.419 ± 0.003	3.9 (6.6)
232.64 ± 0.62	$+17.87 \pm 1.57$	0.283 ± 0.004	22.3 (11.2)	233.32 ± 0.52	$+15.06 \pm 0.80$	0.372 ± 0.002	21.1 (6.3)
270.28 ± 0.62	-7.15 ± 0.90	0.262 ± 0.003	26.7 (11.9)	269.27 ± 0.52	-1.97 ± 1.37	0.346 ± 0.004	26.1 (9.3)
305.49 ± 0.62	-15.23 ± 1.09	0.283 ± 0.004	17.5 (10.1)	306.92 ± 0.52	-13.40 ± 1.84	0.374 ± 0.005	16.7 (11.2)
337.26 ± 0.62	-6.25 ± 1.19	0.321 ± 0.005	9.6 (7.7)	337.30 ± 0.41	-4.54 ± 0.89	0.421 ± 0.006	7.3 (7.5)
IP = 100 m				**IP = 120 m**			
359.99 ± 0.31	$+0.34 \pm 0.69$	0.544 ± 0.007	2.7 (8.7)	0.29 ± 0.21	$+0.93 \pm 0.40$	0.624 ± 0.008	3.1 (2.7)
25.23 ± 0.41	$+6.01 \pm 0.98$	0.524 ± 0.008	8.3 (3.6)	24.97 ± 0.31	$+3.83 \pm 0.79$	0.607 ± 0.002	2.3 (1.9)
52.56 ± 0.41	$+9.18 \pm 1.17$	0.470 ± 0.004	12.7 (4.2)	53.42 ± 0.31	$+5.47 \pm 0.78$	0.558 ± 0.006	11.4 (3.2)
90.71 ± 0.52	-0.92 ± 1.75	0.441 ± 0.005	22.6 (3.9)	90.27 ± 0.21	-0.59 ± 0.78	0.524 ± 0.005	20.6 (3.7)
126.90 ± 0.31	-10.54 ± 0.50	0.469 ± 0.004	16.1 (5.1)	126.89 ± 0.41	-7.37 ± 1.08	0.554 ± 0.006	11.6 (5.3)
156.29 ± 0.31	-4.17 ± 0.78	0.523 ± 0.002	6.5 (3.7)	156.23 ± 0.31	-2.85 ± 0.60	0.606 ± 0.003	7.6 (2.4)
179.92 ± 0.41	$+0.29 \pm 0.70$	0.541 ± 0.004	2.7 (2.9)	179.95 ± 0.21	$+0.12 \pm 0.49$	0.627 ± 0.007	2.9 (2.6)
203.57 ± 0.41	$+4.38 \pm 0.89$	0.518 ± 0.006	2.3 (2.7)	203.14 ± 0.21	$+2.01 \pm 0.59$	0.600 ± 0.004	2.3 (2.6)
232.85 ± 0.52	$+11.71 \pm 1.18$	0.459 ± 0.006	14.3 (9.5)	232.26 ± 0.41	$+6.66 \pm 1.08$	0.539 ± 0.006	14.8 (10.2)
270.28 ± 0.31	-0.31 ± 0.98	0.427 ± 0.002	23.7 (6.5)	270.20 ± 0.21	-1.18 ± 0.78	0.503 ± 0.005	19.1 (3.5)
307.19 ± 0.41	-9.09 ± 1.08	0.461 ± 0.005	15.7 (5.7)	307.18 ± 0.31	-4.93 ± 0.78	0.538 ± 0.007	10.6 (4.1)
336.92 ± 0.41	-3.44 ± 0.89	0.516 ± 0.006	8.2 (4.8)	336.47 ± 0.21	-2.51 ± 0.68	0.599 ± 0.005	5.6 (2.4)

Table 5: The nominal angle δ_n, average displacement $\Delta\delta$, average value of the parameter DIST, RMS of the ALPHA distribution for enabled GF and impact parameters between 60 m and 120 m. The RMS of the ALPHA distribution for disabled GF is given parentheses. The MC γ-ray energy was set to 450 GeV, the ZA to 40° and the azimuth angle to 180°.

$E_\gamma = 1000\,\mathrm{GeV}$, Az = 180°, ZA = 40°, Hard Image Cleaning

δ_n[°]	$\Delta\delta$[°]	DIST[°]	$\mathrm{RMS}_{\lvert\mathrm{ALPHA}\rvert}$[°]	δ_n[°]	$\Delta\delta$[°]	DIST[°]	$\mathrm{RMS}_{\lvert\mathrm{ALPHA}\rvert}$[°]
IP = 60 m				IP = 80 m			
358.63 ± 0.82	-0.27 ± 1.44	0.396 ± 0.008	2.8 (2.8)	359.67 ± 0.49	$+0.39 \pm 0.80$	0.511 ± 0.006	16.1 (2.8)
22.11 ± 0.33	$+4.83 \pm 0.64$	0.382 ± 0.008	26.9 (15.6)	22.49 ± 0.49	$+1.11 \pm 1.11$	0.490 ± 0.006	19.7 (11.2)
53.83 ± 0.66	$+19.08 \pm 1.43$	0.343 ± 0.005	8.4 (3.2)	54.27 ± 0.66	$+10.44 \pm 1.58$	0.444 ± 0.008	2.5 (2.3)
92.44 ± 0.66	$+7.62 \pm 1.90$	0.323 ± 0.003	26.7 (5.1)	89.86 ± 0.49	$+1.32 \pm 1.73$	0.419 ± 0.006	19.0 (11.3)
130.17 ± 0.33	-13.24 ± 0.79	0.347 ± 0.006	16.1 (3.9)	129.09 ± 0.33	-5.64 ± 1.10	0.450 ± 0.004	15.5 (2.4)
156.80 ± 0.82	-3.46 ± 1.29	0.392 ± 0.004	9.5 (3.9)	155.85 ± 0.33	-3.55 ± 0.79	0.506 ± 0.004	4.8 (2.8)
179.17 ± 0.66	-0.40 ± 1.58	0.398 ± 0.006	8.1 (4.6)	179.80 ± 0.33	-2.14 ± 0.64	0.523 ± 0.005	6.8 (2.3)
202.94 ± 0.66	$+3.17 \pm 1.12$	0.380 ± 0.003	4.5 (4.1)	203.07 ± 0.66	$+2.13 \pm 1.12$	0.492 ± 0.006	25.3 (2.7)
234.62 ± 0.16	$+17.57 \pm 0.32$	0.331 ± 0.004	22.6 (2.2)	232.78 ± 0.49	$+10.93 \pm 0.80$	0.434 ± 0.003	28.0 (2.5)
271.62 ± 0.99	-1.10 ± 2.53	0.307 ± 0.004	21.3 (3.7)	269.97 ± 0.66	-1.11 ± 1.27	0.401 ± 0.003	18.2 (2.4)
307.40 ± 0.49	-8.65 ± 1.57	0.328 ± 0.006	13.5 (2.9)	306.70 ± 0.66	-8.21 ± 1.43	0.427 ± 0.004	13.4 (1.8)
337.31 ± 0.33	-2.73 ± 0.94	0.372 ± 0.005	10.9 (2.8)	336.72 ± 0.49	-2.26 ± 0.96	0.486 ± 0.008	3.7 (1.6)
IP = 100 m				IP = 120 m			
359.64 ± 0.33	-1.00 ± 0.64	0.619 ± 0.012	13.6 (1.2)	0.20 ± 0.33	$+0.64 \pm 0.48$	0.707 ± 0.012	12.2 (1.2)
23.77 ± 0.33	$+2.87 \pm 0.94$	0.601 ± 0.009	25.2 (5.2)	23.80 ± 0.33	$+2.82 \pm 0.48$	0.689 ± 0.005	6.8 (1.1)
51.70 ± 0.49	$+5.04 \pm 0.80$	0.538 ± 0.008	4.0 (13.0)	52.19 ± 0.33	$+5.53 \pm 0.94$	0.633 ± 0.003	2.3 (6.6)
89.48 ± 0.66	$+1.34 \pm 0.97$	0.507 ± 0.005	12.5 (16.6)	90.11 ± 0.33	$+3.62 \pm 0.79$	0.596 ± 0.004	7.6 (2.0)
127.48 ± 0.49	-5.64 ± 1.27	0.549 ± 0.006	9.1 (1.8)	127.02 ± 0.49	-0.52 ± 0.96	0.631 ± 0.005	7.7 (1.7)
155.16 ± 0.33	-0.69 ± 0.48	0.606 ± 0.008	3.0 (1.9)	155.56 ± 0.33	$+0.21 \pm 0.79$	0.696 ± 0.004	4.4 (1.4)
179.63 ± 0.49	-2.20 ± 0.80	0.627 ± 0.006	7.8 (1.6)	179.98 ± 0.33	-1.30 ± 0.64	0.709 ± 0.010	1.2 (1.1)
203.51 ± 0.66	$+1.25 \pm 1.12$	0.598 ± 0.004	11.7 (2.1)	203.30 ± 0.33	$+0.36 \pm 0.79$	0.680 ± 0.006	1.2 (1.8)
232.90 ± 0.33	$+5.85 \pm 0.94$	0.530 ± 0.004	17.2 (2.5)	232.41 ± 0.16	$+3.39 \pm 0.63$	0.615 ± 0.004	5.9 (1.7)
270.06 ± 0.33	-1.00 ± 0.48	0.489 ± 0.004	12.5 (1.9)	270.09 ± 0.33	-0.92 ± 1.25	0.573 ± 0.005	7.8 (1.9)
307.87 ± 0.49	-5.91 ± 1.57	0.527 ± 0.010	8.8 (2.5)	307.92 ± 0.16	-3.20 ± 1.09	0.606 ± 0.006	5.9 (1.3)
335.93 ± 0.33	-2.49 ± 0.94	0.586 ± 0.008	10.8 (2.4)	336.58 ± 0.33	-0.75 ± 0.79	0.678 ± 0.006	7.0 (1.4)

Table 6: The nominal angle δ_n, average displacement $\Delta\delta$, average value of the parameter DIST, RMS of the ALPHA distribution for enabled GF and impact parameters between 60 m and 120 m. The RMS of the ALPHA distribution for disabled GF is given parentheses. The MC γ-ray energy was set to 1000 GeV, the ZA to 40° and the azimuth angle to 180°.

$E_\gamma = 1000\,\mathrm{GeV}$, Az = 180°, ZA = 60°, Hard Image Cleaning

δ_n[°]	$\Delta\delta$[°]	DIST[°]	$\mathrm{RMS}_{\lvert\mathrm{ALPHA}\rvert}$[°]	δ_n[°]	$\Delta\delta$[°]	DIST[°]	$\mathrm{RMS}_{\lvert\mathrm{ALPHA}\rvert}$[°]
IP = 60 m				IP = 80 m			
358.63 ± 0.62	-1.53 ± 1.21	0.172 ± 0.001	6.4 (14.7)	358.23 ± 0.53	-2.21 ± 1.03	0.224 ± 0.002	6.2 (12.0)
14.29 ± 0.36	$+6.42 \pm 0.95$	0.158 ± 0.001	17.0 (19.1)	13.79 ± 0.63	$+7.13 \pm 1.04$	0.207 ± 0.001	8.7 (12.3)
38.95 ± 0.10	$+26.90 \pm 1.04$	0.127 ± 0.001	28.6 (23.4)	36.95 ± 0.89	$+19.52 \pm 1.73$	0.157 ± 0.001	30.1 (18.6)
96.85 ± 0.38	-0.29 ± 0.90	0.112 ± 0.001	21.0 (11.5)	90.92 ± 0.11	$+3.99 \pm 0.61$	0.129 ± 0.001	25.2 (25.1)
136.33 ± 0.32	-30.31 ± 1.41	0.130 ± 0.001	17.3 (23.5)	138.76 ± 0.98	-25.15 ± 1.90	0.158 ± 0.001	16.8 (18.8)
160.93 ± 0.45	-10.52 ± 1.04	0.161 ± 0.002	10.4 (19.4)	165.91 ± 0.98	-5.01 ± 1.31	0.206 ± 0.003	9.9 (11.5)
180.96 ± 0.62	$+1.56 \pm 1.22$	0.172 ± 0.001	10.2 (13.5)	180.99 ± 0.80	$+1.07 \pm 1.38$	0.226 ± 0.002	6.3 (13.0)
198.77 ± 0.36	$+11.72 \pm 0.86$	0.158 ± 0.001	9.8 (21.0)	196.90 ± 0.36	$+8.36 \pm 1.02$	0.203 ± 0.001	11.7 (8.4)
219.20 ± 0.09	$+27.00 \pm 0.70$	0.123 ± 0.001	23.8 (22.9)	219.36 ± 0.89	$+22.99 \pm 1.72$	0.149 ± 0.001	24.3 (17.8)
272.72 ± 2.84	$+5.94 \pm 2.95$	0.111 ± 0.002	27.7 (25.5)	268.08 ± 0.63	-0.57 ± 0.96	0.116 ± 0.001	23.6 (21.3)
320.67 ± 0.18	-18.11 ± 0.96	0.121 ± 0.001	18.0 (24.6)	319.37 ± 0.18	-15.54 ± 1.08	0.146 ± 0.001	16.4 (18.8)
340.89 ± 1.07	-7.02 ± 1.48	0.154 ± 0.001	10.2 (17.5)	343.47 ± 0.36	-4.59 ± 0.85	0.201 ± 0.001	7.0 (16.5)
IP = 100 m				IP = 120 m			
0.83 ± 0.71	$+0.80 \pm 1.20$	0.282 ± 0.003	4.9 (11.1)	0.15 ± 0.53	-0.39 ± 0.78	0.336 ± 0.002	5.7 (7.5)
17.09 ± 0.36	$+9.68 \pm 1.01$	0.258 ± 0.003	12.2 (13.8)	14.72 ± 0.71	$+6.23 \pm 1.37$	0.309 ± 0.003	5.2 (12.6)
38.32 ± 0.98	$+17.16 \pm 2.06$	0.195 ± 0.002	15.3 (15.3)	40.38 ± 0.36	$+15.12 \pm 1.68$	0.235 ± 0.002	21.7 (16.9)
91.32 ± 0.27	$+3.84 \pm 0.36$	0.156 ± 0.001	28.4 (19.9)	92.19 ± 1.25	$+3.17 \pm 1.58$	0.183 ± 0.001	27.8 (18.7)
135.78 ± 0.27	-19.90 ± 1.19	0.193 ± 0.002	16.8 (11.7)	136.43 ± 0.27	-19.59 ± 1.19	0.234 ± 0.002	15.3 (9.0)
162.47 ± 0.54	-8.70 ± 1.11	0.259 ± 0.002	8.6 (15.6)	161.98 ± 0.53	-9.06 ± 1.03	0.308 ± 0.003	8.1 (10.5)
179.19 ± 0.71	$+0.26 \pm 1.12$	0.281 ± 0.003	6.6 (11.3)	178.03 ± 0.62	-1.55 ± 1.03	0.338 ± 0.003	6.0 (8.1)
193.15 ± 0.53	$+4.72 \pm 0.86$	0.251 ± 0.003	6.2 (11.4)	194.90 ± 0.53	$+5.79 \pm 1.11$	0.304 ± 0.003	3.9 (8.2)
220.64 ± 0.99	$+19.46 \pm 1.73$	0.180 ± 0.001	9.5 (14.6)	220.45 ± 0.45	$+17.79 \pm 0.70$	0.216 ± 0.002	16.5 (13.6)
269.42 ± 0.99	$+6.65 \pm 1.40$	0.135 ± 0.001	27.1 (23.5)	272.09 ± 0.63	-0.95 ± 0.95	0.160 ± 0.001	27.9 (14.0)
317.76 ± 0.27	-15.96 ± 1.18	0.180 ± 0.001	15.5 (14.2)	319.39 ± 0.62	-12.62 ± 1.29	0.216 ± 0.002	15.7 (14.0)
348.75 ± 0.18	-0.07 ± 0.59	0.253 ± 0.001	7.6 (10.6)	346.65 ± 0.53	-1.37 ± 1.02	0.303 ± 0.002	8.7 (12.5)

Table 7: The nominal angle δ_n, average displacement $\Delta\delta$, average value of the parameter DIST, RMS of the ALPHA distribution for enabled GF and impact parameters between 60 m and 120 m. The RMS of the ALPHA distribution for disabled GF is given parentheses. The MC γ-ray energy was set to 1000 GeV, the ZA to 60° and the azimuth angle to 180°.

Table 2 and table 3 list some of the parameters which can be strongly affected by the influence of the GF: the nominal angle δ_n (orientation of the images for disabled GF), the average rotation angle $\Delta\delta$, the average value of the parameter DIST, and the RMS of the ALPHA distribution obtained for enabled GF and four impact parameter windows. The RMS of the ALPHA distribution obtained for disabled GF is given in parentheses. The MC γ-ray energy was set to 170 GeV, the ZA to 40° and the azimuth angle to 0° (small influence of the GF) and 180° (maximum influence of the GF).
The green-colored rows in table 2 and 3 correspond to arrangements that are favorable with regard to the pointing of the shower images, i.e. the telescope is situated on the y-axis of the CORSIKA coordinate system, pointing to the west, perpendicular to the direction of the GF. For impact parameters above 60 m, the RMS values of the ALPHA distributions obtained for enabled GF are significantly smaller than the ones obtained for disabled GF. This effect is very pronounced for 180° azimuth angle (table 3).
The red-colored rows correspond to the most unfavorable arrangements where the telescope is situated on the x-axis of the CORSIKA coordinate system, pointing to the north, parallel to the direction of the GF. Compared to the case of disabled GF the RMS of the ALPHA distribution obtained for enabled GF are significantly increased, while the average pointing remains unchanged. On average, there is only a small rotation $\Delta\delta$ of the shower images. The intermediate positions (blue-colored rows) at δ_n around 90° and 270° suffer from small rotations $\Delta\delta$ of the shower images, and the error on the rotation angle is comparatively large. As a result, the de-rotation of the shower images at γ-ray energies ~ 170 GeV may not help to enhance the ALPHA distribution. The RMS of the ALPHA distribution obtained for enabled GF at intermediate positions is significantly increased but in most cases smaller than the ones obtained for $\delta = 90°$ and $\delta = 180°$.
Tables 4 and 5 show the rotation angles $\Delta\delta$ for MC γ-rays of 450 GeV energy, 40° as well as 0° and 180° azimuth angle. For 180° azimuth angle and 60 m impact parameter the maximum rotation angle is in the order of $\sim 17°$, while its error is rather small. Tables 6 and 7 show the rotation angles $\Delta\delta$ for MC γ-rays of 1 TeV energy, 40° and 60° ZA as well as 180° azimuth angle. As for lower energies, the rotation of the shower images can be sizeable for unfavorable directions with regard to the influence of the GF (blue-colored rows). The list of tables for all MC input parameters can be found in appendix B.
Figures 131 - 133 show the ALPHA distribution for MC γ-rays of 170 GeV energy, impact parameters between 60 m and 120 m, 40° ZA and 180° azimuth angle. While the black distributions were obtained for disabled GF, the red distributions correspond to the case of enabled GF. The green-colored ALPHA distributions were obtained by the de-rotation of shower images (enabled GF). The de-rotation was done using the average displacement $\Delta\delta$, which is listed in table 3. For the distributions shown in figure 131 all angles φ between 0° and 330° were considered. As expected, the de-rotation of shower images does not enhance the ALPHA distributions significantly. Even if the most unfavorable arrangements ($\varphi = 0°$ and $\varphi = 180°$) are removed from the dataset there is no significant enhancement due to de-rotation (figure 132). Instead, it may be better to simply reject the unfavorable arrangements $\varphi = 0°$ and 180° which are shown in figure 133. As already mentioned, the GF changes not only the average pointing of γ-ray shower images, but significantly disturbs the ALPHA distribution.
Figure 134 shows the normalized ALPHA distributions for MC γ-rays of 450 GeV energy, impact parameters between 60 m and 120 m, 40° ZA and 180° azimuth angle. The angle φ was varied between 0° and 330°. The ALPHA distributions of the de-rotated shower images are in most cases improved with regard to the original distributions, i.e. the percentage of events lying within $|\mathrm{ALPHA}| \leq 9°$ is greater than for the untouched ALPHA distributions. The percentage of recovered events increases for lower impact parameters. However, the recovery of the pointing by changing the orientation of the images is not possible for all events. The ALPHA distributions are strongly disturbed, and the

pointing information of shower images at around 60 m impact parameter is completely lost due to the influence of the GF.
The removal of events collected at the most unfavorable orientations with regard to the influence of the GF further enhances the pointing. The normalized ALPHA distributions shown in figure 135 were obtained for MC γ-rays of 450 GeV energy, impact parameters between 60 m and 120 m, 40° ZA and 180° azimuth angle. The most unfavorable orientations with regard to the influence of the GF, $\varphi = 0°$ and 180° ($\delta = 90°$ and 270°) were not considered. As can be seen from the figures, the removal of events that are disturbed strongest by the influence of the GF further enhances the ALPHA distributions.
Figure 136 shows the normalized ALPHA distributions that were obtained for similar MC input parameters as before. The telescope was situated at the most unfavorable positions with regard to the influence of the GF, $\varphi = 0°$ and 180°. Apparently, the pointing of the shower images obtained for enabled GF cannot be recovered by the de-rotation. The ALPHA distributions are strongly disturbed, and the pointing information of shower images at around 60 m impact parameter is completely lost due to the influence of the GF. Thus, for unfavorable orientations of the telescope, it may be appropriate to remove those events from the data sample.
Figure 137 shows the normalized ALPHA distributions for MC γ-rays of 1 TeV energy, impact parameters between 100 m and 120 m, 40° and 60° ZA and 180° azimuth angle. The angle φ was varied between 0° and 330°. At 40° ZA and 100 m impact parameter (figure 137 (a)), the percentage of events recovered by de-rotation is rather low, and for 120 m impact parameter (figure 137 (b)) the de-rotation slightly worsens the ALPHA distribution. Table 159 was used to de-rotate the shower images.
For 60° ZA (figure 137 (c) - (d)), the de-rotation of shower images helps to enhance the percentage of events lying within $|\text{ALPHA}| \leq 9°$. Similar to the case of lower energies, the ALPHA distributions can be further enhanced by rejecting the most unfavorable orientations with regard to the influence of the GF $\varphi = 0°$ and $\varphi = 180°$ (figure 138 (a) - (d)).
Figure 139 (a) - (d) shows the ALPHA distributions of events collected at the most unfavorable orientation with regard to the influence of the GF. The pointing of the shower images cannot be recovered by de-rotation. For 60° ZA the ALPHA distributions obtained for enabled GF look background-like.
In general, for large angles α (strong GF), the most unfavorable arrangements with regard to the influence of the GF are the ones that correspond to shower images oriented parallel to the direction of the GF in the camera whereas the most favorable are the ones that correspond to shower images oriented vertical to the projection of the GF.
The results from this section show that the enhancement of the ALPHA distribution by de-rotation of shower images is only possible if the rotation angle is large compared to its error and if the γ-ray energy is well above 100 GeV. It is noteworthy that the figures 131 - 139 were obtained under the most optimistic scenario where the impact parameter is well known. In reality, the impact parameter is only known with an accuracy of $\sim 20\,\%$ [27].

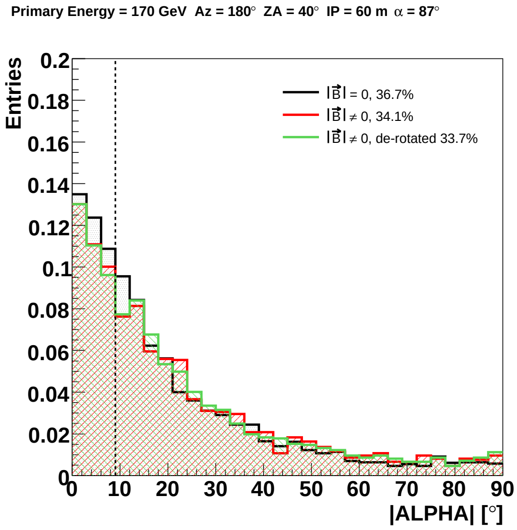

(a) Hard image cleaning, ZA 40°, azimuth angle 180°, impact parameter 60 m, $\varphi = 0° \dots 330°$.

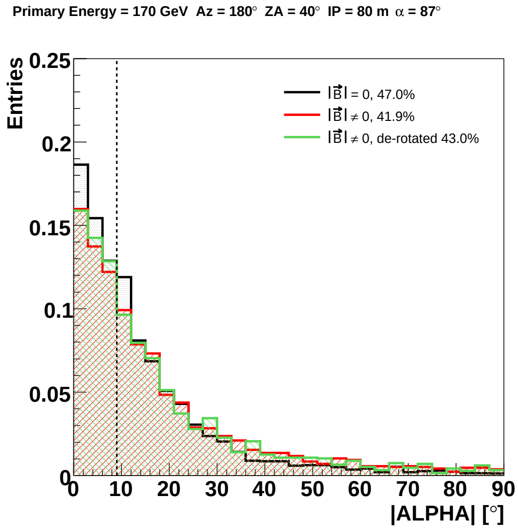

(b) Hard image cleaning, ZA 40°, azimuth angle 180°, impact parameter 80 m, $\varphi = 0° \dots 330°$.

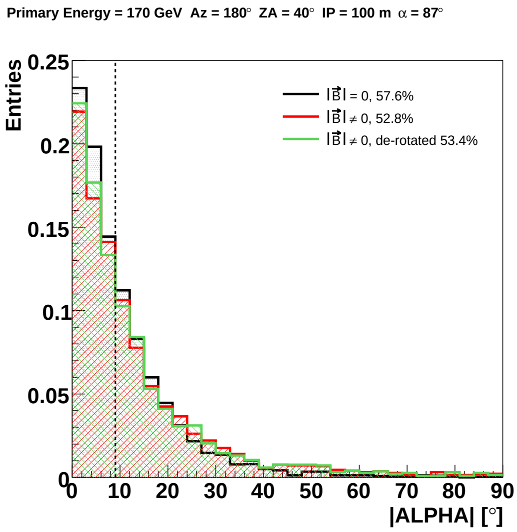

(c) Hard image cleaning, ZA 40°, azimuth angle 180°, impact parameter 100 m, $\varphi = 0° \dots 330°$.

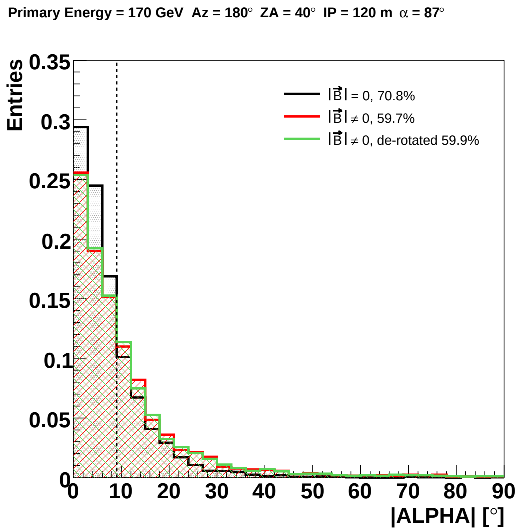

(d) Hard image cleaning, ZA 40°, azimuth angle 180°, impact parameter 120 m, $\varphi = 0° \dots 330°$.

Figure 131: Normalized distributions of the image parameter ALPHA for MC γ-rays of 170 GeV energy, impact parameters between 60 m and 120 m, 40° ZA and 180° azimuth angle. The angle φ was varied between 0° and 330°.

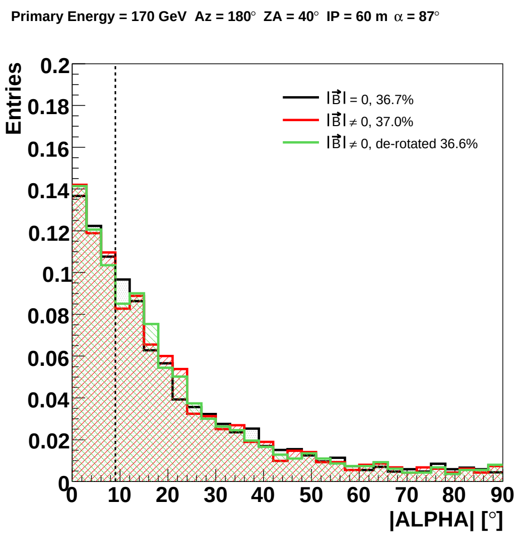

(a) Hard image cleaning, ZA 40°, azimuth angle 180°, impact parameter 60 m, $\varphi \neq 0°, 180°$.

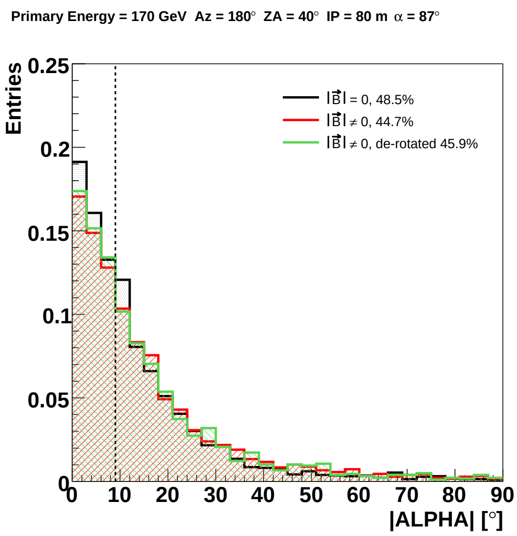

(b) Hard image cleaning, ZA 40°, azimuth angle 180°, impact parameter 80 m, $\varphi \neq 0°, 180°$.

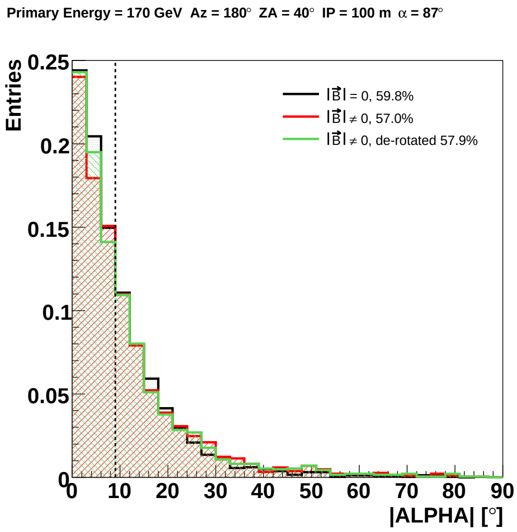

(c) Hard image cleaning, ZA 40°, azimuth angle 180°, impact parameter 100 m, $\varphi \neq 0°, 180°$.

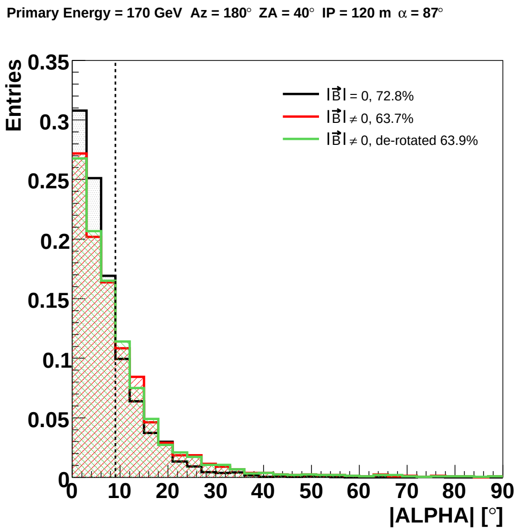

(d) Hard image cleaning, ZA 40°, azimuth angle 180°, impact parameter 120 m, $\varphi \neq 0°, 180°$.

Figure 132: Normalized distributions of the image parameter ALPHA for MC γ-rays of 170 GeV energy, impact parameters between 60 m and 120 m, 40° ZA and 180° azimuth angle. The most unfavorable orientations with regard to the influence of the GF, $\varphi = 0°$ and 180° were not considered.

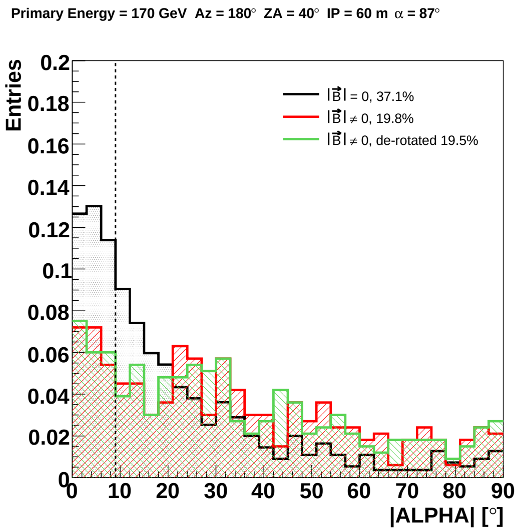

(a) Hard image cleaning, ZA 40°, azimuth angle 180°, impact parameter 60 m, $\varphi = 0°, 180°$.

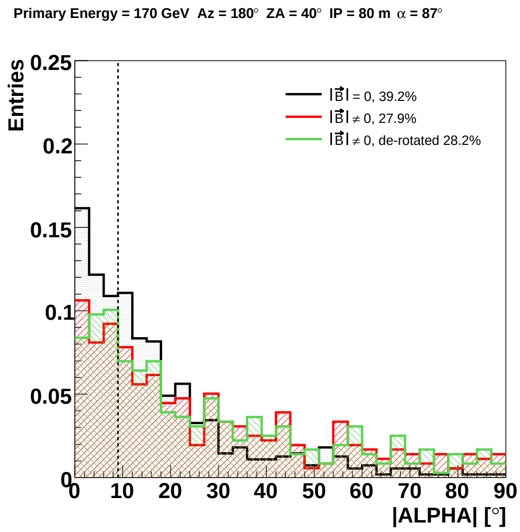

(b) Hard image cleaning, ZA 40°, azimuth angle 180°, impact parameter 80 m, $\varphi = 0°, 180°$.

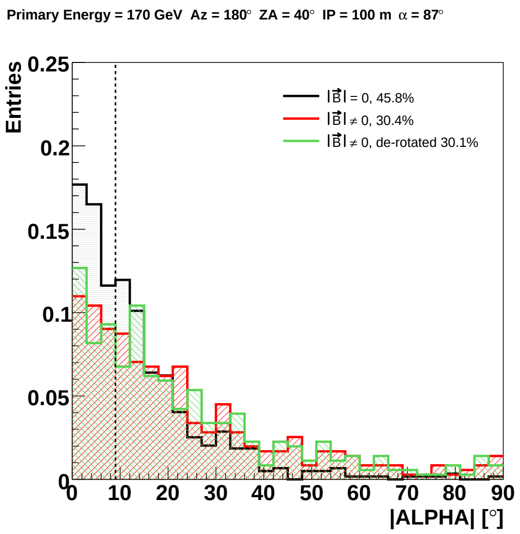

(c) Hard image cleaning, ZA 40°, azimuth angle 180°, impact parameter 100 m, $\varphi = 0°, 180°$.

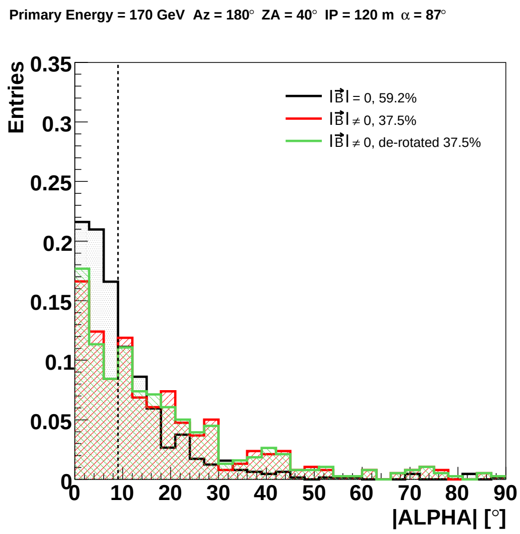

(d) Hard image cleaning, ZA 40°, azimuth angle 180°, impact parameter 120 m, $\varphi = 0°, 180°$.

Figure 133: Normalized distributions of the image parameter ALPHA for MC γ-rays of 170 GeV energy, impact parameters between 60 m and 120 m, 40° ZA and 180° azimuth angle. The angle φ was set to 0° and 180°, respectively.

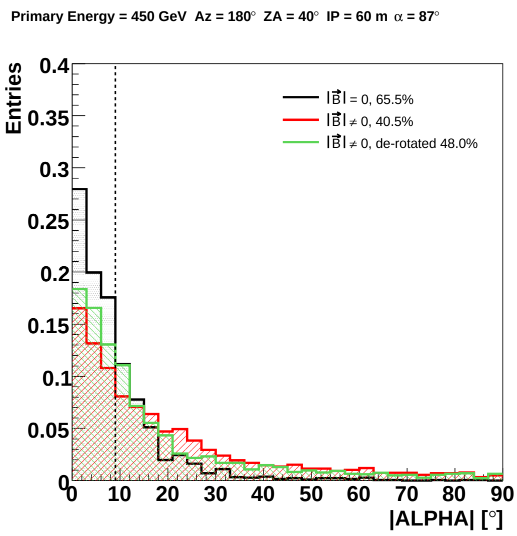

(a) Hard image cleaning, ZA 40°, azimuth angle 180°, impact parameter 60 m, $\varphi = 0° \dots 330°$.

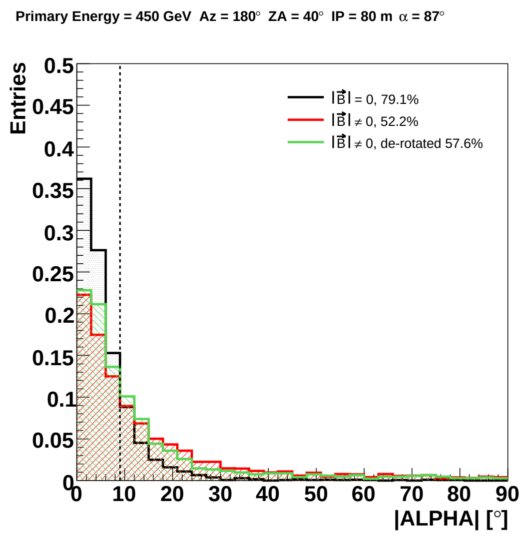

(b) Hard image cleaning, ZA 40°, azimuth angle 180°, impact parameter 80 m, $\varphi = 0° \dots 330°$.

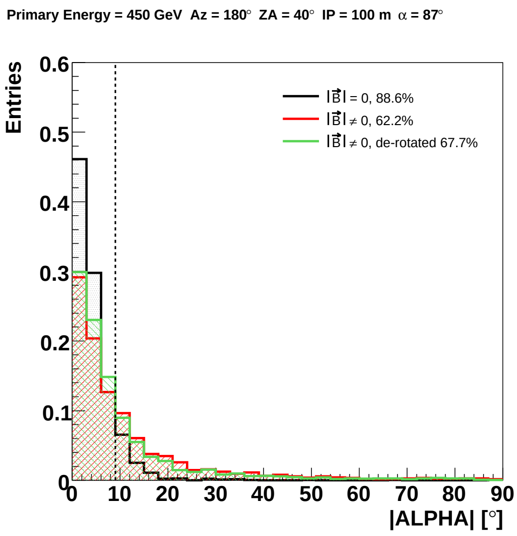

(c) Hard image cleaning, ZA 40°, azimuth angle 180°, impact parameter 100 m, $\varphi = 0° \dots 330°$.

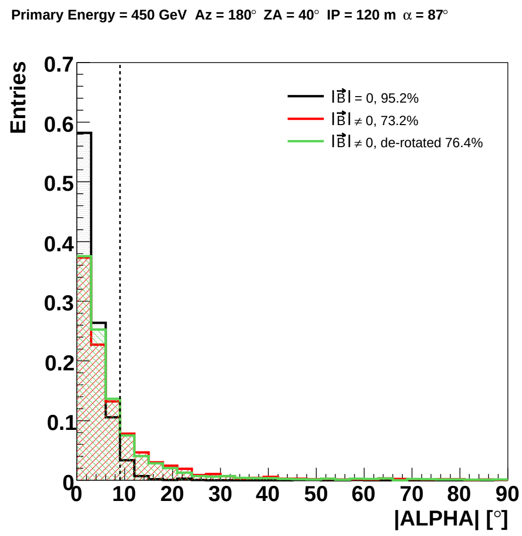

(d) Hard image cleaning, ZA 40°, azimuth angle 180°, impact parameter 120 m, $\varphi = 0° \dots 330°$.

Figure 134: Normalized distributions of the image parameter ALPHA for MC γ-rays of 450 GeV energy, impact parameters between 60 m and 120 m, 40° ZA and 180° azimuth angle. The angle φ was varied between 0° and 330°.

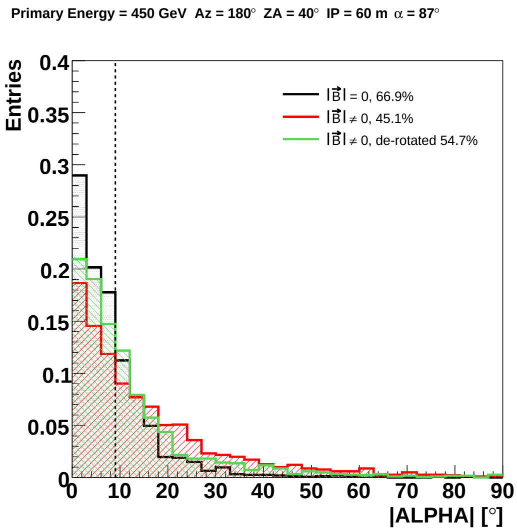

(a) Hard image cleaning, ZA 40°, azimuth angle 180°, impact parameter 60 m, $\varphi \neq 0°, 180°$.

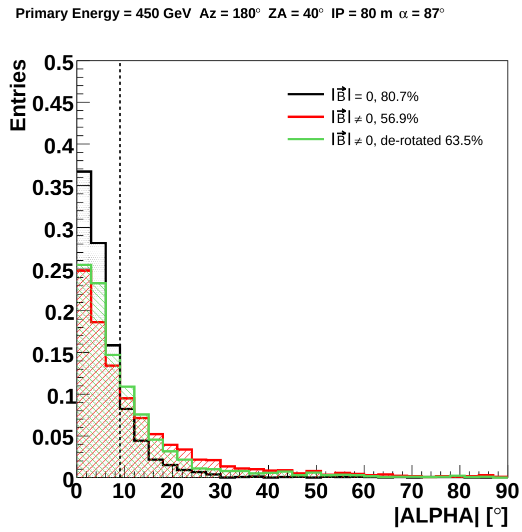

(b) Hard image cleaning, ZA 40°, azimuth angle 180°, impact parameter 80 m, $\varphi \neq 0°, 180°$.

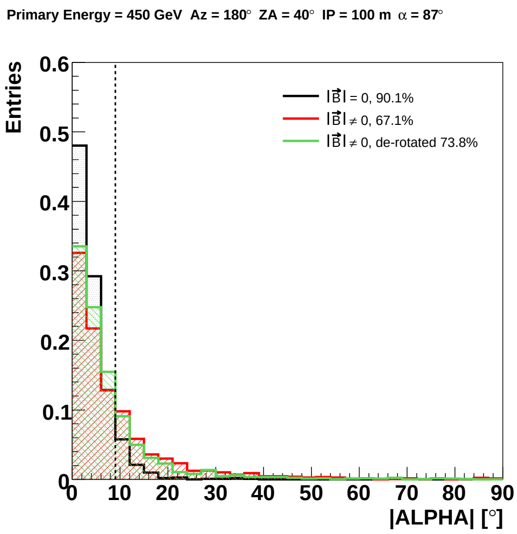

(c) Hard image cleaning, ZA 40°, azimuth angle 180°, impact parameter 100 m, $\varphi \neq 0°, 180°$.

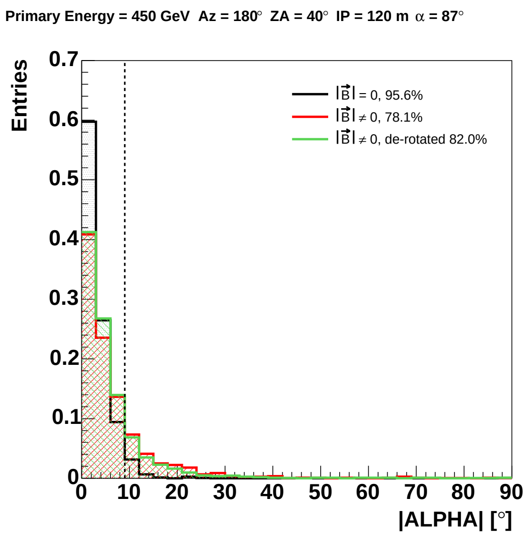

(d) Hard image cleaning, ZA 40°, azimuth angle 180°, impact parameter 120 m, $\varphi \neq 0°, 180°$.

Figure 135: Normalized distributions of the image parameter ALPHA for MC γ-rays of 450 GeV energy, impact parameters between 60 m and 120 m, 40° ZA and 180° azimuth angle. The most unfavorable orientations with regard to the influence of the GF, $\varphi = 0°$ and 180° were not considered.

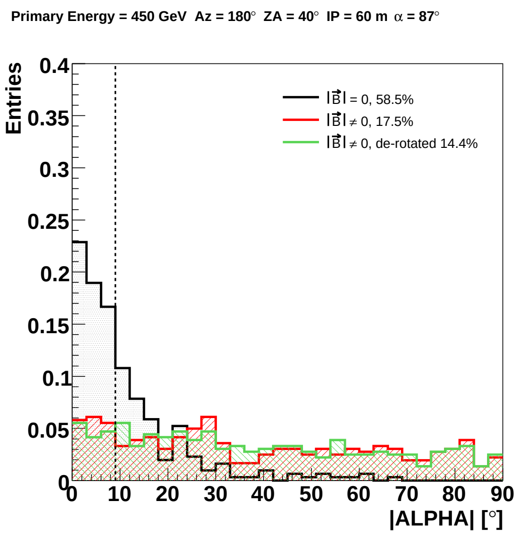

(a) Hard image cleaning, ZA 40°, azimuth angle 180°, impact parameter 60 m, $\varphi = 0°, 180°$.

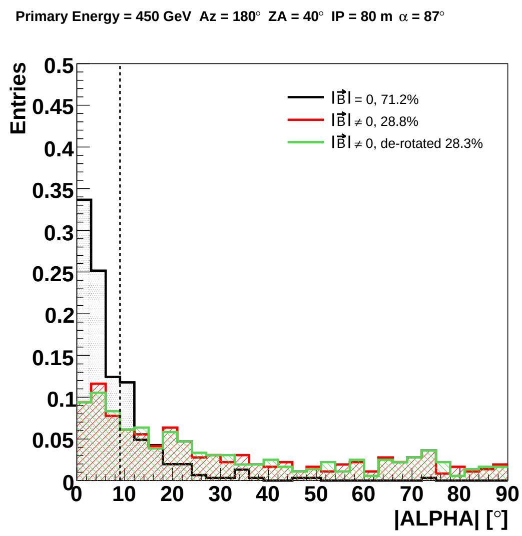

(b) Hard image cleaning, ZA 40°, azimuth angle 180°, impact parameter 80 m, $\varphi = 0°, 180°$.

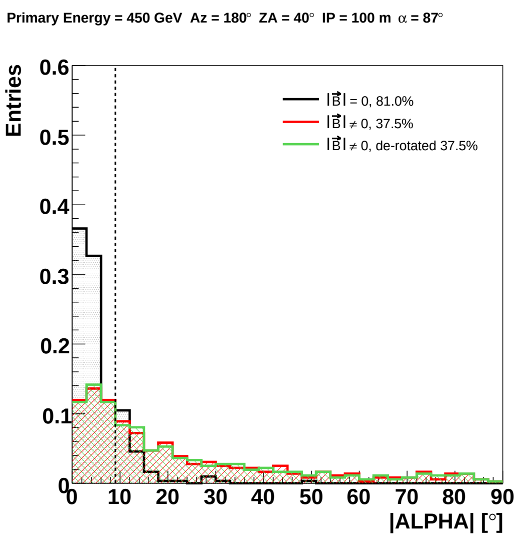

(c) Hard image cleaning, ZA 40°, azimuth angle 180°, impact parameter 100 m, $\varphi = 0°, 180°$.

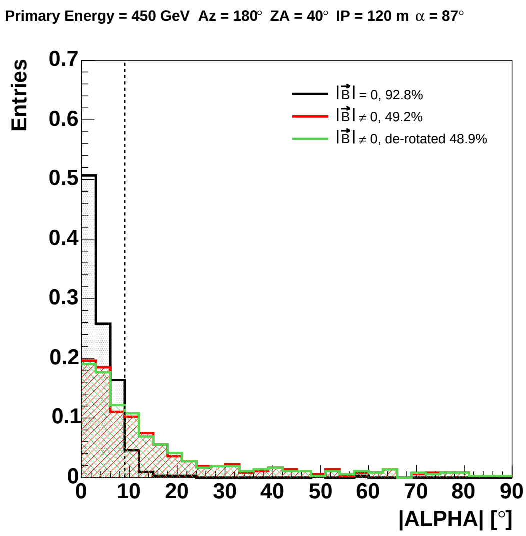

(d) Hard image cleaning, ZA 40°, azimuth angle 180°, impact parameter 120 m, $\varphi = 0°, 180°$.

Figure 136: Normalized distributions of the image parameter ALPHA for MC γ-rays of 450 GeV energy, impact parameters between 60 m and 120 m, 40° ZA and 180° azimuth angle. The angle φ was set to 0° and 180°, respectively.

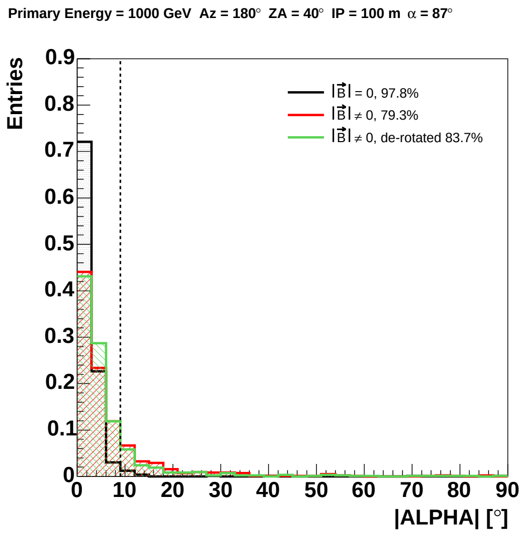

(a) Hard image cleaning, ZA 40°, azimuth angle 180°, impact parameter 100 m, $\varphi = 0° \ldots 330°$.

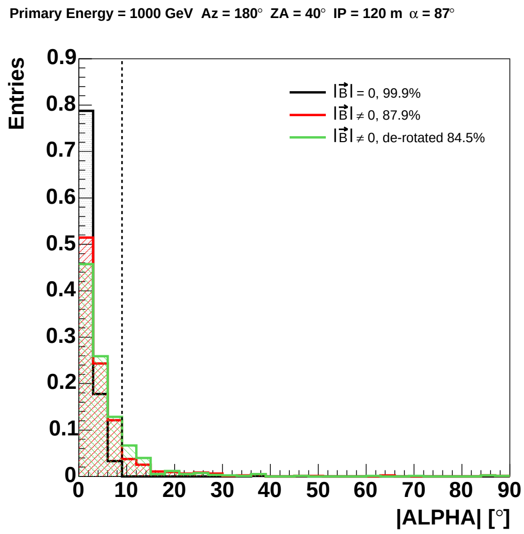

(b) Hard image cleaning, ZA 40°, azimuth angle 180°, impact parameter 120 m, $\varphi = 0° \ldots 330°$.

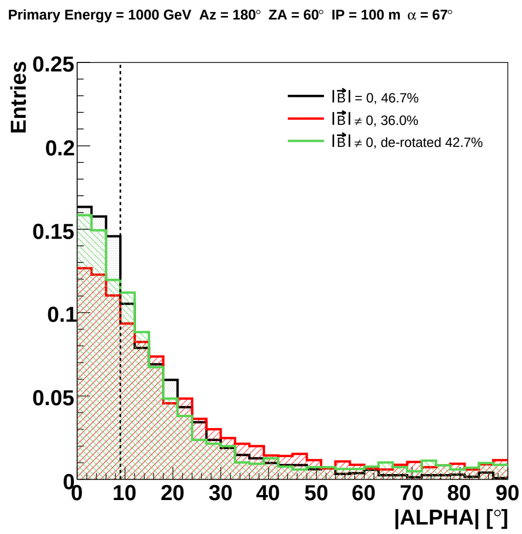

(c) Hard image cleaning, ZA 60°, azimuth angle 180°, impact parameter 100 m, $\varphi = 0° \ldots 330°$.

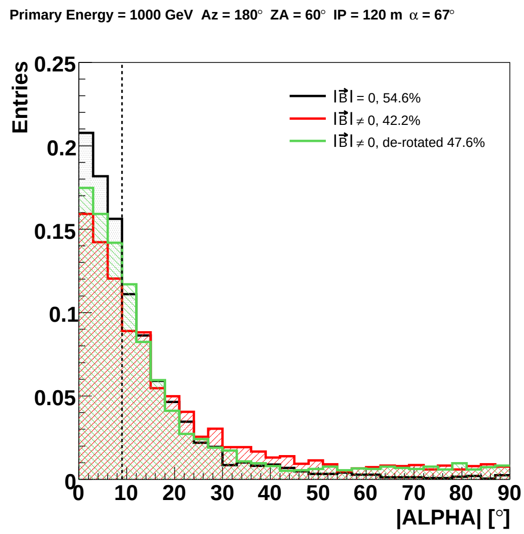

(d) Hard image cleaning, ZA 60°, azimuth angle 180°, impact parameter 120 m, $\varphi = 0° \ldots 330°$.

Figure 137: Normalized distributions of the image parameter ALPHA for MC γ-rays of 1000 GeV energy, impact parameters between 100 m and 120 m, 40° and 60° ZA and 180° azimuth angle. The angle φ was varied between 0° and 330°.

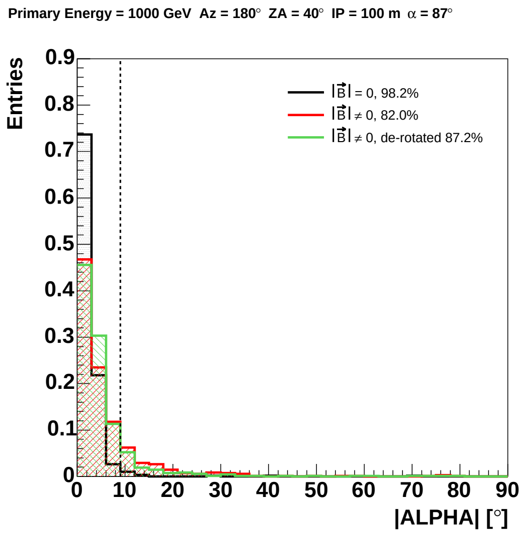

(a) Hard image cleaning, ZA 40°, azimuth angle 180°, impact parameter 100 m, $\varphi \neq 0°, 180°$.

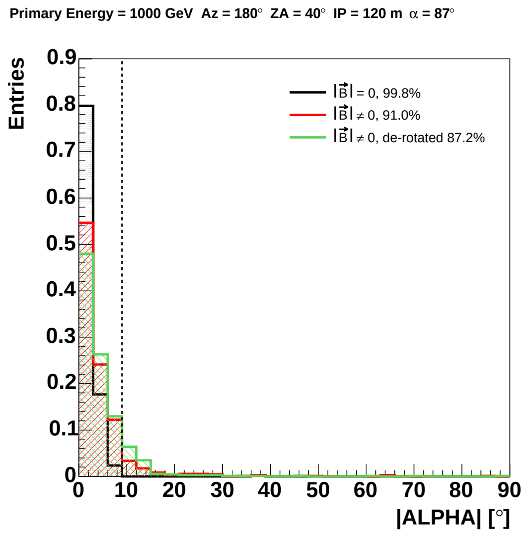

(b) Hard image cleaning, ZA 40°, azimuth angle 180°, impact parameter 120 m, $\varphi \neq 0°, 180°$.

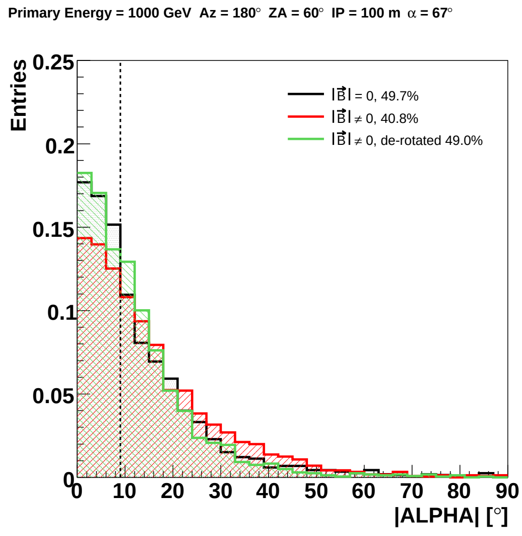

(c) Hard image cleaning, ZA 60°, azimuth angle 180°, impact parameter 100 m, $\varphi \neq 0°, 180°$.

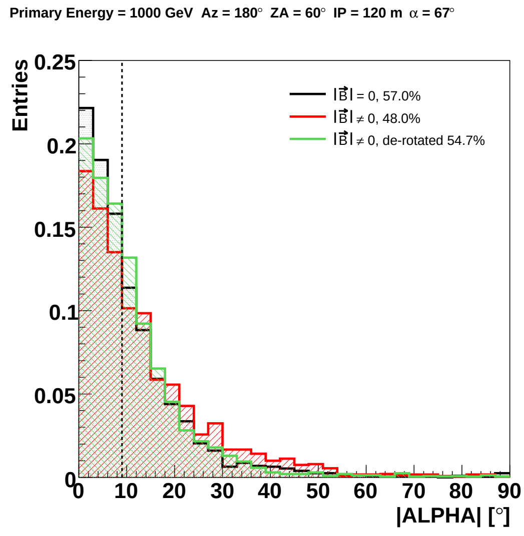

(d) Hard image cleaning, ZA 60°, azimuth angle 180°, impact parameter 120 m, $\varphi \neq 0°, 180°$.

Figure 138: Normalized distributions of the image parameter ALPHA for MC γ-rays of 1000 GeV energy, impact parameters between 100 m and 120 m, 40° and 60° ZA and 180° azimuth angle. The most unfavorable orientations with regard to the influence of the GF, $\varphi = 0°$ and 180° were not considered.

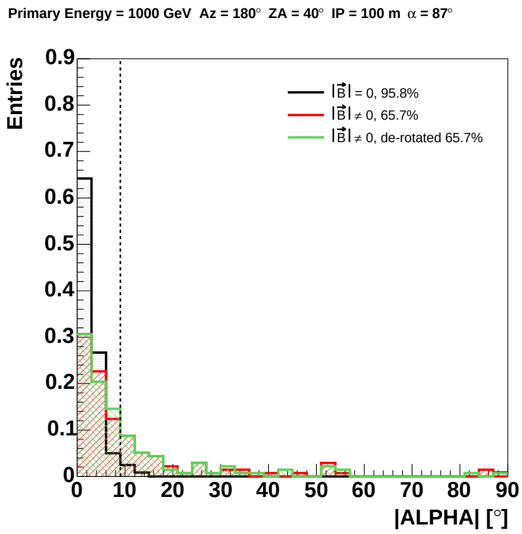

(a) Hard image cleaning, ZA 40°, azimuth angle 180°, impact parameter 100 m, $\varphi = 0°, 180°$.

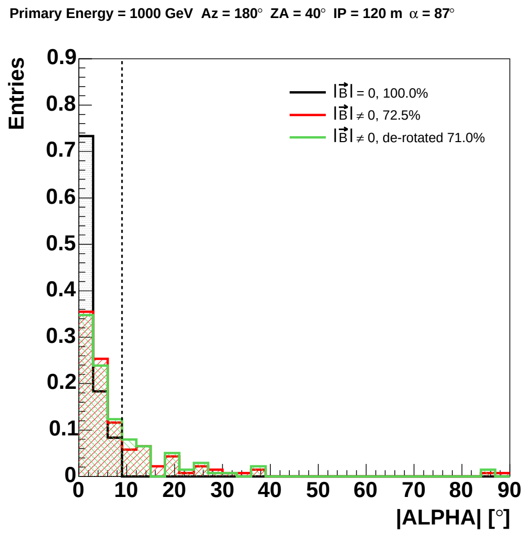

(b) Hard image cleaning, ZA 40°, azimuth angle 180°, impact parameter 120 m, $\varphi = 0°, 180°$.

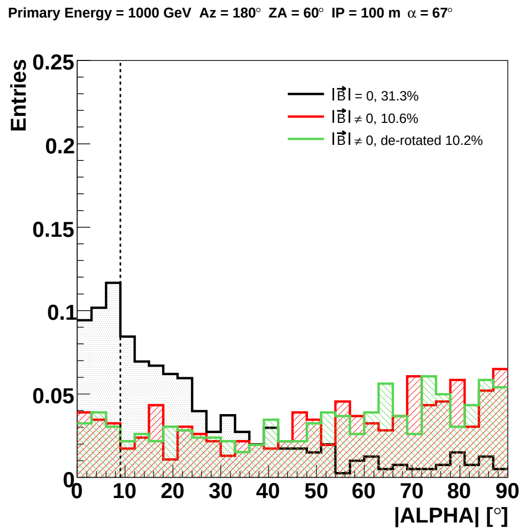

(c) Hard image cleaning, ZA 60°, azimuth angle 180°, impact parameter 100 m, $\varphi = 0°, 180°$.

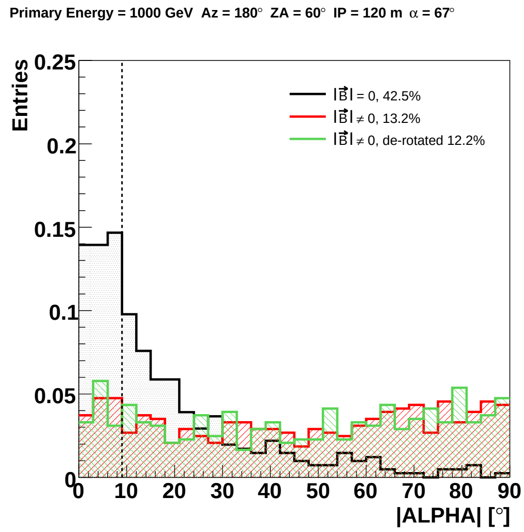

(d) Hard image cleaning, ZA 60°, azimuth angle 180°, impact parameter 120 m, $\varphi = 0°, 180°$.

Figure 139: Normalized distributions of the image parameter ALPHA for MC γ-rays of 1000 GeV energy, impact parameters between 100 m and 120 m, 40° and 60° ZA and 180° azimuth angle. The angle φ was set to 0° and 180°, respectively.

3.1.3 The Influence of the GF on the DISP Analysis

The Influence of the GF on the DISP-Reconstructed Arrival Direction

The findings discussed in the previous sections suggest that the GF affects also the DISP method. The DISP method makes use of the shape of reconstructed shower images to estimate the position of the source located on the major axis of the Hillas ellipse at a certain distance (DISP) from the COG of the Cherenkov light distribution in the camera [20].
The main ingredient to the DISP method is the ellipticity WIDTH/LENGTH of shower images, which is related to the distance of the shower image to the source position. To account for the SIZE dependence of the image parameters WIDTH and LENGTH the DISP parameter is parameterized by a function of the image parameters WIDTH, LENGTH, SIZE and LEAKAGE. The coefficients of this parameterization are usually obtained from MC simulated γ-ray showers by minimizing the average angular distance between the real and estimated source position in the camera.
It was shown in the preceding sections that the GF significantly alters both the shape and the orientation of γ-ray shower images. Therefore, the GF is expected to significantly affect also the DISP method.
For the optimization of the DISP parameters, dedicated MC γ-ray samples with continuous impact parameter distribution between 0 m and 500 m were produced. As for the production of standard MC data the EAS core location was randomly placed somewhere in a circle on the plane perpendicular to the direction of the EAS. Furthermore, the GF was always switched off. This approach allows to demonstrate the influence of the GF on the DISP method while the required computing time for the production of the MC dataset is kept to a minimum, since the MC data had to be produced only for $0°$ azimuth angle. The MC samples were produced for the same energies, ZAs and image cleaning levels as the MC data which were used for the preceding studies (section 2).
The first step of the DISP analysis was the optimization of the DISP parameters using the standard tools provided by the MARS package and the MC γ-ray samples that were produced for this purpose. The next step was the estimation of the DISP parameter for the MC events. This was done for the MC data which were used already for the preceding studies.
The influence of the GF on the DISP method is shown in terms of two-dimensional frequency distributions. The distribution of the DISP-reconstructed arrival directions for MC γ-ray showers between 50 GeV and 1 TeV energy, different ZAs and azimuth angles and impact parameters between 60 m and 160 m are shown in figures 140 - 162. The intermediate image cleaning was applied. In case of enabled GF the projected direction of the GF in the camera is always indicated in the lower right part of the histograms. The ellipticity of the DISP distributions is shown in the lower left part of the histograms. The semi-minor and the semi-major axis of the ellipse corresponds to the sigma of a Gaussian fit to the DISP distribution using bands of $\Delta_{X',Y'} = \pm 0.035°$ parallel and perpendicular to the projected direction of the GF in the camera. The result from the Gauss fit is also shown in the legend.
As expected, for disabled GF the peak of the DISP distribution is always circularly and centered at the source position (camera center). A certain ellipticity can be attributed to the fact that the true impact parameter in direction of the telescopes' inclination scales like cos(ZA) (figure 16). The angular distance to the EAS is lower than for other configurations, which may result in a certain degradation of the DISP-estimated arrival directions of the shower images, even if the GF is disabled.
In case of enabled GF the DISP distribution appears to be significantly elongated perpendicular to the projected direction of the GF in the camera. However, the peak of the DISP distribution is always centered at the source position (camera center). The extent of the elongation depends basically on the angle α between the shower axis and the direction of the GF.

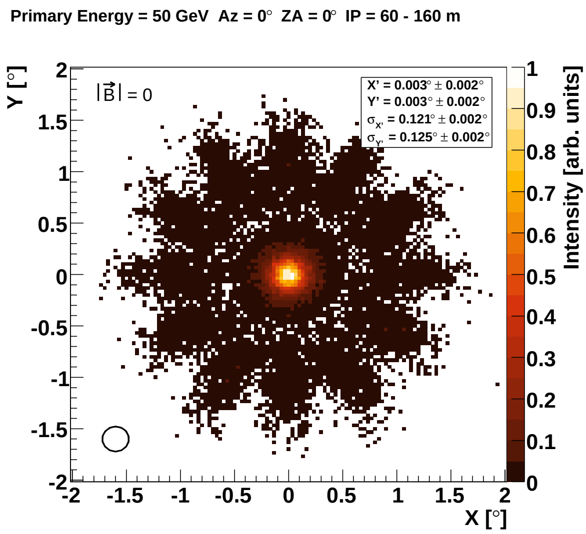

(a) 50 GeV energy, GF disabled.

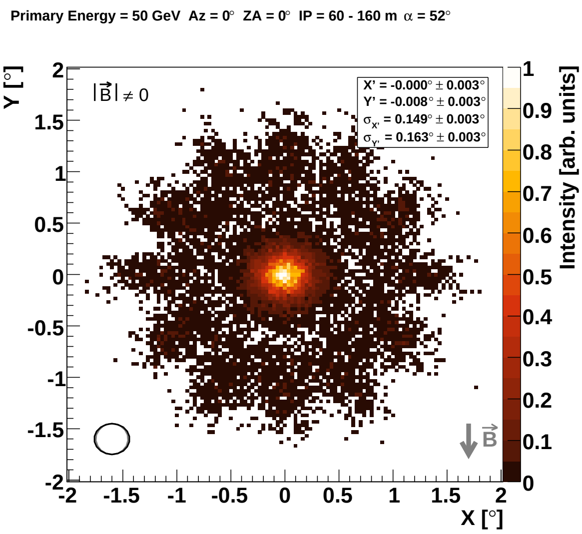

(b) 50 GeV energy, GF enabled.

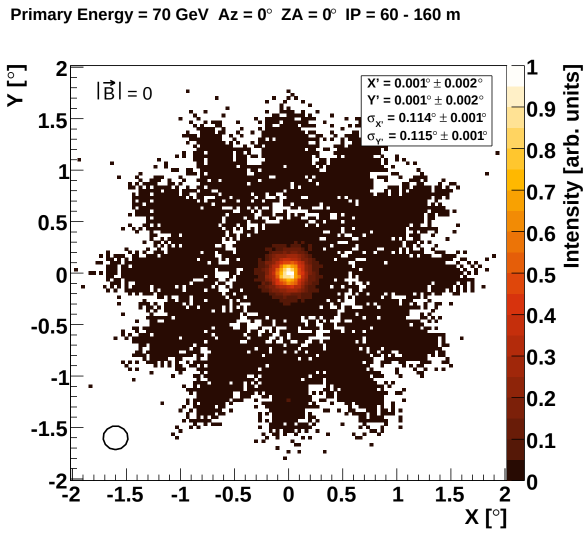

(c) 70 GeV energy, GF disabled.

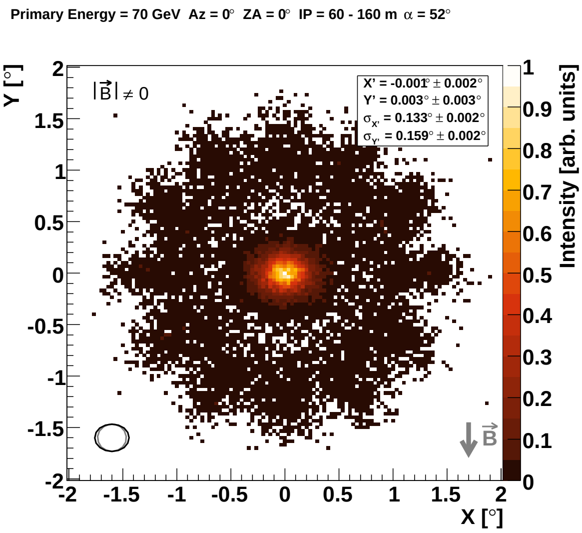

(d) 70 GeV energy, GF enabled.

Figure 140: DISP-reconstructed arrival directions for MC γ-rays of 50 GeV and 70 GeV energy, impact parameters between 60 m and 160 m, 0° ZA and 0° azimuth angle. The intermediate image cleaning was applied.

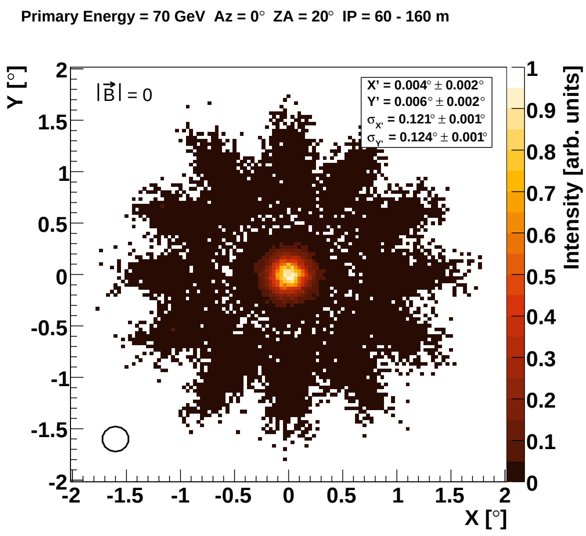

(a) 0° azimuth angle, GF disabled.

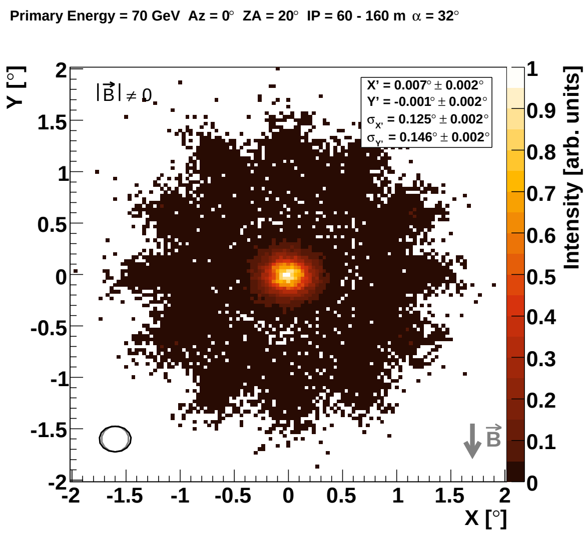

(b) 0° azimuth angle.

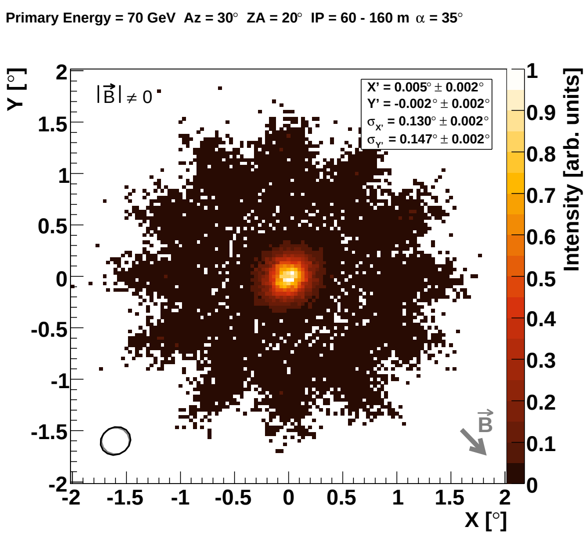

(c) 30° azimuth angle.

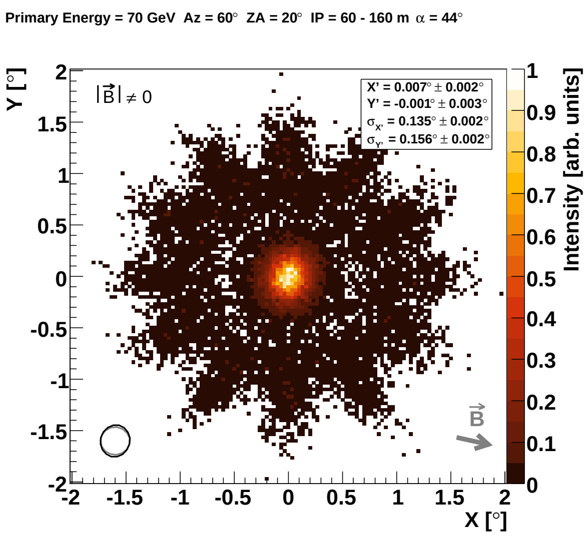

(d) 60° azimuth angle.

Figure 141: DISP-reconstructed arrival directions for MC γ-rays of 70 GeV energy, impact parameters between 60 m and 160 m, 20° ZA and different azimuth angles. The intermediate image cleaning was applied.

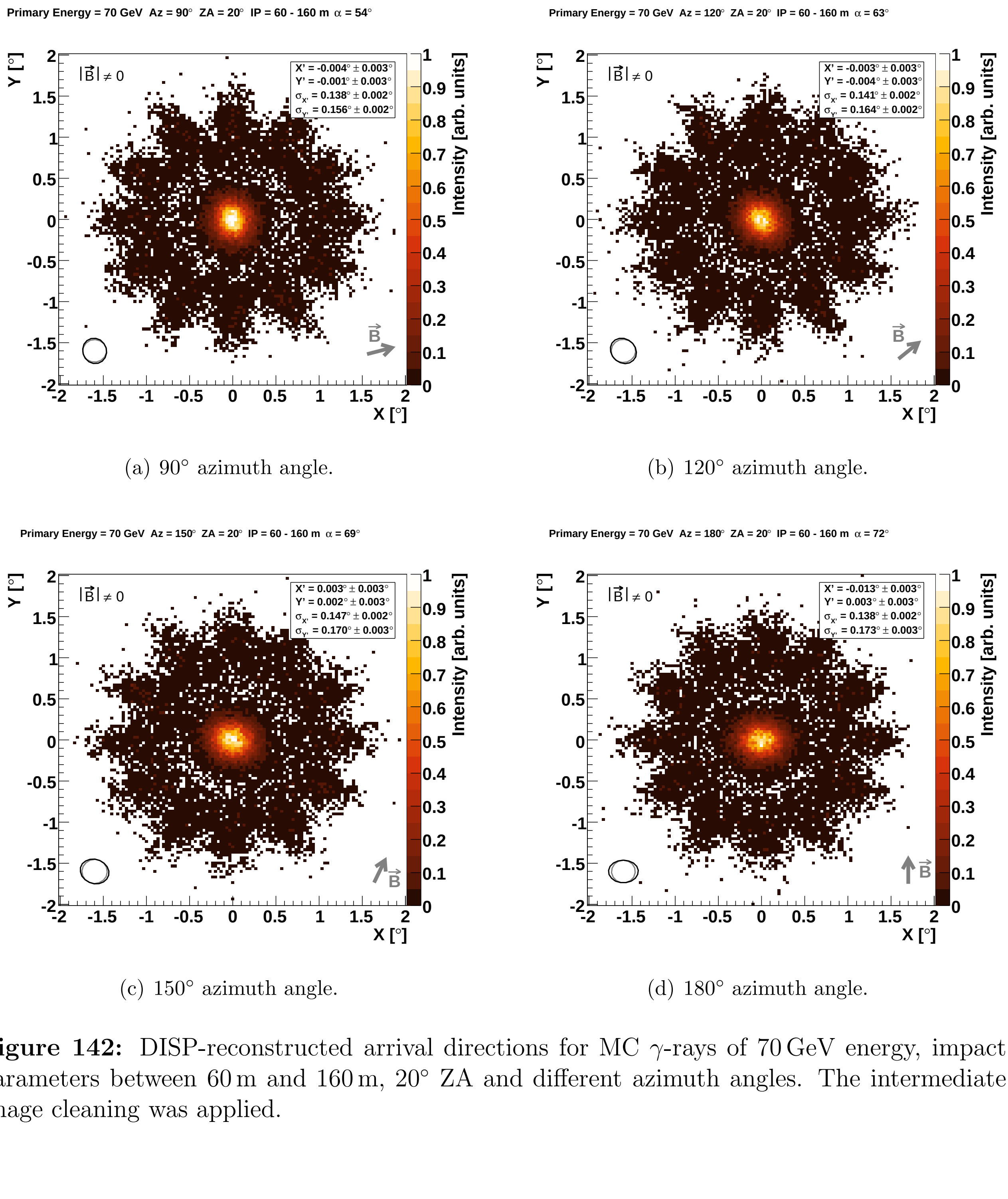

(a) 90° azimuth angle.

(b) 120° azimuth angle.

(c) 150° azimuth angle.

(d) 180° azimuth angle.

Figure 142: DISP-reconstructed arrival directions for MC γ-rays of 70 GeV energy, impact parameters between 60 m and 160 m, 20° ZA and different azimuth angles. The intermediate image cleaning was applied.

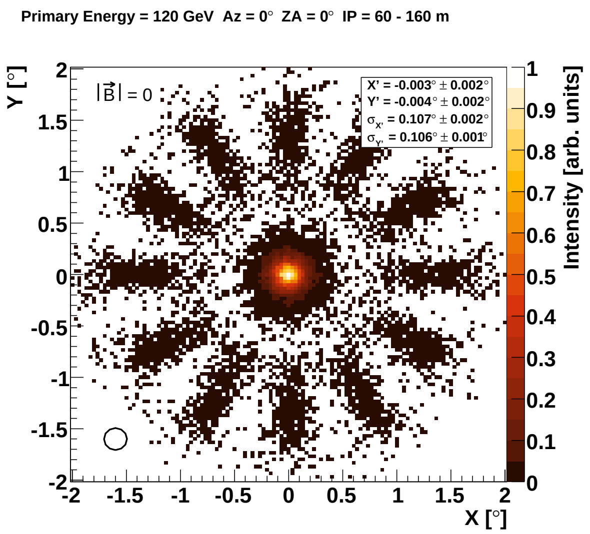

(a) GF disabled.

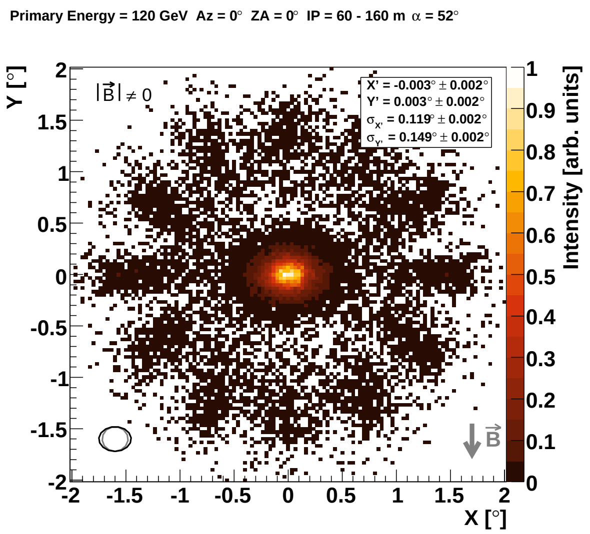

(b) GF enabled.

Figure 143: DISP-reconstructed arrival directions for MC γ-rays of 120 GeV energy, impact parameters between 60 m and 160 m, 0° ZA and 0° azimuth angle. The intermediate image cleaning was applied.

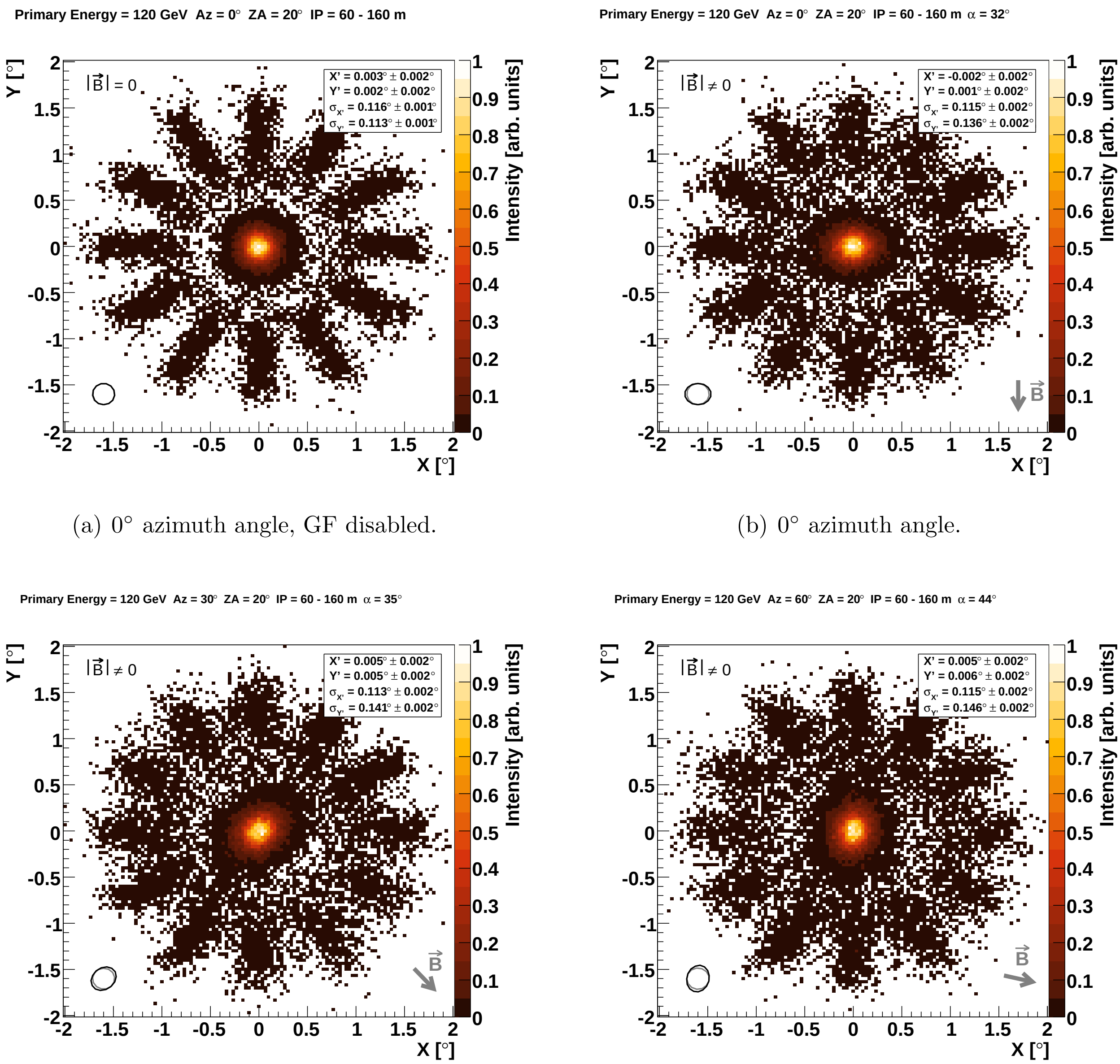

(a) 0° azimuth angle, GF disabled.

(b) 0° azimuth angle.

(c) 30° azimuth angle.

(d) 60° azimuth angle.

Figure 144: DISP-reconstructed arrival directions for MC γ-rays of 120 GeV energy, impact parameters between 60 m and 160 m, 20° ZA and different azimuth angles. The intermediate image cleaning was applied.

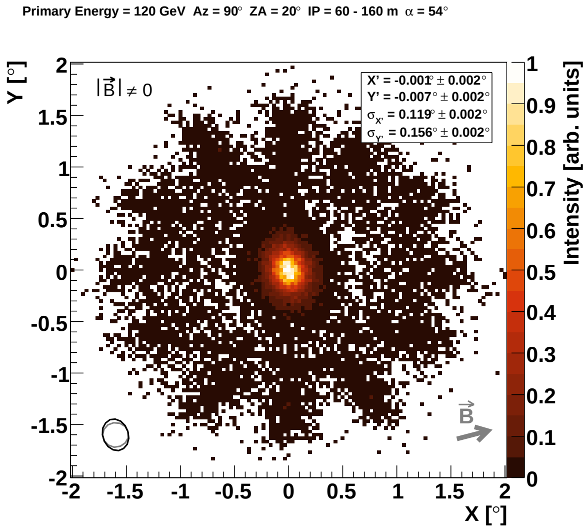

(a) 90° azimuth angle.

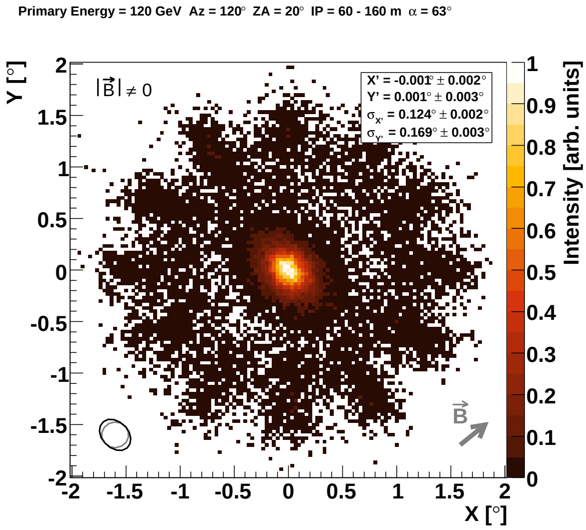

(b) 120° azimuth angle.

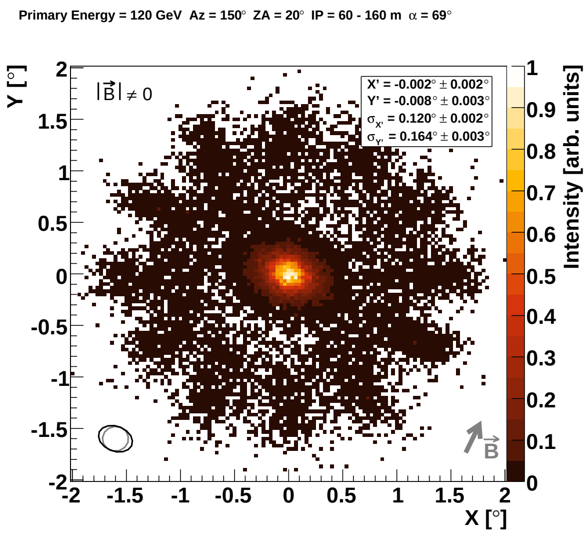

(c) 150° azimuth angle.

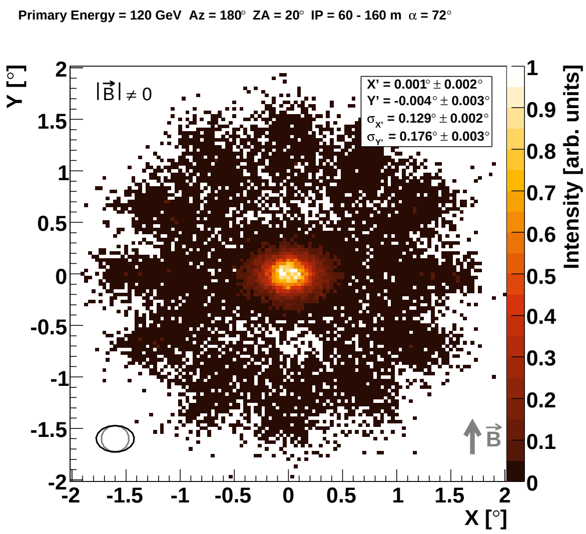

(d) 180° azimuth angle.

Figure 145: DISP-reconstructed arrival directions for MC γ-rays of 120 GeV energy, impact parameters between 60 m and 160 m, 20° ZA and different azimuth angles. The intermediate image cleaning was applied.

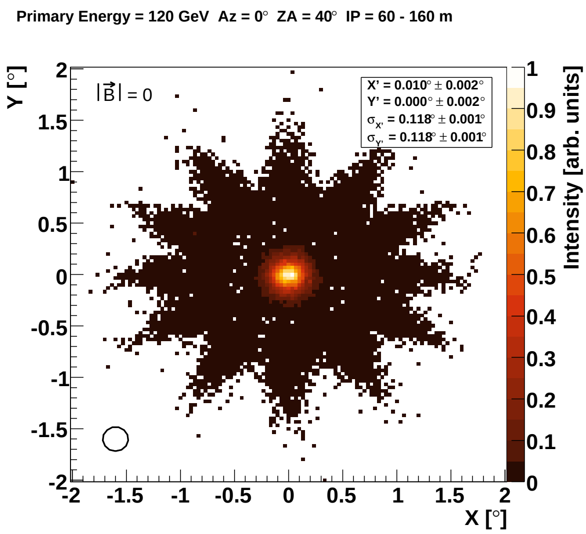

(a) 0° azimuth angle, GF disabled.

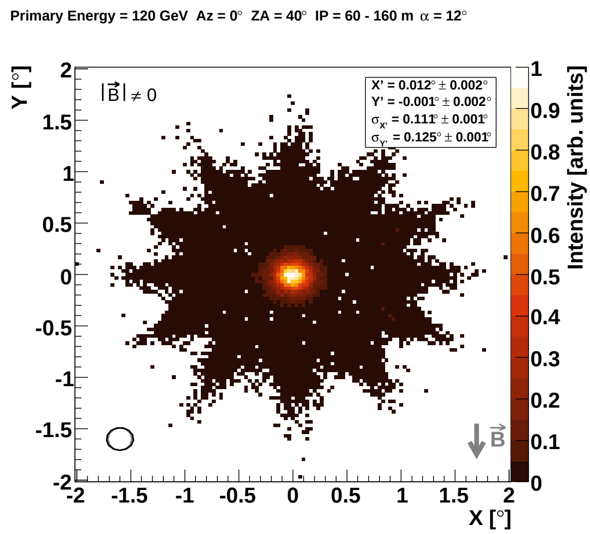

(b) 0° azimuth angle.

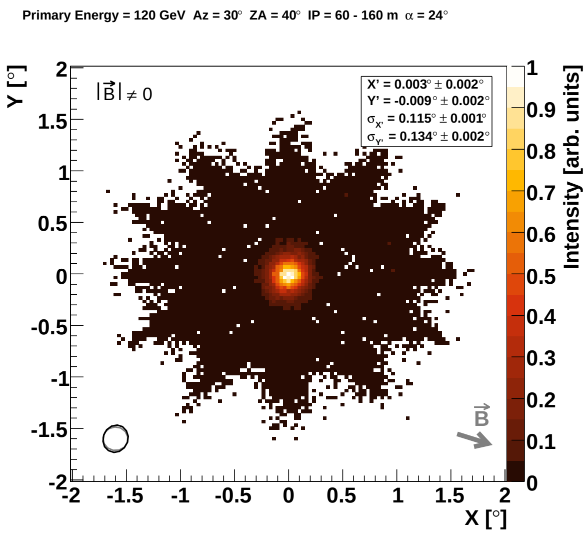

(c) 30° azimuth angle.

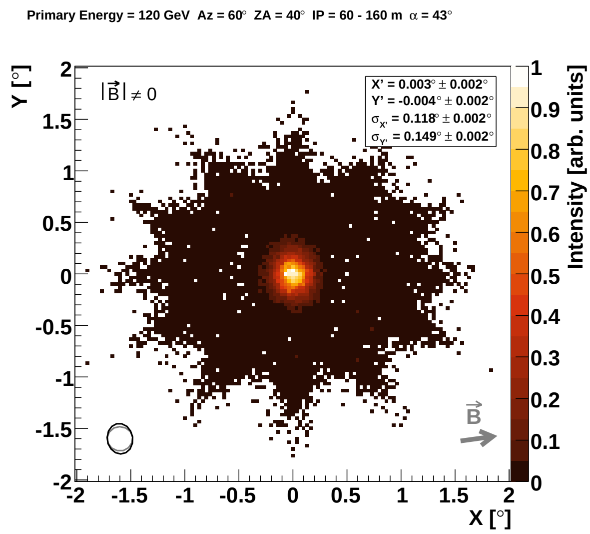

(d) 60° azimuth angle.

Figure 146: DISP-reconstructed arrival directions for MC γ-rays of 120 GeV energy, impact parameters between 60 m and 160 m, 40° ZA and different azimuth angles. The intermediate image cleaning was applied.

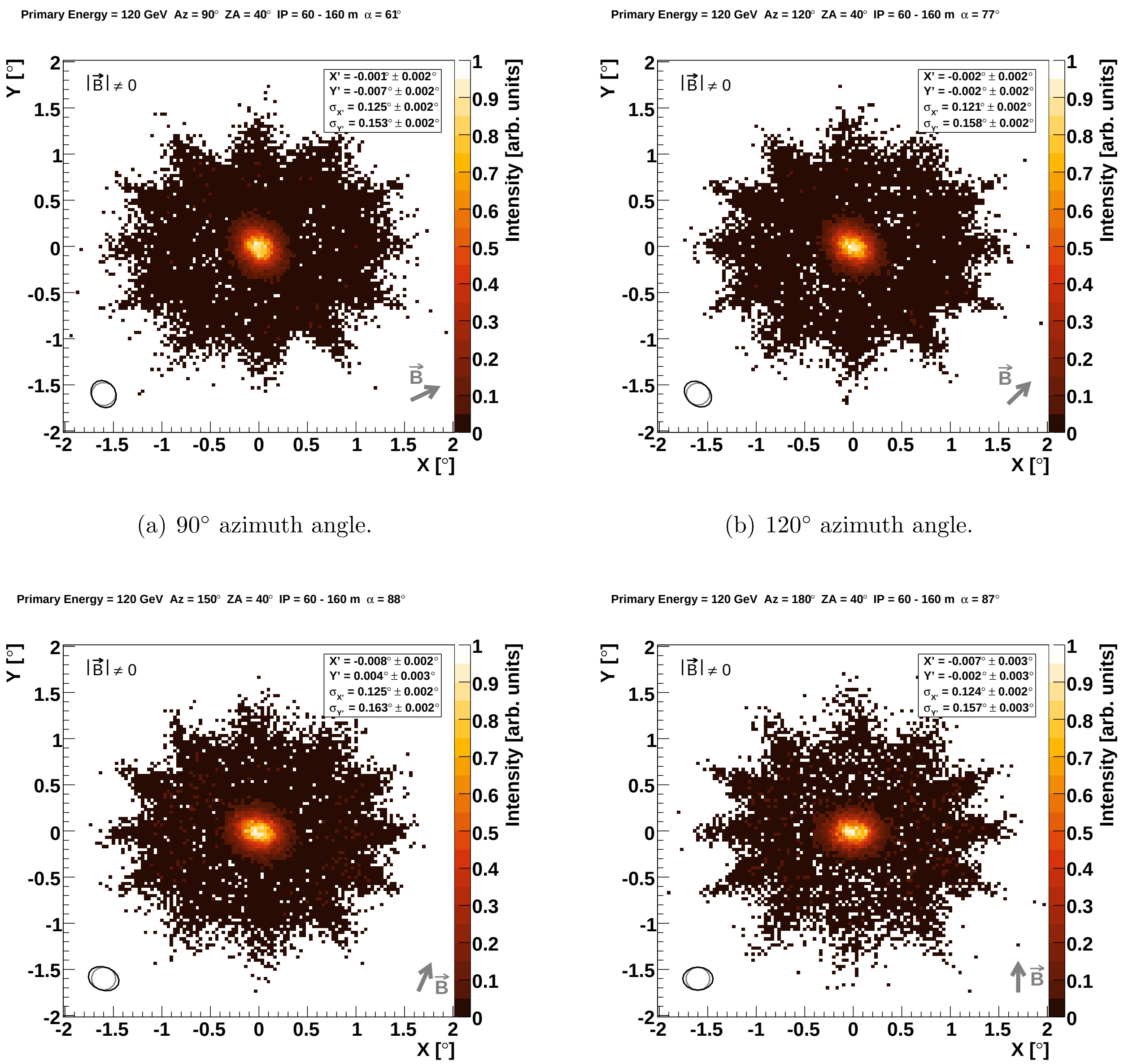

(a) 90° azimuth angle. (b) 120° azimuth angle.

(c) 150° azimuth angle. (d) 180° azimuth angle.

Figure 147: DISP-reconstructed arrival directions for MC γ-rays of 120 GeV energy, impact parameters between 60 m and 160 m, 40° ZA and different azimuth angles. The intermediate image cleaning was applied.

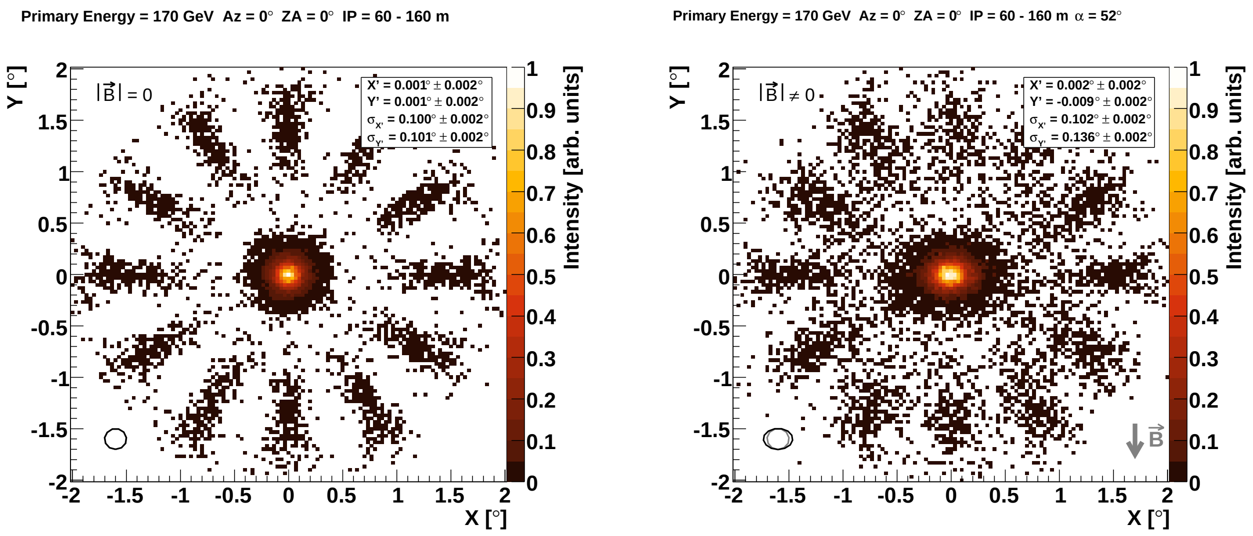

(a) GF disabled. (b) GF enabled.

Figure 148: DISP-reconstructed arrival directions for MC γ-rays of 170 GeV energy, impact parameters between 60 m and 160 m, 0° ZA and 0° azimuth angle. The intermediate image cleaning was applied.

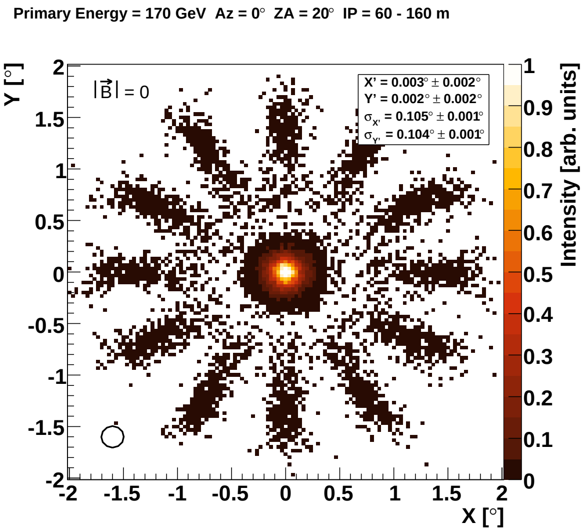

(a) 0° azimuth angle, GF disabled.

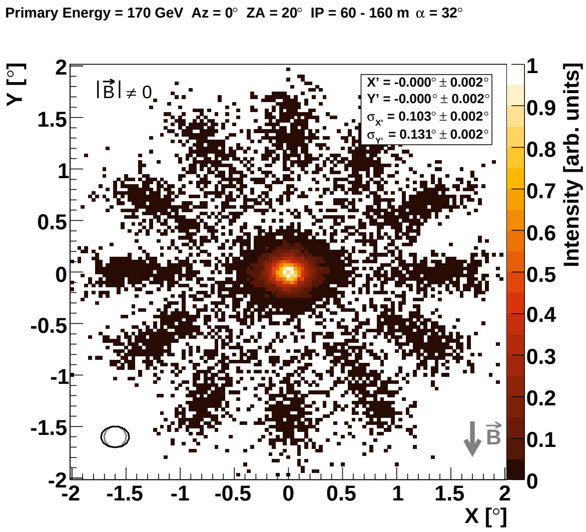

(b) 0° azimuth angle.

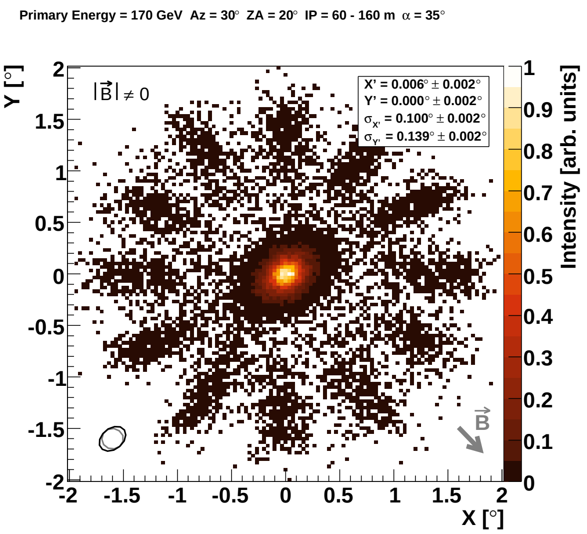

(c) 30° azimuth angle.

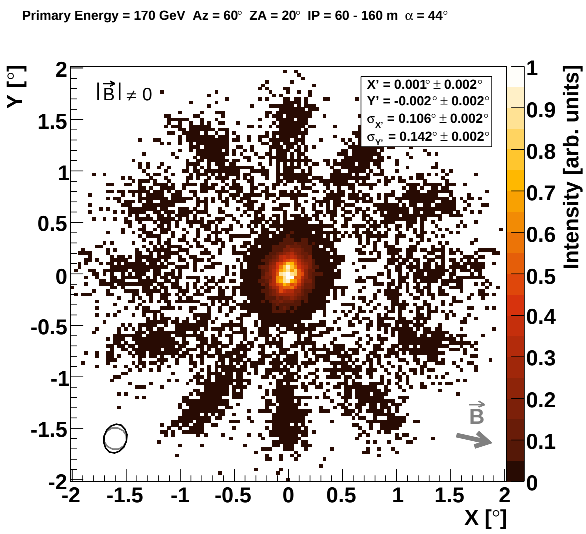

(d) 60° azimuth angle.

Figure 149: DISP-reconstructed arrival directions for MC γ-rays of 170 GeV energy, impact parameters between 60 m and 160 m, 20° ZA and different azimuth angles. The intermediate image cleaning was applied.

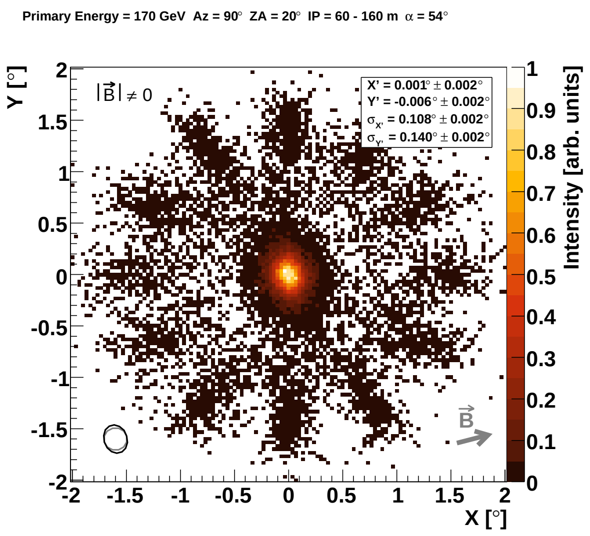

(a) 90° azimuth angle.

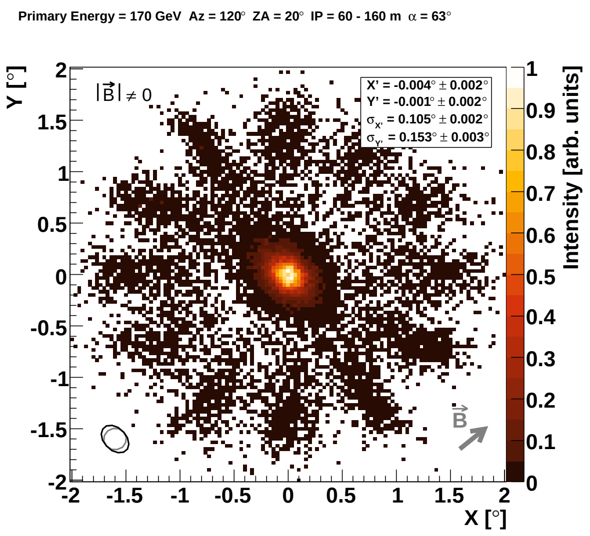

(b) 120° azimuth angle.

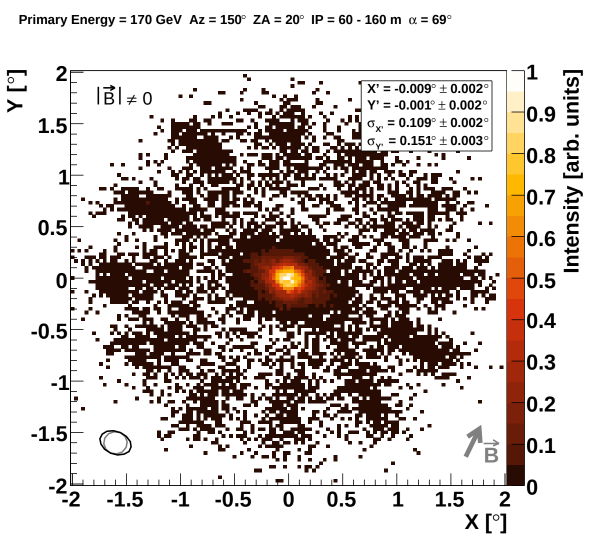

(c) 150° azimuth angle.

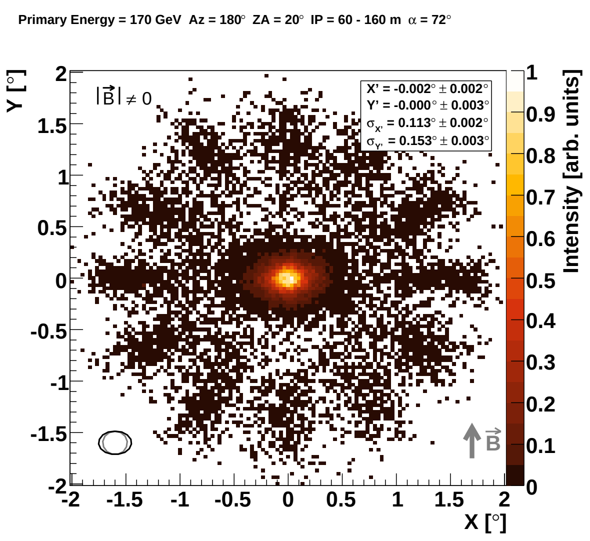

(d) 180° azimuth angle.

Figure 150: DISP-reconstructed arrival directions for MC γ-rays of 170 GeV energy, impact parameters between 60 m and 160 m, 20° ZA and different azimuth angles. The intermediate image cleaning was applied.

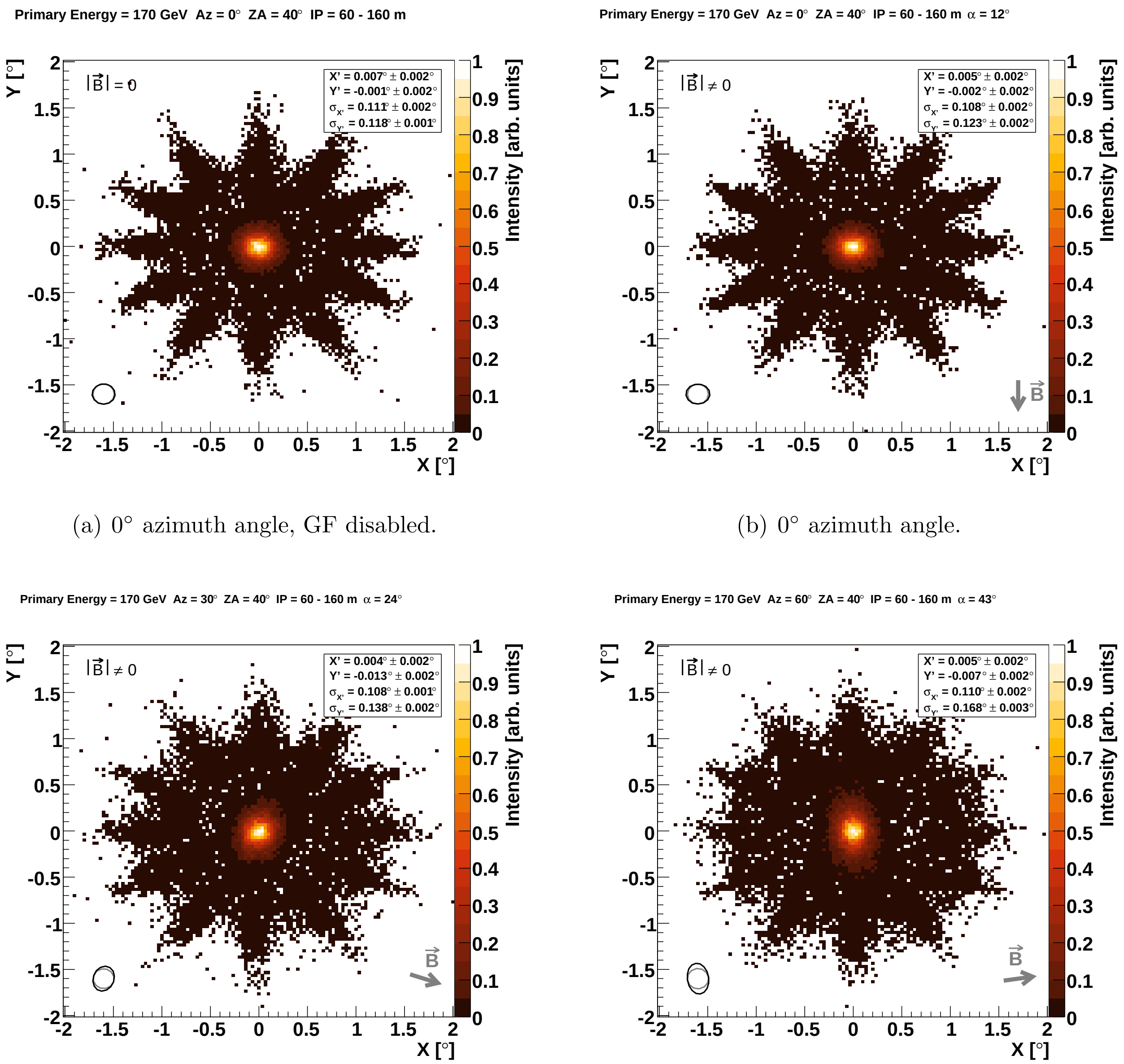

(a) 0° azimuth angle, GF disabled.

(b) 0° azimuth angle.

(c) 30° azimuth angle.

(d) 60° azimuth angle.

Figure 151: DISP-reconstructed arrival directions for MC γ-rays of 170 GeV energy, impact parameters between 60 m and 160 m, 40° ZA and different azimuth angles. The intermediate image cleaning was applied.

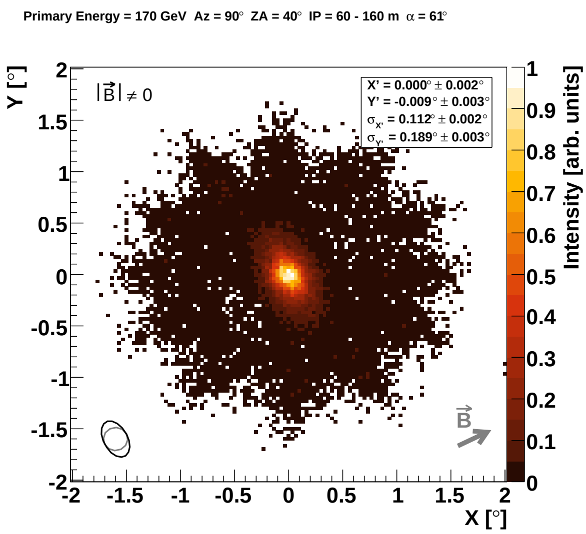

(a) 90° azimuth angle.

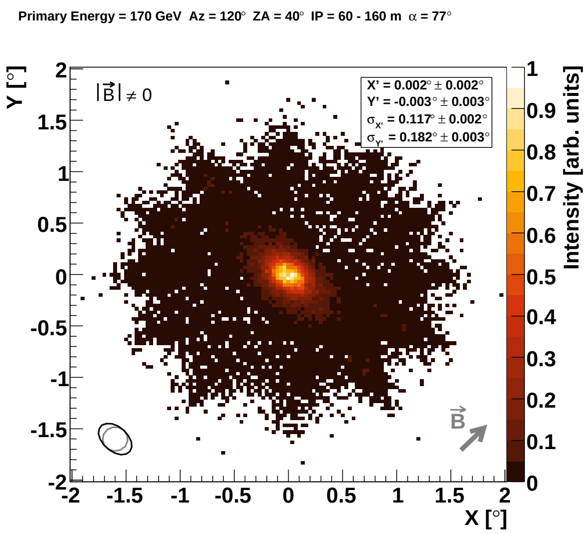

(b) 120° azimuth angle.

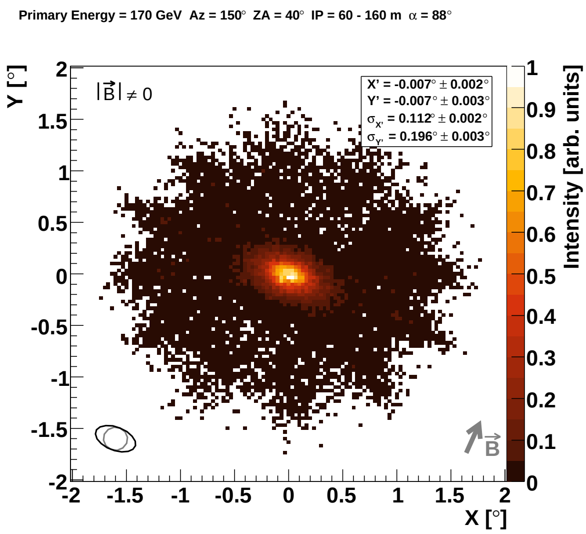

(c) 150° azimuth angle.

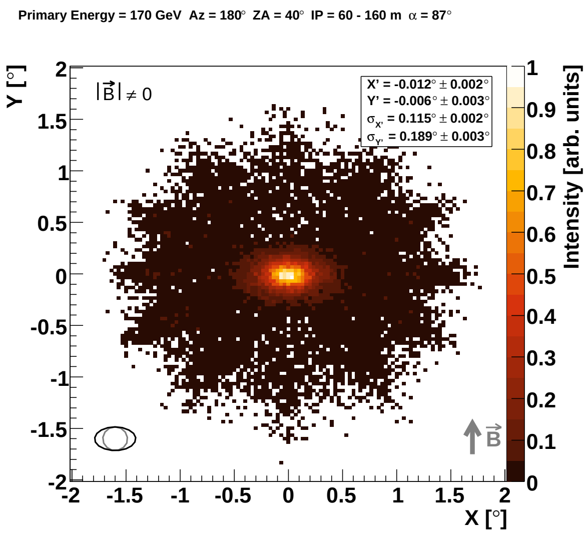

(d) 180° azimuth angle.

Figure 152: DISP-reconstructed arrival directions for MC γ-rays of 170 GeV energy, impact parameters between 60 m and 160 m, 40° ZA and different azimuth angles. The intermediate image cleaning was applied.

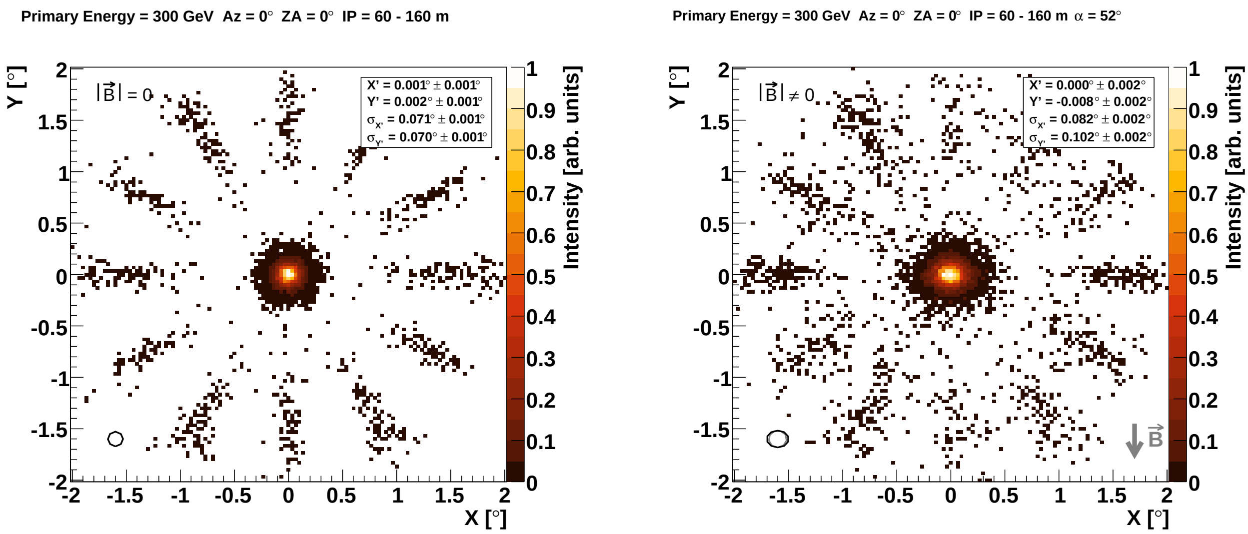

(a) GF disabled. (b) GF enabled.

Figure 153: DISP-reconstructed arrival directions for MC γ-rays of 300 GeV energy, impact parameters between 60 m and 160 m, 0° ZA and 0° azimuth angle. The intermediate image cleaning was applied.

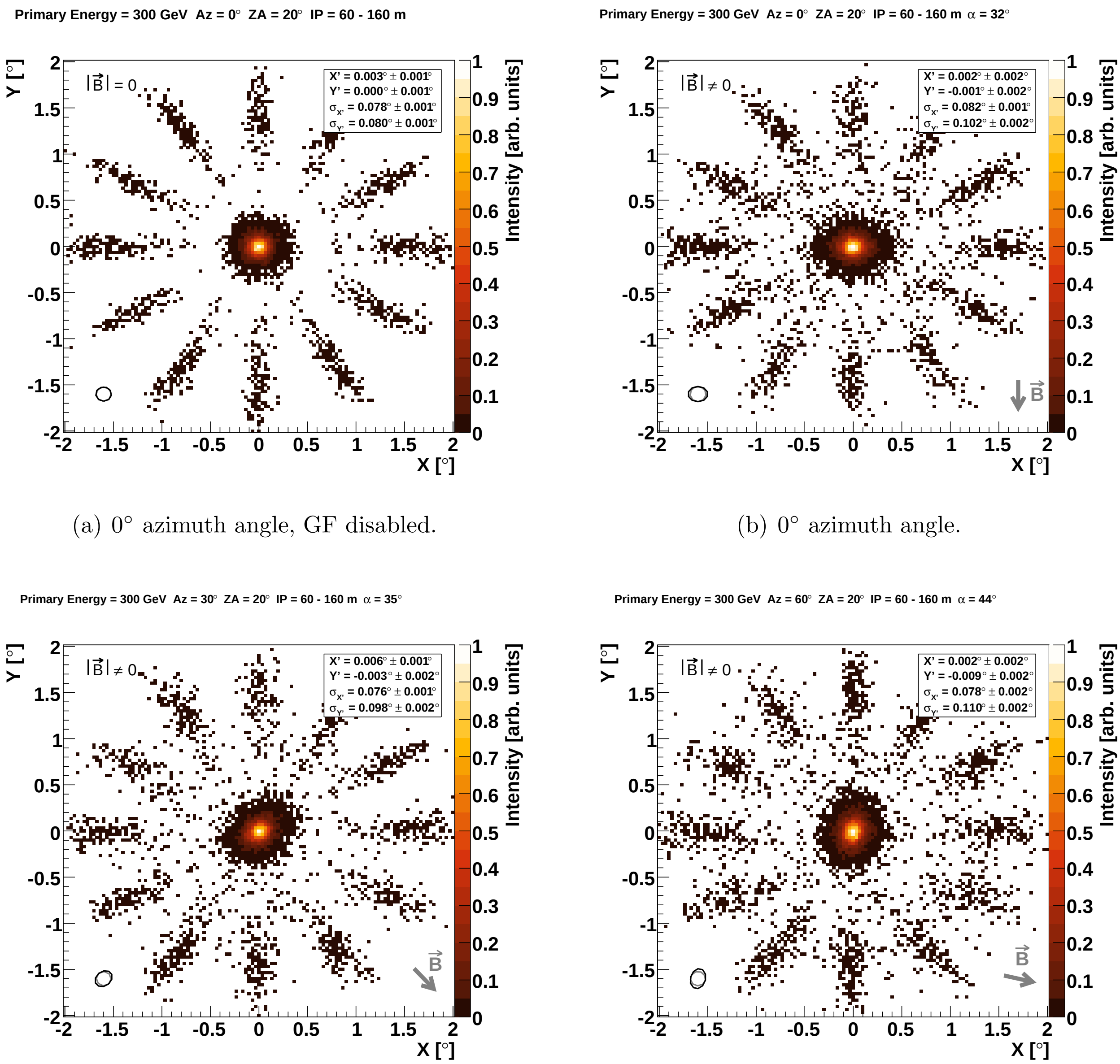

(a) 0° azimuth angle, GF disabled.

(b) 0° azimuth angle.

(c) 30° azimuth angle.

(d) 60° azimuth angle.

Figure 154: DISP-reconstructed arrival directions for MC γ-rays of 300 GeV energy, impact parameters between 60 m and 160 m, 20° ZA and different azimuth angles. The intermediate image cleaning was applied.

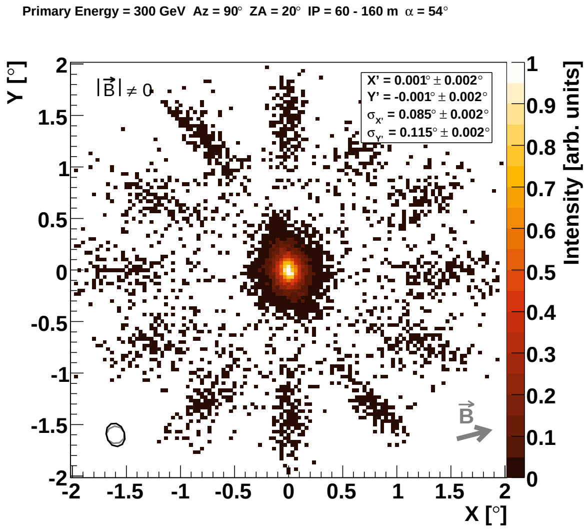

(a) 90° azimuth angle.

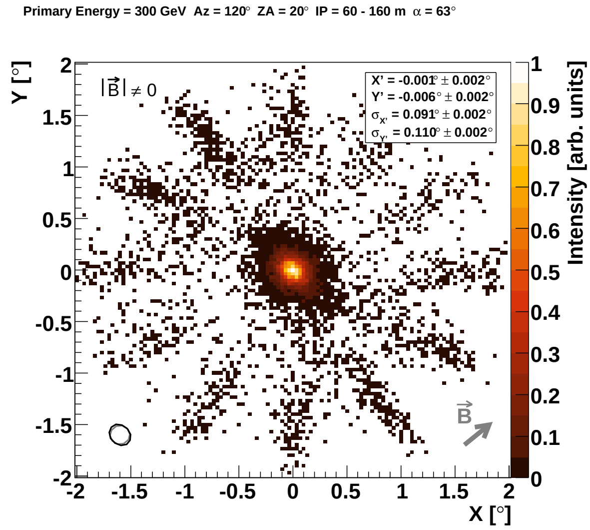

(b) 120° azimuth angle.

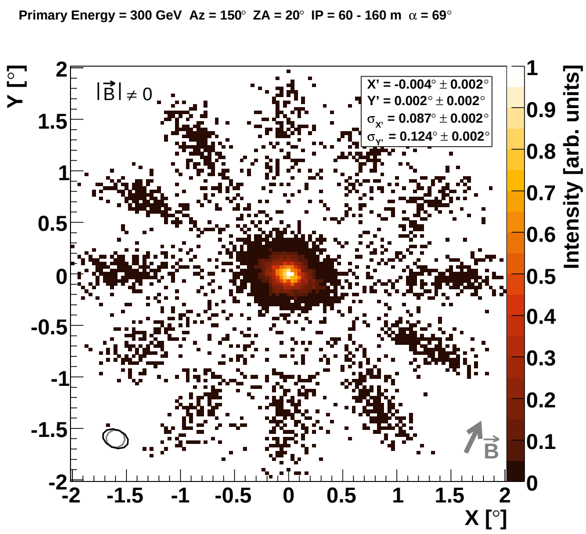

(c) 150° azimuth angle.

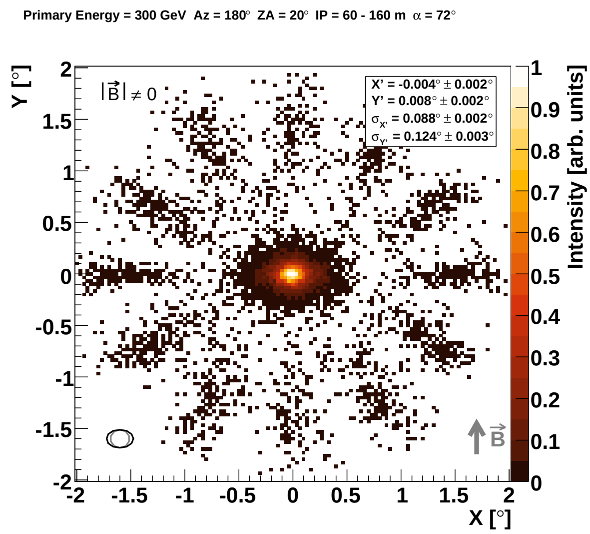

(d) 180° azimuth angle.

Figure 155: DISP-reconstructed arrival directions for MC γ-rays of 300 GeV energy, impact parameters between 60 m and 160 m, 20° ZA and different azimuth angles. The intermediate image cleaning was applied.

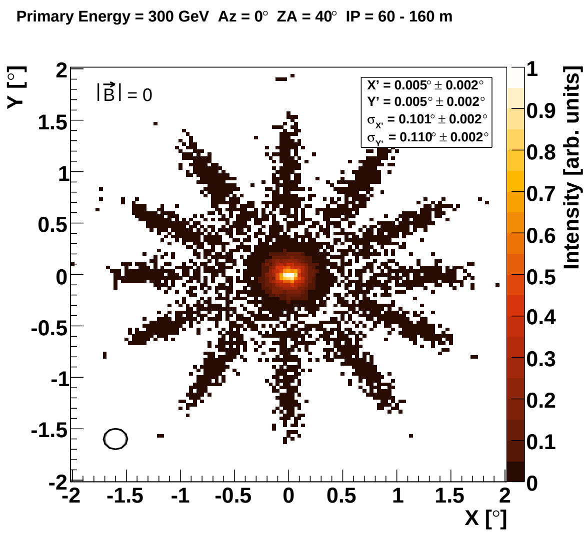

(a) 0° azimuth angle, GF disabled.

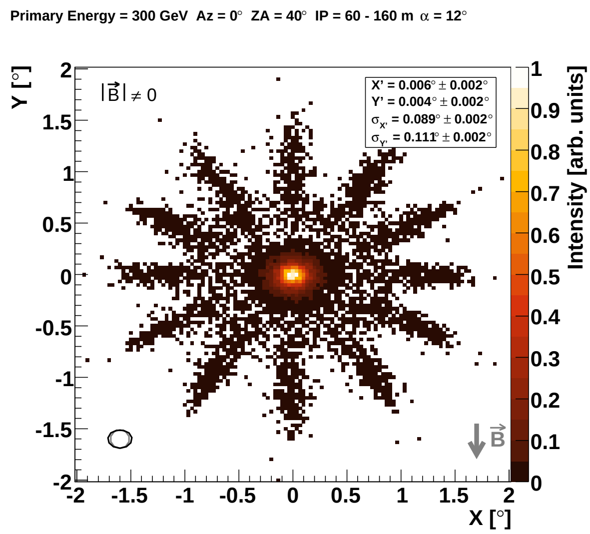

(b) 0° azimuth angle.

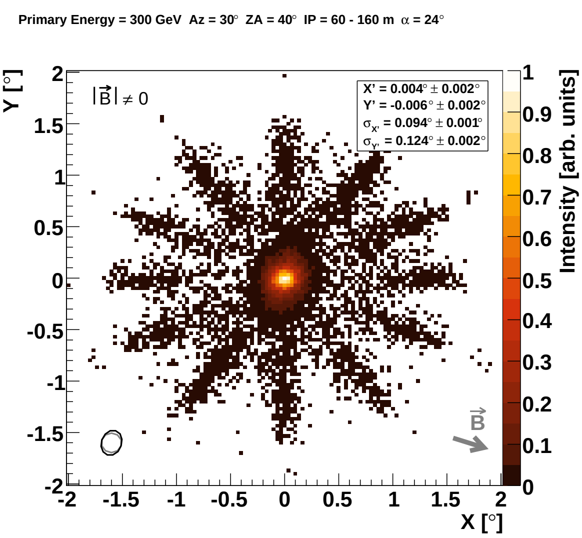

(c) 30° azimuth angle.

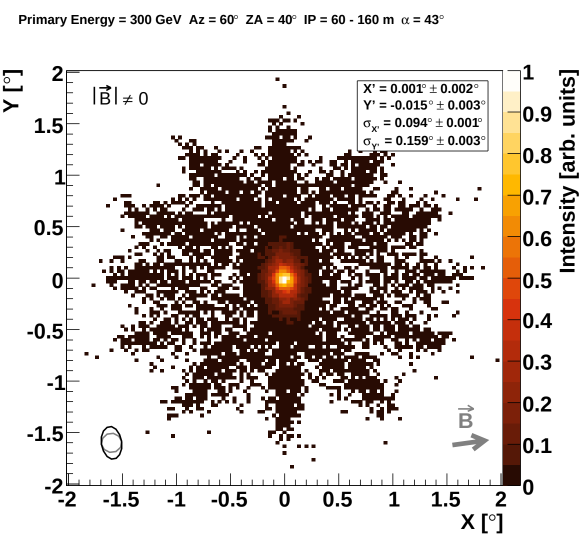

(d) 60° azimuth angle.

Figure 156: DISP-reconstructed arrival directions for MC γ-rays of 300 GeV energy, impact parameters between 60 m and 160 m, 40° ZA and different azimuth angles. The intermediate image cleaning was applied.

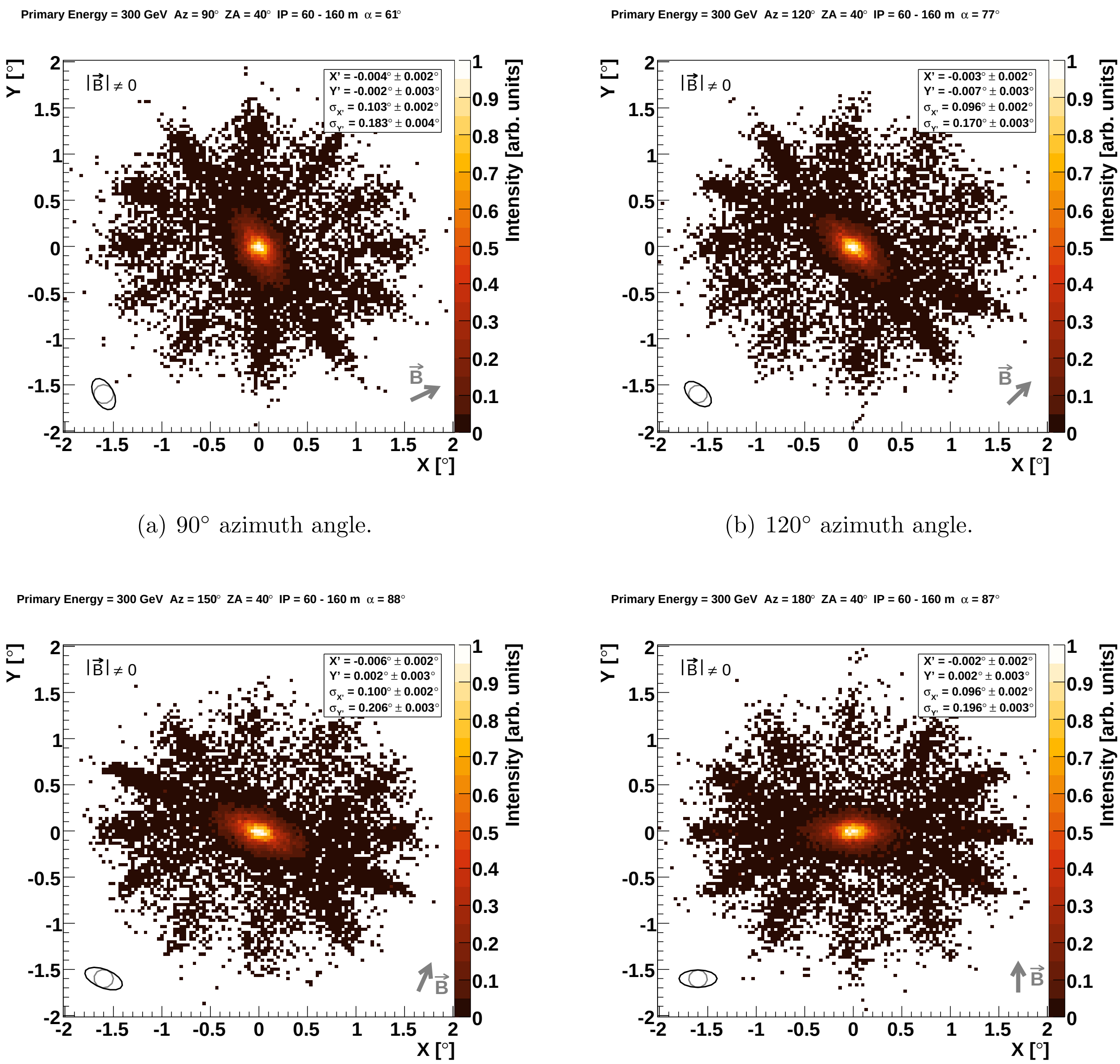

(a) 90° azimuth angle.

(b) 120° azimuth angle.

(c) 150° azimuth angle.

(d) 180° azimuth angle.

Figure 157: DISP-reconstructed arrival directions for MC γ-rays of 300 GeV energy, impact parameters between 60 m and 160 m, 40° ZA and different azimuth angles. The intermediate image cleaning was applied.

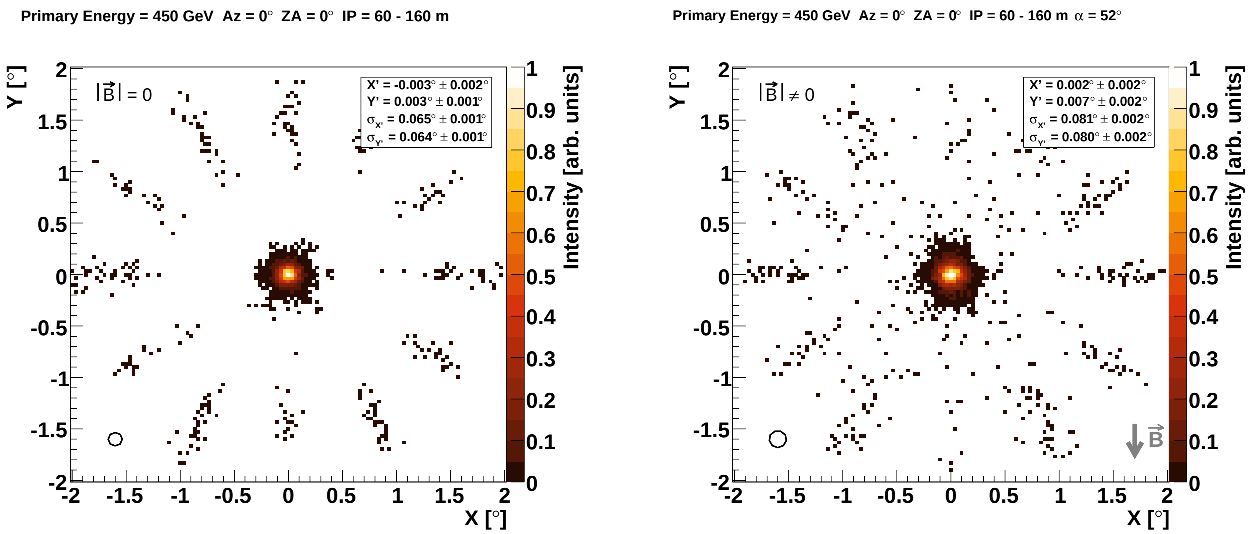

(a) GF disabled.

(b) GF enabled.

Figure 158: DISP-reconstructed arrival directions for MC γ-rays of 450 GeV energy, impact parameters between 60 m and 160 m, 0° ZA and 0° azimuth angle. The intermediate image cleaning was applied.

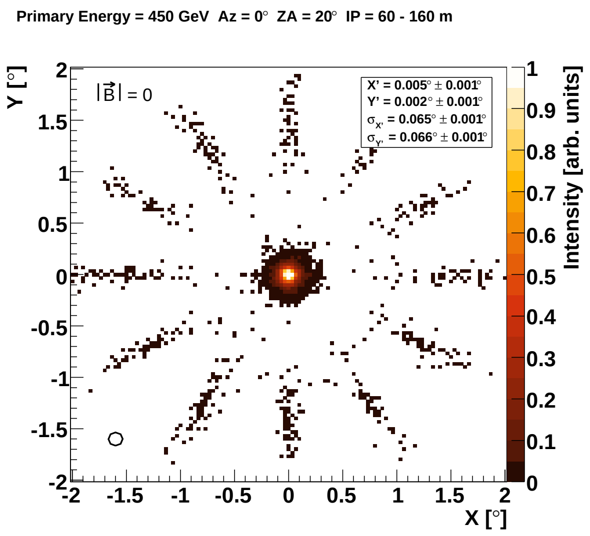

(a) 0° azimuth angle, GF disabled.

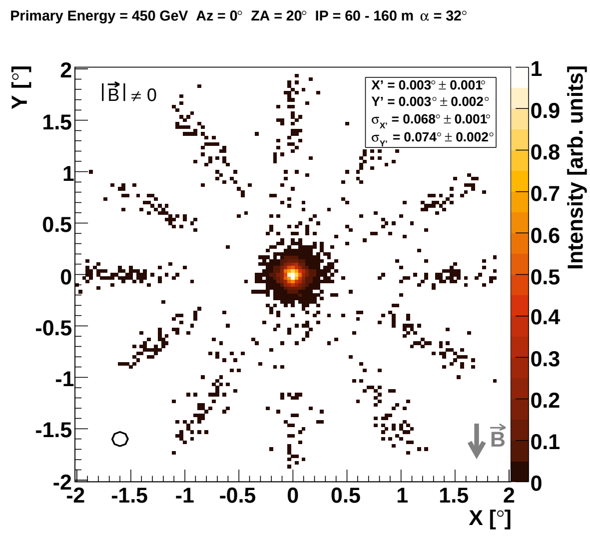

(b) 0° azimuth angle.

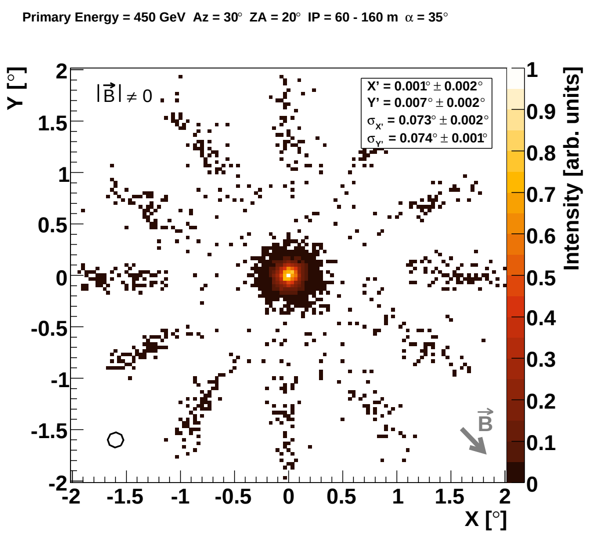

(c) 30° azimuth angle.

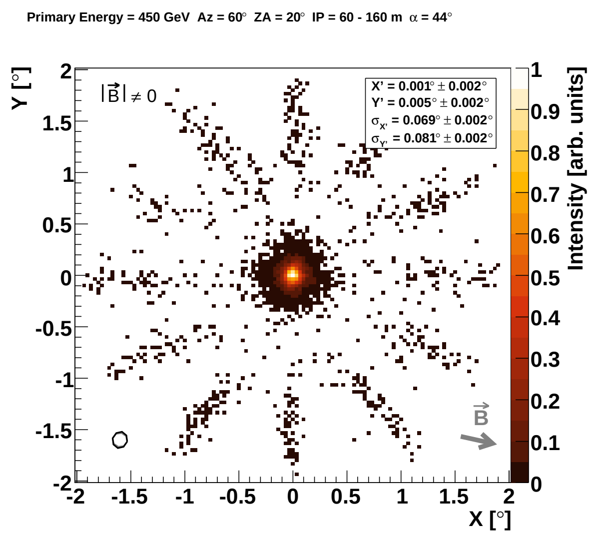

(d) 60° azimuth angle.

Figure 159: DISP-reconstructed arrival directions for MC γ-rays of 450 GeV energy, impact parameters between 60 m and 160 m, 20° ZA and different azimuth angles. The intermediate image cleaning was applied.

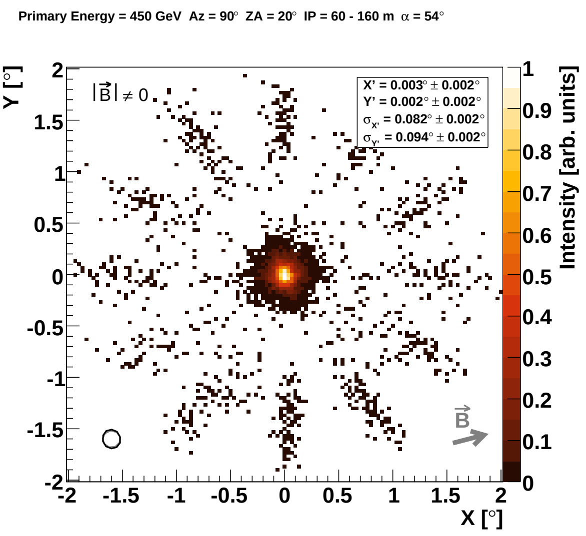

(a) 90° azimuth angle.

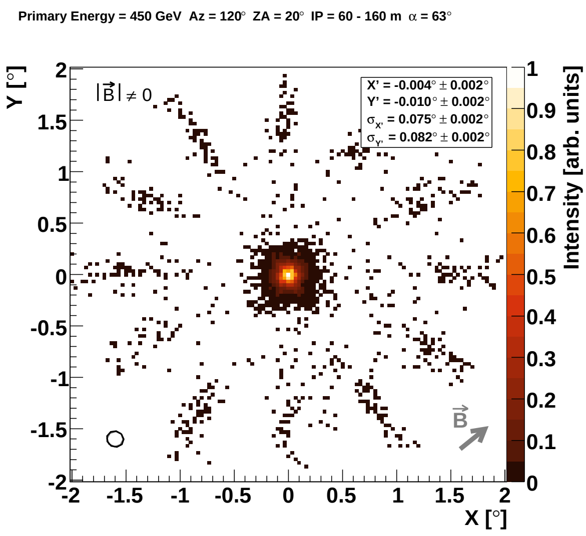

(b) 120° azimuth angle.

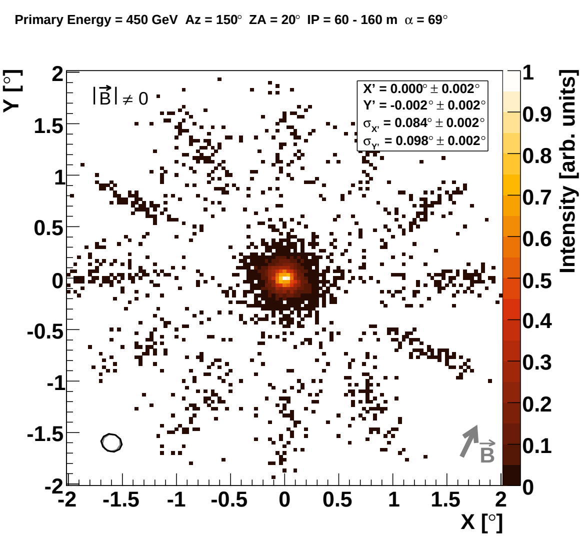

(c) 150° azimuth angle.

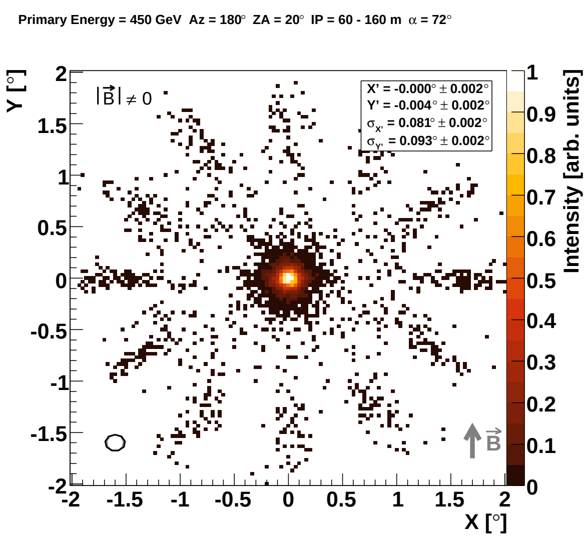

(d) 180° azimuth angle.

Figure 160: DISP-reconstructed arrival directions for MC γ-rays of 450 GeV energy, impact parameters between 60 m and 160 m, 20° ZA and different azimuth angles. The intermediate image cleaning was applied.

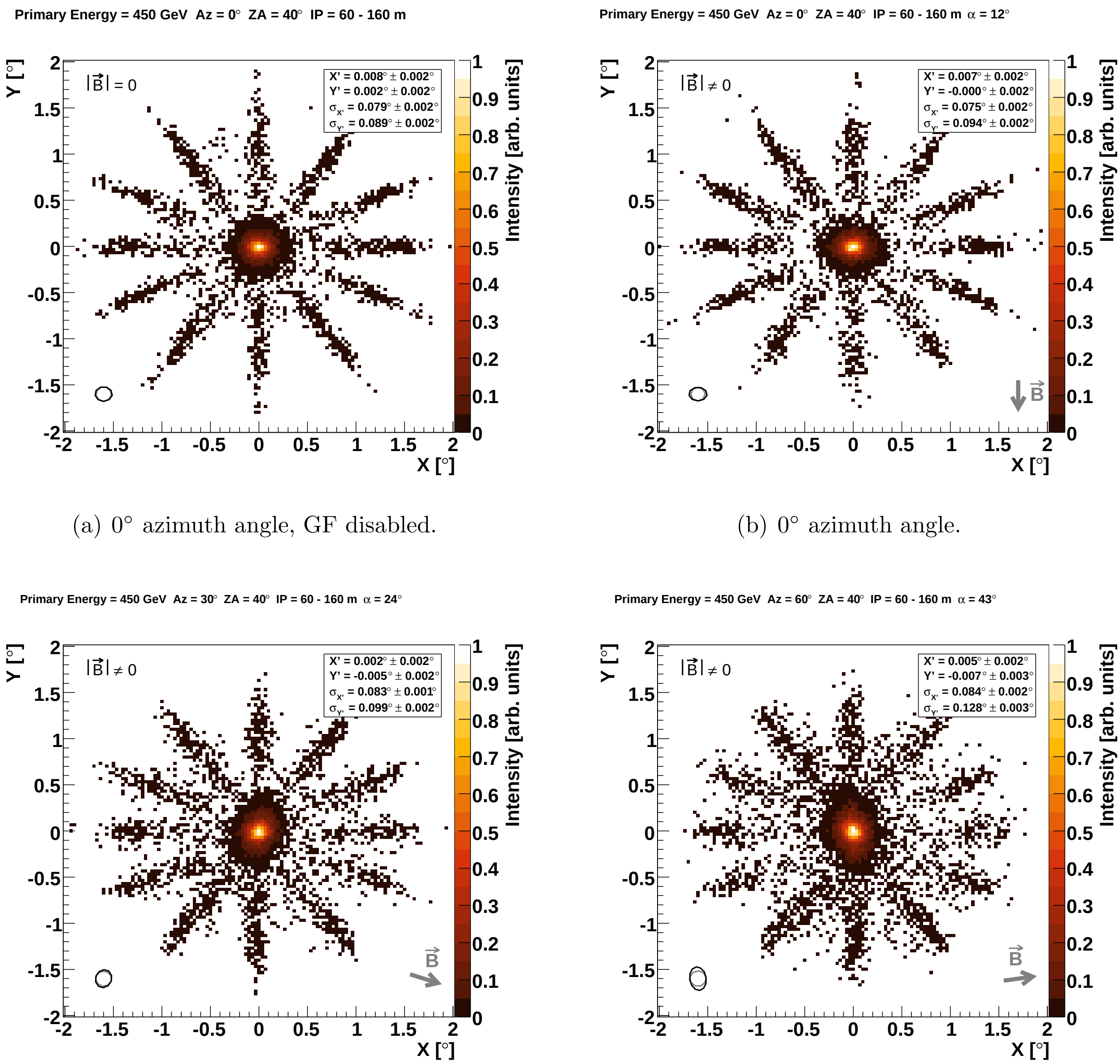

(a) 0° azimuth angle, GF disabled.

(b) 0° azimuth angle.

(c) 30° azimuth angle.

(d) 60° azimuth angle.

Figure 161: DISP-reconstructed arrival directions for MC γ-rays of 450 GeV energy, impact parameters between 60 m and 160 m, 40° ZA and different azimuth angles. The intermediate image cleaning was applied.

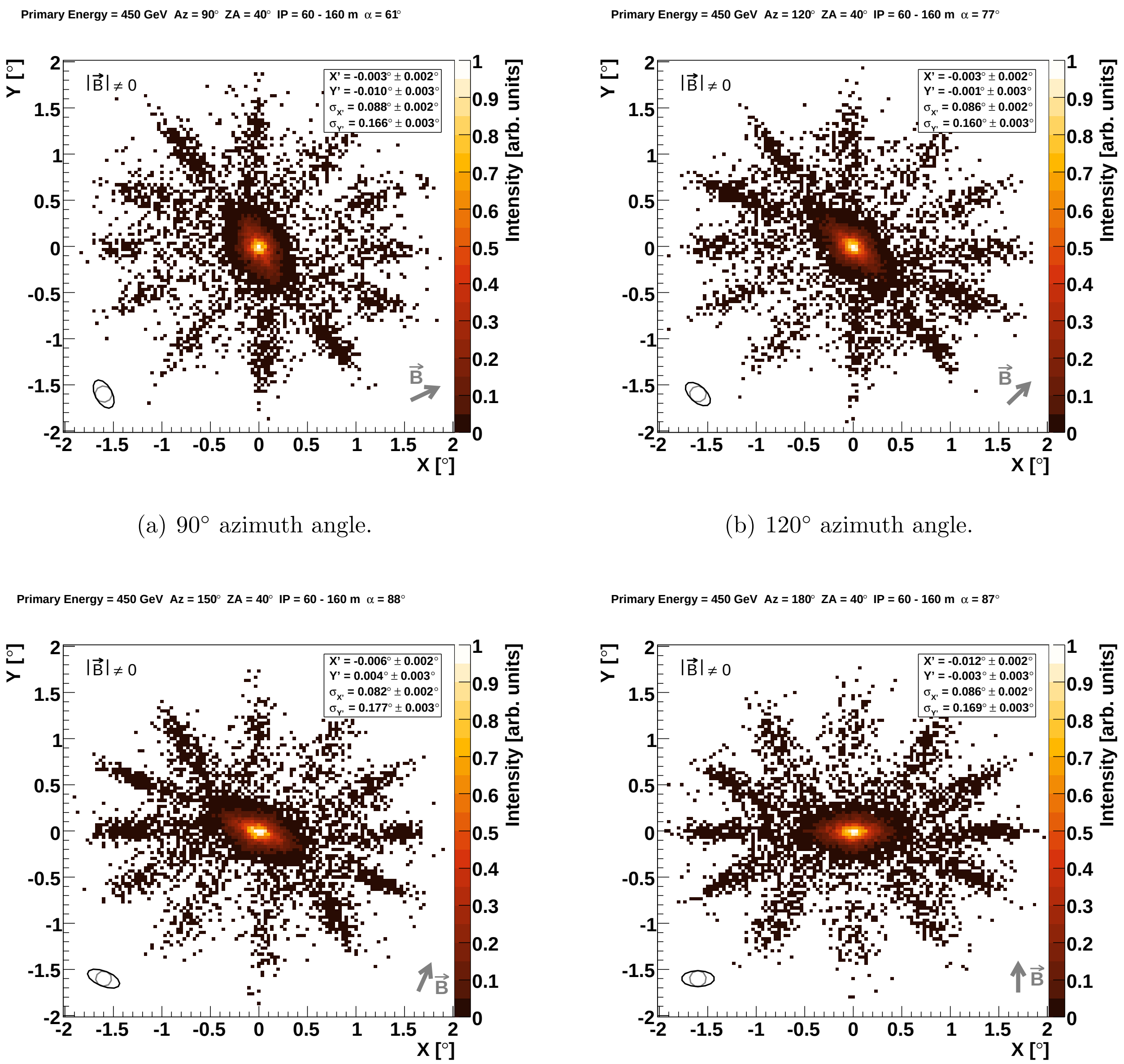

(a) 90° azimuth angle.

(b) 120° azimuth angle.

(c) 150° azimuth angle.

(d) 180° azimuth angle.

Figure 162: DISP-reconstructed arrival directions for MC γ-rays of 450 GeV energy, impact parameters between 60 m and 160 m, 40° ZA and different azimuth angles. The intermediate image cleaning was applied.

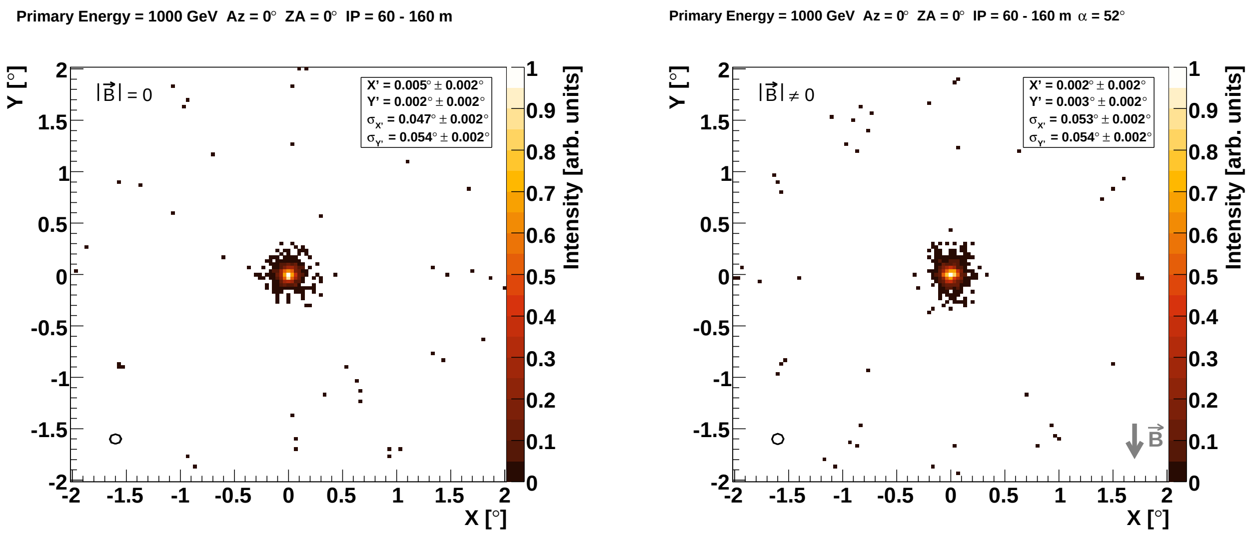

(a) GF disabled.

(b) GF enabled.

Figure 163: DISP-reconstructed arrival directions for MC γ-rays of 1000 GeV energy, impact parameters between 60 m and 160 m, 0° ZA and 0° azimuth angle. The intermediate image cleaning was applied.

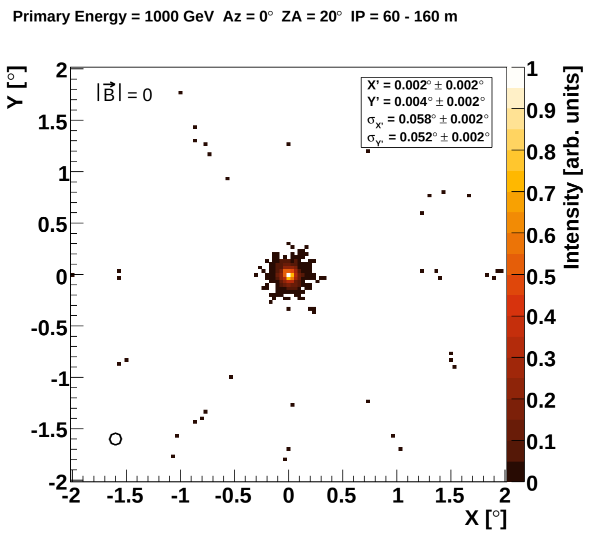

(a) 0° azimuth angle, GF disabled.

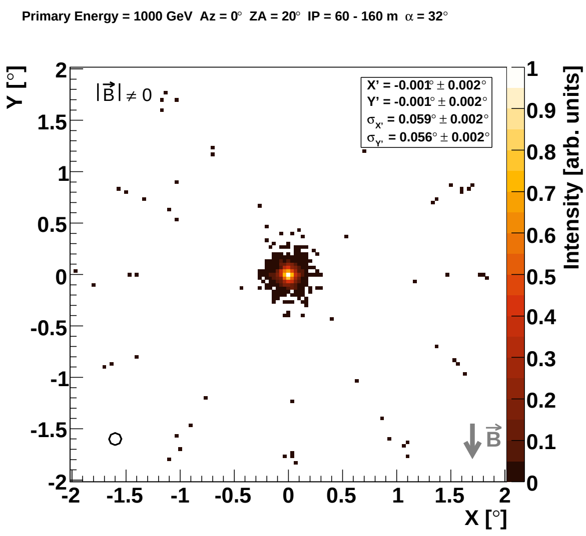

(b) 0° azimuth angle.

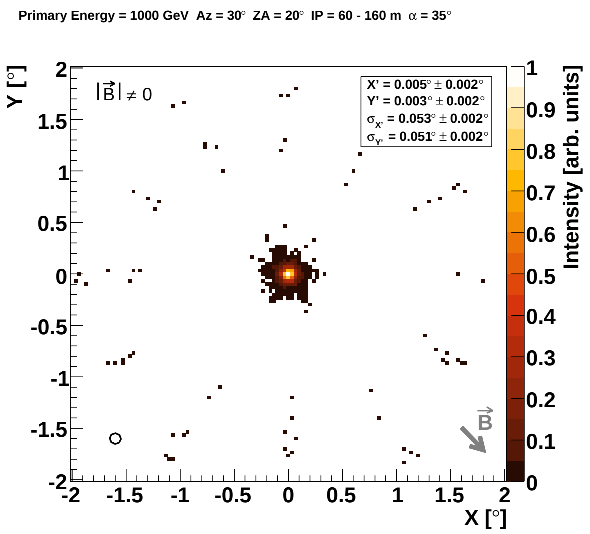

(c) 30° azimuth angle.

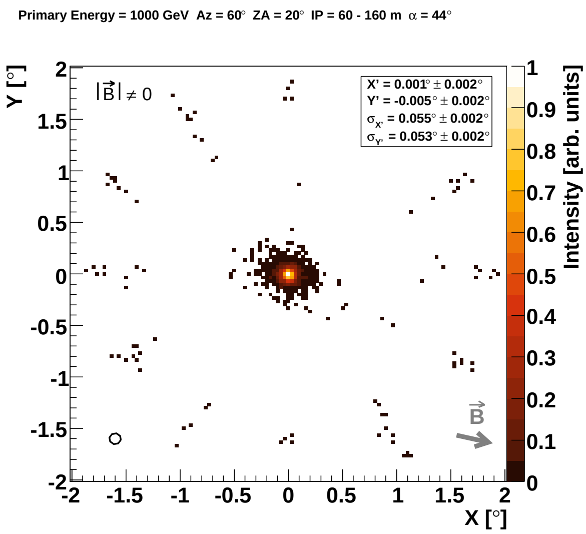

(d) 60° azimuth angle.

Figure 164: DISP-reconstructed arrival directions for MC γ-rays of 1000 GeV energy, impact parameters between 60 m and 160 m, 20° ZA and different azimuth angles. The intermediate image cleaning was applied.

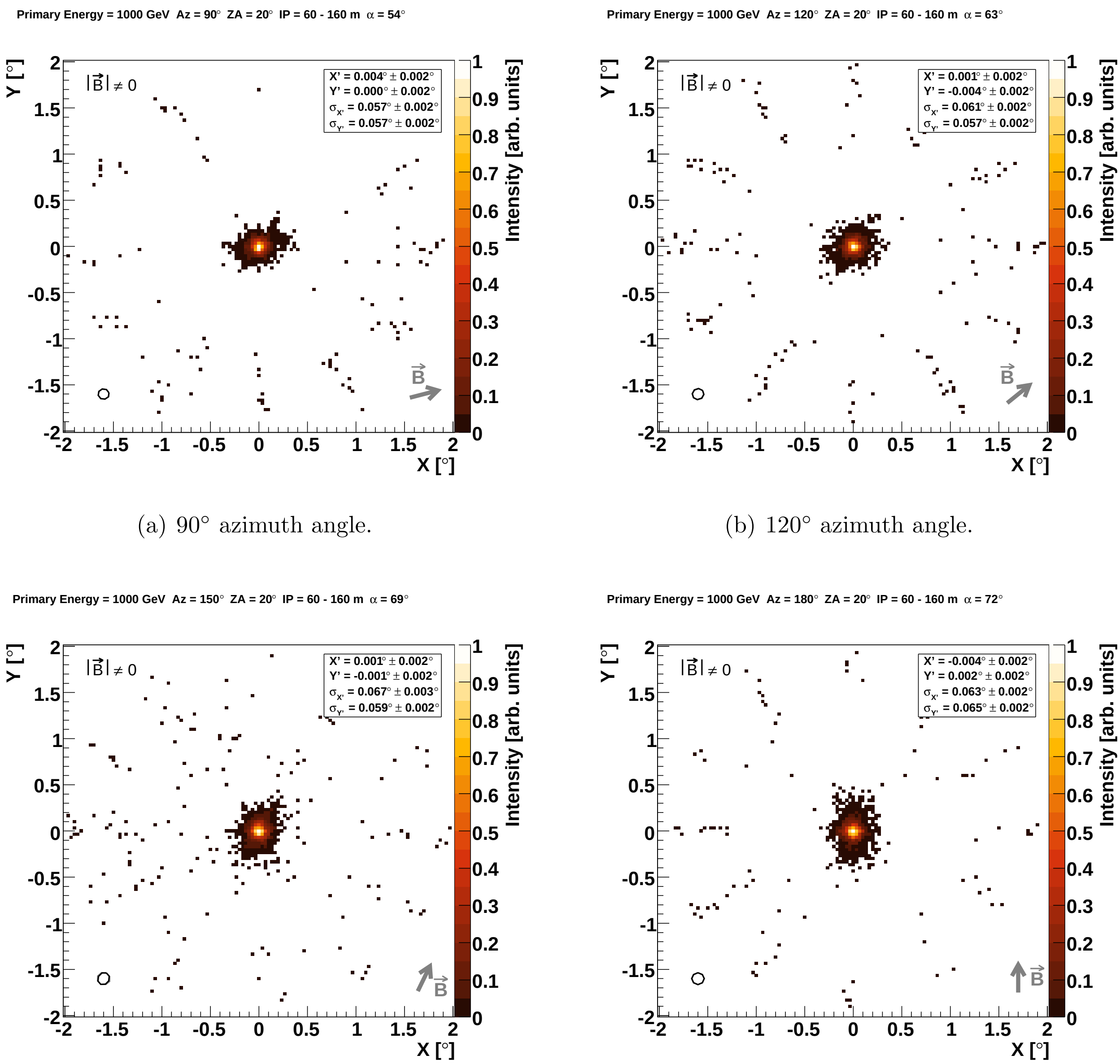

(a) 90° azimuth angle.

(b) 120° azimuth angle.

(c) 150° azimuth angle.

(d) 180° azimuth angle.

Figure 165: DISP-reconstructed arrival directions for MC γ-rays of 1000 GeV energy, impact parameters between 60 m and 160 m, 20° ZA and different azimuth angles. The intermediate image cleaning was applied.

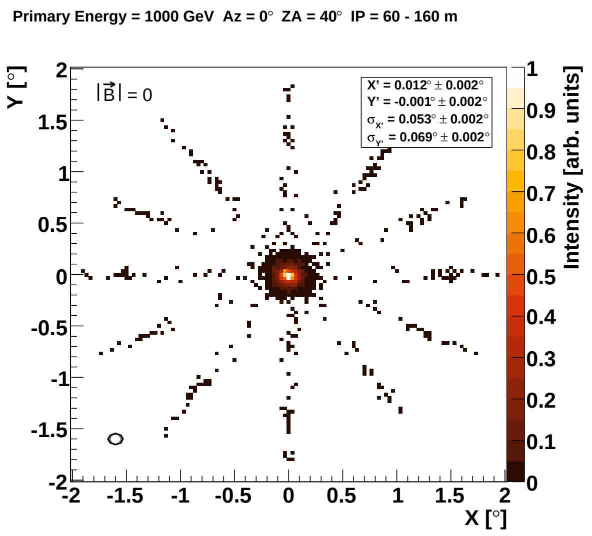

(a) 0° azimuth angle, GF disabled.

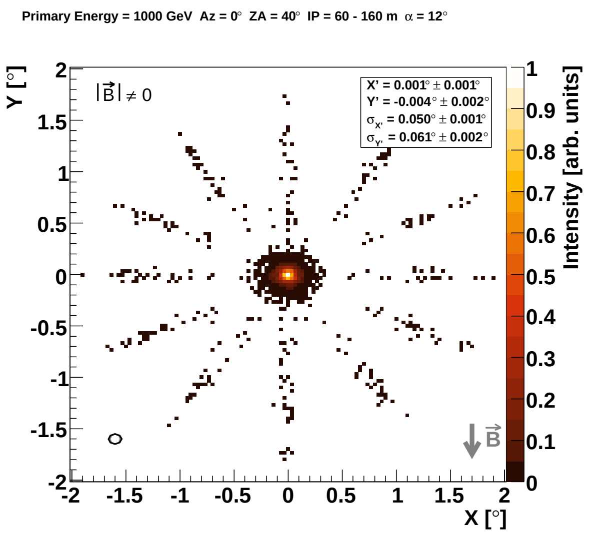

(b) 0° azimuth angle.

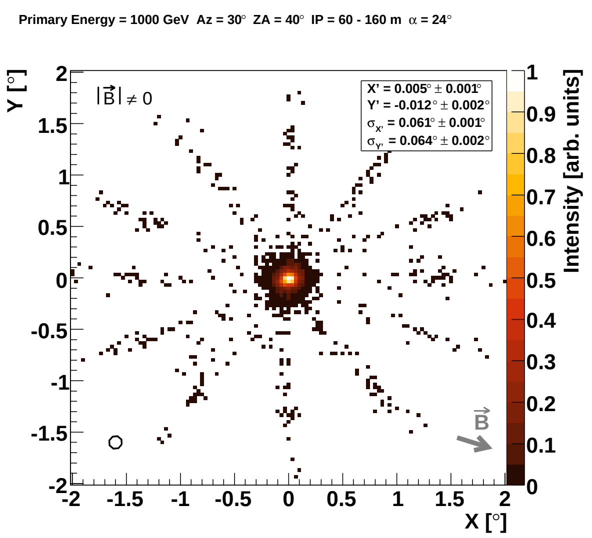

(c) 30° azimuth angle.

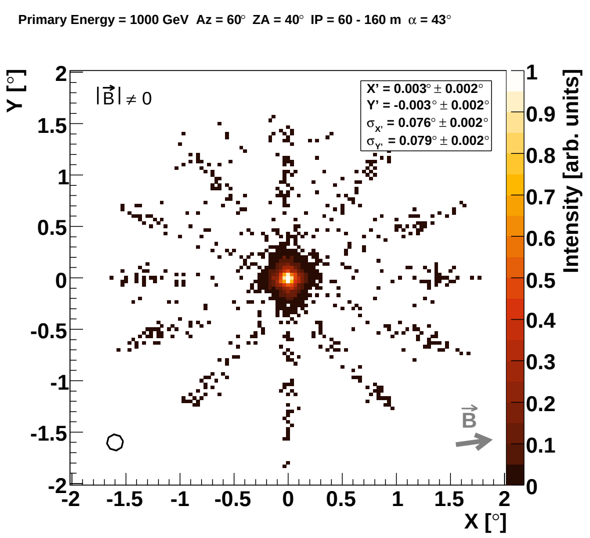

(d) 60° azimuth angle.

Figure 166: DISP-reconstructed arrival directions for MC γ-rays of 1000 GeV energy, impact parameters between 60 m and 160 m, 40° ZA and different azimuth angles. The intermediate image cleaning was applied.

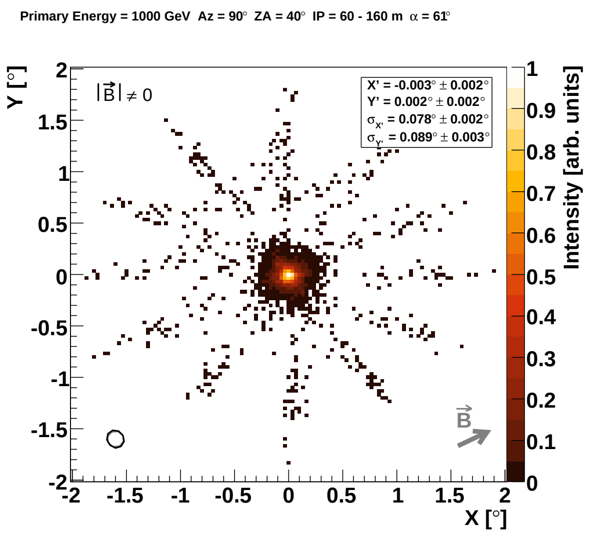

(a) 90° azimuth angle.

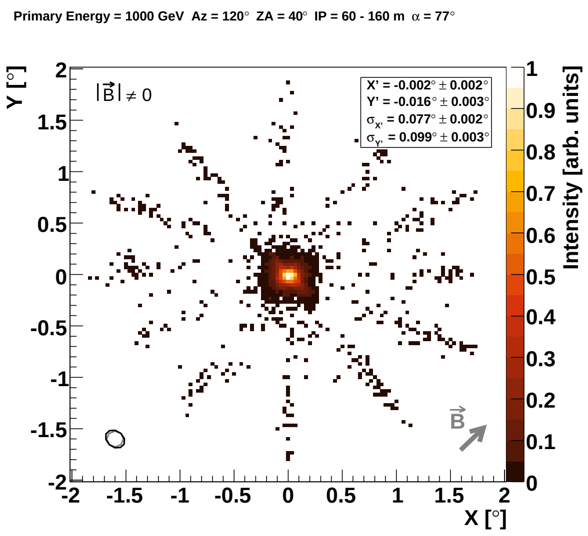

(b) 120° azimuth angle.

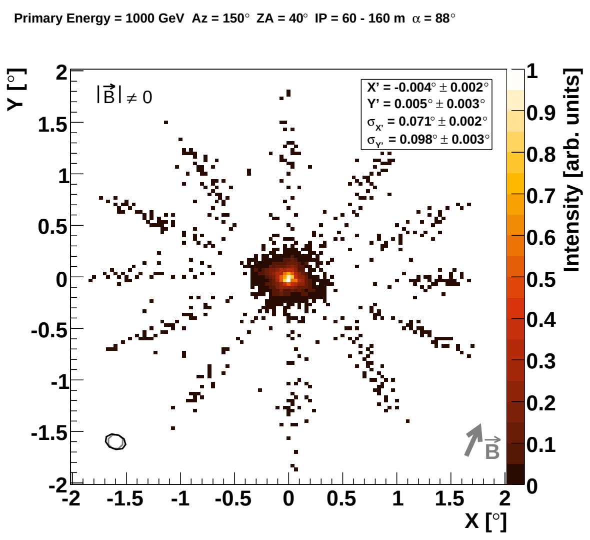

(c) 150° azimuth angle.

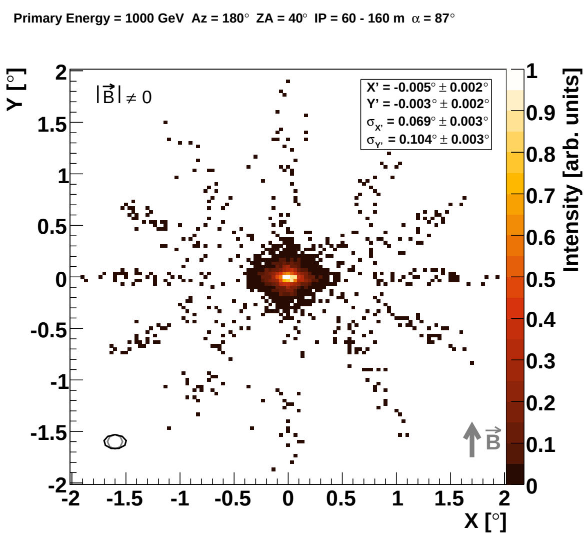

(d) 180° azimuth angle.

Figure 167: DISP-reconstructed arrival directions for MC γ-rays of 1000 GeV energy, impact parameters between 60 m and 160 m, 40° ZA and different azimuth angles. The intermediate image cleaning was applied.

The Influence of the GF on the Lateral and Longitudinal Spread of the DISP Distribution

Figures 168 - 175 show the lateral and longitudinal spread versus γ-ray energy for different orientations of the telescope. The spreads are defined as the sigma of a Gaussian fit to the DISP distribution using bands of $\Delta_{X',Y'} = \pm 0.035°$ parallel and perpendicular to the projected direction of the GF in the camera. All impact parameters between 60 m and 160 m were considered. Both the intermediate and the hard image cleaning were applied. As can be seen in the figures, compared to the case of disabled GF, the spread of the DISP distribution increases significantly with increasing angle α. The maximum spread occurs always perpendicular to the direction of the GF in the camera. The DISP distributions obtained for the hard image cleaning (figures 172 - 175) have a larger spread than the ones obtained for the intermediate image cleaning (figures 168 - 171). It should be kept in mind that for ZA $> 0°$ and azimuth angle $\neq 0°$, $180°$ the figures are not fully compatible in the strict sense since geometrical and GF effects are entangled (figure 20). Furthermore, depending on the inclination of the telescope, the true impact parameter can vary significantly between the different telescope positions (r, φ) (figure 16 (b)). Nevertheless, the figures clearly show that the GF affects the spread of the DISP distribution perpendicular to the direction of the GF in the camera.
Figures 176 - 183 show the lateral and longitudinal spread of the DISP distribution versus azimuth angle for different γ-ray energies, ZAs and image cleanings. All impact parameters between 60 m and 160 m were considered. For ZA $> 0°$, the spread of the DISP distribution perpendicular to the direction of the GF increases significantly with increasing azimuth angle, while the spread in direction of the GF is always comparable to the one obtained for disabled GF (drawn as a straight line). The largest spread occurs for γ-rays of 300 GeV - 450 GeV energy at $180°$ azimuth angle and $40°$ ZA (figure 180 (a) and 181 (c)).
Figures 184 - 198 show the spread of the DISP distribution perpendicular and parallel to the direction of the GF versus impact parameter for different telescope orientations and γ-rays between 50 GeV and 1 TeV. The intermediate and the hard image cleaning was applied. For energies below 120 GeV and impact parameters greater than ~ 100 m the lateral and longitudinal spreads of the DISP distribution are comparable to the ones for disabled GF. For greater energies the influence of the GF on the spread perpendicular to the direction of the GF is clearly visible. For all energies between 50 GeV and 1 TeV the spread increases with decreasing impact parameter. This is also the case for showers that were generated with disabled GF. However, showers with small impact parameters are generally more affected by the GF than the ones at larger impact parameters (compare e.g. figures 194 (a) and (b)).

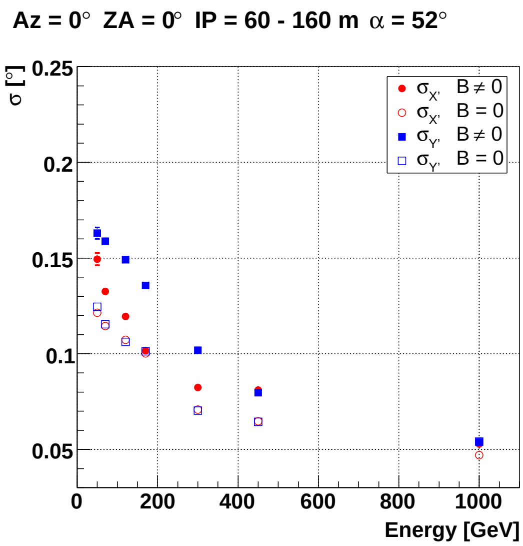

(a) 0° azimuth angle.

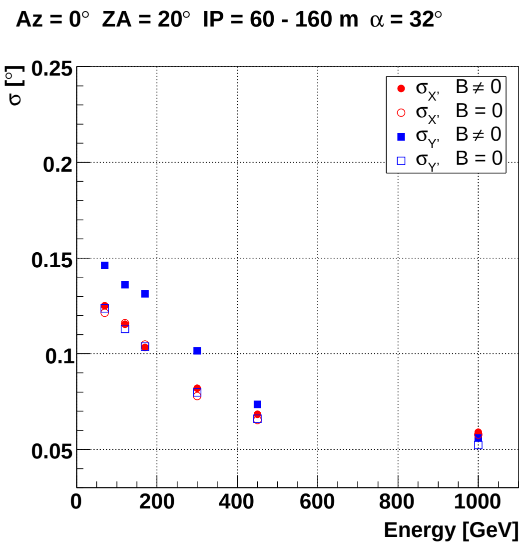

(b) 0° azimuth angle.

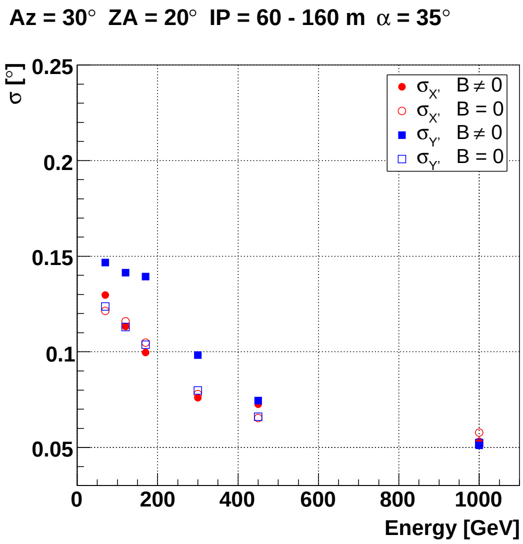

(c) 30° azimuth angle.

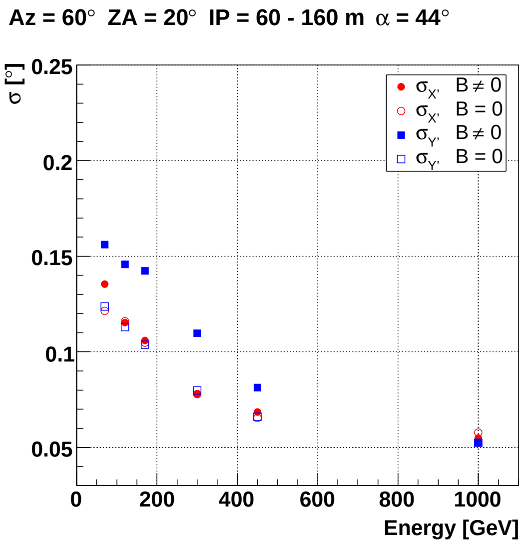

(d) 60° azimuth angle.

Figure 168: Lateral and longitudinal spread of the distribution of the DISP-reconstructed arrival directions for impact parameters between 60 m and 160 m, 0° and 20° ZA, different azimuth angles and γ-ray energies. The intermediate image cleaning was applied.

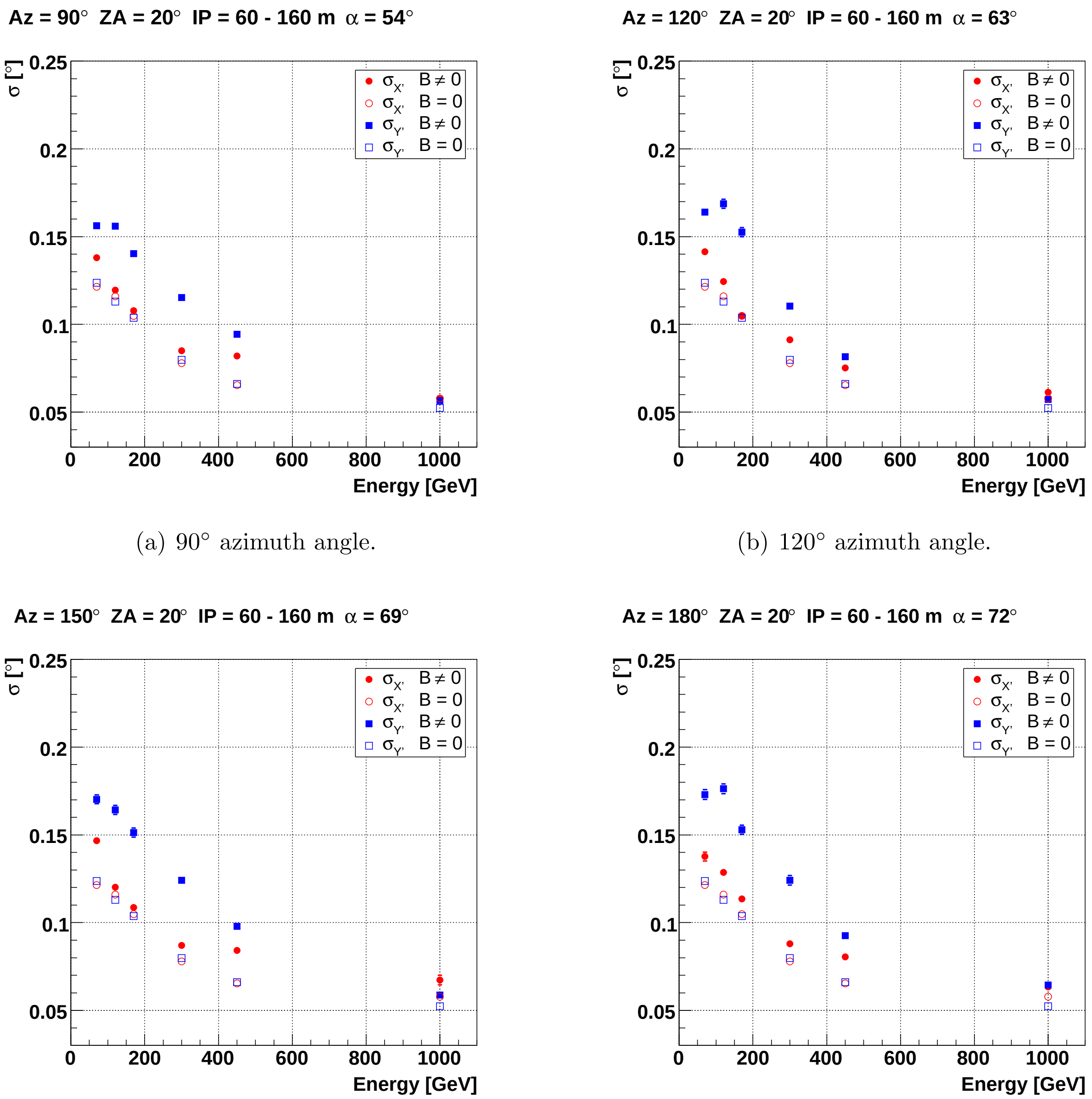

(a) 90° azimuth angle.

(b) 120° azimuth angle.

(c) 150° azimuth angle.

(d) 180° azimuth angle.

Figure 169: Lateral and longitudinal spread of the distribution of the DISP-reconstructed arrival directions for impact parameters between 60 m and 160 m, 20° ZA, different azimuth angles and γ-ray energies. The intermediate image cleaning was applied.

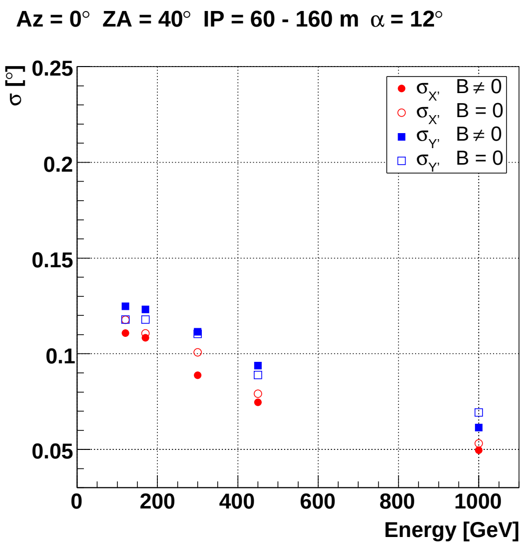

(a) 0° azimuth angle.

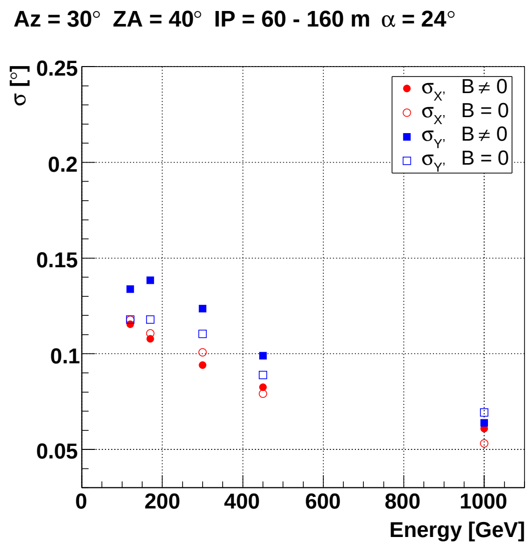

(b) 30° azimuth angle.

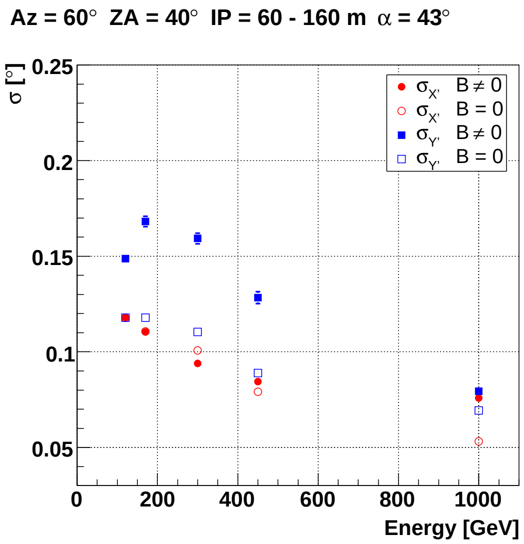

(c) 60° azimuth angle.

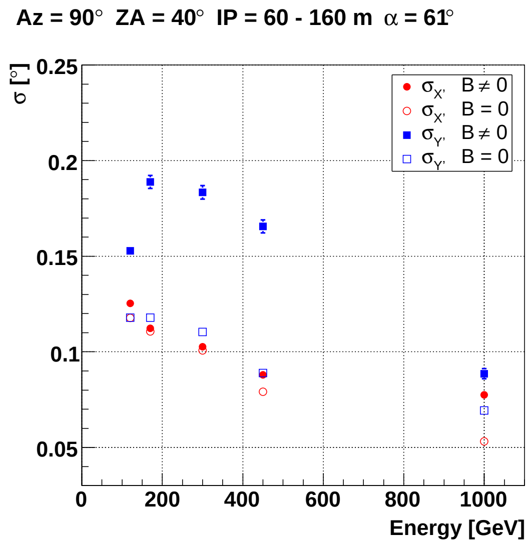

(d) 90° azimuth angle.

Figure 170: Lateral and longitudinal spread of the distribution of the DISP-reconstructed arrival directions for impact parameters between 60 m and 160 m, 40° ZA, different azimuth angles and γ-ray energies. The intermediate image cleaning was applied.

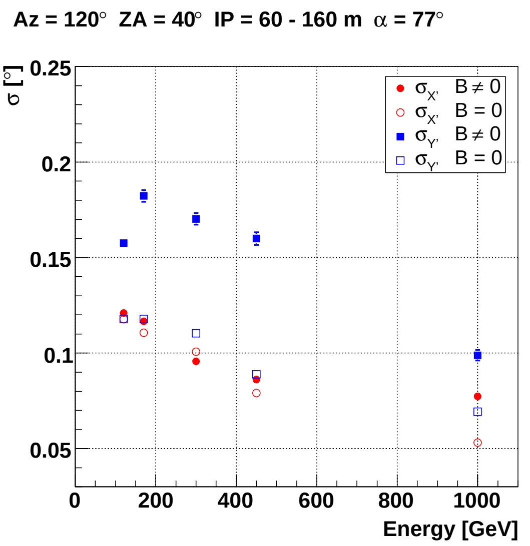

(a) 120° azimuth angle.

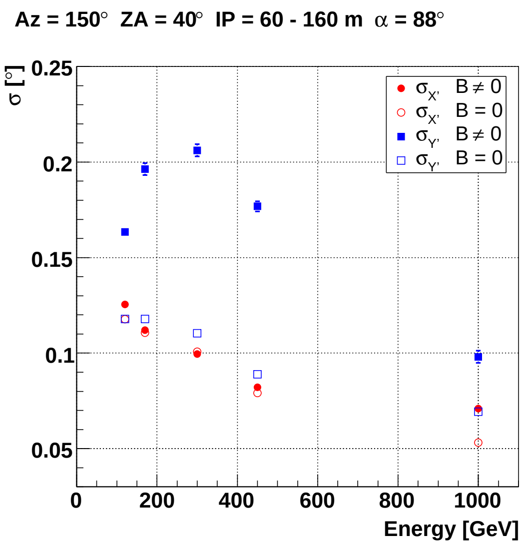

(b) 150° azimuth angle.

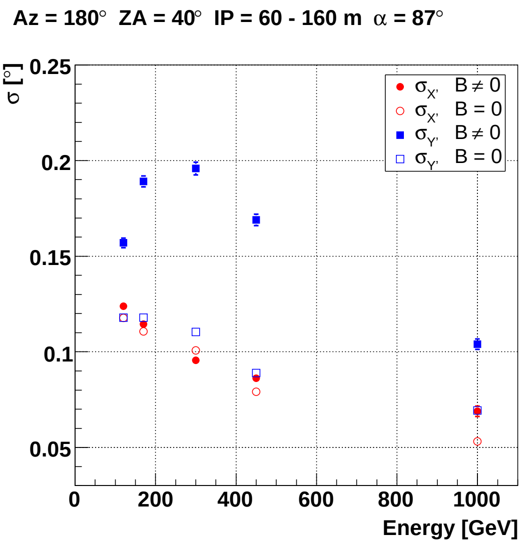

(c) 180° azimuth angle.

Figure 171: Lateral and longitudinal spread of the distribution of the DISP-reconstructed arrival directions for impact parameters between 60 m and 160 m, 40° ZA, different azimuth angles and γ-ray energies. The intermediate image cleaning was applied.

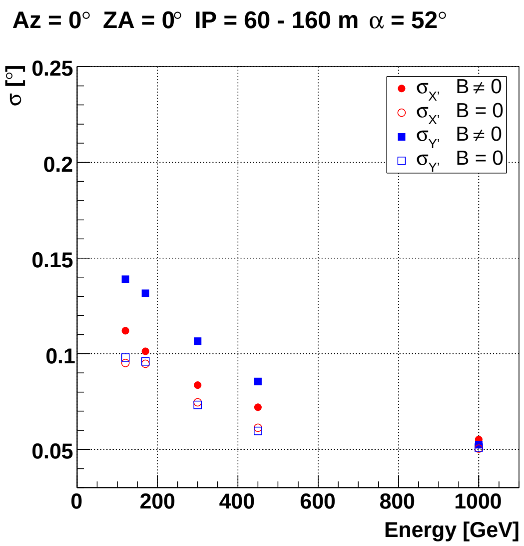

(a) 0° azimuth angle.

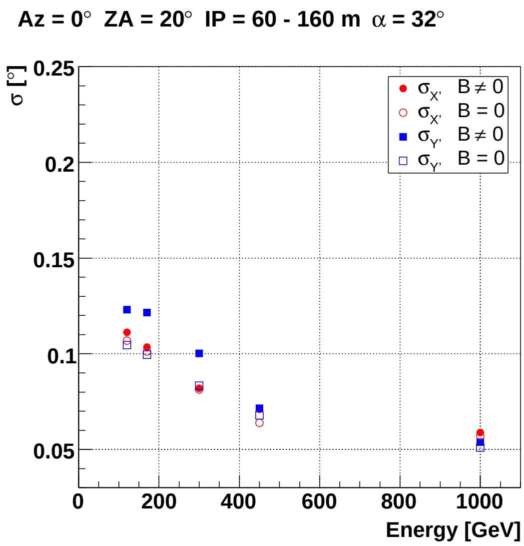

(b) 0° azimuth angle.

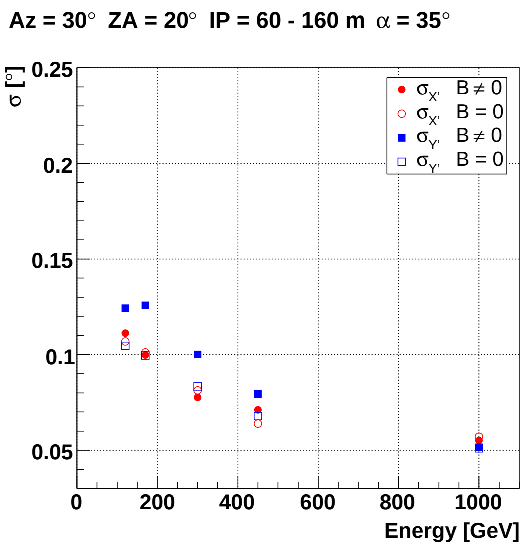

(c) 30° azimuth angle.

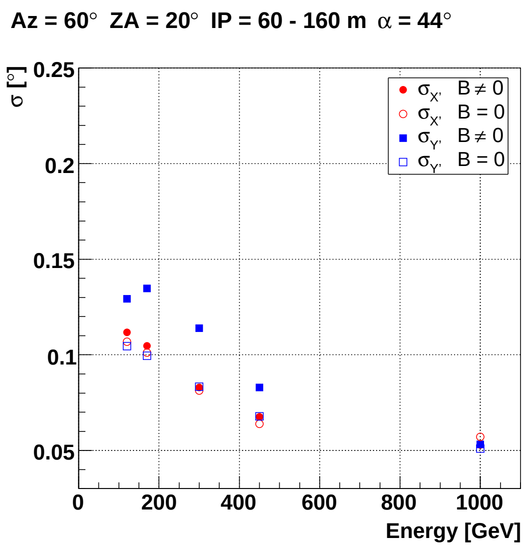

(d) 60° azimuth angle.

Figure 172: Lateral and longitudinal spread of the distribution of the DISP-reconstructed arrival directions for impact parameters between 60 m and 160 m, 0° and 20° ZA, different azimuth angles and γ-ray energies. The hard image cleaning was applied.

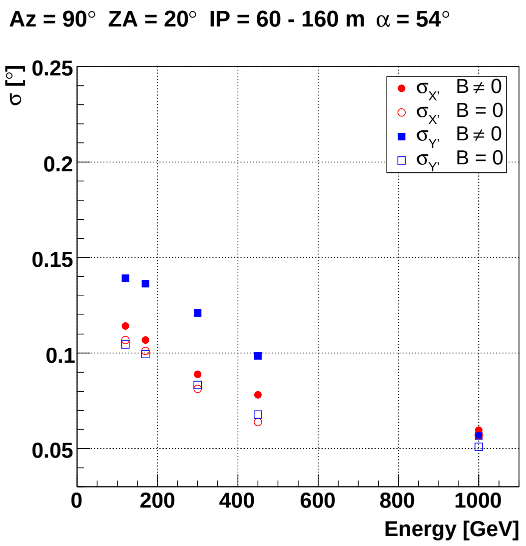

(a) 90° azimuth angle.

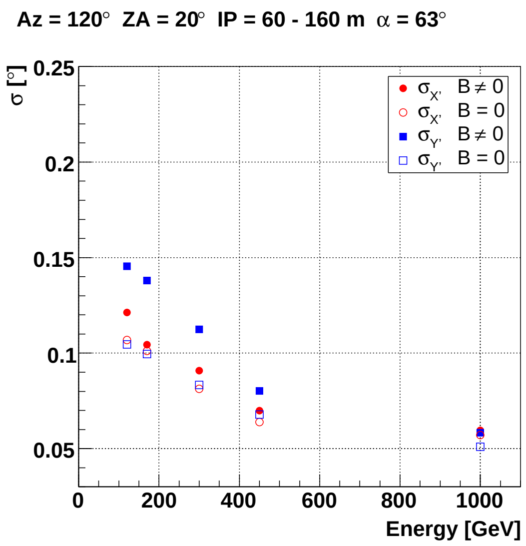

(b) 120° azimuth angle.

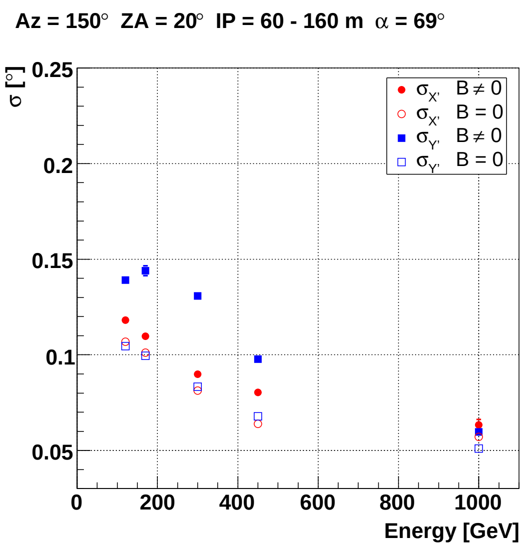

(c) 150° azimuth angle.

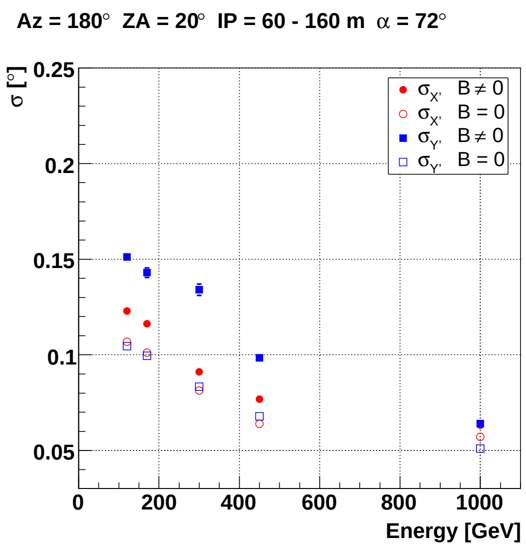

(d) 180° azimuth angle.

Figure 173: Lateral and longitudinal spread of the distribution of the DISP-reconstructed arrival directions for impact parameters between 60 m and 160 m, 20° ZA, different azimuth angles and γ-ray energies. The hard image cleaning was applied.

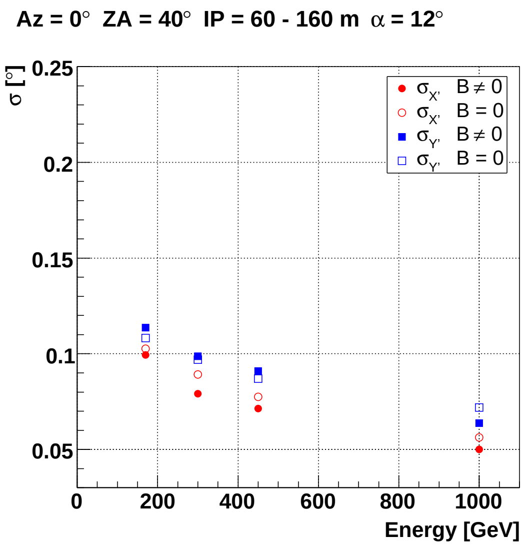

(a) 0° azimuth angle.

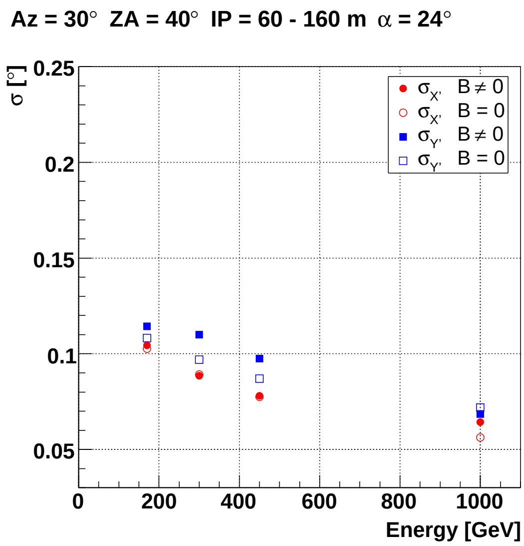

(b) 30° azimuth angle.

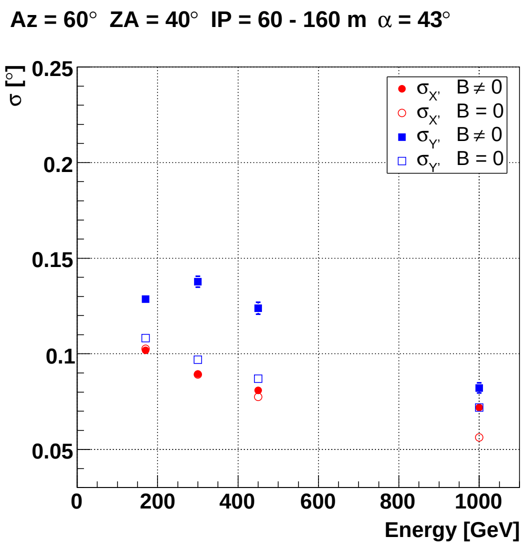

(c) 60° azimuth angle.

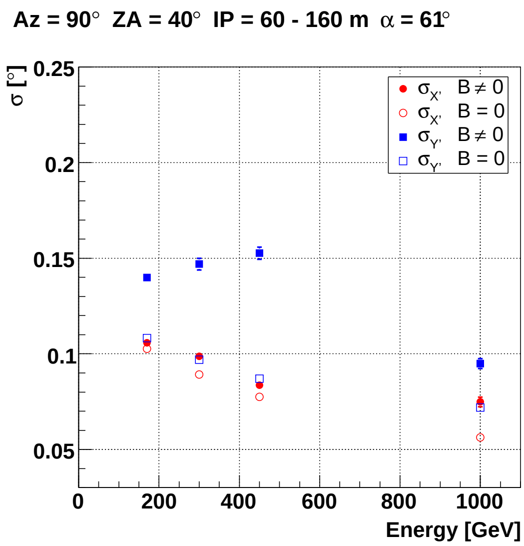

(d) 90° azimuth angle.

Figure 174: Lateral and longitudinal spread of the distribution of the DISP-reconstructed arrival directions for impact parameters between 60 m and 160 m, 40° ZA, different azimuth angles and γ-ray energies. The hard image cleaning was applied.

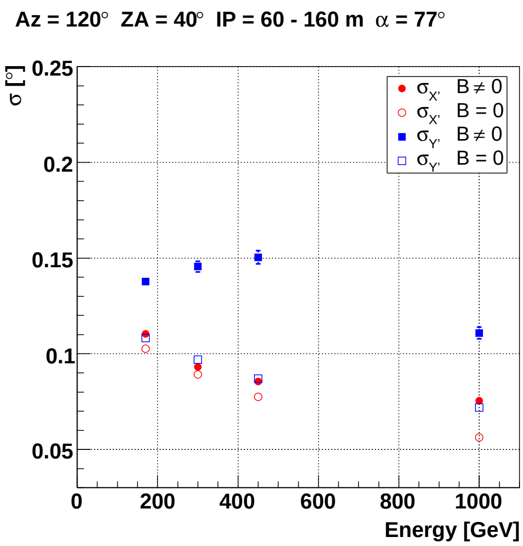

(a) 120° azimuth angle.

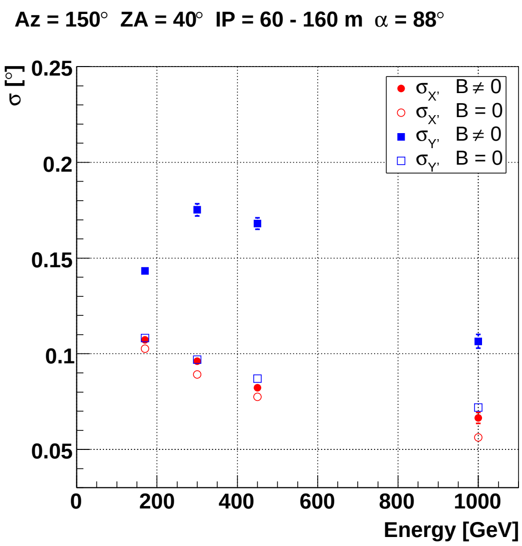

(b) 150° azimuth angle.

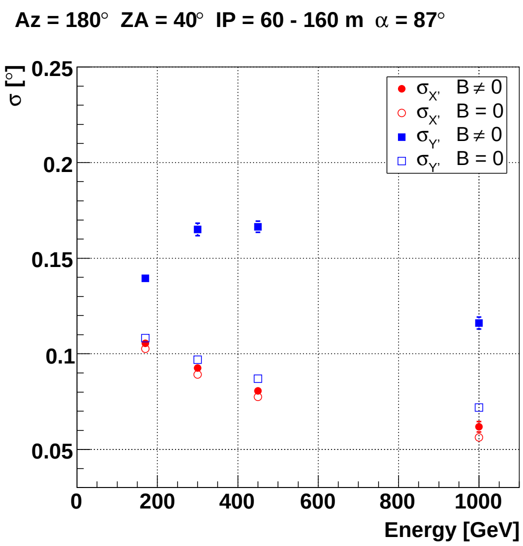

(c) 180° azimuth angle.

Figure 175: Lateral and longitudinal spread of the distribution of the DISP-reconstructed arrival directions for impact parameters between 60 m and 160 m, 40° ZA, different azimuth angles and γ-ray energies. The hard image cleaning was applied.

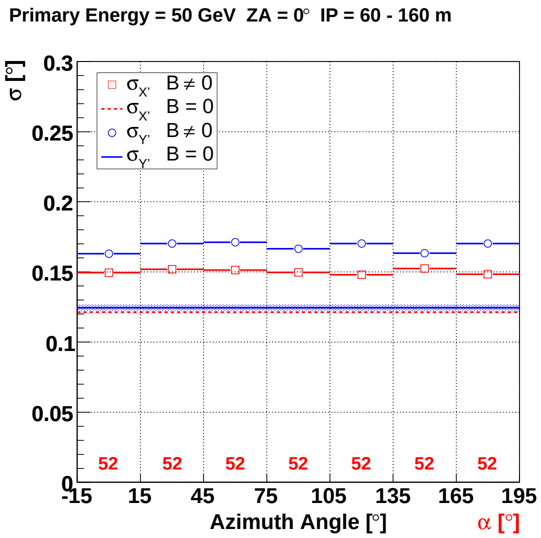

(a) 0° ZA, 50 GeV energy.

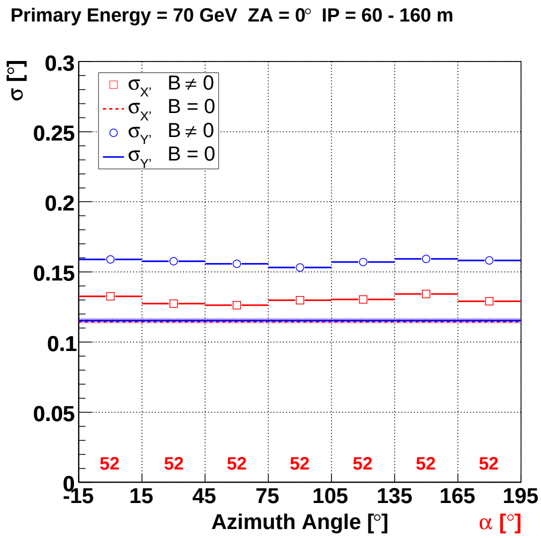

(b) 0° ZA, 70 GeV energy.

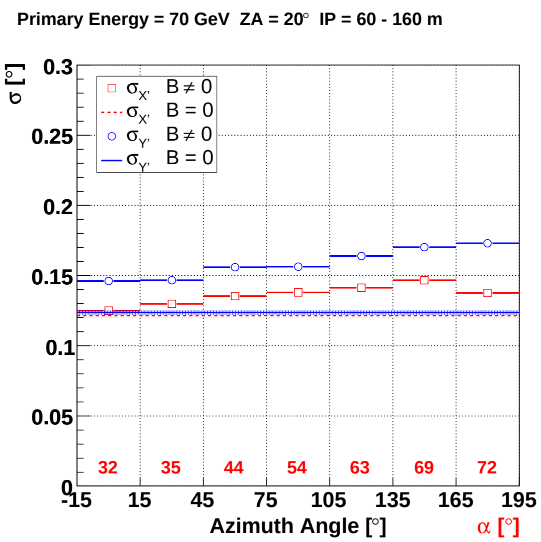

(c) 20° ZA, 70 GeV energy.

Figure 176: Lateral and longitudinal spread of the DISP-reconstructed arrival directions for MC γ-rays of 50 GeV and 70 GeV energy, impact parameters between 60 m and 160 m, and azimuth angles between 0° and 180°. The intermediate image cleaning was applied.

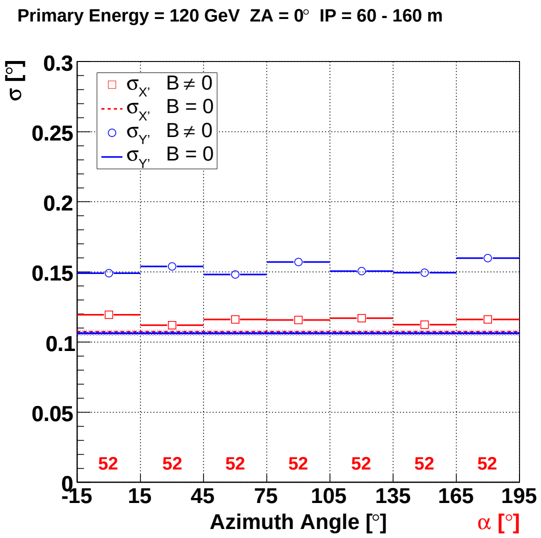

(a) 0° ZA, 120 GeV energy, intermediate image cleaning.

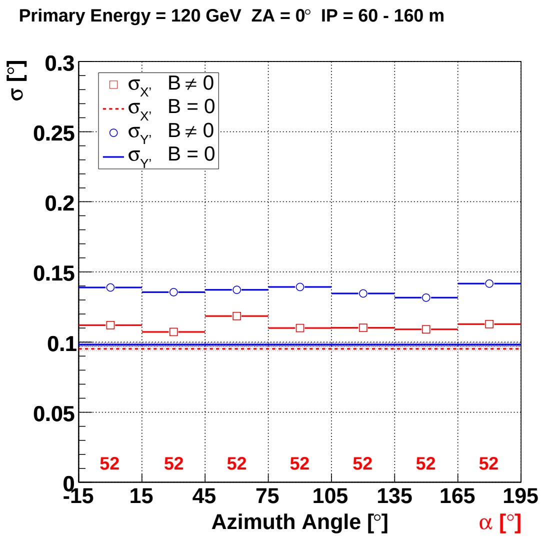

(b) 0° ZA, 120 GeV energy, hard image cleaning.

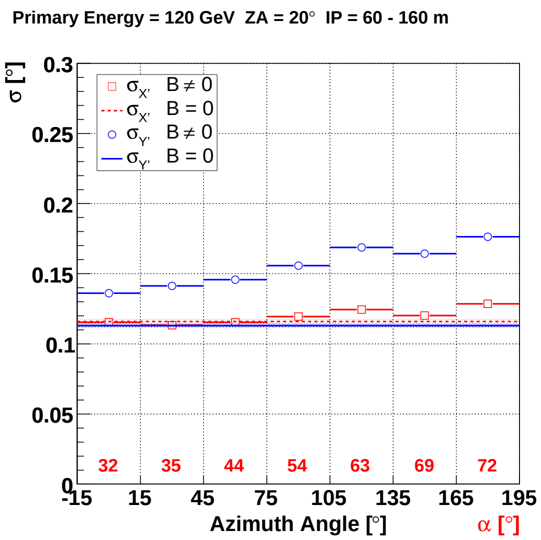

(c) 20° ZA, 120 GeV energy, intermediate image cleaning.

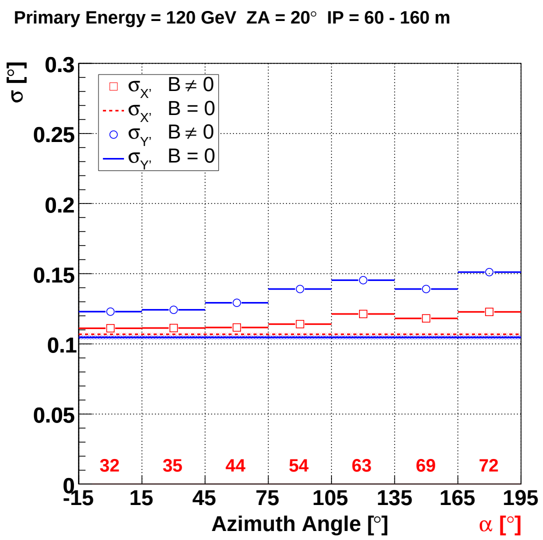

(d) 20° ZA, 120 GeV energy, hard image cleaning.

Figure 177: Lateral and longitudinal spread of the DISP-reconstructed arrival directions for MC γ-rays of 120 GeV energy, impact parameters between 60 m and 160 m, and azimuth angles between 0° and 180°. The intermediate and the hard image cleaning was applied.

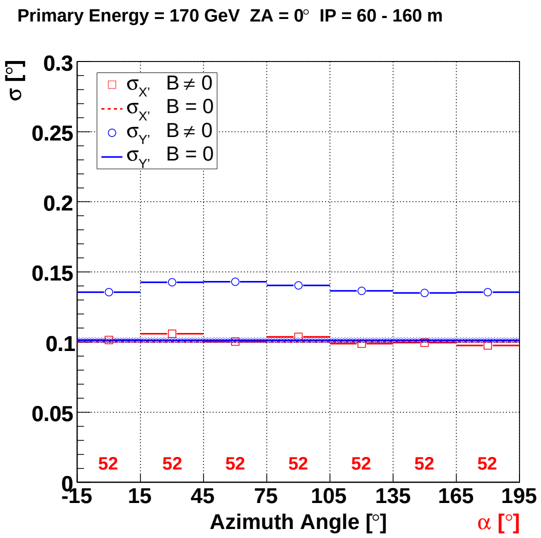

(a) 0° ZA, 170 GeV energy, intermediate image cleaning.

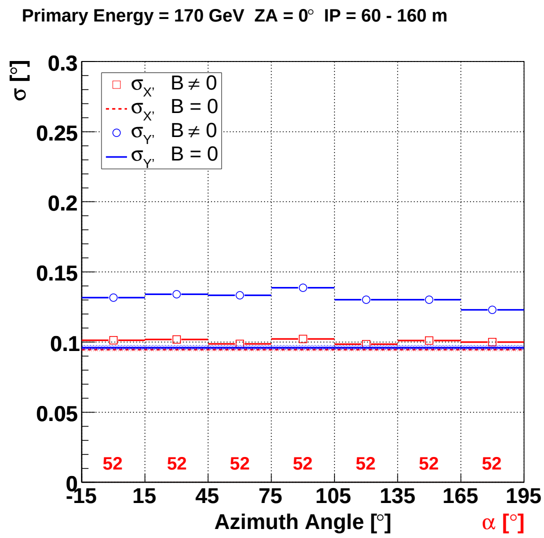

(b) 0° ZA, 170 GeV energy, hard image cleaning.

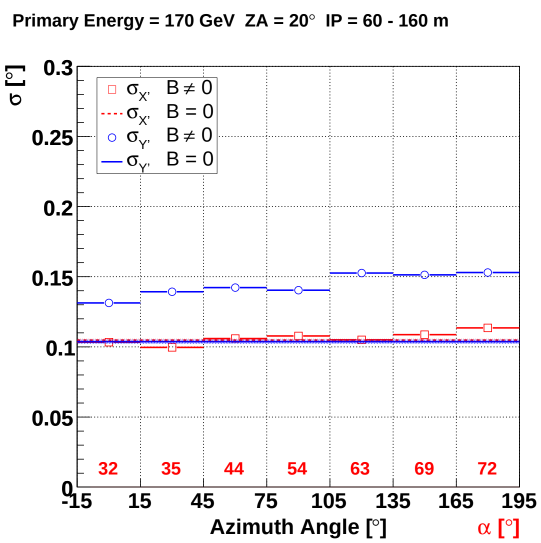

(c) 20° ZA, 170 GeV energy, intermediate image cleaning.

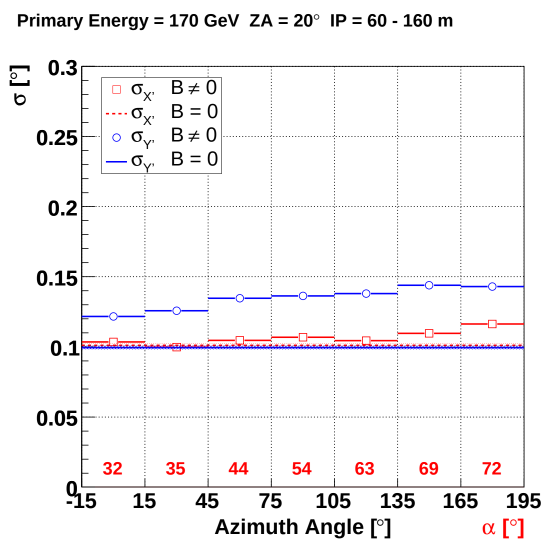

(d) 20° ZA, 170 GeV energy, hard image cleaning.

Figure 178: Lateral and longitudinal spread of the DISP-reconstructed arrival directions for MC γ-rays of 170 GeV energy, impact parameters between 60 m and 160 m, and azimuth angles between 0° and 180°. The intermediate and the hard image cleaning was applied.

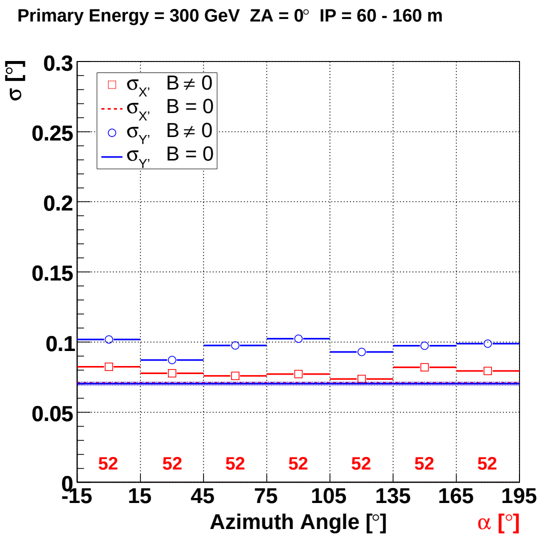

(a) 0° ZA, 300 GeV energy, intermediate image cleaning.

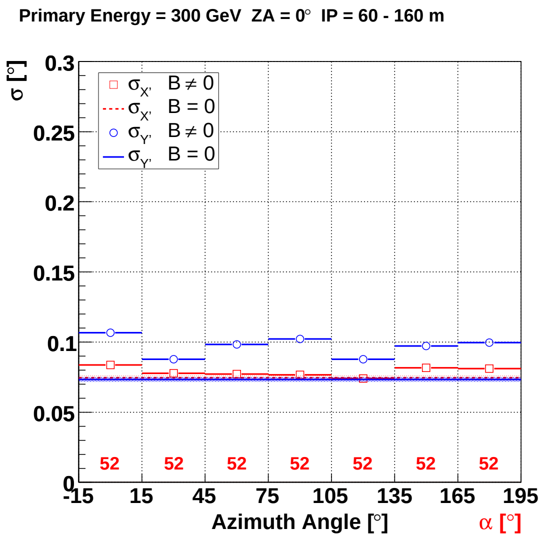

(b) 0° ZA, 300 GeV energy, hard image cleaning.

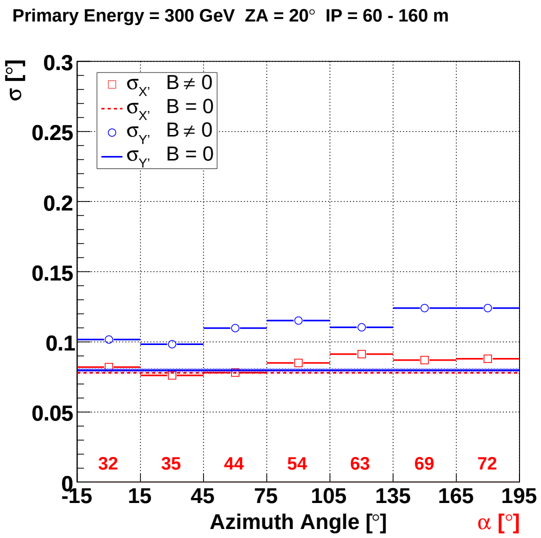

(c) 20° ZA, 300 GeV energy, intermediate image cleaning.

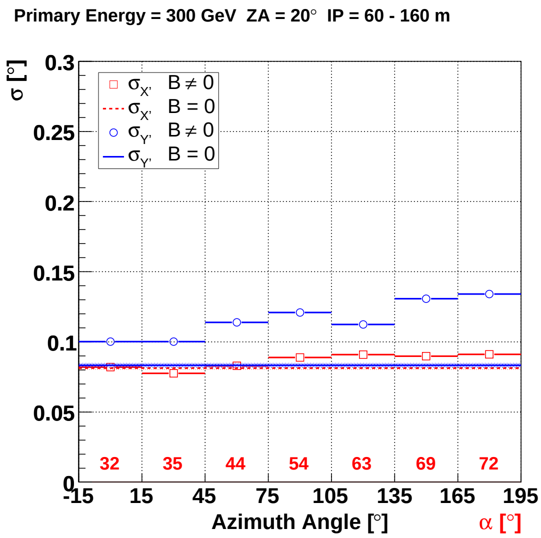

(d) 20° ZA, 300 GeV energy, hard image cleaning.

Figure 179: Lateral and longitudinal spread of the DISP-reconstructed arrival directions for MC γ-rays of 300 GeV energy, impact parameters between 60 m and 160 m, and azimuth angles between 0° and 180°. The intermediate and the hard image cleaning was applied.

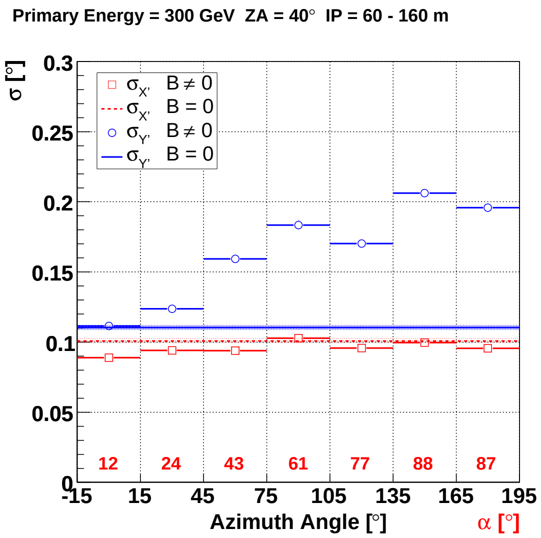

(a) 40° ZA, 300 GeV energy, intermediate image cleaning.

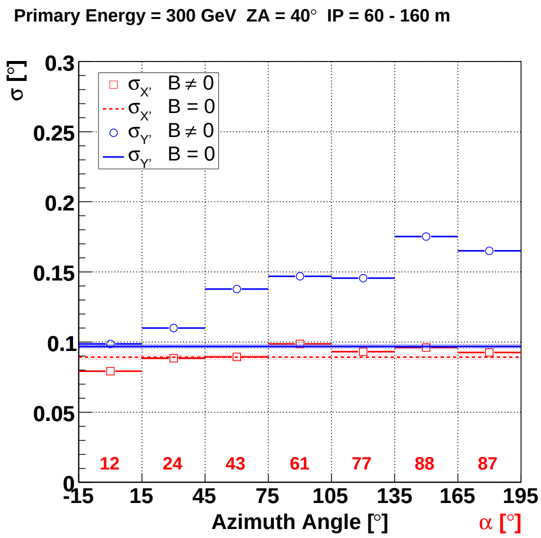

(b) 40° ZA, 300 GeV energy, hard image cleaning.

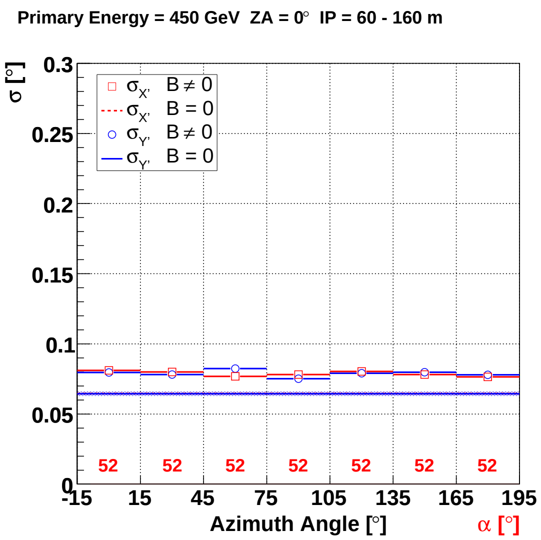

(c) 0° ZA, 450 GeV energy, intermediate image cleaning.

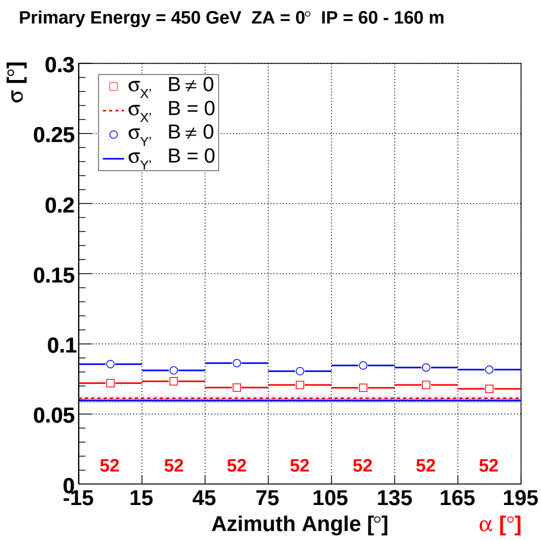

(d) 0° ZA, 450 GeV energy, hard image cleaning.

Figure 180: Lateral and longitudinal spread of the DISP-reconstructed arrival directions for MC γ-rays of 300 GeV and 450 GeV energy, impact parameters between 60 m and 160 m, and azimuth angles between 0° and 180°. The intermediate and the hard image cleaning was applied.

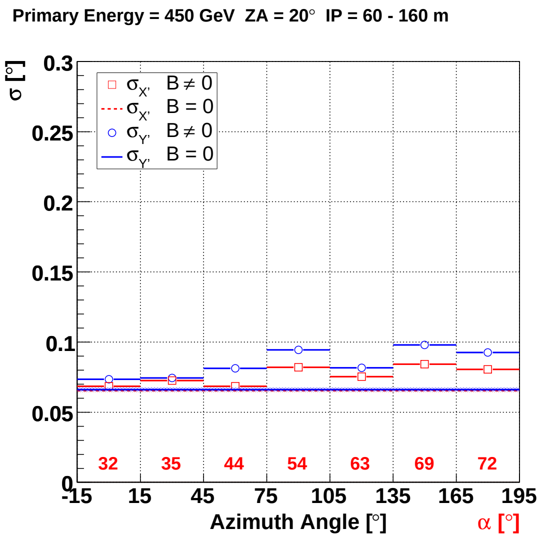

(a) 20° ZA, 450 GeV energy, intermediate image cleaning.

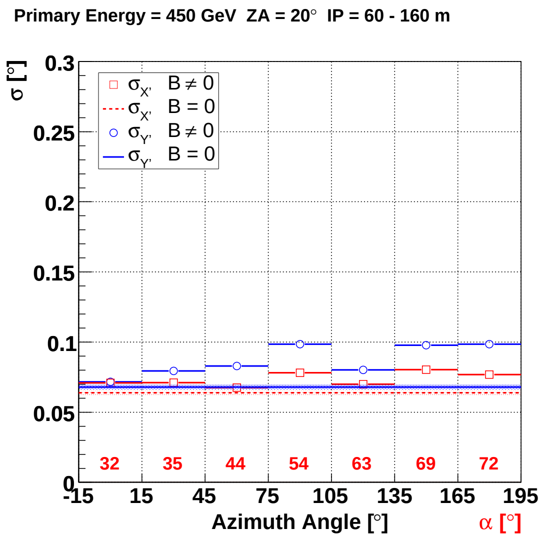

(b) 20° ZA, 450 GeV energy, hard image cleaning.

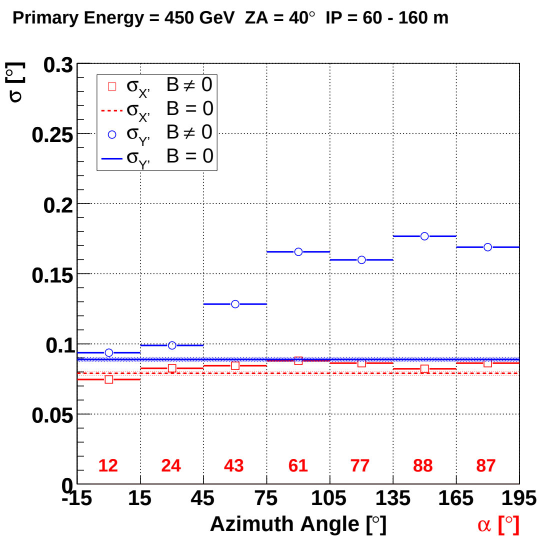

(c) 40° ZA, 450 GeV energy, intermediate image cleaning.

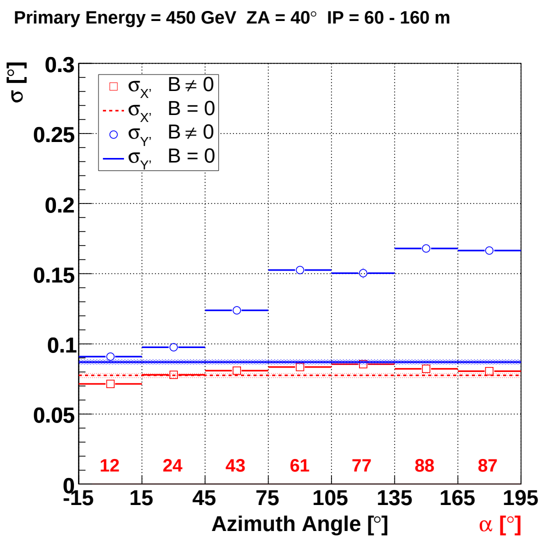

(d) 40° ZA, 450 GeV energy, hard image cleaning.

Figure 181: Lateral and longitudinal spread of the DISP-reconstructed arrival directions for MC γ-rays of 450 GeV energy, impact parameters between 60 m and 160 m, and azimuth angles between 0° and 180°. The intermediate and the hard image cleaning was applied.

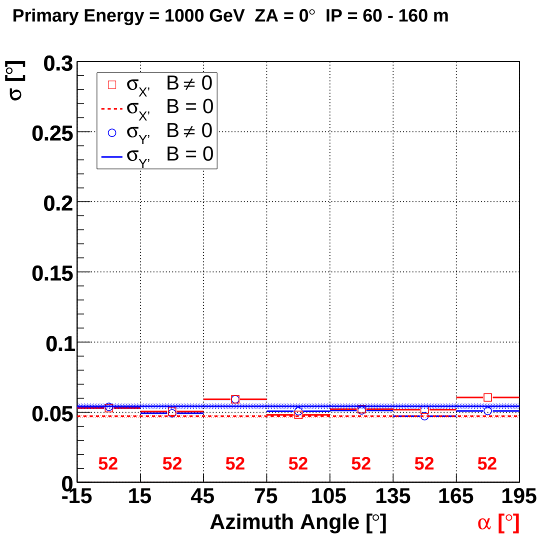

(a) 0° ZA, 1 TeV energy, intermediate image cleaning.

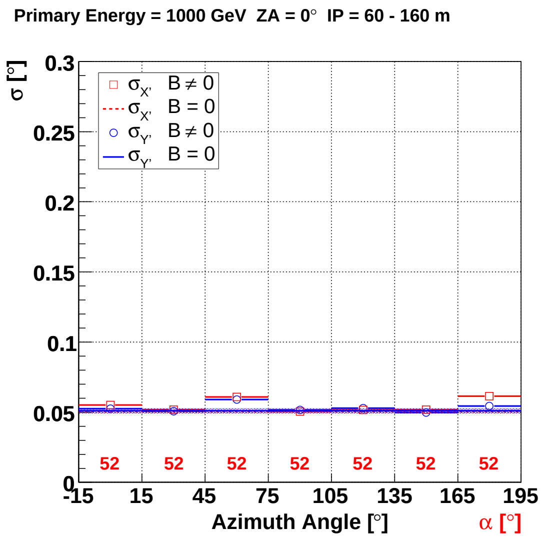

(b) 0° ZA, 1 TeV energy, hard image cleaning.

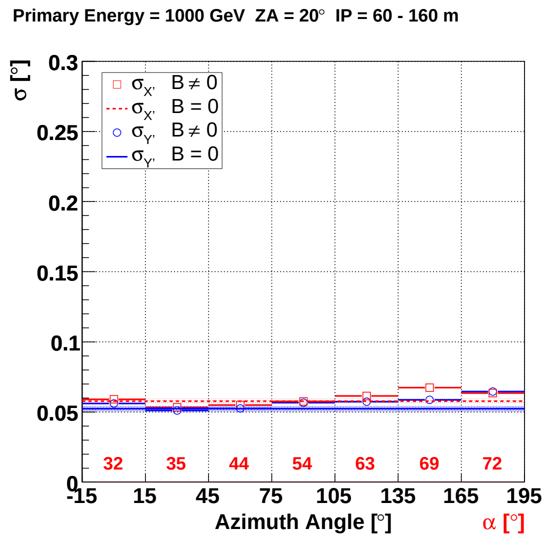

(c) 20° ZA, 1 TeV energy, intermediate image cleaning.

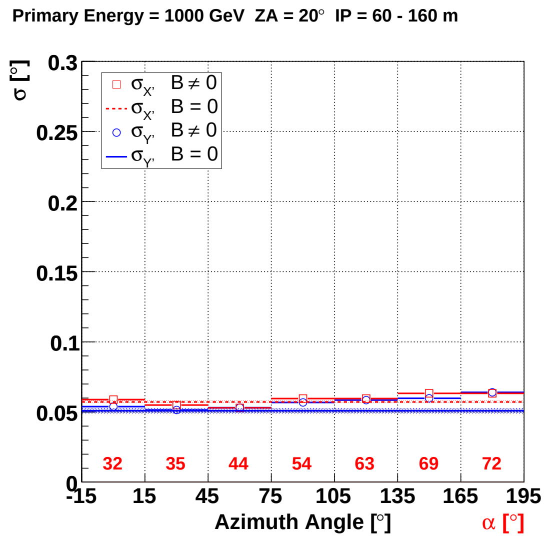

(d) 20° ZA, 1 TeV energy, hard image cleaning.

Figure 182: Lateral and longitudinal spread of the DISP-reconstructed arrival directions for MC γ-rays of 1 TeV energy, impact parameters between 60 m and 160 m, and azimuth angles between 0° and 180°. The intermediate and the hard image cleaning was applied.

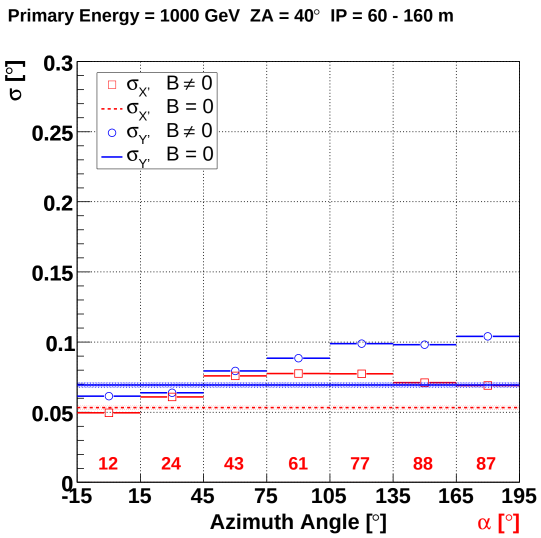

(a) 40° ZA, 1 TeV energy, intermediate image cleaning.

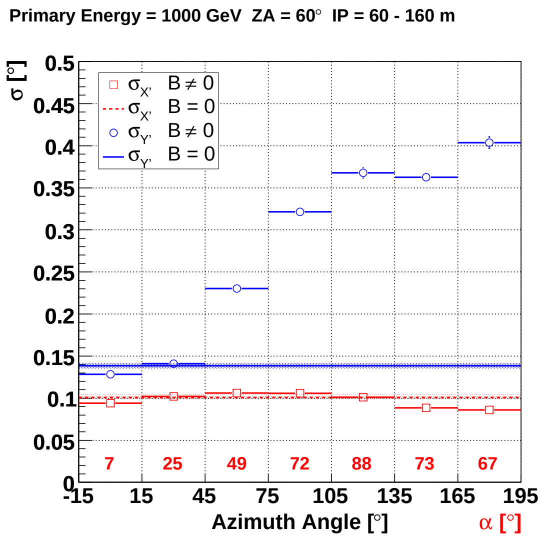

(b) 60° ZA, 1 TeV energy, intermediate image cleaning.

Figure 183: Lateral and longitudinal spread of the DISP-reconstructed arrival directions for MC γ-rays of 1 TeV energy, impact parameters between 60 m and 160 m, and azimuth angles between 0° and 180°. The intermediate image cleaning was applied.

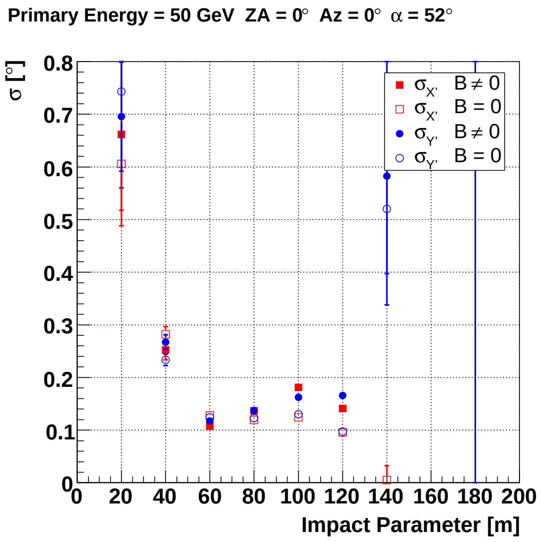

(a) 0° azimuth angle, 0° ZA, 50 GeV energy.

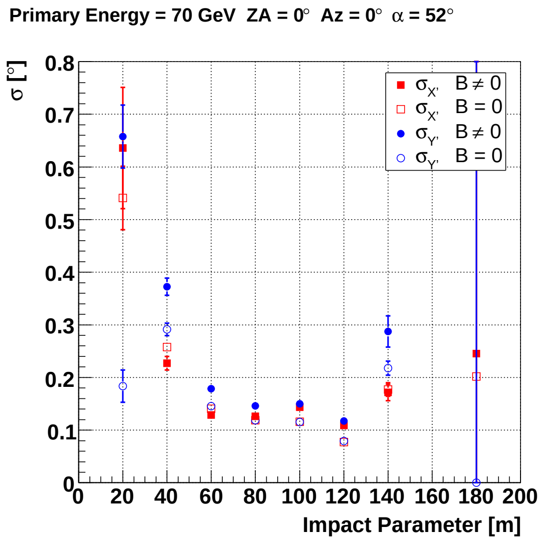

(b) 0° azimuth angle, 0° ZA, 70 GeV energy.

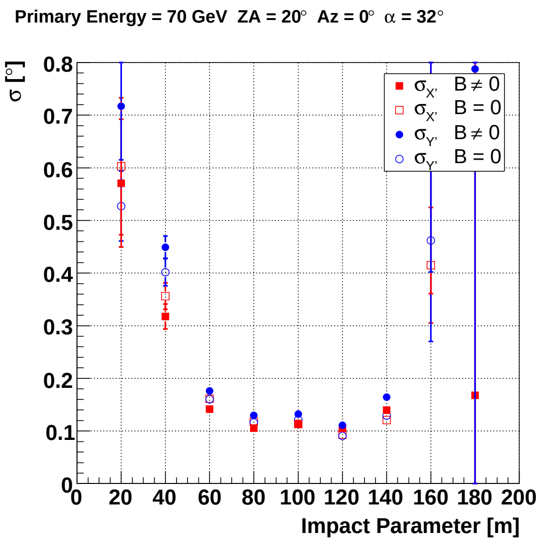

(c) 0° azimuth angle, 20° ZA, 70 GeV energy.

Figure 184: Lateral and longitudinal spread of the DISP-reconstructed arrival directions versus impact parameter for MC γ-rays of 50 GeV and 70 GeV energy, 0° azimuth angle and different ZAs. The intermediate image cleaning was applied.

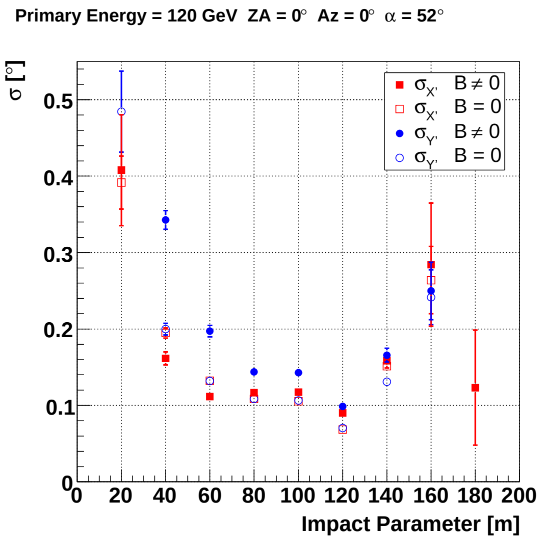

(a) 0° azimuth angle, 0° ZA, 120 GeV energy, intermediate image cleaning.

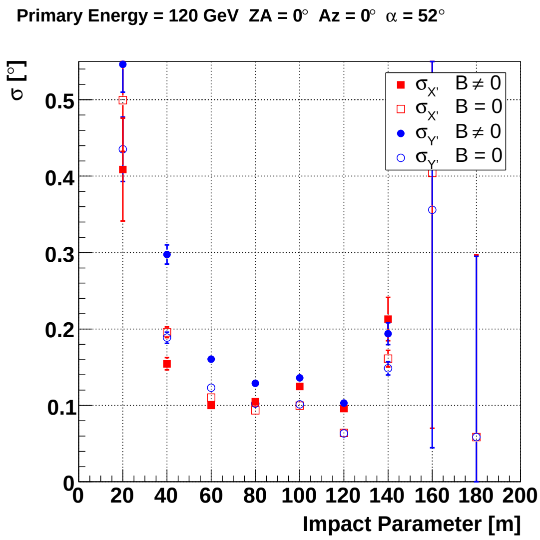

(b) 0° azimuth angle, 0° ZA, 120 GeV energy, hard image cleaning.

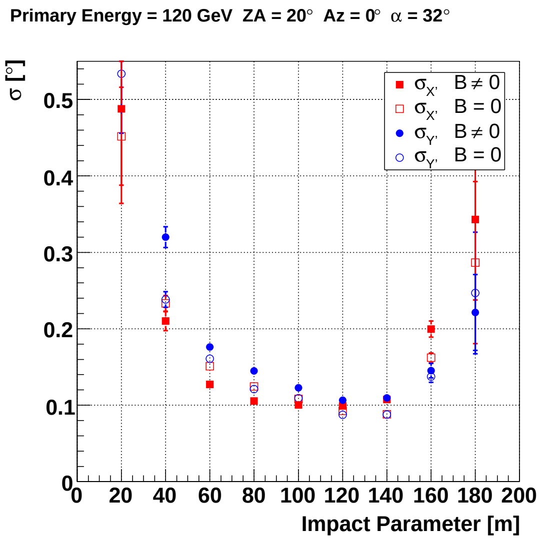

(c) 0° azimuth angle, 20° ZA, 120 GeV energy, intermediate image cleaning.

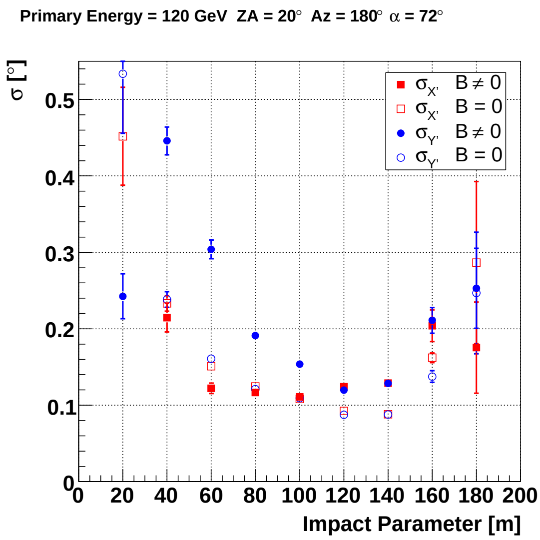

(d) 180° azimuth angle, 20° ZA, 120 GeV energy, intermediate image cleaning.

Figure 185: Lateral and longitudinal spread of the DISP-reconstructed arrival directions versus impact parameter for MC γ-rays of 120 GeV energy, 0° and 180° azimuth angle, different ZAs and different image cleaning levels.

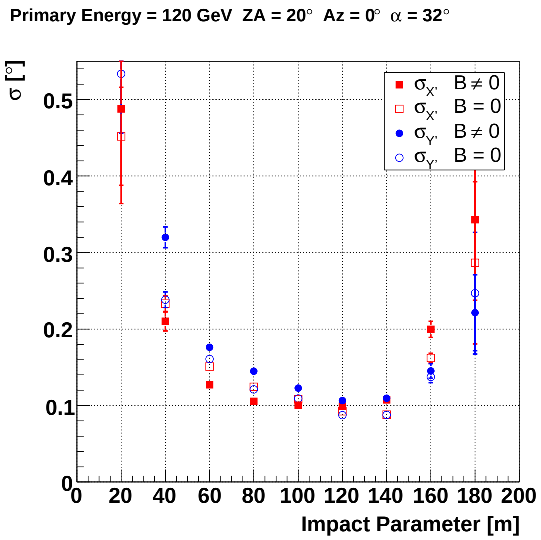

(a) 0° azimuth angle, 20° ZA, 120 GeV energy.

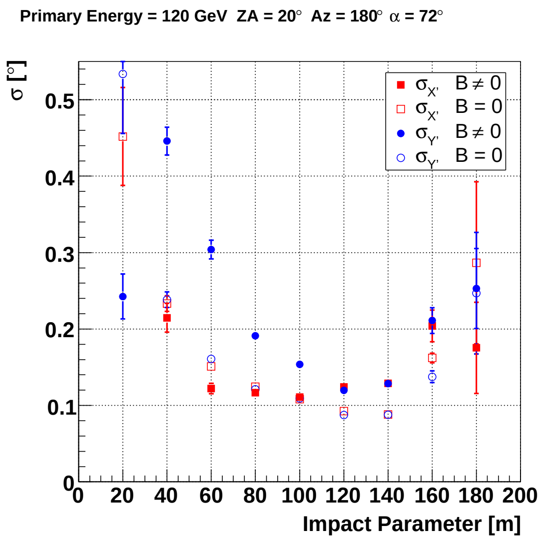

(b) 180° azimuth angle, 20° ZA, 120 GeV energy.

Figure 186: Lateral and longitudinal spread of the DISP-reconstructed arrival directions versus impact parameter for MC γ-rays of 120 GeV energy, 0° and 180° azimuth angle, 20° ZA and the hard image cleaning.

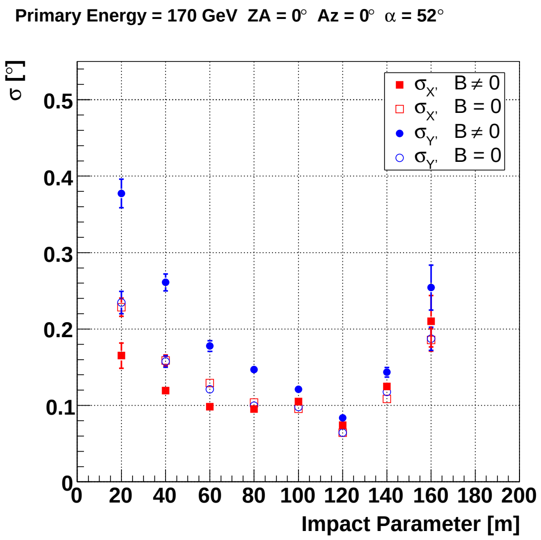

(a) 0° azimuth angle, 0° ZA, 170 GeV energy, intermediate image cleaning.

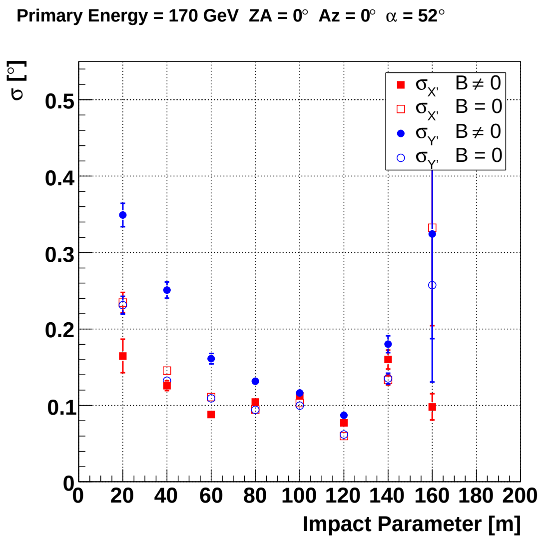

(b) 0° azimuth angle, 0° ZA, 170 GeV energy, hard image cleaning.

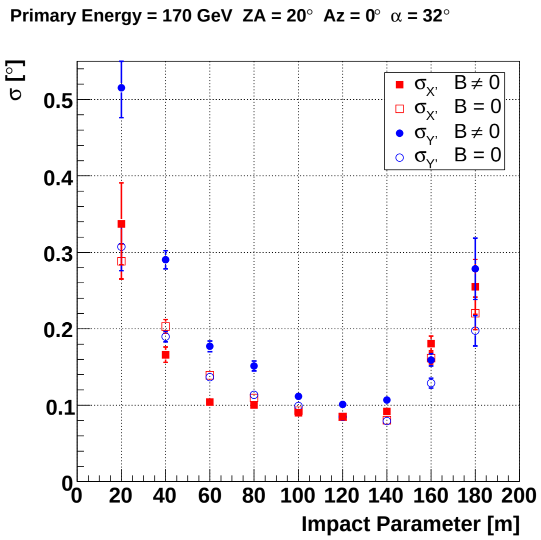

(c) 0° azimuth angle, 20° ZA, 170 GeV energy, intermediate image cleaning.

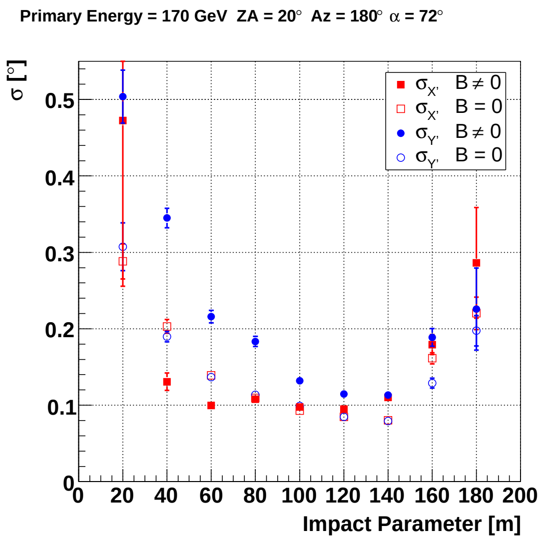

(d) 180° azimuth angle, 20° ZA, 170 GeV energy, intermediate image cleaning.

Figure 187: Lateral and longitudinal spread of the DISP-reconstructed arrival directions versus impact parameter for MC γ-rays of 170 GeV energy, 0° and 180° azimuth angle, different ZAs and different image cleaning levels.

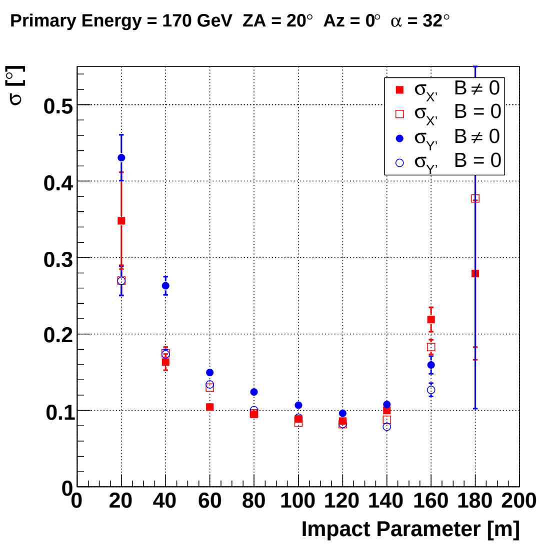

(a) 0° azimuth angle, 20° ZA, 170 GeV energy, hard image cleaning.

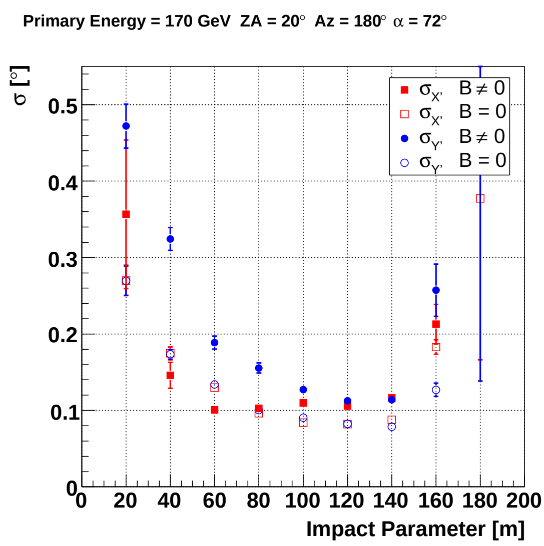

(b) 180° azimuth angle, 20° ZA, 170 GeV energy, hard image cleaning.

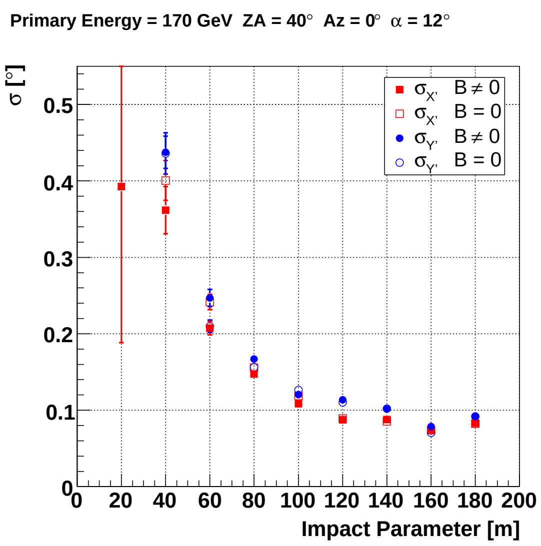

(c) 0° azimuth angle, 40° ZA, 170 GeV energy, intermediate image cleaning.

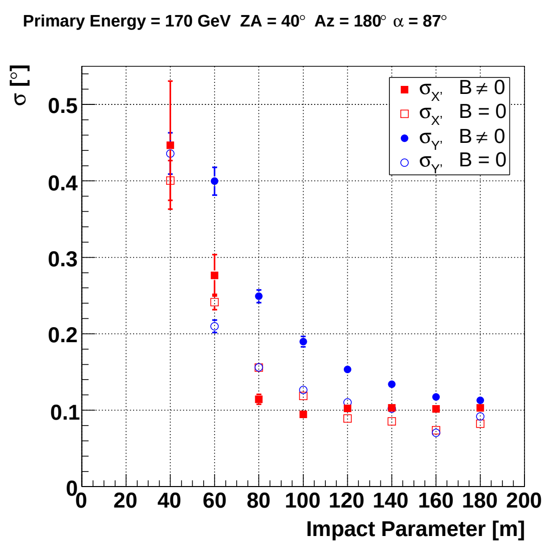

(d) 180° azimuth angle, 40° ZA, 170 GeV energy, intermediate image cleaning.

Figure 188: Lateral and longitudinal spread of the DISP-reconstructed arrival directions versus impact parameter for MC γ-rays of 170 GeV energy, 0° and 180° azimuth angle, different ZAs and different image cleaning levels.

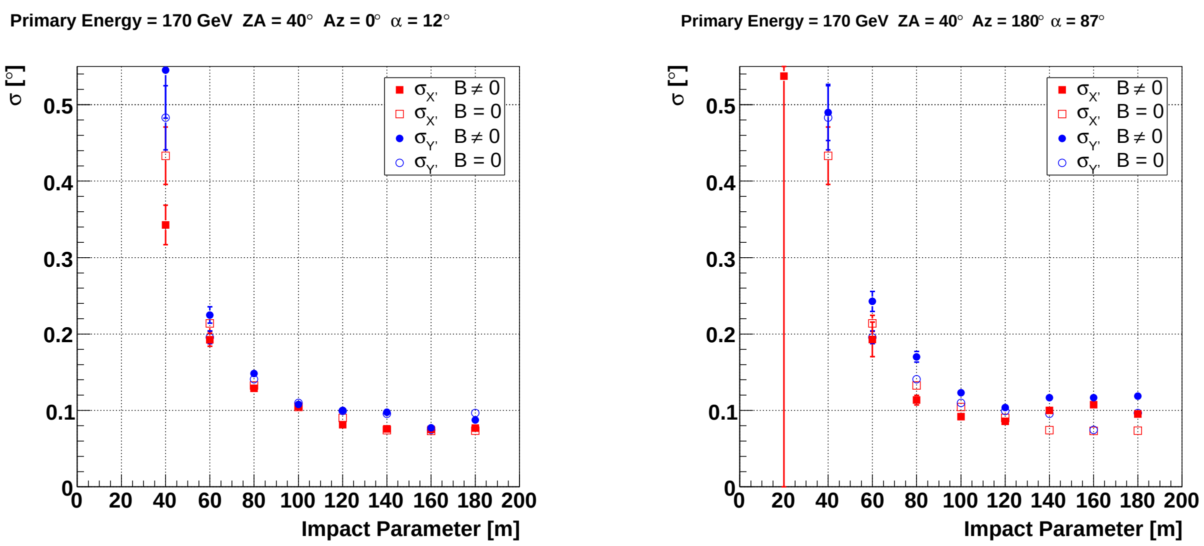

(a) 0° azimuth angle, 40° ZA, 170 GeV energy. (b) 180° azimuth angle, 40° ZA, 170 GeV energy.

Figure 189: Lateral and longitudinal spread of the DISP-reconstructed arrival directions versus impact parameter for MC γ-rays of 170 GeV energy, 0° and 180° azimuth angle, 40° ZA and the hard image cleaning.

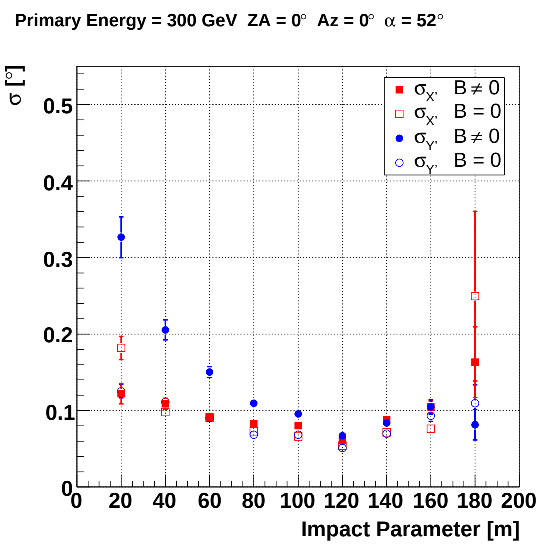

(a) 0° azimuth angle, 0° ZA, 300 GeV energy, intermediate image cleaning.

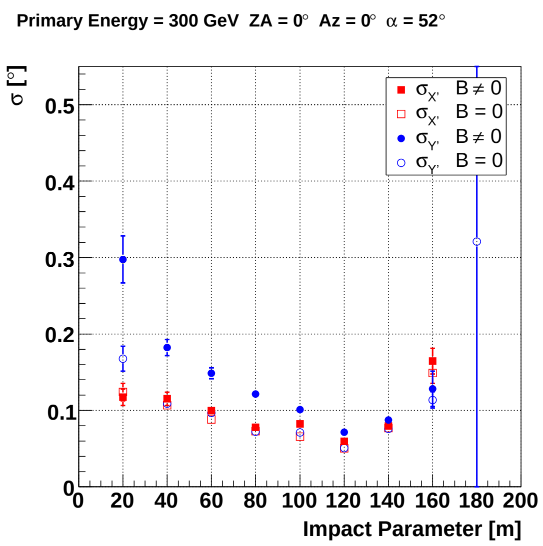

(b) 0° azimuth angle, 0° ZA, 300 GeV energy, hard image cleaning.

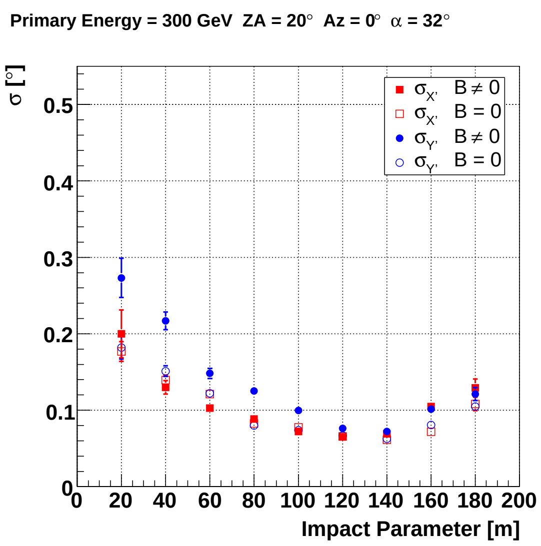

(c) 0° azimuth angle, 20° ZA, 300 GeV energy, intermediate image cleaning.

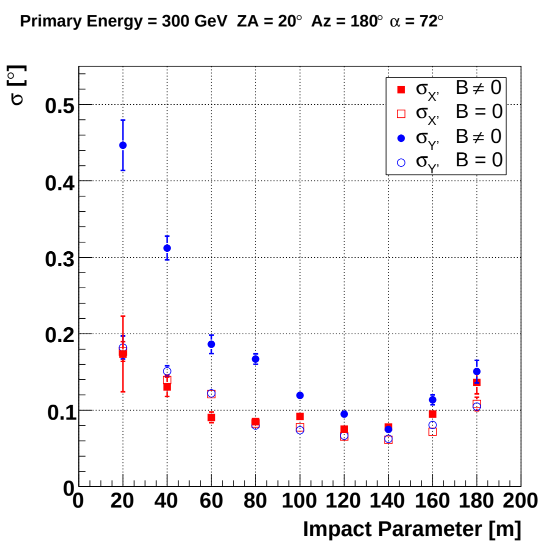

(d) 180° azimuth angle, 20° ZA, 300 GeV energy, intermediate image cleaning.

Figure 190: Lateral and longitudinal spread of the DISP-reconstructed arrival directions versus impact parameter for MC γ-rays of 300 GeV energy, 0° and 180° azimuth angle, different ZAs and different image cleaning levels.

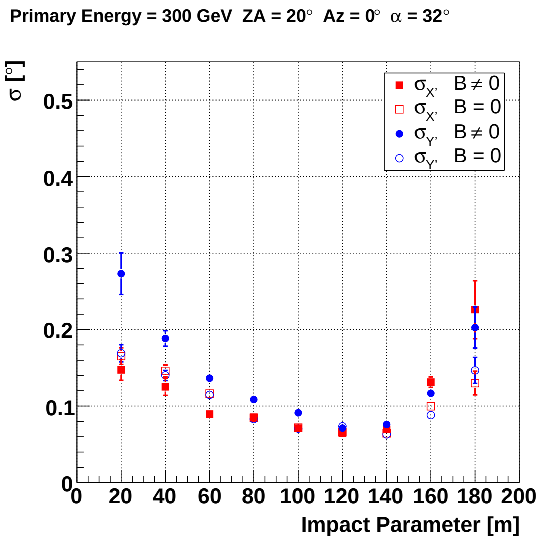

(a) 0° azimuth angle, 20° ZA, 300 GeV energy, hard image cleaning.

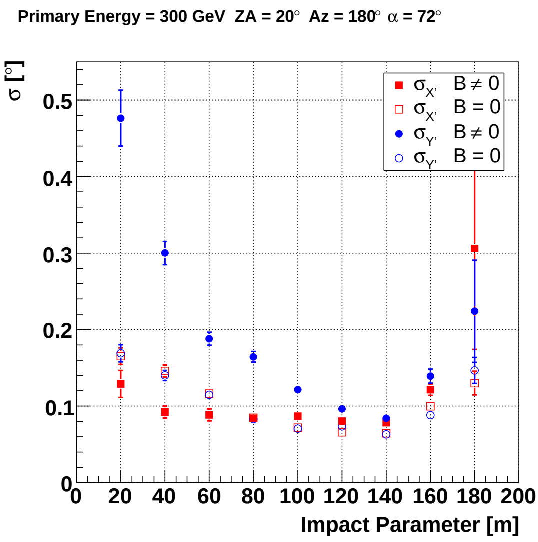

(b) 180° azimuth angle, 20° ZA, 300 GeV energy, hard image cleaning.

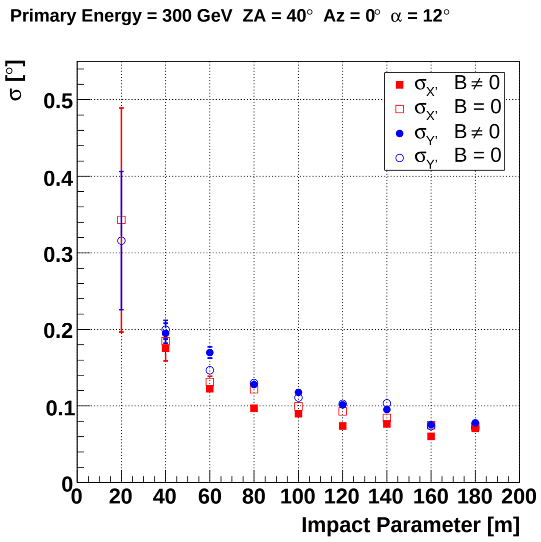

(c) 0° azimuth angle, 40° ZA, 300 GeV energy, intermediate image cleaning.

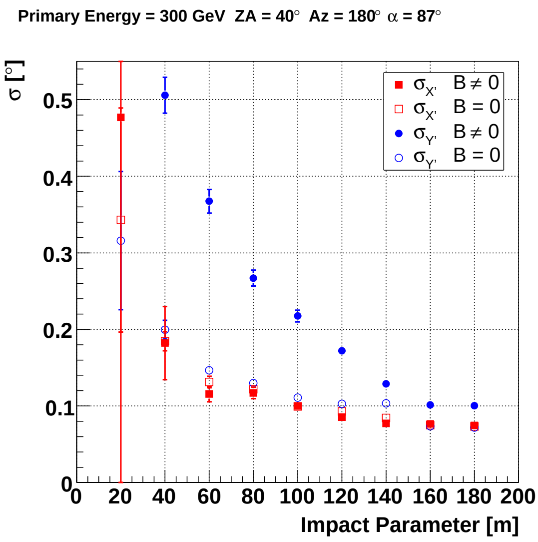

(d) 180° azimuth angle, 40° ZA, 300 GeV energy, intermediate image cleaning.

Figure 191: Lateral and longitudinal spread of the DISP-reconstructed arrival directions versus impact parameter for MC γ-rays of 300 GeV energy, 0° and 180° azimuth angle, different ZAs and different image cleaning levels.

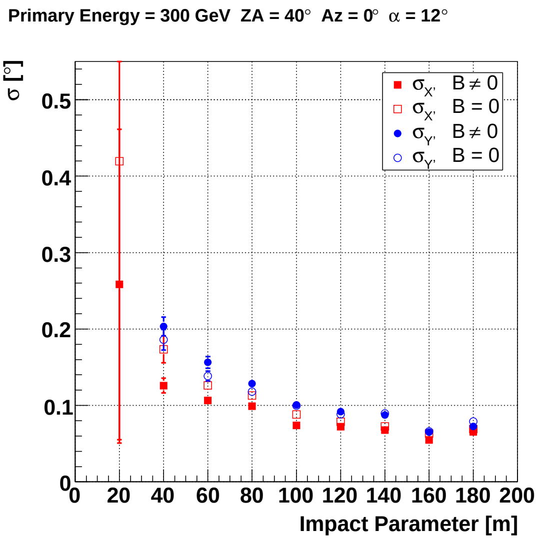

(a) 0° azimuth angle, 40° ZA, 300 GeV energy.

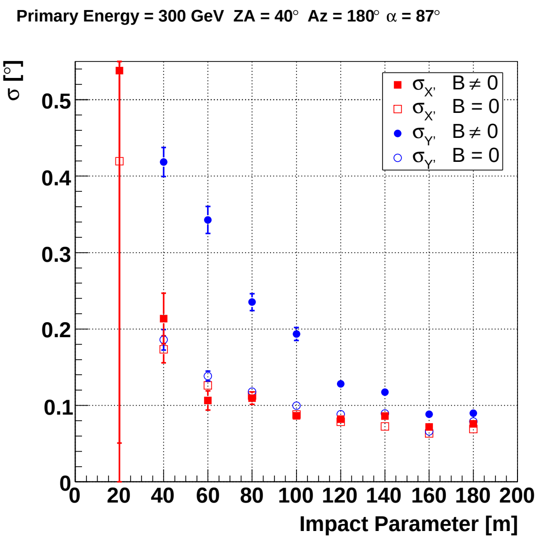

(b) 180° azimuth angle, 40° ZA, 300 GeV energy.

Figure 192: Lateral and longitudinal spread of the DISP-reconstructed arrival directions versus impact parameter for MC γ-rays of 300 GeV energy, 0° and 180° azimuth angle, 40° ZA and the hard image cleaning.

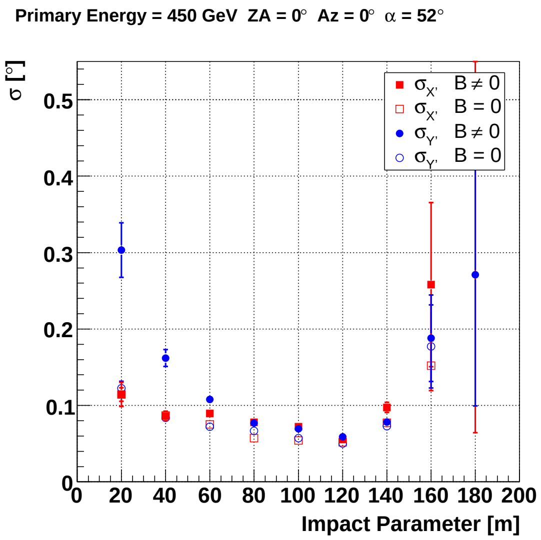

(a) 0° azimuth angle, 0° ZA, 450 GeV energy, intermediate image cleaning.

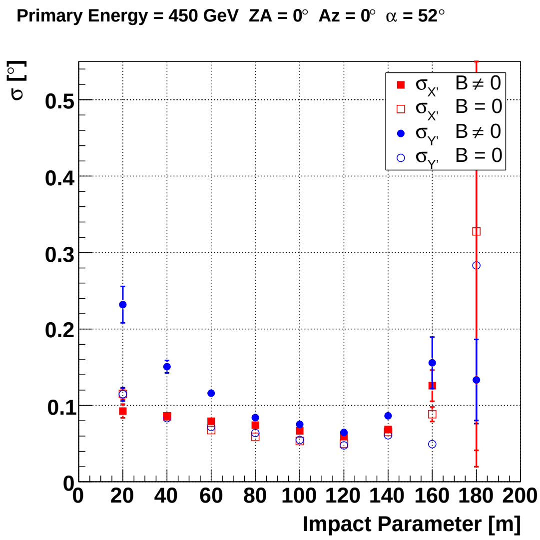

(b) 0° azimuth angle, 0° ZA, 450 GeV energy, hard image cleaning.

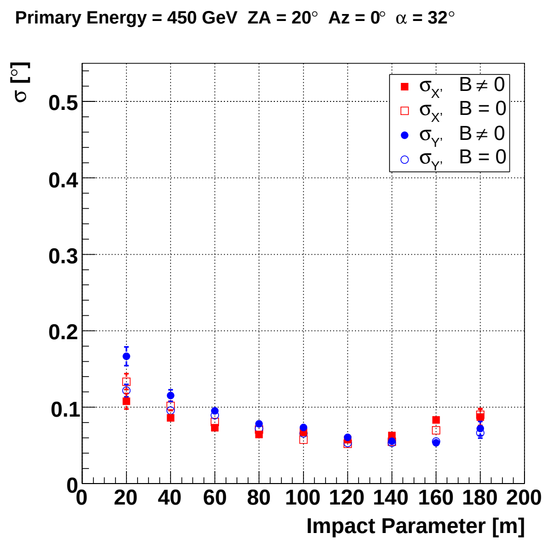

(c) 0° azimuth angle, 20° ZA, 450 GeV energy, intermediate image cleaning.

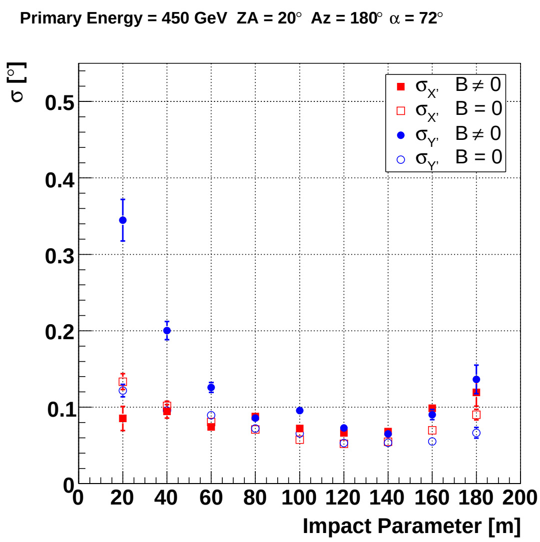

(d) 180° azimuth angle, 20° ZA, 450 GeV energy, intermediate image cleaning.

Figure 193: Lateral and longitudinal spread of the DISP-reconstructed arrival directions versus impact parameter for MC γ-rays of 450 GeV energy, 0° and 180° azimuth angle, different ZAs and different image cleaning levels.

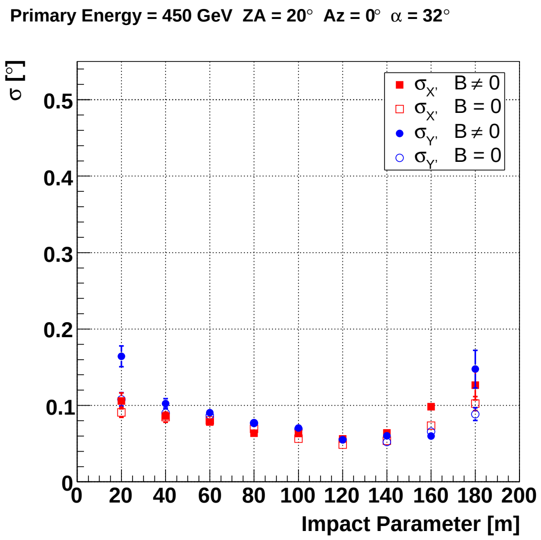

(a) 0° azimuth angle, 20° ZA, 450 GeV energy, hard image cleaning.

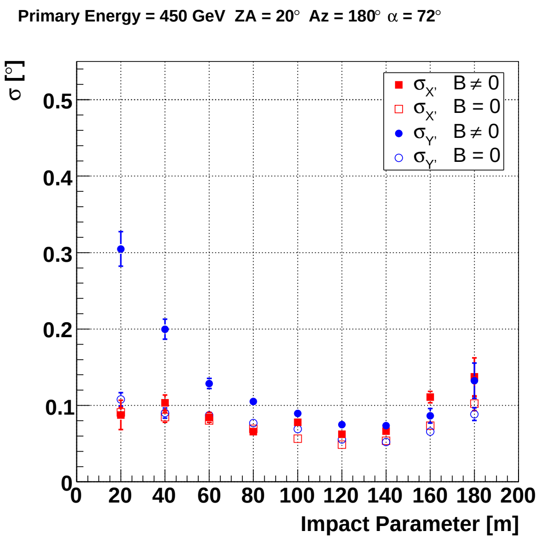

(b) 180° azimuth angle, 20° ZA, 450 GeV energy, hard image cleaning.

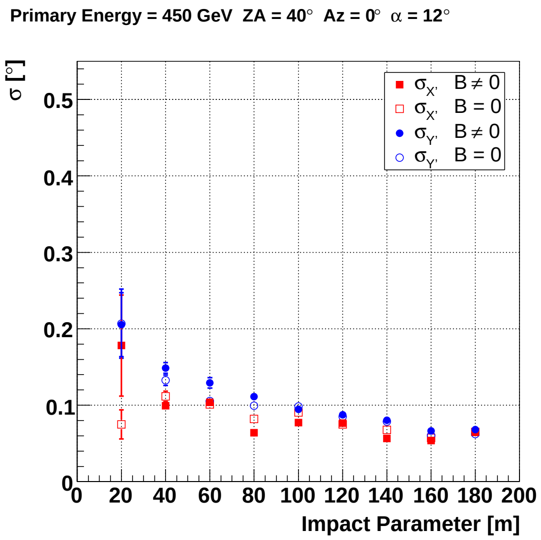

(c) 0° azimuth angle, 40° ZA, 450 GeV energy, intermediate image cleaning.

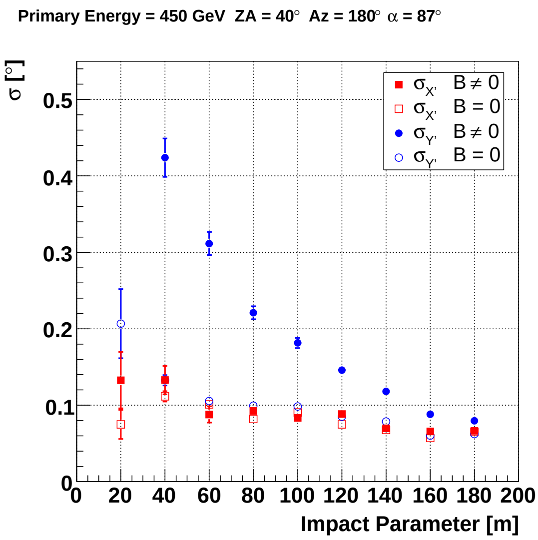

(d) 180° azimuth angle, 40° ZA, 450 GeV energy, intermediate image cleaning.

Figure 194: Lateral and longitudinal spread of the DISP-reconstructed arrival directions versus impact parameter for MC γ-rays of 450 GeV energy, 0° and 180° azimuth angle, different ZAs and different image cleaning levels.

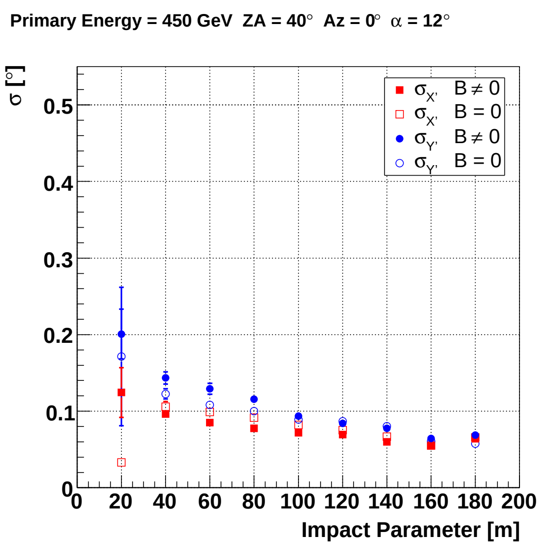

(a) 0° azimuth angle, 40° ZA, 450 GeV energy.

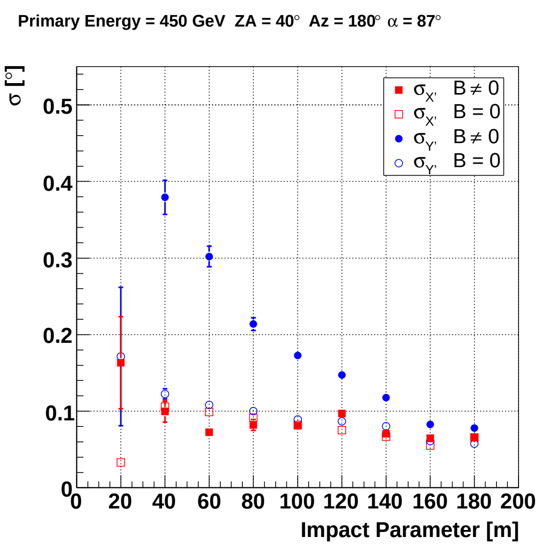

(b) 180° azimuth angle, 40° ZA, 450 GeV energy.

Figure 195: Lateral and longitudinal spread of the DISP-reconstructed arrival directions versus impact parameter for MC γ-rays of 450 GeV energy, 0° and 180° azimuth angle, 40° ZA and the hard image cleaning.

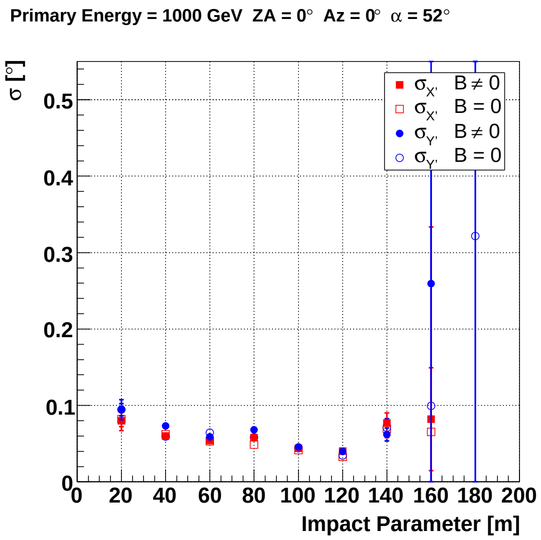

(a) 0° azimuth angle, 0° ZA, 1 TeV energy, intermediate image cleaning.

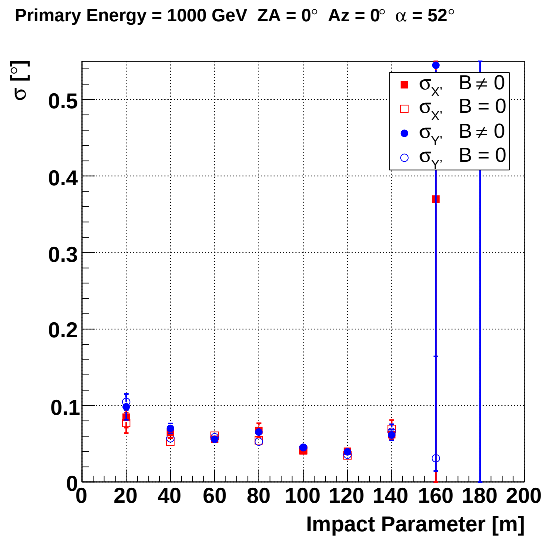

(b) 0° azimuth angle, 0° ZA, 1 TeV energy, hard image cleaning.

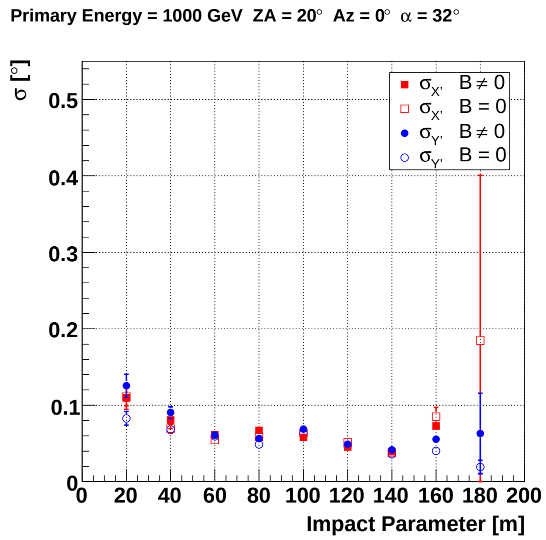

(c) 0° azimuth angle, 20° ZA, 1 TeV energy, intermediate image cleaning.

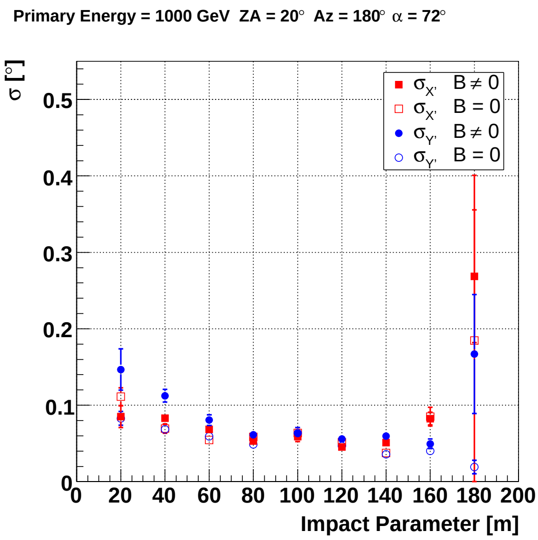

(d) 180° azimuth angle, 20° ZA, 1 TeV energy, intermediate image cleaning.

Figure 196: Lateral and longitudinal spread of the DISP-reconstructed arrival directions versus impact parameter for MC γ-rays of 1 TeV energy, 0° and 180° azimuth angle, different ZAs and different image cleaning levels.

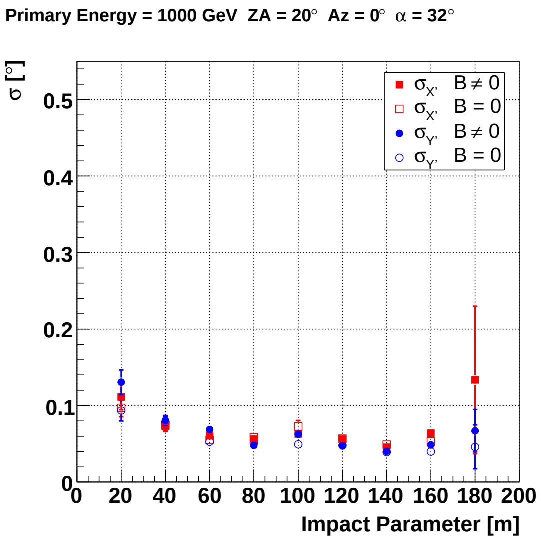

(a) 0° azimuth angle, 20° ZA, 1 TeV energy, hard image cleaning.

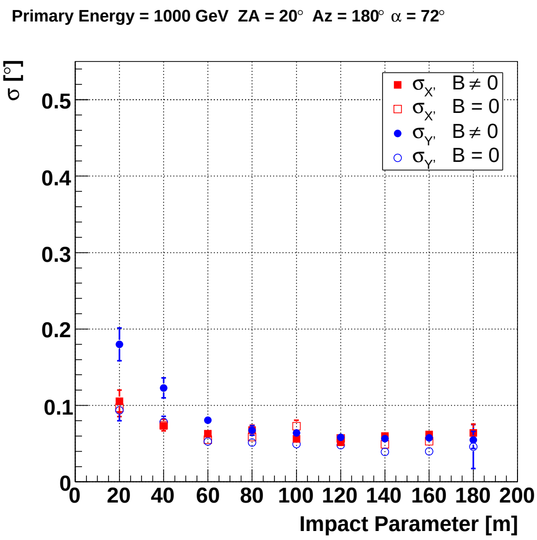

(b) 180° azimuth angle, 20° ZA, 1 TeV energy, hard image cleaning.

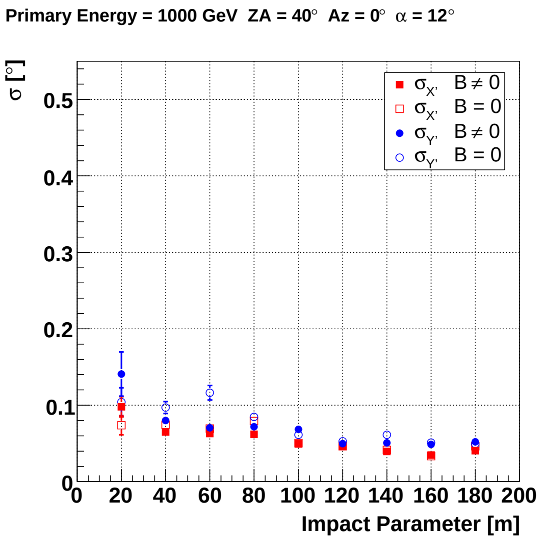

(c) 0° azimuth angle, 40° ZA, 1 TeV energy, intermediate image cleaning.

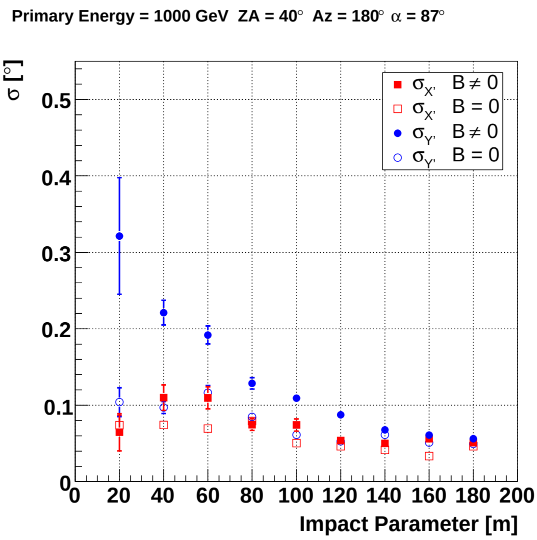

(d) 180° azimuth angle, 40° ZA, 1 TeV energy, intermediate image cleaning.

Figure 197: Lateral and longitudinal spread of the DISP-reconstructed arrival directions versus impact parameter for MC γ-rays of 1 TeV energy, 0° and 180° azimuth angle, different ZAs and different image cleaning levels.

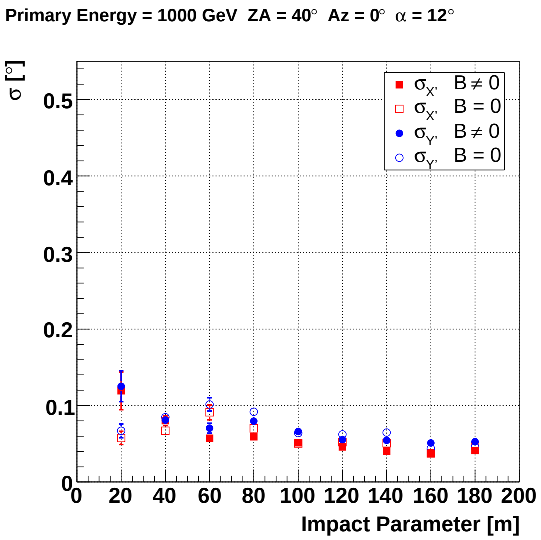

(a) 0° azimuth angle, 40° ZA, 1 TeV energy, hard image cleaning.

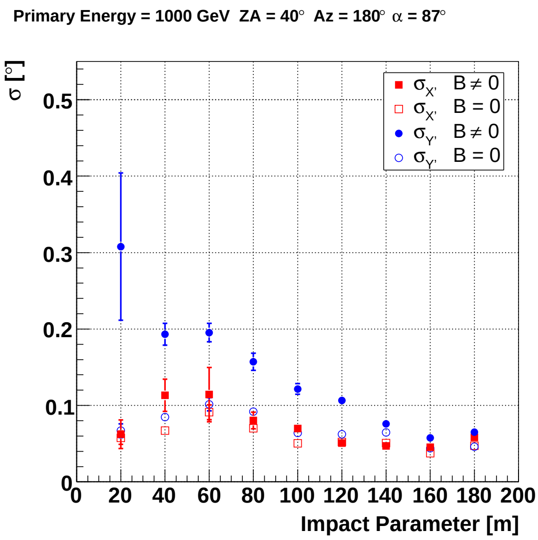

(b) 180° azimuth angle, 40° ZA, 1 TeV energy, hard image cleaning.

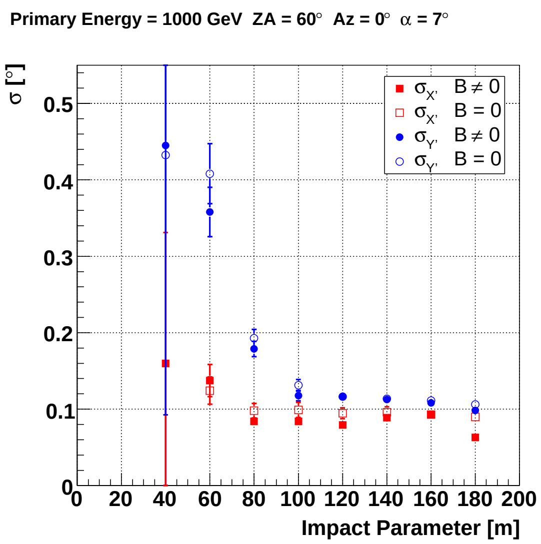

(c) 0° azimuth angle, 60° ZA, 1 TeV energy, intermediate image cleaning.

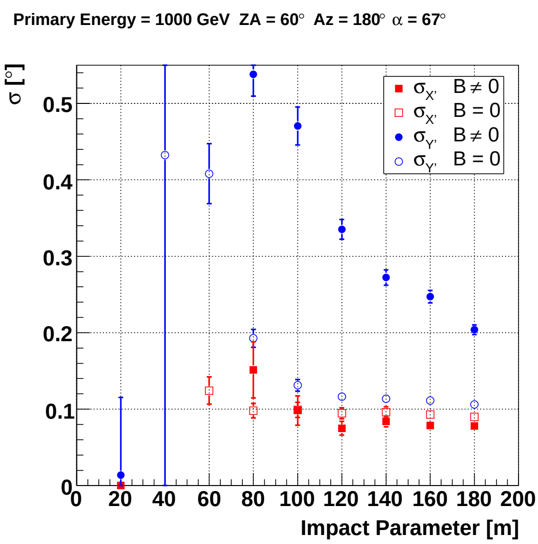

(d) 180° azimuth angle, 60° ZA, 1 TeV energy, intermediate image cleaning.

Figure 198: Lateral and longitudinal spread of the DISP-reconstructed arrival directions versus impact parameter for MC γ-rays of 1 TeV energy, 0° and 180° azimuth angle, 40° ZA and different image cleaning levels.

3.1.4 The Influence of the GF on the Image Parameter SIZE and the γ Efficiency

In the simplest approach, the estimation of the energy of a γ-ray candidate is done using only the image parameter SIZE, which is the total reconstructed integrated light of a shower image. Because the photon yield on ground is directly related to the shower energy, the parameter SIZE is a measure for the energy of a γ-ray candidate. The energy estimation is basically done by comparing the SIZE of real shower images with the one of MC simulated γ-ray events. In general, the energy estimation incorporates additional image parameters. For instance, the SIZE of an event depends also on the image parameter DIST which is related to the impact parameter of a primary γ-ray.
The influence of the GF on the Cherenkov light distribution on ground was briefly discussed in section 1.3. It was shown that the shape and intensity of the distribution of Cherenkov photons on ground and also in the telescope plane strongly depend on the orientation of the primary γ-ray with respect to the direction of the GF [39]. The thinning of the Cherenkov light distribution on ground is expected to have an influence on the image parameter SIZE. For unfavorable orientations with regard to the influence of the GF the SIZE parameter presumably takes smaller values than in case of favorable orientations. Thus, if the effect of the GF is not properly taken into account, the reconstructed energy will be underestimated. It is therefore important to investigate the influence of the GF on the image parameter SIZE.
The γ efficiency, defined as

$$\varepsilon_{\gamma,\mathrm{Trigger}}(E, r, \mathrm{ZA}, \mathrm{Az}) = \frac{N^{\mathrm{Trigger,Image\ Cleaning}}(E, r, \mathrm{ZA}, \mathrm{Az})}{N^{\mathrm{Generated}}(E, r, \mathrm{ZA}, \mathrm{Az})}, \tag{14}$$

is another important impact parameter to look at. Therein, $N^{\mathrm{Trigger,Image\ Cleaning}}(E, r, \mathrm{ZA}, \mathrm{Az})$ denotes the number of MC simulated γ-rays surviving the trigger level as well as the subsequent image cleaning procedure. $N^{\mathrm{Generated}}(E, r, \mathrm{ZA}, \mathrm{Az})$ is the number of MC simulated γ-rays at a certain energy E, impact parameter r and orientation of the telescope $(\mathrm{ZA}, \mathrm{Az})$. The γ efficiency is used to determine the effective collection area, which is in turn used to estimate the flux from a γ-ray source. However, the influence of the GF is expected to affect the γ efficiency only close to the analysis threshold, where the thinned-out distributions of Cherenkov photons on ground have a lower probability to survive the trigger level and the image cleaning.
Figure 199 shows the mean value of the image parameter SIZE and the γ efficiency as a function of the azimuth angle for a MC γ-ray of 30 GeV energy. The impact parameter was set to $r = 120\,\mathrm{m}$ and the ZA to $0°$ and $20°$. The soft image cleaning was applied. For the hard image cleaning, the γ efficiency is at most $\sim 4\,\%$. The angle α between the direction of the primary γ-ray and the direction of the GF is written on top of the abscissa. To disentangle both the geometrical effect and the effect of the GF (figure 23, section 3.1), the telescope is always placed at angles $\varphi = \text{azimuth angle} + 90°$. Thereby, the telescope is always located on top of the maximum of the Cherenkov light distribution on ground or at the same distance with respect to the latter.
For $0°$ ZA (left panel of figure 199), both the mean SIZE and the γ efficiency are reduced in case of enabled GF. As expected, there is no dependency on the azimuth angle, as the angle α stays constant. The corresponding values that were obtained for disabled GF are drawn as solid lines, because the MC data was generated only for $0°$ azimuth angle. For $20°$ ZA (right panel of figure 199), the mean SIZE as well as the γ efficiency decrease with increasing azimuth angle, as the angle α increases, too. The effect on the γ efficiency is stronger, which is expected for γ-rays being close to the analysis threshold. Events lying below the analysis threshold do not survive the trigger level or the image cleaning and therefore do not contribute to the average of the image parameter SIZE. Figure 200 was obtained for

similar MC input parameters as the preceding figure, but the impact parameter range was enlarged to $r = 20 \ldots 200\,\mathrm{m}$. From the comparison of figure 199 and figure 200 it can be seen that both the mean value of the parameter SIZE and the γ efficiency are smaller if the impact parameter range is enlarged. The latter is expected, as in case of figure 199 the telescope was always placed on the maximum of the Cherenkov light distribution on ground. Nevertheless, the influence of the GF on the mean SIZE and the γ efficiency is comparable.

Figures 201 - 214 show the mean value of the image parameter SIZE and the γ efficiency for energies between 50 GeV and 1 TeV and two impact parameter windows. As can be seen from the figures the average SIZE and the γ efficiency can be significantly affected by the influence of the GF. The average SIZE can be reduced by up to 20 % (e.g. figure 211, lower left panel). Depending on the threshold energy (telescope orientation) the influence of the GF on the γ efficiency is greater than the one on the average SIZE, and vice versa. In case the MC generated γ-ray showers lie well above the analysis/trigger threshold the γ efficiency is not affected due to the influence of the GF although the shower images are fainter. However, close to the threshold only images whose SIZE is not affected too much survive the trigger level/image cleaning. Therefore, the average SIZE can be largely unchanged while the γ efficiency decreases significantly (figure 208, lower left panel), and vice versa. The influence of the GF on the image parameter SIZE is clearly visible only for those energies and orientations of the primary γ-ray where the γ efficiency is not altered too much. The latter depends of course on the image cleaning levels which are applied to the shower images.

It is noteworthy that not only low-energy γ-rays are affected by the influence of the GF but also high-energy γ-rays of at least 1 TeV.

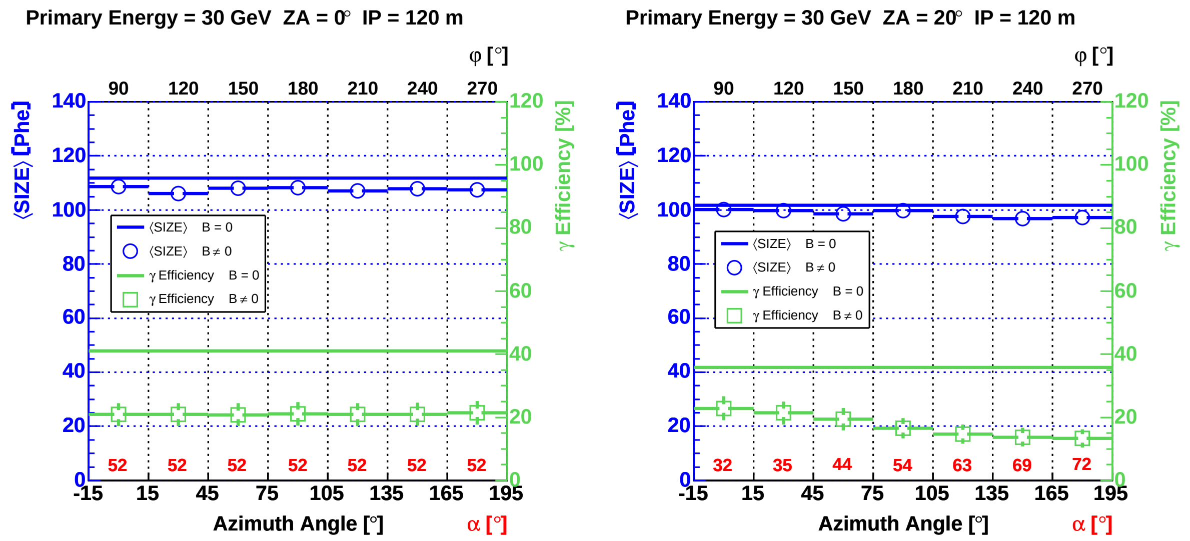

Figure 199: The mean value of the image parameter SIZE and the γ efficiency as a function of the azimuth angle for 30 GeV γ-rays and ZA between $0°$ and $20°$. The telescope is always placed at angles φ = azimuth angle + $90°$. The impact parameter was set to $r = 120$ m. The soft image cleaning was applied.

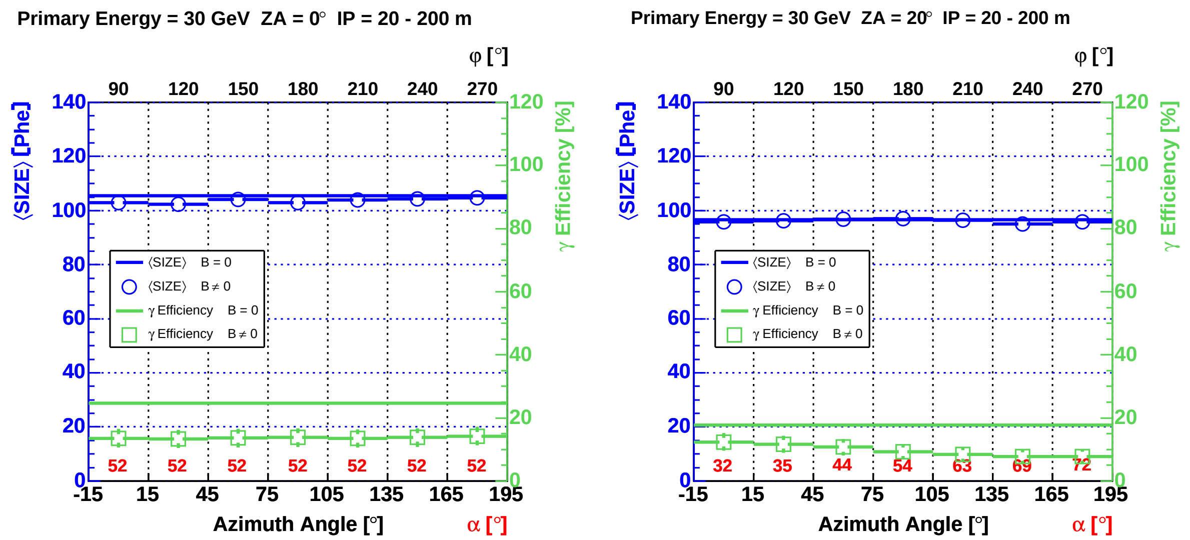

Figure 200: The mean value of the image parameter SIZE and the γ efficiency as a function of the azimuth angle for 30 GeV γ-rays and ZA between $0°$ and $20°$. The telescope is always placed at angles φ = azimuth angle + $90°$. The impact parameters were set to $r = 20 \ldots 200$ m. The soft image cleaning was applied.

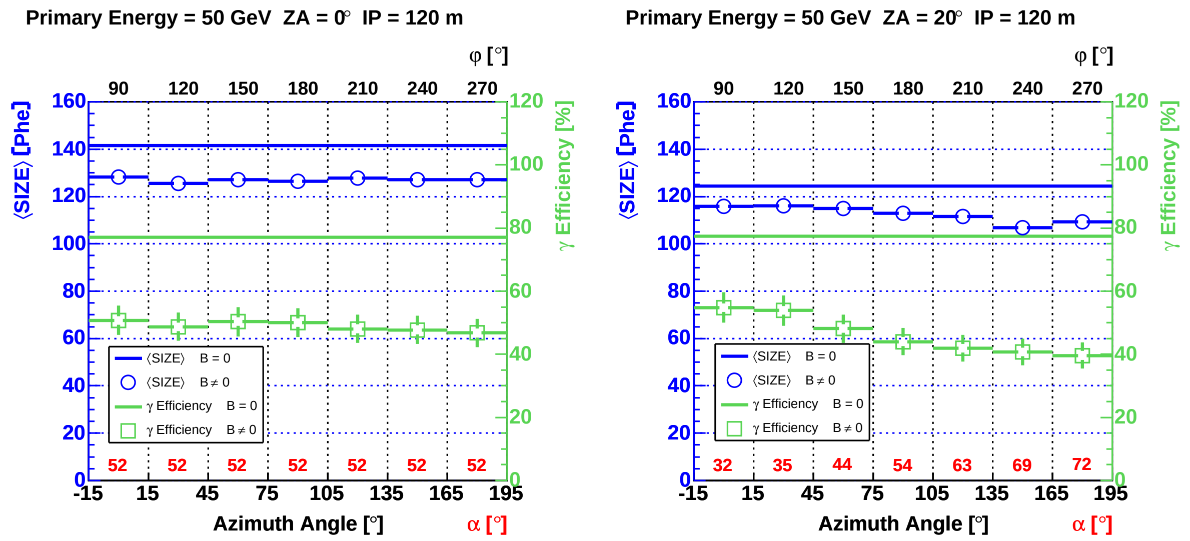

Figure 201: The mean value of the image parameter SIZE and the γ efficiency as a function of the azimuth angle for 50 GeV γ-rays and ZA between $0°$ and $20°$. The telescope is always placed at angles φ = azimuth angle + $90°$. The impact parameter was set to $r = 120$ m. The soft image cleaning was applied.

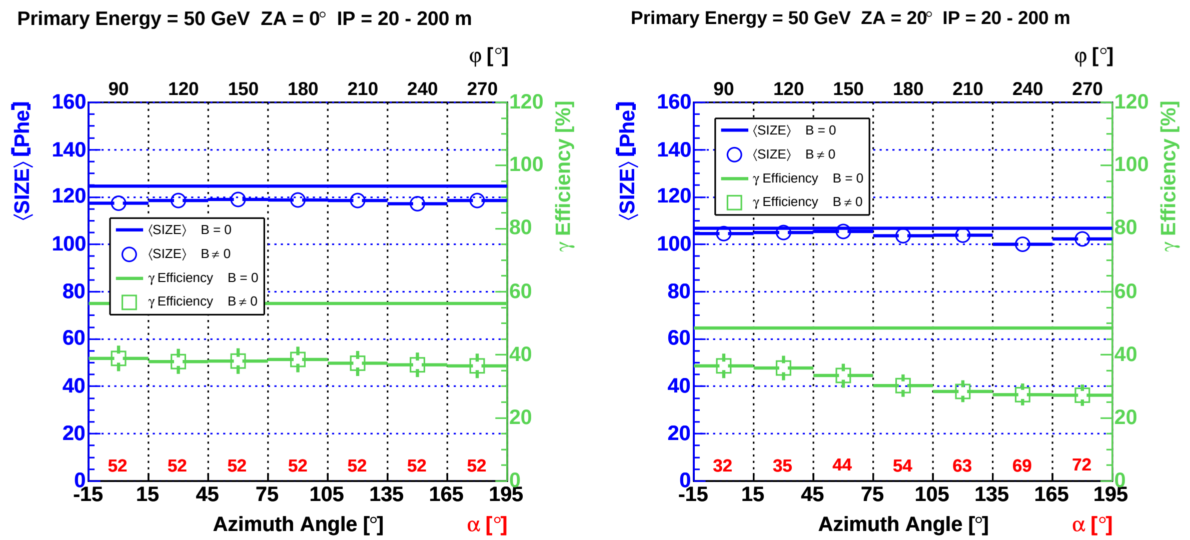

Figure 202: The mean value of the image parameter SIZE and the γ efficiency as a function of the azimuth angle for 50 GeV γ-rays and ZA between $0°$ and $20°$. The telescope is always placed at angles φ = azimuth angle + $90°$. The impact parameters were set to $r = 20 \ldots 200$ m. The soft image cleaning was applied.

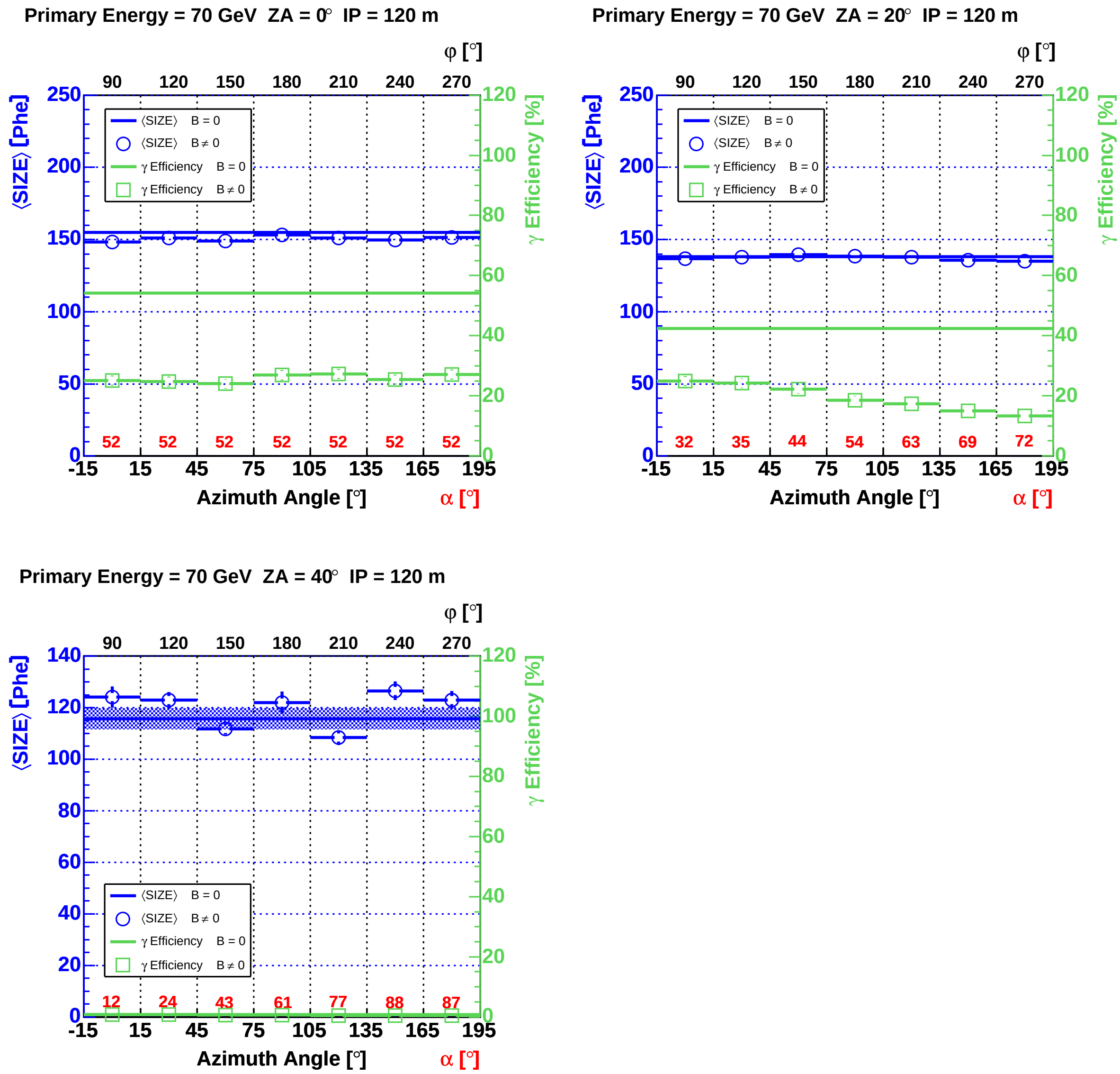

Figure 203: The mean value of the image parameter SIZE and the γ efficiency as a function of the azimuth angle for 70 GeV γ-rays and ZA between 0° and 40°. The telescope is always placed at angles φ = azimuth angle + 90°. The impact parameter was set to r = 120 m. The hard image cleaning was applied.

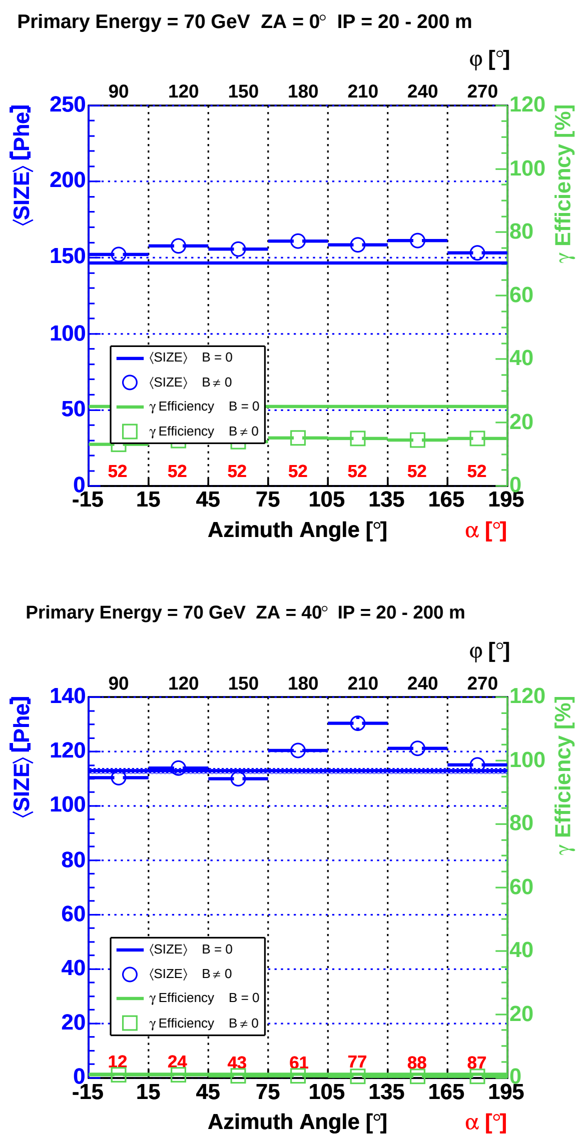

Figure 204: The mean value of the image parameter SIZE and the γ efficiency as a function of the azimuth angle for 70 GeV γ-rays and ZA between 0° and 40°. The telescope is always placed at angles φ = azimuth angle + 90°. The impact parameters were set to $r = 20 \ldots 200$ m. The hard image cleaning was applied.

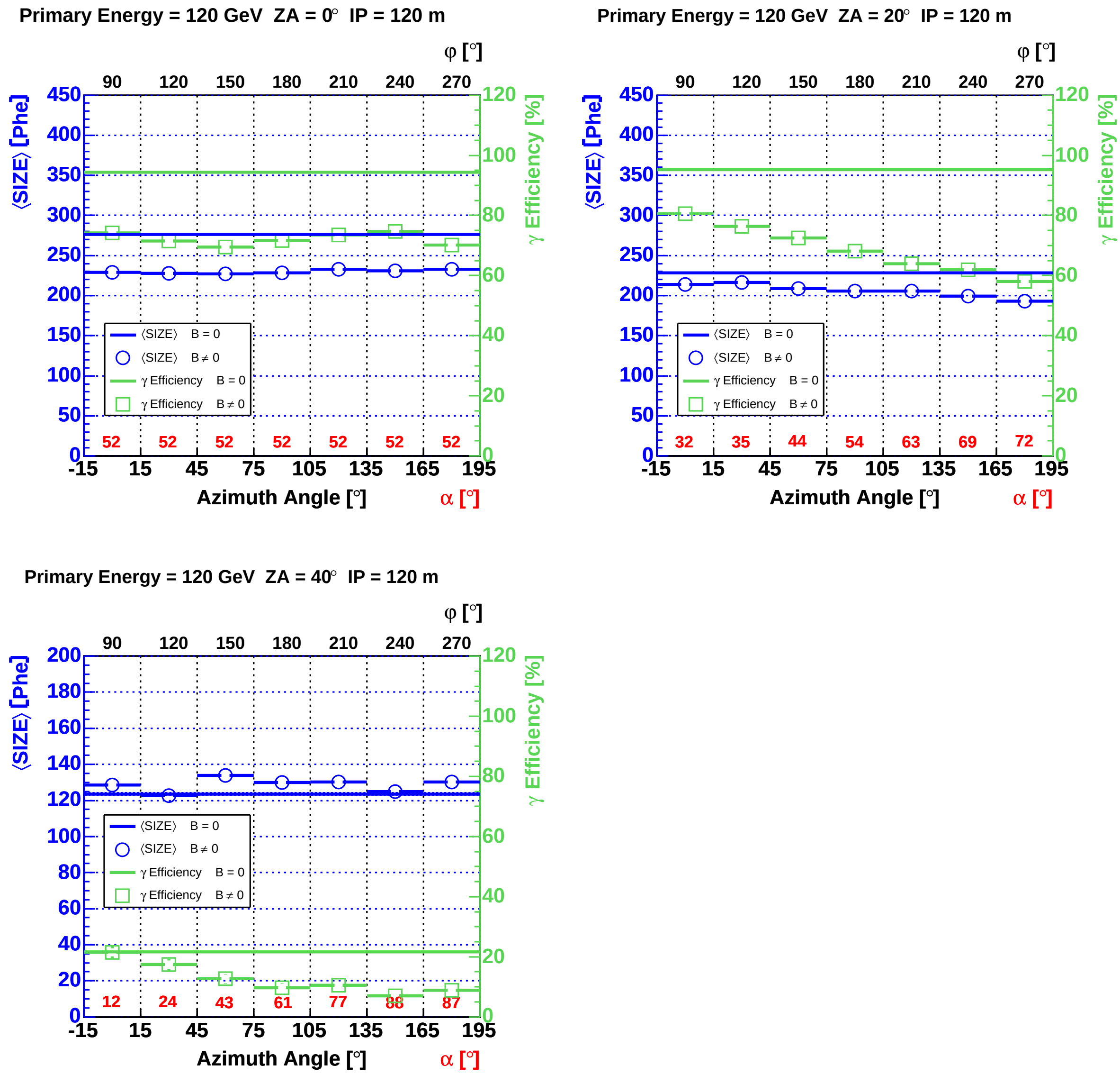

Figure 205: The mean value of the image parameter SIZE and the γ efficiency as a function of the azimuth angle for 120 GeV γ-rays and ZA between 0° and 40°. The telescope is always placed at angles φ = azimuth angle + 90°. The impact parameter was set to r = 120 m. The hard image cleaning was applied.

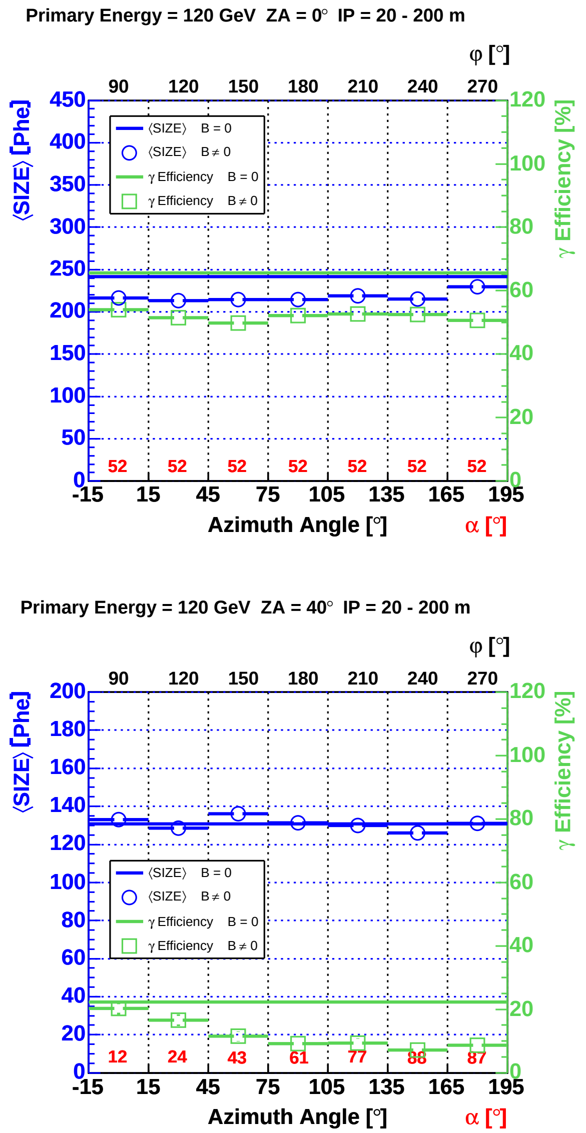

Figure 206: The mean value of the image parameter SIZE and the γ efficiency as a function of the azimuth angle for 120 GeV γ-rays and ZA between 0° and 40°. The telescope is always placed at angles $\varphi =$ azimuth angle $+ 90°$. The impact parameters were set to $r = 20 \ldots 200$ m. The hard image cleaning was applied.

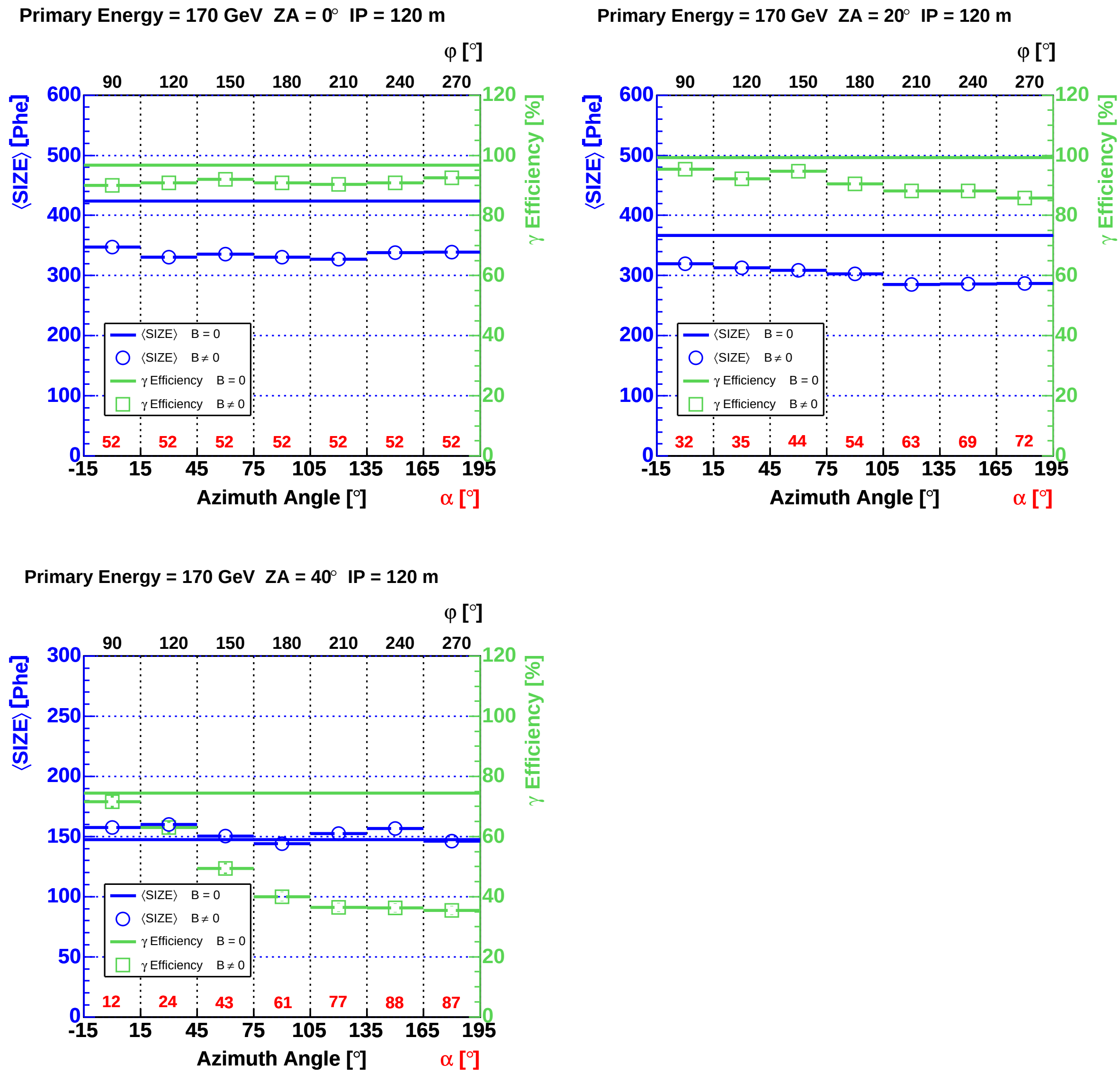

Figure 207: The mean value of the image parameter SIZE and the γ efficiency as a function of the azimuth angle for 170 GeV γ-rays and ZA between $0°$ and $40°$. The telescope is always placed at angles φ = azimuth angle + $90°$. The impact parameter was set to $r = 120\,\mathrm{m}$. The hard image cleaning was applied.

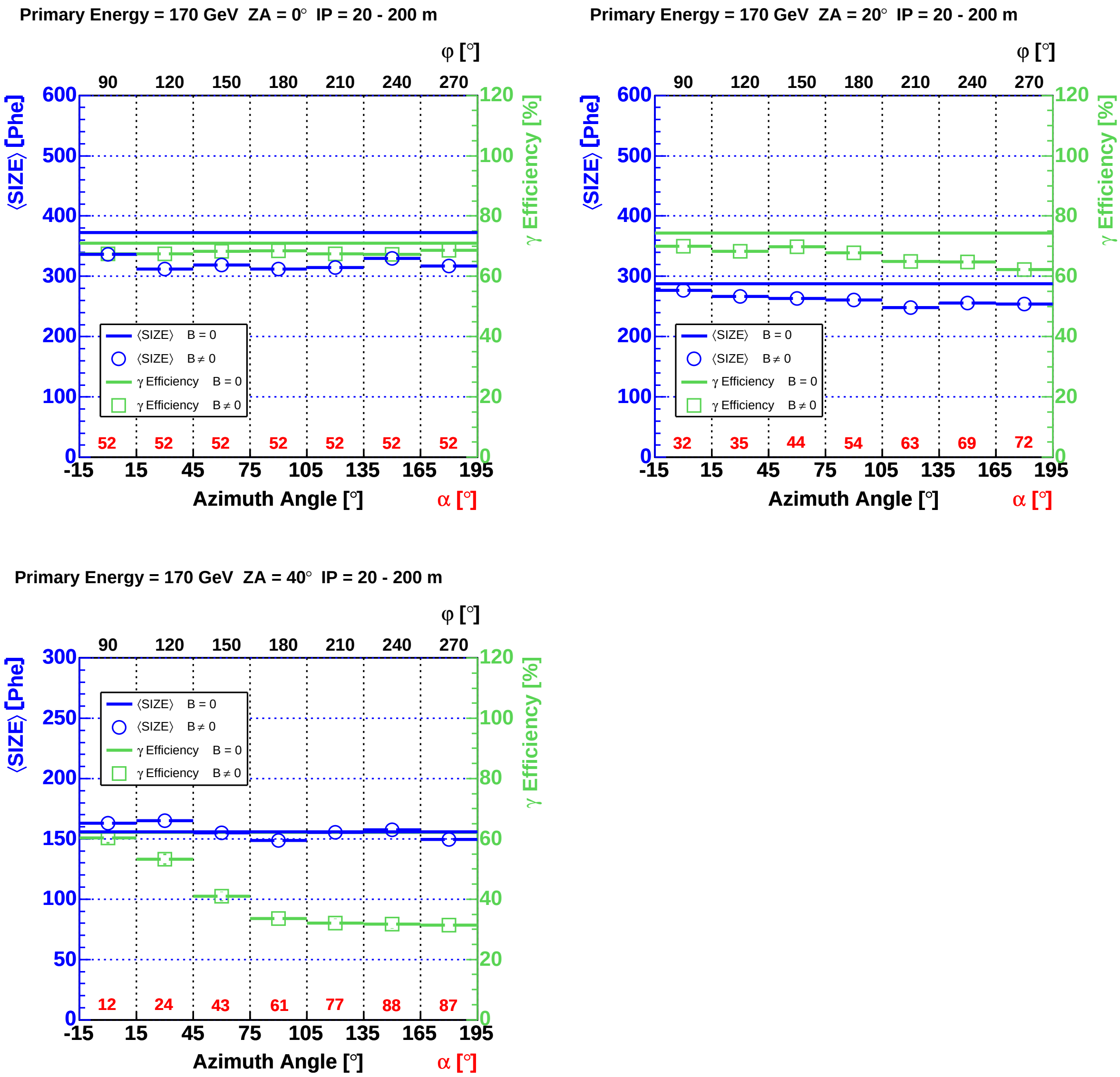

Figure 208: The mean value of the image parameter SIZE and the γ efficiency as a function of the azimuth angle for 170 GeV γ-rays and ZA between $0°$ and $40°$. The telescope is always placed at angles $\varphi =$ azimuth angle $+ 90°$. The impact parameters were set to $r = 20 \ldots 200$ m. The hard image cleaning was applied.

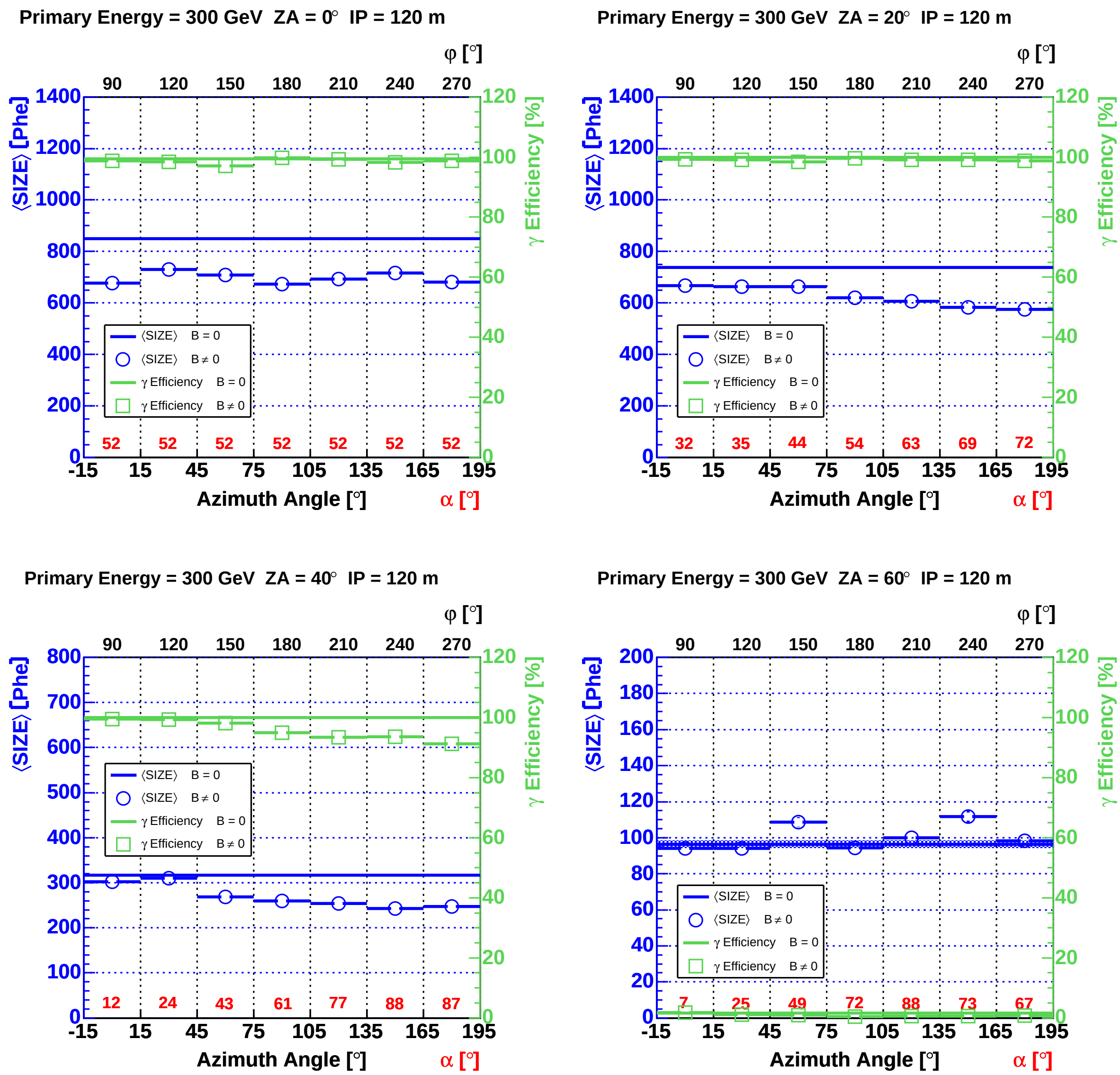

Figure 209: The mean value of the image parameter SIZE and the γ efficiency as a function of the azimuth angle for 300 GeV γ-rays and ZA between 0° and 60°. The telescope is always placed at angles φ = azimuth angle + 90°. The impact parameter was set to $r = 120$ m. The hard image cleaning was applied.

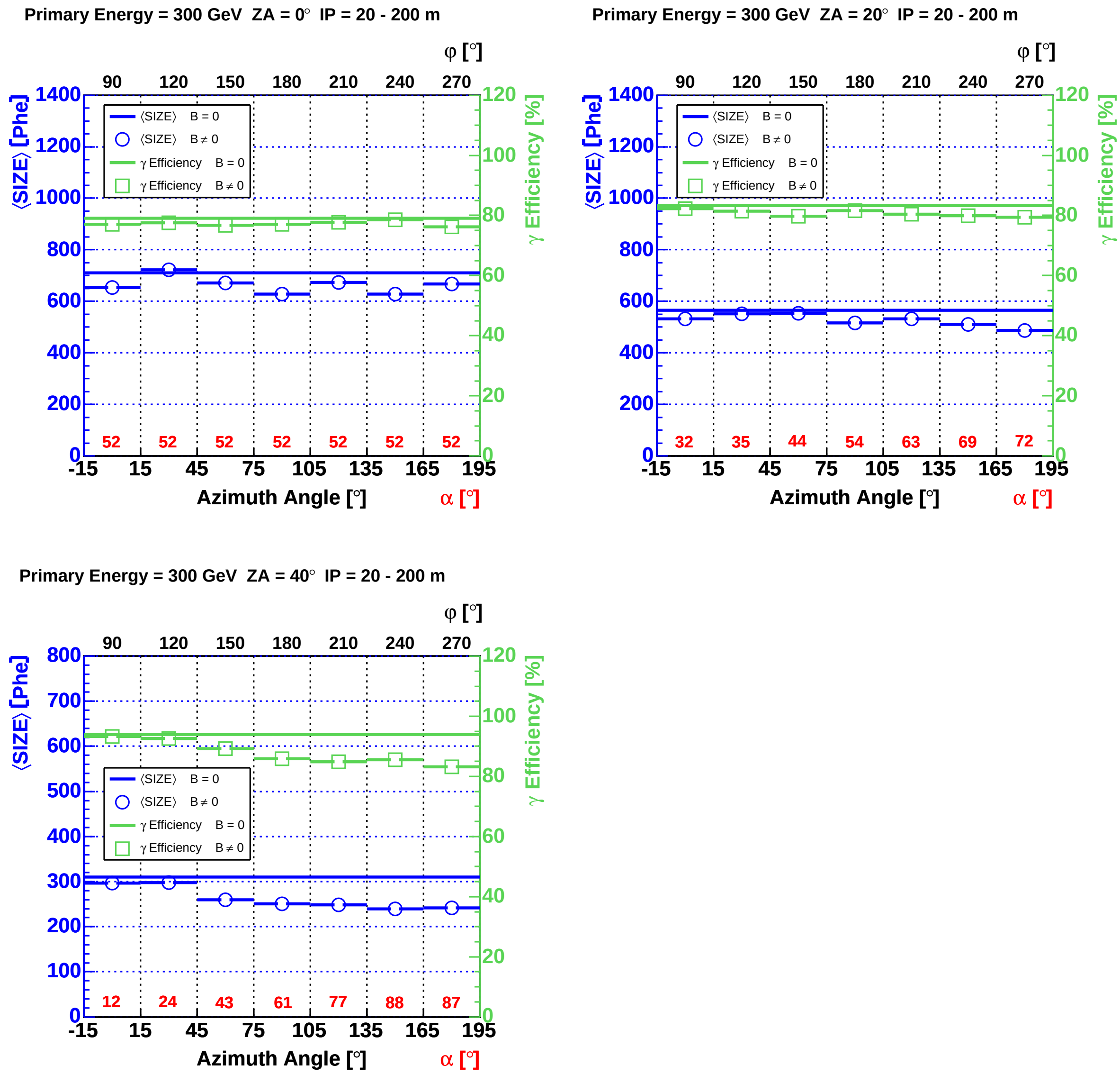

Figure 210: The mean value of the image parameter SIZE and the γ efficiency as a function of the azimuth angle for 300 GeV γ-rays and ZA between 0° and 60°. The telescope is always placed at angles φ = azimuth angle + 90°. The impact parameters were set to $r = 20 \ldots 200$ m. The hard image cleaning was applied.

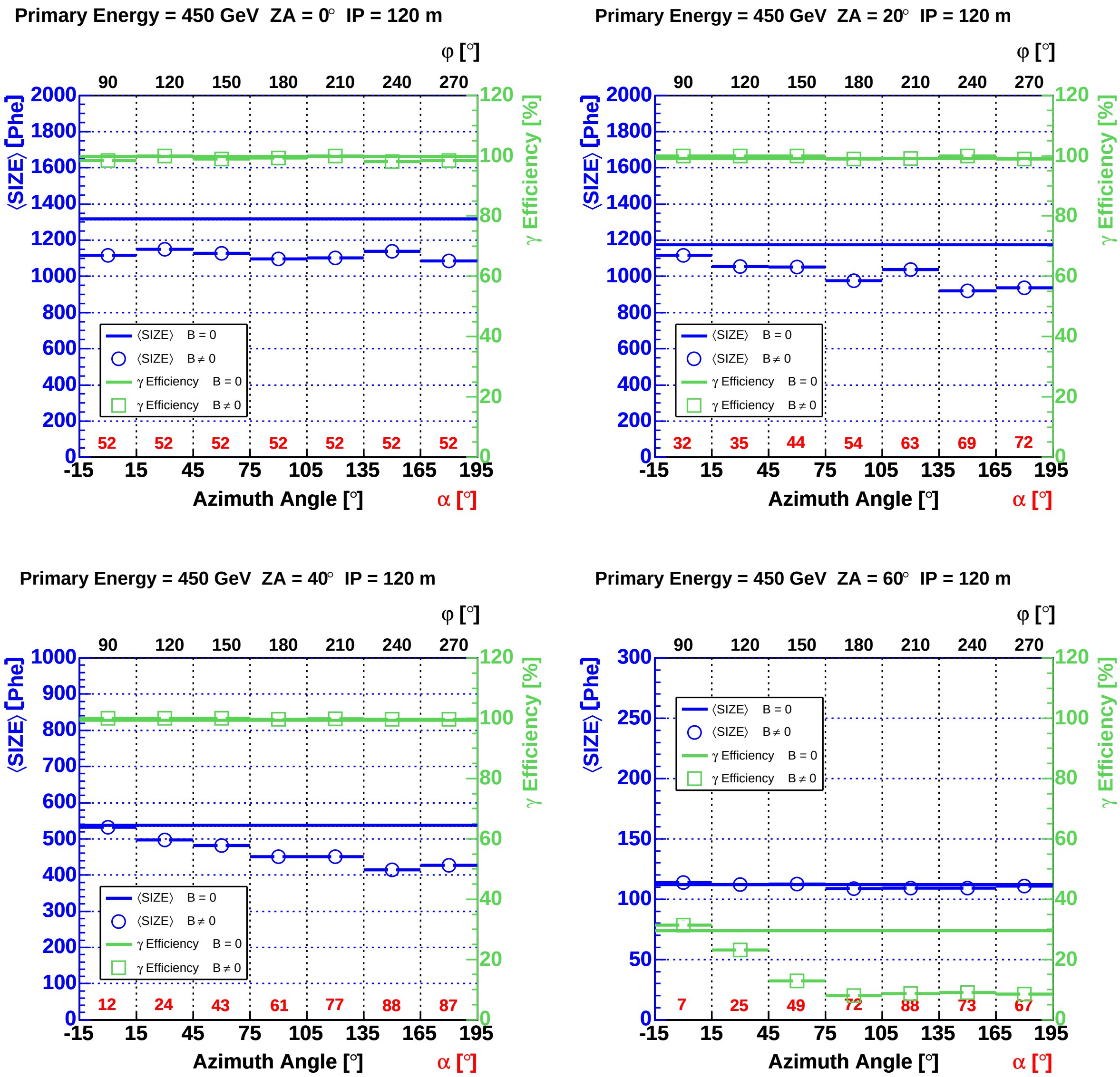

Figure 211: The mean value of the image parameter SIZE and the γ efficiency as a function of the azimuth angle for 450 GeV γ-rays and ZA between 0° and 60°. The telescope is always placed at angles φ = azimuth angle + 90°. The impact parameter was set to r = 120 m. The hard image cleaning was applied.

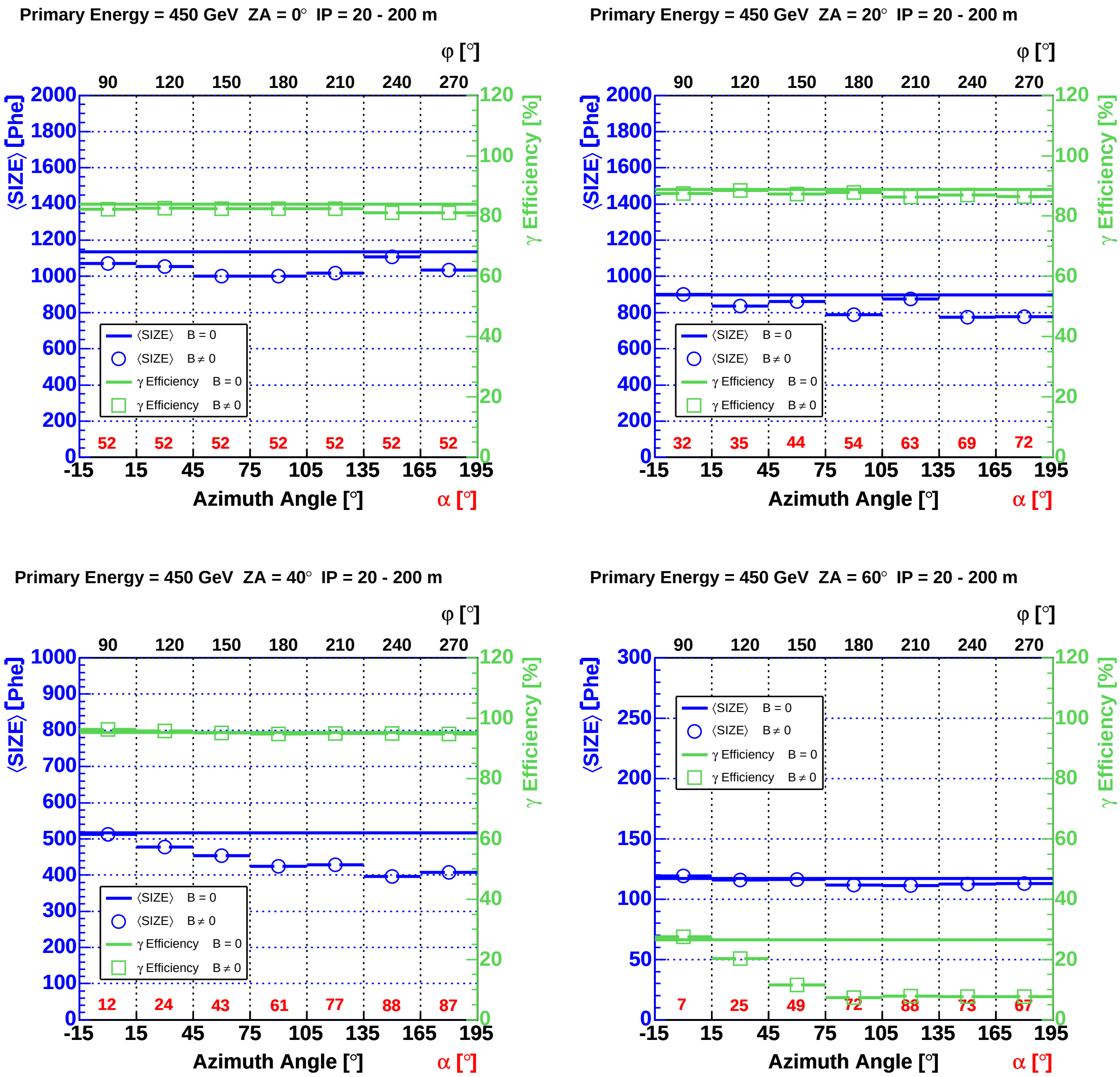

Figure 212: The mean value of the image parameter SIZE and the γ efficiency as a function of the azimuth angle for 450 GeV γ-rays and ZA between $0°$ and $60°$. The telescope is always placed at angles $\varphi =$ azimuth angle $+ 90°$. The impact parameters were set to $r = 20 \ldots 200$ m. The hard image cleaning was applied.

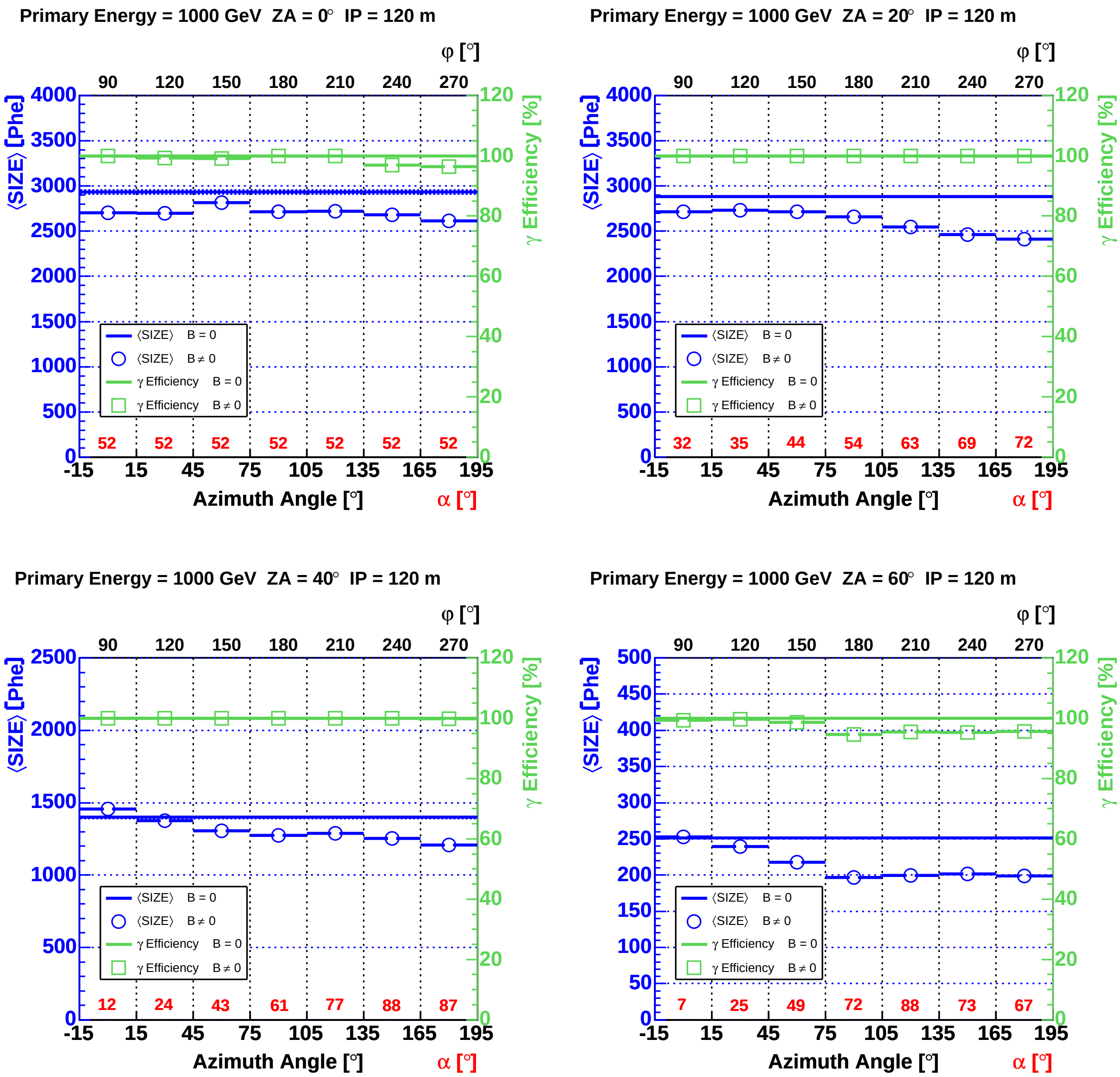

Figure 213: The mean value of the image parameter SIZE and the γ efficiency as a function of the azimuth angle for 1 TeV γ-rays and ZA between $0°$ and $60°$. The telescope is always placed at angles φ = azimuth angle $+\ 90°$. The impact parameter was set to $r = 120$ m. The hard image cleaning was applied.

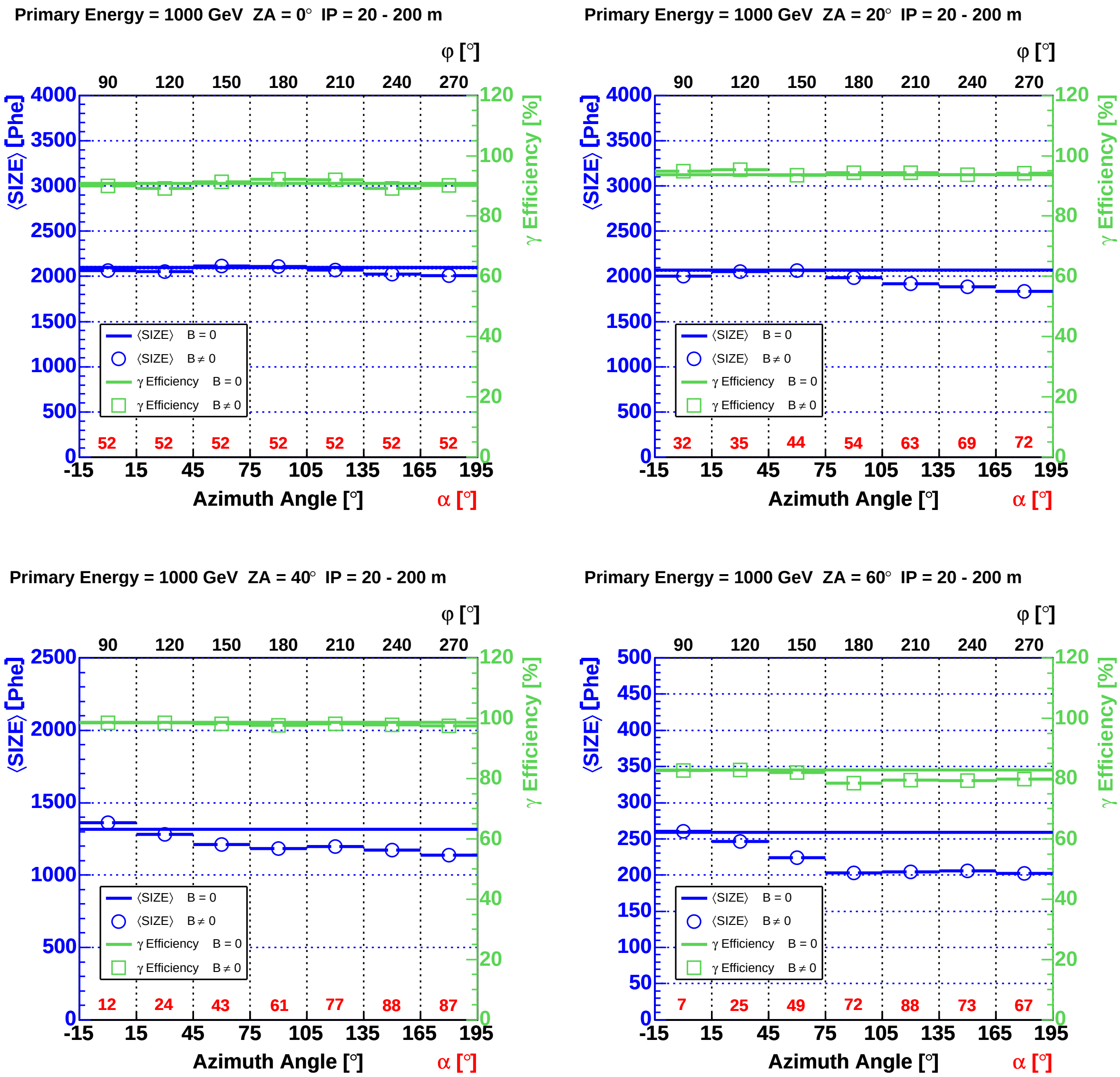

Figure 214: The mean value of the image parameter SIZE and the γ efficiency as a function of the azimuth angle for 1 TeV γ-rays and ZA between $0°$ and $60°$. The telescope is always placed at angles φ = azimuth angle + $90°$. The impact parameters were set to $r = 20 \ldots 200$ m. The hard image cleaning was applied.

4 Discussion & Conclusions

From the results presented in section 3 it is evident that the GF can severely affect both the shape and the orientation of shower images recorded with MAGIC. It was demonstrated that the extend of the influence not only depends on the orientation of the telescope with respect to the direction of the GF, but also on the position of the telescope with respect to the primary γ-ray's impact point on ground. Shower images are not only rotated away from the projected direction of the GF in the telescope camera plane but can also be rotated towards the latter direction, contrary to what was reported in [14].
It is remarkable that the GF effects not only occur at very low energies but also at high energies around 1 TeV. The GF effects seem to be rather pronounced at γ-ray energies around 450 GeV. The reason for the occurrence of GF effects at high energies is presumably linked to a characteristic feature in the development of a γ-ray induced EAS. The process of multiplication in EAS continues until the average energy of the shower particles is insufficient to further produce secondary particles in subsequent collisions. At this stage of the shower development, the shower maximum is reached (largest number of secondary particles) and the average energy of the secondaries is close to the so-called critical energy below which secondary electrons and positrons lose their energy predominantly through ionization of air molecules. At the shower maximum, the average energy of the secondary particles is independent of the primary γ-ray energy and the GF has on average the same influence on the secondary particles. However, the average slant depth at which the shower maximum occurs logarithmically increases with increasing energy of the primary γ-ray, and therefore the distance along which secondary electrons and positrons suffer from Lorentz deflection increases, too.
Another point worthy of mentioning is the fact that the threshold energy for a charged particle to emit Cherenkov light decreases with increasing slant depth. Hence, in high-energy EAS, even charged secondaries of lower energy suffering strong Lorentz deflection may additionally contribute to the Cherenkov light pool on ground.
The main findings of the studies on the GF effects can be summarized as follows:

- **GF effects on the image parameters WIDTH and LENGTH**: On average, the influence of the GF on the image parameters WIDTH and LENGTH is rather small. While γ-ray shower images are elongated perpendicular to the direction of the GF, they appear to be compressed parallel to the direction of the GF. The shape of high-energy γ-ray showers (~ 1 TeV) as well as the one of low-energy γ-ray showers (~ 100 GeV) is affected. For γ-ray energies around 100 GeV, the average WIDTH is changed by $\sim 5\,\%$, while for energies around 1 TeV the average WIDTH can be changed by up to $\sim 15\,\%$, depending on the orientation of the EAS. The effect on the image parameter LENGTH is in the order of $5\,\%$, for γ-ray energies around 100 GeV as well as 1 TeV. These numbers were derived from the figures in paragraph 3.1.1.
  It remains to be shown how the GF effects on the image parameters WIDTH and LENGTH degrade the RF-based γ/hadron separation capability [9] of the analysis.

- **GF effects on the image parameters δ and ALPHA**: The influence of the GF on EAS can significantly alter the pointing of γ-ray shower images and therefore degrades the ALPHA analysis. The disturbance of the pointing can result in a strong broadening of the ALPHA distribution. Some orientations of the primary γ-ray with respect to the direction of the GF result in shower images which are systematically rotated away from the nominal source position in the camera. In general, γ-ray images close to the camera center are more affected, as they are characteristically less elongated. It is remarkable that also TeV γ-ray shower images are rotated due to the influence of the GF.

The rotation of shower images away from the camera center can significantly degrade the ALPHA-based γ/hadron separation. The extent of the rotation is directly related to the image parameter δ (the angular distance between the x-axis of the camera coordinate system and the major image axis) and can be therefore partly corrected. The recovery of the γ-ray signal by correcting for the GF effects is expected to increase the sensitivity of the telescope as well as the significance of a detection.However, the correction for the GF effects requires the knowledge of the rotation angle, which depends on various parameters such as the energy of the primary γ-ray, its impact parameter and orientation.
It was shown that the de-rotation of the shower images does not help to recover the pointing entirely. Thus, for unfavorable orientations with regard to the influence of the GF, a simple procedure could be to remove those regions in the camera which are expected to be affected strongest. The isolation of the camera sectors that belong to arrangements that are affected least of all or most of all by the influence of the GF requires the knowledge of the projection of the GF in the camera coordinate system. With $\delta_B(\mathrm{Az},\mathrm{ZA}) = \sphericalangle(\vec{B}_{\mathrm{Camera}}(\mathrm{Az},\mathrm{ZA}), \vec{e}_{x,\mathrm{Camera}})$ the angle between the projection of the GF in the camera coordinate system and the x-axis of the camera coordinate system (see section 3.1) and using the definitions $\delta_\pm = \Delta\delta \pm \delta_B(\mathrm{Az},\mathrm{ZA})$, images from a real data sample surviving the condition

$$\begin{gathered}
[\{\tan(\delta_+)\,\mathrm{sgn}(\sin(\delta_+))\,y > -\mathrm{sgn}(\sin(\delta_+))\,x\} \quad \wedge \quad \{\tan(\delta_-)\,\mathrm{sgn}(\sin(\delta_-))\,y < \mathrm{sgn}(\sin(\delta_-))\,x\}] \\
\vee \\
[\{\tan(\delta_+)\,\mathrm{sgn}(\sin(\delta_+))\,y < -\mathrm{sgn}(\sin(\delta_+))\,x\} \quad \wedge \quad \{\tan(\delta_-)\,\mathrm{sgn}(\sin(\delta_-))\,y > \mathrm{sgn}(\sin(\delta_-))\,x\}]\,.
\end{gathered} \tag{15}$$

correspond to the most favorable arrangements. Therein $\Delta\delta$ defines the opening angle of the considered camera sectors. x and y denote the coordinates of the centroid of a shower image and $\mathrm{sgn}(x)$ the sign function being defined as

$$\mathrm{sgn}(x) = \begin{cases} +1, & x \geq 0 \\ -1, & x < 0. \end{cases}$$

The pointing of events surviving the condition 15 are affected least by the influence of the GF. Instead, events surviving the condition

$$\begin{gathered}
[\{\mathrm{sgn}(\cos(\delta_-))\,y > -\tan(\delta_-)\,\mathrm{sgn}(\cos(\delta_-))\,x\} \quad \wedge \quad \{\mathrm{sgn}(\cos(\delta_+))\,y < \tan(\delta_+)\,\mathrm{sgn}(\cos(\delta_+))\,x\}] \\
\vee \\
[\{\mathrm{sgn}(\cos(\delta_-))\,y < -\tan(\delta_-)\,\mathrm{sgn}(\cos(\delta_-))\,x\} \quad \wedge \quad \{\mathrm{sgn}(\cos(\delta_+))\,y > \tan(\delta_+)\,\mathrm{sgn}(\cos(\delta_+))\,x\}]\,.
\end{gathered} \tag{16}$$

are expected to be affected strongest by the influence of the GF. For $\Delta\delta = 30^\circ$ one third of all events is kept. To remove only those images from a real dataset that are affected strongest by the influence of the GF, the interval $\Delta\delta$ must be considered as impact parameter-, azimuth angle- and ZA-dependent. For the analysis of a real dataset the best value for the interval $\Delta\delta$ should be determined from an appropriate MC sample.
An example for a `ROOT` implementation of the cut shown above is given in appendix A.

- **GF effects on the image parameter SIZE and the γ-ray efficiency**: It was shown that the GF can significantly affect the image parameter SIZE and the γ efficiency. However, both the GF effects on the γ efficiency and the one on the SIZE parameter are entangled. In case of low-energy showers and unfavorable orientations with regard to the strength of the GF, the Cherenkov light distribution on ground can be thinned out in a way that most of the events do not survive the trigger level. While the mean SIZE of the events surviving the trigger level and the image cleaning remains unchanged, the efficiency can be significantly altered. Thus, if the effect is not taken into account at low energies, the γ efficiency will be overestimated, which in turn affects the effective area calculation and the determination of the flux from a γ-ray source. For low energies close to the analysis threshold, the γ efficiency also depends on the position of the telescope in the Cherenkov light pool (figure 22).
  At higher energies, the γ efficiency is affected only at large ZA, where the telescope threshold energy is significantly increased. Depending on the energy of the γ-ray, the average SIZE can be reduced by up to $\sim 20\,\%$ (for γ-rays of $\sim 300 - 1000\,\mathrm{GeV}$) compared to the case of favorable directions with regard to the influence of the GF. Therfore, the energy of γ candidates will be systematically underestimated if the GF effects are not taken into account.
  To avoid the effects mentioned beforehand, it is essential to use appropriate MC data covering the same ZA range and azimuth angle range as the dataset being analyzed. By using appropriate MC, the GF effects on the SIZE parameter and the γ efficiency are automatically corrected, except for very low energies close to the trigger/analysis threshold where the efficiency depends on the impact point of the γ-ray with respect to the telescope (figure 22).

- **GF effects on the DISP method**: It was shown that the GF can affect the distribution of the DISP-estimated arrival direction of MC generated γ-rays. Due to the influence of the GF on the development of EAS the DISP distribution can be significantly elongated perpendicular to the projection of the GF in the camera. However, the peak of the DISP distribution is always centered at the source position. The extent of the elongation depends basically on the angle α between the shower axis and the direction of the GF. The influence of the GF on the DISP method is expected to degrade the quality of sky maps in a way that a point-like source appears to be extended. Apart from that the determination of the most probable source location from the DISP method should not be affected.

- **GF effects on the hadron induced background**: The influence of the GF on the other components of EAS is expected to be much smaller. The scattering angles of nuclear interactions result in a lateral displacement which is typically much larger than that produced by the influence of the GF [16].
  It is impossible to show the rotation effect using shower images from hadron candidates of real data, because they do not point to any source. Therefore, it is difficult to investigate the influence of the GF on the hadron induced background. However, possible GF effects on the hadron induced background presumably do not degrade the background discrimination.

The result from the MC studies presented in this note suggest that the influence of the GF can significantly reduce the γ/hadron separation capability, the imaging performance as well as the energy estimation of an IACT. Altogether, the GF is expected to affect the γ-ray sensitivity of an instrument and the determination of the γ-ray flux from a source. Furthermore, the MC studies on the GF effect indicate that appropriate MC datasets are not only required for the analysis of low-energy data but also for the reconstruction of VHE γ-rays of at least $1\,\mathrm{TeV}$. Therefore, the MAGIC MC library which is accessible for the standard analysis is certainly incomplete if the GF effects on EAS are taken into

consideration. So far, MC data were produced only for 0° and 90° azimuth angle, which is insufficient regarding the strong azimuthal dependence of the GF effects. The findings summarized in this note support that the standard MC library has to be extended to account for the GF effects. MC data should be produced with continuous ZA and azimuth angle distribution.
GF effects in real data from MAGIC were studied in [17, 18]. Is was shown that the pointing resolution of MAGIC enables us to demonstrate GF effects in real data even for a very low vertical component of the GF ($|\vec{B}_{\perp}| \approx 33\,\mu\mathrm{T}$). A more detailed study on GF effects in real data will be presented in a dedicated TDAS note.

A The ROOT implementation of a Cut to find GF Effects on the ALPHA Distribution in Real Data

```
void DrawALPHA(){

   TH1F *hAlphaBad  = (TH1F*)new TH1F("hAlphaBad","",45,0,90);
   TH1F *hAlphaGood = (TH1F*)new TH1F("hAlphaGood","",45,0,90);

   MGeomCamMagic mgeom;
   Double_t mm2deg = mgeom.GetConvMm2Deg();

   MHillas* mhillas = new MHillas();

   Float_t X = mm2deg*mhillas->GetMeanX();
   Float_t Y = mm2deg*mhillas->GetMeanY();

   MPointingPos* mpointingpos = new MPointingPos();

   // Get the current telescope pointing position
   Float_t az = mpointingpos->GetAz();
   Float_t zd = mpointingpos->GetZd();

   // Project the GF to the camera plane and determine the angle enclosed by
   // the projection of the GF and the x-axis of the camera coordinate system
   Float_t azb = btocam2(az,zd);

   Float_t d = 5; // Sectors have 10 deg opening angle


   // Fill histogram for the most unfavorable sector
   if(((TMath::Sign(1.,cos(TMath::DegToRad()*(d-azb)))*Y>-tan(TMath::DegToRad()*(d-azb))*TMath::Sign(1.,cos(TMath::DegToRad()*(d-azb)))*X) &&
       (TMath::Sign(1.,cos(TMath::DegToRad()*(d+azb)))*Y<tan(TMath::DegToRad()*(d+azb))*TMath::Sign(1.,cos(TMath::DegToRad()*(d+azb)))*X)) ||
      ((TMath::Sign(1.,cos(TMath::DegToRad()*(d-azb)))*Y<-tan(TMath::DegToRad()*(d-azb))*TMath::Sign(1.,cos(TMath::DegToRad()*(d-azb)))*X) &&
       (TMath::Sign(1.,cos(TMath::DegToRad()*(d+azb)))*Y>tan(TMath::DegToRad()*(d+azb))*TMath::Sign(1.,cos(TMath::DegToRad()*(d+azb)))*X)))
         hAlphaBad->Fill(TMath::Abs(Alpha));


   // Fill histogram for the favorable sector
   if(((tan(TMath::DegToRad()*(d+azb))*TMath::Sign(1.,sin(TMath::DegToRad()*(d+azb)))*Y>-TMath::Sign(1.,sin(TMath::DegToRad()*(d+azb)))*X) &&
       (tan(TMath::DegToRad()*(d-azb))*TMath::Sign(1.,sin(TMath::DegToRad()*(d-azb)))*Y<TMath::Sign(1.,sin(TMath::DegToRad()*(d-azb)))*X)) ||
      ((tan(TMath::DegToRad()*(d+azb))*TMath::Sign(1.,sin(TMath::DegToRad()*(d+azb)))*Y<-TMath::Sign(1.,sin(TMath::DegToRad()*(d+azb)))*X) &&
       (tan(TMath::DegToRad()*(d-azb))*TMath::Sign(1.,sin(TMath::DegToRad()*(d-azb)))*Y>TMath::Sign(1.,sin(TMath::DegToRad()*(d-azb)))*X)))
         hAlphaGood->Fill(TMath::Abs(Alpha));

}
```

```
Double_t btocam2(const Float_t phi = 0, const Float_t theta = 0)
{
    // Project the B-field to the camera plane and calculate the angle between
    // the B-field vector and the x-axis of the camera coordinate system

    // Relevant GF components at La Palma
    Float_t Bx = 29.5; // [muT]
    Float_t Bz = 23.0; // [muT]

    // Project the B-field and ransform from the reflector to the camera coordinate system
    Float_t Bx_r = TMath::Cos(TMath::DegToRad()*theta)*TMath::Cos(TMath::DegToRad()*phi)*Bx
                   -TMath::Sin(TMath::DegToRad()*theta)*Bz;
    Float_t By_r = -TMath::Sin(TMath::DegToRad()*phi)*Bx;

    Float_t Bx_c = -By_r;
    Float_t By_c = -Bx_r;


    // Normalize vector
    Float_t normB = TMath::Sqrt(Bx_c**2+By_c**2);

    if(normB>0)
    {
        Bx_c/=normB;
        By_c/=normB;
    }

    // Calculate the angle between the B-field vector and the x-axis of the camera coordinate system
    Double_t bangle = TMath::RadToDeg()*TMath::ASin(By_c);

    if(phi>180.)
        bangle=180.-bangle;

    return bangle;
}
```

B The Spreadsheets for Selected Image Parameters

$E_\gamma = 30\,\mathrm{GeV}$, Az = 0°, ZA = 0°, Intermediate Image Cleaning

$\delta_n[°]$	$\Delta\delta[°]$	DIST[°]	$\mathrm{RMS}_{\lvert\mathrm{ALPHA}\rvert}[°]$	$\delta_n[°]$	$\Delta\delta[°]$	DIST[°]	$\mathrm{RMS}_{\lvert\mathrm{ALPHA}\rvert}[°]$
IP = 60 m				**IP = 80 m**			
2.31 ± 0.44	$+6.39 \pm 0.83$	0.607 ± 0.015	18.6 (18.2)	0.75 ± 0.73	-2.56 ± 1.23	0.696 ± 0.017	20.5 (14.3)
25.79 ± 0.74	-5.18 ± 1.05	0.578 ± 0.004	22.3 (19.1)	29.41 ± 1.42	-3.51 ± 2.11	0.685 ± 0.012	16.4 (16.7)
58.39 ± 0.80	-6.62 ± 2.03	0.574 ± 0.015	21.6 (15.7)	58.75 ± 0.98	-0.74 ± 2.41	0.716 ± 0.016	13.1 (17.9)
87.34 ± 0.29	-11.60 ± 1.00	0.599 ± 0.006	19.4 (18.8)	88.58 ± 0.76	-0.05 ± 1.51	0.702 ± 0.007	15.9 (18.0)
125.13 ± 1.08	$+3.58 \pm 1.26$	0.583 ± 0.008	22.3 (8.9)	123.32 ± 0.41	$+0.50 \pm 0.96$	0.706 ± 0.002	18.8 (9.7)
151.76 ± 0.28	$+3.31 \pm 0.97$	0.588 ± 0.001	19.3 (13.1)	153.16 ± 0.14	$+2.34 \pm 1.41$	0.647 ± 0.012	14.0 (14.3)
177.93 ± 0.81	$+0.34 \pm 0.98$	0.568 ± 0.007	16.0 (16.2)	180.95 ± 0.68	-4.02 ± 1.48	0.683 ± 0.012	14.3 (17.2)
215.89 ± 0.62	$+8.14 \pm 1.32$	0.563 ± 0.004	20.4 (15.2)	215.05 ± 0.65	$+2.75 \pm 1.72$	0.681 ± 0.006	8.3 (13.1)
238.40 ± 1.07	-3.63 ± 1.42	0.581 ± 0.003	18.9 (18.7)	243.94 ± 0.67	$+7.29 \pm 0.98$	0.685 ± 0.014	18.8 (19.5)
271.53 ± 0.13	$+10.02 \pm 0.33$	0.599 ± 0.002	22.0 (23.0)	276.92 ± 1.84	$+3.57 \pm 2.18$	0.660 ± 0.006	23.1 (10.3)
300.62 ± 1.19	$+0.01 \pm 1.72$	0.578 ± 0.001	17.6 (18.3)	301.26 ± 1.49	-3.70 ± 1.80	0.676 ± 0.005	12.6 (12.3)
326.06 ± 0.57	-2.06 ± 1.59	0.598 ± 0.006	24.5 (19.1)	328.03 ± 0.27	$+2.49 \pm 1.49$	0.694 ± 0.004	17.5 (14.1)
IP = 100 m				**IP = 120 m**			
357.33 ± 0.61	-5.69 ± 1.29	0.782 ± 0.006	12.5 (12.9)	358.96 ± 0.91	-4.81 ± 2.08	0.755 ± 0.001	7.4 (8.6)
31.68 ± 0.54	-0.70 ± 2.32	0.745 ± 0.005	12.2 (15.0)	28.54 ± 0.70	-2.06 ± 1.86	0.756 ± 0.013	13.6 (12.3)
60.93 ± 1.00	$+2.58 \pm 1.15$	0.751 ± 0.001	19.1 (12.2)	60.48 ± 0.56	-1.95 ± 1.96	0.734 ± 0.007	10.8 (11.9)
87.96 ± 1.59	-4.62 ± 3.00	0.707 ± 0.007	16.1 (13.6)	89.83 ± 0.61	-0.85 ± 0.94	0.719 ± 0.006	9.4 (10.0)
121.65 ± 0.46	$+0.72 \pm 1.58$	0.716 ± 0.005	11.2 (10.6)	122.36 ± 0.80	$+3.95 \pm 1.54$	0.725 ± 0.012	9.8 (14.8)
151.72 ± 0.83	$+9.89 \pm 2.00$	0.741 ± 0.010	15.9 (11.5)	150.90 ± 0.84	$+7.49 \pm 1.26$	0.728 ± 0.006	8.9 (9.3)
182.29 ± 0.57	-4.36 ± 0.90	0.758 ± 0.010	13.7 (16.1)	180.86 ± 0.84	-0.91 ± 1.97	0.769 ± 0.005	13.0 (10.4)
211.19 ± 0.96	$+2.61 \pm 1.94$	0.750 ± 0.008	11.7 (13.4)	210.83 ± 1.00	-0.36 ± 1.67	0.728 ± 0.007	9.2 (10.6)
238.44 ± 0.42	-1.04 ± 1.78	0.740 ± 0.005	10.1 (13.5)	240.39 ± 0.71	-1.86 ± 1.65	0.726 ± 0.006	10.3 (9.5)
267.08 ± 0.87	-3.16 ± 1.43	0.729 ± 0.002	14.1 (17.0)	270.36 ± 0.82	$+1.66 \pm 2.15$	0.708 ± 0.009	11.3 (11.2)
298.88 ± 1.22	$+2.04 \pm 1.89$	0.747 ± 0.008	15.1 (12.8)	299.61 ± 0.30	$+6.23 \pm 0.99$	0.736 ± 0.011	14.5 (7.5)
330.59 ± 1.20	$+6.56 \pm 2.15$	0.755 ± 0.007	16.4 (18.2)	329.41 ± 0.36	$+3.69 \pm 2.10$	0.761 ± 0.009	11.3 (7.9)

Table 8: The nominal angle δ_n, average displacement $\Delta\delta$, average value of the parameter DIST, RMS of the ALPHA distribution for enabled GF and impact parameters between 60 m and 120 m. The RMS of the ALPHA distribution for disabled GF is given parentheses. The primary γ-ray energy was set to 30 GeV, the ZA to 0° and the azimuth angle to 0°.

$E_\gamma = 30\,\mathrm{GeV}$, Az = 0°, ZA = 20°, Intermediate Image Cleaning

$\delta_n[°]$	$\Delta\delta[°]$	DIST[°]	$\mathrm{RMS}_{\lvert\mathrm{ALPHA}\rvert}[°]$	$\delta_n[°]$	$\Delta\delta[°]$	DIST[°]	$\mathrm{RMS}_{\lvert\mathrm{ALPHA}\rvert}[°]$
IP = 60 m				**IP = 80 m**			
1.02 ± 1.17	-5.25 ± 1.86	0.524 ± 0.002	15.9 (20.2)	357.87 ± 0.22	-3.14 ± 0.46	0.695 ± 0.010	24.6 (15.3)
25.76 ± 0.49	-7.55 ± 0.71	0.523 ± 0.004	21.7 (16.8)	30.29 ± 1.01	$+10.40 \pm 1.45$	0.670 ± 0.002	21.8 (17.6)
59.25 ± 0.39	$+0.68 \pm 0.67$	0.588 ± 0.007	16.4 (21.1)	54.64 ± 2.13	$+0.72 \pm 2.36$	0.681 ± 0.012	20.5 (8.1)
80.50 ± 1.58	-6.53 ± 2.02	0.528 ± 0.005	15.9 (21.8)	96.26 ± 0.20	$+9.03 \pm 1.43$	0.665 ± 0.003	17.3 (12.7)
116.09 ± 0.22	-4.44 ± 0.84	0.530 ± 0.003	22.9 (19.5)	129.02 ± 1.04	$+10.41 \pm 1.27$	0.652 ± 0.002	15.1 (14.5)
159.77 ± 0.20	$+4.13 \pm 0.68$	0.528 ± 0.016	26.1 (14.0)	152.09 ± 1.14	-0.24 ± 1.82	0.673 ± 0.004	14.5 (14.5)
184.17 ± 0.43	-3.80 ± 0.96	0.609 ± 0.002	10.4 (8.8)	182.83 ± 0.20	-2.32 ± 1.39	0.717 ± 0.002	6.6 (10.1)
207.80 ± 2.10	$+9.51 \pm 4.27$	0.578 ± 0.006	23.5 (15.2)	214.11 ± 0.37	$+4.77 \pm 1.08$	0.682 ± 0.008	13.5 (19.6)
232.03 ± 0.84	-3.35 ± 1.07	0.574 ± 0.019	20.3 (14.6)	233.85 ± 0.67	-5.51 ± 2.04	0.700 ± 0.008	20.7 (16.6)
267.21 ± 0.24	$+1.05 \pm 0.48$	0.554 ± 0.004	19.3 (14.3)	273.15 ± 0.37	$+5.69 \pm 1.41$	0.695 ± 0.002	12.1 (11.0)
295.36 ± 0.48	-13.35 ± 1.76	0.614 ± 0.011	19.6 (20.2)	302.33 ± 0.20	-0.92 ± 0.73	0.713 ± 0.007	13.2 (19.4)
332.12 ± 0.40	$+7.42 \pm 0.65$	0.560 ± 0.002	15.1 (20.4)	338.81 ± 0.97	$+7.57 \pm 1.45$	0.719 ± 0.004	9.1 (12.4)
IP = 100 m				**IP = 120 m**			
359.26 ± 1.09	$+6.12 \pm 2.85$	0.758 ± 0.005	18.1 (11.5)	359.28 ± 1.19	-1.28 ± 1.89	0.736 ± 0.013	8.9 (13.8)
30.78 ± 1.28	$+2.18 \pm 1.66$	0.750 ± 0.021	12.5 (9.5)	28.75 ± 0.46	-0.70 ± 1.91	0.716 ± 0.002	13.6 (13.2)
58.84 ± 0.19	$+1.55 \pm 0.56$	0.720 ± 0.011	11.9 (12.7)	59.36 ± 0.13	-0.98 ± 1.52	0.733 ± 0.003	18.7 (15.8)
94.78 ± 0.88	$+2.62 \pm 1.45$	0.729 ± 0.014	14.9 (18.6)	89.29 ± 0.72	$+2.49 \pm 1.58$	0.698 ± 0.001	17.8 (10.8)
125.30 ± 0.19	$+2.85 \pm 2.87$	0.713 ± 0.003	17.5 (10.4)	122.09 ± 1.44	$+0.32 \pm 2.41$	0.732 ± 0.003	10.6 (8.2)
153.00 ± 1.06	$+0.68 \pm 1.24$	0.707 ± 0.015	14.0 (16.7)	153.40 ± 0.61	-1.21 ± 1.05	0.740 ± 0.007	15.4 (13.7)
173.93 ± 0.90	-7.06 ± 3.35	0.790 ± 0.002	6.0 (20.3)	179.01 ± 0.52	$+0.47 \pm 1.15$	0.737 ± 0.003	17.0 (10.9)
208.32 ± 1.01	$+3.59 \pm 3.78$	0.754 ± 0.012	10.3 (12.0)	207.93 ± 0.36	-1.78 ± 0.51	0.722 ± 0.013	9.4 (11.5)
239.79 ± 0.83	$+0.52 \pm 1.97$	0.723 ± 0.010	9.9 (12.3)	239.70 ± 0.65	-3.91 ± 0.96	0.749 ± 0.001	10.9 (10.4)
262.07 ± 0.55	-10.89 ± 1.69	0.741 ± 0.010	20.8 (21.8)	268.91 ± 0.57	-4.87 ± 1.28	0.672 ± 0.009	14.8 (16.7)
302.75 ± 0.95	$+1.89 \pm 1.75$	0.716 ± 0.012	15.6 (10.1)	301.15 ± 0.41	$+4.33 \pm 1.66$	0.716 ± 0.007	17.6 (12.5)
333.24 ± 1.09	$+4.26 \pm 1.28$	0.730 ± 0.002	15.6 (9.4)	330.92 ± 0.51	-2.21 ± 1.34	0.720 ± 0.007	11.8 (14.0)

Table 9: The nominal angle δ_n, average displacement $\Delta\delta$, average value of the parameter DIST, RMS of the ALPHA distribution for enabled GF and impact parameters between 60 m and 120 m. The RMS of the ALPHA distribution for disabled GF is given parentheses. The primary γ-ray energy was set to 30 GeV, the ZA to 20° and the azimuth angle to 0°.

$E_\gamma = 30\,\mathrm{GeV}$, Az = 30°, ZA = 20°, Intermediate Image Cleaning

$\delta_n[°]$	$\Delta\delta[°]$	DIST[°]	$\mathrm{RMS}_{\lvert\mathrm{ALPHA}\rvert}[°]$	$\delta_n[°]$	$\Delta\delta[°]$	DIST[°]	$\mathrm{RMS}_{\lvert\mathrm{ALPHA}\rvert}[°]$
IP = 60 m				**IP = 80 m**			
1.02 ± 1.17	$+1.32 \pm 1.84$	0.550 ± 0.004	17.5 (20.2)	357.87 ± 0.22	-1.26 ± 1.09	0.731 ± 0.006	19.9 (15.3)
25.76 ± 0.49	-7.34 ± 2.18	0.610 ± 0.004	13.7 (16.8)	30.29 ± 1.01	$+8.99 \pm 2.59$	0.726 ± 0.009	17.0 (17.6)
59.25 ± 0.39	$+5.55 \pm 1.93$	0.643 ± 0.029	14.7 (21.1)	54.64 ± 2.13	$+0.19 \pm 2.38$	0.722 ± 0.006	15.9 (8.1)
80.50 ± 1.58	-12.16 ± 1.87	0.629 ± 0.004	19.3 (21.8)	96.26 ± 0.20	-2.35 ± 0.70	0.664 ± 0.008	17.6 (12.7)
116.09 ± 0.22	-5.06 ± 0.48	0.634 ± 0.002	18.8 (19.5)	129.02 ± 1.04	$+6.95 \pm 1.28$	0.711 ± 0.005	16.9 (14.5)
159.77 ± 0.20	$+12.97 \pm 2.07$	0.609 ± 0.017	17.9 (14.0)	152.09 ± 1.14	$+7.83 \pm 2.67$	0.730 ± 0.002	19.3 (14.5)
184.17 ± 0.43	-2.59 ± 0.66	0.563 ± 0.012	16.4 (8.8)	182.83 ± 0.20	$+10.95 \pm 0.93$	0.725 ± 0.012	19.4 (10.1)
207.80 ± 2.10	-7.60 ± 2.83	0.608 ± 0.004	17.6 (15.2)	214.11 ± 0.37	$+5.07 \pm 0.62$	0.679 ± 0.002	18.5 (19.6)
232.03 ± 0.84	-10.03 ± 1.08	0.619 ± 0.010	17.0 (14.6)	233.85 ± 0.67	-5.29 ± 0.89	0.676 ± 0.013	15.5 (16.6)
267.21 ± 0.24	-13.10 ± 2.45	0.638 ± 0.002	19.5 (14.3)	273.15 ± 0.37	$+6.30 \pm 1.28$	0.676 ± 0.009	18.5 (11.0)
295.36 ± 0.48	-7.36 ± 0.95	0.615 ± 0.005	18.4 (20.2)	302.33 ± 0.20	-13.69 ± 0.76	0.666 ± 0.005	17.9 (19.4)
332.12 ± 0.40	$+2.32 \pm 0.61$	0.595 ± 0.002	17.3 (20.4)	338.81 ± 0.97	$+4.19 \pm 2.23$	0.693 ± 0.009	15.9 (12.4)
IP = 100 m				**IP = 120 m**			
359.26 ± 1.09	$+3.98 \pm 1.31$	0.766 ± 0.005	15.0 (11.5)	359.28 ± 1.19	-0.99 ± 1.78	0.733 ± 0.005	15.3 (13.8)
30.78 ± 1.28	$+6.30 \pm 2.33$	0.719 ± 0.012	14.2 (9.5)	28.75 ± 0.46	-0.22 ± 1.71	0.740 ± 0.001	16.6 (13.2)
58.84 ± 0.19	-4.58 ± 1.21	0.702 ± 0.002	16.4 (12.7)	59.36 ± 0.13	$+4.18 \pm 0.62$	0.739 ± 0.012	14.8 (15.8)
94.78 ± 0.88	$+4.32 \pm 2.23$	0.701 ± 0.006	24.1 (18.6)	89.29 ± 0.72	-0.40 ± 2.13	0.701 ± 0.010	17.4 (10.8)
125.30 ± 0.19	$+4.64 \pm 1.54$	0.696 ± 0.019	19.1 (10.4)	122.09 ± 1.44	$+0.02 \pm 1.85$	0.678 ± 0.010	14.8 (8.2)
153.00 ± 1.06	-1.41 ± 1.26	0.761 ± 0.004	12.5 (16.7)	153.40 ± 0.61	$+0.53 \pm 1.34$	0.704 ± 0.009	15.8 (13.7)
173.93 ± 0.90	-13.69 ± 1.12	0.748 ± 0.006	16.2 (20.3)	179.01 ± 0.52	$+0.11 \pm 1.87$	0.738 ± 0.006	14.4 (10.9)
208.32 ± 1.01	-2.85 ± 1.40	0.714 ± 0.003	17.6 (12.0)	207.93 ± 0.36	$+1.36 \pm 1.29$	0.779 ± 0.004	11.4 (11.5)
239.79 ± 0.83	$+0.67 \pm 3.66$	0.743 ± 0.003	12.7 (12.3)	239.70 ± 0.65	$+2.96 \pm 1.16$	0.711 ± 0.006	15.6 (10.4)
262.07 ± 0.55	-10.06 ± 1.38	0.706 ± 0.007	17.0 (21.8)	268.91 ± 0.57	-2.63 ± 1.92	0.692 ± 0.009	14.3 (16.7)
302.75 ± 0.95	$+2.02 \pm 2.89$	0.708 ± 0.005	19.6 (10.1)	301.15 ± 0.41	$+0.34 \pm 1.35$	0.693 ± 0.003	16.5 (12.5)
333.24 ± 1.09	$+2.59 \pm 1.31$	0.758 ± 0.013	18.0 (9.4)	330.92 ± 0.51	$+0.15 \pm 1.76$	0.735 ± 0.009	12.5 (14.0)

Table 10: The nominal angle δ_n, average displacement $\Delta\delta$, average value of the parameter DIST, RMS of the ALPHA distribution for enabled GF and impact parameters between 60 m and 120 m. The RMS of the ALPHA distribution for disabled GF is given parentheses. The primary γ-ray energy was set to 30 GeV, the ZA to 20° and the azimuth angle to 30°.

$E_\gamma = 30\,\mathrm{GeV}$, Az = 60°, ZA = 20°, Intermediate Image Cleaning

$\delta_n[°]$	$\Delta\delta[°]$	DIST[°]	$\mathrm{RMS}_{\lvert\mathrm{ALPHA}\rvert}[°]$	$\delta_n[°]$	$\Delta\delta[°]$	DIST[°]	$\mathrm{RMS}_{\lvert\mathrm{ALPHA}\rvert}[°]$
IP = 60 m				**IP = 80 m**			
1.02 ± 1.17	-2.28 ± 1.65	0.632 ± 0.004	18.2 (20.2)	357.87 ± 0.22	$+10.63 \pm 1.94$	0.685 ± 0.004	16.4 (15.3)
25.76 ± 0.49	-1.90 ± 0.73	0.618 ± 0.020	20.2 (16.8)	30.29 ± 1.01	-0.09 ± 2.27	0.725 ± 0.011	14.0 (17.6)
59.25 ± 0.39	$+3.17 \pm 0.85$	0.685 ± 0.012	22.4 (21.1)	54.64 ± 2.13	-2.72 ± 4.29	0.721 ± 0.003	16.5 (8.1)
80.50 ± 1.58	-10.00 ± 1.99	0.626 ± 0.010	17.7 (21.8)	96.26 ± 0.20	$+11.49 \pm 0.89$	0.719 ± 0.008	20.4 (12.7)
116.09 ± 0.22	-14.28 ± 0.92	0.648 ± 0.010	17.8 (19.5)	129.02 ± 1.04	$+4.17 \pm 2.47$	0.747 ± 0.011	14.3 (14.5)
159.77 ± 0.20	$+6.78 \pm 1.67$	0.686 ± 0.002	16.5 (14.0)	152.09 ± 1.14	$+4.37 \pm 1.85$	0.767 ± 0.010	12.2 (14.5)
184.17 ± 0.43	$+3.18 \pm 2.27$	0.632 ± 0.010	22.5 (8.8)	182.83 ± 0.20	$+1.06 \pm 0.43$	0.748 ± 0.004	12.9 (10.1)
207.80 ± 2.10	-0.26 ± 2.75	0.636 ± 0.004	21.0 (15.2)	214.11 ± 0.37	$+6.01 \pm 0.57$	0.701 ± 0.002	19.1 (19.6)
232.03 ± 0.84	-12.21 ± 1.46	0.633 ± 0.002	16.5 (14.6)	233.85 ± 0.67	-3.40 ± 1.31	0.728 ± 0.007	16.6 (16.6)
267.21 ± 0.24	-1.67 ± 1.09	0.632 ± 0.009	19.1 (14.3)	273.15 ± 0.37	$+7.74 \pm 0.58$	0.736 ± 0.007	19.6 (11.0)
295.36 ± 0.48	$+3.87 \pm 1.99$	0.666 ± 0.004	21.3 (20.2)	302.33 ± 0.20	$+4.86 \pm 0.61$	0.739 ± 0.013	17.4 (19.4)
332.12 ± 0.40	$+8.51 \pm 0.62$	0.623 ± 0.004	19.5 (20.4)	338.81 ± 0.97	$+6.26 \pm 2.18$	0.749 ± 0.017	20.8 (12.4)
IP = 100 m				**IP = 120 m**			
359.26 ± 1.09	-3.04 ± 1.69	0.771 ± 0.014	12.4 (11.5)	359.28 ± 1.19	$+2.05 \pm 2.82$	0.780 ± 0.010	10.2 (13.8)
30.78 ± 1.28	$+3.19 \pm 2.05$	0.765 ± 0.007	18.4 (9.5)	28.75 ± 0.46	$+0.72 \pm 1.04$	0.767 ± 0.004	12.1 (13.2)
58.84 ± 0.19	-0.24 ± 1.22	0.775 ± 0.004	20.8 (12.7)	59.36 ± 0.13	-3.44 ± 0.91	0.770 ± 0.006	13.8 (15.8)
94.78 ± 0.88	-1.51 ± 1.53	0.725 ± 0.002	18.6 (18.6)	89.29 ± 0.72	-2.42 ± 1.08	0.702 ± 0.006	14.4 (10.8)
125.30 ± 0.19	-2.13 ± 1.08	0.728 ± 0.008	16.5 (10.4)	122.09 ± 1.44	$+1.51 \pm 2.51$	0.692 ± 0.001	11.8 (8.2)
153.00 ± 1.06	$+7.03 \pm 4.21$	0.738 ± 0.003	16.1 (16.7)	153.40 ± 0.61	$+0.46 \pm 2.39$	0.722 ± 0.002	12.8 (13.7)
173.93 ± 0.90	-8.60 ± 3.24	0.791 ± 0.002	13.9 (20.3)	179.01 ± 0.52	$+0.77 \pm 1.09$	0.778 ± 0.002	15.4 (10.9)
208.32 ± 1.01	-2.26 ± 1.20	0.766 ± 0.002	18.2 (12.0)	207.93 ± 0.36	$+2.46 \pm 1.81$	0.764 ± 0.005	13.3 (11.5)
239.79 ± 0.83	-0.96 ± 1.98	0.778 ± 0.004	17.8 (12.3)	239.70 ± 0.65	$+1.81 \pm 0.84$	0.745 ± 0.013	16.1 (10.4)
262.07 ± 0.55	-4.12 ± 0.76	0.715 ± 0.002	21.0 (21.8)	268.91 ± 0.57	-1.67 ± 0.77	0.687 ± 0.002	17.7 (16.7)
302.75 ± 0.95	$+1.76 \pm 1.84$	0.744 ± 0.005	18.5 (10.1)	301.15 ± 0.41	$+5.21 \pm 2.17$	0.722 ± 0.001	16.8 (12.5)
333.24 ± 1.09	$+5.75 \pm 1.84$	0.750 ± 0.010	18.2 (9.4)	330.92 ± 0.51	-2.92 ± 1.44	0.731 ± 0.006	13.5 (14.0)

Table 11: The nominal angle δ_n, average displacement $\Delta\delta$, average value of the parameter DIST, RMS of the ALPHA distribution for enabled GF and impact parameters between 60 m and 120 m. The RMS of the ALPHA distribution for disabled GF is given parentheses. The primary γ-ray energy was set to 30 GeV, the ZA to 20° and the azimuth angle to 60°.

$E_\gamma = 30\,\mathrm{GeV}$, Az = 90°, ZA = 20°, Intermediate Image Cleaning

$\delta_n[°]$	$\Delta\delta[°]$	DIST[°]	$\mathrm{RMS}_{\lvert\mathrm{ALPHA}\rvert}[°]$	$\delta_n[°]$	$\Delta\delta[°]$	DIST[°]	$\mathrm{RMS}_{\lvert\mathrm{ALPHA}\rvert}[°]$
IP = 60 m				**IP = 80 m**			
1.02 ± 1.17	-1.67 ± 1.43	0.672 ± 0.002	21.6 (20.2)	357.87 ± 0.22	-9.24 ± 0.45	0.678 ± 0.004	12.1 (15.3)
25.76 ± 0.49	$+0.45 \pm 0.91$	0.587 ± 0.006	19.8 (16.8)	30.29 ± 1.01	$+0.34 \pm 1.22$	0.668 ± 0.006	16.5 (17.6)
59.25 ± 0.39	-1.45 ± 1.87	0.610 ± 0.005	16.5 (21.1)	54.64 ± 2.13	-11.59 ± 3.31	0.719 ± 0.006	14.1 (8.1)
80.50 ± 1.58	-11.98 ± 5.15	0.602 ± 0.002	18.9 (21.8)	96.26 ± 0.20	$+0.98 \pm 1.38$	0.725 ± 0.004	19.2 (12.7)
116.09 ± 0.22	-12.44 ± 1.66	0.596 ± 0.013	24.0 (19.5)	129.02 ± 1.04	$+9.40 \pm 1.49$	0.761 ± 0.013	14.5 (14.5)
159.77 ± 0.20	$+8.12 \pm 1.59$	0.577 ± 0.004	25.7 (14.0)	152.09 ± 1.14	$+5.76 \pm 3.01$	0.673 ± 0.012	13.2 (14.5)
184.17 ± 0.43	-5.64 ± 5.19	0.570 ± 0.008	24.3 (8.8)	182.83 ± 0.20	-1.90 ± 0.86	0.700 ± 0.002	10.3 (10.1)
207.80 ± 2.10	-2.39 ± 3.93	0.578 ± 0.022	26.3 (15.2)	214.11 ± 0.37	-2.91 ± 0.62	0.726 ± 0.004	13.4 (19.6)
232.03 ± 0.84	$+4.12 \pm 1.58$	0.640 ± 0.013	18.7 (14.6)	233.85 ± 0.67	-6.17 ± 1.29	0.718 ± 0.009	15.0 (16.6)
267.21 ± 0.24	-3.48 ± 0.48	0.644 ± 0.004	19.7 (14.3)	273.15 ± 0.37	$+6.42 \pm 1.75$	0.688 ± 0.016	20.4 (11.0)
295.36 ± 0.48	-13.04 ± 0.72	0.593 ± 0.014	25.2 (20.2)	302.33 ± 0.20	$+2.66 \pm 0.45$	0.761 ± 0.002	16.2 (19.4)
332.12 ± 0.40	$+0.89 \pm 1.73$	0.588 ± 0.014	13.5 (20.4)	338.81 ± 0.97	-1.69 ± 2.94	0.674 ± 0.016	16.8 (12.4)
IP = 100 m				**IP = 120 m**			
359.26 ± 1.09	$+1.37 \pm 1.28$	0.759 ± 0.008	18.8 (11.5)	359.28 ± 1.19	-0.35 ± 2.64	0.781 ± 0.003	15.9 (13.8)
30.78 ± 1.28	$+1.66 \pm 2.04$	0.740 ± 0.011	14.8 (9.5)	28.75 ± 0.46	$+2.84 \pm 1.83$	0.788 ± 0.012	16.2 (13.2)
58.84 ± 0.19	-2.68 ± 0.82	0.761 ± 0.008	17.5 (12.7)	59.36 ± 0.13	$+0.89 \pm 0.46$	0.717 ± 0.006	13.9 (15.8)
94.78 ± 0.88	$+7.65 \pm 1.68$	0.742 ± 0.008	16.7 (18.6)	89.29 ± 0.72	$+3.46 \pm 1.11$	0.724 ± 0.004	15.4 (10.8)
125.30 ± 0.19	$+2.09 \pm 1.94$	0.773 ± 0.010	22.0 (10.4)	122.09 ± 1.44	$+2.90 \pm 2.66$	0.737 ± 0.010	10.2 (8.2)
153.00 ± 1.06	-1.19 ± 1.26	0.790 ± 0.008	15.2 (16.7)	153.40 ± 0.61	-0.91 ± 1.08	0.795 ± 0.004	9.8 (13.7)
173.93 ± 0.90	-10.08 ± 1.30	0.750 ± 0.005	17.2 (20.3)	179.01 ± 0.52	-1.72 ± 1.45	0.801 ± 0.002	11.7 (10.9)
208.32 ± 1.01	-1.35 ± 1.79	0.777 ± 0.005	13.9 (12.0)	207.93 ± 0.36	-0.43 ± 1.51	0.790 ± 0.004	13.2 (11.5)
239.79 ± 0.83	-2.26 ± 2.11	0.795 ± 0.013	15.0 (12.3)	239.70 ± 0.65	$+4.12 \pm 1.52$	0.749 ± 0.008	11.2 (10.4)
262.07 ± 0.55	-6.19 ± 1.57	0.758 ± 0.009	10.7 (21.8)	268.91 ± 0.57	-0.96 ± 1.16	0.710 ± 0.004	15.0 (16.7)
302.75 ± 0.95	$+4.26 \pm 1.92$	0.735 ± 0.006	16.1 (10.1)	301.15 ± 0.41	-1.15 ± 0.58	0.690 ± 0.006	10.7 (12.5)
333.24 ± 1.09	-1.36 ± 2.69	0.772 ± 0.011	15.2 (9.4)	330.92 ± 0.51	$+1.39 \pm 0.67$	0.784 ± 0.015	11.0 (14.0)

Table 12: The nominal angle δ_n, average displacement $\Delta\delta$, average value of the parameter DIST, RMS of the ALPHA distribution for enabled GF and impact parameters between 60 m and 120 m. The RMS of the ALPHA distribution for disabled GF is given parentheses. The primary γ-ray energy was set to 30 GeV, the ZA to 20° and the azimuth angle to 90°.

$E_\gamma = 30\,\mathrm{GeV}$, Az = 120°, ZA = 20°, Intermediate Image Cleaning

$\delta_n[°]$	$\Delta\delta[°]$	DIST[°]	$\mathrm{RMS}_{\lvert\mathrm{ALPHA}\rvert}[°]$	$\delta_n[°]$	$\Delta\delta[°]$	DIST[°]	$\mathrm{RMS}_{\lvert\mathrm{ALPHA}\rvert}[°]$
IP = 60 m				**IP = 80 m**			
1.02 ± 1.17	$+0.87 \pm 2.21$	0.559 ± 0.007	26.3 (20.2)	357.87 ± 0.22	$+1.09 \pm 0.97$	0.701 ± 0.002	12.4 (15.3)
25.76 ± 0.49	-4.73 ± 1.70	0.611 ± 0.010	18.7 (16.8)	30.29 ± 1.01	$+3.33 \pm 1.62$	0.733 ± 0.006	18.0 (17.6)
59.25 ± 0.39	$+8.84 \pm 0.67$	0.672 ± 0.002	22.1 (21.1)	54.64 ± 2.13	$+0.62 \pm 2.62$	0.743 ± 0.007	15.6 (8.1)
80.50 ± 1.58	-6.90 ± 2.06	0.661 ± 0.002	23.1 (21.8)	96.26 ± 0.20	$+10.30 \pm 0.94$	0.739 ± 0.006	20.5 (12.7)
116.09 ± 0.22	-13.67 ± 0.43	0.664 ± 0.007	17.5 (19.5)	129.02 ± 1.04	$+0.19 \pm 2.46$	0.768 ± 0.005	14.2 (14.5)
159.77 ± 0.20	$+16.64 \pm 1.68$	0.618 ± 0.009	21.5 (14.0)	152.09 ± 1.14	-5.22 ± 2.67	0.709 ± 0.010	18.8 (14.5)
184.17 ± 0.43	-0.70 ± 0.96	0.594 ± 0.012	17.3 (8.8)	182.83 ± 0.20	-6.73 ± 1.09	0.696 ± 0.006	13.9 (10.1)
207.80 ± 2.10	$+0.23 \pm 2.36$	0.621 ± 0.004	18.1 (15.2)	214.11 ± 0.37	$+16.63 \pm 0.61$	0.756 ± 0.002	10.6 (19.6)
232.03 ± 0.84	-16.32 ± 2.14	0.657 ± 0.013	23.5 (14.6)	233.85 ± 0.67	-11.20 ± 1.48	0.706 ± 0.004	14.4 (16.6)
267.21 ± 0.24	$+1.72 \pm 1.87$	0.624 ± 0.008	19.2 (14.3)	273.15 ± 0.37	-0.17 ± 1.06	0.711 ± 0.002	20.2 (11.0)
295.36 ± 0.48	-15.54 ± 0.72	0.619 ± 0.007	21.6 (20.2)	302.33 ± 0.20	$+5.89 \pm 1.16$	0.721 ± 0.002	16.4 (19.4)
332.12 ± 0.40	-4.50 ± 4.57	0.613 ± 0.002	17.7 (20.4)	338.81 ± 0.97	-4.04 ± 1.51	0.731 ± 0.004	15.1 (12.4)
IP = 100 m				**IP = 120 m**			
359.26 ± 1.09	-4.32 ± 1.58	0.756 ± 0.002	18.0 (11.5)	359.28 ± 1.19	$+1.46 \pm 1.76$	0.780 ± 0.006	13.9 (13.8)
30.78 ± 1.28	$+8.28 \pm 3.47$	0.807 ± 0.008	14.0 (9.5)	28.75 ± 0.46	-2.42 ± 0.63	0.743 ± 0.004	14.4 (13.2)
58.84 ± 0.19	-1.15 ± 0.40	0.841 ± 0.009	11.9 (12.7)	59.36 ± 0.13	$+3.95 \pm 0.77$	0.719 ± 0.008	14.9 (15.8)
94.78 ± 0.88	$+14.50 \pm 1.10$	0.789 ± 0.004	20.4 (18.6)	89.29 ± 0.72	$+1.32 \pm 2.30$	0.710 ± 0.003	18.6 (10.8)
125.30 ± 0.19	$+6.23 \pm 0.80$	0.800 ± 0.003	20.4 (10.4)	122.09 ± 1.44	-0.95 ± 2.66	0.744 ± 0.018	15.9 (8.2)
153.00 ± 1.06	$+6.36 \pm 1.30$	0.788 ± 0.007	18.5 (16.7)	153.40 ± 0.61	$+0.31 \pm 1.05$	0.778 ± 0.009	18.1 (13.7)
173.93 ± 0.90	-9.95 ± 1.58	0.786 ± 0.002	13.2 (20.3)	179.01 ± 0.52	-3.05 ± 0.71	0.759 ± 0.017	12.2 (10.9)
208.32 ± 1.01	-5.13 ± 2.50	0.756 ± 0.004	16.1 (12.0)	207.93 ± 0.36	$+1.95 \pm 1.72$	0.767 ± 0.016	17.5 (11.5)
239.79 ± 0.83	$+1.75 \pm 1.45$	0.780 ± 0.010	13.1 (12.3)	239.70 ± 0.65	$+2.46 \pm 1.33$	0.747 ± 0.003	10.4 (10.4)
262.07 ± 0.55	-14.70 ± 0.78	0.802 ± 0.004	14.2 (21.8)	268.91 ± 0.57	$+1.72 \pm 1.69$	0.698 ± 0.004	13.3 (16.7)
302.75 ± 0.95	$+1.53 \pm 3.24$	0.790 ± 0.011	13.8 (10.1)	301.15 ± 0.41	-6.73 ± 1.99	0.731 ± 0.008	15.9 (12.5)
333.24 ± 1.09	-5.04 ± 1.52	0.784 ± 0.017	16.8 (9.4)	330.92 ± 0.51	-3.77 ± 1.68	0.758 ± 0.020	16.7 (14.0)

Table 13: The nominal angle δ_n, average displacement $\Delta\delta$, average value of the parameter DIST, RMS of the ALPHA distribution for enabled GF and impact parameters between 60 m and 120 m. The RMS of the ALPHA distribution for disabled GF is given parentheses. The primary γ-ray energy was set to 30 GeV, the ZA to 20° and the azimuth angle to 120°.

$E_\gamma = 30\,\mathrm{GeV}$, Az = 150°, ZA = 20°, Intermediate Image Cleaning

$\delta_n[°]$	$\Delta\delta[°]$	DIST[°]	$\mathrm{RMS}_{\vert\mathrm{ALPHA}\vert}[°]$	$\delta_n[°]$	$\Delta\delta[°]$	DIST[°]	$\mathrm{RMS}_{\vert\mathrm{ALPHA}\vert}[°]$
IP = 60 m				**IP = 80 m**			
1.02 ± 1.17	$+2.94 \pm 1.47$	0.631 ± 0.008	17.7 (20.2)	357.87 ± 0.22	-15.58 ± 1.00	0.779 ± 0.002	18.4 (15.3)
25.76 ± 0.49	-5.48 ± 0.75	0.645 ± 0.002	16.7 (16.8)	30.29 ± 1.01	$+6.47 \pm 1.23$	0.725 ± 0.015	19.1 (17.6)
59.25 ± 0.39	$+16.91 \pm 0.64$	0.638 ± 0.004	14.4 (21.1)	54.64 ± 2.13	$+1.80 \pm 3.03$	0.734 ± 0.004	18.9 (8.1)
80.50 ± 1.58	-10.06 ± 3.27	0.618 ± 0.002	17.6 (21.8)	96.26 ± 0.20	$+8.36 \pm 0.47$	0.700 ± 0.032	19.2 (12.7)
116.09 ± 0.22	-0.56 ± 1.85	0.600 ± 0.005	10.6 (19.5)	129.02 ± 1.04	$+5.34 \pm 1.31$	0.717 ± 0.002	19.9 (14.5)
159.77 ± 0.20	$+5.70 \pm 1.15$	0.596 ± 0.005	17.6 (14.0)	152.09 ± 1.14	$+0.59 \pm 5.13$	0.720 ± 0.004	14.1 (14.5)
184.17 ± 0.43	-2.16 ± 3.65	0.654 ± 0.005	16.9 (8.8)	182.83 ± 0.20	-0.89 ± 0.56	0.781 ± 0.002	12.0 (10.1)
207.80 ± 2.10	-7.54 ± 3.40	0.674 ± 0.013	16.4 (15.2)	214.11 ± 0.37	$+0.93 \pm 2.27$	0.774 ± 0.002	16.1 (19.6)
232.03 ± 0.84	-11.55 ± 1.56	0.691 ± 0.002	16.2 (14.6)	233.85 ± 0.67	-4.62 ± 2.36	0.673 ± 0.006	17.1 (16.6)
267.21 ± 0.24	-4.56 ± 4.34	0.596 ± 0.010	23.1 (14.3)	273.15 ± 0.37	-4.69 ± 1.11	0.782 ± 0.013	11.3 (11.0)
295.36 ± 0.48	-9.00 ± 1.57	0.605 ± 0.012	23.9 (20.2)	302.33 ± 0.20	$+3.68 \pm 0.94$	0.747 ± 0.005	15.0 (19.4)
332.12 ± 0.40	-1.17 ± 0.96	0.668 ± 0.007	15.4 (20.4)	338.81 ± 0.97	$+7.96 \pm 2.04$	0.736 ± 0.002	22.3 (12.4)
IP = 100 m				**IP = 120 m**			
359.26 ± 1.09	-4.21 ± 1.67	0.782 ± 0.007	12.4 (11.5)	359.28 ± 1.19	-0.96 ± 2.97	0.782 ± 0.002	16.7 (13.8)
30.78 ± 1.28	$+16.91 \pm 2.48$	0.807 ± 0.004	16.2 (9.5)	28.75 ± 0.46	$+2.48 \pm 0.95$	0.792 ± 0.003	11.6 (13.2)
58.84 ± 0.19	$+6.59 \pm 1.17$	0.798 ± 0.004	16.4 (12.7)	59.36 ± 0.13	$+3.40 \pm 0.75$	0.746 ± 0.005	15.0 (15.8)
94.78 ± 0.88	$+11.06 \pm 1.60$	0.752 ± 0.002	17.0 (18.6)	89.29 ± 0.72	$+3.23 \pm 0.91$	0.738 ± 0.004	14.9 (10.8)
125.30 ± 0.19	$+16.06 \pm 4.19$	0.745 ± 0.018	18.8 (10.4)	122.09 ± 1.44	$+0.20 \pm 2.60$	0.762 ± 0.006	15.1 (8.2)
153.00 ± 1.06	$+2.24 \pm 1.32$	0.766 ± 0.002	12.8 (16.7)	153.40 ± 0.61	-2.04 ± 1.01	0.792 ± 0.005	13.5 (13.7)
173.93 ± 0.90	-0.08 ± 1.14	0.709 ± 0.006	19.9 (20.3)	179.01 ± 0.52	-1.12 ± 2.20	0.774 ± 0.009	17.0 (10.9)
208.32 ± 1.01	-1.13 ± 1.92	0.769 ± 0.010	18.9 (12.0)	207.93 ± 0.36	-3.39 ± 1.45	0.771 ± 0.015	14.6 (11.5)
239.79 ± 0.83	-3.57 ± 1.44	0.734 ± 0.002	15.7 (12.3)	239.70 ± 0.65	$+2.44 \pm 0.80$	0.747 ± 0.008	14.9 (10.4)
262.07 ± 0.55	-11.88 ± 0.98	0.736 ± 0.006	17.1 (21.8)	268.91 ± 0.57	$+0.34 \pm 1.47$	0.732 ± 0.004	14.5 (16.7)
302.75 ± 0.95	-0.94 ± 2.23	0.738 ± 0.010	21.6 (10.1)	301.15 ± 0.41	-2.04 ± 0.82	0.745 ± 0.006	16.6 (12.5)
333.24 ± 1.09	$+1.68 \pm 2.08$	0.767 ± 0.002	20.8 (9.4)	330.92 ± 0.51	-5.71 ± 1.14	0.755 ± 0.008	16.7 (14.0)

Table 14: The nominal angle δ_n, average displacement $\Delta\delta$, average value of the parameter DIST, RMS of the ALPHA distribution for enabled GF and impact parameters between 60 m and 120 m. The RMS of the ALPHA distribution for disabled GF is given parentheses. The primary γ-ray energy was set to 30 GeV, the ZA to 20° and the azimuth angle to 150°.

$E_\gamma = 30\,\mathrm{GeV}$, Az = 180°, ZA = 20°, Intermediate Image Cleaning

$\delta_n[°]$	$\Delta\delta[°]$	DIST[°]	$\mathrm{RMS}_{\vert\mathrm{ALPHA}\vert}[°]$	$\delta_n[°]$	$\Delta\delta[°]$	DIST[°]	$\mathrm{RMS}_{\vert\mathrm{ALPHA}\vert}[°]$
IP = 60 m				**IP = 80 m**			
1.02 ± 1.17	$+18.90 \pm 3.33$	0.582 ± 0.010	9.4 (20.2)	357.87 ± 0.22	-10.14 ± 0.47	0.690 ± 0.044	10.2 (15.3)
25.76 ± 0.49	-9.85 ± 1.41	0.638 ± 0.023	17.2 (16.8)	30.29 ± 1.01	-5.95 ± 1.25	0.769 ± 0.002	23.3 (17.6)
59.25 ± 0.39	-0.81 ± 0.67	0.626 ± 0.009	21.7 (21.1)	54.64 ± 2.13	-5.41 ± 2.86	0.694 ± 0.002	10.5 (8.1)
80.50 ± 1.58	-14.48 ± 2.32	0.617 ± 0.004	16.4 (21.8)	96.26 ± 0.20	$+13.58 \pm 0.68$	0.701 ± 0.008	20.0 (12.7)
116.09 ± 0.22	-15.71 ± 2.21	0.660 ± 0.017	21.0 (19.5)	129.02 ± 1.04	$+18.87 \pm 1.31$	0.736 ± 0.015	15.8 (14.5)
159.77 ± 0.20	$+13.85 \pm 0.89$	0.627 ± 0.017	18.5 (14.0)	152.09 ± 1.14	$+5.81 \pm 1.61$	0.734 ± 0.008	16.5 (14.5)
184.17 ± 0.43	$+6.05 \pm 2.30$	0.593 ± 0.028	5.8 (8.8)	182.83 ± 0.20	$+5.65 \pm 0.74$	0.694 ± 0.004	18.2 (10.1)
207.80 ± 2.10	$+7.67 \pm 4.06$	0.598 ± 0.002	22.0 (15.2)	214.11 ± 0.37	$+1.94 \pm 0.60$	0.730 ± 0.002	12.2 (19.6)
232.03 ± 0.84	-10.26 ± 1.68	0.647 ± 0.011	15.0 (14.6)	233.85 ± 0.67	-1.41 ± 1.38	0.711 ± 0.002	17.1 (16.6)
267.21 ± 0.24	$+4.68 \pm 1.66$	0.636 ± 0.002	22.8 (14.3)	273.15 ± 0.37	$+12.77 \pm 2.88$	0.728 ± 0.004	10.1 (11.0)
295.36 ± 0.48	$+7.68 \pm 0.74$	0.630 ± 0.029	22.4 (20.2)	302.33 ± 0.20	$+6.06 \pm 0.43$	0.699 ± 0.002	13.6 (19.4)
332.12 ± 0.40	$+7.55 \pm 4.74$	0.605 ± 0.015	26.3 (20.4)	338.81 ± 0.97	$+16.19 \pm 1.42$	0.684 ± 0.002	12.9 (12.4)
IP = 100 m				**IP = 120 m**			
359.26 ± 1.09	$+0.84 \pm 2.30$	0.804 ± 0.017	13.6 (11.5)	359.28 ± 1.19	-0.03 ± 2.40	0.794 ± 0.007	19.9 (13.8)
30.78 ± 1.28	-2.55 ± 1.74	0.767 ± 0.022	9.2 (9.5)	28.75 ± 0.46	$+1.77 \pm 0.68$	0.770 ± 0.005	20.4 (13.2)
58.84 ± 0.19	-4.73 ± 1.39	0.786 ± 0.002	16.9 (12.7)	59.36 ± 0.13	$+2.05 \pm 0.65$	0.759 ± 0.004	16.4 (15.8)
94.78 ± 0.88	$+8.03 \pm 1.09$	0.788 ± 0.006	18.4 (18.6)	89.29 ± 0.72	-6.14 ± 1.25	0.733 ± 0.002	8.0 (10.8)
125.30 ± 0.19	$+6.63 \pm 0.76$	0.777 ± 0.006	18.9 (10.4)	122.09 ± 1.44	$+4.73 \pm 2.01$	0.777 ± 0.003	12.2 (8.2)
153.00 ± 1.06	$+3.76 \pm 1.31$	0.759 ± 0.015	18.2 (16.7)	153.40 ± 0.61	$+2.87 \pm 0.83$	0.781 ± 0.009	13.8 (13.7)
173.93 ± 0.90	-3.62 ± 1.95	0.816 ± 0.012	14.0 (20.3)	179.01 ± 0.52	-3.68 ± 1.40	0.777 ± 0.020	8.9 (10.9)
208.32 ± 1.01	-0.24 ± 2.79	0.800 ± 0.010	16.7 (12.0)	207.93 ± 0.36	-1.77 ± 1.13	0.751 ± 0.011	14.1 (11.5)
239.79 ± 0.83	$+6.54 \pm 1.89$	0.801 ± 0.002	9.2 (12.3)	239.70 ± 0.65	-4.41 ± 2.01	0.780 ± 0.009	14.5 (10.4)
262.07 ± 0.55	-8.29 ± 2.39	0.739 ± 0.005	20.2 (21.8)	268.91 ± 0.57	$+5.46 \pm 1.33$	0.749 ± 0.015	15.1 (16.7)
302.75 ± 0.95	-0.35 ± 1.20	0.760 ± 0.014	10.3 (10.1)	301.15 ± 0.41	$+0.99 \pm 2.31$	0.726 ± 0.005	12.7 (12.5)
333.24 ± 1.09	$+7.19 \pm 1.55$	0.774 ± 0.010	13.3 (9.4)	330.92 ± 0.51	$+2.78 \pm 0.88$	0.784 ± 0.016	18.6 (14.0)

Table 15: The nominal angle δ_n, average displacement $\Delta\delta$, average value of the parameter DIST, RMS of the ALPHA distribution for enabled GF and impact parameters between 60 m and 120 m. The RMS of the ALPHA distribution for disabled GF is given parentheses. The primary γ-ray energy was set to 30 GeV, the ZA to 20° and the azimuth angle to 180°.

$E_\gamma = 50\,\mathrm{GeV}$, Az = 0°, ZA = 0°, Intermediate Image Cleaning

δ_n[°]	$\Delta\delta$[°]	DIST[°]	RMS$_{\lvert\mathrm{ALPHA}\rvert}$[°]	δ_n[°]	$\Delta\delta$[°]	DIST[°]	RMS$_{\lvert\mathrm{ALPHA}\rvert}$[°]
IP = 60 m				IP = 80 m			
0.41 ± 0.89	+4.73 ± 1.37	0.507 ± 0.005	16.8 (18.4)	359.76 ± 0.56	−0.96 ± 1.20	0.620 ± 0.009	12.3 (14.5)
29.40 ± 0.65	−1.04 ± 1.51	0.507 ± 0.004	16.8 (19.1)	29.42 ± 0.54	+1.85 ± 1.22	0.611 ± 0.006	17.2 (14.1)
60.39 ± 0.72	+2.08 ± 1.37	0.510 ± 0.006	19.7 (16.3)	59.22 ± 0.64	+2.10 ± 1.33	0.613 ± 0.007	17.7 (13.7)
90.69 ± 0.92	+0.16 ± 1.40	0.513 ± 0.005	19.4 (17.0)	89.75 ± 0.54	+2.74 ± 1.22	0.623 ± 0.007	16.2 (13.0)
118.21 ± 0.58	−2.21 ± 1.59	0.496 ± 0.006	21.9 (19.7)	119.92 ± 0.57	−1.83 ± 1.27	0.608 ± 0.009	17.6 (14.8)
148.09 ± 0.59	−2.86 ± 1.19	0.502 ± 0.007	18.2 (17.9)	150.66 ± 0.62	−1.62 ± 1.31	0.609 ± 0.006	14.8 (14.9)
178.54 ± 0.67	−0.74 ± 1.56	0.502 ± 0.007	16.1 (17.3)	181.37 ± 0.56	+0.01 ± 1.22	0.624 ± 0.003	15.2 (11.9)
209.17 ± 0.92	+4.01 ± 1.87	0.497 ± 0.007	21.2 (20.0)	208.97 ± 0.18	−1.93 ± 0.78	0.612 ± 0.008	12.9 (12.9)
238.73 ± 0.66	−1.50 ± 1.32	0.513 ± 0.004	20.2 (20.7)	240.80 ± 0.50	+1.90 ± 1.26	0.615 ± 0.004	16.9 (13.7)
269.45 ± 0.88	−2.54 ± 1.76	0.506 ± 0.008	21.3 (18.3)	270.98 ± 0.62	−0.69 ± 1.60	0.611 ± 0.006	15.5 (13.6)
299.75 ± 0.75	−2.04 ± 1.41	0.514 ± 0.006	21.8 (19.9)	298.30 ± 0.63	−3.60 ± 1.24	0.613 ± 0.006	16.0 (16.2)
329.78 ± 0.84	−2.89 ± 1.95	0.490 ± 0.007	20.4 (21.1)	330.53 ± 0.43	+2.10 ± 0.97	0.614 ± 0.006	18.8 (14.4)
IP = 100 m				IP = 120 m			
359.85 ± 0.44	−0.74 ± 1.08	0.702 ± 0.009	8.2 (9.8)	0.59 ± 0.33	+1.73 ± 1.00	0.741 ± 0.006	9.3 (8.1)
31.07 ± 0.37	+1.51 ± 1.16	0.699 ± 0.008	12.2 (10.2)	31.00 ± 0.37	−0.96 ± 0.98	0.726 ± 0.005	8.8 (7.1)
60.18 ± 0.44	+1.90 ± 1.22	0.669 ± 0.006	13.3 (11.3)	60.44 ± 0.38	−2.28 ± 0.96	0.707 ± 0.005	10.4 (7.8)
90.59 ± 0.37	+1.22 ± 1.02	0.657 ± 0.006	11.3 (11.9)	90.29 ± 0.42	+1.20 ± 1.06	0.690 ± 0.005	10.1 (8.0)
119.95 ± 0.44	+1.68 ± 1.21	0.672 ± 0.006	16.6 (9.6)	119.77 ± 0.34	+3.08 ± 0.75	0.693 ± 0.006	11.2 (8.3)
148.52 ± 0.42	−1.42 ± 1.01	0.685 ± 0.004	14.1 (11.1)	150.57 ± 0.41	+3.78 ± 1.07	0.713 ± 0.006	8.4 (8.7)
180.83 ± 0.44	−1.22 ± 1.07	0.703 ± 0.007	11.4 (9.7)	179.49 ± 0.28	−1.30 ± 0.94	0.743 ± 0.003	12.4 (7.4)
209.08 ± 0.42	−1.00 ± 0.79	0.690 ± 0.006	12.4 (9.9)	208.92 ± 0.37	−1.71 ± 0.83	0.719 ± 0.004	7.6 (7.3)
238.69 ± 0.44	−2.57 ± 1.08	0.684 ± 0.009	13.6 (11.7)	240.89 ± 0.33	−2.94 ± 0.79	0.692 ± 0.006	8.3 (8.8)
269.40 ± 0.36	−0.66 ± 1.19	0.660 ± 0.008	13.2 (10.2)	269.32 ± 0.31	−0.78 ± 0.83	0.688 ± 0.006	9.1 (7.5)
299.62 ± 0.44	−0.59 ± 0.87	0.681 ± 0.008	14.0 (9.6)	299.89 ± 0.33	+2.31 ± 0.87	0.697 ± 0.006	9.9 (7.4)
330.27 ± 0.53	−0.17 ± 1.37	0.707 ± 0.007	12.3 (10.7)	329.23 ± 0.37	+0.94 ± 1.06	0.729 ± 0.006	8.5 (8.3)

Table 16: The nominal angle δ_n, average displacement $\Delta\delta$, average value of the parameter DIST, RMS of the ALPHA distribution for enabled GF and impact parameters between 60 m and 120 m. The RMS of the ALPHA distribution for disabled GF is given parentheses. The primary γ-ray energy was set to 50 GeV, the ZA to 0° and the azimuth angle to 0°.

$E_\gamma = 50\,\mathrm{GeV}$, Az = 0°, ZA = 20°, Intermediate Image Cleaning

δ_n[°]	$\Delta\delta$[°]	DIST[°]	RMS$_{\lvert\mathrm{ALPHA}\rvert}$[°]	δ_n[°]	$\Delta\delta$[°]	DIST[°]	RMS$_{\lvert\mathrm{ALPHA}\rvert}$[°]
IP = 60 m				IP = 80 m			
0.23 ± 1.09	−0.91 ± 1.83	0.474 ± 0.006	19.4 (17.7)	357.22 ± 0.26	−2.69 ± 0.54	0.586 ± 0.008	15.8 (15.1)
30.31 ± 0.52	+3.00 ± 0.61	0.479 ± 0.007	18.6 (17.8)	30.80 ± 0.56	+4.10 ± 1.36	0.581 ± 0.007	16.1 (11.4)
59.60 ± 1.11	+1.32 ± 1.73	0.475 ± 0.004	22.8 (18.4)	55.63 ± 0.68	+0.27 ± 1.61	0.573 ± 0.004	17.4 (15.8)
89.00 ± 0.71	+0.93 ± 1.40	0.457 ± 0.007	21.4 (24.8)	87.60 ± 0.24	−6.31 ± 1.16	0.554 ± 0.006	18.0 (13.9)
121.14 ± 0.36	−0.74 ± 0.75	0.443 ± 0.006	20.0 (21.3)	118.63 ± 0.70	−6.96 ± 1.35	0.558 ± 0.008	15.2 (15.1)
151.40 ± 1.02	−1.12 ± 2.06	0.465 ± 0.002	21.2 (16.5)	151.55 ± 0.75	+1.25 ± 1.62	0.561 ± 0.005	17.0 (15.7)
182.39 ± 0.47	+1.78 ± 0.77	0.485 ± 0.002	17.1 (18.9)	178.23 ± 0.52	−3.04 ± 1.17	0.588 ± 0.005	15.9 (19.1)
209.59 ± 0.27	+5.62 ± 1.08	0.466 ± 0.004	16.5 (18.2)	207.41 ± 0.58	+0.20 ± 1.29	0.575 ± 0.007	13.5 (17.6)
238.08 ± 0.71	+4.26 ± 1.90	0.477 ± 0.006	20.8 (19.6)	239.74 ± 0.92	+1.04 ± 1.84	0.565 ± 0.006	16.0 (14.9)
269.11 ± 0.44	−2.36 ± 1.10	0.457 ± 0.005	20.0 (18.9)	269.53 ± 0.63	+4.81 ± 1.09	0.567 ± 0.005	21.9 (18.4)
303.30 ± 0.18	−4.57 ± 1.13	0.482 ± 0.006	23.8 (19.4)	303.38 ± 0.75	+1.40 ± 1.58	0.555 ± 0.008	22.3 (14.3)
326.91 ± 1.14	−5.26 ± 1.72	0.481 ± 0.007	18.2 (22.0)	330.81 ± 0.16	−2.39 ± 0.98	0.598 ± 0.007	15.7 (12.9)
IP = 100 m				IP = 120 m			
1.37 ± 0.41	+0.89 ± 1.03	0.667 ± 0.005	9.4 (10.1)	0.08 ± 0.34	−0.22 ± 0.96	0.697 ± 0.006	9.2 (10.3)
27.51 ± 0.53	+0.81 ± 1.25	0.648 ± 0.008	14.4 (16.0)	28.79 ± 0.32	+1.09 ± 0.81	0.671 ± 0.008	11.8 (11.5)
58.13 ± 0.57	+2.28 ± 1.14	0.631 ± 0.007	13.1 (11.4)	58.69 ± 0.41	−0.18 ± 0.76	0.651 ± 0.006	8.5 (7.5)
90.71 ± 0.58	+1.05 ± 1.31	0.620 ± 0.004	14.1 (14.6)	89.29 ± 0.52	+0.35 ± 0.91	0.628 ± 0.007	10.6 (8.5)
123.10 ± 0.65	+2.51 ± 1.52	0.614 ± 0.003	19.7 (11.3)	122.18 ± 0.41	+0.71 ± 0.89	0.651 ± 0.008	13.0 (8.6)
151.32 ± 0.60	+0.76 ± 0.85	0.638 ± 0.007	13.7 (12.6)	152.16 ± 0.43	+2.62 ± 0.86	0.673 ± 0.004	10.8 (10.0)
178.72 ± 0.49	−0.37 ± 1.18	0.651 ± 0.006	9.8 (13.2)	179.49 ± 0.34	−1.44 ± 0.80	0.693 ± 0.006	9.2 (8.6)
209.81 ± 0.54	+2.66 ± 1.01	0.647 ± 0.008	11.3 (10.1)	208.61 ± 0.37	+0.94 ± 0.72	0.672 ± 0.003	8.5 (7.0)
237.89 ± 0.55	+0.53 ± 1.14	0.638 ± 0.008	17.0 (12.7)	238.94 ± 0.40	+0.83 ± 0.87	0.657 ± 0.006	14.3 (9.8)
271.05 ± 0.57	−0.06 ± 1.49	0.622 ± 0.009	16.0 (9.2)	270.28 ± 0.41	+0.15 ± 0.91	0.635 ± 0.006	13.7 (7.5)
301.74 ± 0.37	−1.74 ± 0.84	0.629 ± 0.008	20.7 (14.3)	301.40 ± 0.46	−1.74 ± 0.75	0.668 ± 0.009	7.8 (9.4)
332.00 ± 0.47	−1.94 ± 1.12	0.650 ± 0.005	13.7 (14.8)	332.90 ± 0.27	−1.15 ± 0.83	0.674 ± 0.008	10.3 (9.0)

Table 17: The nominal angle δ_n, average displacement $\Delta\delta$, average value of the parameter DIST, RMS of the ALPHA distribution for enabled GF and impact parameters between 60 m and 120 m. The RMS of the ALPHA distribution for disabled GF is given parentheses. The primary γ-ray energy was set to 50 GeV, the ZA to 20° and the azimuth angle to 0°.

$E_\gamma = 50\,\mathrm{GeV}$, Az $= 30°$, ZA $= 20°$, Intermediate Image Cleaning

$\delta_n\,[°]$	$\Delta\delta\,[°]$	DIST[°]	$\mathrm{RMS}_{\lvert\mathrm{ALPHA}\rvert}\,[°]$	$\delta_n\,[°]$	$\Delta\delta\,[°]$	DIST[°]	$\mathrm{RMS}_{\lvert\mathrm{ALPHA}\rvert}\,[°]$
IP = 60 m				**IP = 80 m**			
0.23 ± 1.09	$+1.53 \pm 1.66$	0.489 ± 0.004	16.2 (17.7)	357.22 ± 0.26	-1.38 ± 1.10	0.594 ± 0.002	15.0 (15.1)
30.31 ± 0.52	$+0.43 \pm 1.11$	0.467 ± 0.005	18.4 (17.8)	30.80 ± 0.56	$+4.55 \pm 1.37$	0.591 ± 0.011	15.6 (11.4)
59.60 ± 1.11	$+1.56 \pm 2.44$	0.467 ± 0.010	20.0 (18.4)	55.63 ± 0.68	-2.54 ± 0.86	0.578 ± 0.007	18.7 (15.8)
89.00 ± 0.71	$+5.03 \pm 1.38$	0.463 ± 0.004	21.4 (24.8)	87.60 ± 0.24	$+1.96 \pm 0.86$	0.580 ± 0.007	19.6 (13.9)
121.14 ± 0.36	$+1.81 \pm 1.00$	0.474 ± 0.003	20.6 (21.3)	118.63 ± 0.70	-2.88 ± 1.83	0.588 ± 0.007	19.1 (15.1)
151.40 ± 1.02	-0.32 ± 1.30	0.504 ± 0.007	17.8 (16.5)	151.55 ± 0.75	-1.24 ± 1.71	0.599 ± 0.006	18.1 (15.7)
182.39 ± 0.47	-2.47 ± 1.35	0.473 ± 0.005	19.3 (18.9)	178.23 ± 0.52	$+0.87 \pm 0.70$	0.601 ± 0.007	16.7 (19.1)
209.59 ± 0.27	$+2.43 \pm 0.91$	0.477 ± 0.008	19.5 (18.2)	207.41 ± 0.58	$+1.52 \pm 1.01$	0.591 ± 0.005	16.8 (17.6)
238.08 ± 0.71	$+0.85 \pm 1.44$	0.470 ± 0.006	19.5 (19.6)	239.74 ± 0.92	$+4.17 \pm 1.63$	0.578 ± 0.003	17.8 (14.9)
269.11 ± 0.44	$+0.96 \pm 1.39$	0.487 ± 0.007	20.6 (18.9)	269.53 ± 0.63	$+1.16 \pm 1.25$	0.582 ± 0.003	20.7 (18.4)
303.30 ± 0.18	-1.66 ± 1.13	0.488 ± 0.006	21.0 (19.4)	303.38 ± 0.75	$+0.77 \pm 1.61$	0.614 ± 0.006	16.7 (14.3)
326.91 ± 1.14	-5.71 ± 1.24	0.502 ± 0.008	19.2 (22.0)	330.81 ± 0.16	-1.03 ± 0.61	0.614 ± 0.004	16.3 (12.9)
IP = 100 m				**IP = 120 m**			
1.37 ± 0.41	$+2.32 \pm 0.83$	0.670 ± 0.008	13.6 (10.1)	0.08 ± 0.34	$+1.31 \pm 0.93$	0.695 ± 0.008	12.5 (10.3)
27.51 ± 0.53	-0.85 ± 1.19	0.663 ± 0.007	15.0 (16.0)	28.79 ± 0.32	$+1.44 \pm 0.82$	0.700 ± 0.004	12.4 (11.5)
58.13 ± 0.57	$+1.27 \pm 1.43$	0.663 ± 0.004	15.9 (11.4)	58.69 ± 0.41	$+1.16 \pm 1.10$	0.677 ± 0.008	13.6 (7.5)
90.71 ± 0.58	$+3.15 \pm 1.46$	0.619 ± 0.007	17.1 (14.6)	89.29 ± 0.52	-0.76 ± 1.17	0.650 ± 0.008	12.9 (8.5)
123.10 ± 0.65	$+1.87 \pm 1.35$	0.643 ± 0.007	14.9 (11.3)	122.18 ± 0.41	-0.04 ± 0.99	0.649 ± 0.007	13.1 (8.6)
151.32 ± 0.60	-0.25 ± 1.38	0.678 ± 0.003	15.5 (12.6)	152.16 ± 0.43	$+2.17 \pm 0.87$	0.695 ± 0.009	12.3 (10.0)
178.72 ± 0.49	-1.87 ± 1.23	0.662 ± 0.009	13.2 (13.2)	179.49 ± 0.34	$+0.87 \pm 0.79$	0.698 ± 0.007	11.9 (8.6)
209.81 ± 0.54	$+1.58 \pm 1.26$	0.660 ± 0.003	14.0 (10.1)	208.61 ± 0.37	$+1.34 \pm 1.04$	0.713 ± 0.008	12.1 (7.0)
237.89 ± 0.55	$+1.35 \pm 1.30$	0.642 ± 0.007	16.3 (12.7)	238.94 ± 0.40	$+1.38 \pm 0.96$	0.681 ± 0.008	13.0 (9.8)
271.05 ± 0.57	$+4.69 \pm 1.40$	0.652 ± 0.008	16.4 (9.2)	270.28 ± 0.41	$+2.62 \pm 0.91$	0.659 ± 0.008	12.6 (7.5)
301.74 ± 0.37	$+0.83 \pm 0.94$	0.658 ± 0.006	15.4 (14.3)	301.40 ± 0.46	-3.25 ± 1.04	0.660 ± 0.006	12.4 (9.4)
332.00 ± 0.47	-1.84 ± 1.17	0.661 ± 0.008	16.3 (14.8)	332.90 ± 0.27	$+1.79 \pm 0.82$	0.688 ± 0.006	12.2 (9.0)

Table 18: The nominal angle δ_n, average displacement $\Delta\delta$, average value of the parameter DIST, RMS of the ALPHA distribution for enabled GF and impact parameters between 60 m and 120 m. The RMS of the ALPHA distribution for disabled GF is given parentheses. The primary γ-ray energy was set to 50 GeV, the ZA to 20° and the azimuth angle to 30°.

$E_\gamma = 50\,\mathrm{GeV}$, Az $= 60°$, ZA $= 20°$, Intermediate Image Cleaning

$\delta_n\,[°]$	$\Delta\delta\,[°]$	DIST[°]	$\mathrm{RMS}_{\lvert\mathrm{ALPHA}\rvert}\,[°]$	$\delta_n\,[°]$	$\Delta\delta\,[°]$	DIST[°]	$\mathrm{RMS}_{\lvert\mathrm{ALPHA}\rvert}\,[°]$
IP = 60 m				**IP = 80 m**			
0.23 ± 1.09	-2.00 ± 1.77	0.475 ± 0.006	18.1 (17.7)	357.22 ± 0.26	-3.79 ± 0.91	0.578 ± 0.007	15.5 (15.1)
30.31 ± 0.52	-0.00 ± 1.21	0.447 ± 0.004	18.8 (17.8)	30.80 ± 0.56	$+0.48 \pm 1.02$	0.578 ± 0.010	17.9 (11.4)
59.60 ± 1.11	$+2.53 \pm 1.41$	0.464 ± 0.004	19.4 (18.4)	55.63 ± 0.68	-4.90 ± 1.37	0.582 ± 0.005	15.8 (15.8)
89.00 ± 0.71	$+0.89 \pm 1.29$	0.480 ± 0.006	21.2 (24.8)	87.60 ± 0.24	-1.30 ± 0.92	0.603 ± 0.005	16.9 (13.9)
121.14 ± 0.36	-2.31 ± 1.12	0.490 ± 0.008	20.5 (21.3)	118.63 ± 0.70	$+0.33 \pm 1.36$	0.597 ± 0.006	19.3 (15.1)
151.40 ± 1.02	$+0.16 \pm 2.02$	0.477 ± 0.007	20.0 (16.5)	151.55 ± 0.75	$+0.34 \pm 1.57$	0.589 ± 0.004	16.4 (15.7)
182.39 ± 0.47	$+4.63 \pm 1.09$	0.476 ± 0.005	18.6 (18.9)	178.23 ± 0.52	-2.62 ± 0.70	0.595 ± 0.005	16.0 (19.1)
209.59 ± 0.27	-1.38 ± 0.47	0.475 ± 0.005	17.0 (18.2)	207.41 ± 0.58	-2.81 ± 1.10	0.584 ± 0.004	15.6 (17.6)
238.08 ± 0.71	-3.81 ± 1.49	0.489 ± 0.003	15.9 (19.6)	239.74 ± 0.92	$+0.87 \pm 1.12$	0.599 ± 0.005	18.0 (14.9)
269.11 ± 0.44	$+0.57 \pm 1.02$	0.486 ± 0.005	19.4 (18.9)	269.53 ± 0.63	$+0.11 \pm 1.44$	0.601 ± 0.002	18.7 (18.4)
303.30 ± 0.18	$+4.05 \pm 0.83$	0.498 ± 0.005	21.9 (19.4)	303.38 ± 0.75	$+1.03 \pm 1.22$	0.610 ± 0.007	18.0 (14.3)
326.91 ± 1.14	-4.02 ± 2.07	0.496 ± 0.006	17.3 (22.0)	330.81 ± 0.16	$+3.34 \pm 0.62$	0.598 ± 0.008	17.2 (12.9)
IP = 100 m				**IP = 120 m**			
1.37 ± 0.41	$+1.69 \pm 1.18$	0.647 ± 0.003	15.4 (10.1)	0.08 ± 0.34	$+0.59 \pm 1.01$	0.714 ± 0.002	11.6 (10.3)
27.51 ± 0.53	-3.19 ± 1.11	0.658 ± 0.002	14.1 (16.0)	28.79 ± 0.32	$+1.91 \pm 0.97$	0.678 ± 0.005	12.1 (11.5)
58.13 ± 0.57	-0.22 ± 1.12	0.648 ± 0.010	15.8 (11.4)	58.69 ± 0.41	$+1.81 \pm 0.83$	0.677 ± 0.007	12.9 (7.5)
90.71 ± 0.58	-1.24 ± 0.94	0.650 ± 0.005	16.6 (14.6)	89.29 ± 0.52	-1.21 ± 1.02	0.645 ± 0.006	14.1 (8.5)
123.10 ± 0.65	$+3.48 \pm 1.54$	0.642 ± 0.004	17.2 (11.3)	122.18 ± 0.41	$+1.28 \pm 1.18$	0.665 ± 0.006	11.5 (8.6)
151.32 ± 0.60	-0.87 ± 1.26	0.665 ± 0.004	14.6 (12.6)	152.16 ± 0.43	-1.57 ± 0.93	0.688 ± 0.007	12.4 (10.0)
178.72 ± 0.49	-3.17 ± 1.11	0.653 ± 0.004	14.5 (13.2)	179.49 ± 0.34	-0.24 ± 0.92	0.713 ± 0.004	13.2 (8.6)
209.81 ± 0.54	-1.07 ± 0.87	0.657 ± 0.008	11.7 (10.1)	208.61 ± 0.37	$+1.42 \pm 1.02$	0.691 ± 0.005	14.2 (7.0)
237.89 ± 0.55	-2.80 ± 1.38	0.678 ± 0.008	16.8 (12.7)	238.94 ± 0.40	-0.38 ± 0.99	0.698 ± 0.004	13.4 (9.8)
271.05 ± 0.57	$+2.07 \pm 1.00$	0.655 ± 0.006	17.4 (9.2)	270.28 ± 0.41	-1.05 ± 1.15	0.660 ± 0.006	12.6 (7.5)
301.74 ± 0.37	-1.62 ± 1.25	0.659 ± 0.004	16.4 (14.3)	301.40 ± 0.46	-1.77 ± 0.84	0.667 ± 0.007	12.7 (9.4)
332.00 ± 0.47	$+0.69 \pm 0.81$	0.663 ± 0.009	16.0 (14.8)	332.90 ± 0.27	$+0.58 \pm 0.84$	0.681 ± 0.008	12.8 (9.0)

Table 19: The nominal angle δ_n, average displacement $\Delta\delta$, average value of the parameter DIST, RMS of the ALPHA distribution for enabled GF and impact parameters between 60 m and 120 m. The RMS of the ALPHA distribution for disabled GF is given parentheses. The primary γ-ray energy was set to 50 GeV, the ZA to 20° and the azimuth angle to 60°.

$E_\gamma = 50\,\mathrm{GeV}$, Az = 90°, ZA = 20°, Intermediate Image Cleaning

$\delta_n[°]$	$\Delta\delta[°]$	DIST[°]	$\mathrm{RMS}_{\lvert\mathrm{ALPHA}\rvert}[°]$	$\delta_n[°]$	$\Delta\delta[°]$	DIST[°]	$\mathrm{RMS}_{\lvert\mathrm{ALPHA}\rvert}[°]$
IP = 60 m				**IP = 80 m**			
0.23 ± 1.09	-1.42 ± 2.11	0.472 ± 0.008	20.0 (17.7)	357.22 ± 0.26	-3.16 ± 0.85	0.579 ± 0.006	14.4 (15.1)
30.31 ± 0.52	-1.84 ± 1.91	0.485 ± 0.004	19.5 (17.8)	30.80 ± 0.56	$+0.85 \pm 1.51$	0.570 ± 0.003	17.8 (11.4)
59.60 ± 1.11	$+1.49 \pm 1.99$	0.489 ± 0.002	19.8 (18.4)	55.63 ± 0.68	-2.69 ± 1.39	0.606 ± 0.005	16.8 (15.8)
89.00 ± 0.71	$+1.56 \pm 1.67$	0.510 ± 0.006	21.4 (24.8)	87.60 ± 0.24	-3.98 ± 0.93	0.613 ± 0.007	19.0 (13.9)
121.14 ± 0.36	$+1.25 \pm 1.47$	0.509 ± 0.006	19.4 (21.3)	118.63 ± 0.70	-1.56 ± 0.90	0.612 ± 0.007	17.0 (15.1)
151.40 ± 1.02	$+3.31 \pm 1.22$	0.495 ± 0.007	19.4 (16.5)	151.55 ± 0.75	-0.22 ± 1.33	0.600 ± 0.008	17.2 (15.7)
182.39 ± 0.47	$+4.10 \pm 0.57$	0.484 ± 0.008	16.9 (18.9)	178.23 ± 0.52	-3.15 ± 0.96	0.594 ± 0.007	19.1 (19.1)
209.59 ± 0.27	$+2.84 \pm 0.67$	0.475 ± 0.005	18.8 (18.2)	207.41 ± 0.58	-2.47 ± 1.67	0.616 ± 0.008	14.0 (17.6)
238.08 ± 0.71	-1.03 ± 1.70	0.500 ± 0.004	20.3 (19.6)	239.74 ± 0.92	$+3.30 \pm 1.02$	0.608 ± 0.006	19.8 (14.9)
269.11 ± 0.44	$+2.06 \pm 1.51$	0.513 ± 0.005	22.5 (18.9)	269.53 ± 0.63	$+0.56 \pm 1.02$	0.620 ± 0.005	20.2 (18.4)
303.30 ± 0.18	-1.82 ± 0.49	0.521 ± 0.006	19.6 (19.4)	303.38 ± 0.75	$+0.30 \pm 1.91$	0.596 ± 0.010	16.5 (14.3)
326.91 ± 1.14	-6.04 ± 1.68	0.487 ± 0.005	22.0 (22.0)	330.81 ± 0.16	-0.98 ± 0.63	0.603 ± 0.011	15.5 (12.9)
IP = 100 m				**IP = 120 m**			
1.37 ± 0.41	-0.03 ± 1.18	0.641 ± 0.009	13.2 (10.1)	0.08 ± 0.34	-3.47 ± 0.90	0.723 ± 0.006	12.4 (10.3)
27.51 ± 0.53	-0.84 ± 1.04	0.669 ± 0.007	15.1 (16.0)	28.79 ± 0.32	$+1.13 \pm 0.78$	0.713 ± 0.007	12.5 (11.5)
58.13 ± 0.57	$+1.47 \pm 1.40$	0.680 ± 0.005	15.8 (11.4)	58.69 ± 0.41	$+2.06 \pm 1.11$	0.698 ± 0.009	11.1 (7.5)
90.71 ± 0.58	$+2.74 \pm 1.03$	0.662 ± 0.003	15.0 (14.6)	89.29 ± 0.52	$+0.74 \pm 1.13$	0.679 ± 0.009	10.7 (8.5)
123.10 ± 0.65	-0.11 ± 1.39	0.679 ± 0.008	14.0 (11.3)	122.18 ± 0.41	-0.09 ± 1.12	0.658 ± 0.009	10.3 (8.6)
151.32 ± 0.60	$+1.32 \pm 1.60$	0.678 ± 0.006	13.1 (12.6)	152.16 ± 0.43	-0.73 ± 1.04	0.722 ± 0.007	9.2 (10.0)
178.72 ± 0.49	-4.99 ± 1.24	0.674 ± 0.003	13.4 (13.2)	179.49 ± 0.34	-2.30 ± 0.83	0.733 ± 0.005	10.1 (8.6)
209.81 ± 0.54	$+0.51 \pm 1.15$	0.688 ± 0.007	12.9 (10.1)	208.61 ± 0.37	$+3.14 \pm 1.01$	0.739 ± 0.007	8.1 (7.0)
237.89 ± 0.55	-3.07 ± 1.44	0.684 ± 0.007	14.9 (12.7)	238.94 ± 0.40	$+1.75 \pm 0.96$	0.703 ± 0.007	11.1 (9.8)
271.05 ± 0.57	$+4.78 \pm 1.21$	0.665 ± 0.008	17.8 (9.2)	270.28 ± 0.41	-0.88 ± 1.04	0.674 ± 0.008	12.5 (7.5)
301.74 ± 0.37	$+0.89 \pm 1.22$	0.657 ± 0.004	14.4 (14.3)	301.40 ± 0.46	$+1.46 \pm 1.00$	0.659 ± 0.009	11.8 (9.4)
332.00 ± 0.47	$+0.60 \pm 1.35$	0.669 ± 0.005	14.6 (14.8)	332.90 ± 0.27	-0.31 ± 0.80	0.692 ± 0.009	10.7 (9.0)

Table 20: The nominal angle δ_n, average displacement $\Delta\delta$, average value of the parameter DIST, RMS of the ALPHA distribution for enabled GF and impact parameters between 60 m and 120 m. The RMS of the ALPHA distribution for disabled GF is given parentheses. The primary γ-ray energy was set to 50 GeV, the ZA to 20° and the azimuth angle to 90°.

$E_\gamma = 50\,\mathrm{GeV}$, Az = 120°, ZA = 20°, Intermediate Image Cleaning

$\delta_n[°]$	$\Delta\delta[°]$	DIST[°]	$\mathrm{RMS}_{\lvert\mathrm{ALPHA}\rvert}[°]$	$\delta_n[°]$	$\Delta\delta[°]$	DIST[°]	$\mathrm{RMS}_{\lvert\mathrm{ALPHA}\rvert}[°]$
IP = 60 m				**IP = 80 m**			
0.23 ± 1.09	$+3.08 \pm 1.65$	0.496 ± 0.006	16.7 (17.7)	357.22 ± 0.26	-3.08 ± 0.76	0.613 ± 0.009	14.4 (15.1)
30.31 ± 0.52	-0.45 ± 1.51	0.497 ± 0.007	16.8 (17.8)	30.80 ± 0.56	$+1.51 \pm 0.66$	0.622 ± 0.007	14.9 (11.4)
59.60 ± 1.11	$+1.68 \pm 1.22$	0.513 ± 0.005	18.1 (18.4)	55.63 ± 0.68	-2.29 ± 1.15	0.634 ± 0.007	16.3 (15.8)
89.00 ± 0.71	$+0.61 \pm 0.91$	0.526 ± 0.008	18.7 (24.8)	87.60 ± 0.24	-2.38 ± 1.25	0.639 ± 0.009	17.0 (13.9)
121.14 ± 0.36	$+0.24 \pm 1.43$	0.507 ± 0.004	19.4 (21.3)	118.63 ± 0.70	-2.68 ± 1.60	0.622 ± 0.003	19.3 (15.1)
151.40 ± 1.02	$+2.55 \pm 1.77$	0.496 ± 0.007	17.7 (16.5)	151.55 ± 0.75	-0.26 ± 1.53	0.608 ± 0.008	16.5 (15.7)
182.39 ± 0.47	$+1.46 \pm 1.24$	0.508 ± 0.006	18.2 (18.9)	178.23 ± 0.52	$+0.49 \pm 1.50$	0.620 ± 0.003	14.6 (19.1)
209.59 ± 0.27	$+5.12 \pm 0.58$	0.524 ± 0.001	19.0 (18.2)	207.41 ± 0.58	-1.58 ± 0.86	0.629 ± 0.003	14.5 (17.6)
238.08 ± 0.71	-2.74 ± 0.91	0.505 ± 0.004	18.3 (19.6)	239.74 ± 0.92	-1.82 ± 1.90	0.643 ± 0.005	15.6 (14.9)
269.11 ± 0.44	-1.41 ± 1.23	0.510 ± 0.003	19.5 (18.9)	269.53 ± 0.63	-0.64 ± 1.53	0.639 ± 0.005	15.7 (18.4)
303.30 ± 0.18	$+6.55 \pm 0.68$	0.499 ± 0.003	20.7 (19.4)	303.38 ± 0.75	$+2.76 \pm 1.57$	0.600 ± 0.006	19.2 (14.3)
326.91 ± 1.14	-5.88 ± 1.54	0.480 ± 0.007	19.1 (22.0)	330.81 ± 0.16	-3.97 ± 1.02	0.604 ± 0.006	17.4 (12.9)
IP = 100 m				**IP = 120 m**			
1.37 ± 0.41	$+0.92 \pm 1.37$	0.679 ± 0.006	13.8 (10.1)	0.08 ± 0.34	-1.78 ± 0.77	0.734 ± 0.006	10.1 (10.3)
27.51 ± 0.53	$+2.97 \pm 1.68$	0.692 ± 0.005	13.2 (16.0)	28.79 ± 0.32	-0.29 ± 0.92	0.730 ± 0.003	11.5 (11.5)
58.13 ± 0.57	$+1.47 \pm 1.03$	0.705 ± 0.009	15.2 (11.4)	58.69 ± 0.41	$+2.65 \pm 1.06$	0.730 ± 0.006	11.1 (7.5)
90.71 ± 0.58	$+2.27 \pm 1.60$	0.682 ± 0.004	15.3 (14.6)	89.29 ± 0.52	$+0.65 \pm 1.04$	0.667 ± 0.007	13.9 (8.5)
123.10 ± 0.65	$+1.25 \pm 1.22$	0.674 ± 0.008	18.0 (11.3)	122.18 ± 0.41	-0.49 ± 1.07	0.691 ± 0.002	14.9 (8.6)
151.32 ± 0.60	$+1.28 \pm 1.24$	0.689 ± 0.010	14.5 (12.6)	152.16 ± 0.43	$+0.22 \pm 0.96$	0.714 ± 0.008	13.8 (10.0)
178.72 ± 0.49	-1.62 ± 1.47	0.697 ± 0.003	13.2 (13.2)	179.49 ± 0.34	-1.91 ± 0.93	0.749 ± 0.009	10.0 (8.6)
209.81 ± 0.54	-0.53 ± 1.21	0.680 ± 0.011	14.8 (10.1)	208.61 ± 0.37	$+0.53 \pm 1.22$	0.751 ± 0.002	12.0 (7.0)
237.89 ± 0.55	-0.88 ± 1.40	0.716 ± 0.010	12.9 (12.7)	238.94 ± 0.40	$+2.23 \pm 1.29$	0.721 ± 0.004	11.9 (9.8)
271.05 ± 0.57	$+0.55 \pm 1.42$	0.665 ± 0.008	16.3 (9.2)	270.28 ± 0.41	-0.25 ± 1.10	0.667 ± 0.006	12.8 (7.5)
301.74 ± 0.37	-0.25 ± 0.67	0.673 ± 0.007	16.4 (14.3)	301.40 ± 0.46	-1.73 ± 1.04	0.678 ± 0.001	14.4 (9.4)
332.00 ± 0.47	-0.68 ± 1.30	0.691 ± 0.009	13.8 (14.8)	332.90 ± 0.27	-0.12 ± 1.10	0.713 ± 0.004	14.1 (9.0)

Table 21: The nominal angle δ_n, average displacement $\Delta\delta$, average value of the parameter DIST, RMS of the ALPHA distribution for enabled GF and impact parameters between 60 m and 120 m. The RMS of the ALPHA distribution for disabled GF is given parentheses. The primary γ-ray energy was set to 50 GeV, the ZA to 20° and the azimuth angle to 120°.

$E_\gamma = 50\,\text{GeV}$, Az = 150°, ZA = 20°, Intermediate Image Cleaning

$\delta_n\,[°]$	$\Delta\delta\,[°]$	DIST[°]	$\text{RMS}_{\lvert\text{ALPHA}\rvert}\,[°]$	$\delta_n\,[°]$	$\Delta\delta\,[°]$	DIST[°]	$\text{RMS}_{\lvert\text{ALPHA}\rvert}\,[°]$
IP = 60 m				**IP = 80 m**			
0.23 ± 1.09	$+5.24 \pm 2.33$	0.496 ± 0.008	19.0 (17.7)	357.22 ± 0.26	-2.65 ± 0.47	0.598 ± 0.007	15.6 (15.1)
30.31 ± 0.52	$+2.24 \pm 0.94$	0.521 ± 0.005	20.2 (17.8)	30.80 ± 0.56	$+1.20 \pm 1.47$	0.619 ± 0.008	16.3 (11.4)
59.60 ± 1.11	$+7.03 \pm 1.33$	0.505 ± 0.007	23.2 (18.4)	55.63 ± 0.68	-7.06 ± 0.99	0.611 ± 0.010	19.6 (15.8)
89.00 ± 0.71	-4.47 ± 0.82	0.509 ± 0.004	21.0 (24.8)	87.60 ± 0.24	-5.17 ± 0.76	0.602 ± 0.004	19.9 (13.9)
121.14 ± 0.36	-5.86 ± 0.90	0.484 ± 0.007	22.9 (21.3)	118.63 ± 0.70	-5.76 ± 1.62	0.612 ± 0.008	19.1 (15.1)
151.40 ± 1.02	-1.68 ± 1.69	0.494 ± 0.003	20.2 (16.5)	151.55 ± 0.75	-1.83 ± 1.48	0.593 ± 0.001	18.3 (15.7)
182.39 ± 0.47	$+5.96 \pm 1.36$	0.511 ± 0.006	15.5 (18.9)	178.23 ± 0.52	-4.83 ± 0.95	0.612 ± 0.008	18.7 (19.1)
209.59 ± 0.27	$+2.45 \pm 1.00$	0.518 ± 0.008	18.3 (18.2)	207.41 ± 0.58	-0.59 ± 0.68	0.600 ± 0.005	16.1 (17.6)
238.08 ± 0.71	$+0.59 \pm 1.03$	0.496 ± 0.005	21.2 (19.6)	239.74 ± 0.92	-5.30 ± 1.80	0.607 ± 0.004	18.4 (14.9)
269.11 ± 0.44	-0.47 ± 0.55	0.502 ± 0.002	19.6 (18.9)	269.53 ± 0.63	-1.05 ± 1.90	0.581 ± 0.002	20.2 (18.4)
303.30 ± 0.18	$+5.28 \pm 0.51$	0.470 ± 0.001	21.6 (19.4)	303.38 ± 0.75	-0.31 ± 2.15	0.596 ± 0.008	19.2 (14.3)
326.91 ± 1.14	-0.97 ± 1.70	0.487 ± 0.004	17.9 (22.0)	330.81 ± 0.16	-2.25 ± 1.15	0.600 ± 0.003	16.6 (12.9)
IP = 100 m				**IP = 120 m**			
1.37 ± 0.41	$+4.62 \pm 1.41$	0.682 ± 0.007	12.8 (10.1)	0.08 ± 0.34	-1.92 ± 0.92	0.723 ± 0.008	10.9 (10.3)
27.51 ± 0.53	-1.25 ± 1.49	0.697 ± 0.004	15.1 (16.0)	28.79 ± 0.32	$+0.13 \pm 0.72$	0.718 ± 0.010	12.2 (11.5)
58.13 ± 0.57	-0.92 ± 1.53	0.672 ± 0.005	17.5 (11.4)	58.69 ± 0.41	$+0.25 \pm 0.99$	0.674 ± 0.006	14.1 (7.5)
90.71 ± 0.58	-2.23 ± 0.88	0.664 ± 0.009	17.6 (14.6)	89.29 ± 0.52	$+0.48 \pm 1.35$	0.661 ± 0.007	15.3 (8.5)
123.10 ± 0.65	$+2.09 \pm 1.49$	0.644 ± 0.003	18.7 (11.3)	122.18 ± 0.41	$+1.17 \pm 1.07$	0.687 ± 0.005	15.7 (8.6)
151.32 ± 0.60	-1.39 ± 1.40	0.679 ± 0.008	15.3 (12.6)	152.16 ± 0.43	$+1.71 \pm 0.82$	0.721 ± 0.004	13.4 (10.0)
178.72 ± 0.49	-1.26 ± 1.11	0.688 ± 0.004	13.1 (13.2)	179.49 ± 0.34	-1.84 ± 1.04	0.720 ± 0.007	13.6 (8.6)
209.81 ± 0.54	$+0.67 \pm 1.29$	0.696 ± 0.002	14.1 (10.1)	208.61 ± 0.37	-0.33 ± 1.17	0.712 ± 0.006	14.6 (7.0)
237.89 ± 0.55	$+0.42 \pm 1.47$	0.675 ± 0.006	15.2 (12.7)	238.94 ± 0.40	-0.78 ± 1.18	0.678 ± 0.007	14.2 (9.8)
271.05 ± 0.57	$+1.75 \pm 1.33$	0.668 ± 0.010	16.4 (9.2)	270.28 ± 0.41	$+2.87 \pm 0.74$	0.658 ± 0.008	14.5 (7.5)
301.74 ± 0.37	$+2.81 \pm 1.08$	0.636 ± 0.005	17.6 (14.3)	301.40 ± 0.46	$+0.49 \pm 1.13$	0.666 ± 0.006	16.7 (9.4)
332.00 ± 0.47	$+1.66 \pm 0.97$	0.667 ± 0.008	12.5 (14.8)	332.90 ± 0.27	-0.44 ± 0.93	0.706 ± 0.005	13.1 (9.0)

Table 22: The nominal angle δ_n, average displacement $\Delta\delta$, average value of the parameter DIST, RMS of the ALPHA distribution for enabled GF and impact parameters between 60 m and 120 m. The RMS of the ALPHA distribution for disabled GF is given parentheses. The primary γ-ray energy was set to 50 GeV, the ZA to 20° and the azimuth angle to 150°.

$E_\gamma = 50\,\text{GeV}$, Az = 180°, ZA = 20°, Intermediate Image Cleaning

$\delta_n\,[°]$	$\Delta\delta\,[°]$	DIST[°]	$\text{RMS}_{\lvert\text{ALPHA}\rvert}\,[°]$	$\delta_n\,[°]$	$\Delta\delta\,[°]$	DIST[°]	$\text{RMS}_{\lvert\text{ALPHA}\rvert}\,[°]$
IP = 60 m				**IP = 80 m**			
0.23 ± 1.09	$+3.34 \pm 1.69$	0.525 ± 0.008	16.0 (17.7)	357.22 ± 0.26	-0.75 ± 1.05	0.626 ± 0.010	14.2 (15.1)
30.31 ± 0.52	$+1.98 \pm 1.32$	0.520 ± 0.005	18.1 (17.8)	30.80 ± 0.56	$+3.17 \pm 1.24$	0.628 ± 0.010	15.3 (11.4)
59.60 ± 1.11	$+0.17 \pm 1.95$	0.505 ± 0.003	22.1 (18.4)	55.63 ± 0.68	-1.09 ± 1.20	0.615 ± 0.010	20.4 (15.8)
89.00 ± 0.71	-6.14 ± 1.14	0.501 ± 0.007	20.7 (24.8)	87.60 ± 0.24	-2.83 ± 0.77	0.593 ± 0.001	21.3 (13.9)
121.14 ± 0.36	-3.77 ± 0.86	0.497 ± 0.011	17.4 (21.3)	118.63 ± 0.70	-5.68 ± 1.20	0.612 ± 0.005	13.1 (15.1)
151.40 ± 1.02	-1.90 ± 1.85	0.516 ± 0.007	17.8 (16.5)	151.55 ± 0.75	-1.48 ± 1.87	0.604 ± 0.007	9.9 (15.7)
182.39 ± 0.47	-0.14 ± 1.30	0.510 ± 0.007	14.1 (18.9)	178.23 ± 0.52	-3.09 ± 1.15	0.642 ± 0.007	14.5 (19.1)
209.59 ± 0.27	$+3.17 \pm 0.48$	0.493 ± 0.008	21.1 (18.2)	207.41 ± 0.58	$+1.98 \pm 1.27$	0.620 ± 0.007	15.9 (17.6)
238.08 ± 0.71	$+2.87 \pm 0.92$	0.495 ± 0.005	21.9 (19.6)	239.74 ± 0.92	$+0.34 \pm 1.61$	0.609 ± 0.003	19.5 (14.9)
269.11 ± 0.44	$+0.13 \pm 0.83$	0.485 ± 0.006	21.9 (18.9)	269.53 ± 0.63	-3.79 ± 0.73	0.605 ± 0.009	13.0 (18.4)
303.30 ± 0.18	-0.44 ± 0.49	0.488 ± 0.006	22.8 (19.4)	303.38 ± 0.75	$+2.57 \pm 1.84$	0.608 ± 0.001	15.7 (14.3)
326.91 ± 1.14	$+0.40 \pm 2.31$	0.506 ± 0.005	20.9 (22.0)	330.81 ± 0.16	-1.06 ± 0.45	0.638 ± 0.013	11.1 (12.9)
IP = 100 m				**IP = 120 m**			
1.37 ± 0.41	$+0.88 \pm 0.82$	0.718 ± 0.010	17.1 (10.1)	0.08 ± 0.34	-0.40 ± 1.06	0.738 ± 0.005	11.8 (10.3)
27.51 ± 0.53	-1.84 ± 0.62	0.704 ± 0.010	10.9 (16.0)	28.79 ± 0.32	$+1.89 \pm 1.02$	0.728 ± 0.007	10.7 (11.5)
58.13 ± 0.57	-0.47 ± 1.78	0.680 ± 0.011	13.1 (11.4)	58.69 ± 0.41	-1.85 ± 0.81	0.714 ± 0.006	12.3 (7.5)
90.71 ± 0.58	-0.26 ± 1.76	0.690 ± 0.013	13.1 (14.6)	89.29 ± 0.52	-0.01 ± 1.46	0.672 ± 0.004	15.0 (8.5)
123.10 ± 0.65	$+2.29 \pm 1.40$	0.673 ± 0.010	11.3 (11.3)	122.18 ± 0.41	$+1.53 \pm 1.16$	0.709 ± 0.007	11.0 (8.6)
151.32 ± 0.60	-1.00 ± 1.59	0.697 ± 0.010	15.1 (12.6)	152.16 ± 0.43	$+1.21 \pm 1.14$	0.729 ± 0.004	8.8 (10.0)
178.72 ± 0.49	-1.15 ± 0.90	0.719 ± 0.007	15.6 (13.2)	179.49 ± 0.34	-0.75 ± 1.08	0.757 ± 0.008	6.1 (8.6)
209.81 ± 0.54	$+2.76 \pm 1.21$	0.705 ± 0.004	11.8 (10.1)	208.61 ± 0.37	-0.72 ± 0.63	0.732 ± 0.006	11.6 (7.0)
237.89 ± 0.55	$+0.91 \pm 1.27$	0.689 ± 0.006	17.2 (12.7)	238.94 ± 0.40	-2.32 ± 0.98	0.713 ± 0.007	15.5 (9.8)
271.05 ± 0.57	$+1.29 \pm 1.23$	0.677 ± 0.005	17.6 (9.2)	270.28 ± 0.41	-1.80 ± 1.14	0.664 ± 0.005	11.5 (7.5)
301.74 ± 0.37	$+0.51 \pm 1.36$	0.685 ± 0.009	10.3 (14.3)	301.40 ± 0.46	$+1.33 \pm 1.02$	0.693 ± 0.007	12.0 (9.4)
332.00 ± 0.47	$+1.20 \pm 1.33$	0.706 ± 0.010	13.9 (14.8)	332.90 ± 0.27	$+3.77 \pm 0.89$	0.714 ± 0.008	9.5 (9.0)

Table 23: The nominal angle δ_n, average displacement $\Delta\delta$, average value of the parameter DIST, RMS of the ALPHA distribution for enabled GF and impact parameters between 60 m and 120 m. The RMS of the ALPHA distribution for disabled GF is given parentheses. The primary γ-ray energy was set to 50 GeV, the ZA to 20° and the azimuth angle to 180°.

$E_\gamma = 70\,\mathrm{GeV}$, Az $= 0°$, ZA $= 0°$, Intermediate Image Cleaning

$\delta_n[°]$	$\Delta\delta[°]$	DIST[°]	$\mathrm{RMS}_{\lvert\mathrm{ALPHA}\rvert}[°]$	$\delta_n[°]$	$\Delta\delta[°]$	DIST[°]	$\mathrm{RMS}_{\lvert\mathrm{ALPHA}\rvert}[°]$
IP = 60 m				**IP = 80 m**			
358.53 ± 0.47	-3.26 ± 0.96	0.457 ± 0.005	13.5 (18.9)	359.18 ± 0.31	-1.91 ± 0.81	0.581 ± 0.007	12.8 (14.0)
28.10 ± 0.47	$+0.41 \pm 0.94$	0.449 ± 0.004	16.7 (18.5)	29.69 ± 0.36	$+2.05 \pm 0.94$	0.568 ± 0.004	15.7 (11.1)
60.29 ± 0.42	$+3.05 \pm 1.14$	0.465 ± 0.003	20.0 (16.4)	60.00 ± 0.36	$+1.20 \pm 1.07$	0.571 ± 0.004	17.4 (12.4)
89.51 ± 0.41	$+1.41 \pm 1.01$	0.466 ± 0.004	23.0 (18.8)	90.46 ± 0.36	$+1.22 \pm 1.10$	0.579 ± 0.004	16.5 (10.3)
121.04 ± 0.52	-3.54 ± 1.35	0.464 ± 0.003	24.0 (16.2)	121.02 ± 0.36	-0.13 ± 1.00	0.573 ± 0.006	19.0 (12.0)
151.37 ± 0.58	-3.19 ± 1.28	0.459 ± 0.002	18.0 (16.0)	151.08 ± 0.40	$+0.10 \pm 0.81$	0.568 ± 0.005	17.0 (12.6)
180.90 ± 0.48	$+2.84 \pm 1.02$	0.462 ± 0.003	16.9 (15.9)	179.53 ± 0.36	$+1.07 \pm 0.85$	0.568 ± 0.006	13.8 (12.0)
209.19 ± 0.57	$+4.78 \pm 0.82$	0.463 ± 0.003	18.0 (16.4)	209.07 ± 0.41	$+2.05 \pm 0.94$	0.572 ± 0.003	13.7 (12.3)
238.96 ± 0.42	$+3.71 \pm 0.91$	0.467 ± 0.003	20.7 (16.9)	239.92 ± 0.46	$+0.58 \pm 1.04$	0.569 ± 0.004	16.5 (10.1)
268.97 ± 0.47	-1.19 ± 1.13	0.466 ± 0.003	20.7 (16.1)	269.42 ± 0.40	$+0.21 \pm 1.16$	0.579 ± 0.004	20.0 (12.0)
301.41 ± 0.42	$+0.08 \pm 0.95$	0.466 ± 0.004	21.5 (15.5)	300.09 ± 0.41	-1.87 ± 1.12	0.580 ± 0.005	17.0 (12.3)
330.30 ± 0.53	-3.65 ± 0.89	0.459 ± 0.004	16.8 (16.7)	330.75 ± 0.46	-1.84 ± 0.87	0.569 ± 0.005	14.6 (11.9)
IP = 100 m				**IP = 120 m**			
359.31 ± 0.30	-0.69 ± 0.67	0.662 ± 0.006	9.2 (10.0)	359.74 ± 0.26	-0.03 ± 0.68	0.714 ± 0.005	8.7 (6.8)
29.15 ± 0.30	-1.42 ± 0.71	0.647 ± 0.006	10.6 (9.3)	29.79 ± 0.25	-2.29 ± 0.69	0.706 ± 0.004	13.1 (7.0)
60.10 ± 0.25	-2.82 ± 0.78	0.650 ± 0.004	9.3 (6.6)	60.38 ± 0.31	-2.51 ± 0.67	0.689 ± 0.005	10.4 (4.9)
90.61 ± 0.34	$+1.36 \pm 0.93$	0.633 ± 0.005	12.1 (5.6)	90.17 ± 0.25	$+0.34 \pm 0.86$	0.683 ± 0.005	8.9 (6.1)
120.69 ± 0.35	$+1.10 \pm 1.02$	0.642 ± 0.005	15.3 (5.9)	120.49 ± 0.26	$+4.72 \pm 0.61$	0.679 ± 0.005	12.3 (5.4)
150.48 ± 0.34	$+2.21 \pm 0.69$	0.654 ± 0.005	12.1 (6.4)	149.92 ± 0.30	$+2.30 \pm 0.81$	0.690 ± 0.005	12.1 (6.7)
179.92 ± 0.30	-0.50 ± 0.61	0.661 ± 0.007	10.6 (6.1)	180.22 ± 0.32	-0.33 ± 0.72	0.707 ± 0.005	10.6 (8.7)
208.81 ± 0.34	-2.15 ± 0.69	0.649 ± 0.005	9.2 (9.2)	210.10 ± 0.30	-2.58 ± 0.68	0.690 ± 0.005	12.2 (5.5)
238.86 ± 0.35	-2.11 ± 0.81	0.651 ± 0.006	13.0 (9.8)	239.73 ± 0.26	-4.73 ± 0.49	0.684 ± 0.006	10.5 (6.0)
269.84 ± 0.29	$+0.43 \pm 0.83$	0.639 ± 0.006	12.0 (6.0)	269.61 ± 0.30	-0.44 ± 0.76	0.691 ± 0.004	9.8 (5.1)
300.61 ± 0.30	$+1.75 \pm 0.93$	0.648 ± 0.006	15.4 (6.0)	299.69 ± 0.21	$+2.83 \pm 0.69$	0.690 ± 0.005	9.4 (6.3)
330.29 ± 0.34	$+2.00 \pm 0.81$	0.655 ± 0.006	13.8 (7.1)	330.07 ± 0.30	$+3.60 \pm 0.75$	0.713 ± 0.005	10.2 (5.2)

Table 24: The nominal angle δ_n, average displacement $\Delta\delta$, average value of the parameter DIST, RMS of the ALPHA distribution for enabled GF and impact parameters between 60 m and 120 m. The RMS of the ALPHA distribution for disabled GF is given parentheses. The primary γ-ray energy was set to 70 GeV, the ZA to 0° and the azimuth angle to 0°.

$E_\gamma = 70\,\mathrm{GeV}$, Az $= 0°$, ZA $= 20°$, Intermediate Image Cleaning

$\delta_n[°]$	$\Delta\delta[°]$	DIST[°]	$\mathrm{RMS}_{\lvert\mathrm{ALPHA}\rvert}[°]$	$\delta_n[°]$	$\Delta\delta[°]$	DIST[°]	$\mathrm{RMS}_{\lvert\mathrm{ALPHA}\rvert}[°]$
IP = 60 m				**IP = 80 m**			
359.95 ± 0.73	$+2.59 \pm 1.54$	0.437 ± 0.003	17.3 (18.2)	0.63 ± 0.59	$+2.60 \pm 1.11$	0.545 ± 0.004	13.4 (14.1)
26.29 ± 0.65	$+0.60 \pm 1.34$	0.430 ± 0.003	17.8 (21.4)	29.12 ± 0.59	$+1.74 \pm 1.08$	0.540 ± 0.002	15.7 (14.0)
61.24 ± 0.61	$+4.79 \pm 1.07$	0.430 ± 0.003	20.4 (20.9)	59.14 ± 0.53	$+2.92 \pm 1.02$	0.518 ± 0.004	18.5 (14.8)
88.38 ± 0.73	$+0.97 \pm 1.30$	0.410 ± 0.003	21.9 (17.9)	91.38 ± 0.47	$+3.91 \pm 1.46$	0.523 ± 0.003	19.9 (15.0)
121.64 ± 0.92	-2.77 ± 1.37	0.411 ± 0.004	19.6 (16.3)	121.65 ± 0.41	$+0.66 \pm 0.91$	0.521 ± 0.004	20.0 (16.7)
153.64 ± 0.72	-0.33 ± 1.50	0.428 ± 0.003	21.0 (18.9)	151.83 ± 0.46	-0.77 ± 1.00	0.529 ± 0.005	14.7 (14.0)
180.25 ± 0.61	$+0.02 \pm 1.25$	0.429 ± 0.004	17.8 (20.2)	178.69 ± 0.52	$+0.03 \pm 1.02$	0.537 ± 0.004	15.3 (14.3)
206.57 ± 0.48	-0.94 ± 1.17	0.426 ± 0.003	17.6 (18.3)	207.35 ± 0.57	$+0.75 \pm 1.06$	0.530 ± 0.004	17.2 (13.4)
237.96 ± 0.41	$+1.06 \pm 0.95$	0.419 ± 0.003	20.0 (18.2)	237.14 ± 0.52	-0.70 ± 0.94	0.527 ± 0.003	19.8 (15.9)
269.68 ± 0.30	-1.72 ± 1.37	0.423 ± 0.003	19.5 (19.3)	268.94 ± 0.41	-4.27 ± 0.90	0.529 ± 0.004	18.5 (15.8)
303.21 ± 0.56	-1.81 ± 1.37	0.423 ± 0.003	21.7 (20.1)	302.03 ± 0.60	-1.39 ± 1.39	0.534 ± 0.003	17.1 (14.1)
331.03 ± 0.68	-4.66 ± 1.19	0.438 ± 0.003	18.5 (18.6)	330.54 ± 0.47	-3.88 ± 0.89	0.538 ± 0.003	15.3 (14.5)
IP = 100 m				**IP = 120 m**			
0.03 ± 0.33	$+0.39 \pm 0.88$	0.631 ± 0.006	9.4 (10.0)	359.61 ± 0.32	-0.37 ± 0.76	0.680 ± 0.004	7.2 (5.9)
29.01 ± 0.37	$+1.34 \pm 0.85$	0.619 ± 0.004	11.7 (10.3)	28.16 ± 0.30	-0.47 ± 0.66	0.663 ± 0.005	8.0 (7.3)
59.42 ± 0.38	$+2.79 \pm 0.91$	0.588 ± 0.003	14.6 (9.2)	58.59 ± 0.35	-0.52 ± 0.82	0.641 ± 0.006	8.8 (7.2)
88.72 ± 0.49	-0.40 ± 1.25	0.599 ± 0.004	14.6 (10.8)	89.92 ± 0.30	$+0.25 \pm 0.77$	0.622 ± 0.005	10.3 (7.7)
121.93 ± 0.43	$+0.85 \pm 1.20$	0.592 ± 0.005	15.0 (11.7)	122.34 ± 0.31	$+2.54 \pm 0.71$	0.639 ± 0.005	12.4 (5.6)
151.09 ± 0.43	-1.00 ± 0.96	0.610 ± 0.005	12.1 (11.8)	151.52 ± 0.30	$+0.85 \pm 0.70$	0.654 ± 0.005	9.3 (8.4)
179.61 ± 0.44	-1.08 ± 0.80	0.616 ± 0.005	10.1 (10.3)	180.29 ± 0.31	-0.04 ± 0.69	0.672 ± 0.005	7.2 (5.8)
207.13 ± 0.47	-0.55 ± 0.82	0.613 ± 0.005	12.1 (10.7)	207.40 ± 0.35	-1.25 ± 0.71	0.663 ± 0.005	9.5 (6.4)
237.33 ± 0.27	-2.27 ± 0.80	0.598 ± 0.004	13.1 (10.2)	238.15 ± 0.26	-1.26 ± 0.59	0.654 ± 0.003	11.7 (8.2)
268.35 ± 0.43	-1.12 ± 0.77	0.598 ± 0.006	15.0 (12.5)	270.00 ± 0.25	$+0.43 \pm 0.67$	0.627 ± 0.006	9.0 (8.8)
302.87 ± 0.50	$+0.93 \pm 0.96$	0.604 ± 0.004	16.9 (9.8)	302.47 ± 0.31	$+1.93 \pm 0.65$	0.650 ± 0.006	11.2 (6.0)
332.10 ± 0.38	-0.36 ± 0.97	0.627 ± 0.003	9.3 (9.2)	331.73 ± 0.30	-0.15 ± 0.66	0.667 ± 0.005	7.1 (7.6)

Table 25: The nominal angle δ_n, average displacement $\Delta\delta$, average value of the parameter DIST, RMS of the ALPHA distribution for enabled GF and impact parameters between 60 m and 120 m. The RMS of the ALPHA distribution for disabled GF is given parentheses. The primary γ-ray energy was set to 70 GeV, the ZA to 20° and the azimuth angle to 0°.

$E_\gamma = 70\,\mathrm{GeV}$, Az = 30°, ZA = 20°, Intermediate Image Cleaning

$\delta_n[°]$	$\Delta\delta[°]$	DIST[°]	$\mathrm{RMS}_{\lvert\mathrm{ALPHA}\rvert}[°]$	$\delta_n[°]$	$\Delta\delta[°]$	DIST[°]	$\mathrm{RMS}_{\lvert\mathrm{ALPHA}\rvert}[°]$
IP = 60 m				**IP = 80 m**			
359.95 ± 0.73	-0.38 ± 1.55	0.434 ± 0.004	17.6 (18.2)	0.63 ± 0.59	-2.19 ± 1.27	0.526 ± 0.004	15.0 (14.1)
26.29 ± 0.65	-2.81 ± 1.16	0.405 ± 0.004	18.1 (21.4)	29.12 ± 0.59	$+1.35 \pm 1.08$	0.513 ± 0.006	15.3 (14.0)
61.24 ± 0.61	$+5.28 \pm 1.30$	0.407 ± 0.003	19.5 (20.9)	59.14 ± 0.53	$+1.74 \pm 0.97$	0.512 ± 0.005	17.1 (14.8)
88.38 ± 0.73	$+0.29 \pm 1.75$	0.417 ± 0.004	22.2 (17.9)	91.38 ± 0.47	$+0.44 \pm 1.06$	0.526 ± 0.004	18.1 (15.0)
121.64 ± 0.92	$+2.17 \pm 1.70$	0.434 ± 0.003	20.4 (16.3)	121.65 ± 0.41	$+1.28 \pm 0.86$	0.543 ± 0.005	17.9 (16.7)
153.64 ± 0.72	$+0.73 \pm 1.82$	0.434 ± 0.005	19.0 (18.9)	151.83 ± 0.46	$+0.85 \pm 0.97$	0.558 ± 0.005	16.8 (14.0)
180.25 ± 0.61	-3.20 ± 1.54	0.434 ± 0.004	17.2 (20.2)	178.69 ± 0.52	-3.08 ± 1.16	0.543 ± 0.004	14.5 (14.3)
206.57 ± 0.48	-1.30 ± 1.00	0.418 ± 0.004	17.3 (18.3)	207.35 ± 0.57	$+0.03 \pm 1.00$	0.531 ± 0.005	15.5 (13.4)
237.96 ± 0.41	$+2.13 \pm 0.97$	0.421 ± 0.003	19.3 (18.2)	237.14 ± 0.52	-0.29 ± 1.02	0.517 ± 0.005	16.8 (15.9)
269.68 ± 0.30	$+3.69 \pm 1.07$	0.429 ± 0.004	21.6 (19.3)	268.94 ± 0.41	$+2.98 \pm 1.03$	0.537 ± 0.004	17.4 (15.8)
303.21 ± 0.56	$+3.34 \pm 1.26$	0.440 ± 0.004	21.1 (20.1)	302.03 ± 0.60	-0.95 ± 1.30	0.543 ± 0.005	16.5 (14.1)
331.03 ± 0.68	-3.03 ± 1.59	0.438 ± 0.004	20.6 (18.6)	330.54 ± 0.47	-2.70 ± 1.02	0.545 ± 0.005	16.0 (14.5)
IP = 100 m				**IP = 120 m**			
0.03 ± 0.33	-2.07 ± 0.76	0.616 ± 0.005	11.2 (10.0)	359.61 ± 0.32	$+1.10 \pm 0.68$	0.667 ± 0.006	9.6 (5.9)
29.01 ± 0.37	$+0.37 \pm 0.73$	0.600 ± 0.007	12.8 (10.3)	28.16 ± 0.30	$+0.17 \pm 0.65$	0.670 ± 0.007	9.0 (7.3)
59.42 ± 0.38	$+1.58 \pm 0.80$	0.608 ± 0.007	14.5 (9.2)	58.59 ± 0.35	-0.65 ± 0.79	0.654 ± 0.007	11.5 (7.2)
88.72 ± 0.49	-1.13 ± 1.04	0.600 ± 0.005	15.0 (10.8)	89.92 ± 0.30	$+0.35 \pm 0.76$	0.626 ± 0.005	11.3 (7.7)
121.93 ± 0.43	$+0.06 \pm 0.84$	0.613 ± 0.005	13.7 (11.7)	122.34 ± 0.31	-0.33 ± 0.76	0.642 ± 0.004	11.3 (5.6)
151.09 ± 0.43	-1.92 ± 0.95	0.630 ± 0.005	13.3 (11.8)	151.52 ± 0.30	$+1.57 \pm 0.62$	0.664 ± 0.005	10.0 (8.4)
179.61 ± 0.44	-0.92 ± 0.86	0.629 ± 0.005	11.9 (10.3)	180.29 ± 0.31	$+1.20 \pm 0.67$	0.671 ± 0.005	10.0 (5.8)
207.13 ± 0.47	-1.91 ± 0.89	0.617 ± 0.006	13.0 (10.7)	207.40 ± 0.35	$+0.62 \pm 0.64$	0.675 ± 0.005	10.1 (6.4)
237.33 ± 0.27	-1.29 ± 0.58	0.609 ± 0.006	13.2 (10.2)	238.15 ± 0.26	-0.20 ± 0.56	0.659 ± 0.005	11.9 (8.2)
268.35 ± 0.43	-0.11 ± 0.78	0.612 ± 0.004	15.7 (12.5)	270.00 ± 0.25	-0.33 ± 0.70	0.646 ± 0.007	12.0 (8.8)
302.87 ± 0.50	$+2.51 \pm 1.10$	0.626 ± 0.006	15.0 (9.8)	302.47 ± 0.31	$+0.34 \pm 0.74$	0.647 ± 0.005	12.5 (6.0)
332.10 ± 0.38	$+0.11 \pm 0.90$	0.638 ± 0.007	12.7 (9.2)	331.73 ± 0.30	$+1.48 \pm 0.68$	0.670 ± 0.006	10.6 (7.6)

Table 26: The nominal angle δ_n, average displacement $\Delta\delta$, average value of the parameter DIST, RMS of the ALPHA distribution for enabled GF and impact parameters between 60 m and 120 m. The RMS of the ALPHA distribution for disabled GF is given parentheses. The primary γ-ray energy was set to 70 GeV, the ZA to 20° and the azimuth angle to 30°.

$E_\gamma = 70\,\mathrm{GeV}$, Az = 60°, ZA = 20°, Intermediate Image Cleaning

$\delta_n[°]$	$\Delta\delta[°]$	DIST[°]	$\mathrm{RMS}_{\lvert\mathrm{ALPHA}\rvert}[°]$	$\delta_n[°]$	$\Delta\delta[°]$	DIST[°]	$\mathrm{RMS}_{\lvert\mathrm{ALPHA}\rvert}[°]$
IP = 60 m				**IP = 80 m**			
359.95 ± 0.73	-7.95 ± 1.77	0.422 ± 0.004	17.0 (18.2)	0.63 ± 0.59	$+1.35 \pm 0.99$	0.532 ± 0.004	14.3 (14.1)
26.29 ± 0.65	-5.17 ± 1.51	0.423 ± 0.004	17.6 (21.4)	29.12 ± 0.59	-3.99 ± 1.21	0.522 ± 0.005	14.7 (14.0)
61.24 ± 0.61	-1.09 ± 1.00	0.431 ± 0.004	18.0 (20.9)	59.14 ± 0.53	-2.03 ± 0.93	0.543 ± 0.007	16.7 (14.8)
88.38 ± 0.73	-1.47 ± 1.53	0.454 ± 0.004	18.4 (17.9)	91.38 ± 0.47	$+0.04 \pm 1.04$	0.559 ± 0.005	17.5 (15.0)
121.64 ± 0.92	$+2.09 \pm 1.91$	0.466 ± 0.004	19.9 (16.3)	121.65 ± 0.41	$+0.45 \pm 0.87$	0.557 ± 0.006	17.6 (16.7)
153.64 ± 0.72	$+1.47 \pm 1.05$	0.445 ± 0.004	18.2 (18.9)	151.83 ± 0.46	$+2.74 \pm 0.97$	0.551 ± 0.006	17.5 (14.0)
180.25 ± 0.61	$+1.13 \pm 1.49$	0.428 ± 0.004	17.0 (20.2)	178.69 ± 0.52	-2.27 ± 1.26	0.537 ± 0.006	14.5 (14.3)
206.57 ± 0.48	-5.52 ± 1.39	0.433 ± 0.004	16.3 (18.3)	207.35 ± 0.57	-3.54 ± 1.18	0.527 ± 0.006	14.6 (13.4)
237.96 ± 0.41	-2.51 ± 0.99	0.440 ± 0.005	18.5 (18.2)	237.14 ± 0.52	-2.08 ± 1.07	0.548 ± 0.006	16.0 (15.9)
269.68 ± 0.30	$+0.89 \pm 0.70$	0.454 ± 0.004	19.9 (19.3)	268.94 ± 0.41	$+1.40 \pm 0.88$	0.562 ± 0.005	18.2 (15.8)
303.21 ± 0.56	$+4.18 \pm 1.36$	0.437 ± 0.005	18.9 (20.1)	302.03 ± 0.60	$+2.97 \pm 1.57$	0.568 ± 0.005	18.3 (14.1)
331.03 ± 0.68	$+2.58 \pm 1.36$	0.436 ± 0.004	19.4 (18.6)	330.54 ± 0.47	$+0.09 \pm 1.29$	0.551 ± 0.004	17.8 (14.5)
IP = 100 m				**IP = 120 m**			
0.03 ± 0.33	-1.52 ± 0.83	0.620 ± 0.005	12.8 (10.0)	359.61 ± 0.32	$+1.30 \pm 0.83$	0.685 ± 0.007	10.3 (5.9)
29.01 ± 0.37	-1.80 ± 1.02	0.608 ± 0.005	13.1 (10.3)	28.16 ± 0.30	$+2.29 \pm 0.66$	0.674 ± 0.004	12.0 (7.3)
59.42 ± 0.38	-0.46 ± 0.86	0.620 ± 0.008	13.9 (9.2)	58.59 ± 0.35	$+1.04 \pm 0.83$	0.668 ± 0.007	11.7 (7.2)
88.72 ± 0.49	-1.98 ± 1.02	0.621 ± 0.006	15.6 (10.8)	89.92 ± 0.30	-1.64 ± 0.57	0.642 ± 0.005	12.6 (7.7)
121.93 ± 0.43	$+0.77 \pm 1.09$	0.618 ± 0.005	16.6 (11.7)	122.34 ± 0.31	-0.17 ± 0.82	0.651 ± 0.003	11.2 (5.6)
151.09 ± 0.43	$+0.76 \pm 0.99$	0.638 ± 0.007	12.9 (11.8)	151.52 ± 0.30	-1.61 ± 0.75	0.667 ± 0.006	11.3 (8.4)
179.61 ± 0.44	-2.00 ± 1.00	0.637 ± 0.005	13.6 (10.3)	180.29 ± 0.31	$+1.92 \pm 0.61$	0.682 ± 0.007	10.6 (5.8)
207.13 ± 0.47	-1.43 ± 1.06	0.623 ± 0.005	12.7 (10.7)	207.40 ± 0.35	$+1.06 \pm 0.78$	0.684 ± 0.005	10.4 (6.4)
237.33 ± 0.27	-2.36 ± 0.75	0.626 ± 0.004	14.7 (10.2)	238.15 ± 0.26	$+0.65 \pm 0.66$	0.682 ± 0.007	11.3 (8.2)
268.35 ± 0.43	-2.02 ± 0.95	0.629 ± 0.006	15.7 (12.5)	270.00 ± 0.25	-0.53 ± 0.78	0.659 ± 0.006	13.0 (8.8)
302.87 ± 0.50	$+2.72 \pm 1.24$	0.624 ± 0.004	15.7 (9.8)	302.47 ± 0.31	-0.73 ± 0.75	0.657 ± 0.004	11.8 (6.0)
332.10 ± 0.38	-0.40 ± 0.81	0.635 ± 0.005	14.4 (9.2)	331.73 ± 0.30	-1.95 ± 0.75	0.671 ± 0.007	11.3 (7.6)

Table 27: The nominal angle δ_n, average displacement $\Delta\delta$, average value of the parameter DIST, RMS of the ALPHA distribution for enabled GF and impact parameters between 60 m and 120 m. The RMS of the ALPHA distribution for disabled GF is given parentheses. The primary γ-ray energy was set to 70 GeV, the ZA to 20° and the azimuth angle to 60°.

$E_\gamma = 70\,\mathrm{GeV}$, Az = 90°, ZA = 20°, Intermediate Image Cleaning

δ_n[°]	$\Delta\delta$[°]	DIST[°]	$\mathrm{RMS}_{\mathrm{|ALPHA|}}$[°]	δ_n[°]	$\Delta\delta$[°]	DIST[°]	$\mathrm{RMS}_{\mathrm{|ALPHA|}}$[°]
IP = 60 m				IP = 80 m			
359.95 ± 0.73	$+0.76 \pm 0.86$	0.438 ± 0.004	18.0 (18.2)	0.63 ± 0.59	$+1.62 \pm 0.92$	0.537 ± 0.007	13.3 (14.1)
26.29 ± 0.65	-3.83 ± 1.48	0.433 ± 0.004	18.0 (21.4)	29.12 ± 0.59	-1.88 ± 0.73	0.535 ± 0.005	13.9 (14.0)
61.24 ± 0.61	$+3.28 \pm 1.24$	0.444 ± 0.004	20.5 (20.9)	59.14 ± 0.53	-1.16 ± 1.01	0.555 ± 0.004	15.7 (14.8)
88.38 ± 0.73	-2.76 ± 1.57	0.466 ± 0.002	21.6 (17.9)	91.38 ± 0.47	-0.06 ± 1.01	0.575 ± 0.006	17.3 (15.0)
121.64 ± 0.92	-0.88 ± 0.99	0.451 ± 0.005	21.3 (16.3)	121.65 ± 0.41	$+0.09 \pm 1.03$	0.563 ± 0.005	20.7 (16.7)
153.64 ± 0.72	$+5.58 \pm 1.55$	0.445 ± 0.004	19.4 (18.9)	151.83 ± 0.46	$+1.77 \pm 1.20$	0.554 ± 0.004	18.0 (14.0)
180.25 ± 0.61	-2.25 ± 1.11	0.429 ± 0.004	19.0 (20.2)	178.69 ± 0.52	-0.49 ± 1.20	0.535 ± 0.006	14.3 (14.3)
206.57 ± 0.48	-4.21 ± 1.16	0.438 ± 0.006	18.6 (18.3)	207.35 ± 0.57	$+0.31 \pm 1.16$	0.554 ± 0.006	12.4 (13.4)
237.96 ± 0.41	-0.25 ± 0.81	0.453 ± 0.005	21.8 (18.2)	237.14 ± 0.52	-2.30 ± 0.98	0.565 ± 0.003	17.2 (15.9)
269.68 ± 0.30	-1.16 ± 0.51	0.465 ± 0.005	19.9 (19.3)	268.94 ± 0.41	-3.21 ± 1.09	0.574 ± 0.007	18.4 (15.8)
303.21 ± 0.56	$+3.14 \pm 1.37$	0.458 ± 0.003	20.7 (20.1)	302.03 ± 0.60	$+1.36 \pm 1.08$	0.568 ± 0.006	17.1 (14.1)
331.03 ± 0.68	$+0.48 \pm 1.30$	0.438 ± 0.005	20.5 (18.6)	330.54 ± 0.47	$+0.80 \pm 0.94$	0.540 ± 0.005	16.9 (14.5)
IP = 100 m				IP = 120 m			
0.03 ± 0.33	$+2.37 \pm 0.94$	0.614 ± 0.007	12.1 (10.0)	359.61 ± 0.32	-2.36 ± 0.77	0.686 ± 0.003	8.8 (5.9)
29.01 ± 0.37	$+0.09 \pm 0.99$	0.625 ± 0.007	12.9 (10.3)	28.16 ± 0.30	$+0.72 \pm 0.79$	0.687 ± 0.003	11.5 (7.3)
59.42 ± 0.38	$+2.14 \pm 0.92$	0.636 ± 0.005	14.8 (9.2)	58.59 ± 0.35	$+1.35 \pm 0.87$	0.683 ± 0.007	8.6 (7.2)
88.72 ± 0.49	-0.17 ± 1.09	0.636 ± 0.006	13.6 (10.8)	89.92 ± 0.30	$+1.08 \pm 0.77$	0.657 ± 0.003	8.6 (7.7)
121.93 ± 0.43	$+0.90 \pm 0.98$	0.618 ± 0.006	14.1 (11.7)	122.34 ± 0.31	$+1.61 \pm 0.71$	0.651 ± 0.006	9.4 (5.6)
151.09 ± 0.43	$+1.24 \pm 1.13$	0.636 ± 0.005	15.4 (11.8)	151.52 ± 0.30	-1.13 ± 0.73	0.685 ± 0.006	10.2 (8.4)
179.61 ± 0.44	-0.03 ± 1.06	0.625 ± 0.006	13.0 (10.3)	180.29 ± 0.31	-0.44 ± 0.83	0.683 ± 0.005	10.4 (5.8)
207.13 ± 0.47	-2.73 ± 1.13	0.636 ± 0.007	13.0 (10.7)	207.40 ± 0.35	$+0.81 \pm 0.90$	0.700 ± 0.008	7.9 (6.4)
237.33 ± 0.27	-1.68 ± 0.79	0.645 ± 0.006	14.2 (10.2)	238.15 ± 0.26	$+0.17 \pm 0.65$	0.683 ± 0.007	10.4 (8.2)
268.35 ± 0.43	-3.86 ± 0.81	0.625 ± 0.008	14.4 (12.5)	270.00 ± 0.25	-1.21 ± 0.70	0.656 ± 0.005	8.8 (8.8)
302.87 ± 0.50	$+0.14 \pm 1.03$	0.624 ± 0.006	14.2 (9.8)	302.47 ± 0.31	$+0.33 \pm 0.77$	0.647 ± 0.005	8.7 (6.0)
332.10 ± 0.38	$+0.56 \pm 0.88$	0.628 ± 0.006	11.9 (9.2)	331.73 ± 0.30	-2.01 ± 0.80	0.679 ± 0.007	10.7 (7.6)

Table 28: The nominal angle δ_n, average displacement $\Delta\delta$, average value of the parameter DIST, RMS of the ALPHA distribution for enabled GF and impact parameters between 60 m and 120 m. The RMS of the ALPHA distribution for disabled GF is given parentheses. The primary γ-ray energy was set to 70 GeV, the ZA to 20° and the azimuth angle to 90°.

$E_\gamma = 70\,\mathrm{GeV}$, Az = 120°, ZA = 20°, Intermediate Image Cleaning

δ_n[°]	$\Delta\delta$[°]	DIST[°]	$\mathrm{RMS}_{\mathrm{|ALPHA|}}$[°]	δ_n[°]	$\Delta\delta$[°]	DIST[°]	$\mathrm{RMS}_{\mathrm{|ALPHA|}}$[°]
IP = 60 m				IP = 80 m			
359.95 ± 0.73	$+6.22 \pm 1.28$	0.425 ± 0.003	16.8 (18.2)	0.63 ± 0.59	$+1.70 \pm 1.34$	0.541 ± 0.004	14.6 (14.1)
26.29 ± 0.65	-0.88 ± 1.40	0.449 ± 0.004	16.6 (21.4)	29.12 ± 0.59	$+0.18 \pm 1.21$	0.555 ± 0.003	13.7 (14.0)
61.24 ± 0.61	-2.25 ± 1.17	0.460 ± 0.005	19.9 (20.9)	59.14 ± 0.53	$+0.22 \pm 1.22$	0.571 ± 0.005	17.1 (14.8)
88.38 ± 0.73	-4.13 ± 1.41	0.457 ± 0.003	20.7 (17.9)	91.38 ± 0.47	-2.85 ± 1.20	0.573 ± 0.006	17.5 (15.0)
121.64 ± 0.92	-0.21 ± 1.47	0.442 ± 0.005	20.4 (16.3)	121.65 ± 0.41	-1.27 ± 0.96	0.555 ± 0.004	18.0 (16.7)
153.64 ± 0.72	$+2.82 \pm 1.40$	0.433 ± 0.004	18.2 (18.9)	151.83 ± 0.46	$+0.28 \pm 0.86$	0.550 ± 0.004	15.6 (14.0)
180.25 ± 0.61	$+7.15 \pm 1.30$	0.435 ± 0.003	15.4 (20.2)	178.69 ± 0.52	$+0.66 \pm 1.08$	0.548 ± 0.006	13.5 (14.3)
206.57 ± 0.48	-0.95 ± 1.88	0.447 ± 0.005	17.1 (18.3)	207.35 ± 0.57	$+1.59 \pm 1.43$	0.567 ± 0.004	14.5 (13.4)
237.96 ± 0.41	-3.97 ± 0.62	0.467 ± 0.004	19.6 (18.2)	237.14 ± 0.52	-4.75 ± 1.19	0.577 ± 0.005	17.2 (15.9)
269.68 ± 0.30	-4.13 ± 0.78	0.452 ± 0.005	19.6 (19.3)	268.94 ± 0.41	-3.52 ± 1.02	0.567 ± 0.006	17.2 (15.8)
303.21 ± 0.56	$+1.06 \pm 1.25$	0.437 ± 0.004	19.9 (20.1)	302.03 ± 0.60	-0.41 ± 1.14	0.549 ± 0.005	19.0 (14.1)
331.03 ± 0.68	$+3.55 \pm 1.56$	0.426 ± 0.005	18.4 (18.6)	330.54 ± 0.47	$+0.91 \pm 0.93$	0.539 ± 0.003	15.9 (14.5)
IP = 100 m				IP = 120 m			
0.03 ± 0.33	-1.65 ± 0.86	0.629 ± 0.004	12.5 (10.0)	359.61 ± 0.32	-2.58 ± 0.82	0.683 ± 0.007	11.5 (5.9)
29.01 ± 0.37	$+1.34 \pm 1.18$	0.645 ± 0.006	12.5 (10.3)	28.16 ± 0.30	-3.24 ± 0.79	0.703 ± 0.006	10.6 (7.3)
59.42 ± 0.38	-0.37 ± 1.26	0.656 ± 0.005	15.6 (9.2)	58.59 ± 0.35	$+1.59 \pm 0.93$	0.694 ± 0.006	11.2 (7.2)
88.72 ± 0.49	-1.05 ± 1.02	0.636 ± 0.005	16.9 (10.8)	89.92 ± 0.30	$+2.06 \pm 0.81$	0.655 ± 0.006	12.4 (7.7)
121.93 ± 0.43	-0.21 ± 0.89	0.629 ± 0.004	17.8 (11.7)	122.34 ± 0.31	$+2.10 \pm 0.79$	0.658 ± 0.007	13.9 (5.6)
151.09 ± 0.43	$+1.18 \pm 0.69$	0.634 ± 0.006	15.4 (11.8)	151.52 ± 0.30	-0.18 ± 0.77	0.686 ± 0.006	12.4 (8.4)
179.61 ± 0.44	-0.34 ± 0.96	0.639 ± 0.004	12.5 (10.3)	180.29 ± 0.31	-1.24 ± 0.77	0.702 ± 0.006	11.1 (5.8)
207.13 ± 0.47	$+0.61 \pm 0.96$	0.646 ± 0.004	11.5 (10.7)	207.40 ± 0.35	-1.59 ± 0.84	0.698 ± 0.006	9.8 (6.4)
237.33 ± 0.27	-0.02 ± 0.96	0.661 ± 0.005	15.0 (10.2)	238.15 ± 0.26	$+2.54 \pm 0.70$	0.690 ± 0.005	12.0 (8.2)
268.35 ± 0.43	-2.82 ± 1.02	0.631 ± 0.005	15.3 (12.5)	270.00 ± 0.25	$+0.59 \pm 0.89$	0.650 ± 0.006	12.0 (8.8)
302.87 ± 0.50	-0.55 ± 1.11	0.629 ± 0.005	16.2 (9.8)	302.47 ± 0.31	$+1.94 \pm 0.79$	0.649 ± 0.006	13.2 (6.0)
332.10 ± 0.38	-0.86 ± 0.90	0.626 ± 0.007	15.7 (9.2)	331.73 ± 0.30	-2.21 ± 0.78	0.679 ± 0.005	11.9 (7.6)

Table 29: The nominal angle δ_n, average displacement $\Delta\delta$, average value of the parameter DIST, RMS of the ALPHA distribution for enabled GF and impact parameters between 60 m and 120 m. The RMS of the ALPHA distribution for disabled GF is given parentheses. The primary γ-ray energy was set to 70 GeV, the ZA to 20° and the azimuth angle to 120°.

$E_\gamma = 70\,\mathrm{GeV}$, Az = 150°, ZA = 20°, Intermediate Image Cleaning

δ_n[°]	$\Delta\delta$[°]	DIST[°]	$\mathrm{RMS}_{\lvert\mathrm{ALPHA}\rvert}$[°]	δ_n[°]	$\Delta\delta$[°]	DIST[°]	$\mathrm{RMS}_{\lvert\mathrm{ALPHA}\rvert}$[°]
IP = 60 m				**IP = 80 m**			
359.95 ± 0.73	$+0.67 \pm 1.00$	0.444 ± 0.004	16.8 (18.2)	0.63 ± 0.59	$+3.11 \pm 1.08$	0.562 ± 0.005	13.9 (14.1)
26.29 ± 0.65	-0.10 ± 1.40	0.461 ± 0.004	17.9 (21.4)	29.12 ± 0.59	$+2.42 \pm 1.62$	0.578 ± 0.006	14.5 (14.0)
61.24 ± 0.61	$+4.39 \pm 1.11$	0.453 ± 0.004	21.9 (20.9)	59.14 ± 0.53	$+2.74 \pm 1.15$	0.570 ± 0.006	19.3 (14.8)
88.38 ± 0.73	-2.85 ± 1.85	0.458 ± 0.004	22.3 (17.9)	91.38 ± 0.47	-0.44 ± 1.14	0.559 ± 0.003	20.1 (15.0)
121.64 ± 0.92	-5.34 ± 1.97	0.455 ± 0.004	21.0 (16.3)	121.65 ± 0.41	-3.11 ± 1.18	0.556 ± 0.004	19.0 (16.7)
153.64 ± 0.72	$+0.26 \pm 1.40$	0.455 ± 0.003	17.5 (18.9)	151.83 ± 0.46	-1.16 ± 0.87	0.564 ± 0.004	16.8 (14.0)
180.25 ± 0.61	$+3.46 \pm 1.25$	0.465 ± 0.003	16.1 (20.2)	178.69 ± 0.52	$+0.04 \pm 0.94$	0.576 ± 0.004	15.1 (14.3)
206.57 ± 0.48	-0.14 ± 1.26	0.462 ± 0.005	18.4 (18.3)	207.35 ± 0.57	$+0.60 \pm 0.98$	0.576 ± 0.005	14.8 (13.4)
237.96 ± 0.41	$+1.28 \pm 1.40$	0.463 ± 0.004	19.2 (18.2)	237.14 ± 0.52	-4.85 ± 0.79	0.580 ± 0.005	18.8 (15.9)
269.68 ± 0.30	$+2.08 \pm 0.94$	0.447 ± 0.003	23.6 (19.3)	268.94 ± 0.41	-2.26 ± 1.29	0.559 ± 0.005	20.1 (15.8)
303.21 ± 0.56	-0.09 ± 1.34	0.438 ± 0.003	21.5 (20.1)	302.03 ± 0.60	-2.32 ± 0.94	0.546 ± 0.005	20.2 (14.1)
331.03 ± 0.68	$+1.21 \pm 1.31$	0.438 ± 0.005	20.5 (18.6)	330.54 ± 0.47	-0.33 ± 1.17	0.543 ± 0.004	17.4 (14.5)
IP = 100 m				**IP = 120 m**			
0.03 ± 0.33	$+0.72 \pm 0.82$	0.653 ± 0.006	11.2 (10.0)	359.61 ± 0.32	-1.74 ± 0.60	0.696 ± 0.005	10.4 (5.9)
29.01 ± 0.37	$+0.13 \pm 0.84$	0.667 ± 0.005	14.4 (10.3)	28.16 ± 0.30	-2.20 ± 0.85	0.711 ± 0.006	10.4 (7.3)
59.42 ± 0.38	$+2.37 \pm 0.83$	0.652 ± 0.005	15.6 (9.2)	58.59 ± 0.35	-0.10 ± 0.92	0.676 ± 0.005	13.3 (7.2)
88.72 ± 0.49	-1.57 ± 0.94	0.631 ± 0.004	17.0 (10.8)	89.92 ± 0.30	$+1.28 \pm 0.84$	0.656 ± 0.005	14.0 (7.7)
121.93 ± 0.43	-0.91 ± 0.91	0.636 ± 0.005	16.4 (11.7)	122.34 ± 0.31	$+1.54 \pm 0.73$	0.670 ± 0.004	13.6 (5.6)
151.09 ± 0.43	-1.49 ± 0.84	0.641 ± 0.005	15.1 (11.8)	151.52 ± 0.30	$+0.89 \pm 0.71$	0.698 ± 0.006	11.6 (8.4)
179.61 ± 0.44	-2.16 ± 0.94	0.660 ± 0.005	13.1 (10.3)	180.29 ± 0.31	-0.39 ± 0.68	0.698 ± 0.006	12.2 (5.8)
207.13 ± 0.47	-0.89 ± 1.07	0.663 ± 0.006	12.6 (10.7)	207.40 ± 0.35	-3.18 ± 0.66	0.716 ± 0.005	11.8 (6.4)
237.33 ± 0.27	-0.41 ± 0.91	0.654 ± 0.006	15.5 (10.2)	238.15 ± 0.26	-1.56 ± 0.83	0.684 ± 0.005	12.2 (8.2)
268.35 ± 0.43	-1.65 ± 1.07	0.635 ± 0.004	16.3 (12.5)	270.00 ± 0.25	$+1.30 \pm 0.66$	0.654 ± 0.004	12.9 (8.8)
302.87 ± 0.50	-0.45 ± 0.82	0.629 ± 0.005	17.3 (9.8)	302.47 ± 0.31	$+2.00 \pm 0.79$	0.666 ± 0.006	13.3 (6.0)
332.10 ± 0.38	$+0.09 \pm 0.78$	0.634 ± 0.005	14.9 (9.2)	331.73 ± 0.30	$+0.69 \pm 0.78$	0.685 ± 0.006	11.8 (7.6)

Table 30: The nominal angle δ_n, average displacement $\Delta\delta$, average value of the parameter DIST, RMS of the ALPHA distribution for enabled GF and impact parameters between 60 m and 120 m. The RMS of the ALPHA distribution for disabled GF is given parentheses. The primary γ-ray energy was set to 70 GeV, the ZA to 20° and the azimuth angle to 150°.

$E_\gamma = 70\,\mathrm{GeV}$, Az = 180°, ZA = 20°, Intermediate Image Cleaning

δ_n[°]	$\Delta\delta$[°]	DIST[°]	$\mathrm{RMS}_{\lvert\mathrm{ALPHA}\rvert}$[°]	δ_n[°]	$\Delta\delta$[°]	DIST[°]	$\mathrm{RMS}_{\lvert\mathrm{ALPHA}\rvert}$[°]
IP = 60 m				**IP = 80 m**			
359.95 ± 0.73	$+2.89 \pm 1.24$	0.452 ± 0.006	16.5 (18.2)	0.63 ± 0.59	$+2.57 \pm 1.16$	0.559 ± 0.006	14.2 (14.1)
26.29 ± 0.65	-3.45 ± 1.22	0.442 ± 0.005	18.6 (21.4)	29.12 ± 0.59	$+0.49 \pm 1.27$	0.552 ± 0.005	17.5 (14.0)
61.24 ± 0.61	$+4.67 \pm 1.25$	0.443 ± 0.005	21.9 (20.9)	59.14 ± 0.53	$+2.48 \pm 0.74$	0.550 ± 0.006	20.6 (14.8)
88.38 ± 0.73	$+1.92 \pm 1.45$	0.444 ± 0.003	23.3 (17.9)	91.38 ± 0.47	$+1.11 \pm 0.96$	0.559 ± 0.004	20.3 (15.0)
121.64 ± 0.92	-1.64 ± 1.42	0.444 ± 0.005	19.4 (16.3)	121.65 ± 0.41	$+0.28 \pm 1.19$	0.553 ± 0.005	16.9 (16.7)
153.64 ± 0.72	$+0.90 \pm 1.38$	0.442 ± 0.004	18.1 (18.9)	151.83 ± 0.46	-1.53 ± 1.03	0.572 ± 0.005	13.9 (14.0)
180.25 ± 0.61	$+0.49 \pm 1.06$	0.462 ± 0.004	15.7 (20.2)	178.69 ± 0.52	-1.85 ± 1.09	0.569 ± 0.004	10.5 (14.3)
206.57 ± 0.48	-0.10 ± 0.91	0.442 ± 0.006	23.7 (18.3)	207.35 ± 0.57	$+0.07 \pm 1.20$	0.551 ± 0.004	18.8 (13.4)
237.96 ± 0.41	$+6.27 \pm 1.06$	0.442 ± 0.005	21.6 (18.2)	237.14 ± 0.52	-1.25 ± 1.21	0.548 ± 0.006	19.2 (15.9)
269.68 ± 0.30	-1.31 ± 1.32	0.443 ± 0.006	23.0 (19.3)	268.94 ± 0.41	$+0.69 \pm 0.77$	0.543 ± 0.006	21.6 (15.8)
303.21 ± 0.56	$+0.19 \pm 1.49$	0.431 ± 0.004	23.1 (20.1)	302.03 ± 0.60	-0.45 ± 1.44	0.547 ± 0.007	17.4 (14.1)
331.03 ± 0.68	$+3.52 \pm 1.44$	0.438 ± 0.005	17.5 (18.6)	330.54 ± 0.47	-1.19 ± 1.26	0.554 ± 0.005	15.1 (14.5)
IP = 100 m				**IP = 120 m**			
0.03 ± 0.33	-1.95 ± 0.85	0.644 ± 0.009	11.8 (10.0)	359.61 ± 0.32	-1.40 ± 0.84	0.718 ± 0.006	9.3 (5.9)
29.01 ± 0.37	-0.81 ± 0.79	0.634 ± 0.006	12.6 (10.3)	28.16 ± 0.30	-1.58 ± 0.85	0.697 ± 0.006	9.2 (7.3)
59.42 ± 0.38	$+1.27 \pm 0.85$	0.633 ± 0.006	19.2 (9.2)	58.59 ± 0.35	-0.10 ± 0.85	0.668 ± 0.007	16.3 (7.2)
88.72 ± 0.49	-1.38 ± 1.26	0.622 ± 0.007	15.6 (10.8)	89.92 ± 0.30	$+0.66 \pm 1.04$	0.640 ± 0.005	9.2 (7.7)
121.93 ± 0.43	$+0.92 \pm 1.17$	0.630 ± 0.007	15.4 (11.7)	122.34 ± 0.31	$+2.16 \pm 0.99$	0.672 ± 0.006	11.6 (5.6)
151.09 ± 0.43	$+0.18 \pm 0.91$	0.657 ± 0.007	11.5 (11.8)	151.52 ± 0.30	$+2.64 \pm 0.71$	0.701 ± 0.006	8.2 (8.4)
179.61 ± 0.44	-1.13 ± 0.96	0.663 ± 0.006	14.7 (10.3)	180.29 ± 0.31	$+0.36 \pm 0.69$	0.704 ± 0.006	10.4 (5.8)
207.13 ± 0.47	$+0.39 \pm 1.02$	0.653 ± 0.005	14.1 (10.7)	207.40 ± 0.35	-0.38 ± 0.84	0.695 ± 0.007	8.9 (6.4)
237.33 ± 0.27	-1.65 ± 0.87	0.624 ± 0.004	17.1 (10.2)	238.15 ± 0.26	-4.19 ± 0.76	0.661 ± 0.006	10.3 (8.2)
268.35 ± 0.43	-1.62 ± 1.27	0.608 ± 0.005	18.8 (12.5)	270.00 ± 0.25	-0.66 ± 0.53	0.629 ± 0.006	10.3 (8.8)
302.87 ± 0.50	$+0.25 \pm 1.17$	0.617 ± 0.006	15.7 (9.8)	302.47 ± 0.31	$+2.82 \pm 0.68$	0.662 ± 0.006	11.3 (6.0)
332.10 ± 0.38	$+1.00 \pm 0.81$	0.635 ± 0.006	12.0 (9.2)	331.73 ± 0.30	$+1.48 \pm 0.86$	0.681 ± 0.005	11.1 (7.6)

Table 31: The nominal angle δ_n, average displacement $\Delta\delta$, average value of the parameter DIST, RMS of the ALPHA distribution for enabled GF and impact parameters between 60 m and 120 m. The RMS of the ALPHA distribution for disabled GF is given parentheses. The primary γ-ray energy was set to 70 GeV, the ZA to 20° and the azimuth angle to 180°.

$E_\gamma = 120\,\mathrm{GeV}$, Az $= 0°$, ZA $= 0°$, Intermediate Image Cleaning

$\delta_n\,[°]$	$\Delta\delta\,[°]$	DIST[°]	RMS$_{\lvert\mathrm{ALPHA}\rvert}$[°]	$\delta_n\,[°]$	$\Delta\delta\,[°]$	DIST[°]	RMS$_{\lvert\mathrm{ALPHA}\rvert}$[°]
IP = 60 m				IP = 80 m			
359.23 ± 0.51	-1.78 ± 0.88	0.473 ± 0.004	9.4 (12.0)	359.17 ± 0.38	-0.69 ± 0.76	0.585 ± 0.006	8.8 (6.9)
30.50 ± 0.38	$+5.78 \pm 0.87$	0.474 ± 0.004	14.1 (11.1)	30.25 ± 0.38	$+3.38 \pm 0.88$	0.592 ± 0.003	13.0 (7.2)
59.71 ± 0.51	$+2.48 \pm 0.94$	0.481 ± 0.004	18.9 (8.0)	59.79 ± 0.38	-1.36 ± 0.81	0.595 ± 0.006	11.9 (6.1)
90.43 ± 0.45	-2.31 ± 0.95	0.483 ± 0.005	20.4 (10.1)	90.23 ± 0.38	-0.31 ± 0.81	0.597 ± 0.006	17.7 (5.6)
119.09 ± 0.51	-5.57 ± 1.00	0.475 ± 0.003	21.2 (11.2)	119.25 ± 0.38	-1.47 ± 1.02	0.589 ± 0.005	19.9 (6.3)
148.64 ± 0.32	-6.48 ± 1.00	0.463 ± 0.005	18.3 (9.7)	150.16 ± 0.38	-2.53 ± 0.75	0.586 ± 0.004	13.8 (6.2)
181.36 ± 0.45	$+1.78 \pm 0.88$	0.465 ± 0.007	11.3 (12.0)	180.87 ± 0.26	$+0.30 \pm 0.63$	0.585 ± 0.007	7.5 (8.5)
211.67 ± 0.45	$+4.92 \pm 0.88$	0.471 ± 0.006	15.2 (11.6)	210.46 ± 0.38	$+3.94 \pm 0.94$	0.582 ± 0.006	13.2 (7.4)
241.49 ± 0.57	$+5.56 \pm 1.00$	0.483 ± 0.006	18.8 (10.2)	240.69 ± 0.38	$+3.55 \pm 1.00$	0.594 ± 0.007	16.9 (5.0)
269.77 ± 0.64	$+0.47 \pm 1.34$	0.489 ± 0.005	22.7 (10.8)	270.62 ± 0.38	$+0.39 \pm 0.83$	0.596 ± 0.007	17.2 (5.0)
299.96 ± 0.32	-4.67 ± 1.06	0.487 ± 0.004	23.4 (10.8)	300.33 ± 0.32	-2.72 ± 0.93	0.598 ± 0.005	17.7 (6.2)
328.72 ± 0.45	-5.84 ± 1.00	0.476 ± 0.004	16.3 (11.4)	330.05 ± 0.32	-2.24 ± 0.63	0.591 ± 0.005	12.4 (6.0)
IP = 100 m				IP = 120 m			
358.83 ± 0.39	-1.55 ± 0.65	0.671 ± 0.006	4.9 (3.8)	359.84 ± 0.26	$+0.47 \pm 0.59$	0.735 ± 0.005	5.9 (5.2)
30.46 ± 0.32	$+0.74 \pm 0.69$	0.678 ± 0.006	9.0 (7.4)	30.31 ± 0.26	-0.61 ± 0.45	0.737 ± 0.004	9.8 (2.8)
59.81 ± 0.39	-0.62 ± 0.70	0.678 ± 0.006	10.1 (6.4)	59.74 ± 0.26	-2.06 ± 0.65	0.723 ± 0.004	10.2 (4.6)
89.97 ± 0.38	$+1.06 \pm 0.88$	0.673 ± 0.008	11.7 (4.0)	89.69 ± 0.26	$+0.74 \pm 0.70$	0.722 ± 0.003	13.2 (3.5)
120.09 ± 0.26	$+0.25 \pm 0.82$	0.672 ± 0.005	13.7 (3.1)	119.82 ± 0.26	$+2.41 \pm 0.64$	0.714 ± 0.004	12.4 (2.6)
149.77 ± 0.26	-1.13 ± 0.63	0.666 ± 0.006	10.2 (3.4)	150.17 ± 0.26	$+2.01 \pm 0.64$	0.726 ± 0.002	12.1 (3.0)
180.58 ± 0.26	$+0.12 \pm 0.64$	0.667 ± 0.006	6.1 (3.4)	180.45 ± 0.26	$+0.01 \pm 0.66$	0.725 ± 0.005	4.5 (3.0)
209.78 ± 0.32	$+1.19 \pm 0.76$	0.671 ± 0.005	9.2 (3.8)	209.85 ± 0.26	-0.33 ± 0.64	0.732 ± 0.004	6.2 (3.4)
240.24 ± 0.26	-0.78 ± 0.69	0.671 ± 0.007	12.7 (3.2)	240.14 ± 0.33	-3.03 ± 0.77	0.719 ± 0.004	8.9 (3.6)
270.12 ± 0.32	$+1.19 \pm 0.81$	0.672 ± 0.006	11.8 (3.8)	270.03 ± 0.39	-0.09 ± 0.82	0.722 ± 0.003	10.7 (3.4)
300.28 ± 0.26	-0.22 ± 0.69	0.679 ± 0.006	10.9 (5.3)	300.20 ± 0.26	$+1.46 \pm 0.65$	0.721 ± 0.004	8.0 (3.6)
329.58 ± 0.26	-0.34 ± 0.69	0.677 ± 0.005	13.8 (5.4)	329.92 ± 0.32	$+0.46 \pm 0.71$	0.736 ± 0.004	8.1 (3.7)

Table 32: The nominal angle δ_n, average displacement $\Delta\delta$, average value of the parameter DIST, RMS of the ALPHA distribution for enabled GF and impact parameters between 60 m and 120 m. The RMS of the ALPHA distribution for disabled GF is given parentheses. The primary γ-ray energy was set to 120 GeV, the ZA to 0° and the azimuth angle to 0°.

$E_\gamma = 120\,\mathrm{GeV}$, Az $= 0°$, ZA $= 20°$, Intermediate Image Cleaning

$\delta_n\,[°]$	$\Delta\delta\,[°]$	DIST[°]	RMS$_{\lvert\mathrm{ALPHA}\rvert}$[°]	$\delta_n\,[°]$	$\Delta\delta\,[°]$	DIST[°]	RMS$_{\lvert\mathrm{ALPHA}\rvert}$[°]
IP = 60 m				IP = 80 m			
1.96 ± 0.48	$+1.33 \pm 0.92$	0.434 ± 0.004	12.8 (11.7)	359.88 ± 0.36	$+0.38 \pm 0.84$	0.545 ± 0.005	7.6 (8.9)
28.75 ± 0.48	$+4.31 \pm 1.04$	0.426 ± 0.003	13.3 (14.7)	28.16 ± 0.53	$+1.88 \pm 0.90$	0.538 ± 0.005	11.0 (9.1)
59.91 ± 0.54	$+8.48 \pm 1.28$	0.414 ± 0.002	19.5 (14.7)	58.28 ± 0.36	$+3.75 \pm 0.90$	0.529 ± 0.004	13.9 (10.9)
90.96 ± 0.54	$+3.24 \pm 1.35$	0.408 ± 0.003	22.4 (16.0)	89.77 ± 0.48	$+1.57 \pm 0.95$	0.512 ± 0.004	19.6 (10.9)
119.88 ± 0.54	-1.40 ± 1.19	0.408 ± 0.003	22.1 (16.0)	121.90 ± 0.30	-2.52 ± 0.78	0.519 ± 0.003	17.7 (8.2)
150.69 ± 0.54	-5.24 ± 1.14	0.414 ± 0.004	14.7 (15.6)	151.04 ± 0.24	-3.42 ± 0.90	0.528 ± 0.005	12.2 (8.2)
178.80 ± 0.48	-1.52 ± 0.96	0.423 ± 0.005	15.4 (15.0)	179.54 ± 0.36	$+0.14 \pm 0.72$	0.536 ± 0.004	10.3 (8.8)
207.09 ± 0.30	$+0.82 \pm 0.72$	0.416 ± 0.004	16.1 (17.3)	206.71 ± 0.36	-0.51 ± 0.78	0.529 ± 0.005	13.0 (7.9)
237.22 ± 0.60	$+1.69 \pm 0.96$	0.417 ± 0.004	19.3 (16.0)	237.32 ± 0.24	$+1.97 \pm 0.84$	0.528 ± 0.004	18.0 (10.1)
270.98 ± 0.48	$+0.45 \pm 0.84$	0.415 ± 0.003	22.0 (13.9)	270.08 ± 0.42	-1.30 ± 1.07	0.525 ± 0.004	15.9 (8.7)
300.89 ± 0.59	-6.09 ± 1.25	0.420 ± 0.003	22.1 (17.9)	302.58 ± 0.42	-2.89 ± 0.84	0.533 ± 0.005	16.2 (10.9)
333.13 ± 0.48	-2.39 ± 1.04	0.428 ± 0.004	13.8 (15.0)	333.17 ± 0.30	-0.09 ± 0.78	0.540 ± 0.004	10.4 (7.1)
IP = 100 m				IP = 120 m			
0.20 ± 0.30	$+0.51 \pm 0.67$	0.634 ± 0.006	8.6 (7.1)	0.15 ± 0.24	$+0.32 \pm 0.49$	0.690 ± 0.006	5.9 (4.4)
29.12 ± 0.36	$+1.02 \pm 0.72$	0.626 ± 0.004	7.2 (4.4)	28.73 ± 0.30	-0.39 ± 0.54	0.689 ± 0.005	6.6 (3.7)
58.05 ± 0.30	$+2.21 \pm 0.72$	0.614 ± 0.007	13.3 (7.7)	58.64 ± 0.30	$+0.96 \pm 0.60$	0.672 ± 0.006	10.2 (3.2)
89.86 ± 0.30	$+2.30 \pm 0.65$	0.605 ± 0.005	14.4 (5.1)	89.65 ± 0.30	$+0.81 \pm 0.77$	0.663 ± 0.006	9.9 (4.0)
121.21 ± 0.30	$+0.13 \pm 0.60$	0.603 ± 0.006	13.9 (6.1)	121.99 ± 0.30	$+1.68 \pm 0.60$	0.668 ± 0.005	10.9 (3.5)
152.06 ± 0.24	-0.19 ± 0.61	0.619 ± 0.005	7.9 (5.8)	151.55 ± 0.30	-0.15 ± 0.54	0.680 ± 0.005	6.3 (4.1)
179.45 ± 0.30	-0.69 ± 0.67	0.629 ± 0.005	10.5 (5.9)	179.87 ± 0.24	$+0.39 \pm 0.63$	0.688 ± 0.005	6.5 (3.4)
207.22 ± 0.24	$+0.15 \pm 0.48$	0.626 ± 0.007	8.1 (5.3)	207.57 ± 0.24	-0.96 ± 0.56	0.691 ± 0.004	7.4 (3.8)
238.49 ± 0.24	$+0.27 \pm 0.66$	0.617 ± 0.006	11.9 (5.3)	238.10 ± 0.24	-1.82 ± 0.55	0.679 ± 0.005	8.6 (3.8)
269.28 ± 0.24	-1.59 ± 0.59	0.612 ± 0.005	11.2 (7.2)	269.58 ± 0.36	-1.38 ± 0.71	0.671 ± 0.005	7.7 (4.3)
302.44 ± 0.36	-1.09 ± 0.72	0.625 ± 0.006	9.7 (8.2)	302.38 ± 0.24	$+0.50 \pm 0.48$	0.683 ± 0.006	9.7 (3.3)
332.26 ± 0.30	$+0.04 \pm 0.68$	0.630 ± 0.005	8.6 (7.9)	331.84 ± 0.24	-0.09 ± 0.54	0.693 ± 0.005	8.3 (3.6)

Table 33: The nominal angle δ_n, average displacement $\Delta\delta$, average value of the parameter DIST, RMS of the ALPHA distribution for enabled GF and impact parameters between 60 m and 120 m. The RMS of the ALPHA distribution for disabled GF is given parentheses. The primary γ-ray energy was set to 120 GeV, the ZA to 20° and the azimuth angle to 0°.

$E_\gamma = 120$ GeV, Az = 30°, ZA = 20°, Intermediate Image Cleaning

δ_n[°]	$\Delta\delta$[°]	DIST[°]	$\mathrm{RMS}_{\lvert\mathrm{ALPHA}\rvert}$[°]	δ_n[°]	$\Delta\delta$[°]	DIST[°]	$\mathrm{RMS}_{\lvert\mathrm{ALPHA}\rvert}$[°]
IP = 60 m				**IP = 80 m**			
1.96 ± 0.48	$+0.99 \pm 1.13$	0.408 ± 0.004	14.3 (11.7)	359.88 ± 0.36	-1.30 ± 0.77	0.520 ± 0.006	11.6 (8.9)
28.75 ± 0.48	$+1.34 \pm 0.96$	0.398 ± 0.003	15.6 (14.7)	28.16 ± 0.53	-0.62 ± 0.89	0.507 ± 0.005	12.9 (9.1)
59.91 ± 0.54	$+3.65 \pm 0.83$	0.395 ± 0.003	20.1 (14.7)	58.28 ± 0.36	$+1.61 \pm 0.80$	0.507 ± 0.004	16.6 (10.9)
90.96 ± 0.54	$+1.72 \pm 0.95$	0.408 ± 0.003	20.8 (16.0)	89.77 ± 0.48	$+1.00 \pm 0.83$	0.518 ± 0.004	17.3 (10.9)
119.88 ± 0.54	-2.00 ± 1.02	0.420 ± 0.004	19.4 (16.0)	121.90 ± 0.30	-1.23 ± 0.83	0.530 ± 0.005	16.5 (8.2)
150.69 ± 0.54	-6.44 ± 1.18	0.427 ± 0.005	16.6 (15.6)	151.04 ± 0.24	-3.78 ± 0.83	0.539 ± 0.005	12.8 (8.2)
178.80 ± 0.48	-6.75 ± 1.13	0.426 ± 0.004	12.6 (15.0)	179.54 ± 0.36	-4.24 ± 0.78	0.536 ± 0.005	10.8 (8.8)
207.09 ± 0.30	-3.56 ± 0.66	0.415 ± 0.004	14.3 (17.3)	206.71 ± 0.36	-1.98 ± 0.78	0.522 ± 0.003	11.6 (7.9)
237.22 ± 0.60	$+1.05 \pm 1.13$	0.409 ± 0.004	18.0 (16.0)	237.32 ± 0.24	$+1.17 \pm 0.54$	0.518 ± 0.004	15.1 (10.1)
270.98 ± 0.48	$+7.93 \pm 1.13$	0.413 ± 0.003	20.3 (13.9)	270.08 ± 0.42	$+5.18 \pm 0.83$	0.526 ± 0.004	18.4 (8.7)
300.89 ± 0.59	$+5.68 \pm 1.19$	0.423 ± 0.003	19.2 (17.9)	302.58 ± 0.42	$+3.65 \pm 0.83$	0.539 ± 0.004	17.6 (10.9)
333.13 ± 0.48	-1.96 ± 1.02	0.418 ± 0.005	17.8 (15.0)	333.17 ± 0.30	$+3.16 \pm 0.71$	0.536 ± 0.005	12.7 (7.1)
IP = 100 m				**IP = 120 m**			
0.20 ± 0.30	$+1.14 \pm 0.73$	0.616 ± 0.007	9.5 (7.1)	0.15 ± 0.24	$+1.28 \pm 0.49$	0.683 ± 0.005	8.3 (4.4)
29.12 ± 0.36	$+0.12 \pm 0.67$	0.608 ± 0.006	9.5 (4.4)	28.73 ± 0.30	$+0.43 \pm 0.60$	0.675 ± 0.006	8.6 (3.7)
58.05 ± 0.30	$+0.52 \pm 0.60$	0.600 ± 0.004	12.5 (7.7)	58.64 ± 0.30	$+0.40 \pm 0.61$	0.666 ± 0.005	10.8 (3.2)
89.86 ± 0.30	-0.87 ± 0.71	0.605 ± 0.004	13.9 (5.1)	89.65 ± 0.30	-1.99 ± 0.65	0.662 ± 0.005	9.7 (4.0)
121.21 ± 0.30	-0.68 ± 0.71	0.623 ± 0.004	12.3 (6.1)	121.99 ± 0.30	-1.80 ± 0.66	0.669 ± 0.004	9.6 (3.5)
152.06 ± 0.24	-1.06 ± 0.59	0.634 ± 0.005	10.5 (5.8)	151.55 ± 0.30	-0.89 ± 0.59	0.682 ± 0.004	8.6 (4.1)
179.45 ± 0.30	-2.69 ± 0.60	0.631 ± 0.006	9.8 (5.9)	179.87 ± 0.24	$+0.04 \pm 0.49$	0.693 ± 0.004	6.9 (3.4)
207.22 ± 0.24	-1.81 ± 0.60	0.623 ± 0.005	9.2 (5.3)	207.57 ± 0.24	-0.20 ± 0.55	0.684 ± 0.004	7.4 (3.8)
238.49 ± 0.24	-0.03 ± 0.48	0.614 ± 0.006	12.3 (5.3)	238.10 ± 0.24	$+0.07 \pm 0.55$	0.684 ± 0.004	8.4 (3.8)
269.28 ± 0.24	$+1.35 \pm 0.72$	0.621 ± 0.004	14.5 (7.2)	269.58 ± 0.36	-0.55 ± 0.66	0.675 ± 0.006	10.2 (4.3)
302.44 ± 0.36	$+2.56 \pm 0.65$	0.629 ± 0.003	13.1 (8.2)	302.38 ± 0.24	$+1.55 \pm 0.54$	0.681 ± 0.005	10.6 (3.3)
332.26 ± 0.30	$+1.46 \pm 0.65$	0.636 ± 0.008	10.6 (7.9)	331.84 ± 0.24	$+1.99 \pm 0.65$	0.694 ± 0.004	10.3 (3.6)

Table 34: The nominal angle δ_n, average displacement $\Delta\delta$, average value of the parameter DIST, RMS of the ALPHA distribution for enabled GF and impact parameters between 60 m and 120 m. The RMS of the ALPHA distribution for disabled GF is given parentheses. The primary γ-ray energy was set to 120 GeV, the ZA to 20° and the azimuth angle to 30°.

$E_\gamma = 120$ GeV, Az = 60°, ZA = 20°, Intermediate Image Cleaning

δ_n[°]	$\Delta\delta$[°]	DIST[°]	$\mathrm{RMS}_{\lvert\mathrm{ALPHA}\rvert}$[°]	δ_n[°]	$\Delta\delta$[°]	DIST[°]	$\mathrm{RMS}_{\lvert\mathrm{ALPHA}\rvert}$[°]
IP = 60 m				**IP = 80 m**			
1.96 ± 0.48	$+1.39 \pm 1.43$	0.399 ± 0.005	14.7 (11.7)	359.88 ± 0.36	$+2.04 \pm 0.72$	0.511 ± 0.005	12.4 (8.9)
28.75 ± 0.48	-3.31 ± 1.26	0.394 ± 0.005	14.1 (14.7)	28.16 ± 0.53	-1.71 ± 0.95	0.502 ± 0.005	12.0 (9.1)
59.91 ± 0.54	-1.44 ± 1.08	0.412 ± 0.004	17.7 (14.7)	58.28 ± 0.36	-1.35 ± 0.83	0.518 ± 0.004	15.3 (10.9)
90.96 ± 0.54	-0.51 ± 0.89	0.426 ± 0.003	18.9 (16.0)	89.77 ± 0.48	-0.13 ± 0.95	0.543 ± 0.004	15.8 (10.9)
119.88 ± 0.54	$+1.48 \pm 1.07$	0.436 ± 0.003	18.8 (16.0)	121.90 ± 0.30	$+1.66 \pm 0.96$	0.552 ± 0.005	17.1 (8.2)
150.69 ± 0.54	-1.64 ± 1.07	0.428 ± 0.004	18.2 (15.6)	151.04 ± 0.24	$+0.86 \pm 0.83$	0.544 ± 0.005	15.0 (8.2)
178.80 ± 0.48	-3.61 ± 1.20	0.418 ± 0.004	14.2 (15.0)	179.54 ± 0.36	-3.22 ± 0.60	0.527 ± 0.005	11.6 (8.8)
207.09 ± 0.30	-8.26 ± 0.84	0.411 ± 0.003	13.2 (17.3)	206.71 ± 0.36	-6.15 ± 0.89	0.518 ± 0.004	11.1 (7.9)
237.22 ± 0.60	-4.79 ± 1.07	0.417 ± 0.003	15.9 (16.0)	237.32 ± 0.24	-2.20 ± 0.66	0.523 ± 0.004	14.2 (10.1)
270.98 ± 0.48	$+2.10 \pm 0.78$	0.429 ± 0.003	18.6 (13.9)	270.08 ± 0.42	$+1.21 \pm 0.77$	0.544 ± 0.004	16.8 (8.7)
300.89 ± 0.59	$+5.99 \pm 1.19$	0.435 ± 0.003	20.0 (17.9)	302.58 ± 0.42	$+3.38 \pm 0.89$	0.545 ± 0.004	15.9 (10.9)
333.13 ± 0.48	$+7.13 \pm 1.01$	0.421 ± 0.003	17.3 (15.0)	333.17 ± 0.30	$+4.15 \pm 0.77$	0.537 ± 0.004	15.5 (7.1)
IP = 100 m				**IP = 120 m**			
0.20 ± 0.30	$+0.15 \pm 0.66$	0.605 ± 0.004	9.7 (7.1)	0.15 ± 0.24	$+1.98 \pm 0.73$	0.680 ± 0.007	8.8 (4.4)
29.12 ± 0.36	$+0.45 \pm 0.78$	0.598 ± 0.004	10.6 (4.4)	28.73 ± 0.30	$+2.36 \pm 0.60$	0.667 ± 0.005	8.6 (3.7)
58.05 ± 0.30	-0.26 ± 0.54	0.610 ± 0.005	12.8 (7.7)	58.64 ± 0.30	$+0.61 \pm 0.61$	0.674 ± 0.007	9.6 (3.2)
89.86 ± 0.30	-0.36 ± 0.72	0.623 ± 0.005	13.5 (5.1)	89.65 ± 0.30	-0.65 ± 0.61	0.675 ± 0.004	9.7 (4.0)
121.21 ± 0.30	$+0.52 \pm 0.72$	0.637 ± 0.006	12.0 (6.1)	121.99 ± 0.30	-0.42 ± 0.67	0.676 ± 0.006	9.8 (3.5)
152.06 ± 0.24	$+0.21 \pm 0.71$	0.634 ± 0.004	13.5 (5.8)	151.55 ± 0.30	-1.14 ± 0.66	0.686 ± 0.006	8.9 (4.1)
179.45 ± 0.30	-0.05 ± 0.78	0.618 ± 0.004	10.2 (5.9)	179.87 ± 0.24	-0.14 ± 0.67	0.684 ± 0.005	8.4 (3.4)
207.22 ± 0.24	-2.83 ± 0.66	0.613 ± 0.005	9.7 (5.3)	207.57 ± 0.24	$+0.57 \pm 0.48$	0.681 ± 0.006	8.2 (3.8)
238.49 ± 0.24	$+0.09 \pm 0.54$	0.624 ± 0.005	12.0 (5.3)	238.10 ± 0.24	-0.14 ± 0.55	0.680 ± 0.007	9.7 (3.8)
269.28 ± 0.24	-0.69 ± 0.60	0.633 ± 0.005	13.2 (7.2)	269.58 ± 0.36	-0.56 ± 0.66	0.680 ± 0.002	10.8 (4.3)
302.44 ± 0.36	$+0.88 \pm 0.78$	0.632 ± 0.005	13.5 (8.2)	302.38 ± 0.24	-0.39 ± 0.69	0.679 ± 0.006	10.0 (3.3)
332.26 ± 0.30	$+2.14 \pm 0.65$	0.629 ± 0.005	12.6 (7.9)	331.84 ± 0.24	-0.01 ± 0.60	0.689 ± 0.007	9.8 (3.6)

Table 35: The nominal angle δ_n, average displacement $\Delta\delta$, average value of the parameter DIST, RMS of the ALPHA distribution for enabled GF and impact parameters between 60 m and 120 m. The RMS of the ALPHA distribution for disabled GF is given parentheses. The primary γ-ray energy was set to 120 GeV, the ZA to 20° and the azimuth angle to 60°.

$E_\gamma = 120\,\mathrm{GeV}$, Az = 90°, ZA = 20°, Intermediate Image Cleaning

δ_n[°]	$\Delta\delta$[°]	DIST[°]	RMS$_{\lvert ALPHA \rvert}$[°]	δ_n[°]	$\Delta\delta$[°]	DIST[°]	RMS$_{\lvert ALPHA \rvert}$[°]
IP = 60 m				IP = 80 m			
1.96 ± 0.48	$+8.14 \pm 1.08$	0.399 ± 0.003	14.4 (11.7)	359.88 ± 0.36	$+2.50 \pm 0.83$	0.507 ± 0.005	12.5 (8.9)
28.75 ± 0.48	$+1.67 \pm 1.02$	0.400 ± 0.005	14.6 (14.7)	28.16 ± 0.53	$+0.21 \pm 1.12$	0.511 ± 0.005	12.5 (9.1)
59.91 ± 0.54	-5.58 ± 1.12	0.424 ± 0.003	18.4 (14.7)	58.28 ± 0.36	-1.93 ± 0.89	0.533 ± 0.004	17.0 (10.9)
90.96 ± 0.54	-1.98 ± 1.08	0.437 ± 0.004	22.1 (16.0)	89.77 ± 0.48	-2.73 ± 0.84	0.551 ± 0.005	18.4 (10.9)
119.88 ± 0.54	$+0.91 \pm 1.07$	0.430 ± 0.002	21.3 (16.0)	121.90 ± 0.30	$+1.32 \pm 0.54$	0.540 ± 0.006	19.9 (8.2)
150.69 ± 0.54	$+4.38 \pm 1.32$	0.412 ± 0.004	21.3 (15.6)	151.04 ± 0.24	$+1.95 \pm 0.77$	0.528 ± 0.005	17.8 (8.2)
178.80 ± 0.48	$+2.41 \pm 0.84$	0.403 ± 0.004	13.2 (15.0)	179.54 ± 0.36	-0.69 ± 0.96	0.516 ± 0.005	11.3 (8.8)
207.09 ± 0.30	-4.80 ± 0.42	0.413 ± 0.004	14.9 (17.3)	206.71 ± 0.36	-3.75 ± 0.89	0.524 ± 0.006	11.6 (7.9)
237.22 ± 0.60	-7.31 ± 1.49	0.427 ± 0.004	19.2 (16.0)	237.32 ± 0.24	-4.83 ± 0.71	0.545 ± 0.005	16.2 (10.1)
270.98 ± 0.48	-2.53 ± 0.95	0.437 ± 0.003	21.9 (13.9)	270.08 ± 0.42	-2.06 ± 0.71	0.552 ± 0.004	17.9 (8.7)
300.89 ± 0.59	$+1.56 \pm 1.13$	0.430 ± 0.003	23.5 (17.9)	302.58 ± 0.42	$+1.74 \pm 0.83$	0.540 ± 0.004	19.6 (10.9)
333.13 ± 0.48	$+9.16 \pm 0.78$	0.408 ± 0.004	20.5 (15.0)	333.17 ± 0.30	$+4.14 \pm 0.89$	0.522 ± 0.005	17.6 (7.1)
IP = 100 m				IP = 120 m			
0.20 ± 0.30	$+0.11 \pm 0.71$	0.597 ± 0.005	10.9 (7.1)	0.15 ± 0.24	-0.41 ± 0.66	0.673 ± 0.005	7.9 (4.4)
29.12 ± 0.36	$+1.54 \pm 0.82$	0.598 ± 0.005	11.1 (4.4)	28.73 ± 0.30	$+0.88 \pm 0.65$	0.673 ± 0.005	10.3 (3.7)
58.05 ± 0.30	-0.27 ± 0.78	0.625 ± 0.004	13.3 (7.7)	58.64 ± 0.30	$+1.69 \pm 0.67$	0.683 ± 0.005	12.8 (3.2)
89.86 ± 0.30	-0.46 ± 0.54	0.631 ± 0.004	14.6 (5.1)	89.65 ± 0.30	-0.18 ± 0.61	0.677 ± 0.005	11.8 (4.0)
121.21 ± 0.30	$+0.43 \pm 0.66$	0.628 ± 0.003	15.1 (6.1)	121.99 ± 0.30	-0.13 ± 0.55	0.678 ± 0.002	11.0 (3.5)
152.06 ± 0.24	$+0.95 \pm 0.65$	0.617 ± 0.006	12.7 (5.8)	151.55 ± 0.30	-1.28 ± 0.72	0.687 ± 0.006	11.7 (4.1)
179.45 ± 0.30	-1.55 ± 0.71	0.613 ± 0.005	6.5 (5.9)	179.87 ± 0.24	-2.34 ± 0.66	0.683 ± 0.006	6.7 (3.4)
207.22 ± 0.24	-0.69 ± 0.83	0.620 ± 0.005	8.6 (5.3)	207.57 ± 0.24	$+1.22 \pm 0.65$	0.692 ± 0.006	7.9 (3.8)
238.49 ± 0.24	$+0.05 \pm 0.72$	0.642 ± 0.005	12.5 (5.3)	238.10 ± 0.24	$+1.77 \pm 0.55$	0.693 ± 0.005	11.0 (3.8)
269.28 ± 0.24	-1.80 ± 0.48	0.629 ± 0.005	12.9 (7.2)	269.58 ± 0.36	-0.39 ± 0.72	0.676 ± 0.005	9.7 (4.3)
302.44 ± 0.36	$+0.49 \pm 0.66$	0.625 ± 0.006	15.1 (8.2)	302.38 ± 0.24	-0.06 ± 0.56	0.670 ± 0.004	10.7 (3.3)
332.26 ± 0.30	$+0.54 \pm 0.78$	0.607 ± 0.006	13.1 (7.9)	331.84 ± 0.24	-1.58 ± 0.55	0.678 ± 0.005	9.7 (3.6)

Table 36: The nominal angle δ_n, average displacement $\Delta\delta$, average value of the parameter DIST, RMS of the ALPHA distribution for enabled GF and impact parameters between 60 m and 120 m. The RMS of the ALPHA distribution for disabled GF is given parentheses. The primary γ-ray energy was set to 120 GeV, the ZA to 20° and the azimuth angle to 90°.

$E_\gamma = 120\,\mathrm{GeV}$, Az = 120°, ZA = 20°, Intermediate Image Cleaning

δ_n[°]	$\Delta\delta$[°]	DIST[°]	RMS$_{\lvert ALPHA \rvert}$[°]	δ_n[°]	$\Delta\delta$[°]	DIST[°]	RMS$_{\lvert ALPHA \rvert}$[°]
IP = 60 m				IP = 80 m			
1.96 ± 0.48	$+5.43 \pm 0.72$	0.410 ± 0.005	13.2 (11.7)	359.88 ± 0.36	$+2.15 \pm 0.84$	0.511 ± 0.005	11.2 (8.9)
28.75 ± 0.48	$+3.19 \pm 1.02$	0.418 ± 0.005	15.2 (14.7)	28.16 ± 0.53	-1.50 ± 1.07	0.534 ± 0.005	12.2 (9.1)
59.91 ± 0.54	$+1.54 \pm 0.71$	0.435 ± 0.004	19.1 (14.7)	58.28 ± 0.36	-0.94 ± 0.89	0.551 ± 0.006	15.8 (10.9)
90.96 ± 0.54	-4.90 ± 1.19	0.438 ± 0.003	20.8 (16.0)	89.77 ± 0.48	-3.41 ± 1.14	0.550 ± 0.004	18.7 (10.9)
119.88 ± 0.54	-3.99 ± 1.02	0.424 ± 0.003	20.5 (16.0)	121.90 ± 0.30	-0.71 ± 0.66	0.531 ± 0.004	19.0 (8.2)
150.69 ± 0.54	$+1.52 \pm 1.08$	0.413 ± 0.004	17.3 (15.6)	151.04 ± 0.24	$+2.18 \pm 0.66$	0.521 ± 0.004	14.5 (8.2)
178.80 ± 0.48	$+4.12 \pm 1.44$	0.416 ± 0.003	13.4 (15.0)	179.54 ± 0.36	$+3.58 \pm 0.66$	0.524 ± 0.006	10.6 (8.8)
207.09 ± 0.30	$+1.92 \pm 1.15$	0.420 ± 0.003	16.0 (17.3)	206.71 ± 0.36	-1.08 ± 0.84	0.533 ± 0.005	12.5 (7.9)
237.22 ± 0.60	-3.32 ± 1.54	0.434 ± 0.005	18.8 (16.0)	237.32 ± 0.24	-2.24 ± 0.77	0.541 ± 0.005	16.5 (10.1)
270.98 ± 0.48	-5.79 ± 1.14	0.434 ± 0.004	20.6 (13.9)	270.08 ± 0.42	-2.13 ± 0.90	0.542 ± 0.005	17.4 (8.7)
300.89 ± 0.59	-2.44 ± 1.02	0.413 ± 0.003	21.4 (17.9)	302.58 ± 0.42	$+0.92 \pm 0.72$	0.526 ± 0.004	16.9 (10.9)
333.13 ± 0.48	$+6.32 \pm 0.78$	0.402 ± 0.003	16.6 (15.0)	333.17 ± 0.30	$+2.22 \pm 0.72$	0.517 ± 0.004	14.9 (7.1)
IP = 100 m				IP = 120 m			
0.20 ± 0.30	$+2.00 \pm 0.72$	0.611 ± 0.004	8.5 (7.1)	0.15 ± 0.24	-1.51 ± 0.62	0.681 ± 0.008	8.7 (4.4)
29.12 ± 0.36	-0.99 ± 0.95	0.624 ± 0.006	10.9 (4.4)	28.73 ± 0.30	-1.10 ± 0.65	0.698 ± 0.005	9.6 (3.7)
58.05 ± 0.30	$+0.67 \pm 0.89$	0.643 ± 0.005	13.0 (7.7)	58.64 ± 0.30	$+2.15 \pm 0.72$	0.695 ± 0.007	11.0 (3.2)
89.86 ± 0.30	-0.81 ± 0.79	0.635 ± 0.005	14.1 (5.1)	89.65 ± 0.30	-0.15 ± 0.73	0.681 ± 0.005	11.7 (4.0)
121.21 ± 0.30	-0.92 ± 0.55	0.619 ± 0.005	15.9 (6.1)	121.99 ± 0.30	-0.26 ± 0.56	0.677 ± 0.005	11.7 (3.5)
152.06 ± 0.24	$+1.04 \pm 0.54$	0.614 ± 0.006	13.4 (5.8)	151.55 ± 0.30	-1.37 ± 0.68	0.684 ± 0.005	9.9 (4.1)
179.45 ± 0.30	-1.58 ± 0.67	0.609 ± 0.003	9.4 (5.9)	179.87 ± 0.24	-3.28 ± 0.62	0.691 ± 0.005	7.9 (3.4)
207.22 ± 0.24	-0.96 ± 0.72	0.630 ± 0.004	10.8 (5.3)	207.57 ± 0.24	-1.25 ± 0.60	0.700 ± 0.006	9.5 (3.8)
238.49 ± 0.24	$+0.45 \pm 0.83$	0.633 ± 0.004	12.9 (5.3)	238.10 ± 0.24	$+0.71 \pm 0.66$	0.686 ± 0.007	10.6 (3.8)
269.28 ± 0.24	-2.63 ± 0.48	0.630 ± 0.006	14.4 (7.2)	269.58 ± 0.36	$+0.61 \pm 0.73$	0.673 ± 0.005	10.9 (4.3)
302.44 ± 0.36	-0.24 ± 0.66	0.619 ± 0.005	15.1 (8.2)	302.38 ± 0.24	$+0.46 \pm 0.50$	0.667 ± 0.007	12.0 (3.3)
332.26 ± 0.30	$+1.77 \pm 0.66$	0.610 ± 0.004	13.0 (7.9)	331.84 ± 0.24	$+0.39 \pm 0.62$	0.675 ± 0.004	11.4 (3.6)

Table 37: The nominal angle δ_n, average displacement $\Delta\delta$, average value of the parameter DIST, RMS of the ALPHA distribution for enabled GF and impact parameters between 60 m and 120 m. The RMS of the ALPHA distribution for disabled GF is given parentheses. The primary γ-ray energy was set to 120 GeV, the ZA to 20° and the azimuth angle to 120°.

$E_\gamma = 120\,\mathrm{GeV}$, Az = 150°, ZA = 20°, Intermediate Image Cleaning

δ_n[°]	$\Delta\delta$[°]	DIST[°]	$\mathrm{RMS}_{\lvert\mathrm{ALPHA}\rvert}$[°]	δ_n[°]	$\Delta\delta$[°]	DIST[°]	$\mathrm{RMS}_{\lvert\mathrm{ALPHA}\rvert}$[°]
IP = 60 m				**IP = 80 m**			
1.96 ± 0.48	$+7.49 \pm 0.90$	0.422 ± 0.004	12.4 (11.7)	359.88 ± 0.36	$+3.27 \pm 0.72$	0.531 ± 0.006	10.5 (8.9)
28.75 ± 0.48	$+6.55 \pm 1.38$	0.429 ± 0.005	15.7 (14.7)	28.16 ± 0.53	$+1.97 \pm 1.07$	0.539 ± 0.005	11.8 (9.1)
59.91 ± 0.54	$+4.14 \pm 0.89$	0.433 ± 0.003	19.1 (14.7)	58.28 ± 0.36	$+2.65 \pm 0.83$	0.543 ± 0.005	16.5 (10.9)
90.96 ± 0.54	-4.65 ± 1.38	0.433 ± 0.004	21.8 (16.0)	89.77 ± 0.48	-1.44 ± 1.31	0.544 ± 0.005	18.5 (10.9)
119.88 ± 0.54	-5.97 ± 1.01	0.420 ± 0.003	21.4 (16.0)	121.90 ± 0.30	-1.07 ± 0.78	0.530 ± 0.005	19.3 (8.2)
150.69 ± 0.54	-1.69 ± 0.96	0.421 ± 0.004	17.2 (15.6)	151.04 ± 0.24	-0.83 ± 0.60	0.532 ± 0.005	15.7 (8.2)
178.80 ± 0.48	$+0.64 \pm 0.90$	0.430 ± 0.005	14.1 (15.0)	179.54 ± 0.36	$+1.95 \pm 0.90$	0.541 ± 0.006	11.4 (8.8)
207.09 ± 0.30	$+4.15 \pm 1.25$	0.434 ± 0.005	13.5 (17.3)	206.71 ± 0.36	$+0.92 \pm 0.71$	0.548 ± 0.006	11.8 (7.9)
237.22 ± 0.60	$+2.37 \pm 1.07$	0.432 ± 0.004	20.6 (16.0)	237.32 ± 0.24	-0.13 ± 0.90	0.544 ± 0.005	16.6 (10.1)
270.98 ± 0.48	-1.85 ± 0.89	0.424 ± 0.003	22.5 (13.9)	270.08 ± 0.42	-2.90 ± 0.95	0.533 ± 0.004	19.1 (8.7)
300.89 ± 0.59	-5.50 ± 1.19	0.414 ± 0.003	21.4 (17.9)	302.58 ± 0.42	-1.00 ± 0.66	0.522 ± 0.002	17.9 (10.9)
333.13 ± 0.48	-0.75 ± 0.78	0.410 ± 0.004	16.7 (15.0)	333.17 ± 0.30	$+2.65 \pm 0.72$	0.519 ± 0.004	14.9 (7.1)
IP = 100 m				**IP = 120 m**			
0.20 ± 0.30	$+0.71 \pm 0.61$	0.622 ± 0.005	10.0 (7.1)	0.15 ± 0.24	-2.30 ± 0.50	0.693 ± 0.006	9.0 (4.4)
29.12 ± 0.36	$+1.60 \pm 0.78$	0.639 ± 0.006	11.3 (4.4)	28.73 ± 0.30	-2.69 ± 0.67	0.699 ± 0.006	11.5 (3.7)
58.05 ± 0.30	-0.09 ± 0.83	0.639 ± 0.006	13.4 (7.7)	58.64 ± 0.30	-0.62 ± 0.72	0.690 ± 0.007	11.3 (3.2)
89.86 ± 0.30	-2.24 ± 0.83	0.629 ± 0.005	15.8 (5.1)	89.65 ± 0.30	$+1.00 \pm 0.72$	0.677 ± 0.005	11.9 (4.0)
121.21 ± 0.30	-1.43 ± 0.60	0.624 ± 0.005	15.5 (6.1)	121.99 ± 0.30	$+2.64 \pm 0.68$	0.679 ± 0.006	12.5 (3.5)
152.06 ± 0.24	$+0.41 \pm 0.54$	0.626 ± 0.006	12.4 (5.8)	151.55 ± 0.30	-1.37 ± 0.55	0.699 ± 0.006	10.2 (4.1)
179.45 ± 0.30	-0.90 ± 0.73	0.631 ± 0.006	9.3 (5.9)	179.87 ± 0.24	-2.64 ± 0.63	0.704 ± 0.006	7.7 (3.4)
207.22 ± 0.24	-0.67 ± 0.60	0.634 ± 0.007	10.9 (5.3)	207.57 ± 0.24	-3.67 ± 0.54	0.696 ± 0.006	9.6 (3.8)
238.49 ± 0.24	$+0.06 \pm 0.83$	0.634 ± 0.006	14.5 (5.3)	238.10 ± 0.24	-1.32 ± 0.72	0.690 ± 0.006	11.8 (3.8)
269.28 ± 0.24	-0.70 ± 0.77	0.618 ± 0.005	15.7 (7.2)	269.58 ± 0.36	$+2.33 \pm 0.78$	0.667 ± 0.006	11.0 (4.3)
302.44 ± 0.36	$+0.41 \pm 0.79$	0.614 ± 0.006	15.6 (8.2)	302.38 ± 0.24	$+2.36 \pm 0.62$	0.672 ± 0.006	12.8 (3.3)
332.26 ± 0.30	$+0.14 \pm 0.60$	0.615 ± 0.006	13.1 (7.9)	331.84 ± 0.24	$+0.44 \pm 0.56$	0.668 ± 0.007	10.2 (3.6)

Table 38: The nominal angle δ_n, average displacement $\Delta\delta$, average value of the parameter DIST, RMS of the ALPHA distribution for enabled GF and impact parameters between 60 m and 120 m. The RMS of the ALPHA distribution for disabled GF is given parentheses. The primary γ-ray energy was set to 120 GeV, the ZA to 20° and the azimuth angle to 150°.

$E_\gamma = 120\,\mathrm{GeV}$, Az = 180°, ZA = 20°, Intermediate Image Cleaning

δ_n[°]	$\Delta\delta$[°]	DIST[°]	$\mathrm{RMS}_{\lvert\mathrm{ALPHA}\rvert}$[°]	δ_n[°]	$\Delta\delta$[°]	DIST[°]	$\mathrm{RMS}_{\lvert\mathrm{ALPHA}\rvert}$[°]
IP = 60 m				**IP = 80 m**			
1.96 ± 0.48	$+0.70 \pm 0.90$	0.421 ± 0.004	14.7 (11.7)	359.88 ± 0.36	$+1.36 \pm 0.78$	0.535 ± 0.001	9.3 (8.9)
28.75 ± 0.48	$+5.00 \pm 0.90$	0.418 ± 0.005	21.6 (14.7)	28.16 ± 0.53	$+2.46 \pm 0.77$	0.530 ± 0.006	15.2 (9.1)
59.91 ± 0.54	$+6.15 \pm 1.60$	0.419 ± 0.003	28.1 (14.7)	58.28 ± 0.36	$+2.48 \pm 0.95$	0.528 ± 0.004	20.8 (10.9)
90.96 ± 0.54	$+0.07 \pm 1.43$	0.416 ± 0.003	24.0 (16.0)	89.77 ± 0.48	-1.29 ± 1.07	0.524 ± 0.003	20.3 (10.9)
119.88 ± 0.54	-7.81 ± 1.60	0.412 ± 0.004	22.1 (16.0)	121.90 ± 0.30	-3.29 ± 1.06	0.527 ± 0.004	17.9 (8.2)
150.69 ± 0.54	-5.01 ± 0.96	0.413 ± 0.004	18.2 (15.6)	151.04 ± 0.24	-5.00 ± 0.60	0.530 ± 0.005	12.9 (8.2)
178.80 ± 0.48	-2.01 ± 0.84	0.417 ± 0.005	13.2 (15.0)	179.54 ± 0.36	$+0.40 \pm 0.66$	0.534 ± 0.006	7.9 (8.8)
207.09 ± 0.30	$+3.26 \pm 0.84$	0.411 ± 0.004	21.1 (17.3)	206.71 ± 0.36	$+3.01 \pm 0.83$	0.524 ± 0.005	14.6 (7.9)
237.22 ± 0.60	$+6.19 \pm 0.95$	0.407 ± 0.003	23.6 (16.0)	237.32 ± 0.24	$+3.72 \pm 0.83$	0.520 ± 0.004	16.3 (10.1)
270.98 ± 0.48	$+5.11 \pm 0.72$	0.410 ± 0.003	22.4 (13.9)	270.08 ± 0.42	$+2.77 \pm 0.95$	0.517 ± 0.003	19.5 (8.7)
300.89 ± 0.59	$+0.14 \pm 1.32$	0.409 ± 0.003	20.0 (17.9)	302.58 ± 0.42	$+0.52 \pm 1.13$	0.514 ± 0.004	17.7 (10.9)
333.13 ± 0.48	$+2.13 \pm 1.19$	0.420 ± 0.004	15.6 (15.0)	333.17 ± 0.30	$+1.88 \pm 0.72$	0.527 ± 0.004	14.5 (7.1)
IP = 100 m				**IP = 120 m**			
0.20 ± 0.30	-0.26 ± 0.61	0.614 ± 0.005	6.9 (7.1)	0.15 ± 0.24	$+0.79 \pm 0.51$	0.691 ± 0.005	5.1 (4.4)
29.12 ± 0.36	$+2.19 \pm 0.72$	0.624 ± 0.006	12.5 (4.4)	28.73 ± 0.30	-1.82 ± 0.61	0.690 ± 0.005	7.8 (3.7)
58.05 ± 0.30	-0.77 ± 0.71	0.614 ± 0.006	17.4 (7.7)	58.64 ± 0.30	-3.08 ± 0.72	0.667 ± 0.007	12.0 (3.2)
89.86 ± 0.30	$+0.02 \pm 0.94$	0.611 ± 0.002	16.9 (5.1)	89.65 ± 0.30	-0.32 ± 0.82	0.659 ± 0.005	11.4 (4.0)
121.21 ± 0.30	-0.07 ± 0.71	0.614 ± 0.003	14.0 (6.1)	121.99 ± 0.30	$+2.01 \pm 0.73$	0.671 ± 0.004	11.2 (3.5)
152.06 ± 0.24	-0.48 ± 0.54	0.626 ± 0.005	12.8 (5.8)	151.55 ± 0.30	-0.28 ± 0.67	0.693 ± 0.004	8.2 (4.1)
179.45 ± 0.30	$+0.05 \pm 0.68$	0.630 ± 0.007	10.3 (5.9)	179.87 ± 0.24	$+0.53 \pm 0.64$	0.699 ± 0.006	4.7 (3.4)
207.22 ± 0.24	$+0.83 \pm 0.61$	0.629 ± 0.007	11.9 (5.3)	207.57 ± 0.24	-0.85 ± 0.62	0.683 ± 0.005	13.3 (3.8)
238.49 ± 0.24	-0.06 ± 0.77	0.609 ± 0.005	15.5 (5.3)	238.10 ± 0.24	-2.36 ± 0.66	0.667 ± 0.006	15.1 (3.8)
269.28 ± 0.24	$+2.55 \pm 1.05$	0.601 ± 0.005	15.8 (7.2)	269.58 ± 0.36	-0.06 ± 0.88	0.652 ± 0.005	10.6 (4.3)
302.44 ± 0.36	$+2.31 \pm 0.66$	0.607 ± 0.003	13.1 (8.2)	302.38 ± 0.24	$+2.96 \pm 0.67$	0.660 ± 0.006	11.9 (3.3)
332.26 ± 0.30	$+1.71 \pm 0.78$	0.621 ± 0.006	10.6 (7.9)	331.84 ± 0.24	$+2.03 \pm 0.62$	0.678 ± 0.005	12.2 (3.6)

Table 39: The nominal angle δ_n, average displacement $\Delta\delta$, average value of the parameter DIST, RMS of the ALPHA distribution for enabled GF and impact parameters between 60 m and 120 m. The RMS of the ALPHA distribution for disabled GF is given parentheses. The primary γ-ray energy was set to 120 GeV, the ZA to 20° and the azimuth angle to 180°.

$E_\gamma = 170\,\mathrm{GeV}$, Az $= 0°$, ZA $= 0°$, Intermediate Image Cleaning

$\delta_n[°]$	$\Delta\delta[°]$	DIST[°]	$\mathrm{RMS}_{\lvert\mathrm{ALPHA}\rvert}[°]$	$\delta_n[°]$	$\Delta\delta[°]$	DIST[°]	$\mathrm{RMS}_{\lvert\mathrm{ALPHA}\rvert}[°]$
IP = 60 m				**IP = 80 m**			
359.79 ± 0.39	$+2.09 \pm 0.77$	0.521 ± 0.005	10.1 (8.8)	359.18 ± 0.39	-0.69 ± 0.62	0.644 ± 0.011	4.4 (4.9)
30.61 ± 0.47	$+6.74 \pm 1.07$	0.521 ± 0.006	15.5 (6.0)	30.70 ± 0.39	$+4.03 \pm 0.69$	0.643 ± 0.008	10.6 (3.5)
60.09 ± 0.47	$+4.30 \pm 1.01$	0.519 ± 0.007	17.4 (8.1)	60.02 ± 0.47	$+1.76 \pm 1.02$	0.651 ± 0.007	11.7 (4.2)
90.58 ± 0.47	$+2.91 \pm 1.14$	0.523 ± 0.006	21.1 (7.9)	90.27 ± 0.47	$+2.78 \pm 0.84$	0.649 ± 0.006	17.6 (4.3)
119.24 ± 0.31	-3.30 ± 0.69	0.525 ± 0.006	18.2 (6.3)	119.47 ± 0.39	-2.55 ± 0.99	0.647 ± 0.006	13.5 (5.0)
149.39 ± 0.62	-4.07 ± 1.15	0.514 ± 0.007	11.7 (7.0)	149.98 ± 0.39	-0.25 ± 0.84	0.639 ± 0.009	11.8 (3.7)
180.02 ± 0.47	-0.00 ± 0.92	0.512 ± 0.006	9.0 (7.4)	180.20 ± 0.31	-1.05 ± 0.62	0.633 ± 0.002	5.1 (3.7)
209.76 ± 0.39	$+2.34 \pm 0.91$	0.516 ± 0.002	14.6 (6.5)	210.03 ± 0.23	$+0.45 \pm 0.61$	0.640 ± 0.006	10.5 (4.2)
240.16 ± 0.47	$+4.01 \pm 0.92$	0.528 ± 0.006	18.6 (5.4)	240.15 ± 0.31	$+2.13 \pm 0.84$	0.643 ± 0.006	13.6 (4.2)
269.07 ± 0.39	-1.87 ± 0.99	0.530 ± 0.006	21.5 (8.5)	269.94 ± 0.39	$+0.51 \pm 0.84$	0.651 ± 0.007	19.1 (4.9)
299.26 ± 0.62	-6.12 ± 1.37	0.528 ± 0.006	18.3 (9.5)	300.04 ± 0.39	-4.07 ± 0.69	0.652 ± 0.008	12.6 (3.9)
329.53 ± 0.54	-2.87 ± 1.07	0.519 ± 0.006	13.7 (8.5)	329.18 ± 0.39	-2.63 ± 0.84	0.645 ± 0.006	13.0 (5.9)
IP = 100 m				**IP = 120 m**			
359.58 ± 0.31	-0.91 ± 0.70	0.727 ± 0.008	3.4 (2.4)	359.91 ± 0.32	-0.41 ± 0.63	0.784 ± 0.007	3.2 (2.2)
30.47 ± 0.23	$+0.57 \pm 0.61$	0.730 ± 0.006	9.7 (2.6)	30.13 ± 0.31	-0.01 ± 0.62	0.794 ± 0.006	7.6 (1.9)
60.13 ± 0.31	$+1.22 \pm 0.84$	0.730 ± 0.007	11.8 (2.7)	59.81 ± 0.31	-1.42 ± 0.77	0.774 ± 0.002	8.0 (2.5)
90.06 ± 0.31	$+0.51 \pm 0.84$	0.735 ± 0.010	11.0 (3.4)	89.92 ± 0.24	-0.49 ± 0.62	0.779 ± 0.006	7.9 (2.3)
119.77 ± 0.31	$+0.24 \pm 0.76$	0.727 ± 0.006	10.4 (2.8)	119.95 ± 0.32	$+1.77 \pm 0.78$	0.764 ± 0.006	7.6 (2.6)
150.23 ± 0.31	$+1.13 \pm 0.54$	0.724 ± 0.008	11.7 (2.8)	149.45 ± 0.24	-0.67 ± 0.46	0.777 ± 0.007	5.9 (2.4)
180.08 ± 0.31	-0.89 ± 0.70	0.717 ± 0.008	6.8 (2.6)	179.93 ± 0.24	$+0.05 \pm 0.55$	0.777 ± 0.005	4.0 (2.2)
209.64 ± 0.31	-0.92 ± 0.69	0.733 ± 0.007	7.1 (2.8)	209.56 ± 0.31	$+0.20 \pm 0.54$	0.782 ± 0.008	9.6 (2.4)
239.58 ± 0.23	-0.29 ± 0.77	0.731 ± 0.012	11.9 (2.8)	240.26 ± 0.32	-1.20 ± 0.78	0.769 ± 0.006	11.8 (2.4)
270.13 ± 0.31	-1.57 ± 0.76	0.733 ± 0.009	10.5 (2.8)	270.11 ± 0.16	-0.88 ± 0.54	0.777 ± 0.003	10.1 (2.3)
300.58 ± 0.31	-0.11 ± 0.77	0.730 ± 0.007	13.5 (2.5)	300.56 ± 0.24	$+0.73 \pm 0.56$	0.767 ± 0.005	6.2 (2.6)
330.08 ± 0.16	$+0.09 \pm 0.46$	0.733 ± 0.009	9.7 (3.3)	330.14 ± 0.24	$+0.15 \pm 0.55$	0.795 ± 0.008	4.4 (2.4)

Table 40: The nominal angle δ_n, average displacement $\Delta\delta$, average value of the parameter DIST, RMS of the ALPHA distribution for enabled GF and impact parameters between 60 m and 120 m. The RMS of the ALPHA distribution for disabled GF is given parentheses. The primary γ-ray energy was set to 170 GeV, the ZA to 0° and the azimuth angle to 0°.

$E_\gamma = 170\,\mathrm{GeV}$, Az $= 0°$, ZA $= 0°$, Hard Image Cleaning

$\delta_n[°]$	$\Delta\delta[°]$	DIST[°]	$\mathrm{RMS}_{\lvert\mathrm{ALPHA}\rvert}[°]$	$\delta_n[°]$	$\Delta\delta[°]$	DIST[°]	$\mathrm{RMS}_{\lvert\mathrm{ALPHA}\rvert}[°]$
IP = 60 m				**IP = 80 m**			
359.85 ± 0.39	$+1.70 \pm 0.69$	0.511 ± 0.006	10.2 (8.1)	359.44 ± 0.39	-0.05 ± 0.70	0.632 ± 0.010	4.3 (4.7)
30.93 ± 0.39	$+6.38 \pm 0.85$	0.510 ± 0.005	13.3 (6.2)	30.85 ± 0.39	$+4.29 \pm 0.85$	0.635 ± 0.010	10.0 (3.5)
59.90 ± 0.47	$+5.13 \pm 0.78$	0.510 ± 0.005	17.4 (8.8)	60.36 ± 0.39	$+1.84 \pm 0.86$	0.639 ± 0.006	10.9 (4.0)
91.03 ± 0.62	$+3.76 \pm 1.38$	0.515 ± 0.007	21.0 (8.2)	90.59 ± 0.39	$+3.19 \pm 0.92$	0.641 ± 0.006	16.4 (4.0)
119.29 ± 0.39	-4.35 ± 0.85	0.514 ± 0.005	17.7 (7.8)	119.76 ± 0.39	-1.58 ± 0.85	0.637 ± 0.008	12.5 (4.5)
149.62 ± 0.39	-2.59 ± 0.85	0.509 ± 0.006	15.9 (6.5)	149.87 ± 0.47	-0.68 ± 1.00	0.627 ± 0.005	12.6 (3.4)
179.40 ± 0.47	-1.19 ± 0.85	0.508 ± 0.009	5.2 (8.5)	180.24 ± 0.23	-0.21 ± 0.54	0.627 ± 0.006	5.0 (3.5)
208.83 ± 0.47	$+0.55 \pm 1.00$	0.505 ± 0.002	12.9 (9.6)	209.62 ± 0.16	$+1.95 \pm 0.46$	0.629 ± 0.005	12.5 (4.1)
240.20 ± 0.31	$+3.91 \pm 0.92$	0.522 ± 0.006	16.5 (5.9)	239.72 ± 0.39	$+1.60 \pm 0.85$	0.638 ± 0.005	12.6 (4.4)
269.64 ± 0.54	-1.02 ± 1.07	0.521 ± 0.006	21.3 (6.1)	269.65 ± 0.39	$+0.18 \pm 0.69$	0.642 ± 0.004	18.4 (4.9)
299.16 ± 0.39	-4.86 ± 0.92	0.516 ± 0.005	20.4 (8.0)	299.65 ± 0.31	-5.04 ± 0.84	0.641 ± 0.006	10.3 (4.0)
329.09 ± 0.47	-4.05 ± 1.07	0.509 ± 0.006	10.8 (9.5)	329.69 ± 0.31	-2.36 ± 0.69	0.638 ± 0.006	11.2 (5.3)
IP = 100 m				**IP = 120 m**			
359.65 ± 0.23	-0.15 ± 0.55	0.723 ± 0.009	3.2 (3.1)	359.97 ± 0.32	$+0.33 \pm 0.64$	0.779 ± 0.007	3.2 (2.6)
30.42 ± 0.31	$+0.90 \pm 0.70$	0.730 ± 0.008	7.6 (2.5)	30.24 ± 0.31	-0.40 ± 0.71	0.775 ± 0.007	6.4 (2.1)
59.75 ± 0.31	$+0.24 \pm 0.85$	0.722 ± 0.011	9.1 (2.6)	59.85 ± 0.16	-0.95 ± 0.63	0.762 ± 0.007	6.5 (2.5)
90.06 ± 0.31	-0.69 ± 0.77	0.720 ± 0.006	8.4 (3.3)	89.79 ± 0.24	-0.13 ± 0.55	0.762 ± 0.004	7.0 (2.7)
119.63 ± 0.31	$+0.04 \pm 0.77$	0.720 ± 0.010	8.1 (2.8)	119.96 ± 0.32	$+2.18 \pm 0.71$	0.750 ± 0.006	10.5 (2.6)
150.30 ± 0.39	$+0.89 \pm 0.78$	0.718 ± 0.007	9.7 (2.7)	149.58 ± 0.31	$+0.17 \pm 0.63$	0.766 ± 0.006	4.4 (2.1)
179.92 ± 0.31	$+0.02 \pm 0.62$	0.707 ± 0.008	4.3 (2.8)	179.82 ± 0.24	$+0.25 \pm 0.56$	0.770 ± 0.006	2.7 (2.2)
210.06 ± 0.31	$+0.13 \pm 0.70$	0.720 ± 0.006	9.3 (2.4)	209.80 ± 0.24	-0.73 ± 0.39	0.768 ± 0.005	9.4 (2.3)
239.58 ± 0.23	-0.55 ± 0.70	0.722 ± 0.010	9.2 (3.1)	240.17 ± 0.24	-2.05 ± 0.63	0.752 ± 0.006	9.5 (2.3)
269.93 ± 0.23	-0.90 ± 0.69	0.721 ± 0.009	11.0 (3.3)	270.32 ± 0.24	-0.84 ± 0.71	0.757 ± 0.005	7.7 (2.6)
300.49 ± 0.31	$+0.38 \pm 0.70$	0.722 ± 0.010	12.8 (3.0)	300.30 ± 0.32	$+0.96 \pm 0.64$	0.762 ± 0.007	5.3 (2.3)
330.49 ± 0.23	-0.44 ± 0.62	0.726 ± 0.009	4.0 (3.0)	330.02 ± 0.16	$+0.57 \pm 0.39$	0.779 ± 0.006	4.7 (2.4)

Table 41: The nominal angle δ_n, average displacement $\Delta\delta$, average value of the parameter DIST, RMS of the ALPHA distribution for enabled GF and impact parameters between 60 m and 120 m. The RMS of the ALPHA distribution for disabled GF is given parentheses. The primary γ-ray energy was set to 170 GeV, the ZA to 0° and the azimuth angle to 0°.

$E_\gamma = 170\,$GeV, Az $= 0°$, ZA $= 20°$, Intermediate Image Cleaning

δ_n[°]	$\Delta\delta$[°]	DIST[°]	RMS$_{\lvert\mathrm{ALPHA}\rvert}$[°]	δ_n[°]	$\Delta\delta$[°]	DIST[°]	RMS$_{\lvert\mathrm{ALPHA}\rvert}$[°]
IP = 60 m				IP = 80 m			
359.25 ± 0.58	$+0.44 \pm 1.01$	0.458 ± 0.004	10.4 (9.0)	359.72 ± 0.51	-0.10 ± 0.94	0.577 ± 0.005	5.4 (5.4)
28.59 ± 0.58	$+5.40 \pm 1.08$	0.453 ± 0.005	14.6 (9.0)	28.93 ± 0.43	$+2.19 \pm 0.86$	0.571 ± 0.004	8.3 (7.4)
58.91 ± 0.22	$+5.13 \pm 0.86$	0.438 ± 0.005	18.5 (11.8)	57.92 ± 0.29	$+3.10 \pm 0.65$	0.557 ± 0.005	12.9 (6.8)
89.34 ± 0.51	-1.87 ± 1.15	0.437 ± 0.005	19.7 (15.5)	90.26 ± 0.36	$+0.29 \pm 0.86$	0.554 ± 0.007	18.2 (5.7)
120.26 ± 0.36	-5.66 ± 1.01	0.442 ± 0.005	20.1 (11.5)	121.02 ± 0.29	-3.44 ± 0.65	0.561 ± 0.004	15.2 (8.5)
149.60 ± 0.73	-6.41 ± 1.25	0.446 ± 0.003	10.2 (14.5)	151.79 ± 0.36	-2.14 ± 0.72	0.568 ± 0.004	10.5 (7.0)
181.33 ± 0.58	$+1.17 \pm 0.94$	0.457 ± 0.003	10.4 (12.8)	181.01 ± 0.43	$+0.65 \pm 0.79$	0.574 ± 0.004	4.3 (4.9)
209.47 ± 0.65	$+4.68 \pm 1.37$	0.456 ± 0.004	11.0 (10.2)	208.54 ± 0.44	$+2.89 \pm 0.94$	0.575 ± 0.005	8.5 (6.9)
237.53 ± 0.58	$+3.67 \pm 1.29$	0.450 ± 0.004	19.3 (8.1)	237.46 ± 0.36	$+1.19 \pm 0.79$	0.566 ± 0.005	13.3 (5.3)
269.49 ± 0.58	-1.03 ± 1.29	0.446 ± 0.005	22.2 (11.6)	269.51 ± 0.43	-0.94 ± 0.86	0.562 ± 0.005	15.4 (5.3)
301.88 ± 0.43	-3.82 ± 1.29	0.452 ± 0.004	23.1 (13.6)	300.67 ± 0.36	-3.85 ± 0.79	0.568 ± 0.005	18.5 (8.3)
332.88 ± 0.43	-1.81 ± 0.86	0.455 ± 0.005	16.8 (12.0)	331.08 ± 0.51	-3.19 ± 1.01	0.576 ± 0.006	9.1 (9.7)
IP = 100 m				IP = 120 m			
359.55 ± 0.29	-0.02 ± 0.65	0.665 ± 0.007	7.6 (3.9)	359.53 ± 0.22	$+0.25 \pm 0.52$	0.720 ± 0.006	6.3 (2.5)
29.26 ± 0.36	$+1.89 \pm 0.72$	0.664 ± 0.005	8.9 (4.0)	28.67 ± 0.29	$+0.61 \pm 0.59$	0.728 ± 0.006	4.9 (3.1)
58.40 ± 0.36	$+2.19 \pm 0.72$	0.649 ± 0.007	9.3 (5.1)	58.28 ± 0.22	-0.36 ± 0.52	0.707 ± 0.008	5.3 (2.6)
89.81 ± 0.36	-0.16 ± 0.93	0.646 ± 0.007	10.9 (4.7)	89.71 ± 0.29	-0.69 ± 0.74	0.707 ± 0.007	7.4 (3.7)
121.59 ± 0.36	-1.20 ± 0.74	0.651 ± 0.004	11.3 (5.5)	122.11 ± 0.22	-0.29 ± 0.60	0.703 ± 0.004	9.1 (2.3)
151.46 ± 0.29	-2.26 ± 0.68	0.664 ± 0.007	4.4 (5.7)	152.00 ± 0.29	-0.32 ± 0.59	0.724 ± 0.006	4.0 (2.7)
180.34 ± 0.44	$+0.16 \pm 0.74$	0.672 ± 0.008	3.5 (3.6)	180.32 ± 0.29	$+0.31 \pm 0.60$	0.723 ± 0.005	3.2 (2.4)
208.62 ± 0.36	$+0.98 \pm 0.74$	0.674 ± 0.007	6.5 (3.6)	207.89 ± 0.22	$+0.31 \pm 0.59$	0.730 ± 0.004	7.9 (2.6)
237.99 ± 0.29	$+0.77 \pm 0.74$	0.665 ± 0.006	9.9 (3.7)	238.04 ± 0.29	-0.09 ± 0.67	0.722 ± 0.004	7.1 (2.4)
269.35 ± 0.36	-0.51 ± 0.96	0.659 ± 0.006	10.6 (3.4)	269.69 ± 0.29	-0.25 ± 0.59	0.714 ± 0.007	8.9 (2.5)
302.07 ± 0.22	-0.81 ± 0.43	0.659 ± 0.008	11.4 (4.4)	302.39 ± 0.29	-0.34 ± 0.59	0.717 ± 0.005	4.4 (2.9)
331.66 ± 0.36	-2.19 ± 0.72	0.670 ± 0.007	5.1 (4.9)	331.38 ± 0.29	-0.02 ± 0.59	0.733 ± 0.007	7.7 (2.5)

Table 42: The nominal angle δ_n, average displacement $\Delta\delta$, average value of the parameter DIST, RMS of the ALPHA distribution for enabled GF and impact parameters between 60 m and 120 m. The RMS of the ALPHA distribution for disabled GF is given parentheses. The primary γ-ray energy was set to 170 GeV, the ZA to 20° and the azimuth angle to 0°.

$E_\gamma = 170\,$GeV, Az $= 0°$, ZA $= 20°$, Hard Image Cleaning

δ_n[°]	$\Delta\delta$[°]	DIST[°]	RMS$_{\lvert\mathrm{ALPHA}\rvert}$[°]	δ_n[°]	$\Delta\delta$[°]	DIST[°]	RMS$_{\lvert\mathrm{ALPHA}\rvert}$[°]
IP = 60 m				IP = 80 m			
359.29 ± 0.44	-0.33 ± 0.87	0.449 ± 0.004	7.9 (8.4)	359.71 ± 0.44	-0.26 ± 0.72	0.570 ± 0.005	4.9 (5.7)
29.38 ± 0.58	$+5.60 \pm 1.30$	0.442 ± 0.004	14.7 (8.6)	29.61 ± 0.44	$+2.73 \pm 0.94$	0.564 ± 0.005	8.3 (4.9)
57.48 ± 0.36	$+3.86 \pm 1.01$	0.430 ± 0.005	18.8 (13.2)	57.74 ± 0.15	$+2.33 \pm 0.51$	0.550 ± 0.005	15.4 (6.6)
90.33 ± 0.73	-0.95 ± 1.23	0.427 ± 0.004	18.8 (11.9)	89.67 ± 0.36	$+0.41 \pm 1.09$	0.546 ± 0.005	17.8 (5.8)
120.64 ± 0.29	-4.03 ± 0.94	0.432 ± 0.005	21.3 (10.8)	121.35 ± 0.36	-2.81 ± 0.87	0.549 ± 0.005	15.4 (9.3)
150.60 ± 0.44	-5.51 ± 0.96	0.435 ± 0.003	11.1 (12.5)	152.51 ± 0.36	-1.10 ± 0.72	0.560 ± 0.006	9.3 (6.1)
181.94 ± 0.58	$+1.27 \pm 1.01$	0.449 ± 0.004	7.2 (9.5)	181.08 ± 0.51	$+0.99 \pm 0.87$	0.562 ± 0.006	4.6 (5.3)
210.01 ± 0.51	$+5.97 \pm 1.16$	0.445 ± 0.005	12.3 (7.5)	208.61 ± 0.44	$+2.99 \pm 0.94$	0.564 ± 0.006	11.0 (6.1)
237.60 ± 0.44	$+4.07 \pm 0.94$	0.439 ± 0.004	19.6 (11.0)	237.28 ± 0.29	$+0.81 \pm 0.87$	0.556 ± 0.006	12.5 (7.6)
269.28 ± 0.51	$+0.38 \pm 1.16$	0.438 ± 0.004	19.5 (11.9)	270.04 ± 0.36	$+0.10 \pm 0.94$	0.550 ± 0.005	15.4 (5.2)
301.22 ± 0.51	-4.21 ± 1.09	0.445 ± 0.004	22.3 (13.4)	300.57 ± 0.36	-4.14 ± 0.87	0.561 ± 0.006	16.2 (6.9)
332.70 ± 0.51	-1.53 ± 1.08	0.445 ± 0.004	17.1 (11.4)	331.14 ± 0.44	-2.96 ± 0.80	0.569 ± 0.007	11.1 (8.7)
IP = 100 m				IP = 120 m			
359.88 ± 0.44	-0.18 ± 0.72	0.659 ± 0.006	3.7 (3.4)	359.63 ± 0.22	-0.30 ± 0.53	0.717 ± 0.006	2.7 (2.4)
29.12 ± 0.29	$+1.71 \pm 0.65$	0.660 ± 0.005	5.7 (2.8)	28.51 ± 0.29	$+0.32 \pm 0.60$	0.710 ± 0.005	3.5 (3.0)
58.39 ± 0.22	$+2.28 \pm 0.58$	0.641 ± 0.007	10.5 (5.2)	58.34 ± 0.29	-0.36 ± 0.59	0.697 ± 0.010	4.0 (2.3)
89.72 ± 0.44	-0.82 ± 0.87	0.638 ± 0.005	8.2 (4.7)	89.85 ± 0.29	-0.40 ± 0.89	0.696 ± 0.006	6.6 (3.3)
121.72 ± 0.22	-1.52 ± 0.60	0.645 ± 0.007	8.3 (3.6)	121.98 ± 0.29	-0.54 ± 0.60	0.693 ± 0.006	6.9 (2.3)
151.34 ± 0.36	-1.81 ± 0.68	0.660 ± 0.008	4.4 (5.7)	151.97 ± 0.29	-0.21 ± 0.60	0.715 ± 0.004	4.4 (2.7)
180.29 ± 0.15	$+0.26 \pm 0.53$	0.663 ± 0.008	3.2 (4.0)	179.93 ± 0.29	-0.44 ± 0.61	0.716 ± 0.005	2.9 (2.5)
208.12 ± 0.29	$+0.81 \pm 0.74$	0.665 ± 0.008	7.3 (3.8)	207.76 ± 0.29	-0.35 ± 0.60	0.721 ± 0.006	4.1 (2.7)
237.93 ± 0.29	$+0.09 \pm 0.74$	0.656 ± 0.006	9.5 (3.5)	238.04 ± 0.22	$+0.59 \pm 0.52$	0.708 ± 0.007	10.1 (2.4)
269.41 ± 0.29	-0.93 ± 0.74	0.649 ± 0.006	11.0 (4.0)	269.82 ± 0.29	$+1.07 \pm 0.59$	0.701 ± 0.007	9.5 (2.6)
301.99 ± 0.22	-0.67 ± 0.65	0.653 ± 0.007	10.8 (3.9)	302.19 ± 0.22	$+0.82 \pm 0.52$	0.707 ± 0.008	6.8 (2.6)
331.65 ± 0.36	-1.29 ± 0.65	0.664 ± 0.006	7.2 (4.8)	331.70 ± 0.29	-0.49 ± 0.60	0.719 ± 0.006	4.2 (2.7)

Table 43: The nominal angle δ_n, average displacement $\Delta\delta$, average value of the parameter DIST, RMS of the ALPHA distribution for enabled GF and impact parameters between 60 m and 120 m. The RMS of the ALPHA distribution for disabled GF is given parentheses. The primary γ-ray energy was set to 170 GeV, the ZA to 20° and the azimuth angle to 0°.

$E_\gamma = 170\,\text{GeV}$, Az = 30°, ZA = 20°, Intermediate Image Cleaning

δ_n[°]	$\Delta\delta$[°]	DIST[°]	RMS$_{\lvert\text{ALPHA}\rvert}$[°]	δ_n[°]	$\Delta\delta$[°]	DIST[°]	RMS$_{\lvert\text{ALPHA}\rvert}$[°]
IP = 60 m				**IP = 80 m**			
359.25 ± 0.58	-6.15 ± 1.07	0.432 ± 0.004	11.0 (9.0)	359.72 ± 0.51	-3.78 ± 1.07	0.547 ± 0.005	8.5 (5.4)
28.59 ± 0.58	-2.60 ± 1.21	0.422 ± 0.004	11.8 (9.0)	28.93 ± 0.43	-0.86 ± 0.72	0.533 ± 0.005	10.4 (7.4)
58.91 ± 0.22	$+1.50 \pm 0.71$	0.416 ± 0.005	18.1 (11.8)	57.92 ± 0.29	$+2.06 \pm 0.64$	0.531 ± 0.004	13.9 (6.8)
89.34 ± 0.51	$+3.61 \pm 1.07$	0.427 ± 0.004	21.6 (15.5)	90.26 ± 0.36	$+2.60 \pm 0.86$	0.543 ± 0.005	16.6 (5.7)
120.26 ± 0.36	$+0.73 \pm 0.86$	0.438 ± 0.004	19.2 (11.5)	121.02 ± 0.29	-0.01 ± 0.50	0.553 ± 0.006	16.7 (8.5)
149.60 ± 0.73	-4.44 ± 1.71	0.441 ± 0.005	14.1 (14.5)	151.79 ± 0.36	$+0.60 \pm 0.71$	0.558 ± 0.006	11.4 (7.0)
181.33 ± 0.58	-4.93 ± 0.93	0.439 ± 0.006	12.0 (12.8)	181.01 ± 0.43	-2.70 ± 0.93	0.552 ± 0.006	8.9 (4.9)
209.47 ± 0.65	-0.90 ± 1.15	0.433 ± 0.006	12.0 (10.2)	208.54 ± 0.44	-1.22 ± 0.86	0.544 ± 0.005	10.3 (6.9)
237.53 ± 0.58	$+2.98 \pm 0.86$	0.426 ± 0.004	16.3 (8.1)	237.46 ± 0.36	$+1.41 \pm 0.78$	0.540 ± 0.005	14.1 (5.3)
269.49 ± 0.58	$+5.74 \pm 1.24$	0.435 ± 0.003	20.1 (11.6)	269.51 ± 0.43	$+4.44 \pm 1.07$	0.555 ± 0.006	15.9 (5.3)
301.88 ± 0.43	$+6.16 \pm 1.07$	0.444 ± 0.005	18.9 (13.6)	300.67 ± 0.36	$+1.06 \pm 0.64$	0.562 ± 0.004	15.4 (8.3)
332.88 ± 0.43	-0.50 ± 1.07	0.450 ± 0.005	16.2 (12.0)	331.08 ± 0.51	$+0.73 \pm 0.72$	0.564 ± 0.008	11.8 (9.7)
IP = 100 m				**IP = 120 m**			
359.55 ± 0.29	-1.34 ± 0.79	0.636 ± 0.006	7.6 (3.9)	359.53 ± 0.22	$+0.41 \pm 0.58$	0.707 ± 0.005	6.6 (2.5)
29.26 ± 0.36	-0.31 ± 0.64	0.621 ± 0.007	7.5 (4.0)	28.67 ± 0.29	$+0.15 \pm 0.57$	0.696 ± 0.007	7.1 (3.1)
58.40 ± 0.36	$+0.22 \pm 0.71$	0.621 ± 0.005	11.4 (5.1)	58.28 ± 0.22	$+0.03 \pm 0.50$	0.691 ± 0.007	9.4 (2.6)
89.81 ± 0.36	-0.00 ± 0.93	0.629 ± 0.006	11.6 (4.7)	89.71 ± 0.29	-0.18 ± 0.71	0.680 ± 0.007	8.8 (3.7)
121.59 ± 0.36	-0.43 ± 0.78	0.640 ± 0.005	11.8 (5.5)	122.11 ± 0.22	$+0.41 \pm 0.58$	0.698 ± 0.005	8.8 (2.3)
151.46 ± 0.29	$+0.20 \pm 0.78$	0.649 ± 0.007	8.3 (5.7)	152.00 ± 0.29	$+0.91 \pm 0.57$	0.706 ± 0.005	7.5 (2.7)
180.34 ± 0.44	-0.96 ± 0.86	0.648 ± 0.004	8.0 (3.6)	180.32 ± 0.29	$+1.12 \pm 0.58$	0.713 ± 0.006	6.2 (2.4)
208.62 ± 0.36	-0.42 ± 0.72	0.633 ± 0.007	9.0 (3.6)	207.89 ± 0.22	-0.23 ± 0.57	0.702 ± 0.006	6.8 (2.6)
237.99 ± 0.29	$+1.46 \pm 0.64$	0.633 ± 0.006	10.0 (3.7)	238.04 ± 0.29	$+0.15 \pm 0.58$	0.699 ± 0.005	8.2 (2.4)
269.35 ± 0.36	-0.54 ± 0.86	0.643 ± 0.002	11.2 (3.4)	269.69 ± 0.29	-0.28 ± 0.57	0.696 ± 0.004	9.0 (2.5)
302.07 ± 0.22	-0.77 ± 0.78	0.653 ± 0.004	11.0 (4.4)	302.39 ± 0.29	$+0.25 \pm 0.65$	0.702 ± 0.006	7.7 (2.9)
331.66 ± 0.36	$+0.55 \pm 0.85$	0.652 ± 0.004	9.4 (4.9)	331.38 ± 0.29	-0.50 ± 0.64	0.706 ± 0.007	7.7 (2.5)

Table 44: The nominal angle δ_n, average displacement $\Delta\delta$, average value of the parameter DIST, RMS of the ALPHA distribution for enabled GF and impact parameters between 60 m and 120 m. The RMS of the ALPHA distribution for disabled GF is given parentheses. The primary γ-ray energy was set to 170 GeV, the ZA to 20° and the azimuth angle to 30°.

$E_\gamma = 170\,\text{GeV}$, Az = 30°, ZA = 20°, Hard Image Cleaning

δ_n[°]	$\Delta\delta$[°]	DIST[°]	RMS$_{\lvert\text{ALPHA}\rvert}$[°]	δ_n[°]	$\Delta\delta$[°]	DIST[°]	RMS$_{\lvert\text{ALPHA}\rvert}$[°]
IP = 60 m				**IP = 80 m**			
359.29 ± 0.44	-4.51 ± 0.94	0.430 ± 0.004	9.9 (8.4)	359.71 ± 0.44	-2.52 ± 1.08	0.543 ± 0.007	9.1 (5.7)
29.38 ± 0.58	-2.04 ± 1.16	0.417 ± 0.004	12.3 (8.6)	29.61 ± 0.44	-0.49 ± 0.79	0.534 ± 0.004	9.0 (4.9)
57.48 ± 0.36	$+1.33 \pm 0.94$	0.412 ± 0.005	18.0 (13.2)	57.74 ± 0.15	$+1.23 \pm 0.51$	0.526 ± 0.004	14.0 (6.6)
90.33 ± 0.73	$+6.47 \pm 1.23$	0.420 ± 0.004	19.8 (11.9)	89.67 ± 0.36	$+2.22 \pm 1.01$	0.536 ± 0.005	15.9 (5.8)
120.64 ± 0.29	-0.34 ± 0.87	0.429 ± 0.002	18.2 (10.8)	121.35 ± 0.36	-0.68 ± 1.15	0.549 ± 0.006	15.3 (9.3)
150.60 ± 0.44	-3.57 ± 1.15	0.436 ± 0.004	13.7 (12.5)	152.51 ± 0.36	$+0.08 \pm 1.01$	0.557 ± 0.005	10.4 (6.1)
181.94 ± 0.58	-2.81 ± 1.30	0.431 ± 0.006	11.6 (9.5)	181.08 ± 0.51	-2.24 ± 0.94	0.550 ± 0.007	8.1 (5.3)
210.01 ± 0.51	-1.68 ± 1.08	0.427 ± 0.005	11.9 (7.5)	208.61 ± 0.44	-2.18 ± 0.87	0.538 ± 0.007	11.1 (6.1)
237.60 ± 0.44	$+4.20 \pm 0.94$	0.418 ± 0.004	16.3 (11.0)	237.28 ± 0.29	$+1.53 \pm 0.65$	0.533 ± 0.005	13.6 (7.6)
269.28 ± 0.51	$+4.12 \pm 1.56$	0.428 ± 0.004	18.8 (11.9)	270.04 ± 0.36	$+3.59 \pm 0.87$	0.549 ± 0.005	14.7 (5.2)
301.22 ± 0.51	$+5.83 \pm 1.37$	0.440 ± 0.005	17.6 (13.4)	300.57 ± 0.36	$+0.39 \pm 1.08$	0.558 ± 0.005	13.5 (6.9)
332.70 ± 0.51	-2.86 ± 1.01	0.444 ± 0.004	15.1 (11.4)	331.14 ± 0.44	-2.88 ± 0.94	0.557 ± 0.006	12.7 (8.7)
IP = 100 m				**IP = 120 m**			
359.88 ± 0.44	-0.79 ± 0.87	0.637 ± 0.005	7.3 (3.4)	359.63 ± 0.22	-0.12 ± 0.59	0.702 ± 0.005	5.7 (2.4)
29.12 ± 0.29	$+0.13 \pm 0.72$	0.622 ± 0.007	7.0 (2.8)	28.51 ± 0.29	$+0.06 \pm 0.58$	0.692 ± 0.007	5.2 (3.0)
58.39 ± 0.22	$+0.79 \pm 0.51$	0.616 ± 0.006	10.3 (5.2)	58.34 ± 0.29	-0.90 ± 0.58	0.686 ± 0.006	8.5 (2.3)
89.72 ± 0.44	$+1.22 \pm 0.94$	0.622 ± 0.007	11.6 (4.7)	89.85 ± 0.29	-0.74 ± 0.65	0.673 ± 0.002	8.1 (3.3)
121.72 ± 0.22	-0.06 ± 0.64	0.636 ± 0.006	11.7 (3.6)	121.98 ± 0.29	-0.27 ± 0.58	0.686 ± 0.007	8.2 (2.3)
151.34 ± 0.36	-0.36 ± 0.94	0.644 ± 0.007	7.8 (5.7)	151.97 ± 0.29	$+0.56 \pm 0.65$	0.698 ± 0.004	6.5 (2.7)
180.29 ± 0.15	-0.59 ± 0.58	0.644 ± 0.006	7.0 (4.0)	179.93 ± 0.29	$+0.36 \pm 0.51$	0.709 ± 0.005	5.4 (2.5)
208.12 ± 0.29	-0.91 ± 0.65	0.631 ± 0.005	8.8 (3.8)	207.76 ± 0.29	-1.01 ± 0.66	0.697 ± 0.007	5.5 (2.7)
237.93 ± 0.29	$+1.26 \pm 0.65$	0.627 ± 0.005	10.2 (3.5)	238.04 ± 0.22	$+0.50 \pm 0.51$	0.690 ± 0.006	7.6 (2.4)
269.41 ± 0.29	$+1.38 \pm 0.72$	0.632 ± 0.006	11.1 (4.0)	269.82 ± 0.29	-0.46 ± 0.73	0.687 ± 0.005	7.9 (2.6)
301.99 ± 0.22	-0.95 ± 0.72	0.647 ± 0.006	11.1 (3.9)	302.19 ± 0.22	-0.97 ± 0.72	0.692 ± 0.004	7.1 (2.6)
331.65 ± 0.36	-1.02 ± 0.86	0.648 ± 0.006	8.8 (4.8)	331.70 ± 0.29	$+0.18 \pm 0.65$	0.699 ± 0.007	7.2 (2.7)

Table 45: The nominal angle δ_n, average displacement $\Delta\delta$, average value of the parameter DIST, RMS of the ALPHA distribution for enabled GF and impact parameters between 60 m and 120 m. The RMS of the ALPHA distribution for disabled GF is given parentheses. The primary γ-ray energy was set to 170 GeV, the ZA to 20° and the azimuth angle to 30°.

$E_\gamma = 170\,\mathrm{GeV}$, Az = 60°, ZA = 20°, Intermediate Image Cleaning

δ_n[°]	$\Delta\delta$[°]	DIST[°]	$\mathrm{RMS}_{\mathrm{\|ALPHA\|}}$[°]	δ_n[°]	$\Delta\delta$[°]	DIST[°]	$\mathrm{RMS}_{\mathrm{\|ALPHA\|}}$[°]
IP = 60 m				**IP = 80 m**			
359.25 ± 0.58	-3.03 ± 1.42	0.431 ± 0.005	11.9 (9.0)	359.72 ± 0.51	-0.26 ± 1.28	0.546 ± 0.005	9.7 (5.4)
28.59 ± 0.58	-4.66 ± 1.00	0.426 ± 0.004	11.4 (9.0)	28.93 ± 0.43	-2.46 ± 0.92	0.538 ± 0.005	8.5 (7.4)
58.91 ± 0.22	-2.86 ± 0.57	0.429 ± 0.005	15.2 (11.8)	57.92 ± 0.29	-2.43 ± 0.71	0.549 ± 0.001	12.8 (6.8)
89.34 ± 0.51	$+1.42 \pm 1.00$	0.450 ± 0.004	18.3 (15.5)	90.26 ± 0.36	$+1.72 \pm 0.78$	0.567 ± 0.005	15.7 (5.7)
120.26 ± 0.36	$+4.70 \pm 0.92$	0.455 ± 0.004	18.3 (11.5)	121.02 ± 0.29	$+2.25 \pm 0.78$	0.574 ± 0.002	15.7 (8.5)
149.60 ± 0.73	$+0.99 \pm 1.43$	0.449 ± 0.005	15.6 (14.5)	151.79 ± 0.36	$+1.74 \pm 0.92$	0.570 ± 0.004	12.4 (7.0)
181.33 ± 0.58	-1.91 ± 0.86	0.434 ± 0.004	11.8 (12.8)	181.01 ± 0.43	-1.25 ± 1.14	0.551 ± 0.004	8.1 (4.9)
209.47 ± 0.65	-6.96 ± 1.36	0.432 ± 0.005	11.6 (10.2)	208.54 ± 0.44	-3.06 ± 1.00	0.544 ± 0.004	8.8 (6.9)
237.53 ± 0.58	-3.84 ± 1.07	0.441 ± 0.004	15.8 (8.1)	237.46 ± 0.36	-2.55 ± 0.78	0.559 ± 0.005	11.5 (5.3)
269.49 ± 0.58	$+1.76 \pm 1.21$	0.454 ± 0.005	17.4 (11.6)	269.51 ± 0.43	$+0.91 \pm 0.79$	0.576 ± 0.005	14.8 (5.3)
301.88 ± 0.43	$+7.65 \pm 1.06$	0.459 ± 0.004	19.8 (13.6)	300.67 ± 0.36	$+2.17 \pm 0.85$	0.580 ± 0.005	15.6 (8.3)
332.88 ± 0.43	$+6.82 \pm 1.13$	0.445 ± 0.004	15.9 (12.0)	331.08 ± 0.51	$+2.84 \pm 1.21$	0.565 ± 0.005	13.2 (9.7)
IP = 100 m				**IP = 120 m**			
359.55 ± 0.29	-0.21 ± 0.78	0.638 ± 0.006	8.0 (3.9)	359.53 ± 0.22	$+0.15 \pm 0.50$	0.706 ± 0.006	6.5 (2.5)
29.26 ± 0.36	$+0.15 \pm 0.85$	0.636 ± 0.005	6.6 (4.0)	28.67 ± 0.29	$+0.25 \pm 0.64$	0.696 ± 0.005	6.5 (3.1)
58.40 ± 0.36	-0.78 ± 0.79	0.637 ± 0.006	10.0 (5.1)	58.28 ± 0.22	-0.06 ± 0.57	0.699 ± 0.006	7.8 (2.6)
89.81 ± 0.36	$+0.66 \pm 0.81$	0.657 ± 0.005	11.5 (4.7)	89.71 ± 0.29	$+0.63 \pm 0.64$	0.709 ± 0.005	8.5 (3.7)
121.59 ± 0.36	$+1.30 \pm 0.73$	0.664 ± 0.006	10.9 (5.5)	122.11 ± 0.22	$+0.65 \pm 0.57$	0.710 ± 0.006	8.0 (2.3)
151.46 ± 0.29	$+1.01 \pm 0.87$	0.663 ± 0.006	9.7 (5.7)	152.00 ± 0.29	$+0.28 \pm 0.71$	0.720 ± 0.006	8.2 (2.7)
180.34 ± 0.44	$+0.14 \pm 1.07$	0.644 ± 0.005	6.3 (3.6)	180.32 ± 0.29	$+1.03 \pm 0.72$	0.713 ± 0.004	7.3 (2.4)
208.62 ± 0.36	-0.86 ± 0.85	0.638 ± 0.005	6.9 (3.6)	207.89 ± 0.22	-0.13 ± 0.64	0.710 ± 0.005	5.3 (2.6)
237.99 ± 0.29	-0.95 ± 0.64	0.650 ± 0.005	9.6 (3.7)	238.04 ± 0.29	-1.02 ± 0.58	0.718 ± 0.006	7.1 (2.4)
269.35 ± 0.36	$+0.56 \pm 0.71$	0.664 ± 0.007	11.4 (3.4)	269.69 ± 0.29	$+1.32 \pm 0.57$	0.717 ± 0.005	7.9 (2.5)
302.07 ± 0.22	$+0.80 \pm 0.71$	0.664 ± 0.005	10.8 (4.4)	302.39 ± 0.29	$+1.11 \pm 0.64$	0.708 ± 0.005	8.1 (2.9)
331.66 ± 0.36	$+0.88 \pm 1.06$	0.657 ± 0.006	9.7 (4.9)	331.38 ± 0.29	-0.39 ± 0.64	0.717 ± 0.004	8.2 (2.5)

Table 46: The nominal angle δ_n, average displacement $\Delta\delta$, average value of the parameter DIST, RMS of the ALPHA distribution for enabled GF and impact parameters between 60 m and 120 m. The RMS of the ALPHA distribution for disabled GF is given parentheses. The primary γ-ray energy was set to 170 GeV, the ZA to 20° and the azimuth angle to 60°.

$E_\gamma = 170\,\mathrm{GeV}$, Az = 60°, ZA = 20°, Hard Image Cleaning

δ_n[°]	$\Delta\delta$[°]	DIST[°]	$\mathrm{RMS}_{\mathrm{\|ALPHA\|}}$[°]	δ_n[°]	$\Delta\delta$[°]	DIST[°]	$\mathrm{RMS}_{\mathrm{\|ALPHA\|}}$[°]
IP = 60 m				**IP = 80 m**			
359.29 ± 0.44	$+1.00 \pm 0.94$	0.421 ± 0.004	11.9 (8.4)	359.71 ± 0.44	-1.01 ± 0.94	0.541 ± 0.007	8.8 (5.7)
29.38 ± 0.58	-4.18 ± 1.22	0.418 ± 0.005	12.6 (8.6)	29.61 ± 0.44	-1.75 ± 0.93	0.528 ± 0.005	9.1 (4.9)
57.48 ± 0.36	-4.10 ± 0.93	0.421 ± 0.004	14.7 (13.2)	57.74 ± 0.15	-2.45 ± 0.57	0.540 ± 0.005	12.9 (6.6)
90.33 ± 0.73	$+1.61 \pm 1.23$	0.438 ± 0.005	17.9 (11.9)	89.67 ± 0.36	$+1.38 \pm 0.72$	0.557 ± 0.005	15.7 (5.8)
120.64 ± 0.29	$+5.91 \pm 1.15$	0.448 ± 0.004	17.7 (10.8)	121.35 ± 0.36	$+3.78 \pm 0.72$	0.565 ± 0.005	14.8 (9.3)
150.60 ± 0.44	$+1.83 \pm 1.43$	0.440 ± 0.002	16.3 (12.5)	152.51 ± 0.36	$+1.63 \pm 0.86$	0.562 ± 0.005	12.1 (6.1)
181.94 ± 0.58	-0.47 ± 1.01	0.426 ± 0.003	12.2 (9.5)	181.08 ± 0.51	-2.21 ± 1.15	0.544 ± 0.005	9.2 (5.3)
210.01 ± 0.51	-5.43 ± 0.87	0.423 ± 0.004	11.4 (7.5)	208.61 ± 0.44	-2.74 ± 1.01	0.536 ± 0.005	8.7 (6.1)
237.60 ± 0.44	-2.96 ± 1.01	0.434 ± 0.003	16.2 (11.0)	237.28 ± 0.29	-2.74 ± 0.72	0.548 ± 0.004	11.9 (7.6)
269.28 ± 0.51	$+1.90 \pm 1.08$	0.450 ± 0.005	16.5 (11.9)	270.04 ± 0.36	$+2.16 \pm 0.72$	0.564 ± 0.005	13.6 (5.2)
301.22 ± 0.51	$+4.61 \pm 1.00$	0.449 ± 0.004	18.6 (13.4)	300.57 ± 0.36	$+2.28 \pm 0.93$	0.572 ± 0.005	15.2 (6.9)
332.70 ± 0.51	$+4.29 \pm 1.44$	0.435 ± 0.004	15.1 (11.4)	331.14 ± 0.44	$+2.30 \pm 1.14$	0.555 ± 0.005	12.2 (8.7)
IP = 100 m				**IP = 120 m**			
359.88 ± 0.44	$+0.42 \pm 1.00$	0.630 ± 0.006	8.3 (3.4)	359.63 ± 0.22	$+0.03 \pm 0.64$	0.699 ± 0.005	6.3 (2.4)
29.12 ± 0.29	-0.06 ± 0.79	0.628 ± 0.006	7.0 (2.8)	28.51 ± 0.29	$+0.50 \pm 0.72$	0.690 ± 0.004	6.0 (3.0)
58.39 ± 0.22	-1.27 ± 0.50	0.628 ± 0.004	10.0 (5.2)	58.34 ± 0.29	$+0.06 \pm 0.65$	0.690 ± 0.007	7.6 (2.3)
89.72 ± 0.44	$+1.12 \pm 0.89$	0.646 ± 0.006	11.9 (4.7)	89.85 ± 0.29	$+0.14 \pm 0.51$	0.699 ± 0.006	8.5 (3.3)
121.72 ± 0.22	$+1.29 \pm 0.81$	0.657 ± 0.004	10.6 (3.6)	121.98 ± 0.29	$+0.38 \pm 0.72$	0.701 ± 0.006	7.0 (2.3)
151.34 ± 0.36	$+0.52 \pm 1.02$	0.654 ± 0.002	9.2 (5.7)	151.97 ± 0.29	$+0.10 \pm 0.64$	0.713 ± 0.004	7.7 (2.7)
180.29 ± 0.15	$+0.62 \pm 0.64$	0.636 ± 0.006	6.4 (4.0)	179.93 ± 0.29	$+1.11 \pm 0.72$	0.705 ± 0.005	5.7 (2.5)
208.12 ± 0.29	-1.33 ± 0.65	0.627 ± 0.005	6.9 (3.8)	207.76 ± 0.29	-0.14 ± 0.73	0.705 ± 0.005	5.8 (2.7)
237.93 ± 0.29	-0.76 ± 0.58	0.643 ± 0.005	9.4 (3.5)	238.04 ± 0.22	-0.21 ± 0.58	0.707 ± 0.005	7.2 (2.4)
269.41 ± 0.29	$+0.28 \pm 0.65$	0.656 ± 0.005	11.5 (4.0)	269.82 ± 0.29	$+0.86 \pm 0.65$	0.708 ± 0.006	8.2 (2.6)
301.99 ± 0.22	$+0.99 \pm 0.65$	0.652 ± 0.007	10.6 (3.9)	302.19 ± 0.22	$+0.23 \pm 0.50$	0.694 ± 0.005	8.5 (2.6)
331.65 ± 0.36	$+0.91 \pm 0.93$	0.645 ± 0.005	9.3 (4.8)	331.70 ± 0.29	-0.43 ± 0.72	0.704 ± 0.007	7.9 (2.7)

Table 47: The nominal angle δ_n, average displacement $\Delta\delta$, average value of the parameter DIST, RMS of the ALPHA distribution for enabled GF and impact parameters between 60 m and 120 m. The RMS of the ALPHA distribution for disabled GF is given parentheses. The primary γ-ray energy was set to 170 GeV, the ZA to 20° and the azimuth angle to 60°.

$E_\gamma = 170\,\mathrm{GeV}$, Az = 90°, ZA = 20°, Intermediate Image Cleaning

δ_n[°]	$\Delta\delta$[°]	DIST[°]	RMS$_{\lvert \mathrm{ALPHA} \rvert}$[°]	δ_n[°]	$\Delta\delta$[°]	DIST[°]	RMS$_{\lvert \mathrm{ALPHA} \rvert}$[°]
IP = 60 m				**IP = 80 m**			
359.25 ± 0.58	$+2.66 \pm 1.28$	0.419 ± 0.003	15.4 (9.0)	359.72 ± 0.51	$+3.17 \pm 1.13$	0.534 ± 0.006	11.2 (5.4)
28.59 ± 0.58	-3.83 ± 1.27	0.423 ± 0.005	10.6 (9.0)	28.93 ± 0.43	-1.18 ± 1.13	0.540 ± 0.005	10.0 (7.4)
58.91 ± 0.22	-5.91 ± 0.63	0.442 ± 0.003	17.9 (11.8)	57.92 ± 0.29	-4.15 ± 0.85	0.558 ± 0.005	13.4 (6.8)
89.34 ± 0.51	-3.65 ± 0.93	0.452 ± 0.002	21.3 (15.5)	90.26 ± 0.36	-1.99 ± 0.78	0.573 ± 0.005	16.5 (5.7)
120.26 ± 0.36	$+0.99 \pm 0.92$	0.451 ± 0.004	22.3 (11.5)	121.02 ± 0.29	$+1.23 \pm 0.71$	0.571 ± 0.004	16.9 (8.5)
149.60 ± 0.73	$+4.20 \pm 1.21$	0.434 ± 0.003	19.2 (14.5)	151.79 ± 0.36	$+2.33 \pm 0.92$	0.552 ± 0.005	14.5 (7.0)
181.33 ± 0.58	$+5.38 \pm 1.35$	0.423 ± 0.004	11.1 (12.8)	181.01 ± 0.43	$+0.18 \pm 0.99$	0.538 ± 0.005	9.7 (4.9)
209.47 ± 0.65	-2.13 ± 0.86	0.432 ± 0.005	12.6 (10.2)	208.54 ± 0.44	-2.35 ± 0.92	0.546 ± 0.006	9.4 (6.9)
237.53 ± 0.58	-8.16 ± 0.86	0.447 ± 0.003	18.3 (8.1)	237.46 ± 0.36	-6.39 ± 0.78	0.565 ± 0.005	13.6 (5.3)
269.49 ± 0.58	-2.76 ± 1.14	0.457 ± 0.003	20.5 (11.6)	269.51 ± 0.43	-2.22 ± 0.78	0.578 ± 0.003	15.9 (5.3)
301.88 ± 0.43	$+3.49 \pm 0.99$	0.449 ± 0.003	22.0 (13.6)	300.67 ± 0.36	$+1.22 \pm 0.71$	0.565 ± 0.005	16.2 (8.3)
332.88 ± 0.43	$+9.64 \pm 1.48$	0.432 ± 0.005	19.2 (12.0)	331.08 ± 0.51	$+1.86 \pm 1.34$	0.549 ± 0.006	18.0 (9.7)
IP = 100 m				**IP = 120 m**			
359.55 ± 0.29	-0.35 ± 0.78	0.631 ± 0.005	7.7 (3.9)	359.53 ± 0.22	-0.80 ± 0.57	0.704 ± 0.004	9.3 (2.5)
29.26 ± 0.36	-0.93 ± 0.92	0.634 ± 0.007	9.8 (4.0)	28.67 ± 0.29	$+0.06 \pm 0.64$	0.697 ± 0.007	8.7 (3.1)
58.40 ± 0.36	-1.93 ± 0.85	0.655 ± 0.005	11.6 (5.1)	58.28 ± 0.22	$+0.53 \pm 0.57$	0.712 ± 0.007	8.4 (2.6)
89.81 ± 0.36	-0.73 ± 0.71	0.662 ± 0.005	10.3 (4.7)	89.71 ± 0.29	-0.70 ± 0.64	0.708 ± 0.004	7.9 (3.7)
121.59 ± 0.36	$+0.66 \pm 0.78$	0.660 ± 0.005	12.8 (5.5)	122.11 ± 0.22	$+0.17 \pm 0.57$	0.714 ± 0.004	11.6 (2.3)
151.46 ± 0.29	$+0.48 \pm 0.78$	0.645 ± 0.006	14.1 (5.7)	152.00 ± 0.29	-0.20 ± 0.64	0.716 ± 0.005	10.0 (2.7)
180.34 ± 0.44	$+0.59 \pm 0.92$	0.636 ± 0.005	5.8 (3.6)	180.32 ± 0.29	-0.39 ± 0.72	0.705 ± 0.006	4.4 (2.4)
208.62 ± 0.36	$+0.50 \pm 0.78$	0.647 ± 0.006	7.3 (3.6)	207.89 ± 0.22	$+0.50 \pm 0.64$	0.716 ± 0.007	6.3 (2.6)
237.99 ± 0.29	-1.11 ± 0.64	0.664 ± 0.005	11.7 (3.7)	238.04 ± 0.29	$+0.00 \pm 0.65$	0.726 ± 0.005	10.1 (2.4)
269.35 ± 0.36	-1.96 ± 0.71	0.667 ± 0.003	12.1 (3.4)	269.69 ± 0.29	-0.55 ± 0.72	0.710 ± 0.005	9.7 (2.5)
302.07 ± 0.22	$+1.34 \pm 0.57$	0.662 ± 0.006	11.8 (4.4)	302.39 ± 0.29	$+0.63 \pm 0.58$	0.711 ± 0.005	9.7 (2.9)
331.66 ± 0.36	$+0.26 \pm 0.71$	0.642 ± 0.006	11.4 (4.9)	331.38 ± 0.29	-1.06 ± 0.65	0.707 ± 0.006	8.5 (2.5)

Table 48: The nominal angle δ_n, average displacement $\Delta\delta$, average value of the parameter DIST, RMS of the ALPHA distribution for enabled GF and impact parameters between 60 m and 120 m. The RMS of the ALPHA distribution for disabled GF is given parentheses. The primary γ-ray energy was set to 170 GeV, the ZA to 20° and the azimuth angle to 90°.

$E_\gamma = 170\,\mathrm{GeV}$, Az = 90°, ZA = 20°, Hard Image Cleaning

δ_n[°]	$\Delta\delta$[°]	DIST[°]	RMS$_{\lvert \mathrm{ALPHA} \rvert}$[°]	δ_n[°]	$\Delta\delta$[°]	DIST[°]	RMS$_{\lvert \mathrm{ALPHA} \rvert}$[°]
IP = 60 m				**IP = 80 m**			
359.29 ± 0.44	$+3.50 \pm 0.86$	0.413 ± 0.004	14.0 (8.4)	359.71 ± 0.44	$+1.60 \pm 0.94$	0.529 ± 0.005	11.1 (5.7)
29.38 ± 0.58	-1.96 ± 0.87	0.420 ± 0.003	11.6 (8.6)	29.61 ± 0.44	-2.14 ± 1.01	0.536 ± 0.004	8.4 (4.9)
57.48 ± 0.36	-7.30 ± 1.44	0.439 ± 0.004	17.1 (13.2)	57.74 ± 0.15	-3.96 ± 0.58	0.556 ± 0.004	14.3 (6.6)
90.33 ± 0.73	-1.68 ± 1.08	0.447 ± 0.003	20.6 (11.9)	89.67 ± 0.36	-2.04 ± 0.65	0.569 ± 0.004	14.6 (5.8)
120.64 ± 0.29	$+1.07 \pm 0.86$	0.446 ± 0.003	22.1 (10.8)	121.35 ± 0.36	$+2.36 \pm 0.86$	0.563 ± 0.005	17.1 (9.3)
150.60 ± 0.44	$+6.27 \pm 1.29$	0.427 ± 0.004	18.6 (12.5)	152.51 ± 0.36	$+3.89 \pm 0.58$	0.550 ± 0.004	13.0 (6.1)
181.94 ± 0.58	$+4.30 \pm 1.23$	0.416 ± 0.004	10.7 (9.5)	181.08 ± 0.51	$+2.93 \pm 1.22$	0.535 ± 0.005	9.0 (5.3)
210.01 ± 0.51	-2.50 ± 1.23	0.424 ± 0.004	12.9 (7.5)	208.61 ± 0.44	-1.04 ± 1.01	0.544 ± 0.005	8.3 (6.1)
237.60 ± 0.44	-9.00 ± 1.37	0.441 ± 0.004	16.7 (11.0)	237.28 ± 0.29	-4.59 ± 0.94	0.564 ± 0.004	13.9 (7.6)
269.28 ± 0.51	-3.51 ± 1.08	0.450 ± 0.004	19.1 (11.9)	270.04 ± 0.36	-2.20 ± 0.79	0.572 ± 0.004	16.1 (5.2)
301.22 ± 0.51	$+2.87 \pm 1.01$	0.443 ± 0.004	21.9 (13.4)	300.57 ± 0.36	$+0.74 \pm 0.79$	0.562 ± 0.005	14.3 (6.9)
332.70 ± 0.51	$+8.88 \pm 1.30$	0.425 ± 0.004	19.7 (11.4)	331.14 ± 0.44	$+1.45 \pm 1.01$	0.547 ± 0.004	14.4 (8.7)
IP = 100 m				**IP = 120 m**			
359.88 ± 0.44	$+0.21 \pm 0.94$	0.627 ± 0.003	7.5 (3.4)	359.63 ± 0.22	-1.58 ± 0.58	0.694 ± 0.005	7.2 (2.4)
29.12 ± 0.29	$+0.05 \pm 0.86$	0.634 ± 0.005	8.1 (2.8)	28.51 ± 0.29	$+0.51 \pm 0.58$	0.698 ± 0.007	4.1 (3.0)
58.39 ± 0.22	-2.02 ± 0.65	0.654 ± 0.005	8.3 (5.2)	58.34 ± 0.29	$+1.61 \pm 0.66$	0.705 ± 0.005	9.1 (2.3)
89.72 ± 0.44	-0.54 ± 0.87	0.657 ± 0.006	10.5 (4.7)	89.85 ± 0.29	-0.22 ± 0.66	0.701 ± 0.004	7.4 (3.3)
121.72 ± 0.22	$+1.31 \pm 0.58$	0.657 ± 0.005	11.5 (3.6)	121.98 ± 0.29	$+0.30 \pm 0.66$	0.709 ± 0.005	7.9 (2.3)
151.34 ± 0.36	$+2.12 \pm 0.94$	0.641 ± 0.006	11.7 (5.7)	151.97 ± 0.29	-1.34 ± 0.58	0.713 ± 0.006	7.9 (2.7)
180.29 ± 0.15	$+0.49 \pm 0.64$	0.633 ± 0.004	6.3 (4.0)	179.93 ± 0.29	-0.82 ± 0.73	0.700 ± 0.005	5.6 (2.5)
208.12 ± 0.29	$+0.56 \pm 0.78$	0.645 ± 0.005	5.9 (3.8)	207.76 ± 0.29	$+0.51 \pm 0.65$	0.713 ± 0.006	4.4 (2.7)
237.93 ± 0.29	-1.46 ± 0.79	0.659 ± 0.007	8.7 (3.5)	238.04 ± 0.22	$+1.02 \pm 0.59$	0.720 ± 0.004	8.0 (2.4)
269.41 ± 0.29	-1.99 ± 0.51	0.662 ± 0.003	9.8 (4.0)	269.82 ± 0.29	$+0.01 \pm 0.65$	0.704 ± 0.005	7.5 (2.6)
301.99 ± 0.22	$+1.59 \pm 0.58$	0.656 ± 0.005	12.4 (3.9)	302.19 ± 0.22	$+0.55 \pm 0.58$	0.704 ± 0.005	8.5 (2.6)
331.65 ± 0.36	$+0.52 \pm 0.86$	0.641 ± 0.005	9.7 (4.8)	331.70 ± 0.29	-1.23 ± 0.66	0.704 ± 0.006	7.9 (2.7)

Table 49: The nominal angle δ_n, average displacement $\Delta\delta$, average value of the parameter DIST, RMS of the ALPHA distribution for enabled GF and impact parameters between 60 m and 120 m. The RMS of the ALPHA distribution for disabled GF is given parentheses. The primary γ-ray energy was set to 170 GeV, the ZA to 20° and the azimuth angle to 90°.

$E_\gamma = 170\,\mathrm{GeV}$, Az = 120°, ZA = 20°, Intermediate Image Cleaning

δ_n[°]	$\Delta\delta$[°]	DIST[°]	$\mathrm{RMS}_{\lvert\mathrm{ALPHA}\rvert}$[°]	δ_n[°]	$\Delta\delta$[°]	DIST[°]	$\mathrm{RMS}_{\lvert\mathrm{ALPHA}\rvert}$[°]
IP = 60 m				**IP = 80 m**			
359.25 ± 0.58	$+6.76 \pm 1.40$	0.427 ± 0.003	10.6 (9.0)	359.72 ± 0.51	$+3.94 \pm 0.99$	0.531 ± 0.004	8.1 (5.4)
28.59 ± 0.58	$+3.00 \pm 0.99$	0.434 ± 0.003	12.7 (9.0)	28.93 ± 0.43	$+1.52 \pm 0.98$	0.546 ± 0.005	10.1 (7.4)
58.91 ± 0.22	-1.92 ± 1.11	0.449 ± 0.005	17.2 (11.8)	57.92 ± 0.29	-2.27 ± 0.70	0.564 ± 0.005	14.1 (6.8)
89.34 ± 0.51	-10.57 ± 1.19	0.447 ± 0.004	18.4 (15.5)	90.26 ± 0.36	-4.87 ± 0.84	0.562 ± 0.006	16.1 (5.7)
120.26 ± 0.36	-3.50 ± 0.78	0.440 ± 0.005	16.8 (11.5)	121.02 ± 0.29	-2.56 ± 0.63	0.549 ± 0.006	17.6 (8.5)
149.60 ± 0.73	$+2.40 \pm 1.34$	0.425 ± 0.005	15.5 (14.5)	151.79 ± 0.36	$+3.69 \pm 0.84$	0.536 ± 0.005	12.6 (7.0)
181.33 ± 0.58	$+8.93 \pm 1.20$	0.426 ± 0.005	9.9 (12.8)	181.01 ± 0.43	$+4.54 \pm 0.85$	0.536 ± 0.006	8.7 (4.9)
209.47 ± 0.65	$+4.66 \pm 1.06$	0.430 ± 0.004	12.8 (10.2)	208.54 ± 0.44	$+2.20 \pm 1.05$	0.552 ± 0.006	10.7 (6.9)
237.53 ± 0.58	-6.05 ± 1.20	0.446 ± 0.004	17.2 (8.1)	237.46 ± 0.36	-0.69 ± 0.91	0.561 ± 0.005	13.8 (5.3)
269.49 ± 0.58	-6.42 ± 1.13	0.442 ± 0.003	18.3 (11.6)	269.51 ± 0.43	-4.05 ± 0.85	0.560 ± 0.005	16.0 (5.3)
301.88 ± 0.43	-4.25 ± 0.99	0.431 ± 0.004	19.6 (13.6)	300.67 ± 0.36	-4.26 ± 0.71	0.544 ± 0.005	16.1 (8.3)
332.88 ± 0.43	$+4.84 \pm 0.98$	0.421 ± 0.003	14.6 (12.0)	331.08 ± 0.51	$+0.34 \pm 0.99$	0.531 ± 0.004	13.5 (9.7)
IP = 100 m				**IP = 120 m**			
359.55 ± 0.29	$+1.39 \pm 0.84$	0.620 ± 0.008	7.6 (3.9)	359.53 ± 0.22	-0.67 ± 0.64	0.691 ± 0.006	6.4 (2.5)
29.26 ± 0.36	-0.72 ± 0.77	0.640 ± 0.005	8.8 (4.0)	28.67 ± 0.29	-2.16 ± 0.63	0.706 ± 0.006	9.1 (3.1)
58.40 ± 0.36	$+0.34 \pm 0.84$	0.648 ± 0.008	12.2 (5.1)	58.28 ± 0.22	$+0.68 \pm 0.63$	0.709 ± 0.005	8.5 (2.6)
89.81 ± 0.36	-0.91 ± 0.78	0.650 ± 0.006	12.8 (4.7)	89.71 ± 0.29	$+1.63 \pm 0.78$	0.703 ± 0.005	10.0 (3.7)
121.59 ± 0.36	-0.74 ± 0.64	0.639 ± 0.007	12.6 (5.5)	122.11 ± 0.22	$+0.15 \pm 0.50$	0.697 ± 0.007	9.9 (2.3)
151.46 ± 0.29	$+2.21 \pm 0.64$	0.630 ± 0.005	10.5 (5.7)	152.00 ± 0.29	$+0.83 \pm 0.57$	0.701 ± 0.005	9.7 (2.7)
180.34 ± 0.44	$+1.60 \pm 0.78$	0.633 ± 0.006	7.9 (3.6)	180.32 ± 0.29	-1.68 ± 0.64	0.708 ± 0.009	5.8 (2.4)
208.62 ± 0.36	-0.54 ± 0.91	0.648 ± 0.007	10.2 (3.6)	207.89 ± 0.22	-2.92 ± 0.49	0.724 ± 0.004	7.4 (2.6)
237.99 ± 0.29	-0.95 ± 0.77	0.651 ± 0.006	10.9 (3.7)	238.04 ± 0.29	$+0.67 \pm 0.57$	0.715 ± 0.002	9.6 (2.4)
269.35 ± 0.36	-2.17 ± 0.77	0.652 ± 0.006	11.8 (3.4)	269.69 ± 0.29	$+0.94 \pm 0.78$	0.700 ± 0.006	9.9 (2.5)
302.07 ± 0.22	-1.00 ± 0.56	0.633 ± 0.006	13.9 (4.4)	302.39 ± 0.29	-0.28 ± 0.58	0.688 ± 0.006	10.8 (2.9)
331.66 ± 0.36	$+1.03 \pm 0.71$	0.623 ± 0.007	11.4 (4.9)	331.38 ± 0.29	-0.19 ± 0.64	0.693 ± 0.006	9.4 (2.5)

Table 50: The nominal angle δ_n, average displacement $\Delta\delta$, average value of the parameter DIST, RMS of the ALPHA distribution for enabled GF and impact parameters between 60 m and 120 m. The RMS of the ALPHA distribution for disabled GF is given parentheses. The primary γ-ray energy was set to 170 GeV, the ZA to 20° and the azimuth angle to 120°.

$E_\gamma = 170\,\mathrm{GeV}$, Az = 120°, ZA = 20°, Hard Image Cleaning

δ_n[°]	$\Delta\delta$[°]	DIST[°]	$\mathrm{RMS}_{\lvert\mathrm{ALPHA}\rvert}$[°]	δ_n[°]	$\Delta\delta$[°]	DIST[°]	$\mathrm{RMS}_{\lvert\mathrm{ALPHA}\rvert}$[°]
IP = 60 m				**IP = 80 m**			
359.29 ± 0.44	$+7.21 \pm 1.00$	0.423 ± 0.004	10.8 (8.4)	359.71 ± 0.44	$+3.56 \pm 1.07$	0.531 ± 0.003	8.1 (5.7)
29.38 ± 0.58	$+1.90 \pm 1.01$	0.433 ± 0.002	10.7 (8.6)	29.61 ± 0.44	$+0.53 \pm 1.00$	0.548 ± 0.005	8.6 (4.9)
57.48 ± 0.36	-5.77 ± 0.93	0.445 ± 0.005	16.5 (13.2)	57.74 ± 0.15	-5.15 ± 0.79	0.568 ± 0.004	13.5 (6.6)
90.33 ± 0.73	-8.43 ± 1.23	0.444 ± 0.004	19.3 (11.9)	89.67 ± 0.36	-1.97 ± 0.87	0.560 ± 0.005	14.9 (5.8)
120.64 ± 0.29	-2.58 ± 0.65	0.433 ± 0.004	17.3 (10.8)	121.35 ± 0.36	-2.33 ± 0.79	0.550 ± 0.006	16.4 (9.3)
150.60 ± 0.44	$+4.56 \pm 1.02$	0.418 ± 0.004	15.5 (12.5)	152.51 ± 0.36	$+4.07 \pm 0.86$	0.531 ± 0.005	12.5 (6.1)
181.94 ± 0.58	$+9.10 \pm 1.15$	0.419 ± 0.005	10.0 (9.5)	181.08 ± 0.51	$+4.16 \pm 0.87$	0.540 ± 0.006	8.9 (5.3)
210.01 ± 0.51	$+4.02 \pm 1.01$	0.430 ± 0.005	13.2 (7.5)	208.61 ± 0.44	$+1.86 \pm 0.87$	0.547 ± 0.007	9.2 (6.1)
237.60 ± 0.44	-3.24 ± 1.09	0.440 ± 0.005	16.7 (11.0)	237.28 ± 0.29	$+0.44 \pm 0.79$	0.559 ± 0.005	12.4 (7.6)
269.28 ± 0.51	-6.42 ± 1.08	0.439 ± 0.003	17.2 (11.9)	270.04 ± 0.36	-3.36 ± 0.79	0.556 ± 0.005	15.2 (5.2)
301.22 ± 0.51	-3.88 ± 1.08	0.428 ± 0.004	18.2 (13.4)	300.57 ± 0.36	-3.68 ± 0.72	0.542 ± 0.006	15.1 (6.9)
332.70 ± 0.51	$+5.37 \pm 1.08$	0.418 ± 0.004	14.7 (11.4)	331.14 ± 0.44	$+1.50 \pm 0.86$	0.532 ± 0.003	12.7 (8.7)
IP = 100 m				**IP = 120 m**			
359.88 ± 0.44	$+1.44 \pm 1.01$	0.622 ± 0.007	7.0 (3.4)	359.63 ± 0.22	-2.55 ± 0.44	0.690 ± 0.006	6.5 (2.4)
29.12 ± 0.29	$+0.10 \pm 0.78$	0.637 ± 0.006	9.1 (2.8)	28.51 ± 0.29	-0.56 ± 0.71	0.708 ± 0.005	7.8 (3.0)
58.39 ± 0.22	$+0.86 \pm 0.64$	0.648 ± 0.007	11.1 (5.2)	58.34 ± 0.29	$+1.12 \pm 0.71$	0.707 ± 0.006	7.6 (2.3)
89.72 ± 0.44	-1.19 ± 0.86	0.646 ± 0.006	11.9 (4.7)	89.85 ± 0.29	$+0.67 \pm 0.72$	0.695 ± 0.005	8.7 (3.3)
121.72 ± 0.22	-0.69 ± 0.50	0.634 ± 0.006	13.3 (3.6)	121.98 ± 0.29	-0.11 ± 0.66	0.692 ± 0.006	9.0 (2.3)
151.34 ± 0.36	$+2.24 \pm 0.72$	0.630 ± 0.006	10.4 (5.7)	151.97 ± 0.29	$+0.17 \pm 0.59$	0.703 ± 0.005	7.6 (2.7)
180.29 ± 0.15	$+0.98 \pm 0.65$	0.637 ± 0.005	7.1 (4.0)	179.93 ± 0.29	-0.67 ± 0.59	0.716 ± 0.006	5.2 (2.5)
208.12 ± 0.29	-0.92 ± 0.92	0.656 ± 0.005	7.7 (3.8)	207.76 ± 0.29	-1.93 ± 0.72	0.724 ± 0.005	7.4 (2.7)
237.93 ± 0.29	-1.13 ± 0.71	0.653 ± 0.006	9.6 (3.5)	238.04 ± 0.22	$+1.71 \pm 0.64$	0.714 ± 0.005	7.6 (2.4)
269.41 ± 0.29	-1.62 ± 0.72	0.648 ± 0.005	11.8 (4.0)	269.82 ± 0.29	-0.39 ± 0.80	0.691 ± 0.005	10.0 (2.6)
301.99 ± 0.22	-1.19 ± 0.51	0.631 ± 0.004	12.8 (3.9)	302.19 ± 0.22	$+0.52 \pm 0.52$	0.680 ± 0.006	9.7 (2.6)
331.65 ± 0.36	$+0.81 \pm 0.72$	0.621 ± 0.007	11.1 (4.8)	331.70 ± 0.29	-0.64 ± 0.58	0.693 ± 0.006	8.3 (2.7)

Table 51: The nominal angle δ_n, average displacement $\Delta\delta$, average value of the parameter DIST, RMS of the ALPHA distribution for enabled GF and impact parameters between 60 m and 120 m. The RMS of the ALPHA distribution for disabled GF is given parentheses. The primary γ-ray energy was set to 170 GeV, the ZA to 20° and the azimuth angle to 120°.

$E_\gamma = 170\,\mathrm{GeV}$, Az = 150°, ZA = 20°, Intermediate Image Cleaning

$\delta_n\,[°]$	$\Delta\delta\,[°]$	DIST[°]	$\mathrm{RMS}_{\lvert\mathrm{ALPHA}\rvert}\,[°]$	$\delta_n\,[°]$	$\Delta\delta\,[°]$	DIST[°]	$\mathrm{RMS}_{\lvert\mathrm{ALPHA}\rvert}\,[°]$
IP = 60 m				IP = 80 m			
359.25 ± 0.58	$+3.77 \pm 1.27$	0.445 ± 0.006	10.1 (9.0)	359.72 ± 0.51	$+2.01 \pm 0.85$	0.558 ± 0.007	8.4 (5.4)
28.59 ± 0.58	$+5.90 \pm 1.06$	0.457 ± 0.005	11.4 (9.0)	28.93 ± 0.43	$+2.68 \pm 0.92$	0.570 ± 0.005	11.9 (7.4)
58.91 ± 0.22	$+0.16 \pm 0.70$	0.456 ± 0.004	17.7 (11.8)	57.92 ± 0.29	-1.62 ± 0.91	0.571 ± 0.006	14.0 (6.8)
89.34 ± 0.51	-7.43 ± 1.20	0.453 ± 0.002	22.5 (15.5)	90.26 ± 0.36	-3.26 ± 0.91	0.567 ± 0.003	17.7 (5.7)
120.26 ± 0.36	-8.45 ± 0.91	0.437 ± 0.005	21.1 (11.5)	121.02 ± 0.29	-4.06 ± 0.84	0.558 ± 0.005	15.6 (8.5)
149.60 ± 0.73	-1.27 ± 1.00	0.432 ± 0.005	16.6 (14.5)	151.79 ± 0.36	$+0.78 \pm 0.64$	0.555 ± 0.005	13.4 (7.0)
181.33 ± 0.58	$+6.90 \pm 1.20$	0.445 ± 0.003	10.8 (12.8)	181.01 ± 0.43	$+3.51 \pm 0.92$	0.565 ± 0.006	8.3 (4.9)
209.47 ± 0.65	$+9.74 \pm 1.55$	0.450 ± 0.004	12.3 (10.2)	208.54 ± 0.44	$+4.95 \pm 0.92$	0.569 ± 0.004	11.2 (6.9)
237.53 ± 0.58	$+3.70 \pm 1.34$	0.448 ± 0.005	17.9 (8.1)	237.46 ± 0.36	$+0.71 \pm 1.12$	0.565 ± 0.006	15.1 (5.3)
269.49 ± 0.58	-7.46 ± 1.47	0.443 ± 0.004	22.6 (11.6)	269.51 ± 0.43	-1.26 ± 1.12	0.560 ± 0.006	17.5 (5.3)
301.88 ± 0.43	-6.40 ± 1.40	0.435 ± 0.004	20.6 (13.6)	300.67 ± 0.36	-4.57 ± 0.98	0.551 ± 0.006	16.6 (8.3)
332.88 ± 0.43	$+2.00 \pm 0.85$	0.439 ± 0.004	15.4 (12.0)	331.08 ± 0.51	-1.64 ± 0.78	0.550 ± 0.005	12.3 (9.7)
IP = 100 m				IP = 120 m			
359.55 ± 0.29	$+1.03 \pm 0.64$	0.651 ± 0.006	6.6 (3.9)	359.53 ± 0.22	-0.89 ± 0.50	0.727 ± 0.005	5.7 (2.5)
29.26 ± 0.36	-0.45 ± 0.64	0.669 ± 0.005	8.7 (4.0)	28.67 ± 0.29	-0.51 ± 0.57	0.728 ± 0.004	7.2 (3.1)
58.40 ± 0.36	$+0.45 \pm 0.84$	0.660 ± 0.003	11.6 (5.1)	58.28 ± 0.22	-0.39 ± 0.63	0.724 ± 0.006	9.5 (2.6)
89.81 ± 0.36	-1.35 ± 0.91	0.654 ± 0.005	14.4 (4.7)	89.71 ± 0.29	-0.98 ± 0.64	0.705 ± 0.004	9.9 (3.7)
121.59 ± 0.36	-2.33 ± 0.71	0.654 ± 0.005	13.9 (5.5)	122.11 ± 0.22	$+0.28 \pm 0.50$	0.707 ± 0.006	10.1 (2.3)
151.46 ± 0.29	$+0.47 \pm 0.57$	0.656 ± 0.006	10.8 (5.7)	152.00 ± 0.29	$+0.39 \pm 0.57$	0.717 ± 0.006	8.5 (2.7)
180.34 ± 0.44	$+1.11 \pm 0.86$	0.662 ± 0.004	6.4 (3.6)	180.32 ± 0.29	$+0.99 \pm 0.65$	0.726 ± 0.005	6.0 (2.4)
208.62 ± 0.36	$+2.67 \pm 0.78$	0.665 ± 0.006	8.5 (3.6)	207.89 ± 0.22	$+0.35 \pm 0.71$	0.723 ± 0.005	7.9 (2.6)
237.99 ± 0.29	$+0.07 \pm 0.77$	0.663 ± 0.006	12.7 (3.7)	238.04 ± 0.29	$+0.86 \pm 0.64$	0.716 ± 0.006	9.9 (2.4)
269.35 ± 0.36	-0.45 ± 0.64	0.645 ± 0.006	13.9 (3.4)	269.69 ± 0.29	$+0.50 \pm 0.70$	0.696 ± 0.006	9.7 (2.5)
302.07 ± 0.22	-1.43 ± 0.50	0.641 ± 0.006	12.6 (4.4)	302.39 ± 0.29	$+1.01 \pm 0.57$	0.697 ± 0.006	10.6 (2.9)
331.66 ± 0.36	$+0.04 \pm 0.71$	0.638 ± 0.005	10.1 (4.9)	331.38 ± 0.29	-0.99 ± 0.57	0.702 ± 0.007	8.1 (2.5)

Table 52: The nominal angle δ_n, average displacement $\Delta\delta$, average value of the parameter DIST, RMS of the ALPHA distribution for enabled GF and impact parameters between 60 m and 120 m. The RMS of the ALPHA distribution for disabled GF is given parentheses. The primary γ-ray energy was set to 170 GeV, the ZA to 20° and the azimuth angle to 150°.

$E_\gamma = 170\,\mathrm{GeV}$, Az = 150°, ZA = 20°, Hard Image Cleaning

$\delta_n\,[°]$	$\Delta\delta\,[°]$	DIST[°]	$\mathrm{RMS}_{\lvert\mathrm{ALPHA}\rvert}\,[°]$	$\delta_n\,[°]$	$\Delta\delta\,[°]$	DIST[°]	$\mathrm{RMS}_{\lvert\mathrm{ALPHA}\rvert}\,[°]$
IP = 60 m				IP = 80 m			
359.29 ± 0.44	$+3.42 \pm 1.00$	0.441 ± 0.003	10.2 (8.4)	359.71 ± 0.44	$+1.52 \pm 0.86$	0.559 ± 0.006	8.2 (5.7)
29.38 ± 0.58	$+6.58 \pm 1.43$	0.456 ± 0.005	11.2 (8.6)	29.61 ± 0.44	$+4.16 \pm 1.08$	0.566 ± 0.007	10.0 (4.9)
57.48 ± 0.36	-1.19 ± 0.94	0.455 ± 0.004	17.3 (13.2)	57.74 ± 0.15	-1.60 ± 0.79	0.570 ± 0.006	14.3 (6.6)
90.33 ± 0.73	-6.57 ± 1.15	0.447 ± 0.003	21.5 (11.9)	89.67 ± 0.36	-6.08 ± 0.93	0.567 ± 0.002	16.4 (5.8)
120.64 ± 0.29	-7.57 ± 0.94	0.432 ± 0.004	20.2 (10.8)	121.35 ± 0.36	-4.17 ± 0.79	0.554 ± 0.004	16.3 (9.3)
150.60 ± 0.44	-0.19 ± 0.86	0.433 ± 0.004	15.8 (12.5)	152.51 ± 0.36	$+0.94 \pm 0.72$	0.561 ± 0.005	11.9 (6.1)
181.94 ± 0.58	$+7.40 \pm 1.01$	0.442 ± 0.004	9.7 (9.5)	181.08 ± 0.51	$+4.88 \pm 1.01$	0.564 ± 0.005	8.4 (5.3)
210.01 ± 0.51	$+8.79 \pm 1.30$	0.445 ± 0.005	12.7 (7.5)	208.61 ± 0.44	$+5.45 \pm 1.01$	0.570 ± 0.001	10.4 (6.1)
237.60 ± 0.44	$+2.99 \pm 1.22$	0.443 ± 0.004	17.2 (11.0)	237.28 ± 0.29	$+1.89 \pm 1.00$	0.565 ± 0.006	14.3 (7.6)
269.28 ± 0.51	-5.51 ± 0.94	0.437 ± 0.004	20.7 (11.9)	270.04 ± 0.36	-1.09 ± 1.22	0.561 ± 0.006	17.1 (5.2)
301.22 ± 0.51	-7.49 ± 1.38	0.430 ± 0.004	20.2 (13.4)	300.57 ± 0.36	-5.61 ± 0.87	0.546 ± 0.003	16.1 (6.9)
332.70 ± 0.51	$+0.48 \pm 1.01$	0.441 ± 0.004	14.9 (11.4)	331.14 ± 0.44	-1.80 ± 0.79	0.546 ± 0.005	11.6 (8.7)
IP = 100 m				IP = 120 m			
359.88 ± 0.44	$+0.77 \pm 0.80$	0.652 ± 0.006	6.7 (3.4)	359.63 ± 0.22	-0.95 ± 0.59	0.723 ± 0.005	5.4 (2.4)
29.12 ± 0.29	$+0.80 \pm 0.65$	0.667 ± 0.006	8.4 (2.8)	28.51 ± 0.29	-1.17 ± 0.58	0.727 ± 0.004	6.4 (3.0)
58.39 ± 0.22	$+0.18 \pm 0.64$	0.665 ± 0.005	10.4 (5.2)	58.34 ± 0.29	-0.22 ± 0.71	0.720 ± 0.005	8.1 (2.3)
89.72 ± 0.44	-2.55 ± 1.07	0.648 ± 0.004	13.9 (4.7)	89.85 ± 0.29	-0.61 ± 0.72	0.697 ± 0.004	10.0 (3.3)
121.72 ± 0.22	-0.87 ± 0.58	0.651 ± 0.006	13.5 (3.6)	121.98 ± 0.29	$+0.89 \pm 0.59$	0.696 ± 0.004	10.2 (2.3)
151.34 ± 0.36	$+0.40 \pm 0.72$	0.659 ± 0.003	9.2 (5.7)	151.97 ± 0.29	$+0.24 \pm 0.59$	0.715 ± 0.009	8.4 (2.7)
180.29 ± 0.15	$+1.70 \pm 0.59$	0.659 ± 0.006	7.1 (4.0)	179.93 ± 0.29	$+0.23 \pm 0.67$	0.723 ± 0.007	6.1 (2.5)
208.12 ± 0.29	$+1.89 \pm 0.80$	0.664 ± 0.008	7.4 (3.8)	207.76 ± 0.29	$+0.39 \pm 0.73$	0.727 ± 0.007	7.5 (2.7)
237.93 ± 0.29	$+0.47 \pm 0.64$	0.663 ± 0.006	11.2 (3.5)	238.04 ± 0.22	$+0.18 \pm 0.64$	0.713 ± 0.007	9.6 (2.4)
269.41 ± 0.29	-1.25 ± 0.79	0.641 ± 0.007	12.9 (4.0)	269.82 ± 0.29	$+0.39 \pm 0.71$	0.689 ± 0.006	9.6 (2.6)
301.99 ± 0.22	-2.11 ± 0.58	0.636 ± 0.007	12.6 (3.9)	302.19 ± 0.22	$+0.46 \pm 0.51$	0.693 ± 0.007	10.0 (2.6)
331.65 ± 0.36	$+0.60 \pm 0.65$	0.639 ± 0.006	9.4 (4.8)	331.70 ± 0.29	-0.50 ± 0.58	0.699 ± 0.007	8.1 (2.7)

Table 53: The nominal angle δ_n, average displacement $\Delta\delta$, average value of the parameter DIST, RMS of the ALPHA distribution for enabled GF and impact parameters between 60 m and 120 m. The RMS of the ALPHA distribution for disabled GF is given parentheses. The primary γ-ray energy was set to 170 GeV, the ZA to 20° and the azimuth angle to 150°.

$E_\gamma = 170\,\mathrm{GeV}$, Az = 180°, ZA = 20°, Intermediate Image Cleaning

$\delta_n\,[^\circ]$	$\Delta\delta\,[^\circ]$	DIST[°]	$\mathrm{RMS}_{\vert\mathrm{ALPHA}\vert}\,[^\circ]$	$\delta_n\,[^\circ]$	$\Delta\delta\,[^\circ]$	DIST[°]	$\mathrm{RMS}_{\vert\mathrm{ALPHA}\vert}\,[^\circ]$
IP = 60 m				**IP = 80 m**			
359.25 ± 0.58	-2.41 ± 0.86	0.452 ± 0.005	8.5 (9.0)	359.72 ± 0.51	-0.09 ± 0.86	0.563 ± 0.004	5.2 (5.4)
28.59 ± 0.58	$+2.58 \pm 1.20$	0.444 ± 0.003	18.8 (9.0)	28.93 ± 0.43	$+0.79 \pm 0.85$	0.566 ± 0.005	19.8 (7.4)
58.91 ± 0.22	$+4.69 \pm 0.56$	0.441 ± 0.005	23.3 (11.8)	57.92 ± 0.29	$+3.17 \pm 0.91$	0.563 ± 0.006	20.5 (6.8)
89.34 ± 0.51	-0.29 ± 1.19	0.437 ± 0.005	21.4 (15.5)	90.26 ± 0.36	$+1.35 \pm 1.12$	0.555 ± 0.005	19.6 (5.7)
120.26 ± 0.36	-5.90 ± 1.26	0.439 ± 0.005	22.3 (11.5)	121.02 ± 0.29	-3.13 ± 1.18	0.555 ± 0.006	14.7 (8.5)
149.60 ± 0.73	-8.15 ± 1.35	0.441 ± 0.006	15.6 (14.5)	151.79 ± 0.36	-3.87 ± 0.78	0.556 ± 0.005	12.7 (7.0)
181.33 ± 0.58	$+0.84 \pm 1.00$	0.446 ± 0.005	8.3 (12.8)	181.01 ± 0.43	-0.02 ± 0.78	0.565 ± 0.006	5.0 (4.9)
209.47 ± 0.65	$+5.84 \pm 1.27$	0.437 ± 0.004	21.3 (10.2)	208.54 ± 0.44	$+2.29 \pm 0.85$	0.554 ± 0.006	14.2 (6.9)
237.53 ± 0.58	$+4.94 \pm 1.54$	0.437 ± 0.004	24.6 (8.1)	237.46 ± 0.36	$+2.17 \pm 1.12$	0.549 ± 0.006	16.8 (5.3)
269.49 ± 0.58	$+3.36 \pm 1.41$	0.435 ± 0.004	22.7 (11.6)	269.51 ± 0.43	$+2.42 \pm 1.12$	0.551 ± 0.005	18.7 (5.3)
301.88 ± 0.43	-0.38 ± 0.98	0.438 ± 0.005	20.3 (13.6)	300.67 ± 0.36	-1.67 ± 0.98	0.557 ± 0.003	14.8 (8.3)
332.88 ± 0.43	$+0.92 \pm 0.98$	0.443 ± 0.005	16.0 (12.0)	331.08 ± 0.51	-0.62 ± 1.06	0.557 ± 0.005	16.1 (9.7)
IP = 100 m				**IP = 120 m**			
359.55 ± 0.29	-0.14 ± 0.57	0.658 ± 0.005	4.2 (3.9)	359.53 ± 0.22	-1.16 ± 0.51	0.727 ± 0.005	3.7 (2.5)
29.26 ± 0.36	$+0.32 \pm 0.71$	0.656 ± 0.006	10.4 (4.0)	28.67 ± 0.29	-0.19 ± 0.57	0.730 ± 0.006	8.4 (3.1)
58.40 ± 0.36	$+0.64 \pm 0.71$	0.656 ± 0.006	16.8 (5.1)	58.28 ± 0.22	-2.22 ± 0.71	0.714 ± 0.006	13.8 (2.6)
89.81 ± 0.36	$+0.48 \pm 0.77$	0.654 ± 0.005	14.2 (4.7)	89.71 ± 0.29	-0.12 ± 0.71	0.707 ± 0.006	12.0 (3.7)
121.59 ± 0.36	$+0.29 \pm 0.64$	0.653 ± 0.007	12.4 (5.5)	122.11 ± 0.22	$+0.88 \pm 0.57$	0.713 ± 0.006	8.5 (2.3)
151.46 ± 0.29	-1.49 ± 0.64	0.654 ± 0.003	13.2 (5.7)	152.00 ± 0.29	$+1.03 \pm 0.57$	0.726 ± 0.007	7.7 (2.7)
180.34 ± 0.44	$+0.78 \pm 0.79$	0.651 ± 0.007	4.9 (3.6)	180.32 ± 0.29	$+0.29 \pm 0.58$	0.722 ± 0.007	5.3 (2.4)
208.62 ± 0.36	$+1.18 \pm 0.64$	0.650 ± 0.006	12.2 (3.6)	207.89 ± 0.22	-0.21 ± 0.57	0.721 ± 0.008	9.2 (2.6)
237.99 ± 0.29	-0.48 ± 0.70	0.642 ± 0.007	10.5 (3.7)	238.04 ± 0.29	-1.42 ± 0.71	0.704 ± 0.004	8.6 (2.4)
269.35 ± 0.36	-0.12 ± 0.71	0.645 ± 0.005	14.2 (3.4)	269.69 ± 0.29	-0.23 ± 0.71	0.695 ± 0.008	9.0 (2.5)
302.07 ± 0.22	-0.03 ± 0.70	0.648 ± 0.004	13.4 (4.4)	302.39 ± 0.29	$+2.49 \pm 0.78$	0.705 ± 0.006	12.1 (2.9)
331.66 ± 0.36	-1.36 ± 0.78	0.657 ± 0.008	11.6 (4.9)	331.38 ± 0.29	$+1.52 \pm 0.71$	0.722 ± 0.005	9.6 (2.5)

Table 54: The nominal angle δ_n, average displacement $\Delta\delta$, average value of the parameter DIST, RMS of the ALPHA distribution for enabled GF and impact parameters between 60 m and 120 m. The RMS of the ALPHA distribution for disabled GF is given parentheses. The primary γ-ray energy was set to 170 GeV, the ZA to 20° and the azimuth angle to 180°.

$E_\gamma = 170\,\mathrm{GeV}$, Az = 180°, ZA = 20°, Hard Image Cleaning

$\delta_n\,[^\circ]$	$\Delta\delta\,[^\circ]$	DIST[°]	$\mathrm{RMS}_{\vert\mathrm{ALPHA}\vert}\,[^\circ]$	$\delta_n\,[^\circ]$	$\Delta\delta\,[^\circ]$	DIST[°]	$\mathrm{RMS}_{\vert\mathrm{ALPHA}\vert}\,[^\circ]$
IP = 60 m				**IP = 80 m**			
359.29 ± 0.44	$+0.41 \pm 0.87$	0.453 ± 0.005	8.6 (8.4)	359.71 ± 0.44	-0.27 ± 0.66	0.568 ± 0.004	6.6 (5.7)
29.38 ± 0.58	$+4.98 \pm 1.01$	0.442 ± 0.004	15.1 (8.6)	29.61 ± 0.44	$+1.95 \pm 0.87$	0.568 ± 0.003	13.8 (4.9)
57.48 ± 0.36	$+3.75 \pm 0.94$	0.441 ± 0.005	22.4 (13.2)	57.74 ± 0.15	$+3.52 \pm 0.79$	0.561 ± 0.004	17.7 (6.6)
90.33 ± 0.73	-0.39 ± 0.94	0.438 ± 0.004	24.0 (11.9)	89.67 ± 0.36	$+2.29 \pm 1.09$	0.555 ± 0.004	19.7 (5.8)
120.64 ± 0.29	-8.55 ± 1.16	0.436 ± 0.005	19.8 (10.8)	121.35 ± 0.36	-2.40 ± 1.09	0.555 ± 0.007	13.9 (9.3)
150.60 ± 0.44	-8.72 ± 1.15	0.443 ± 0.005	14.4 (12.5)	152.51 ± 0.36	-2.64 ± 0.87	0.555 ± 0.006	11.4 (6.1)
181.94 ± 0.58	$+1.78 \pm 0.87$	0.450 ± 0.004	7.9 (9.5)	181.08 ± 0.51	$+0.73 \pm 0.72$	0.569 ± 0.007	5.9 (5.3)
210.01 ± 0.51	$+6.48 \pm 1.08$	0.437 ± 0.005	16.3 (7.5)	208.61 ± 0.44	$+3.68 \pm 0.87$	0.555 ± 0.005	12.5 (6.1)
237.60 ± 0.44	$+4.70 \pm 1.23$	0.432 ± 0.004	22.1 (11.0)	237.28 ± 0.29	$+2.15 \pm 0.94$	0.550 ± 0.007	12.0 (7.6)
269.28 ± 0.51	-0.24 ± 1.16	0.432 ± 0.004	23.4 (11.9)	270.04 ± 0.36	$+2.75 \pm 0.72$	0.549 ± 0.005	14.9 (5.2)
301.22 ± 0.51	-1.95 ± 0.94	0.436 ± 0.005	20.5 (13.4)	300.57 ± 0.36	-2.30 ± 0.65	0.559 ± 0.004	14.4 (6.9)
332.70 ± 0.51	$+0.01 \pm 0.87$	0.438 ± 0.003	16.0 (11.4)	331.14 ± 0.44	-0.99 ± 1.01	0.558 ± 0.005	14.3 (8.7)
IP = 100 m				**IP = 120 m**			
359.88 ± 0.44	$+0.26 \pm 0.81$	0.661 ± 0.007	3.9 (3.4)	359.63 ± 0.22	-0.53 ± 0.52	0.729 ± 0.006	3.6 (2.4)
29.12 ± 0.29	$+0.30 \pm 0.51$	0.660 ± 0.008	10.5 (2.8)	28.51 ± 0.29	-0.44 ± 0.58	0.730 ± 0.002	6.9 (3.0)
58.39 ± 0.22	$+0.02 \pm 0.72$	0.660 ± 0.006	10.6 (5.2)	58.34 ± 0.29	-3.45 ± 0.65	0.712 ± 0.006	11.0 (2.3)
89.72 ± 0.44	-0.06 ± 1.07	0.648 ± 0.006	11.9 (4.7)	89.85 ± 0.29	-1.08 ± 0.64	0.699 ± 0.008	11.2 (3.3)
121.72 ± 0.22	-0.36 ± 0.65	0.654 ± 0.007	11.1 (3.6)	121.98 ± 0.29	$+0.46 \pm 0.58$	0.709 ± 0.006	6.5 (2.3)
151.34 ± 0.36	-0.67 ± 0.73	0.654 ± 0.006	10.9 (5.7)	151.97 ± 0.29	$+0.69 \pm 0.59$	0.726 ± 0.006	4.0 (2.7)
180.29 ± 0.15	$+0.63 \pm 0.59$	0.660 ± 0.007	5.1 (4.0)	179.93 ± 0.29	-0.03 ± 0.60	0.728 ± 0.007	3.9 (2.5)
208.12 ± 0.29	$+1.15 \pm 0.65$	0.653 ± 0.004	12.1 (3.8)	207.76 ± 0.29	-0.19 ± 0.59	0.726 ± 0.007	7.7 (2.7)
237.93 ± 0.29	$+1.08 \pm 0.65$	0.640 ± 0.007	12.1 (3.5)	238.04 ± 0.22	-1.81 ± 0.65	0.696 ± 0.004	11.7 (2.4)
269.41 ± 0.29	-0.32 ± 0.85	0.639 ± 0.006	13.6 (4.0)	269.82 ± 0.29	$+0.25 \pm 0.79$	0.690 ± 0.007	9.7 (2.6)
301.99 ± 0.22	-0.39 ± 0.58	0.648 ± 0.007	11.3 (3.9)	302.19 ± 0.22	$+2.57 \pm 0.65$	0.701 ± 0.006	9.2 (2.6)
331.65 ± 0.36	-1.72 ± 0.72	0.661 ± 0.005	6.1 (4.8)	331.70 ± 0.29	$+1.54 \pm 0.66$	0.729 ± 0.007	4.3 (2.7)

Table 55: The nominal angle δ_n, average displacement $\Delta\delta$, average value of the parameter DIST, RMS of the ALPHA distribution for enabled GF and impact parameters between 60 m and 120 m. The RMS of the ALPHA distribution for disabled GF is given parentheses. The primary γ-ray energy was set to 170 GeV, the ZA to 20° and the azimuth angle to 180°.

$E_\gamma = 170\,\mathrm{GeV}$, Az $= 0°$, ZA $= 40°$, Intermediate Image Cleaning

δ_n[°]	$\Delta\delta$[°]	DIST[°]	RMS$_{\vert\mathrm{ALPHA}\vert}$[°]	δ_n[°]	$\Delta\delta$[°]	DIST[°]	RMS$_{\vert\mathrm{ALPHA}\vert}$[°]
IP = 60 m				IP = 80 m			
359.63 ± 0.55	-1.29 ± 0.98	0.310 ± 0.002	16.1 (19.2)	1.16 ± 0.60	$+2.24 \pm 0.90$	0.403 ± 0.003	13.3 (13.1)
23.58 ± 0.73	$+4.83 \pm 1.65$	0.290 ± 0.002	18.3 (19.4)	22.12 ± 0.48	$+1.08 \pm 0.84$	0.378 ± 0.003	13.6 (14.9)
54.50 ± 0.30	$+4.58 \pm 0.91$	0.250 ± 0.002	22.0 (19.2)	52.07 ± 0.73	$+2.41 \pm 1.22$	0.332 ± 0.002	18.0 (18.3)
89.51 ± 0.90	-4.73 ± 1.87	0.230 ± 0.003	21.5 (20.1)	91.38 ± 0.72	-3.10 ± 1.34	0.306 ± 0.002	18.7 (20.0)
129.10 ± 0.72	-0.92 ± 1.16	0.251 ± 0.003	20.7 (17.0)	125.90 ± 0.55	-2.77 ± 1.28	0.333 ± 0.002	18.5 (15.9)
155.32 ± 0.79	-1.75 ± 1.24	0.288 ± 0.003	20.2 (16.9)	156.33 ± 0.42	-0.63 ± 1.03	0.378 ± 0.004	14.6 (14.2)
177.25 ± 0.72	$+0.35 \pm 1.28$	0.308 ± 0.003	18.5 (18.0)	179.45 ± 0.36	$+1.55 \pm 0.79$	0.400 ± 0.003	14.2 (12.9)
205.76 ± 0.91	$+3.86 \pm 1.66$	0.290 ± 0.002	18.3 (21.2)	204.46 ± 0.48	$+2.84 \pm 1.09$	0.382 ± 0.002	15.3 (13.4)
233.10 ± 0.73	$+3.82 \pm 1.47$	0.263 ± 0.002	23.1 (20.7)	233.47 ± 0.55	$+2.17 \pm 1.04$	0.344 ± 0.002	18.2 (16.4)
269.47 ± 0.48	$+0.75 \pm 1.28$	0.244 ± 0.002	23.0 (20.8)	271.60 ± 0.73	$+0.31 \pm 1.77$	0.322 ± 0.002	21.4 (15.1)
308.01 ± 0.60	-3.32 ± 1.28	0.263 ± 0.002	21.7 (20.0)	307.93 ± 0.42	-3.35 ± 1.09	0.344 ± 0.003	17.0 (16.9)
334.69 ± 0.61	-2.82 ± 1.33	0.294 ± 0.002	19.6 (21.0)	335.42 ± 0.36	-1.92 ± 0.73	0.385 ± 0.003	15.5 (14.2)
IP = 100 m				IP = 120 m			
359.98 ± 0.36	$+1.47 \pm 0.78$	0.485 ± 0.004	10.1 (10.6)	359.77 ± 0.30	$+0.42 \pm 0.60$	0.564 ± 0.005	5.8 (4.7)
23.79 ± 0.36	$+0.78 \pm 0.72$	0.460 ± 0.003	9.0 (12.2)	23.45 ± 0.35	$+0.77 \pm 0.59$	0.535 ± 0.004	9.4 (6.7)
52.66 ± 0.48	$+1.65 \pm 1.03$	0.410 ± 0.003	14.7 (12.8)	51.96 ± 0.30	-0.08 ± 0.72	0.479 ± 0.004	9.3 (8.9)
88.49 ± 0.60	-2.78 ± 1.08	0.376 ± 0.003	18.5 (17.2)	90.81 ± 0.42	-0.19 ± 0.99	0.447 ± 0.003	13.8 (10.0)
126.22 ± 0.36	-4.18 ± 0.96	0.408 ± 0.003	13.4 (12.1)	127.96 ± 0.35	$+0.47 \pm 0.78$	0.479 ± 0.003	13.2 (8.6)
156.51 ± 0.36	-1.66 ± 0.66	0.459 ± 0.004	10.9 (11.3)	156.43 ± 0.18	$+0.15 \pm 0.48$	0.535 ± 0.005	7.1 (6.0)
180.32 ± 0.30	$+1.16 \pm 0.66$	0.486 ± 0.005	9.0 (7.8)	180.52 ± 0.36	$+0.45 \pm 0.60$	0.560 ± 0.005	6.9 (5.0)
202.73 ± 0.53	$+0.13 \pm 0.96$	0.464 ± 0.004	11.2 (11.5)	202.61 ± 0.35	$+0.53 \pm 0.73$	0.545 ± 0.005	8.6 (7.6)
232.48 ± 0.42	$+1.03 \pm 0.96$	0.419 ± 0.003	14.5 (13.5)	233.49 ± 0.41	$+1.26 \pm 0.78$	0.494 ± 0.004	11.5 (9.4)
271.97 ± 0.42	$+2.23 \pm 1.03$	0.392 ± 0.003	16.4 (14.3)	270.82 ± 0.42	$+0.48 \pm 0.96$	0.459 ± 0.004	12.8 (9.6)
308.21 ± 0.24	-1.03 ± 0.84	0.422 ± 0.003	14.2 (10.6)	306.90 ± 0.36	-1.93 ± 0.78	0.493 ± 0.004	9.3 (10.8)
337.76 ± 0.30	-0.27 ± 0.72	0.469 ± 0.004	9.2 (10.2)	336.52 ± 0.24	$+0.24 \pm 0.54$	0.547 ± 0.004	9.4 (7.7)

Table 56: The nominal angle δ_n, average displacement $\Delta\delta$, average value of the parameter DIST, RMS of the ALPHA distribution for enabled GF and impact parameters between 60 m and 120 m. The RMS of the ALPHA distribution for disabled GF is given parentheses. The primary γ-ray energy was set to 170 GeV, the ZA to 40° and the azimuth angle to 0°.

$E_\gamma = 170\,\mathrm{GeV}$, Az $= 0°$, ZA $= 40°$, Hard Image Cleaning

δ_n[°]	$\Delta\delta$[°]	DIST[°]	RMS$_{\vert\mathrm{ALPHA}\vert}$[°]	δ_n[°]	$\Delta\delta$[°]	DIST[°]	RMS$_{\vert\mathrm{ALPHA}\vert}$[°]
IP = 60 m				IP = 80 m			
1.73 ± 0.76	$+1.02 \pm 1.53$	0.329 ± 0.002	16.4 (17.9)	0.92 ± 0.61	$+1.89 \pm 1.14$	0.425 ± 0.004	13.4 (14.1)
22.43 ± 0.70	-0.38 ± 0.93	0.305 ± 0.002	15.8 (19.2)	23.43 ± 0.61	$+1.50 \pm 1.00$	0.396 ± 0.004	13.1 (13.5)
54.48 ± 0.85	$+2.87 \pm 1.70$	0.268 ± 0.003	19.5 (20.3)	53.20 ± 0.55	$+2.52 \pm 1.16$	0.347 ± 0.003	17.7 (16.7)
88.81 ± 0.71	-4.13 ± 1.59	0.247 ± 0.003	20.1 (21.1)	92.10 ± 0.77	-1.76 ± 1.68	0.321 ± 0.003	18.8 (16.0)
127.37 ± 0.15	$+0.36 \pm 0.62$	0.267 ± 0.003	20.3 (17.3)	125.58 ± 0.62	-1.57 ± 1.42	0.357 ± 0.003	16.2 (13.7)
151.50 ± 0.24	-6.55 ± 0.98	0.310 ± 0.003	18.2 (19.8)	157.83 ± 0.69	-0.05 ± 1.31	0.397 ± 0.004	10.6 (12.5)
179.60 ± 0.76	$+3.29 \pm 1.53$	0.325 ± 0.003	17.3 (17.5)	179.08 ± 0.69	$+0.09 \pm 1.15$	0.426 ± 0.004	11.1 (14.1)
207.69 ± 0.62	$+2.46 \pm 1.75$	0.312 ± 0.003	17.3 (19.8)	204.98 ± 0.37	$+1.38 \pm 0.75$	0.403 ± 0.004	11.9 (14.8)
235.25 ± 0.47	$+1.89 \pm 1.34$	0.278 ± 0.003	22.3 (19.7)	233.34 ± 0.68	$+3.64 \pm 1.44$	0.362 ± 0.003	15.9 (16.5)
269.83 ± 0.60	-0.98 ± 1.69	0.258 ± 0.003	20.3 (19.5)	271.67 ± 0.54	$+1.72 \pm 1.29$	0.341 ± 0.002	18.0 (17.2)
308.62 ± 0.62	$+0.39 \pm 1.39$	0.277 ± 0.003	19.9 (20.4)	307.97 ± 0.59	$+1.01 \pm 0.90$	0.364 ± 0.003	16.3 (15.0)
337.80 ± 0.85	$+1.38 \pm 1.33$	0.315 ± 0.003	18.0 (20.2)	336.93 ± 0.84	-0.03 ± 1.38	0.408 ± 0.004	13.5 (11.5)
IP = 100 m				IP = 120 m			
0.50 ± 0.29	$+1.44 \pm 0.72$	0.506 ± 0.004	8.8 (9.8)	360.00 ± 0.33	$+0.36 \pm 0.67$	0.579 ± 0.005	5.7 (5.9)
24.78 ± 0.35	$+1.11 \pm 0.78$	0.479 ± 0.004	9.7 (11.9)	23.48 ± 0.26	$+0.21 \pm 0.53$	0.549 ± 0.004	6.4 (6.6)
52.87 ± 0.74	$+0.75 \pm 1.26$	0.425 ± 0.003	13.0 (13.4)	51.52 ± 0.50	-0.33 ± 1.00	0.498 ± 0.004	10.5 (7.7)
90.32 ± 0.30	$+2.02 \pm 0.91$	0.391 ± 0.003	19.9 (14.3)	89.77 ± 0.51	-0.10 ± 1.31	0.469 ± 0.005	10.7 (12.4)
125.81 ± 0.51	-4.13 ± 1.03	0.426 ± 0.003	13.6 (11.6)	128.65 ± 0.35	$+1.51 \pm 0.93$	0.500 ± 0.004	12.7 (7.3)
157.01 ± 0.51	-0.93 ± 0.95	0.477 ± 0.004	9.4 (9.8)	156.02 ± 0.40	$+0.69 \pm 0.68$	0.550 ± 0.005	8.0 (7.5)
180.55 ± 0.57	$+0.93 \pm 0.86$	0.501 ± 0.004	9.2 (8.4)	180.20 ± 0.27	$+0.04 \pm 0.54$	0.576 ± 0.004	5.2 (5.2)
203.79 ± 0.57	$+1.31 \pm 1.00$	0.483 ± 0.004	10.9 (9.2)	203.03 ± 0.33	$+0.64 \pm 0.62$	0.557 ± 0.005	7.4 (7.6)
233.09 ± 0.50	$+2.08 \pm 1.16$	0.439 ± 0.004	12.2 (10.3)	234.04 ± 0.48	$+2.04 \pm 0.83$	0.508 ± 0.004	10.6 (6.8)
271.84 ± 0.80	$+3.60 \pm 1.32$	0.407 ± 0.004	16.3 (13.3)	271.55 ± 0.56	$+0.42 \pm 0.99$	0.473 ± 0.004	8.7 (8.2)
307.25 ± 0.52	-1.50 ± 1.11	0.440 ± 0.002	8.7 (8.8)	306.83 ± 0.42	-1.97 ± 0.91	0.506 ± 0.005	9.9 (7.1)
337.14 ± 0.35	-0.99 ± 1.00	0.484 ± 0.004	9.9 (9.9)	336.99 ± 0.34	$+1.05 \pm 0.61$	0.563 ± 0.005	8.7 (6.0)

Table 57: The nominal angle δ_n, average displacement $\Delta\delta$, average value of the parameter DIST, RMS of the ALPHA distribution for enabled GF and impact parameters between 60 m and 120 m. The RMS of the ALPHA distribution for disabled GF is given parentheses. The primary γ-ray energy was set to 170 GeV, the ZA to 40° and the azimuth angle to 0°.

$E_\gamma = 170\,\mathrm{GeV}$, Az = 30°, ZA = 40°, Intermediate Image Cleaning

$\delta_n[°]$	$\Delta\delta[°]$	DIST[°]	$\mathrm{RMS}_{\lvert\mathrm{ALPHA}\rvert}[°]$	$\delta_n[°]$	$\Delta\delta[°]$	DIST[°]	$\mathrm{RMS}_{\lvert\mathrm{ALPHA}\rvert}[°]$
IP = 60 m				**IP = 80 m**			
359.63 ± 0.55	-6.60 ± 0.80	0.298 ± 0.003	20.3 (19.2)	1.16 ± 0.60	-1.43 ± 1.08	0.387 ± 0.003	18.2 (13.1)
23.58 ± 0.73	-6.01 ± 1.51	0.262 ± 0.003	18.4 (19.4)	22.12 ± 0.48	-4.82 ± 1.02	0.342 ± 0.003	16.0 (14.9)
54.50 ± 0.30	-5.36 ± 0.80	0.244 ± 0.003	19.3 (19.2)	52.07 ± 0.73	-3.70 ± 1.21	0.313 ± 0.003	17.1 (18.3)
89.51 ± 0.90	$+2.30 \pm 1.63$	0.260 ± 0.003	21.4 (20.1)	91.38 ± 0.72	$+1.60 \pm 1.15$	0.341 ± 0.003	19.3 (20.0)
129.10 ± 0.72	$+8.09 \pm 1.21$	0.300 ± 0.002	22.0 (17.0)	125.90 ± 0.55	$+5.38 \pm 1.34$	0.390 ± 0.003	20.1 (15.9)
155.32 ± 0.79	-0.38 ± 1.71	0.318 ± 0.003	22.6 (16.9)	156.33 ± 0.42	-0.03 ± 1.09	0.409 ± 0.002	18.9 (14.2)
177.25 ± 0.72	-6.16 ± 1.33	0.303 ± 0.003	21.1 (18.0)	179.45 ± 0.36	$+0.21 \pm 0.90$	0.391 ± 0.002	17.7 (12.9)
205.76 ± 0.91	-6.31 ± 1.04	0.273 ± 0.003	20.0 (21.2)	204.46 ± 0.48	-3.05 ± 0.96	0.356 ± 0.003	15.4 (13.4)
233.10 ± 0.73	-2.81 ± 1.52	0.256 ± 0.003	18.5 (20.7)	233.47 ± 0.55	-2.95 ± 1.05	0.330 ± 0.003	17.1 (16.4)
269.47 ± 0.48	$+2.29 \pm 0.99$	0.276 ± 0.002	22.9 (20.8)	271.60 ± 0.73	$+7.19 \pm 1.28$	0.353 ± 0.003	20.1 (15.1)
308.01 ± 0.60	$+9.94 \pm 1.22$	0.309 ± 0.002	22.7 (20.0)	307.93 ± 0.42	$+5.49 \pm 0.97$	0.395 ± 0.003	21.2 (16.9)
334.69 ± 0.61	-1.45 ± 0.79	0.323 ± 0.003	21.1 (21.0)	335.42 ± 0.36	$+2.50 \pm 0.90$	0.410 ± 0.003	17.2 (14.2)
IP = 100 m				**IP = 120 m**			
359.98 ± 0.36	-2.91 ± 0.89	0.469 ± 0.003	14.9 (10.6)	359.77 ± 0.30	-1.06 ± 0.65	0.542 ± 0.005	11.9 (4.7)
23.79 ± 0.36	-2.59 ± 0.71	0.416 ± 0.004	14.3 (12.2)	23.45 ± 0.35	-2.43 ± 0.71	0.483 ± 0.004	10.5 (6.7)
52.66 ± 0.48	-0.82 ± 0.90	0.384 ± 0.004	15.7 (12.8)	51.96 ± 0.30	-1.94 ± 0.59	0.444 ± 0.003	14.4 (8.9)
88.49 ± 0.60	-0.29 ± 1.08	0.416 ± 0.004	17.0 (17.2)	90.81 ± 0.42	$+2.15 \pm 0.79$	0.484 ± 0.004	15.2 (10.0)
126.22 ± 0.36	$+3.39 \pm 0.84$	0.473 ± 0.003	16.7 (12.1)	127.96 ± 0.35	$+3.55 \pm 0.83$	0.543 ± 0.004	14.1 (8.6)
156.51 ± 0.36	$+0.91 \pm 0.96$	0.494 ± 0.004	15.6 (11.3)	156.43 ± 0.18	$+2.53 \pm 0.53$	0.566 ± 0.005	11.4 (6.0)
180.32 ± 0.30	-0.11 ± 0.95	0.475 ± 0.004	14.1 (7.8)	180.52 ± 0.36	$+0.23 \pm 0.89$	0.548 ± 0.004	11.5 (5.0)
202.73 ± 0.53	-2.74 ± 0.78	0.427 ± 0.004	13.3 (11.5)	202.61 ± 0.35	-2.34 ± 0.65	0.495 ± 0.003	12.2 (7.6)
232.48 ± 0.42	-3.48 ± 0.77	0.399 ± 0.003	16.0 (13.5)	233.49 ± 0.41	-1.26 ± 0.71	0.467 ± 0.004	12.6 (9.4)
271.97 ± 0.42	$+3.74 \pm 1.02$	0.431 ± 0.003	16.6 (14.3)	270.82 ± 0.42	$+3.03 \pm 0.77$	0.504 ± 0.003	14.0 (9.6)
308.21 ± 0.24	$+4.67 \pm 0.60$	0.480 ± 0.004	15.8 (10.6)	306.90 ± 0.36	$+0.53 \pm 0.65$	0.552 ± 0.003	13.2 (10.8)
337.76 ± 0.30	$+1.63 \pm 0.71$	0.498 ± 0.002	14.4 (10.2)	336.52 ± 0.24	-0.75 ± 0.70	0.567 ± 0.005	12.1 (7.7)

Table 58: The nominal angle δ_n, average displacement $\Delta\delta$, average value of the parameter DIST, RMS of the ALPHA distribution for enabled GF and impact parameters between 60 m and 120 m. The RMS of the ALPHA distribution for disabled GF is given parentheses. The primary γ-ray energy was set to 170 GeV, the ZA to 40° and the azimuth angle to 30°.

$E_\gamma = 170\,\mathrm{GeV}$, Az = 30°, ZA = 40°, Hard Image Cleaning

$\delta_n[°]$	$\Delta\delta[°]$	DIST[°]	$\mathrm{RMS}_{\lvert\mathrm{ALPHA}\rvert}[°]$	$\delta_n[°]$	$\Delta\delta[°]$	DIST[°]	$\mathrm{RMS}_{\lvert\mathrm{ALPHA}\rvert}[°]$
IP = 60 m				**IP = 80 m**			
1.73 ± 0.76	-4.32 ± 1.41	0.317 ± 0.003	19.3 (17.9)	0.92 ± 0.61	-0.37 ± 0.93	0.411 ± 0.003	15.8 (14.1)
22.43 ± 0.70	-8.46 ± 1.47	0.285 ± 0.003	16.2 (19.2)	23.43 ± 0.61	-3.90 ± 1.24	0.364 ± 0.003	16.5 (13.5)
54.48 ± 0.85	-2.59 ± 1.60	0.265 ± 0.003	21.1 (20.3)	53.20 ± 0.55	-0.78 ± 1.11	0.335 ± 0.004	16.8 (16.7)
88.81 ± 0.71	$+0.48 \pm 1.71$	0.284 ± 0.003	19.4 (21.1)	92.10 ± 0.77	$+3.54 \pm 1.32$	0.360 ± 0.003	18.0 (16.0)
127.37 ± 0.15	$+8.05 \pm 0.57$	0.318 ± 0.003	19.5 (17.3)	125.58 ± 0.62	$+3.44 \pm 1.54$	0.417 ± 0.003	18.6 (13.7)
151.50 ± 0.24	-5.62 ± 1.18	0.340 ± 0.003	22.0 (19.8)	157.83 ± 0.69	$+3.61 \pm 1.33$	0.438 ± 0.003	15.9 (12.5)
179.60 ± 0.76	-1.36 ± 1.31	0.326 ± 0.002	19.3 (17.5)	179.08 ± 0.69	-2.01 ± 1.16	0.423 ± 0.002	15.3 (14.1)
207.69 ± 0.62	-0.40 ± 1.82	0.293 ± 0.003	19.2 (19.8)	204.98 ± 0.37	$+0.56 \pm 0.69$	0.382 ± 0.004	14.9 (14.8)
235.25 ± 0.47	$+0.97 \pm 1.43$	0.277 ± 0.003	19.2 (19.7)	233.34 ± 0.68	-2.90 ± 1.19	0.356 ± 0.003	16.6 (16.5)
269.83 ± 0.60	$+0.95 \pm 1.37$	0.291 ± 0.002	22.4 (19.5)	271.67 ± 0.54	$+2.22 \pm 1.32$	0.380 ± 0.004	18.5 (17.2)
308.62 ± 0.62	$+7.18 \pm 1.34$	0.331 ± 0.003	20.8 (20.4)	307.97 ± 0.59	$+4.91 \pm 1.14$	0.425 ± 0.004	17.5 (15.0)
337.80 ± 0.85	$+2.06 \pm 1.26$	0.342 ± 0.003	17.6 (20.2)	336.93 ± 0.84	$+3.52 \pm 1.40$	0.443 ± 0.005	14.5 (11.5)
IP = 100 m				**IP = 120 m**			
0.50 ± 0.29	-0.42 ± 0.58	0.499 ± 0.004	13.0 (9.8)	360.00 ± 0.33	-1.89 ± 0.75	0.571 ± 0.004	11.5 (5.9)
24.78 ± 0.35	$+0.76 \pm 0.73$	0.444 ± 0.003	13.3 (11.9)	23.48 ± 0.26	-1.48 ± 0.70	0.507 ± 0.005	10.6 (6.6)
52.87 ± 0.74	-0.94 ± 1.34	0.410 ± 0.004	14.0 (13.4)	51.52 ± 0.50	-2.10 ± 0.92	0.480 ± 0.005	12.9 (7.7)
90.32 ± 0.30	$+2.29 \pm 0.92$	0.441 ± 0.003	13.1 (14.3)	89.77 ± 0.51	$+0.11 \pm 1.07$	0.510 ± 0.004	13.2 (12.4)
125.81 ± 0.51	$+1.06 \pm 1.04$	0.508 ± 0.003	12.3 (11.6)	128.65 ± 0.35	$+3.50 \pm 0.71$	0.565 ± 0.004	12.7 (7.3)
157.01 ± 0.51	$+0.57 \pm 0.97$	0.524 ± 0.006	15.4 (9.8)	156.02 ± 0.40	$+2.53 \pm 0.89$	0.586 ± 0.005	10.2 (7.5)
180.55 ± 0.57	$+1.78 \pm 1.02$	0.505 ± 0.004	13.2 (8.4)	180.20 ± 0.27	-0.43 ± 0.55	0.576 ± 0.004	9.7 (5.2)
203.79 ± 0.57	-0.83 ± 0.88	0.460 ± 0.004	11.5 (9.2)	203.03 ± 0.33	-2.46 ± 0.76	0.517 ± 0.005	10.7 (7.6)
233.09 ± 0.50	-1.01 ± 0.96	0.421 ± 0.004	15.4 (10.3)	234.04 ± 0.48	$+0.36 \pm 0.98$	0.497 ± 0.005	11.5 (6.8)
271.84 ± 0.80	$+3.28 \pm 1.54$	0.458 ± 0.003	13.7 (13.3)	271.55 ± 0.56	$+2.74 \pm 1.09$	0.535 ± 0.003	13.0 (8.2)
307.25 ± 0.52	$+1.71 \pm 0.97$	0.516 ± 0.004	14.8 (8.8)	306.83 ± 0.42	$+0.30 \pm 0.79$	0.581 ± 0.005	10.9 (7.1)
337.14 ± 0.35	$+1.67 \pm 0.74$	0.523 ± 0.003	13.9 (9.9)	336.99 ± 0.34	-0.21 ± 0.77	0.591 ± 0.004	11.1 (6.0)

Table 59: The nominal angle δ_n, average displacement $\Delta\delta$, average value of the parameter DIST, RMS of the ALPHA distribution for enabled GF and impact parameters between 60 m and 120 m. The RMS of the ALPHA distribution for disabled GF is given parentheses. The primary γ-ray energy was set to 170 GeV, the ZA to 40° and the azimuth angle to 30°.

$E_\gamma = 170\,\mathrm{GeV}$, Az = 60°, ZA = 40°, Intermediate Image Cleaning

δ_n[°]	$\Delta\delta$[°]	DIST[°]	RMS$_{\lvert\mathrm{ALPHA}\rvert}$[°]	δ_n[°]	$\Delta\delta$[°]	DIST[°]	RMS$_{\lvert\mathrm{ALPHA}\rvert}$[°]
IP = 60 m				**IP = 80 m**			
359.63 ± 0.55	$+4.92 \pm 0.61$	0.258 ± 0.003	20.6 (19.2)	1.16 ± 0.60	$+4.41 \pm 0.96$	0.335 ± 0.002	20.3 (13.1)
23.58 ± 0.73	-1.18 ± 0.79	0.239 ± 0.002	17.1 (19.4)	22.12 ± 0.48	-4.26 ± 0.66	0.312 ± 0.003	16.0 (14.9)
54.50 ± 0.30	-8.71 ± 0.60	0.257 ± 0.003	16.8 (19.2)	52.07 ± 0.73	-9.92 ± 0.97	0.335 ± 0.003	15.5 (18.3)
89.51 ± 0.90	-3.01 ± 1.64	0.292 ± 0.002	19.0 (20.1)	91.38 ± 0.72	-0.43 ± 1.35	0.383 ± 0.003	18.6 (20.0)
129.10 ± 0.72	$+11.89 \pm 1.58$	0.314 ± 0.003	23.0 (17.0)	125.90 ± 0.55	$+8.02 \pm 1.28$	0.406 ± 0.002	19.0 (15.9)
155.32 ± 0.79	$+6.73 \pm 1.83$	0.301 ± 0.002	21.9 (16.9)	156.33 ± 0.42	$+5.81 \pm 0.85$	0.392 ± 0.003	20.5 (14.2)
177.25 ± 0.72	-2.13 ± 1.39	0.269 ± 0.002	20.9 (18.0)	179.45 ± 0.36	$+1.15 \pm 1.02$	0.349 ± 0.002	18.3 (12.9)
205.76 ± 0.91	-4.29 ± 2.42	0.255 ± 0.003	16.1 (21.2)	204.46 ± 0.48	-6.49 ± 1.39	0.325 ± 0.004	15.1 (13.4)
233.10 ± 0.73	-7.49 ± 1.64	0.272 ± 0.003	16.8 (20.7)	233.47 ± 0.55	-4.76 ± 1.14	0.349 ± 0.003	15.7 (16.4)
269.47 ± 0.48	-1.08 ± 1.17	0.304 ± 0.003	20.2 (20.8)	271.60 ± 0.73	$+0.78 \pm 1.15$	0.397 ± 0.002	17.6 (15.1)
308.01 ± 0.60	$+11.22 \pm 1.27$	0.317 ± 0.002	21.1 (20.0)	307.93 ± 0.42	$+7.73 \pm 1.15$	0.408 ± 0.002	18.6 (16.9)
334.69 ± 0.61	$+9.09 \pm 1.35$	0.295 ± 0.002	20.8 (21.0)	335.42 ± 0.36	$+6.68 \pm 1.15$	0.382 ± 0.002	20.5 (14.2)
IP = 100 m				**IP = 120 m**			
359.98 ± 0.36	$+2.75 \pm 1.13$	0.411 ± 0.003	17.4 (10.6)	359.77 ± 0.30	$+0.35 \pm 0.76$	0.475 ± 0.003	15.4 (4.7)
23.79 ± 0.36	-1.46 ± 0.89	0.374 ± 0.003	14.2 (12.2)	23.45 ± 0.35	-1.78 ± 0.76	0.443 ± 0.003	11.5 (6.7)
52.66 ± 0.48	-6.63 ± 1.20	0.411 ± 0.003	14.1 (12.8)	51.96 ± 0.30	-4.95 ± 0.65	0.479 ± 0.003	12.9 (8.9)
88.49 ± 0.60	-4.60 ± 1.02	0.466 ± 0.003	16.1 (17.2)	90.81 ± 0.42	-0.69 ± 0.65	0.537 ± 0.004	13.7 (10.0)
126.22 ± 0.36	$+5.04 \pm 0.83$	0.489 ± 0.003	16.8 (12.1)	127.96 ± 0.35	$+3.50 \pm 0.71$	0.557 ± 0.004	14.1 (8.6)
156.51 ± 0.36	$+4.78 \pm 0.78$	0.472 ± 0.002	17.7 (11.3)	156.43 ± 0.18	$+2.98 \pm 0.59$	0.543 ± 0.003	14.5 (6.0)
180.32 ± 0.30	$+1.63 \pm 0.83$	0.427 ± 0.003	16.2 (7.8)	180.52 ± 0.36	$+1.13 \pm 0.64$	0.494 ± 0.003	14.1 (5.0)
202.73 ± 0.53	-4.17 ± 0.89	0.398 ± 0.003	12.5 (11.5)	202.61 ± 0.35	-1.11 ± 0.82	0.461 ± 0.002	11.5 (7.6)
232.48 ± 0.42	-5.39 ± 1.01	0.423 ± 0.004	13.9 (13.5)	233.49 ± 0.41	-3.01 ± 1.00	0.497 ± 0.003	12.0 (9.4)
271.97 ± 0.42	$+0.92 \pm 0.91$	0.476 ± 0.003	16.2 (14.3)	270.82 ± 0.42	-0.07 ± 0.83	0.550 ± 0.003	13.6 (9.6)
308.21 ± 0.24	$+7.07 \pm 0.78$	0.490 ± 0.002	17.5 (10.6)	306.90 ± 0.36	$+3.03 \pm 0.71$	0.559 ± 0.003	14.5 (10.8)
337.76 ± 0.30	$+6.28 \pm 0.60$	0.467 ± 0.002	18.4 (10.2)	336.52 ± 0.24	$+3.72 \pm 0.76$	0.535 ± 0.004	15.8 (7.7)

Table 60: The nominal angle δ_n, average displacement $\Delta\delta$, average value of the parameter DIST, RMS of the ALPHA distribution for enabled GF and impact parameters between 60 m and 120 m. The RMS of the ALPHA distribution for disabled GF is given parentheses. The primary γ-ray energy was set to 170 GeV, the ZA to 40° and the azimuth angle to 60°.

$E_\gamma = 170\,\mathrm{GeV}$, Az = 60°, ZA = 40°, Hard Image Cleaning

δ_n[°]	$\Delta\delta$[°]	DIST[°]	RMS$_{\lvert\mathrm{ALPHA}\rvert}$[°]	δ_n[°]	$\Delta\delta$[°]	DIST[°]	RMS$_{\lvert\mathrm{ALPHA}\rvert}$[°]
IP = 60 m				**IP = 80 m**			
1.73 ± 0.76	$+1.76 \pm 1.57$	0.282 ± 0.003	19.3 (17.9)	0.92 ± 0.61	$+1.53 \pm 0.87$	0.367 ± 0.003	17.7 (14.1)
22.43 ± 0.70	$+0.90 \pm 1.23$	0.263 ± 0.004	17.1 (19.2)	23.43 ± 0.61	-4.08 ± 1.22	0.337 ± 0.003	15.6 (13.5)
54.48 ± 0.85	-5.91 ± 1.72	0.281 ± 0.004	16.7 (20.3)	53.20 ± 0.55	-5.58 ± 1.34	0.370 ± 0.004	12.9 (16.7)
88.81 ± 0.71	-0.16 ± 1.35	0.318 ± 0.004	17.1 (21.1)	92.10 ± 0.77	$+1.14 \pm 1.47$	0.419 ± 0.004	15.7 (16.0)
127.37 ± 0.15	$+9.01 \pm 1.41$	0.345 ± 0.004	18.8 (17.3)	125.58 ± 0.62	$+3.19 \pm 1.39$	0.439 ± 0.004	16.2 (13.7)
151.50 ± 0.24	$+2.35 \pm 1.12$	0.331 ± 0.004	20.6 (19.8)	157.83 ± 0.69	$+5.60 \pm 1.38$	0.428 ± 0.004	17.5 (12.5)
179.60 ± 0.76	-1.58 ± 1.65	0.292 ± 0.004	19.2 (17.5)	179.08 ± 0.69	$+0.83 \pm 1.28$	0.381 ± 0.003	17.6 (14.1)
207.69 ± 0.62	-2.24 ± 1.23	0.281 ± 0.004	16.8 (19.8)	204.98 ± 0.37	-1.52 ± 1.05	0.355 ± 0.003	14.7 (14.8)
235.25 ± 0.47	-2.62 ± 1.50	0.296 ± 0.003	14.5 (19.7)	233.34 ± 0.68	-1.98 ± 1.80	0.385 ± 0.003	14.0 (16.5)
269.83 ± 0.60	-3.92 ± 0.69	0.330 ± 0.004	18.5 (19.5)	271.67 ± 0.54	$+2.62 \pm 1.13$	0.435 ± 0.004	16.0 (17.2)
308.62 ± 0.62	$+8.29 \pm 1.61$	0.344 ± 0.003	20.6 (20.4)	307.97 ± 0.59	$+4.84 \pm 1.01$	0.442 ± 0.004	18.3 (15.0)
337.80 ± 0.85	$+9.72 \pm 2.43$	0.323 ± 0.004	19.7 (20.2)	336.93 ± 0.84	$+6.43 \pm 2.09$	0.421 ± 0.005	18.7 (11.5)
IP = 100 m				**IP = 120 m**			
0.50 ± 0.29	$+1.11 \pm 1.18$	0.446 ± 0.004	14.6 (9.8)	360.00 ± 0.33	$+0.53 \pm 0.70$	0.508 ± 0.004	12.9 (5.9)
24.78 ± 0.35	-0.67 ± 0.76	0.407 ± 0.003	12.7 (11.9)	23.48 ± 0.26	-3.35 ± 0.71	0.478 ± 0.005	11.2 (6.6)
52.87 ± 0.74	-3.57 ± 1.50	0.440 ± 0.004	12.6 (13.4)	51.52 ± 0.50	-5.26 ± 1.04	0.510 ± 0.004	11.1 (7.7)
90.32 ± 0.30	-1.92 ± 0.89	0.502 ± 0.005	15.1 (14.3)	89.77 ± 0.51	-0.25 ± 0.98	0.571 ± 0.006	11.4 (12.4)
125.81 ± 0.51	$+1.95 \pm 0.84$	0.532 ± 0.006	15.6 (11.6)	128.65 ± 0.35	$+4.26 \pm 0.97$	0.587 ± 0.005	12.8 (7.3)
157.01 ± 0.51	$+2.77 \pm 1.33$	0.508 ± 0.003	16.0 (9.8)	156.02 ± 0.40	$+4.38 \pm 0.95$	0.572 ± 0.005	13.3 (7.5)
180.55 ± 0.57	$+1.10 \pm 1.32$	0.463 ± 0.003	15.0 (8.4)	180.20 ± 0.27	-0.17 ± 0.71	0.523 ± 0.003	13.0 (5.2)
203.79 ± 0.57	-1.53 ± 0.89	0.425 ± 0.003	11.8 (9.2)	203.03 ± 0.33	-1.53 ± 0.94	0.489 ± 0.005	12.0 (7.6)
233.09 ± 0.50	-4.65 ± 0.99	0.460 ± 0.003	11.9 (10.3)	234.04 ± 0.48	-2.63 ± 1.02	0.539 ± 0.003	10.3 (6.8)
271.84 ± 0.80	$+0.90 \pm 1.20$	0.506 ± 0.005	14.1 (13.3)	271.55 ± 0.56	$+1.88 \pm 1.11$	0.583 ± 0.002	11.1 (8.2)
307.25 ± 0.52	$+2.27 \pm 0.93$	0.530 ± 0.003	14.9 (8.8)	306.83 ± 0.42	$+3.10 \pm 1.00$	0.592 ± 0.005	12.7 (7.1)
337.14 ± 0.35	$+2.60 \pm 0.99$	0.502 ± 0.004	16.1 (9.9)	336.99 ± 0.34	$+4.73 \pm 0.87$	0.567 ± 0.006	14.3 (6.0)

Table 61: The nominal angle δ_n, average displacement $\Delta\delta$, average value of the parameter DIST, RMS of the ALPHA distribution for enabled GF and impact parameters between 60 m and 120 m. The RMS of the ALPHA distribution for disabled GF is given parentheses. The primary γ-ray energy was set to 170 GeV, the ZA to 40° and the azimuth angle to 60°.

$E_\gamma = 170\,\mathrm{GeV}$, Az = 90°, ZA = 40°, Intermediate Image Cleaning

$\delta_n[°]$	$\Delta\delta[°]$	DIST[°]	$\mathrm{RMS}_{\lvert\mathrm{ALPHA}\rvert}[°]$	$\delta_n[°]$	$\Delta\delta[°]$	DIST[°]	$\mathrm{RMS}_{\lvert\mathrm{ALPHA}\rvert}[°]$
IP = 60 m				**IP = 80 m**			
359.63 ± 0.55	$+7.68 \pm 1.70$	0.245 ± 0.003	19.4 (19.2)	1.16 ± 0.60	$+7.97 \pm 0.92$	0.313 ± 0.003	18.5 (13.1)
23.58 ± 0.73	$+1.14 \pm 0.85$	0.265 ± 0.002	16.9 (19.4)	22.12 ± 0.48	-0.70 ± 1.11	0.336 ± 0.003	14.8 (14.9)
54.50 ± 0.30	-9.10 ± 1.53	0.294 ± 0.003	20.8 (19.2)	52.07 ± 0.73	-12.35 ± 1.67	0.388 ± 0.003	19.0 (18.3)
89.51 ± 0.90	-9.85 ± 1.68	0.318 ± 0.002	24.4 (20.1)	91.38 ± 0.72	-7.09 ± 1.35	0.406 ± 0.002	20.8 (20.0)
129.10 ± 0.72	$+4.36 \pm 1.18$	0.306 ± 0.002	26.2 (17.0)	125.90 ± 0.55	$+1.20 \pm 0.99$	0.391 ± 0.003	23.7 (15.9)
155.32 ± 0.79	$+8.11 \pm 1.75$	0.270 ± 0.002	24.9 (16.9)	156.33 ± 0.42	$+6.32 \pm 0.87$	0.347 ± 0.003	24.1 (14.2)
177.25 ± 0.72	$+7.19 \pm 1.30$	0.247 ± 0.003	20.0 (18.0)	179.45 ± 0.36	$+6.78 \pm 0.98$	0.320 ± 0.003	16.4 (12.9)
205.76 ± 0.91	$+2.98 \pm 1.62$	0.264 ± 0.003	16.2 (21.2)	204.46 ± 0.48	$+2.49 \pm 1.05$	0.344 ± 0.003	15.3 (13.4)
233.10 ± 0.73	-7.85 ± 1.35	0.301 ± 0.002	21.2 (20.7)	233.47 ± 0.55	-6.34 ± 1.48	0.386 ± 0.003	19.7 (16.4)
269.47 ± 0.48	-10.84 ± 1.07	0.316 ± 0.002	25.1 (20.8)	271.60 ± 0.73	-6.16 ± 1.36	0.413 ± 0.003	22.5 (15.1)
308.01 ± 0.60	$+4.50 \pm 1.37$	0.301 ± 0.001	25.9 (20.0)	307.93 ± 0.42	$+3.21 \pm 1.06$	0.385 ± 0.003	23.9 (16.9)
334.69 ± 0.61	$+10.59 \pm 1.51$	0.264 ± 0.002	24.4 (21.0)	335.42 ± 0.36	$+7.21 \pm 1.24$	0.341 ± 0.003	23.7 (14.2)
IP = 100 m				**IP = 120 m**			
359.98 ± 0.36	$+3.52 \pm 1.16$	0.377 ± 0.003	18.1 (10.6)	359.77 ± 0.30	$+2.15 \pm 0.60$	0.446 ± 0.004	13.0 (4.7)
23.79 ± 0.36	$+2.24 \pm 0.85$	0.408 ± 0.003	11.5 (12.2)	23.45 ± 0.35	-0.91 ± 0.94	0.481 ± 0.004	9.5 (6.7)
52.66 ± 0.48	-6.67 ± 1.16	0.466 ± 0.003	15.7 (12.8)	51.96 ± 0.30	-3.94 ± 1.16	0.536 ± 0.004	11.6 (8.9)
88.49 ± 0.60	-9.52 ± 1.10	0.489 ± 0.004	19.1 (17.2)	90.81 ± 0.42	-4.61 ± 0.91	0.564 ± 0.003	14.4 (10.0)
126.22 ± 0.36	$+0.22 \pm 0.79$	0.475 ± 0.003	21.0 (12.1)	127.96 ± 0.35	$+1.27 \pm 0.73$	0.544 ± 0.003	15.6 (8.6)
156.51 ± 0.36	$+4.70 \pm 0.91$	0.427 ± 0.003	21.0 (11.3)	156.43 ± 0.18	$+4.20 \pm 0.55$	0.498 ± 0.003	17.1 (6.0)
180.32 ± 0.30	$+2.71 \pm 0.67$	0.388 ± 0.003	16.2 (7.8)	180.52 ± 0.36	$+1.95 \pm 0.84$	0.460 ± 0.004	14.5 (5.0)
202.73 ± 0.53	-1.01 ± 1.09	0.422 ± 0.003	14.0 (11.5)	202.61 ± 0.35	$+0.97 \pm 0.89$	0.494 ± 0.003	9.7 (7.6)
232.48 ± 0.42	-6.69 ± 1.10	0.475 ± 0.003	15.8 (13.5)	233.49 ± 0.41	-3.53 ± 1.03	0.548 ± 0.003	11.8 (9.4)
271.97 ± 0.42	-3.66 ± 1.11	0.492 ± 0.003	17.5 (14.3)	270.82 ± 0.42	-2.63 ± 0.92	0.562 ± 0.002	14.4 (9.6)
308.21 ± 0.24	$+2.02 \pm 0.61$	0.469 ± 0.003	20.8 (10.6)	306.90 ± 0.36	$+0.55 \pm 0.67$	0.535 ± 0.004	15.0 (10.8)
337.76 ± 0.30	$+5.79 \pm 0.92$	0.412 ± 0.003	21.0 (10.2)	336.52 ± 0.24	$+1.14 \pm 0.67$	0.483 ± 0.003	19.3 (7.7)

Table 62: The nominal angle δ_n, average displacement $\Delta\delta$, average value of the parameter DIST, RMS of the ALPHA distribution for enabled GF and impact parameters between 60 m and 120 m. The RMS of the ALPHA distribution for disabled GF is given parentheses. The primary γ-ray energy was set to 170 GeV, the ZA to 40° and the azimuth angle to 90°.

$E_\gamma = 170\,\mathrm{GeV}$, Az = 90°, ZA = 40°, Hard Image Cleaning

$\delta_n[°]$	$\Delta\delta[°]$	DIST[°]	$\mathrm{RMS}_{\lvert\mathrm{ALPHA}\rvert}[°]$	$\delta_n[°]$	$\Delta\delta[°]$	DIST[°]	$\mathrm{RMS}_{\lvert\mathrm{ALPHA}\rvert}[°]$
IP = 60 m				**IP = 80 m**			
1.73 ± 0.76	$+10.00 \pm 0.95$	0.269 ± 0.004	18.3 (17.9)	0.92 ± 0.61	$+5.44 \pm 1.53$	0.347 ± 0.004	17.1 (14.1)
22.43 ± 0.70	$+4.36 \pm 1.91$	0.298 ± 0.001	13.0 (19.2)	23.43 ± 0.61	$+0.85 \pm 1.45$	0.366 ± 0.005	12.7 (13.5)
54.48 ± 0.85	-2.49 ± 1.77	0.326 ± 0.004	18.0 (20.3)	53.20 ± 0.55	-8.31 ± 1.77	0.430 ± 0.006	15.9 (16.7)
88.81 ± 0.71	-11.86 ± 1.41	0.350 ± 0.003	20.6 (21.1)	92.10 ± 0.77	-3.44 ± 1.88	0.451 ± 0.006	17.2 (16.0)
127.37 ± 0.15	$+5.47 \pm 1.31$	0.332 ± 0.004	22.7 (17.3)	125.58 ± 0.62	$+1.14 \pm 0.98$	0.426 ± 0.006	21.9 (13.7)
151.50 ± 0.24	$+0.55 \pm 1.12$	0.293 ± 0.003	22.5 (19.8)	157.83 ± 0.69	$+6.02 \pm 1.39$	0.379 ± 0.005	22.2 (12.5)
179.60 ± 0.76	$+8.73 \pm 1.43$	0.267 ± 0.003	17.9 (17.5)	179.08 ± 0.69	$+4.64 \pm 1.36$	0.354 ± 0.003	14.1 (14.1)
207.69 ± 0.62	$+4.37 \pm 1.39$	0.290 ± 0.004	16.2 (19.8)	204.98 ± 0.37	$+3.03 \pm 0.57$	0.373 ± 0.004	15.6 (14.8)
235.25 ± 0.47	-5.70 ± 0.67	0.331 ± 0.006	19.8 (19.7)	233.34 ± 0.68	-4.72 ± 1.63	0.434 ± 0.004	17.8 (16.5)
269.83 ± 0.60	-6.79 ± 1.20	0.341 ± 0.005	23.0 (19.5)	271.67 ± 0.54	-5.07 ± 1.39	0.448 ± 0.005	19.6 (17.2)
308.62 ± 0.62	$+2.42 \pm 1.01$	0.326 ± 0.003	25.1 (20.4)	307.97 ± 0.59	$+3.85 \pm 1.39$	0.426 ± 0.003	21.0 (15.0)
337.80 ± 0.85	$+8.82 \pm 1.44$	0.292 ± 0.003	22.7 (20.2)	336.93 ± 0.84	$+3.02 \pm 1.42$	0.372 ± 0.004	22.8 (11.5)
IP = 100 m				**IP = 120 m**			
0.50 ± 0.29	$+0.34 \pm 0.99$	0.418 ± 0.006	15.8 (9.8)	360.00 ± 0.33	$+2.15 \pm 0.73$	0.486 ± 0.006	9.0 (5.9)
24.78 ± 0.35	$+2.45 \pm 0.72$	0.448 ± 0.005	10.0 (11.9)	23.48 ± 0.26	$+0.67 \pm 0.75$	0.518 ± 0.003	8.8 (6.6)
52.87 ± 0.74	-2.84 ± 1.89	0.508 ± 0.002	13.0 (13.4)	51.52 ± 0.50	-3.72 ± 0.94	0.573 ± 0.006	8.6 (7.7)
90.32 ± 0.30	-5.82 ± 0.85	0.540 ± 0.007	15.6 (14.3)	89.77 ± 0.51	-4.51 ± 0.95	0.598 ± 0.007	10.3 (12.4)
125.81 ± 0.51	$+2.98 \pm 1.14$	0.509 ± 0.004	17.0 (11.6)	128.65 ± 0.35	$+1.20 \pm 0.76$	0.582 ± 0.004	12.0 (7.3)
157.01 ± 0.51	$+4.48 \pm 1.41$	0.459 ± 0.005	16.2 (9.8)	156.02 ± 0.40	$+4.14 \pm 0.90$	0.539 ± 0.005	14.3 (7.5)
180.55 ± 0.57	$+2.13 \pm 1.01$	0.420 ± 0.005	13.4 (8.4)	180.20 ± 0.27	$+0.41 \pm 0.92$	0.492 ± 0.004	7.8 (5.2)
203.79 ± 0.57	$+0.42 \pm 1.19$	0.456 ± 0.005	10.9 (9.2)	203.03 ± 0.33	$+1.71 \pm 0.74$	0.535 ± 0.006	10.1 (7.6)
233.09 ± 0.50	-1.62 ± 0.76	0.512 ± 0.007	12.8 (10.3)	234.04 ± 0.48	-2.49 ± 1.26	0.595 ± 0.005	10.4 (6.8)
271.84 ± 0.80	-3.83 ± 1.61	0.533 ± 0.005	15.2 (13.3)	271.55 ± 0.56	-0.39 ± 1.26	0.598 ± 0.005	9.9 (8.2)
307.25 ± 0.52	$+0.69 \pm 1.14$	0.521 ± 0.004	15.8 (8.8)	306.83 ± 0.42	-0.39 ± 0.75	0.575 ± 0.006	13.7 (7.1)
337.14 ± 0.35	$+4.52 \pm 1.24$	0.455 ± 0.003	16.3 (9.9)	336.99 ± 0.34	$+3.16 \pm 0.59$	0.524 ± 0.006	15.2 (6.0)

Table 63: The nominal angle δ_n, average displacement $\Delta\delta$, average value of the parameter DIST, RMS of the ALPHA distribution for enabled GF and impact parameters between 60 m and 120 m. The RMS of the ALPHA distribution for disabled GF is given parentheses. The primary γ-ray energy was set to 170 GeV, the ZA to 40° and the azimuth angle to 90°.

$E_\gamma = 170\,\mathrm{GeV}$, Az = 120°, ZA = 40°, Intermediate Image Cleaning

$\delta_n[°]$	$\Delta\delta[°]$	DIST[°]	$\mathrm{RMS}_{\lvert\mathrm{ALPHA}\rvert}[°]$	$\delta_n[°]$	$\Delta\delta[°]$	DIST[°]	$\mathrm{RMS}_{\lvert\mathrm{ALPHA}\rvert}[°]$
IP = 60 m				IP = 80 m			
359.63 ± 0.55	$+11.59 \pm 1.20$	0.271 ± 0.003	15.2 (19.2)	1.16 ± 0.60	$+7.19 \pm 1.37$	0.348 ± 0.004	13.4 (13.1)
23.58 ± 0.73	$+10.60 \pm 1.63$	0.305 ± 0.003	16.6 (19.4)	22.12 ± 0.48	$+4.50 \pm 1.43$	0.394 ± 0.005	14.9 (14.9)
54.50 ± 0.30	$+2.49 \pm 0.69$	0.327 ± 0.004	19.0 (19.2)	52.07 ± 0.73	-2.46 ± 1.24	0.412 ± 0.003	17.6 (18.3)
89.51 ± 0.90	-14.12 ± 1.74	0.314 ± 0.003	21.9 (20.1)	91.38 ± 0.72	-11.43 ± 1.62	0.405 ± 0.003	19.9 (20.0)
129.10 ± 0.72	-0.98 ± 1.45	0.283 ± 0.002	23.0 (17.0)	125.90 ± 0.55	-2.39 ± 0.94	0.366 ± 0.003	20.1 (15.9)
155.32 ± 0.79	$+4.30 \pm 1.50$	0.265 ± 0.003	18.9 (16.9)	156.33 ± 0.42	$+3.44 \pm 0.94$	0.340 ± 0.003	17.1 (14.2)
177.25 ± 0.72	$+5.80 \pm 1.31$	0.279 ± 0.003	15.2 (18.0)	179.45 ± 0.36	$+6.52 \pm 0.87$	0.358 ± 0.003	12.8 (12.9)
205.76 ± 0.91	$+9.68 \pm 1.63$	0.311 ± 0.003	16.5 (21.2)	204.46 ± 0.48	$+4.62 \pm 1.06$	0.398 ± 0.004	15.2 (13.4)
233.10 ± 0.73	-2.85 ± 0.98	0.322 ± 0.003	20.3 (20.7)	233.47 ± 0.55	-3.20 ± 1.56	0.418 ± 0.004	16.9 (16.4)
269.47 ± 0.48	-11.14 ± 1.59	0.311 ± 0.003	22.0 (20.8)	271.60 ± 0.73	-7.97 ± 1.64	0.399 ± 0.003	21.2 (15.1)
308.01 ± 0.60	-0.38 ± 1.00	0.271 ± 0.003	23.4 (20.0)	307.93 ± 0.42	-0.43 ± 1.00	0.354 ± 0.002	22.7 (16.9)
334.69 ± 0.61	$+4.56 \pm 1.12$	0.249 ± 0.003	17.2 (21.0)	335.42 ± 0.36	$+3.92 \pm 0.88$	0.323 ± 0.003	17.7 (14.2)
IP = 100 m				IP = 120 m			
359.98 ± 0.36	$+6.02 \pm 0.80$	0.418 ± 0.004	11.9 (10.6)	359.77 ± 0.30	$+1.36 \pm 0.61$	0.487 ± 0.004	10.3 (4.7)
23.79 ± 0.36	$+2.52 \pm 0.93$	0.481 ± 0.005	13.0 (12.2)	23.45 ± 0.35	-0.20 ± 0.90	0.555 ± 0.005	11.1 (6.7)
52.66 ± 0.48	-3.46 ± 1.29	0.503 ± 0.004	15.6 (12.8)	51.96 ± 0.30	-0.70 ± 0.91	0.584 ± 0.004	12.9 (8.9)
88.49 ± 0.60	-9.17 ± 1.43	0.483 ± 0.003	17.8 (17.2)	90.81 ± 0.42	-6.75 ± 0.85	0.561 ± 0.004	15.3 (10.0)
126.22 ± 0.36	-4.02 ± 0.73	0.438 ± 0.004	19.5 (12.1)	127.96 ± 0.35	-1.40 ± 0.79	0.512 ± 0.004	17.6 (8.6)
156.51 ± 0.36	$+2.17 \pm 0.87$	0.410 ± 0.004	15.7 (11.3)	156.43 ± 0.18	$+2.43 \pm 0.56$	0.479 ± 0.005	14.9 (6.0)
180.32 ± 0.30	$+4.40 \pm 0.93$	0.433 ± 0.004	12.2 (7.8)	180.52 ± 0.36	$+1.44 \pm 0.80$	0.501 ± 0.005	10.6 (5.0)
202.73 ± 0.53	$+0.65 \pm 0.97$	0.481 ± 0.004	13.0 (11.5)	202.61 ± 0.35	-0.40 ± 1.03	0.561 ± 0.005	11.4 (7.6)
232.48 ± 0.42	-4.03 ± 1.16	0.504 ± 0.005	15.6 (13.5)	233.49 ± 0.41	-1.23 ± 1.14	0.578 ± 0.003	13.5 (9.4)
271.97 ± 0.42	-7.02 ± 1.12	0.483 ± 0.003	18.1 (14.3)	270.82 ± 0.42	-5.14 ± 1.05	0.551 ± 0.004	16.0 (9.6)
308.21 ± 0.24	$+0.37 \pm 0.68$	0.425 ± 0.004	21.7 (10.6)	306.90 ± 0.36	-1.17 ± 0.73	0.495 ± 0.004	18.9 (10.8)
337.76 ± 0.30	$+5.43 \pm 0.68$	0.395 ± 0.004	17.6 (10.2)	336.52 ± 0.24	$+3.02 \pm 0.49$	0.460 ± 0.004	15.7 (7.7)

Table 64: The nominal angle δ_n, average displacement $\Delta\delta$, average value of the parameter DIST, RMS of the ALPHA distribution for enabled GF and impact parameters between 60 m and 120 m. The RMS of the ALPHA distribution for disabled GF is given parentheses. The primary γ-ray energy was set to 170 GeV, the ZA to 40° and the azimuth angle to 120°.

$E_\gamma = 170\,\mathrm{GeV}$, Az = 120°, ZA = 40°, Hard Image Cleaning

$\delta_n[°]$	$\Delta\delta[°]$	DIST[°]	$\mathrm{RMS}_{\lvert\mathrm{ALPHA}\rvert}[°]$	$\delta_n[°]$	$\Delta\delta[°]$	DIST[°]	$\mathrm{RMS}_{\lvert\mathrm{ALPHA}\rvert}[°]$
IP = 60 m				IP = 80 m			
1.73 ± 0.76	$+9.26 \pm 1.60$	0.294 ± 0.005	14.3 (17.9)	0.92 ± 0.61	$+5.89 \pm 1.35$	0.379 ± 0.004	11.9 (14.1)
22.43 ± 0.70	$+6.75 \pm 2.20$	0.336 ± 0.004	16.8 (19.2)	23.43 ± 0.61	$+3.06 \pm 0.80$	0.435 ± 0.006	14.0 (13.5)
54.48 ± 0.85	$+1.80 \pm 1.50$	0.362 ± 0.004	18.2 (20.3)	53.20 ± 0.55	-4.68 ± 1.38	0.455 ± 0.005	14.7 (16.7)
88.81 ± 0.71	-16.53 ± 1.49	0.345 ± 0.004	19.7 (21.1)	92.10 ± 0.77	-10.17 ± 1.67	0.440 ± 0.005	17.4 (16.0)
127.37 ± 0.15	-1.40 ± 0.99	0.308 ± 0.004	21.3 (17.3)	125.58 ± 0.62	-2.52 ± 1.24	0.391 ± 0.004	19.1 (13.7)
151.50 ± 0.24	-1.46 ± 0.70	0.290 ± 0.003	18.2 (19.8)	157.83 ± 0.69	$+1.64 \pm 1.62$	0.361 ± 0.005	15.9 (12.5)
179.60 ± 0.76	$+5.93 \pm 1.79$	0.303 ± 0.004	14.5 (17.5)	179.08 ± 0.69	$+3.32 \pm 1.16$	0.388 ± 0.004	12.0 (14.1)
207.69 ± 0.62	$+4.36 \pm 1.22$	0.335 ± 0.006	16.4 (19.8)	204.98 ± 0.37	$+3.82 \pm 1.01$	0.443 ± 0.005	12.8 (14.8)
235.25 ± 0.47	-3.10 ± 0.57	0.356 ± 0.004	18.4 (19.7)	233.34 ± 0.68	$+1.22 \pm 1.04$	0.463 ± 0.006	14.9 (16.5)
269.83 ± 0.60	-5.39 ± 1.18	0.336 ± 0.004	20.5 (19.5)	271.67 ± 0.54	-7.19 ± 1.54	0.433 ± 0.002	18.5 (17.2)
308.62 ± 0.62	-1.08 ± 1.38	0.298 ± 0.003	20.5 (20.4)	307.97 ± 0.59	$+0.29 \pm 1.32$	0.381 ± 0.005	19.5 (15.0)
337.80 ± 0.85	$+9.57 \pm 1.88$	0.275 ± 0.003	17.5 (20.2)	336.93 ± 0.84	$+2.45 \pm 1.40$	0.346 ± 0.004	16.8 (11.5)
IP = 100 m				IP = 120 m			
0.50 ± 0.29	$+4.87 \pm 1.00$	0.461 ± 0.005	10.8 (9.8)	360.00 ± 0.33	$+2.48 \pm 0.93$	0.535 ± 0.007	9.0 (5.9)
24.78 ± 0.35	$+4.08 \pm 1.00$	0.529 ± 0.005	11.5 (11.9)	23.48 ± 0.26	$+0.61 \pm 0.61$	0.603 ± 0.007	9.8 (6.6)
52.87 ± 0.74	-2.49 ± 1.39	0.559 ± 0.006	13.8 (13.4)	51.52 ± 0.50	-1.59 ± 1.21	0.632 ± 0.007	9.7 (7.7)
90.32 ± 0.30	-5.64 ± 0.76	0.539 ± 0.007	15.0 (14.3)	89.77 ± 0.51	-4.16 ± 0.97	0.608 ± 0.008	13.8 (12.4)
125.81 ± 0.51	-4.85 ± 1.05	0.479 ± 0.005	17.7 (11.6)	128.65 ± 0.35	$+0.52 \pm 0.78$	0.562 ± 0.007	14.6 (7.3)
157.01 ± 0.51	$+0.67 \pm 1.24$	0.442 ± 0.004	14.6 (9.8)	156.02 ± 0.40	$+1.82 \pm 0.74$	0.514 ± 0.006	13.6 (7.5)
180.55 ± 0.57	$+2.88 \pm 1.37$	0.471 ± 0.006	10.4 (8.4)	180.20 ± 0.27	$+2.08 \pm 0.61$	0.546 ± 0.006	8.1 (5.2)
203.79 ± 0.57	$+3.24 \pm 1.13$	0.520 ± 0.005	11.8 (9.2)	203.03 ± 0.33	$+0.41 \pm 0.92$	0.612 ± 0.006	9.6 (7.6)
233.09 ± 0.50	-0.38 ± 0.77	0.557 ± 0.005	12.4 (10.3)	234.04 ± 0.48	-0.03 ± 1.18	0.625 ± 0.007	10.9 (6.8)
271.84 ± 0.80	-5.64 ± 1.61	0.531 ± 0.004	14.9 (13.3)	271.55 ± 0.56	-1.43 ± 1.62	0.605 ± 0.007	15.3 (8.2)
307.25 ± 0.52	-2.47 ± 1.14	0.465 ± 0.005	17.3 (8.8)	306.83 ± 0.42	-0.71 ± 0.68	0.544 ± 0.006	16.0 (7.1)
337.14 ± 0.35	$+3.98 \pm 0.71$	0.438 ± 0.005	15.5 (9.9)	336.99 ± 0.34	$+2.87 \pm 0.87$	0.508 ± 0.006	14.4 (6.0)

Table 65: The nominal angle δ_n, average displacement $\Delta\delta$, average value of the parameter DIST, RMS of the ALPHA distribution for enabled GF and impact parameters between 60 m and 120 m. The RMS of the ALPHA distribution for disabled GF is given parentheses. The primary γ-ray energy was set to 170 GeV, the ZA to 40° and the azimuth angle to 120°.

$E_\gamma = 170\,\mathrm{GeV}$, Az = 150°, ZA = 40°, Intermediate Image Cleaning

δ_n[°]	$\Delta\delta$[°]	DIST[°]	RMS$_{\lvert ALPHA \rvert}$[°]	δ_n[°]	$\Delta\delta$[°]	DIST[°]	RMS$_{\lvert ALPHA \rvert}$[°]
IP = 60 m				**IP = 80 m**			
359.63 ± 0.55	$+7.83 \pm 1.26$	0.309 ± 0.003	13.1 (19.2)	1.16 ± 0.60	$+7.74 \pm 1.04$	0.399 ± 0.003	13.3 (13.1)
23.58 ± 0.73	$+7.35 \pm 1.69$	0.331 ± 0.003	15.0 (19.4)	22.12 ± 0.48	$+3.33 \pm 1.18$	0.416 ± 0.003	13.6 (14.9)
54.50 ± 0.30	$+6.46 \pm 0.87$	0.321 ± 0.002	20.9 (19.2)	52.07 ± 0.73	-1.93 ± 1.43	0.404 ± 0.004	18.7 (18.3)
89.51 ± 0.90	-11.84 ± 1.35	0.285 ± 0.002	26.5 (20.1)	91.38 ± 0.72	-7.65 ± 1.04	0.367 ± 0.003	25.1 (20.0)
129.10 ± 0.72	-5.91 ± 1.31	0.260 ± 0.002	23.6 (17.0)	125.90 ± 0.55	-9.07 ± 0.99	0.337 ± 0.003	22.6 (15.9)
155.32 ± 0.79	$+2.39 \pm 1.31$	0.275 ± 0.003	21.0 (16.9)	156.33 ± 0.42	$+0.76 \pm 0.87$	0.356 ± 0.003	18.6 (14.2)
177.25 ± 0.72	$+6.49 \pm 1.24$	0.310 ± 0.002	16.3 (18.0)	179.45 ± 0.36	$+6.45 \pm 0.93$	0.400 ± 0.004	12.4 (12.9)
205.76 ± 0.91	$+15.79 \pm 1.97$	0.319 ± 0.003	15.5 (21.2)	204.46 ± 0.48	$+7.60 \pm 1.31$	0.416 ± 0.004	14.6 (13.4)
233.10 ± 0.73	$+8.13 \pm 2.27$	0.303 ± 0.002	22.8 (20.7)	233.47 ± 0.55	$+5.08 \pm 1.05$	0.393 ± 0.003	19.9 (16.4)
269.47 ± 0.48	-8.78 ± 1.19	0.272 ± 0.002	26.0 (20.8)	271.60 ± 0.73	-3.43 ± 0.98	0.353 ± 0.003	24.7 (15.1)
308.01 ± 0.60	-4.55 ± 1.38	0.254 ± 0.002	21.6 (20.0)	307.93 ± 0.42	-6.70 ± 1.00	0.327 ± 0.002	22.8 (16.9)
334.69 ± 0.61	-3.01 ± 1.14	0.272 ± 0.002	18.6 (21.0)	335.42 ± 0.36	-2.14 ± 0.75	0.349 ± 0.002	17.0 (14.2)
IP = 100 m				**IP = 120 m**			
359.98 ± 0.36	$+0.55 \pm 0.86$	0.482 ± 0.004	11.1 (10.6)	359.77 ± 0.30	$+1.82 \pm 0.62$	0.558 ± 0.004	9.4 (4.7)
23.79 ± 0.36	$+1.85 \pm 0.99$	0.509 ± 0.005	12.7 (12.2)	23.45 ± 0.35	$+0.42 \pm 0.91$	0.588 ± 0.005	10.4 (6.7)
52.66 ± 0.48	$+1.57 \pm 1.04$	0.492 ± 0.004	15.8 (12.8)	51.96 ± 0.30	-3.13 ± 1.03	0.563 ± 0.004	14.7 (8.9)
88.49 ± 0.60	-7.80 ± 1.43	0.441 ± 0.003	21.6 (17.2)	90.81 ± 0.42	-4.88 ± 0.85	0.512 ± 0.004	18.2 (10.0)
126.22 ± 0.36	-5.56 ± 0.80	0.410 ± 0.003	21.8 (12.1)	127.96 ± 0.35	-3.38 ± 0.73	0.479 ± 0.003	20.0 (8.6)
156.51 ± 0.36	$+1.22 \pm 0.80$	0.433 ± 0.003	16.8 (11.3)	156.43 ± 0.18	$+1.06 \pm 0.56$	0.504 ± 0.004	14.0 (6.0)
180.32 ± 0.30	$+3.90 \pm 0.74$	0.484 ± 0.003	11.2 (7.8)	180.52 ± 0.36	$+2.68 \pm 0.75$	0.555 ± 0.003	9.5 (5.0)
202.73 ± 0.53	$+5.46 \pm 1.23$	0.502 ± 0.004	13.2 (11.5)	202.61 ± 0.35	$+2.97 \pm 0.73$	0.578 ± 0.004	9.8 (7.6)
232.48 ± 0.42	$+4.47 \pm 1.21$	0.480 ± 0.004	17.3 (13.5)	233.49 ± 0.41	$+3.60 \pm 0.84$	0.552 ± 0.004	14.2 (9.4)
271.97 ± 0.42	-2.84 ± 1.24	0.427 ± 0.003	21.8 (14.3)	270.82 ± 0.42	$+1.45 \pm 1.16$	0.497 ± 0.003	18.9 (9.6)
308.21 ± 0.24	-4.52 ± 0.74	0.399 ± 0.003	21.1 (10.6)	306.90 ± 0.36	-2.73 ± 0.73	0.467 ± 0.004	17.6 (10.8)
337.76 ± 0.30	$+2.39 \pm 0.74$	0.428 ± 0.003	15.6 (10.2)	336.52 ± 0.24	$+0.19 \pm 0.55$	0.494 ± 0.004	14.5 (7.7)

Table 66: The nominal angle δ_n, average displacement $\Delta\delta$, average value of the parameter DIST, RMS of the ALPHA distribution for enabled GF and impact parameters between 60 m and 120 m. The RMS of the ALPHA distribution for disabled GF is given parentheses. The primary γ-ray energy was set to 170 GeV, the ZA to 40° and the azimuth angle to 150°.

$E_\gamma = 170\,\mathrm{GeV}$, Az = 150°, ZA = 40°, Hard Image Cleaning

δ_n[°]	$\Delta\delta$[°]	DIST[°]	RMS$_{\lvert ALPHA \rvert}$[°]	δ_n[°]	$\Delta\delta$[°]	DIST[°]	RMS$_{\lvert ALPHA \rvert}$[°]
IP = 60 m				**IP = 80 m**			
1.73 ± 0.76	$+11.02 \pm 1.42$	0.341 ± 0.005	13.5 (17.9)	0.92 ± 0.61	$+5.90 \pm 1.19$	0.440 ± 0.004	10.6 (14.1)
22.43 ± 0.70	$+7.45 \pm 1.09$	0.361 ± 0.003	16.8 (19.2)	23.43 ± 0.61	$+4.58 \pm 0.71$	0.464 ± 0.004	11.8 (13.5)
54.48 ± 0.85	$+10.92 \pm 1.72$	0.350 ± 0.002	18.3 (20.3)	53.20 ± 0.55	$+1.75 \pm 1.27$	0.445 ± 0.004	16.0 (16.7)
88.81 ± 0.71	-9.64 ± 0.81	0.309 ± 0.005	25.8 (21.1)	92.10 ± 0.77	-4.96 ± 1.34	0.396 ± 0.004	21.7 (16.0)
127.37 ± 0.15	-5.31 ± 1.20	0.287 ± 0.002	22.4 (17.3)	125.58 ± 0.62	-9.83 ± 1.34	0.375 ± 0.005	21.2 (13.7)
151.50 ± 0.24	-5.21 ± 1.03	0.302 ± 0.005	20.1 (19.8)	157.83 ± 0.69	$+3.51 \pm 0.98$	0.396 ± 0.005	18.4 (12.5)
179.60 ± 0.76	$+5.62 \pm 1.04$	0.340 ± 0.002	14.4 (17.5)	179.08 ± 0.69	$+4.64 \pm 1.45$	0.444 ± 0.007	11.7 (14.1)
207.69 ± 0.62	$+15.27 \pm 1.30$	0.351 ± 0.003	14.9 (19.8)	204.98 ± 0.37	$+6.00 \pm 0.92$	0.470 ± 0.004	14.4 (14.8)
235.25 ± 0.47	$+13.64 \pm 1.76$	0.339 ± 0.005	18.6 (19.7)	233.34 ± 0.68	$+4.93 \pm 1.87$	0.444 ± 0.006	16.4 (16.5)
269.83 ± 0.60	-6.57 ± 1.26	0.298 ± 0.004	22.7 (19.5)	271.67 ± 0.54	-6.01 ± 0.73	0.384 ± 0.005	22.4 (17.2)
308.62 ± 0.62	-2.89 ± 1.96	0.282 ± 0.004	21.5 (20.4)	307.97 ± 0.59	-5.79 ± 1.34	0.363 ± 0.004	19.3 (15.0)
337.80 ± 0.85	$+1.00 \pm 1.52$	0.301 ± 0.006	17.2 (20.2)	336.93 ± 0.84	-0.92 ± 1.51	0.389 ± 0.003	16.1 (11.5)
IP = 100 m				**IP = 120 m**			
0.50 ± 0.29	$+2.13 \pm 0.76$	0.530 ± 0.007	9.6 (9.8)	360.00 ± 0.33	$+0.77 \pm 0.95$	0.603 ± 0.005	8.2 (5.9)
24.78 ± 0.35	$+2.02 \pm 0.80$	0.564 ± 0.003	11.8 (11.9)	23.48 ± 0.26	$+0.66 \pm 0.77$	0.642 ± 0.006	9.3 (6.6)
52.87 ± 0.74	$+0.20 \pm 1.50$	0.541 ± 0.003	13.8 (13.4)	51.52 ± 0.50	-1.53 ± 1.04	0.617 ± 0.003	11.6 (7.7)
90.32 ± 0.30	-2.71 ± 0.40	0.487 ± 0.003	17.8 (14.3)	89.77 ± 0.51	-6.95 ± 0.97	0.561 ± 0.005	16.0 (12.4)
125.81 ± 0.51	-4.83 ± 1.14	0.448 ± 0.003	18.7 (11.6)	128.65 ± 0.35	-2.42 ± 1.04	0.524 ± 0.005	17.5 (7.3)
157.01 ± 0.51	$+0.93 \pm 1.15$	0.481 ± 0.005	14.1 (9.8)	156.02 ± 0.40	-0.31 ± 0.91	0.559 ± 0.005	10.8 (7.5)
180.55 ± 0.57	$+2.14 \pm 1.11$	0.534 ± 0.005	10.9 (8.4)	180.20 ± 0.27	$+0.92 \pm 0.61$	0.613 ± 0.006	9.1 (5.2)
203.79 ± 0.57	$+4.39 \pm 0.93$	0.569 ± 0.002	11.0 (9.2)	203.03 ± 0.33	$+3.01 \pm 0.83$	0.642 ± 0.008	9.5 (7.6)
233.09 ± 0.50	$+3.35 \pm 1.03$	0.531 ± 0.006	12.9 (10.3)	234.04 ± 0.48	$+0.88 \pm 0.82$	0.609 ± 0.007	12.3 (6.8)
271.84 ± 0.80	-5.76 ± 1.82	0.482 ± 0.005	17.3 (13.3)	271.55 ± 0.56	-1.23 ± 0.83	0.556 ± 0.007	13.9 (8.2)
307.25 ± 0.52	-2.52 ± 1.06	0.438 ± 0.006	18.6 (8.8)	306.83 ± 0.42	-3.07 ± 0.95	0.522 ± 0.006	14.5 (7.1)
337.14 ± 0.35	$+0.32 \pm 0.98$	0.473 ± 0.003	13.0 (9.9)	336.99 ± 0.34	-0.23 ± 0.76	0.548 ± 0.003	11.0 (6.0)

Table 67: The nominal angle δ_n, average displacement $\Delta\delta$, average value of the parameter DIST, RMS of the ALPHA distribution for enabled GF and impact parameters between 60 m and 120 m. The RMS of the ALPHA distribution for disabled GF is given parentheses. The primary γ-ray energy was set to 170 GeV, the ZA to 40° and the azimuth angle to 150°.

$E_\gamma = 170\,\mathrm{GeV}$, Az = 180°, ZA = 40°, Intermediate Image Cleaning

$\delta_n[°]$	$\Delta\delta[°]$	DIST[°]	$\mathrm{RMS}_{\lvert\mathrm{ALPHA}\rvert}[°]$	$\delta_n[°]$	$\Delta\delta[°]$	DIST[°]	$\mathrm{RMS}_{\lvert\mathrm{ALPHA}\rvert}[°]$
IP = 60 m				**IP = 80 m**			
359.63 ± 0.55	−1.67 ± 1.07	0.320 ± 0.003	13.0 (19.2)	1.16 ± 0.60	−0.18 ± 1.06	0.411 ± 0.004	11.8 (13.1)
23.58 ± 0.73	+5.85 ± 1.23	0.305 ± 0.003	22.5 (19.4)	22.12 ± 0.48	+5.07 ± 0.98	0.393 ± 0.004	16.5 (14.9)
54.50 ± 0.30	+11.64 ± 1.25	0.276 ± 0.003	28.9 (19.2)	52.07 ± 0.73	+6.61 ± 1.43	0.361 ± 0.003	24.4 (18.3)
89.51 ± 0.90	−1.71 ± 1.66	0.259 ± 0.002	26.7 (20.1)	91.38 ± 0.72	−2.21 ± 1.04	0.332 ± 0.001	25.7 (20.0)
129.10 ± 0.72	−6.95 ± 1.62	0.272 ± 0.002	22.1 (17.0)	125.90 ± 0.55	−11.49 ± 1.12	0.350 ± 0.003	20.2 (15.9)
155.32 ± 0.79	−8.07 ± 1.52	0.299 ± 0.003	16.1 (16.9)	156.33 ± 0.42	−5.14 ± 0.94	0.387 ± 0.003	16.5 (14.2)
177.25 ± 0.72	−1.75 ± 1.11	0.313 ± 0.002	14.1 (18.0)	179.45 ± 0.36	+0.52 ± 0.68	0.407 ± 0.003	10.0 (12.9)
205.76 ± 0.91	+8.85 ± 1.49	0.296 ± 0.003	18.8 (21.2)	204.46 ± 0.48	+6.89 ± 1.19	0.377 ± 0.003	16.8 (13.4)
233.10 ± 0.73	+12.47 ± 1.62	0.260 ± 0.003	28.1 (20.7)	233.47 ± 0.55	+12.76 ± 1.62	0.337 ± 0.003	25.6 (16.4)
269.47 ± 0.48	+1.44 ± 0.67	0.246 ± 0.002	23.3 (20.8)	271.60 ± 0.73	+4.09 ± 1.42	0.316 ± 0.002	25.5 (15.1)
308.01 ± 0.60	−0.64 ± 1.56	0.265 ± 0.002	21.7 (20.0)	307.93 ± 0.42	−3.50 ± 0.62	0.350 ± 0.003	19.7 (16.9)
334.69 ± 0.61	+0.28 ± 1.19	0.301 ± 0.003	17.0 (21.0)	335.42 ± 0.36	−0.62 ± 0.87	0.391 ± 0.004	13.6 (14.2)
IP = 100 m				**IP = 120 m**			
359.98 ± 0.36	+0.18 ± 0.87	0.491 ± 0.004	11.2 (10.6)	359.77 ± 0.30	+0.06 ± 0.55	0.566 ± 0.004	6.2 (4.7)
23.79 ± 0.36	+4.02 ± 0.85	0.469 ± 0.004	18.2 (12.2)	23.45 ± 0.35	+0.96 ± 0.91	0.550 ± 0.004	7.2 (6.7)
52.66 ± 0.48	+6.02 ± 1.30	0.435 ± 0.002	23.5 (12.8)	51.96 ± 0.30	+0.91 ± 0.85	0.503 ± 0.004	21.0 (8.9)
88.49 ± 0.60	−6.55 ± 1.48	0.406 ± 0.003	24.2 (17.2)	90.81 ± 0.42	−2.56 ± 1.15	0.475 ± 0.003	23.6 (10.0)
126.22 ± 0.36	−7.10 ± 0.48	0.427 ± 0.003	18.4 (12.1)	127.96 ± 0.35	−6.65 ± 1.04	0.502 ± 0.004	16.2 (8.6)
156.51 ± 0.36	−5.14 ± 0.87	0.471 ± 0.003	15.0 (11.3)	156.43 ± 0.18	−1.74 ± 0.55	0.551 ± 0.004	10.9 (6.0)
180.32 ± 0.30	+0.56 ± 0.61	0.488 ± 0.003	10.0 (7.8)	180.52 ± 0.36	+2.10 ± 0.62	0.558 ± 0.005	7.4 (5.0)
202.73 ± 0.53	+2.93 ± 0.90	0.460 ± 0.004	13.9 (11.5)	202.61 ± 0.35	+3.65 ± 0.72	0.534 ± 0.005	11.2 (7.6)
232.48 ± 0.42	+9.06 ± 1.22	0.413 ± 0.003	21.3 (13.5)	233.49 ± 0.41	+5.90 ± 0.84	0.484 ± 0.004	21.5 (9.4)
271.97 ± 0.42	+3.04 ± 1.53	0.390 ± 0.002	24.1 (14.3)	270.82 ± 0.42	+2.57 ± 0.66	0.450 ± 0.003	21.7 (9.6)
308.21 ± 0.24	−3.69 ± 0.80	0.419 ± 0.003	18.2 (10.6)	306.90 ± 0.36	−1.29 ± 1.03	0.489 ± 0.003	16.7 (10.8)
337.76 ± 0.30	+0.74 ± 0.68	0.474 ± 0.004	12.4 (10.2)	336.52 ± 0.24	+0.03 ± 0.49	0.539 ± 0.005	10.2 (7.7)

Table 68: The nominal angle δ_n, average displacement $\Delta\delta$, average value of the parameter DIST, RMS of the ALPHA distribution for enabled GF and impact parameters between 60 m and 120 m. The RMS of the ALPHA distribution for disabled GF is given parentheses. The primary γ-ray energy was set to 170 GeV, the ZA to 40° and the azimuth angle to 180°.

$E_\gamma = 170\,\mathrm{GeV}$, Az = 180°, ZA = 40°, Hard Image Cleaning

$\delta_n[°]$	$\Delta\delta[°]$	DIST[°]	$\mathrm{RMS}_{\lvert\mathrm{ALPHA}\rvert}[°]$	$\delta_n[°]$	$\Delta\delta[°]$	DIST[°]	$\mathrm{RMS}_{\lvert\mathrm{ALPHA}\rvert}[°]$
IP = 60 m				**IP = 80 m**			
1.73 ± 0.76	−1.29 ± 1.25	0.350 ± 0.003	11.5 (17.9)	0.92 ± 0.61	+1.25 ± 1.21	0.441 ± 0.004	8.7 (14.1)
22.43 ± 0.70	+3.72 ± 1.67	0.324 ± 0.004	16.8 (19.2)	23.43 ± 0.61	+3.82 ± 1.45	0.426 ± 0.005	14.6 (13.5)
54.48 ± 0.85	+12.57 ± 1.95	0.292 ± 0.003	27.4 (20.3)	53.20 ± 0.55	+7.20 ± 0.84	0.381 ± 0.004	22.3 (16.7)
88.81 ± 0.71	−3.61 ± 1.21	0.280 ± 0.003	21.7 (21.1)	92.10 ± 0.77	−1.30 ± 0.87	0.355 ± 0.005	21.8 (16.0)
127.37 ± 0.15	−6.58 ± 0.56	0.296 ± 0.004	20.9 (17.3)	125.58 ± 0.62	−9.71 ± 1.74	0.383 ± 0.004	17.7 (13.7)
151.50 ± 0.24	−6.94 ± 1.70	0.324 ± 0.004	14.4 (19.8)	157.83 ± 0.69	−3.32 ± 1.16	0.425 ± 0.005	11.7 (12.5)
179.60 ± 0.76	−0.71 ± 1.06	0.343 ± 0.004	13.3 (17.5)	179.08 ± 0.69	−0.25 ± 1.26	0.448 ± 0.005	10.9 (14.1)
207.69 ± 0.62	+9.99 ± 1.30	0.321 ± 0.003	13.6 (19.8)	204.98 ± 0.37	+3.76 ± 1.12	0.419 ± 0.005	13.7 (14.8)
235.25 ± 0.47	+10.78 ± 0.98	0.286 ± 0.003	25.1 (19.7)	233.34 ± 0.68	+11.72 ± 1.63	0.369 ± 0.003	23.6 (16.5)
269.83 ± 0.60	+1.69 ± 0.99	0.262 ± 0.003	23.9 (19.5)	271.67 ± 0.54	+1.41 ± 1.22	0.338 ± 0.003	25.3 (17.2)
308.62 ± 0.62	−5.01 ± 1.43	0.287 ± 0.003	20.9 (20.4)	307.97 ± 0.59	−9.17 ± 1.18	0.366 ± 0.003	19.3 (15.0)
337.80 ± 0.85	+0.27 ± 1.24	0.333 ± 0.005	12.7 (20.2)	336.93 ± 0.84	−1.74 ± 1.52	0.424 ± 0.003	10.7 (11.5)
IP = 100 m				**IP = 120 m**			
0.50 ± 0.29	+1.56 ± 0.58	0.537 ± 0.006	5.7 (9.8)	360.00 ± 0.33	+0.60 ± 0.78	0.615 ± 0.002	5.2 (5.9)
24.78 ± 0.35	+1.80 ± 0.72	0.515 ± 0.004	8.1 (11.9)	23.48 ± 0.26	+0.06 ± 0.79	0.582 ± 0.007	5.5 (6.6)
52.87 ± 0.74	+4.77 ± 1.43	0.471 ± 0.003	15.0 (13.4)	51.52 ± 0.50	+3.90 ± 1.05	0.543 ± 0.006	18.1 (7.7)
90.32 ± 0.30	−0.58 ± 1.36	0.434 ± 0.004	22.0 (14.3)	89.77 ± 0.51	+1.38 ± 1.84	0.510 ± 0.005	21.2 (12.4)
125.81 ± 0.51	−2.37 ± 1.19	0.469 ± 0.004	15.5 (11.6)	128.65 ± 0.35	−3.08 ± 0.87	0.540 ± 0.005	13.3 (7.3)
157.01 ± 0.51	−2.77 ± 1.15	0.523 ± 0.005	8.7 (9.8)	156.02 ± 0.40	−0.94 ± 1.18	0.599 ± 0.006	9.4 (7.5)
180.55 ± 0.57	+3.18 ± 1.02	0.539 ± 0.006	6.4 (8.4)	180.20 ± 0.27	+1.59 ± 0.62	0.616 ± 0.006	4.7 (5.2)
203.79 ± 0.57	+3.68 ± 1.19	0.508 ± 0.005	11.4 (9.2)	203.03 ± 0.33	+2.00 ± 0.66	0.590 ± 0.006	7.5 (7.6)
233.09 ± 0.50	+7.48 ± 1.69	0.462 ± 0.004	14.0 (10.3)	234.04 ± 0.48	+1.82 ± 1.01	0.533 ± 0.005	12.6 (6.8)
271.84 ± 0.80	+3.82 ± 1.18	0.427 ± 0.003	20.3 (13.3)	271.55 ± 0.56	+2.22 ± 0.84	0.496 ± 0.005	16.3 (8.2)
307.25 ± 0.52	−4.88 ± 1.19	0.457 ± 0.005	12.7 (8.8)	306.83 ± 0.42	−3.25 ± 0.96	0.529 ± 0.006	14.6 (7.1)
337.14 ± 0.35	+0.41 ± 0.92	0.514 ± 0.005	8.5 (9.9)	336.99 ± 0.34	−0.24 ± 0.96	0.590 ± 0.007	7.9 (6.0)

Table 69: The nominal angle δ_n, average displacement $\Delta\delta$, average value of the parameter DIST, RMS of the ALPHA distribution for enabled GF and impact parameters between 60 m and 120 m. The RMS of the ALPHA distribution for disabled GF is given parentheses. The primary γ-ray energy was set to 170 GeV, the ZA to 40° and the azimuth angle to 180°.

$E_\gamma = 300\,\mathrm{GeV}$, Az $= 0°$, ZA $= 0°$, Intermediate Image Cleaning

$\delta_n[°]$	$\Delta\delta[°]$	DIST[°]	$\mathrm{RMS}_{\lvert\mathrm{ALPHA}\rvert}[°]$	$\delta_n[°]$	$\Delta\delta[°]$	DIST[°]	$\mathrm{RMS}_{\lvert\mathrm{ALPHA}\rvert}[°]$
IP = 60 m				**IP = 80 m**			
358.82 ± 0.63	-0.36 ± 1.15	0.581 ± 0.005	4.0 (11.1)	359.61 ± 0.42	$+0.43 \pm 0.63$	0.698 ± 0.009	3.8 (9.7)
31.21 ± 0.53	$+5.79 \pm 1.04$	0.579 ± 0.006	8.8 (3.0)	30.26 ± 0.42	$+3.51 \pm 0.63$	0.706 ± 0.006	9.1 (4.4)
59.51 ± 0.53	$+7.94 \pm 1.25$	0.580 ± 0.009	17.5 (6.7)	59.88 ± 0.32	$+4.38 \pm 1.04$	0.700 ± 0.008	10.7 (2.5)
90.25 ± 0.42	$+0.96 \pm 1.45$	0.578 ± 0.006	17.3 (4.7)	89.86 ± 0.42	-1.08 ± 0.73	0.707 ± 0.009	10.3 (4.6)
119.72 ± 0.42	-6.27 ± 1.04	0.575 ± 0.005	9.9 (5.3)	120.59 ± 0.42	-0.79 ± 0.84	0.703 ± 0.006	9.9 (3.2)
149.85 ± 0.53	-2.67 ± 1.14	0.577 ± 0.005	4.9 (9.7)	149.02 ± 0.42	-2.45 ± 0.83	0.700 ± 0.008	4.0 (4.5)
179.41 ± 0.53	$+0.27 \pm 0.84$	0.576 ± 0.006	5.1 (7.0)	179.40 ± 0.42	-0.53 ± 0.83	0.695 ± 0.003	3.4 (4.5)
208.77 ± 0.53	$+3.10 \pm 1.04$	0.579 ± 0.005	9.3 (11.3)	208.79 ± 0.32	$+2.15 \pm 0.73$	0.706 ± 0.010	9.3 (8.2)
240.39 ± 0.42	$+6.40 \pm 0.94$	0.583 ± 0.003	15.3 (10.9)	240.64 ± 0.21	$+4.09 \pm 0.72$	0.705 ± 0.006	12.2 (7.1)
270.14 ± 0.32	$+0.25 \pm 1.03$	0.586 ± 0.004	21.2 (3.6)	269.61 ± 0.42	$+0.63 \pm 0.63$	0.704 ± 0.008	17.4 (6.0)
299.07 ± 0.42	-10.73 ± 0.94	0.582 ± 0.006	15.7 (4.0)	299.81 ± 0.42	-4.65 ± 1.04	0.701 ± 0.005	13.6 (8.2)
329.77 ± 0.53	-6.05 ± 1.04	0.580 ± 0.009	3.5 (5.2)	329.70 ± 0.42	-3.45 ± 0.73	0.703 ± 0.009	2.3 (3.1)
IP = 100 m				**IP = 120 m**			
359.28 ± 0.42	-0.32 ± 0.73	0.789 ± 0.007	2.1 (6.6)	0.15 ± 0.21	$+0.58 \pm 0.42$	0.845 ± 0.006	2.2 (1.4)
30.51 ± 0.21	$+1.76 \pm 0.52$	0.794 ± 0.001	4.0 (2.3)	30.30 ± 0.21	$+1.40 \pm 0.42$	0.852 ± 0.008	3.8 (1.2)
60.23 ± 0.32	$+2.19 \pm 0.73$	0.783 ± 0.003	8.5 (2.0)	60.40 ± 0.32	$+1.55 \pm 0.73$	0.833 ± 0.005	7.6 (1.5)
89.78 ± 0.32	-1.27 ± 0.42	0.790 ± 0.011	6.9 (1.9)	89.89 ± 0.21	$+0.79 \pm 0.52$	0.843 ± 0.003	9.5 (1.8)
119.77 ± 0.21	-1.22 ± 0.73	0.782 ± 0.010	6.9 (2.4)	120.10 ± 0.21	-0.20 ± 0.52	0.831 ± 0.006	3.4 (1.8)
149.86 ± 0.21	-1.24 ± 0.52	0.791 ± 0.011	1.9 (1.9)	149.99 ± 0.21	-0.51 ± 0.42	0.856 ± 0.008	1.8 (1.7)
179.95 ± 0.21	-0.17 ± 0.62	0.784 ± 0.004	2.4 (3.5)	179.75 ± 0.21	-0.16 ± 0.62	0.845 ± 0.007	2.0 (3.2)
209.06 ± 0.21	$+0.08 \pm 0.52$	0.789 ± 0.009	4.9 (6.0)	209.09 ± 0.21	-0.43 ± 0.42	0.855 ± 0.007	3.9 (4.0)
238.15 ± 0.42	-0.66 ± 0.84	0.787 ± 0.009	10.5 (4.6)	239.09 ± 0.32	$+0.42 \pm 0.73$	0.825 ± 0.004	11.1 (4.4)
269.96 ± 0.32	-0.95 ± 0.62	0.789 ± 0.009	13.4 (10.2)	270.45 ± 0.21	$+0.27 \pm 0.62$	0.836 ± 0.006	8.9 (2.3)
300.00 ± 0.42	-2.62 ± 0.84	0.781 ± 0.003	7.6 (4.7)	300.07 ± 0.21	-0.03 ± 0.63	0.831 ± 0.004	7.4 (3.2)
330.02 ± 0.21	-1.90 ± 0.52	0.795 ± 0.010	2.7 (2.1)	330.32 ± 0.21	-0.47 ± 0.42	0.853 ± 0.009	3.0 (1.5)

Table 70: The nominal angle δ_n, average displacement $\Delta\delta$, average value of the parameter DIST, RMS of the ALPHA distribution for enabled GF and impact parameters between 60 m and 120 m. The RMS of the ALPHA distribution for disabled GF is given parentheses. The primary γ-ray energy was set to 300 GeV, the ZA to 0° and the azimuth angle to 0°.

$E_\gamma = 300\,\mathrm{GeV}$, Az $= 0°$, ZA $= 0°$, Hard Image Cleaning

$\delta_n[°]$	$\Delta\delta[°]$	DIST[°]	$\mathrm{RMS}_{\lvert\mathrm{ALPHA}\rvert}[°]$	$\delta_n[°]$	$\Delta\delta[°]$	DIST[°]	$\mathrm{RMS}_{\lvert\mathrm{ALPHA}\rvert}[°]$
IP = 60 m				**IP = 80 m**			
0.09 ± 0.42	$+0.79 \pm 0.83$	0.568 ± 0.005	3.3 (6.9)	0.11 ± 0.42	$+0.36 \pm 0.84$	0.686 ± 0.007	2.8 (2.3)
31.12 ± 0.42	$+6.50 \pm 0.94$	0.566 ± 0.005	8.8 (3.9)	30.49 ± 0.21	$+3.21 \pm 0.62$	0.695 ± 0.009	7.8 (3.4)
59.72 ± 0.53	$+8.14 \pm 0.94$	0.566 ± 0.007	16.4 (3.8)	60.11 ± 0.32	$+3.88 \pm 0.93$	0.691 ± 0.006	11.8 (2.3)
90.11 ± 0.42	$+0.48 \pm 0.94$	0.566 ± 0.007	16.9 (4.9)	90.09 ± 0.42	-1.08 ± 1.04	0.698 ± 0.008	9.0 (3.3)
119.44 ± 0.42	-5.91 ± 1.35	0.566 ± 0.006	9.0 (5.4)	120.52 ± 0.42	-1.18 ± 0.84	0.691 ± 0.005	10.5 (2.9)
150.53 ± 0.42	-1.70 ± 0.63	0.565 ± 0.005	4.6 (4.0)	149.55 ± 0.32	-2.03 ± 0.63	0.688 ± 0.006	3.9 (2.8)
179.13 ± 0.53	-0.32 ± 0.94	0.566 ± 0.003	3.7 (6.9)	179.54 ± 0.21	-0.43 ± 0.42	0.685 ± 0.003	2.8 (4.4)
210.26 ± 0.42	$+3.82 \pm 1.04$	0.568 ± 0.005	7.7 (5.5)	208.75 ± 0.32	$+2.24 \pm 0.83$	0.693 ± 0.009	9.0 (8.2)
238.99 ± 0.53	$+3.20 \pm 1.15$	0.571 ± 0.004	13.4 (6.6)	240.43 ± 0.32	$+3.81 \pm 0.63$	0.686 ± 0.010	12.3 (7.2)
269.73 ± 0.42	-1.28 ± 0.83	0.569 ± 0.004	19.4 (3.1)	269.43 ± 0.42	$+0.12 \pm 0.94$	0.693 ± 0.009	16.6 (4.4)
299.35 ± 0.42	-10.02 ± 1.24	0.568 ± 0.006	12.9 (3.6)	299.63 ± 0.42	-4.76 ± 0.83	0.688 ± 0.004	13.7 (6.7)
330.34 ± 0.53	-4.56 ± 1.25	0.567 ± 0.006	4.4 (3.9)	329.71 ± 0.42	-3.40 ± 0.73	0.691 ± 0.006	3.1 (2.5)
IP = 100 m				**IP = 120 m**			
359.59 ± 0.32	-0.22 ± 0.63	0.778 ± 0.009	2.5 (2.4)	359.92 ± 0.21	$+0.78 \pm 0.52$	0.825 ± 0.006	2.2 (1.4)
30.56 ± 0.21	$+1.34 \pm 0.31$	0.779 ± 0.009	4.2 (2.3)	30.47 ± 0.21	$+1.11 \pm 0.42$	0.837 ± 0.007	3.6 (1.3)
60.19 ± 0.21	$+1.49 \pm 0.73$	0.773 ± 0.005	7.8 (1.6)	60.08 ± 0.32	$+0.51 \pm 0.63$	0.816 ± 0.005	3.9 (1.7)
89.93 ± 0.32	-0.95 ± 0.63	0.779 ± 0.013	5.9 (1.6)	90.19 ± 0.21	-0.03 ± 0.62	0.826 ± 0.003	5.6 (1.8)
119.66 ± 0.42	-1.23 ± 1.04	0.772 ± 0.010	6.0 (2.0)	120.22 ± 0.32	-0.22 ± 0.73	0.819 ± 0.005	3.4 (1.7)
150.04 ± 0.21	-1.07 ± 0.42	0.781 ± 0.011	2.1 (1.8)	149.78 ± 0.21	-0.57 ± 0.52	0.837 ± 0.004	1.8 (1.8)
179.71 ± 0.21	-0.30 ± 0.42	0.775 ± 0.003	2.4 (3.4)	179.93 ± 0.21	$+0.07 \pm 0.62$	0.830 ± 0.004	1.9 (1.7)
209.04 ± 0.21	$+0.89 \pm 0.52$	0.779 ± 0.009	8.9 (6.1)	209.47 ± 0.21	$+0.02 \pm 0.42$	0.839 ± 0.005	6.1 (2.0)
238.42 ± 0.42	-0.24 ± 0.94	0.775 ± 0.010	9.7 (4.3)	239.12 ± 0.42	-0.99 ± 0.84	0.806 ± 0.006	8.9 (4.3)
269.64 ± 0.32	-0.14 ± 0.73	0.776 ± 0.008	11.0 (9.4)	269.83 ± 0.21	-0.86 ± 0.42	0.815 ± 0.007	8.0 (2.1)
300.06 ± 0.21	-2.14 ± 0.83	0.770 ± 0.002	5.8 (4.5)	300.62 ± 0.21	$+0.28 \pm 0.52$	0.811 ± 0.005	4.0 (1.5)
330.04 ± 0.21	-1.54 ± 0.52	0.784 ± 0.007	2.2 (2.2)	330.43 ± 0.21	-0.43 ± 0.42	0.837 ± 0.005	2.6 (1.5)

Table 71: The nominal angle δ_n, average displacement $\Delta\delta$, average value of the parameter DIST, RMS of the ALPHA distribution for enabled GF and impact parameters between 60 m and 120 m. The RMS of the ALPHA distribution for disabled GF is given parentheses. The primary γ-ray energy was set to 300 GeV, the ZA to 0° and the azimuth angle to 0°.

$E_\gamma = 300\,\mathrm{GeV}$, Az = 0°, ZA = 20°, Intermediate Image Cleaning

δ_n [°]	$\Delta\delta$ [°]	DIST [°]	$\mathrm{RMS}_{\lvert\mathrm{ALPHA}\rvert}$ [°]	δ_n [°]	$\Delta\delta$ [°]	DIST [°]	$\mathrm{RMS}_{\lvert\mathrm{ALPHA}\rvert}$ [°]
IP = 60 m				IP = 80 m			
359.53 ± 0.40	$+0.44 \pm 0.69$	0.497 ± 0.004	5.8 (5.3)	0.01 ± 0.40	$+0.69 \pm 0.79$	0.623 ± 0.006	7.9 (2.6)
28.14 ± 0.40	$+3.20 \pm 0.69$	0.484 ± 0.004	8.8 (5.8)	28.34 ± 0.40	$+1.87 \pm 0.79$	0.613 ± 0.006	7.5 (3.2)
55.92 ± 0.40	$+3.32 \pm 0.99$	0.471 ± 0.006	16.1 (10.7)	57.41 ± 0.40	$+1.81 \pm 0.89$	0.595 ± 0.007	12.6 (2.9)
88.89 ± 0.50	-4.09 ± 0.79	0.466 ± 0.006	15.1 (6.3)	89.21 ± 0.60	-0.65 ± 1.09	0.591 ± 0.009	13.4 (4.0)
120.72 ± 0.60	-7.18 ± 1.38	0.475 ± 0.007	13.2 (5.2)	120.45 ± 0.30	-3.63 ± 0.79	0.594 ± 0.004	11.9 (3.5)
151.94 ± 0.60	-3.46 ± 1.29	0.484 ± 0.006	7.8 (5.5)	151.37 ± 0.40	-2.96 ± 0.79	0.611 ± 0.007	3.5 (3.1)
181.08 ± 0.40	$+0.09 \pm 0.99$	0.494 ± 0.006	5.3 (5.5)	180.89 ± 0.40	$+0.80 \pm 0.79$	0.624 ± 0.008	3.2 (3.6)
210.41 ± 0.40	$+4.54 \pm 1.08$	0.494 ± 0.004	8.3 (7.0)	209.35 ± 0.40	$+2.78 \pm 0.89$	0.617 ± 0.010	5.7 (3.3)
239.49 ± 0.50	$+8.47 \pm 1.18$	0.487 ± 0.007	17.2 (4.5)	239.34 ± 0.60	$+5.42 \pm 1.19$	0.609 ± 0.009	11.5 (3.0)
271.89 ± 0.30	$+0.92 \pm 0.50$	0.477 ± 0.006	18.0 (7.5)	270.81 ± 0.40	$+2.72 \pm 0.79$	0.603 ± 0.007	18.8 (2.9)
302.78 ± 0.60	-3.93 ± 1.19	0.481 ± 0.006	10.2 (5.7)	302.57 ± 0.40	-1.82 ± 0.89	0.609 ± 0.008	10.6 (3.3)
331.61 ± 0.50	-3.43 ± 1.18	0.491 ± 0.006	12.1 (5.5)	331.97 ± 0.50	-1.77 ± 0.89	0.618 ± 0.007	10.7 (2.7)
IP = 100 m				IP = 120 m			
359.56 ± 0.40	-0.86 ± 0.79	0.714 ± 0.006	2.3 (1.8)	0.01 ± 0.40	$+0.64 \pm 0.79$	0.769 ± 0.003	2.0 (1.6)
28.33 ± 0.40	$+0.65 \pm 0.79$	0.710 ± 0.006	5.9 (2.4)	28.62 ± 0.20	$+0.32 \pm 0.49$	0.772 ± 0.005	4.3 (1.5)
57.30 ± 0.40	$+0.05 \pm 0.69$	0.694 ± 0.008	8.9 (2.3)	57.47 ± 0.20	$+0.42 \pm 0.40$	0.755 ± 0.007	9.4 (1.8)
89.52 ± 0.30	-1.07 ± 0.59	0.693 ± 0.006	9.6 (2.7)	89.80 ± 0.20	-0.04 ± 0.49	0.757 ± 0.008	12.3 (1.7)
121.24 ± 0.30	-2.71 ± 0.79	0.694 ± 0.008	3.5 (2.4)	121.72 ± 0.30	-1.69 ± 0.69	0.753 ± 0.002	3.5 (2.2)
151.23 ± 0.30	-1.83 ± 0.69	0.710 ± 0.006	3.2 (2.5)	151.57 ± 0.10	-0.79 ± 0.39	0.773 ± 0.007	2.2 (1.8)
180.44 ± 0.30	$+0.25 \pm 0.59$	0.715 ± 0.007	2.3 (2.2)	180.26 ± 0.40	-0.07 ± 0.79	0.769 ± 0.007	2.4 (1.7)
208.57 ± 0.30	$+1.32 \pm 0.59$	0.716 ± 0.008	5.3 (2.3)	208.39 ± 0.30	$+0.60 \pm 0.59$	0.774 ± 0.007	6.7 (1.7)
238.50 ± 0.30	$+2.47 \pm 0.89$	0.704 ± 0.006	10.4 (2.6)	238.21 ± 0.20	$+1.20 \pm 0.49$	0.761 ± 0.007	11.1 (1.8)
270.43 ± 0.40	$+1.72 \pm 0.79$	0.701 ± 0.007	15.4 (2.2)	270.14 ± 0.30	$+1.27 \pm 0.69$	0.765 ± 0.005	12.8 (1.7)
302.23 ± 0.30	-1.69 ± 0.69	0.706 ± 0.010	12.2 (2.1)	302.27 ± 0.20	-1.27 ± 0.49	0.769 ± 0.004	5.2 (1.9)
331.75 ± 0.30	-1.19 ± 0.59	0.716 ± 0.007	5.2 (2.4)	331.83 ± 0.30	-0.90 ± 0.50	0.781 ± 0.005	3.4 (1.7)

Table 72: The nominal angle δ_n, average displacement $\Delta\delta$, average value of the parameter DIST, RMS of the ALPHA distribution for enabled GF and impact parameters between 60 m and 120 m. The RMS of the ALPHA distribution for disabled GF is given parentheses. The primary γ-ray energy was set to 300 GeV, the ZA to 20° and the azimuth angle to 0°.

$E_\gamma = 300\,\mathrm{GeV}$, Az = 0°, ZA = 20°, Hard Image Cleaning

δ_n [°]	$\Delta\delta$ [°]	DIST [°]	$\mathrm{RMS}_{\lvert\mathrm{ALPHA}\rvert}$ [°]	δ_n [°]	$\Delta\delta$ [°]	DIST [°]	$\mathrm{RMS}_{\lvert\mathrm{ALPHA}\rvert}$ [°]
IP = 60 m				IP = 80 m			
359.48 ± 0.40	-0.17 ± 0.89	0.484 ± 0.004	3.7 (5.0)	0.47 ± 0.30	$+0.83 \pm 0.59$	0.612 ± 0.007	3.6 (2.8)
28.29 ± 0.40	$+3.19 \pm 1.28$	0.474 ± 0.007	9.0 (5.2)	28.22 ± 0.30	$+1.08 \pm 0.79$	0.600 ± 0.006	6.6 (3.0)
56.42 ± 0.50	$+2.32 \pm 0.79$	0.458 ± 0.005	15.9 (9.9)	57.27 ± 0.40	$+1.72 \pm 0.79$	0.585 ± 0.007	12.8 (2.9)
88.99 ± 0.60	-2.89 ± 0.70	0.453 ± 0.008	14.8 (5.6)	88.99 ± 0.40	-0.63 ± 0.89	0.578 ± 0.007	13.1 (3.7)
120.48 ± 0.60	-7.83 ± 1.48	0.462 ± 0.006	11.7 (5.3)	120.64 ± 0.40	-3.63 ± 0.99	0.582 ± 0.006	10.3 (3.4)
151.58 ± 0.50	-4.02 ± 1.28	0.473 ± 0.006	4.7 (6.2)	150.99 ± 0.50	-3.36 ± 0.89	0.601 ± 0.007	4.1 (3.7)
180.83 ± 0.40	-0.23 ± 0.99	0.483 ± 0.010	4.6 (6.2)	180.91 ± 0.30	$+0.62 \pm 0.59$	0.612 ± 0.001	3.2 (3.4)
209.96 ± 0.40	$+3.48 \pm 0.89$	0.482 ± 0.007	7.3 (5.1)	208.99 ± 0.40	$+2.65 \pm 0.89$	0.605 ± 0.005	5.9 (4.3)
239.56 ± 0.30	$+8.24 \pm 0.79$	0.472 ± 0.007	15.8 (5.2)	239.25 ± 0.40	$+5.89 \pm 0.69$	0.596 ± 0.010	12.8 (3.0)
271.59 ± 0.40	$+1.39 \pm 1.38$	0.462 ± 0.005	17.9 (5.1)	270.56 ± 0.20	$+2.06 \pm 0.88$	0.590 ± 0.005	15.9 (2.9)
302.51 ± 0.60	-4.53 ± 1.09	0.471 ± 0.004	10.9 (5.5)	302.34 ± 0.30	-1.79 ± 0.98	0.597 ± 0.006	6.0 (3.1)
331.53 ± 0.50	-3.77 ± 0.79	0.481 ± 0.005	5.9 (5.1)	332.02 ± 0.50	-1.62 ± 1.09	0.605 ± 0.007	10.3 (2.2)
IP = 100 m				IP = 120 m			
359.57 ± 0.40	-0.47 ± 0.79	0.705 ± 0.008	2.3 (2.1)	359.96 ± 0.30	$+0.21 \pm 0.69$	0.759 ± 0.007	1.7 (1.4)
28.03 ± 0.30	$+0.32 \pm 0.59$	0.701 ± 0.006	5.2 (2.4)	28.30 ± 0.30	$+0.08 \pm 0.59$	0.763 ± 0.007	4.6 (1.6)
57.61 ± 0.30	$+0.64 \pm 0.59$	0.687 ± 0.004	8.1 (2.1)	57.30 ± 0.20	$+0.18 \pm 0.40$	0.747 ± 0.004	10.2 (1.8)
89.24 ± 0.40	-0.37 ± 0.60	0.681 ± 0.006	12.2 (2.9)	89.64 ± 0.20	-0.11 ± 0.49	0.747 ± 0.006	10.5 (1.9)
121.34 ± 0.30	-1.90 ± 0.79	0.685 ± 0.008	4.6 (2.3)	121.82 ± 0.30	-1.32 ± 0.69	0.741 ± 0.006	3.7 (2.1)
151.44 ± 0.30	-1.59 ± 0.69	0.701 ± 0.007	2.7 (2.3)	151.54 ± 0.30	-0.92 ± 0.59	0.761 ± 0.007	2.3 (1.7)
180.50 ± 0.40	$+0.88 \pm 0.79$	0.705 ± 0.008	2.6 (2.1)	179.98 ± 0.30	$+0.13 \pm 0.60$	0.758 ± 0.007	2.6 (1.8)
208.49 ± 0.30	$+1.32 \pm 0.59$	0.707 ± 0.007	5.8 (2.2)	208.11 ± 0.30	$+0.17 \pm 0.59$	0.762 ± 0.007	6.7 (1.6)
238.40 ± 0.20	$+2.30 \pm 0.69$	0.697 ± 0.011	10.6 (2.6)	238.26 ± 0.30	$+0.56 \pm 0.59$	0.749 ± 0.007	11.6 (1.5)
270.08 ± 0.30	$+0.39 \pm 0.59$	0.692 ± 0.006	13.4 (2.2)	270.24 ± 0.40	$+0.99 \pm 0.69$	0.756 ± 0.010	11.9 (1.7)
302.41 ± 0.30	-1.09 ± 0.59	0.697 ± 0.010	4.6 (1.9)	302.48 ± 0.20	-0.35 ± 0.49	0.756 ± 0.007	3.5 (1.7)
331.70 ± 0.30	-1.29 ± 0.59	0.706 ± 0.009	4.2 (2.1)	332.00 ± 0.30	-0.02 ± 0.50	0.768 ± 0.007	3.7 (1.7)

Table 73: The nominal angle δ_n, average displacement $\Delta\delta$, average value of the parameter DIST, RMS of the ALPHA distribution for enabled GF and impact parameters between 60 m and 120 m. The RMS of the ALPHA distribution for disabled GF is given parentheses. The primary γ-ray energy was set to 300 GeV, the ZA to 20° and the azimuth angle to 0°.

$E_\gamma = 300\,\mathrm{GeV}$, Az $= 30°$, ZA $= 20°$, Intermediate Image Cleaning

$\delta_n[°]$	$\Delta\delta[°]$	DIST[°]	$\mathrm{RMS}_{\lvert\mathrm{ALPHA}\rvert}[°]$	$\delta_n[°]$	$\Delta\delta[°]$	DIST[°]	$\mathrm{RMS}_{\lvert\mathrm{ALPHA}\rvert}[°]$
IP = 60 m				**IP = 80 m**			
359.53 ± 0.40	-2.88 ± 0.90	0.509 ± 0.002	7.7 (5.3)	0.01 ± 0.40	-1.35 ± 0.80	0.636 ± 0.004	7.4 (2.6)
28.14 ± 0.40	-1.73 ± 0.80	0.498 ± 0.008	7.7 (5.8)	28.34 ± 0.40	-0.95 ± 0.80	0.619 ± 0.008	6.1 (3.2)
55.92 ± 0.40	-0.88 ± 0.80	0.495 ± 0.007	12.9 (10.7)	57.41 ± 0.40	-0.78 ± 0.80	0.614 ± 0.004	8.8 (2.9)
88.89 ± 0.50	$+1.08 \pm 1.09$	0.496 ± 0.007	13.9 (6.3)	89.21 ± 0.60	-0.09 ± 1.10	0.621 ± 0.003	11.0 (4.0)
120.72 ± 0.60	-0.25 ± 1.00	0.511 ± 0.007	12.4 (5.2)	120.45 ± 0.30	-1.48 ± 0.70	0.636 ± 0.004	9.0 (3.5)
151.94 ± 0.60	-3.14 ± 1.29	0.517 ± 0.006	10.4 (5.5)	151.37 ± 0.40	-1.75 ± 0.80	0.642 ± 0.007	9.2 (3.1)
181.08 ± 0.40	-0.99 ± 1.19	0.515 ± 0.007	7.2 (5.5)	180.89 ± 0.40	$+0.49 \pm 0.80$	0.638 ± 0.002	5.6 (3.6)
210.41 ± 0.40	$+0.23 \pm 0.90$	0.502 ± 0.007	7.8 (7.0)	209.35 ± 0.40	$+0.13 \pm 0.80$	0.627 ± 0.007	5.0 (3.3)
239.49 ± 0.50	$+3.89 \pm 1.00$	0.496 ± 0.005	12.9 (4.5)	239.34 ± 0.60	$+2.17 \pm 0.90$	0.622 ± 0.007	8.6 (3.0)
271.89 ± 0.30	$+6.67 \pm 0.89$	0.503 ± 0.007	15.4 (7.5)	270.81 ± 0.40	$+3.68 \pm 0.90$	0.633 ± 0.009	11.2 (2.9)
302.78 ± 0.60	$+3.94 \pm 1.19$	0.517 ± 0.007	11.1 (5.7)	302.57 ± 0.40	$+2.48 \pm 0.70$	0.645 ± 0.007	9.2 (3.3)
331.61 ± 0.50	-3.25 ± 0.80	0.520 ± 0.006	11.2 (5.5)	331.97 ± 0.50	-1.04 ± 0.90	0.648 ± 0.006	7.6 (2.7)
IP = 100 m				**IP = 120 m**			
359.56 ± 0.40	-1.00 ± 0.80	0.732 ± 0.007	4.0 (1.8)	0.01 ± 0.40	$+0.34 \pm 0.60$	0.785 ± 0.003	3.2 (1.6)
28.33 ± 0.40	-1.46 ± 0.70	0.710 ± 0.005	5.1 (2.4)	28.62 ± 0.20	-0.56 ± 0.50	0.770 ± 0.005	3.2 (1.5)
57.30 ± 0.40	-1.17 ± 0.70	0.713 ± 0.005	7.0 (2.3)	57.47 ± 0.20	-0.52 ± 0.40	0.774 ± 0.003	6.0 (1.8)
89.52 ± 0.30	$+0.78 \pm 0.50$	0.713 ± 0.005	6.3 (2.7)	89.80 ± 0.20	$+0.14 \pm 0.40$	0.763 ± 0.005	4.4 (1.7)
121.24 ± 0.30	-1.57 ± 0.79	0.731 ± 0.002	5.6 (2.4)	121.72 ± 0.30	-1.15 ± 0.70	0.774 ± 0.005	4.0 (2.2)
151.23 ± 0.30	-1.04 ± 0.40	0.737 ± 0.002	5.6 (2.5)	151.57 ± 0.10	-0.82 ± 0.40	0.781 ± 0.004	4.1 (1.8)
180.44 ± 0.30	-0.19 ± 0.60	0.737 ± 0.004	4.1 (2.2)	180.26 ± 0.40	-0.29 ± 0.80	0.798 ± 0.008	3.5 (1.7)
208.57 ± 0.30	-0.16 ± 0.60	0.723 ± 0.009	4.2 (2.3)	208.39 ± 0.30	$+0.22 \pm 0.60$	0.780 ± 0.003	3.6 (1.7)
238.50 ± 0.30	$+1.10 \pm 0.70$	0.723 ± 0.001	6.2 (2.6)	238.21 ± 0.20	$+0.74 \pm 0.40$	0.780 ± 0.006	4.6 (1.8)
270.43 ± 0.40	$+1.36 \pm 0.80$	0.725 ± 0.005	8.8 (2.2)	270.14 ± 0.30	$+1.05 \pm 0.70$	0.773 ± 0.007	6.7 (1.7)
302.23 ± 0.30	$+0.93 \pm 0.70$	0.738 ± 0.004	6.8 (2.1)	302.27 ± 0.20	$+1.22 \pm 0.50$	0.784 ± 0.006	5.7 (1.9)
331.75 ± 0.30	-0.69 ± 0.60	0.740 ± 0.008	5.0 (2.4)	331.83 ± 0.30	$+0.62 \pm 0.60$	0.780 ± 0.007	4.0 (1.7)

Table 74: The nominal angle δ_n, average displacement $\Delta\delta$, average value of the parameter DIST, RMS of the ALPHA distribution for enabled GF and impact parameters between 60 m and 120 m. The RMS of the ALPHA distribution for disabled GF is given parentheses. The primary γ-ray energy was set to 300 GeV, the ZA to 20° and the azimuth angle to 30°.

$E_\gamma = 300\,\mathrm{GeV}$, Az $= 30°$, ZA $= 20°$, Hard Image Cleaning

$\delta_n[°]$	$\Delta\delta[°]$	DIST[°]	$\mathrm{RMS}_{\lvert\mathrm{ALPHA}\rvert}[°]$	$\delta_n[°]$	$\Delta\delta[°]$	DIST[°]	$\mathrm{RMS}_{\lvert\mathrm{ALPHA}\rvert}[°]$
IP = 60 m				**IP = 80 m**			
359.48 ± 0.40	-3.32 ± 1.09	0.499 ± 0.002	6.9 (5.0)	0.47 ± 0.30	-1.67 ± 0.60	0.624 ± 0.007	7.0 (2.8)
28.29 ± 0.40	-1.15 ± 0.80	0.486 ± 0.003	7.3 (5.2)	28.22 ± 0.30	-0.74 ± 0.70	0.607 ± 0.004	6.1 (3.0)
56.42 ± 0.50	-0.55 ± 1.00	0.480 ± 0.007	10.9 (9.9)	57.27 ± 0.40	-0.94 ± 0.70	0.601 ± 0.007	8.9 (2.9)
88.99 ± 0.60	$+0.41 \pm 1.19$	0.481 ± 0.002	13.0 (5.6)	88.99 ± 0.40	-0.30 ± 0.99	0.610 ± 0.004	9.8 (3.7)
120.48 ± 0.60	-2.11 ± 1.00	0.499 ± 0.007	12.6 (5.3)	120.64 ± 0.40	-1.76 ± 0.99	0.626 ± 0.004	8.5 (3.4)
151.58 ± 0.50	-2.06 ± 1.19	0.504 ± 0.006	10.7 (6.2)	150.99 ± 0.50	-2.34 ± 0.90	0.635 ± 0.009	7.8 (3.7)
180.83 ± 0.40	-1.03 ± 0.99	0.501 ± 0.005	7.3 (6.2)	180.91 ± 0.30	-0.34 ± 0.70	0.628 ± 0.003	5.4 (3.4)
209.96 ± 0.40	$+0.25 \pm 0.80$	0.490 ± 0.005	8.0 (5.1)	208.99 ± 0.40	-0.34 ± 0.80	0.617 ± 0.003	5.2 (4.3)
239.56 ± 0.30	$+3.47 \pm 0.79$	0.484 ± 0.005	12.4 (5.2)	239.25 ± 0.40	$+1.93 \pm 0.80$	0.611 ± 0.005	7.9 (3.0)
271.59 ± 0.40	$+6.98 \pm 0.99$	0.492 ± 0.007	14.9 (5.1)	270.56 ± 0.20	$+3.12 \pm 0.60$	0.622 ± 0.007	10.2 (2.9)
302.51 ± 0.60	$+3.15 \pm 1.59$	0.506 ± 0.008	11.5 (5.5)	302.34 ± 0.30	$+1.79 \pm 0.70$	0.633 ± 0.003	7.5 (3.1)
331.53 ± 0.50	-1.84 ± 1.00	0.507 ± 0.007	10.7 (5.1)	332.02 ± 0.50	-2.13 ± 0.90	0.637 ± 0.006	6.5 (2.2)
IP = 100 m				**IP = 120 m**			
359.57 ± 0.40	-1.00 ± 0.80	0.722 ± 0.002	4.1 (2.1)	359.96 ± 0.30	$+0.32 \pm 0.70$	0.775 ± 0.002	3.3 (1.4)
28.03 ± 0.30	-1.56 ± 0.60	0.703 ± 0.004	4.5 (2.4)	28.30 ± 0.30	-0.71 ± 0.60	0.759 ± 0.007	3.4 (1.6)
57.61 ± 0.30	-0.86 ± 0.70	0.701 ± 0.007	5.6 (2.1)	57.30 ± 0.30	-1.04 ± 0.50	0.763 ± 0.009	5.7 (1.8)
89.24 ± 0.40	-0.79 ± 0.80	0.704 ± 0.008	6.9 (2.9)	89.64 ± 0.20	-0.54 ± 0.50	0.753 ± 0.004	4.3 (1.9)
121.34 ± 0.30	-1.15 ± 0.70	0.719 ± 0.005	5.8 (2.3)	121.82 ± 0.30	-0.97 ± 0.70	0.760 ± 0.005	4.3 (2.1)
151.44 ± 0.30	-1.17 ± 0.60	0.726 ± 0.003	4.8 (2.3)	151.54 ± 0.30	-1.05 ± 0.60	0.769 ± 0.004	4.5 (1.7)
180.50 ± 0.40	$+0.10 \pm 0.80$	0.729 ± 0.005	4.4 (2.1)	179.98 ± 0.30	-0.17 ± 0.70	0.789 ± 0.005	3.8 (1.8)
208.49 ± 0.30	-0.67 ± 0.60	0.711 ± 0.008	3.8 (2.2)	208.11 ± 0.30	-0.10 ± 0.60	0.767 ± 0.004	3.6 (1.6)
238.40 ± 0.20	$+1.02 \pm 0.50$	0.713 ± 0.002	6.2 (2.6)	238.26 ± 0.30	$+0.89 \pm 0.70$	0.770 ± 0.004	4.5 (1.5)
270.08 ± 0.30	$+1.43 \pm 0.70$	0.714 ± 0.005	8.9 (2.2)	270.24 ± 0.40	$+1.04 \pm 0.80$	0.764 ± 0.005	5.9 (1.7)
302.41 ± 0.30	$+1.06 \pm 0.70$	0.729 ± 0.007	6.6 (1.9)	302.48 ± 0.20	$+1.01 \pm 0.60$	0.770 ± 0.004	4.6 (1.7)
331.70 ± 0.30	-0.45 ± 0.70	0.729 ± 0.005	4.9 (2.1)	332.00 ± 0.30	$+0.92 \pm 0.70$	0.771 ± 0.004	3.6 (1.7)

Table 75: The nominal angle δ_n, average displacement $\Delta\delta$, average value of the parameter DIST, RMS of the ALPHA distribution for enabled GF and impact parameters between 60 m and 120 m. The RMS of the ALPHA distribution for disabled GF is given parentheses. The primary γ-ray energy was set to 300 GeV, the ZA to 20° and the azimuth angle to 30°.

$E_\gamma = 300\,\mathrm{GeV}$, Az = 60°, ZA = 20°, Intermediate Image Cleaning

$\delta_n\,[°]$	$\Delta\delta\,[°]$	DIST[°]	$\mathrm{RMS}_{\lvert\mathrm{ALPHA}\rvert}\,[°]$	$\delta_n\,[°]$	$\Delta\delta\,[°]$	DIST[°]	$\mathrm{RMS}_{\lvert\mathrm{ALPHA}\rvert}\,[°]$
IP = 60 m				IP = 80 m			
359.53 ± 0.40	-4.83 ± 1.39	0.499 ± 0.007	10.0 (5.3)	0.01 ± 0.40	-2.54 ± 0.99	0.620 ± 0.007	5.1 (2.6)
28.14 ± 0.40	-3.93 ± 0.79	0.491 ± 0.007	8.4 (5.8)	28.34 ± 0.40	-1.58 ± 0.89	0.611 ± 0.008	5.4 (3.2)
55.92 ± 0.40	-4.44 ± 1.09	0.499 ± 0.007	11.6 (10.7)	57.41 ± 0.40	-2.99 ± 0.79	0.622 ± 0.008	9.3 (2.9)
88.89 ± 0.50	$+0.50 \pm 0.90$	0.517 ± 0.007	15.9 (6.3)	89.21 ± 0.60	$+0.94 \pm 1.00$	0.645 ± 0.005	11.6 (4.0)
120.72 ± 0.60	$+3.73 \pm 1.00$	0.523 ± 0.008	15.2 (5.2)	120.45 ± 0.30	-0.26 ± 0.89	0.653 ± 0.009	12.0 (3.5)
151.94 ± 0.60	$+4.84 \pm 0.90$	0.514 ± 0.006	12.8 (5.5)	151.37 ± 0.40	$+0.66 \pm 0.99$	0.646 ± 0.005	12.7 (3.1)
181.08 ± 0.40	-0.61 ± 0.80	0.502 ± 0.009	8.3 (5.5)	180.89 ± 0.40	$+0.11 \pm 0.80$	0.626 ± 0.005	7.1 (3.6)
210.41 ± 0.40	-3.59 ± 0.90	0.496 ± 0.003	7.3 (7.0)	209.35 ± 0.40	-2.32 ± 1.19	0.621 ± 0.007	6.2 (3.3)
239.49 ± 0.50	-0.91 ± 1.09	0.506 ± 0.007	12.8 (4.5)	239.34 ± 0.60	-0.25 ± 1.10	0.631 ± 0.007	9.3 (3.0)
271.89 ± 0.30	$+3.74 \pm 0.90$	0.522 ± 0.005	13.2 (7.5)	270.81 ± 0.40	$+1.86 \pm 0.70$	0.652 ± 0.003	10.8 (2.9)
302.78 ± 0.60	$+5.27 \pm 1.19$	0.526 ± 0.007	15.1 (5.7)	302.57 ± 0.40	$+2.95 \pm 1.19$	0.656 ± 0.008	10.9 (3.3)
331.61 ± 0.50	$+3.47 \pm 0.99$	0.521 ± 0.006	12.8 (5.5)	331.97 ± 0.50	$+3.58 \pm 0.99$	0.649 ± 0.003	9.1 (2.7)
IP = 100 m				IP = 120 m			
359.56 ± 0.40	-0.05 ± 0.89	0.713 ± 0.004	6.3 (1.8)	0.01 ± 0.40	$+0.47 \pm 0.80$	0.783 ± 0.003	5.7 (1.6)
28.33 ± 0.40	$+0.35 \pm 0.89$	0.710 ± 0.007	5.5 (2.4)	28.62 ± 0.20	$+0.28 \pm 0.50$	0.780 ± 0.004	5.5 (1.5)
57.30 ± 0.40	-2.61 ± 0.70	0.718 ± 0.006	8.8 (2.3)	57.47 ± 0.20	-0.71 ± 0.50	0.781 ± 0.002	5.4 (1.8)
89.52 ± 0.30	$+1.08 \pm 0.60$	0.740 ± 0.009	7.7 (2.7)	89.80 ± 0.20	-0.17 ± 0.40	0.788 ± 0.007	5.8 (1.7)
121.24 ± 0.30	-0.20 ± 0.69	0.749 ± 0.007	8.6 (2.4)	121.72 ± 0.30	$+0.22 \pm 0.60$	0.785 ± 0.007	6.5 (2.2)
151.23 ± 0.30	$+0.26 \pm 0.60$	0.749 ± 0.007	8.5 (2.5)	151.57 ± 0.10	-0.59 ± 0.49	0.805 ± 0.012	5.3 (1.8)
180.44 ± 0.30	-1.24 ± 0.89	0.728 ± 0.007	4.9 (2.2)	180.26 ± 0.40	$+0.74 \pm 0.80$	0.790 ± 0.011	4.7 (1.7)
208.57 ± 0.30	-1.18 ± 0.70	0.725 ± 0.007	4.5 (2.3)	208.39 ± 0.30	$+0.80 \pm 0.60$	0.794 ± 0.003	4.0 (1.7)
238.50 ± 0.30	-0.39 ± 0.79	0.735 ± 0.007	6.9 (2.6)	238.21 ± 0.20	-0.30 ± 0.50	0.791 ± 0.005	5.0 (1.8)
270.43 ± 0.40	$+1.52 \pm 0.60$	0.752 ± 0.005	7.1 (2.2)	270.14 ± 0.30	$+1.19 \pm 0.50$	0.795 ± 0.006	5.4 (1.7)
302.23 ± 0.30	$+2.82 \pm 0.79$	0.752 ± 0.008	7.4 (2.1)	302.27 ± 0.20	$+0.54 \pm 0.50$	0.787 ± 0.006	5.8 (1.9)
331.75 ± 0.30	$+1.92 \pm 0.79$	0.743 ± 0.007	6.0 (2.4)	331.83 ± 0.30	$+1.80 \pm 0.60$	0.798 ± 0.007	5.6 (1.7)

Table 76: The nominal angle δ_n, average displacement $\Delta\delta$, average value of the parameter DIST, RMS of the ALPHA distribution for enabled GF and impact parameters between 60 m and 120 m. The RMS of the ALPHA distribution for disabled GF is given parentheses. The primary γ-ray energy was set to 300 GeV, the ZA to 20° and the azimuth angle to 60°.

$E_\gamma = 300\,\mathrm{GeV}$, Az = 60°, ZA = 20°, Hard Image Cleaning

$\delta_n\,[°]$	$\Delta\delta\,[°]$	DIST[°]	$\mathrm{RMS}_{\lvert\mathrm{ALPHA}\rvert}\,[°]$	$\delta_n\,[°]$	$\Delta\delta\,[°]$	DIST[°]	$\mathrm{RMS}_{\lvert\mathrm{ALPHA}\rvert}\,[°]$
IP = 60 m				IP = 80 m			
359.48 ± 0.40	-5.03 ± 0.50	0.487 ± 0.008	8.6 (5.0)	0.47 ± 0.30	-1.17 ± 0.70	0.607 ± 0.006	5.5 (2.8)
28.29 ± 0.40	-3.92 ± 0.89	0.479 ± 0.005	8.8 (5.2)	28.22 ± 0.30	-1.25 ± 0.69	0.599 ± 0.008	5.9 (3.0)
56.42 ± 0.50	-3.74 ± 1.19	0.488 ± 0.006	10.3 (9.9)	57.27 ± 0.40	-2.03 ± 0.89	0.612 ± 0.006	7.9 (2.9)
88.99 ± 0.60	-0.43 ± 0.80	0.505 ± 0.007	14.4 (5.6)	88.99 ± 0.40	$+1.03 \pm 0.89$	0.635 ± 0.006	10.0 (3.7)
120.48 ± 0.60	$+3.40 \pm 1.00$	0.510 ± 0.007	15.2 (5.3)	120.64 ± 0.40	$+1.10 \pm 0.89$	0.643 ± 0.009	11.7 (3.4)
151.58 ± 0.50	$+4.89 \pm 1.39$	0.502 ± 0.004	11.8 (6.2)	150.99 ± 0.50	$+0.50 \pm 1.00$	0.635 ± 0.004	11.4 (3.7)
180.83 ± 0.40	-3.42 ± 0.99	0.493 ± 0.005	8.3 (6.2)	180.91 ± 0.30	-1.40 ± 0.99	0.619 ± 0.005	6.1 (3.4)
209.96 ± 0.40	-2.73 ± 0.99	0.487 ± 0.004	6.3 (5.1)	208.99 ± 0.40	-2.44 ± 1.00	0.610 ± 0.008	5.0 (4.3)
239.56 ± 0.30	-0.34 ± 0.89	0.496 ± 0.007	11.9 (5.2)	239.25 ± 0.40	-0.14 ± 0.90	0.624 ± 0.007	10.3 (3.0)
271.59 ± 0.40	$+2.94 \pm 0.80$	0.512 ± 0.006	12.4 (5.1)	270.56 ± 0.20	$+1.85 \pm 0.69$	0.643 ± 0.007	10.2 (2.9)
302.51 ± 0.60	$+4.85 \pm 1.49$	0.515 ± 0.007	13.8 (5.5)	302.34 ± 0.30	$+2.84 \pm 0.99$	0.649 ± 0.007	10.9 (3.1)
331.53 ± 0.50	$+5.01 \pm 1.09$	0.505 ± 0.007	11.7 (5.1)	332.02 ± 0.50	$+3.27 \pm 0.90$	0.638 ± 0.004	8.2 (2.2)
IP = 100 m				IP = 120 m			
359.57 ± 0.40	$+0.22 \pm 0.80$	0.703 ± 0.006	6.1 (2.1)	359.96 ± 0.30	$+0.17 \pm 0.80$	0.775 ± 0.002	4.7 (1.4)
28.03 ± 0.30	-0.98 ± 0.79	0.698 ± 0.007	5.4 (2.4)	28.30 ± 0.30	$+0.52 \pm 0.60$	0.770 ± 0.005	3.6 (1.6)
57.61 ± 0.30	-1.82 ± 0.60	0.709 ± 0.004	8.0 (2.1)	57.30 ± 0.20	-1.06 ± 0.50	0.770 ± 0.008	5.7 (1.8)
89.24 ± 0.40	$+0.80 \pm 0.70$	0.728 ± 0.009	7.9 (2.9)	89.64 ± 0.20	-0.57 ± 0.40	0.775 ± 0.006	5.5 (1.9)
121.34 ± 0.30	-0.41 ± 0.69	0.736 ± 0.007	8.4 (2.3)	121.82 ± 0.30	-0.09 ± 0.50	0.773 ± 0.010	5.8 (2.1)
151.44 ± 0.30	-0.41 ± 0.89	0.741 ± 0.007	8.1 (2.3)	151.54 ± 0.30	-0.28 ± 0.60	0.794 ± 0.008	5.4 (1.7)
180.50 ± 0.40	$+0.91 \pm 0.99$	0.720 ± 0.006	6.9 (2.1)	179.98 ± 0.30	-0.01 ± 0.70	0.784 ± 0.010	3.9 (1.8)
208.49 ± 0.30	-1.58 ± 0.80	0.714 ± 0.007	5.4 (2.2)	208.11 ± 0.30	$+0.66 \pm 0.60$	0.781 ± 0.007	4.1 (1.6)
238.40 ± 0.20	-0.26 ± 0.69	0.726 ± 0.007	6.4 (2.6)	238.26 ± 0.30	$+0.42 \pm 0.60$	0.780 ± 0.008	5.2 (1.5)
270.08 ± 0.30	$+1.00 \pm 0.60$	0.743 ± 0.010	7.0 (2.2)	270.24 ± 0.40	$+1.04 \pm 0.60$	0.780 ± 0.004	5.3 (1.7)
302.41 ± 0.30	$+1.77 \pm 0.79$	0.739 ± 0.004	6.2 (1.9)	302.48 ± 0.20	$+0.68 \pm 0.50$	0.775 ± 0.005	5.5 (1.7)
331.70 ± 0.30	$+0.72 \pm 0.89$	0.731 ± 0.007	6.0 (2.1)	332.00 ± 0.30	$+1.91 \pm 0.50$	0.786 ± 0.007	5.0 (1.7)

Table 77: The nominal angle δ_n, average displacement $\Delta\delta$, average value of the parameter DIST, RMS of the ALPHA distribution for enabled GF and impact parameters between 60 m and 120 m. The RMS of the ALPHA distribution for disabled GF is given parentheses. The primary γ-ray energy was set to 300 GeV, the ZA to 20° and the azimuth angle to 60°.

$E_\gamma = 300\,\mathrm{GeV}$, Az = 90°, ZA = 20°, Intermediate Image Cleaning

δ_n[°]	$\Delta\delta$[°]	DIST[°]	$\mathrm{RMS}_{\vert\mathrm{ALPHA}\vert}$[°]	δ_n[°]	$\Delta\delta$[°]	DIST[°]	$\mathrm{RMS}_{\vert\mathrm{ALPHA}\vert}$[°]
IP = 60 m				IP = 80 m			
359.53 ± 0.40	$+4.48 \pm 0.98$	0.469 ± 0.007	7.6 (5.3)	0.01 ± 0.40	$+2.40 \pm 1.17$	0.595 ± 0.006	4.2 (2.6)
28.14 ± 0.40	-4.76 ± 0.69	0.475 ± 0.008	6.7 (5.8)	28.34 ± 0.40	-1.93 ± 1.27	0.600 ± 0.006	4.8 (3.2)
55.92 ± 0.40	-9.41 ± 1.17	0.492 ± 0.008	14.7 (10.7)	57.41 ± 0.40	-4.27 ± 0.69	0.622 ± 0.008	10.6 (2.9)
88.89 ± 0.50	-4.91 ± 1.08	0.507 ± 0.007	20.8 (6.3)	89.21 ± 0.60	-2.96 ± 0.99	0.634 ± 0.009	13.2 (4.0)
120.72 ± 0.60	$+3.17 \pm 1.28$	0.504 ± 0.007	20.0 (5.2)	120.45 ± 0.30	$+0.42 \pm 0.78$	0.631 ± 0.008	11.1 (3.5)
151.94 ± 0.60	$+9.47 \pm 1.47$	0.489 ± 0.004	15.8 (5.5)	151.37 ± 0.40	$+2.82 \pm 0.79$	0.615 ± 0.003	9.1 (3.1)
181.08 ± 0.40	$+2.77 \pm 0.98$	0.478 ± 0.007	6.6 (5.5)	180.89 ± 0.40	$+2.41 \pm 0.88$	0.605 ± 0.008	5.2 (3.6)
210.41 ± 0.40	-4.25 ± 1.17	0.484 ± 0.006	5.9 (7.0)	209.35 ± 0.40	-2.66 ± 0.69	0.612 ± 0.009	4.2 (3.3)
239.49 ± 0.50	-7.05 ± 1.08	0.504 ± 0.007	13.7 (4.5)	239.34 ± 0.60	-2.52 ± 1.08	0.628 ± 0.008	9.5 (3.0)
271.89 ± 0.30	-0.39 ± 0.69	0.513 ± 0.007	21.5 (7.5)	270.81 ± 0.40	-1.25 ± 0.79	0.634 ± 0.007	11.7 (2.9)
302.78 ± 0.60	$+4.56 \pm 1.18$	0.499 ± 0.006	20.5 (5.7)	302.57 ± 0.40	$+2.96 \pm 0.88$	0.626 ± 0.009	13.1 (3.3)
331.61 ± 0.50	$+9.85 \pm 1.27$	0.480 ± 0.006	16.7 (5.5)	331.97 ± 0.50	$+5.27 \pm 0.89$	0.604 ± 0.010	9.7 (2.7)
IP = 100 m				IP = 120 m			
359.56 ± 0.40	$+0.85 \pm 1.08$	0.697 ± 0.006	2.9 (1.8)	0.01 ± 0.40	$+0.72 \pm 0.69$	0.772 ± 0.011	2.5 (1.6)
28.33 ± 0.40	-0.55 ± 0.79	0.697 ± 0.010	3.1 (2.4)	28.62 ± 0.20	$+0.86 \pm 0.49$	0.767 ± 0.006	3.0 (1.5)
57.30 ± 0.40	-2.68 ± 0.89	0.718 ± 0.008	6.3 (2.3)	57.47 ± 0.20	-0.71 ± 0.59	0.778 ± 0.008	4.9 (1.8)
89.52 ± 0.30	-1.50 ± 0.69	0.726 ± 0.009	5.9 (2.7)	89.80 ± 0.20	-0.82 ± 0.49	0.765 ± 0.006	4.2 (1.7)
121.24 ± 0.30	$+0.66 \pm 0.59$	0.728 ± 0.006	6.5 (2.4)	121.72 ± 0.30	$+0.32 \pm 0.59$	0.770 ± 0.006	4.3 (2.2)
151.23 ± 0.30	$+0.41 \pm 0.78$	0.709 ± 0.008	6.4 (2.5)	151.57 ± 0.10	$+0.58 \pm 0.29$	0.772 ± 0.007	4.7 (1.8)
180.44 ± 0.30	$+0.26 \pm 0.98$	0.703 ± 0.012	3.4 (2.2)	180.26 ± 0.40	-0.23 ± 0.79	0.780 ± 0.009	2.7 (1.7)
208.57 ± 0.30	-0.83 ± 0.88	0.711 ± 0.011	3.3 (2.3)	208.39 ± 0.30	-0.48 ± 0.78	0.779 ± 0.006	2.1 (1.7)
238.50 ± 0.30	-2.44 ± 0.69	0.725 ± 0.006	5.4 (2.6)	238.21 ± 0.20	-0.82 ± 0.59	0.788 ± 0.010	3.8 (1.8)
270.43 ± 0.40	-0.77 ± 0.88	0.725 ± 0.007	7.9 (2.2)	270.14 ± 0.30	-0.26 ± 0.49	0.767 ± 0.003	5.1 (1.7)
302.23 ± 0.30	$+1.83 \pm 0.69$	0.724 ± 0.007	7.7 (2.1)	302.27 ± 0.20	$+0.61 \pm 0.49$	0.772 ± 0.009	6.7 (1.9)
331.75 ± 0.30	$+2.09 \pm 0.88$	0.706 ± 0.010	4.8 (2.4)	331.83 ± 0.30	$+0.79 \pm 0.59$	0.767 ± 0.010	3.9 (1.7)

Table 78: The nominal angle δ_n, average displacement $\Delta\delta$, average value of the parameter DIST, RMS of the ALPHA distribution for enabled GF and impact parameters between 60 m and 120 m. The RMS of the ALPHA distribution for disabled GF is given parentheses. The primary γ-ray energy was set to 300 GeV, the ZA to 20° and the azimuth angle to 90°.

$E_\gamma = 300\,\mathrm{GeV}$, Az = 90°, ZA = 20°, Hard Image Cleaning

δ_n[°]	$\Delta\delta$[°]	DIST[°]	$\mathrm{RMS}_{\vert\mathrm{ALPHA}\vert}$[°]	δ_n[°]	$\Delta\delta$[°]	DIST[°]	$\mathrm{RMS}_{\vert\mathrm{ALPHA}\vert}$[°]
IP = 60 m				IP = 80 m			
359.48 ± 0.40	$+3.82 \pm 1.37$	0.460 ± 0.005	6.9 (5.0)	0.47 ± 0.30	$+4.18 \pm 1.17$	0.585 ± 0.006	4.4 (2.8)
28.29 ± 0.40	-3.85 ± 1.17	0.466 ± 0.006	6.3 (5.2)	28.22 ± 0.30	-1.53 ± 0.69	0.590 ± 0.005	4.7 (3.0)
56.42 ± 0.50	-10.30 ± 0.98	0.480 ± 0.007	16.0 (9.9)	57.27 ± 0.40	-4.37 ± 0.88	0.611 ± 0.007	10.4 (2.9)
88.99 ± 0.60	-4.02 ± 1.28	0.494 ± 0.006	20.3 (5.6)	88.99 ± 0.40	-2.78 ± 0.69	0.621 ± 0.006	11.1 (3.7)
120.48 ± 0.60	$+3.04 \pm 1.18$	0.491 ± 0.004	19.7 (5.3)	120.64 ± 0.40	$+0.73 \pm 0.79$	0.619 ± 0.008	10.8 (3.4)
151.58 ± 0.50	$+7.06 \pm 1.08$	0.478 ± 0.005	15.1 (6.2)	150.99 ± 0.50	$+2.97 \pm 0.98$	0.606 ± 0.007	8.0 (3.7)
180.83 ± 0.40	$+4.47 \pm 0.79$	0.468 ± 0.007	7.2 (6.2)	180.91 ± 0.30	$+2.48 \pm 0.88$	0.594 ± 0.006	4.3 (3.4)
209.96 ± 0.40	-3.50 ± 0.50	0.473 ± 0.006	6.3 (5.1)	208.99 ± 0.40	-2.45 ± 0.98	0.600 ± 0.010	4.2 (4.3)
239.56 ± 0.30	-6.77 ± 0.88	0.492 ± 0.006	14.6 (5.2)	239.25 ± 0.40	-2.99 ± 1.08	0.616 ± 0.008	10.1 (3.0)
271.59 ± 0.40	-0.77 ± 0.88	0.499 ± 0.006	20.1 (5.1)	270.56 ± 0.20	-1.24 ± 0.59	0.622 ± 0.007	13.1 (2.9)
302.51 ± 0.60	$+4.38 \pm 1.08$	0.487 ± 0.006	20.0 (5.5)	302.34 ± 0.30	$+2.75 \pm 0.59$	0.615 ± 0.002	13.5 (3.1)
331.53 ± 0.50	$+9.36 \pm 1.18$	0.467 ± 0.006	15.6 (5.1)	332.02 ± 0.50	$+5.69 \pm 0.60$	0.594 ± 0.009	10.0 (2.2)
IP = 100 m				IP = 120 m			
359.57 ± 0.40	$+0.42 \pm 1.08$	0.686 ± 0.009	2.5 (2.1)	359.96 ± 0.30	$+0.72 \pm 0.69$	0.757 ± 0.010	2.4 (1.4)
28.03 ± 0.30	-0.12 ± 0.98	0.686 ± 0.010	2.9 (2.4)	28.30 ± 0.30	$+0.37 \pm 0.69$	0.756 ± 0.007	2.8 (1.6)
57.61 ± 0.30	-2.31 ± 0.78	0.708 ± 0.009	5.3 (2.1)	57.30 ± 0.20	-0.70 ± 0.49	0.766 ± 0.003	4.8 (1.8)
89.24 ± 0.40	-1.77 ± 0.79	0.714 ± 0.009	6.9 (2.9)	89.64 ± 0.20	-0.93 ± 0.49	0.752 ± 0.006	4.4 (1.9)
121.34 ± 0.30	$+0.75 \pm 0.69$	0.717 ± 0.010	6.4 (2.3)	121.82 ± 0.30	$+0.36 \pm 0.59$	0.759 ± 0.006	4.5 (2.1)
151.44 ± 0.30	$+0.12 \pm 0.78$	0.700 ± 0.009	6.0 (2.3)	151.54 ± 0.30	$+0.56 \pm 0.49$	0.761 ± 0.008	4.6 (1.7)
180.50 ± 0.40	-0.51 ± 0.98	0.695 ± 0.010	3.1 (2.1)	179.98 ± 0.30	-0.37 ± 0.79	0.767 ± 0.002	2.4 (1.8)
208.49 ± 0.30	-1.15 ± 0.69	0.697 ± 0.006	3.3 (2.2)	208.11 ± 0.30	-0.68 ± 0.59	0.768 ± 0.007	2.5 (1.6)
238.40 ± 0.20	-2.82 ± 0.68	0.714 ± 0.006	5.7 (2.6)	238.26 ± 0.30	-0.92 ± 0.78	0.776 ± 0.008	4.1 (1.5)
270.08 ± 0.30	-0.66 ± 0.59	0.715 ± 0.008	7.3 (2.2)	270.24 ± 0.40	-0.17 ± 0.59	0.753 ± 0.003	5.2 (1.7)
302.41 ± 0.30	$+1.60 \pm 0.78$	0.713 ± 0.007	8.5 (1.9)	302.48 ± 0.20	$+0.65 \pm 0.49$	0.760 ± 0.010	6.0 (1.7)
331.70 ± 0.30	$+2.15 \pm 0.88$	0.694 ± 0.009	5.3 (2.1)	332.00 ± 0.30	$+1.37 \pm 0.59$	0.757 ± 0.009	4.0 (1.7)

Table 79: The nominal angle δ_n, average displacement $\Delta\delta$, average value of the parameter DIST, RMS of the ALPHA distribution for enabled GF and impact parameters between 60 m and 120 m. The RMS of the ALPHA distribution for disabled GF is given parentheses. The primary γ-ray energy was set to 300 GeV, the ZA to 20° and the azimuth angle to 90°.

$E_\gamma = 300\,\mathrm{GeV}$, Az = 120°, ZA = 20°, Intermediate Image Cleaning

δ_n[°]	$\Delta\delta$[°]	DIST[°]	$\mathrm{RMS}_{\lvert\mathrm{ALPHA}\rvert}$[°]	δ_n[°]	$\Delta\delta$[°]	DIST[°]	$\mathrm{RMS}_{\lvert\mathrm{ALPHA}\rvert}$[°]
IP = 60 m				IP = 80 m			
359.53 ± 0.40	+7.22 ± 0.69	0.503 ± 0.007	8.2 (5.3)	0.01 ± 0.40	+5.65 ± 0.79	0.615 ± 0.005	5.9 (2.6)
28.14 ± 0.40	−2.73 ± 0.69	0.514 ± 0.006	9.8 (5.8)	28.34 ± 0.40	+1.04 ± 0.99	0.630 ± 0.007	7.4 (3.2)
55.92 ± 0.40	−7.73 ± 1.28	0.520 ± 0.007	15.2 (10.7)	57.41 ± 0.40	−7.39 ± 1.18	0.639 ± 0.005	12.7 (2.9)
88.89 ± 0.50	−7.94 ± 1.18	0.514 ± 0.007	16.1 (6.3)	89.21 ± 0.60	−5.58 ± 1.19	0.639 ± 0.006	13.5 (4.0)
120.72 ± 0.60	−2.07 ± 1.09	0.499 ± 0.004	15.3 (5.2)	120.45 ± 0.30	−2.80 ± 0.50	0.622 ± 0.003	11.8 (3.5)
151.94 ± 0.60	+5.06 ± 1.09	0.491 ± 0.008	13.5 (5.5)	151.37 ± 0.40	+3.77 ± 0.89	0.609 ± 0.009	11.6 (3.1)
181.08 ± 0.40	+9.07 ± 0.99	0.494 ± 0.003	8.3 (5.5)	180.89 ± 0.40	+6.97 ± 0.99	0.611 ± 0.011	6.9 (3.6)
210.41 ± 0.40	+5.47 ± 0.89	0.507 ± 0.003	11.1 (7.0)	209.35 ± 0.40	+4.30 ± 0.89	0.629 ± 0.007	8.7 (3.3)
239.49 ± 0.50	−3.87 ± 1.28	0.512 ± 0.007	15.7 (4.5)	239.34 ± 0.60	+0.57 ± 1.38	0.638 ± 0.001	11.8 (3.0)
271.89 ± 0.30	−4.16 ± 0.89	0.511 ± 0.007	15.6 (7.5)	270.81 ± 0.40	−4.19 ± 0.99	0.640 ± 0.006	11.7 (2.9)
302.78 ± 0.60	−0.42 ± 0.99	0.499 ± 0.006	15.7 (5.7)	302.57 ± 0.40	+1.34 ± 0.79	0.624 ± 0.008	12.3 (3.3)
331.61 ± 0.50	+1.29 ± 0.79	0.498 ± 0.003	14.0 (5.5)	331.97 ± 0.50	+1.22 ± 0.79	0.614 ± 0.009	11.3 (2.7)
IP = 100 m				IP = 120 m			
359.56 ± 0.40	+1.01 ± 0.89	0.702 ± 0.006	4.4 (1.8)	0.01 ± 0.40	+1.12 ± 0.89	0.774 ± 0.003	4.4 (1.6)
28.33 ± 0.40	−3.23 ± 1.08	0.722 ± 0.005	7.1 (2.4)	28.62 ± 0.20	−0.75 ± 0.49	0.794 ± 0.007	7.5 (1.5)
57.30 ± 0.40	−4.68 ± 0.79	0.732 ± 0.011	12.8 (2.3)	57.47 ± 0.20	−2.15 ± 0.59	0.785 ± 0.002	9.7 (1.8)
89.52 ± 0.30	−2.21 ± 0.79	0.734 ± 0.011	11.3 (2.7)	89.80 ± 0.20	−0.49 ± 0.69	0.790 ± 0.008	9.7 (1.7)
121.24 ± 0.30	−1.71 ± 0.59	0.720 ± 0.002	11.1 (2.4)	121.72 ± 0.30	−0.60 ± 0.50	0.780 ± 0.007	8.1 (2.2)
151.23 ± 0.30	+2.57 ± 0.59	0.714 ± 0.008	10.8 (2.5)	151.57 ± 0.10	+0.79 ± 0.39	0.784 ± 0.007	9.4 (1.8)
180.44 ± 0.30	+4.32 ± 0.89	0.716 ± 0.010	6.3 (2.2)	180.26 ± 0.40	+1.71 ± 0.80	0.782 ± 0.002	5.0 (1.7)
208.57 ± 0.30	+2.40 ± 0.79	0.727 ± 0.007	6.7 (2.3)	208.39 ± 0.30	+2.08 ± 0.59	0.797 ± 0.008	7.8 (1.7)
238.50 ± 0.30	+0.17 ± 0.98	0.735 ± 0.005	10.1 (2.6)	238.21 ± 0.20	−0.77 ± 0.59	0.791 ± 0.007	9.2 (1.8)
270.43 ± 0.40	−1.60 ± 0.99	0.734 ± 0.010	9.7 (2.2)	270.14 ± 0.30	+0.28 ± 0.69	0.788 ± 0.002	8.2 (1.7)
302.23 ± 0.30	−0.93 ± 0.69	0.715 ± 0.010	10.1 (2.1)	302.27 ± 0.20	−0.57 ± 0.49	0.774 ± 0.004	8.3 (1.9)
331.75 ± 0.30	+2.43 ± 0.59	0.707 ± 0.011	9.4 (2.4)	331.83 ± 0.30	+0.90 ± 0.59	0.775 ± 0.011	8.7 (1.7)

Table 80: The nominal angle δ_n, average displacement $\Delta\delta$, average value of the parameter DIST, RMS of the ALPHA distribution for enabled GF and impact parameters between 60 m and 120 m. The RMS of the ALPHA distribution for disabled GF is given parentheses. The primary γ-ray energy was set to 300 GeV, the ZA to 20° and the azimuth angle to 120°.

$E_\gamma = 300\,\mathrm{GeV}$, Az = 120°, ZA = 20°, Hard Image Cleaning

δ_n[°]	$\Delta\delta$[°]	DIST[°]	$\mathrm{RMS}_{\lvert\mathrm{ALPHA}\rvert}$[°]	δ_n[°]	$\Delta\delta$[°]	DIST[°]	$\mathrm{RMS}_{\lvert\mathrm{ALPHA}\rvert}$[°]
IP = 60 m				IP = 80 m			
359.48 ± 0.40	+5.35 ± 1.08	0.491 ± 0.006	7.2 (5.0)	0.47 ± 0.30	+5.24 ± 0.69	0.605 ± 0.009	5.6 (2.8)
28.29 ± 0.40	−2.48 ± 0.69	0.506 ± 0.007	8.7 (5.2)	28.22 ± 0.30	+1.02 ± 0.69	0.622 ± 0.003	7.3 (3.0)
56.42 ± 0.50	−9.60 ± 1.38	0.510 ± 0.007	13.9 (9.9)	57.27 ± 0.40	−8.34 ± 1.08	0.628 ± 0.008	13.2 (2.9)
88.99 ± 0.60	−7.81 ± 1.38	0.501 ± 0.007	16.0 (5.6)	88.99 ± 0.40	−5.54 ± 0.99	0.628 ± 0.006	13.4 (3.7)
120.48 ± 0.60	−2.56 ± 0.99	0.486 ± 0.007	15.7 (5.3)	120.64 ± 0.40	−2.00 ± 0.79	0.614 ± 0.009	12.6 (3.4)
151.58 ± 0.50	+4.76 ± 1.09	0.482 ± 0.007	12.4 (6.2)	150.99 ± 0.50	+2.84 ± 0.89	0.597 ± 0.006	10.4 (3.7)
180.83 ± 0.40	+9.09 ± 0.89	0.488 ± 0.006	8.0 (6.2)	180.91 ± 0.30	+7.20 ± 0.89	0.607 ± 0.007	5.8 (3.4)
209.96 ± 0.40	+5.19 ± 0.99	0.496 ± 0.007	9.4 (5.1)	208.99 ± 0.40	+3.29 ± 0.79	0.618 ± 0.011	8.7 (4.3)
239.56 ± 0.30	−3.66 ± 0.79	0.500 ± 0.006	15.3 (5.2)	239.25 ± 0.40	+1.93 ± 1.08	0.631 ± 0.006	10.8 (3.0)
271.59 ± 0.40	−4.57 ± 1.28	0.502 ± 0.003	15.2 (5.1)	270.56 ± 0.20	−3.63 ± 0.79	0.632 ± 0.007	12.7 (2.9)
302.51 ± 0.60	−1.15 ± 0.99	0.487 ± 0.007	14.9 (5.5)	302.34 ± 0.30	−0.56 ± 0.69	0.613 ± 0.001	11.9 (3.1)
331.53 ± 0.50	+1.66 ± 0.99	0.487 ± 0.007	12.1 (5.1)	332.02 ± 0.50	+2.22 ± 0.79	0.606 ± 0.009	10.1 (2.2)
IP = 100 m				IP = 120 m			
359.57 ± 0.40	+1.93 ± 0.79	0.694 ± 0.001	4.5 (2.1)	359.96 ± 0.30	−1.64 ± 0.69	0.764 ± 0.009	4.5 (1.4)
28.03 ± 0.30	−2.42 ± 0.79	0.711 ± 0.008	5.8 (2.4)	28.30 ± 0.30	−1.92 ± 0.69	0.785 ± 0.006	5.8 (1.6)
57.61 ± 0.30	−5.15 ± 0.89	0.727 ± 0.011	11.4 (2.1)	57.30 ± 0.20	−1.60 ± 0.59	0.774 ± 0.003	8.2 (1.8)
89.24 ± 0.40	−2.69 ± 0.99	0.725 ± 0.007	11.7 (2.9)	89.64 ± 0.20	−0.47 ± 0.79	0.780 ± 0.007	8.8 (1.9)
121.34 ± 0.30	−0.65 ± 0.50	0.712 ± 0.010	10.9 (2.3)	121.82 ± 0.30	−0.54 ± 0.50	0.768 ± 0.009	8.3 (2.1)
151.44 ± 0.30	+2.26 ± 0.59	0.704 ± 0.011	8.0 (2.3)	151.54 ± 0.30	−0.11 ± 0.60	0.771 ± 0.007	8.1 (1.7)
180.50 ± 0.40	+2.33 ± 0.90	0.704 ± 0.011	6.2 (2.1)	179.98 ± 0.30	−0.21 ± 0.70	0.768 ± 0.008	4.8 (1.8)
208.49 ± 0.30	+1.21 ± 0.69	0.720 ± 0.003	7.1 (2.2)	208.11 ± 0.30	−0.31 ± 0.79	0.785 ± 0.007	7.2 (1.6)
238.40 ± 0.20	+1.97 ± 0.79	0.728 ± 0.005	8.8 (2.6)	238.26 ± 0.30	+0.66 ± 0.69	0.778 ± 0.002	8.6 (1.5)
270.08 ± 0.30	−3.23 ± 0.79	0.725 ± 0.006	11.1 (2.2)	270.24 ± 0.40	−0.13 ± 0.79	0.775 ± 0.007	7.8 (1.7)
302.41 ± 0.30	−0.59 ± 0.60	0.707 ± 0.007	9.5 (1.9)	302.48 ± 0.20	−0.44 ± 0.59	0.766 ± 0.006	6.2 (1.7)
331.70 ± 0.30	+1.44 ± 0.59	0.700 ± 0.011	8.8 (2.1)	332.00 ± 0.30	+0.44 ± 0.59	0.766 ± 0.004	7.8 (1.7)

Table 81: The nominal angle δ_n, average displacement $\Delta\delta$, average value of the parameter DIST, RMS of the ALPHA distribution for enabled GF and impact parameters between 60 m and 120 m. The RMS of the ALPHA distribution for disabled GF is given parentheses. The primary γ-ray energy was set to 300 GeV, the ZA to 20° and the azimuth angle to 120°.

$E_\gamma = 300\,\mathrm{GeV}$, Az = 150°, ZA = 20°, Intermediate Image Cleaning

$\delta_n[^\circ]$	$\Delta\delta[^\circ]$	DIST[°]	$\mathrm{RMS}_{\lvert\mathrm{ALPHA}\rvert}[^\circ]$	$\delta_n[^\circ]$	$\Delta\delta[^\circ]$	DIST[°]	$\mathrm{RMS}_{\lvert\mathrm{ALPHA}\rvert}[^\circ]$
IP = 60 m				IP = 80 m			
359.53 ± 0.40	$+4.83 \pm 0.97$	0.505 ± 0.007	6.3 (5.3)	0.01 ± 0.40	$+3.72 \pm 0.97$	0.621 ± 0.005	6.2 (2.6)
28.14 ± 0.40	$+8.06 \pm 0.78$	0.505 ± 0.009	11.2 (5.8)	28.34 ± 0.40	$+5.43 \pm 0.88$	0.632 ± 0.006	9.0 (3.2)
55.92 ± 0.40	$+4.89 \pm 0.69$	0.510 ± 0.004	14.8 (10.7)	57.41 ± 0.40	$+2.79 \pm 0.97$	0.637 ± 0.005	13.0 (2.9)
88.89 ± 0.50	-6.02 ± 1.84	0.504 ± 0.002	18.9 (6.3)	89.21 ± 0.60	-3.69 ± 1.27	0.627 ± 0.005	14.8 (4.0)
120.72 ± 0.60	-6.88 ± 1.17	0.496 ± 0.002	18.4 (5.2)	120.45 ± 0.30	-2.84 ± 0.78	0.619 ± 0.004	15.0 (3.5)
151.94 ± 0.60	$+0.63 \pm 0.99$	0.496 ± 0.003	10.9 (5.5)	151.37 ± 0.40	$+0.19 \pm 0.69$	0.620 ± 0.005	9.6 (3.1)
181.08 ± 0.40	$+3.81 \pm 1.16$	0.505 ± 0.004	6.8 (5.5)	180.89 ± 0.40	$+2.09 \pm 0.69$	0.632 ± 0.004	5.2 (3.6)
210.41 ± 0.40	$+7.54 \pm 1.07$	0.513 ± 0.003	11.0 (7.0)	209.35 ± 0.40	$+3.36 \pm 0.97$	0.631 ± 0.003	7.4 (3.3)
239.49 ± 0.50	-0.57 ± 1.84	0.507 ± 0.005	14.4 (4.5)	239.34 ± 0.60	$+0.53 \pm 1.08$	0.636 ± 0.006	9.6 (3.0)
271.89 ± 0.30	-6.39 ± 1.26	0.495 ± 0.004	18.2 (7.5)	270.81 ± 0.40	-4.84 ± 1.16	0.619 ± 0.006	14.8 (2.9)
302.78 ± 0.60	-5.90 ± 1.27	0.489 ± 0.006	19.3 (5.7)	302.57 ± 0.40	-4.38 ± 0.69	0.610 ± 0.007	15.6 (3.3)
331.61 ± 0.50	-2.11 ± 0.98	0.486 ± 0.006	13.1 (5.5)	331.97 ± 0.50	-0.44 ± 0.79	0.606 ± 0.005	9.8 (2.7)
IP = 100 m				IP = 120 m			
359.56 ± 0.40	$+1.79 \pm 0.69$	0.720 ± 0.005	5.0 (1.8)	0.01 ± 0.40	$+1.24 \pm 0.69$	0.801 ± 0.005	4.4 (1.6)
28.33 ± 0.40	$+1.35 \pm 0.97$	0.730 ± 0.006	6.5 (2.4)	28.62 ± 0.20	$+0.14 \pm 0.49$	0.793 ± 0.004	5.8 (1.5)
57.30 ± 0.40	-0.26 ± 0.88	0.730 ± 0.005	8.5 (2.3)	57.47 ± 0.20	$+0.31 \pm 0.77$	0.794 ± 0.005	6.3 (1.8)
89.52 ± 0.30	-0.93 ± 0.78	0.715 ± 0.005	10.1 (2.7)	89.80 ± 0.20	-0.37 ± 0.58	0.776 ± 0.009	8.0 (1.7)
121.24 ± 0.30	-2.49 ± 0.68	0.715 ± 0.006	10.4 (2.4)	121.72 ± 0.30	-0.25 ± 0.68	0.777 ± 0.007	9.0 (2.2)
151.23 ± 0.30	-0.89 ± 0.59	0.713 ± 0.006	8.0 (2.5)	151.57 ± 0.10	-0.16 ± 0.39	0.786 ± 0.006	6.6 (1.8)
180.44 ± 0.30	$+1.79 \pm 0.59$	0.726 ± 0.005	4.7 (2.2)	180.26 ± 0.40	$+0.97 \pm 0.79$	0.802 ± 0.003	3.6 (1.7)
208.57 ± 0.30	$+1.80 \pm 0.68$	0.729 ± 0.010	6.2 (2.3)	208.39 ± 0.30	$+0.44 \pm 0.68$	0.793 ± 0.004	5.1 (1.7)
238.50 ± 0.30	-0.40 ± 0.78	0.731 ± 0.005	9.6 (2.6)	238.21 ± 0.20	-0.22 ± 0.58	0.787 ± 0.006	6.6 (1.8)
270.43 ± 0.40	-3.31 ± 0.69	0.710 ± 0.006	12.1 (2.2)	270.14 ± 0.30	-0.94 ± 0.68	0.766 ± 0.007	8.1 (1.7)
302.23 ± 0.30	-2.67 ± 0.78	0.708 ± 0.006	10.9 (2.1)	302.27 ± 0.20	-1.11 ± 0.58	0.768 ± 0.005	8.4 (1.9)
331.75 ± 0.30	$+0.31 \pm 0.59$	0.706 ± 0.006	8.2 (2.4)	331.83 ± 0.30	-0.12 ± 0.59	0.770 ± 0.007	6.3 (1.7)

Table 82: The nominal angle δ_n, average displacement $\Delta\delta$, average value of the parameter DIST, RMS of the ALPHA distribution for enabled GF and impact parameters between 60 m and 120 m. The RMS of the ALPHA distribution for disabled GF is given parentheses. The primary γ-ray energy was set to 300 GeV, the ZA to 20° and the azimuth angle to 150°.

$E_\gamma = 300\,\mathrm{GeV}$, Az = 150°, ZA = 20°, Hard Image Cleaning

$\delta_n[^\circ]$	$\Delta\delta[^\circ]$	DIST[°]	$\mathrm{RMS}_{\lvert\mathrm{ALPHA}\rvert}[^\circ]$	$\delta_n[^\circ]$	$\Delta\delta[^\circ]$	DIST[°]	$\mathrm{RMS}_{\lvert\mathrm{ALPHA}\rvert}[^\circ]$
IP = 60 m				IP = 80 m			
359.48 ± 0.40	$+3.87 \pm 0.78$	0.494 ± 0.008	6.0 (5.0)	0.47 ± 0.30	$+4.07 \pm 0.78$	0.609 ± 0.006	6.3 (2.8)
28.29 ± 0.40	$+8.27 \pm 1.26$	0.498 ± 0.003	10.4 (5.2)	28.22 ± 0.30	$+4.71 \pm 0.49$	0.620 ± 0.003	8.9 (3.0)
56.42 ± 0.50	$+6.25 \pm 1.36$	0.500 ± 0.005	14.6 (9.9)	57.27 ± 0.40	$+2.04 \pm 0.97$	0.626 ± 0.004	11.0 (2.9)
88.99 ± 0.60	-6.67 ± 1.46	0.493 ± 0.003	18.6 (5.6)	88.99 ± 0.40	-4.41 ± 1.07	0.616 ± 0.005	14.1 (3.7)
120.48 ± 0.60	-6.56 ± 1.27	0.484 ± 0.004	18.2 (5.3)	120.64 ± 0.40	-3.50 ± 0.88	0.607 ± 0.006	16.0 (3.4)
151.58 ± 0.50	$+0.51 \pm 0.98$	0.486 ± 0.005	10.7 (6.2)	150.99 ± 0.50	$+0.03 \pm 0.79$	0.609 ± 0.006	8.3 (3.7)
180.83 ± 0.40	$+3.17 \pm 0.88$	0.495 ± 0.005	6.3 (6.2)	180.91 ± 0.30	$+2.72 \pm 0.68$	0.626 ± 0.006	4.7 (3.4)
209.96 ± 0.40	$+7.58 \pm 0.97$	0.500 ± 0.003	10.8 (5.1)	208.99 ± 0.40	$+5.02 \pm 1.07$	0.620 ± 0.006	7.0 (4.3)
239.56 ± 0.30	$+0.69 \pm 1.26$	0.496 ± 0.004	14.6 (5.2)	239.25 ± 0.40	$+0.06 \pm 0.78$	0.625 ± 0.002	9.4 (3.0)
271.59 ± 0.40	-6.51 ± 0.59	0.481 ± 0.006	19.2 (5.1)	270.56 ± 0.20	-4.85 ± 0.68	0.606 ± 0.006	14.3 (2.9)
302.51 ± 0.60	-5.92 ± 0.79	0.476 ± 0.005	18.2 (5.5)	302.34 ± 0.30	-4.69 ± 0.68	0.598 ± 0.009	16.2 (3.1)
331.53 ± 0.50	-2.01 ± 1.08	0.477 ± 0.007	12.4 (5.1)	332.02 ± 0.50	-0.17 ± 0.88	0.595 ± 0.008	9.2 (2.2)
IP = 100 m				IP = 120 m			
359.57 ± 0.40	$+1.26 \pm 0.78$	0.712 ± 0.006	5.0 (2.1)	359.96 ± 0.30	$+0.22 \pm 0.69$	0.784 ± 0.005	4.4 (1.4)
28.03 ± 0.30	$+0.64 \pm 0.97$	0.721 ± 0.006	6.9 (2.4)	28.30 ± 0.30	$+0.10 \pm 0.59$	0.780 ± 0.003	5.5 (1.6)
57.61 ± 0.30	$+0.06 \pm 0.49$	0.719 ± 0.005	8.4 (2.1)	57.30 ± 0.20	-0.58 ± 0.49	0.782 ± 0.006	6.0 (1.8)
89.24 ± 0.40	-1.70 ± 0.97	0.705 ± 0.005	10.8 (2.9)	89.64 ± 0.20	-0.11 ± 0.39	0.765 ± 0.008	7.5 (1.9)
121.34 ± 0.30	-2.05 ± 0.68	0.705 ± 0.002	11.5 (2.3)	121.82 ± 0.30	$+0.54 \pm 0.68$	0.767 ± 0.007	9.0 (2.1)
151.44 ± 0.30	-0.59 ± 0.59	0.706 ± 0.007	7.5 (2.3)	151.54 ± 0.30	$+0.03 \pm 0.59$	0.773 ± 0.006	5.6 (1.7)
180.50 ± 0.40	$+1.17 \pm 0.78$	0.717 ± 0.009	4.5 (2.1)	179.98 ± 0.30	$+0.78 \pm 0.69$	0.789 ± 0.004	3.7 (1.8)
208.49 ± 0.30	$+1.07 \pm 0.68$	0.718 ± 0.010	5.9 (2.2)	208.11 ± 0.30	-0.34 ± 0.68	0.782 ± 0.006	4.9 (1.6)
238.40 ± 0.20	-0.87 ± 0.77	0.721 ± 0.002	9.3 (2.6)	238.26 ± 0.30	-0.40 ± 0.78	0.777 ± 0.007	5.7 (1.5)
270.08 ± 0.30	-3.56 ± 0.78	0.701 ± 0.006	11.0 (2.2)	270.24 ± 0.40	-0.97 ± 0.59	0.753 ± 0.007	9.0 (1.7)
302.41 ± 0.30	-1.55 ± 0.78	0.697 ± 0.004	10.6 (1.9)	302.48 ± 0.20	-0.33 ± 0.39	0.757 ± 0.004	7.5 (1.7)
331.70 ± 0.30	$+0.11 \pm 0.59$	0.698 ± 0.004	7.9 (2.1)	332.00 ± 0.30	$+0.02 \pm 0.59$	0.762 ± 0.006	5.4 (1.7)

Table 83: The nominal angle δ_n, average displacement $\Delta\delta$, average value of the parameter DIST, RMS of the ALPHA distribution for enabled GF and impact parameters between 60 m and 120 m. The RMS of the ALPHA distribution for disabled GF is given parentheses. The primary γ-ray energy was set to 300 GeV, the ZA to 20° and the azimuth angle to 150°.

$E_\gamma = 300\,\mathrm{GeV}$, Az = 180°, ZA = 20°, Intermediate Image Cleaning

$\delta_n[°]$	$\Delta\delta[°]$	DIST[°]	$\mathrm{RMS}_{\lvert\mathrm{ALPHA}\rvert}[°]$	$\delta_n[°]$	$\Delta\delta[°]$	DIST[°]	$\mathrm{RMS}_{\lvert\mathrm{ALPHA}\rvert}[°]$
IP = 60 m				**IP = 80 m**			
359.53 ± 0.40	$+0.23 \pm 0.78$	0.478 ± 0.006	9.4 (5.3)	0.01 ± 0.40	$+1.14 \pm 0.78$	0.606 ± 0.008	2.8 (2.6)
28.14 ± 0.40	$+5.84 \pm 1.07$	0.475 ± 0.005	8.7 (5.8)	28.34 ± 0.40	$+4.03 \pm 0.88$	0.603 ± 0.006	12.3 (3.2)
55.92 ± 0.40	$+5.45 \pm 0.88$	0.474 ± 0.006	15.0 (10.7)	57.41 ± 0.40	$+5.69 \pm 1.07$	0.600 ± 0.007	14.9 (2.9)
88.89 ± 0.50	-1.36 ± 0.79	0.468 ± 0.006	23.2 (6.3)	89.21 ± 0.60	$+0.87 \pm 1.17$	0.595 ± 0.006	14.7 (4.0)
120.72 ± 0.60	-10.23 ± 0.70	0.475 ± 0.006	21.6 (5.2)	120.45 ± 0.30	-4.24 ± 0.87	0.603 ± 0.008	15.8 (3.5)
151.94 ± 0.60	-4.97 ± 1.36	0.487 ± 0.005	11.0 (5.5)	151.37 ± 0.40	-3.11 ± 1.07	0.612 ± 0.007	10.0 (3.1)
181.08 ± 0.40	$+0.75 \pm 0.88$	0.493 ± 0.001	5.3 (5.5)	180.89 ± 0.40	$+0.43 \pm 0.69$	0.616 ± 0.006	3.0 (3.6)
210.41 ± 0.40	$+6.47 \pm 0.97$	0.479 ± 0.006	7.5 (7.0)	209.35 ± 0.40	$+1.96 \pm 0.88$	0.605 ± 0.006	4.8 (3.3)
239.49 ± 0.50	$+10.47 \pm 1.64$	0.470 ± 0.006	26.1 (4.5)	239.34 ± 0.60	$+4.01 \pm 1.08$	0.593 ± 0.007	14.6 (3.0)
271.89 ± 0.30	$+3.15 \pm 1.25$	0.463 ± 0.004	22.5 (7.5)	270.81 ± 0.40	$+2.04 \pm 1.16$	0.585 ± 0.006	15.6 (2.9)
302.78 ± 0.60	-10.61 ± 1.27	0.463 ± 0.007	17.3 (5.7)	302.57 ± 0.40	-6.47 ± 1.07	0.588 ± 0.006	13.9 (3.3)
331.61 ± 0.50	-5.96 ± 1.17	0.470 ± 0.004	9.3 (5.5)	331.97 ± 0.50	-4.27 ± 1.07	0.599 ± 0.008	5.9 (2.7)
IP = 100 m				**IP = 120 m**			
359.56 ± 0.40	$+0.70 \pm 0.59$	0.705 ± 0.006	3.1 (1.8)	0.01 ± 0.40	-0.55 ± 0.59	0.777 ± 0.009	2.1 (1.6)
28.33 ± 0.40	$+0.95 \pm 0.78$	0.711 ± 0.002	6.0 (2.4)	28.62 ± 0.20	$+0.61 \pm 0.58$	0.785 ± 0.007	4.0 (1.5)
57.30 ± 0.40	$+2.64 \pm 0.78$	0.698 ± 0.007	11.0 (2.3)	57.47 ± 0.20	-0.71 ± 0.58	0.762 ± 0.006	9.2 (1.8)
89.52 ± 0.30	$+1.50 \pm 0.87$	0.699 ± 0.008	9.0 (2.7)	89.80 ± 0.20	$+0.73 \pm 0.68$	0.758 ± 0.004	6.0 (1.7)
121.24 ± 0.30	$+0.25 \pm 0.78$	0.701 ± 0.004	8.0 (2.4)	121.72 ± 0.30	$+0.78 \pm 0.78$	0.763 ± 0.006	4.2 (2.2)
151.23 ± 0.30	-1.69 ± 0.68	0.710 ± 0.003	5.1 (2.5)	151.57 ± 0.10	-0.47 ± 0.39	0.784 ± 0.004	4.7 (1.8)
180.44 ± 0.30	-0.56 ± 0.59	0.710 ± 0.006	2.2 (2.2)	180.26 ± 0.40	$+0.06 \pm 0.69$	0.779 ± 0.006	2.3 (1.7)
208.57 ± 0.30	$+0.74 \pm 0.68$	0.705 ± 0.002	3.7 (2.3)	208.39 ± 0.30	$+0.63 \pm 0.68$	0.779 ± 0.006	3.9 (1.7)
238.50 ± 0.30	$+1.26 \pm 0.87$	0.691 ± 0.008	10.7 (2.6)	238.21 ± 0.20	-0.77 ± 0.68	0.753 ± 0.001	8.4 (1.8)
270.43 ± 0.40	-0.27 ± 0.78	0.687 ± 0.005	10.4 (2.2)	270.14 ± 0.30	-0.76 ± 0.78	0.753 ± 0.008	4.5 (1.7)
302.23 ± 0.30	-3.22 ± 0.68	0.690 ± 0.008	7.1 (2.1)	302.27 ± 0.20	-0.96 ± 0.39	0.754 ± 0.008	5.7 (1.9)
331.75 ± 0.30	-1.47 ± 0.78	0.700 ± 0.010	4.4 (2.4)	331.83 ± 0.30	-0.52 ± 0.68	0.779 ± 0.009	4.8 (1.7)

Table 84: The nominal angle δ_n, average displacement $\Delta\delta$, average value of the parameter DIST, RMS of the ALPHA distribution for enabled GF and impact parameters between 60 m and 120 m. The RMS of the ALPHA distribution for disabled GF is given parentheses. The primary γ-ray energy was set to 300 GeV, the ZA to 20° and the azimuth angle to 180°.

$E_\gamma = 300\,\mathrm{GeV}$, Az = 180°, ZA = 20°, Hard Image Cleaning

$\delta_n[°]$	$\Delta\delta[°]$	DIST[°]	$\mathrm{RMS}_{\lvert\mathrm{ALPHA}\rvert}[°]$	$\delta_n[°]$	$\Delta\delta[°]$	DIST[°]	$\mathrm{RMS}_{\lvert\mathrm{ALPHA}\rvert}[°]$
IP = 60 m				**IP = 80 m**			
359.48 ± 0.40	$+0.30 \pm 0.78$	0.465 ± 0.004	3.5 (5.0)	0.47 ± 0.30	$+1.81 \pm 0.59$	0.597 ± 0.006	3.2 (2.8)
28.29 ± 0.40	$+6.19 \pm 0.97$	0.466 ± 0.006	8.2 (5.2)	28.22 ± 0.30	$+3.32 \pm 0.68$	0.593 ± 0.007	11.1 (3.0)
56.42 ± 0.50	$+7.03 \pm 1.07$	0.462 ± 0.005	15.1 (9.9)	57.27 ± 0.40	$+7.57 \pm 0.78$	0.589 ± 0.007	12.2 (2.9)
88.99 ± 0.60	-1.96 ± 1.17	0.456 ± 0.006	22.1 (5.6)	88.99 ± 0.40	-0.48 ± 1.16	0.584 ± 0.008	18.4 (3.7)
120.48 ± 0.60	-9.59 ± 0.89	0.465 ± 0.006	21.0 (5.3)	120.64 ± 0.40	-3.32 ± 0.69	0.590 ± 0.007	15.2 (3.4)
151.58 ± 0.50	-4.39 ± 1.26	0.476 ± 0.004	9.8 (6.2)	150.99 ± 0.50	-2.55 ± 0.98	0.601 ± 0.001	8.3 (3.7)
180.83 ± 0.40	$+0.96 \pm 0.78$	0.480 ± 0.006	4.0 (6.2)	180.91 ± 0.30	$+0.39 \pm 0.68$	0.604 ± 0.007	2.8 (3.4)
209.96 ± 0.40	$+5.74 \pm 0.78$	0.470 ± 0.006	7.7 (5.1)	208.99 ± 0.40	$+1.60 \pm 0.97$	0.593 ± 0.003	3.9 (4.3)
239.56 ± 0.30	$+10.28 \pm 0.59$	0.460 ± 0.006	25.4 (5.2)	239.25 ± 0.40	$+5.22 \pm 0.88$	0.581 ± 0.007	7.6 (3.0)
271.59 ± 0.40	$+2.65 \pm 1.26$	0.449 ± 0.006	25.3 (5.1)	270.56 ± 0.20	$+1.13 \pm 0.96$	0.575 ± 0.005	16.6 (2.9)
302.51 ± 0.60	-10.32 ± 1.55	0.454 ± 0.006	17.3 (5.5)	302.34 ± 0.30	-7.53 ± 0.78	0.577 ± 0.006	13.7 (3.1)
331.53 ± 0.50	-5.78 ± 1.07	0.459 ± 0.005	8.6 (5.1)	332.02 ± 0.50	-3.74 ± 0.98	0.587 ± 0.008	5.7 (2.2)
IP = 100 m				**IP = 120 m**			
359.57 ± 0.40	-1.61 ± 0.69	0.697 ± 0.009	2.5 (2.1)	359.96 ± 0.30	-0.96 ± 0.49	0.768 ± 0.006	2.1 (1.4)
28.03 ± 0.30	$+0.49 \pm 0.68$	0.698 ± 0.009	9.3 (2.4)	28.30 ± 0.30	$+0.51 \pm 0.68$	0.777 ± 0.007	5.2 (1.6)
57.61 ± 0.30	$+2.25 \pm 0.68$	0.690 ± 0.008	10.5 (2.1)	57.30 ± 0.20	-0.29 ± 0.58	0.750 ± 0.002	8.9 (1.8)
89.24 ± 0.40	$+1.71 \pm 0.97$	0.689 ± 0.005	8.5 (2.9)	89.64 ± 0.20	$+0.10 \pm 0.68$	0.746 ± 0.006	6.3 (1.9)
121.34 ± 0.30	$+0.20 \pm 0.68$	0.688 ± 0.008	8.5 (2.3)	121.82 ± 0.30	$+1.56 \pm 0.78$	0.753 ± 0.007	4.9 (2.1)
151.44 ± 0.30	-1.27 ± 0.59	0.702 ± 0.004	5.0 (2.3)	151.54 ± 0.30	-0.52 ± 0.59	0.775 ± 0.003	3.7 (1.7)
180.50 ± 0.40	-0.15 ± 0.69	0.698 ± 0.006	2.2 (2.1)	179.98 ± 0.30	-0.18 ± 0.59	0.770 ± 0.006	2.4 (1.8)
208.49 ± 0.30	$+0.21 \pm 0.78$	0.696 ± 0.007	3.7 (2.2)	208.11 ± 0.30	$+0.02 \pm 0.59$	0.768 ± 0.007	2.7 (1.6)
238.40 ± 0.20	$+0.71 \pm 0.77$	0.680 ± 0.004	10.2 (2.6)	238.26 ± 0.30	-0.78 ± 0.68	0.745 ± 0.007	7.0 (1.5)
270.08 ± 0.30	-0.82 ± 0.87	0.678 ± 0.006	11.1 (2.2)	270.24 ± 0.40	-0.72 ± 0.69	0.741 ± 0.009	5.1 (1.7)
302.41 ± 0.30	-2.66 ± 0.49	0.681 ± 0.010	5.1 (1.9)	302.48 ± 0.20	-0.74 ± 0.39	0.744 ± 0.008	4.3 (1.7)
331.70 ± 0.30	-1.61 ± 0.59	0.692 ± 0.010	4.1 (2.1)	332.00 ± 0.30	$+0.11 \pm 0.59$	0.765 ± 0.005	4.5 (1.7)

Table 85: The nominal angle δ_n, average displacement $\Delta\delta$, average value of the parameter DIST, RMS of the ALPHA distribution for enabled GF and impact parameters between 60 m and 120 m. The RMS of the ALPHA distribution for disabled GF is given parentheses. The primary γ-ray energy was set to 300 GeV, the ZA to 20° and the azimuth angle to 180°.

$E_\gamma = 300\,\mathrm{GeV}$, Az = 0°, ZA = 40°, Intermediate Image Cleaning

$\delta_n[^\circ]$	$\Delta\delta[^\circ]$	DIST[°]	$\mathrm{RMS}_{\lvert\mathrm{ALPHA}\rvert}[^\circ]$	$\delta_n[^\circ]$	$\Delta\delta[^\circ]$	DIST[°]	$\mathrm{RMS}_{\lvert\mathrm{ALPHA}\rvert}[^\circ]$
IP = 60 m				**IP = 80 m**			
359.40 ± 0.33	-0.99 ± 0.90	0.326 ± 0.003	11.5 (13.8)	359.69 ± 0.49	-0.43 ± 0.98	0.428 ± 0.005	9.9 (8.8)
23.84 ± 0.49	$+2.00 \pm 1.22$	0.307 ± 0.003	11.2 (9.9)	25.63 ± 0.16	$+1.92 \pm 0.57$	0.402 ± 0.003	7.1 (5.9)
53.40 ± 0.74	$+0.47 \pm 1.31$	0.268 ± 0.003	14.8 (17.8)	54.12 ± 0.58	$+2.34 \pm 0.98$	0.353 ± 0.004	11.3 (8.9)
91.68 ± 0.74	$+0.19 \pm 0.98$	0.245 ± 0.003	20.3 (13.2)	90.95 ± 0.49	-1.47 ± 1.06	0.325 ± 0.003	19.6 (11.3)
128.29 ± 0.66	-3.55 ± 1.39	0.269 ± 0.003	13.7 (13.1)	127.99 ± 0.66	-2.54 ± 1.47	0.356 ± 0.004	7.7 (8.2)
156.26 ± 0.82	-1.71 ± 1.47	0.308 ± 0.004	13.3 (14.2)	156.09 ± 0.49	-0.51 ± 1.14	0.405 ± 0.004	9.3 (8.8)
179.86 ± 0.66	$+0.40 \pm 1.06$	0.328 ± 0.003	11.5 (11.4)	180.10 ± 0.49	$+0.24 \pm 1.06$	0.430 ± 0.004	6.0 (6.7)
203.58 ± 0.49	$+0.88 \pm 1.22$	0.314 ± 0.003	13.1 (12.6)	204.48 ± 0.33	$+2.66 \pm 0.82$	0.413 ± 0.005	7.4 (6.9)
231.70 ± 0.74	$+2.83 \pm 1.63$	0.278 ± 0.004	14.4 (11.8)	232.03 ± 0.49	$+2.89 \pm 1.14$	0.369 ± 0.003	13.3 (9.7)
270.41 ± 0.49	$+2.23 \pm 1.06$	0.260 ± 0.003	19.1 (12.0)	268.87 ± 0.58	$+1.58 \pm 1.14$	0.340 ± 0.003	16.9 (13.1)
304.61 ± 0.58	-3.26 ± 1.14	0.275 ± 0.002	17.1 (13.5)	306.03 ± 0.58	-2.13 ± 0.98	0.366 ± 0.004	17.1 (13.8)
335.78 ± 0.74	-4.43 ± 1.55	0.313 ± 0.003	10.1 (13.8)	335.91 ± 0.16	-1.93 ± 0.41	0.410 ± 0.003	10.7 (7.0)
IP = 100 m				**IP = 120 m**			
359.93 ± 0.41	$+0.22 \pm 0.90$	0.522 ± 0.005	5.7 (8.1)	359.85 ± 0.33	$+0.50 \pm 0.65$	0.608 ± 0.007	5.6 (2.7)
25.54 ± 0.25	$+1.78 \pm 0.57$	0.496 ± 0.005	4.1 (5.1)	25.10 ± 0.33	$+1.07 \pm 0.65$	0.581 ± 0.005	3.6 (2.6)
53.11 ± 0.41	$+1.27 \pm 0.82$	0.439 ± 0.003	7.7 (6.0)	53.22 ± 0.25	$+1.48 \pm 0.65$	0.517 ± 0.004	5.8 (3.7)
91.70 ± 0.58	$+0.66 \pm 1.06$	0.403 ± 0.005	10.5 (9.8)	91.66 ± 0.25	$+0.88 \pm 0.73$	0.478 ± 0.005	9.8 (4.5)
127.23 ± 0.41	-1.06 ± 0.90	0.440 ± 0.005	7.4 (6.9)	127.46 ± 0.41	$+0.07 \pm 0.82$	0.517 ± 0.005	7.9 (4.0)
155.76 ± 0.41	-0.14 ± 0.82	0.496 ± 0.005	5.8 (4.8)	156.53 ± 0.33	$+0.07 \pm 0.65$	0.579 ± 0.005	3.8 (3.3)
180.39 ± 0.41	$+0.04 \pm 0.74$	0.526 ± 0.005	4.8 (5.0)	179.90 ± 0.33	-0.22 ± 0.66	0.608 ± 0.005	3.2 (3.3)
203.35 ± 0.33	$+0.37 \pm 0.74$	0.505 ± 0.005	4.7 (5.6)	203.02 ± 0.33	$+1.05 \pm 0.65$	0.590 ± 0.005	3.4 (3.6)
231.42 ± 0.41	$+0.23 \pm 0.90$	0.452 ± 0.005	6.8 (7.3)	232.83 ± 0.33	$+1.72 \pm 0.73$	0.531 ± 0.005	7.0 (4.4)
269.02 ± 0.33	-0.59 ± 0.82	0.420 ± 0.004	11.8 (8.2)	268.73 ± 0.41	-0.13 ± 0.90	0.495 ± 0.003	8.9 (5.9)
307.00 ± 0.49	-1.87 ± 0.90	0.451 ± 0.005	7.4 (8.4)	306.86 ± 0.25	-1.33 ± 0.73	0.532 ± 0.003	5.4 (8.0)
335.87 ± 0.41	-0.42 ± 0.74	0.503 ± 0.005	4.9 (4.3)	335.70 ± 0.33	-0.91 ± 0.65	0.587 ± 0.005	4.0 (3.3)

Table 86: The nominal angle δ_n, average displacement $\Delta\delta$, average value of the parameter DIST, RMS of the ALPHA distribution for enabled GF and impact parameters between 60 m and 120 m. The RMS of the ALPHA distribution for disabled GF is given parentheses. The primary γ-ray energy was set to 300 GeV, the ZA to 40° and the azimuth angle to 0°.

$E_\gamma = 300\,\mathrm{GeV}$, Az = 0°, ZA = 40°, Hard Image Cleaning

$\delta_n[^\circ]$	$\Delta\delta[^\circ]$	DIST[°]	$\mathrm{RMS}_{\lvert\mathrm{ALPHA}\rvert}[^\circ]$	$\delta_n[^\circ]$	$\Delta\delta[^\circ]$	DIST[°]	$\mathrm{RMS}_{\lvert\mathrm{ALPHA}\rvert}[^\circ]$
IP = 60 m				**IP = 80 m**			
358.33 ± 0.49	-2.80 ± 0.98	0.319 ± 0.003	10.9 (15.1)	359.29 ± 0.41	-0.59 ± 0.98	0.421 ± 0.004	9.6 (8.5)
23.11 ± 0.41	$+2.00 \pm 1.06$	0.302 ± 0.003	13.0 (12.1)	25.27 ± 0.49	$+2.05 \pm 0.90$	0.396 ± 0.005	8.4 (6.8)
53.48 ± 0.74	$+1.62 \pm 1.55$	0.262 ± 0.003	16.9 (15.9)	54.85 ± 0.58	$+3.80 \pm 1.06$	0.348 ± 0.005	12.1 (9.3)
92.44 ± 0.74	$+2.20 \pm 1.55$	0.241 ± 0.003	22.2 (12.2)	91.87 ± 0.58	$+2.40 \pm 1.23$	0.319 ± 0.003	21.2 (11.2)
126.41 ± 0.66	-4.66 ± 1.63	0.266 ± 0.003	18.0 (14.5)	126.96 ± 0.49	-3.02 ± 1.23	0.350 ± 0.003	7.6 (8.3)
155.69 ± 0.58	-2.17 ± 1.31	0.304 ± 0.004	14.8 (15.1)	156.81 ± 0.58	$+0.21 \pm 1.23$	0.398 ± 0.005	10.7 (7.9)
181.16 ± 0.25	$+0.78 \pm 0.82$	0.321 ± 0.003	11.7 (11.2)	179.23 ± 0.41	-0.28 ± 0.74	0.423 ± 0.005	6.7 (6.4)
204.44 ± 0.58	$+1.43 \pm 1.15$	0.309 ± 0.003	13.4 (13.5)	204.00 ± 0.33	$+1.77 \pm 0.82$	0.404 ± 0.005	6.9 (7.2)
233.27 ± 0.33	$+4.11 \pm 1.06$	0.274 ± 0.003	15.8 (11.8)	231.00 ± 0.58	$+0.98 \pm 1.31$	0.363 ± 0.004	12.3 (12.7)
268.53 ± 0.82	$+0.07 \pm 1.72$	0.256 ± 0.003	20.2 (16.1)	268.63 ± 0.74	-1.28 ± 1.63	0.335 ± 0.003	14.1 (14.3)
306.17 ± 0.49	-3.55 ± 0.90	0.273 ± 0.001	16.3 (13.0)	307.95 ± 0.49	$+0.82 \pm 0.90$	0.360 ± 0.004	14.8 (9.0)
336.52 ± 0.41	-3.39 ± 1.14	0.306 ± 0.003	11.3 (10.8)	335.34 ± 0.49	-1.81 ± 0.74	0.404 ± 0.005	8.3 (6.9)
IP = 100 m				**IP = 120 m**			
0.15 ± 0.49	$+0.37 \pm 0.82$	0.515 ± 0.006	3.9 (8.3)	0.52 ± 0.33	$+0.77 \pm 0.65$	0.600 ± 0.003	6.4 (2.6)
25.81 ± 0.33	$+1.89 \pm 0.74$	0.489 ± 0.004	4.3 (3.8)	25.13 ± 0.41	$+0.90 \pm 0.74$	0.574 ± 0.006	3.7 (2.9)
53.48 ± 0.33	$+1.99 \pm 0.65$	0.430 ± 0.005	8.3 (5.5)	53.10 ± 0.25	$+0.56 \pm 0.73$	0.509 ± 0.003	5.4 (3.7)
91.90 ± 0.49	$+1.93 \pm 1.06$	0.397 ± 0.004	12.4 (9.1)	91.97 ± 0.41	$+1.01 \pm 0.90$	0.470 ± 0.004	7.6 (4.7)
128.36 ± 0.41	-0.39 ± 1.06	0.433 ± 0.005	7.0 (7.8)	127.86 ± 0.25	-0.24 ± 0.65	0.511 ± 0.005	6.3 (4.0)
155.22 ± 0.25	-0.82 ± 0.73	0.490 ± 0.005	6.8 (5.0)	156.05 ± 0.33	-0.21 ± 0.65	0.572 ± 0.006	4.1 (3.5)
179.87 ± 0.41	-0.18 ± 0.65	0.519 ± 0.005	5.3 (4.4)	179.89 ± 0.25	-0.08 ± 0.57	0.600 ± 0.005	3.4 (3.1)
203.73 ± 0.33	$+0.56 \pm 0.74$	0.498 ± 0.005	4.6 (5.5)	203.29 ± 0.25	$+0.76 \pm 0.49$	0.582 ± 0.006	3.7 (3.2)
231.19 ± 0.41	$+0.40 \pm 0.82$	0.446 ± 0.004	7.2 (7.2)	231.71 ± 0.33	$+0.15 \pm 0.74$	0.523 ± 0.005	5.3 (7.2)
268.56 ± 0.41	-0.00 ± 0.98	0.414 ± 0.005	10.0 (8.1)	268.88 ± 0.41	$+0.39 \pm 0.74$	0.488 ± 0.004	9.9 (4.9)
307.12 ± 0.33	-2.29 ± 0.98	0.445 ± 0.005	8.6 (6.4)	307.31 ± 0.25	-0.61 ± 0.65	0.524 ± 0.002	5.8 (4.3)
335.70 ± 0.33	-0.83 ± 0.74	0.495 ± 0.005	5.0 (4.2)	335.77 ± 0.33	-1.14 ± 0.74	0.581 ± 0.007	2.8 (3.3)

Table 87: The nominal angle δ_n, average displacement $\Delta\delta$, average value of the parameter DIST, RMS of the ALPHA distribution for enabled GF and impact parameters between 60 m and 120 m. The RMS of the ALPHA distribution for disabled GF is given parentheses. The primary γ-ray energy was set to 300 GeV, the ZA to 40° and the azimuth angle to 0°.

$E_\gamma = 300\,\mathrm{GeV}$, Az = 30°, ZA = 40°, Intermediate Image Cleaning

$\delta_n\,[°]$	$\Delta\delta\,[°]$	DIST[°]	$\mathrm{RMS}_{\lvert\mathrm{ALPHA}\rvert}\,[°]$	$\delta_n\,[°]$	$\Delta\delta\,[°]$	DIST[°]	$\mathrm{RMS}_{\lvert\mathrm{ALPHA}\rvert}\,[°]$
IP = 60 m				**IP = 80 m**			
359.40 ± 0.33	-4.38 ± 1.13	0.320 ± 0.003	15.4 (13.8)	359.69 ± 0.49	-3.20 ± 0.97	0.423 ± 0.002	11.3 (8.8)
23.84 ± 0.49	-6.90 ± 1.21	0.281 ± 0.002	14.0 (9.9)	25.63 ± 0.16	-2.52 ± 0.64	0.370 ± 0.004	10.9 (5.9)
53.40 ± 0.74	-3.46 ± 1.46	0.257 ± 0.002	13.7 (17.8)	54.12 ± 0.58	-1.36 ± 1.06	0.339 ± 0.003	11.0 (8.9)
91.68 ± 0.74	$+2.42 \pm 1.38$	0.277 ± 0.003	18.8 (13.2)	90.95 ± 0.49	$+2.19 \pm 0.97$	0.373 ± 0.003	16.7 (11.3)
128.29 ± 0.66	$+7.49 \pm 1.06$	0.322 ± 0.004	20.3 (13.1)	127.99 ± 0.66	$+6.56 \pm 1.14$	0.423 ± 0.003	14.9 (8.2)
156.26 ± 0.82	$+7.58 \pm 1.30$	0.342 ± 0.003	16.8 (14.2)	156.09 ± 0.49	$+2.97 \pm 0.97$	0.445 ± 0.005	13.0 (8.8)
179.86 ± 0.66	-4.68 ± 1.30	0.328 ± 0.004	15.1 (11.4)	180.10 ± 0.49	-4.74 ± 1.05	0.427 ± 0.004	11.9 (6.7)
203.58 ± 0.49	-9.45 ± 1.13	0.292 ± 0.003	14.0 (12.6)	204.48 ± 0.33	-4.70 ± 0.89	0.384 ± 0.005	11.3 (6.9)
231.70 ± 0.74	-5.43 ± 1.54	0.272 ± 0.003	13.0 (11.8)	232.03 ± 0.49	-3.46 ± 1.13	0.354 ± 0.004	11.1 (9.7)
270.41 ± 0.49	$+4.17 \pm 1.05$	0.292 ± 0.003	19.7 (12.0)	268.87 ± 0.58	$+2.18 \pm 1.14$	0.384 ± 0.004	17.7 (13.1)
304.61 ± 0.58	$+9.05 \pm 1.06$	0.331 ± 0.003	21.0 (13.5)	306.03 ± 0.58	$+6.66 \pm 1.22$	0.429 ± 0.004	15.5 (13.8)
335.78 ± 0.74	$+1.33 \pm 1.54$	0.345 ± 0.003	18.6 (13.8)	335.91 ± 0.16	$+2.39 \pm 0.72$	0.450 ± 0.004	14.1 (7.0)
IP = 100 m				**IP = 120 m**			
359.93 ± 0.41	-0.81 ± 0.73	0.517 ± 0.004	9.3 (8.1)	359.85 ± 0.33	-0.65 ± 0.81	0.600 ± 0.006	7.9 (2.7)
25.54 ± 0.25	-1.35 ± 0.81	0.455 ± 0.005	7.7 (5.1)	25.10 ± 0.33	-0.69 ± 0.65	0.532 ± 0.006	6.5 (2.6)
53.11 ± 0.41	-2.48 ± 0.89	0.420 ± 0.005	9.7 (6.0)	53.22 ± 0.25	-1.15 ± 0.65	0.495 ± 0.005	7.9 (3.7)
91.70 ± 0.58	$+2.73 \pm 1.06$	0.458 ± 0.005	13.0 (9.8)	91.66 ± 0.25	$+2.66 \pm 0.65$	0.536 ± 0.005	10.1 (4.5)
127.23 ± 0.41	$+4.85 \pm 0.57$	0.513 ± 0.005	13.0 (6.9)	127.46 ± 0.41	$+3.62 \pm 0.89$	0.597 ± 0.005	9.8 (4.0)
155.76 ± 0.41	$+1.25 \pm 0.89$	0.543 ± 0.005	10.4 (4.8)	156.53 ± 0.33	$+0.62 \pm 0.73$	0.621 ± 0.005	8.3 (3.3)
180.39 ± 0.41	-1.72 ± 0.81	0.523 ± 0.005	9.7 (5.0)	179.90 ± 0.33	-1.23 ± 0.73	0.606 ± 0.004	7.8 (3.3)
203.35 ± 0.33	-3.38 ± 0.65	0.467 ± 0.005	9.1 (5.6)	203.02 ± 0.33	-2.46 ± 0.65	0.546 ± 0.006	7.5 (3.6)
231.42 ± 0.41	-2.98 ± 0.81	0.435 ± 0.003	8.9 (7.3)	232.83 ± 0.33	-0.79 ± 0.73	0.512 ± 0.005	7.9 (4.4)
269.02 ± 0.33	$+1.26 \pm 0.81$	0.468 ± 0.004	12.7 (8.2)	268.73 ± 0.41	$+0.89 \pm 0.81$	0.551 ± 0.004	10.8 (5.9)
307.00 ± 0.49	$+4.91 \pm 0.73$	0.528 ± 0.005	11.8 (8.4)	306.86 ± 0.25	$+3.15 \pm 0.65$	0.610 ± 0.003	9.7 (8.0)
335.87 ± 0.41	$+0.80 \pm 0.73$	0.548 ± 0.004	11.1 (4.3)	335.70 ± 0.33	$+0.53 \pm 0.49$	0.631 ± 0.007	7.8 (3.3)

Table 88: The nominal angle δ_n, average displacement $\Delta\delta$, average value of the parameter DIST, RMS of the ALPHA distribution for enabled GF and impact parameters between 60 m and 120 m. The RMS of the ALPHA distribution for disabled GF is given parentheses. The primary γ-ray energy was set to 300 GeV, the ZA to 40° and the azimuth angle to 30°.

$E_\gamma = 300\,\mathrm{GeV}$, Az = 30°, ZA = 40°, Hard Image Cleaning

$\delta_n\,[°]$	$\Delta\delta\,[°]$	DIST[°]	$\mathrm{RMS}_{\lvert\mathrm{ALPHA}\rvert}\,[°]$	$\delta_n\,[°]$	$\Delta\delta\,[°]$	DIST[°]	$\mathrm{RMS}_{\lvert\mathrm{ALPHA}\rvert}\,[°]$
IP = 60 m				**IP = 80 m**			
358.33 ± 0.49	-6.36 ± 1.54	0.316 ± 0.003	15.6 (15.1)	359.29 ± 0.41	-4.35 ± 0.97	0.416 ± 0.003	11.9 (8.5)
23.11 ± 0.41	-6.77 ± 1.29	0.277 ± 0.003	14.1 (12.1)	25.27 ± 0.49	-3.14 ± 0.81	0.364 ± 0.003	11.1 (6.8)
53.48 ± 0.74	-2.91 ± 1.30	0.252 ± 0.003	13.3 (15.9)	54.85 ± 0.58	$+0.04 \pm 0.74$	0.333 ± 0.003	10.8 (9.3)
92.44 ± 0.74	$+2.66 \pm 1.38$	0.275 ± 0.003	19.3 (12.2)	91.87 ± 0.58	$+1.56 \pm 1.14$	0.366 ± 0.003	16.4 (11.2)
126.41 ± 0.66	$+6.43 \pm 1.22$	0.317 ± 0.003	20.2 (14.5)	126.96 ± 0.49	$+4.96 \pm 1.05$	0.415 ± 0.004	14.5 (8.3)
155.69 ± 0.58	$+2.86 \pm 1.30$	0.335 ± 0.004	18.0 (15.1)	156.81 ± 0.58	$+2.30 \pm 1.06$	0.438 ± 0.004	14.6 (7.9)
181.16 ± 0.25	-2.83 ± 0.97	0.322 ± 0.003	16.2 (11.2)	179.23 ± 0.41	-1.94 ± 0.81	0.419 ± 0.003	11.8 (6.4)
204.44 ± 0.58	-9.03 ± 0.98	0.287 ± 0.003	14.0 (13.5)	204.00 ± 0.33	-5.45 ± 0.81	0.375 ± 0.004	11.8 (7.2)
233.27 ± 0.33	-2.89 ± 0.89	0.267 ± 0.003	13.2 (11.8)	231.00 ± 0.58	-3.77 ± 1.06	0.347 ± 0.003	10.9 (12.7)
268.53 ± 0.82	$+2.49 \pm 1.14$	0.288 ± 0.003	19.6 (16.1)	268.63 ± 0.74	$+0.84 \pm 1.14$	0.377 ± 0.003	17.9 (14.3)
306.17 ± 0.49	$+8.90 \pm 0.89$	0.322 ± 0.003	21.8 (13.0)	307.95 ± 0.49	$+7.68 \pm 1.14$	0.424 ± 0.004	14.6 (9.0)
336.52 ± 0.41	$+2.11 \pm 0.73$	0.338 ± 0.003	18.0 (10.8)	335.34 ± 0.49	$+1.19 \pm 0.89$	0.441 ± 0.005	12.2 (6.9)
IP = 100 m				**IP = 120 m**			
0.15 ± 0.49	-1.94 ± 0.73	0.509 ± 0.005	8.8 (8.3)	0.52 ± 0.33	-0.91 ± 0.65	0.593 ± 0.007	7.8 (2.6)
25.81 ± 0.33	-0.41 ± 0.81	0.446 ± 0.004	9.1 (3.8)	25.13 ± 0.41	$+0.09 \pm 0.81$	0.528 ± 0.006	6.6 (2.9)
53.48 ± 0.33	-2.36 ± 0.89	0.413 ± 0.004	9.3 (5.5)	53.10 ± 0.25	-1.28 ± 0.57	0.487 ± 0.005	7.3 (3.7)
91.90 ± 0.49	$+2.11 \pm 1.05$	0.450 ± 0.003	11.8 (9.1)	91.97 ± 0.41	$+2.56 \pm 0.81$	0.528 ± 0.005	10.8 (4.7)
128.36 ± 0.41	$+5.23 \pm 0.89$	0.506 ± 0.005	12.7 (7.8)	127.86 ± 0.25	$+4.41 \pm 0.65$	0.587 ± 0.006	9.3 (4.0)
155.22 ± 0.25	$+0.54 \pm 0.57$	0.535 ± 0.004	10.1 (5.0)	156.05 ± 0.33	$+0.01 \pm 0.73$	0.614 ± 0.007	8.6 (3.5)
179.87 ± 0.41	-1.69 ± 0.65	0.515 ± 0.005	10.4 (4.4)	179.89 ± 0.25	-0.59 ± 0.65	0.598 ± 0.004	8.0 (3.1)
203.73 ± 0.33	-2.03 ± 0.73	0.460 ± 0.004	9.1 (5.5)	203.29 ± 0.25	-1.14 ± 0.49	0.543 ± 0.003	6.3 (3.2)
231.19 ± 0.41	-2.95 ± 0.89	0.430 ± 0.004	9.6 (7.2)	231.71 ± 0.33	-2.30 ± 0.65	0.506 ± 0.004	7.1 (7.2)
268.56 ± 0.41	$+0.96 \pm 0.97$	0.464 ± 0.003	12.1 (8.1)	268.88 ± 0.41	$+0.53 \pm 0.81$	0.544 ± 0.004	10.3 (4.9)
307.12 ± 0.33	$+4.57 \pm 0.81$	0.521 ± 0.005	12.0 (6.4)	307.31 ± 0.25	$+3.06 \pm 0.65$	0.602 ± 0.003	9.4 (4.3)
335.70 ± 0.33	-0.50 ± 0.57	0.540 ± 0.005	9.5 (4.2)	335.77 ± 0.33	$+0.29 \pm 0.65$	0.623 ± 0.004	6.8 (3.3)

Table 89: The nominal angle δ_n, average displacement $\Delta\delta$, average value of the parameter DIST, RMS of the ALPHA distribution for enabled GF and impact parameters between 60 m and 120 m. The RMS of the ALPHA distribution for disabled GF is given parentheses. The primary γ-ray energy was set to 300 GeV, the ZA to 40° and the azimuth angle to 30°.

$E_\gamma = 300\,\mathrm{GeV}$, Az = 60°, ZA = 40°, Intermediate Image Cleaning

$\delta_n[^\circ]$	$\Delta\delta[^\circ]$	DIST[°]	$\mathrm{RMS}_{\lvert\mathrm{ALPHA}\rvert}[^\circ]$	$\delta_n[^\circ]$	$\Delta\delta[^\circ]$	DIST[°]	$\mathrm{RMS}_{\lvert\mathrm{ALPHA}\rvert}[^\circ]$
IP = 60 m				**IP = 80 m**			
359.40 ± 0.33	$+1.10 \pm 1.01$	0.271 ± 0.003	17.3 (13.8)	359.69 ± 0.49	$+1.31 \pm 0.95$	0.356 ± 0.003	15.5 (8.8)
23.84 ± 0.49	-12.03 ± 1.02	0.250 ± 0.003	12.8 (9.9)	25.63 ± 0.16	-4.58 ± 0.77	0.330 ± 0.003	10.0 (5.9)
53.40 ± 0.74	-13.76 ± 1.57	0.270 ± 0.003	12.0 (17.8)	54.12 ± 0.58	-9.83 ± 1.18	0.357 ± 0.004	11.8 (8.9)
91.68 ± 0.74	-2.10 ± 1.27	0.307 ± 0.004	18.6 (13.2)	90.95 ± 0.49	-1.66 ± 0.95	0.404 ± 0.003	14.7 (11.3)
128.29 ± 0.66	$+10.64 \pm 1.41$	0.327 ± 0.004	19.8 (13.1)	127.99 ± 0.66	$+8.38 \pm 1.49$	0.426 ± 0.004	16.3 (8.2)
156.26 ± 0.82	$+12.73 \pm 0.97$	0.309 ± 0.003	21.2 (14.2)	156.09 ± 0.49	$+9.73 \pm 0.95$	0.407 ± 0.004	18.6 (8.8)
179.86 ± 0.66	$+9.70 \pm 1.41$	0.276 ± 0.003	18.2 (11.4)	180.10 ± 0.49	$+6.72 \pm 1.02$	0.364 ± 0.004	16.1 (6.7)
203.58 ± 0.49	-10.02 ± 1.17	0.257 ± 0.003	12.1 (12.6)	204.48 ± 0.33	-4.77 ± 0.93	0.332 ± 0.004	9.5 (6.9)
231.70 ± 0.74	-15.30 ± 1.65	0.275 ± 0.003	13.6 (11.8)	232.03 ± 0.49	-8.65 ± 0.95	0.358 ± 0.004	11.8 (9.7)
270.41 ± 0.49	-1.57 ± 1.03	0.311 ± 0.004	17.6 (12.0)	268.87 ± 0.58	-2.63 ± 0.73	0.407 ± 0.004	14.5 (13.1)
304.61 ± 0.58	$+8.82 \pm 0.88$	0.330 ± 0.003	20.7 (13.5)	306.03 ± 0.58	$+5.46 \pm 1.26$	0.427 ± 0.004	18.2 (13.8)
335.78 ± 0.74	$+8.88 \pm 2.02$	0.309 ± 0.004	21.2 (13.8)	335.91 ± 0.16	$+7.41 \pm 0.62$	0.405 ± 0.003	17.9 (7.0)
IP = 100 m				**IP = 120 m**			
359.93 ± 0.41	$+0.39 \pm 0.79$	0.439 ± 0.003	14.2 (8.1)	359.85 ± 0.33	-0.15 ± 0.63	0.512 ± 0.005	11.4 (2.7)
25.54 ± 0.25	-2.91 ± 0.70	0.407 ± 0.004	8.3 (5.1)	25.10 ± 0.33	-2.77 ± 0.63	0.477 ± 0.005	6.8 (2.6)
53.11 ± 0.41	-8.93 ± 0.94	0.438 ± 0.004	10.2 (6.0)	53.22 ± 0.25	-4.53 ± 0.85	0.512 ± 0.004	9.2 (3.7)
91.70 ± 0.58	-1.56 ± 0.95	0.491 ± 0.004	12.8 (9.8)	91.66 ± 0.25	$+0.82 \pm 0.70$	0.573 ± 0.006	9.2 (4.5)
127.23 ± 0.41	$+5.28 \pm 1.02$	0.520 ± 0.004	13.3 (6.9)	127.46 ± 0.41	$+4.22 \pm 0.86$	0.598 ± 0.005	9.8 (4.0)
155.76 ± 0.41	$+6.25 \pm 1.09$	0.502 ± 0.004	15.9 (4.8)	156.53 ± 0.33	$+4.38 \pm 0.56$	0.582 ± 0.005	12.6 (3.3)
180.39 ± 0.41	$+3.82 \pm 0.86$	0.445 ± 0.004	13.6 (5.0)	179.90 ± 0.33	$+2.06 \pm 0.56$	0.522 ± 0.005	11.4 (3.3)
203.35 ± 0.33	-2.36 ± 0.71	0.411 ± 0.005	8.7 (5.6)	203.02 ± 0.33	-0.19 ± 0.71	0.482 ± 0.006	6.9 (3.6)
231.42 ± 0.41	-6.17 ± 1.09	0.442 ± 0.005	10.4 (7.3)	232.83 ± 0.33	-3.61 ± 0.78	0.527 ± 0.006	8.2 (4.4)
269.02 ± 0.33	-2.45 ± 0.71	0.499 ± 0.004	13.1 (8.2)	268.73 ± 0.41	-2.33 ± 0.71	0.581 ± 0.004	10.9 (5.9)
307.00 ± 0.49	$+4.07 \pm 1.02$	0.521 ± 0.004	15.3 (8.4)	306.86 ± 0.25	$+2.98 \pm 0.47$	0.600 ± 0.004	10.9 (8.0)
335.87 ± 0.41	$+2.93 \pm 0.86$	0.496 ± 0.004	13.9 (4.3)	335.70 ± 0.33	$+1.84 \pm 0.56$	0.572 ± 0.004	12.0 (3.3)

Table 90: The nominal angle δ_n, average displacement $\Delta\delta$, average value of the parameter DIST, RMS of the ALPHA distribution for enabled GF and impact parameters between 60 m and 120 m. The RMS of the ALPHA distribution for disabled GF is given parentheses. The primary γ-ray energy was set to 300 GeV, the ZA to 40° and the azimuth angle to 60°.

$E_\gamma = 300\,\mathrm{GeV}$, Az = 60°, ZA = 40°, Hard Image Cleaning

$\delta_n[^\circ]$	$\Delta\delta[^\circ]$	DIST[°]	$\mathrm{RMS}_{\lvert\mathrm{ALPHA}\rvert}[^\circ]$	$\delta_n[^\circ]$	$\Delta\delta[^\circ]$	DIST[°]	$\mathrm{RMS}_{\lvert\mathrm{ALPHA}\rvert}[^\circ]$
IP = 60 m				**IP = 80 m**			
358.33 ± 0.49	-2.12 ± 1.34	0.268 ± 0.004	17.1 (15.1)	359.29 ± 0.41	-1.55 ± 0.87	0.352 ± 0.003	14.7 (8.5)
23.11 ± 0.41	-10.31 ± 0.95	0.247 ± 0.003	12.0 (12.1)	25.27 ± 0.49	-5.26 ± 0.88	0.322 ± 0.003	10.2 (6.8)
53.48 ± 0.74	-14.36 ± 1.58	0.268 ± 0.003	12.5 (15.9)	54.85 ± 0.58	-8.86 ± 1.49	0.350 ± 0.003	12.0 (9.3)
92.44 ± 0.74	-0.99 ± 1.27	0.302 ± 0.004	18.0 (12.2)	91.87 ± 0.58	-2.33 ± 1.11	0.397 ± 0.004	14.5 (11.2)
126.41 ± 0.66	$+9.01 \pm 1.35$	0.321 ± 0.003	19.8 (14.5)	126.96 ± 0.49	$+7.75 \pm 1.18$	0.420 ± 0.003	16.4 (8.3)
155.69 ± 0.58	$+10.48 \pm 1.03$	0.305 ± 0.002	22.2 (15.1)	156.81 ± 0.58	$+9.55 \pm 1.18$	0.400 ± 0.003	18.3 (7.9)
181.16 ± 0.25	$+8.26 \pm 0.93$	0.273 ± 0.003	17.6 (11.2)	179.23 ± 0.41	$+4.79 \pm 0.94$	0.356 ± 0.003	15.5 (6.4)
204.44 ± 0.58	-9.25 ± 1.87	0.253 ± 0.003	11.9 (13.5)	204.00 ± 0.33	-4.42 ± 1.09	0.329 ± 0.003	9.7 (7.2)
233.27 ± 0.33	-12.88 ± 1.55	0.271 ± 0.003	13.0 (11.8)	231.00 ± 0.58	-7.70 ± 1.34	0.354 ± 0.003	12.4 (12.7)
268.53 ± 0.82	-4.18 ± 1.28	0.304 ± 0.004	18.3 (16.1)	268.63 ± 0.74	-3.65 ± 1.13	0.403 ± 0.004	14.5 (14.3)
306.17 ± 0.49	$+10.17 \pm 1.03$	0.324 ± 0.003	19.8 (13.0)	307.95 ± 0.49	$+8.18 \pm 1.18$	0.420 ± 0.004	18.2 (9.0)
336.52 ± 0.41	$+6.89 \pm 0.79$	0.306 ± 0.003	19.6 (10.8)	335.34 ± 0.49	$+7.99 \pm 1.03$	0.400 ± 0.004	17.8 (6.9)
IP = 100 m				**IP = 120 m**			
0.15 ± 0.49	$+1.05 \pm 1.03$	0.434 ± 0.003	13.6 (8.3)	0.52 ± 0.33	-0.35 ± 0.79	0.505 ± 0.004	11.9 (2.6)
25.81 ± 0.33	-2.37 ± 0.78	0.398 ± 0.004	8.9 (3.8)	25.13 ± 0.41	-1.98 ± 0.79	0.470 ± 0.005	7.2 (2.9)
53.48 ± 0.33	-7.25 ± 0.71	0.430 ± 0.004	10.5 (5.5)	53.10 ± 0.25	-5.01 ± 0.78	0.506 ± 0.005	8.8 (3.7)
91.90 ± 0.49	-0.49 ± 0.87	0.485 ± 0.004	12.3 (9.1)	91.97 ± 0.41	$+0.53 \pm 0.79$	0.565 ± 0.005	10.6 (4.7)
128.36 ± 0.41	$+5.84 \pm 0.79$	0.513 ± 0.005	12.4 (7.8)	127.86 ± 0.25	$+4.73 \pm 0.70$	0.592 ± 0.005	9.8 (4.0)
155.22 ± 0.25	$+5.40 \pm 0.55$	0.495 ± 0.003	16.2 (5.0)	156.05 ± 0.33	$+3.46 \pm 0.48$	0.576 ± 0.005	12.6 (3.5)
179.87 ± 0.41	$+4.57 \pm 0.86$	0.438 ± 0.004	13.7 (4.4)	179.89 ± 0.25	$+1.55 \pm 0.63$	0.517 ± 0.004	11.4 (3.1)
203.73 ± 0.33	-2.72 ± 0.94	0.406 ± 0.005	8.9 (5.5)	203.29 ± 0.25	-0.14 ± 0.71	0.475 ± 0.006	7.4 (3.2)
231.19 ± 0.41	-5.94 ± 0.95	0.439 ± 0.004	10.6 (7.2)	231.71 ± 0.33	-4.99 ± 0.86	0.519 ± 0.006	8.7 (7.2)
268.56 ± 0.41	-3.14 ± 0.80	0.493 ± 0.006	12.9 (8.1)	268.88 ± 0.41	-1.68 ± 0.64	0.576 ± 0.004	11.7 (4.9)
307.12 ± 0.33	$+3.81 \pm 0.79$	0.515 ± 0.003	14.6 (6.4)	307.31 ± 0.25	$+3.05 \pm 0.55$	0.592 ± 0.004	10.8 (4.3)
335.70 ± 0.33	$+2.30 \pm 0.79$	0.489 ± 0.005	14.9 (4.2)	335.77 ± 0.33	$+0.70 \pm 0.63$	0.566 ± 0.005	11.5 (3.3)

Table 91: The nominal angle δ_n, average displacement $\Delta\delta$, average value of the parameter DIST, RMS of the ALPHA distribution for enabled GF and impact parameters between 60 m and 120 m. The RMS of the ALPHA distribution for disabled GF is given parentheses. The primary γ-ray energy was set to 300 GeV, the ZA to 40° and the azimuth angle to 60°.

$E_\gamma = 300\,\mathrm{GeV}$, Az = 90°, ZA = 40°, Intermediate Image Cleaning

$\delta_n[°]$	$\Delta\delta[°]$	DIST[°]	$\mathrm{RMS}_{\lvert\mathrm{ALPHA}\rvert}[°]$	$\delta_n[°]$	$\Delta\delta[°]$	DIST[°]	$\mathrm{RMS}_{\lvert\mathrm{ALPHA}\rvert}[°]$
IP = 60 m				**IP = 80 m**			
359.40 ± 0.33	$+6.71 \pm 0.86$	0.256 ± 0.002	14.5 (13.8)	359.69 ± 0.49	$+4.11 \pm 1.18$	0.332 ± 0.003	13.9 (8.8)
23.84 ± 0.49	-5.74 ± 1.33	0.282 ± 0.002	9.9 (9.9)	25.63 ± 0.16	$+1.51 \pm 0.47$	0.360 ± 0.003	7.5 (5.9)
53.40 ± 0.74	-17.44 ± 2.03	0.316 ± 0.001	17.6 (17.8)	54.12 ± 0.58	-13.57 ± 1.56	0.408 ± 0.003	14.7 (8.9)
91.68 ± 0.74	-10.66 ± 1.12	0.336 ± 0.003	23.6 (13.2)	90.95 ± 0.49	-9.83 ± 1.18	0.433 ± 0.003	21.6 (11.3)
128.29 ± 0.66	$+6.70 \pm 1.27$	0.320 ± 0.002	25.8 (13.1)	127.99 ± 0.66	$+4.69 \pm 1.11$	0.415 ± 0.004	24.4 (8.2)
156.26 ± 0.82	$+14.49 \pm 1.73$	0.281 ± 0.003	25.6 (14.2)	156.09 ± 0.49	$+11.01 \pm 1.02$	0.369 ± 0.004	22.9 (8.8)
179.86 ± 0.66	$+15.31 \pm 1.79$	0.256 ± 0.003	14.9 (11.4)	180.10 ± 0.49	$+10.79 \pm 1.02$	0.334 ± 0.004	13.8 (6.7)
203.58 ± 0.49	$+0.38 \pm 0.80$	0.275 ± 0.003	10.8 (12.6)	204.48 ± 0.33	$+5.03 \pm 1.09$	0.359 ± 0.003	9.8 (6.9)
231.70 ± 0.74	-12.38 ± 1.19	0.307 ± 0.003	19.3 (11.8)	232.03 ± 0.49	-7.03 ± 1.10	0.406 ± 0.004	16.8 (9.7)
270.41 ± 0.49	-8.83 ± 1.03	0.328 ± 0.003	24.1 (12.0)	268.87 ± 0.58	-7.18 ± 1.18	0.429 ± 0.003	19.3 (13.1)
304.61 ± 0.58	$+0.57 \pm 1.03$	0.315 ± 0.003	25.8 (13.5)	306.03 ± 0.58	$+0.36 \pm 1.03$	0.409 ± 0.003	23.1 (13.8)
335.78 ± 0.74	$+8.35 \pm 0.97$	0.278 ± 0.003	23.2 (13.8)	335.91 ± 0.16	$+8.19 \pm 0.70$	0.360 ± 0.003	23.0 (7.0)
IP = 100 m				**IP = 120 m**			
359.93 ± 0.41	$+3.87 \pm 1.02$	0.407 ± 0.004	11.6 (8.1)	359.85 ± 0.33	$+2.03 \pm 0.78$	0.482 ± 0.004	11.5 (2.7)
25.54 ± 0.25	-0.33 ± 0.70	0.439 ± 0.004	7.0 (5.1)	25.10 ± 0.33	-0.02 ± 0.86	0.511 ± 0.004	5.8 (2.6)
53.11 ± 0.41	-6.75 ± 0.79	0.497 ± 0.004	13.5 (6.0)	53.22 ± 0.25	-4.66 ± 0.70	0.571 ± 0.005	10.2 (3.7)
91.70 ± 0.58	-6.82 ± 1.03	0.527 ± 0.004	16.6 (9.8)	91.66 ± 0.25	-4.28 ± 0.78	0.602 ± 0.005	13.9 (4.5)
127.23 ± 0.41	$+3.28 \pm 0.71$	0.506 ± 0.004	21.2 (6.9)	127.46 ± 0.41	$+2.92 \pm 0.79$	0.583 ± 0.004	14.1 (4.0)
155.76 ± 0.41	$+7.48 \pm 0.79$	0.451 ± 0.004	20.1 (4.8)	156.53 ± 0.33	$+5.54 \pm 0.71$	0.528 ± 0.003	15.7 (3.3)
180.39 ± 0.41	$+4.91 \pm 0.94$	0.410 ± 0.004	12.2 (5.0)	179.90 ± 0.33	$+4.02 \pm 0.78$	0.485 ± 0.003	9.4 (3.3)
203.35 ± 0.33	$+3.19 \pm 0.93$	0.438 ± 0.006	8.6 (5.6)	203.02 ± 0.33	$+0.01 \pm 0.56$	0.513 ± 0.004	6.7 (3.6)
231.42 ± 0.41	-7.13 ± 0.71	0.496 ± 0.003	13.5 (7.3)	232.83 ± 0.33	-3.96 ± 0.78	0.574 ± 0.004	8.5 (4.4)
269.02 ± 0.33	-6.35 ± 1.09	0.522 ± 0.004	14.3 (8.2)	268.73 ± 0.41	-4.49 ± 0.94	0.599 ± 0.005	12.4 (5.9)
307.00 ± 0.49	$+0.58 \pm 0.95$	0.497 ± 0.004	19.4 (8.4)	306.86 ± 0.25	$+0.47 \pm 0.55$	0.574 ± 0.004	13.0 (8.0)
335.87 ± 0.41	$+2.35 \pm 1.02$	0.442 ± 0.003	19.7 (4.3)	335.70 ± 0.33	$+0.99 \pm 0.63$	0.518 ± 0.005	15.8 (3.3)

Table 92: The nominal angle δ_n, average displacement $\Delta\delta$, average value of the parameter DIST, RMS of the ALPHA distribution for enabled GF and impact parameters between 60 m and 120 m. The RMS of the ALPHA distribution for disabled GF is given parentheses. The primary γ-ray energy was set to 300 GeV, the ZA to 40° and the azimuth angle to 90°.

$E_\gamma = 300\,\mathrm{GeV}$, Az = 90°, ZA = 40°, Hard Image Cleaning

$\delta_n[°]$	$\Delta\delta[°]$	DIST[°]	$\mathrm{RMS}_{\lvert\mathrm{ALPHA}\rvert}[°]$	$\delta_n[°]$	$\Delta\delta[°]$	DIST[°]	$\mathrm{RMS}_{\lvert\mathrm{ALPHA}\rvert}[°]$
IP = 60 m				**IP = 80 m**			
358.33 ± 0.49	$+7.32 \pm 0.89$	0.255 ± 0.003	15.2 (15.1)	359.29 ± 0.41	$+1.83 \pm 1.12$	0.329 ± 0.003	14.4 (8.5)
23.11 ± 0.41	-0.06 ± 0.88	0.275 ± 0.003	9.6 (12.1)	25.27 ± 0.49	$+1.19 \pm 1.50$	0.357 ± 0.003	9.1 (6.8)
53.48 ± 0.74	-17.68 ± 1.28	0.312 ± 0.002	17.7 (15.9)	54.85 ± 0.58	-9.58 ± 1.43	0.406 ± 0.004	14.2 (9.3)
92.44 ± 0.74	-10.58 ± 1.37	0.331 ± 0.003	23.5 (12.2)	91.87 ± 0.58	-9.74 ± 1.19	0.430 ± 0.002	20.6 (11.2)
126.41 ± 0.66	$+4.86 \pm 1.28$	0.317 ± 0.002	26.5 (14.5)	126.96 ± 0.49	$+4.59 \pm 1.11$	0.410 ± 0.004	24.1 (8.3)
155.69 ± 0.58	$+13.04 \pm 1.27$	0.279 ± 0.003	26.8 (15.1)	156.81 ± 0.58	$+10.79 \pm 1.27$	0.362 ± 0.003	23.5 (7.9)
181.16 ± 0.25	$+15.13 \pm 1.10$	0.254 ± 0.003	14.5 (11.2)	179.23 ± 0.41	$+10.73 \pm 1.03$	0.332 ± 0.003	12.9 (6.4)
204.44 ± 0.58	$+3.30 \pm 0.96$	0.273 ± 0.004	11.5 (13.5)	204.00 ± 0.33	$+7.87 \pm 1.03$	0.361 ± 0.003	8.5 (7.2)
233.27 ± 0.33	-13.37 ± 0.56	0.307 ± 0.003	19.4 (11.8)	231.00 ± 0.58	-4.59 ± 1.66	0.401 ± 0.004	14.9 (12.7)
268.53 ± 0.82	-10.03 ± 1.45	0.324 ± 0.002	23.7 (16.1)	268.63 ± 0.74	-8.45 ± 1.29	0.427 ± 0.004	19.5 (14.3)
306.17 ± 0.49	$+3.11 \pm 1.04$	0.310 ± 0.003	25.9 (13.0)	307.95 ± 0.49	$+4.13 \pm 1.13$	0.402 ± 0.002	22.0 (9.0)
336.52 ± 0.41	$+10.82 \pm 1.04$	0.274 ± 0.003	23.1 (10.8)	335.34 ± 0.49	$+5.44 \pm 1.19$	0.355 ± 0.003	22.9 (6.9)
IP = 100 m				**IP = 120 m**			
0.15 ± 0.49	$+1.99 \pm 1.03$	0.404 ± 0.004	12.5 (8.3)	0.52 ± 0.33	$+1.38 \pm 0.64$	0.478 ± 0.005	8.0 (2.6)
25.81 ± 0.33	-1.68 ± 0.71	0.436 ± 0.003	7.0 (3.8)	25.13 ± 0.41	$+0.06 \pm 0.87$	0.508 ± 0.003	4.5 (2.9)
53.48 ± 0.33	-7.84 ± 0.41	0.492 ± 0.005	12.2 (5.5)	53.10 ± 0.25	-5.98 ± 0.48	0.567 ± 0.004	10.9 (3.7)
91.90 ± 0.49	-5.99 ± 1.03	0.522 ± 0.004	14.7 (9.1)	91.97 ± 0.41	-3.46 ± 0.96	0.598 ± 0.003	11.3 (4.7)
128.36 ± 0.41	$+4.71 \pm 0.87$	0.500 ± 0.003	19.5 (7.8)	127.86 ± 0.25	$+2.78 \pm 0.64$	0.576 ± 0.004	12.6 (4.0)
155.22 ± 0.25	$+5.76 \pm 0.79$	0.447 ± 0.004	19.4 (5.0)	156.05 ± 0.33	$+5.01 \pm 0.71$	0.522 ± 0.002	14.1 (3.5)
179.87 ± 0.41	$+5.65 \pm 0.96$	0.407 ± 0.005	12.6 (4.4)	179.89 ± 0.25	$+3.73 \pm 0.48$	0.481 ± 0.004	10.3 (3.1)
203.73 ± 0.33	$+3.37 \pm 0.56$	0.435 ± 0.003	7.8 (5.5)	203.29 ± 0.25	$+0.61 \pm 0.94$	0.510 ± 0.005	4.9 (3.2)
231.19 ± 0.41	-5.99 ± 0.80	0.490 ± 0.003	13.8 (7.2)	231.71 ± 0.33	-3.32 ± 0.79	0.573 ± 0.004	8.1 (7.2)
268.56 ± 0.41	-5.95 ± 1.03	0.516 ± 0.004	14.4 (8.1)	268.88 ± 0.41	-3.80 ± 0.87	0.595 ± 0.004	9.9 (4.9)
307.12 ± 0.33	$+1.54 \pm 0.72$	0.489 ± 0.004	17.7 (6.4)	307.31 ± 0.25	$+0.77 \pm 0.55$	0.568 ± 0.004	13.1 (4.3)
335.70 ± 0.33	$+2.55 \pm 0.79$	0.435 ± 0.003	17.7 (4.2)	335.77 ± 0.33	$+1.95 \pm 0.72$	0.513 ± 0.004	14.3 (3.3)

Table 93: The nominal angle δ_n, average displacement $\Delta\delta$, average value of the parameter DIST, RMS of the ALPHA distribution for enabled GF and impact parameters between 60 m and 120 m. The RMS of the ALPHA distribution for disabled GF is given parentheses. The primary γ-ray energy was set to 300 GeV, the ZA to 40° and the azimuth angle to 90°.

$E_\gamma = 300\,\mathrm{GeV}$, Az = 120°, ZA = 40°, Intermediate Image Cleaning

δ_n[°]	$\Delta\delta$[°]	DIST[°]	RMS$_{\vert\mathrm{ALPHA}\vert}$[°]	δ_n[°]	$\Delta\delta$[°]	DIST[°]	RMS$_{\vert\mathrm{ALPHA}\vert}$[°]
IP = 60 m				**IP = 80 m**			
359.40 ± 0.33	$+13.82 \pm 1.38$	0.280 ± 0.003	11.1 (13.8)	359.69 ± 0.49	$+9.47 \pm 0.94$	0.364 ± 0.003	9.3 (8.8)
23.84 ± 0.49	$+11.95 \pm 2.22$	0.317 ± 0.003	12.7 (9.9)	25.63 ± 0.16	$+11.32 \pm 0.99$	0.406 ± 0.003	12.2 (5.9)
53.40 ± 0.74	-10.98 ± 0.89	0.338 ± 0.004	17.9 (17.8)	54.12 ± 0.58	-7.84 ± 1.02	0.434 ± 0.004	15.0 (8.9)
91.68 ± 0.74	-13.07 ± 1.34	0.325 ± 0.003	21.5 (13.2)	90.95 ± 0.49	-9.49 ± 1.24	0.422 ± 0.004	20.1 (11.3)
128.29 ± 0.66	-2.00 ± 0.96	0.290 ± 0.002	22.0 (13.1)	127.99 ± 0.66	-1.70 ± 1.11	0.380 ± 0.002	21.1 (8.2)
156.26 ± 0.82	$+7.53 \pm 1.43$	0.265 ± 0.002	16.6 (14.2)	156.09 ± 0.49	$+5.22 \pm 1.02$	0.347 ± 0.003	15.7 (8.8)
179.86 ± 0.66	$+13.93 \pm 1.56$	0.284 ± 0.004	10.6 (11.4)	180.10 ± 0.49	$+8.97 \pm 1.25$	0.369 ± 0.004	8.4 (6.7)
203.58 ± 0.49	$+7.11 \pm 1.84$	0.316 ± 0.004	14.0 (12.6)	204.48 ± 0.33	$+8.31 \pm 0.40$	0.412 ± 0.004	10.6 (6.9)
231.70 ± 0.74	-5.93 ± 0.81	0.332 ± 0.004	17.9 (11.8)	232.03 ± 0.49	-2.01 ± 1.01	0.437 ± 0.004	14.6 (9.7)
270.41 ± 0.49	-15.57 ± 1.54	0.320 ± 0.004	20.4 (12.0)	268.87 ± 0.58	-18.61 ± 1.55	0.412 ± 0.003	20.1 (13.1)
304.61 ± 0.58	-5.01 ± 0.95	0.283 ± 0.002	21.2 (13.5)	306.03 ± 0.58	-4.38 ± 0.95	0.367 ± 0.003	19.6 (13.8)
335.78 ± 0.74	$+7.45 \pm 1.42$	0.257 ± 0.003	17.0 (13.8)	335.91 ± 0.16	$+5.99 \pm 0.61$	0.332 ± 0.003	16.5 (7.0)
IP = 100 m				**IP = 120 m**			
359.93 ± 0.41	$+5.89 \pm 0.94$	0.440 ± 0.006	8.4 (8.1)	359.85 ± 0.33	$+3.32 \pm 0.63$	0.512 ± 0.003	8.3 (2.7)
25.54 ± 0.25	$+8.02 \pm 0.85$	0.489 ± 0.004	9.9 (5.1)	25.10 ± 0.33	$+3.95 \pm 0.55$	0.572 ± 0.004	8.2 (2.6)
53.11 ± 0.41	-2.87 ± 0.86	0.524 ± 0.004	13.0 (6.0)	53.22 ± 0.25	-1.48 ± 0.84	0.604 ± 0.006	10.6 (3.7)
91.70 ± 0.58	-8.30 ± 1.55	0.511 ± 0.005	16.6 (9.8)	91.66 ± 0.25	-5.26 ± 1.00	0.592 ± 0.006	13.8 (4.5)
127.23 ± 0.41	-2.37 ± 0.79	0.463 ± 0.004	17.9 (6.9)	127.46 ± 0.41	-1.15 ± 0.64	0.539 ± 0.003	17.0 (4.0)
155.76 ± 0.41	$+3.02 \pm 0.71$	0.425 ± 0.003	13.7 (4.8)	156.53 ± 0.33	$+4.50 \pm 0.63$	0.496 ± 0.004	12.3 (3.3)
180.39 ± 0.41	$+4.13 \pm 0.86$	0.452 ± 0.005	7.4 (5.0)	179.90 ± 0.33	$+3.40 \pm 0.86$	0.530 ± 0.006	6.1 (3.3)
203.35 ± 0.33	$+3.87 \pm 1.00$	0.505 ± 0.006	8.2 (5.6)	203.02 ± 0.33	$+1.87 \pm 0.85$	0.585 ± 0.004	7.5 (3.6)
231.42 ± 0.41	-3.30 ± 1.16	0.526 ± 0.004	12.7 (7.3)	232.83 ± 0.33	-0.24 ± 0.78	0.608 ± 0.006	11.2 (4.4)
269.02 ± 0.33	-10.71 ± 1.00	0.501 ± 0.004	16.4 (8.2)	268.73 ± 0.41	-9.44 ± 0.86	0.582 ± 0.004	13.2 (5.9)
307.00 ± 0.49	-2.47 ± 0.79	0.448 ± 0.004	17.3 (8.4)	306.86 ± 0.25	-2.54 ± 0.55	0.521 ± 0.004	15.9 (8.0)
335.87 ± 0.41	$+2.41 \pm 0.71$	0.411 ± 0.004	14.4 (4.3)	335.70 ± 0.33	$+1.60 \pm 0.63$	0.481 ± 0.004	12.9 (3.3)

Table 94: The nominal angle δ_n, average displacement $\Delta\delta$, average value of the parameter DIST, RMS of the ALPHA distribution for enabled GF and impact parameters between 60 m and 120 m. The RMS of the ALPHA distribution for disabled GF is given parentheses. The primary γ-ray energy was set to 300 GeV, the ZA to 40° and the azimuth angle to 120°.

$E_\gamma = 300\,\mathrm{GeV}$, Az = 120°, ZA = 40°, Hard Image Cleaning

δ_n[°]	$\Delta\delta$[°]	DIST[°]	RMS$_{\vert\mathrm{ALPHA}\vert}$[°]	δ_n[°]	$\Delta\delta$[°]	DIST[°]	RMS$_{\vert\mathrm{ALPHA}\vert}$[°]
IP = 60 m				**IP = 80 m**			
358.33 ± 0.49	$+11.25 \pm 1.42$	0.278 ± 0.003	11.2 (15.1)	359.29 ± 0.41	$+7.86 \pm 0.95$	0.364 ± 0.003	9.4 (8.5)
23.11 ± 0.41	$+11.20 \pm 0.88$	0.316 ± 0.003	12.3 (12.1)	25.27 ± 0.49	$+10.24 \pm 0.88$	0.407 ± 0.004	10.9 (6.8)
53.48 ± 0.74	-9.20 ± 2.06	0.332 ± 0.003	17.3 (15.9)	54.85 ± 0.58	-2.28 ± 0.81	0.435 ± 0.005	14.6 (9.3)
92.44 ± 0.74	-10.54 ± 1.51	0.322 ± 0.003	21.3 (12.2)	91.87 ± 0.58	-10.25 ± 1.20	0.420 ± 0.003	19.3 (11.2)
126.41 ± 0.66	-3.73 ± 0.89	0.287 ± 0.002	22.4 (14.5)	126.96 ± 0.49	-2.83 ± 1.04	0.378 ± 0.003	20.7 (8.3)
155.69 ± 0.58	$+7.24 \pm 1.13$	0.259 ± 0.003	15.1 (15.1)	156.81 ± 0.58	$+6.12 \pm 1.04$	0.345 ± 0.004	15.9 (7.9)
181.16 ± 0.25	$+14.61 \pm 0.71$	0.284 ± 0.004	10.3 (11.2)	179.23 ± 0.41	$+7.18 \pm 1.11$	0.369 ± 0.004	8.8 (6.4)
204.44 ± 0.58	$+11.48 \pm 1.42$	0.314 ± 0.004	13.9 (13.5)	204.00 ± 0.33	$+9.06 \pm 1.65$	0.412 ± 0.003	11.0 (7.2)
233.27 ± 0.33	-2.97 ± 0.48	0.333 ± 0.004	17.8 (11.8)	231.00 ± 0.58	-3.56 ± 1.11	0.433 ± 0.004	14.6 (12.7)
268.53 ± 0.82	-16.54 ± 1.74	0.316 ± 0.003	21.0 (16.1)	268.63 ± 0.74	-13.64 ± 1.21	0.413 ± 0.003	18.2 (14.3)
306.17 ± 0.49	-3.36 ± 0.81	0.281 ± 0.003	20.4 (13.0)	307.95 ± 0.49	-1.87 ± 0.88	0.364 ± 0.003	18.8 (9.0)
336.52 ± 0.41	$+7.91 \pm 0.95$	0.254 ± 0.003	15.6 (10.8)	335.34 ± 0.49	$+4.32 \pm 1.03$	0.332 ± 0.004	14.4 (6.9)
IP = 100 m				**IP = 120 m**			
0.15 ± 0.49	$+5.20 \pm 0.88$	0.437 ± 0.004	7.7 (8.3)	0.52 ± 0.33	$+4.15 \pm 0.56$	0.512 ± 0.005	6.9 (2.6)
25.81 ± 0.33	$+7.85 \pm 1.10$	0.492 ± 0.003	8.7 (3.8)	25.13 ± 0.41	$+4.07 \pm 0.64$	0.575 ± 0.005	7.1 (2.9)
53.48 ± 0.33	-3.82 ± 1.03	0.529 ± 0.005	12.1 (5.5)	53.10 ± 0.25	-3.69 ± 0.86	0.603 ± 0.006	9.5 (3.7)
91.90 ± 0.49	-8.43 ± 1.19	0.508 ± 0.004	14.5 (9.1)	91.97 ± 0.41	-3.86 ± 0.80	0.588 ± 0.006	12.7 (4.7)
128.36 ± 0.41	-1.28 ± 0.80	0.461 ± 0.004	17.7 (7.8)	127.86 ± 0.25	-1.05 ± 0.56	0.536 ± 0.005	16.0 (4.0)
155.22 ± 0.25	$+2.52 \pm 0.48$	0.423 ± 0.004	13.4 (5.0)	156.05 ± 0.33	$+3.56 \pm 0.64$	0.493 ± 0.004	12.0 (3.5)
179.87 ± 0.41	$+5.62 \pm 1.03$	0.447 ± 0.005	8.5 (4.4)	179.89 ± 0.25	$+2.51 \pm 0.71$	0.526 ± 0.006	6.2 (3.1)
203.73 ± 0.33	$+5.15 \pm 0.64$	0.506 ± 0.006	7.8 (5.5)	203.29 ± 0.25	$+1.37 \pm 0.71$	0.590 ± 0.005	6.8 (3.2)
231.19 ± 0.41	-3.54 ± 1.03	0.523 ± 0.006	12.3 (7.2)	231.71 ± 0.33	-2.01 ± 0.86	0.609 ± 0.006	9.9 (7.2)
268.56 ± 0.41	-10.80 ± 1.02	0.498 ± 0.004	14.7 (8.1)	268.88 ± 0.41	-7.31 ± 0.95	0.581 ± 0.005	12.7 (4.9)
307.12 ± 0.33	-2.66 ± 0.64	0.446 ± 0.005	17.1 (6.4)	307.31 ± 0.25	-1.86 ± 0.55	0.519 ± 0.004	14.9 (4.3)
335.70 ± 0.33	$+2.69 \pm 0.79$	0.407 ± 0.004	13.2 (4.2)	335.77 ± 0.33	$+1.76 \pm 0.56$	0.481 ± 0.004	12.1 (3.3)

Table 95: The nominal angle δ_n, average displacement $\Delta\delta$, average value of the parameter DIST, RMS of the ALPHA distribution for enabled GF and impact parameters between 60 m and 120 m. The RMS of the ALPHA distribution for disabled GF is given parentheses. The primary γ-ray energy was set to 300 GeV, the ZA to 40° and the azimuth angle to 120°.

$E_\gamma = 300\,\mathrm{GeV}$, Az = 150°, ZA = 40°, Intermediate Image Cleaning

δ_n[°]	$\Delta\delta$[°]	DIST[°]	$\mathrm{RMS}_{\mathrm{\lvert ALPHA\rvert}}$[°]	δ_n[°]	$\Delta\delta$[°]	DIST[°]	$\mathrm{RMS}_{\mathrm{\lvert ALPHA\rvert}}$[°]
IP = 60 m				**IP = 80 m**			
359.40 ± 0.33	$+7.65 \pm 1.00$	0.304 ± 0.004	10.6 (13.8)	359.69 ± 0.49	$+5.55 \pm 1.09$	0.395 ± 0.004	8.5 (8.8)
23.84 ± 0.49	$+17.37 \pm 1.45$	0.326 ± 0.004	12.9 (9.9)	25.63 ± 0.16	$+12.73 \pm 0.75$	0.418 ± 0.004	10.6 (5.9)
53.40 ± 0.74	$+10.94 \pm 0.89$	0.311 ± 0.003	19.8 (17.8)	54.12 ± 0.58	$+8.09 \pm 1.02$	0.406 ± 0.004	16.2 (8.9)
91.68 ± 0.74	-12.13 ± 0.89	0.286 ± 0.002	25.7 (13.2)	90.95 ± 0.49	-13.96 ± 1.08	0.368 ± 0.003	24.5 (11.3)
128.29 ± 0.66	-10.44 ± 1.25	0.269 ± 0.002	21.8 (13.1)	127.99 ± 0.66	-7.88 ± 1.39	0.344 ± 0.004	22.1 (8.2)
156.26 ± 0.82	$+1.88 \pm 1.34$	0.279 ± 0.003	14.9 (14.2)	156.09 ± 0.49	$+1.75 \pm 0.86$	0.366 ± 0.003	14.6 (8.8)
179.86 ± 0.66	$+7.30 \pm 1.25$	0.316 ± 0.004	9.9 (11.4)	180.10 ± 0.49	$+5.19 \pm 1.01$	0.411 ± 0.004	7.7 (6.7)
203.58 ± 0.49	$+14.11 \pm 1.23$	0.330 ± 0.003	11.4 (12.6)	204.48 ± 0.33	$+12.16 \pm 0.99$	0.428 ± 0.004	10.5 (6.9)
231.70 ± 0.74	$+8.62 \pm 2.73$	0.311 ± 0.002	18.5 (11.8)	232.03 ± 0.49	$+6.28 \pm 0.71$	0.405 ± 0.002	15.3 (9.7)
270.41 ± 0.49	-11.22 ± 1.45	0.278 ± 0.002	25.9 (12.0)	268.87 ± 0.58	-16.06 ± 1.38	0.363 ± 0.002	23.6 (13.1)
304.61 ± 0.58	-14.20 ± 1.39	0.255 ± 0.002	22.7 (13.5)	306.03 ± 0.58	-10.85 ± 1.24	0.331 ± 0.002	22.3 (13.8)
335.78 ± 0.74	-1.46 ± 1.19	0.271 ± 0.003	15.3 (13.8)	335.91 ± 0.16	-1.18 ± 0.46	0.352 ± 0.004	15.2 (7.0)
IP = 100 m				**IP = 120 m**			
359.93 ± 0.41	$+4.48 \pm 0.78$	0.481 ± 0.005	7.6 (8.1)	359.85 ± 0.33	$+2.79 \pm 0.70$	0.559 ± 0.006	5.8 (2.7)
25.54 ± 0.25	$+7.85 \pm 0.69$	0.511 ± 0.006	9.6 (5.1)	25.10 ± 0.33	$+4.56 \pm 0.70$	0.588 ± 0.007	7.7 (2.6)
53.11 ± 0.41	$+7.10 \pm 1.44$	0.491 ± 0.005	15.1 (6.0)	53.22 ± 0.25	$+4.10 \pm 0.91$	0.574 ± 0.006	12.6 (3.7)
91.70 ± 0.58	-7.49 ± 0.80	0.453 ± 0.003	20.4 (9.8)	91.66 ± 0.25	-2.99 ± 1.05	0.526 ± 0.005	16.7 (4.5)
127.23 ± 0.41	-5.61 ± 0.93	0.424 ± 0.003	21.6 (6.9)	127.46 ± 0.41	-2.96 ± 0.85	0.490 ± 0.005	18.0 (4.0)
155.76 ± 0.41	$+1.03 \pm 0.71$	0.447 ± 0.004	13.2 (4.8)	156.53 ± 0.33	$+0.98 \pm 0.55$	0.522 ± 0.005	11.0 (3.3)
180.39 ± 0.41	$+4.44 \pm 0.78$	0.497 ± 0.004	7.2 (5.0)	179.90 ± 0.33	$+1.46 \pm 0.77$	0.573 ± 0.003	5.5 (3.3)
203.35 ± 0.33	$+4.39 \pm 0.92$	0.518 ± 0.004	9.9 (5.6)	203.02 ± 0.33	$+1.88 \pm 0.77$	0.594 ± 0.006	7.0 (3.6)
231.42 ± 0.41	$+3.14 \pm 1.14$	0.491 ± 0.004	14.2 (7.3)	232.83 ± 0.33	$+3.76 \pm 0.99$	0.568 ± 0.005	10.7 (4.4)
269.02 ± 0.33	-15.24 ± 0.40	0.440 ± 0.004	19.8 (8.2)	268.73 ± 0.41	-9.58 ± 1.37	0.515 ± 0.006	16.6 (5.9)
307.00 ± 0.49	-7.54 ± 1.16	0.404 ± 0.004	20.8 (8.4)	306.86 ± 0.25	-5.42 ± 0.69	0.476 ± 0.004	17.2 (8.0)
335.87 ± 0.41	-1.38 ± 0.71	0.429 ± 0.004	13.4 (4.3)	335.70 ± 0.33	-0.32 ± 0.62	0.503 ± 0.005	11.5 (3.3)

Table 96: The nominal angle δ_n, average displacement $\Delta\delta$, average value of the parameter DIST, RMS of the ALPHA distribution for enabled GF and impact parameters between 60 m and 120 m. The RMS of the ALPHA distribution for disabled GF is given parentheses. The primary γ-ray energy was set to 300 GeV, the ZA to 40° and the azimuth angle to 150°.

$E_\gamma = 300\,\mathrm{GeV}$, Az = 150°, ZA = 40°, Hard Image Cleaning

δ_n[°]	$\Delta\delta$[°]	DIST[°]	$\mathrm{RMS}_{\mathrm{\lvert ALPHA\rvert}}$[°]	δ_n[°]	$\Delta\delta$[°]	DIST[°]	$\mathrm{RMS}_{\mathrm{\lvert ALPHA\rvert}}$[°]
IP = 60 m				**IP = 80 m**			
358.33 ± 0.49	$+6.40 \pm 1.10$	0.301 ± 0.003	11.1 (15.1)	359.29 ± 0.41	$+4.40 \pm 0.94$	0.389 ± 0.004	9.4 (8.5)
23.11 ± 0.41	$+15.00 \pm 0.79$	0.316 ± 0.004	13.3 (12.1)	25.27 ± 0.49	$+10.99 \pm 1.02$	0.413 ± 0.004	10.1 (6.8)
53.48 ± 0.74	$+7.07 \pm 0.82$	0.308 ± 0.003	20.8 (15.9)	54.85 ± 0.58	$+7.72 \pm 1.42$	0.401 ± 0.004	16.3 (9.3)
92.44 ± 0.74	-11.88 ± 1.94	0.283 ± 0.003	24.4 (12.2)	91.87 ± 0.58	-8.86 ± 1.80	0.364 ± 0.003	24.6 (11.2)
126.41 ± 0.66	-11.54 ± 1.34	0.266 ± 0.003	22.6 (14.5)	126.96 ± 0.49	-8.79 ± 1.03	0.339 ± 0.003	21.4 (8.3)
155.69 ± 0.58	-0.89 ± 0.96	0.276 ± 0.003	16.0 (15.1)	156.81 ± 0.58	$+1.32 \pm 1.03$	0.365 ± 0.004	15.0 (7.9)
181.16 ± 0.25	$+7.79 \pm 0.77$	0.313 ± 0.004	10.5 (11.2)	179.23 ± 0.41	$+4.98 \pm 0.94$	0.408 ± 0.002	8.8 (6.4)
204.44 ± 0.58	$+14.11 \pm 1.64$	0.329 ± 0.003	11.3 (13.5)	204.00 ± 0.33	$+9.88 \pm 1.16$	0.425 ± 0.004	10.9 (7.2)
233.27 ± 0.33	$+8.34 \pm 0.56$	0.309 ± 0.003	18.1 (11.8)	231.00 ± 0.58	$+0.17 \pm 1.11$	0.400 ± 0.003	15.2 (12.7)
268.53 ± 0.82	-17.19 ± 1.74	0.271 ± 0.002	26.2 (16.1)	268.63 ± 0.74	-15.39 ± 1.12	0.354 ± 0.003	22.7 (14.3)
306.17 ± 0.49	-12.55 ± 1.17	0.249 ± 0.003	21.8 (13.0)	307.95 ± 0.49	-9.26 ± 1.17	0.329 ± 0.004	22.4 (9.0)
336.52 ± 0.41	-0.12 ± 1.02	0.268 ± 0.004	16.2 (10.8)	335.34 ± 0.49	-1.21 ± 0.95	0.350 ± 0.004	13.9 (6.9)
IP = 100 m				**IP = 120 m**			
0.15 ± 0.49	$+4.36 \pm 0.87$	0.480 ± 0.006	8.0 (8.3)	0.52 ± 0.33	$+3.03 \pm 0.63$	0.556 ± 0.005	5.9 (2.6)
25.81 ± 0.33	$+9.83 \pm 0.94$	0.510 ± 0.006	8.5 (3.8)	25.13 ± 0.41	$+4.57 \pm 0.87$	0.585 ± 0.004	7.8 (2.9)
53.48 ± 0.33	$+5.33 \pm 1.01$	0.487 ± 0.004	16.1 (5.5)	53.10 ± 0.25	$+4.88 \pm 0.55$	0.570 ± 0.006	12.7 (3.7)
91.90 ± 0.49	-4.57 ± 1.09	0.447 ± 0.003	19.7 (9.1)	91.97 ± 0.41	$+0.37 \pm 1.02$	0.520 ± 0.005	17.0 (4.7)
128.36 ± 0.41	-3.65 ± 0.94	0.419 ± 0.001	19.6 (7.8)	127.86 ± 0.25	-2.23 ± 0.62	0.485 ± 0.003	18.0 (4.0)
155.22 ± 0.25	$+0.39 \pm 0.55$	0.442 ± 0.005	13.0 (5.0)	156.05 ± 0.33	$+0.98 \pm 0.48$	0.523 ± 0.003	10.4 (3.5)
179.87 ± 0.41	$+3.65 \pm 0.87$	0.490 ± 0.004	8.0 (4.4)	179.89 ± 0.25	$+2.07 \pm 0.55$	0.573 ± 0.006	5.7 (3.1)
203.73 ± 0.33	$+4.03 \pm 1.01$	0.512 ± 0.003	9.8 (5.5)	203.29 ± 0.25	$+2.57 \pm 0.77$	0.591 ± 0.007	7.4 (3.2)
231.19 ± 0.41	$+1.73 \pm 0.86$	0.491 ± 0.004	12.0 (7.2)	231.71 ± 0.33	-0.35 ± 0.93	0.565 ± 0.005	11.0 (7.2)
268.56 ± 0.41	-15.51 ± 1.17	0.435 ± 0.003	19.5 (8.1)	268.88 ± 0.41	-6.70 ± 1.02	0.510 ± 0.006	14.9 (4.9)
307.12 ± 0.33	-7.51 ± 0.94	0.399 ± 0.004	20.8 (6.4)	307.31 ± 0.25	-4.51 ± 0.70	0.472 ± 0.003	16.2 (4.3)
335.70 ± 0.33	-0.65 ± 0.55	0.422 ± 0.004	13.1 (4.2)	335.77 ± 0.33	-0.16 ± 0.63	0.504 ± 0.005	10.4 (3.3)

Table 97: The nominal angle δ_n, average displacement $\Delta\delta$, average value of the parameter DIST, RMS of the ALPHA distribution for enabled GF and impact parameters between 60 m and 120 m. The RMS of the ALPHA distribution for disabled GF is given parentheses. The primary γ-ray energy was set to 300 GeV, the ZA to 40° and the azimuth angle to 150°.

$E_\gamma = 300\,\mathrm{GeV}$, Az = 180°, ZA = 40°, Intermediate Image Cleaning

δ_n[°]	$\Delta\delta$[°]	DIST[°]	RMS$_{\lvert ALPHA \rvert}$[°]	δ_n[°]	$\Delta\delta$[°]	DIST[°]	RMS$_{\lvert ALPHA \rvert}$[°]
IP = 60 m				**IP = 80 m**			
359.40 ± 0.33	-0.53 ± 0.71	0.324 ± 0.004	8.4 (13.8)	359.69 ± 0.49	$+0.26 \pm 0.79$	0.419 ± 0.004	5.4 (8.8)
23.84 ± 0.49	$+8.55 \pm 0.94$	0.314 ± 0.003	16.3 (9.9)	25.63 ± 0.16	$+8.82 \pm 0.84$	0.402 ± 0.003	21.1 (5.9)
53.40 ± 0.74	$+15.09 \pm 2.01$	0.288 ± 0.003	29.1 (17.8)	54.12 ± 0.58	$+14.38 \pm 1.62$	0.371 ± 0.004	23.2 (8.9)
91.68 ± 0.74	$+1.96 \pm 1.71$	0.274 ± 0.003	27.9 (13.2)	90.95 ± 0.49	$+0.38 \pm 0.72$	0.351 ± 0.002	26.9 (11.3)
128.29 ± 0.66	-12.80 ± 1.93	0.287 ± 0.002	19.4 (13.1)	127.99 ± 0.66	-9.09 ± 1.41	0.372 ± 0.003	20.0 (8.2)
156.26 ± 0.82	-7.16 ± 1.35	0.317 ± 0.003	13.7 (14.2)	156.09 ± 0.49	-6.67 ± 1.02	0.415 ± 0.004	10.2 (8.8)
179.86 ± 0.66	$+0.03 \pm 1.04$	0.336 ± 0.004	9.9 (11.4)	180.10 ± 0.49	-0.95 ± 0.79	0.427 ± 0.003	7.5 (6.7)
203.58 ± 0.49	$+8.83 \pm 0.87$	0.315 ± 0.004	16.7 (12.6)	204.48 ± 0.33	$+6.21 \pm 0.85$	0.407 ± 0.004	11.5 (6.9)
231.70 ± 0.74	$+10.23 \pm 1.26$	0.279 ± 0.002	23.7 (11.8)	232.03 ± 0.49	$+13.12 \pm 0.79$	0.362 ± 0.003	26.7 (9.7)
270.41 ± 0.49	-4.43 ± 0.81	0.258 ± 0.002	26.0 (12.0)	268.87 ± 0.58	-4.67 ± 1.62	0.341 ± 0.003	25.3 (13.1)
304.61 ± 0.58	-11.42 ± 0.95	0.272 ± 0.002	21.0 (13.5)	306.03 ± 0.58	-10.40 ± 0.72	0.359 ± 0.003	21.1 (13.8)
335.78 ± 0.74	-5.20 ± 1.19	0.307 ± 0.003	10.8 (13.8)	335.91 ± 0.16	-4.06 ± 0.62	0.394 ± 0.004	12.2 (7.0)
IP = 100 m				**IP = 120 m**			
359.93 ± 0.41	$+1.28 \pm 0.71$	0.511 ± 0.004	4.0 (8.1)	359.85 ± 0.33	$+0.90 \pm 0.56$	0.595 ± 0.006	3.3 (2.7)
25.54 ± 0.25	$+5.84 \pm 0.62$	0.494 ± 0.004	19.1 (5.1)	25.10 ± 0.33	$+3.67 \pm 0.63$	0.577 ± 0.005	11.4 (2.6)
53.11 ± 0.41	$+7.71 \pm 1.01$	0.454 ± 0.004	21.8 (6.0)	53.22 ± 0.25	$+7.27 \pm 0.77$	0.530 ± 0.004	17.5 (3.7)
91.70 ± 0.58	$+2.67 \pm 1.02$	0.429 ± 0.003	25.4 (9.8)	91.66 ± 0.25	$+2.50 \pm 0.99$	0.499 ± 0.004	19.6 (4.5)
127.23 ± 0.41	-7.54 ± 1.01	0.455 ± 0.002	17.2 (6.9)	127.46 ± 0.41	-4.36 ± 1.01	0.535 ± 0.003	16.0 (4.0)
155.76 ± 0.41	-4.19 ± 0.78	0.500 ± 0.004	10.3 (4.8)	156.53 ± 0.33	-2.12 ± 0.63	0.579 ± 0.004	9.7 (3.3)
180.39 ± 0.41	$+0.96 \pm 0.71$	0.513 ± 0.003	4.9 (5.0)	179.90 ± 0.33	-0.24 ± 0.63	0.592 ± 0.005	4.0 (3.3)
203.35 ± 0.33	$+3.21 \pm 0.78$	0.489 ± 0.004	9.0 (5.6)	203.02 ± 0.33	$+2.42 \pm 0.78$	0.569 ± 0.004	5.8 (3.6)
231.42 ± 0.41	$+7.30 \pm 1.31$	0.443 ± 0.004	24.1 (7.3)	232.83 ± 0.33	$+4.38 \pm 0.93$	0.516 ± 0.005	14.8 (4.4)
269.02 ± 0.33	-2.80 ± 1.52	0.415 ± 0.003	23.3 (8.2)	268.73 ± 0.41	-1.42 ± 0.78	0.485 ± 0.003	22.0 (5.9)
307.00 ± 0.49	-6.18 ± 1.32	0.438 ± 0.004	17.6 (8.4)	306.86 ± 0.25	-5.15 ± 1.07	0.514 ± 0.004	14.3 (8.0)
335.87 ± 0.41	-3.60 ± 0.86	0.482 ± 0.003	10.7 (4.3)	335.70 ± 0.33	-2.34 ± 0.63	0.563 ± 0.005	7.0 (3.3)

Table 98: The nominal angle δ_n, average displacement $\Delta\delta$, average value of the parameter DIST, RMS of the ALPHA distribution for enabled GF and impact parameters between 60 m and 120 m. The RMS of the ALPHA distribution for disabled GF is given parentheses. The primary γ-ray energy was set to 300 GeV, the ZA to 40° and the azimuth angle to 180°.

$E_\gamma = 300\,\mathrm{GeV}$, Az = 180°, ZA = 40°, Hard Image Cleaning

δ_n[°]	$\Delta\delta$[°]	DIST[°]	RMS$_{\lvert ALPHA \rvert}$[°]	δ_n[°]	$\Delta\delta$[°]	DIST[°]	RMS$_{\lvert ALPHA \rvert}$[°]
IP = 60 m				**IP = 80 m**			
358.33 ± 0.49	-0.82 ± 0.81	0.322 ± 0.003	7.0 (15.1)	359.29 ± 0.41	$+0.38 \pm 0.73$	0.421 ± 0.004	5.4 (8.5)
23.11 ± 0.41	$+8.35 \pm 0.96$	0.311 ± 0.003	18.5 (12.1)	25.27 ± 0.49	$+8.18 \pm 0.96$	0.405 ± 0.003	12.8 (6.8)
53.48 ± 0.74	$+13.42 \pm 1.99$	0.284 ± 0.003	27.7 (15.9)	54.85 ± 0.58	$+11.76 \pm 1.59$	0.370 ± 0.004	26.8 (9.3)
92.44 ± 0.74	$+1.58 \pm 0.89$	0.272 ± 0.003	27.3 (12.2)	91.87 ± 0.58	-1.78 ± 2.76	0.348 ± 0.002	24.6 (11.2)
126.41 ± 0.66	-16.07 ± 1.82	0.290 ± 0.003	18.6 (14.5)	126.96 ± 0.49	-9.46 ± 1.73	0.374 ± 0.003	18.5 (8.3)
155.69 ± 0.58	-8.24 ± 1.12	0.318 ± 0.003	13.8 (15.1)	156.81 ± 0.58	-6.85 ± 1.19	0.415 ± 0.005	11.1 (7.9)
181.16 ± 0.25	$+1.08 \pm 0.63$	0.333 ± 0.005	10.1 (11.2)	179.23 ± 0.41	-0.68 ± 0.72	0.430 ± 0.005	8.0 (6.4)
204.44 ± 0.58	$+9.41 \pm 1.19$	0.313 ± 0.002	11.1 (13.5)	204.00 ± 0.33	$+5.36 \pm 0.72$	0.405 ± 0.003	12.8 (7.2)
233.27 ± 0.33	$+11.16 \pm 0.56$	0.278 ± 0.003	26.6 (11.8)	231.00 ± 0.58	$+7.64 \pm 1.50$	0.361 ± 0.004	24.9 (12.7)
268.53 ± 0.82	-5.21 ± 1.31	0.256 ± 0.002	25.3 (16.1)	268.63 ± 0.74	-3.77 ± 1.91	0.336 ± 0.003	24.0 (14.3)
306.17 ± 0.49	-9.21 ± 1.52	0.270 ± 0.003	20.1 (13.0)	307.95 ± 0.49	-6.25 ± 1.66	0.358 ± 0.003	20.2 (9.0)
336.52 ± 0.41	-3.73 ± 0.80	0.304 ± 0.003	11.4 (10.8)	335.34 ± 0.49	-4.59 ± 0.96	0.397 ± 0.003	11.8 (6.9)
IP = 100 m				**IP = 120 m**			
0.15 ± 0.49	$+1.04 \pm 0.81$	0.511 ± 0.004	4.0 (8.3)	0.52 ± 0.33	$+1.97 \pm 0.65$	0.596 ± 0.006	3.1 (2.6)
25.81 ± 0.33	$+6.70 \pm 0.72$	0.496 ± 0.005	12.4 (3.8)	25.13 ± 0.41	$+3.13 \pm 0.64$	0.576 ± 0.006	13.3 (2.9)
53.48 ± 0.33	$+8.41 \pm 0.95$	0.454 ± 0.003	18.3 (5.5)	53.10 ± 0.25	$+5.39 \pm 0.56$	0.533 ± 0.004	11.9 (3.7)
91.90 ± 0.49	$+5.07 \pm 1.27$	0.426 ± 0.003	24.1 (9.1)	91.97 ± 0.41	-0.04 ± 0.96	0.496 ± 0.003	18.8 (4.7)
128.36 ± 0.41	-7.45 ± 1.10	0.453 ± 0.003	15.2 (7.8)	127.86 ± 0.25	-6.48 ± 0.93	0.531 ± 0.003	15.0 (4.0)
155.22 ± 0.25	-3.65 ± 0.71	0.503 ± 0.005	9.9 (5.0)	156.05 ± 0.33	-2.21 ± 0.64	0.580 ± 0.004	9.7 (3.5)
179.87 ± 0.41	-0.37 ± 0.72	0.515 ± 0.004	4.5 (4.4)	179.89 ± 0.25	$+0.51 \pm 0.56$	0.596 ± 0.004	4.0 (3.1)
203.73 ± 0.33	$+2.94 \pm 0.72$	0.491 ± 0.003	5.2 (5.5)	203.29 ± 0.25	$+1.92 \pm 0.63$	0.568 ± 0.005	6.0 (3.2)
231.19 ± 0.41	$+6.60 \pm 1.33$	0.438 ± 0.003	19.5 (7.2)	231.71 ± 0.33	$+3.57 \pm 1.10$	0.517 ± 0.003	12.9 (7.2)
268.56 ± 0.41	-2.28 ± 1.27	0.409 ± 0.003	20.8 (8.1)	268.88 ± 0.41	-0.13 ± 0.80	0.484 ± 0.004	19.7 (4.9)
307.12 ± 0.33	-5.13 ± 1.18	0.436 ± 0.003	15.4 (6.4)	307.31 ± 0.25	-4.32 ± 0.71	0.514 ± 0.004	15.0 (4.3)
335.70 ± 0.33	-3.54 ± 0.72	0.486 ± 0.005	7.7 (4.2)	335.77 ± 0.33	-1.84 ± 0.64	0.566 ± 0.005	7.5 (3.3)

Table 99: The nominal angle δ_n, average displacement $\Delta\delta$, average value of the parameter DIST, RMS of the ALPHA distribution for enabled GF and impact parameters between 60 m and 120 m. The RMS of the ALPHA distribution for disabled GF is given parentheses. The primary γ-ray energy was set to 300 GeV, the ZA to 40° and the azimuth angle to 180°.

$E_\gamma = 450\,\mathrm{GeV}$, Az = 0°, ZA = 0°, Intermediate Image Cleaning

$\delta_n[°]$	$\Delta\delta[°]$	DIST[°]	$\mathrm{RMS}_{\lvert\mathrm{ALPHA}\rvert}[°]$	$\delta_n[°]$	$\Delta\delta[°]$	DIST[°]	$\mathrm{RMS}_{\lvert\mathrm{ALPHA}\rvert}[°]$
IP = 60 m				IP = 80 m			
359.00 ± 0.54	-0.19 ± 1.08	0.625 ± 0.007	3.4 (3.3)	359.58 ± 0.54	-0.31 ± 0.81	0.752 ± 0.007	1.9 (2.0)
29.58 ± 0.54	$+1.36 \pm 0.94$	0.627 ± 0.008	7.9 (3.9)	30.31 ± 0.54	$+2.30 \pm 1.08$	0.756 ± 0.008	6.4 (1.8)
59.27 ± 0.41	$+3.96 \pm 1.08$	0.636 ± 0.007	14.3 (2.6)	59.26 ± 0.41	$+1.76 \pm 0.67$	0.759 ± 0.007	11.4 (2.1)
89.81 ± 0.68	-2.34 ± 1.21	0.635 ± 0.006	12.5 (2.4)	89.75 ± 0.41	-1.95 ± 0.94	0.765 ± 0.001	6.1 (1.6)
120.32 ± 0.41	-5.09 ± 0.81	0.634 ± 0.008	4.3 (3.6)	119.60 ± 0.41	-2.39 ± 0.94	0.757 ± 0.003	3.3 (2.0)
150.12 ± 0.54	-3.41 ± 1.08	0.633 ± 0.002	3.1 (3.8)	150.41 ± 0.27	-1.56 ± 0.67	0.766 ± 0.001	1.2 (2.8)
180.29 ± 0.41	$+0.23 \pm 0.94$	0.635 ± 0.003	2.0 (4.0)	179.65 ± 0.27	-0.16 ± 0.67	0.762 ± 0.006	2.4 (2.4)
211.03 ± 0.54	$+4.58 \pm 0.94$	0.636 ± 0.009	6.3 (4.2)	210.13 ± 0.54	$+1.29 \pm 0.94$	0.766 ± 0.010	4.2 (3.0)
239.47 ± 0.41	$+3.56 \pm 1.08$	0.639 ± 0.013	10.0 (4.7)	239.69 ± 0.27	$+2.78 \pm 0.54$	0.760 ± 0.010	8.0 (2.1)
269.51 ± 0.81	$+1.85 \pm 0.95$	0.632 ± 0.012	17.8 (5.2)	269.88 ± 0.27	$+0.95 \pm 0.81$	0.761 ± 0.006	12.7 (2.4)
300.28 ± 0.27	-3.52 ± 0.94	0.629 ± 0.013	6.4 (2.9)	299.60 ± 0.54	-2.05 ± 1.48	0.762 ± 0.001	4.2 (3.9)
329.29 ± 0.54	-3.78 ± 1.08	0.624 ± 0.006	2.7 (2.8)	329.84 ± 0.27	-2.20 ± 0.94	0.758 ± 0.003	2.7 (1.9)
IP = 100 m				IP = 120 m			
359.55 ± 0.27	-0.67 ± 0.54	0.838 ± 0.008	1.3 (1.5)	359.71 ± 0.27	-0.37 ± 0.67	0.901 ± 0.006	1.4 (1.1)
29.67 ± 0.27	$+0.16 \pm 0.54$	0.843 ± 0.008	4.9 (1.3)	29.74 ± 0.27	-0.17 ± 0.54	0.902 ± 0.007	4.2 (1.2)
59.43 ± 0.27	-1.72 ± 0.54	0.837 ± 0.006	4.4 (1.7)	59.57 ± 0.27	-0.08 ± 0.81	0.879 ± 0.011	11.7 (1.6)
89.36 ± 0.41	-1.63 ± 0.81	0.840 ± 0.008	2.6 (1.5)	90.08 ± 0.27	-0.67 ± 0.54	0.877 ± 0.002	2.3 (1.2)
120.06 ± 0.41	-1.45 ± 0.81	0.837 ± 0.004	2.2 (2.0)	120.01 ± 0.27	-1.59 ± 0.82	0.870 ± 0.006	1.2 (1.1)
150.76 ± 0.27	-0.84 ± 0.54	0.846 ± 0.004	1.6 (1.0)	150.34 ± 0.27	-0.80 ± 0.54	0.899 ± 0.002	1.2 (1.0)
180.57 ± 0.54	$+0.58 \pm 0.81$	0.842 ± 0.003	1.4 (1.9)	180.19 ± 0.27	$+0.49 \pm 0.54$	0.885 ± 0.008	1.7 (1.4)
210.23 ± 0.27	$+1.33 \pm 0.67$	0.848 ± 0.006	5.0 (1.2)	210.01 ± 0.27	$+0.66 \pm 0.54$	0.907 ± 0.009	3.8 (1.0)
239.79 ± 0.27	$+2.26 \pm 0.54$	0.837 ± 0.004	8.2 (1.4)	240.13 ± 0.27	$+1.75 \pm 0.81$	0.881 ± 0.004	8.1 (1.2)
269.84 ± 0.27	$+1.91 \pm 0.54$	0.840 ± 0.007	11.9 (1.6)	269.97 ± 0.27	$+1.77 \pm 0.67$	0.883 ± 0.007	11.3 (1.1)
300.02 ± 0.27	-1.02 ± 0.81	0.842 ± 0.008	3.8 (1.6)	299.92 ± 0.27	-0.62 ± 0.54	0.877 ± 0.007	2.6 (1.5)
329.71 ± 0.27	-1.20 ± 0.54	0.843 ± 0.011	1.5 (1.6)	329.98 ± 0.27	-0.33 ± 0.54	0.901 ± 0.004	1.4 (1.1)

Table 100: The nominal angle δ_n, average displacement $\Delta\delta$, average value of the parameter DIST, RMS of the ALPHA distribution for enabled GF and impact parameters between 60 m and 120 m. The RMS of the ALPHA distribution for disabled GF is given parentheses. The primary γ-ray energy was set to 450 GeV, the ZA to 0° and the azimuth angle to 0°.

$E_\gamma = 450\,\mathrm{GeV}$, Az = 0°, ZA = 0°, Hard Image Cleaning

$\delta_n[°]$	$\Delta\delta[°]$	DIST[°]	$\mathrm{RMS}_{\lvert\mathrm{ALPHA}\rvert}[°]$	$\delta_n[°]$	$\Delta\delta[°]$	DIST[°]	$\mathrm{RMS}_{\lvert\mathrm{ALPHA}\rvert}[°]$
IP = 60 m				IP = 80 m			
359.43 ± 0.68	-0.13 ± 1.08	0.615 ± 0.008	2.8 (3.0)	359.94 ± 0.54	$+0.06 \pm 0.81$	0.742 ± 0.006	1.9 (1.8)
29.81 ± 0.54	$+3.30 \pm 0.94$	0.617 ± 0.006	11.2 (2.4)	30.16 ± 0.54	$+2.10 \pm 0.94$	0.747 ± 0.008	6.6 (1.3)
59.46 ± 0.68	$+4.52 \pm 1.35$	0.622 ± 0.007	13.8 (2.7)	59.48 ± 0.41	$+1.64 \pm 0.94$	0.750 ± 0.008	11.2 (2.0)
89.86 ± 0.27	-5.23 ± 0.54	0.623 ± 0.008	7.4 (2.6)	89.58 ± 0.41	-2.01 ± 0.94	0.754 ± 0.007	5.7 (1.6)
120.49 ± 0.27	-4.62 ± 0.40	0.623 ± 0.008	4.3 (3.7)	119.87 ± 0.41	-2.70 ± 0.81	0.746 ± 0.003	2.3 (2.0)
149.53 ± 0.54	-3.70 ± 1.08	0.623 ± 0.002	2.8 (2.7)	150.29 ± 0.54	-1.45 ± 0.94	0.758 ± 0.008	1.3 (1.6)
180.00 ± 0.27	-0.36 ± 0.54	0.625 ± 0.002	2.5 (3.6)	180.26 ± 0.54	$+0.18 \pm 0.81$	0.753 ± 0.006	1.8 (2.2)
210.60 ± 0.54	$+4.51 \pm 0.81$	0.624 ± 0.008	6.2 (6.0)	210.29 ± 0.27	$+1.77 \pm 0.67$	0.757 ± 0.006	4.2 (2.6)
239.62 ± 0.41	$+5.34 \pm 1.21$	0.624 ± 0.001	10.5 (4.0)	239.80 ± 0.27	$+2.78 \pm 0.94$	0.749 ± 0.007	7.4 (2.3)
269.41 ± 0.68	-0.36 ± 0.94	0.624 ± 0.010	15.0 (4.5)	269.88 ± 0.27	$+1.33 \pm 0.81$	0.752 ± 0.006	12.6 (2.1)
300.31 ± 0.27	-3.74 ± 1.34	0.618 ± 0.012	5.9 (2.1)	299.75 ± 0.41	-2.37 ± 1.08	0.751 ± 0.008	5.2 (1.8)
329.62 ± 0.41	-3.60 ± 0.94	0.616 ± 0.012	2.0 (1.9)	329.87 ± 0.27	-1.89 ± 0.81	0.751 ± 0.001	2.1 (1.8)
IP = 100 m				IP = 120 m			
359.66 ± 0.41	-0.37 ± 0.67	0.828 ± 0.008	1.3 (1.4)	359.67 ± 0.27	-0.38 ± 0.67	0.887 ± 0.004	1.5 (1.2)
29.67 ± 0.27	$+0.07 \pm 0.54$	0.834 ± 0.007	5.5 (1.2)	29.79 ± 0.27	-0.24 ± 0.54	0.893 ± 0.008	4.1 (1.2)
59.41 ± 0.27	-1.49 ± 0.67	0.828 ± 0.003	4.5 (1.6)	59.37 ± 0.27	-0.07 ± 0.81	0.867 ± 0.009	11.7 (1.6)
89.41 ± 0.27	-1.37 ± 0.67	0.830 ± 0.004	3.1 (1.6)	90.04 ± 0.27	-0.61 ± 0.54	0.866 ± 0.007	2.2 (1.0)
120.21 ± 0.27	-1.51 ± 0.81	0.828 ± 0.004	1.9 (1.2)	119.97 ± 0.27	-1.62 ± 0.68	0.854 ± 0.005	1.4 (1.3)
150.57 ± 0.27	-0.74 ± 0.67	0.840 ± 0.003	1.5 (1.0)	150.33 ± 0.27	-0.38 ± 0.54	0.887 ± 0.004	1.2 (1.1)
180.32 ± 0.54	$+0.55 \pm 0.81$	0.831 ± 0.003	1.5 (1.9)	180.26 ± 0.27	$+0.55 \pm 0.54$	0.871 ± 0.008	1.5 (1.4)
210.25 ± 0.27	$+1.20 \pm 0.67$	0.840 ± 0.017	4.8 (1.2)	210.01 ± 0.27	$+0.60 \pm 0.54$	0.897 ± 0.003	4.8 (1.0)
239.69 ± 0.41	$+2.02 \pm 0.81$	0.827 ± 0.004	8.5 (1.3)	240.14 ± 0.27	$+1.66 \pm 0.81$	0.869 ± 0.006	8.1 (1.2)
269.73 ± 0.27	-0.01 ± 0.54	0.832 ± 0.006	4.3 (1.5)	269.88 ± 0.27	$+1.53 \pm 0.67$	0.874 ± 0.006	10.0 (1.1)
299.99 ± 0.27	-0.86 ± 0.81	0.830 ± 0.004	3.6 (1.3)	299.83 ± 0.27	-0.82 ± 0.68	0.863 ± 0.008	2.5 (1.4)
329.68 ± 0.27	-0.80 ± 0.54	0.834 ± 0.010	1.6 (1.6)	329.83 ± 0.27	-0.14 ± 0.54	0.889 ± 0.008	1.5 (1.1)

Table 101: The nominal angle δ_n, average displacement $\Delta\delta$, average value of the parameter DIST, RMS of the ALPHA distribution for enabled GF and impact parameters between 60 m and 120 m. The RMS of the ALPHA distribution for disabled GF is given parentheses. The primary γ-ray energy was set to 450 GeV, the ZA to 0° and the azimuth angle to 0°.

$E_\gamma = 450\,\mathrm{GeV}$, Az = 0°, ZA = 20°, Intermediate Image Cleaning

$\delta_n[°]$	$\Delta\delta[°]$	DIST[°]	$\mathrm{RMS}_{\lvert\mathrm{ALPHA}\rvert}[°]$	$\delta_n[°]$	$\Delta\delta[°]$	DIST[°]	$\mathrm{RMS}_{\lvert\mathrm{ALPHA}\rvert}[°]$
IP = 60 m				**IP = 80 m**			
0.00 ± 0.51	$+0.03 \pm 1.14$	0.551 ± 0.007	2.6 (8.8)	359.56 ± 0.38	-0.16 ± 0.88	0.685 ± 0.004	2.0 (7.5)
28.62 ± 0.51	$+2.22 \pm 1.01$	0.542 ± 0.002	7.0 (11.1)	28.91 ± 0.25	$+1.96 \pm 0.63$	0.679 ± 0.002	4.9 (5.8)
61.21 ± 0.76	$+6.11 \pm 1.64$	0.531 ± 0.006	12.8 (3.9)	58.58 ± 0.51	$+2.52 \pm 1.01$	0.659 ± 0.006	10.7 (2.1)
92.00 ± 0.76	-2.34 ± 1.14	0.524 ± 0.005	6.0 (3.2)	89.76 ± 0.51	-1.62 ± 1.01	0.655 ± 0.005	3.5 (2.6)
121.84 ± 0.63	-2.52 ± 1.14	0.532 ± 0.006	7.3 (3.2)	121.43 ± 0.38	-2.20 ± 0.76	0.659 ± 0.006	2.8 (2.6)
150.93 ± 0.51	-2.39 ± 1.01	0.545 ± 0.006	7.6 (4.7)	151.47 ± 0.38	-2.02 ± 0.76	0.677 ± 0.007	1.7 (3.9)
178.79 ± 0.38	-1.16 ± 0.88	0.552 ± 0.002	4.3 (9.9)	179.55 ± 0.51	$+0.02 \pm 1.01$	0.685 ± 0.008	3.6 (7.7)
208.14 ± 0.63	$+2.23 \pm 1.14$	0.549 ± 0.004	7.2 (11.3)	209.16 ± 0.38	$+2.54 \pm 0.88$	0.686 ± 0.005	5.2 (2.7)
238.32 ± 0.63	$+4.41 \pm 1.52$	0.537 ± 0.004	11.9 (3.0)	238.68 ± 0.51	$+3.96 \pm 0.88$	0.667 ± 0.007	9.5 (2.3)
269.69 ± 0.63	$+0.31 \pm 1.26$	0.532 ± 0.004	16.8 (4.7)	269.52 ± 0.51	$+0.49 \pm 0.88$	0.662 ± 0.005	10.7 (3.0)
301.42 ± 0.25	-5.79 ± 0.76	0.534 ± 0.005	4.5 (4.8)	301.31 ± 0.38	-3.51 ± 0.76	0.664 ± 0.007	3.6 (4.0)
331.78 ± 0.51	-3.29 ± 0.88	0.544 ± 0.005	3.2 (9.2)	331.95 ± 0.38	-1.47 ± 0.63	0.683 ± 0.007	1.9 (8.8)
IP = 100 m				**IP = 120 m**			
359.98 ± 0.25	$+0.11 \pm 0.51$	0.787 ± 0.006	1.7 (4.5)	359.45 ± 0.25	-0.62 ± 0.51	0.838 ± 0.007	1.2 (2.4)
28.66 ± 0.38	$+0.73 \pm 0.76$	0.785 ± 0.008	4.3 (3.5)	28.63 ± 0.25	$+0.60 \pm 0.51$	0.838 ± 0.008	4.2 (1.4)
57.65 ± 0.38	-0.16 ± 0.63	0.762 ± 0.006	8.8 (1.9)	58.17 ± 0.38	$+0.65 \pm 0.63$	0.823 ± 0.002	8.1 (1.6)
89.63 ± 0.38	-1.72 ± 0.76	0.755 ± 0.004	3.1 (2.3)	89.78 ± 0.25	-1.29 ± 0.51	0.821 ± 0.005	2.1 (1.6)
121.65 ± 0.38	-1.86 ± 0.88	0.762 ± 0.005	2.3 (2.2)	121.93 ± 0.38	-1.54 ± 0.63	0.818 ± 0.002	1.8 (1.3)
152.02 ± 0.25	-0.93 ± 0.63	0.780 ± 0.002	1.3 (1.5)	151.37 ± 0.13	-0.81 ± 0.38	0.835 ± 0.005	1.5 (1.6)
179.63 ± 0.25	-0.12 ± 0.51	0.782 ± 0.007	2.0 (1.8)	179.97 ± 0.25	$+0.17 \pm 0.63$	0.832 ± 0.006	1.7 (1.5)
208.96 ± 0.38	$+1.75 \pm 0.76$	0.788 ± 0.003	4.1 (2.1)	208.07 ± 0.25	$+0.38 \pm 0.38$	0.843 ± 0.004	3.0 (1.2)
238.05 ± 0.38	$+1.83 \pm 0.76$	0.771 ± 0.013	9.7 (2.2)	237.88 ± 0.25	$+1.54 \pm 0.63$	0.833 ± 0.007	6.2 (1.6)
270.21 ± 0.38	$+2.08 \pm 0.63$	0.771 ± 0.003	14.7 (1.4)	269.99 ± 0.25	$+1.32 \pm 0.51$	0.830 ± 0.012	10.4 (1.3)
301.65 ± 0.38	-2.12 ± 0.88	0.775 ± 0.007	2.4 (4.3)	302.04 ± 0.25	-0.63 ± 0.63	0.832 ± 0.007	2.4 (3.6)
331.28 ± 0.25	-1.62 ± 0.63	0.789 ± 0.012	1.3 (7.3)	331.48 ± 0.13	-1.27 ± 0.38	0.847 ± 0.008	1.0 (5.3)

Table 102: The nominal angle δ_n, average displacement $\Delta\delta$, average value of the parameter DIST, RMS of the ALPHA distribution for enabled GF and impact parameters between 60 m and 120 m. The RMS of the ALPHA distribution for disabled GF is given parentheses. The primary γ-ray energy was set to 450 GeV, the ZA to 20° and the azimuth angle to 0°.

$E_\gamma = 450\,\mathrm{GeV}$, Az = 0°, ZA = 20°, Hard Image Cleaning

$\delta_n[°]$	$\Delta\delta[°]$	DIST[°]	$\mathrm{RMS}_{\lvert\mathrm{ALPHA}\rvert}[°]$	$\delta_n[°]$	$\Delta\delta[°]$	DIST[°]	$\mathrm{RMS}_{\lvert\mathrm{ALPHA}\rvert}[°]$
IP = 60 m				**IP = 80 m**			
359.62 ± 0.51	-0.23 ± 0.76	0.541 ± 0.006	3.0 (10.0)	359.66 ± 0.51	$+0.20 \pm 0.88$	0.674 ± 0.005	1.9 (7.0)
28.49 ± 0.51	$+2.60 \pm 1.14$	0.532 ± 0.007	6.7 (10.3)	28.76 ± 0.38	$+1.83 \pm 0.76$	0.670 ± 0.005	4.6 (4.2)
59.28 ± 0.76	$+4.13 \pm 1.52$	0.519 ± 0.008	10.8 (4.2)	58.30 ± 0.63	$+2.43 \pm 1.14$	0.651 ± 0.009	12.1 (2.9)
90.53 ± 0.63	-2.77 ± 1.14	0.512 ± 0.006	6.3 (3.2)	89.60 ± 0.25	-1.12 ± 0.51	0.647 ± 0.006	3.5 (2.4)
121.56 ± 0.63	-3.55 ± 1.01	0.519 ± 0.004	6.0 (3.1)	121.39 ± 0.38	-2.75 ± 0.76	0.651 ± 0.006	2.6 (2.5)
150.42 ± 0.51	-2.94 ± 1.14	0.536 ± 0.009	3.6 (4.6)	151.31 ± 0.38	-1.88 ± 0.76	0.669 ± 0.006	1.8 (3.4)
179.05 ± 0.63	-1.07 ± 1.14	0.542 ± 0.004	3.3 (10.1)	179.53 ± 0.51	-0.05 ± 1.01	0.677 ± 0.002	2.6 (7.9)
208.11 ± 0.63	$+2.29 \pm 1.01$	0.539 ± 0.007	6.9 (11.5)	209.14 ± 0.38	$+2.53 \pm 0.88$	0.678 ± 0.004	6.7 (2.6)
238.47 ± 0.63	$+5.42 \pm 1.14$	0.524 ± 0.006	11.3 (3.6)	238.69 ± 0.51	$+3.79 \pm 0.88$	0.659 ± 0.006	8.5 (2.1)
269.54 ± 0.51	$+0.52 \pm 0.76$	0.519 ± 0.004	14.3 (4.0)	269.72 ± 0.38	$+1.37 \pm 0.76$	0.654 ± 0.005	13.7 (2.2)
301.62 ± 0.63	-4.99 ± 1.14	0.525 ± 0.005	4.1 (5.0)	301.60 ± 0.38	-3.23 ± 0.76	0.655 ± 0.007	2.9 (2.5)
331.53 ± 0.38	-3.18 ± 1.01	0.535 ± 0.005	4.3 (8.7)	331.48 ± 0.25	-2.06 ± 0.76	0.674 ± 0.009	1.9 (8.4)
IP = 100 m				**IP = 120 m**			
0.22 ± 0.38	$+0.19 \pm 0.63$	0.777 ± 0.005	1.3 (4.4)	359.49 ± 0.25	-0.70 ± 0.63	0.828 ± 0.006	1.3 (3.0)
28.67 ± 0.38	$+0.62 \pm 0.76$	0.779 ± 0.006	4.6 (2.8)	28.39 ± 0.38	$+0.22 \pm 0.63$	0.831 ± 0.008	4.4 (1.4)
57.78 ± 0.25	$+0.38 \pm 0.63$	0.754 ± 0.007	9.2 (1.8)	58.11 ± 0.38	$+1.10 \pm 0.76$	0.810 ± 0.006	8.9 (1.2)
89.76 ± 0.51	-1.91 ± 0.76	0.744 ± 0.001	2.9 (1.8)	89.76 ± 0.25	-1.77 ± 0.51	0.812 ± 0.007	1.6 (1.5)
121.52 ± 0.38	-1.87 ± 0.76	0.754 ± 0.007	2.2 (1.9)	121.96 ± 0.25	-1.71 ± 0.63	0.808 ± 0.007	1.9 (1.3)
151.63 ± 0.25	-1.36 ± 0.63	0.773 ± 0.005	1.2 (1.5)	151.05 ± 0.25	-0.93 ± 0.38	0.826 ± 0.008	1.5 (1.4)
179.62 ± 0.38	-0.22 ± 0.63	0.773 ± 0.011	1.7 (1.8)	179.87 ± 0.25	$+0.21 \pm 0.51$	0.823 ± 0.006	1.7 (1.6)
209.09 ± 0.13	$+1.55 \pm 0.51$	0.781 ± 0.012	4.3 (1.6)	208.30 ± 0.25	$+0.80 \pm 0.38$	0.834 ± 0.004	3.8 (1.1)
238.14 ± 0.25	$+2.32 \pm 0.51$	0.761 ± 0.011	9.2 (2.1)	237.57 ± 0.25	$+1.24 \pm 0.51$	0.820 ± 0.007	6.7 (1.8)
270.12 ± 0.25	$+2.07 \pm 0.51$	0.763 ± 0.003	15.8 (1.4)	269.91 ± 0.25	$+1.15 \pm 0.51$	0.822 ± 0.008	11.1 (1.2)
301.97 ± 0.25	-2.11 ± 0.63	0.767 ± 0.004	2.2 (4.0)	302.28 ± 0.25	$+0.03 \pm 0.51$	0.824 ± 0.007	12.7 (1.2)
331.43 ± 0.38	-1.52 ± 0.76	0.783 ± 0.007	1.3 (7.0)	331.66 ± 0.38	-0.90 ± 0.63	0.839 ± 0.009	1.0 (5.4)

Table 103: The nominal angle δ_n, average displacement $\Delta\delta$, average value of the parameter DIST, RMS of the ALPHA distribution for enabled GF and impact parameters between 60 m and 120 m. The RMS of the ALPHA distribution for disabled GF is given parentheses. The primary γ-ray energy was set to 450 GeV, the ZA to 20° and the azimuth angle to 0°.

$E_\gamma = 450\,\mathrm{GeV}$, Az = 30°, ZA = 20°, Intermediate Image Cleaning

$\delta_n[°]$	$\Delta\delta[°]$	DIST[°]	$\mathrm{RMS}_{\lvert\mathrm{ALPHA}\rvert}[°]$	$\delta_n[°]$	$\Delta\delta[°]$	DIST[°]	$\mathrm{RMS}_{\lvert\mathrm{ALPHA}\rvert}[°]$
IP = 60 m				**IP = 80 m**			
0.00 ± 0.51	−1.39 ± 1.24	0.528 ± 0.007	6.4 (8.8)	359.56 ± 0.38	−1.79 ± 1.12	0.657 ± 0.002	7.4 (7.5)
28.62 ± 0.51	−2.37 ± 1.00	0.509 ± 0.008	9.0 (11.1)	28.91 ± 0.25	+0.70 ± 0.87	0.645 ± 0.008	7.2 (5.8)
61.21 ± 0.76	+6.13 ± 1.37	0.504 ± 0.003	12.4 (3.9)	58.58 ± 0.51	+3.06 ± 1.00	0.637 ± 0.005	7.7 (2.1)
92.00 ± 0.76	+5.99 ± 1.25	0.516 ± 0.008	14.8 (3.2)	89.76 ± 0.51	+0.86 ± 0.75	0.641 ± 0.004	9.6 (2.6)
121.84 ± 0.63	−0.55 ± 1.25	0.536 ± 0.008	8.6 (3.2)	121.43 ± 0.38	−2.07 ± 0.87	0.662 ± 0.010	6.1 (2.6)
150.93 ± 0.51	−7.32 ± 1.00	0.544 ± 0.006	7.2 (4.7)	151.47 ± 0.38	−4.30 ± 0.75	0.670 ± 0.005	4.8 (3.9)
178.79 ± 0.38	−8.34 ± 0.99	0.540 ± 0.007	6.3 (9.9)	179.55 ± 0.51	−3.93 ± 0.87	0.667 ± 0.002	5.6 (7.7)
208.14 ± 0.63	−2.33 ± 1.25	0.530 ± 0.009	8.1 (11.3)	209.16 ± 0.38	−0.50 ± 0.87	0.657 ± 0.008	7.5 (2.7)
238.32 ± 0.63	+2.88 ± 1.25	0.526 ± 0.007	12.6 (3.0)	238.68 ± 0.51	+3.60 ± 0.87	0.651 ± 0.011	9.0 (2.3)
269.69 ± 0.63	+7.46 ± 1.61	0.529 ± 0.001	15.5 (4.7)	269.52 ± 0.51	+4.45 ± 0.87	0.663 ± 0.009	11.5 (3.0)
301.42 ± 0.25	+6.49 ± 0.62	0.543 ± 0.003	10.3 (4.8)	301.31 ± 0.38	+3.94 ± 1.24	0.665 ± 0.007	8.5 (4.0)
331.78 ± 0.51	−2.99 ± 0.87	0.543 ± 0.005	10.6 (9.2)	331.95 ± 0.38	+0.46 ± 0.87	0.667 ± 0.007	7.9 (8.8)
IP = 100 m				**IP = 120 m**			
359.98 ± 0.25	−0.70 ± 0.62	0.756 ± 0.006	3.6 (4.5)	359.45 ± 0.25	−0.31 ± 0.62	0.820 ± 0.004	2.5 (2.4)
28.66 ± 0.38	+0.12 ± 0.87	0.739 ± 0.007	4.3 (3.5)	28.63 ± 0.25	−0.53 ± 0.38	0.804 ± 0.003	3.2 (1.4)
57.65 ± 0.38	+0.79 ± 0.87	0.737 ± 0.005	5.7 (1.9)	58.17 ± 0.38	+0.51 ± 0.63	0.803 ± 0.004	4.4 (1.6)
89.63 ± 0.38	+0.15 ± 0.75	0.737 ± 0.006	7.7 (2.3)	89.78 ± 0.25	+0.32 ± 0.50	0.792 ± 0.008	4.1 (1.6)
121.65 ± 0.38	−1.08 ± 0.62	0.757 ± 0.010	5.5 (2.2)	121.93 ± 0.38	−1.33 ± 0.87	0.800 ± 0.008	4.0 (1.3)
152.02 ± 0.25	−2.03 ± 0.62	0.757 ± 0.009	4.6 (1.5)	151.37 ± 0.13	−1.60 ± 0.50	0.806 ± 0.007	3.1 (1.6)
179.63 ± 0.25	−2.64 ± 0.87	0.761 ± 0.002	3.0 (1.8)	179.97 ± 0.25	−1.18 ± 0.62	0.818 ± 0.009	2.3 (1.5)
208.96 ± 0.38	−0.30 ± 0.62	0.749 ± 0.004	3.5 (2.1)	208.07 ± 0.25	−0.70 ± 0.62	0.806 ± 0.007	2.9 (1.2)
238.05 ± 0.38	+1.02 ± 0.62	0.748 ± 0.007	5.6 (2.2)	237.88 ± 0.25	+0.60 ± 0.50	0.807 ± 0.008	3.8 (1.6)
270.21 ± 0.38	+3.08 ± 0.75	0.750 ± 0.009	6.7 (1.4)	269.99 ± 0.25	+1.27 ± 0.62	0.802 ± 0.006	3.5 (1.3)
301.65 ± 0.38	+1.93 ± 0.87	0.760 ± 0.006	6.4 (4.3)	302.04 ± 0.25	+1.29 ± 0.62	0.808 ± 0.001	3.9 (3.6)
331.28 ± 0.25	+0.18 ± 0.62	0.762 ± 0.007	5.1 (7.3)	331.48 ± 0.13	+0.89 ± 0.50	0.812 ± 0.008	4.4 (5.3)

Table 104: The nominal angle δ_n, average displacement $\Delta\delta$, average value of the parameter DIST, RMS of the ALPHA distribution for enabled GF and impact parameters between 60 m and 120 m. The RMS of the ALPHA distribution for disabled GF is given parentheses. The primary γ-ray energy was set to 450 GeV, the ZA to 20° and the azimuth angle to 30°.

$E_\gamma = 450\,\mathrm{GeV}$, Az = 30°, ZA = 20°, Hard Image Cleaning

$\delta_n[°]$	$\Delta\delta[°]$	DIST[°]	$\mathrm{RMS}_{\lvert\mathrm{ALPHA}\rvert}[°]$	$\delta_n[°]$	$\Delta\delta[°]$	DIST[°]	$\mathrm{RMS}_{\lvert\mathrm{ALPHA}\rvert}[°]$
IP = 60 m				**IP = 80 m**			
359.62 ± 0.51	−1.30 ± 1.12	0.517 ± 0.007	5.6 (10.0)	359.66 ± 0.51	−1.76 ± 1.00	0.648 ± 0.011	7.3 (7.0)
28.49 ± 0.51	−1.60 ± 1.00	0.499 ± 0.008	9.2 (10.3)	28.76 ± 0.38	+0.28 ± 0.99	0.630 ± 0.009	6.1 (4.2)
59.28 ± 0.76	+4.63 ± 1.37	0.497 ± 0.007	12.2 (4.2)	58.30 ± 0.63	+2.02 ± 1.12	0.622 ± 0.007	7.0 (2.9)
90.53 ± 0.63	+3.16 ± 1.37	0.506 ± 0.008	13.4 (3.2)	89.60 ± 0.25	+1.81 ± 0.87	0.629 ± 0.002	9.5 (2.4)
121.56 ± 0.63	−2.12 ± 1.12	0.522 ± 0.002	8.2 (3.1)	121.39 ± 0.38	−1.75 ± 0.99	0.652 ± 0.008	6.1 (2.5)
150.42 ± 0.51	−7.48 ± 1.00	0.535 ± 0.004	7.2 (4.6)	151.31 ± 0.38	−4.44 ± 0.87	0.658 ± 0.006	4.7 (3.4)
179.05 ± 0.63	−7.20 ± 1.25	0.529 ± 0.004	6.3 (10.1)	179.53 ± 0.51	−4.13 ± 1.00	0.659 ± 0.005	4.0 (7.9)
208.11 ± 0.63	−2.17 ± 1.25	0.519 ± 0.010	7.4 (11.5)	209.14 ± 0.38	−1.10 ± 0.87	0.647 ± 0.009	4.5 (2.6)
238.47 ± 0.63	+2.97 ± 1.00	0.518 ± 0.004	11.6 (3.6)	238.69 ± 0.51	+2.14 ± 0.87	0.641 ± 0.005	8.3 (2.1)
269.54 ± 0.51	+6.21 ± 1.00	0.518 ± 0.010	15.0 (4.0)	269.72 ± 0.38	+4.53 ± 0.87	0.652 ± 0.009	9.9 (2.2)
301.62 ± 0.63	+5.70 ± 1.12	0.531 ± 0.008	9.3 (5.0)	301.60 ± 0.38	+3.03 ± 0.87	0.656 ± 0.005	9.1 (2.5)
331.53 ± 0.38	−4.54 ± 0.87	0.530 ± 0.002	9.9 (8.7)	331.48 ± 0.25	−0.53 ± 0.74	0.658 ± 0.003	8.3 (8.4)
IP = 100 m				**IP = 120 m**			
0.22 ± 0.38	+0.54 ± 0.62	0.748 ± 0.011	3.4 (4.4)	359.49 ± 0.25	+0.02 ± 0.62	0.813 ± 0.007	2.5 (3.0)
28.67 ± 0.38	+0.19 ± 0.75	0.727 ± 0.009	3.7 (2.8)	28.39 ± 0.38	−0.51 ± 0.50	0.795 ± 0.002	2.7 (1.4)
57.78 ± 0.25	+0.74 ± 0.74	0.729 ± 0.008	5.8 (1.8)	58.11 ± 0.38	+0.49 ± 0.63	0.793 ± 0.004	4.0 (1.2)
89.76 ± 0.51	+0.52 ± 0.87	0.728 ± 0.009	7.5 (1.8)	89.76 ± 0.25	+0.34 ± 0.50	0.783 ± 0.009	4.0 (1.5)
121.52 ± 0.38	−1.44 ± 0.62	0.746 ± 0.003	4.8 (1.9)	121.96 ± 0.25	−1.42 ± 0.75	0.790 ± 0.008	3.3 (1.3)
151.63 ± 0.25	−2.39 ± 0.74	0.748 ± 0.007	4.2 (1.5)	151.05 ± 0.25	−1.75 ± 0.62	0.798 ± 0.006	2.8 (1.4)
179.62 ± 0.38	−2.57 ± 0.87	0.750 ± 0.010	3.1 (1.8)	179.87 ± 0.25	−1.37 ± 0.62	0.806 ± 0.010	2.2 (1.6)
209.09 ± 0.13	−0.22 ± 0.49	0.738 ± 0.005	5.2 (1.6)	208.30 ± 0.25	−0.51 ± 0.50	0.794 ± 0.006	2.8 (1.1)
238.14 ± 0.25	+1.27 ± 0.50	0.739 ± 0.007	5.5 (2.1)	237.57 ± 0.25	+0.22 ± 0.62	0.796 ± 0.008	3.6 (1.8)
270.12 ± 0.25	+3.27 ± 0.62	0.741 ± 0.008	6.1 (1.4)	269.91 ± 0.25	+0.93 ± 0.62	0.791 ± 0.007	3.6 (1.2)
301.97 ± 0.25	+2.19 ± 0.62	0.753 ± 0.007	5.7 (4.0)	302.28 ± 0.25	+1.12 ± 0.62	0.803 ± 0.002	3.9 (1.2)
331.43 ± 0.38	+0.58 ± 0.75	0.753 ± 0.006	6.9 (7.0)	331.66 ± 0.38	+0.85 ± 0.63	0.802 ± 0.008	3.9 (5.4)

Table 105: The nominal angle δ_n, average displacement $\Delta\delta$, average value of the parameter DIST, RMS of the ALPHA distribution for enabled GF and impact parameters between 60 m and 120 m. The RMS of the ALPHA distribution for disabled GF is given parentheses. The primary γ-ray energy was set to 450 GeV, the ZA to 20° and the azimuth angle to 30°.

$E_\gamma = 450\,\mathrm{GeV}$, Az = 60°, ZA = 20°, Intermediate Image Cleaning

δ_n[°]	$\Delta\delta$[°]	DIST[°]	$\mathrm{RMS}_{\lvert\mathrm{ALPHA}\rvert}$[°]	δ_n[°]	$\Delta\delta$[°]	DIST[°]	$\mathrm{RMS}_{\lvert\mathrm{ALPHA}\rvert}$[°]
IP = 60 m				**IP = 80 m**			
0.00 ± 0.51	-0.45 ± 0.75	0.514 ± 0.007	7.3 (8.8)	359.56 ± 0.38	-2.11 ± 0.75	0.643 ± 0.004	5.4 (7.5)
28.62 ± 0.51	-5.08 ± 1.00	0.508 ± 0.006	6.6 (11.1)	28.91 ± 0.25	-2.01 ± 0.62	0.636 ± 0.009	4.2 (5.8)
61.21 ± 0.76	$+0.58 \pm 1.50$	0.513 ± 0.005	10.2 (3.9)	58.58 ± 0.51	-1.23 ± 1.00	0.642 ± 0.008	8.2 (2.1)
92.00 ± 0.76	$+4.18 \pm 1.37$	0.530 ± 0.007	13.4 (3.2)	89.76 ± 0.51	$+2.06 \pm 0.87$	0.662 ± 0.011	10.0 (2.6)
121.84 ± 0.63	$+6.16 \pm 1.00$	0.539 ± 0.007	15.3 (3.2)	121.43 ± 0.38	$+3.74 \pm 0.75$	0.674 ± 0.010	10.7 (2.6)
150.93 ± 0.51	$+4.63 \pm 1.12$	0.538 ± 0.005	11.9 (4.7)	151.47 ± 0.38	$+3.14 \pm 0.75$	0.669 ± 0.003	8.2 (3.9)
178.79 ± 0.38	-10.06 ± 1.36	0.526 ± 0.007	7.3 (9.9)	179.55 ± 0.51	-4.06 ± 1.00	0.655 ± 0.008	5.6 (7.7)
208.14 ± 0.63	-9.96 ± 1.74	0.519 ± 0.003	6.4 (11.3)	209.16 ± 0.38	-4.72 ± 0.75	0.648 ± 0.004	4.5 (2.7)
238.32 ± 0.63	-3.95 ± 1.00	0.529 ± 0.007	9.1 (3.0)	238.68 ± 0.51	-1.67 ± 1.00	0.653 ± 0.005	9.5 (2.3)
269.69 ± 0.63	$+2.17 \pm 1.12$	0.543 ± 0.006	12.3 (4.7)	269.52 ± 0.51	$+1.46 \pm 1.12$	0.672 ± 0.004	10.9 (3.0)
301.42 ± 0.25	$+6.51 \pm 0.74$	0.543 ± 0.006	14.0 (4.8)	301.31 ± 0.38	$+4.16 \pm 0.62$	0.674 ± 0.013	11.2 (4.0)
331.78 ± 0.51	$+7.87 \pm 0.75$	0.530 ± 0.007	12.8 (9.2)	331.95 ± 0.38	$+4.29 \pm 0.87$	0.663 ± 0.010	8.9 (8.8)
IP = 100 m				**IP = 120 m**			
359.98 ± 0.25	-0.88 ± 0.50	0.747 ± 0.013	4.1 (4.5)	359.45 ± 0.25	$+0.93 \pm 0.62$	0.813 ± 0.008	4.0 (2.4)
28.66 ± 0.38	-1.81 ± 0.75	0.746 ± 0.012	4.4 (3.5)	28.63 ± 0.25	-1.19 ± 0.62	0.816 ± 0.008	3.6 (1.4)
57.65 ± 0.38	-0.89 ± 0.87	0.748 ± 0.010	6.6 (1.9)	58.17 ± 0.38	-0.31 ± 0.63	0.807 ± 0.007	5.4 (1.6)
89.63 ± 0.38	$+1.43 \pm 0.75$	0.766 ± 0.003	6.9 (2.3)	89.78 ± 0.25	$+0.42 \pm 0.50$	0.813 ± 0.010	5.0 (1.6)
121.65 ± 0.38	$+2.23 \pm 0.75$	0.764 ± 0.005	7.2 (2.2)	121.93 ± 0.38	$+1.27 \pm 0.63$	0.811 ± 0.002	4.9 (1.3)
152.02 ± 0.25	$+0.31 \pm 0.62$	0.763 ± 0.002	6.1 (1.5)	151.37 ± 0.13	$+0.02 \pm 0.37$	0.825 ± 0.008	4.1 (1.6)
179.63 ± 0.25	-1.74 ± 0.75	0.750 ± 0.008	4.3 (1.8)	179.97 ± 0.25	-0.18 ± 0.50	0.813 ± 0.003	3.0 (1.5)
208.96 ± 0.38	-2.13 ± 0.62	0.748 ± 0.006	3.2 (2.1)	208.07 ± 0.25	-1.27 ± 0.38	0.815 ± 0.010	2.5 (1.2)
238.05 ± 0.38	-0.75 ± 0.75	0.752 ± 0.004	5.5 (2.2)	237.88 ± 0.25	-0.67 ± 0.62	0.815 ± 0.009	5.1 (1.6)
270.21 ± 0.38	$+1.55 \pm 0.75$	0.769 ± 0.010	6.0 (1.4)	269.99 ± 0.25	$+0.54 \pm 0.50$	0.817 ± 0.010	5.5 (1.3)
301.65 ± 0.38	$+1.68 \pm 0.75$	0.765 ± 0.010	7.4 (4.3)	302.04 ± 0.25	$+0.65 \pm 0.50$	0.813 ± 0.009	5.0 (3.6)
331.28 ± 0.25	$+1.07 \pm 0.62$	0.764 ± 0.012	7.9 (7.3)	331.48 ± 0.13	$+0.41 \pm 0.25$	0.824 ± 0.008	4.7 (5.3)

Table 106: The nominal angle δ_n, average displacement $\Delta\delta$, average value of the parameter DIST, RMS of the ALPHA distribution for enabled GF and impact parameters between 60 m and 120 m. The RMS of the ALPHA distribution for disabled GF is given parentheses. The primary γ-ray energy was set to 450 GeV, the ZA to 20° and the azimuth angle to 60°.

$E_\gamma = 450\,\mathrm{GeV}$, Az = 60°, ZA = 20°, Hard Image Cleaning

δ_n[°]	$\Delta\delta$[°]	DIST[°]	$\mathrm{RMS}_{\lvert\mathrm{ALPHA}\rvert}$[°]	δ_n[°]	$\Delta\delta$[°]	DIST[°]	$\mathrm{RMS}_{\lvert\mathrm{ALPHA}\rvert}$[°]
IP = 60 m				**IP = 80 m**			
359.62 ± 0.51	$+0.26 \pm 1.12$	0.505 ± 0.007	7.4 (10.0)	359.66 ± 0.51	-1.21 ± 0.87	0.634 ± 0.003	4.9 (7.0)
28.49 ± 0.51	-5.87 ± 0.63	0.500 ± 0.006	6.1 (10.3)	28.76 ± 0.38	-2.58 ± 0.75	0.627 ± 0.008	4.4 (4.2)
59.28 ± 0.76	-1.86 ± 1.37	0.503 ± 0.006	10.3 (4.2)	58.30 ± 0.63	-1.28 ± 1.00	0.632 ± 0.001	8.3 (2.9)
90.53 ± 0.63	$+2.56 \pm 1.00$	0.519 ± 0.006	13.1 (3.2)	89.60 ± 0.25	$+2.03 \pm 0.62$	0.654 ± 0.008	9.2 (2.4)
121.56 ± 0.63	$+6.65 \pm 1.00$	0.530 ± 0.008	14.4 (3.1)	121.39 ± 0.38	$+3.33 \pm 0.75$	0.664 ± 0.004	8.6 (2.5)
150.42 ± 0.51	$+5.17 \pm 0.87$	0.529 ± 0.007	12.4 (4.6)	151.31 ± 0.38	$+2.41 \pm 0.87$	0.660 ± 0.012	8.0 (3.4)
179.05 ± 0.63	-12.76 ± 1.12	0.517 ± 0.007	7.8 (10.1)	179.53 ± 0.51	-2.14 ± 0.87	0.646 ± 0.008	5.4 (7.9)
208.11 ± 0.63	-9.63 ± 1.37	0.513 ± 0.005	6.4 (11.5)	209.14 ± 0.38	-4.59 ± 0.75	0.640 ± 0.006	4.2 (2.6)
238.47 ± 0.63	-3.60 ± 1.00	0.517 ± 0.008	9.4 (3.6)	238.69 ± 0.51	-1.59 ± 1.00	0.641 ± 0.004	8.6 (2.1)
269.54 ± 0.51	$+2.17 \pm 1.12$	0.535 ± 0.005	11.2 (4.0)	269.72 ± 0.38	$+1.69 \pm 0.87$	0.662 ± 0.005	8.8 (2.2)
301.62 ± 0.63	$+8.11 \pm 1.00$	0.534 ± 0.005	14.5 (5.0)	301.60 ± 0.38	$+4.40 \pm 0.62$	0.665 ± 0.012	9.5 (2.5)
331.53 ± 0.38	$+7.01 \pm 0.75$	0.523 ± 0.006	13.2 (8.7)	331.48 ± 0.25	$+2.89 \pm 0.74$	0.655 ± 0.005	8.5 (8.4)
IP = 100 m				**IP = 120 m**			
0.22 ± 0.38	-0.69 ± 0.75	0.739 ± 0.011	4.3 (4.4)	359.49 ± 0.25	-0.99 ± 0.62	0.806 ± 0.008	3.6 (3.0)
28.67 ± 0.38	-1.56 ± 0.75	0.738 ± 0.011	3.6 (2.8)	28.39 ± 0.38	-1.52 ± 0.63	0.809 ± 0.009	3.7 (1.4)
57.78 ± 0.25	-0.85 ± 0.62	0.740 ± 0.009	6.5 (1.8)	58.11 ± 0.38	-0.16 ± 0.63	0.798 ± 0.002	5.0 (1.2)
89.76 ± 0.51	$+1.18 \pm 0.87$	0.758 ± 0.003	6.6 (1.8)	89.76 ± 0.25	$+0.39 \pm 0.50$	0.804 ± 0.004	4.7 (1.5)
121.52 ± 0.38	$+1.81 \pm 0.62$	0.756 ± 0.008	5.9 (1.9)	121.96 ± 0.25	$+1.02 \pm 0.50$	0.802 ± 0.003	4.7 (1.3)
151.63 ± 0.25	$+1.71 \pm 0.62$	0.755 ± 0.004	6.7 (1.5)	151.05 ± 0.25	-0.19 ± 0.62	0.816 ± 0.009	4.1 (1.4)
179.62 ± 0.38	-1.11 ± 0.75	0.742 ± 0.008	3.9 (1.8)	179.87 ± 0.25	-0.52 ± 0.62	0.804 ± 0.010	3.2 (1.6)
209.09 ± 0.13	-2.00 ± 0.37	0.739 ± 0.008	3.3 (1.6)	208.30 ± 0.25	-1.56 ± 0.50	0.807 ± 0.003	2.5 (1.1)
238.14 ± 0.25	-0.95 ± 0.62	0.743 ± 0.010	4.9 (2.1)	237.57 ± 0.25	-0.91 ± 0.62	0.807 ± 0.003	5.4 (1.8)
270.12 ± 0.25	$+1.30 \pm 0.62$	0.761 ± 0.006	7.6 (1.4)	269.91 ± 0.25	$+0.44 \pm 0.50$	0.809 ± 0.010	5.5 (1.2)
301.97 ± 0.25	$+0.90 \pm 0.62$	0.758 ± 0.008	7.4 (4.0)	302.28 ± 0.25	$+1.76 \pm 0.62$	0.803 ± 0.010	5.2 (1.2)
331.43 ± 0.38	$+1.26 \pm 0.62$	0.757 ± 0.005	7.7 (7.0)	331.66 ± 0.38	$+0.55 \pm 0.63$	0.816 ± 0.008	5.2 (5.4)

Table 107: The nominal angle δ_n, average displacement $\Delta\delta$, average value of the parameter DIST, RMS of the ALPHA distribution for enabled GF and impact parameters between 60 m and 120 m. The RMS of the ALPHA distribution for disabled GF is given parentheses. The primary γ-ray energy was set to 450 GeV, the ZA to 20° and the azimuth angle to 60°.

$E_\gamma = 450\,\mathrm{GeV}$, Az = 90°, ZA = 20°, Intermediate Image Cleaning

$\delta_n[°]$	$\Delta\delta[°]$	DIST[°]	$\mathrm{RMS}_{\mathrm{\vert ALPHA\vert}}[°]$	$\delta_n[°]$	$\Delta\delta[°]$	DIST[°]	$\mathrm{RMS}_{\mathrm{\vert ALPHA\vert}}[°]$
IP = 60 m				IP = 80 m			
0.00 ± 0.51	$+2.41 \pm 0.99$	0.500 ± 0.004	5.5 (8.8)	359.56 ± 0.38	$+3.32 \pm 0.98$	0.623 ± 0.005	3.8 (7.5)
28.62 ± 0.51	-3.63 ± 0.75	0.502 ± 0.009	4.8 (11.1)	28.91 ± 0.25	-0.97 ± 0.97	0.626 ± 0.006	3.4 (5.8)
61.21 ± 0.76	-5.75 ± 1.48	0.518 ± 0.008	13.8 (3.9)	58.58 ± 0.51	-3.66 ± 0.75	0.645 ± 0.007	10.7 (2.1)
92.00 ± 0.76	-1.21 ± 1.24	0.531 ± 0.007	18.5 (3.2)	89.76 ± 0.51	-2.06 ± 0.99	0.659 ± 0.006	12.6 (2.6)
121.84 ± 0.63	$+3.51 \pm 1.11$	0.532 ± 0.007	18.9 (3.2)	121.43 ± 0.38	$+1.72 \pm 0.98$	0.654 ± 0.002	10.9 (2.6)
150.93 ± 0.51	$+6.62 \pm 1.23$	0.525 ± 0.007	8.6 (4.7)	151.47 ± 0.38	$+3.66 \pm 0.98$	0.645 ± 0.005	6.6 (3.9)
178.79 ± 0.38	$+1.93 \pm 1.22$	0.511 ± 0.002	4.8 (9.9)	179.55 ± 0.51	$+0.59 \pm 1.11$	0.634 ± 0.006	2.8 (7.7)
208.14 ± 0.63	-6.51 ± 0.87	0.517 ± 0.008	5.9 (11.3)	209.16 ± 0.38	-2.41 ± 0.62	0.643 ± 0.009	7.7 (2.7)
238.32 ± 0.63	-6.53 ± 1.95	0.530 ± 0.002	9.7 (3.0)	238.68 ± 0.51	-3.42 ± 1.23	0.658 ± 0.011	7.0 (2.3)
269.69 ± 0.63	-2.44 ± 1.35	0.536 ± 0.007	18.7 (4.7)	269.52 ± 0.51	-1.71 ± 1.23	0.665 ± 0.008	9.7 (3.0)
301.42 ± 0.25	$+3.41 \pm 0.85$	0.528 ± 0.007	19.5 (4.8)	301.31 ± 0.38	$+1.41 \pm 0.86$	0.653 ± 0.008	11.7 (4.0)
331.78 ± 0.51	$+7.89 \pm 0.87$	0.509 ± 0.010	16.7 (9.2)	331.95 ± 0.38	$+4.81 \pm 0.74$	0.628 ± 0.010	10.5 (8.8)
IP = 100 m				IP = 120 m			
359.98 ± 0.25	$+2.61 \pm 0.85$	0.722 ± 0.008	3.0 (4.5)	359.45 ± 0.25	$+1.83 \pm 0.62$	0.792 ± 0.007	2.0 (2.4)
28.66 ± 0.38	$+0.32 \pm 0.74$	0.725 ± 0.009	2.6 (3.5)	28.63 ± 0.25	$+0.92 \pm 0.62$	0.783 ± 0.005	2.1 (1.4)
57.65 ± 0.38	-2.08 ± 0.62	0.746 ± 0.006	4.3 (1.9)	58.17 ± 0.38	$+0.18 \pm 0.74$	0.804 ± 0.006	3.3 (1.6)
89.63 ± 0.38	-1.35 ± 0.62	0.750 ± 0.007	7.4 (2.3)	89.78 ± 0.25	-0.46 ± 0.50	0.793 ± 0.002	4.1 (1.6)
121.65 ± 0.38	$+1.29 \pm 0.62$	0.755 ± 0.004	7.3 (2.2)	121.93 ± 0.38	$+0.50 \pm 0.74$	0.793 ± 0.005	4.7 (1.3)
152.02 ± 0.25	$+2.41 \pm 0.73$	0.738 ± 0.005	5.5 (1.5)	151.37 ± 0.13	-0.35 ± 0.37	0.793 ± 0.004	4.8 (1.6)
179.63 ± 0.25	-0.12 ± 0.73	0.733 ± 0.006	2.8 (1.8)	179.97 ± 0.25	-0.87 ± 0.74	0.806 ± 0.008	2.3 (1.5)
208.96 ± 0.38	-1.05 ± 0.98	0.741 ± 0.008	3.0 (2.1)	208.07 ± 0.25	-1.61 ± 0.50	0.802 ± 0.006	2.2 (1.2)
238.05 ± 0.38	-2.83 ± 0.98	0.753 ± 0.006	5.4 (2.2)	237.88 ± 0.25	-1.73 ± 0.62	0.808 ± 0.004	5.0 (1.6)
270.21 ± 0.38	-0.79 ± 0.74	0.752 ± 0.007	5.9 (1.4)	269.99 ± 0.25	-0.96 ± 0.61	0.787 ± 0.007	6.9 (1.3)
301.65 ± 0.38	$+0.76 \pm 0.86$	0.747 ± 0.004	8.5 (4.3)	302.04 ± 0.25	$+0.62 \pm 0.62$	0.791 ± 0.013	4.6 (3.6)
331.28 ± 0.25	$+2.13 \pm 0.73$	0.730 ± 0.003	5.6 (7.3)	331.48 ± 0.13	$+1.38 \pm 0.49$	0.787 ± 0.007	3.7 (5.3)

Table 108: The nominal angle δ_n, average displacement $\Delta\delta$, average value of the parameter DIST, RMS of the ALPHA distribution for enabled GF and impact parameters between 60 m and 120 m. The RMS of the ALPHA distribution for disabled GF is given parentheses. The primary γ-ray energy was set to 450 GeV, the ZA to 20° and the azimuth angle to 90°.

$E_\gamma = 450\,\mathrm{GeV}$, Az = 90°, ZA = 20°, Hard Image Cleaning

$\delta_n[°]$	$\Delta\delta[°]$	DIST[°]	$\mathrm{RMS}_{\mathrm{\vert ALPHA\vert}}[°]$	$\delta_n[°]$	$\Delta\delta[°]$	DIST[°]	$\mathrm{RMS}_{\mathrm{\vert ALPHA\vert}}[°]$
IP = 60 m				IP = 80 m			
359.62 ± 0.51	$+3.07 \pm 0.75$	0.490 ± 0.008	5.2 (10.0)	359.66 ± 0.51	$+2.87 \pm 0.99$	0.611 ± 0.007	3.7 (7.0)
28.49 ± 0.51	-0.73 ± 0.75	0.492 ± 0.009	4.9 (10.3)	28.76 ± 0.38	-1.99 ± 0.86	0.617 ± 0.009	3.4 (4.2)
59.28 ± 0.76	-6.07 ± 1.48	0.507 ± 0.006	14.1 (4.2)	58.30 ± 0.63	-3.69 ± 1.23	0.637 ± 0.004	10.0 (2.9)
90.53 ± 0.63	-2.94 ± 1.11	0.521 ± 0.007	19.3 (3.2)	89.60 ± 0.25	-2.29 ± 0.61	0.646 ± 0.006	11.5 (2.4)
121.56 ± 0.63	$+3.13 \pm 1.35$	0.518 ± 0.006	17.2 (3.1)	121.39 ± 0.38	$+1.19 \pm 0.86$	0.643 ± 0.007	10.7 (2.5)
150.42 ± 0.51	$+6.52 \pm 1.11$	0.511 ± 0.008	9.1 (4.6)	151.31 ± 0.38	$+3.26 \pm 0.86$	0.634 ± 0.006	6.9 (3.4)
179.05 ± 0.63	$+2.71 \pm 0.87$	0.500 ± 0.003	4.6 (10.1)	179.53 ± 0.51	-0.33 ± 1.11	0.622 ± 0.006	3.1 (7.9)
208.11 ± 0.63	-6.09 ± 1.47	0.506 ± 0.008	6.8 (11.5)	209.14 ± 0.38	-3.12 ± 0.98	0.633 ± 0.005	3.8 (2.6)
238.47 ± 0.63	-6.55 ± 1.23	0.522 ± 0.007	9.9 (3.6)	238.69 ± 0.51	-3.33 ± 0.99	0.645 ± 0.004	7.1 (2.1)
269.54 ± 0.51	-2.77 ± 1.11	0.524 ± 0.006	16.4 (4.0)	269.72 ± 0.38	-1.98 ± 0.74	0.654 ± 0.007	11.2 (2.2)
301.62 ± 0.63	$+2.99 \pm 0.99$	0.512 ± 0.007	21.0 (5.0)	301.60 ± 0.38	$+2.38 \pm 0.74$	0.642 ± 0.006	12.1 (2.5)
331.53 ± 0.38	$+8.25 \pm 0.98$	0.498 ± 0.006	17.7 (8.7)	331.48 ± 0.25	$+4.57 \pm 0.73$	0.618 ± 0.009	10.6 (8.4)
IP = 100 m				IP = 120 m			
0.22 ± 0.38	$+2.81 \pm 0.86$	0.711 ± 0.008	2.5 (4.4)	359.49 ± 0.25	$+1.77 \pm 0.62$	0.780 ± 0.007	1.8 (3.0)
28.67 ± 0.38	$+0.71 \pm 0.86$	0.717 ± 0.011	2.5 (2.8)	28.39 ± 0.38	$+0.85 \pm 0.74$	0.773 ± 0.006	2.0 (1.4)
57.78 ± 0.25	-1.93 ± 0.61	0.738 ± 0.005	4.5 (1.8)	58.11 ± 0.38	$+0.21 \pm 0.86$	0.790 ± 0.006	4.0 (1.2)
89.76 ± 0.51	-0.83 ± 0.87	0.743 ± 0.009	6.9 (1.8)	89.76 ± 0.25	-0.65 ± 0.62	0.783 ± 0.003	4.1 (1.5)
121.52 ± 0.38	$+0.73 \pm 0.74$	0.746 ± 0.007	5.7 (1.9)	121.96 ± 0.25	$+0.38 \pm 0.62$	0.782 ± 0.008	4.6 (1.3)
151.63 ± 0.25	$+1.04 \pm 0.73$	0.727 ± 0.006	5.7 (1.5)	151.05 ± 0.25	-0.32 ± 0.50	0.781 ± 0.005	4.8 (1.4)
179.62 ± 0.38	-0.90 ± 0.74	0.721 ± 0.004	2.6 (1.8)	179.87 ± 0.25	-0.85 ± 0.74	0.790 ± 0.007	2.3 (1.6)
209.09 ± 0.13	-1.68 ± 0.61	0.731 ± 0.006	2.7 (1.6)	208.30 ± 0.25	-1.42 ± 0.62	0.790 ± 0.008	2.4 (1.1)
238.14 ± 0.25	-2.87 ± 0.73	0.744 ± 0.004	5.1 (2.1)	237.57 ± 0.25	-2.12 ± 0.62	0.796 ± 0.004	5.3 (1.8)
270.12 ± 0.25	-0.94 ± 0.49	0.742 ± 0.008	5.3 (1.4)	269.91 ± 0.25	-0.98 ± 0.50	0.778 ± 0.007	6.5 (1.2)
301.97 ± 0.25	$+1.18 \pm 0.61$	0.740 ± 0.005	8.0 (4.0)	302.28 ± 0.25	$+0.63 \pm 0.62$	0.782 ± 0.007	4.7 (1.2)
331.43 ± 0.38	$+2.89 \pm 0.86$	0.719 ± 0.002	5.2 (7.0)	331.66 ± 0.38	$+1.46 \pm 0.74$	0.777 ± 0.005	4.1 (5.4)

Table 109: The nominal angle δ_n, average displacement $\Delta\delta$, average value of the parameter DIST, RMS of the ALPHA distribution for enabled GF and impact parameters between 60 m and 120 m. The RMS of the ALPHA distribution for disabled GF is given parentheses. The primary γ-ray energy was set to 450 GeV, the ZA to 20° and the azimuth angle to 90°.

$E_\gamma = 450\,\mathrm{GeV}$, Az = 120°, ZA = 20°, Intermediate Image Cleaning

δ_n[°]	$\Delta\delta$[°]	DIST[°]	RMS$_{\lvert ALPHA \rvert}$[°]	δ_n[°]	$\Delta\delta$[°]	DIST[°]	RMS$_{\lvert ALPHA \rvert}$[°]
IP = 60 m				**IP = 80 m**			
0.00 ± 0.51	$+6.72 \pm 1.13$	0.547 ± 0.009	5.4 (8.8)	359.56 ± 0.38	$+3.90 \pm 0.50$	0.673 ± 0.004	4.4 (7.5)
28.62 ± 0.51	$+2.04 \pm 0.63$	0.567 ± 0.003	7.1 (11.1)	28.91 ± 0.25	$+0.35 \pm 1.00$	0.694 ± 0.006	4.8 (5.8)
61.21 ± 0.76	-0.79 ± 1.63	0.570 ± 0.004	10.0 (3.9)	58.58 ± 0.51	-5.25 ± 1.25	0.702 ± 0.005	8.5 (2.1)
92.00 ± 0.76	-4.81 ± 1.38	0.566 ± 0.004	13.9 (3.2)	89.76 ± 0.51	-3.49 ± 0.88	0.701 ± 0.006	10.6 (2.6)
121.84 ± 0.63	-1.45 ± 1.01	0.556 ± 0.002	10.5 (3.2)	121.43 ± 0.38	-0.96 ± 0.75	0.686 ± 0.013	9.1 (2.6)
150.93 ± 0.51	$+3.47 \pm 1.13$	0.546 ± 0.008	9.0 (4.7)	151.47 ± 0.38	$+1.67 \pm 0.88$	0.672 ± 0.003	6.7 (3.9)
178.79 ± 0.38	$+4.01 \pm 0.88$	0.550 ± 0.010	5.3 (9.9)	179.55 ± 0.51	$+3.28 \pm 0.88$	0.678 ± 0.007	3.8 (7.7)
208.14 ± 0.63	$+3.84 \pm 1.25$	0.565 ± 0.002	7.8 (11.3)	209.16 ± 0.38	$+4.40 \pm 1.00$	0.690 ± 0.004	5.3 (2.7)
238.32 ± 0.63	-3.49 ± 1.38	0.567 ± 0.005	11.7 (3.0)	238.68 ± 0.51	-2.18 ± 1.00	0.696 ± 0.007	9.6 (2.3)
269.69 ± 0.63	-6.08 ± 1.01	0.565 ± 0.010	11.5 (4.7)	269.52 ± 0.51	-2.42 ± 1.00	0.693 ± 0.003	7.0 (3.0)
301.42 ± 0.25	-0.63 ± 0.50	0.553 ± 0.007	13.4 (4.8)	301.31 ± 0.38	-1.25 ± 0.75	0.677 ± 0.011	7.8 (4.0)
331.78 ± 0.51	$+4.15 \pm 1.25$	0.547 ± 0.008	7.9 (9.2)	331.95 ± 0.38	$+2.71 \pm 0.88$	0.672 ± 0.007	7.3 (8.8)
IP = 100 m				**IP = 120 m**			
359.98 ± 0.25	$+1.75 \pm 0.63$	0.775 ± 0.003	3.5 (4.5)	359.45 ± 0.25	$+0.70 \pm 0.75$	0.836 ± 0.002	3.0 (2.4)
28.66 ± 0.38	$+0.49 \pm 0.75$	0.794 ± 0.005	3.9 (3.5)	28.63 ± 0.25	-0.34 ± 0.50	0.850 ± 0.002	2.8 (1.4)
57.65 ± 0.38	-3.32 ± 0.75	0.787 ± 0.005	6.5 (1.9)	58.17 ± 0.38	-0.54 ± 0.63	0.837 ± 0.003	3.5 (1.6)
89.63 ± 0.38	-2.38 ± 0.75	0.797 ± 0.006	8.6 (2.3)	89.78 ± 0.25	-1.06 ± 0.63	0.834 ± 0.006	5.6 (1.6)
121.65 ± 0.38	-0.66 ± 0.63	0.772 ± 0.013	6.4 (2.2)	121.93 ± 0.38	-0.63 ± 0.76	0.831 ± 0.002	4.3 (1.3)
152.02 ± 0.25	$+1.28 \pm 0.63$	0.773 ± 0.007	5.5 (1.5)	151.37 ± 0.13	$+0.43 \pm 0.25$	0.835 ± 0.014	5.6 (1.6)
179.63 ± 0.25	$+1.29 \pm 0.63$	0.770 ± 0.013	2.9 (1.8)	179.97 ± 0.25	$+0.51 \pm 0.75$	0.842 ± 0.002	2.7 (1.5)
208.96 ± 0.38	$+1.70 \pm 0.75$	0.795 ± 0.004	3.9 (2.1)	208.07 ± 0.25	$+1.38 \pm 0.50$	0.857 ± 0.004	3.4 (1.2)
238.05 ± 0.38	$+0.17 \pm 0.75$	0.787 ± 0.004	7.2 (2.2)	237.88 ± 0.25	$+0.59 \pm 0.63$	0.840 ± 0.006	6.0 (1.6)
270.21 ± 0.38	-0.82 ± 0.63	0.796 ± 0.003	6.3 (1.4)	269.99 ± 0.25	-0.65 ± 0.50	0.836 ± 0.009	4.2 (1.3)
301.65 ± 0.38	-1.25 ± 0.75	0.778 ± 0.004	6.3 (4.3)	302.04 ± 0.25	-0.35 ± 0.50	0.823 ± 0.005	4.9 (3.6)
331.28 ± 0.25	$+1.27 \pm 0.50$	0.774 ± 0.001	5.6 (7.3)	331.48 ± 0.13	$+0.10 \pm 0.38$	0.834 ± 0.007	3.9 (5.3)

Table 110: The nominal angle δ_n, average displacement $\Delta\delta$, average value of the parameter DIST, RMS of the ALPHA distribution for enabled GF and impact parameters between 60 m and 120 m. The RMS of the ALPHA distribution for disabled GF is given parentheses. The primary γ-ray energy was set to 450 GeV, the ZA to 20° and the azimuth angle to 120°.

$E_\gamma = 450\,\mathrm{GeV}$, Az = 120°, ZA = 20°, Hard Image Cleaning

δ_n[°]	$\Delta\delta$[°]	DIST[°]	RMS$_{\lvert ALPHA \rvert}$[°]	δ_n[°]	$\Delta\delta$[°]	DIST[°]	RMS$_{\lvert ALPHA \rvert}$[°]
IP = 60 m				**IP = 80 m**			
359.62 ± 0.51	$+5.95 \pm 1.25$	0.537 ± 0.007	5.0 (10.0)	359.66 ± 0.51	$+3.47 \pm 1.13$	0.664 ± 0.006	3.8 (7.0)
28.49 ± 0.51	$+0.95 \pm 1.25$	0.557 ± 0.004	6.6 (10.3)	28.76 ± 0.38	$+0.55 \pm 0.88$	0.686 ± 0.005	4.7 (4.2)
59.28 ± 0.76	-3.94 ± 2.13	0.559 ± 0.006	11.2 (4.2)	58.30 ± 0.63	-4.88 ± 1.25	0.692 ± 0.007	6.6 (2.9)
90.53 ± 0.63	-5.91 ± 1.25	0.557 ± 0.005	12.2 (3.2)	89.60 ± 0.25	-3.99 ± 0.63	0.692 ± 0.011	9.7 (2.4)
121.56 ± 0.63	-1.64 ± 1.01	0.545 ± 0.004	13.2 (3.1)	121.39 ± 0.38	-1.02 ± 0.75	0.675 ± 0.008	8.4 (2.5)
150.42 ± 0.51	$+2.68 \pm 0.88$	0.536 ± 0.006	9.1 (4.6)	151.31 ± 0.38	$+1.35 \pm 0.75$	0.664 ± 0.003	6.6 (3.4)
179.05 ± 0.63	$+5.22 \pm 1.25$	0.541 ± 0.009	4.8 (10.1)	179.53 ± 0.51	$+2.37 \pm 0.88$	0.669 ± 0.008	3.7 (7.9)
208.11 ± 0.63	$+2.01 \pm 1.25$	0.556 ± 0.007	6.8 (11.5)	209.14 ± 0.38	$+1.60 \pm 0.63$	0.682 ± 0.003	5.5 (2.6)
238.47 ± 0.63	-4.64 ± 1.01	0.558 ± 0.005	11.7 (3.6)	238.69 ± 0.51	-2.58 ± 1.00	0.688 ± 0.006	9.4 (2.1)
269.54 ± 0.51	-5.16 ± 1.25	0.554 ± 0.005	13.4 (4.0)	269.72 ± 0.38	-2.35 ± 0.88	0.683 ± 0.004	8.6 (2.2)
301.62 ± 0.63	-0.56 ± 1.13	0.542 ± 0.007	10.6 (5.0)	301.60 ± 0.38	-0.76 ± 0.63	0.667 ± 0.009	8.7 (2.5)
331.53 ± 0.38	$+3.46 \pm 1.13$	0.536 ± 0.008	7.8 (8.7)	331.48 ± 0.25	$+2.06 \pm 0.50$	0.661 ± 0.004	7.1 (8.4)
IP = 100 m				**IP = 120 m**			
0.22 ± 0.38	$+1.89 \pm 0.88$	0.765 ± 0.007	3.2 (4.4)	359.49 ± 0.25	$+0.37 \pm 0.50$	0.826 ± 0.008	2.9 (3.0)
28.67 ± 0.38	$+0.62 \pm 0.88$	0.784 ± 0.005	3.9 (2.8)	28.39 ± 0.38	-0.39 ± 0.76	0.841 ± 0.006	2.7 (1.4)
57.78 ± 0.25	-1.61 ± 0.75	0.778 ± 0.002	5.3 (1.8)	58.11 ± 0.38	-0.39 ± 0.63	0.824 ± 0.004	3.5 (1.2)
89.76 ± 0.51	-2.15 ± 0.88	0.789 ± 0.006	6.4 (1.8)	89.76 ± 0.25	-1.19 ± 0.63	0.826 ± 0.007	4.3 (1.5)
121.52 ± 0.38	-0.89 ± 0.75	0.763 ± 0.006	6.4 (1.9)	121.96 ± 0.25	-0.76 ± 0.63	0.821 ± 0.001	4.4 (1.3)
151.63 ± 0.25	$+0.93 \pm 0.63$	0.765 ± 0.008	5.4 (1.5)	151.05 ± 0.25	$+0.03 \pm 0.50$	0.829 ± 0.007	5.3 (1.4)
179.62 ± 0.38	$+1.26 \pm 0.76$	0.762 ± 0.008	3.0 (1.8)	179.87 ± 0.25	$+0.48 \pm 0.50$	0.830 ± 0.009	2.6 (1.6)
209.09 ± 0.13	$+1.38 \pm 0.50$	0.788 ± 0.003	3.5 (1.6)	208.30 ± 0.25	$+0.92 \pm 0.63$	0.847 ± 0.005	3.6 (1.1)
238.14 ± 0.25	$+0.28 \pm 0.63$	0.779 ± 0.005	5.9 (2.1)	237.57 ± 0.25	$+0.50 \pm 0.50$	0.828 ± 0.010	7.1 (1.8)
270.12 ± 0.25	-0.73 ± 0.50	0.785 ± 0.004	6.4 (1.4)	269.91 ± 0.25	-0.46 ± 0.50	0.827 ± 0.001	4.1 (1.2)
301.97 ± 0.25	-0.75 ± 0.63	0.767 ± 0.004	7.6 (4.0)	302.28 ± 0.25	-0.31 ± 0.50	0.814 ± 0.006	4.7 (1.2)
331.43 ± 0.38	$+1.36 \pm 0.75$	0.768 ± 0.006	5.4 (7.0)	331.66 ± 0.38	$+0.60 \pm 0.76$	0.825 ± 0.006	3.7 (5.4)

Table 111: The nominal angle δ_n, average displacement $\Delta\delta$, average value of the parameter DIST, RMS of the ALPHA distribution for enabled GF and impact parameters between 60 m and 120 m. The RMS of the ALPHA distribution for disabled GF is given parentheses. The primary γ-ray energy was set to 450 GeV, the ZA to 20° and the azimuth angle to 120°.

$E_\gamma = 450\,\mathrm{GeV}$, Az = 150°, ZA = 20°, Intermediate Image Cleaning

δ_n[°]	$\Delta\delta$[°]	DIST[°]	RMS$_{\lvert\mathrm{ALPHA}\rvert}$[°]	δ_n[°]	$\Delta\delta$[°]	DIST[°]	RMS$_{\lvert\mathrm{ALPHA}\rvert}$[°]
IP = 60 m				IP = 80 m			
0.00 ± 0.51	$+5.93 \pm 1.11$	0.529 ± 0.005	5.1 (8.8)	359.56 ± 0.38	$+3.14 \pm 0.74$	0.644 ± 0.004	4.1 (7.5)
28.62 ± 0.51	$+3.67 \pm 1.23$	0.530 ± 0.003	8.0 (11.1)	28.91 ± 0.25	$+2.33 \pm 0.73$	0.648 ± 0.003	5.6 (5.8)
61.21 ± 0.76	$+3.96 \pm 1.36$	0.531 ± 0.007	14.1 (3.9)	58.58 ± 0.51	$+0.43 \pm 1.47$	0.654 ± 0.008	8.8 (2.1)
92.00 ± 0.76	-5.03 ± 1.24	0.529 ± 0.004	16.6 (3.2)	89.76 ± 0.51	-5.43 ± 0.99	0.648 ± 0.004	12.8 (2.6)
121.84 ± 0.63	-6.52 ± 1.59	0.516 ± 0.008	16.8 (3.2)	121.43 ± 0.38	-3.79 ± 0.98	0.640 ± 0.007	14.3 (2.6)
150.93 ± 0.51	-0.90 ± 0.99	0.522 ± 0.004	12.5 (4.7)	151.47 ± 0.38	-0.30 ± 0.62	0.642 ± 0.007	11.2 (3.9)
178.79 ± 0.38	$+4.56 \pm 0.86$	0.529 ± 0.009	4.8 (9.9)	179.55 ± 0.51	$+3.00 \pm 0.87$	0.649 ± 0.007	3.6 (7.7)
208.14 ± 0.63	$+7.08 \pm 1.35$	0.533 ± 0.008	7.2 (11.3)	209.16 ± 0.38	$+5.56 \pm 0.98$	0.652 ± 0.004	5.5 (2.7)
238.32 ± 0.63	$+3.98 \pm 1.71$	0.535 ± 0.008	13.5 (3.0)	238.68 ± 0.51	$+0.10 \pm 1.47$	0.656 ± 0.010	11.8 (2.3)
269.69 ± 0.63	-6.82 ± 0.99	0.518 ± 0.007	17.7 (4.7)	269.52 ± 0.51	-3.34 ± 0.99	0.637 ± 0.009	14.3 (3.0)
301.42 ± 0.25	-7.11 ± 0.61	0.515 ± 0.006	17.9 (4.8)	301.31 ± 0.38	-4.93 ± 0.74	0.627 ± 0.006	14.8 (4.0)
331.78 ± 0.51	-0.71 ± 0.87	0.514 ± 0.008	10.7 (9.2)	331.95 ± 0.38	$+0.02 \pm 0.74$	0.632 ± 0.005	9.3 (8.8)
IP = 100 m				IP = 120 m			
359.98 ± 0.25	$+2.52 \pm 0.61$	0.744 ± 0.007	3.3 (4.5)	359.45 ± 0.25	$+0.56 \pm 0.61$	0.813 ± 0.008	2.4 (2.4)
28.66 ± 0.38	$+0.45 \pm 0.74$	0.749 ± 0.008	5.1 (3.5)	28.63 ± 0.25	-0.19 ± 0.61	0.808 ± 0.004	5.1 (1.4)
57.65 ± 0.38	-0.31 ± 0.86	0.754 ± 0.011	8.8 (1.9)	58.17 ± 0.38	$+0.79 \pm 0.62$	0.805 ± 0.010	6.7 (1.6)
89.63 ± 0.38	-2.86 ± 0.98	0.738 ± 0.005	10.4 (2.3)	89.78 ± 0.25	-0.89 ± 0.73	0.794 ± 0.011	10.0 (1.6)
121.65 ± 0.38	-2.83 ± 0.74	0.736 ± 0.004	11.7 (2.2)	121.93 ± 0.38	-2.33 ± 0.86	0.798 ± 0.012	7.8 (1.3)
152.02 ± 0.25	$+0.31 \pm 0.61$	0.737 ± 0.003	8.6 (1.5)	151.37 ± 0.13	-0.50 ± 0.49	0.804 ± 0.006	4.8 (1.6)
179.63 ± 0.25	$+2.00 \pm 0.73$	0.749 ± 0.001	3.4 (1.8)	179.97 ± 0.25	$+1.48 \pm 0.61$	0.818 ± 0.011	2.6 (1.5)
208.96 ± 0.38	$+2.35 \pm 0.50$	0.748 ± 0.006	4.3 (2.1)	208.07 ± 0.25	$+1.68 \pm 0.49$	0.815 ± 0.009	3.8 (1.2)
238.05 ± 0.38	$+1.13 \pm 0.74$	0.745 ± 0.011	8.1 (2.2)	237.88 ± 0.25	$+0.26 \pm 0.61$	0.806 ± 0.007	5.2 (1.6)
270.21 ± 0.38	-1.84 ± 0.98	0.729 ± 0.008	10.2 (1.4)	269.99 ± 0.25	-0.41 ± 0.61	0.787 ± 0.006	7.3 (1.3)
301.65 ± 0.38	-3.14 ± 0.74	0.723 ± 0.009	11.6 (4.3)	302.04 ± 0.25	-0.84 ± 0.73	0.788 ± 0.007	8.9 (3.6)
331.28 ± 0.25	-0.51 ± 0.61	0.729 ± 0.007	8.8 (7.3)	331.48 ± 0.13	-0.41 ± 0.49	0.794 ± 0.006	8.1 (5.3)

Table 112: The nominal angle δ_n, average displacement $\Delta\delta$, average value of the parameter DIST, RMS of the ALPHA distribution for enabled GF and impact parameters between 60 m and 120 m. The RMS of the ALPHA distribution for disabled GF is given parentheses. The primary γ-ray energy was set to 450 GeV, the ZA to 20° and the azimuth angle to 150°.

$E_\gamma = 450\,\mathrm{GeV}$, Az = 150°, ZA = 20°, Hard Image Cleaning

δ_n[°]	$\Delta\delta$[°]	DIST[°]	RMS$_{\lvert\mathrm{ALPHA}\rvert}$[°]	δ_n[°]	$\Delta\delta$[°]	DIST[°]	RMS$_{\lvert\mathrm{ALPHA}\rvert}$[°]
IP = 60 m				IP = 80 m			
359.62 ± 0.51	$+3.07 \pm 1.11$	0.520 ± 0.010	4.8 (10.0)	359.66 ± 0.51	$+2.30 \pm 0.87$	0.635 ± 0.007	4.2 (7.0)
28.49 ± 0.51	$+4.47 \pm 1.11$	0.524 ± 0.005	6.7 (10.3)	28.76 ± 0.38	$+1.87 \pm 0.86$	0.640 ± 0.010	5.7 (4.2)
59.28 ± 0.76	$+2.57 \pm 1.24$	0.521 ± 0.010	13.7 (4.2)	58.30 ± 0.63	-0.00 ± 1.35	0.644 ± 0.009	8.6 (2.9)
90.53 ± 0.63	-5.86 ± 1.47	0.516 ± 0.002	15.6 (3.2)	89.60 ± 0.25	-3.87 ± 0.97	0.635 ± 0.007	12.7 (2.4)
121.56 ± 0.63	-6.16 ± 1.35	0.505 ± 0.007	17.0 (3.1)	121.39 ± 0.38	-3.89 ± 0.98	0.628 ± 0.002	13.5 (2.5)
150.42 ± 0.51	-0.78 ± 0.99	0.514 ± 0.007	10.5 (4.6)	151.31 ± 0.38	-0.60 ± 0.74	0.630 ± 0.005	9.0 (3.4)
179.05 ± 0.63	$+4.61 \pm 1.11$	0.518 ± 0.009	4.5 (10.1)	179.53 ± 0.51	$+3.28 \pm 0.99$	0.643 ± 0.009	3.6 (7.9)
208.11 ± 0.63	$+6.69 \pm 1.47$	0.521 ± 0.007	9.9 (11.5)	209.14 ± 0.38	$+5.57 \pm 1.22$	0.644 ± 0.008	5.8 (2.6)
238.47 ± 0.63	$+5.03 \pm 1.11$	0.523 ± 0.007	13.3 (3.6)	238.69 ± 0.51	$+2.18 \pm 1.23$	0.648 ± 0.003	11.6 (2.1)
269.54 ± 0.51	-8.52 ± 1.35	0.509 ± 0.009	15.7 (4.0)	269.72 ± 0.38	-4.71 ± 1.22	0.629 ± 0.007	12.7 (2.2)
301.62 ± 0.63	-4.70 ± 1.11	0.505 ± 0.005	17.4 (5.0)	301.60 ± 0.38	-3.58 ± 0.74	0.618 ± 0.009	13.9 (2.5)
331.53 ± 0.38	-0.87 ± 0.74	0.502 ± 0.005	10.2 (8.7)	331.48 ± 0.25	-0.21 ± 0.61	0.624 ± 0.005	8.4 (8.4)
IP = 100 m				IP = 120 m			
0.22 ± 0.38	$+1.27 \pm 0.74$	0.735 ± 0.001	3.4 (4.4)	359.49 ± 0.25	-0.78 ± 0.61	0.799 ± 0.003	2.5 (3.0)
28.67 ± 0.38	$+0.45 \pm 0.62$	0.739 ± 0.005	5.1 (2.8)	28.39 ± 0.38	-1.10 ± 0.74	0.796 ± 0.004	5.0 (1.4)
57.78 ± 0.25	$+0.19 \pm 0.85$	0.744 ± 0.013	7.3 (1.8)	58.11 ± 0.38	$+0.87 \pm 0.86$	0.794 ± 0.004	6.9 (1.2)
89.76 ± 0.51	-4.01 ± 0.99	0.728 ± 0.008	10.7 (1.8)	89.76 ± 0.25	-1.44 ± 0.61	0.786 ± 0.011	10.0 (1.5)
121.52 ± 0.38	-3.44 ± 0.74	0.725 ± 0.007	11.1 (1.9)	121.96 ± 0.25	-1.56 ± 0.61	0.790 ± 0.009	6.8 (1.3)
151.63 ± 0.25	-0.30 ± 0.61	0.724 ± 0.008	5.8 (1.5)	151.05 ± 0.25	-0.82 ± 0.49	0.792 ± 0.007	5.4 (1.4)
179.62 ± 0.38	$+2.19 \pm 0.86$	0.734 ± 0.007	3.0 (1.8)	179.87 ± 0.25	$+1.03 \pm 0.49$	0.808 ± 0.010	2.5 (1.6)
209.09 ± 0.13	$+4.12 \pm 0.49$	0.741 ± 0.006	6.0 (1.6)	208.30 ± 0.25	$+1.75 \pm 0.37$	0.801 ± 0.006	4.5 (1.1)
238.14 ± 0.25	$+1.11 \pm 0.97$	0.737 ± 0.009	8.6 (2.1)	237.57 ± 0.25	$+0.01 \pm 0.61$	0.797 ± 0.006	5.9 (1.8)
270.12 ± 0.25	-1.36 ± 0.73	0.720 ± 0.010	9.9 (1.4)	269.91 ± 0.25	-0.14 ± 0.61	0.779 ± 0.004	5.9 (1.2)
301.97 ± 0.25	-1.05 ± 0.61	0.715 ± 0.009	12.0 (4.0)	302.28 ± 0.25	-0.19 ± 0.73	0.776 ± 0.007	10.2 (1.2)
331.43 ± 0.38	-0.06 ± 0.62	0.721 ± 0.004	8.3 (7.0)	331.66 ± 0.38	-0.28 ± 0.74	0.785 ± 0.006	5.9 (5.4)

Table 113: The nominal angle δ_n, average displacement $\Delta\delta$, average value of the parameter DIST, RMS of the ALPHA distribution for enabled GF and impact parameters between 60 m and 120 m. The RMS of the ALPHA distribution for disabled GF is given parentheses. The primary γ-ray energy was set to 450 GeV, the ZA to 20° and the azimuth angle to 150°.

$E_\gamma = 450\,\mathrm{GeV}$, Az = 180°, ZA = 20°, Intermediate Image Cleaning

δ_n[°]	$\Delta\delta$[°]	DIST[°]	RMS$_{\lvert ALPHA \rvert}$[°]	δ_n[°]	$\Delta\delta$[°]	DIST[°]	RMS$_{\lvert ALPHA \rvert}$[°]
IP = 60 m				**IP = 80 m**			
0.00 ± 0.51	-1.40 ± 0.87	0.522 ± 0.005	3.9 (8.8)	359.56 ± 0.38	$+0.07 \pm 0.62$	0.649 ± 0.008	6.0 (7.5)
28.62 ± 0.51	$+4.29 \pm 1.23$	0.521 ± 0.009	9.8 (11.1)	28.91 ± 0.25	$+3.13 \pm 0.74$	0.651 ± 0.008	3.8 (5.8)
61.21 ± 0.76	$+13.35 \pm 1.36$	0.520 ± 0.003	13.1 (3.9)	58.58 ± 0.51	$+7.26 \pm 0.87$	0.641 ± 0.012	8.9 (2.1)
92.00 ± 0.76	$+5.24 \pm 1.48$	0.517 ± 0.007	25.9 (3.2)	89.76 ± 0.51	$+0.79 \pm 1.23$	0.640 ± 0.009	13.7 (2.6)
121.84 ± 0.63	-8.70 ± 1.48	0.524 ± 0.008	19.1 (3.2)	121.43 ± 0.38	-4.67 ± 1.10	0.645 ± 0.010	16.0 (2.6)
150.93 ± 0.51	-6.02 ± 0.99	0.530 ± 0.010	12.1 (4.7)	151.47 ± 0.38	-3.55 ± 0.98	0.656 ± 0.005	8.3 (3.9)
178.79 ± 0.38	-0.82 ± 0.86	0.532 ± 0.010	4.1 (9.9)	179.55 ± 0.51	-1.82 ± 0.87	0.657 ± 0.006	3.2 (7.7)
208.14 ± 0.63	$+6.26 \pm 1.36$	0.525 ± 0.007	11.9 (11.3)	209.16 ± 0.38	$+4.16 \pm 0.74$	0.648 ± 0.007	7.4 (2.7)
238.32 ± 0.63	$+11.42 \pm 1.24$	0.517 ± 0.005	14.2 (3.0)	238.68 ± 0.51	$+6.33 \pm 0.99$	0.635 ± 0.011	8.0 (2.3)
269.69 ± 0.63	$+2.97 \pm 1.11$	0.506 ± 0.002	22.3 (4.7)	269.52 ± 0.51	$+2.23 \pm 1.23$	0.628 ± 0.010	19.8 (3.0)
301.42 ± 0.25	-9.43 ± 1.46	0.509 ± 0.002	17.7 (4.8)	301.31 ± 0.38	-6.03 ± 0.74	0.629 ± 0.008	14.8 (4.0)
331.78 ± 0.51	-4.11 ± 1.23	0.518 ± 0.008	11.2 (9.2)	331.95 ± 0.38	-2.10 ± 0.98	0.641 ± 0.004	8.4 (8.8)
IP = 100 m				**IP = 120 m**			
359.98 ± 0.25	$+0.32 \pm 0.61$	0.749 ± 0.007	2.9 (4.5)	359.45 ± 0.25	-0.12 ± 0.50	0.810 ± 0.007	2.0 (2.4)
28.66 ± 0.38	$+1.19 \pm 0.74$	0.754 ± 0.010	11.3 (3.5)	28.63 ± 0.25	$+0.02 \pm 0.61$	0.825 ± 0.009	2.5 (1.4)
57.65 ± 0.38	$+1.61 \pm 0.86$	0.742 ± 0.008	13.4 (1.9)	58.17 ± 0.38	-0.34 ± 0.86	0.802 ± 0.008	13.5 (1.6)
89.63 ± 0.38	-2.69 ± 1.10	0.740 ± 0.007	9.4 (2.3)	89.78 ± 0.25	$+0.14 \pm 0.86$	0.794 ± 0.004	6.2 (1.6)
121.65 ± 0.38	-1.71 ± 0.62	0.743 ± 0.007	12.8 (2.2)	121.93 ± 0.38	-0.52 ± 0.86	0.797 ± 0.011	5.8 (1.3)
152.02 ± 0.25	-0.47 ± 0.49	0.756 ± 0.011	5.2 (1.5)	151.37 ± 0.13	-1.52 ± 0.37	0.827 ± 0.010	3.6 (1.6)
179.63 ± 0.25	-0.98 ± 0.62	0.761 ± 0.007	1.8 (1.8)	179.97 ± 0.25	-0.46 ± 0.50	0.821 ± 0.009	1.7 (1.5)
208.96 ± 0.38	$+0.92 \pm 0.86$	0.755 ± 0.002	7.7 (2.1)	208.07 ± 0.25	$+0.46 \pm 0.50$	0.821 ± 0.008	6.5 (1.2)
238.05 ± 0.38	$+2.84 \pm 0.74$	0.733 ± 0.010	13.7 (2.2)	237.88 ± 0.25	$+0.29 \pm 0.86$	0.796 ± 0.001	12.6 (1.6)
270.21 ± 0.38	$+1.12 \pm 0.86$	0.734 ± 0.007	18.1 (1.4)	269.99 ± 0.25	$+1.29 \pm 0.85$	0.790 ± 0.010	7.5 (1.3)
301.65 ± 0.38	-2.59 ± 0.98	0.730 ± 0.002	10.2 (4.3)	302.04 ± 0.25	-0.52 ± 0.74	0.792 ± 0.008	8.5 (3.6)
331.28 ± 0.25	-1.41 ± 0.74	0.745 ± 0.011	5.0 (7.3)	331.48 ± 0.13	-0.57 ± 0.49	0.816 ± 0.007	8.1 (5.3)

Table 114: The nominal angle δ_n, average displacement $\Delta\delta$, average value of the parameter DIST, RMS of the ALPHA distribution for enabled GF and impact parameters between 60 m and 120 m. The RMS of the ALPHA distribution for disabled GF is given parentheses. The primary γ-ray energy was set to 450 GeV, the ZA to 20° and the azimuth angle to 180°.

$E_\gamma = 450\,\mathrm{GeV}$, Az = 180°, ZA = 20°, Hard Image Cleaning

δ_n[°]	$\Delta\delta$[°]	DIST[°]	RMS$_{\lvert ALPHA \rvert}$[°]	δ_n[°]	$\Delta\delta$[°]	DIST[°]	RMS$_{\lvert ALPHA \rvert}$[°]
IP = 60 m				**IP = 80 m**			
359.62 ± 0.51	-1.41 ± 0.63	0.512 ± 0.008	4.1 (10.0)	359.66 ± 0.51	-0.13 ± 0.99	0.644 ± 0.008	2.3 (7.0)
28.49 ± 0.51	$+4.20 \pm 1.11$	0.513 ± 0.010	9.4 (10.3)	28.76 ± 0.38	$+2.48 \pm 0.86$	0.641 ± 0.012	3.3 (4.2)
59.28 ± 0.76	$+11.32 \pm 1.36$	0.508 ± 0.009	21.9 (4.2)	58.30 ± 0.63	$+6.37 \pm 1.48$	0.629 ± 0.009	16.4 (2.9)
90.53 ± 0.63	$+3.95 \pm 1.24$	0.508 ± 0.006	25.5 (3.2)	89.60 ± 0.25	-0.57 ± 1.22	0.631 ± 0.011	17.7 (2.4)
121.56 ± 0.63	-8.41 ± 1.84	0.513 ± 0.007	17.8 (3.1)	121.39 ± 0.38	-3.34 ± 1.10	0.636 ± 0.010	15.8 (2.5)
150.42 ± 0.51	-6.95 ± 0.87	0.518 ± 0.010	9.2 (4.6)	151.31 ± 0.38	-2.57 ± 0.98	0.647 ± 0.001	5.5 (3.4)
179.05 ± 0.63	$+0.94 \pm 1.11$	0.523 ± 0.001	4.1 (10.1)	179.53 ± 0.51	-0.85 ± 0.99	0.646 ± 0.011	2.4 (7.9)
208.11 ± 0.63	$+5.16 \pm 1.24$	0.514 ± 0.010	11.9 (11.5)	209.14 ± 0.38	$+4.15 \pm 0.74$	0.640 ± 0.013	8.1 (2.6)
238.47 ± 0.63	$+10.21 \pm 0.99$	0.500 ± 0.009	10.5 (3.6)	238.69 ± 0.51	$+4.35 \pm 1.11$	0.627 ± 0.008	11.5 (2.1)
269.54 ± 0.51	$+3.77 \pm 1.23$	0.495 ± 0.007	23.5 (4.0)	269.72 ± 0.38	$+2.91 \pm 0.98$	0.618 ± 0.009	20.3 (2.2)
301.62 ± 0.63	-9.15 ± 1.24	0.498 ± 0.003	15.3 (5.0)	301.60 ± 0.38	-5.15 ± 1.10	0.620 ± 0.010	11.4 (2.5)
331.53 ± 0.38	-4.36 ± 1.59	0.509 ± 0.008	11.2 (8.7)	331.48 ± 0.25	-1.47 ± 0.86	0.634 ± 0.011	5.6 (8.4)
IP = 100 m				**IP = 120 m**			
0.22 ± 0.38	$+0.65 \pm 0.74$	0.742 ± 0.002	2.5 (4.4)	359.49 ± 0.25	-0.38 ± 0.62	0.795 ± 0.007	2.0 (3.0)
28.67 ± 0.38	$+1.14 \pm 0.74$	0.744 ± 0.004	11.9 (2.8)	28.39 ± 0.38	$+0.76 \pm 0.74$	0.810 ± 0.005	14.3 (1.4)
57.78 ± 0.25	-0.21 ± 0.74	0.733 ± 0.010	5.2 (1.8)	58.11 ± 0.38	$+0.16 \pm 0.50$	0.790 ± 0.005	4.8 (1.2)
89.76 ± 0.51	-1.97 ± 1.23	0.732 ± 0.001	10.2 (1.8)	89.76 ± 0.25	-0.89 ± 0.74	0.786 ± 0.004	6.9 (1.5)
121.52 ± 0.38	-2.91 ± 0.86	0.733 ± 0.006	8.7 (1.9)	121.96 ± 0.25	$+0.09 \pm 0.74$	0.787 ± 0.007	5.7 (1.3)
151.63 ± 0.25	-1.22 ± 0.61	0.747 ± 0.010	4.4 (1.5)	151.05 ± 0.25	-0.42 ± 0.62	0.821 ± 0.005	6.9 (1.4)
179.62 ± 0.38	-0.79 ± 0.62	0.752 ± 0.003	1.8 (1.8)	179.87 ± 0.25	-0.59 ± 0.50	0.807 ± 0.009	1.5 (1.6)
209.09 ± 0.13	$+0.88 \pm 0.61$	0.749 ± 0.008	2.3 (1.6)	208.30 ± 0.25	-0.63 ± 0.62	0.815 ± 0.008	2.0 (1.1)
238.14 ± 0.25	$+1.96 \pm 0.74$	0.727 ± 0.008	18.5 (2.1)	237.57 ± 0.25	$+0.33 \pm 0.74$	0.787 ± 0.002	7.7 (1.8)
270.12 ± 0.25	$+0.97 \pm 0.86$	0.725 ± 0.007	15.2 (1.4)	269.91 ± 0.25	$+0.42 \pm 0.73$	0.780 ± 0.008	7.4 (1.2)
301.97 ± 0.25	-1.50 ± 0.98	0.722 ± 0.009	10.0 (4.0)	302.28 ± 0.25	$+0.26 \pm 0.50$	0.784 ± 0.010	9.0 (1.2)
331.43 ± 0.38	-0.95 ± 0.86	0.736 ± 0.006	4.8 (7.0)	331.66 ± 0.38	-1.16 ± 0.74	0.801 ± 0.010	4.6 (5.4)

Table 115: The nominal angle δ_n, average displacement $\Delta\delta$, average value of the parameter DIST, RMS of the ALPHA distribution for enabled GF and impact parameters between 60 m and 120 m. The RMS of the ALPHA distribution for disabled GF is given parentheses. The primary γ-ray energy was set to 450 GeV, the ZA to 20° and the azimuth angle to 180°.

$E_\gamma = 450\,\mathrm{GeV}$, Az = 0°, ZA = 40°, Intermediate Image Cleaning

$\delta_n[°]$	$\Delta\delta[°]$	DIST[°]	$\mathrm{RMS}_{\lvert\mathrm{ALPHA}\rvert}[°]$	$\delta_n[°]$	$\Delta\delta[°]$	DIST[°]	$\mathrm{RMS}_{\lvert\mathrm{ALPHA}\rvert}[°]$
IP = 60 m				**IP = 80 m**			
0.99 ± 0.62	+1.53 ± 0.82	0.364 ± 0.004	6.4 (9.3)	0.46 ± 0.51	+0.53 ± 0.93	0.477 ± 0.004	4.9 (7.7)
24.64 ± 0.62	+3.00 ± 1.13	0.342 ± 0.004	9.6 (9.6)	25.33 ± 0.31	+2.15 ± 0.72	0.449 ± 0.005	8.2 (7.7)
54.32 ± 0.93	+3.48 ± 1.45	0.297 ± 0.003	13.2 (10.2)	54.16 ± 0.41	+1.57 ± 0.93	0.392 ± 0.003	10.7 (6.9)
89.85 ± 0.52	+1.25 ± 1.45	0.272 ± 0.003	15.9 (14.0)	91.37 ± 0.52	+1.19 ± 1.14	0.361 ± 0.004	12.0 (5.4)
127.93 ± 0.52	−3.12 ± 1.03	0.299 ± 0.003	11.5 (10.3)	127.89 ± 0.52	−1.80 ± 0.93	0.393 ± 0.003	6.0 (5.6)
156.43 ± 0.72	−0.61 ± 1.55	0.342 ± 0.003	6.1 (7.0)	155.12 ± 0.52	−1.60 ± 0.93	0.448 ± 0.004	3.9 (7.2)
179.11 ± 0.72	−1.48 ± 1.45	0.364 ± 0.004	5.7 (7.0)	179.89 ± 0.31	−0.41 ± 0.72	0.473 ± 0.003	3.9 (7.7)
203.44 ± 0.52	+0.04 ± 1.14	0.347 ± 0.003	7.1 (10.0)	203.70 ± 0.41	−0.00 ± 0.72	0.456 ± 0.003	5.5 (6.8)
231.67 ± 0.41	+1.81 ± 1.03	0.311 ± 0.003	13.9 (13.7)	233.75 ± 0.52	+2.93 ± 0.93	0.410 ± 0.003	8.6 (5.5)
270.10 ± 0.31	+0.53 ± 1.03	0.289 ± 0.003	14.7 (11.1)	267.95 ± 0.52	−2.77 ± 1.14	0.380 ± 0.004	7.6 (15.2)
306.10 ± 0.31	−1.35 ± 0.93	0.309 ± 0.003	10.9 (9.6)	306.37 ± 0.62	−1.11 ± 1.03	0.411 ± 0.003	6.4 (12.8)
337.79 ± 0.41	+0.67 ± 0.83	0.352 ± 0.004	6.6 (9.0)	337.80 ± 0.41	+1.42 ± 0.93	0.457 ± 0.003	5.0 (7.5)
IP = 100 m				**IP = 120 m**			
359.07 ± 0.41	−0.30 ± 0.83	0.578 ± 0.005	4.3 (8.1)	359.58 ± 0.31	−0.01 ± 0.72	0.658 ± 0.007	3.1 (4.8)
26.26 ± 0.41	+2.81 ± 0.62	0.548 ± 0.005	3.4 (2.9)	26.08 ± 0.21	+2.29 ± 0.62	0.632 ± 0.004	2.8 (2.0)
53.31 ± 0.41	+2.00 ± 1.03	0.484 ± 0.003	5.9 (6.3)	53.28 ± 0.31	+0.62 ± 0.52	0.567 ± 0.005	5.1 (3.4)
91.06 ± 0.62	+0.62 ± 1.03	0.447 ± 0.004	11.5 (4.1)	90.63 ± 0.41	−0.54 ± 0.72	0.525 ± 0.004	3.7 (3.3)
127.15 ± 0.52	−1.42 ± 0.83	0.483 ± 0.004	3.6 (5.0)	126.46 ± 0.52	−0.69 ± 0.93	0.562 ± 0.006	2.6 (5.5)
155.82 ± 0.41	−1.41 ± 0.62	0.545 ± 0.005	2.3 (6.6)	156.04 ± 0.31	−0.38 ± 0.62	0.628 ± 0.007	2.8 (6.0)
180.16 ± 0.41	−0.50 ± 0.83	0.574 ± 0.005	2.8 (3.1)	180.06 ± 0.31	−0.09 ± 0.52	0.655 ± 0.005	2.6 (2.4)
203.41 ± 0.41	−0.10 ± 0.83	0.553 ± 0.003	4.9 (3.0)	203.04 ± 0.31	−0.38 ± 0.62	0.641 ± 0.005	2.7 (2.5)
233.75 ± 0.41	+2.00 ± 0.72	0.498 ± 0.005	6.3 (4.3)	232.02 ± 0.41	−0.76 ± 0.72	0.584 ± 0.005	4.2 (9.5)
269.48 ± 0.31	+0.47 ± 0.72	0.465 ± 0.003	6.9 (6.5)	270.36 ± 0.21	−0.58 ± 0.52	0.546 ± 0.003	3.6 (4.5)
306.63 ± 0.31	−1.74 ± 0.62	0.503 ± 0.004	4.8 (5.4)	307.08 ± 0.31	−0.17 ± 0.62	0.588 ± 0.006	3.7 (3.6)
336.98 ± 0.31	+0.40 ± 0.62	0.555 ± 0.003	3.4 (5.5)	336.80 ± 0.31	+0.58 ± 0.62	0.641 ± 0.005	2.8 (2.3)

Table 116: The nominal angle δ_n, average displacement $\Delta\delta$, average value of the parameter DIST, RMS of the ALPHA distribution for enabled GF and impact parameters between 60 m and 120 m. The RMS of the ALPHA distribution for disabled GF is given parentheses. The primary γ-ray energy was set to 450 GeV, the ZA to 40° and the azimuth angle to 0°.

$E_\gamma = 450\,\mathrm{GeV}$, Az = 0°, ZA = 40°, Hard Image Cleaning

$\delta_n[°]$	$\Delta\delta[°]$	DIST[°]	$\mathrm{RMS}_{\lvert\mathrm{ALPHA}\rvert}[°]$	$\delta_n[°]$	$\Delta\delta[°]$	DIST[°]	$\mathrm{RMS}_{\lvert\mathrm{ALPHA}\rvert}[°]$
IP = 60 m				**IP = 80 m**			
0.10 ± 0.31	+0.13 ± 0.93	0.358 ± 0.004	7.6 (12.1)	0.74 ± 0.51	+0.91 ± 0.93	0.468 ± 0.003	6.2 (10.6)
23.41 ± 0.62	+1.50 ± 1.14	0.335 ± 0.003	8.4 (9.1)	24.35 ± 0.52	+1.49 ± 0.93	0.441 ± 0.006	9.1 (3.9)
54.65 ± 0.93	+2.49 ± 1.24	0.292 ± 0.003	12.5 (7.8)	53.60 ± 0.52	+1.64 ± 0.93	0.387 ± 0.003	13.0 (4.7)
91.52 ± 0.83	+2.71 ± 1.24	0.267 ± 0.003	16.3 (11.6)	90.85 ± 0.62	+1.42 ± 1.14	0.357 ± 0.004	16.4 (5.9)
128.06 ± 0.52	−1.00 ± 1.03	0.293 ± 0.003	11.2 (6.2)	128.44 ± 0.52	−0.51 ± 0.93	0.388 ± 0.004	6.4 (5.0)
156.64 ± 0.62	−1.00 ± 1.24	0.337 ± 0.003	5.7 (6.8)	154.96 ± 0.52	−1.69 ± 1.03	0.440 ± 0.004	3.9 (6.7)
179.48 ± 0.41	+0.09 ± 1.34	0.356 ± 0.003	7.1 (8.2)	180.59 ± 0.41	+0.65 ± 0.83	0.466 ± 0.004	3.7 (3.9)
203.50 ± 0.41	+0.66 ± 0.83	0.342 ± 0.003	8.3 (9.0)	203.95 ± 0.52	+0.88 ± 0.83	0.448 ± 0.004	5.4 (6.6)
232.64 ± 0.62	+1.64 ± 1.55	0.305 ± 0.002	12.0 (11.2)	233.32 ± 0.52	+2.20 ± 0.93	0.404 ± 0.003	8.5 (6.3)
270.28 ± 0.62	+0.17 ± 0.93	0.283 ± 0.003	12.2 (11.9)	269.27 ± 0.52	−2.12 ± 1.24	0.372 ± 0.004	7.9 (9.3)
305.49 ± 0.62	−3.15 ± 1.34	0.303 ± 0.003	9.4 (10.1)	306.92 ± 0.52	+0.12 ± 1.03	0.405 ± 0.003	10.0 (11.2)
337.26 ± 0.62	+0.63 ± 1.24	0.345 ± 0.003	5.4 (7.7)	337.30 ± 0.41	+0.96 ± 0.83	0.451 ± 0.004	5.0 (7.5)
IP = 100 m				**IP = 120 m**			
359.99 ± 0.31	+0.67 ± 0.72	0.570 ± 0.007	4.5 (8.7)	0.29 ± 0.21	+0.55 ± 0.62	0.650 ± 0.008	2.7 (2.7)
25.23 ± 0.41	+1.40 ± 0.72	0.541 ± 0.005	3.7 (3.6)	24.97 ± 0.31	+0.94 ± 0.52	0.623 ± 0.006	2.4 (1.9)
52.56 ± 0.41	+0.67 ± 0.72	0.477 ± 0.003	6.2 (4.2)	53.42 ± 0.31	+0.55 ± 0.62	0.560 ± 0.005	4.1 (3.2)
90.71 ± 0.52	−0.38 ± 0.93	0.441 ± 0.005	9.1 (3.9)	90.27 ± 0.21	−0.67 ± 0.72	0.519 ± 0.005	3.8 (3.7)
126.90 ± 0.31	−1.15 ± 0.72	0.476 ± 0.006	3.5 (5.1)	126.89 ± 0.41	−0.29 ± 0.62	0.556 ± 0.005	2.6 (5.3)
156.29 ± 0.31	−0.97 ± 0.72	0.537 ± 0.005	2.3 (3.7)	156.23 ± 0.31	−0.02 ± 0.52	0.622 ± 0.007	2.3 (2.4)
179.92 ± 0.41	−0.74 ± 0.83	0.567 ± 0.004	2.5 (2.9)	179.95 ± 0.21	−0.29 ± 0.41	0.648 ± 0.004	2.2 (2.6)
203.57 ± 0.41	+0.27 ± 0.83	0.546 ± 0.006	5.0 (2.7)	203.14 ± 0.21	−0.55 ± 0.41	0.632 ± 0.007	2.8 (2.6)
232.85 ± 0.52	+1.40 ± 0.83	0.491 ± 0.004	6.6 (9.5)	232.26 ± 0.41	−0.60 ± 0.83	0.577 ± 0.005	5.0 (10.2)
270.28 ± 0.31	+0.59 ± 0.72	0.458 ± 0.003	6.4 (6.5)	270.20 ± 0.21	−0.46 ± 0.62	0.539 ± 0.006	4.0 (3.5)
307.19 ± 0.41	−1.51 ± 0.83	0.495 ± 0.003	5.0 (5.7)	307.18 ± 0.31	+0.37 ± 0.62	0.579 ± 0.005	4.0 (4.1)
336.92 ± 0.41	+0.26 ± 0.72	0.549 ± 0.007	3.1 (4.8)	336.47 ± 0.21	+0.24 ± 0.41	0.633 ± 0.005	2.3 (2.4)

Table 117: The nominal angle δ_n, average displacement $\Delta\delta$, average value of the parameter DIST, RMS of the ALPHA distribution for enabled GF and impact parameters between 60 m and 120 m. The RMS of the ALPHA distribution for disabled GF is given parentheses. The primary γ-ray energy was set to 450 GeV, the ZA to 40° and the azimuth angle to 0°.

$E_\gamma = 450\,\mathrm{GeV}$, Az = 30°, ZA = 40°, Intermediate Image Cleaning

δ_n[°]	$\Delta\delta$[°]	DIST[°]	$\mathrm{RMS}_{\lvert\mathrm{ALPHA}\rvert}$[°]	δ_n[°]	$\Delta\delta$[°]	DIST[°]	$\mathrm{RMS}_{\lvert\mathrm{ALPHA}\rvert}$[°]
IP = 60 m				IP = 80 m			
0.99 ± 0.62	−0.90 ± 1.41	0.331 ± 0.003	13.2 (9.3)	0.46 ± 0.51	−0.66 ± 0.91	0.434 ± 0.003	8.1 (7.7)
24.64 ± 0.62	−4.07 ± 1.51	0.289 ± 0.003	10.8 (9.6)	25.33 ± 0.31	−3.61 ± 0.90	0.378 ± 0.003	8.2 (7.7)
54.32 ± 0.93	−2.52 ± 1.62	0.266 ± 0.002	12.1 (10.2)	54.16 ± 0.41	−1.43 ± 0.91	0.349 ± 0.003	9.0 (6.9)
89.85 ± 0.52	+3.23 ± 1.11	0.291 ± 0.002	16.9 (14.0)	91.37 ± 0.52	+3.69 ± 1.01	0.379 ± 0.003	14.0 (5.4)
127.93 ± 0.52	+6.30 ± 0.91	0.332 ± 0.003	16.1 (10.3)	127.89 ± 0.52	+4.68 ± 0.81	0.433 ± 0.003	13.0 (5.6)
156.43 ± 0.72	+1.43 ± 1.02	0.352 ± 0.002	14.4 (7.0)	155.12 ± 0.52	+1.54 ± 1.21	0.459 ± 0.004	10.7 (7.2)
179.11 ± 0.72	−7.02 ± 1.71	0.338 ± 0.003	10.9 (7.0)	179.89 ± 0.31	−2.25 ± 0.51	0.441 ± 0.004	10.3 (7.7)
203.44 ± 0.52	−7.82 ± 1.50	0.301 ± 0.002	10.5 (10.0)	203.70 ± 0.41	−4.34 ± 0.91	0.398 ± 0.003	8.4 (6.8)
231.67 ± 0.41	−3.58 ± 0.91	0.279 ± 0.002	11.8 (13.7)	233.75 ± 0.52	−0.37 ± 1.01	0.365 ± 0.003	9.1 (5.5)
270.10 ± 0.31	+4.45 ± 0.51	0.301 ± 0.003	15.9 (11.1)	267.95 ± 0.52	+0.55 ± 1.01	0.396 ± 0.004	13.5 (15.2)
306.10 ± 0.31	+6.88 ± 1.20	0.339 ± 0.003	19.9 (9.6)	306.37 ± 0.62	+5.21 ± 1.61	0.441 ± 0.003	13.3 (12.8)
337.79 ± 0.41	+6.23 ± 0.91	0.353 ± 0.002	16.2 (9.0)	337.80 ± 0.41	+4.60 ± 0.91	0.459 ± 0.004	11.8 (7.5)
IP = 100 m				IP = 120 m			
359.07 ± 0.41	−2.33 ± 0.71	0.526 ± 0.005	6.7 (8.1)	359.58 ± 0.31	−0.03 ± 0.51	0.613 ± 0.005	5.0 (4.8)
26.26 ± 0.41	−0.95 ± 0.91	0.470 ± 0.003	5.9 (2.9)	26.08 ± 0.21	+0.45 ± 0.40	0.546 ± 0.007	4.8 (2.0)
53.31 ± 0.41	−1.84 ± 0.91	0.431 ± 0.003	7.3 (6.3)	53.28 ± 0.31	−1.00 ± 0.61	0.506 ± 0.004	5.5 (3.4)
91.06 ± 0.62	+2.39 ± 1.11	0.465 ± 0.003	10.1 (4.1)	90.63 ± 0.41	+1.39 ± 0.81	0.543 ± 0.005	8.5 (3.3)
127.15 ± 0.52	+3.74 ± 0.91	0.527 ± 0.005	10.2 (5.0)	126.46 ± 0.52	+1.44 ± 0.81	0.611 ± 0.006	7.8 (5.5)
155.82 ± 0.41	+1.12 ± 0.61	0.555 ± 0.006	6.0 (6.6)	156.04 ± 0.31	+0.66 ± 0.61	0.639 ± 0.004	5.6 (6.0)
180.16 ± 0.41	−1.75 ± 0.71	0.537 ± 0.004	7.7 (3.1)	180.06 ± 0.31	−0.81 ± 0.61	0.619 ± 0.005	5.0 (2.4)
203.41 ± 0.41	−3.81 ± 0.71	0.484 ± 0.004	6.4 (3.0)	203.04 ± 0.31	−2.77 ± 0.70	0.565 ± 0.004	5.0 (2.5)
233.75 ± 0.41	−0.10 ± 0.91	0.450 ± 0.004	6.7 (4.3)	232.02 ± 0.41	−1.72 ± 0.81	0.529 ± 0.004	5.7 (9.5)
269.48 ± 0.31	+1.87 ± 0.80	0.484 ± 0.005	9.9 (6.5)	270.36 ± 0.21	+2.01 ± 0.50	0.565 ± 0.005	8.1 (4.5)
306.63 ± 0.31	+3.42 ± 0.70	0.537 ± 0.003	9.6 (5.4)	307.08 ± 0.31	+2.20 ± 0.80	0.620 ± 0.007	7.8 (3.6)
336.98 ± 0.31	+1.24 ± 0.70	0.560 ± 0.005	7.6 (5.5)	336.80 ± 0.31	+0.94 ± 0.60	0.641 ± 0.006	6.4 (2.3)

Table 118: The nominal angle δ_n, average displacement $\Delta\delta$, average value of the parameter DIST, RMS of the ALPHA distribution for enabled GF and impact parameters between 60 m and 120 m. The RMS of the ALPHA distribution for disabled GF is given parentheses. The primary γ-ray energy was set to 450 GeV, the ZA to 40° and the azimuth angle to 30°.

$E_\gamma = 450\,\mathrm{GeV}$, Az = 30°, ZA = 40°, Hard Image Cleaning

δ_n[°]	$\Delta\delta$[°]	DIST[°]	$\mathrm{RMS}_{\lvert\mathrm{ALPHA}\rvert}$[°]	δ_n[°]	$\Delta\delta$[°]	DIST[°]	$\mathrm{RMS}_{\lvert\mathrm{ALPHA}\rvert}$[°]
IP = 60 m				IP = 80 m			
0.10 ± 0.31	−0.80 ± 0.90	0.325 ± 0.003	11.5 (12.1)	0.74 ± 0.51	−0.56 ± 0.91	0.428 ± 0.003	8.4 (10.6)
23.41 ± 0.62	−5.46 ± 1.11	0.285 ± 0.003	11.0 (9.1)	24.35 ± 0.52	−4.70 ± 1.11	0.373 ± 0.003	8.7 (3.9)
54.65 ± 0.93	−2.83 ± 1.52	0.262 ± 0.002	11.3 (7.8)	53.60 ± 0.52	−1.85 ± 1.11	0.343 ± 0.002	8.7 (4.7)
91.52 ± 0.83	+4.73 ± 1.62	0.285 ± 0.002	15.5 (11.6)	90.85 ± 0.62	+3.04 ± 1.11	0.373 ± 0.003	13.8 (5.9)
128.06 ± 0.52	+5.80 ± 1.21	0.326 ± 0.002	16.9 (6.2)	128.44 ± 0.52	+5.53 ± 0.81	0.425 ± 0.004	13.1 (5.0)
156.64 ± 0.62	+0.69 ± 1.01	0.346 ± 0.002	13.7 (6.8)	154.96 ± 0.52	+0.90 ± 1.01	0.452 ± 0.003	10.0 (6.7)
179.48 ± 0.41	−7.19 ± 0.91	0.332 ± 0.003	12.4 (8.2)	180.59 ± 0.41	−1.32 ± 0.61	0.435 ± 0.003	9.7 (3.9)
203.50 ± 0.41	−8.05 ± 0.81	0.297 ± 0.002	10.2 (9.0)	203.95 ± 0.52	−3.85 ± 0.91	0.391 ± 0.003	8.4 (6.6)
232.64 ± 0.62	−1.64 ± 1.01	0.276 ± 0.002	11.6 (11.2)	233.32 ± 0.52	−1.00 ± 1.11	0.358 ± 0.003	8.3 (6.3)
270.28 ± 0.62	+3.46 ± 1.31	0.297 ± 0.003	15.5 (11.9)	269.27 ± 0.52	+2.27 ± 1.21	0.390 ± 0.004	12.4 (9.3)
305.49 ± 0.62	+5.87 ± 0.92	0.334 ± 0.002	18.9 (10.1)	306.92 ± 0.52	+5.56 ± 1.11	0.435 ± 0.003	12.7 (11.2)
337.26 ± 0.62	+3.84 ± 1.31	0.348 ± 0.002	15.6 (7.7)	337.30 ± 0.41	+3.74 ± 0.91	0.453 ± 0.004	11.2 (7.5)
IP = 100 m				IP = 120 m			
359.99 ± 0.31	−0.51 ± 0.61	0.519 ± 0.006	6.4 (8.7)	0.29 ± 0.21	−0.32 ± 0.40	0.607 ± 0.004	4.9 (2.7)
25.23 ± 0.41	−1.72 ± 0.91	0.461 ± 0.004	6.2 (3.6)	24.97 ± 0.31	−0.72 ± 0.61	0.539 ± 0.006	4.8 (1.9)
52.56 ± 0.41	−2.70 ± 0.71	0.424 ± 0.004	7.4 (4.2)	53.42 ± 0.31	−0.97 ± 0.70	0.499 ± 0.004	5.4 (3.2)
90.71 ± 0.52	+2.04 ± 1.01	0.458 ± 0.003	8.9 (3.9)	90.27 ± 0.21	+1.13 ± 0.60	0.536 ± 0.005	8.4 (3.7)
126.90 ± 0.31	+3.34 ± 0.70	0.517 ± 0.004	9.8 (5.1)	126.89 ± 0.41	+1.45 ± 0.71	0.603 ± 0.005	6.9 (5.3)
156.29 ± 0.31	+1.19 ± 0.51	0.549 ± 0.005	5.9 (3.7)	156.23 ± 0.31	+0.71 ± 0.51	0.634 ± 0.004	5.0 (2.4)
179.92 ± 0.41	−1.63 ± 0.81	0.529 ± 0.004	6.8 (2.9)	179.95 ± 0.21	−1.44 ± 0.50	0.614 ± 0.004	4.9 (2.6)
203.57 ± 0.41	−3.46 ± 0.71	0.478 ± 0.005	6.2 (2.7)	203.14 ± 0.21	−2.45 ± 0.60	0.558 ± 0.004	5.1 (2.6)
232.85 ± 0.52	−1.28 ± 0.91	0.443 ± 0.004	7.0 (9.5)	232.26 ± 0.41	−1.64 ± 0.81	0.522 ± 0.004	5.9 (10.2)
270.28 ± 0.31	+2.20 ± 0.70	0.477 ± 0.004	10.1 (6.5)	270.20 ± 0.21	+1.92 ± 0.50	0.557 ± 0.006	7.9 (3.5)
307.19 ± 0.41	+3.68 ± 0.71	0.530 ± 0.004	9.8 (5.7)	307.18 ± 0.31	+2.52 ± 0.80	0.613 ± 0.005	7.4 (4.1)
336.92 ± 0.41	+1.64 ± 0.81	0.552 ± 0.005	7.8 (4.8)	336.47 ± 0.21	+0.71 ± 0.60	0.633 ± 0.005	5.5 (2.4)

Table 119: The nominal angle δ_n, average displacement $\Delta\delta$, average value of the parameter DIST, RMS of the ALPHA distribution for enabled GF and impact parameters between 60 m and 120 m. The RMS of the ALPHA distribution for disabled GF is given parentheses. The primary γ-ray energy was set to 450 GeV, the ZA to 40° and the azimuth angle to 30°.

$E_\gamma = 450\,\mathrm{GeV}$, Az = 60°, ZA = 40°, Intermediate Image Cleaning

$\delta_n[°]$	$\Delta\delta[°]$	DIST[°]	$\mathrm{RMS}_{\|\mathrm{ALPHA}\|}[°]$	$\delta_n[°]$	$\Delta\delta[°]$	DIST[°]	$\mathrm{RMS}_{\|\mathrm{ALPHA}\|}[°]$
IP = 60 m				**IP = 80 m**			
0.99 ± 0.62	$+5.94 \pm 1.93$	0.290 ± 0.003	15.7 (9.3)	0.46 ± 0.51	$+7.79 \pm 1.12$	0.385 ± 0.005	14.0 (7.7)
24.64 ± 0.62	-6.23 ± 1.22	0.268 ± 0.003	11.1 (9.6)	25.33 ± 0.31	-2.96 ± 1.01	0.349 ± 0.006	7.7 (7.7)
54.32 ± 0.93	-13.60 ± 1.63	0.291 ± 0.004	10.2 (10.2)	54.16 ± 0.41	-8.01 ± 1.42	0.382 ± 0.005	8.7 (6.9)
89.85 ± 0.52	-3.91 ± 1.22	0.330 ± 0.006	13.9 (14.0)	91.37 ± 0.52	-2.25 ± 1.12	0.435 ± 0.004	11.3 (5.4)
127.93 ± 0.52	$+9.91 \pm 1.12$	0.352 ± 0.006	17.9 (10.3)	127.89 ± 0.52	$+7.63 \pm 1.32$	0.459 ± 0.005	16.3 (5.6)
156.43 ± 0.72	$+14.50 \pm 1.33$	0.340 ± 0.004	20.2 (7.0)	155.12 ± 0.52	$+9.06 \pm 0.92$	0.439 ± 0.005	18.4 (7.2)
179.11 ± 0.72	$+4.71 \pm 1.53$	0.303 ± 0.003	16.7 (7.0)	179.89 ± 0.31	$+1.06 \pm 1.01$	0.396 ± 0.005	14.9 (7.7)
203.44 ± 0.52	-15.22 ± 1.32	0.286 ± 0.003	10.4 (10.0)	203.70 ± 0.41	-9.89 ± 1.12	0.372 ± 0.004	6.9 (6.8)
231.67 ± 0.41	-13.92 ± 1.12	0.303 ± 0.003	12.3 (13.7)	233.75 ± 0.52	-9.28 ± 1.22	0.397 ± 0.004	11.1 (5.5)
270.10 ± 0.31	-1.80 ± 1.02	0.339 ± 0.003	14.2 (11.1)	267.95 ± 0.52	-4.29 ± 1.12	0.445 ± 0.006	12.0 (15.2)
306.10 ± 0.31	$+8.41 \pm 1.22$	0.356 ± 0.003	16.8 (9.6)	306.37 ± 0.62	$+5.47 \pm 0.72$	0.464 ± 0.005	13.3 (12.8)
337.79 ± 0.41	$+13.11 \pm 1.32$	0.336 ± 0.005	18.2 (9.0)	337.80 ± 0.41	$+10.20 \pm 0.91$	0.438 ± 0.005	15.3 (7.5)
IP = 100 m				**IP = 120 m**			
359.07 ± 0.41	$+2.29 \pm 1.02$	0.470 ± 0.008	11.6 (8.1)	359.58 ± 0.31	$+2.26 \pm 0.81$	0.552 ± 0.008	11.4 (4.8)
26.26 ± 0.41	-1.76 ± 1.02	0.434 ± 0.006	6.3 (2.9)	26.08 ± 0.21	$+0.43 \pm 0.61$	0.511 ± 0.003	4.8 (2.0)
53.31 ± 0.41	-6.55 ± 0.71	0.470 ± 0.003	9.5 (6.3)	53.28 ± 0.31	-4.52 ± 0.81	0.548 ± 0.008	6.4 (3.4)
91.06 ± 0.62	-2.09 ± 1.22	0.529 ± 0.007	10.3 (4.1)	90.63 ± 0.41	-0.63 ± 0.92	0.614 ± 0.008	7.4 (3.3)
127.15 ± 0.52	$+5.33 \pm 0.82$	0.561 ± 0.006	12.5 (5.0)	126.46 ± 0.52	$+3.06 \pm 1.02$	0.642 ± 0.008	8.6 (5.5)
155.82 ± 0.41	$+4.36 \pm 1.02$	0.540 ± 0.006	13.4 (6.6)	156.04 ± 0.31	$+2.36 \pm 0.71$	0.625 ± 0.008	9.8 (6.0)
180.16 ± 0.41	$+0.51 \pm 0.82$	0.482 ± 0.005	11.7 (3.1)	180.06 ± 0.31	$+0.89 \pm 0.81$	0.566 ± 0.007	8.5 (2.4)
203.41 ± 0.41	-7.74 ± 0.92	0.449 ± 0.006	6.2 (3.0)	203.04 ± 0.31	-4.18 ± 0.81	0.531 ± 0.008	4.9 (2.5)
233.75 ± 0.41	-5.13 ± 0.82	0.484 ± 0.006	7.7 (4.3)	232.02 ± 0.41	-6.04 ± 0.71	0.567 ± 0.008	6.0 (9.5)
269.48 ± 0.31	-2.46 ± 0.71	0.542 ± 0.006	9.1 (6.5)	270.36 ± 0.21	-0.90 ± 0.51	0.630 ± 0.008	7.0 (4.5)
306.63 ± 0.31	$+5.04 \pm 0.61$	0.564 ± 0.007	10.9 (5.4)	307.08 ± 0.31	$+3.53 \pm 0.51$	0.648 ± 0.006	7.9 (3.6)
336.98 ± 0.31	$+4.78 \pm 0.71$	0.534 ± 0.007	11.3 (5.5)	336.80 ± 0.31	$+3.92 \pm 0.71$	0.620 ± 0.009	9.6 (2.3)

Table 120: The nominal angle δ_n, average displacement $\Delta\delta$, average value of the parameter DIST, RMS of the ALPHA distribution for enabled GF and impact parameters between 60 m and 120 m. The RMS of the ALPHA distribution for disabled GF is given parentheses. The primary γ-ray energy was set to 450 GeV, the ZA to 40° and the azimuth angle to 60°.

$E_\gamma = 450\,\mathrm{GeV}$, Az = 60°, ZA = 40°, Hard Image Cleaning

$\delta_n[°]$	$\Delta\delta[°]$	DIST[°]	$\mathrm{RMS}_{\|\mathrm{ALPHA}\|}[°]$	$\delta_n[°]$	$\Delta\delta[°]$	DIST[°]	$\mathrm{RMS}_{\|\mathrm{ALPHA}\|}[°]$
IP = 60 m				**IP = 80 m**			
0.10 ± 0.31	$+5.54 \pm 1.01$	0.285 ± 0.003	16.1 (12.1)	0.74 ± 0.51	$+6.35 \pm 1.22$	0.379 ± 0.004	13.2 (10.6)
23.41 ± 0.62	-5.63 ± 0.82	0.265 ± 0.004	9.7 (9.1)	24.35 ± 0.52	-3.84 ± 1.22	0.344 ± 0.006	8.1 (3.9)
54.65 ± 0.93	-11.08 ± 1.43	0.286 ± 0.005	10.3 (7.8)	53.60 ± 0.52	-7.88 ± 1.32	0.376 ± 0.006	9.9 (4.7)
91.52 ± 0.83	-1.90 ± 1.53	0.325 ± 0.006	14.5 (11.6)	90.85 ± 0.62	-2.19 ± 1.33	0.429 ± 0.005	11.4 (5.9)
128.06 ± 0.52	$+11.05 \pm 1.22$	0.346 ± 0.005	17.7 (6.2)	128.44 ± 0.52	$+8.31 \pm 1.32$	0.452 ± 0.005	15.7 (5.0)
156.64 ± 0.62	$+11.80 \pm 1.32$	0.333 ± 0.004	18.8 (6.8)	154.96 ± 0.52	$+9.78 \pm 0.92$	0.433 ± 0.004	18.2 (6.7)
179.48 ± 0.41	$+4.22 \pm 0.92$	0.298 ± 0.004	16.2 (8.2)	180.59 ± 0.41	$+0.97 \pm 0.92$	0.389 ± 0.006	14.8 (3.9)
203.50 ± 0.41	-14.16 ± 1.12	0.282 ± 0.003	9.6 (9.0)	203.95 ± 0.52	-6.84 ± 0.92	0.366 ± 0.005	7.8 (6.6)
232.64 ± 0.62	-12.35 ± 1.32	0.296 ± 0.003	11.4 (11.2)	233.32 ± 0.52	-10.15 ± 1.32	0.392 ± 0.004	10.1 (6.3)
270.28 ± 0.62	-1.54 ± 1.22	0.334 ± 0.003	14.5 (11.9)	269.27 ± 0.52	-2.92 ± 1.12	0.437 ± 0.006	12.5 (9.3)
305.49 ± 0.62	$+7.60 \pm 1.42$	0.349 ± 0.005	16.3 (10.1)	306.92 ± 0.52	$+6.68 \pm 1.22$	0.456 ± 0.005	12.3 (11.2)
337.26 ± 0.62	$+13.32 \pm 1.42$	0.328 ± 0.004	18.7 (7.7)	337.30 ± 0.41	$+10.26 \pm 1.22$	0.429 ± 0.005	13.7 (7.5)
IP = 100 m				**IP = 120 m**			
359.99 ± 0.31	$+3.93 \pm 0.71$	0.463 ± 0.007	10.9 (8.7)	0.29 ± 0.21	$+2.94 \pm 0.81$	0.544 ± 0.009	10.8 (2.7)
25.23 ± 0.41	-2.11 ± 0.82	0.426 ± 0.007	7.4 (3.6)	24.97 ± 0.31	-0.91 ± 0.71	0.505 ± 0.008	5.1 (1.9)
52.56 ± 0.41	-6.76 ± 1.12	0.463 ± 0.005	9.7 (4.2)	53.42 ± 0.31	-4.41 ± 0.81	0.543 ± 0.008	6.5 (3.2)
90.71 ± 0.52	-2.20 ± 1.02	0.522 ± 0.007	9.7 (3.9)	90.27 ± 0.21	-0.80 ± 0.61	0.609 ± 0.008	7.5 (3.7)
126.90 ± 0.31	$+4.78 \pm 0.91$	0.554 ± 0.007	11.6 (5.1)	126.89 ± 0.41	$+3.34 \pm 0.92$	0.636 ± 0.008	9.1 (5.3)
156.29 ± 0.31	$+4.86 \pm 0.71$	0.533 ± 0.006	12.1 (3.7)	156.23 ± 0.31	$+2.58 \pm 0.61$	0.616 ± 0.008	7.9 (2.4)
179.92 ± 0.41	$+0.35 \pm 0.92$	0.475 ± 0.005	11.4 (2.9)	179.95 ± 0.21	$+1.13 \pm 0.51$	0.559 ± 0.006	8.5 (2.6)
203.57 ± 0.41	-6.82 ± 1.02	0.442 ± 0.006	6.1 (2.7)	203.14 ± 0.21	-3.73 ± 0.61	0.524 ± 0.006	4.7 (2.6)
232.85 ± 0.52	-5.79 ± 1.12	0.477 ± 0.006	7.2 (9.5)	232.26 ± 0.41	-5.35 ± 1.02	0.562 ± 0.007	5.9 (10.2)
270.28 ± 0.31	-1.48 ± 0.71	0.532 ± 0.007	10.1 (6.5)	270.20 ± 0.21	-0.72 ± 0.61	0.623 ± 0.007	7.2 (3.5)
307.19 ± 0.41	$+5.09 \pm 0.71$	0.555 ± 0.008	10.0 (5.7)	307.18 ± 0.31	$+3.75 \pm 0.71$	0.640 ± 0.008	8.4 (4.1)
336.92 ± 0.41	$+4.41 \pm 0.92$	0.525 ± 0.007	11.5 (4.8)	336.47 ± 0.21	$+3.85 \pm 0.61$	0.613 ± 0.009	9.6 (2.4)

Table 121: The nominal angle δ_n, average displacement $\Delta\delta$, average value of the parameter DIST, RMS of the ALPHA distribution for enabled GF and impact parameters between 60 m and 120 m. The RMS of the ALPHA distribution for disabled GF is given parentheses. The primary γ-ray energy was set to 450 GeV, the ZA to 40° and the azimuth angle to 60°.

$E_\gamma = 450$ GeV, Az = 90°, ZA = 40°, Intermediate Image Cleaning

δ_n[°]	$\Delta\delta$[°]	DIST[°]	RMS$_{\lvert\mathrm{ALPHA}\rvert}$[°]	δ_n[°]	$\Delta\delta$[°]	DIST[°]	RMS$_{\lvert\mathrm{ALPHA}\rvert}$[°]
IP = 60 m				**IP = 80 m**			
0.99 ± 0.62	$+13.78 \pm 1.10$	0.268 ± 0.003	13.3 (9.3)	0.46 ± 0.51	$+8.19 \pm 1.09$	0.352 ± 0.003	11.5 (7.7)
24.64 ± 0.62	$+2.31 \pm 1.67$	0.289 ± 0.002	7.3 (9.6)	25.33 ± 0.31	$+4.46 \pm 1.27$	0.382 ± 0.006	6.5 (7.7)
54.32 ± 0.93	-14.96 ± 1.50	0.331 ± 0.003	14.9 (10.2)	54.16 ± 0.41	-12.25 ± 1.28	0.435 ± 0.006	10.1 (6.9)
89.85 ± 0.52	-8.81 ± 1.28	0.355 ± 0.003	21.4 (14.0)	91.37 ± 0.52	-6.52 ± 1.00	0.463 ± 0.006	17.3 (5.4)
127.93 ± 0.52	$+5.26 \pm 1.19$	0.339 ± 0.003	27.8 (10.3)	127.89 ± 0.52	$+4.59 \pm 1.09$	0.445 ± 0.006	21.7 (5.6)
156.43 ± 0.72	$+14.60 \pm 1.49$	0.303 ± 0.003	22.9 (7.0)	155.12 ± 0.52	$+7.93 \pm 1.28$	0.400 ± 0.003	20.5 (7.2)
179.11 ± 0.72	$+14.58 \pm 1.39$	0.284 ± 0.003	10.9 (7.0)	179.89 ± 0.31	$+11.20 \pm 0.69$	0.369 ± 0.002	7.8 (7.7)
203.44 ± 0.52	$+1.55 \pm 1.00$	0.304 ± 0.002	6.3 (10.0)	203.70 ± 0.41	$+0.26 \pm 0.70$	0.395 ± 0.005	5.2 (6.8)
231.67 ± 0.41	-16.98 ± 1.37	0.342 ± 0.005	12.7 (13.7)	233.75 ± 0.52	-10.83 ± 1.48	0.445 ± 0.005	10.3 (5.5)
270.10 ± 0.31	-8.26 ± 1.37	0.359 ± 0.004	19.4 (11.1)	267.95 ± 0.52	-9.66 ± 1.00	0.465 ± 0.006	14.9 (15.2)
306.10 ± 0.31	$+2.58 \pm 0.41$	0.338 ± 0.004	24.3 (9.6)	306.37 ± 0.62	$+0.65 \pm 1.19$	0.438 ± 0.005	21.5 (12.8)
337.79 ± 0.41	$+12.53 \pm 1.08$	0.295 ± 0.003	23.1 (9.0)	337.80 ± 0.41	$+9.45 \pm 1.28$	0.387 ± 0.005	21.5 (7.5)
IP = 100 m				**IP = 120 m**			
359.07 ± 0.41	$+3.47 \pm 1.08$	0.434 ± 0.006	7.9 (8.1)	359.58 ± 0.31	$+1.46 \pm 0.98$	0.507 ± 0.006	6.7 (4.8)
26.26 ± 0.41	$+2.65 \pm 1.28$	0.465 ± 0.007	4.1 (2.9)	26.08 ± 0.21	$+2.28 \pm 0.59$	0.545 ± 0.006	3.4 (2.0)
53.31 ± 0.41	-7.51 ± 0.60	0.525 ± 0.007	9.3 (6.3)	53.28 ± 0.31	-3.69 ± 0.79	0.608 ± 0.006	7.9 (3.4)
91.06 ± 0.62	-5.24 ± 1.10	0.563 ± 0.006	14.6 (4.1)	90.63 ± 0.41	-3.57 ± 0.89	0.645 ± 0.006	9.7 (3.3)
127.15 ± 0.52	$+2.63 \pm 0.80$	0.544 ± 0.006	14.9 (5.0)	126.46 ± 0.52	$+1.72 \pm 0.80$	0.625 ± 0.006	11.2 (5.5)
155.82 ± 0.41	$+6.20 \pm 0.99$	0.488 ± 0.006	16.3 (6.6)	156.04 ± 0.31	$+4.93 \pm 0.60$	0.567 ± 0.005	12.3 (6.0)
180.16 ± 0.41	$+5.56 \pm 1.18$	0.453 ± 0.006	6.6 (3.1)	180.06 ± 0.31	$+4.31 \pm 1.08$	0.529 ± 0.003	6.2 (2.4)
203.41 ± 0.41	$+2.26 \pm 0.80$	0.486 ± 0.005	4.3 (3.0)	203.04 ± 0.31	$+1.43 \pm 0.69$	0.567 ± 0.007	3.7 (2.5)
233.75 ± 0.41	-6.29 ± 1.08	0.542 ± 0.006	6.6 (4.3)	232.02 ± 0.41	-5.33 ± 0.89	0.624 ± 0.005	6.1 (9.5)
269.48 ± 0.31	-6.25 ± 0.60	0.563 ± 0.004	12.6 (6.5)	270.36 ± 0.21	-4.12 ± 0.69	0.646 ± 0.007	9.9 (4.5)
306.63 ± 0.31	$+0.08 \pm 0.60$	0.536 ± 0.001	15.6 (5.4)	307.08 ± 0.31	$+2.32 \pm 0.50$	0.618 ± 0.007	12.2 (3.6)
336.98 ± 0.31	$+4.52 \pm 0.98$	0.474 ± 0.004	17.4 (5.5)	336.80 ± 0.31	$+2.83 \pm 0.69$	0.553 ± 0.006	12.0 (2.3)

Table 122: The nominal angle δ_n, average displacement $\Delta\delta$, average value of the parameter DIST, RMS of the ALPHA distribution for enabled GF and impact parameters between 60 m and 120 m. The RMS of the ALPHA distribution for disabled GF is given parentheses. The primary γ-ray energy was set to 450 GeV, the ZA to 40° and the azimuth angle to 90°.

$E_\gamma = 450$ GeV, Az = 90°, ZA = 40°, Hard Image Cleaning

δ_n[°]	$\Delta\delta$[°]	DIST[°]	RMS$_{\lvert\mathrm{ALPHA}\rvert}$[°]	δ_n[°]	$\Delta\delta$[°]	DIST[°]	RMS$_{\lvert\mathrm{ALPHA}\rvert}$[°]
IP = 60 m				**IP = 80 m**			
0.10 ± 0.31	$+11.41 \pm 0.69$	0.259 ± 0.004	12.1 (12.1)	0.74 ± 0.51	$+8.84 \pm 1.28$	0.343 ± 0.003	9.7 (10.6)
23.41 ± 0.62	$+3.74 \pm 1.29$	0.283 ± 0.002	6.9 (9.1)	24.35 ± 0.52	$+1.06 \pm 1.09$	0.370 ± 0.006	6.3 (3.9)
54.65 ± 0.93	-15.77 ± 1.60	0.324 ± 0.004	14.3 (7.8)	53.60 ± 0.52	-11.68 ± 1.76	0.425 ± 0.005	9.7 (4.7)
91.52 ± 0.83	-8.59 ± 1.79	0.348 ± 0.005	21.6 (11.6)	90.85 ± 0.62	-7.47 ± 1.29	0.453 ± 0.006	15.6 (5.9)
128.06 ± 0.52	$+5.23 \pm 1.00$	0.333 ± 0.003	27.1 (6.2)	128.44 ± 0.52	$+5.30 \pm 1.00$	0.437 ± 0.003	21.0 (5.0)
156.64 ± 0.62	$+15.09 \pm 1.58$	0.297 ± 0.003	23.8 (6.8)	154.96 ± 0.52	$+7.36 \pm 1.09$	0.392 ± 0.004	20.4 (6.7)
179.48 ± 0.41	$+14.31 \pm 0.70$	0.280 ± 0.003	9.6 (8.2)	180.59 ± 0.41	$+10.11 \pm 0.51$	0.363 ± 0.002	8.2 (3.9)
203.50 ± 0.41	-0.52 ± 0.70	0.299 ± 0.002	8.6 (9.0)	203.95 ± 0.52	$+3.49 \pm 1.00$	0.390 ± 0.002	5.2 (6.6)
232.64 ± 0.62	-15.13 ± 2.06	0.336 ± 0.003	12.8 (11.2)	233.32 ± 0.52	-10.92 ± 0.90	0.438 ± 0.005	10.9 (6.3)
270.28 ± 0.62	-8.47 ± 1.00	0.352 ± 0.003	19.2 (11.9)	269.27 ± 0.52	-8.24 ± 1.19	0.456 ± 0.004	15.1 (9.3)
305.49 ± 0.62	$+1.76 \pm 1.19$	0.331 ± 0.003	24.3 (10.1)	306.92 ± 0.52	$+1.76 \pm 0.80$	0.430 ± 0.003	19.1 (11.2)
337.26 ± 0.62	$+12.72 \pm 1.10$	0.287 ± 0.003	22.8 (7.7)	337.30 ± 0.41	$+8.33 \pm 1.18$	0.380 ± 0.005	19.5 (7.5)
IP = 100 m				**IP = 120 m**			
359.99 ± 0.31	$+4.37 \pm 0.89$	0.424 ± 0.006	7.2 (8.7)	0.29 ± 0.21	$+2.66 \pm 0.59$	0.499 ± 0.006	6.5 (2.7)
25.23 ± 0.41	$+2.50 \pm 0.70$	0.458 ± 0.007	4.0 (3.6)	24.97 ± 0.31	$+0.86 \pm 0.79$	0.538 ± 0.007	3.3 (1.9)
52.56 ± 0.41	-8.04 ± 0.80	0.517 ± 0.007	9.3 (4.2)	53.42 ± 0.31	-3.52 ± 0.89	0.602 ± 0.007	7.3 (3.2)
90.71 ± 0.52	-4.78 ± 1.00	0.555 ± 0.005	11.7 (3.9)	90.27 ± 0.21	-4.01 ± 0.59	0.637 ± 0.007	9.5 (3.7)
126.90 ± 0.31	$+2.09 \pm 0.60$	0.537 ± 0.006	13.2 (5.1)	126.89 ± 0.41	$+2.13 \pm 0.80$	0.617 ± 0.006	11.6 (5.3)
156.29 ± 0.31	$+6.90 \pm 0.79$	0.481 ± 0.006	14.6 (3.7)	156.23 ± 0.31	$+4.74 \pm 0.69$	0.558 ± 0.002	11.2 (2.4)
179.92 ± 0.41	$+5.21 \pm 0.51$	0.443 ± 0.005	7.4 (2.9)	179.95 ± 0.21	$+3.74 \pm 0.88$	0.520 ± 0.005	6.0 (2.6)
203.57 ± 0.41	$+2.57 \pm 0.70$	0.478 ± 0.006	3.6 (2.7)	203.14 ± 0.21	$+1.29 \pm 0.69$	0.559 ± 0.007	3.4 (2.6)
232.85 ± 0.52	-4.74 ± 0.80	0.534 ± 0.006	6.4 (9.5)	232.26 ± 0.41	-4.65 ± 0.80	0.616 ± 0.004	5.7 (10.2)
270.28 ± 0.31	-5.62 ± 0.79	0.553 ± 0.003	11.0 (6.5)	270.20 ± 0.21	-3.80 ± 0.69	0.639 ± 0.008	8.9 (3.5)
307.19 ± 0.41	$+0.66 \pm 0.70$	0.526 ± 0.002	15.3 (5.7)	307.18 ± 0.31	$+0.50 \pm 0.50$	0.611 ± 0.007	11.8 (4.1)
336.92 ± 0.41	$+4.16 \pm 0.89$	0.465 ± 0.003	15.2 (4.8)	336.47 ± 0.21	$+2.36 \pm 0.69$	0.544 ± 0.001	10.9 (2.4)

Table 123: The nominal angle δ_n, average displacement $\Delta\delta$, average value of the parameter DIST, RMS of the ALPHA distribution for enabled GF and impact parameters between 60 m and 120 m. The RMS of the ALPHA distribution for disabled GF is given parentheses. The primary γ-ray energy was set to 450 GeV, the ZA to 40° and the azimuth angle to 90°.

$E_\gamma = 450\,\mathrm{GeV}$, Az = 120°, ZA = 40°, Intermediate Image Cleaning

$\delta_n[°]$	$\Delta\delta[°]$	DIST[°]	$\mathrm{RMS}_{\lvert\mathrm{ALPHA}\rvert}[°]$	$\delta_n[°]$	$\Delta\delta[°]$	DIST[°]	$\mathrm{RMS}_{\lvert\mathrm{ALPHA}\rvert}[°]$
IP = 60 m				**IP = 80 m**			
0.99 ± 0.62	$+16.52 \pm 1.38$	0.299 ± 0.005	8.2 (9.3)	0.46 ± 0.51	$+10.81 \pm 0.99$	0.389 ± 0.005	8.3 (7.7)
24.64 ± 0.62	$+15.68 \pm 1.10$	0.337 ± 0.005	9.8 (9.6)	25.33 ± 0.31	$+8.51 \pm 1.07$	0.441 ± 0.006	9.1 (7.7)
54.32 ± 0.93	-7.31 ± 1.89	0.358 ± 0.003	14.9 (10.2)	54.16 ± 0.41	-5.57 ± 0.89	0.468 ± 0.005	13.7 (6.9)
89.85 ± 0.52	-19.09 ± 1.19	0.346 ± 0.003	18.9 (14.0)	91.37 ± 0.52	-15.45 ± 1.76	0.450 ± 0.006	17.8 (5.4)
127.93 ± 0.52	-4.26 ± 1.19	0.308 ± 0.002	19.7 (10.3)	127.89 ± 0.52	-2.06 ± 1.09	0.404 ± 0.005	19.0 (5.6)
156.43 ± 0.72	$+8.86 \pm 1.39$	0.284 ± 0.004	13.3 (7.0)	155.12 ± 0.52	$+5.71 \pm 1.09$	0.371 ± 0.003	12.5 (7.2)
179.11 ± 0.72	$+13.56 \pm 1.30$	0.308 ± 0.004	10.2 (7.0)	179.89 ± 0.31	$+11.13 \pm 0.41$	0.399 ± 0.006	7.4 (7.7)
203.44 ± 0.52	$+10.32 \pm 0.99$	0.341 ± 0.005	10.8 (10.0)	203.70 ± 0.41	$+9.99 \pm 0.99$	0.446 ± 0.006	8.4 (6.8)
231.67 ± 0.41	-14.50 ± 0.89	0.360 ± 0.002	15.6 (13.7)	233.75 ± 0.52	-3.32 ± 1.47	0.470 ± 0.005	14.3 (5.5)
270.10 ± 0.31	-16.87 ± 1.27	0.341 ± 0.005	20.4 (11.1)	267.95 ± 0.52	-15.76 ± 1.38	0.444 ± 0.004	16.2 (15.2)
306.10 ± 0.31	-4.37 ± 0.89	0.298 ± 0.003	20.8 (9.6)	306.37 ± 0.62	-3.30 ± 1.10	0.392 ± 0.006	19.0 (12.8)
337.79 ± 0.41	$+8.45 \pm 0.99$	0.273 ± 0.002	12.5 (9.0)	337.80 ± 0.41	$+7.38 \pm 0.79$	0.361 ± 0.004	11.2 (7.5)
IP = 100 m				**IP = 120 m**			
359.07 ± 0.41	$+6.18 \pm 0.99$	0.474 ± 0.006	5.8 (8.1)	359.58 ± 0.31	$+3.82 \pm 0.69$	0.555 ± 0.005	4.7 (4.8)
26.26 ± 0.41	$+8.48 \pm 0.99$	0.533 ± 0.006	8.2 (2.9)	26.08 ± 0.21	$+5.00 \pm 0.68$	0.619 ± 0.008	6.2 (2.0)
53.31 ± 0.41	-1.97 ± 1.08	0.565 ± 0.003	11.4 (6.3)	53.28 ± 0.31	-2.49 ± 0.88	0.647 ± 0.004	9.3 (3.4)
91.06 ± 0.62	-9.13 ± 1.00	0.549 ± 0.003	14.7 (4.1)	90.63 ± 0.41	-7.74 ± 1.08	0.633 ± 0.006	11.8 (3.3)
127.15 ± 0.52	-1.80 ± 0.90	0.494 ± 0.002	15.4 (5.0)	126.46 ± 0.52	-1.36 ± 0.80	0.580 ± 0.006	14.3 (5.5)
155.82 ± 0.41	$+4.70 \pm 0.89$	0.458 ± 0.003	11.5 (6.6)	156.04 ± 0.31	$+2.86 \pm 0.60$	0.536 ± 0.007	10.5 (6.0)
180.16 ± 0.41	$+7.01 \pm 0.80$	0.489 ± 0.004	5.7 (3.1)	180.06 ± 0.31	$+4.02 \pm 0.88$	0.571 ± 0.008	4.7 (2.4)
203.41 ± 0.41	$+3.81 \pm 0.80$	0.544 ± 0.002	7.4 (3.0)	203.04 ± 0.31	$+2.26 \pm 0.69$	0.632 ± 0.008	6.2 (2.5)
233.75 ± 0.41	-0.42 ± 0.99	0.567 ± 0.005	12.2 (4.3)	232.02 ± 0.41	-3.09 ± 0.80	0.654 ± 0.007	9.6 (9.5)
269.48 ± 0.31	-9.70 ± 1.17	0.543 ± 0.006	14.1 (6.5)	270.36 ± 0.21	-8.45 ± 0.97	0.628 ± 0.008	11.5 (4.5)
306.63 ± 0.31	-2.68 ± 0.50	0.483 ± 0.004	14.5 (5.4)	307.08 ± 0.31	-1.36 ± 0.69	0.566 ± 0.006	13.7 (3.6)
336.98 ± 0.31	$+3.71 \pm 0.60$	0.448 ± 0.006	11.0 (5.5)	336.80 ± 0.31	$+3.26 \pm 0.60$	0.522 ± 0.005	9.5 (2.3)

Table 124: The nominal angle δ_n, average displacement $\Delta\delta$, average value of the parameter DIST, RMS of the ALPHA distribution for enabled GF and impact parameters between 60 m and 120 m. The RMS of the ALPHA distribution for disabled GF is given parentheses. The primary γ-ray energy was set to 450 GeV, the ZA to 40° and the azimuth angle to 120°.

$E_\gamma = 450\,\mathrm{GeV}$, Az = 120°, ZA = 40°, Hard Image Cleaning

$\delta_n[°]$	$\Delta\delta[°]$	DIST[°]	$\mathrm{RMS}_{\lvert\mathrm{ALPHA}\rvert}[°]$	$\delta_n[°]$	$\Delta\delta[°]$	DIST[°]	$\mathrm{RMS}_{\lvert\mathrm{ALPHA}\rvert}[°]$
IP = 60 m				**IP = 80 m**			
0.10 ± 0.31	$+15.64 \pm 1.07$	0.295 ± 0.005	8.0 (12.1)	0.74 ± 0.51	$+10.93 \pm 0.99$	0.386 ± 0.005	7.7 (10.6)
23.41 ± 0.62	$+17.71 \pm 1.00$	0.331 ± 0.004	9.8 (9.1)	24.35 ± 0.52	$+9.60 \pm 1.19$	0.436 ± 0.003	8.1 (3.9)
54.65 ± 0.93	-3.85 ± 1.02	0.353 ± 0.002	15.7 (7.8)	53.60 ± 0.52	-3.45 ± 0.71	0.462 ± 0.003	13.6 (4.7)
91.52 ± 0.83	-16.91 ± 1.30	0.339 ± 0.002	20.0 (11.6)	90.85 ± 0.62	-15.00 ± 1.67	0.443 ± 0.005	17.1 (5.9)
128.06 ± 0.52	-3.45 ± 1.10	0.303 ± 0.004	20.0 (6.2)	128.44 ± 0.52	-1.45 ± 1.00	0.395 ± 0.005	19.2 (5.0)
156.64 ± 0.62	$+9.13 \pm 1.29$	0.278 ± 0.004	12.7 (6.8)	154.96 ± 0.52	$+5.29 \pm 1.00$	0.366 ± 0.003	11.7 (6.7)
179.48 ± 0.41	$+11.04 \pm 1.47$	0.303 ± 0.004	8.3 (8.2)	180.59 ± 0.41	$+10.45 \pm 0.60$	0.393 ± 0.007	6.7 (3.9)
203.50 ± 0.41	$+9.41 \pm 0.99$	0.338 ± 0.004	10.8 (9.0)	203.95 ± 0.52	$+7.86 \pm 1.28$	0.440 ± 0.003	8.3 (6.6)
232.64 ± 0.62	-10.39 ± 1.48	0.355 ± 0.005	15.1 (11.2)	233.32 ± 0.52	-2.10 ± 1.28	0.462 ± 0.006	14.1 (6.3)
270.28 ± 0.62	-17.43 ± 1.10	0.335 ± 0.004	20.7 (11.9)	269.27 ± 0.52	-14.37 ± 1.47	0.437 ± 0.003	17.0 (9.3)
305.49 ± 0.62	-5.19 ± 1.10	0.293 ± 0.003	20.2 (10.1)	306.92 ± 0.52	-3.01 ± 1.00	0.387 ± 0.003	19.5 (11.2)
337.26 ± 0.62	$+8.56 \pm 1.29$	0.269 ± 0.002	13.1 (7.7)	337.30 ± 0.41	$+6.73 \pm 0.80$	0.355 ± 0.003	11.7 (7.5)
IP = 100 m				**IP = 120 m**			
359.99 ± 0.31	$+6.37 \pm 0.88$	0.471 ± 0.006	5.1 (8.7)	0.29 ± 0.21	$+3.68 \pm 0.59$	0.549 ± 0.004	4.5 (2.7)
25.23 ± 0.41	$+5.23 \pm 0.89$	0.528 ± 0.002	7.8 (3.6)	24.97 ± 0.31	$+4.64 \pm 0.79$	0.612 ± 0.005	6.2 (1.9)
52.56 ± 0.41	-2.75 ± 1.08	0.560 ± 0.006	10.6 (4.2)	53.42 ± 0.31	-1.24 ± 0.79	0.638 ± 0.004	9.3 (3.2)
90.71 ± 0.52	-8.64 ± 1.28	0.542 ± 0.006	15.1 (3.9)	90.27 ± 0.21	-6.02 ± 0.78	0.626 ± 0.007	11.1 (3.7)
126.90 ± 0.31	-1.89 ± 0.69	0.486 ± 0.006	16.0 (5.1)	126.89 ± 0.41	-0.92 ± 0.80	0.572 ± 0.006	13.6 (5.3)
156.29 ± 0.31	$+4.79 \pm 0.50$	0.450 ± 0.006	11.3 (3.7)	156.23 ± 0.31	$+3.24 \pm 0.60$	0.528 ± 0.006	10.9 (2.4)
179.92 ± 0.41	$+4.61 \pm 0.99$	0.483 ± 0.003	5.5 (2.9)	179.95 ± 0.21	$+3.90 \pm 0.68$	0.563 ± 0.005	5.1 (2.6)
203.57 ± 0.41	$+4.26 \pm 0.89$	0.539 ± 0.005	6.2 (2.7)	203.14 ± 0.21	$+2.15 \pm 0.49$	0.624 ± 0.008	5.6 (2.6)
232.85 ± 0.52	$+0.14 \pm 0.99$	0.560 ± 0.008	12.2 (9.5)	232.26 ± 0.41	-2.79 ± 0.80	0.645 ± 0.008	10.7 (10.2)
270.28 ± 0.31	-10.18 ± 1.08	0.535 ± 0.004	13.0 (6.5)	270.20 ± 0.21	-6.96 ± 0.88	0.621 ± 0.005	11.5 (3.5)
307.19 ± 0.41	-2.14 ± 0.80	0.477 ± 0.003	15.8 (5.7)	307.18 ± 0.31	-1.27 ± 0.69	0.559 ± 0.008	13.5 (4.1)
336.92 ± 0.41	$+3.57 \pm 0.80$	0.440 ± 0.004	10.3 (4.8)	336.47 ± 0.21	$+2.87 \pm 0.49$	0.512 ± 0.002	9.4 (2.4)

Table 125: The nominal angle δ_n, average displacement $\Delta\delta$, average value of the parameter DIST, RMS of the ALPHA distribution for enabled GF and impact parameters between 60 m and 120 m. The RMS of the ALPHA distribution for disabled GF is given parentheses. The primary γ-ray energy was set to 450 GeV, the ZA to 40° and the azimuth angle to 120°.

$E_\gamma = 450\,\mathrm{GeV}$, Az = 150°, ZA = 40°, Intermediate Image Cleaning

δ_n[°]	$\Delta\delta$[°]	DIST[°]	$\mathrm{RMS}_{\lvert\mathrm{ALPHA}\rvert}$[°]	δ_n[°]	$\Delta\delta$[°]	DIST[°]	$\mathrm{RMS}_{\lvert\mathrm{ALPHA}\rvert}$[°]
IP = 60 m				IP = 80 m			
0.99 ± 0.62	$+9.65 \pm 1.17$	0.324 ± 0.003	8.4 (9.3)	0.46 ± 0.51	$+7.05 \pm 0.98$	0.422 ± 0.002	5.9 (7.7)
24.64 ± 0.62	$+16.15 \pm 1.27$	0.341 ± 0.004	9.3 (9.6)	25.33 ± 0.31	$+12.03 \pm 0.96$	0.446 ± 0.005	8.0 (7.7)
54.32 ± 0.93	$+11.77 \pm 1.49$	0.329 ± 0.002	15.5 (10.2)	54.16 ± 0.41	$+10.86 \pm 0.69$	0.430 ± 0.004	13.0 (6.9)
89.85 ± 0.52	-19.23 ± 2.74	0.298 ± 0.003	26.7 (14.0)	91.37 ± 0.52	-12.65 ± 1.17	0.387 ± 0.003	21.7 (5.4)
127.93 ± 0.52	-10.36 ± 0.89	0.275 ± 0.002	19.5 (10.3)	127.89 ± 0.52	-8.57 ± 1.35	0.362 ± 0.002	20.7 (5.6)
156.43 ± 0.72	$+2.21 \pm 1.19$	0.294 ± 0.003	12.5 (7.0)	155.12 ± 0.52	$+0.37 \pm 0.89$	0.387 ± 0.005	10.7 (7.2)
179.11 ± 0.72	$+6.94 \pm 0.91$	0.333 ± 0.004	7.5 (7.0)	179.89 ± 0.31	$+6.39 \pm 0.77$	0.436 ± 0.005	6.2 (7.7)
203.44 ± 0.52	$+15.83 \pm 1.35$	0.348 ± 0.004	8.6 (10.0)	203.70 ± 0.41	$+11.45 \pm 1.06$	0.452 ± 0.005	7.3 (6.8)
231.67 ± 0.41	$+8.20 \pm 1.62$	0.327 ± 0.003	14.1 (13.7)	233.75 ± 0.52	$+6.64 \pm 0.89$	0.428 ± 0.004	11.8 (5.5)
270.10 ± 0.31	-23.20 ± 0.96	0.286 ± 0.003	24.8 (11.1)	267.95 ± 0.52	-21.09 ± 1.35	0.376 ± 0.003	19.8 (15.2)
306.10 ± 0.31	-12.74 ± 0.87	0.262 ± 0.002	21.9 (9.6)	306.37 ± 0.62	-10.02 ± 1.27	0.347 ± 0.004	21.5 (12.8)
337.79 ± 0.41	$+0.33 \pm 0.88$	0.286 ± 0.004	12.3 (9.0)	337.80 ± 0.41	$+1.24 \pm 0.60$	0.373 ± 0.004	11.4 (7.5)
IP = 100 m				IP = 120 m			
359.07 ± 0.41	$+3.35 \pm 0.97$	0.508 ± 0.005	4.5 (8.1)	359.58 ± 0.31	$+1.96 \pm 0.49$	0.596 ± 0.005	4.3 (4.8)
26.26 ± 0.41	$+9.74 \pm 0.60$	0.543 ± 0.005	6.9 (2.9)	26.08 ± 0.21	$+6.56 \pm 0.58$	0.623 ± 0.006	6.2 (2.0)
53.31 ± 0.41	$+7.16 \pm 1.25$	0.525 ± 0.005	9.1 (6.3)	53.28 ± 0.31	$+3.27 \pm 0.96$	0.609 ± 0.004	7.1 (3.4)
91.06 ± 0.62	-11.16 ± 1.45	0.477 ± 0.005	16.6 (4.1)	90.63 ± 0.41	-7.58 ± 0.88	0.556 ± 0.006	14.2 (3.3)
127.15 ± 0.52	-5.32 ± 0.89	0.445 ± 0.005	18.6 (5.0)	126.46 ± 0.52	-4.12 ± 0.98	0.524 ± 0.003	15.1 (5.5)
155.82 ± 0.41	$+1.15 \pm 0.60$	0.476 ± 0.005	9.6 (6.6)	156.04 ± 0.31	$+0.69 \pm 0.59$	0.556 ± 0.005	7.1 (6.0)
180.16 ± 0.41	$+3.82 \pm 0.97$	0.529 ± 0.004	4.4 (3.1)	180.06 ± 0.31	$+1.87 \pm 0.68$	0.615 ± 0.005	3.7 (2.4)
203.41 ± 0.41	$+7.15 \pm 0.78$	0.551 ± 0.005	6.3 (3.0)	203.04 ± 0.31	$+2.71 \pm 0.59$	0.631 ± 0.006	4.9 (2.5)
233.75 ± 0.41	$+5.57 \pm 0.97$	0.524 ± 0.005	9.9 (4.3)	232.02 ± 0.41	$+1.22 \pm 1.25$	0.604 ± 0.006	7.2 (9.5)
269.48 ± 0.31	-13.40 ± 1.15	0.467 ± 0.004	16.6 (6.5)	270.36 ± 0.21	-7.16 ± 0.86	0.544 ± 0.005	12.3 (4.5)
306.63 ± 0.31	-8.02 ± 0.96	0.427 ± 0.005	18.5 (5.4)	307.08 ± 0.31	-4.81 ± 0.87	0.503 ± 0.005	14.9 (3.6)
336.98 ± 0.31	$+0.27 \pm 0.59$	0.459 ± 0.005	8.7 (5.5)	336.80 ± 0.31	$+0.10 \pm 0.49$	0.532 ± 0.005	6.5 (2.3)

Table 126: The nominal angle δ_n, average displacement $\Delta\delta$, average value of the parameter DIST, RMS of the ALPHA distribution for enabled GF and impact parameters between 60 m and 120 m. The RMS of the ALPHA distribution for disabled GF is given parentheses. The primary γ-ray energy was set to 450 GeV, the ZA to 40° and the azimuth angle to 150°.

$E_\gamma = 450\,\mathrm{GeV}$, Az = 150°, ZA = 40°, Hard Image Cleaning

δ_n[°]	$\Delta\delta$[°]	DIST[°]	$\mathrm{RMS}_{\lvert\mathrm{ALPHA}\rvert}$[°]	δ_n[°]	$\Delta\delta$[°]	DIST[°]	$\mathrm{RMS}_{\lvert\mathrm{ALPHA}\rvert}$[°]
IP = 60 m				IP = 80 m			
0.10 ± 0.31	$+9.10 \pm 0.96$	0.319 ± 0.003	8.0 (12.1)	0.74 ± 0.51	$+7.08 \pm 1.07$	0.414 ± 0.004	5.8 (10.6)
23.41 ± 0.62	$+14.72 \pm 1.08$	0.336 ± 0.004	9.2 (9.1)	24.35 ± 0.52	$+9.94 \pm 1.26$	0.438 ± 0.004	7.8 (3.9)
54.65 ± 0.93	$+8.81 \pm 1.30$	0.323 ± 0.002	15.8 (7.8)	53.60 ± 0.52	$+11.96 \pm 0.79$	0.422 ± 0.004	13.2 (4.7)
91.52 ± 0.83	-17.70 ± 1.75	0.293 ± 0.003	26.6 (11.6)	90.85 ± 0.62	-16.42 ± 1.08	0.382 ± 0.003	21.3 (5.9)
128.06 ± 0.52	-8.67 ± 1.17	0.271 ± 0.002	19.6 (6.2)	128.44 ± 0.52	-7.25 ± 1.17	0.354 ± 0.003	19.5 (5.0)
156.64 ± 0.62	$+1.92 \pm 1.09$	0.291 ± 0.003	11.7 (6.8)	154.96 ± 0.52	$+0.39 \pm 0.89$	0.379 ± 0.003	10.9 (6.7)
179.48 ± 0.41	$+6.87 \pm 0.78$	0.324 ± 0.003	7.8 (8.2)	180.59 ± 0.41	$+6.58 \pm 0.69$	0.426 ± 0.004	5.4 (3.9)
203.50 ± 0.41	$+15.15 \pm 1.43$	0.339 ± 0.004	9.0 (9.0)	203.95 ± 0.52	$+10.27 \pm 0.98$	0.445 ± 0.003	7.2 (6.6)
232.64 ± 0.62	$+10.41 \pm 0.71$	0.319 ± 0.003	14.3 (11.2)	233.32 ± 0.52	$+10.04 \pm 1.17$	0.419 ± 0.005	12.5 (6.3)
270.28 ± 0.62	-23.06 ± 1.55	0.281 ± 0.003	24.9 (11.9)	269.27 ± 0.52	-18.12 ± 0.89	0.370 ± 0.004	19.2 (9.3)
305.49 ± 0.62	-13.76 ± 1.18	0.257 ± 0.003	21.2 (10.1)	306.92 ± 0.52	-9.55 ± 1.26	0.339 ± 0.004	20.7 (11.2)
337.26 ± 0.62	$+0.50 \pm 1.18$	0.279 ± 0.004	11.7 (7.7)	337.30 ± 0.41	$+0.87 \pm 0.69$	0.367 ± 0.004	11.3 (7.5)
IP = 100 m				IP = 120 m			
359.99 ± 0.31	$+3.67 \pm 0.68$	0.502 ± 0.005	5.1 (8.7)	0.29 ± 0.21	$+2.48 \pm 0.49$	0.589 ± 0.005	4.0 (2.7)
25.23 ± 0.41	$+7.85 \pm 0.97$	0.534 ± 0.005	6.6 (3.6)	24.97 ± 0.31	$+4.47 \pm 0.68$	0.617 ± 0.002	6.1 (1.9)
52.56 ± 0.41	$+4.90 \pm 0.97$	0.517 ± 0.005	9.8 (4.2)	53.42 ± 0.31	$+4.66 \pm 0.96$	0.601 ± 0.005	7.3 (3.2)
90.71 ± 0.52	-8.65 ± 0.89	0.469 ± 0.004	16.8 (3.9)	90.27 ± 0.21	-6.17 ± 0.76	0.548 ± 0.005	12.3 (3.7)
126.90 ± 0.31	-5.28 ± 0.77	0.438 ± 0.005	17.9 (5.1)	126.89 ± 0.41	-3.13 ± 0.88	0.514 ± 0.005	14.7 (5.3)
156.29 ± 0.31	$+1.37 \pm 0.68$	0.467 ± 0.003	9.8 (3.7)	156.23 ± 0.31	$+0.97 \pm 0.50$	0.549 ± 0.006	7.5 (2.4)
179.92 ± 0.41	$+3.21 \pm 0.88$	0.521 ± 0.009	4.6 (2.9)	179.95 ± 0.21	$+1.97 \pm 0.67$	0.605 ± 0.005	3.5 (2.6)
203.57 ± 0.41	$+5.27 \pm 0.88$	0.540 ± 0.005	6.0 (2.7)	203.14 ± 0.21	$+2.43 \pm 0.76$	0.621 ± 0.007	5.1 (2.6)
232.85 ± 0.52	$+5.65 \pm 1.17$	0.515 ± 0.005	10.4 (9.5)	232.26 ± 0.41	$+3.03 \pm 0.88$	0.596 ± 0.007	6.8 (10.2)
270.28 ± 0.31	-11.57 ± 1.15	0.457 ± 0.005	16.6 (6.5)	270.20 ± 0.21	-6.20 ± 0.86	0.535 ± 0.005	11.0 (3.5)
307.19 ± 0.41	-7.72 ± 1.06	0.419 ± 0.005	19.1 (5.7)	307.18 ± 0.31	-4.96 ± 0.87	0.492 ± 0.005	14.4 (4.1)
336.92 ± 0.41	$+0.50 \pm 0.69$	0.451 ± 0.004	8.5 (4.8)	336.47 ± 0.21	-0.00 ± 0.49	0.525 ± 0.003	6.4 (2.4)

Table 127: The nominal angle δ_n, average displacement $\Delta\delta$, average value of the parameter DIST, RMS of the ALPHA distribution for enabled GF and impact parameters between 60 m and 120 m. The RMS of the ALPHA distribution for disabled GF is given parentheses. The primary γ-ray energy was set to 450 GeV, the ZA to 40° and the azimuth angle to 150°.

$E_\gamma = 450\,\mathrm{GeV}$, Az = 180°, ZA = 40°, Intermediate Image Cleaning

$\delta_n[°]$	$\Delta\delta[°]$	DIST[°]	$\mathrm{RMS}_{\vert\mathrm{ALPHA}\vert}[°]$	$\delta_n[°]$	$\Delta\delta[°]$	DIST[°]	$\mathrm{RMS}_{\vert\mathrm{ALPHA}\vert}[°]$
IP = 60 m				IP = 80 m			
0.99 ± 0.62	$+1.04 \pm 1.09$	0.347 ± 0.005	5.2 (9.3)	0.46 ± 0.51	$+0.70 \pm 0.89$	0.451 ± 0.005	4.1 (7.7)
24.64 ± 0.62	$+9.75 \pm 1.19$	0.333 ± 0.004	17.6 (9.6)	25.33 ± 0.31	$+7.83 \pm 0.69$	0.433 ± 0.004	5.1 (7.7)
54.32 ± 0.93	$+17.37 \pm 1.21$	0.298 ± 0.002	26.2 (10.2)	54.16 ± 0.41	$+15.68 \pm 1.65$	0.392 ± 0.005	23.1 (6.9)
89.85 ± 0.52	$+0.39 \pm 0.61$	0.280 ± 0.003	27.5 (14.0)	91.37 ± 0.52	$+2.72 \pm 0.99$	0.364 ± 0.004	27.9 (5.4)
127.93 ± 0.52	-18.12 ± 1.37	0.296 ± 0.003	17.4 (10.3)	127.89 ± 0.52	-13.91 ± 1.65	0.388 ± 0.005	17.1 (5.6)
156.43 ± 0.72	-7.65 ± 1.39	0.331 ± 0.004	11.1 (7.0)	155.12 ± 0.52	-7.35 ± 1.28	0.432 ± 0.005	7.4 (7.2)
179.11 ± 0.72	-0.06 ± 1.10	0.345 ± 0.004	4.7 (7.0)	179.89 ± 0.31	$+0.49 \pm 0.59$	0.452 ± 0.006	3.1 (7.7)
203.44 ± 0.52	$+8.25 \pm 1.09$	0.327 ± 0.004	8.6 (10.0)	203.70 ± 0.41	$+7.75 \pm 0.98$	0.424 ± 0.005	3.3 (6.8)
231.67 ± 0.41	$+17.68 \pm 1.55$	0.286 ± 0.003	24.4 (13.7)	233.75 ± 0.52	$+17.32 \pm 1.37$	0.378 ± 0.005	21.3 (5.5)
270.10 ± 0.31	-0.42 ± 0.50	0.267 ± 0.002	26.3 (11.1)	267.95 ± 0.52	-3.25 ± 0.99	0.353 ± 0.005	26.0 (15.2)
306.10 ± 0.31	-14.08 ± 0.97	0.290 ± 0.002	17.1 (9.6)	306.37 ± 0.62	-14.71 ± 1.47	0.379 ± 0.006	16.7 (12.8)
337.79 ± 0.41	-6.03 ± 0.98	0.327 ± 0.005	10.2 (9.0)	337.80 ± 0.41	-4.04 ± 0.98	0.426 ± 0.006	9.9 (7.5)
IP = 100 m				IP = 120 m			
359.07 ± 0.41	-0.37 ± 0.79	0.548 ± 0.006	2.7 (8.1)	359.58 ± 0.31	$+0.31 \pm 0.69$	0.630 ± 0.006	2.5 (4.8)
26.26 ± 0.41	$+7.08 \pm 0.89$	0.531 ± 0.006	4.2 (2.9)	26.08 ± 0.21	$+5.16 \pm 0.59$	0.616 ± 0.007	2.2 (2.0)
53.31 ± 0.41	$+10.12 \pm 0.70$	0.477 ± 0.003	24.3 (6.3)	53.28 ± 0.31	$+6.79 \pm 0.69$	0.565 ± 0.006	11.5 (3.4)
91.06 ± 0.62	-0.65 ± 1.38	0.449 ± 0.005	25.1 (4.1)	90.63 ± 0.41	-0.11 ± 0.79	0.531 ± 0.004	22.7 (3.3)
127.15 ± 0.52	-9.90 ± 1.28	0.476 ± 0.003	16.1 (5.0)	126.46 ± 0.52	-8.12 ± 1.09	0.561 ± 0.002	12.1 (5.5)
155.82 ± 0.41	-4.79 ± 0.60	0.531 ± 0.006	6.3 (6.6)	156.04 ± 0.31	-3.35 ± 0.59	0.614 ± 0.007	8.2 (6.0)
180.16 ± 0.41	$+0.38 \pm 0.79$	0.547 ± 0.004	3.8 (3.1)	180.06 ± 0.31	-0.04 ± 0.59	0.636 ± 0.008	2.3 (2.4)
203.41 ± 0.41	$+5.02 \pm 0.89$	0.521 ± 0.006	2.5 (3.0)	203.04 ± 0.31	$+2.34 \pm 0.69$	0.606 ± 0.004	2.7 (2.5)
233.75 ± 0.41	$+11.68 \pm 0.98$	0.464 ± 0.004	14.5 (4.3)	232.02 ± 0.41	$+6.76 \pm 0.98$	0.546 ± 0.005	10.5 (9.5)
269.48 ± 0.31	-1.51 ± 0.69	0.434 ± 0.006	23.8 (6.5)	270.36 ± 0.21	-2.85 ± 0.87	0.512 ± 0.002	19.8 (4.5)
306.63 ± 0.31	-8.90 ± 1.07	0.468 ± 0.006	15.9 (5.4)	307.08 ± 0.31	-5.09 ± 0.78	0.544 ± 0.006	12.1 (3.6)
336.98 ± 0.31	-4.10 ± 0.78	0.521 ± 0.005	7.2 (5.5)	336.80 ± 0.31	-2.14 ± 0.78	0.606 ± 0.008	5.7 (2.3)

Table 128: The nominal angle δ_n, average displacement $\Delta\delta$, average value of the parameter DIST, RMS of the ALPHA distribution for enabled GF and impact parameters between 60 m and 120 m. The RMS of the ALPHA distribution for disabled GF is given parentheses. The primary γ-ray energy was set to 450 GeV, the ZA to 40° and the azimuth angle to 180°.

$E_\gamma = 450\,\mathrm{GeV}$, Az = 180°, ZA = 40°, Hard Image Cleaning

$\delta_n[°]$	$\Delta\delta[°]$	DIST[°]	$\mathrm{RMS}_{\vert\mathrm{ALPHA}\vert}[°]$	$\delta_n[°]$	$\Delta\delta[°]$	DIST[°]	$\mathrm{RMS}_{\vert\mathrm{ALPHA}\vert}[°]$
IP = 60 m				IP = 80 m			
0.10 ± 0.31	$+0.50 \pm 0.59$	0.340 ± 0.005	5.3 (12.1)	0.74 ± 0.51	$+1.17 \pm 0.80$	0.444 ± 0.005	3.3 (10.6)
23.41 ± 0.62	$+8.06 \pm 0.81$	0.328 ± 0.004	18.6 (9.1)	24.35 ± 0.52	$+6.86 \pm 0.90$	0.428 ± 0.002	3.7 (3.9)
54.65 ± 0.93	$+16.67 \pm 1.88$	0.294 ± 0.002	25.7 (7.8)	53.60 ± 0.52	$+13.23 \pm 1.18$	0.386 ± 0.005	26.1 (4.7)
91.52 ± 0.83	$+0.07 \pm 1.21$	0.275 ± 0.003	25.3 (11.6)	90.85 ± 0.62	$+0.88 \pm 1.76$	0.359 ± 0.004	26.7 (5.9)
128.06 ± 0.52	-17.44 ± 1.18	0.293 ± 0.004	17.7 (6.2)	128.44 ± 0.52	-12.50 ± 1.94	0.382 ± 0.004	17.2 (5.0)
156.64 ± 0.62	-7.71 ± 1.38	0.325 ± 0.005	10.6 (6.8)	154.96 ± 0.52	-6.79 ± 1.09	0.428 ± 0.005	7.7 (6.7)
179.48 ± 0.41	$+0.06 \pm 0.70$	0.342 ± 0.005	4.6 (8.2)	180.59 ± 0.41	$+0.78 \pm 0.79$	0.445 ± 0.005	3.2 (3.9)
203.50 ± 0.41	$+9.53 \pm 0.98$	0.322 ± 0.004	15.0 (9.0)	203.95 ± 0.52	$+8.06 \pm 0.99$	0.419 ± 0.003	3.9 (6.6)
232.64 ± 0.62	$+17.87 \pm 1.57$	0.283 ± 0.004	22.3 (11.2)	233.32 ± 0.52	$+15.06 \pm 0.80$	0.372 ± 0.002	21.1 (6.3)
270.28 ± 0.62	-7.15 ± 0.90	0.262 ± 0.003	26.7 (11.9)	269.27 ± 0.52	-1.97 ± 1.37	0.346 ± 0.004	26.1 (9.3)
305.49 ± 0.62	-15.23 ± 1.09	0.283 ± 0.004	17.5 (10.1)	306.92 ± 0.52	-13.40 ± 1.84	0.374 ± 0.005	16.7 (11.2)
337.26 ± 0.62	-6.25 ± 1.19	0.321 ± 0.005	9.6 (7.7)	337.30 ± 0.41	-4.54 ± 0.89	0.421 ± 0.006	7.3 (7.5)
IP = 100 m				IP = 120 m			
359.99 ± 0.31	$+0.34 \pm 0.69$	0.544 ± 0.007	2.7 (8.7)	0.29 ± 0.21	$+0.93 \pm 0.40$	0.624 ± 0.008	3.1 (2.7)
25.23 ± 0.41	$+6.01 \pm 0.98$	0.524 ± 0.008	8.3 (3.6)	24.97 ± 0.31	$+3.83 \pm 0.79$	0.607 ± 0.002	2.3 (1.9)
52.56 ± 0.41	$+9.18 \pm 1.17$	0.470 ± 0.004	12.7 (4.2)	53.42 ± 0.31	$+5.47 \pm 0.78$	0.558 ± 0.006	11.4 (3.2)
90.71 ± 0.52	-0.92 ± 1.75	0.441 ± 0.005	22.6 (3.9)	90.27 ± 0.21	-0.59 ± 0.78	0.524 ± 0.005	20.6 (3.7)
126.90 ± 0.31	-10.54 ± 0.50	0.469 ± 0.004	16.1 (5.1)	126.89 ± 0.41	-7.37 ± 1.08	0.554 ± 0.006	11.6 (5.3)
156.29 ± 0.31	-4.17 ± 0.78	0.523 ± 0.002	6.5 (3.7)	156.23 ± 0.31	-2.85 ± 0.60	0.606 ± 0.003	7.6 (2.4)
179.92 ± 0.41	$+0.29 \pm 0.70$	0.541 ± 0.004	2.7 (2.9)	179.95 ± 0.21	$+0.12 \pm 0.49$	0.627 ± 0.007	2.9 (2.6)
203.57 ± 0.41	$+4.38 \pm 0.89$	0.518 ± 0.006	2.3 (2.7)	203.14 ± 0.21	$+2.01 \pm 0.59$	0.600 ± 0.004	2.3 (2.6)
232.85 ± 0.52	$+11.71 \pm 1.18$	0.459 ± 0.006	14.3 (9.5)	232.26 ± 0.41	$+6.66 \pm 1.08$	0.539 ± 0.006	14.8 (10.2)
270.28 ± 0.31	-0.31 ± 0.98	0.427 ± 0.002	23.7 (6.5)	270.20 ± 0.21	-1.18 ± 0.78	0.503 ± 0.005	19.1 (3.5)
307.19 ± 0.41	-9.09 ± 1.08	0.461 ± 0.005	15.7 (5.7)	307.18 ± 0.31	-4.93 ± 0.78	0.538 ± 0.007	10.6 (4.1)
336.92 ± 0.41	-3.44 ± 0.89	0.516 ± 0.006	8.2 (4.8)	336.47 ± 0.21	-2.51 ± 0.68	0.599 ± 0.005	5.6 (2.4)

Table 129: The nominal angle δ_n, average displacement $\Delta\delta$, average value of the parameter DIST, RMS of the ALPHA distribution for enabled GF and impact parameters between 60 m and 120 m. The RMS of the ALPHA distribution for disabled GF is given parentheses. The primary γ-ray energy was set to 450 GeV, the ZA to 40° and the azimuth angle to 180°.

$E_\gamma = 1000\,\mathrm{GeV}$, Az = 0°, ZA = 0°, Intermediate Image Cleaning

$\delta_n\,[°]$	$\Delta\delta\,[°]$	DIST[°]	$\mathrm{RMS}_{\lvert\mathrm{ALPHA}\rvert}\,[°]$	$\delta_n\,[°]$	$\Delta\delta\,[°]$	DIST[°]	$\mathrm{RMS}_{\lvert\mathrm{ALPHA}\rvert}\,[°]$
IP = 60 m				**IP = 80 m**			
357.07 ± 0.22	-1.92 ± 0.66	0.756 ± 0.005	2.0 (16.0)	358.63 ± 0.22	-0.68 ± 0.66	0.872 ± 0.002	1.6 (2.9)
28.83 ± 0.44	-0.41 ± 1.31	0.749 ± 0.002	2.6 (5.9)	29.94 ± 0.44	$+0.09 \pm 0.88$	0.872 ± 0.004	1.8 (1.8)
61.79 ± 0.44	$+2.18 \pm 0.66$	0.747 ± 0.002	4.5 (2.0)	59.27 ± 0.44	-0.10 ± 1.09	0.865 ± 0.004	3.0 (2.0)
91.44 ± 0.88	$+0.91 \pm 1.31$	0.754 ± 0.002	3.3 (1.6)	90.71 ± 0.44	$+0.25 \pm 0.88$	0.871 ± 0.004	2.0 (1.2)
119.97 ± 0.22	-1.11 ± 0.88	0.752 ± 0.002	2.5 (4.2)	120.59 ± 0.44	-0.31 ± 1.09	0.870 ± 0.026	1.8 (1.4)
151.67 ± 0.88	-0.88 ± 1.53	0.752 ± 0.011	1.1 (2.1)	150.85 ± 0.44	-0.50 ± 1.09	0.871 ± 0.002	1.4 (1.2)
180.10 ± 0.88	-0.78 ± 1.31	0.750 ± 0.004	0.9 (1.8)	180.46 ± 0.66	-0.36 ± 1.09	0.871 ± 0.013	1.7 (1.4)
210.08 ± 0.44	$+1.02 \pm 0.88$	0.753 ± 0.015	2.6 (1.7)	210.15 ± 0.66	$+0.97 \pm 1.09$	0.874 ± 0.022	1.9 (1.5)
240.10 ± 0.66	$+2.12 \pm 1.31$	0.758 ± 0.004	4.0 (2.5)	240.41 ± 0.44	$+1.58 \pm 1.09$	0.874 ± 0.002	3.5 (1.5)
270.24 ± 0.66	$+1.21 \pm 1.53$	0.751 ± 0.002	3.8 (2.6)	269.90 ± 0.44	-0.28 ± 1.31	0.872 ± 0.002	2.9 (0.9)
299.84 ± 0.66	-0.78 ± 1.09	0.755 ± 0.007	1.9 (2.3)	299.81 ± 0.44	-1.24 ± 0.66	0.875 ± 0.004	2.3 (1.7)
327.67 ± 0.44	-2.05 ± 1.09	0.756 ± 0.007	4.0 (18.0)	329.41 ± 0.44	-1.04 ± 0.88	0.873 ± 0.020	1.3 (3.2)
IP = 100 m				**IP = 120 m**			
358.64 ± 0.44	-0.47 ± 0.88	0.947 ± 0.018	1.5 (2.8)	359.39 ± 0.44	-0.01 ± 0.88	0.992 ± 0.005	1.5 (4.2)
29.87 ± 0.44	-0.07 ± 0.88	0.941 ± 0.004	1.3 (1.1)	30.46 ± 0.44	$+0.55 \pm 0.88$	0.986 ± 0.011	1.4 (0.9)
59.57 ± 0.44	-0.11 ± 0.88	0.945 ± 0.002	1.9 (2.9)	59.40 ± 0.44	-0.51 ± 0.88	0.979 ± 0.002	1.3 (1.3)
90.26 ± 0.44	-0.06 ± 0.88	0.941 ± 0.002	1.3 (2.6)	90.58 ± 0.44	-0.14 ± 0.88	0.964 ± 0.002	0.5 (4.0)
120.97 ± 0.44	$+0.80 \pm 0.66$	0.943 ± 0.004	1.1 (1.0)	120.06 ± 0.44	-0.06 ± 0.88	0.982 ± 0.011	0.9 (0.9)
150.76 ± 0.44	-0.36 ± 0.88	0.942 ± 0.004	0.7 (1.1)	150.42 ± 0.44	$+0.07 \pm 0.88$	0.984 ± 0.018	0.6 (0.6)
180.01 ± 0.44	-0.30 ± 0.88	0.943 ± 0.005	2.0 (1.0)	180.26 ± 0.44	$+0.52 \pm 0.88$	0.991 ± 0.002	1.5 (0.9)
210.23 ± 0.44	$+0.61 \pm 0.88$	0.939 ± 0.002	0.9 (0.7)	209.96 ± 0.44	$+0.12 \pm 0.88$	0.979 ± 0.013	1.2 (0.7)
239.97 ± 0.44	$+0.86 \pm 1.09$	0.938 ± 0.009	2.6 (0.8)	239.42 ± 0.22	-0.15 ± 0.66	0.972 ± 0.009	1.4 (1.0)
269.89 ± 0.44	$+0.28 \pm 0.88$	0.941 ± 0.011	2.0 (0.8)	270.03 ± 0.44	$+0.32 \pm 0.88$	0.968 ± 0.005	0.9 (0.7)
299.69 ± 0.44	-0.29 ± 0.88	0.947 ± 0.015	1.9 (1.4)	299.56 ± 0.44	-0.50 ± 0.88	0.977 ± 0.011	1.3 (1.2)
329.68 ± 0.44	-0.75 ± 0.88	0.946 ± 0.005	1.0 (2.2)	329.80 ± 0.22	-0.16 ± 0.66	0.980 ± 0.009	0.8 (4.0)

Table 130: The nominal angle δ_n, average displacement $\Delta\delta$, average value of the parameter DIST, RMS of the ALPHA distribution for enabled GF and impact parameters between 60 m and 120 m. The RMS of the ALPHA distribution for disabled GF is given parentheses. The primary γ-ray energy was set to 1000 GeV, the ZA to 0° and the azimuth angle to 0°.

$E_\gamma = 1000\,\mathrm{GeV}$, Az = 0°, ZA = 0°, Hard Image Cleaning

$\delta_n\,[°]$	$\Delta\delta\,[°]$	DIST[°]	$\mathrm{RMS}_{\lvert\mathrm{ALPHA}\rvert}\,[°]$	$\delta_n\,[°]$	$\Delta\delta\,[°]$	DIST[°]	$\mathrm{RMS}_{\lvert\mathrm{ALPHA}\rvert}\,[°]$
IP = 60 m				**IP = 80 m**			
358.72 ± 0.66	-0.45 ± 0.88	0.751 ± 0.004	2.1 (1.7)	358.87 ± 0.22	-0.96 ± 0.66	0.866 ± 0.016	1.2 (3.1)
28.82 ± 0.44	-0.38 ± 1.31	0.744 ± 0.016	2.2 (4.7)	30.15 ± 0.44	$+0.56 \pm 1.09$	0.870 ± 0.005	1.9 (1.6)
61.59 ± 0.66	$+2.23 \pm 0.88$	0.740 ± 0.004	3.5 (1.8)	58.08 ± 0.44	-1.16 ± 0.66	0.859 ± 0.005	3.0 (10.9)
91.03 ± 0.44	$+0.62 \pm 1.09$	0.746 ± 0.002	4.2 (1.4)	90.33 ± 0.44	$+0.13 \pm 0.88$	0.868 ± 0.002	2.2 (1.0)
120.05 ± 0.44	-1.27 ± 1.09	0.745 ± 0.007	1.8 (3.9)	121.00 ± 0.44	-0.05 ± 1.31	0.864 ± 0.018	2.1 (1.0)
151.82 ± 0.44	-0.74 ± 0.88	0.747 ± 0.004	1.1 (1.8)	150.55 ± 0.44	-0.65 ± 1.09	0.867 ± 0.004	1.4 (0.9)
180.08 ± 0.88	-0.63 ± 1.31	0.743 ± 0.002	1.2 (1.6)	180.21 ± 0.66	-0.50 ± 1.31	0.864 ± 0.026	1.2 (1.3)
210.34 ± 0.44	$+1.41 \pm 1.09$	0.747 ± 0.004	2.7 (1.8)	210.22 ± 0.44	$+0.64 \pm 0.88$	0.870 ± 0.022	1.7 (1.5)
240.18 ± 0.44	$+2.02 \pm 1.31$	0.750 ± 0.004	4.1 (2.3)	240.15 ± 0.66	$+1.30 \pm 1.31$	0.868 ± 0.005	3.5 (1.3)
269.97 ± 0.66	$+0.81 \pm 1.09$	0.748 ± 0.022	3.7 (2.4)	270.01 ± 0.44	-0.09 ± 1.09	0.869 ± 0.002	2.8 (0.8)
299.78 ± 0.22	-0.78 ± 0.88	0.750 ± 0.002	2.4 (2.2)	299.72 ± 0.44	-0.99 ± 1.31	0.867 ± 0.016	1.9 (1.3)
327.66 ± 0.44	-2.09 ± 1.09	0.751 ± 0.002	2.4 (18.3)	329.43 ± 0.44	-1.01 ± 1.31	0.871 ± 0.004	1.2 (2.3)
IP = 100 m				**IP = 120 m**			
358.79 ± 0.44	-0.37 ± 0.88	0.940 ± 0.020	1.2 (3.0)	359.54 ± 0.44	-0.18 ± 0.88	0.985 ± 0.011	1.2 (4.6)
29.76 ± 0.44	-0.15 ± 0.88	0.940 ± 0.004	1.5 (2.8)	30.43 ± 0.44	$+0.63 \pm 0.88$	0.985 ± 0.011	1.4 (1.0)
59.91 ± 0.66	$+0.11 \pm 1.31$	0.938 ± 0.005	1.7 (1.5)	59.65 ± 0.44	-0.02 ± 0.88	0.972 ± 0.002	1.7 (1.3)
90.18 ± 0.44	$+0.00 \pm 0.88$	0.937 ± 0.002	1.4 (2.6)	90.53 ± 0.44	$+0.06 \pm 0.88$	0.962 ± 0.007	0.8 (2.6)
120.94 ± 0.44	$+0.63 \pm 0.88$	0.938 ± 0.004	1.2 (1.3)	120.23 ± 0.44	$+0.25 \pm 0.88$	0.975 ± 0.002	1.1 (1.0)
150.59 ± 0.22	-0.12 ± 0.66	0.940 ± 0.004	0.9 (0.9)	150.55 ± 0.44	$+0.39 \pm 0.88$	0.982 ± 0.005	0.6 (0.7)
180.14 ± 0.44	-0.07 ± 0.88	0.936 ± 0.005	2.0 (1.3)	180.12 ± 0.44	$+0.51 \pm 0.88$	0.985 ± 0.011	1.1 (1.0)
210.37 ± 0.44	$+0.85 \pm 0.88$	0.937 ± 0.011	1.0 (1.0)	210.39 ± 0.44	$+0.64 \pm 0.88$	0.976 ± 0.007	1.2 (0.8)
240.13 ± 0.44	$+0.51 \pm 1.09$	0.932 ± 0.015	2.4 (0.9)	239.15 ± 0.44	-0.60 ± 0.88	0.965 ± 0.015	1.7 (1.0)
269.89 ± 0.44	$+0.27 \pm 0.88$	0.938 ± 0.004	1.9 (0.9)	269.93 ± 0.44	$+0.10 \pm 0.88$	0.965 ± 0.005	1.0 (0.9)
299.76 ± 0.44	-0.41 ± 1.09	0.940 ± 0.005	1.3 (1.5)	299.65 ± 0.44	-0.57 ± 0.88	0.971 ± 0.002	1.2 (1.2)
329.51 ± 0.44	-0.65 ± 0.88	0.944 ± 0.005	1.0 (2.5)	329.69 ± 0.44	-0.22 ± 0.88	0.977 ± 0.007	0.7 (3.6)

Table 131: The nominal angle δ_n, average displacement $\Delta\delta$, average value of the parameter DIST, RMS of the ALPHA distribution for enabled GF and impact parameters between 60 m and 120 m. The RMS of the ALPHA distribution for disabled GF is given parentheses. The primary γ-ray energy was set to 1000 GeV, the ZA to 0° and the azimuth angle to 0°.

$E_\gamma = 1000\,\text{GeV},\ \text{Az} = 0°,\ \text{ZA} = 20°$, Intermediate Image Cleaning

δ_n[°]	$\Delta\delta$[°]	DIST[°]	$\text{RMS}_{\lvert\text{ALPHA}\rvert}$[°]	δ_n[°]	$\Delta\delta$[°]	DIST[°]	$\text{RMS}_{\lvert\text{ALPHA}\rvert}$[°]
IP = 60 m				**IP = 80 m**			
1.31 ± 0.89	$+2.21 \pm 1.28$	0.612 ± 0.003	2.7 (1.9)	0.27 ± 0.67	$+1.23 \pm 1.06$	0.748 ± 0.010	2.0 (1.8)
28.82 ± 1.11	$+3.31 \pm 1.50$	0.607 ± 0.015	9.8 (3.7)	28.68 ± 0.67	$+1.96 \pm 1.25$	0.740 ± 0.006	7.9 (1.6)
58.76 ± 1.33	$+3.23 \pm 1.92$	0.595 ± 0.010	8.8 (3.5)	57.49 ± 0.67	$+0.76 \pm 1.06$	0.720 ± 0.006	3.0 (2.3)
89.38 ± 0.89	-0.75 ± 1.47	0.585 ± 0.005	5.8 (2.6)	90.40 ± 0.44	$+0.62 \pm 0.83$	0.713 ± 0.008	2.1 (1.1)
121.81 ± 0.67	-1.62 ± 1.45	0.591 ± 0.010	4.0 (1.9)	121.89 ± 0.44	-1.41 ± 0.83	0.720 ± 0.002	1.5 (2.0)
151.36 ± 0.67	-1.15 ± 1.45	0.609 ± 0.006	3.0 (2.0)	151.95 ± 0.44	-0.38 ± 1.03	0.745 ± 0.005	3.7 (1.3)
179.41 ± 0.67	-0.29 ± 1.25	0.621 ± 0.011	3.1 (2.7)	180.25 ± 0.67	$+0.62 \pm 1.06$	0.753 ± 0.010	3.4 (1.2)
208.00 ± 0.89	-0.64 ± 1.47	0.616 ± 0.008	3.0 (2.3)	208.75 ± 0.22	-0.39 ± 0.81	0.749 ± 0.002	1.8 (1.7)
237.70 ± 1.11	-1.33 ± 1.70	0.599 ± 0.002	2.9 (2.4)	237.62 ± 0.44	-0.40 ± 1.03	0.734 ± 0.006	2.4 (1.9)
269.33 ± 0.67	-1.66 ± 1.45	0.596 ± 0.006	3.9 (2.2)	269.06 ± 0.67	-1.46 ± 1.06	0.725 ± 0.005	2.6 (2.2)
301.07 ± 0.67	-2.26 ± 1.25	0.602 ± 0.010	2.5 (2.7)	301.28 ± 0.44	-1.26 ± 0.83	0.732 ± 0.005	2.0 (2.0)
331.97 ± 0.67	-0.83 ± 1.45	0.611 ± 0.005	2.4 (2.8)	332.59 ± 0.44	-0.40 ± 0.83	0.745 ± 0.005	1.4 (1.5)
IP = 100 m				**IP = 120 m**			
0.16 ± 0.44	$+0.70 \pm 0.64$	0.839 ± 0.003	1.2 (0.9)	359.28 ± 0.22	-0.34 ± 0.61	0.887 ± 0.010	1.0 (0.8)
28.70 ± 0.22	$+0.70 \pm 0.81$	0.834 ± 0.005	2.1 (1.5)	28.92 ± 0.22	$+0.62 \pm 0.42$	0.884 ± 0.010	0.8 (0.6)
57.64 ± 0.89	$+0.44 \pm 1.28$	0.819 ± 0.011	1.8 (1.7)	57.76 ± 0.22	$+0.58 \pm 0.61$	0.870 ± 0.011	1.3 (1.2)
90.47 ± 0.44	$+0.00 \pm 1.03$	0.815 ± 0.006	1.3 (1.2)	90.66 ± 0.22	$+0.25 \pm 0.61$	0.869 ± 0.010	0.9 (1.0)
122.35 ± 0.44	-0.64 ± 0.83	0.817 ± 0.005	1.8 (1.1)	122.52 ± 0.44	-0.51 ± 0.83	0.869 ± 0.005	1.0 (0.9)
151.91 ± 0.44	$+0.22 \pm 0.83$	0.835 ± 0.005	8.9 (0.6)	151.88 ± 0.22	$+0.76 \pm 0.42$	0.882 ± 0.002	7.3 (0.6)
180.36 ± 0.44	$+0.40 \pm 1.03$	0.842 ± 0.002	1.7 (1.1)	180.63 ± 0.44	$+0.56 \pm 0.83$	0.881 ± 0.010	1.1 (0.7)
208.56 ± 0.44	$+0.51 \pm 0.83$	0.841 ± 0.006	1.2 (1.2)	208.54 ± 0.22	$+0.04 \pm 0.42$	0.884 ± 0.005	1.1 (1.3)
238.34 ± 0.67	$+0.18 \pm 1.06$	0.830 ± 0.005	1.5 (1.3)	238.03 ± 0.22	$+0.11 \pm 0.61$	0.878 ± 0.010	1.2 (1.1)
269.90 ± 0.44	-0.51 ± 0.64	0.825 ± 0.016	1.5 (0.9)	269.96 ± 0.44	$+0.30 \pm 0.83$	0.876 ± 0.010	1.1 (0.5)
301.20 ± 0.44	-1.40 ± 0.83	0.827 ± 0.005	0.7 (1.1)	301.69 ± 0.22	-0.74 ± 0.61	0.879 ± 0.010	0.9 (0.9)
331.78 ± 0.22	$+0.27 \pm 0.61$	0.840 ± 0.010	1.7 (0.9)	332.07 ± 0.22	$+0.72 \pm 0.61$	0.887 ± 0.008	1.3 (0.7)

Table 132: The nominal angle δ_n, average displacement $\Delta\delta$, average value of the parameter DIST, RMS of the ALPHA distribution for enabled GF and impact parameters between 60 m and 120 m. The RMS of the ALPHA distribution for disabled GF is given parentheses. The primary γ-ray energy was set to 1000 GeV, the ZA to 20° and the azimuth angle to 0°.

$E_\gamma = 1000\,\text{GeV},\ \text{Az} = 0°,\ \text{ZA} = 20°$, Hard Image Cleaning

δ_n[°]	$\Delta\delta$[°]	DIST[°]	$\text{RMS}_{\lvert\text{ALPHA}\rvert}$[°]	δ_n[°]	$\Delta\delta$[°]	DIST[°]	$\text{RMS}_{\lvert\text{ALPHA}\rvert}$[°]
IP = 60 m				**IP = 80 m**			
0.86 ± 0.67	$+1.83 \pm 1.25$	0.607 ± 0.008	2.6 (1.5)	0.43 ± 0.44	$+1.02 \pm 1.03$	0.740 ± 0.005	1.5 (1.3)
28.97 ± 0.89	$+2.86 \pm 1.28$	0.602 ± 0.011	7.8 (3.1)	29.08 ± 0.44	$+2.58 \pm 0.83$	0.735 ± 0.003	7.2 (1.5)
58.79 ± 0.89	$+3.43 \pm 1.47$	0.586 ± 0.008	8.3 (3.6)	57.73 ± 0.67	$+1.06 \pm 1.06$	0.714 ± 0.006	2.3 (2.2)
89.28 ± 0.67	-1.09 ± 1.25	0.579 ± 0.002	4.7 (2.2)	89.99 ± 0.44	$+0.41 \pm 0.83$	0.705 ± 0.010	1.8 (1.2)
122.33 ± 0.44	-1.52 ± 1.42	0.584 ± 0.010	2.9 (2.0)	122.34 ± 0.44	-1.35 ± 0.83	0.713 ± 0.003	1.5 (1.3)
151.76 ± 0.44	-1.03 ± 0.83	0.603 ± 0.008	3.1 (1.9)	151.90 ± 0.44	-0.37 ± 1.03	0.739 ± 0.005	3.4 (1.2)
179.33 ± 0.67	-0.44 ± 0.86	0.613 ± 0.002	3.6 (2.4)	180.24 ± 0.67	$+0.50 \pm 1.25$	0.746 ± 0.008	3.6 (1.2)
208.41 ± 0.89	-0.61 ± 1.28	0.609 ± 0.006	3.0 (2.4)	208.83 ± 0.22	$+0.34 \pm 0.81$	0.741 ± 0.003	1.8 (1.6)
237.44 ± 0.22	-1.11 ± 0.81	0.592 ± 0.013	3.0 (2.4)	237.45 ± 0.44	-0.57 ± 1.03	0.727 ± 0.002	2.1 (1.5)
268.90 ± 0.67	-2.13 ± 1.45	0.590 ± 0.006	3.4 (2.1)	269.18 ± 0.67	-1.31 ± 0.86	0.720 ± 0.006	2.4 (1.9)
301.17 ± 0.89	-1.81 ± 1.47	0.595 ± 0.010	2.0 (3.1)	301.51 ± 0.67	-1.19 ± 1.06	0.724 ± 0.006	1.6 (1.4)
331.69 ± 0.67	-1.29 ± 1.45	0.605 ± 0.010	1.6 (3.2)	332.37 ± 0.22	$+0.71 \pm 0.61$	0.739 ± 0.006	1.1 (1.5)
IP = 100 m				**IP = 120 m**			
0.24 ± 0.44	$+0.93 \pm 0.83$	0.831 ± 0.005	1.2 (1.1)	359.22 ± 0.22	-0.39 ± 0.61	0.879 ± 0.006	1.1 (0.6)
28.67 ± 0.22	$+0.47 \pm 0.81$	0.829 ± 0.005	1.6 (1.3)	28.78 ± 0.22	$+0.34 \pm 0.42$	0.881 ± 0.008	0.7 (0.5)
57.47 ± 0.44	$+0.51 \pm 0.83$	0.814 ± 0.016	1.4 (1.5)	57.67 ± 0.44	$+0.32 \pm 0.83$	0.864 ± 0.003	1.3 (1.2)
90.10 ± 0.44	-0.14 ± 0.83	0.810 ± 0.005	1.3 (0.8)	90.47 ± 0.22	$+0.15 \pm 0.61$	0.864 ± 0.008	1.0 (1.3)
122.58 ± 0.44	-0.17 ± 0.83	0.810 ± 0.006	1.7 (0.7)	122.74 ± 0.44	$+0.35 \pm 1.03$	0.862 ± 0.010	0.7 (0.8)
151.77 ± 0.22	$+0.21 \pm 0.61$	0.830 ± 0.019	9.5 (0.6)	151.85 ± 0.22	$+0.16 \pm 0.42$	0.879 ± 0.002	0.9 (0.8)
180.17 ± 0.44	-0.14 ± 0.83	0.834 ± 0.005	1.5 (1.4)	180.22 ± 0.44	$+0.20 \pm 0.83$	0.875 ± 0.010	0.9 (0.8)
208.63 ± 0.44	$+0.68 \pm 0.83$	0.834 ± 0.006	1.6 (1.3)	208.67 ± 0.22	$+0.27 \pm 0.61$	0.879 ± 0.002	0.9 (0.9)
238.02 ± 0.44	$+0.21 \pm 0.83$	0.822 ± 0.008	1.6 (1.1)	237.83 ± 0.44	-0.19 ± 0.83	0.873 ± 0.008	1.5 (1.1)
270.00 ± 0.44	-0.10 ± 0.83	0.820 ± 0.006	1.4 (1.0)	269.75 ± 0.44	$+0.11 \pm 0.83$	0.871 ± 0.013	1.1 (0.8)
301.25 ± 0.44	-1.51 ± 0.83	0.820 ± 0.006	0.9 (1.2)	301.89 ± 0.22	-0.56 ± 0.61	0.871 ± 0.002	0.5 (1.1)
331.68 ± 0.22	$+0.55 \pm 0.42$	0.833 ± 0.005	1.5 (1.1)	331.92 ± 0.22	$+0.54 \pm 0.42$	0.883 ± 0.010	0.8 (0.7)

Table 133: The nominal angle δ_n, average displacement $\Delta\delta$, average value of the parameter DIST, RMS of the ALPHA distribution for enabled GF and impact parameters between 60 m and 120 m. The RMS of the ALPHA distribution for disabled GF is given parentheses. The primary γ-ray energy was set to 1000 GeV, the ZA to 20° and the azimuth angle to 0°.

$E_\gamma = 1000$ GeV, Az = 30°, ZA = 20°, Intermediate Image Cleaning

δ_n[°]	$\Delta\delta$[°]	DIST[°]	RMS$_{\lvert ALPHA \rvert}$[°]	δ_n[°]	$\Delta\delta$[°]	DIST[°]	RMS$_{\lvert ALPHA \rvert}$[°]
IP = 60 m				IP = 80 m			
1.31 ± 0.89	$+0.34 \pm 1.50$	0.632 ± 0.003	3.6 (1.9)	0.27 ± 0.67	-0.32 ± 1.08	0.757 ± 0.005	2.7 (1.8)
28.82 ± 1.11	-1.44 ± 1.52	0.613 ± 0.002	3.8 (3.7)	28.68 ± 0.67	$+0.08 \pm 1.08$	0.736 ± 0.010	3.3 (1.6)
58.76 ± 1.33	$+0.96 \pm 1.95$	0.606 ± 0.009	3.8 (3.5)	57.49 ± 0.67	$+0.25 \pm 1.08$	0.739 ± 0.003	2.3 (2.3)
89.38 ± 0.89	$+1.77 \pm 1.50$	0.611 ± 0.007	6.3 (2.6)	90.40 ± 0.44	$+1.30 \pm 0.85$	0.740 ± 0.005	3.7 (1.1)
121.81 ± 0.67	$+0.55 \pm 1.48$	0.628 ± 0.005	5.7 (1.9)	121.89 ± 0.44	$+1.14 \pm 0.65$	0.761 ± 0.003	3.4 (2.0)
151.36 ± 0.67	-1.56 ± 1.08	0.629 ± 0.003	4.2 (2.0)	151.95 ± 0.44	-0.15 ± 0.85	0.765 ± 0.002	3.4 (1.3)
179.41 ± 0.67	-2.22 ± 1.48	0.632 ± 0.007	4.1 (2.7)	180.25 ± 0.67	-0.36 ± 1.08	0.762 ± 0.010	2.8 (1.2)
208.00 ± 0.89	-0.89 ± 1.50	0.621 ± 0.002	4.2 (2.3)	208.75 ± 0.22	$+0.49 \pm 0.84$	0.748 ± 0.003	2.6 (1.7)
237.70 ± 1.11	$+1.50 \pm 1.72$	0.618 ± 0.020	4.6 (2.4)	237.62 ± 0.44	$+0.37 \pm 0.85$	0.744 ± 0.003	2.8 (1.9)
269.33 ± 0.67	$+1.49 \pm 1.28$	0.629 ± 0.005	5.3 (2.2)	269.06 ± 0.67	-0.14 ± 1.28	0.753 ± 0.007	3.8 (2.2)
301.07 ± 0.67	-0.00 ± 0.87	0.642 ± 0.002	6.0 (2.7)	301.28 ± 0.44	-0.36 ± 0.65	0.768 ± 0.024	3.5 (2.0)
331.97 ± 0.67	-1.59 ± 1.08	0.639 ± 0.003	5.3 (2.8)	332.59 ± 0.44	-0.45 ± 1.06	0.767 ± 0.005	3.3 (1.5)
IP = 100 m				IP = 120 m			
0.16 ± 0.44	$+0.55 \pm 0.85$	0.854 ± 0.012	2.4 (0.9)	359.28 ± 0.22	-0.40 ± 0.63	0.894 ± 0.010	1.3 (0.8)
28.70 ± 0.22	$+0.53 \pm 0.84$	0.832 ± 0.010	1.8 (1.5)	28.92 ± 0.22	$+0.78 \pm 0.43$	0.889 ± 0.007	1.4 (0.6)
57.64 ± 0.89	$+0.28 \pm 1.30$	0.830 ± 0.014	3.0 (1.7)	57.76 ± 0.22	$+0.20 \pm 0.63$	0.885 ± 0.009	1.7 (1.2)
90.47 ± 0.44	$+0.50 \pm 0.85$	0.833 ± 0.005	2.7 (1.2)	90.66 ± 0.22	$+0.44 \pm 0.63$	0.886 ± 0.014	2.4 (1.0)
122.35 ± 0.44	$+1.15 \pm 0.85$	0.847 ± 0.012	1.9 (1.1)	122.52 ± 0.44	$+0.65 \pm 0.65$	0.888 ± 0.002	1.7 (0.9)
151.91 ± 0.44	-0.36 ± 0.85	0.856 ± 0.019	2.4 (0.6)	151.88 ± 0.22	-0.15 ± 0.63	0.892 ± 0.005	1.8 (0.6)
180.36 ± 0.44	$+0.02 \pm 0.85$	0.857 ± 0.002	1.3 (1.1)	180.63 ± 0.44	$+0.76 \pm 0.85$	0.900 ± 0.005	1.2 (0.7)
208.56 ± 0.44	$+0.32 \pm 0.65$	0.843 ± 0.007	2.0 (1.2)	208.54 ± 0.22	$+0.17 \pm 0.43$	0.897 ± 0.007	1.4 (1.3)
238.34 ± 0.67	$+0.64 \pm 1.08$	0.841 ± 0.009	1.7 (1.3)	238.03 ± 0.22	$+0.43 \pm 0.43$	0.896 ± 0.010	1.5 (1.1)
269.90 ± 0.44	$+0.30 \pm 0.85$	0.843 ± 0.007	1.9 (0.9)	269.96 ± 0.44	-0.24 ± 0.85	0.891 ± 0.009	1.7 (0.5)
301.20 ± 0.44	-1.15 ± 0.85	0.858 ± 0.014	2.8 (1.1)	301.69 ± 0.22	-0.53 ± 0.43	0.891 ± 0.014	1.9 (0.9)
331.78 ± 0.22	-0.14 ± 0.63	0.855 ± 0.009	2.5 (0.9)	332.07 ± 0.22	$+0.14 \pm 0.43$	0.889 ± 0.014	1.4 (0.7)

Table 134: The nominal angle δ_n, average displacement $\Delta\delta$, average value of the parameter DIST, RMS of the ALPHA distribution for enabled GF and impact parameters between 60 m and 120 m. The RMS of the ALPHA distribution for disabled GF is given parentheses. The primary γ-ray energy was set to 1000 GeV, the ZA to 20° and the azimuth angle to 30°.

$E_\gamma = 1000$ GeV, Az = 30°, ZA = 20°, Hard Image Cleaning

δ_n[°]	$\Delta\delta$[°]	DIST[°]	RMS$_{\lvert ALPHA \rvert}$[°]	δ_n[°]	$\Delta\delta$[°]	DIST[°]	RMS$_{\lvert ALPHA \rvert}$[°]
IP = 60 m				IP = 80 m			
0.86 ± 0.67	-0.26 ± 1.48	0.624 ± 0.014	3.2 (1.5)	0.43 ± 0.44	-0.43 ± 1.06	0.755 ± 0.005	2.3 (1.3)
28.97 ± 0.89	-0.59 ± 1.50	0.604 ± 0.009	3.0 (3.1)	29.08 ± 0.44	$+0.54 \pm 0.85$	0.727 ± 0.012	2.3 (1.5)
58.79 ± 0.89	$+1.69 \pm 1.50$	0.598 ± 0.002	3.6 (3.6)	57.73 ± 0.67	$+0.24 \pm 1.28$	0.733 ± 0.002	2.5 (2.2)
89.28 ± 0.67	$+2.13 \pm 1.28$	0.602 ± 0.020	7.3 (2.2)	89.99 ± 0.44	$+1.39 \pm 1.06$	0.733 ± 0.009	3.6 (1.2)
122.33 ± 0.44	$+1.67 \pm 1.26$	0.621 ± 0.022	4.7 (2.0)	122.34 ± 0.44	$+1.54 \pm 1.26$	0.755 ± 0.002	3.7 (1.3)
151.76 ± 0.44	-0.01 ± 1.06	0.623 ± 0.003	3.8 (1.9)	151.90 ± 0.44	-0.09 ± 0.65	0.758 ± 0.002	3.1 (1.2)
179.33 ± 0.67	-2.47 ± 1.48	0.625 ± 0.007	3.3 (2.4)	180.24 ± 0.67	-0.24 ± 1.28	0.757 ± 0.012	2.3 (1.2)
208.41 ± 0.89	-0.75 ± 1.50	0.612 ± 0.010	3.6 (2.4)	208.83 ± 0.22	$+0.52 \pm 0.84$	0.739 ± 0.014	2.4 (1.6)
237.44 ± 0.22	$+0.90 \pm 0.84$	0.608 ± 0.003	3.8 (2.4)	237.45 ± 0.44	-0.20 ± 1.06	0.738 ± 0.002	2.3 (1.5)
268.90 ± 0.67	$+0.78 \pm 1.08$	0.619 ± 0.007	5.2 (2.1)	269.18 ± 0.67	-0.18 ± 1.08	0.743 ± 0.015	2.6 (1.9)
301.17 ± 0.89	-0.33 ± 1.71	0.632 ± 0.002	7.0 (3.1)	301.51 ± 0.67	-0.61 ± 1.28	0.761 ± 0.003	3.1 (1.4)
331.69 ± 0.67	-1.90 ± 1.28	0.626 ± 0.002	4.8 (3.2)	332.37 ± 0.22	-0.22 ± 0.84	0.759 ± 0.022	3.2 (1.5)
IP = 100 m				IP = 120 m			
0.24 ± 0.44	$+0.57 \pm 1.06$	0.850 ± 0.002	2.0 (1.1)	359.22 ± 0.22	-0.39 ± 0.63	0.892 ± 0.014	1.3 (0.6)
28.67 ± 0.22	$+0.71 \pm 0.63$	0.825 ± 0.002	1.7 (1.3)	28.78 ± 0.22	$+0.77 \pm 0.43$	0.882 ± 0.012	1.5 (0.5)
57.47 ± 0.44	$+0.13 \pm 0.85$	0.826 ± 0.014	2.4 (1.5)	57.67 ± 0.44	$+0.31 \pm 0.85$	0.879 ± 0.002	1.7 (1.2)
90.10 ± 0.44	$+0.24 \pm 0.85$	0.825 ± 0.015	2.8 (0.8)	90.47 ± 0.22	$+0.42 \pm 0.63$	0.879 ± 0.014	2.0 (1.3)
122.58 ± 0.44	$+0.76 \pm 1.06$	0.844 ± 0.012	2.1 (0.7)	122.74 ± 0.44	$+0.53 \pm 0.85$	0.883 ± 0.002	1.4 (0.8)
151.77 ± 0.22	-0.34 ± 0.63	0.851 ± 0.014	2.1 (0.6)	151.85 ± 0.22	-0.03 ± 0.43	0.885 ± 0.005	1.9 (0.8)
180.17 ± 0.44	-0.15 ± 0.85	0.853 ± 0.007	1.4 (1.4)	180.22 ± 0.44	$+0.69 \pm 0.85$	0.897 ± 0.005	1.3 (0.8)
208.63 ± 0.44	$+0.26 \pm 0.65$	0.836 ± 0.007	2.1 (1.3)	208.67 ± 0.22	$+0.06 \pm 0.43$	0.889 ± 0.007	1.5 (0.9)
238.02 ± 0.44	$+0.15 \pm 0.65$	0.835 ± 0.007	1.5 (1.1)	237.83 ± 0.44	$+0.15 \pm 0.85$	0.893 ± 0.014	1.6 (1.1)
270.00 ± 0.44	$+0.46 \pm 0.85$	0.834 ± 0.007	2.3 (1.0)	269.75 ± 0.44	-0.51 ± 0.85	0.885 ± 0.009	1.8 (0.8)
301.25 ± 0.44	-1.20 ± 0.85	0.854 ± 0.009	2.5 (1.2)	301.89 ± 0.22	-0.39 ± 0.63	0.885 ± 0.014	1.9 (1.1)
331.68 ± 0.22	-0.17 ± 0.84	0.848 ± 0.007	2.6 (1.1)	331.92 ± 0.22	-0.12 ± 0.43	0.881 ± 0.002	1.7 (0.7)

Table 135: The nominal angle δ_n, average displacement $\Delta\delta$, average value of the parameter DIST, RMS of the ALPHA distribution for enabled GF and impact parameters between 60 m and 120 m. The RMS of the ALPHA distribution for disabled GF is given parentheses. The primary γ-ray energy was set to 1000 GeV, the ZA to 20° and the azimuth angle to 30°.

$E_\gamma = 1000$ GeV, Az = 60°, ZA = 20°, Intermediate Image Cleaning

$\delta_n\,[°]$	$\Delta\delta\,[°]$	DIST[°]	RMS$_{\lvert ALPHA \rvert}$[°]	$\delta_n\,[°]$	$\Delta\delta\,[°]$	DIST[°]	RMS$_{\lvert ALPHA \rvert}$[°]
IP = 60 m				**IP = 80 m**			
1.31 ± 0.89	$+0.81 \pm 1.71$	0.628 ± 0.002	3.8 (1.9)	0.27 ± 0.67	-1.13 ± 1.28	0.769 ± 0.005	2.9 (1.8)
28.82 ± 1.11	-2.26 ± 1.52	0.625 ± 0.003	3.1 (3.7)	28.68 ± 0.67	-1.39 ± 1.08	0.761 ± 0.007	4.6 (1.6)
58.76 ± 1.33	-1.06 ± 2.15	0.625 ± 0.005	4.7 (3.5)	57.49 ± 0.67	-1.53 ± 1.28	0.764 ± 0.017	3.4 (2.3)
89.38 ± 0.89	$+1.04 \pm 1.30$	0.643 ± 0.007	6.9 (2.6)	90.40 ± 0.44	$+0.81 \pm 1.06$	0.783 ± 0.012	3.4 (1.1)
121.81 ± 0.67	$+1.32 \pm 1.28$	0.650 ± 0.003	9.4 (1.9)	121.89 ± 0.44	$+0.45 \pm 0.65$	0.784 ± 0.005	5.5 (2.0)
151.36 ± 0.67	$+0.24 \pm 1.69$	0.644 ± 0.014	5.5 (2.0)	151.95 ± 0.44	$+0.57 \pm 0.85$	0.779 ± 0.003	4.8 (1.3)
179.41 ± 0.67	-4.13 ± 1.28	0.632 ± 0.014	3.6 (2.7)	180.25 ± 0.67	$+1.20 \pm 1.08$	0.765 ± 0.009	2.9 (1.2)
208.00 ± 0.89	-2.81 ± 1.71	0.626 ± 0.002	3.5 (2.3)	208.75 ± 0.22	-1.12 ± 0.43	0.758 ± 0.007	2.4 (1.7)
237.70 ± 1.11	-1.89 ± 1.72	0.637 ± 0.002	4.7 (2.4)	237.62 ± 0.44	-1.37 ± 1.06	0.770 ± 0.005	4.5 (1.9)
269.33 ± 0.67	$+0.81 \pm 1.08$	0.655 ± 0.002	5.4 (2.2)	269.06 ± 0.67	-0.11 ± 1.08	0.783 ± 0.005	9.6 (2.2)
301.07 ± 0.67	$+2.69 \pm 1.48$	0.656 ± 0.002	6.0 (2.7)	301.28 ± 0.44	$+1.36 \pm 0.85$	0.791 ± 0.005	6.2 (2.0)
331.97 ± 0.67	$+2.26 \pm 1.48$	0.650 ± 0.005	5.5 (2.8)	332.59 ± 0.44	$+0.14 \pm 0.65$	0.784 ± 0.003	3.5 (1.5)
IP = 100 m				**IP = 120 m**			
0.16 ± 0.44	-0.65 ± 0.85	0.860 ± 0.003	2.5 (0.9)	359.28 ± 0.22	-1.01 ± 0.63	0.918 ± 0.007	1.5 (0.8)
28.70 ± 0.22	-1.07 ± 0.63	0.858 ± 0.005	1.7 (1.5)	28.92 ± 0.22	-0.25 ± 0.43	0.918 ± 0.005	2.2 (0.6)
57.64 ± 0.89	-0.74 ± 1.50	0.863 ± 0.003	2.1 (1.7)	57.76 ± 0.22	-0.37 ± 0.43	0.918 ± 0.002	2.8 (1.2)
90.47 ± 0.44	$+0.02 \pm 0.85$	0.875 ± 0.003	3.6 (1.2)	90.66 ± 0.22	$+0.86 \pm 0.63$	0.912 ± 0.009	1.8 (1.0)
122.35 ± 0.44	$+1.06 \pm 0.85$	0.880 ± 0.003	3.7 (1.1)	122.52 ± 0.44	$+0.63 \pm 0.85$	0.914 ± 0.002	2.1 (0.9)
151.91 ± 0.44	$+0.80 \pm 0.65$	0.879 ± 0.003	3.2 (0.6)	151.88 ± 0.22	$+0.26 \pm 0.43$	0.923 ± 0.002	1.8 (0.6)
180.36 ± 0.44	$+1.00 \pm 0.85$	0.875 ± 0.007	2.7 (1.1)	180.63 ± 0.44	$+0.56 \pm 0.85$	0.922 ± 0.002	1.6 (0.7)
208.56 ± 0.44	-0.21 ± 0.65	0.864 ± 0.005	2.0 (1.2)	208.54 ± 0.22	$+0.46 \pm 0.43$	0.924 ± 0.012	1.4 (1.3)
238.34 ± 0.67	$+0.13 \pm 0.87$	0.869 ± 0.005	3.9 (1.3)	238.03 ± 0.22	$+0.32 \pm 0.43$	0.924 ± 0.007	2.0 (1.1)
269.90 ± 0.44	$+0.62 \pm 0.85$	0.878 ± 0.003	2.5 (0.9)	269.96 ± 0.44	$+0.33 \pm 0.65$	0.917 ± 0.003	2.2 (0.5)
301.20 ± 0.44	$+0.45 \pm 1.06$	0.880 ± 0.007	3.8 (1.1)	301.69 ± 0.22	-0.49 ± 0.63	0.914 ± 0.015	2.0 (0.9)
331.78 ± 0.22	-0.06 ± 0.84	0.879 ± 0.002	2.9 (0.9)	332.07 ± 0.22	-0.43 ± 0.43	0.918 ± 0.007	1.6 (0.7)

Table 136: The nominal angle δ_n, average displacement $\Delta\delta$, average value of the parameter DIST, RMS of the ALPHA distribution for enabled GF and impact parameters between 60 m and 120 m. The RMS of the ALPHA distribution for disabled GF is given parentheses. The primary γ-ray energy was set to 1000 GeV, the ZA to 20° and the azimuth angle to 60°.

$E_\gamma = 1000$ GeV, Az = 60°, ZA = 20°, Hard Image Cleaning

$\delta_n\,[°]$	$\Delta\delta\,[°]$	DIST[°]	RMS$_{\lvert ALPHA \rvert}$[°]	$\delta_n\,[°]$	$\Delta\delta\,[°]$	DIST[°]	RMS$_{\lvert ALPHA \rvert}$[°]
IP = 60 m				**IP = 80 m**			
0.86 ± 0.67	$+0.35 \pm 1.08$	0.622 ± 0.007	3.8 (1.5)	0.43 ± 0.44	-0.59 ± 1.06	0.763 ± 0.005	3.0 (1.3)
28.97 ± 0.89	-2.07 ± 1.30	0.620 ± 0.009	2.8 (3.1)	29.08 ± 0.44	-1.04 ± 0.85	0.757 ± 0.009	2.3 (1.5)
58.79 ± 0.89	-0.69 ± 1.50	0.617 ± 0.005	4.7 (3.6)	57.73 ± 0.67	-0.93 ± 1.28	0.756 ± 0.015	3.0 (2.2)
89.28 ± 0.67	-0.63 ± 1.08	0.636 ± 0.002	6.3 (2.2)	89.99 ± 0.44	-0.09 ± 0.85	0.777 ± 0.002	2.8 (1.2)
122.33 ± 0.44	$+2.09 \pm 1.26$	0.641 ± 0.007	7.4 (2.0)	122.34 ± 0.44	$+0.99 \pm 1.06$	0.777 ± 0.009	4.8 (1.3)
151.76 ± 0.44	$+1.04 \pm 1.47$	0.637 ± 0.002	5.6 (1.9)	151.90 ± 0.44	$+0.88 \pm 0.85$	0.774 ± 0.002	4.5 (1.2)
179.33 ± 0.67	-3.27 ± 1.08	0.625 ± 0.002	3.8 (2.4)	180.24 ± 0.67	$+1.20 \pm 1.28$	0.759 ± 0.002	3.1 (1.2)
208.41 ± 0.89	-2.54 ± 1.50	0.620 ± 0.007	3.0 (2.4)	208.83 ± 0.22	-0.82 ± 0.63	0.753 ± 0.003	2.5 (1.6)
237.44 ± 0.22	-2.08 ± 1.04	0.631 ± 0.002	4.5 (2.4)	237.45 ± 0.44	-1.71 ± 1.06	0.762 ± 0.005	4.7 (1.5)
268.90 ± 0.67	$+0.09 \pm 1.08$	0.647 ± 0.014	5.7 (2.1)	269.18 ± 0.67	-0.19 ± 1.08	0.778 ± 0.009	7.9 (1.9)
301.17 ± 0.89	$+2.44 \pm 1.30$	0.649 ± 0.003	5.1 (3.1)	301.51 ± 0.67	$+1.41 \pm 0.87$	0.783 ± 0.002	6.1 (1.4)
331.69 ± 0.67	$+3.04 \pm 1.28$	0.641 ± 0.002	5.4 (3.2)	332.37 ± 0.22	$+0.24 \pm 0.43$	0.779 ± 0.002	3.3 (1.5)
IP = 100 m				**IP = 120 m**			
0.24 ± 0.44	-0.42 ± 0.85	0.855 ± 0.009	2.1 (1.1)	359.22 ± 0.22	-0.95 ± 0.63	0.913 ± 0.007	1.4 (0.6)
28.67 ± 0.22	-0.76 ± 0.63	0.855 ± 0.024	1.7 (1.3)	28.78 ± 0.22	-0.24 ± 0.43	0.913 ± 0.002	2.2 (0.5)
57.47 ± 0.44	-0.74 ± 0.65	0.855 ± 0.002	2.0 (1.5)	57.67 ± 0.44	-0.47 ± 0.65	0.912 ± 0.003	2.9 (1.2)
90.10 ± 0.44	-0.29 ± 0.85	0.872 ± 0.002	3.4 (0.8)	90.47 ± 0.22	$+0.82 \pm 0.63$	0.910 ± 0.009	1.8 (1.3)
122.58 ± 0.44	$+1.13 \pm 1.06$	0.873 ± 0.002	5.3 (0.7)	122.74 ± 0.44	$+0.77 \pm 1.06$	0.906 ± 0.009	2.2 (0.8)
151.77 ± 0.22	$+0.73 \pm 0.63$	0.876 ± 0.002	3.0 (0.6)	151.85 ± 0.22	$+0.30 \pm 0.43$	0.918 ± 0.012	2.2 (0.8)
180.17 ± 0.44	$+0.89 \pm 0.85$	0.867 ± 0.009	2.6 (1.4)	180.22 ± 0.44	$+0.07 \pm 0.85$	0.916 ± 0.012	1.7 (0.8)
208.63 ± 0.44	-0.26 ± 1.06	0.860 ± 0.005	2.0 (1.3)	208.67 ± 0.22	$+0.73 \pm 0.43$	0.920 ± 0.015	1.4 (0.9)
238.02 ± 0.44	-0.25 ± 0.65	0.862 ± 0.005	3.8 (1.1)	237.83 ± 0.44	$+0.09 \pm 0.85$	0.918 ± 0.003	2.0 (1.1)
270.00 ± 0.44	$+0.44 \pm 0.85$	0.875 ± 0.010	2.8 (1.0)	269.75 ± 0.44	$+0.30 \pm 0.65$	0.913 ± 0.003	3.2 (0.8)
301.25 ± 0.44	$+0.30 \pm 0.85$	0.875 ± 0.014	3.5 (1.2)	301.89 ± 0.22	-0.73 ± 0.63	0.908 ± 0.015	1.9 (1.1)
331.68 ± 0.22	$+0.41 \pm 0.84$	0.876 ± 0.007	2.9 (1.1)	331.92 ± 0.22	-0.58 ± 0.63	0.916 ± 0.007	1.6 (0.7)

Table 137: The nominal angle δ_n, average displacement $\Delta\delta$, average value of the parameter DIST, RMS of the ALPHA distribution for enabled GF and impact parameters between 60 m and 120 m. The RMS of the ALPHA distribution for disabled GF is given parentheses. The primary γ-ray energy was set to 1000 GeV, the ZA to 20° and the azimuth angle to 60°.

$E_\gamma = 1000$ GeV, Az = 90°, ZA = 20°, Intermediate Image Cleaning

δ_n[°]	$\Delta\delta$[°]	DIST[°]	RMS$_{\lvert ALPHA\rvert}$[°]	δ_n[°]	$\Delta\delta$[°]	DIST[°]	RMS$_{\lvert ALPHA\rvert}$[°]
IP = 60 m				IP = 80 m			
1.31 ± 0.89	$+4.28 \pm 1.29$	0.616 ± 0.020	4.2 (1.9)	0.27 ± 0.67	$+2.01 \pm 1.07$	0.750 ± 0.002	1.8 (1.8)
28.82 ± 1.11	-1.47 ± 2.32	0.620 ± 0.002	2.8 (3.7)	28.68 ± 0.67	-0.73 ± 1.27	0.756 ± 0.002	2.5 (1.6)
58.76 ± 1.33	-1.23 ± 2.54	0.641 ± 0.002	6.7 (3.5)	57.49 ± 0.67	-1.83 ± 1.27	0.777 ± 0.002	4.1 (2.3)
89.38 ± 0.89	-2.19 ± 1.70	0.645 ± 0.007	4.8 (2.6)	90.40 ± 0.44	-0.02 ± 0.85	0.786 ± 0.007	3.1 (1.1)
121.81 ± 0.67	$+1.82 \pm 1.27$	0.645 ± 0.025	5.3 (1.9)	121.89 ± 0.44	$+1.42 \pm 0.85$	0.777 ± 0.003	3.7 (2.0)
151.36 ± 0.67	$+3.24 \pm 1.07$	0.625 ± 0.002	4.6 (2.0)	151.95 ± 0.44	$+1.61 \pm 1.05$	0.760 ± 0.002	3.3 (1.3)
179.41 ± 0.67	$+0.56 \pm 1.27$	0.619 ± 0.008	3.0 (2.7)	180.25 ± 0.67	$+0.85 \pm 1.47$	0.754 ± 0.002	2.0 (1.2)
208.00 ± 0.89	-4.10 ± 1.49	0.625 ± 0.010	2.4 (2.3)	208.75 ± 0.22	-2.04 ± 0.83	0.760 ± 0.005	1.7 (1.7)
237.70 ± 1.11	-5.14 ± 2.12	0.644 ± 0.002	6.3 (2.4)	237.62 ± 0.44	-2.92 ± 0.65	0.779 ± 0.002	3.4 (1.9)
269.33 ± 0.67	-2.77 ± 0.87	0.644 ± 0.002	6.2 (2.2)	269.06 ± 0.67	-2.20 ± 1.27	0.780 ± 0.013	4.4 (2.2)
301.07 ± 0.67	$+0.61 \pm 1.27$	0.639 ± 0.010	7.3 (2.7)	301.28 ± 0.44	$+0.21 \pm 1.05$	0.773 ± 0.005	3.2 (2.0)
331.97 ± 0.67	$+3.85 \pm 1.88$	0.617 ± 0.002	4.4 (2.8)	332.59 ± 0.44	$+3.00 \pm 1.45$	0.755 ± 0.017	2.9 (1.5)
IP = 100 m				IP = 120 m			
0.16 ± 0.44	$+1.27 \pm 0.85$	0.849 ± 0.012	1.4 (0.9)	359.28 ± 0.22	-0.29 ± 0.63	0.913 ± 0.007	1.0 (0.8)
28.70 ± 0.22	-0.00 ± 0.42	0.853 ± 0.003	1.6 (1.5)	28.92 ± 0.22	$+0.63 \pm 0.63$	0.916 ± 0.007	1.2 (0.6)
57.64 ± 0.89	-1.03 ± 1.29	0.867 ± 0.013	2.0 (1.7)	57.76 ± 0.22	-0.01 ± 0.83	0.919 ± 0.002	1.2 (1.2)
90.47 ± 0.44	$+0.71 \pm 0.85$	0.874 ± 0.010	2.0 (1.2)	90.66 ± 0.22	$+0.51 \pm 0.63$	0.912 ± 0.013	1.5 (1.0)
122.35 ± 0.44	$+0.96 \pm 1.05$	0.870 ± 0.010	1.9 (1.1)	122.52 ± 0.44	$+0.53 \pm 1.05$	0.910 ± 0.002	1.4 (0.9)
151.91 ± 0.44	$+0.67 \pm 1.05$	0.859 ± 0.005	2.8 (0.6)	151.88 ± 0.22	$+0.89 \pm 0.83$	0.916 ± 0.015	2.1 (0.6)
180.36 ± 0.44	$+0.34 \pm 1.05$	0.853 ± 0.003	1.7 (1.1)	180.63 ± 0.44	$+0.25 \pm 1.05$	0.916 ± 0.003	1.2 (0.7)
208.56 ± 0.44	-0.68 ± 1.05	0.860 ± 0.024	1.7 (1.2)	208.54 ± 0.22	-0.18 ± 0.42	0.918 ± 0.013	1.4 (1.3)
238.34 ± 0.67	-1.52 ± 0.87	0.873 ± 0.002	2.0 (1.3)	238.03 ± 0.22	-0.44 ± 0.63	0.917 ± 0.012	1.3 (1.1)
269.90 ± 0.44	-0.64 ± 0.85	0.872 ± 0.012	2.3 (0.9)	269.96 ± 0.44	-0.14 ± 0.85	0.903 ± 0.012	1.3 (0.5)
301.20 ± 0.44	-0.14 ± 1.05	0.868 ± 0.008	1.4 (1.1)	301.69 ± 0.22	-0.54 ± 0.63	0.906 ± 0.010	1.3 (0.9)
331.78 ± 0.22	$+0.52 \pm 0.63$	0.857 ± 0.005	2.8 (0.9)	332.07 ± 0.22	$+0.30 \pm 0.63$	0.912 ± 0.008	1.2 (0.7)

Table 138: The nominal angle δ_n, average displacement $\Delta\delta$, average value of the parameter DIST, RMS of the ALPHA distribution for enabled GF and impact parameters between 60 m and 120 m. The RMS of the ALPHA distribution for disabled GF is given parentheses. The primary γ-ray energy was set to 1000 GeV, the ZA to 20° and the azimuth angle to 90°.

$E_\gamma = 1000$ GeV, Az = 90°, ZA = 20°, Hard Image Cleaning

δ_n[°]	$\Delta\delta$[°]	DIST[°]	RMS$_{\lvert ALPHA\rvert}$[°]	δ_n[°]	$\Delta\delta$[°]	DIST[°]	RMS$_{\lvert ALPHA\rvert}$[°]
IP = 60 m				IP = 80 m			
0.86 ± 0.67	$+3.55 \pm 1.07$	0.607 ± 0.013	3.4 (1.5)	0.43 ± 0.44	$+2.53 \pm 0.85$	0.745 ± 0.002	1.9 (1.3)
28.97 ± 0.89	-0.58 ± 1.90	0.612 ± 0.003	2.3 (3.1)	29.08 ± 0.44	-0.19 ± 1.05	0.749 ± 0.003	2.3 (1.5)
58.79 ± 0.89	-1.05 ± 1.70	0.635 ± 0.020	6.0 (3.6)	57.73 ± 0.67	-1.57 ± 0.87	0.771 ± 0.005	3.6 (2.2)
89.28 ± 0.67	-1.79 ± 1.47	0.639 ± 0.017	5.9 (2.2)	89.99 ± 0.44	-0.41 ± 0.85	0.780 ± 0.003	2.9 (1.2)
122.33 ± 0.44	$+1.98 \pm 1.05$	0.638 ± 0.025	5.8 (2.0)	122.34 ± 0.44	$+1.06 \pm 0.85$	0.771 ± 0.005	3.6 (1.3)
151.76 ± 0.44	$+3.31 \pm 0.65$	0.620 ± 0.002	4.2 (1.9)	151.90 ± 0.44	$+1.24 \pm 1.05$	0.754 ± 0.005	3.0 (1.2)
179.33 ± 0.67	$+0.80 \pm 1.07$	0.613 ± 0.002	2.5 (2.4)	180.24 ± 0.67	$+0.62 \pm 1.47$	0.750 ± 0.005	2.0 (1.2)
208.41 ± 0.89	-3.35 ± 1.29	0.618 ± 0.005	2.0 (2.4)	208.83 ± 0.22	-1.96 ± 0.83	0.755 ± 0.002	1.9 (1.6)
237.44 ± 0.22	-5.33 ± 1.03	0.635 ± 0.020	7.4 (2.4)	237.45 ± 0.44	-2.96 ± 0.85	0.773 ± 0.007	3.2 (1.5)
268.90 ± 0.67	-2.84 ± 1.27	0.635 ± 0.003	4.6 (2.1)	269.18 ± 0.67	-2.18 ± 1.07	0.774 ± 0.007	4.1 (1.9)
301.17 ± 0.89	$+0.43 \pm 1.29$	0.631 ± 0.002	5.2 (3.1)	301.51 ± 0.67	$+0.32 \pm 1.07$	0.765 ± 0.017	2.1 (1.4)
331.69 ± 0.67	$+4.26 \pm 1.68$	0.610 ± 0.002	3.6 (3.2)	332.37 ± 0.22	$+2.46 \pm 0.42$	0.749 ± 0.002	2.9 (1.5)
IP = 100 m				IP = 120 m			
0.24 ± 0.44	$+1.28 \pm 0.85$	0.845 ± 0.013	1.4 (1.1)	359.22 ± 0.22	-0.32 ± 0.63	0.908 ± 0.008	0.9 (0.6)
28.67 ± 0.22	-0.03 ± 0.42	0.846 ± 0.005	1.4 (1.3)	28.78 ± 0.22	$+0.55 \pm 0.42$	0.910 ± 0.008	1.3 (0.5)
57.47 ± 0.44	-1.10 ± 0.65	0.862 ± 0.012	1.9 (1.5)	57.67 ± 0.44	$+0.27 \pm 0.85$	0.916 ± 0.002	1.5 (1.2)
90.10 ± 0.44	$+0.11 \pm 0.85$	0.869 ± 0.005	2.1 (0.8)	90.47 ± 0.22	$+0.41 \pm 0.63$	0.905 ± 0.012	1.4 (1.3)
122.58 ± 0.44	$+1.07 \pm 0.85$	0.867 ± 0.010	1.9 (0.7)	122.74 ± 0.44	$+0.73 \pm 0.85$	0.908 ± 0.002	1.3 (0.8)
151.77 ± 0.22	$+0.74 \pm 0.63$	0.853 ± 0.003	2.3 (0.6)	151.85 ± 0.22	$+0.64 \pm 0.83$	0.910 ± 0.002	2.0 (0.8)
180.17 ± 0.44	$+0.38 \pm 0.85$	0.851 ± 0.002	1.6 (1.4)	180.22 ± 0.44	-0.02 ± 0.85	0.913 ± 0.015	1.3 (0.8)
208.63 ± 0.44	-0.56 ± 0.85	0.855 ± 0.025	1.5 (1.3)	208.67 ± 0.22	-0.13 ± 0.42	0.912 ± 0.005	1.5 (0.9)
238.02 ± 0.44	-1.62 ± 0.65	0.867 ± 0.015	1.7 (1.1)	237.83 ± 0.44	-0.69 ± 0.85	0.912 ± 0.012	1.4 (1.1)
270.00 ± 0.44	-0.52 ± 0.85	0.866 ± 0.008	1.9 (1.0)	269.75 ± 0.44	-0.31 ± 0.85	0.899 ± 0.012	1.4 (0.8)
301.25 ± 0.44	-0.42 ± 1.05	0.865 ± 0.008	1.3 (1.2)	301.89 ± 0.22	-0.66 ± 0.63	0.903 ± 0.007	1.2 (1.1)
331.68 ± 0.22	$+0.48 \pm 0.63$	0.851 ± 0.007	2.2 (1.1)	331.92 ± 0.22	$+0.20 \pm 0.42$	0.906 ± 0.008	0.9 (0.7)

Table 139: The nominal angle δ_n, average displacement $\Delta\delta$, average value of the parameter DIST, RMS of the ALPHA distribution for enabled GF and impact parameters between 60 m and 120 m. The RMS of the ALPHA distribution for disabled GF is given parentheses. The primary γ-ray energy was set to 1000 GeV, the ZA to 20° and the azimuth angle to 90°.

$E_\gamma = 1000\,\mathrm{GeV}$, Az = 120°, ZA = 20°, Intermediate Image Cleaning

$\delta_n[°]$	$\Delta\delta[°]$	DIST[°]	$\mathrm{RMS}_{\lvert\mathrm{ALPHA}\rvert}[°]$	$\delta_n[°]$	$\Delta\delta[°]$	DIST[°]	$\mathrm{RMS}_{\lvert\mathrm{ALPHA}\rvert}[°]$
IP = 60 m				**IP = 80 m**			
1.31 ± 0.89	$+5.16 \pm 1.47$	0.628 ± 0.006	3.6 (1.9)	0.27 ± 0.67	$+2.86 \pm 1.25$	0.757 ± 0.013	3.0 (1.8)
28.82 ± 1.11	$+2.68 \pm 1.70$	0.648 ± 0.016	3.7 (3.7)	28.68 ± 0.67	$+0.99 \pm 1.25$	0.769 ± 0.015	2.8 (1.6)
58.76 ± 1.33	-0.10 ± 2.11	0.651 ± 0.013	5.0 (3.5)	57.49 ± 0.67	-1.82 ± 1.25	0.774 ± 0.010	3.4 (2.3)
89.38 ± 0.89	-4.35 ± 1.08	0.647 ± 0.006	5.1 (2.6)	90.40 ± 0.44	-1.84 ± 0.83	0.772 ± 0.011	4.5 (1.1)
121.81 ± 0.67	-1.43 ± 1.45	0.636 ± 0.015	6.5 (1.9)	121.89 ± 0.44	-1.35 ± 1.03	0.757 ± 0.016	5.6 (2.0)
151.36 ± 0.67	$+0.49 \pm 1.64$	0.625 ± 0.005	5.6 (2.0)	151.95 ± 0.44	$+0.81 \pm 1.03$	0.755 ± 0.019	4.3 (1.3)
179.41 ± 0.67	$+2.05 \pm 1.25$	0.630 ± 0.006	3.8 (2.7)	180.25 ± 0.67	$+1.75 \pm 1.25$	0.759 ± 0.002	2.6 (1.2)
208.00 ± 0.89	-0.81 ± 1.86	0.641 ± 0.015	4.0 (2.3)	208.75 ± 0.22	$+0.85 \pm 0.61$	0.774 ± 0.013	3.0 (1.7)
237.70 ± 1.11	-3.06 ± 1.70	0.649 ± 0.005	7.0 (2.4)	237.62 ± 0.44	-2.17 ± 1.03	0.782 ± 0.008	5.7 (1.9)
269.33 ± 0.67	-3.74 ± 1.45	0.642 ± 0.005	7.9 (2.2)	269.06 ± 0.67	-1.99 ± 1.25	0.774 ± 0.010	4.9 (2.2)
301.07 ± 0.67	-0.69 ± 1.45	0.623 ± 0.008	10.7 (2.7)	301.28 ± 0.44	-0.29 ± 0.83	0.751 ± 0.010	4.7 (2.0)
331.97 ± 0.67	$+3.22 \pm 1.45$	0.624 ± 0.008	5.5 (2.8)	332.59 ± 0.44	$+2.64 \pm 0.83$	0.745 ± 0.002	3.3 (1.5)
IP = 100 m				**IP = 120 m**			
0.16 ± 0.44	$+1.92 \pm 0.83$	0.847 ± 0.015	2.3 (0.9)	359.28 ± 0.22	$+0.38 \pm 0.81$	0.902 ± 0.013	2.0 (0.8)
28.70 ± 0.22	$+0.71 \pm 0.42$	0.864 ± 0.015	2.0 (1.5)	28.92 ± 0.22	$+0.40 \pm 0.42$	0.911 ± 0.013	1.6 (0.6)
57.64 ± 0.89	-0.66 ± 1.47	0.868 ± 0.013	3.0 (1.7)	57.76 ± 0.22	-0.20 ± 0.61	0.907 ± 0.010	2.5 (1.2)
90.47 ± 0.44	-1.09 ± 1.03	0.864 ± 0.010	3.3 (1.2)	90.66 ± 0.22	-0.49 ± 0.81	0.900 ± 0.015	2.3 (1.0)
122.35 ± 0.44	-0.31 ± 0.83	0.852 ± 0.006	4.4 (1.1)	122.52 ± 0.44	-0.12 ± 0.83	0.903 ± 0.015	3.0 (0.9)
151.91 ± 0.44	$+0.46 \pm 1.03$	0.854 ± 0.002	4.0 (0.6)	151.88 ± 0.22	$+0.18 \pm 0.42$	0.908 ± 0.006	3.5 (0.6)
180.36 ± 0.44	$+1.33 \pm 0.83$	0.861 ± 0.015	2.5 (1.1)	180.63 ± 0.44	$+0.56 \pm 0.83$	0.920 ± 0.018	1.7 (0.7)
208.56 ± 0.44	$+0.67 \pm 1.03$	0.867 ± 0.008	2.8 (1.2)	208.54 ± 0.22	$+0.49 \pm 0.42$	0.922 ± 0.011	1.9 (1.3)
238.34 ± 0.67	$+0.00 \pm 1.25$	0.866 ± 0.002	5.0 (1.3)	238.03 ± 0.22	-0.14 ± 0.61	0.908 ± 0.002	3.7 (1.1)
269.90 ± 0.44	-1.19 ± 0.83	0.863 ± 0.013	3.4 (0.9)	269.96 ± 0.44	-0.01 ± 0.83	0.900 ± 0.003	2.4 (0.5)
301.20 ± 0.44	-1.12 ± 0.64	0.841 ± 0.003	3.8 (1.1)	301.69 ± 0.22	-0.74 ± 0.61	0.895 ± 0.003	2.6 (0.9)
331.78 ± 0.22	$+1.13 \pm 0.61$	0.847 ± 0.013	2.5 (0.9)	332.07 ± 0.22	$+1.07 \pm 0.42$	0.901 ± 0.010	2.2 (0.7)

Table 140: The nominal angle δ_n, average displacement $\Delta\delta$, average value of the parameter DIST, RMS of the ALPHA distribution for enabled GF and impact parameters between 60 m and 120 m. The RMS of the ALPHA distribution for disabled GF is given parentheses. The primary γ-ray energy was set to 1000 GeV, the ZA to 20° and the azimuth angle to 120°.

$E_\gamma = 1000\,\mathrm{GeV}$, Az = 120°, ZA = 20°, Hard Image Cleaning

$\delta_n[°]$	$\Delta\delta[°]$	DIST[°]	$\mathrm{RMS}_{\lvert\mathrm{ALPHA}\rvert}[°]$	$\delta_n[°]$	$\Delta\delta[°]$	DIST[°]	$\mathrm{RMS}_{\lvert\mathrm{ALPHA}\rvert}[°]$
IP = 60 m				**IP = 80 m**			
0.86 ± 0.67	$+4.64 \pm 1.25$	0.621 ± 0.003	3.6 (1.5)	0.43 ± 0.44	$+2.74 \pm 0.83$	0.750 ± 0.010	2.9 (1.3)
28.97 ± 0.89	$+2.65 \pm 1.28$	0.639 ± 0.008	3.1 (3.1)	29.08 ± 0.44	$+1.81 \pm 1.03$	0.763 ± 0.015	2.4 (1.5)
58.79 ± 0.89	$+0.11 \pm 1.67$	0.642 ± 0.015	4.6 (3.6)	57.73 ± 0.67	-1.27 ± 1.25	0.768 ± 0.011	3.5 (2.2)
89.28 ± 0.67	-4.10 ± 0.86	0.638 ± 0.005	5.3 (2.2)	89.99 ± 0.44	-2.18 ± 1.03	0.765 ± 0.005	4.8 (1.2)
122.33 ± 0.44	-0.27 ± 1.22	0.626 ± 0.008	6.9 (2.0)	122.34 ± 0.44	-0.44 ± 0.83	0.751 ± 0.016	5.2 (1.3)
151.76 ± 0.44	$+1.50 \pm 1.03$	0.619 ± 0.008	5.1 (1.9)	151.90 ± 0.44	$+0.71 \pm 0.83$	0.750 ± 0.021	4.6 (1.2)
179.33 ± 0.67	$+1.69 \pm 1.06$	0.623 ± 0.013	3.6 (2.4)	180.24 ± 0.67	$+1.68 \pm 1.06$	0.752 ± 0.002	2.8 (1.2)
208.41 ± 0.89	$+0.80 \pm 1.08$	0.636 ± 0.008	3.7 (2.4)	208.83 ± 0.22	$+0.52 \pm 0.81$	0.768 ± 0.006	2.6 (1.6)
237.44 ± 0.22	-3.05 ± 0.81	0.640 ± 0.011	6.2 (2.4)	237.45 ± 0.44	-2.23 ± 1.03	0.774 ± 0.008	5.3 (1.5)
268.90 ± 0.67	-3.99 ± 1.45	0.632 ± 0.006	7.4 (2.1)	269.18 ± 0.67	-1.93 ± 1.45	0.769 ± 0.010	4.4 (1.9)
301.17 ± 0.89	-0.60 ± 1.47	0.616 ± 0.008	9.8 (3.1)	301.51 ± 0.67	-0.25 ± 1.25	0.746 ± 0.005	5.0 (1.4)
331.69 ± 0.67	$+2.40 \pm 1.06$	0.617 ± 0.011	5.7 (3.2)	332.37 ± 0.22	$+2.32 \pm 0.61$	0.739 ± 0.011	3.3 (1.5)
IP = 100 m				**IP = 120 m**			
0.24 ± 0.44	$+1.79 \pm 1.03$	0.841 ± 0.016	2.4 (1.1)	359.22 ± 0.22	$+0.00 \pm 0.61$	0.898 ± 0.013	1.9 (0.6)
28.67 ± 0.22	$+1.02 \pm 0.42$	0.858 ± 0.015	1.9 (1.3)	28.78 ± 0.22	$+0.25 \pm 0.42$	0.909 ± 0.015	1.5 (0.5)
57.47 ± 0.44	-0.85 ± 0.83	0.859 ± 0.016	3.1 (1.5)	57.67 ± 0.44	-0.25 ± 1.03	0.900 ± 0.010	2.5 (1.2)
90.10 ± 0.44	-1.19 ± 0.83	0.860 ± 0.018	3.0 (0.8)	90.47 ± 0.22	-0.58 ± 0.81	0.896 ± 0.003	2.3 (1.3)
122.58 ± 0.44	-0.10 ± 0.83	0.847 ± 0.006	4.1 (0.7)	122.74 ± 0.44	-0.06 ± 0.83	0.898 ± 0.016	3.1 (0.8)
151.77 ± 0.22	$+0.37 \pm 0.42$	0.849 ± 0.003	3.6 (0.6)	151.85 ± 0.22	$+0.31 \pm 0.42$	0.905 ± 0.015	3.6 (0.8)
180.17 ± 0.44	$+1.16 \pm 0.83$	0.853 ± 0.008	2.5 (1.4)	180.22 ± 0.44	$+0.43 \pm 0.83$	0.914 ± 0.015	1.7 (0.8)
208.63 ± 0.44	$+0.66 \pm 1.03$	0.864 ± 0.015	2.5 (1.3)	208.67 ± 0.22	$+0.16 \pm 0.42$	0.917 ± 0.011	1.8 (0.9)
238.02 ± 0.44	-0.34 ± 1.03	0.861 ± 0.018	4.7 (1.1)	237.83 ± 0.44	-0.07 ± 0.83	0.902 ± 0.003	3.3 (1.1)
270.00 ± 0.44	-0.98 ± 0.83	0.858 ± 0.013	3.6 (1.0)	269.75 ± 0.44	-0.51 ± 0.83	0.896 ± 0.005	2.3 (0.8)
301.25 ± 0.44	-1.20 ± 0.64	0.837 ± 0.015	3.4 (1.2)	301.89 ± 0.22	-0.38 ± 0.61	0.887 ± 0.011	2.8 (1.1)
331.68 ± 0.22	$+1.14 \pm 0.61$	0.842 ± 0.015	2.5 (1.1)	331.92 ± 0.22	$+0.83 \pm 0.42$	0.896 ± 0.011	2.0 (0.7)

Table 141: The nominal angle δ_n, average displacement $\Delta\delta$, average value of the parameter DIST, RMS of the ALPHA distribution for enabled GF and impact parameters between 60 m and 120 m. The RMS of the ALPHA distribution for disabled GF is given parentheses. The primary γ-ray energy was set to 1000 GeV, the ZA to 20° and the azimuth angle to 120°.

$E_\gamma = 1000\,\mathrm{GeV}$, Az = 150°, ZA = 20°, Intermediate Image Cleaning

δ_n[°]	$\Delta\delta$[°]	DIST[°]	$\mathrm{RMS}_{\lvert\mathrm{ALPHA}\rvert}$[°]	δ_n[°]	$\Delta\delta$[°]	DIST[°]	$\mathrm{RMS}_{\lvert\mathrm{ALPHA}\rvert}$[°]
IP = 60 m				**IP = 80 m**			
1.31 ± 0.89	$+4.30 \pm 1.09$	0.621 ± 0.015	5.4 (1.9)	0.27 ± 0.67	$+1.73 \pm 1.26$	0.743 ± 0.015	2.3 (1.8)
28.82 ± 1.11	$+5.26 \pm 1.70$	0.635 ± 0.008	4.7 (3.7)	28.68 ± 0.67	$+1.30 \pm 1.26$	0.758 ± 0.003	3.7 (1.6)
58.76 ± 1.33	-0.39 ± 1.92	0.636 ± 0.007	7.4 (3.5)	57.49 ± 0.67	-1.89 ± 1.06	0.759 ± 0.008	5.3 (2.3)
89.38 ± 0.89	-8.76 ± 2.07	0.631 ± 0.010	10.0 (2.6)	90.40 ± 0.44	-2.79 ± 1.04	0.754 ± 0.015	6.8 (1.1)
121.81 ± 0.67	-3.24 ± 1.85	0.618 ± 0.008	10.1 (1.9)	121.89 ± 0.44	-2.02 ± 1.04	0.743 ± 0.007	7.9 (2.0)
151.36 ± 0.67	$+0.28 \pm 0.86$	0.627 ± 0.007	9.2 (2.0)	151.95 ± 0.44	$+1.02 \pm 1.04$	0.742 ± 0.002	4.1 (1.3)
179.41 ± 0.67	$+3.74 \pm 1.45$	0.631 ± 0.011	6.3 (2.7)	180.25 ± 0.67	$+2.89 \pm 1.45$	0.752 ± 0.007	3.9 (1.2)
208.00 ± 0.89	$+6.03 \pm 1.48$	0.626 ± 0.011	5.8 (2.3)	208.75 ± 0.22	$+2.79 \pm 0.62$	0.752 ± 0.005	4.0 (1.7)
237.70 ± 1.11	$+0.62 \pm 1.70$	0.617 ± 0.015	9.3 (2.4)	237.62 ± 0.44	$+1.60 \pm 0.84$	0.750 ± 0.013	4.9 (1.9)
269.33 ± 0.67	-3.50 ± 1.65	0.600 ± 0.011	12.4 (2.2)	269.06 ± 0.67	-3.73 ± 0.86	0.731 ± 0.015	10.7 (2.2)
301.07 ± 0.67	-3.95 ± 1.26	0.594 ± 0.005	12.1 (2.7)	301.28 ± 0.44	-3.25 ± 0.64	0.722 ± 0.023	8.5 (2.0)
331.97 ± 0.67	-2.55 ± 1.45	0.602 ± 0.013	6.3 (2.8)	332.59 ± 0.44	$+0.59 \pm 0.84$	0.725 ± 0.002	5.5 (1.5)
IP = 100 m				**IP = 120 m**			
0.16 ± 0.44	$+1.24 \pm 1.04$	0.846 ± 0.005	2.3 (0.9)	359.28 ± 0.22	-0.16 ± 0.62	0.904 ± 0.013	1.3 (0.8)
28.70 ± 0.22	$+0.92 \pm 0.62$	0.854 ± 0.015	3.1 (1.5)	28.92 ± 0.22	$+0.92 \pm 0.62$	0.898 ± 0.018	2.8 (0.6)
57.64 ± 0.89	-0.28 ± 1.48	0.854 ± 0.011	6.1 (1.7)	57.76 ± 0.22	-1.04 ± 0.81	0.896 ± 0.003	4.2 (1.2)
90.47 ± 0.44	-1.63 ± 1.04	0.848 ± 0.005	4.3 (1.2)	90.66 ± 0.22	-0.43 ± 0.62	0.889 ± 0.011	4.1 (1.0)
122.35 ± 0.44	-0.48 ± 0.84	0.838 ± 0.010	7.5 (1.1)	122.52 ± 0.44	$+0.66 \pm 0.84$	0.891 ± 0.005	4.2 (0.9)
151.91 ± 0.44	$+0.96 \pm 1.04$	0.842 ± 0.011	2.8 (0.6)	151.88 ± 0.22	$+1.21 \pm 0.42$	0.898 ± 0.016	4.9 (0.6)
180.36 ± 0.44	$+1.76 \pm 0.84$	0.853 ± 0.005	2.4 (1.1)	180.63 ± 0.44	$+1.36 \pm 0.84$	0.902 ± 0.015	3.4 (0.7)
208.56 ± 0.44	$+1.74 \pm 1.04$	0.847 ± 0.013	3.0 (1.2)	208.54 ± 0.22	$+1.15 \pm 0.62$	0.890 ± 0.015	2.5 (1.3)
238.34 ± 0.67	$+1.23 \pm 1.45$	0.846 ± 0.005	3.5 (1.3)	238.03 ± 0.22	$+0.34 \pm 0.62$	0.888 ± 0.015	3.2 (1.1)
269.90 ± 0.44	-1.46 ± 1.04	0.824 ± 0.005	6.9 (0.9)	269.96 ± 0.44	-0.69 ± 0.84	0.876 ± 0.003	7.7 (0.5)
301.20 ± 0.44	-2.46 ± 1.04	0.819 ± 0.003	7.4 (1.1)	301.69 ± 0.22	-1.29 ± 0.62	0.875 ± 0.008	8.8 (0.9)
331.78 ± 0.22	$+0.06 \pm 0.42$	0.821 ± 0.013	3.6 (0.9)	332.07 ± 0.22	$+0.64 \pm 0.42$	0.879 ± 0.003	3.2 (0.7)

Table 142: The nominal angle δ_n, average displacement $\Delta\delta$, average value of the parameter DIST, RMS of the ALPHA distribution for enabled GF and impact parameters between 60 m and 120 m. The RMS of the ALPHA distribution for disabled GF is given parentheses. The primary γ-ray energy was set to 1000 GeV, the ZA to 20° and the azimuth angle to 150°.

$E_\gamma = 1000\,\mathrm{GeV}$, Az = 150°, ZA = 20°, Hard Image Cleaning

δ_n[°]	$\Delta\delta$[°]	DIST[°]	$\mathrm{RMS}_{\lvert\mathrm{ALPHA}\rvert}$[°]	δ_n[°]	$\Delta\delta$[°]	DIST[°]	$\mathrm{RMS}_{\lvert\mathrm{ALPHA}\rvert}$[°]
IP = 60 m				**IP = 80 m**			
0.86 ± 0.67	$+4.08 \pm 1.65$	0.612 ± 0.007	5.1 (1.5)	0.43 ± 0.44	$+1.78 \pm 1.04$	0.738 ± 0.007	2.3 (1.3)
28.97 ± 0.89	$+5.44 \pm 1.48$	0.626 ± 0.015	4.4 (3.1)	29.08 ± 0.44	$+1.69 \pm 1.23$	0.752 ± 0.003	3.4 (1.5)
58.79 ± 0.89	-0.58 ± 1.48	0.628 ± 0.011	6.9 (3.6)	57.73 ± 0.67	-0.89 ± 1.26	0.753 ± 0.007	5.4 (2.2)
89.28 ± 0.67	-7.64 ± 1.65	0.620 ± 0.002	9.7 (2.2)	89.99 ± 0.44	-2.61 ± 1.04	0.744 ± 0.007	6.8 (1.2)
122.33 ± 0.44	-2.68 ± 1.23	0.605 ± 0.008	9.9 (2.0)	122.34 ± 0.44	-1.39 ± 0.84	0.737 ± 0.005	7.3 (1.3)
151.76 ± 0.44	$+0.57 \pm 1.04$	0.620 ± 0.005	8.7 (1.9)	151.90 ± 0.44	$+0.85 \pm 0.64$	0.739 ± 0.003	4.7 (1.2)
179.33 ± 0.67	$+1.87 \pm 1.45$	0.626 ± 0.003	5.8 (2.4)	180.24 ± 0.67	$+2.71 \pm 1.45$	0.746 ± 0.007	3.2 (1.2)
208.41 ± 0.89	$+6.12 \pm 1.48$	0.618 ± 0.002	5.5 (2.4)	208.83 ± 0.22	$+2.98 \pm 0.42$	0.746 ± 0.003	3.8 (1.6)
237.44 ± 0.22	$+1.76 \pm 0.62$	0.611 ± 0.003	9.0 (2.4)	237.45 ± 0.44	$+1.17 \pm 1.63$	0.745 ± 0.015	4.9 (1.5)
268.90 ± 0.67	-1.80 ± 1.26	0.594 ± 0.003	11.7 (2.1)	269.18 ± 0.67	-3.53 ± 1.26	0.724 ± 0.016	10.1 (1.9)
301.17 ± 0.89	-4.37 ± 1.68	0.585 ± 0.005	10.6 (3.1)	301.51 ± 0.67	-2.34 ± 1.26	0.718 ± 0.026	6.8 (1.4)
331.69 ± 0.67	-2.74 ± 1.45	0.593 ± 0.013	5.9 (3.2)	332.37 ± 0.22	-0.02 ± 0.62	0.719 ± 0.005	5.0 (1.5)
IP = 100 m				**IP = 120 m**			
0.24 ± 0.44	$+0.72 \pm 0.84$	0.841 ± 0.008	2.0 (1.1)	359.22 ± 0.22	-0.21 ± 0.62	0.899 ± 0.013	1.2 (0.6)
28.67 ± 0.22	$+1.31 \pm 0.81$	0.845 ± 0.008	2.8 (1.3)	28.78 ± 0.22	$+0.68 \pm 0.62$	0.890 ± 0.002	3.0 (0.5)
57.47 ± 0.44	-0.10 ± 0.84	0.848 ± 0.013	5.9 (1.5)	57.67 ± 0.44	-0.97 ± 0.84	0.891 ± 0.007	4.0 (1.2)
90.10 ± 0.44	-1.31 ± 1.04	0.840 ± 0.002	4.4 (0.8)	90.47 ± 0.22	-0.36 ± 0.62	0.882 ± 0.013	4.2 (1.3)
122.58 ± 0.44	-0.19 ± 0.64	0.831 ± 0.023	5.1 (0.7)	122.74 ± 0.44	$+0.87 \pm 0.84$	0.884 ± 0.003	3.1 (0.8)
151.77 ± 0.22	$+1.16 \pm 0.42$	0.835 ± 0.002	2.9 (0.6)	151.85 ± 0.22	$+2.14 \pm 0.42$	0.892 ± 0.007	4.7 (0.8)
180.17 ± 0.44	$+1.56 \pm 0.84$	0.847 ± 0.005	2.2 (1.4)	180.22 ± 0.44	$+0.86 \pm 0.84$	0.898 ± 0.013	3.4 (0.8)
208.63 ± 0.44	$+2.11 \pm 1.04$	0.841 ± 0.011	2.7 (1.3)	208.67 ± 0.22	$+1.17 \pm 0.62$	0.883 ± 0.013	2.2 (0.9)
238.02 ± 0.44	$+0.96 \pm 1.43$	0.839 ± 0.002	3.6 (1.1)	237.83 ± 0.44	-0.10 ± 1.04	0.885 ± 0.015	2.8 (1.1)
270.00 ± 0.44	-0.64 ± 0.84	0.817 ± 0.013	7.4 (1.0)	269.75 ± 0.44	-0.11 ± 1.04	0.869 ± 0.002	7.3 (0.8)
301.25 ± 0.44	-2.14 ± 0.84	0.816 ± 0.016	6.2 (1.2)	301.89 ± 0.22	-0.99 ± 0.62	0.872 ± 0.003	8.4 (1.1)
331.68 ± 0.22	-0.53 ± 0.42	0.818 ± 0.011	5.3 (1.1)	331.92 ± 0.22	$+0.53 \pm 0.42$	0.874 ± 0.013	3.1 (0.7)

Table 143: The nominal angle δ_n, average displacement $\Delta\delta$, average value of the parameter DIST, RMS of the ALPHA distribution for enabled GF and impact parameters between 60 m and 120 m. The RMS of the ALPHA distribution for disabled GF is given parentheses. The primary γ-ray energy was set to 1000 GeV, the ZA to 20° and the azimuth angle to 150°.

$E_\gamma = 1000\,\mathrm{GeV}$, Az $= 180°$, ZA $= 20°$, Intermediate Image Cleaning

$\delta_n\,[°]$	$\Delta\delta\,[°]$	DIST[°]	$\mathrm{RMS}_{\lvert\mathrm{ALPHA}\rvert}\,[°]$	$\delta_n\,[°]$	$\Delta\delta\,[°]$	DIST[°]	$\mathrm{RMS}_{\lvert\mathrm{ALPHA}\rvert}\,[°]$
IP = 60 m				IP = 80 m			
1.31 ± 0.89	$+0.86 \pm 1.28$	0.622 ± 0.008	1.4 (1.9)	0.27 ± 0.67	$+0.03 \pm 1.06$	0.759 ± 0.008	1.4 (1.8)
28.82 ± 1.11	$+3.23 \pm 1.50$	0.619 ± 0.002	1.5 (3.7)	28.68 ± 0.67	$+2.57 \pm 1.06$	0.755 ± 0.002	1.9 (1.6)
58.76 ± 1.33	$+9.01 \pm 1.92$	0.606 ± 0.006	2.6 (3.5)	57.49 ± 0.67	$+3.35 \pm 0.86$	0.742 ± 0.002	2.1 (2.3)
89.38 ± 0.89	-2.01 ± 1.67	0.605 ± 0.010	15.9 (2.6)	90.40 ± 0.44	-0.42 ± 1.03	0.738 ± 0.006	4.6 (1.1)
121.81 ± 0.67	-4.44 ± 1.64	0.613 ± 0.008	8.3 (1.9)	121.89 ± 0.44	-2.07 ± 1.22	0.749 ± 0.013	6.3 (2.0)
151.36 ± 0.67	-2.75 ± 1.25	0.623 ± 0.021	6.5 (2.0)	151.95 ± 0.44	-1.19 ± 0.64	0.754 ± 0.006	4.1 (1.3)
179.41 ± 0.67	$+0.05 \pm 1.45$	0.618 ± 0.002	2.9 (2.7)	180.25 ± 0.67	$+1.09 \pm 1.06$	0.754 ± 0.023	1.8 (1.2)
208.00 ± 0.89	$+3.36 \pm 1.08$	0.615 ± 0.002	1.6 (2.3)	208.75 ± 0.22	$+1.95 \pm 0.61$	0.745 ± 0.002	0.6 (1.7)
237.70 ± 1.11	$+4.17 \pm 1.89$	0.598 ± 0.008	1.4 (2.4)	237.62 ± 0.44	$+1.88 \pm 1.22$	0.726 ± 0.002	2.8 (1.9)
269.33 ± 0.67	-6.29 ± 1.25	0.595 ± 0.003	19.7 (2.2)	269.06 ± 0.67	-0.88 ± 1.25	0.723 ± 0.021	11.0 (2.2)
301.07 ± 0.67	-3.78 ± 1.64	0.601 ± 0.024	10.6 (2.7)	301.28 ± 0.44	-4.85 ± 1.03	0.729 ± 0.005	5.8 (2.0)
331.97 ± 0.67	-4.04 ± 1.25	0.618 ± 0.002	4.9 (2.8)	332.59 ± 0.44	-2.21 ± 1.03	0.751 ± 0.006	2.7 (1.5)
IP = 100 m				IP = 120 m			
0.16 ± 0.44	$+0.36 \pm 0.83$	0.845 ± 0.010	1.2 (0.9)	359.28 ± 0.22	-0.57 ± 0.61	0.888 ± 0.019	0.9 (0.8)
28.70 ± 0.22	$+2.02 \pm 0.61$	0.843 ± 0.005	1.0 (1.5)	28.92 ± 0.22	$+1.29 \pm 0.42$	0.891 ± 0.011	0.8 (0.6)
57.64 ± 0.89	$+1.93 \pm 1.47$	0.833 ± 0.002	1.5 (1.7)	57.76 ± 0.22	$+1.11 \pm 0.61$	0.878 ± 0.002	1.3 (1.2)
90.47 ± 0.44	$+0.32 \pm 0.83$	0.829 ± 0.002	3.7 (1.2)	90.66 ± 0.22	$+0.82 \pm 0.61$	0.871 ± 0.003	2.5 (1.0)
122.35 ± 0.44	-0.98 ± 0.83	0.837 ± 0.010	3.4 (1.1)	122.52 ± 0.44	-0.18 ± 0.83	0.882 ± 0.010	2.8 (0.9)
151.91 ± 0.44	-0.92 ± 1.22	0.845 ± 0.002	2.5 (0.6)	151.88 ± 0.22	$+0.09 \pm 0.42$	0.889 ± 0.018	2.0 (0.6)
180.36 ± 0.44	$+0.44 \pm 0.83$	0.839 ± 0.005	1.1 (1.1)	180.63 ± 0.44	$+0.86 \pm 0.83$	0.891 ± 0.019	1.1 (0.7)
208.56 ± 0.44	$+0.88 \pm 0.83$	0.833 ± 0.002	1.0 (1.2)	208.54 ± 0.22	$+0.80 \pm 0.42$	0.886 ± 0.005	1.0 (1.3)
238.34 ± 0.67	$+1.67 \pm 1.25$	0.816 ± 0.005	1.4 (1.3)	238.03 ± 0.22	$+0.14 \pm 1.00$	0.869 ± 0.005	2.0 (1.1)
269.90 ± 0.44	-0.27 ± 0.83	0.813 ± 0.002	6.9 (0.9)	269.96 ± 0.44	-0.02 ± 0.83	0.863 ± 0.013	3.2 (0.5)
301.20 ± 0.44	-2.50 ± 1.03	0.820 ± 0.003	4.0 (1.1)	301.69 ± 0.22	-1.19 ± 0.81	0.869 ± 0.002	2.9 (0.9)
331.78 ± 0.22	-1.52 ± 0.61	0.841 ± 0.008	1.9 (0.9)	332.07 ± 0.22	-0.56 ± 0.42	0.887 ± 0.010	1.7 (0.7)

Table 144: The nominal angle δ_n, average displacement $\Delta\delta$, average value of the parameter DIST, RMS of the ALPHA distribution for enabled GF and impact parameters between 60 m and 120 m. The RMS of the ALPHA distribution for disabled GF is given parentheses. The primary γ-ray energy was set to 1000 GeV, the ZA to 20° and the azimuth angle to 180°.

$E_\gamma = 1000\,\mathrm{GeV}$, Az $= 180°$, ZA $= 20°$, Hard Image Cleaning

$\delta_n\,[°]$	$\Delta\delta\,[°]$	DIST[°]	$\mathrm{RMS}_{\lvert\mathrm{ALPHA}\rvert}\,[°]$	$\delta_n\,[°]$	$\Delta\delta\,[°]$	DIST[°]	$\mathrm{RMS}_{\lvert\mathrm{ALPHA}\rvert}\,[°]$
IP = 60 m				IP = 80 m			
0.86 ± 0.67	$+0.78 \pm 1.06$	0.616 ± 0.002	1.3 (1.5)	0.43 ± 0.44	$+0.40 \pm 0.83$	0.751 ± 0.021	0.9 (1.3)
28.97 ± 0.89	$+3.52 \pm 1.28$	0.612 ± 0.002	1.4 (3.1)	29.08 ± 0.44	$+2.46 \pm 0.64$	0.750 ± 0.005	0.9 (1.5)
58.79 ± 0.89	$+8.65 \pm 1.67$	0.599 ± 0.002	3.3 (3.6)	57.73 ± 0.67	$+3.49 \pm 1.45$	0.737 ± 0.006	2.4 (2.2)
89.28 ± 0.67	-1.65 ± 1.06	0.598 ± 0.011	17.2 (2.2)	89.99 ± 0.44	-0.74 ± 0.83	0.731 ± 0.005	4.2 (1.2)
122.33 ± 0.44	-3.77 ± 1.61	0.606 ± 0.023	15.8 (2.0)	122.34 ± 0.44	-1.50 ± 1.22	0.742 ± 0.019	6.3 (1.3)
151.76 ± 0.44	-1.89 ± 1.03	0.616 ± 0.003	6.4 (1.9)	151.90 ± 0.44	-1.19 ± 0.83	0.748 ± 0.005	3.6 (1.2)
179.33 ± 0.67	$+0.08 \pm 1.45$	0.612 ± 0.006	2.2 (2.4)	180.24 ± 0.67	$+1.24 \pm 1.06$	0.745 ± 0.023	1.6 (1.2)
208.41 ± 0.89	$+3.28 \pm 1.28$	0.607 ± 0.008	2.2 (2.4)	208.83 ± 0.22	$+2.25 \pm 0.61$	0.741 ± 0.006	0.9 (1.6)
237.44 ± 0.22	$+3.59 \pm 0.81$	0.591 ± 0.002	1.0 (2.4)	237.45 ± 0.44	$+1.51 \pm 1.22$	0.721 ± 0.002	1.2 (1.5)
268.90 ± 0.67	-6.99 ± 1.45	0.586 ± 0.011	18.9 (2.1)	269.18 ± 0.67	-0.65 ± 0.86	0.716 ± 0.010	9.8 (1.9)
301.17 ± 0.89	-6.60 ± 1.67	0.593 ± 0.010	9.2 (3.1)	301.51 ± 0.67	-4.48 ± 0.86	0.721 ± 0.006	6.1 (1.4)
331.69 ± 0.67	-4.79 ± 1.06	0.612 ± 0.026	4.6 (3.2)	332.37 ± 0.22	-2.23 ± 0.81	0.744 ± 0.003	2.8 (1.5)
IP = 100 m				IP = 120 m			
0.24 ± 0.44	$+0.71 \pm 0.83$	0.834 ± 0.005	1.0 (1.1)	359.22 ± 0.22	-0.66 ± 0.61	0.881 ± 0.005	0.9 (0.6)
28.67 ± 0.22	$+1.69 \pm 0.61$	0.837 ± 0.005	0.9 (1.3)	28.78 ± 0.22	$+1.10 \pm 0.61$	0.886 ± 0.011	0.8 (0.5)
57.47 ± 0.44	$+2.14 \pm 0.64$	0.825 ± 0.005	1.8 (1.5)	57.67 ± 0.44	$+0.95 \pm 0.83$	0.871 ± 0.003	1.8 (1.2)
90.10 ± 0.44	$+0.23 \pm 0.83$	0.824 ± 0.003	2.7 (0.8)	90.47 ± 0.22	$+0.50 \pm 0.61$	0.866 ± 0.005	2.1 (1.3)
122.58 ± 0.44	-0.65 ± 0.83	0.828 ± 0.005	4.3 (0.7)	122.74 ± 0.44	-0.17 ± 0.83	0.876 ± 0.021	2.9 (0.8)
151.77 ± 0.22	-0.89 ± 0.61	0.839 ± 0.010	2.5 (0.6)	151.85 ± 0.22	$+0.26 \pm 0.42$	0.884 ± 0.011	1.9 (0.8)
180.17 ± 0.44	$+0.41 \pm 0.83$	0.833 ± 0.021	1.2 (1.4)	180.22 ± 0.44	$+0.52 \pm 0.83$	0.882 ± 0.013	1.1 (0.8)
208.63 ± 0.44	$+0.81 \pm 0.83$	0.830 ± 0.002	1.0 (1.3)	208.67 ± 0.22	$+0.71 \pm 0.61$	0.881 ± 0.005	1.1 (0.9)
238.02 ± 0.44	$+1.50 \pm 1.03$	0.808 ± 0.028	1.2 (1.1)	237.83 ± 0.44	-0.34 ± 0.83	0.860 ± 0.005	3.9 (1.1)
270.00 ± 0.44	-0.32 ± 1.03	0.807 ± 0.003	5.8 (1.0)	269.75 ± 0.44	-0.31 ± 0.83	0.857 ± 0.002	3.6 (0.8)
301.25 ± 0.44	-2.55 ± 1.22	0.813 ± 0.002	3.8 (1.2)	301.89 ± 0.22	-1.00 ± 0.61	0.861 ± 0.002	2.7 (1.1)
331.68 ± 0.22	-1.52 ± 0.42	0.833 ± 0.005	1.8 (1.1)	331.92 ± 0.22	-0.45 ± 0.42	0.880 ± 0.008	1.3 (0.7)

Table 145: The nominal angle δ_n, average displacement $\Delta\delta$, average value of the parameter DIST, RMS of the ALPHA distribution for enabled GF and impact parameters between 60 m and 120 m. The RMS of the ALPHA distribution for disabled GF is given parentheses. The primary γ-ray energy was set to 1000 GeV, the ZA to 20° and the azimuth angle to 180°.

$E_\gamma = 1000\,\mathrm{GeV}$, Az $= 0°$, ZA $= 40°$, Intermediate Image Cleaning

$\delta_n[°]$	$\Delta\delta[°]$	DIST[°]	$\mathrm{RMS}_{\mid\mathrm{ALPHA}\mid}[°]$	$\delta_n[°]$	$\Delta\delta[°]$	DIST[°]	$\mathrm{RMS}_{\mid\mathrm{ALPHA}\mid}[°]$
IP = 60 m				IP = 80 m			
359.29 ± 0.34	$+0.54 \pm 0.84$	0.422 ± 0.010	2.8 (2.2)	359.70 ± 0.34	-0.31 ± 1.01	0.543 ± 0.011	1.7 (2.8)
22.19 ± 0.52	$+0.77 \pm 1.35$	0.398 ± 0.008	4.5 (15.6)	22.42 ± 0.69	-0.11 ± 1.19	0.519 ± 0.012	3.3 (11.8)
54.60 ± 0.69	$+5.23 \pm 1.69$	0.348 ± 0.008	6.7 (5.4)	54.47 ± 0.52	$+3.48 \pm 1.18$	0.456 ± 0.011	3.4 (3.2)
91.41 ± 0.17	$+1.61 \pm 0.50$	0.317 ± 0.006	12.7 (5.4)	90.32 ± 0.34	$+2.06 \pm 0.84$	0.419 ± 0.010	8.1 (12.7)
130.18 ± 0.34	$+2.10 \pm 1.01$	0.348 ± 0.008	6.9 (3.2)	129.36 ± 0.69	$+0.92 \pm 1.02$	0.453 ± 0.011	3.2 (2.9)
156.32 ± 0.86	$+0.16 \pm 1.69$	0.396 ± 0.010	5.1 (3.4)	155.81 ± 0.34	-0.35 ± 1.01	0.518 ± 0.004	3.2 (2.5)
179.46 ± 0.34	-1.13 ± 0.84	0.418 ± 0.006	3.6 (4.5)	179.69 ± 0.34	-0.71 ± 0.68	0.544 ± 0.003	2.5 (2.7)
203.23 ± 0.86	-1.14 ± 1.36	0.404 ± 0.008	4.3 (4.2)	203.79 ± 0.52	-0.62 ± 1.02	0.521 ± 0.007	3.4 (3.0)
235.82 ± 0.34	$+1.96 \pm 1.18$	0.362 ± 0.007	6.8 (2.3)	232.88 ± 0.69	-0.56 ± 1.19	0.471 ± 0.007	4.5 (2.5)
272.21 ± 0.34	$+2.91 \pm 0.68$	0.340 ± 0.007	10.9 (4.6)	269.32 ± 0.69	-1.97 ± 1.35	0.441 ± 0.010	5.6 (3.3)
307.19 ± 0.69	$+0.45 \pm 1.35$	0.365 ± 0.008	8.4 (5.3)	306.85 ± 0.69	-0.90 ± 1.35	0.475 ± 0.011	4.3 (1.8)
337.26 ± 0.34	$+0.15 \pm 1.34$	0.405 ± 0.008	2.6 (2.9)	336.91 ± 0.34	$+0.07 \pm 1.01$	0.524 ± 0.011	1.8 (2.0)
IP = 100 m				IP = 120 m			
359.78 ± 0.34	-0.08 ± 0.68	0.649 ± 0.012	1.5 (1.9)	0.11 ± 0.34	$+0.24 \pm 0.68$	0.734 ± 0.015	1.6 (1.4)
24.57 ± 0.34	$+0.81 \pm 0.68$	0.623 ± 0.012	2.1 (4.7)	24.03 ± 0.34	-0.20 ± 0.68	0.712 ± 0.004	1.6 (1.4)
51.26 ± 0.52	-0.33 ± 0.85	0.557 ± 0.008	2.1 (12.5)	51.84 ± 0.34	$+0.35 \pm 0.84$	0.645 ± 0.007	2.1 (7.6)
92.56 ± 0.34	$+3.48 \pm 0.84$	0.513 ± 0.010	3.7 (2.2)	91.81 ± 0.34	$+2.88 \pm 1.01$	0.604 ± 0.011	3.4 (1.9)
127.47 ± 0.52	-0.28 ± 1.02	0.553 ± 0.011	2.5 (2.1)	127.18 ± 0.52	$+0.63 \pm 1.02$	0.641 ± 0.011	2.2 (1.6)
155.36 ± 0.34	-0.89 ± 0.68	0.618 ± 0.010	2.2 (2.0)	155.54 ± 0.34	-0.46 ± 0.68	0.707 ± 0.011	1.5 (1.3)
179.26 ± 0.52	-0.89 ± 0.85	0.649 ± 0.014	1.7 (1.8)	180.12 ± 0.34	$+0.18 \pm 0.68$	0.732 ± 0.001	1.3 (1.1)
203.35 ± 0.69	-0.86 ± 1.02	0.625 ± 0.008	2.5 (1.9)	202.74 ± 0.17	-1.36 ± 0.50	0.719 ± 0.010	1.8 (2.3)
232.75 ± 0.17	-0.04 ± 0.67	0.570 ± 0.001	3.9 (2.3)	232.09 ± 0.34	-0.79 ± 0.84	0.662 ± 0.012	2.7 (1.9)
270.49 ± 0.69	-0.19 ± 1.19	0.535 ± 0.006	3.5 (2.1)	269.93 ± 0.34	-0.18 ± 1.01	0.621 ± 0.012	2.2 (2.2)
307.89 ± 0.52	$+0.44 \pm 0.85$	0.573 ± 0.008	2.6 (2.0)	307.70 ± 0.17	-0.17 ± 0.67	0.663 ± 0.012	1.7 (1.5)
335.60 ± 0.34	-1.07 ± 0.68	0.631 ± 0.010	2.3 (2.5)	336.68 ± 0.34	$+0.07 \pm 0.51$	0.719 ± 0.010	1.6 (1.1)

Table 146: The nominal angle δ_n, average displacement $\Delta\delta$, average value of the parameter DIST, RMS of the ALPHA distribution for enabled GF and impact parameters between 60 m and 120 m. The RMS of the ALPHA distribution for disabled GF is given parentheses. The primary γ-ray energy was set to 1000 GeV, the ZA to 40° and the azimuth angle to 0°.

$E_\gamma = 1000\,\mathrm{GeV}$, Az $= 0°$, ZA $= 40°$, Hard Image Cleaning

$\delta_n[°]$	$\Delta\delta[°]$	DIST[°]	$\mathrm{RMS}_{\mid\mathrm{ALPHA}\mid}[°]$	$\delta_n[°]$	$\Delta\delta[°]$	DIST[°]	$\mathrm{RMS}_{\mid\mathrm{ALPHA}\mid}[°]$
IP = 60 m				IP = 80 m			
358.63 ± 0.82	-0.63 ± 1.49	0.415 ± 0.006	2.1 (2.8)	359.67 ± 0.49	-0.40 ± 0.99	0.539 ± 0.011	1.4 (2.8)
22.11 ± 0.33	$+0.37 \pm 1.16$	0.393 ± 0.007	4.2 (15.6)	22.49 ± 0.49	-0.20 ± 1.16	0.513 ± 0.010	3.2 (11.2)
53.83 ± 0.66	$+3.59 \pm 1.16$	0.343 ± 0.008	5.3 (3.2)	54.27 ± 0.66	$+3.36 \pm 1.32$	0.451 ± 0.011	3.2 (2.3)
92.44 ± 0.66	$+2.36 \pm 1.49$	0.313 ± 0.008	11.0 (5.1)	89.86 ± 0.49	$+1.83 \pm 0.83$	0.412 ± 0.007	7.8 (11.3)
130.17 ± 0.33	$+1.12 \pm 0.83$	0.343 ± 0.008	4.5 (3.9)	129.09 ± 0.33	$+0.82 \pm 0.66$	0.448 ± 0.006	2.2 (2.4)
156.80 ± 0.82	$+0.28 \pm 1.49$	0.388 ± 0.010	3.7 (3.9)	155.85 ± 0.33	-0.49 ± 0.99	0.509 ± 0.010	2.7 (2.8)
179.17 ± 0.66	-1.17 ± 1.49	0.413 ± 0.010	3.2 (4.6)	179.80 ± 0.33	-0.45 ± 0.99	0.537 ± 0.012	2.5 (2.3)
202.94 ± 0.66	$+0.09 \pm 0.99$	0.398 ± 0.008	4.3 (4.1)	203.07 ± 0.66	-0.95 ± 1.32	0.517 ± 0.008	3.5 (2.7)
234.62 ± 0.16	$+1.21 \pm 1.00$	0.355 ± 0.008	6.0 (2.2)	232.78 ± 0.49	-0.33 ± 0.99	0.465 ± 0.010	5.1 (2.5)
271.62 ± 0.99	$+2.33 \pm 1.65$	0.335 ± 0.006	9.7 (3.7)	269.97 ± 0.66	-1.12 ± 1.66	0.434 ± 0.008	4.5 (2.4)
307.40 ± 0.49	-0.88 ± 0.99	0.356 ± 0.007	4.1 (2.9)	306.70 ± 0.66	-1.72 ± 1.32	0.468 ± 0.011	2.3 (1.8)
337.31 ± 0.33	$+0.16 \pm 0.99$	0.397 ± 0.004	2.5 (2.8)	336.72 ± 0.49	-0.09 ± 1.16	0.519 ± 0.010	2.0 (1.6)
IP = 100 m				IP = 120 m			
359.64 ± 0.33	-0.28 ± 0.66	0.642 ± 0.010	1.4 (1.2)	0.20 ± 0.33	$+0.36 \pm 0.66$	0.729 ± 0.001	1.2 (1.2)
23.77 ± 0.33	$+0.16 \pm 0.66$	0.617 ± 0.017	2.0 (5.2)	23.80 ± 0.33	-0.17 ± 0.66	0.706 ± 0.008	1.3 (1.1)
51.70 ± 0.49	-0.34 ± 0.99	0.552 ± 0.008	2.4 (13.0)	52.19 ± 0.33	$+0.52 \pm 0.66$	0.639 ± 0.007	2.0 (6.6)
89.48 ± 0.66	-0.09 ± 1.16	0.508 ± 0.007	3.7 (16.6)	90.11 ± 0.33	$+1.22 \pm 0.99$	0.597 ± 0.003	3.3 (2.0)
127.48 ± 0.49	-0.03 ± 1.16	0.547 ± 0.007	2.0 (1.8)	127.02 ± 0.49	$+0.45 \pm 0.99$	0.638 ± 0.011	2.0 (1.7)
155.16 ± 0.33	-0.98 ± 0.66	0.612 ± 0.010	1.9 (1.9)	155.56 ± 0.33	-0.49 ± 0.66	0.702 ± 0.004	1.6 (1.4)
179.63 ± 0.49	-0.20 ± 0.83	0.643 ± 0.014	1.6 (1.6)	179.98 ± 0.33	$+0.02 \pm 0.66$	0.726 ± 0.001	1.4 (1.1)
203.51 ± 0.66	-0.22 ± 0.99	0.621 ± 0.003	2.5 (2.1)	203.30 ± 0.33	-0.81 ± 0.66	0.712 ± 0.010	1.9 (1.8)
232.90 ± 0.33	-0.02 ± 0.66	0.565 ± 0.001	3.5 (2.5)	232.41 ± 0.16	-0.24 ± 0.50	0.657 ± 0.011	2.8 (1.7)
270.06 ± 0.33	-0.61 ± 0.66	0.530 ± 0.011	3.5 (1.9)	270.09 ± 0.33	-0.05 ± 0.83	0.616 ± 0.012	2.2 (1.9)
307.87 ± 0.49	-0.20 ± 0.99	0.567 ± 0.010	1.3 (2.5)	307.92 ± 0.16	-0.10 ± 0.66	0.656 ± 0.014	1.0 (1.3)
335.93 ± 0.33	-0.90 ± 0.66	0.627 ± 0.014	2.0 (2.4)	336.58 ± 0.33	-0.15 ± 0.66	0.714 ± 0.010	1.6 (1.4)

Table 147: The nominal angle δ_n, average displacement $\Delta\delta$, average value of the parameter DIST, RMS of the ALPHA distribution for enabled GF and impact parameters between 60 m and 120 m. The RMS of the ALPHA distribution for disabled GF is given parentheses. The primary γ-ray energy was set to 1000 GeV, the ZA to 40° and the azimuth angle to 0°.

$E_\gamma = 1000\,\mathrm{GeV}$, Az = 30°, ZA = 40°, Intermediate Image Cleaning

$\delta_n[^\circ]$	$\Delta\delta[^\circ]$	DIST[°]	$\mathrm{RMS}_{\lvert\mathrm{ALPHA}\rvert}[^\circ]$	$\delta_n[^\circ]$	$\Delta\delta[^\circ]$	DIST[°]	$\mathrm{RMS}_{\lvert\mathrm{ALPHA}\rvert}[^\circ]$
IP = 60 m				IP = 80 m			
359.29 ± 0.34	-2.71 ± 1.31	0.404 ± 0.005	7.6 (2.2)	359.70 ± 0.34	-1.88 ± 0.83	0.513 ± 0.004	6.4 (2.8)
22.19 ± 0.52	-5.27 ± 1.00	0.357 ± 0.007	6.9 (15.6)	22.42 ± 0.69	-3.34 ± 1.17	0.460 ± 0.005	8.3 (11.8)
54.60 ± 0.69	-0.89 ± 1.33	0.334 ± 0.005	7.3 (5.4)	54.47 ± 0.52	$+0.84 \pm 0.84$	0.425 ± 0.009	5.9 (3.2)
91.41 ± 0.17	$+2.96 \pm 1.14$	0.354 ± 0.005	9.0 (5.4)	90.32 ± 0.34	$+1.35 \pm 0.83$	0.457 ± 0.005	6.1 (12.7)
130.18 ± 0.34	$+6.45 \pm 0.83$	0.401 ± 0.005	11.1 (3.2)	129.36 ± 0.69	$+3.91 \pm 0.85$	0.514 ± 0.004	5.9 (2.9)
156.32 ± 0.86	$+4.03 \pm 1.34$	0.422 ± 0.004	7.4 (3.4)	155.81 ± 0.34	$+1.07 \pm 0.83$	0.541 ± 0.004	6.6 (2.5)
179.46 ± 0.34	-2.39 ± 0.99	0.404 ± 0.003	8.7 (4.5)	179.69 ± 0.34	-1.34 ± 0.67	0.515 ± 0.005	4.3 (2.7)
203.23 ± 0.86	-3.35 ± 1.50	0.363 ± 0.003	7.2 (4.2)	203.79 ± 0.52	-1.69 ± 1.00	0.468 ± 0.003	4.5 (3.0)
235.82 ± 0.34	$+1.94 \pm 0.83$	0.338 ± 0.004	9.6 (2.3)	232.88 ± 0.69	-0.79 ± 1.17	0.438 ± 0.008	7.9 (2.5)
272.21 ± 0.34	$+6.64 \pm 1.31$	0.365 ± 0.004	10.4 (4.6)	269.32 ± 0.69	$+1.63 \pm 1.17$	0.470 ± 0.003	6.5 (3.3)
307.19 ± 0.69	$+3.99 \pm 1.81$	0.411 ± 0.001	8.8 (5.3)	306.85 ± 0.69	$+1.34 \pm 1.01$	0.521 ± 0.005	5.4 (1.8)
337.26 ± 0.34	$+0.33 \pm 1.15$	0.426 ± 0.004	7.4 (2.9)	336.91 ± 0.34	-0.76 ± 0.83	0.541 ± 0.004	5.5 (2.0)
IP = 100 m				IP = 120 m			
359.78 ± 0.34	-0.96 ± 0.83	0.613 ± 0.001	5.4 (1.9)	0.11 ± 0.34	-0.84 ± 0.83	0.702 ± 0.007	6.4 (1.4)
24.57 ± 0.34	-0.90 ± 0.51	0.549 ± 0.007	6.2 (4.7)	24.03 ± 0.34	-0.70 ± 0.67	0.635 ± 0.011	5.1 (1.4)
51.26 ± 0.52	-1.60 ± 0.84	0.512 ± 0.005	4.6 (12.5)	51.84 ± 0.34	-0.52 ± 0.83	0.594 ± 0.005	3.2 (7.6)
92.56 ± 0.34	$+3.00 \pm 0.83$	0.553 ± 0.011	4.1 (2.2)	91.81 ± 0.34	$+2.86 \pm 0.83$	0.632 ± 0.005	3.3 (1.9)
127.47 ± 0.52	$+2.09 \pm 1.00$	0.616 ± 0.005	3.3 (2.1)	127.18 ± 0.52	$+1.50 \pm 0.84$	0.703 ± 0.001	3.2 (1.6)
155.36 ± 0.34	-0.04 ± 0.67	0.642 ± 0.005	4.0 (2.0)	155.54 ± 0.34	-0.29 ± 0.67	0.727 ± 0.007	3.6 (1.3)
179.26 ± 0.52	-1.01 ± 1.00	0.622 ± 0.003	3.5 (1.8)	180.12 ± 0.34	$+0.20 \pm 0.67$	0.713 ± 0.004	2.9 (1.1)
203.35 ± 0.69	-1.66 ± 1.01	0.566 ± 0.007	4.4 (1.9)	202.74 ± 0.17	-1.88 ± 0.49	0.654 ± 0.007	4.6 (2.3)
232.75 ± 0.17	-0.48 ± 0.49	0.529 ± 0.004	6.8 (2.3)	232.09 ± 0.34	-0.36 ± 0.67	0.617 ± 0.005	3.3 (1.9)
270.49 ± 0.69	$+2.14 \pm 1.33$	0.570 ± 0.004	4.3 (2.1)	269.93 ± 0.34	$+1.05 \pm 0.83$	0.659 ± 0.001	3.7 (2.2)
307.89 ± 0.52	$+1.51 \pm 1.00$	0.624 ± 0.007	4.0 (2.0)	307.70 ± 0.17	$+0.59 \pm 0.49$	0.712 ± 0.001	4.0 (1.5)
335.60 ± 0.34	-2.03 ± 0.67	0.641 ± 0.007	3.9 (2.5)	336.68 ± 0.34	$+0.01 \pm 0.67$	0.723 ± 0.012	4.2 (1.1)

Table 148: The nominal angle δ_n, average displacement $\Delta\delta$, average value of the parameter DIST, RMS of the ALPHA distribution for enabled GF and impact parameters between 60 m and 120 m. The RMS of the ALPHA distribution for disabled GF is given parentheses. The primary γ-ray energy was set to 1000 GeV, the ZA to 40° and the azimuth angle to 30°.

$E_\gamma = 1000\,\mathrm{GeV}$, Az = 30°, ZA = 40°, Hard Image Cleaning

$\delta_n[^\circ]$	$\Delta\delta[^\circ]$	DIST[°]	$\mathrm{RMS}_{\lvert\mathrm{ALPHA}\rvert}[^\circ]$	$\delta_n[^\circ]$	$\Delta\delta[^\circ]$	DIST[°]	$\mathrm{RMS}_{\lvert\mathrm{ALPHA}\rvert}[^\circ]$
IP = 60 m				IP = 80 m			
358.63 ± 0.82	-3.63 ± 1.63	0.398 ± 0.004	6.7 (2.8)	359.67 ± 0.49	-2.14 ± 0.82	0.506 ± 0.004	6.3 (2.8)
22.11 ± 0.33	-5.66 ± 0.65	0.349 ± 0.005	5.4 (15.6)	22.49 ± 0.49	-3.57 ± 0.98	0.454 ± 0.004	4.7 (11.2)
53.83 ± 0.66	-2.67 ± 1.30	0.327 ± 0.004	5.9 (3.2)	54.27 ± 0.66	-0.14 ± 0.98	0.420 ± 0.004	5.9 (2.3)
92.44 ± 0.66	$+4.25 \pm 1.46$	0.349 ± 0.004	8.4 (5.1)	89.86 ± 0.49	$+1.10 \pm 0.98$	0.452 ± 0.008	5.8 (11.3)
130.17 ± 0.33	$+6.64 \pm 1.29$	0.392 ± 0.007	11.3 (3.9)	129.09 ± 0.33	$+3.46 \pm 0.81$	0.509 ± 0.004	5.5 (2.4)
156.80 ± 0.82	$+4.72 \pm 1.47$	0.414 ± 0.004	9.8 (3.9)	155.85 ± 0.33	$+1.02 \pm 0.49$	0.534 ± 0.003	5.4 (2.8)
179.17 ± 0.66	-1.05 ± 1.46	0.397 ± 0.003	6.9 (4.6)	179.80 ± 0.33	-0.86 ± 0.65	0.511 ± 0.003	4.6 (2.3)
202.94 ± 0.66	-3.73 ± 1.46	0.359 ± 0.001	7.8 (4.1)	203.07 ± 0.66	-2.14 ± 1.14	0.463 ± 0.004	4.4 (2.7)
234.62 ± 0.16	$+1.29 \pm 0.97$	0.329 ± 0.005	10.1 (2.2)	232.78 ± 0.49	-0.58 ± 0.98	0.433 ± 0.004	7.1 (2.5)
271.62 ± 0.99	$+6.37 \pm 1.63$	0.357 ± 0.004	10.8 (3.7)	269.97 ± 0.66	$+2.35 \pm 0.98$	0.466 ± 0.005	6.8 (2.4)
307.40 ± 0.49	$+5.71 \pm 1.30$	0.404 ± 0.003	7.7 (2.9)	306.70 ± 0.66	$+1.19 \pm 1.14$	0.514 ± 0.005	6.5 (1.8)
337.31 ± 0.33	-0.31 ± 1.13	0.421 ± 0.003	6.9 (2.8)	336.72 ± 0.49	-0.69 ± 0.98	0.536 ± 0.005	5.0 (1.6)
IP = 100 m				IP = 120 m			
359.64 ± 0.33	-1.41 ± 0.65	0.607 ± 0.007	5.0 (1.2)	0.20 ± 0.33	-1.02 ± 0.81	0.697 ± 0.007	6.1 (1.2)
23.77 ± 0.33	-1.66 ± 0.81	0.544 ± 0.005	5.8 (5.2)	23.80 ± 0.33	-1.09 ± 0.65	0.628 ± 0.007	5.1 (1.1)
51.70 ± 0.49	-1.77 ± 0.82	0.505 ± 0.001	4.2 (13.0)	52.19 ± 0.33	-0.46 ± 0.81	0.589 ± 0.012	3.2 (6.6)
89.48 ± 0.66	-0.39 ± 1.30	0.545 ± 0.007	3.9 (16.6)	90.11 ± 0.33	$+0.99 \pm 0.81$	0.627 ± 0.005	3.5 (2.0)
127.48 ± 0.49	$+1.73 \pm 0.98$	0.610 ± 0.003	3.3 (1.8)	127.02 ± 0.49	$+1.12 \pm 0.82$	0.696 ± 0.005	3.1 (1.7)
155.16 ± 0.33	-0.02 ± 0.49	0.637 ± 0.005	4.2 (1.9)	155.56 ± 0.33	-0.05 ± 0.65	0.721 ± 0.007	3.0 (1.4)
179.63 ± 0.49	-0.93 ± 0.82	0.617 ± 0.007	4.0 (1.6)	179.98 ± 0.33	$+0.46 \pm 0.65$	0.709 ± 0.005	2.9 (1.1)
203.51 ± 0.66	-1.49 ± 0.98	0.561 ± 0.004	3.8 (2.1)	203.30 ± 0.33	-1.17 ± 0.65	0.649 ± 0.009	4.3 (1.8)
232.90 ± 0.33	$+0.02 \pm 0.65$	0.523 ± 0.008	6.2 (2.5)	232.41 ± 0.16	-0.15 ± 0.65	0.612 ± 0.007	3.0 (1.7)
270.06 ± 0.33	$+1.76 \pm 0.81$	0.563 ± 0.005	4.6 (1.9)	270.09 ± 0.33	$+0.97 \pm 0.81$	0.651 ± 0.007	3.4 (1.9)
307.87 ± 0.49	$+1.75 \pm 0.66$	0.620 ± 0.008	4.0 (2.5)	307.92 ± 0.16	$+0.99 \pm 0.33$	0.708 ± 0.001	2.9 (1.3)
335.93 ± 0.33	-1.36 ± 0.49	0.637 ± 0.001	3.6 (2.4)	336.58 ± 0.33	$+0.31 \pm 0.81$	0.717 ± 0.011	4.1 (1.4)

Table 149: The nominal angle δ_n, average displacement $\Delta\delta$, average value of the parameter DIST, RMS of the ALPHA distribution for enabled GF and impact parameters between 60 m and 120 m. The RMS of the ALPHA distribution for disabled GF is given parentheses. The primary γ-ray energy was set to 1000 GeV, the ZA to 40° and the azimuth angle to 30°.

$E_\gamma = 1000\,\mathbf{GeV}$, Az $= 60°$, ZA $= 40°$, Intermediate Image Cleaning

$\delta_n[°]$	$\Delta\delta[°]$	DIST[°]	$\mathrm{RMS}_{\vert\mathrm{ALPHA}\vert}[°]$	$\delta_n[°]$	$\Delta\delta[°]$	DIST[°]	$\mathrm{RMS}_{\vert\mathrm{ALPHA}\vert}[°]$
IP = 60 m				IP = 80 m			
359.29 ± 0.34	$+2.75 \pm 1.27$	0.336 ± 0.006	11.4 (2.2)	359.70 ± 0.34	$+0.92 \pm 0.81$	0.441 ± 0.006	7.5 (2.8)
22.19 ± 0.52	-9.02 ± 0.82	0.305 ± 0.008	6.1 (15.6)	22.42 ± 0.69	-4.49 ± 1.61	0.406 ± 0.006	5.6 (11.8)
54.60 ± 0.69	-8.65 ± 1.61	0.331 ± 0.009	7.2 (5.4)	54.47 ± 0.52	-3.78 ± 1.90	0.437 ± 0.008	6.1 (3.2)
91.41 ± 0.17	$+0.71 \pm 1.09$	0.377 ± 0.005	11.5 (5.4)	90.32 ± 0.34	-0.59 ± 0.81	0.497 ± 0.009	7.8 (12.7)
130.18 ± 0.34	$+9.74 \pm 1.27$	0.401 ± 0.008	10.5 (3.2)	129.36 ± 0.69	$+6.05 \pm 1.15$	0.525 ± 0.009	7.2 (2.9)
156.32 ± 0.86	$+8.86 \pm 1.63$	0.388 ± 0.006	9.8 (3.4)	155.81 ± 0.34	$+4.22 \pm 0.81$	0.503 ± 0.009	7.8 (2.5)
179.46 ± 0.34	$+1.53 \pm 0.96$	0.346 ± 0.005	10.5 (4.5)	179.69 ± 0.34	$+2.78 \pm 1.11$	0.449 ± 0.005	6.4 (2.7)
203.23 ± 0.86	-5.39 ± 1.32	0.329 ± 0.005	5.8 (4.2)	203.79 ± 0.52	-2.56 ± 0.67	0.420 ± 0.005	4.6 (3.0)
235.82 ± 0.34	-4.53 ± 1.42	0.348 ± 0.004	7.6 (2.3)	232.88 ± 0.69	-6.88 ± 1.46	0.453 ± 0.006	6.3 (2.5)
272.21 ± 0.34	-1.15 ± 0.81	0.388 ± 0.006	9.6 (4.6)	269.32 ± 0.69	-2.63 ± 1.46	0.505 ± 0.004	7.5 (3.3)
307.19 ± 0.69	$+7.24 \pm 1.30$	0.408 ± 0.005	10.8 (5.3)	306.85 ± 0.69	$+4.69 \pm 1.30$	0.528 ± 0.009	9.2 (1.8)
337.26 ± 0.34	$+5.81 \pm 0.96$	0.386 ± 0.005	11.8 (2.9)	336.91 ± 0.34	$+4.44 \pm 0.81$	0.500 ± 0.006	9.6 (2.0)
IP = 100 m				IP = 120 m			
359.78 ± 0.34	-0.16 ± 0.96	0.538 ± 0.009	5.6 (1.9)	0.11 ± 0.34	-0.03 ± 0.65	0.629 ± 0.012	4.8 (1.4)
24.57 ± 0.34	-1.27 ± 0.81	0.498 ± 0.006	4.4 (4.7)	24.03 ± 0.34	-1.61 ± 0.81	0.582 ± 0.006	3.8 (1.4)
51.26 ± 0.52	-4.87 ± 1.13	0.537 ± 0.009	4.5 (12.5)	51.84 ± 0.34	-2.53 ± 0.81	0.626 ± 0.012	4.0 (7.6)
92.56 ± 0.34	$+0.85 \pm 0.65$	0.603 ± 0.009	7.5 (2.2)	91.81 ± 0.34	$+1.74 \pm 0.81$	0.694 ± 0.014	5.7 (1.9)
127.47 ± 0.52	$+2.78 \pm 0.98$	0.631 ± 0.005	7.1 (2.1)	127.18 ± 0.52	$+1.69 \pm 0.98$	0.712 ± 0.004	4.8 (1.6)
155.36 ± 0.34	$+0.56 \pm 1.11$	0.608 ± 0.005	5.8 (2.0)	155.54 ± 0.34	$+1.05 \pm 0.81$	0.702 ± 0.010	4.6 (1.3)
179.26 ± 0.52	-0.29 ± 0.98	0.549 ± 0.009	4.9 (1.8)	180.12 ± 0.34	$+1.68 \pm 0.81$	0.641 ± 0.009	4.7 (1.1)
203.35 ± 0.69	-1.94 ± 1.15	0.512 ± 0.009	3.9 (1.9)	202.74 ± 0.17	$+0.08 \pm 0.63$	0.596 ± 0.009	3.3 (2.3)
232.75 ± 0.17	-3.95 ± 0.79	0.548 ± 0.010	4.7 (2.3)	232.09 ± 0.34	-2.26 ± 0.96	0.637 ± 0.008	3.5 (1.9)
270.49 ± 0.69	-0.62 ± 1.15	0.611 ± 0.003	4.5 (2.1)	269.93 ± 0.34	-0.72 ± 0.65	0.697 ± 0.009	5.1 (2.2)
307.89 ± 0.52	$+3.91 \pm 1.13$	0.632 ± 0.009	7.9 (2.0)	307.70 ± 0.17	$+2.56 \pm 0.63$	0.718 ± 0.008	5.1 (1.5)
335.60 ± 0.34	$+1.02 \pm 0.81$	0.608 ± 0.005	7.9 (2.5)	336.68 ± 0.34	-0.01 ± 0.65	0.693 ± 0.009	5.5 (1.1)

Table 150: The nominal angle δ_n, average displacement $\Delta\delta$, average value of the parameter DIST, RMS of the ALPHA distribution for enabled GF and impact parameters between 60 m and 120 m. The RMS of the ALPHA distribution for disabled GF is given parentheses. The primary γ-ray energy was set to 1000 GeV, the ZA to 40° and the azimuth angle to 60°.

$E_\gamma = 1000\,\mathbf{GeV}$, Az $= 60°$, ZA $= 40°$, Hard Image Cleaning

$\delta_n[°]$	$\Delta\delta[°]$	DIST[°]	$\mathrm{RMS}_{\vert\mathrm{ALPHA}\vert}[°]$	$\delta_n[°]$	$\Delta\delta[°]$	DIST[°]	$\mathrm{RMS}_{\vert\mathrm{ALPHA}\vert}[°]$
IP = 60 m				IP = 80 m			
358.63 ± 0.82	$+1.38 \pm 1.59$	0.331 ± 0.006	10.9 (2.8)	359.67 ± 0.49	$+0.20 \pm 1.26$	0.436 ± 0.005	7.7 (2.8)
22.11 ± 0.33	-8.87 ± 1.41	0.302 ± 0.008	5.5 (15.6)	22.49 ± 0.49	-3.84 ± 1.26	0.401 ± 0.010	4.3 (11.2)
53.83 ± 0.66	-9.46 ± 1.89	0.327 ± 0.006	7.4 (3.2)	54.27 ± 0.66	-4.17 ± 1.58	0.433 ± 0.008	6.0 (2.3)
92.44 ± 0.66	$+1.76 \pm 1.12$	0.372 ± 0.008	10.7 (5.1)	89.86 ± 0.49	-1.03 ± 1.26	0.490 ± 0.008	7.2 (11.3)
130.17 ± 0.33	$+9.68 \pm 0.94$	0.396 ± 0.006	11.5 (3.9)	129.09 ± 0.33	$+5.70 \pm 1.10$	0.521 ± 0.012	6.9 (2.4)
156.80 ± 0.82	$+9.01 \pm 1.75$	0.380 ± 0.008	9.5 (3.9)	155.85 ± 0.33	$+3.93 \pm 0.94$	0.497 ± 0.004	7.2 (2.8)
179.17 ± 0.66	$+1.02 \pm 1.27$	0.340 ± 0.006	10.8 (4.6)	179.80 ± 0.33	$+1.92 \pm 1.10$	0.445 ± 0.006	5.5 (2.3)
202.94 ± 0.66	-5.71 ± 1.12	0.324 ± 0.005	5.5 (4.1)	203.07 ± 0.66	-2.67 ± 1.43	0.419 ± 0.008	3.8 (2.7)
234.62 ± 0.16	-5.69 ± 1.09	0.341 ± 0.005	6.9 (2.2)	232.78 ± 0.49	-6.06 ± 1.11	0.447 ± 0.005	6.3 (2.5)
271.62 ± 0.99	-1.49 ± 1.76	0.380 ± 0.005	8.9 (3.7)	269.97 ± 0.66	-1.73 ± 1.12	0.497 ± 0.006	7.7 (2.4)
307.40 ± 0.49	$+7.61 \pm 0.96$	0.402 ± 0.005	13.0 (2.9)	306.70 ± 0.66	$+3.81 \pm 1.12$	0.520 ± 0.012	9.7 (1.8)
337.31 ± 0.33	$+6.45 \pm 0.64$	0.379 ± 0.006	8.7 (2.8)	336.72 ± 0.49	$+3.85 \pm 1.11$	0.494 ± 0.008	9.5 (1.6)
IP = 100 m				IP = 120 m			
359.64 ± 0.33	-0.19 ± 0.64	0.534 ± 0.009	5.4 (1.2)	0.20 ± 0.33	$+0.58 \pm 0.64$	0.623 ± 0.012	4.6 (1.2)
23.77 ± 0.33	-1.86 ± 0.79	0.493 ± 0.001	4.4 (5.2)	23.80 ± 0.33	-1.60 ± 0.79	0.577 ± 0.010	3.0 (1.1)
51.70 ± 0.49	-4.64 ± 1.26	0.532 ± 0.001	4.8 (13.0)	52.19 ± 0.33	-2.35 ± 0.64	0.620 ± 0.010	3.9 (6.6)
89.48 ± 0.66	-2.40 ± 1.12	0.596 ± 0.010	6.5 (16.6)	90.11 ± 0.33	$+0.22 \pm 0.64$	0.688 ± 0.014	5.4 (2.0)
127.48 ± 0.49	$+2.71 \pm 0.96$	0.625 ± 0.009	5.8 (1.8)	127.02 ± 0.49	$+1.73 \pm 0.80$	0.708 ± 0.005	5.2 (1.7)
155.16 ± 0.33	$+1.47 \pm 0.79$	0.601 ± 0.003	6.1 (1.9)	155.56 ± 0.33	$+1.00 \pm 0.79$	0.697 ± 0.010	3.7 (1.4)
179.63 ± 0.49	$+0.14 \pm 0.96$	0.543 ± 0.009	4.2 (1.6)	179.98 ± 0.33	$+1.64 \pm 0.64$	0.636 ± 0.009	4.5 (1.1)
203.51 ± 0.66	-1.59 ± 1.12	0.506 ± 0.008	3.7 (2.1)	203.30 ± 0.33	$+0.19 \pm 0.64$	0.590 ± 0.010	3.7 (1.8)
232.90 ± 0.33	-3.61 ± 0.94	0.542 ± 0.010	5.4 (2.5)	232.41 ± 0.16	-2.18 ± 0.78	0.632 ± 0.001	3.3 (1.7)
270.06 ± 0.33	-0.69 ± 0.64	0.606 ± 0.006	4.5 (1.9)	270.09 ± 0.33	-0.56 ± 0.64	0.689 ± 0.009	5.0 (1.9)
307.87 ± 0.49	$+3.01 \pm 0.96$	0.626 ± 0.001	5.3 (2.5)	307.92 ± 0.16	$+2.80 \pm 0.78$	0.713 ± 0.010	3.6 (1.3)
335.93 ± 0.33	$+1.10 \pm 0.79$	0.601 ± 0.010	7.4 (2.4)	336.58 ± 0.33	-0.27 ± 0.64	0.688 ± 0.009	5.3 (1.4)

Table 151: The nominal angle δ_n, average displacement $\Delta\delta$, average value of the parameter DIST, RMS of the ALPHA distribution for enabled GF and impact parameters between 60 m and 120 m. The RMS of the ALPHA distribution for disabled GF is given parentheses. The primary γ-ray energy was set to 1000 GeV, the ZA to 40° and the azimuth angle to 60°.

$E_\gamma = 1000\,\mathrm{GeV}$, Az = 90°, ZA = 40°, Intermediate Image Cleaning

δ_n[°]	$\Delta\delta$[°]	DIST[°]	$\mathrm{RMS}_{\lvert\mathrm{ALPHA}\rvert}$[°]	δ_n[°]	$\Delta\delta$[°]	DIST[°]	$\mathrm{RMS}_{\lvert\mathrm{ALPHA}\rvert}$[°]
IP = 60 m				**IP = 80 m**			
359.29 ± 0.34	$+10.38 \pm 0.81$	0.302 ± 0.004	8.0 (2.2)	359.70 ± 0.34	$+6.27 \pm 0.97$	0.398 ± 0.003	5.5 (2.8)
22.19 ± 0.52	-0.26 ± 1.30	0.331 ± 0.004	10.8 (15.6)	22.42 ± 0.69	-2.01 ± 1.31	0.433 ± 0.004	10.5 (11.8)
54.60 ± 0.69	-11.65 ± 1.78	0.375 ± 0.004	9.6 (5.4)	54.47 ± 0.52	-6.47 ± 1.14	0.487 ± 0.005	11.8 (3.2)
91.41 ± 0.17	-6.75 ± 1.58	0.397 ± 0.004	14.9 (5.4)	90.32 ± 0.34	-4.21 ± 1.12	0.514 ± 0.005	13.3 (12.7)
130.18 ± 0.34	$+8.24 \pm 1.12$	0.384 ± 0.003	25.3 (3.2)	129.36 ± 0.69	$+5.58 \pm 1.31$	0.499 ± 0.006	14.3 (2.9)
156.32 ± 0.86	$+9.16 \pm 2.11$	0.343 ± 0.005	21.2 (3.4)	155.81 ± 0.34	$+5.11 \pm 0.97$	0.451 ± 0.005	13.8 (2.5)
179.46 ± 0.34	$+11.59 \pm 0.81$	0.318 ± 0.004	8.1 (4.5)	179.69 ± 0.34	$+4.56 \pm 0.81$	0.420 ± 0.003	5.5 (2.7)
203.23 ± 0.86	$+2.62 \pm 1.95$	0.346 ± 0.001	6.1 (4.2)	203.79 ± 0.52	$+1.45 \pm 1.14$	0.450 ± 0.005	3.0 (3.0)
235.82 ± 0.34	-19.01 ± 0.50	0.391 ± 0.005	10.3 (2.3)	232.88 ± 0.69	-8.47 ± 2.40	0.504 ± 0.006	6.6 (2.5)
272.21 ± 0.34	-7.69 ± 0.81	0.407 ± 0.003	15.8 (4.6)	269.32 ± 0.69	-6.88 ± 1.00	0.520 ± 0.006	11.7 (3.3)
307.19 ± 0.69	$+4.31 \pm 1.62$	0.380 ± 0.003	22.3 (5.3)	306.85 ± 0.69	$+2.39 \pm 1.16$	0.496 ± 0.010	18.0 (1.8)
337.26 ± 0.34	$+10.48 \pm 1.44$	0.333 ± 0.004	17.8 (2.9)	336.91 ± 0.34	$+7.46 \pm 0.50$	0.433 ± 0.003	14.8 (2.0)
IP = 100 m				**IP = 120 m**			
359.78 ± 0.34	$+3.80 \pm 1.12$	0.493 ± 0.006	4.2 (1.9)	0.11 ± 0.34	$+1.98 \pm 0.50$	0.575 ± 0.006	4.4 (1.4)
24.57 ± 0.34	$+1.79 \pm 0.81$	0.527 ± 0.008	7.7 (4.7)	24.03 ± 0.34	-0.88 ± 0.66	0.618 ± 0.008	3.1 (1.4)
51.26 ± 0.52	-6.98 ± 1.14	0.594 ± 0.005	7.1 (12.5)	51.84 ± 0.34	-4.89 ± 0.81	0.685 ± 0.006	3.9 (7.6)
92.56 ± 0.34	-0.99 ± 0.81	0.629 ± 0.009	6.1 (2.2)	91.81 ± 0.34	-1.40 ± 1.12	0.713 ± 0.004	5.0 (1.9)
127.47 ± 0.52	$+3.05 \pm 1.14$	0.605 ± 0.004	8.4 (2.1)	127.18 ± 0.52	$+1.12 \pm 0.98$	0.694 ± 0.004	6.0 (1.6)
155.36 ± 0.34	$+3.69 \pm 0.97$	0.546 ± 0.006	10.7 (2.0)	155.54 ± 0.34	$+2.07 \pm 0.81$	0.636 ± 0.003	5.5 (1.3)
179.26 ± 0.52	$+2.99 \pm 0.98$	0.513 ± 0.004	5.0 (1.8)	180.12 ± 0.34	$+1.62 \pm 0.66$	0.596 ± 0.004	4.2 (1.1)
203.35 ± 0.69	$+0.78 \pm 1.47$	0.546 ± 0.005	2.6 (1.9)	202.74 ± 0.17	$+0.25 \pm 0.33$	0.634 ± 0.003	2.0 (2.3)
232.75 ± 0.17	-5.80 ± 0.95	0.611 ± 0.003	3.8 (2.3)	232.09 ± 0.34	-2.54 ± 1.12	0.695 ± 0.006	3.0 (1.9)
270.49 ± 0.69	-4.38 ± 1.47	0.631 ± 0.005	9.6 (2.1)	269.93 ± 0.34	-3.64 ± 0.97	0.714 ± 0.004	3.4 (2.2)
307.89 ± 0.52	$+2.56 \pm 1.14$	0.603 ± 0.006	11.1 (2.0)	307.70 ± 0.17	$+1.59 \pm 0.48$	0.691 ± 0.005	4.8 (1.5)
335.60 ± 0.34	$+3.16 \pm 0.81$	0.532 ± 0.005	9.3 (2.5)	336.68 ± 0.34	$+2.80 \pm 0.66$	0.622 ± 0.005	7.3 (1.1)

Table 152: The nominal angle δ_n, average displacement $\Delta\delta$, average value of the parameter DIST, RMS of the ALPHA distribution for enabled GF and impact parameters between 60 m and 120 m. The RMS of the ALPHA distribution for disabled GF is given parentheses. The primary γ-ray energy was set to 1000 GeV, the ZA to 40° and the azimuth angle to 90°.

$E_\gamma = 1000\,\mathrm{GeV}$, Az = 90°, ZA = 40°, Hard Image Cleaning

δ_n[°]	$\Delta\delta$[°]	DIST[°]	$\mathrm{RMS}_{\lvert\mathrm{ALPHA}\rvert}$[°]	δ_n[°]	$\Delta\delta$[°]	DIST[°]	$\mathrm{RMS}_{\lvert\mathrm{ALPHA}\rvert}$[°]
IP = 60 m				**IP = 80 m**			
358.63 ± 0.82	$+9.78 \pm 1.45$	0.298 ± 0.003	8.0 (2.8)	359.67 ± 0.49	$+5.29 \pm 0.81$	0.392 ± 0.004	5.5 (2.8)
22.11 ± 0.33	-5.89 ± 1.42	0.327 ± 0.003	10.9 (15.6)	22.49 ± 0.49	-3.41 ± 1.12	0.426 ± 0.005	10.9 (11.2)
53.83 ± 0.66	-13.32 ± 1.28	0.370 ± 0.004	9.0 (3.2)	54.27 ± 0.66	-7.38 ± 1.28	0.482 ± 0.005	11.1 (2.3)
92.44 ± 0.66	-6.35 ± 2.06	0.391 ± 0.004	16.1 (5.1)	89.86 ± 0.49	-5.04 ± 0.81	0.508 ± 0.004	13.6 (11.3)
130.17 ± 0.33	$+8.49 \pm 1.11$	0.380 ± 0.004	22.7 (3.9)	129.09 ± 0.33	$+5.88 \pm 0.80$	0.492 ± 0.005	13.2 (2.4)
156.80 ± 0.82	$+9.53 \pm 1.29$	0.339 ± 0.001	19.1 (3.9)	155.85 ± 0.33	$+5.09 \pm 0.95$	0.445 ± 0.005	15.8 (2.8)
179.17 ± 0.66	$+11.84 \pm 1.13$	0.314 ± 0.001	7.7 (4.6)	179.80 ± 0.33	$+6.83 \pm 0.80$	0.413 ± 0.005	5.8 (2.3)
202.94 ± 0.66	$+1.12 \pm 1.28$	0.339 ± 0.001	5.6 (4.1)	203.07 ± 0.66	$+1.92 \pm 1.13$	0.445 ± 0.006	2.9 (2.7)
234.62 ± 0.16	-14.68 ± 0.63	0.383 ± 0.008	9.9 (2.2)	232.78 ± 0.49	-8.23 ± 1.27	0.497 ± 0.005	7.3 (2.5)
271.62 ± 0.99	-7.71 ± 1.92	0.400 ± 0.004	15.9 (3.7)	269.97 ± 0.66	-6.42 ± 0.97	0.515 ± 0.004	10.1 (2.4)
307.40 ± 0.49	$+4.47 \pm 1.12$	0.375 ± 0.004	18.8 (2.9)	306.70 ± 0.66	$+1.89 \pm 1.13$	0.490 ± 0.010	14.7 (1.8)
337.31 ± 0.33	$+10.25 \pm 1.42$	0.328 ± 0.004	18.0 (2.8)	336.72 ± 0.49	$+7.61 \pm 1.12$	0.429 ± 0.003	12.8 (1.6)
IP = 100 m				**IP = 120 m**			
359.64 ± 0.33	$+3.28 \pm 0.80$	0.488 ± 0.005	4.3 (1.2)	0.20 ± 0.33	$+1.49 \pm 0.64$	0.572 ± 0.005	4.0 (1.2)
23.77 ± 0.33	-2.20 ± 0.95	0.523 ± 0.008	7.1 (5.2)	23.80 ± 0.33	-1.25 ± 0.64	0.612 ± 0.001	2.6 (1.1)
51.70 ± 0.49	-7.58 ± 1.12	0.589 ± 0.004	7.2 (13.0)	52.19 ± 0.33	-5.07 ± 0.80	0.680 ± 0.008	3.8 (6.6)
89.48 ± 0.66	-4.24 ± 1.44	0.622 ± 0.008	6.0 (16.6)	90.11 ± 0.33	-2.91 ± 0.95	0.706 ± 0.004	4.9 (2.0)
127.48 ± 0.49	$+2.84 \pm 1.12$	0.599 ± 0.004	7.9 (1.8)	127.02 ± 0.49	$+1.02 \pm 0.81$	0.689 ± 0.004	5.9 (1.7)
155.16 ± 0.33	$+3.81 \pm 0.80$	0.538 ± 0.003	10.0 (1.9)	155.56 ± 0.33	$+2.24 \pm 0.49$	0.631 ± 0.004	6.2 (1.4)
179.63 ± 0.49	$+3.24 \pm 0.96$	0.508 ± 0.006	4.8 (1.6)	179.98 ± 0.33	$+1.94 \pm 0.64$	0.588 ± 0.004	3.8 (1.1)
203.51 ± 0.66	$+0.76 \pm 1.28$	0.541 ± 0.005	2.5 (2.1)	203.30 ± 0.33	$+0.90 \pm 0.80$	0.629 ± 0.005	1.9 (1.8)
232.90 ± 0.33	-5.48 ± 1.27	0.607 ± 0.003	3.4 (2.5)	232.41 ± 0.16	-1.94 ± 0.94	0.690 ± 0.006	2.7 (1.7)
270.06 ± 0.33	-4.50 ± 0.95	0.625 ± 0.005	8.4 (1.9)	270.09 ± 0.33	-3.61 ± 0.80	0.709 ± 0.001	3.0 (1.9)
307.87 ± 0.49	$+2.36 \pm 0.96$	0.597 ± 0.004	11.0 (2.5)	307.92 ± 0.16	$+1.61 \pm 0.63$	0.684 ± 0.005	4.4 (1.3)
335.93 ± 0.33	$+3.16 \pm 0.64$	0.526 ± 0.005	9.6 (2.4)	336.58 ± 0.33	$+2.60 \pm 0.64$	0.615 ± 0.005	9.9 (1.4)

Table 153: The nominal angle δ_n, average displacement $\Delta\delta$, average value of the parameter DIST, RMS of the ALPHA distribution for enabled GF and impact parameters between 60 m and 120 m. The RMS of the ALPHA distribution for disabled GF is given parentheses. The primary γ-ray energy was set to 1000 GeV, the ZA to 40° and the azimuth angle to 90°.

$E_\gamma = 1000\,\mathrm{GeV}$, Az = 120°, ZA = 40°, Intermediate Image Cleaning

$\delta_n[°]$	$\Delta\delta[°]$	DIST[°]	$\mathrm{RMS}_{\vert\mathrm{ALPHA}\vert}[°]$	$\delta_n[°]$	$\Delta\delta[°]$	DIST[°]	$\mathrm{RMS}_{\vert\mathrm{ALPHA}\vert}[°]$
IP = 60 m				**IP = 80 m**			
359.29 ± 0.34	$+9.65 \pm 1.12$	0.357 ± 0.008	5.0 (2.2)	359.70 ± 0.34	$+4.64 \pm 0.81$	0.457 ± 0.006	4.3 (2.8)
22.19 ± 0.52	$+8.44 \pm 0.67$	0.401 ± 0.009	7.2 (15.6)	22.42 ± 0.69	$+1.51 \pm 1.15$	0.516 ± 0.005	4.7 (11.8)
54.60 ± 0.69	-3.79 ± 1.62	0.423 ± 0.004	8.6 (5.4)	54.47 ± 0.52	-2.35 ± 0.98	0.543 ± 0.010	9.3 (3.2)
91.41 ± 0.17	-15.35 ± 0.79	0.409 ± 0.005	17.0 (5.4)	90.32 ± 0.34	-11.60 ± 1.74	0.521 ± 0.004	10.1 (12.7)
130.18 ± 0.34	-0.72 ± 0.81	0.365 ± 0.003	15.9 (3.2)	129.36 ± 0.69	-0.27 ± 1.31	0.470 ± 0.005	14.3 (2.9)
156.32 ± 0.86	$+6.76 \pm 1.79$	0.336 ± 0.001	12.3 (3.4)	155.81 ± 0.34	$+3.90 \pm 0.81$	0.439 ± 0.005	9.3 (2.5)
179.46 ± 0.34	$+10.28 \pm 1.74$	0.361 ± 0.005	5.8 (4.5)	179.69 ± 0.34	$+6.63 \pm 1.27$	0.466 ± 0.003	4.6 (2.7)
203.23 ± 0.86	$+11.24 \pm 1.79$	0.406 ± 0.005	6.4 (4.2)	203.79 ± 0.52	$+5.63 \pm 1.45$	0.520 ± 0.006	4.1 (3.0)
235.82 ± 0.34	-1.63 ± 1.27	0.420 ± 0.006	9.6 (2.3)	232.88 ± 0.69	-4.20 ± 1.46	0.547 ± 0.005	6.8 (2.5)
272.21 ± 0.34	-10.58 ± 1.74	0.400 ± 0.006	17.9 (4.6)	269.32 ± 0.69	-8.62 ± 1.31	0.522 ± 0.005	10.0 (3.3)
307.19 ± 0.69	-2.10 ± 1.46	0.350 ± 0.005	13.7 (5.3)	306.85 ± 0.69	-0.98 ± 1.31	0.464 ± 0.006	14.6 (1.8)
337.26 ± 0.34	$+6.20 \pm 0.96$	0.329 ± 0.005	10.3 (2.9)	336.91 ± 0.34	$+3.23 \pm 1.12$	0.426 ± 0.009	10.0 (2.0)
IP = 100 m				**IP = 120 m**			
359.78 ± 0.34	$+1.90 \pm 0.81$	0.555 ± 0.012	3.3 (1.9)	0.11 ± 0.34	$+0.81 \pm 0.81$	0.642 ± 0.012	2.7 (1.4)
24.57 ± 0.34	$+2.17 \pm 0.81$	0.625 ± 0.013	4.1 (4.7)	24.03 ± 0.34	-0.39 ± 0.96	0.708 ± 0.001	2.8 (1.4)
51.26 ± 0.52	-4.43 ± 1.45	0.648 ± 0.003	5.8 (12.5)	51.84 ± 0.34	-2.06 ± 1.12	0.733 ± 0.008	3.4 (7.6)
92.56 ± 0.34	-4.55 ± 1.12	0.629 ± 0.006	7.1 (2.2)	91.81 ± 0.34	-3.35 ± 0.96	0.718 ± 0.003	5.9 (1.9)
127.47 ± 0.52	-1.20 ± 0.83	0.570 ± 0.003	7.6 (2.1)	127.18 ± 0.52	-1.00 ± 0.98	0.656 ± 0.004	7.2 (1.6)
155.36 ± 0.34	$+1.64 \pm 0.96$	0.530 ± 0.003	7.4 (2.0)	155.54 ± 0.34	$+1.16 \pm 0.81$	0.617 ± 0.004	5.5 (1.3)
179.26 ± 0.52	$+3.30 \pm 1.14$	0.570 ± 0.003	2.8 (1.8)	180.12 ± 0.34	$+2.46 \pm 0.96$	0.659 ± 0.009	2.5 (1.1)
203.35 ± 0.69	$+4.56 \pm 1.15$	0.629 ± 0.006	3.2 (1.9)	202.74 ± 0.17	$+1.25 \pm 0.79$	0.719 ± 0.009	2.4 (2.3)
232.75 ± 0.17	$+0.40 \pm 0.79$	0.651 ± 0.006	5.6 (2.3)	232.09 ± 0.34	-0.26 ± 1.12	0.733 ± 0.006	4.1 (1.9)
270.49 ± 0.69	-4.73 ± 1.31	0.624 ± 0.006	7.9 (2.1)	269.93 ± 0.34	-3.17 ± 0.81	0.711 ± 0.006	5.7 (2.2)
307.89 ± 0.52	-0.18 ± 0.67	0.564 ± 0.006	11.5 (2.0)	307.70 ± 0.17	-0.59 ± 0.48	0.646 ± 0.001	8.2 (1.5)
335.60 ± 0.34	$+0.75 \pm 0.81$	0.519 ± 0.008	8.0 (2.5)	336.68 ± 0.34	$+1.41 \pm 0.65$	0.601 ± 0.009	5.4 (1.1)

Table 154: The nominal angle δ_n, average displacement $\Delta\delta$, average value of the parameter DIST, RMS of the ALPHA distribution for enabled GF and impact parameters between 60 m and 120 m. The RMS of the ALPHA distribution for disabled GF is given parentheses. The primary γ-ray energy was set to 1000 GeV, the ZA to 40° and the azimuth angle to 120°.

$E_\gamma = 1000\,\mathrm{GeV}$, Az = 120°, ZA = 40°, Hard Image Cleaning

$\delta_n[°]$	$\Delta\delta[°]$	DIST[°]	$\mathrm{RMS}_{\vert\mathrm{ALPHA}\vert}[°]$	$\delta_n[°]$	$\Delta\delta[°]$	DIST[°]	$\mathrm{RMS}_{\vert\mathrm{ALPHA}\vert}[°]$
IP = 60 m				**IP = 80 m**			
358.63 ± 0.82	$+7.93 \pm 1.60$	0.351 ± 0.004	4.9 (2.8)	359.67 ± 0.49	$+4.15 \pm 1.27$	0.451 ± 0.010	4.0 (2.8)
22.11 ± 0.33	$+7.09 \pm 0.95$	0.396 ± 0.009	6.5 (15.6)	22.49 ± 0.49	$+1.47 \pm 1.27$	0.509 ± 0.009	4.8 (11.2)
53.83 ± 0.66	-5.93 ± 1.28	0.417 ± 0.004	8.3 (3.2)	54.27 ± 0.66	-0.12 ± 1.59	0.537 ± 0.003	8.9 (2.3)
92.44 ± 0.66	-12.13 ± 1.74	0.399 ± 0.005	14.6 (5.1)	89.86 ± 0.49	-10.96 ± 1.11	0.514 ± 0.008	10.2 (11.3)
130.17 ± 0.33	-0.02 ± 0.95	0.357 ± 0.003	16.4 (3.9)	129.09 ± 0.33	-0.69 ± 0.79	0.463 ± 0.003	14.1 (2.4)
156.80 ± 0.82	$+6.83 \pm 1.60$	0.329 ± 0.004	10.4 (3.9)	155.85 ± 0.33	$+3.59 \pm 0.79$	0.430 ± 0.004	9.2 (2.8)
179.17 ± 0.66	$+10.32 \pm 1.90$	0.353 ± 0.005	5.8 (4.6)	179.80 ± 0.33	$+6.19 \pm 1.26$	0.462 ± 0.003	4.1 (2.3)
202.94 ± 0.66	$+10.99 \pm 1.74$	0.399 ± 0.004	6.1 (4.1)	203.07 ± 0.66	$+3.18 \pm 1.43$	0.515 ± 0.003	4.4 (2.7)
234.62 ± 0.16	-2.30 ± 0.78	0.413 ± 0.004	9.6 (2.2)	232.78 ± 0.49	$+0.67 \pm 1.27$	0.539 ± 0.005	6.6 (2.5)
271.62 ± 0.99	-11.25 ± 1.61	0.393 ± 0.004	13.7 (3.7)	269.97 ± 0.66	-8.03 ± 1.74	0.515 ± 0.005	10.6 (2.4)
307.40 ± 0.49	-0.69 ± 1.11	0.344 ± 0.006	15.3 (2.9)	306.70 ± 0.66	-1.24 ± 1.12	0.455 ± 0.005	15.9 (1.8)
337.31 ± 0.33	$+5.66 \pm 1.41$	0.320 ± 0.006	9.3 (2.8)	336.72 ± 0.49	$+3.03 \pm 0.96$	0.419 ± 0.006	8.4 (1.6)
IP = 100 m				**IP = 120 m**			
359.64 ± 0.33	$+1.43 \pm 0.79$	0.548 ± 0.005	2.8 (1.2)	0.20 ± 0.33	$+1.00 \pm 0.79$	0.635 ± 0.005	2.8 (1.2)
23.77 ± 0.33	$+1.17 \pm 0.95$	0.616 ± 0.006	3.8 (5.2)	23.80 ± 0.33	-0.41 ± 0.48	0.703 ± 0.012	2.7 (1.1)
51.70 ± 0.49	-3.37 ± 1.11	0.643 ± 0.001	6.0 (13.0)	52.19 ± 0.33	-1.60 ± 0.95	0.730 ± 0.005	3.5 (6.6)
89.48 ± 0.66	-7.28 ± 1.59	0.622 ± 0.008	7.0 (16.6)	90.11 ± 0.33	-4.95 ± 0.95	0.714 ± 0.003	5.6 (2.0)
127.48 ± 0.49	-1.03 ± 0.96	0.562 ± 0.006	8.7 (1.8)	127.02 ± 0.49	-0.89 ± 0.96	0.651 ± 0.005	6.7 (1.7)
155.16 ± 0.33	$+1.47 \pm 0.79$	0.524 ± 0.001	7.2 (1.9)	155.56 ± 0.33	$+1.09 \pm 0.79$	0.611 ± 0.004	5.3 (1.4)
179.63 ± 0.49	$+3.24 \pm 1.11$	0.563 ± 0.004	2.7 (1.6)	179.98 ± 0.33	$+2.09 \pm 0.79$	0.652 ± 0.004	2.1 (1.1)
203.51 ± 0.66	$+4.26 \pm 1.28$	0.624 ± 0.004	3.1 (2.1)	203.30 ± 0.33	$+2.04 \pm 0.95$	0.713 ± 0.004	2.2 (1.8)
232.90 ± 0.33	$+0.85 \pm 0.79$	0.645 ± 0.006	5.4 (2.5)	232.41 ± 0.16	$+0.21 \pm 0.78$	0.727 ± 0.004	4.1 (1.7)
270.06 ± 0.33	-5.18 ± 1.26	0.618 ± 0.006	7.7 (1.9)	270.09 ± 0.33	-2.64 ± 0.95	0.703 ± 0.005	5.7 (1.9)
307.87 ± 0.49	-0.41 ± 1.11	0.553 ± 0.009	12.1 (2.5)	307.92 ± 0.16	-0.27 ± 0.47	0.639 ± 0.005	7.6 (1.3)
335.93 ± 0.33	$+1.15 \pm 0.79$	0.512 ± 0.013	8.4 (2.4)	336.58 ± 0.33	$+1.23 \pm 0.64$	0.593 ± 0.004	5.0 (1.4)

Table 155: The nominal angle δ_n, average displacement $\Delta\delta$, average value of the parameter DIST, RMS of the ALPHA distribution for enabled GF and impact parameters between 60 m and 120 m. The RMS of the ALPHA distribution for disabled GF is given parentheses. The primary γ-ray energy was set to 1000 GeV, the ZA to 40° and the azimuth angle to 120°.

$E_\gamma = 1000\,\mathrm{GeV}$, Az $= 150°$, ZA $= 40°$, Intermediate Image Cleaning

$\delta_n[°]$	$\Delta\delta[°]$	DIST[°]	$\mathrm{RMS}_{\lvert\mathrm{ALPHA}\rvert}[°]$	$\delta_n[°]$	$\Delta\delta[°]$	DIST[°]	$\mathrm{RMS}_{\lvert\mathrm{ALPHA}\rvert}[°]$
IP = 60 m				**IP = 80 m**			
359.29 ± 0.34	$+4.26 \pm 0.97$	0.384 ± 0.006	5.2 (2.2)	359.70 ± 0.34	$+3.64 \pm 0.97$	0.500 ± 0.004	3.7 (2.8)
22.19 ± 0.52	$+10.21 \pm 1.30$	0.407 ± 0.009	5.9 (15.6)	22.42 ± 0.69	$+6.13 \pm 1.62$	0.527 ± 0.005	4.2 (11.8)
54.60 ± 0.69	$+10.98 \pm 1.62$	0.392 ± 0.008	8.8 (5.4)	54.47 ± 0.52	$+7.81 \pm 0.83$	0.511 ± 0.005	7.7 (3.2)
91.41 ± 0.17	-15.84 ± 1.11	0.354 ± 0.005	14.0 (5.4)	90.32 ± 0.34	-8.20 ± 1.12	0.464 ± 0.006	14.0 (12.7)
130.18 ± 0.34	-6.44 ± 1.44	0.339 ± 0.004	19.4 (3.2)	129.36 ± 0.69	-2.86 ± 1.62	0.440 ± 0.008	16.3 (2.9)
156.32 ± 0.86	$+1.23 \pm 1.17$	0.364 ± 0.008	9.6 (3.4)	155.81 ± 0.34	$+0.36 \pm 0.66$	0.472 ± 0.010	6.9 (2.5)
179.46 ± 0.34	$+6.10 \pm 0.81$	0.405 ± 0.010	4.9 (4.5)	179.69 ± 0.34	$+3.84 \pm 0.66$	0.520 ± 0.005	3.2 (2.7)
203.23 ± 0.86	$+12.51 \pm 1.48$	0.422 ± 0.005	6.5 (4.2)	203.79 ± 0.52	$+6.45 \pm 0.83$	0.538 ± 0.012	4.3 (3.0)
235.82 ± 0.34	$+17.04 \pm 0.66$	0.396 ± 0.009	10.1 (2.3)	232.88 ± 0.69	$+3.67 \pm 1.16$	0.511 ± 0.005	7.1 (2.5)
272.21 ± 0.34	-16.81 ± 1.44	0.348 ± 0.003	16.9 (4.6)	269.32 ± 0.69	-13.32 ± 1.31	0.454 ± 0.004	16.4 (3.3)
307.19 ± 0.69	-9.77 ± 2.09	0.320 ± 0.008	20.1 (5.3)	306.85 ± 0.69	-7.31 ± 1.16	0.415 ± 0.010	14.7 (1.8)
337.26 ± 0.34	-0.71 ± 0.81	0.342 ± 0.008	9.0 (2.9)	336.91 ± 0.34	-0.75 ± 0.81	0.444 ± 0.010	6.3 (2.0)
IP = 100 m				**IP = 120 m**			
359.78 ± 0.34	$+2.57 \pm 0.66$	0.606 ± 0.013	3.4 (1.9)	0.11 ± 0.34	$+1.04 \pm 0.81$	0.697 ± 0.004	2.5 (1.4)
24.57 ± 0.34	$+4.85 \pm 0.81$	0.635 ± 0.003	3.6 (4.7)	24.03 ± 0.34	$+2.75 \pm 0.81$	0.728 ± 0.009	2.5 (1.4)
51.26 ± 0.52	$+3.35 \pm 0.83$	0.615 ± 0.003	5.6 (12.5)	51.84 ± 0.34	$+2.22 \pm 0.66$	0.707 ± 0.004	4.0 (7.6)
92.56 ± 0.34	-2.69 ± 0.81	0.562 ± 0.003	6.7 (2.2)	91.81 ± 0.34	$+0.06 \pm 0.81$	0.651 ± 0.005	7.9 (1.9)
127.47 ± 0.52	-2.42 ± 1.14	0.532 ± 0.009	10.8 (2.1)	127.18 ± 0.52	-1.64 ± 0.83	0.614 ± 0.003	8.4 (1.6)
155.36 ± 0.34	-0.30 ± 0.81	0.569 ± 0.004	5.7 (2.0)	155.54 ± 0.34	-0.25 ± 0.81	0.654 ± 0.003	4.5 (1.3)
179.26 ± 0.52	$+2.10 \pm 0.98$	0.624 ± 0.001	2.0 (1.8)	180.12 ± 0.34	$+1.91 \pm 0.81$	0.714 ± 0.001	1.9 (1.1)
203.35 ± 0.69	$+3.09 \pm 1.31$	0.644 ± 0.004	3.2 (1.9)	202.74 ± 0.17	$+1.37 \pm 0.64$	0.728 ± 0.004	2.5 (2.3)
232.75 ± 0.17	$+5.14 \pm 0.95$	0.613 ± 0.006	5.4 (2.3)	232.09 ± 0.34	$+0.28 \pm 0.97$	0.703 ± 0.012	4.2 (1.9)
270.49 ± 0.69	-7.53 ± 1.94	0.552 ± 0.012	10.5 (2.1)	269.93 ± 0.34	-5.37 ± 1.12	0.639 ± 0.016	6.5 (2.2)
307.89 ± 0.52	-4.33 ± 0.83	0.508 ± 0.005	10.7 (2.0)	307.70 ± 0.17	-3.63 ± 0.48	0.592 ± 0.009	7.4 (1.5)
335.60 ± 0.34	-1.35 ± 0.66	0.540 ± 0.003	5.6 (2.5)	336.68 ± 0.34	$+0.08 \pm 0.66$	0.631 ± 0.005	4.0 (1.1)

Table 156: The nominal angle δ_n, average displacement $\Delta\delta$, average value of the parameter DIST, RMS of the ALPHA distribution for enabled GF and impact parameters between 60 m and 120 m. The RMS of the ALPHA distribution for disabled GF is given parentheses. The primary γ-ray energy was set to 1000 GeV, the ZA to 40° and the azimuth angle to 150°.

$E_\gamma = 1000\,\mathrm{GeV}$, Az $= 150°$, ZA $= 40°$, Hard Image Cleaning

$\delta_n[°]$	$\Delta\delta[°]$	DIST[°]	$\mathrm{RMS}_{\lvert\mathrm{ALPHA}\rvert}[°]$	$\delta_n[°]$	$\Delta\delta[°]$	DIST[°]	$\mathrm{RMS}_{\lvert\mathrm{ALPHA}\rvert}[°]$
IP = 60 m				**IP = 80 m**			
358.63 ± 0.82	$+3.68 \pm 1.76$	0.379 ± 0.009	3.5 (2.8)	359.67 ± 0.49	$+3.40 \pm 1.12$	0.494 ± 0.008	3.7 (2.8)
22.11 ± 0.33	$+10.13 \pm 0.49$	0.403 ± 0.006	5.9 (15.6)	22.49 ± 0.49	$+5.86 \pm 1.43$	0.523 ± 0.009	4.4 (11.2)
53.83 ± 0.66	$+10.92 \pm 0.82$	0.388 ± 0.008	9.1 (3.2)	54.27 ± 0.66	$+9.40 \pm 1.13$	0.504 ± 0.008	7.6 (2.3)
92.44 ± 0.66	-13.88 ± 1.59	0.349 ± 0.006	18.4 (5.1)	89.86 ± 0.49	-9.17 ± 0.96	0.457 ± 0.003	12.8 (11.3)
130.17 ± 0.33	-5.20 ± 1.42	0.332 ± 0.004	19.9 (3.9)	129.09 ± 0.33	-3.08 ± 1.11	0.432 ± 0.005	16.2 (2.4)
156.80 ± 0.82	$+1.46 \pm 1.29$	0.359 ± 0.008	9.4 (3.9)	155.85 ± 0.33	$+0.49 \pm 0.80$	0.467 ± 0.004	6.7 (2.8)
179.17 ± 0.66	$+5.67 \pm 1.44$	0.399 ± 0.009	4.3 (4.6)	179.80 ± 0.33	$+3.60 \pm 0.64$	0.513 ± 0.008	3.0 (2.3)
202.94 ± 0.66	$+10.75 \pm 1.13$	0.418 ± 0.009	5.9 (4.1)	203.07 ± 0.66	$+6.04 \pm 1.13$	0.531 ± 0.012	4.2 (2.7)
234.62 ± 0.16	$+11.65 \pm 1.26$	0.391 ± 0.009	10.1 (2.2)	232.78 ± 0.49	$+2.38 \pm 1.12$	0.506 ± 0.004	7.2 (2.5)
271.62 ± 0.99	-17.49 ± 1.61	0.342 ± 0.006	15.1 (3.7)	269.97 ± 0.66	-12.56 ± 0.82	0.446 ± 0.003	12.9 (2.4)
307.40 ± 0.49	-9.53 ± 1.74	0.315 ± 0.005	19.9 (2.9)	306.70 ± 0.66	-7.52 ± 1.44	0.410 ± 0.009	13.3 (1.8)
337.31 ± 0.33	-0.41 ± 0.95	0.336 ± 0.008	8.3 (2.8)	336.72 ± 0.49	-0.70 ± 0.96	0.439 ± 0.006	6.4 (1.6)
IP = 100 m				**IP = 120 m**			
359.64 ± 0.33	$+2.64 \pm 0.64$	0.599 ± 0.004	3.3 (1.2)	0.20 ± 0.33	$+1.23 \pm 0.80$	0.692 ± 0.009	2.3 (1.2)
23.77 ± 0.33	$+4.07 \pm 0.80$	0.629 ± 0.004	3.6 (5.2)	23.80 ± 0.33	$+2.23 \pm 0.80$	0.721 ± 0.004	2.5 (1.1)
51.70 ± 0.49	$+3.76 \pm 0.81$	0.609 ± 0.001	5.2 (13.0)	52.19 ± 0.33	$+2.27 \pm 0.64$	0.700 ± 0.001	4.8 (6.6)
89.48 ± 0.66	-6.48 ± 1.13	0.555 ± 0.008	6.4 (16.6)	90.11 ± 0.33	-1.47 ± 0.80	0.645 ± 0.014	6.2 (2.0)
127.48 ± 0.49	-3.02 ± 0.96	0.527 ± 0.005	10.0 (1.8)	127.02 ± 0.49	-2.29 ± 0.81	0.607 ± 0.005	7.3 (1.7)
155.16 ± 0.33	$+0.01 \pm 0.80$	0.563 ± 0.008	5.4 (1.9)	155.56 ± 0.33	-0.17 ± 0.64	0.646 ± 0.008	4.2 (1.4)
179.63 ± 0.49	$+2.23 \pm 0.96$	0.615 ± 0.004	2.0 (1.6)	179.98 ± 0.33	$+1.91 \pm 0.80$	0.708 ± 0.009	1.7 (1.1)
203.51 ± 0.66	$+3.24 \pm 1.28$	0.637 ± 0.008	2.9 (2.1)	203.30 ± 0.33	$+2.10 \pm 0.80$	0.723 ± 0.008	2.5 (1.8)
232.90 ± 0.33	$+4.22 \pm 0.95$	0.608 ± 0.008	5.3 (2.5)	232.41 ± 0.16	$+0.46 \pm 0.63$	0.698 ± 0.009	4.0 (1.7)
270.06 ± 0.33	-7.65 ± 1.27	0.546 ± 0.009	10.3 (1.9)	270.09 ± 0.33	-5.35 ± 0.80	0.632 ± 0.004	6.0 (1.9)
307.87 ± 0.49	-4.47 ± 1.27	0.500 ± 0.010	10.3 (2.5)	307.92 ± 0.16	-3.51 ± 0.63	0.586 ± 0.004	7.1 (1.3)
335.93 ± 0.33	-0.77 ± 0.64	0.534 ± 0.009	4.6 (2.4)	336.58 ± 0.33	$+0.06 \pm 0.64$	0.626 ± 0.005	4.4 (1.4)

Table 157: The nominal angle δ_n, average displacement $\Delta\delta$, average value of the parameter DIST, RMS of the ALPHA distribution for enabled GF and impact parameters between 60 m and 120 m. The RMS of the ALPHA distribution for disabled GF is given parentheses. The primary γ-ray energy was set to 1000 GeV, the ZA to 40° and the azimuth angle to 150°.

$E_\gamma = 1000\,$GeV, Az = 180°, ZA = 40°, Intermediate Image Cleaning

$\delta_n[°]$	$\Delta\delta[°]$	DIST[°]	$\text{RMS}_{\lvert\text{ALPHA}\rvert}[°]$	$\delta_n[°]$	$\Delta\delta[°]$	DIST[°]	$\text{RMS}_{\lvert\text{ALPHA}\rvert}[°]$
IP = 60 m				**IP = 80 m**			
359.29 ± 0.34	-2.14 ± 0.81	0.399 ± 0.006	17.7 (2.2)	359.70 ± 0.34	$+0.68 \pm 0.65$	0.516 ± 0.008	1.4 (2.8)
22.19 ± 0.52	$+4.32 \pm 0.98$	0.386 ± 0.008	26.4 (15.6)	22.42 ± 0.69	$+1.11 \pm 1.15$	0.496 ± 0.005	23.2 (11.8)
54.60 ± 0.69	$+21.10 \pm 2.07$	0.349 ± 0.006	11.8 (5.4)	54.47 ± 0.52	$+9.17 \pm 1.28$	0.453 ± 0.006	16.5 (3.2)
91.41 ± 0.17	$+5.69 \pm 1.57$	0.328 ± 0.004	24.2 (5.4)	90.32 ± 0.34	-1.48 ± 1.11	0.427 ± 0.004	18.9 (12.7)
130.18 ± 0.34	-12.65 ± 0.96	0.352 ± 0.005	17.2 (3.2)	129.36 ± 0.69	-8.95 ± 1.46	0.460 ± 0.003	11.2 (2.9)
156.32 ± 0.86	-2.93 ± 1.63	0.396 ± 0.006	10.5 (3.4)	155.81 ± 0.34	-4.21 ± 0.81	0.510 ± 0.004	11.1 (2.5)
179.46 ± 0.34	-2.11 ± 0.65	0.408 ± 0.005	8.5 (4.5)	179.69 ± 0.34	$+0.44 \pm 0.65$	0.530 ± 0.005	7.6 (2.7)
203.23 ± 0.86	$+3.53 \pm 1.32$	0.386 ± 0.004	16.9 (4.2)	203.79 ± 0.52	$+2.78 \pm 0.98$	0.499 ± 0.005	24.3 (3.0)
235.82 ± 0.34	$+16.62 \pm 0.96$	0.338 ± 0.001	13.2 (2.3)	232.88 ± 0.69	$+8.16 \pm 1.30$	0.444 ± 0.001	33.6 (2.5)
272.21 ± 0.34	$+0.05 \pm 0.81$	0.311 ± 0.004	23.9 (4.6)	269.32 ± 0.69	-1.96 ± 0.84	0.403 ± 0.006	25.8 (3.3)
307.19 ± 0.69	-9.52 ± 1.30	0.333 ± 0.004	13.3 (5.3)	306.85 ± 0.69	-6.77 ± 1.46	0.436 ± 0.005	10.5 (1.8)
337.26 ± 0.34	-2.88 ± 1.27	0.375 ± 0.005	11.0 (2.9)	336.91 ± 0.34	-2.25 ± 0.96	0.490 ± 0.008	3.5 (2.0)
IP = 100 m				**IP = 120 m**			
359.78 ± 0.34	$+0.12 \pm 0.65$	0.623 ± 0.008	13.3 (1.9)	0.11 ± 0.34	-0.56 ± 0.65	0.710 ± 0.012	10.0 (1.4)
24.57 ± 0.34	$+2.01 \pm 0.96$	0.607 ± 0.009	18.5 (4.7)	24.03 ± 0.34	$+2.65 \pm 0.81$	0.694 ± 0.006	4.7 (1.4)
51.26 ± 0.52	$+3.47 \pm 0.82$	0.547 ± 0.004	5.1 (12.5)	51.84 ± 0.34	$+2.92 \pm 0.96$	0.638 ± 0.001	2.5 (7.6)
92.56 ± 0.34	$+5.47 \pm 0.81$	0.516 ± 0.006	16.1 (2.2)	91.81 ± 0.34	$+5.47 \pm 0.96$	0.603 ± 0.006	7.4 (1.9)
127.47 ± 0.52	-4.16 ± 1.28	0.555 ± 0.006	9.7 (2.1)	127.18 ± 0.52	-0.40 ± 0.98	0.641 ± 0.005	7.8 (1.6)
155.36 ± 0.34	-0.73 ± 0.81	0.617 ± 0.008	3.6 (2.0)	155.54 ± 0.34	-0.17 ± 0.96	0.701 ± 0.003	4.3 (1.3)
179.26 ± 0.52	-2.47 ± 0.82	0.634 ± 0.006	7.9 (1.8)	180.12 ± 0.34	-0.74 ± 0.65	0.715 ± 0.006	11.0 (1.1)
203.35 ± 0.69	$+1.26 \pm 1.00$	0.604 ± 0.003	19.1 (1.9)	202.74 ± 0.17	-0.03 ± 0.63	0.687 ± 0.010	4.7 (2.3)
232.75 ± 0.17	$+5.71 \pm 0.79$	0.539 ± 0.004	22.4 (2.3)	232.09 ± 0.34	$+3.68 \pm 0.96$	0.624 ± 0.004	18.7 (1.9)
270.49 ± 0.69	$+0.43 \pm 1.61$	0.495 ± 0.003	18.1 (2.1)	269.93 ± 0.34	-0.46 ± 1.42	0.579 ± 0.005	7.7 (2.2)
307.89 ± 0.52	-4.36 ± 1.59	0.527 ± 0.010	8.6 (2.0)	307.70 ± 0.17	-2.68 ± 0.94	0.612 ± 0.010	6.0 (1.5)
335.60 ± 0.34	-1.85 ± 0.81	0.592 ± 0.010	11.6 (2.5)	336.68 ± 0.34	-0.60 ± 0.81	0.685 ± 0.010	6.3 (1.1)

Table 158: The nominal angle δ_n, average displacement $\Delta\delta$, average value of the parameter DIST, RMS of the ALPHA distribution for enabled GF and impact parameters between 60 m and 120 m. The RMS of the ALPHA distribution for disabled GF is given parentheses. The primary γ-ray energy was set to 1000 GeV, the ZA to 40° and the azimuth angle to 180°.

$E_\gamma = 1000\,$GeV, Az = 180°, ZA = 40°, Hard Image Cleaning

$\delta_n[°]$	$\Delta\delta[°]$	DIST[°]	$\text{RMS}_{\lvert\text{ALPHA}\rvert}[°]$	$\delta_n[°]$	$\Delta\delta[°]$	DIST[°]	$\text{RMS}_{\lvert\text{ALPHA}\rvert}[°]$
IP = 60 m				**IP = 80 m**			
358.63 ± 0.82	-0.27 ± 1.44	0.396 ± 0.008	2.8 (2.8)	359.67 ± 0.49	$+0.39 \pm 0.80$	0.511 ± 0.006	16.1 (2.8)
22.11 ± 0.33	$+4.83 \pm 0.64$	0.382 ± 0.008	26.9 (15.6)	22.49 ± 0.49	$+1.11 \pm 1.11$	0.490 ± 0.006	19.7 (11.2)
53.83 ± 0.66	$+19.08 \pm 1.43$	0.343 ± 0.005	8.4 (3.2)	54.27 ± 0.66	$+10.44 \pm 1.58$	0.444 ± 0.008	2.5 (2.3)
92.44 ± 0.66	$+7.62 \pm 1.90$	0.323 ± 0.003	26.7 (5.1)	89.86 ± 0.49	$+1.32 \pm 1.73$	0.419 ± 0.006	19.0 (11.3)
130.17 ± 0.33	-13.24 ± 0.79	0.347 ± 0.006	16.1 (3.9)	129.09 ± 0.33	-5.64 ± 1.10	0.450 ± 0.004	15.5 (2.4)
156.80 ± 0.82	-3.46 ± 1.29	0.392 ± 0.004	9.5 (3.9)	155.85 ± 0.33	-3.55 ± 0.79	0.506 ± 0.004	4.8 (2.8)
179.17 ± 0.66	-0.40 ± 1.58	0.398 ± 0.006	8.1 (4.6)	179.80 ± 0.33	-2.14 ± 0.64	0.523 ± 0.005	6.8 (2.3)
202.94 ± 0.66	$+3.17 \pm 1.12$	0.380 ± 0.003	4.5 (4.1)	203.07 ± 0.66	$+2.13 \pm 1.12$	0.492 ± 0.006	25.3 (2.7)
234.62 ± 0.16	$+17.57 \pm 0.32$	0.331 ± 0.004	22.6 (2.2)	232.78 ± 0.49	$+10.93 \pm 0.80$	0.434 ± 0.003	28.0 (2.5)
271.62 ± 0.99	-1.10 ± 2.53	0.307 ± 0.004	21.3 (3.7)	269.97 ± 0.66	-1.11 ± 1.27	0.401 ± 0.003	18.2 (2.4)
307.40 ± 0.49	-8.65 ± 1.57	0.328 ± 0.006	13.5 (2.9)	306.70 ± 0.66	-8.21 ± 1.43	0.427 ± 0.004	13.4 (1.8)
337.31 ± 0.33	-2.73 ± 0.94	0.372 ± 0.005	10.9 (2.8)	336.72 ± 0.49	-2.26 ± 0.96	0.486 ± 0.008	3.7 (1.6)
IP = 100 m				**IP = 120 m**			
359.64 ± 0.33	-1.00 ± 0.64	0.619 ± 0.012	13.6 (1.2)	0.20 ± 0.33	$+0.64 \pm 0.48$	0.707 ± 0.012	12.2 (1.2)
23.77 ± 0.33	$+2.87 \pm 0.94$	0.601 ± 0.009	25.2 (5.2)	23.80 ± 0.33	$+2.82 \pm 0.48$	0.689 ± 0.005	6.8 (1.1)
51.70 ± 0.49	$+5.04 \pm 0.80$	0.538 ± 0.008	4.0 (13.0)	52.19 ± 0.33	$+5.53 \pm 0.94$	0.633 ± 0.003	2.3 (6.6)
89.48 ± 0.66	$+1.34 \pm 0.97$	0.507 ± 0.005	12.5 (16.6)	90.11 ± 0.33	$+3.62 \pm 0.79$	0.596 ± 0.004	7.6 (2.0)
127.48 ± 0.49	-5.64 ± 1.27	0.549 ± 0.006	9.1 (1.8)	127.02 ± 0.49	-0.52 ± 0.96	0.631 ± 0.005	7.7 (1.7)
155.16 ± 0.33	-0.69 ± 0.48	0.606 ± 0.008	3.0 (1.9)	155.56 ± 0.33	$+0.21 \pm 0.79$	0.696 ± 0.004	4.4 (1.4)
179.63 ± 0.49	-2.20 ± 0.80	0.627 ± 0.006	7.8 (1.6)	179.98 ± 0.33	-1.30 ± 0.64	0.709 ± 0.010	1.2 (1.1)
203.51 ± 0.66	$+1.25 \pm 1.12$	0.598 ± 0.004	11.7 (2.1)	203.30 ± 0.33	$+0.36 \pm 0.79$	0.680 ± 0.006	1.2 (1.8)
232.90 ± 0.33	$+5.85 \pm 0.94$	0.530 ± 0.004	17.2 (2.5)	232.41 ± 0.16	$+3.39 \pm 0.63$	0.615 ± 0.004	5.9 (1.7)
270.06 ± 0.33	-1.00 ± 0.48	0.489 ± 0.004	12.5 (1.9)	270.09 ± 0.33	-0.92 ± 1.25	0.573 ± 0.005	7.8 (1.9)
307.87 ± 0.49	-5.91 ± 1.57	0.527 ± 0.010	8.8 (2.5)	307.92 ± 0.16	-3.20 ± 1.09	0.606 ± 0.006	5.9 (1.3)
335.93 ± 0.33	-2.49 ± 0.94	0.586 ± 0.008	10.8 (2.4)	336.58 ± 0.33	-0.75 ± 0.79	0.678 ± 0.006	7.0 (1.4)

Table 159: The nominal angle δ_n, average displacement $\Delta\delta$, average value of the parameter DIST, RMS of the ALPHA distribution for enabled GF and impact parameters between 60 m and 120 m. The RMS of the ALPHA distribution for disabled GF is given parentheses. The primary γ-ray energy was set to 1000 GeV, the ZA to 40° and the azimuth angle to 180°.

$E_\gamma = 1000\,\mathrm{GeV}$, Az $= 0°$, ZA $= 60°$, Intermediate Image Cleaning

δ_n[°]	$\Delta\delta$[°]	DIST[°]	RMS$_{\lvert\mathrm{ALPHA}\rvert}$[°]	δ_n[°]	$\Delta\delta$[°]	DIST[°]	RMS$_{\lvert\mathrm{ALPHA}\rvert}$[°]
IP = 60 m				**IP = 80 m**			
1.00 ± 0.47	$+0.17 \pm 0.73$	0.171 ± 0.001	20.6 (16.4)	358.94 ± 0.56	$+0.02 \pm 1.36$	0.226 ± 0.002	11.7 (10.1)
17.32 ± 0.47	-1.35 ± 1.18	0.155 ± 0.001	18.2 (17.6)	16.99 ± 0.65	-0.68 ± 1.54	0.202 ± 0.001	10.9 (11.8)
39.99 ± 1.68	$+3.94 \pm 4.02$	0.120 ± 0.001	24.2 (24.4)	38.65 ± 1.12	-0.48 ± 1.74	0.148 ± 0.001	23.5 (20.1)
99.27 ± 0.74	-5.51 ± 1.69	0.144 ± 0.003	31.1 (14.1)	98.86 ± 1.96	$+4.86 \pm 4.78$	0.117 ± 0.001	26.9 (23.1)
134.90 ± 0.45	$+0.88 \pm 1.87$	0.121 ± 0.001	21.4 (20.9)	140.61 ± 1.30	-5.60 ± 2.82	0.144 ± 0.001	18.5 (17.6)
158.90 ± 1.30	-3.28 ± 2.37	0.150 ± 0.001	18.5 (20.4)	163.25 ± 0.74	$+0.15 \pm 1.28$	0.200 ± 0.001	11.0 (12.9)
179.57 ± 0.28	$+4.63 \pm 1.08$	0.169 ± 0.001	14.9 (14.1)	179.64 ± 0.93	$+4.14 \pm 1.38$	0.227 ± 0.001	11.9 (11.8)
195.95 ± 0.74	-2.86 ± 1.73	0.157 ± 0.001	16.6 (19.6)	195.94 ± 0.37	$+3.80 \pm 1.00$	0.205 ± 0.001	13.5 (9.7)
216.53 ± 0.29	$+2.11 \pm 1.20$	0.124 ± 0.002	24.1 (23.0)	215.94 ± 0.56	-2.03 ± 1.45	0.158 ± 0.001	16.5 (20.0)
270.56 ± 0.26	$+1.17 \pm 0.49$	0.110 ± 0.001	25.4 (21.5)	272.67 ± 0.47	$+5.05 \pm 0.74$	0.130 ± 0.001	22.4 (22.8)
320.08 ± 0.47	-5.04 ± 2.91	0.126 ± 0.002	23.2 (23.3)	320.21 ± 0.09	-4.68 ± 1.16	0.160 ± 0.001	17.8 (21.1)
343.77 ± 0.47	-0.16 ± 1.00	0.159 ± 0.001	22.6 (20.6)	342.87 ± 0.47	-4.02 ± 0.73	0.207 ± 0.001	17.0 (15.2)
IP = 100 m				**IP = 120 m**			
0.74 ± 0.74	$+0.19 \pm 1.19$	0.287 ± 0.003	11.2 (9.5)	0.29 ± 0.37	-2.05 ± 0.91	0.345 ± 0.002	5.2 (8.0)
16.28 ± 0.74	-0.33 ± 1.46	0.253 ± 0.002	7.4 (9.7)	15.20 ± 0.47	-0.11 ± 1.09	0.305 ± 0.002	6.1 (8.1)
40.58 ± 0.56	-0.65 ± 1.00	0.181 ± 0.001	14.5 (13.9)	42.68 ± 0.28	$+0.12 \pm 0.90$	0.218 ± 0.001	8.4 (13.2)
90.82 ± 0.85	-3.53 ± 1.83	0.135 ± 0.001	21.2 (20.0)	89.41 ± 0.65	-1.89 ± 1.54	0.161 ± 0.001	17.7 (20.5)
137.40 ± 0.56	-3.44 ± 1.00	0.180 ± 0.001	11.7 (11.2)	137.89 ± 0.65	-2.18 ± 1.10	0.217 ± 0.002	7.3 (9.2)
163.11 ± 0.56	$+2.64 \pm 0.83$	0.253 ± 0.002	9.6 (11.9)	162.15 ± 0.47	-0.44 ± 0.91	0.306 ± 0.002	9.3 (8.1)
177.59 ± 0.47	-0.39 ± 1.36	0.285 ± 0.001	8.8 (10.3)	177.73 ± 0.65	$+0.77 \pm 1.37$	0.340 ± 0.003	10.0 (9.3)
193.94 ± 0.56	-0.05 ± 1.27	0.261 ± 0.001	9.0 (10.5)	195.20 ± 0.56	$+0.69 \pm 1.36$	0.312 ± 0.001	11.0 (8.4)
219.60 ± 0.65	$+2.11 \pm 1.10$	0.193 ± 0.001	13.4 (17.5)	220.74 ± 0.56	$+3.62 \pm 1.18$	0.234 ± 0.001	14.3 (12.3)
270.21 ± 1.12	$+5.88 \pm 2.91$	0.156 ± 0.001	22.5 (21.1)	269.72 ± 0.84	-0.48 ± 1.56	0.182 ± 0.001	17.6 (16.3)
317.85 ± 0.65	-3.97 ± 1.28	0.197 ± 0.001	12.8 (15.7)	318.97 ± 0.47	-2.29 ± 1.18	0.235 ± 0.001	7.4 (12.4)
345.44 ± 0.47	-2.23 ± 1.27	0.261 ± 0.001	13.5 (15.5)	346.89 ± 0.74	-0.25 ± 1.46	0.316 ± 0.002	12.5 (12.8)

Table 160: The nominal angle δ_n, average displacement $\Delta\delta$, average value of the parameter DIST, RMS of the ALPHA distribution for enabled GF and impact parameters between 60 m and 120 m. The RMS of the ALPHA distribution for disabled GF is given parentheses. The primary γ-ray energy was set to 1000 GeV, the ZA to 60° and the azimuth angle to 0°.

$E_\gamma = 1000\,\mathrm{GeV}$, Az $= 0°$, ZA $= 60°$, Hard Image Cleaning

δ_n[°]	$\Delta\delta$[°]	DIST[°]	RMS$_{\lvert\mathrm{ALPHA}\rvert}$[°]	δ_n[°]	$\Delta\delta$[°]	DIST[°]	RMS$_{\lvert\mathrm{ALPHA}\rvert}$[°]
IP = 60 m				**IP = 80 m**			
358.63 ± 0.62	$+0.23 \pm 1.25$	0.171 ± 0.001	16.7 (14.7)	358.23 ± 0.53	-1.30 ± 0.98	0.226 ± 0.002	12.9 (12.0)
14.29 ± 0.36	-3.59 ± 0.89	0.154 ± 0.001	16.2 (19.1)	13.79 ± 0.63	-0.44 ± 1.52	0.201 ± 0.001	9.8 (12.3)
38.95 ± 0.10	$+4.09 \pm 0.92$	0.119 ± 0.001	23.7 (23.4)	36.95 ± 0.89	$+0.63 \pm 1.16$	0.146 ± 0.001	19.6 (18.6)
96.85 ± 0.38	-11.21 ± 1.31	0.111 ± 0.003	36.0 (11.5)	90.92 ± 0.11	-1.86 ± 0.43	0.116 ± 0.001	23.1 (25.1)
136.33 ± 0.32	-1.77 ± 1.54	0.116 ± 0.001	21.3 (23.5)	138.76 ± 0.98	-6.76 ± 2.14	0.144 ± 0.001	14.5 (18.8)
160.93 ± 0.45	-2.22 ± 0.53	0.149 ± 0.001	16.6 (19.4)	165.91 ± 0.98	-0.06 ± 1.52	0.199 ± 0.001	10.9 (11.5)
180.96 ± 0.62	$+3.69 \pm 1.69$	0.169 ± 0.001	12.9 (13.5)	180.99 ± 0.80	$+3.65 \pm 1.07$	0.226 ± 0.001	15.1 (13.0)
198.77 ± 0.36	-2.67 ± 0.89	0.156 ± 0.001	16.8 (21.0)	196.90 ± 0.36	$+2.01 \pm 0.98$	0.205 ± 0.001	11.0 (8.4)
219.20 ± 0.09	$+3.75 \pm 0.91$	0.124 ± 0.002	24.0 (22.9)	219.36 ± 0.89	-0.23 ± 1.61	0.156 ± 0.001	16.5 (17.8)
272.72 ± 2.84	-3.74 ± 3.08	0.111 ± 0.001	22.5 (25.5)	268.08 ± 0.63	-2.05 ± 0.72	0.129 ± 0.002	20.5 (21.3)
320.67 ± 0.18	-5.79 ± 1.53	0.124 ± 0.002	22.2 (24.6)	319.37 ± 0.18	-1.99 ± 0.53	0.159 ± 0.001	21.6 (18.8)
340.89 ± 1.07	-4.25 ± 1.87	0.157 ± 0.001	18.2 (17.5)	343.47 ± 0.36	-2.01 ± 1.07	0.207 ± 0.001	16.9 (16.5)
IP = 100 m				**IP = 120 m**			
0.83 ± 0.71	-0.20 ± 1.34	0.286 ± 0.001	12.5 (11.1)	0.15 ± 0.53	-1.57 ± 1.07	0.343 ± 0.002	4.4 (7.5)
17.09 ± 0.36	-0.55 ± 0.80	0.253 ± 0.002	9.0 (13.8)	14.72 ± 0.71	-0.33 ± 1.16	0.304 ± 0.002	7.5 (12.6)
38.32 ± 0.98	-2.13 ± 1.60	0.180 ± 0.001	11.0 (15.3)	40.38 ± 0.36	-0.85 ± 0.89	0.217 ± 0.001	12.4 (16.9)
91.32 ± 0.27	-1.23 ± 0.90	0.135 ± 0.001	21.5 (19.9)	92.19 ± 1.25	$+2.23 \pm 1.69$	0.160 ± 0.001	21.1 (18.7)
135.78 ± 0.27	-1.00 ± 1.07	0.179 ± 0.001	13.2 (11.7)	136.43 ± 0.27	-1.39 ± 0.80	0.216 ± 0.002	9.9 (9.0)
162.47 ± 0.54	$+3.10 \pm 0.98$	0.252 ± 0.002	13.9 (15.6)	161.98 ± 0.53	-1.93 ± 0.89	0.305 ± 0.002	8.7 (10.5)
179.19 ± 0.71	$+0.65 \pm 1.52$	0.284 ± 0.001	8.3 (11.3)	178.03 ± 0.62	-0.25 ± 1.34	0.338 ± 0.003	7.5 (8.1)
193.15 ± 0.53	-0.07 ± 0.89	0.260 ± 0.001	12.3 (11.4)	194.90 ± 0.53	$+0.33 \pm 1.07$	0.311 ± 0.001	10.4 (8.2)
220.64 ± 0.99	$+1.57 \pm 1.43$	0.191 ± 0.001	13.7 (14.6)	220.45 ± 0.45	$+4.27 \pm 0.80$	0.234 ± 0.001	16.4 (13.6)
269.42 ± 0.99	$+1.25 \pm 1.70$	0.155 ± 0.001	18.9 (23.5)	272.09 ± 0.63	$+1.93 \pm 1.25$	0.181 ± 0.001	17.6 (14.0)
317.76 ± 0.27	-1.81 ± 0.89	0.196 ± 0.001	14.5 (14.2)	319.39 ± 0.62	-0.31 ± 1.52	0.233 ± 0.001	11.6 (14.0)
348.75 ± 0.18	$+0.97 \pm 0.89$	0.261 ± 0.002	9.8 (10.6)	346.65 ± 0.53	-1.05 ± 1.07	0.314 ± 0.002	10.6 (12.5)

Table 161: The nominal angle δ_n, average displacement $\Delta\delta$, average value of the parameter DIST, RMS of the ALPHA distribution for enabled GF and impact parameters between 60 m and 120 m. The RMS of the ALPHA distribution for disabled GF is given parentheses. The primary γ-ray energy was set to 1000 GeV, the ZA to 60° and the azimuth angle to 0°.

$E_\gamma = 1000\,\text{GeV}$, Az = 30°, ZA = 60°, Intermediate Image Cleaning

δ_n[°]	$\Delta\delta$[°]	DIST[°]	$\text{RMS}_{\lvert\text{ALPHA}\rvert}$[°]	δ_n[°]	$\Delta\delta$[°]	DIST[°]	$\text{RMS}_{\lvert\text{ALPHA}\rvert}$[°]
IP = 60 m				**IP = 80 m**			
1.00 ± 0.47	$+12.83 \pm 0.80$	0.154 ± 0.001	25.0 (16.4)	358.94 ± 0.56	$+9.47 \pm 1.23$	0.203 ± 0.001	20.3 (10.1)
17.32 ± 0.47	$+2.98 \pm 1.05$	0.118 ± 0.001	27.4 (17.6)	16.99 ± 0.65	$+4.77 \pm 1.41$	0.146 ± 0.001	23.1 (11.8)
39.99 ± 1.68	-11.46 ± 2.35	0.112 ± 0.002	22.1 (24.4)	38.65 ± 1.12	-13.83 ± 2.46	0.118 ± 0.001	22.1 (20.1)
99.27 ± 0.74	$+9.48 \pm 1.00$	0.119 ± 0.001	19.5 (14.1)	98.86 ± 1.96	-2.32 ± 3.09	0.145 ± 0.001	18.4 (23.1)
134.90 ± 0.45	$+0.41 \pm 1.36$	0.150 ± 0.001	19.9 (20.9)	140.61 ± 1.30	$+8.95 \pm 1.47$	0.200 ± 0.001	16.5 (17.6)
158.90 ± 1.30	$+10.82 \pm 2.15$	0.169 ± 0.001	20.1 (20.4)	163.25 ± 0.74	$+9.67 \pm 1.33$	0.227 ± 0.001	18.2 (12.9)
179.57 ± 0.28	$+14.73 \pm 0.78$	0.157 ± 0.001	23.4 (14.1)	179.64 ± 0.93	$+10.96 \pm 1.18$	0.207 ± 0.001	21.1 (11.8)
195.95 ± 0.74	$+7.81 \pm 2.00$	0.126 ± 0.001	26.3 (19.6)	195.94 ± 0.37	$+6.67 \pm 1.13$	0.159 ± 0.001	21.7 (9.7)
216.53 ± 0.29	-19.61 ± 0.72	0.115 ± 0.001	25.9 (23.0)	215.94 ± 0.56	-19.82 ± 0.81	0.133 ± 0.001	20.7 (20.0)
270.56 ± 0.26	-7.53 ± 0.59	0.129 ± 0.001	23.3 (21.5)	272.67 ± 0.47	-8.06 ± 1.07	0.162 ± 0.001	17.7 (22.8)
320.08 ± 0.47	$+12.03 \pm 1.24$	0.161 ± 0.001	22.3 (23.3)	320.21 ± 0.09	$+8.96 \pm 0.68$	0.208 ± 0.001	17.8 (21.1)
343.77 ± 0.47	$+14.75 \pm 0.80$	0.171 ± 0.001	22.8 (20.6)	342.87 ± 0.47	$+8.01 \pm 1.30$	0.228 ± 0.001	18.5 (15.2)
IP = 100 m				**IP = 120 m**			
0.74 ± 0.74	$+9.08 \pm 1.42$	0.255 ± 0.002	17.7 (9.5)	0.29 ± 0.37	$+6.60 \pm 1.04$	0.307 ± 0.002	17.6 (8.0)
16.28 ± 0.74	$+2.27 \pm 1.33$	0.182 ± 0.001	20.0 (9.7)	15.20 ± 0.47	$+2.36 \pm 0.80$	0.218 ± 0.002	16.4 (8.1)
40.58 ± 0.56	-12.29 ± 0.64	0.136 ± 0.001	18.3 (13.9)	42.68 ± 0.28	-8.03 ± 0.95	0.160 ± 0.001	15.8 (13.2)
90.82 ± 0.85	-15.00 ± 2.03	0.180 ± 0.001	14.0 (20.0)	89.41 ± 0.65	-9.56 ± 0.99	0.217 ± 0.001	12.0 (20.5)
137.40 ± 0.56	$+5.12 \pm 1.06$	0.253 ± 0.002	15.7 (11.2)	137.89 ± 0.65	$+5.13 \pm 1.15$	0.306 ± 0.002	13.7 (9.2)
163.11 ± 0.56	$+10.11 \pm 0.98$	0.287 ± 0.001	17.4 (11.9)	162.15 ± 0.47	$+7.73 \pm 1.05$	0.343 ± 0.002	14.8 (8.1)
177.59 ± 0.47	$+4.80 \pm 1.05$	0.263 ± 0.001	19.5 (10.3)	177.73 ± 0.65	$+3.71 \pm 1.32$	0.314 ± 0.002	19.3 (9.3)
193.94 ± 0.56	-1.99 ± 1.48	0.195 ± 0.001	18.5 (10.5)	195.20 ± 0.56	$+3.27 \pm 0.98$	0.235 ± 0.002	18.4 (8.4)
219.60 ± 0.65	-12.04 ± 1.41	0.158 ± 0.001	16.7 (17.5)	220.74 ± 0.56	-7.73 ± 1.40	0.186 ± 0.001	12.9 (12.3)
270.21 ± 1.12	-6.24 ± 2.06	0.197 ± 0.001	14.5 (21.1)	269.72 ± 0.84	-9.76 ± 1.34	0.236 ± 0.001	14.1 (16.3)
317.85 ± 0.65	$+7.23 \pm 1.32$	0.263 ± 0.002	15.7 (15.7)	318.97 ± 0.47	$+7.49 \pm 0.97$	0.316 ± 0.001	14.2 (12.4)
345.44 ± 0.47	$+8.41 \pm 1.05$	0.288 ± 0.001	17.6 (15.5)	346.89 ± 0.74	$+8.30 \pm 1.25$	0.346 ± 0.002	14.8 (12.8)

Table 162: The nominal angle δ_n, average displacement $\Delta\delta$, average value of the parameter DIST, RMS of the ALPHA distribution for enabled GF and impact parameters between 60 m and 120 m. The RMS of the ALPHA distribution for disabled GF is given parentheses. The primary γ-ray energy was set to 1000 GeV, the ZA to 60° and the azimuth angle to 30°.

$E_\gamma = 1000\,\text{GeV}$, Az = 30°, ZA = 60°, Hard Image Cleaning

δ_n[°]	$\Delta\delta$[°]	DIST[°]	$\text{RMS}_{\lvert\text{ALPHA}\rvert}$[°]	δ_n[°]	$\Delta\delta$[°]	DIST[°]	$\text{RMS}_{\lvert\text{ALPHA}\rvert}$[°]
IP = 60 m				**IP = 80 m**			
358.63 ± 0.62	$+10.69 \pm 1.55$	0.154 ± 0.001	24.5 (14.7)	358.23 ± 0.53	$+8.08 \pm 0.79$	0.202 ± 0.001	21.3 (12.0)
14.29 ± 0.36	$+4.62 \pm 0.94$	0.118 ± 0.001	29.7 (19.1)	13.79 ± 0.63	$+3.84 \pm 1.46$	0.145 ± 0.001	25.3 (12.3)
38.95 ± 0.10	-9.07 ± 0.77	0.111 ± 0.002	20.7 (23.4)	36.95 ± 0.89	-10.83 ± 0.98	0.117 ± 0.001	19.6 (18.6)
96.85 ± 0.38	-1.27 ± 3.17	0.118 ± 0.001	18.8 (11.5)	90.92 ± 0.11	-16.09 ± 1.36	0.145 ± 0.001	18.3 (25.1)
136.33 ± 0.32	$+6.73 \pm 1.40$	0.149 ± 0.001	19.7 (23.5)	138.76 ± 0.98	$+7.62 \pm 2.17$	0.200 ± 0.001	17.0 (18.8)
160.93 ± 0.45	$+12.95 \pm 1.21$	0.168 ± 0.001	20.7 (19.4)	165.91 ± 0.98	$+11.44 \pm 1.23$	0.227 ± 0.001	18.9 (11.5)
180.96 ± 0.62	$+15.23 \pm 1.29$	0.157 ± 0.001	23.1 (13.5)	180.99 ± 0.80	$+8.07 \pm 1.31$	0.207 ± 0.001	20.5 (13.0)
198.77 ± 0.36	$+12.44 \pm 0.52$	0.125 ± 0.001	24.5 (21.0)	196.90 ± 0.36	$+6.08 \pm 0.86$	0.158 ± 0.001	21.2 (8.4)
219.20 ± 0.09	-13.62 ± 1.05	0.114 ± 0.001	23.0 (22.9)	219.36 ± 0.89	-15.08 ± 2.07	0.132 ± 0.001	19.8 (17.8)
272.72 ± 2.84	-6.45 ± 4.06	0.128 ± 0.001	22.2 (25.5)	268.08 ± 0.63	-14.11 ± 0.72	0.160 ± 0.001	18.8 (21.3)
320.67 ± 0.18	$+13.25 \pm 1.04$	0.160 ± 0.001	19.2 (24.6)	319.37 ± 0.18	$+8.54 \pm 1.19$	0.208 ± 0.001	17.0 (18.8)
340.89 ± 1.07	$+10.31 \pm 2.08$	0.170 ± 0.001	21.5 (17.5)	343.47 ± 0.36	$+7.08 \pm 1.03$	0.227 ± 0.001	18.2 (16.5)
IP = 100 m				**IP = 120 m**			
0.83 ± 0.71	$+8.87 \pm 1.38$	0.254 ± 0.001	19.8 (11.1)	0.15 ± 0.53	$+8.23 \pm 0.79$	0.306 ± 0.002	17.2 (7.5)
17.09 ± 0.36	$+6.85 \pm 0.44$	0.181 ± 0.001	20.0 (13.8)	14.72 ± 0.71	$+1.31 \pm 1.47$	0.216 ± 0.002	16.2 (12.6)
38.32 ± 0.98	-7.50 ± 1.74	0.136 ± 0.001	19.2 (15.3)	40.38 ± 0.36	-8.68 ± 0.94	0.160 ± 0.001	14.5 (16.9)
91.32 ± 0.27	-12.21 ± 0.78	0.179 ± 0.001	14.1 (19.9)	92.19 ± 1.25	-8.11 ± 2.17	0.216 ± 0.002	12.6 (18.7)
135.78 ± 0.27	$+4.91 \pm 0.94$	0.254 ± 0.001	16.9 (11.7)	136.43 ± 0.27	$+4.70 \pm 0.94$	0.304 ± 0.002	14.3 (9.0)
162.47 ± 0.54	$+9.30 \pm 1.29$	0.286 ± 0.001	17.6 (15.6)	161.98 ± 0.53	$+5.98 \pm 1.29$	0.341 ± 0.002	14.5 (10.5)
179.19 ± 0.71	$+4.56 \pm 1.30$	0.262 ± 0.001	21.1 (11.3)	178.03 ± 0.62	$+3.33 \pm 1.21$	0.313 ± 0.001	18.6 (8.1)
193.15 ± 0.53	-1.38 ± 1.12	0.195 ± 0.001	18.7 (11.4)	194.90 ± 0.53	$+4.35 \pm 1.46$	0.235 ± 0.002	19.8 (8.2)
220.64 ± 0.99	-7.89 ± 1.57	0.158 ± 0.001	16.2 (14.6)	220.45 ± 0.45	-6.55 ± 0.95	0.185 ± 0.001	13.0 (13.6)
269.42 ± 0.99	-6.72 ± 1.66	0.196 ± 0.001	13.3 (23.5)	272.09 ± 0.63	-6.96 ± 1.13	0.236 ± 0.001	13.5 (14.0)
317.76 ± 0.27	$+5.77 \pm 0.69$	0.264 ± 0.001	15.9 (14.2)	319.39 ± 0.62	$+6.98 \pm 0.96$	0.314 ± 0.001	14.2 (14.0)
348.75 ± 0.18	$+11.96 \pm 0.77$	0.288 ± 0.001	18.1 (10.6)	346.65 ± 0.53	$+7.63 \pm 1.12$	0.343 ± 0.002	15.7 (12.5)

Table 163: The nominal angle δ_n, average displacement $\Delta\delta$, average value of the parameter DIST, RMS of the ALPHA distribution for enabled GF and impact parameters between 60 m and 120 m. The RMS of the ALPHA distribution for disabled GF is given parentheses. The primary γ-ray energy was set to 1000 GeV, the ZA to 60° and the azimuth angle to 30°.

$E_\gamma = 1000\,\mathrm{GeV}$, Az = 60°, ZA = 60°, Intermediate Image Cleaning

δ_n[°]	$\Delta\delta$[°]	DIST[°]	$\mathrm{RMS}_{\lvert\mathrm{ALPHA}\rvert}$[°]	δ_n[°]	$\Delta\delta$[°]	DIST[°]	$\mathrm{RMS}_{\lvert\mathrm{ALPHA}\rvert}$[°]
IP = 60 m				**IP = 80 m**			
1.00 ± 0.47	$+21.99 \pm 2.31$	0.118 ± 0.001	25.0 (16.4)	358.94 ± 0.56	$+17.23 \pm 1.20$	0.147 ± 0.001	22.7 (10.1)
17.32 ± 0.47	$+16.08 \pm 1.11$	0.116 ± 0.002	20.4 (17.6)	16.99 ± 0.65	$+14.93 \pm 1.21$	0.122 ± 0.001	19.7 (11.8)
39.99 ± 1.68	-9.79 ± 1.78	0.121 ± 0.001	15.7 (24.4)	38.65 ± 1.12	-19.53 ± 1.44	0.148 ± 0.001	13.0 (20.1)
99.27 ± 0.74	-15.51 ± 1.13	0.151 ± 0.001	13.8 (14.1)	98.86 ± 1.96	-7.18 ± 2.36	0.199 ± 0.002	12.8 (23.1)
134.90 ± 0.45	$+13.04 \pm 1.32$	0.168 ± 0.002	18.6 (20.9)	140.61 ± 1.30	$+15.47 \pm 1.88$	0.226 ± 0.002	15.0 (17.6)
158.90 ± 1.30	$+18.73 \pm 2.35$	0.157 ± 0.001	21.9 (20.4)	163.25 ± 0.74	$+16.31 \pm 1.55$	0.207 ± 0.001	21.5 (12.9)
179.57 ± 0.28	$+19.44 \pm 0.36$	0.126 ± 0.001	25.7 (14.1)	179.64 ± 0.93	$+14.29 \pm 2.22$	0.159 ± 0.001	23.0 (11.8)
195.95 ± 0.74	$+1.67 \pm 1.87$	0.116 ± 0.001	20.7 (19.6)	195.94 ± 0.37	$+6.85 \pm 0.53$	0.135 ± 0.001	18.4 (9.7)
216.53 ± 0.29	-31.02 ± 0.79	0.131 ± 0.001	18.0 (23.0)	215.94 ± 0.56	-25.24 ± 0.80	0.162 ± 0.002	15.0 (20.0)
270.56 ± 0.26	-17.92 ± 2.03	0.159 ± 0.001	15.6 (21.5)	272.67 ± 0.47	-14.29 ± 0.88	0.208 ± 0.001	15.3 (22.8)
320.08 ± 0.47	$+15.98 \pm 1.39$	0.172 ± 0.001	18.7 (23.3)	320.21 ± 0.09	$+14.34 \pm 0.98$	0.230 ± 0.002	17.3 (21.1)
343.77 ± 0.47	$+24.72 \pm 1.11$	0.155 ± 0.001	20.6 (20.6)	342.87 ± 0.47	$+15.80 \pm 0.95$	0.203 ± 0.001	19.4 (15.2)
IP = 100 m				**IP = 120 m**			
0.74 ± 0.74	$+18.07 \pm 1.31$	0.183 ± 0.001	21.1 (9.5)	0.29 ± 0.37	$+13.50 \pm 0.85$	0.219 ± 0.002	20.5 (8.0)
16.28 ± 0.74	$+9.71 \pm 1.79$	0.137 ± 0.001	17.0 (9.7)	15.20 ± 0.47	$+7.08 \pm 1.19$	0.161 ± 0.002	15.2 (8.1)
40.58 ± 0.56	-11.12 ± 1.36	0.183 ± 0.001	12.0 (13.9)	42.68 ± 0.28	-17.38 ± 0.92	0.219 ± 0.002	10.7 (13.2)
90.82 ± 0.85	-16.09 ± 1.26	0.257 ± 0.003	13.7 (20.0)	89.41 ± 0.65	-14.64 ± 1.54	0.307 ± 0.002	12.4 (20.5)
137.40 ± 0.56	$+9.58 \pm 1.04$	0.287 ± 0.002	14.8 (11.2)	137.89 ± 0.65	$+9.35 \pm 1.21$	0.343 ± 0.003	14.3 (9.2)
163.11 ± 0.56	$+16.33 \pm 1.36$	0.262 ± 0.002	20.9 (11.9)	162.15 ± 0.47	$+12.54 \pm 1.19$	0.315 ± 0.002	19.5 (8.1)
177.59 ± 0.47	$+18.55 \pm 1.27$	0.195 ± 0.002	22.5 (10.3)	177.73 ± 0.65	$+12.29 \pm 1.21$	0.236 ± 0.002	23.9 (9.3)
193.94 ± 0.56	$+4.85 \pm 0.72$	0.160 ± 0.001	15.1 (10.5)	195.20 ± 0.56	$+5.89 \pm 1.20$	0.186 ± 0.001	13.9 (8.4)
219.60 ± 0.65	-19.71 ± 1.78	0.199 ± 0.001	12.3 (17.5)	220.74 ± 0.56	-9.84 ± 0.96	0.236 ± 0.002	12.6 (12.3)
270.21 ± 1.12	-13.14 ± 1.37	0.263 ± 0.003	14.7 (21.1)	269.72 ± 0.84	-10.64 ± 1.41	0.318 ± 0.003	11.9 (16.3)
317.85 ± 0.65	$+9.98 \pm 1.46$	0.290 ± 0.002	15.5 (15.7)	318.97 ± 0.47	$+9.46 \pm 1.11$	0.346 ± 0.002	14.8 (12.4)
345.44 ± 0.47	$+17.08 \pm 1.43$	0.257 ± 0.001	19.5 (15.5)	346.89 ± 0.74	$+14.39 \pm 1.07$	0.307 ± 0.002	17.5 (12.8)

Table 164: The nominal angle δ_n, average displacement $\Delta\delta$, average value of the parameter DIST, RMS of the ALPHA distribution for enabled GF and impact parameters between 60 m and 120 m. The RMS of the ALPHA distribution for disabled GF is given parentheses. The primary γ-ray energy was set to 1000 GeV, the ZA to 60° and the azimuth angle to 60°.

$E_\gamma = 1000\,\mathrm{GeV}$, Az = 60°, ZA = 60°, Hard Image Cleaning

δ_n[°]	$\Delta\delta$[°]	DIST[°]	$\mathrm{RMS}_{\lvert\mathrm{ALPHA}\rvert}$[°]	δ_n[°]	$\Delta\delta$[°]	DIST[°]	$\mathrm{RMS}_{\lvert\mathrm{ALPHA}\rvert}$[°]
IP = 60 m				**IP = 80 m**			
358.63 ± 0.62	$+20.82 \pm 1.28$	0.118 ± 0.001	25.1 (14.7)	358.23 ± 0.53	$+17.23 \pm 0.70$	0.146 ± 0.001	24.0 (12.0)
14.29 ± 0.36	$+15.30 \pm 0.68$	0.116 ± 0.002	17.1 (19.1)	13.79 ± 0.63	$+13.76 \pm 1.36$	0.121 ± 0.001	18.6 (12.3)
38.95 ± 0.10	-14.08 ± 0.93	0.120 ± 0.001	16.3 (23.4)	36.95 ± 0.89	-18.80 ± 1.46	0.148 ± 0.001	11.8 (18.6)
96.85 ± 0.38	-16.40 ± 0.59	0.150 ± 0.001	14.6 (11.5)	90.92 ± 0.11	-16.21 ± 0.81	0.199 ± 0.001	14.1 (25.1)
136.33 ± 0.32	$+10.57 \pm 1.68$	0.169 ± 0.001	18.6 (23.5)	138.76 ± 0.98	$+13.04 \pm 1.64$	0.226 ± 0.003	16.1 (18.8)
160.93 ± 0.45	$+18.25 \pm 1.92$	0.157 ± 0.001	22.7 (19.4)	165.91 ± 0.98	$+17.64 \pm 2.04$	0.207 ± 0.001	20.2 (11.5)
180.96 ± 0.62	$+19.92 \pm 2.01$	0.125 ± 0.001	25.8 (13.5)	180.99 ± 0.80	$+12.59 \pm 1.45$	0.159 ± 0.001	24.2 (13.0)
198.77 ± 0.36	$+1.40 \pm 0.44$	0.115 ± 0.001	19.4 (21.0)	196.90 ± 0.36	$+8.87 \pm 1.08$	0.135 ± 0.001	17.8 (8.4)
219.20 ± 0.09	-24.64 ± 0.18	0.130 ± 0.001	18.3 (22.9)	219.36 ± 0.89	-23.68 ± 1.87	0.162 ± 0.001	14.8 (17.8)
272.72 ± 2.84	-14.09 ± 3.36	0.159 ± 0.001	14.9 (25.5)	268.08 ± 0.63	-19.76 ± 1.47	0.208 ± 0.002	14.8 (21.3)
320.67 ± 0.18	$+14.95 \pm 0.52$	0.171 ± 0.001	16.4 (24.6)	319.37 ± 0.18	$+12.53 \pm 0.91$	0.229 ± 0.002	17.1 (18.8)
340.89 ± 1.07	$+20.12 \pm 2.28$	0.154 ± 0.001	21.8 (17.5)	343.47 ± 0.36	$+14.95 \pm 0.92$	0.203 ± 0.001	19.6 (16.5)
IP = 100 m				**IP = 120 m**			
0.83 ± 0.71	$+17.63 \pm 1.44$	0.182 ± 0.001	21.1 (11.1)	0.15 ± 0.53	$+12.41 \pm 0.94$	0.218 ± 0.002	19.3 (7.5)
17.09 ± 0.36	$+11.86 \pm 1.00$	0.138 ± 0.001	17.0 (13.8)	14.72 ± 0.71	$+6.61 \pm 1.12$	0.162 ± 0.002	15.7 (12.6)
38.32 ± 0.98	-11.30 ± 1.55	0.183 ± 0.001	11.3 (15.3)	40.38 ± 0.36	-16.30 ± 0.76	0.217 ± 0.002	10.8 (16.9)
91.32 ± 0.27	-15.28 ± 0.94	0.256 ± 0.003	14.0 (19.9)	92.19 ± 1.25	-12.17 ± 1.98	0.306 ± 0.002	12.1 (18.7)
135.78 ± 0.27	$+8.89 \pm 0.92$	0.285 ± 0.003	15.4 (11.7)	136.43 ± 0.27	$+8.34 \pm 1.00$	0.341 ± 0.003	15.0 (9.0)
162.47 ± 0.54	$+13.23 \pm 1.34$	0.262 ± 0.001	20.0 (15.6)	161.98 ± 0.53	$+10.53 \pm 1.26$	0.312 ± 0.003	19.3 (10.5)
179.19 ± 0.71	$+15.94 \pm 1.76$	0.195 ± 0.002	21.4 (11.3)	178.03 ± 0.62	$+10.58 \pm 1.27$	0.236 ± 0.002	22.9 (8.1)
193.15 ± 0.53	$+3.32 \pm 1.26$	0.160 ± 0.001	15.6 (11.4)	194.90 ± 0.53	$+4.55 \pm 1.34$	0.186 ± 0.001	14.3 (8.2)
220.64 ± 0.99	-16.41 ± 1.39	0.197 ± 0.001	12.4 (14.6)	220.45 ± 0.45	-9.70 ± 1.17	0.236 ± 0.002	13.0 (13.6)
269.42 ± 0.99	-15.08 ± 1.72	0.263 ± 0.002	15.3 (23.5)	272.09 ± 0.63	-9.48 ± 1.28	0.315 ± 0.003	13.0 (14.0)
317.76 ± 0.27	$+9.06 \pm 0.75$	0.289 ± 0.001	14.4 (14.2)	319.39 ± 0.62	$+10.74 \pm 1.35$	0.345 ± 0.002	15.0 (14.0)
348.75 ± 0.18	$+20.05 \pm 0.74$	0.257 ± 0.001	23.0 (10.6)	346.65 ± 0.53	$+14.12 \pm 1.26$	0.307 ± 0.002	16.8 (12.5)

Table 165: The nominal angle δ_n, average displacement $\Delta\delta$, average value of the parameter DIST, RMS of the ALPHA distribution for enabled GF and impact parameters between 60 m and 120 m. The RMS of the ALPHA distribution for disabled GF is given parentheses. The primary γ-ray energy was set to 1000 GeV, the ZA to 60° and the azimuth angle to 60°.

$E_\gamma = 1000\,\mathrm{GeV}$, Az = 90°, ZA = 60°, Intermediate Image Cleaning

$\delta_n[°]$	$\Delta\delta[°]$	DIST[°]	$\mathrm{RMS}_{\lvert\mathrm{ALPHA}\rvert}[°]$	$\delta_n[°]$	$\Delta\delta[°]$	DIST[°]	$\mathrm{RMS}_{\lvert\mathrm{ALPHA}\rvert}[°]$
IP = 60 m				**IP = 80 m**			
1.00 ± 0.47	$+29.00 \pm 0.78$	0.129 ± 0.002	18.3 (16.4)	358.94 ± 0.56	$+19.70 \pm 1.19$	0.129 ± 0.001	18.6 (10.1)
17.32 ± 0.47	$+25.62 \pm 0.78$	0.131 ± 0.001	16.4 (17.6)	16.99 ± 0.65	$+24.86 \pm 0.89$	0.151 ± 0.001	12.4 (11.8)
39.99 ± 1.68	$+2.40 \pm 2.42$	0.151 ± 0.001	16.2 (24.4)	38.65 ± 1.12	-11.20 ± 1.20	0.200 ± 0.002	16.1 (20.1)
99.27 ± 0.74	-14.62 ± 0.92	0.167 ± 0.002	21.5 (14.1)	98.86 ± 1.96	-15.57 ± 2.55	0.225 ± 0.002	21.2 (23.1)
134.90 ± 0.45	$+5.65 \pm 1.33$	0.158 ± 0.001	25.3 (20.9)	140.61 ± 1.30	$+11.76 \pm 2.04$	0.206 ± 0.001	25.3 (17.6)
158.90 ± 1.30	$+18.25 \pm 2.03$	0.127 ± 0.001	22.9 (20.4)	163.25 ± 0.74	$+16.80 \pm 1.54$	0.156 ± 0.001	25.7 (12.9)
179.57 ± 0.28	$+24.06 \pm 0.68$	0.130 ± 0.001	15.9 (14.1)	179.64 ± 0.93	$+22.46 \pm 1.64$	0.142 ± 0.001	16.2 (11.8)
195.95 ± 0.74	$+22.16 \pm 1.14$	0.141 ± 0.001	13.0 (19.6)	195.94 ± 0.37	$+12.91 \pm 1.09$	0.165 ± 0.001	12.0 (9.7)
216.53 ± 0.29	-28.30 ± 0.79	0.160 ± 0.001	17.4 (23.0)	215.94 ± 0.56	-22.69 ± 0.96	0.208 ± 0.001	15.6 (20.0)
270.56 ± 0.26	-23.25 ± 1.20	0.169 ± 0.002	21.3 (21.5)	272.67 ± 0.47	-21.70 ± 1.23	0.225 ± 0.002	22.3 (22.8)
320.08 ± 0.47	$+13.80 \pm 1.32$	0.152 ± 0.001	26.0 (23.3)	320.21 ± 0.09	$+10.95 \pm 0.83$	0.201 ± 0.002	24.8 (21.1)
343.77 ± 0.47	$+26.65 \pm 1.11$	0.121 ± 0.001	24.6 (20.6)	342.87 ± 0.47	$+18.21 \pm 1.50$	0.148 ± 0.001	26.1 (15.2)
IP = 100 m				**IP = 120 m**			
0.74 ± 0.74	$+23.81 \pm 1.54$	0.138 ± 0.001	16.3 (9.5)	0.29 ± 0.37	$+16.25 \pm 0.61$	0.163 ± 0.002	14.5 (8.0)
16.28 ± 0.74	$+19.69 \pm 1.14$	0.184 ± 0.003	8.8 (9.7)	15.20 ± 0.47	$+16.94 \pm 0.86$	0.218 ± 0.002	9.1 (8.1)
40.58 ± 0.56	-9.94 ± 1.20	0.250 ± 0.002	14.9 (13.9)	42.68 ± 0.28	-5.86 ± 1.71	0.301 ± 0.002	14.1 (13.2)
90.82 ± 0.85	-23.74 ± 1.67	0.285 ± 0.002	20.7 (20.0)	89.41 ± 0.65	-19.02 ± 1.30	0.339 ± 0.002	18.3 (20.5)
137.40 ± 0.56	$+9.36 \pm 1.04$	0.260 ± 0.001	25.8 (11.2)	137.89 ± 0.65	$+6.45 \pm 1.13$	0.310 ± 0.002	23.7 (9.2)
163.11 ± 0.56	$+16.28 \pm 1.43$	0.195 ± 0.001	27.5 (11.9)	162.15 ± 0.47	$+11.90 \pm 1.10$	0.233 ± 0.001	26.7 (8.1)
177.59 ± 0.47	$+20.98 \pm 1.58$	0.162 ± 0.001	15.4 (10.3)	177.73 ± 0.65	$+16.08 \pm 1.53$	0.186 ± 0.001	14.4 (9.3)
193.94 ± 0.56	$+14.42 \pm 0.88$	0.197 ± 0.001	9.1 (10.5)	195.20 ± 0.56	$+20.09 \pm 1.27$	0.230 ± 0.001	10.2 (8.4)
219.60 ± 0.65	-15.39 ± 1.05	0.257 ± 0.001	16.3 (17.5)	220.74 ± 0.56	-17.43 ± 0.72	0.311 ± 0.003	15.6 (12.3)
270.21 ± 1.12	-19.56 ± 2.09	0.283 ± 0.003	21.1 (21.1)	269.72 ± 0.84	-17.67 ± 1.56	0.339 ± 0.002	18.3 (16.3)
317.85 ± 0.65	$+7.90 \pm 1.37$	0.252 ± 0.002	25.5 (15.7)	318.97 ± 0.47	$+7.45 \pm 1.02$	0.301 ± 0.002	25.5 (12.4)
345.44 ± 0.47	$+20.04 \pm 1.50$	0.180 ± 0.001	25.7 (15.5)	346.89 ± 0.74	$+18.36 \pm 1.54$	0.216 ± 0.002	26.2 (12.8)

Table 166: The nominal angle δ_n, average displacement $\Delta\delta$, average value of the parameter DIST, RMS of the ALPHA distribution for enabled GF and impact parameters between 60 m and 120 m. The RMS of the ALPHA distribution for disabled GF is given parentheses. The primary γ-ray energy was set to 1000 GeV, the ZA to 60° and the azimuth angle to 90°.

$E_\gamma = 1000\,\mathrm{GeV}$, Az = 90°, ZA = 60°, Hard Image Cleaning

$\delta_n[°]$	$\Delta\delta[°]$	DIST[°]	$\mathrm{RMS}_{\lvert\mathrm{ALPHA}\rvert}[°]$	$\delta_n[°]$	$\Delta\delta[°]$	DIST[°]	$\mathrm{RMS}_{\lvert\mathrm{ALPHA}\rvert}[°]$
IP = 60 m				**IP = 80 m**			
358.63 ± 0.62	$+25.55 \pm 2.11$	0.119 ± 0.002	23.2 (14.7)	358.23 ± 0.53	$+18.83 \pm 1.35$	0.130 ± 0.001	18.2 (12.0)
14.29 ± 0.36	$+21.62 \pm 1.59$	0.133 ± 0.001	13.8 (19.1)	13.79 ± 0.63	$+18.79 \pm 1.28$	0.152 ± 0.001	11.8 (12.3)
38.95 ± 0.10	-9.59 ± 0.77	0.150 ± 0.001	16.9 (23.4)	36.95 ± 0.89	-6.49 ± 1.06	0.199 ± 0.002	15.7 (18.6)
96.85 ± 0.38	-24.26 ± 1.64	0.168 ± 0.001	21.6 (11.5)	90.92 ± 0.11	-23.62 ± 0.42	0.225 ± 0.002	22.6 (25.1)
136.33 ± 0.32	$+7.22 \pm 1.24$	0.157 ± 0.001	24.7 (23.5)	138.76 ± 0.98	$+11.93 \pm 1.24$	0.205 ± 0.001	26.6 (18.8)
160.93 ± 0.45	$+20.41 \pm 1.11$	0.126 ± 0.001	24.0 (19.4)	165.91 ± 0.98	$+20.19 \pm 1.81$	0.156 ± 0.001	27.5 (11.5)
180.96 ± 0.62	$+23.69 \pm 1.04$	0.128 ± 0.001	17.0 (13.5)	180.99 ± 0.80	$+21.97 \pm 1.29$	0.139 ± 0.001	16.1 (13.0)
198.77 ± 0.36	$+19.66 \pm 1.68$	0.138 ± 0.001	12.5 (21.0)	196.90 ± 0.36	$+14.99 \pm 0.76$	0.166 ± 0.001	13.5 (8.4)
219.20 ± 0.09	-23.32 ± 0.69	0.158 ± 0.001	15.4 (22.9)	219.36 ± 0.89	-19.72 ± 1.55	0.205 ± 0.001	14.4 (17.8)
272.72 ± 2.84	-22.10 ± 3.16	0.169 ± 0.002	20.1 (25.5)	268.08 ± 0.63	-24.88 ± 1.51	0.226 ± 0.002	21.9 (21.3)
320.67 ± 0.18	$+13.31 \pm 0.97$	0.151 ± 0.001	26.2 (24.6)	319.37 ± 0.18	$+10.97 \pm 0.43$	0.202 ± 0.001	23.8 (18.8)
340.89 ± 1.07	$+19.01 \pm 1.90$	0.121 ± 0.001	25.0 (17.5)	343.47 ± 0.36	$+17.90 \pm 0.77$	0.147 ± 0.001	25.8 (16.5)
IP = 100 m				**IP = 120 m**			
0.83 ± 0.71	$+19.43 \pm 1.12$	0.139 ± 0.001	15.5 (11.1)	0.15 ± 0.53	$+17.85 \pm 1.50$	0.164 ± 0.001	15.0 (7.5)
17.09 ± 0.36	$+23.20 \pm 1.01$	0.183 ± 0.002	9.7 (13.8)	14.72 ± 0.71	$+16.46 \pm 1.12$	0.216 ± 0.002	9.4 (12.6)
38.32 ± 0.98	-11.86 ± 1.23	0.252 ± 0.002	15.4 (15.3)	40.38 ± 0.36	-1.70 ± 0.44	0.303 ± 0.002	15.5 (16.9)
91.32 ± 0.27	-20.87 ± 0.95	0.286 ± 0.002	20.3 (19.9)	92.19 ± 1.25	-16.71 ± 1.83	0.337 ± 0.001	17.3 (18.7)
135.78 ± 0.27	$+8.99 \pm 0.68$	0.260 ± 0.001	25.3 (11.7)	136.43 ± 0.27	$+5.37 \pm 0.76$	0.309 ± 0.002	25.1 (9.0)
162.47 ± 0.54	$+17.00 \pm 1.61$	0.194 ± 0.001	26.9 (15.6)	161.98 ± 0.53	$+11.47 \pm 1.19$	0.234 ± 0.001	27.3 (10.5)
179.19 ± 0.71	$+20.58 \pm 1.61$	0.161 ± 0.001	14.9 (11.3)	178.03 ± 0.62	$+17.00 \pm 1.10$	0.185 ± 0.001	15.1 (8.1)
193.15 ± 0.53	$+16.42 \pm 0.62$	0.197 ± 0.001	8.2 (11.4)	194.90 ± 0.53	$+16.88 \pm 1.02$	0.233 ± 0.002	8.9 (8.2)
220.64 ± 0.99	-14.25 ± 1.07	0.258 ± 0.001	15.7 (14.6)	220.45 ± 0.45	-12.74 ± 0.77	0.307 ± 0.003	16.7 (13.6)
269.42 ± 0.99	-20.78 ± 1.58	0.284 ± 0.001	21.0 (23.5)	272.09 ± 0.63	-14.84 ± 1.53	0.337 ± 0.001	19.8 (14.0)
317.76 ± 0.27	$+7.05 \pm 0.85$	0.253 ± 0.002	25.2 (14.2)	319.39 ± 0.62	$+7.68 \pm 1.12$	0.303 ± 0.002	23.4 (14.0)
348.75 ± 0.18	$+21.75 \pm 0.75$	0.180 ± 0.001	26.5 (10.6)	346.65 ± 0.53	$+17.13 \pm 1.18$	0.218 ± 0.001	27.2 (12.5)

Table 167: The nominal angle δ_n, average displacement $\Delta\delta$, average value of the parameter DIST, RMS of the ALPHA distribution for enabled GF and impact parameters between 60 m and 120 m. The RMS of the ALPHA distribution for disabled GF is given parentheses. The primary γ-ray energy was set to 1000 GeV, the ZA to 60° and the azimuth angle to 90°.

$E_\gamma = 1000\,\mathrm{GeV}$, Az = 120°, ZA = 60°, Intermediate Image Cleaning

$\delta_n[°]$	$\Delta\delta[°]$	DIST[°]	$\mathrm{RMS}_{\lvert\mathrm{ALPHA}\rvert}[°]$	$\delta_n[°]$	$\Delta\delta[°]$	DIST[°]	$\mathrm{RMS}_{\lvert\mathrm{ALPHA}\rvert}[°]$
IP = 60 m				**IP = 80 m**			
1.00 ± 0.47	$+23.68 \pm 1.55$	0.126 ± 0.001	14.4 (16.4)	358.94 ± 0.56	$+17.89 \pm 1.25$	0.152 ± 0.001	13.3 (10.1)
17.32 ± 0.47	$+31.71 \pm 1.16$	0.156 ± 0.001	14.5 (17.6)	16.99 ± 0.65	$+24.33 \pm 2.03$	0.202 ± 0.002	11.8 (11.8)
39.99 ± 1.68	$+25.59 \pm 2.29$	0.170 ± 0.002	15.3 (24.4)	38.65 ± 1.12	$+15.16 \pm 1.42$	0.227 ± 0.002	15.1 (20.1)
99.27 ± 0.74	-24.37 ± 1.07	0.159 ± 0.001	20.4 (14.1)	98.86 ± 1.96	-23.35 ± 2.53	0.208 ± 0.001	19.0 (23.1)
134.90 ± 0.45	$+1.90 \pm 1.38$	0.128 ± 0.001	23.8 (20.9)	140.61 ± 1.30	$+4.22 \pm 1.79$	0.161 ± 0.001	21.6 (17.6)
158.90 ± 1.30	$+12.94 \pm 1.94$	0.120 ± 0.001	18.2 (20.4)	163.25 ± 0.74	$+12.88 \pm 1.36$	0.137 ± 0.001	14.7 (12.9)
179.57 ± 0.28	$+20.54 \pm 0.89$	0.135 ± 0.001	15.0 (14.1)	179.64 ± 0.93	$+17.90 \pm 1.78$	0.166 ± 0.001	14.3 (11.8)
195.95 ± 0.74	$+23.97 \pm 1.28$	0.164 ± 0.002	16.7 (19.6)	195.94 ± 0.37	$+22.38 \pm 1.14$	0.210 ± 0.002	14.6 (9.7)
216.53 ± 0.29	-2.91 ± 1.24	0.174 ± 0.002	16.8 (23.0)	215.94 ± 0.56	-6.11 ± 0.64	0.230 ± 0.002	16.3 (20.0)
270.56 ± 0.26	-31.03 ± 0.65	0.156 ± 0.001	21.3 (21.5)	272.67 ± 0.47	-28.99 ± 1.27	0.206 ± 0.001	19.9 (22.8)
320.08 ± 0.47	$+1.94 \pm 1.12$	0.123 ± 0.001	24.6 (23.3)	320.21 ± 0.09	$+3.66 \pm 0.72$	0.149 ± 0.001	23.4 (21.1)
343.77 ± 0.47	$+17.11 \pm 1.17$	0.126 ± 0.001	14.3 (20.6)	342.87 ± 0.47	$+11.03 \pm 1.24$	0.125 ± 0.001	14.8 (15.2)
IP = 100 m				**IP = 120 m**			
0.74 ± 0.74	$+19.52 \pm 1.59$	0.185 ± 0.003	10.9 (9.5)	0.29 ± 0.37	$+14.63 \pm 0.99$	0.219 ± 0.002	8.8 (8.0)
16.28 ± 0.74	$+23.22 \pm 1.13$	0.253 ± 0.002	10.7 (9.7)	15.20 ± 0.47	$+18.65 \pm 1.23$	0.304 ± 0.002	10.8 (8.1)
40.58 ± 0.56	$+8.22 \pm 0.87$	0.285 ± 0.002	15.1 (13.9)	42.68 ± 0.28	$+6.33 \pm 0.74$	0.341 ± 0.003	14.2 (13.2)
90.82 ± 0.85	-26.10 ± 1.80	0.262 ± 0.002	18.3 (20.0)	89.41 ± 0.65	-26.36 ± 1.65	0.315 ± 0.002	19.6 (20.5)
137.40 ± 0.56	$+1.24 \pm 1.26$	0.197 ± 0.001	22.7 (11.2)	137.89 ± 0.65	$+1.16 \pm 1.27$	0.238 ± 0.002	20.4 (9.2)
163.11 ± 0.56	$+11.43 \pm 1.10$	0.161 ± 0.001	13.0 (11.9)	162.15 ± 0.47	$+9.16 \pm 1.00$	0.188 ± 0.002	14.1 (8.1)
177.59 ± 0.47	$+16.41 \pm 1.39$	0.201 ± 0.001	11.1 (10.3)	177.73 ± 0.65	$+13.97 \pm 1.11$	0.237 ± 0.001	10.0 (9.3)
193.94 ± 0.56	$+22.46 \pm 1.25$	0.262 ± 0.002	13.7 (10.5)	195.20 ± 0.56	$+19.36 \pm 1.02$	0.313 ± 0.001	12.4 (8.4)
219.60 ± 0.65	$+3.85 \pm 1.04$	0.286 ± 0.003	16.4 (17.5)	220.74 ± 0.56	$+3.85 \pm 1.10$	0.344 ± 0.003	15.3 (12.3)
270.21 ± 1.12	-26.17 ± 1.74	0.258 ± 0.003	19.8 (21.1)	269.72 ± 0.84	-22.97 ± 1.76	0.309 ± 0.003	17.7 (16.3)
317.85 ± 0.65	-0.37 ± 1.27	0.185 ± 0.001	24.2 (15.7)	318.97 ± 0.47	$+1.30 \pm 0.85$	0.223 ± 0.002	22.9 (12.4)
345.44 ± 0.47	$+12.36 \pm 1.00$	0.142 ± 0.001	14.4 (15.5)	346.89 ± 0.74	$+12.84 \pm 1.44$	0.163 ± 0.001	13.0 (12.8)

Table 168: The nominal angle δ_n, average displacement $\Delta\delta$, average value of the parameter DIST, RMS of the ALPHA distribution for enabled GF and impact parameters between 60 m and 120 m. The RMS of the ALPHA distribution for disabled GF is given parentheses. The primary γ-ray energy was set to 1000 GeV, the ZA to 60° and the azimuth angle to 120°.

$E_\gamma = 1000\,\mathrm{GeV}$, Az = 120°, ZA = 60°, Hard Image Cleaning

$\delta_n[°]$	$\Delta\delta[°]$	DIST[°]	$\mathrm{RMS}_{\lvert\mathrm{ALPHA}\rvert}[°]$	$\delta_n[°]$	$\Delta\delta[°]$	DIST[°]	$\mathrm{RMS}_{\lvert\mathrm{ALPHA}\rvert}[°]$
IP = 60 m				**IP = 80 m**			
358.63 ± 0.62	$+19.81 \pm 1.58$	0.127 ± 0.002	16.5 (14.7)	358.23 ± 0.53	$+15.76 \pm 1.08$	0.154 ± 0.001	13.5 (12.0)
14.29 ± 0.36	$+28.29 \pm 0.92$	0.155 ± 0.001	14.9 (19.1)	13.79 ± 0.63	$+21.27 \pm 1.42$	0.203 ± 0.002	12.7 (12.3)
38.95 ± 0.10	$+23.38 \pm 0.64$	0.171 ± 0.001	15.8 (23.4)	36.95 ± 0.89	$+13.14 \pm 0.97$	0.227 ± 0.002	16.4 (18.6)
96.85 ± 0.38	-20.56 ± 0.76	0.159 ± 0.001	20.6 (11.5)	90.92 ± 0.11	-30.78 ± 0.70	0.209 ± 0.001	18.2 (25.1)
136.33 ± 0.32	$+0.77 \pm 1.10$	0.126 ± 0.001	22.5 (23.5)	138.76 ± 0.98	$+2.77 \pm 1.32$	0.161 ± 0.001	22.6 (18.8)
160.93 ± 0.45	$+13.24 \pm 1.27$	0.120 ± 0.001	18.9 (19.4)	165.91 ± 0.98	$+15.52 \pm 1.31$	0.136 ± 0.001	16.5 (11.5)
180.96 ± 0.62	$+21.90 \pm 1.58$	0.136 ± 0.001	15.8 (13.5)	180.99 ± 0.80	$+18.73 \pm 1.27$	0.166 ± 0.002	13.7 (13.0)
198.77 ± 0.36	$+22.28 \pm 1.23$	0.164 ± 0.002	16.3 (21.0)	196.90 ± 0.36	$+22.51 \pm 0.83$	0.212 ± 0.002	13.8 (8.4)
219.20 ± 0.09	$+0.14 \pm 0.33$	0.174 ± 0.002	16.9 (22.9)	219.36 ± 0.89	-3.73 ± 1.37	0.231 ± 0.002	16.1 (17.8)
272.72 ± 2.84	-27.42 ± 3.86	0.157 ± 0.001	20.1 (25.5)	268.08 ± 0.63	-31.53 ± 1.38	0.208 ± 0.001	18.8 (21.3)
320.67 ± 0.18	$+3.63 \pm 0.93$	0.124 ± 0.001	23.7 (24.6)	319.37 ± 0.18	$+3.18 \pm 0.91$	0.151 ± 0.001	24.8 (18.8)
340.89 ± 1.07	$+11.84 \pm 1.87$	0.122 ± 0.002	18.6 (17.5)	343.47 ± 0.36	$+10.12 \pm 1.07$	0.123 ± 0.001	16.2 (16.5)
IP = 100 m				**IP = 120 m**			
0.83 ± 0.71	$+17.97 \pm 1.50$	0.184 ± 0.002	11.3 (11.1)	0.15 ± 0.53	$+13.57 \pm 1.00$	0.220 ± 0.003	9.7 (7.5)
17.09 ± 0.36	$+25.06 \pm 1.54$	0.253 ± 0.002	12.5 (13.8)	14.72 ± 0.71	$+16.65 \pm 1.65$	0.303 ± 0.002	10.6 (12.6)
38.32 ± 0.98	$+11.71 \pm 2.40$	0.285 ± 0.002	14.4 (15.3)	40.38 ± 0.36	$+6.45 \pm 0.75$	0.340 ± 0.003	14.4 (16.9)
91.32 ± 0.27	-23.84 ± 0.69	0.264 ± 0.002	18.8 (19.9)	92.19 ± 1.25	-21.47 ± 2.28	0.313 ± 0.002	18.7 (18.7)
135.78 ± 0.27	$+0.29 \pm 0.83$	0.198 ± 0.001	22.8 (11.7)	136.43 ± 0.27	$+0.21 \pm 0.51$	0.240 ± 0.002	23.1 (9.0)
162.47 ± 0.54	$+10.91 \pm 1.24$	0.160 ± 0.001	12.6 (15.6)	161.98 ± 0.53	$+8.10 \pm 1.16$	0.188 ± 0.002	14.4 (10.5)
179.19 ± 0.71	$+16.32 \pm 1.03$	0.203 ± 0.001	11.6 (11.3)	178.03 ± 0.62	$+12.30 \pm 1.25$	0.241 ± 0.002	10.7 (8.1)
193.15 ± 0.53	$+21.05 \pm 0.77$	0.265 ± 0.002	13.3 (11.4)	194.90 ± 0.53	$+13.49 \pm 1.16$	0.314 ± 0.002	12.1 (8.2)
220.64 ± 0.99	$+2.78 \pm 1.06$	0.289 ± 0.002	15.0 (14.6)	220.45 ± 0.45	$+5.37 \pm 0.60$	0.344 ± 0.002	15.4 (13.6)
269.42 ± 0.99	-25.44 ± 1.54	0.259 ± 0.002	19.4 (23.5)	272.09 ± 0.63	-19.32 ± 1.41	0.309 ± 0.003	18.2 (14.0)
317.76 ± 0.27	$+0.85 \pm 0.59$	0.186 ± 0.001	23.6 (14.2)	319.39 ± 0.62	$+0.89 \pm 1.02$	0.221 ± 0.002	23.2 (14.0)
348.75 ± 0.18	$+15.34 \pm 0.73$	0.143 ± 0.001	14.3 (10.6)	346.65 ± 0.53	$+12.02 \pm 1.16$	0.162 ± 0.001	13.6 (12.5)

Table 169: The nominal angle δ_n, average displacement $\Delta\delta$, average value of the parameter DIST, RMS of the ALPHA distribution for enabled GF and impact parameters between 60 m and 120 m. The RMS of the ALPHA distribution for disabled GF is given parentheses. The primary γ-ray energy was set to 1000 GeV, the ZA to 60° and the azimuth angle to 120°.

$E_\gamma = 1000\,\mathrm{GeV}$, Az = 150°, ZA = 60°, Intermediate Image Cleaning

$\delta_n[°]$	$\Delta\delta[°]$	DIST[°]	$\mathrm{RMS}_{\mid\mathrm{ALPHA}\mid}[°]$	$\delta_n[°]$	$\Delta\delta[°]$	DIST[°]	$\mathrm{RMS}_{\mid\mathrm{ALPHA}\mid}[°]$
IP = 60 m				IP = 80 m			
1.00 ± 0.47	$+12.99 \pm 1.24$	0.157 ± 0.001	10.7 (16.4)	358.94 ± 0.56	$+9.28 \pm 0.95$	0.205 ± 0.003	9.5 (10.1)
17.32 ± 0.47	$+24.66 \pm 1.33$	0.173 ± 0.002	9.5 (17.6)	16.99 ± 0.65	$+19.16 \pm 1.43$	0.225 ± 0.002	10.0 (11.8)
39.99 ± 1.68	$+38.47 \pm 1.95$	0.158 ± 0.001	18.9 (24.4)	38.65 ± 1.12	$+32.11 \pm 1.82$	0.206 ± 0.001	11.6 (20.1)
99.27 ± 0.74	-10.15 ± 1.34	0.128 ± 0.001	30.2 (14.1)	98.86 ± 1.96	-25.99 ± 2.24	0.159 ± 0.001	29.6 (23.1)
134.90 ± 0.45	-14.40 ± 1.11	0.117 ± 0.001	17.2 (20.9)	140.61 ± 1.30	-7.89 ± 1.79	0.133 ± 0.001	16.2 (17.6)
158.90 ± 1.30	$+2.08 \pm 1.78$	0.132 ± 0.001	17.4 (20.4)	163.25 ± 0.74	$+4.37 \pm 1.21$	0.162 ± 0.001	13.9 (12.9)
179.57 ± 0.28	$+15.00 \pm 0.83$	0.165 ± 0.002	13.6 (14.1)	179.64 ± 0.93	$+11.57 \pm 1.63$	0.209 ± 0.001	10.4 (11.8)
195.95 ± 0.74	$+24.05 \pm 1.37$	0.174 ± 0.001	13.2 (19.6)	195.94 ± 0.37	$+20.55 \pm 1.38$	0.228 ± 0.002	10.5 (9.7)
216.53 ± 0.29	$+22.10 \pm 1.25$	0.157 ± 0.001	13.1 (23.0)	215.94 ± 0.56	$+18.48 \pm 0.79$	0.204 ± 0.001	11.4 (20.0)
270.56 ± 0.26	-36.12 ± 0.57	0.122 ± 0.001	27.4 (21.5)	272.67 ± 0.47	-34.58 ± 1.34	0.148 ± 0.001	26.6 (22.8)
320.08 ± 0.47	-10.19 ± 1.13	0.122 ± 0.002	22.2 (23.3)	320.21 ± 0.09	-10.78 ± 0.56	0.120 ± 0.001	19.7 (21.1)
343.77 ± 0.47	$+3.81 \pm 0.94$	0.126 ± 0.002	17.7 (20.6)	342.87 ± 0.47	$+2.11 \pm 1.01$	0.153 ± 0.001	13.8 (15.2)
IP = 100 m				IP = 120 m			
0.74 ± 0.74	$+9.88 \pm 1.36$	0.252 ± 0.003	9.0 (9.5)	0.29 ± 0.37	$+8.22 \pm 0.91$	0.304 ± 0.002	8.6 (8.0)
16.28 ± 0.74	$+14.69 \pm 1.36$	0.285 ± 0.003	9.8 (9.7)	15.20 ± 0.47	$+12.86 \pm 1.16$	0.341 ± 0.003	9.3 (8.1)
40.58 ± 0.56	$+21.65 \pm 1.41$	0.259 ± 0.003	11.2 (13.9)	42.68 ± 0.28	$+22.21 \pm 0.36$	0.312 ± 0.003	11.9 (13.2)
90.82 ± 0.85	-31.30 ± 1.64	0.195 ± 0.002	25.4 (20.0)	89.41 ± 0.65	-28.66 ± 0.88	0.235 ± 0.002	22.7 (20.5)
137.40 ± 0.56	-8.92 ± 1.11	0.158 ± 0.001	20.3 (11.2)	137.89 ± 0.65	-6.87 ± 1.04	0.185 ± 0.001	21.5 (9.2)
163.11 ± 0.56	$+4.44 \pm 0.87$	0.199 ± 0.002	10.8 (11.9)	162.15 ± 0.47	$+2.27 \pm 1.01$	0.235 ± 0.001	11.0 (8.1)
177.59 ± 0.47	$+9.57 \pm 1.08$	0.260 ± 0.002	9.9 (10.3)	177.73 ± 0.65	$+8.52 \pm 1.12$	0.312 ± 0.003	9.0 (9.3)
193.94 ± 0.56	$+18.38 \pm 1.18$	0.283 ± 0.003	10.9 (10.5)	195.20 ± 0.56	$+17.31 \pm 1.10$	0.339 ± 0.002	9.9 (8.4)
219.60 ± 0.65	$+19.57 \pm 1.58$	0.252 ± 0.002	13.3 (17.5)	220.74 ± 0.56	$+25.94 \pm 0.95$	0.305 ± 0.003	11.8 (12.3)
270.21 ± 1.12	-27.78 ± 2.13	0.182 ± 0.001	23.5 (21.1)	269.72 ± 0.84	-28.83 ± 2.01	0.220 ± 0.002	24.1 (16.3)
317.85 ± 0.65	-9.76 ± 1.28	0.138 ± 0.001	20.4 (15.7)	318.97 ± 0.47	-7.29 ± 0.93	0.162 ± 0.001	18.5 (12.4)
345.44 ± 0.47	$+3.01 \pm 0.85$	0.185 ± 0.002	11.5 (15.5)	346.89 ± 0.74	$+4.26 \pm 1.13$	0.219 ± 0.003	11.9 (12.8)

Table 170: The nominal angle δ_n, average displacement $\Delta\delta$, average value of the parameter DIST, RMS of the ALPHA distribution for enabled GF and impact parameters between 60 m and 120 m. The RMS of the ALPHA distribution for disabled GF is given parentheses. The primary γ-ray energy was set to 1000 GeV, the ZA to 60° and the azimuth angle to 150°.

$E_\gamma = 1000\,\mathrm{GeV}$, Az = 150°, ZA = 60°, Hard Image Cleaning

$\delta_n[°]$	$\Delta\delta[°]$	DIST[°]	$\mathrm{RMS}_{\mid\mathrm{ALPHA}\mid}[°]$	$\delta_n[°]$	$\Delta\delta[°]$	DIST[°]	$\mathrm{RMS}_{\mid\mathrm{ALPHA}\mid}[°]$
IP = 60 m				IP = 80 m			
358.63 ± 0.62	$+11.01 \pm 1.19$	0.156 ± 0.001	11.8 (14.7)	358.23 ± 0.53	$+8.16 \pm 0.94$	0.209 ± 0.003	10.1 (12.0)
14.29 ± 0.36	$+22.05 \pm 1.42$	0.174 ± 0.002	9.2 (19.1)	13.79 ± 0.63	$+17.01 \pm 1.10$	0.225 ± 0.002	8.9 (12.3)
38.95 ± 0.10	$+33.73 \pm 1.00$	0.159 ± 0.001	17.2 (23.4)	36.95 ± 0.89	$+26.07 \pm 1.53$	0.207 ± 0.003	11.9 (18.6)
96.85 ± 0.38	-25.89 ± 1.15	0.127 ± 0.001	30.1 (11.5)	90.92 ± 0.11	-32.85 ± 0.88	0.158 ± 0.001	27.0 (25.1)
136.33 ± 0.32	-11.07 ± 0.91	0.115 ± 0.001	16.6 (23.5)	138.76 ± 0.98	-8.36 ± 1.49	0.132 ± 0.001	17.1 (18.8)
160.93 ± 0.45	$+3.20 \pm 0.95$	0.131 ± 0.001	16.3 (19.4)	165.91 ± 0.98	$+6.68 \pm 1.74$	0.161 ± 0.001	14.6 (11.5)
180.96 ± 0.62	$+14.37 \pm 1.19$	0.165 ± 0.001	13.4 (13.5)	180.99 ± 0.80	$+12.10 \pm 1.12$	0.210 ± 0.001	10.3 (13.0)
198.77 ± 0.36	$+26.41 \pm 0.92$	0.176 ± 0.001	11.2 (21.0)	196.90 ± 0.36	$+19.23 \pm 1.07$	0.230 ± 0.002	10.0 (8.4)
219.20 ± 0.09	$+23.75 \pm 0.59$	0.158 ± 0.001	12.7 (22.9)	219.36 ± 0.89	$+21.13 \pm 1.76$	0.205 ± 0.001	11.3 (17.8)
272.72 ± 2.84	-39.06 ± 3.80	0.120 ± 0.001	28.6 (25.5)	268.08 ± 0.63	-36.42 ± 1.36	0.148 ± 0.001	26.2 (21.3)
320.67 ± 0.18	-9.97 ± 0.69	0.114 ± 0.002	19.9 (24.6)	319.37 ± 0.18	-10.52 ± 0.74	0.120 ± 0.001	20.1 (18.8)
340.89 ± 1.07	$+1.74 \pm 1.96$	0.126 ± 0.002	16.3 (17.5)	343.47 ± 0.36	$+1.31 \pm 0.84$	0.151 ± 0.001	13.0 (16.5)
IP = 100 m				IP = 120 m			
0.83 ± 0.71	$+9.98 \pm 1.34$	0.254 ± 0.003	9.9 (11.1)	0.15 ± 0.53	$+8.13 \pm 1.01$	0.303 ± 0.003	8.7 (7.5)
17.09 ± 0.36	$+18.64 \pm 0.91$	0.285 ± 0.003	9.5 (13.8)	14.72 ± 0.71	$+11.89 \pm 1.34$	0.339 ± 0.003	8.7 (12.6)
38.32 ± 0.98	$+20.06 \pm 1.94$	0.260 ± 0.002	12.1 (15.3)	40.38 ± 0.36	$+20.52 \pm 0.75$	0.311 ± 0.003	11.2 (16.9)
91.32 ± 0.27	-28.04 ± 0.93	0.196 ± 0.002	24.9 (19.9)	92.19 ± 1.25	-25.06 ± 2.53	0.236 ± 0.002	25.7 (18.7)
135.78 ± 0.27	-11.17 ± 1.00	0.158 ± 0.001	19.8 (11.7)	136.43 ± 0.27	-6.85 ± 0.67	0.183 ± 0.001	21.8 (9.0)
162.47 ± 0.54	$+3.21 \pm 1.02$	0.199 ± 0.001	10.6 (15.6)	161.98 ± 0.53	$+1.86 \pm 0.93$	0.237 ± 0.001	12.7 (10.5)
179.19 ± 0.71	$+10.32 \pm 1.43$	0.262 ± 0.003	9.5 (11.3)	178.03 ± 0.62	$+7.92 \pm 1.18$	0.314 ± 0.003	9.2 (8.1)
193.15 ± 0.53	$+15.58 \pm 1.40$	0.283 ± 0.002	10.8 (11.4)	194.90 ± 0.53	$+15.61 \pm 1.25$	0.341 ± 0.003	9.6 (8.2)
220.64 ± 0.99	$+20.85 \pm 1.15$	0.254 ± 0.002	11.7 (14.6)	220.45 ± 0.45	$+26.35 \pm 1.62$	0.304 ± 0.002	12.0 (13.6)
269.42 ± 0.99	-27.23 ± 1.55	0.182 ± 0.001	22.6 (23.5)	272.09 ± 0.63	-24.63 ± 0.94	0.221 ± 0.002	24.5 (14.0)
317.76 ± 0.27	-9.13 ± 0.84	0.137 ± 0.001	20.7 (14.2)	319.39 ± 0.62	-8.61 ± 1.26	0.162 ± 0.001	19.7 (14.0)
348.75 ± 0.18	$+5.67 \pm 0.74$	0.185 ± 0.001	12.7 (10.6)	346.65 ± 0.53	$+3.34 \pm 1.01$	0.220 ± 0.003	12.6 (12.5)

Table 171: The nominal angle δ_n, average displacement $\Delta\delta$, average value of the parameter DIST, RMS of the ALPHA distribution for enabled GF and impact parameters between 60 m and 120 m. The RMS of the ALPHA distribution for disabled GF is given parentheses. The primary γ-ray energy was set to 1000 GeV, the ZA to 60° and the azimuth angle to 150°.

$E_\gamma = 1000\,\mathrm{GeV}$, Az = 180°, ZA = 60°, Intermediate Image Cleaning

δ_n[°]	$\Delta\delta$[°]	DIST[°]	$\mathrm{RMS}_{\lvert\mathrm{ALPHA}\rvert}$[°]	δ_n[°]	$\Delta\delta$[°]	DIST[°]	$\mathrm{RMS}_{\lvert\mathrm{ALPHA}\rvert}$[°]
IP = 60 m				IP = 80 m			
1.00 ± 0.47	$+1.41 \pm 1.03$	0.171 ± 0.001	6.1 (16.4)	358.94 ± 0.56	-1.65 ± 0.96	0.225 ± 0.002	6.8 (10.1)
17.32 ± 0.47	$+8.74 \pm 1.12$	0.158 ± 0.001	10.3 (17.6)	16.99 ± 0.65	$+9.46 \pm 1.22$	0.207 ± 0.001	5.8 (11.8)
39.99 ± 1.68	$+30.45 \pm 1.87$	0.127 ± 0.001	26.7 (24.4)	38.65 ± 1.12	$+23.46 \pm 2.02$	0.159 ± 0.001	27.6 (20.1)
99.27 ± 0.74	$+8.81 \pm 1.00$	0.112 ± 0.001	19.6 (14.1)	98.86 ± 1.96	$+4.59 \pm 2.46$	0.130 ± 0.001	25.1 (23.1)
134.90 ± 0.45	-34.01 ± 1.43	0.130 ± 0.001	18.2 (20.9)	140.61 ± 1.30	-23.47 ± 2.12	0.160 ± 0.001	17.3 (17.6)
158.90 ± 1.30	-12.88 ± 1.79	0.161 ± 0.002	11.8 (20.4)	163.25 ± 0.74	-7.97 ± 1.47	0.206 ± 0.001	9.0 (12.9)
179.57 ± 0.28	$+0.75 \pm 0.85$	0.171 ± 0.001	9.7 (14.1)	179.64 ± 0.93	$+1.56 \pm 1.50$	0.224 ± 0.002	6.6 (11.8)
195.95 ± 0.74	$+11.73 \pm 1.48$	0.157 ± 0.001	9.5 (19.6)	195.94 ± 0.37	$+7.98 \pm 0.94$	0.201 ± 0.002	6.6 (9.7)
216.53 ± 0.29	$+26.53 \pm 1.22$	0.124 ± 0.001	21.3 (23.0)	215.94 ± 0.56	$+18.53 \pm 1.37$	0.148 ± 0.001	17.6 (20.0)
270.56 ± 0.26	$+5.92 \pm 0.81$	0.111 ± 0.002	24.8 (21.5)	272.67 ± 0.47	$+8.69 \pm 0.71$	0.116 ± 0.001	22.5 (22.8)
320.08 ± 0.47	-17.54 ± 1.06	0.122 ± 0.001	19.0 (23.3)	320.21 ± 0.09	-15.76 ± 0.74	0.145 ± 0.001	16.5 (21.1)
343.77 ± 0.47	-3.71 ± 0.63	0.153 ± 0.001	10.2 (20.6)	342.87 ± 0.47	-5.29 ± 0.95	0.199 ± 0.002	7.3 (15.2)
IP = 100 m				IP = 120 m			
0.74 ± 0.74	$+1.03 \pm 1.31$	0.282 ± 0.003	5.2 (9.5)	0.29 ± 0.37	$+0.35 \pm 0.86$	0.337 ± 0.003	7.4 (8.0)
16.28 ± 0.74	$+7.39 \pm 1.31$	0.258 ± 0.003	10.5 (9.7)	15.20 ± 0.47	$+6.30 \pm 0.79$	0.308 ± 0.002	4.0 (8.1)
40.58 ± 0.56	$+17.92 \pm 1.44$	0.195 ± 0.002	14.3 (13.9)	42.68 ± 0.28	$+17.24 \pm 1.09$	0.233 ± 0.003	28.3 (13.2)
90.82 ± 0.85	$+4.92 \pm 1.59$	0.156 ± 0.001	27.9 (20.0)	89.41 ± 0.65	-2.38 ± 0.89	0.183 ± 0.001	29.4 (20.5)
137.40 ± 0.56	-20.34 ± 1.61	0.193 ± 0.002	17.1 (11.2)	137.89 ± 0.65	-18.49 ± 1.38	0.231 ± 0.002	16.1 (9.2)
163.11 ± 0.56	-7.52 ± 0.96	0.257 ± 0.003	8.6 (11.9)	162.15 ± 0.47	-7.96 ± 1.03	0.309 ± 0.003	8.7 (8.1)
177.59 ± 0.47	$+0.08 \pm 0.87$	0.281 ± 0.003	9.0 (10.3)	177.73 ± 0.65	-0.95 ± 1.05	0.337 ± 0.003	6.1 (9.3)
193.94 ± 0.56	$+4.69 \pm 1.12$	0.251 ± 0.003	6.4 (10.5)	195.20 ± 0.56	$+6.99 \pm 0.96$	0.303 ± 0.002	5.1 (8.4)
219.60 ± 0.65	$+18.84 \pm 1.62$	0.178 ± 0.001	15.5 (17.5)	220.74 ± 0.56	$+19.39 \pm 1.28$	0.214 ± 0.002	19.5 (12.3)
270.21 ± 1.12	$+9.73 \pm 1.20$	0.134 ± 0.001	25.8 (21.1)	269.72 ± 0.84	$+1.70 \pm 1.32$	0.160 ± 0.001	26.7 (16.3)
317.85 ± 0.65	-16.11 ± 1.14	0.180 ± 0.001	14.7 (15.7)	318.97 ± 0.47	-14.46 ± 0.55	0.215 ± 0.002	14.6 (12.4)
345.44 ± 0.47	-3.11 ± 0.87	0.252 ± 0.002	8.2 (15.5)	346.89 ± 0.74	-1.09 ± 1.31	0.302 ± 0.003	7.8 (12.8)

Table 172: The nominal angle δ_n, average displacement $\Delta\delta$, average value of the parameter DIST, RMS of the ALPHA distribution for enabled GF and impact parameters between 60 m and 120 m. The RMS of the ALPHA distribution for disabled GF is given parentheses. The primary γ-ray energy was set to 1000 GeV, the ZA to 60° and the azimuth angle to 180°.

$E_\gamma = 1000\,\mathrm{GeV}$, Az = 180°, ZA = 60°, Hard Image Cleaning

δ_n[°]	$\Delta\delta$[°]	DIST[°]	$\mathrm{RMS}_{\lvert\mathrm{ALPHA}\rvert}$[°]	δ_n[°]	$\Delta\delta$[°]	DIST[°]	$\mathrm{RMS}_{\lvert\mathrm{ALPHA}\rvert}$[°]
IP = 60 m				IP = 80 m			
358.63 ± 0.62	-1.53 ± 1.21	0.172 ± 0.001	6.4 (14.7)	358.23 ± 0.53	-2.21 ± 1.03	0.224 ± 0.002	6.2 (12.0)
14.29 ± 0.36	$+6.42 \pm 0.95$	0.158 ± 0.001	17.0 (19.1)	13.79 ± 0.63	$+7.13 \pm 1.04$	0.207 ± 0.001	8.7 (12.3)
38.95 ± 0.10	$+26.90 \pm 1.04$	0.127 ± 0.001	28.6 (23.4)	36.95 ± 0.89	$+19.52 \pm 1.73$	0.157 ± 0.001	30.1 (18.6)
96.85 ± 0.38	-0.29 ± 0.90	0.112 ± 0.001	21.0 (11.5)	90.92 ± 0.11	$+3.99 \pm 0.61$	0.129 ± 0.001	25.2 (25.1)
136.33 ± 0.32	-30.31 ± 1.41	0.130 ± 0.001	17.3 (23.5)	138.76 ± 0.98	-25.15 ± 1.90	0.158 ± 0.001	16.8 (18.8)
160.93 ± 0.45	-10.52 ± 1.04	0.161 ± 0.002	10.4 (19.4)	165.91 ± 0.98	-5.01 ± 1.31	0.206 ± 0.003	9.9 (11.5)
180.96 ± 0.62	$+1.56 \pm 1.22$	0.172 ± 0.001	10.2 (13.5)	180.99 ± 0.80	$+1.07 \pm 1.38$	0.226 ± 0.002	6.3 (13.0)
198.77 ± 0.36	$+11.72 \pm 0.86$	0.158 ± 0.001	9.8 (21.0)	196.90 ± 0.36	$+8.36 \pm 1.02$	0.203 ± 0.001	11.7 (8.4)
219.20 ± 0.09	$+27.00 \pm 0.70$	0.123 ± 0.001	23.8 (22.9)	219.36 ± 0.89	$+22.99 \pm 1.72$	0.149 ± 0.001	24.3 (17.8)
272.72 ± 2.84	$+5.94 \pm 2.95$	0.111 ± 0.002	27.7 (25.5)	268.08 ± 0.63	-0.57 ± 0.96	0.116 ± 0.001	23.6 (21.3)
320.67 ± 0.18	-18.11 ± 0.96	0.121 ± 0.001	18.0 (24.6)	319.37 ± 0.18	-15.54 ± 1.08	0.146 ± 0.001	16.4 (18.8)
340.89 ± 1.07	-7.02 ± 1.48	0.154 ± 0.001	10.2 (17.5)	343.47 ± 0.36	-4.59 ± 0.85	0.201 ± 0.001	7.0 (16.5)
IP = 100 m				IP = 120 m			
0.83 ± 0.71	$+0.80 \pm 1.20$	0.282 ± 0.003	4.9 (11.1)	0.15 ± 0.53	-0.39 ± 0.78	0.336 ± 0.002	5.7 (7.5)
17.09 ± 0.36	$+9.68 \pm 1.01$	0.258 ± 0.003	12.2 (13.8)	14.72 ± 0.71	$+6.23 \pm 1.37$	0.309 ± 0.003	5.2 (12.6)
38.32 ± 0.98	$+17.16 \pm 2.06$	0.195 ± 0.002	15.3 (15.3)	40.38 ± 0.36	$+15.12 \pm 1.68$	0.235 ± 0.002	21.7 (16.9)
91.32 ± 0.27	$+3.84 \pm 0.36$	0.156 ± 0.001	28.4 (19.9)	92.19 ± 1.25	$+3.17 \pm 1.58$	0.183 ± 0.001	27.8 (18.7)
135.78 ± 0.27	-19.90 ± 1.19	0.193 ± 0.002	16.8 (11.7)	136.43 ± 0.27	-19.59 ± 1.19	0.234 ± 0.002	15.3 (9.0)
162.47 ± 0.54	-8.70 ± 1.11	0.259 ± 0.002	8.6 (15.6)	161.98 ± 0.53	-9.06 ± 1.03	0.308 ± 0.003	8.1 (10.5)
179.19 ± 0.71	$+0.26 \pm 1.12$	0.281 ± 0.003	6.6 (11.3)	178.03 ± 0.62	-1.55 ± 1.03	0.338 ± 0.003	6.0 (8.1)
193.15 ± 0.53	$+4.72 \pm 0.86$	0.251 ± 0.003	6.2 (11.4)	194.90 ± 0.53	$+5.79 \pm 1.11$	0.304 ± 0.003	3.9 (8.2)
220.64 ± 0.99	$+19.46 \pm 1.73$	0.180 ± 0.001	9.5 (14.6)	220.45 ± 0.45	$+17.79 \pm 0.70$	0.216 ± 0.002	16.5 (13.6)
269.42 ± 0.99	$+6.65 \pm 1.40$	0.135 ± 0.001	27.1 (23.5)	272.09 ± 0.63	-0.95 ± 0.95	0.160 ± 0.001	27.9 (14.0)
317.76 ± 0.27	-15.96 ± 1.18	0.180 ± 0.001	15.5 (14.2)	319.39 ± 0.62	-12.62 ± 1.29	0.216 ± 0.002	15.7 (14.0)
348.75 ± 0.18	-0.07 ± 0.59	0.253 ± 0.001	7.6 (10.6)	346.65 ± 0.53	-1.37 ± 1.02	0.303 ± 0.002	8.7 (12.5)

Table 173: The nominal angle δ_n, average displacement $\Delta\delta$, average value of the parameter DIST, RMS of the ALPHA distribution for enabled GF and impact parameters between 60 m and 120 m. The RMS of the ALPHA distribution for disabled GF is given parentheses. The primary γ-ray energy was set to 1000 GeV, the ZA to 60° and the azimuth angle to 180°.

References

[1] J. Albert et al. (MAGIC collaboration), First Observation of the Giant Radio Galaxy M87 in the 100 GeV Energy Domain with the MAGIC Telescope, 29th International Cosmic Ray Conference Pune, India (2005) 4, 295-298.

[2] J. Albert at al. (MAGIC collaboration), Observation of Gamma Rays from the Galactic Center with the MAGIC Telescope, Astrophys. J., 638:L101-L104, 2006 February 20.

[3] J. Albert et al. (MAGIC collaboration), Observation of VHE Gamma Radiation from HESS J1834-087/W41 with the MAGIC Telescope, Astrophys. J., 643:L53-L56, 2006 May 20.

[4] J. Albert et al. (MAGIC collaboration), Variable Very-High-Energy Gamma-Ray Emission from the Microquasar LS I +61 303, Science 312:1771-1773, June 2006 23.

[5] H. Anderhub, private communication.

[6] J.A. Barrio et al., The MAGIC telescope design report, Max-Planck-Institut für Physik, Munich, report MPI-PhE/98-5 (1998).

[7] A. Unsöld, B. Baschek, Der Neue Kosmos, 6. Auflage, Springer-Verlag, 1999.

[8] O. Blanch, A. Moralejo, How To Use The Camera Simulation Program 0.7, MAGIC-TDAS 04-07/040906.

[9] R.K. Bock et al., Methods for multidimensional event classification: a case study using images from a Cherenkov gamma-ray telescope, Nucl. Instr. & Methods A 516 (2004) 511-528.

[10] C.C.G. Bowden et al., The effect of the geomagnetic field on TeV γ-ray detection, J. Phys. G: Nucl. Part. Phys. 18 (1992) L55-L60.

[11] T. Bretz et al., The MAGIC Analysis And Reconstruction Software, 28th International Cosmic Ray Conference Tsukuba, Japan (2003) 2947-2950.

[12] I.N. Bronstein, K.A. Semendjajew, G. Musiol, H. Mühlig, Taschenbuch der Mathematik, 4. Auflage, Verlag Harri Deutsch, 1999.

[13] W.H. Campbell, Introduction to Geomagnetic Fields, Cambridge University Press, 2nd edition (2003).

[14] P.M. Chadwick et al., Geomagnetic effects on atmospheric Čerenkov images, J. Phys. G: Nucl. Part. Phys. 25 (1999) 1223-1233.

[15] P.M. Chadwick et al., The correction of atmospheric Čherenkov images for the effect of the geomagnetic field, J. Phys. G: Nucl. Part. Phys. 26 (2000) L5-L9.

[16] G. Cocconi, Influence of the Earth's Magnetic Field on the Extensive Air Showers, Phys. Rev. 93:646-647 (1953).

[17] S. Commichau, PhD Dissertation, ETH-17118 (2007).

[18] S. Commichau et al., Geomagnetic Field Effects on the Imaging Air Shower Cherenkov Technique, 30th International Cosmic Ray Conference Mérida, México (2007), `http://arxiv.org/abs/0709.1251`.

[19] J. Cortina et al., Technical Performance of the MAGIC Telescope, 29th International Cosmic Ray Conference Pune, India (2005) 5, 359-362.

[20] E. Domingo-Santamaria et al., The DISP analysis method for point-like or extended γ source searches/studies with the MAGIC Telescope, Proc. 29th International Cosmic Ray Conference Pune, India (2005) 5, 363-366.

[21] D. Heck et al., CORSIKA, A Monte Carlo code to simulate extensive air showers, Forschungszentrum Karlsruhe, Report FZKA 6019, (1998).

[22] A.M. Hillas, Cerenkov light images of EAS produced by primary gamma rays and by nuclei, 19th International Cosmic Ray Conference (1985) 445-448.

[23] Web pages of the International Real-time Magnetic Observatory Network (INTERMAGNET), `http://www.intermagnet.org/`.

[24] P. Jaco'n, D. Sobczyńska, T. Wibig, A data analysis preprocessing; the effect of the Earth magnetic field on MAGIC shower images, MAGIC-TDAS 04-02/040520.

[25] M. Kasztelan, T. Wibig and D. Sobczyńska, Effect of the Earth Magnetic Field on MAGIC Shower Images, MAGIC-TDAS 02-13/021217.

[26] M.H. Kräber, Feasibility Study of a Synchrotron Radiation Detector for AMS on the International Space Station, PhD thesis, ETH Zurich, 2002.

[27] D. Kranich, Temporal and spectral characteristics of the active galactic nucleus Mkn 501 during a phase of high activity in the TeV range, PhD thesis, TU Munich, 2000.

[28] M.J. Lang, A search for a geomagnetic effect on the sensitivity of the atmospheric Cherenkov imaging technique, J. Phys. G: Nucl. Part. Phys. 20 (1994) 1841-1850.

[29] The MARS web pages, University of Würzburg, Germany, `http://magic.astro.uni-wuerzburg.de:81/mars/`.

[30] The MARS IFAE web pages, UAB Bellaterra, Barcelona, Spain, `http://cvs.ifae.es`.

[31] A. Moralejo, The Reflector Simulation Program V 0.6, MAGIC-TDAS 02-11/030120.

[32] M. Mori et al., The Cangaroo-III Project, Proc. GeV-TeV Gamma-Ray Astrophysics Workshop, "Towards a Major Atmospheric Cherenkov Detector VI Snowbird", Utah, August 13-16, 1999.

[33] Web pages of the National Geophysical Data Center (NGDC), `http://www.ngdc.noaa.gov/seg/geomag/`.

[34] R. de los Reyes, Effect of earth magnetic field in the MAGIC Telescope effective area for gammas, MAGIC-TDAS 03-05/030511.

[35] The ROOT website, CERN, `http://root.cern.ch`.

[36] D. Sobczyńska, MMcs from CORSIKA 6.014, MAGIC-TDAS 02-10/020730.

[37] D. Sobczyńska, Characteristics of a few GeV γ showers, MAGIC-TDAS 03-05/03052003.

[38] R.M. Wagner et al., Observations of the Crab nebula with the MAGIC telescope, 29th International Cosmic Ray Conference Pune, India (2005) 4, 163-166.

[39] A. Wenger, The effect of the earth's magnetic field on extensive air showers, diploma thesis, Institute for Particle Physics, ETH Zürich 2004.